

APPLIED PROCESS DESIGN

FOR CHEMICAL AND PETROCHEMICAL PLANTS

Volume 2, Third Edition

Covers distillation and packed towers, and shows how to apply techniques of process design and interpret results into mechanical equipment details



Ernest E. Ludwig

**A P P L I E D
P R O C E S S
D E S I G N**

FOR CHEMICAL AND PETROCHEMICAL PLANTS

Volume 2, Third Edition

- Volume 1:**
1. Process Planning, Scheduling, Flowsheet Design
 2. Fluid Flow
 3. Pumping of Liquids
 4. Mechanical Separations
 5. Mixing of Liquids
 6. Ejectors
 7. Process Safety and Pressure-Relieving Devices
- Appendix of Conversion Factors
- Volume 2:**
8. Distillation
 9. Packed Towers
- Volume 3:**
10. Heat Transfer
 11. Refrigeration Systems
 12. Compression Equipment
 13. Compression Surge Drums
 14. Mechanical Drivers



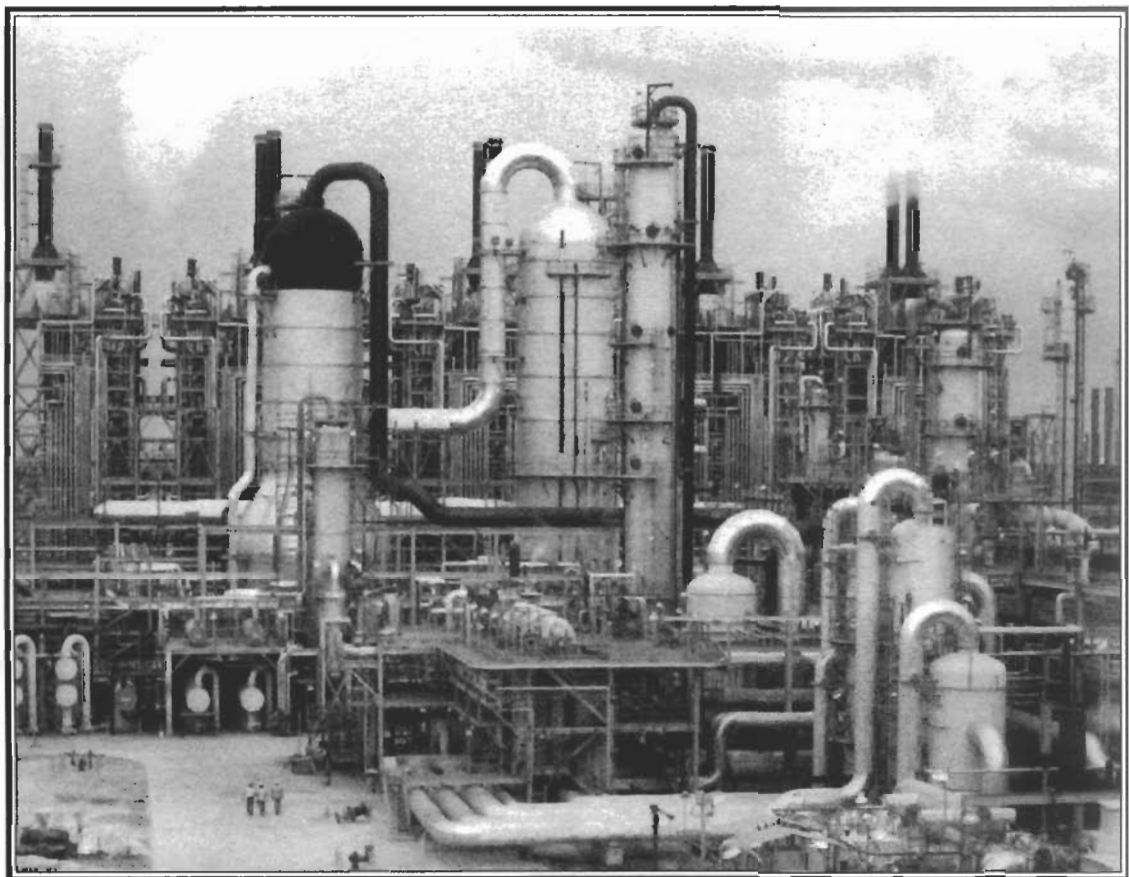
Gulf Professional Publishing
an imprint of Butterworth-Heinemann

A P P L I E D P R O C E S S D E S I G N

FOR CHEMICAL AND PETROCHEMICAL PLANTS

Volume 2, Third Edition

Covers distillation and packed towers, and shows how to apply techniques of process design and interpret results into mechanical equipment details



Ernest E. Ludwig

*To my wife, Sue, for her
patient encouragement and help*



Disclaimer

The material in this book was prepared in good faith and carefully reviewed and edited. The author and publisher, however, cannot be held liable for errors of any sort in these chapters. Furthermore, because the author has no means of checking the reliability of some of the data presented in the public literature, but can only examine it for suitability for the intended purpose herein, this information cannot be warranted. Also because the author cannot vouch for the experience or technical capability of the user of the information and the suitability of the information for the user's purpose, the use of the contents must be at the best judgment of the user.

Copyright © 1964, 1979 by Butterworth-Heinemann.
Copyright © 1997 by Ernest E. Ludwig. All rights reserved.
Printed in the United States of America.
This book, or parts thereof, may not be reproduced in any form
without permission of the publisher.

Originally published by Gulf Publishing Company,
Houston, TX.

10 9 8 7 6 5 4 3 2

For information, please contact:
Manager of Special Sales
Butterworth-Heinemann
225 Wildwood Avenue
Woburn, MA 01801-2041
Tel: 781-904-2500
Fax: 781-904-2620
For information on all Butterworth-Heinemann publications available,
contact our World Wide Web home page at: <http://www.bh.com>

Library of Congress Cataloging-in-Publication Data

Ludwig, Ernest E.
Applied process design for chemical and petrochemical
plants / Ernest E. Ludwig. — 3rd ed.
p. cm.
Includes bibliographical references and index.
ISBN 0-88415-025-9 (v. 1)
1. Chemical plants—Equipment and supplies. 2.
Petroleum industry and trade—Equipment and supplies.
I. Title.
TP 155.5.L8 1994
660'.283—dc20

94-13383
CIP

Printed on Acid-Free Paper (∞)

Contents

Preface to Third Edition	v	
8. Distillation	1	
Part 1		
Distillation Process Performance	1	
Equilibrium Basic Consideration, 1; Ideal Systems, 2; K-Factor Hydrocarbon Equilibrium Charts, 4; Non-Ideal Systems, 5; Example 8-1: Raoult's Law, 14; Binary System Material Balance: Constant Molal Overflow Tray to Tray, 15; Example 8-2: Bubble Point and Dew Point, 17; Example 8-3: Flashing Composition; Distillation Operating Pressures, 18; Total Condenser, 19; Partial Condenser, 20; Thermal Condition of Feed, 20; Total Reflux, Minimum Plates, 21; Fenske Equation: Overall Minimum Total Tray with Total Condenser, 22; Relative Volatility, 22; Example 8-4: Determine Minimum Number of Trays by Winn's Method, 24; Example 8-5: Boiling Point Curve and Equilibrium Diagram for Benzene-Toluene Mixture, 26; Example 8-7: Flash Vaporization of a Hydrocarbon Liquid Mixture, 27; Quick Estimate of Relative Volatility, 28; Example 8-8: Relative Volatility Estimate by Wagle's Method, 29; Minimum Reflux Ratio: Infinite Plates, 29; Theoretical Trays at Actual Reflux, 30; Example 8-9: Solving Gilliland's Equation for Determining Minimum Theoretical Plates for Setting Actual Reflux, 32; "Pinch Conditions" on x-y Diagram at High Pressure, 32; Example 8-10: Graphical Design for Binary Systems, 33; Example 8-11: Thermal Condition of Feed, 35; Example 8-12: Minimum Theoretical Trays/Plates/Stages at Total Reflux, 38; Tray Efficiency, 40; Example 8-13: Estimating Distillation Tray Efficiency, 42; Batch Distillation, 45; Differential Distillation, 46; Simple Batch Distillation, 47; Fixed Number Theoretical Trays, 48; Batch with Constant Reflux Ratio, 48; Batch with Variable Reflux Rate Rectification, 50; Example 8-14: Batch Distillation, Constant Reflux; Following the Procedure of Block, 51; Example 8-15: Vapor Boil-up Rate for Fixed Trays, 53; Example 8-16: Binary Batch Differential Distillation, 54; Example 8-17: Multicomponent Batch Distillation, 55; Steam Distillation, 57; Example 8-18: Multicomponent Steam Flash, 59; Example 8-18: Continuous Steam Flash Separation Process — Separation of Non-Volatile Component from Organics, 61; Example 8-20: Open Steam Stripping of Heavy Absorber Rich Oil of Light Hydrocarbon Content, 62; Distillation with Heat Balance,		63; Unequal Molal Flow, 63; Ponchon-Savarit Method, 63; Example 8-21: Ponchon Unequal Molal Overflow, 65; Multicomponent Distillation, 68; Minimum Reflux Ratio — Infinite Plates, 68; Example 8-22: Multicomponent Distillation by Yaw's Method, 70; Algebraic Plate-to-Plate Method, 70; Underwood Algebraic Method, 71; Example 8-23: Minimum Reflux Ratio Using Underwood Equation, 73; Minimum Reflux Colburn Method, 74; Example 8-24: Using the Colburn Equation to Calculate Minimum Reflux Ratio, 76; Scheibel-Montross Empirical: Adjacent Key Systems, 79; Example 8-25: Scheibel-Montross Minimum Reflux, 80; Minimum Number of Trays: Total Reflux — Constant Volatility, 80; Chou and Yaws Method, 81; Example 8-26: Distillation with Two Sidestream Feeds, 82; Theoretical Trays at Operating Reflux, 83; Example 8-27: Operating Reflux Ratio, 84; Estimating Multicomponent Recoveries, 85; Example 8-28: Estimated Multicomponent Recoveries by Yaw's Method, 87; Tray-by-Tray Using a Computer, 90; Example 8-29: Tray-to-Tray Design Multicomponent Mixture, 90; Example 8-30: Tray-by-Tray Multicomponent Mixture Using a Computer, 95; Computer Printout for Multicomponent Distillation, 95; Example 8-31: Multicomponent Examination of Reflux Ratio and Distillate to Feed Ratio, 99; Example 8-32: Stripping Dissolved Organics from Water in a Packed Tower Using Method of Li and Hsiao, 100; Troubleshooting, Predictive Maintenance, and Controls for Distillation Columns, 101; Nomenclature for Part 1, 102
		Part 2
		Hydrocarbon Absorption and Stripping
		108
		Kremser-Brown-Sherwood Method — No Heat of Absorption, 108; Absorption — Determine Component Absorption in Fixed Tray Tower, 108; Absorption — Determine Number of Trays for Specified Product Absorption, 109; Stripping — Determine Theoretical Trays and Stripping or Gas Rate for a Component Recovery, 110; Stripping — Determine Stripping-Medium Rate for Fixed Recovery, 111; Absorption — Edmister Method, 112; Example 8-33: Absorption of Hydrocarbons with Lean Oil, 114; Intercooling for Absorbers, 116; Absorption and Stripping Efficiency, 118; Example 8-34: Determine Number of Trays for Specified Product Absorption, 118; Example 8-35: Determine Component Absorption in Fixed-Tray Tower, 119; Nomenclature for Part 2, 121

Part 3
Mechanical Designs
for Tray Performance 122

Contacting Trays, 122; Tray Types and Distinguishing Application Features, 122; **Bubble Cap Tray Design**, 124; **Tray Layouts**, 130; Flow Paths, 130; Liquid Distribution: Feed, Side Streams, Reflux, 131; Liquid By-Pass Baffles, 135; Liquid Drainage or Weep Holes, 154; Bottom Tray Seal Pan, 154; Turndown Ratio, 155; **Bubble Caps**, 155; Slots, 156; Shroud Ring, 156; **Tray Performance — Bubble Caps**, 158; Tray Capacity Related to Vapor-Liquid Loads, 156; Tray Balance, Flexibility, and Stability, 157; Flooding, 157; Pulsing, 157; Blowing, 158; Coning, 158, Entrainment, 158; Overdesign, 158; Total Tray Pressure Drop, 158; Liquid Height Over Outlet Weir, 158; Slot Opening, 158; Riser and Reversal Drop, 166; Total Pressure Drop Through Tray, 167; Downcomer Pressure Drop, 167; Liquid Height in Downcomer, 168; Downcomer Seal, 168; Tray Spacing, 168; Residence Time in Downcomers, 169; Liquid Entrainment from Bubble Cap Trays, 169; Free Height in Downcomer, 170; Slot Seal, 170; Inlet Weir, 170; Bottom Tray Seal Pan, 170; Throw Over Outlet Segmental Weir, 170; Vapor Distribution, 171; **Bubble Cap Tray Design and Evaluation**, 171; Example 8-36: Bubble Cap Tray Design, 171; **Sieve Trays with Downcomers**, 174; Tower Diameter, 176; Tray Spacing, 177; Downcomer, 177; Hole Size and Spacing, 178; Tray Hydraulics, 179; Height of Liquid Over Outlet Weir, 179; Hydraulic Gradient, 179; Dry Tray Pressure Drop, 180; Fair's Method, 181; Static Liquid Seal on Tray, or Submergence, 181; Dynamic Liquid Seal, 182; Total Wet Tray Pressure Drop, 182; Pressure Drop Through Downcomer, 183; Free Height in Downcomer, 183; Minimum Vapor Velocity: Weep Point, 183; Entrainment Flooding, 187; Example 8-37: Sieve Tray Splitter Design for Entrainment Flooding Using Fair's Method, 191; Maximum Hole Velocity: Flooding, 193; Design Hole Velocity, 193; Tray Stability, 193; Vapor Cross-Flow Channeling on Sieve Trays, 194; Tray Layout, 195; Example 8-38: Sieve Tray Design (Perforated) with Downcomer, 195; Example 8-39: Tower Diameter Following Fair's Recommendation, 199; **Perforated Plates Without Downcomers**, 202; Diameter, 203; Capacity, 203; Pressure Drop, 203; Dry Pressure Drop, 203; Effective Head, 203; Total Wet Tray Pressure Drop, 203; Hole Size, Spacing, Percent Open Area, 203; Tray Spacing, 204; Entrainment, 204; Dump Point, Plate Activation Point, or Load Point, 204; Efficiency, 204; Flood Point, 205; Tray Designs and Layout, 205; Example 8-40: Design of Perforated Trays Without Downcomers, 206; Proprietary Valve Trays Design and Selection, 207; Example 8-41: Procedure for Calculating Valve Tray Pressure Drop, 210; Proprietary Designs, 211; Baffle Tray Columns, 213; Example 8-42: Mass Transfer Efficiency Calculation for Baffle Tray Column, 215; **Tower Specifications**, 215; Mechanical Problems in Tray Distillation Columns, 220; Troubleshooting Distillation Columns, 221; Nomenclature for Part 3, 221; References, 223; Bibliography, 226

9. Packed Towers230

Shell, 234; **Random Packing**, 234; **Packing Supports**, 236; **Liquid Distribution**, 246; Redistributors, 269; Packing Installation, 270; Stacked, 270; Dumped, 270; **Packing Selection and Performance**, 272; Guidelines: Trays vs. Packings, 272; Minimum Liquid Wetting Rates, 281; Loading Point—Loading Region, 282; Flooding Point, 288; Foaming Liquid Systems, 288; Surface Tension Effects, 289; **Packing Factors**, 290; **Recommended Design Capacity and Pressure Drop**, 292; Pressure Drop Design Criteria and Guide: Random Packings Only, 293; Proprietary Random Packing Design Guides, 301; Example 9-1: Hydrocarbon Stripper Design, 302; **Dumped Packing: Gas-Liquid System Below Loading**, 310; Loading and Flooding Regions, 310; Pressure Drop at Flooding, 311; Pressure Drop Below and at Flood Point, Liquid Continuous Range, 311; Pressure Drop Across Packing Supports and Redistribution Plates, 312; Example 9-2: Evaluation of Tower Condition and Pressure Drop, 313; Example 9-3: Alternate Evaluation of Tower Condition and Pressure Drop, 315; Example 9-4: Change of Performance with Change in Packing in Existing Tower, 315; Example 9-5: Stacked Packing Pressure Drop, 316; Liquid Hold-Up, 317; Corrections Factors for Liquid Other Than Water, 318; Packed Wetted Area, 320; Effective Interfacial Area, 320; Entrainment from Packing Surface, 320; Example 9-6: Operation at Low Rate, Liquid Hold-Up, 320; **Structured Packing**, 322; Example 9-7: Koch-Sulzer Packing Tower Sizing, 326; Example 9-8: Heavy Gas-Oil Fractionation of a Crude Tower Using Glitsch's Gempak, 331; Technical Performance Features, 337; Guidelines for Structured Packings, 342; Structured Packing Scale-Up, 342; **Mass and Heat Transfer in Packed Towers**, 343; Number of Transfer Units, 343; Example 9-9: Number of Transfer Units for Dilute Solutions, 346; Example 9-10: Use of Colburn's Chart for Transfer Units, 348; Example 9-11: Number Transfer Units—Concentrated Solutions, 348; Gas and Liquid-Phase Coefficients, 349; Height of a Transfer Unit, 350; Example 9-12: Design of Ammonia Absorption Tower, 352; **Mass Transfer with Chemical Reaction**, 361; Carbon Dioxide or Sulfur Dioxide in Alkaline Solutions, 361; Example 9-13: Design a Packed Tower Using Caustic to Remove Carbon Dioxide from Vent Stream, 364; NH₃-Air-H₂O System, 367; SO₂-H₂O System (Dilute Gas), 368; Air-Water System, 369; Hydrogen Chloride-Water System, 369; **Distillation in Packed Towers**, 370; Height Equivalent to a Theoretical Plate (HETP), 370; HETP Guidelines, 375; Transfer Unit, 375; Example 9-14: Transfer Units in Distillation, 377; **Cooling Water with Air**, 379; Atmospheric, 380; Natural Drafts, 380; Forced Draft, 380; Induced Draft, 380; General Construction, 380; **Cooling Tower Terminology**, 381; Specifications, 383; Performance, 387; Ground Area vs. Height, 391; Pressure Losses, 393; Fan Horsepower for Mechanical Draft Tower, 392; Water Rates and Distribution, 393; Blow-Down and Continuation Build-Up, 394; Example 9-15: Determining Approximate Blow-Down for Cooling Tower, 395; Pre-

liminary Design Estimate of New Tower, 396; Performance Evaluation of Existing Tower, 396; Example 9-16: Wood Packed Cooling Tower with Recirculation, Induced Draft, 396; Nomenclature, 408; References, 411; Bibliography, 414

Appendix416

A-1: Alphabetical Conversion Factors, 416; A-2: Physical Property Conversion Factors, 423; A-3: Synchronous Speeds, 426; A-4: Conversion Factors, 427; A-5: Temperature Conversion, 429; A-6: Altitude and Atmospheric Pressures, 430; A-7: Vapor Pressure Curves, 431; A-8: Pressure Conversion Chart, 432; A-9: Vacuum Conversion, 433; A-10: Decimal and Millimeter Equivalents of Fractions, 434; A-11: Particle Size Measurement, 434; A-12: Viscosity Conversions, 435; A-13: Viscosity Conversions, 436; A-14: Commercial Wrought Steel Pipe Data, 437; A-15: Stainless Steel Pipe Data, 440; A-16: Properties of Pipe, 441; A-17: Equation of Pipes, 450; A-18: Circumferences and Areas of Circles, 451; A-19: Capacities of Cylinders and Spheres, 457; A-20: Tank Capacities, Horizontal Cylindrical—Contents of Tanks with Flat Ends When Filled to Various Depths, 461; A-21: Tank Capacities, Horizontal Cylindri-

cal—Contents of Standard Dished Heads When Filled to Various Depths, 461; A-22: Miscellaneous Formulas, 462; A-23: Decimal Equivalents in Inches, Feet and Millimeters, 463; A-24: Properties of the Circle, Area of Plane Figures, and Volume of a Wedge, 464; A-24: A-24 (continued): Trigonometric Formulas, 465; A-24 (continued): Properties of Sections, 465; A-25: Wind Chill Equivalent Temperatures on Exposed Flesh at Varying Velocity, 469; A-26: Impurities in Water, 469; A-27: Water Analysis Conversions for Units Employed: Equivalents, 470; A-28: Parts Per Million to Grains Per U.S. Gallon, 470; A-29: Formulas, Molecular and Equivalent Weights, and Conversion Factors to CaCO₃ of Substances Frequently Appearing in the Chemistry of Water Softening, 471; A-30: Grains Per U.S. Gallons—Pounds Per 1000 Gallons, 473; A-31: Parts Per Million—Pounds Per 1000 Gallons, 473; A-32: Coagulant, Acid, and Sulfate—1 ppm Equivalents, 473; A-33: Alkali and Lime—1ppm Equivalents, 474; A-34: Sulfuric, Hydrochloric Acid Equivalent, 474; A-35: ASME Flanged and Dished Heads IDD Chart, 475; A-35 (continued): Elliptical Heads, 476; A-35 (continued): 80-10 Heads, 477.

Index.....478

Preface to the Third Edition

The techniques of process design continue to improve as the science of chemical engineering develops new and better interpretations of fundamentals. Accordingly, this third edition presents additional, reliable design methods based on proven techniques and supported by pertinent data. Since the first edition, much progress has been made in standardizing and improving the design techniques for the hardware components that are used in designing process equipment. This standardization has been incorporated in the previous and this latest edition, as much as practically possible. Although most of the chapters have been expanded to include new material, some obsolete information has been removed. Chapter 8 on Distillation has incorporated additional multicomponent systems information and enlarged batch separation fundamentals. The variety of the mechanical hardware now applied to distillation separations has greatly expanded, and Chapter 9 has been significantly updated to reflect developments in the rapidly expanding packed tower field. References are also updated.

The many aspects of process design are essential to the proper performance of the work of chemical engineers, and other engineers engaged in the process engineering design details for chemical and petrochemical plants. Process design has developed by necessity into a unique section of the scope of work for the broad spectrum of chemical engineering.

The purpose of these 3 volumes is to present techniques of process design and to interpret the results into mechanical equipment details. There is no attempt to present theoretical developments of the design equations. The equations recommended have practically all been used in actual plant equipment design, and are considered to be the most reasonable available to the author, and still capable of being handled by both the inexperienced as well as the experienced engineer. A conscious effort has been made to offer guidelines to judgment, decisions and selections, and some of this will be found in the illustrative problems.

The text material assumes that the reader is a graduate or equivalent chemical or related engineer, having a

sound knowledge of the fundamentals of the profession. From this background the reader is led into the techniques of design required to actually design as well as mechanically detail and specify. It is my philosophy that the process engineer has not adequately performed his/her function unless the results of a process calculation for equipment are specified in terms of something that can be economically built, and which can by visual or mental techniques be *mechanically interpreted* to actually perform the process function for which it is being designed. This concept is stressed to a reasonable degree in the various chapters.

As a part of the objective, the chapters are developed by the *design function* of the designing engineer and not in accordance with previously suggested standards for unit operations. In fact some chapters use the same principles, but require different interpretations when recognized in relation to the *process* and the function the equipment performs in this process.

Due to the magnitude of the task of preparing such material in proper detail, it has been necessary to drop several important topics with which every designing engineer must be acquainted, such as corrosion, cost estimating, economics and several others. These are now left to the more specialized works of several fine authors. Recognizing this reduction in content, I'm confident that in many petrochemical and chemical processes the designer will find design techniques adaptable to 75–80 percent of his/her requirements. Thus, an effort has been made to place this book in a position of utilization somewhere between a handbook and an applied teaching text. The present work is considered suitable for graduate courses in detailed process design, and particularly if a general course in plant design is available to fill in the broader factors associated with overall plant layout and planning. Also see Volumes 1 and 3 of this series.

I am indebted to the many industrial firms that have so generously made available certain valuable design data and information. This credit is acknowledged at the appropriate locations in the text, except for the few cases where a specific request was made to omit this credit.

I was encouraged to undertake this work by Dr. James Villbrandt, together with the late Dr. W. A. Cunningham and Dr. J. J. McKetta. The latter two, together with the late Dr. K. A. Kobe, offered many suggestions to help establish the usefulness of the material to the broadest group of engineers. Dr. P. A. Bryant, a professor at Louisiana State University, contributed significantly to updating the second edition's Absorption and Stripping section.

In addition, I am deeply appreciative of the courtesy of The Dow Chemical Co. for the use of certain noncredited materials, and their release for publication. In this regard, particular thanks are given to Mr. N. D. Griswold and Mr. J. E. Ross. The valuable contribution of associates in

checking material and making suggestions is gratefully acknowledged to H. F. Hasenbeck, L. T. McBeth, E. R. Ketchum, J. D. Hajek, W. J. Evers, D. A. Gibson.

The contribution of Western Supply Co. through Mr. James E. Hughes is also acknowledged with appreciation.

The courtesy of the Rexall Chemical Co. to encourage continuation of this work is also gratefully appreciated.

I have incorporated my 27+ years of broad industrial consulting in process design, project management, and industrial safety relating to fires and explosions as may be applicable.

Ernest E. Ludwig, P. E.
Baton Rouge, Louisiana

Distillation

Part 1: Distillation Process Performance

Efficient and economical performance of distillation equipment is vital to many processes. Although the art and science of distillation has been practiced for many years, studies still continue to determine the best design procedures for multicomponent, azeotropic, batch, multidraw, multifeed and other types. Some shortcut procedures are adequate for many systems, yet have limitations in others; in fact the same might be said even for more detailed procedures.

The methods outlined in this chapter are considered adequate for the stated conditions, yet some specific systems may be exceptions to these generalizations. The process engineer often “double checks” his results by using a second method to verify the “ball-park” results, or shortcut recognized as being inadequate for fine detail.

Current design techniques using computer programs allow excellent prediction of performance for complicated multicomponent systems such as azeotropic or high hydrogen hydrocarbon as well as extremely high purity of one or more product streams. Of course, the more straightforward, uncomplicated systems are being predicted with excellent accuracy also. The use of computers provides capability to examine a useful array of variables, which is invaluable in selecting optimum or at least preferred modes or conditions of operation.

The expense of fabrication and erection of this equipment certainly warrants recognition of the quality of methods as well as extra checking time prior to initiating fabrication. The general process symbol diagram of Figure 8-1 will be used as reference for the systems and methods pre-

sented. Nomenclature for (1) distillation performance and design is on page 102 (2) absorption and stripping on page 121 and (3) tray hydraulic design on page 221.

Equilibrium Basic Considerations

Distillation design is based on the theoretical consideration that heat and mass transfer from stage to stage (theoretical) are in equilibrium [225–229]. Actual columns with actual trays are designed by establishing column tray efficiencies, and applying these to the theoretical trays or stages determined by the calculation methods to be presented in later sections.

Dechman [109] illustrates a modification to the usual McCabe-Thiele diagram that assumes constant molal overflow in a diagram that recognizes unequal molal overflow.

Distillation, extractive distillation, liquid-liquid extraction and absorption are all techniques used to separate binary and multicomponent mixtures of liquids and vapors. Reference 121 examines approaches to determine optimum process sequences for separating components from a mixture, primarily by distillation.

It is essential to calculate, predict or experimentally determine vapor-liquid equilibrium data in order to adequately perform distillation calculations. These data need to relate composition, temperature, and system pressure.

Basically there are two types of systems: ideal and non-ideal. These terms apply to the simpler binary or two component systems as well as to the often more complex multicomponent systems.

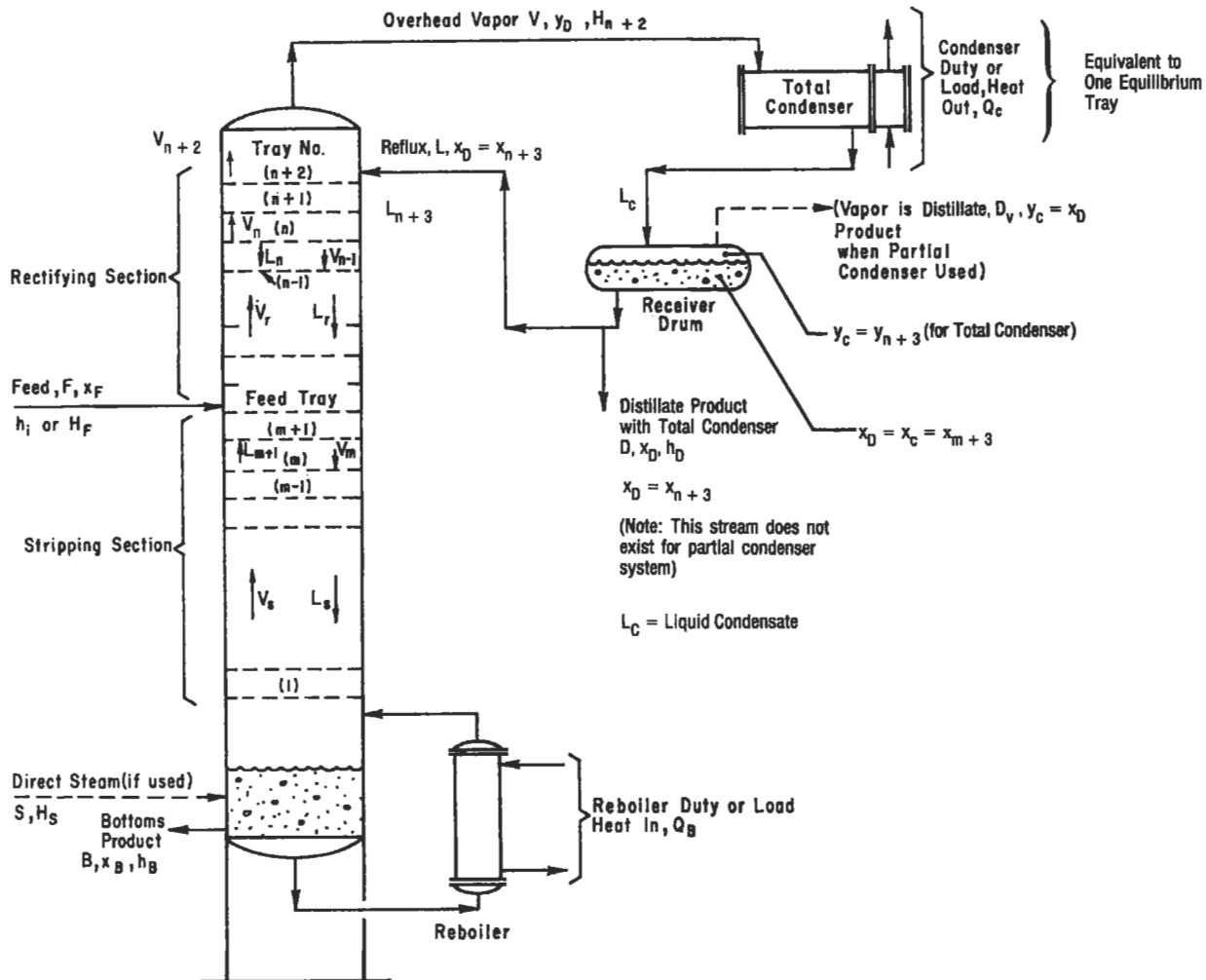


Figure 8-1. Schematic distillation tower/column arrangement with total condenser.

Figure 8-2 illustrates a typical normal volatility vapor-liquid equilibrium curve for a particular component of interest in a distillation separation, usually for the more volatile of the binary mixture, or the one where separation is important in a multicomponent mixture.

Ideal Systems

The separation performance of these systems (usually low-pressure, not close to critical conditions, and with similar components) can be predicted by Raoult's Law, applying to vapor and liquid in equilibrium.

When one liquid is dissolved (totally miscible) in another, the partial pressure of each is decreased. Raoult's Law states that for any mixture the partial pressure of any component will equal the vapor pressure of that component in the pure state times its mol fraction in the liquid mixture.

$$p_i = p_i^* x_i = P_i x_i \quad (8-1)$$

$$p_{ii} = P_{ii} x_{ii} \quad (\text{for a second component, } ii, \text{ in the system}) \quad (8-2)$$

where p_i = partial pressure, absolute, of one component in the liquid solution

x_i = mol fraction of component, i , in the liquid solution

$p_i^* = P_i$ = vapor pressure of component, i , in its pure state; p_{ii}^* similar by analogy

There are many mixtures of liquids that do not follow Raoult's Law, which represents the performance of ideal mixtures. For those systems following the ideal gas law and Raoult's Law for the liquid, for each component,

$$y_i = \frac{p_i}{\pi} = \frac{P_i^* x_i}{\pi} \quad (8-3)$$

(Raoult's Law combined with Dalton's Law)

y_i = mol fraction of component, i , in vapor
 π = system total pressure

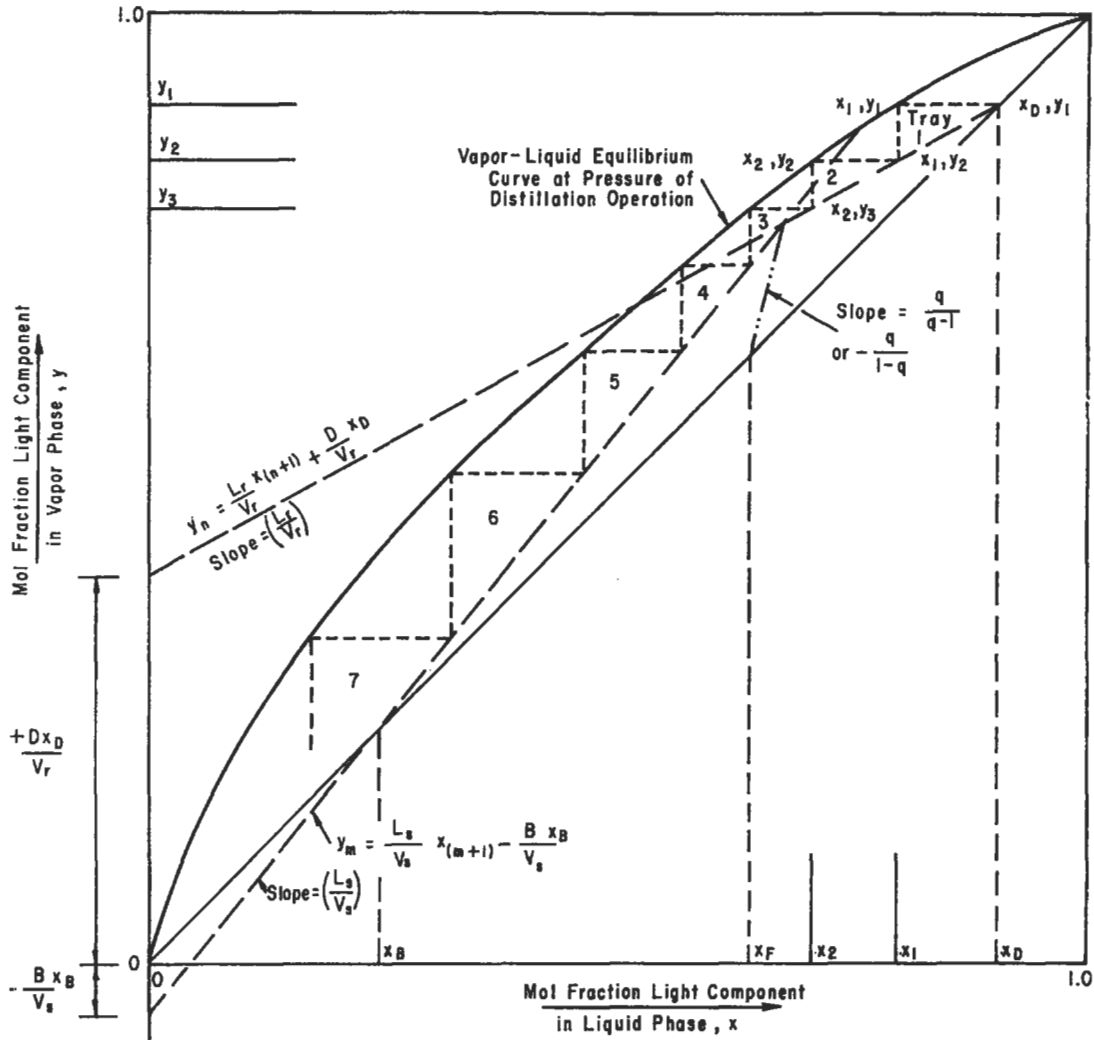


Figure 8-2. Continuous fractionation of binary mixtures; McCabe-Thiele Diagram with total condenser.

Raoult's Law is not applicable as the conditions approach critical, and for hydrocarbon mixtures accuracy is lost above about 60 psig [81].

Dalton's Law relates composition of the vapor phase to the pressure and temperature well below the critical pressure, that is, total pressure of a system is the sum of its component's partial pressure:

$$\pi = p_1 + p_2 + p_3 + \dots \quad (8 - 4)$$

where p_1, p_2, \dots = partial pressures of components numbered 1, 2, ...

Therefore, for Raoult's and Dalton's Laws to apply, the relationship between the vapor and liquid composition for a given component of a mixture is a function only of pressure and temperature, and independent of the other components in the mixture.

Henry's Law applies to the vapor pressure of the solute in dilute solutions, and is a modification of Raoult's Law:

Henry's Law—

$$p_i = k x_i \quad (8 - 5)$$

where p_i = partial pressure of the solute
 x_i = mol fraction solute in solution
 k = experimentally determined Henry's constant

Referring to Figure 8-2, Henry's Law would usually be expected to apply on the vaporization curve for about the first 1 in. of length, starting with zero, because this is the dilute end, while Raoult's Law applies to the upper end of the curve.

Carroll [82] discusses Henry's Law in detail and explains the limitations. This constant is a function of the solute-solvent pair and the temperature, but not the pres-

sure, because it is only a valid concept in the stage of infinite dilution. It is equal to the reference fugacity only at infinite dilution. From [82]:

Strict Henry's Law

$$x_i H_{ij} = y_i P \quad (8-6)$$

for restrictions of: $x_i < 0.01$ and $P < 200$ kPa

Simple Henry's Law

$$x_i H_{ij} = P \quad (8-7)$$

for restrictions of: $x_i < 0.01$, $y_j \approx 0$, and $P < 200$ kPa

$$K = \frac{y_i}{x_i} = \frac{P_i^*}{P} \quad (8-8)$$

where H_{ij} = Henry's constant
 x_i = mol fraction of solute component, i, in liquid
 P = pressure, absolute
 y_i = mol fraction of solute component, i, in vapor
 y_j = mol fraction solvent component, j, in vapor
 kPa = metric pressure

Care must be exercised that the appropriate assumptions are made, which may require experience and/or experimentation.

Carroll [83] presents Henry's Law constant evaluation for several multicomponent mixtures, i.e., (1) a non-volatile substance (such as a solid) dissolved in a solvent, (2) solubility of a gas in solution of aqueous electrolytes, (3) mixed electrolytes, (4) mixed solvents, i.e., a gas in equilibrium with a solvent composed of two or more components, (5) two or more gaseous solutes in equilibrium with a single solvent, (6) complex, simultaneous phase and chemical equilibrium.

Values of K-equilibrium factors are usually associated with hydrocarbon systems for which most data have been developed. See following paragraph on K-factor charts. For systems of chemical components where such factors are not developed, the basic relation is:

$$K_i = \frac{y_i}{x_i} = \frac{v_i}{\Omega_i} \frac{P_i^*}{P} \quad (8-9)$$

For ideal systems: $v_i = \Omega_i$

where K_i = mol fraction of component, i, in vapor phase in equilibrium divided by mol fraction of component, i, in liquid phase in equilibrium
 Ω_i = equilibrium distribution coefficient for system's component, i
 P_i^* = vapor pressure of component, i, at temperature
 P = total pressure of system = π

v = activity coefficient
 Ω = fugacity coefficient

The ideal concept is usually a good approximation for close boiling components of a system, wherein the components are all of the same "family" of hydrocarbons or chemicals; for example paraffin hydrocarbons. When "odd" or non-family components are present, the possibility of deviations from non-ideality becomes greater, or if the system is a wide boiling range of components.

Often for preliminary calculation, the ideal conditions are assumed, followed by more rigorous design methods. The first approximation ideal basis calculations may be completely satisfactory, particularly when the activities of the individual components are 1.0 or nearly so.

Although it is not the intent of this chapter to evaluate the methods and techniques for establishing the equilibrium relationships, selected references will be given for the benefit of the designer's pursuit of more detail. This subject is so detailed as to require specialized books for adequate reference such as Prausnitz [54].

Many process components do not conform to the ideal gas laws for pressure, volume and temperature relationships. Therefore, when ideal concepts are applied by calculation, erroneous results are obtained—some not serious when the deviation from ideal is not significant, but some can be quite serious. Therefore, when data are available to confirm the ideality or non-ideality of a system, then the choice of approach is much more straightforward and can proceed with a high degree of confidence.

K-Factor Hydrocarbon Equilibrium Charts

K-factors for vapor-liquid equilibrium ratios are usually associated with various hydrocarbons and some common impurities as nitrogen, carbon dioxide, and hydrogen sulfide [48]. The K-factor is the *equilibrium* ratio of the mole fraction of a component in the vapor phase divided by the mole fraction of the same component in the liquid phase. K is generally considered a function of the mixture composition in which a specific component occurs, plus the temperature and pressure of the system at equilibrium.

The Gas Processors Suppliers Association [79] provides a more detailed background development of the K-factors and the use of *convergence pressure*. Convergence pressure alone does not represent a system's composition effects in hydrocarbon mixtures, but the concept does provide a rather rapid approach for systems calculations and is used for many industrial calculations. These are not well adapted for very low temperature separation systems.

The charts of reference [79] are for binary systems unless noted otherwise. Within a reasonable degree of accuracy the convergence can usually represent the com-

position of the equilibrium for the vapor and liquid phases, and is the critical pressure for a system at a specific temperature. The convergence pressure represents the pressure of system at a temperature when the vapor-liquid separation is no longer possible [79]. The convergence pressure generally is a function of the liquid phase, and assumes that the liquid composition is known from a flash calculation using a first estimate for convergence pressure, and is usually the critical pressure of a system at a given temperature. The following procedure is recommended by Reference 79:

Step 1. Assume the liquid phase composition or make an approximation. (If there is no guide, use the total feed composition.)

Step 2. Identify the lightest hydrocarbon component that is present at least 0.1 mole % in the liquid phase.

Step 3. Calculate the weight average critical temperature and critical pressure for the remaining heavier components to form a pseudo binary system. (A shortcut approach good for most hydrocarbon systems is to calculate the weight average T_c only.)

Step 4. Trace the critical locus of the binary consisting of the light component and pseudo heavy component. When the averaged pseudo heavy component is between two real hydrocarbons, an interpolation of the two critical loci must be made.

Step 5. Read the convergence pressure (ordinate) at the temperature (abscissa) corresponding to that of the desired flash conditions, from Figure 8-3A [79].

Step 6. Using the convergence pressure determined in Step 5, together with the system temperature and system pressure, obtain K-values for the components from the appropriate convergence-pressure K-charts.

Step 7. Make a flash calculation with the feed composition and the K-values from Step 6.

Step 8. Repeat Steps 2 through 7 until the assumed and calculated convergence pressures check within an acceptable tolerance, or until the two successive calculations for the same light and pseudo heavy components agree within an acceptable tolerance.

The calculation procedure can be iterative after starting with the first "guess." Refer to Figure 8-3A to determine the most representative convergence pressure, using methane as the light component (see Figure 8-3B for selecting K values convergence pressure.)

For a temperature of 100°F, the convergence pressure is approximately 2,500 psia (dotted line) for the pseudo system methane-n-pentane (see Figure 8-3C). For n-pentane at convergence pressure of 3,000 psia (nearest chart) the K-value reads 0.19. The DePriester charts [80] check this quite well (see Figures 8-4A and B, and Figure 8-3D).

Interpolation between charts of convergence pressure can be calculated, depending on how close the operating pressure is to the convergence pressure. The K-factor (or K-values) do not change rapidly with convergence pressure, P_k (psia) [79].

The use of the K-factor charts represents pure components and pseudo binary systems of a light hydrocarbon plus a calculated pseudo heavy component in a mixture, when several components are present. It is necessary to determine the average molecular weight of the system on a methane-free basis, and then interpolate the K-value between the two binaries whose heavy component lies on either side of the pseudo-components. If nitrogen is present by more than 3–5 mol%, the accuracy becomes poor. See Reference 79 to obtain more detailed explanation and a more complete set of charts.

Non-Ideal Systems

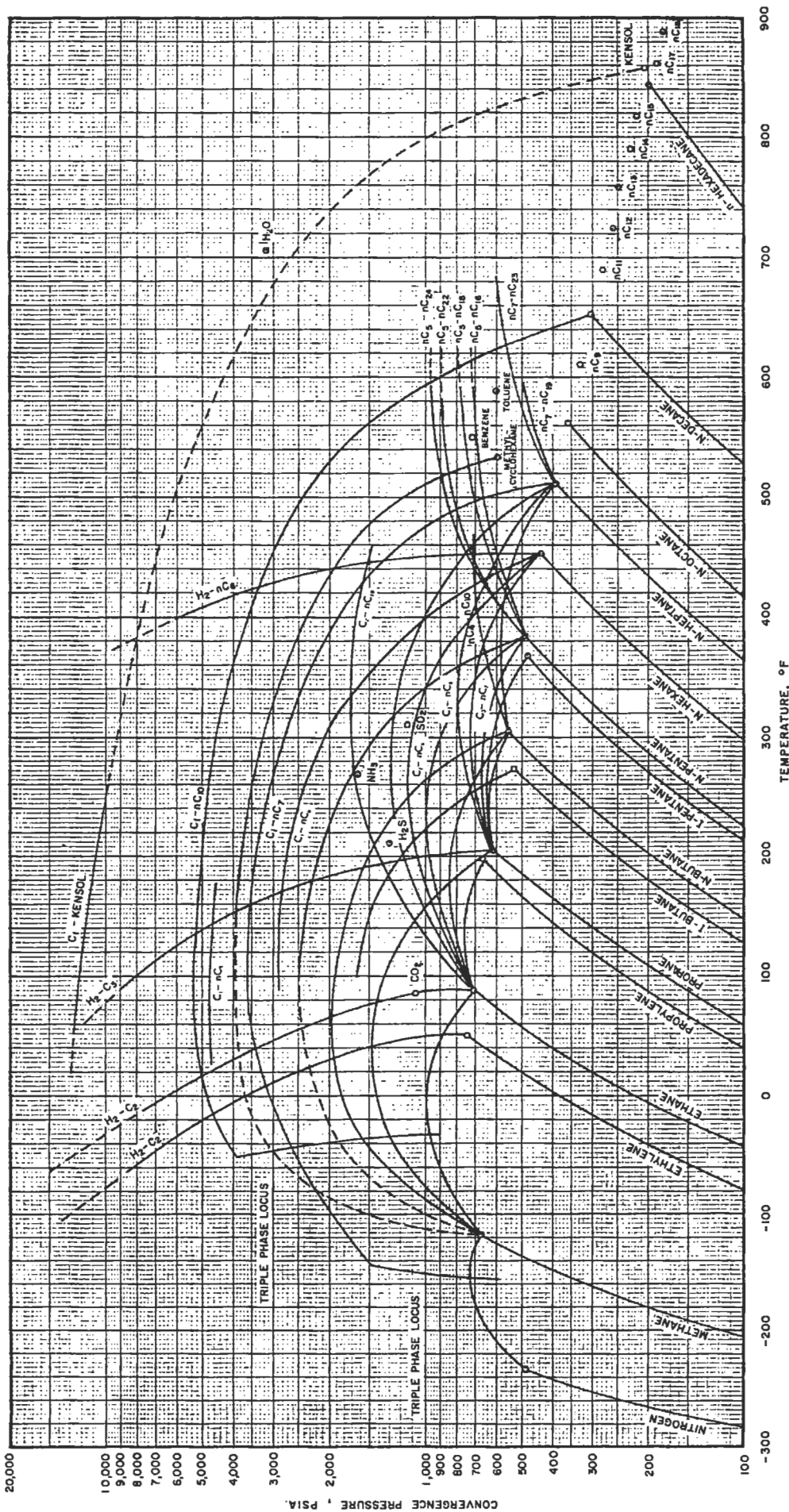
Systems of two or more hydrocarbon, chemical and water components may be non-ideal for a variety of reasons. In order to accurately predict the distillation performance of these systems, accurate, experimental data are necessary. Second best is the use of specific empirical relationships that predict with varying degrees of accuracy the vapor pressure-concentration relationships at specific temperatures and pressures.

Prausnitz [54] presents a thorough analysis of the application of empirical techniques in the absence of experimental data.

The heart of the question of non-ideality deals with the determination of the distribution of the respective system components between the liquid and gaseous phases. The concepts of fugacity and activity are fundamental to the interpretation of the non-ideal systems. For a pure ideal gas the fugacity is equal to the pressure, and for a component, i , in a mixture of ideal gases it is equal to its partial pressure $y_i P$, where P is the system pressure. As the system pressure approaches zero, the fugacity approaches ideal. For many systems the deviations from unity are minor at system pressures less than 25 psig.

The ratio f/f° is called activity, a . **Note:** This is *not* the activity coefficient. The activity is an indication of how "active" a substance is relative to its standard state (not necessarily zero pressure), f° . The standard state is the reference condition, which may be anything; however, most references are to constant temperature, with composition and pressure varying as required. Fugacity becomes a corrected pressure, representing a specific component's deviation from ideal. The fugacity coefficient is:

(text continued on page 12)



Note: These convergence pressures are the basis for the convergence charts. Later data do not necessarily agree.

Rev. 1976

Figure 8-3A. Convergence pressures for hydrocarbons (critical locus). Used by permission, Gas Processors Suppliers Association Data Book, 9th Ed. V. 1 and 2 (1972-1987), Tulsa, Okla.

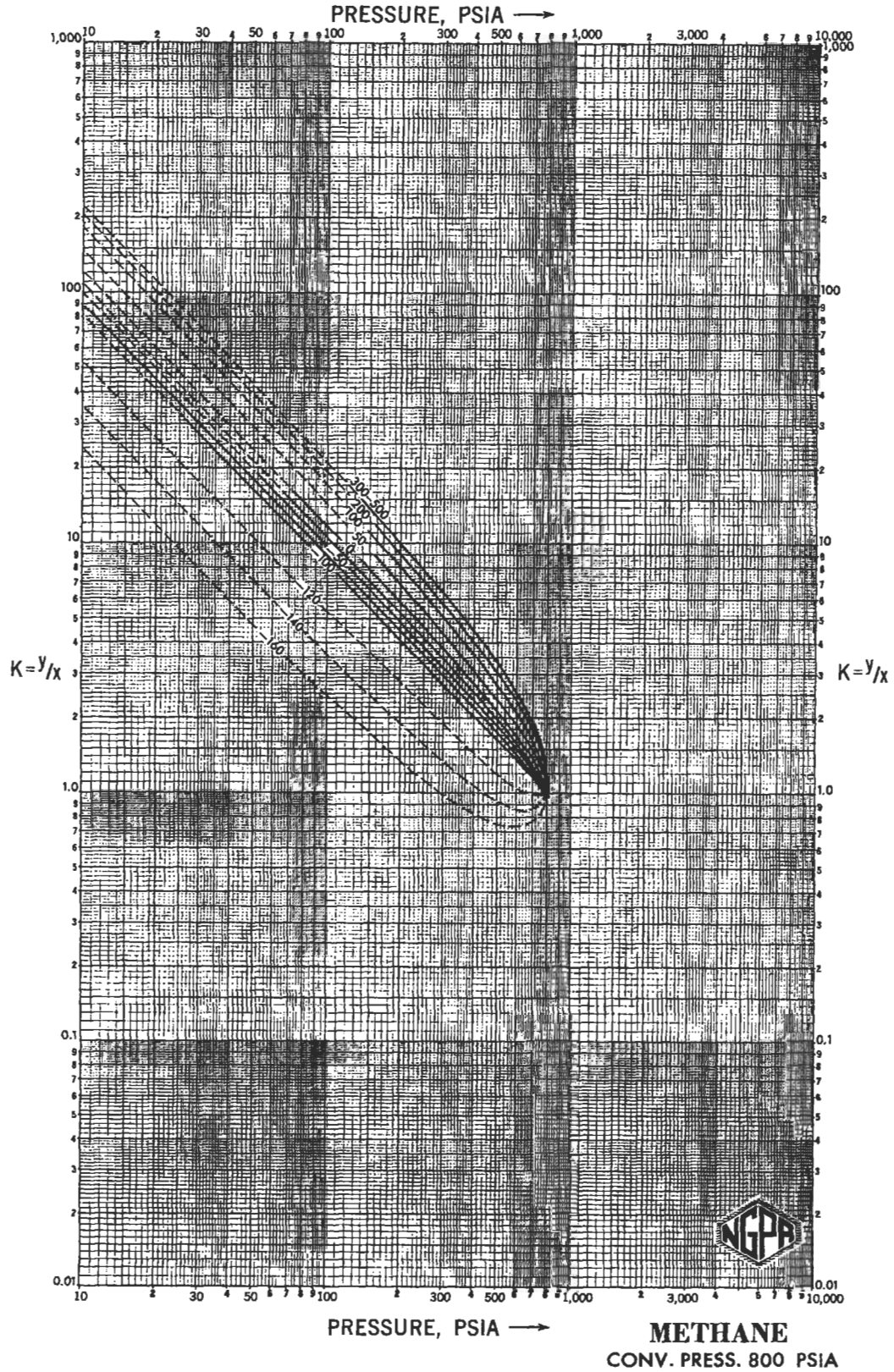


Figure 8-3B. Pressure vs. K for methane at convergence pressure of 800 psia. Used by permission, Gas Processors Suppliers Association Data Book, 9th Ed. V. 1 and 2 (1972-1987), Tulsa, Okla.

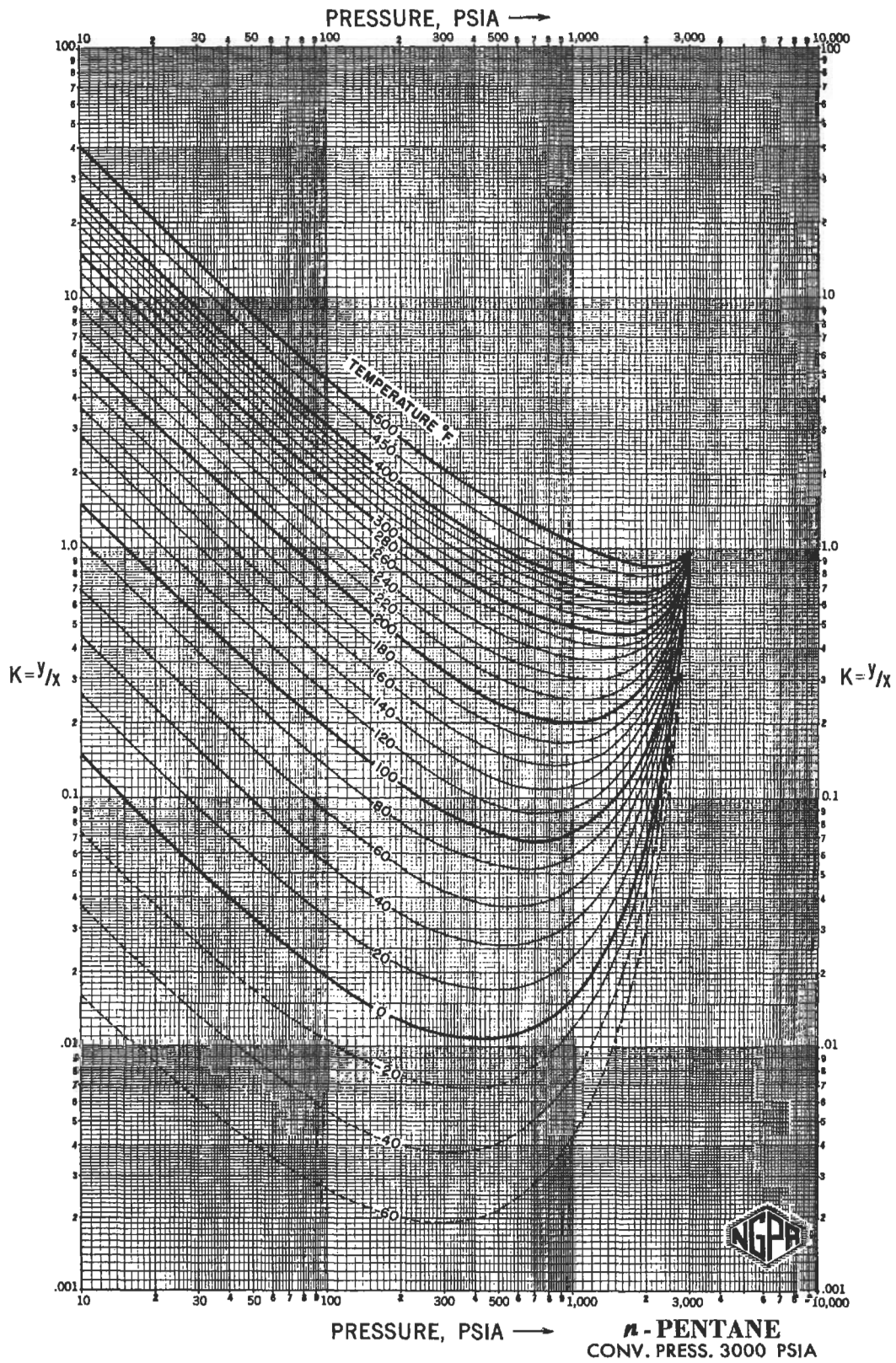


Figure 8-3C. Pressure vs. K for n-pentane at convergence pressure of 3,000 psia. Used by permission, Gas Processors Suppliers Association Data Book, 9th Ed. V. 1 and 2 (1972-1987), Tulsa, Okla.

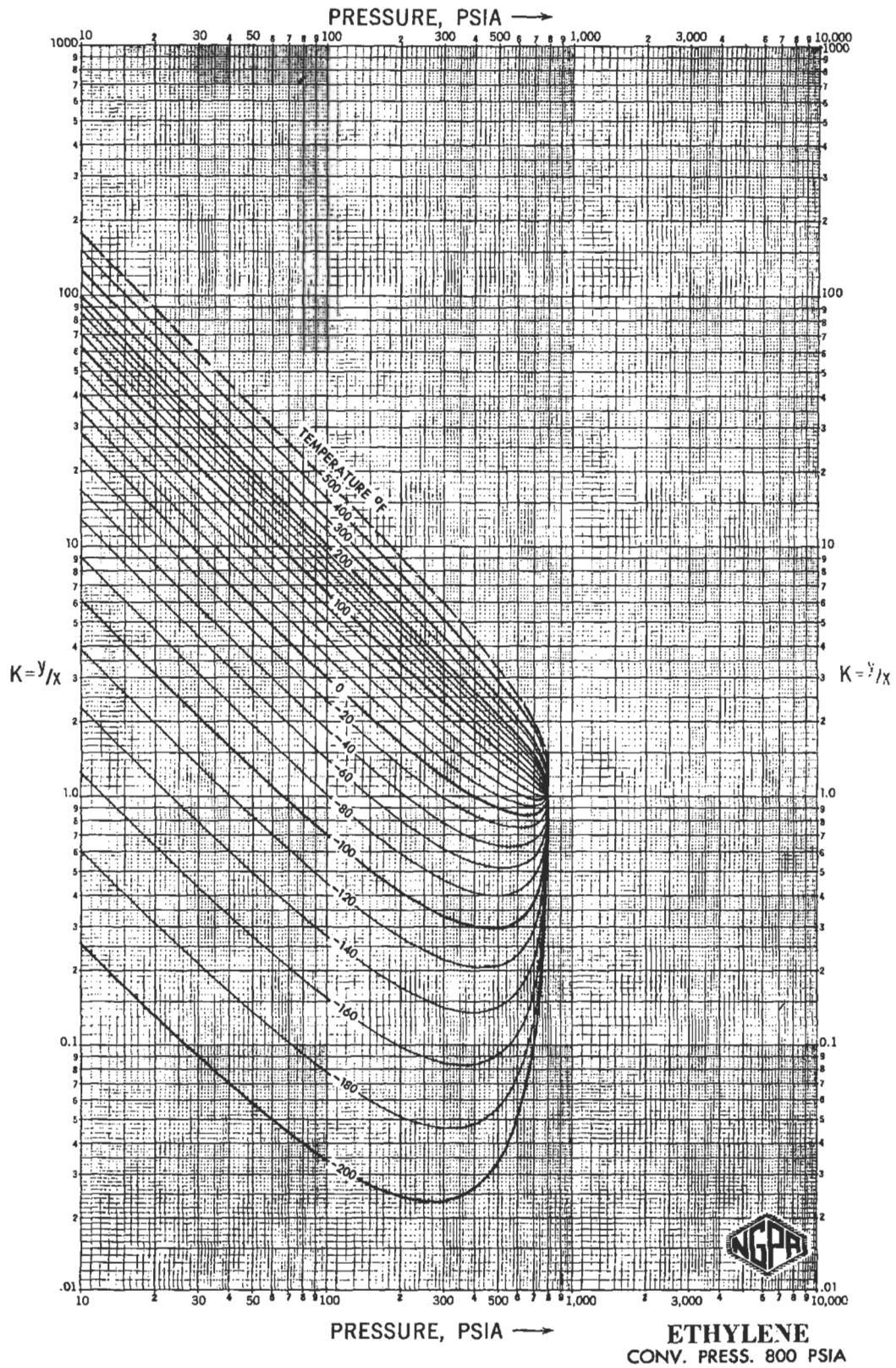


Figure 8-3D. Pressure vs. K for ethylene at convergence pressure of 800 psia. Used by permission, *Gas Processors Suppliers Association Data Book*, 9th Ed. V. 1 and 2 (1972-1987), Tulsa, Okla.

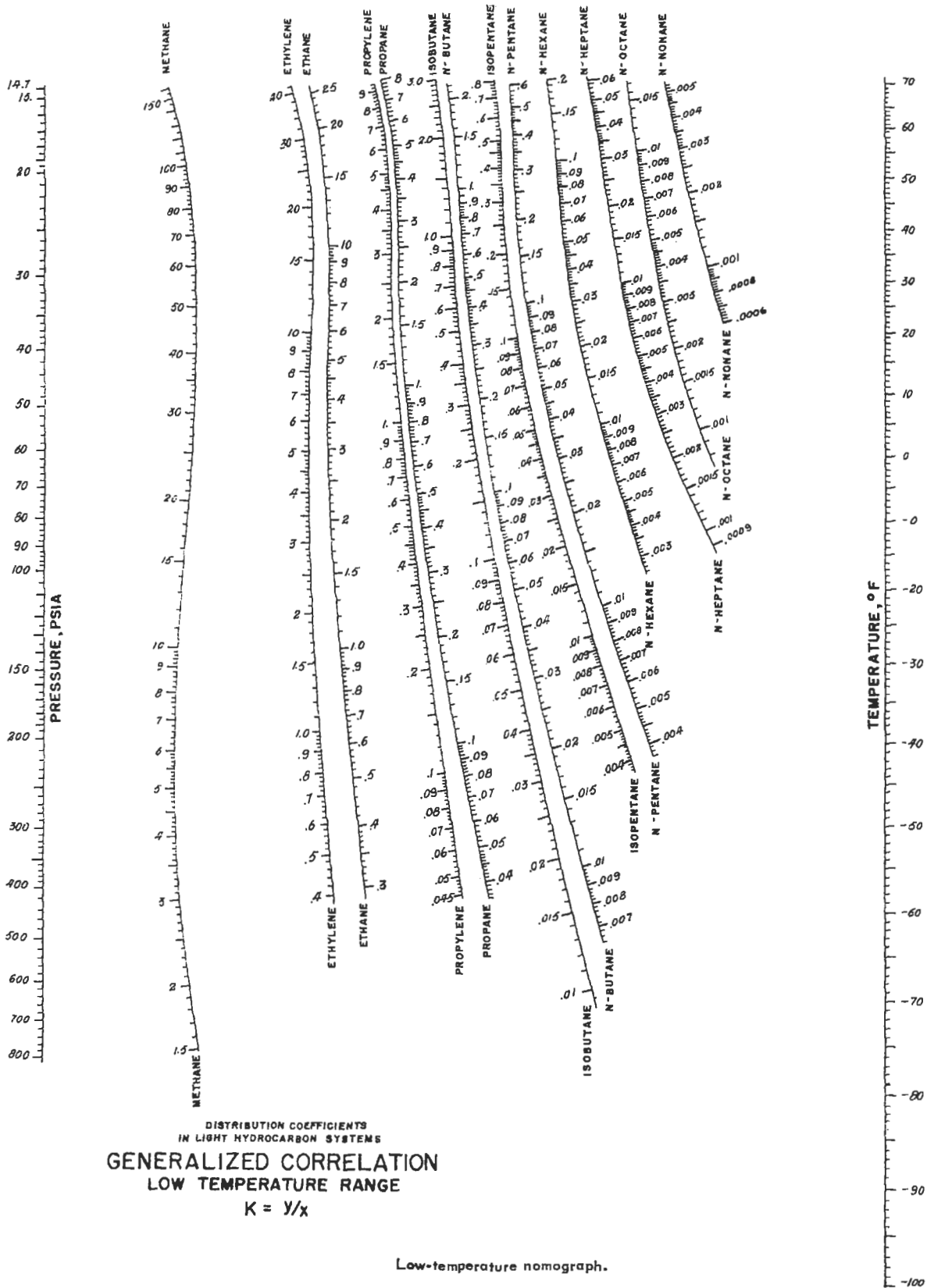


Figure 8-4A. DePriester Charts; K-Values of light hydrocarbon systems, generalized correlations, low-temperature range. Used by permission, DePriester, C.L., The American Institute of Chemical Engineers, *Chemical Eng. Prog.* Ser. 49 No. 7 (1953), all rights reserved.

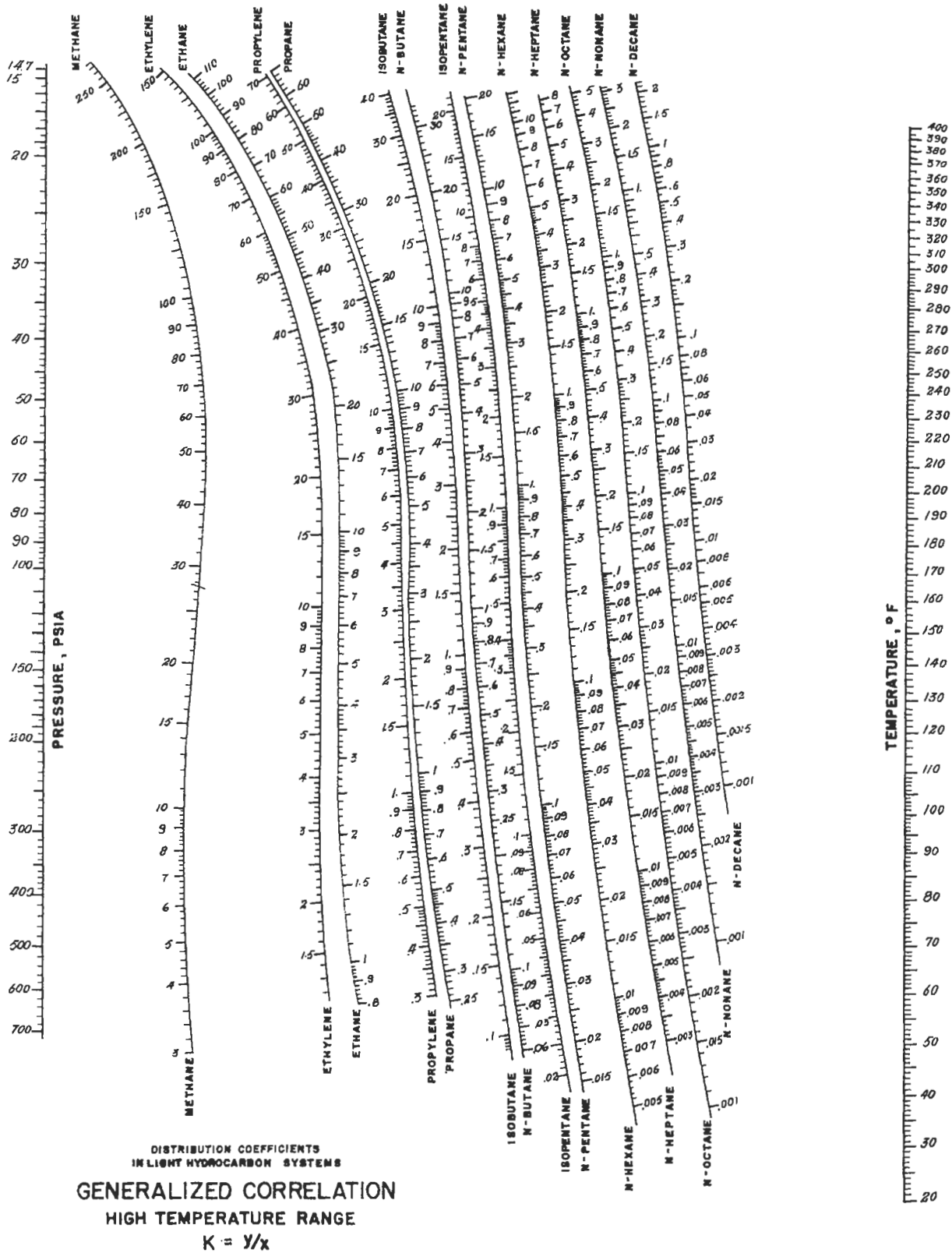


Figure 8-4B. DePriester Charts; K-Values of light hydrocarbon systems, generalized correlations, high-temperature range. Used by permission, The American Institute of Chemical Engineers, *Chemical Engineering Progress* Ser. 49, No. 7 (1953), all rights reserved.

(text continued from page 5)

$$\Omega_i = \frac{f_i}{y_i P} \quad (8-10)$$

The Virial Equation of State for gases is generally:

$$Z = \frac{Pv}{RT} = 1 + \frac{B}{v} + \frac{C}{v^2} + \frac{D}{v^3} + \dots \quad (8-11)$$

where B, C, D, etc. = virial coefficients, independent of pressure or density, and for pure components are functions of temperature only

v = molar volume

Z = compressibility factor

Fugacities and activities can be determined using this concept.

Other important equations of state which can be related to fugacity and activity have been developed by Redlich-Kwong [56] with Chueh [10], which is an improvement over the original Redlich-Kwong, and Palmer's summary of activity coefficient methods [51].

Activity coefficients are equal to 1.0 for an ideal solution when the mole fraction is equal to the activity. The activity (a) of a component, i , at a specific temperature, pressure and composition is defined as the ratio of the fugacity of i at these conditions to the fugacity of i at the standard state [54].

$$a(T, P, x) = \frac{f_i(T, P, x)}{f_i(T, P^\circ, x^\circ)}, \text{ liquid phase}$$

(Zero superscript indicates a specific pressure and composition)

The activity coefficient γ_i is

$$\gamma_i = \frac{a_i}{x_i} = 1.0 \text{ for ideal solution}$$

The ideal solution law, Henry's Law, also enters into the establishment of performance of ideal and non-ideal solutions.

The Redlich-Kister [55, 57] equations provide a good technique for representing liquid phase activity and classifying solutions.

The Gibbs-Duhem equation allows the determination of activity coefficients for one component from data for those of other components.

Wilson's [77] equation has been found to be quite accurate in predicting the vapor-liquid relationships and activity coefficients for miscible liquid systems. The results can be expanded to as many components in a multicomponent system as may be needed without any additional data other than for a binary system. This makes Wilson's and

Renon's techniques valuable for the complexities of multicomponent systems and in particular the solution by digital computer.

Renon's [58] technique for predicting vapor-liquid relationships is applicable to partially miscible systems as well as those with complete miscibility. This is described in the reference above and in Reference 54.

There are many other specific techniques applicable to particular situations, and these should often be investigated to select the method for developing the vapor-liquid relationships most reliable for the system. These are often expressed in calculation terms as the effective "K" for the components, i , of a system. Frequently used methods are: Chao-Seader, Peng-Robinson, Renon, Redlich-Kwong, Soave Redlich-Kwong, Wilson.

Azeotropes

Azeotrope mixtures consist of two or more components, and are surprisingly common in distillation systems. Therefore it is essential to determine if the possibility of an azeotrope exists. Fortunately, if experimental data are not available, there is an excellent reference that lists known azeotropic systems, with vapor pressure information [20, 28, 43]. Typical forms of representation of azeotropic data are shown in Figures 8-5 and 8-6. These are homogeneous, being of one liquid phase at the azeotrope point. Figure 8-7 illustrates a heterogeneous azeotrope where two liquid phases are in equilibrium with one vapor phase. The system butanol-water is an example of the latter, while chloroform-methanol and acetone-chloroform are examples of homogeneous azeotropes with "minimal boiling point" and "maximum boiling point" respectively.

A "minimum" boiling azeotrope exhibits a constant composition as shown by its crossing of the $x = y$, 45° line in Figure 8-8, which boils at a lower temperature than either of its pure components. This class of azeotrope results from positive deviations from Raoult's Law. Likewise, the "maximum" (Figure 8-9) boiling azeotrope represents negative deviations from Raoult's Law and exhibits a constant boiling point greater than either pure component. At the point where the equilibrium curve crosses $x = y$, 45° line, the composition is constant and cannot be further purified by normal distillation. Both the minimum and maximum azeotropes can be modified by changing the system pressure and/or addition of a third component, which should form a minimum boiling azeotrope with one of the original pair. To be effective the new azeotrope should boil well below or above the original azeotrope. By this technique one of the original components can often be recovered as a pure product, while still obtaining the second azeotrope for separate purification.

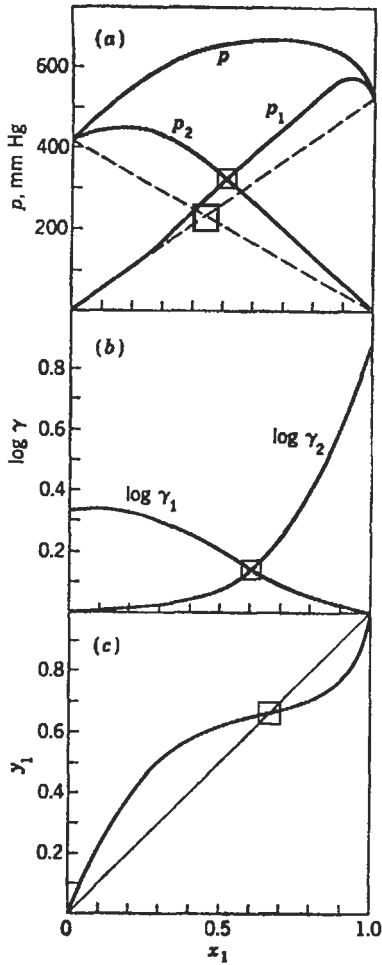


Figure 8-5. Chloroform (1)-methanol (2) system at 50°C. Azeotrope formed by positive deviations from Raoult's Law (dashed lines). Data of Sesonke, dissertation, University of Delaware, used by permission, Smith, B.D., *Design of Equilibrium Stage Processes*, McGraw-Hill New York, (1963), all rights reserved.

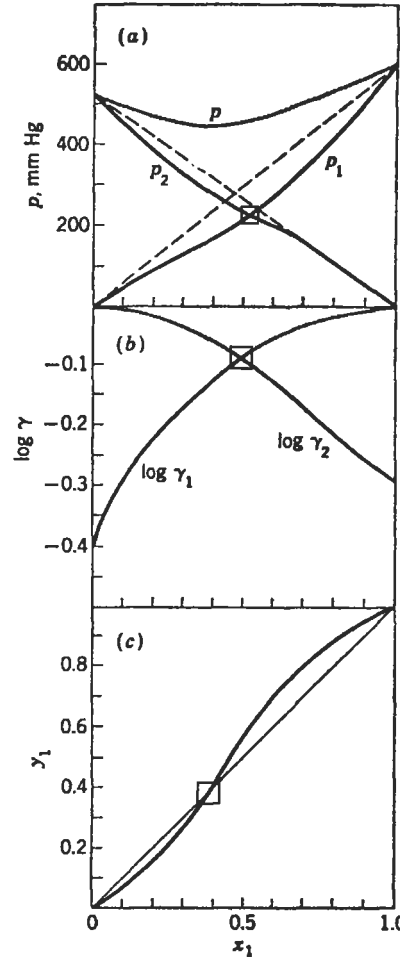


Figure 8-6. Acetone (1)-Chloroform (2) system at 50°C. Azeotrope formed by negative deviations from Raoult's Law (dashed lines). Data of Sesonke, dissertation, University of Delaware, used by permission, Smith, B.D., *Design of Equilibrium Stage Processes*, McGraw-Hill New York (1963), all rights reserved.

For a "minimum" boiling azeotrope the partial pressures of the components will be greater than predicted by Raoult's Law, and the activity coefficients will be greater than 1.0.

$$\gamma = (y_i p) / (x_i p_i^*) \quad (8-12)$$

where p_i^* = vapor pressure of component i, at temperature
 $p = P =$ total pressure = π
 $\gamma = a_i / x_i =$ activity coefficient of component, i
 $p_i =$ partial pressure of component i.
 Raoult's Law: $p_i = x_i p_i^* = x_i P_1 = y_1 P$

For "maximum" boiling azeotropes the partial pressures will be less than predicted by Raoult's Law and the activity coefficients will be less than 1.0.

In reference to distillation conditions, the azeotrope represents a point in the system where the relative volatilities reverse. This applies to either type of azeotrope, the direction of reversal is just opposite. For example in Figure 8-5 the lower portion of the x-y diagram shows that $y_i > x_i$, while at the upper part, the $y_i < x_i$. In actual distilla-

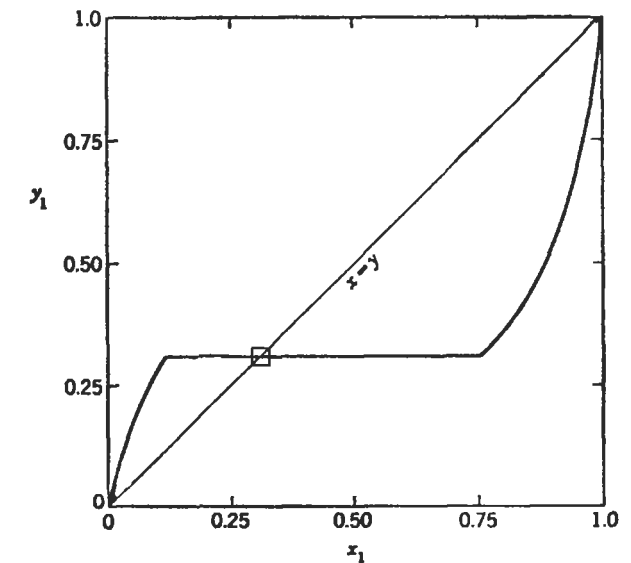


Figure 8-7. System with heterogeneous azeotrope—two liquid phases in the equilibrium with one vapor phase. Used by permission, Smith, B.D., *Design of Equilibrium Stage Processes*, McGraw-Hill, New York (1963), all rights reserved.

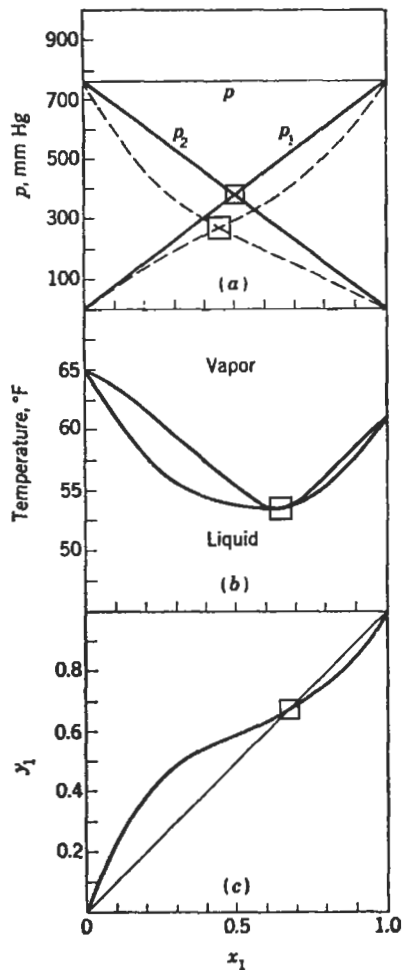


Figure 8-8. Chloroform (1)-methanol (2) system at 757 mm Hg. Minimum boiling azeotrope formed by positive deviations from Raoult's Law (dashed lines). Used by permission, Smith, B.D., *Design of Equilibrium Stage Processes*, McGraw-Hill, New York (1963), all rights reserved.

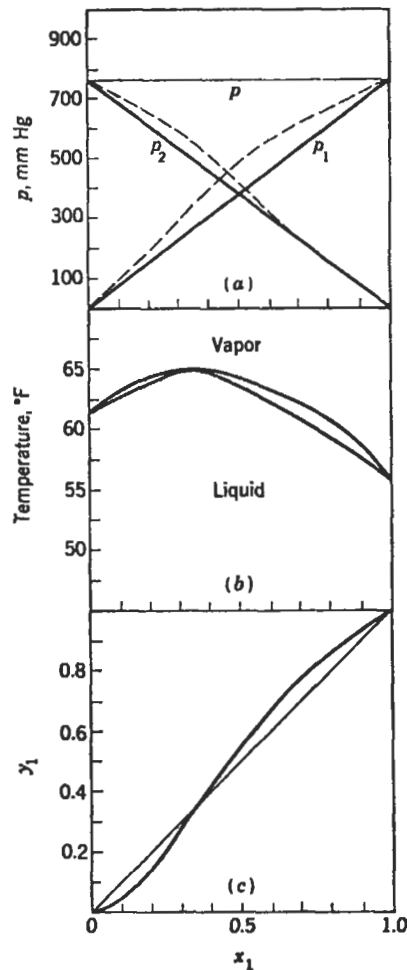


Figure 8-9. Acetone (1)-chloroform (2) system at 760 mm Hg. Maximum boiling azeotrope formed by negative deviations from Raoult's Law (dashed lines). Used by permission, Smith, B.D., *Design of Equilibrium Stage Processes*, McGraw-Hill, New York, (1963), all rights reserved.

tion, without addition of an azeotrope "breaker" or solvent to change the system characteristics, if a feed of composition 30% x_1 were used, the column could only produce (or approach) pure x_2 out the bottom while producing the azeotrope composition of about 65% x_1 and 35% x_2 at the top. The situation would be changed only to the extent of recognizing that if the feed came in above the azeotropic point, the bottoms product would be the azeotrope composition, Smith [65] discusses azeotropic distillation in detail. References 153–157, 171, and 172 describe azeotropic design techniques.

Example 8-1: Raoult's Law

A hydrocarbon liquid is a mixture at 55°F of:

- (a) 41.5 mol % iso-butane
- (b) 46.5 mol % pentane
- (c) 12.0 mol % n-hexane

A vaporizer is to heat the mixture to 190°F at 110 psia. Data from vapor pressure charts such as [48]:

- (a) vapor pressure of iso-butane at 190°F = 235 psia
- (b) vapor pressure of pentane at 190°F = 65 psia
- (c) vapor pressure of n-hexane at 190°F = 26 psia

Specific gravity of pure liquid at 55°F [79]:

- (a) iso-butane = 0.575
- (b) pentane = 0.638
- (c) n-hexane = 0.678

Moles in original liquid. Basis 100 gallons liquid. Assume Raoult's Law:

$$\begin{aligned}
 \text{Mols iso-butane} &= 41.5 (8.33 \times 0.575) / \text{MW} = 198.77 / 58.12 \\
 &= 3.42 \\
 \text{Mols pentane} &= 46.5 (8.33 \times 0.638) / \text{MW} = 247.12 / 72.146 \\
 &= 3.425 \\
 \text{Mols n-hexane} &= 12 (8.33 \times 0.678) / \text{MW} = 67.77 / 86.172 \\
 &= 0.786 \\
 \text{Total Mols} &= 7.631 \\
 \text{Mol fraction iso-butane in liquid} = x_1 &= 3.42 / 7.631 = 0.448 \\
 \text{Mol fraction pentane in liquid} = x_2 &= 3.425 / 7.63 = 0.449
 \end{aligned}$$

Mol fraction n-hexane in liquid = $x_3 = 0.786/7.631 = \frac{0.103}{1.000}$

Mol fraction in vapor phase at 190°F. Raoult's Law:

$y_i = p_i/\pi = (p_i^* x_i)/\pi$ (for a binary system) (8 - 3)

$y_i = (x_i P_i)/(x_1 P_1 + x_2 P_2 + x_3 P_3)$ (for multicomponent mixtures) (8 - 13)

$y_1 = 0.448 (235)/[(0.448) (65) + (0.448) (235) + (0.103) (26)]$
 $= 105.28/[29.185 + 105.28 + 2.678] = 105.28/[137.143]$
 $= 0.767$

$y_2 = 0.449 (65)/137.143 = 0.212$
 $y_3 = 0.103 (26)/137.143 = \underline{0.0195}$
 $\Sigma y_i = 0.998$ (not rounded)

Because, $P_{total} = (0.448) (235) + 0.449 (65) + 0.103 (26)$
 $= 137.14$ psia

This is greater than the selected pressure of 110 psia, therefore, for a binary the results will work out without a trial-and-error solution. But, for the case of other mixtures of 3 or more components, the trial-and-error assumption of the temperature for the vapor pressure will require a new temperature, redetermination of the component's vapor pressure, and repetition of the process until a closer match with the pressure is obtained.

Binary System Material Balance: Constant Molal Overflow Tray to Tray

Refer to Figure 8-1. (For an overall review see Reference 173.)

• Rectifying Section:

$V_r = L_r + D$ (8 - 14)

For any component in the mixture; using total condenser see Figures 8-2 and 8-13.

$V_n y_{ni} = L_{n+1} x_{(n+1)i} + D x_{Di}$ (8 - 15)

$y_{ni} = \frac{L_{n+1}}{V_n} x_{(n+1)i} + \frac{D}{V_n} x_{Di}$ (8 - 16)

• Operating Line Equation:

$y_{ni} = \frac{L_r}{V_r} x_{(n+1)i} + \frac{D}{V_r} x_{Di}$ (8 - 17)

For total condenser: y (top plate) = x_D

• Stripping Section:

$L_s = V_s + B$ (8 - 18)

$L_{(m+1)} x_{(m+1)i} = V_m y_{mi} + B x_{Bi}$ (8 - 19)

• Operating Line Equation:

$y_{mi} = \frac{L_s}{V_s} x_{(m+1)i} - \frac{B}{V_s} x_{Bi}$ (8 - 20)

Conditions of Operation (usually fixed):

1. Feed composition, and quantity.
2. Reflux Ratio (this may be a part of the initial unknowns).
3. Thermal condition of feed (at boiling point, all vapor, sub-cooled liquid).
4. Degree, type or amount of fractionation or separation, including compositions of overhead or bottoms.
5. Column operating pressure or temperature of condensation of overhead (determined by temperature of cooling medium), including type of condensation, i.e., total or partial.
6. Constant molal overflow from stage to stage (theoretical) for simple ideal systems following Raoult's Law. More complicated techniques apply for non-ideal systems.

Flash Vaporization (see Figure 8-10)

At a total pressure, P , the temperature of flash must be between the dew point and the bubble point of a mixture [144–148]. Thus:

T (Bubble Point) < T (Flash) < T (Dew Point)

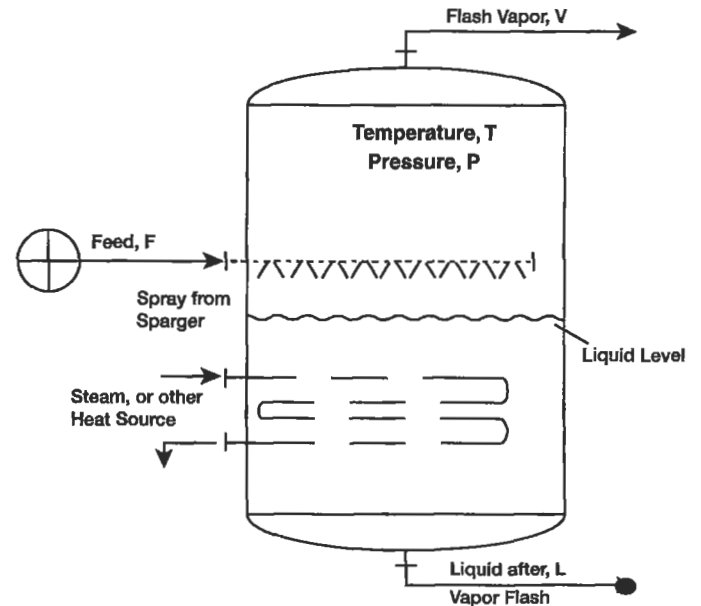


Figure 8-10. Schematic liquid flash tank. Note: Feed can be pre-heated to vaporize feed partially.

For binary mixtures [147]:

1. Set the temperature and pressure of the flash chamber.
2. Make a material balance on a single component.

$$F_t X_i = V y_i + L x_i \quad (8-21)$$

3. Knowing F , calculate amount and composition of V and L .

$$F_t = F + V_s = \text{mols of feed plus mols of non-condensable gases}$$

From Henry's Law:

$$F_t X_{fi} = V y_i + L (y_i / K_i) \quad (8-22)$$

$$V_t = V + V_s = \text{mols of vapor formed plus mols non-condensed gases}$$

$$y_i = K_i x_i$$

4. $F_t = V_t + L$ (8-22A)

$$y_i = \frac{F_t X_{fi}}{V_t + \frac{L}{K_i}} = \frac{F_t X_{fi}}{F_t - L + \frac{L}{K_i}} \quad (8-23)$$

$$y_i = \frac{X_{fi}}{1 - \frac{L}{F_t} \left(1 - \frac{1}{K_i}\right)} \quad (8-23A)$$

After calculating V , calculate the x_i 's and y_i 's:

$$y_i V = \frac{F X_i}{1 + \frac{L}{K_i V}} \quad (8-23B)$$

Then,

$$y_i = \frac{\left(\frac{F X_i}{V}\right)}{1 + \frac{L}{K_i V}} \quad (8-23C)$$

Calculate each y_i ; after calculating the y_i 's, calculate x_i 's as follows:

$$y_i = K_i x_i \quad (8-8)$$

so, $x_i = y_i / K_i$

$$K_i = P_i / \pi \quad (8-23D)$$

Relation for K_i :

$$y_i = K_i x_i \quad (8-8)$$

$$P_i = P_i x_i \quad (8-23E)$$

$$P_i = \pi y_i \quad (8-23F)$$

$$\pi y_i = P_i x_i \quad (8-23G)$$

$$\frac{y_i}{x_i} = \frac{P_i}{\pi}$$

where X_i = mols of a component i in vapor plus mols of same component in liquid, divided by total mols of feed (both liquid and vapor)
= total mol fraction, regardless of whether component is in liquid or vapor.

$$F X_i = V y_i + L x_i \quad (8-23H)$$

$$x_i = y_i / K_i$$

$$y_i = V + L / K_i \quad (8-23I)$$

$$y_i V = V \left(1 + \frac{L}{K_i V}\right) \quad (8-23J)$$

$$\Sigma y_i = 1.0$$

$$\sum_{i=1}^c y_i V = \sum_{i=1}^c \left(\frac{F X_i}{1 + \frac{L}{K_i V}} \right) \quad (8-23K)$$

To calculate, V , L , y_i 's, and x_i 's:

1. Assume: V
2. Calculate: $L = F - V$
3. Calculate: L/V
4. Look up K_i 's at temperature and total pressure of system
5. Substitute in:

$$V = \sum_{i=1}^c \frac{F X_i}{1 + \frac{L}{K_i V}} \quad (8-24)$$

6. If an equality is obtained from:

$V_{\text{calc}} = V_{\text{assumed}}$ the amount of vapor was satisfactory as assumed.

$$V = \frac{F X_1}{1 + \frac{L}{K_1 V}} + \frac{F X_2}{1 + \frac{L}{K_2 V}} + \frac{F X_3}{1 + \frac{L}{K_3 V}} + \dots + \frac{F X_i}{1 + \frac{L}{K_i V}} \quad (8-25)$$

$$7. V y_i = \frac{F X_i}{1 + \frac{L}{K_i V}} \quad (8-23B)$$

$$\text{and } y_i = \frac{F X_i / V}{1 + \frac{L}{K_i V}} \quad (8-23C)$$

8. Calculate each y_i as in (7) above, then the x_i 's are determined:

$$y_i = K_i x_i$$

or, $x_i = y_i / K_i$

9. $K_i = P_i/\pi$ (8-23D)

Calculate the Bubble Point: Assume composition is liquid.

where π = total system pressure absolute

P_i = vapor pressure of individual component at temperature, abs

$X_i = X$ = mols of a component, i, in vapor phase plus mols of same component in liquid divided by the total mols of feed (both liquid and vapor)

x_f = mol fraction of a component in feed

x_f = mol fraction of any component in the feed, F_t where $X_f = F x_f/F_t$ for all components in F; for the non-condensable gases, $x_f = V_s/F_t$

F = mols of feed entering flash zone per unit time contains all components except non-condensable gases

$F_t = F + V_s$

$V_t = V + V_s$ mols of vapor at a specific temperature and pressure, leaving flash zone per unit time

V_s = mols of non-condensable gases entering with the feed, F, and leaving with the vapor, V, per unit time

V = mols of vapor produced from F per unit time, $F = V + L$

L = mols of liquid at a specific temperature and pressure, from F, per unit time

i = specific individual component in mixture

K_i = equilibrium K values for a specific component at a specific temperature and pressure, from References 18, 65, 79, 99, 131, 235

T = temperature, abs

x_i = mol fraction of a specific component in liquid mixture as may be associated with feed, distillate, or bottoms, respectively

y_i = mol fraction of a specific component in vapor mixture as may be associated with the feed, distillate or bottoms, respectively

10. For the simplified case of a mixture free of non-condensable gases, see Equation 8-23A, where $X_f = x_f$.

Example 8-2: Bubble Point and Dew Point

From the hydrocarbon feed stock listed, calculate the bubble point and dew point of the mixture at 165 psia, and using K values as listed, which can be read from a chart in 3rd edition Perry's, *Chemical Engineer's Handbook*.

Feed Stock:

Composition	Mol Fraction
C ₂ H ₆	0.15
C ₃ H ₈	0.15
n-C ₄ H ₁₀	0.30
i-C ₄ H ₁₀	0.25
n-C ₅ H ₁₂	<u>0.15</u>
	1.00

Composition	Mol Fraction	K, at		Assume T = 100°F,	
		assumed T = 90°F	T = 90°F	K _x	K
C ₂ H ₆	0.15	3.1	0.465	3.4	0.51
C ₃ H ₈	0.15	1.0	0.150	1.2	0.18
n-C ₄ H ₁₀	0.30	0.35	0.105	0.39	0.117
i-C ₄ H ₁₀	0.25	0.46	0.115	0.52	0.13
n-C ₅ H ₁₂	<u>0.15</u>	0.12	<u>0.018</u>	0.13	<u>0.0195</u>
	1.00		0.853		0.956

(Too low)

Assume T = 105°F

K	K _x
3.45	0.517
1.25	0.187
0.41	0.123
0.55	0.137
0.15	<u>0.022</u>
	0.986

By interpolation:

$$\frac{0.986 - 0.956}{105 - 100} = \frac{1.000 - 0.986}{x}$$

$$x = 2.34^\circ\text{F}$$

So, T = 105 + 2.34 = 107°F Bubble point at 165 psia

Calculation of Dew Point

Composition	Mol Frac. in Vapor	Assume, T = 160°F K (from charts)	x = y/k
C ₂ H ₆	0.15	5.1	0.0294
C ₃ H ₈	0.15	1.85	0.081
n-C ₄ H ₁₀	0.30	0.80	0.375
i-C ₄ H ₁₀	0.25	1.00	0.250
n-C ₅ H ₁₂	<u>0.15</u>	0.32	<u>0.469</u>
	1.00		1.204 = $\Sigma y/K = 1$

Assume T = 180°F, K	x = y/K	Assume T = 175°F, K	x = y/K
5.95	0.0252	5.6	0.0268
2.25	0.0666	2.2	0.0682
0.98	0.3060	0.91	0.330
1.30	0.1920	1.2	0.208
0.41	<u>0.3660</u>	0.39	<u>0.385</u>
	0.9558 = $\Sigma y/K = 1$		1.018 = $\Sigma y/K = 1.0$

Dew point is essentially 175°F at 165 psia

Example 8-3: Flashing Composition

If the mixture shown in Example 8-2 is flashed at a temperature midway between the bubble point and dew point,

and at a pressure of 75 psia, calculate the amounts and compositions of the gas and liquid phases.

Referring to Example 8-2:

Composition	Mol Fraction
C ₂ H ₆	0.15
C ₃ H ₈	0.15
n-C ₄ H ₁₀	0.30
i-C ₄ H ₁₀	0.25
n-C ₅ H ₁₂	<u>0.15</u>
	1.00

Must Calculate Bubble Point at 75 psia:

Composition	Mol Frac.	K@50°F	y = Kx	K@40°F	y = Kx
C ₂ H ₆	0.15	5.0	0.75	4.5	0.675
C ₃ H ₈	0.15	1.2	0.18	1.07	0.1603
n-C ₄ H ₁₀	0.30	0.325	0.0975	0.28	0.084
i-C ₄ H ₁₀	0.25	0.48	0.12	0.415	0.104
n-C ₅ H ₁₂	0.15	0.089	<u>0.0133</u>	0.074	<u>0.011</u>
			1.16		1.0344

Bubble point = 40°F (as close as K curves can be read)

$$\text{Extrapolating} = \left(\frac{1.00 - 1.03}{1.16 - 1.03} \right) (50^\circ - 40^\circ) = 2.3^\circ$$

Therefore, a close value of bubble point would be: 40° - 2° = 38°F

Calculate Dew Point at 75 psia

Compo- sition	Mol Frac.	K @ 70°F	Σx = y/K	K @ 100°F	Σx = y/K	K @ 130°F	Σx = y/K
C ₂ H ₆	0.15	5.9	0.0254	7.6	0.0197	9.5	0.0158
C ₃ H ₈	0.15	1.55	0.0969	2.18	0.0688	3.0	0.050
n-C ₄ H ₁₀	0.30	0.45	0.668	0.70	0.428	1.06	0.283
i-C ₄ H ₁₀	0.25	0.58	0.43	1.0	0.250	1.45	0.172
n-C ₅ H ₁₂	0.15	0.13	<u>1.15</u>	0.225	<u>0.665</u>	0.37	<u>0.405</u>
			2.37		1.4315		0.9258

(too low temp.)

Refer to extrapolation curve, Figure 8-11.

At Σx = y/K = 1.0, dew point = 124°F

Flash this mixture at temperature midway between bubble point and dew point, or flash temperature = $\frac{38 + 124}{2} = 81^\circ\text{F}$

Assume: F (feed) = 100

Pressure: = 75 psia; then tabulating the calculations:

Compo- sition	Feed Mol. Frac., x	Fx	L/V	K@81°F	$\frac{L}{VK}$	$\frac{L}{1+VK}$	$\frac{Fx}{\Sigma yV = 1 + L/VK}$
C ₂ H ₆	0.15	15	2.34	6.6	0.352	1.352	11.1
C ₃ H ₈	0.15	15		1.78	1.31	2.31	6.5
n-C ₄ H ₁₀	0.30	30		0.54	4.32	5.32	5.65
i-C ₄ H ₁₀	0.25	25		0.77	3.02	4.02	6.22
n-C ₅ H ₁₂	0.15	15		0.16	14.6	15.6	<u>0.96</u>
							30.43

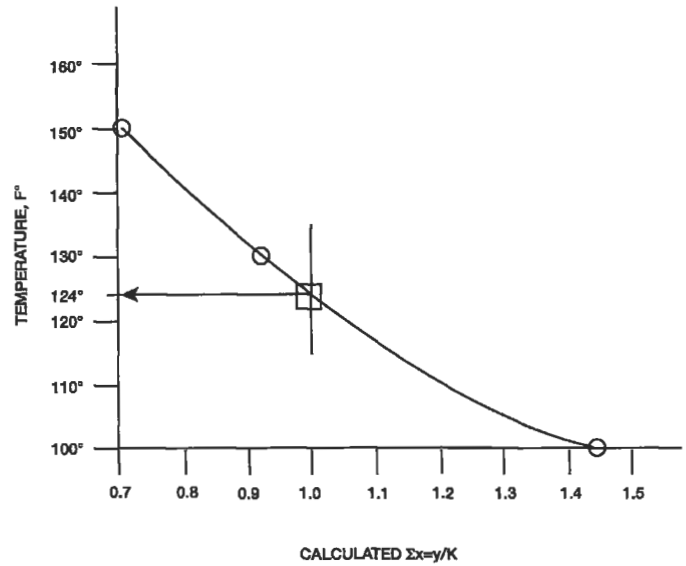


Figure 8-11. Extrapolation curve for dew point for Example 8-3.

Vapor phase after flashing at 75 psia and 81°F = 30.4% of original feed.

Liquid phase = 100 - 30 = 70% of original feed

Composition of Vapor

Composition	Mol Fraction
C ₂ H ₆	11.1/30.43 = 0.365
C ₃ H ₈	6.5/30.43 = 0.214
n-C ₄ H ₁₀	5.65/30.43 = 0.186
i-C ₄ H ₁₀	6.22/30.43 = 0.204
n-C ₅ H ₁₂	0.96/30.43 = <u>0.031</u>
	1.000

Composition of Liquid

Feed Composition	K@81°F	Mol Fraction = x = y/K
C ₂ H ₆	6.6	0.365/6.6 = 0.0554
C ₃ H ₈	1.78	0.214/1.78 = 0.120
n-C ₄ H ₁₀	0.54	0.186/0.54 = 0.345
i-C ₄ H ₁₀	0.77	0.204/0.77 = 0.265
n-C ₅ H ₁₂	0.16	0.031/0.16 = <u>0.1935</u>
		0.9789

This should be = 1.00. Inaccuracy in reading K values probably accounts for most of the difference.

Distillation Operating Pressures

To determine the proper operating pressure for a distillation system, whether trays or packed column, exam-

ine the conditions following the pattern of Figure 8-12 [149]. It is essential to realistically establish the condensing conditions of the distillation overhead vapors, and any limitations on bottoms temperature at an estimated pressure drop through the system. Preliminary calculations for the number of trays or amount of packing must be performed to develop a fairly reasonable system pressure drop. With this accomplished, the top and bottom column conditions can be established, and more detailed calculations performed. For trays this can be 0.1 psi/actual tray to be installed [149] whether atmospheric or above, and use 0.05 psi/tray equivalent for low vacuum (not low absolute pressure).

Because low-pressure operations require larger diameter columns, use pressures for operations only as low as required to accomplish the separation.

For high vacuum distillation, Eckles et al. [150] suggest using a thin film or conventional batch process for industrial type installations; however, there are many tray and packed columns operating as low as 4 mm Hg, abs Eckles [150] suggests "high vacuum" be taken as 5mm Hg, and that molecular distillation be 0.3 – 0.003 mm Hg pressure, and unobstructed path distillation occur at 0.5 – 0.02 mm Hg. These latter two can be classed as evaporation processes. Eckles' [150] rules of thumb can be summarized:

1. Do not use a lower pressure than necessary, because separation efficiency and throughput decrease as pressure decreases.

The requirement of bottoms temperature to avoid overheating heat sensitive materials may become controlling.

2. When separating volatile components such as a single stream from low-volatility bottoms, use a molecular or unobstructed path process, either thin film or batch.
3. When separating a volatile product from volatile impurities, batch distillation is usually best.
4. Do not add a packed column to a thin film evaporator system, because complications arise.

Note that good vapor-liquid equilibrium data for low pressure conditions are very scarce and difficult to locate. However, for proper calculations they are essential. See References 151 and 152 dealing with this.

Studies with high-pressure distillation by Brierley [239] provide insight into some FRI studies and the effects of pressure on performance as well as the impacts of errors in physical properties, relative volatility, etc. This work provides important contributions to understanding and setting operating pressures.

Total Condenser

In a total condenser all of the overhead vapor is condensed to the liquid state. When the heat load or duty on the condenser is exactly equal to the latent heat of the saturated or dew point of the overhead vapor from the distillation column, the condensed liquid will be a saturated bubble point liquid. The condenser and accumulator

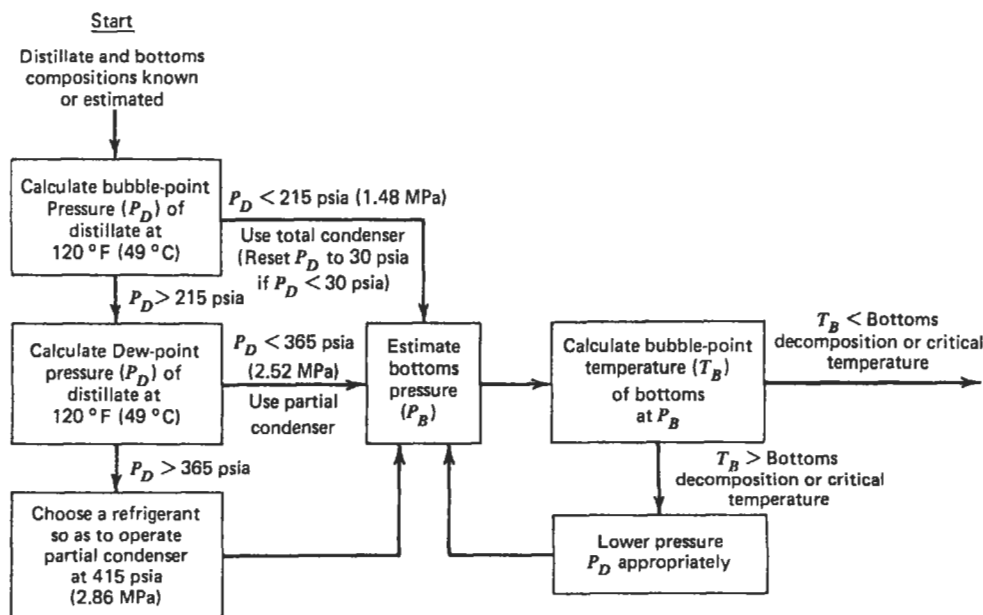


Figure 8-12. Algorithm for establishing distillation column pressure and type condenser. Used by permission, Henley, E. J. and Seader, J. D., *Equilibrium Stage Separation Operations in Chemical Engineering*, John Wiley, © (1981), p. 43, all rights reserved.

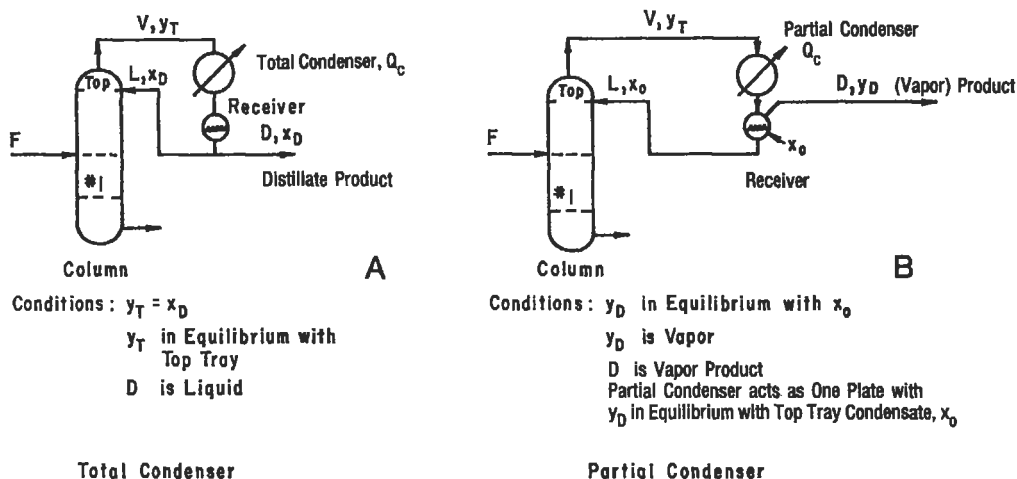


Figure 8-13. Total and partial condenser arrangements.

pressure will be the total vapor pressure of the condensate. If an inert gas is present the system total pressure will be affected accordingly. When using a total condenser, the condensed stream is split into one going back into the column as reflux and the remaining portion leaving the system as distillate product.

Partial Condenser

The effect of the partial condenser is indicated in Figure 8-13 and is otherwise represented by the relations for the rectifying and stripping sections as just given. The key point to note is that the product is a vapor that is in *equilibrium* with the reflux to the column top tray, and hence the partial condenser is actually serving as an "external" tray for the system and should be considered as the *top* tray when using the equations for total reflux conditions. This requires just a little care in step-wise calculation of the column performance.

In a partial condenser there are two general conditions of operation:

1. All condensed liquid is returned to column as reflux, while all vapor is withdrawn from the accumulator as product. In this case the vapor $y_c = x_D$; Figure 8-1 and Figure 8-14.
2. Both liquid and vapor products are withdrawn, with liquid reflux composition being equal to liquid product composition. Note that on an equilibrium diagram the partial condenser liquid and vapor stream's respective compositions are in equilibrium, but only when *combined* do they represent the intersection of the operating line with the 45° slope (Figure 8-14).

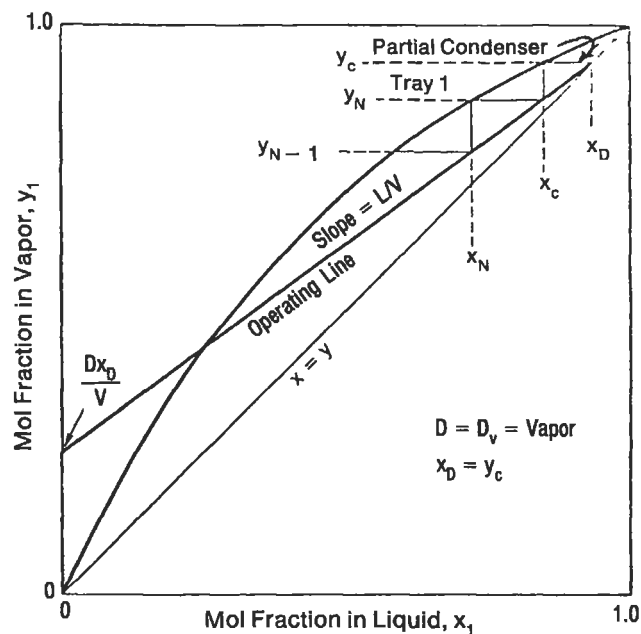


Figure 8-14. Diagram of partial condenser; only a vapor product is withdrawn.

Thermal Condition of Feed

The condition of the feed as it enters the column has an effect on the number of trays, reflux requirements and heat duties for a given separation. Figure 8-15 illustrates the possible situations, i.e., sub-cooled liquid feed, feed at the boiling point of the column feed tray, part vapor and part liquid, all vapor but not superheated, and superheated vapor. The thermal condition is designated as "q," and

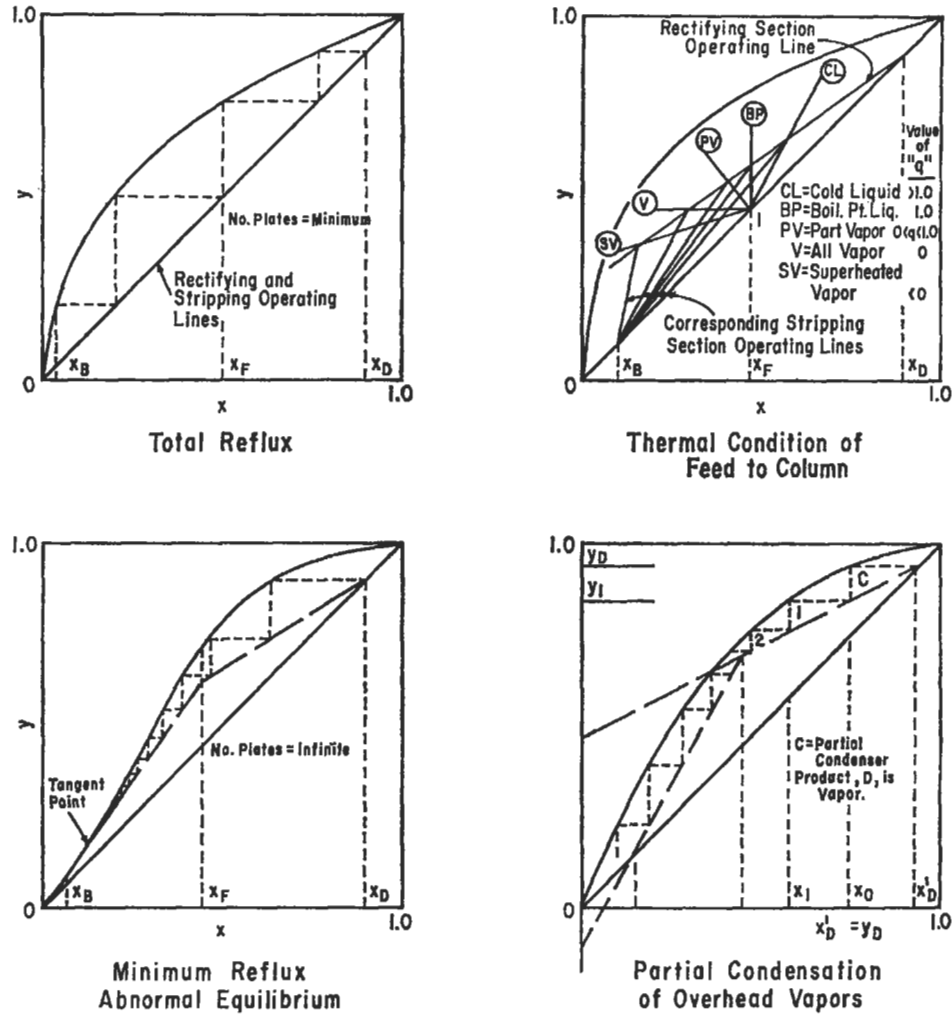


Figure 8-15. Operating characteristics of distillation columns.

is approximately the amount of heat required to vaporize one mol of feed at the feed tray conditions, divided by the latent heat of vaporization of the feed.

$$L_s = L_r + qF \tag{8-26}$$

$$q = (L_s - L_r)/F \tag{8-27}$$

The slope of a line from the intersection point of the feed composition, x_F , with the 45° line on Figure 8-2 is given by $q/(q - 1) = -q/(1 - q)$. Physically this gives a good approximation of the mols of saturated liquid that will form on the feed plate by the introduction of the feed, keeping in mind that under some thermal conditions the feed may vaporize liquid on the feed plate rather than condense any.

Liebert [218] studied feed preheat conditions and the effects on the energy requirements of a column. This topic is essential to the efficient design of a distillation system.

As an alternate to locating the “q” line, any value of x_i may be substituted in the “q” line equation below, and a corresponding value of y_i determined, which when plotted will allow the “q” line to be drawn in. This is the line for SV - I, V - I, PV - I, BP - I and CL - I of Figure 8-15.

$$y_i = -\frac{q}{1-q} x_i + \frac{x_F}{1-q} \tag{8-28}$$

Total Reflux, Minimum Plates

Total reflux exists in a distillation column, whether a binary or multicomponent system, when all the overhead vapor from the top tray or stage is condensed and returned to the top tray. Usually a column is brought to equilibrium at total reflux for test or for a temporary plant condition which requires discontinuing feed. Rather than shut down, drain and then re-establish operating conditions later, it is usually more convenient and requires less

energy in the form of reboiler heat and condenser coolant to maintain a total reflux condition with no feed, no overhead and no bottoms products or withdrawals.

The conditions of total liquid reflux in a column also represent the minimum number of plates required for a given separation. Under such conditions the column has zero production of product, and infinite heat requirements, and $L_s/V_s = 1.0$ as shown in Figure 8-15. This is the limiting condition for the number of trays and is a convenient measure of the complexity or difficulty of separation.

Fenske Equation: Overall Minimum Total Trays with Total Condenser

$$S_m = (N_{\min} + 1) = \frac{\log \left(\frac{x_{Di}}{x_{Dh}} \right) \left(\frac{x_{Bh}}{x_{Bl}} \right)}{\log \alpha_{\text{avg}}} \quad (8-29)$$

This includes the bottoms reboiler as a tray in the system. See tabulation below.

N_{\min} includes only the required trays in the column itself, and not the reboiler.

$$\alpha_{\text{avg}} = (\alpha_{lk/hk})_{\text{avg}}$$

D refers to overhead distillate

B refers to bottoms

$$S_m = N_{\min} = \frac{\log [(x_{lk}/x_{hk})_D (x_{hk}/x_{lk})_B]}{\log (\alpha_{lk/hk})_{\text{avg}}} \quad (8-30)$$

This applies to any pair of components. My experience suggests adding +1 theoretical tray for the reboiler, thus making the total *theoretical* trays perhaps a bit conservative. But, they must be included when converting to actual trays using the selected or calculated tray efficiency:

$$S_m + 1 = N_{\min} \quad (8-31)$$

For a condition of overall total trays allowance is to be made for feed tray effect, *then add one more theoretical tray to the total*. As demonstrated in the tabulation to follow, allowance should be made for the reboiler and condenser.

	Total Condenser	Reboiler	Partial Condenser	Total
S_m	+1	0	+0	$N_m + 1$
	+1	+1	+0	$N_m + 2$
	+0	+1	+1	$N_m + 2$

Note that the approach recommended here is not in agreement with Van Winkle [74], because he assumes the reboiler and partial condenser are included in the overall calculation for N_{\min} .

Various average values of α for use in these calculations are suggested in the following section on "Relative Volatility."

Because the feed tray is essentially non-effective it is suggested that an additional theoretical tray be added to allow for this. This can be conveniently solved by the nomographs [21] of Figures 8-16 and 17. If the minimum number of trays in the rectifying section are needed, they can be calculated by the Fenske equation substituting the limits of x_{F1} for x_{Bh} and x_{B1} , and the stripping section can be calculated by difference.

From Fenske's equation, the minimum number of equilibrium stages at total reflux is related to their bottoms (B) and distillate or overhead (D) compositions using the average relative volatility, see Equation 8-29.

To solve for the component split [100] in distillate or bottoms:

$$\left(\frac{x_{LK}}{x_{HK}} \right)_D = \left(\frac{x_{LK}}{x_{HK}} \right)_B (\alpha_{LK-HK})^{S_m} \quad (8-32)$$

where S_m = total number of calculated theoretical trays at total reflux, from Equation 8-30

$x_{lk} = x_{LK}$ = liquid mol fraction of light key

$x_{hk} = x_{HK}$ = liquid mol fraction of heavy key

lk - hk = LK - HK = average relative volatility of column (top to bottom)

Because a column cannot operate at total reflux and produce net product from the column, a reflux ratio of about 1.1 to 1.5 times the *minimum* reflux will usually give practical results. Be aware that as the reflux ratio comes down approaching the minimum, the number of theoretical and then corresponding *actual* trays must increase.

Relative Volatility

Relative volatility is the volatility separation factor in a vapor-liquid system, i.e., the volatility of one component divided by the volatility of the other. It is the tendency for one component in a liquid mixture to separate upon distillation from the other. The term is expressed as the ratio of vapor pressure of the more volatile to the less volatile in the liquid mixture, and therefore $\alpha_{1,2}$ is always equal to 1.0 or greater. $\alpha_{1,2}$ means the relationship of the more volatile or low boiler to the less volatile or high boiler at a constant specific temperature. The greater the value of α , the easier will be the desired separation. Relative volatility can be calculated between any two components in a mixture, binary or multicomponent. One of the substances is chosen as the reference to which the other component is compared.

Definition of Relative Volatility: Relative Volatility of Component 1 with respect to component 2.

$$\alpha_{1,2} = (p_1 x_2) / (p_2 x_1) = (y_1 x_2) / (y_2 x_1) \quad (8-33)$$

where 1,2, etc. are component identification
p = partial pressure of a component

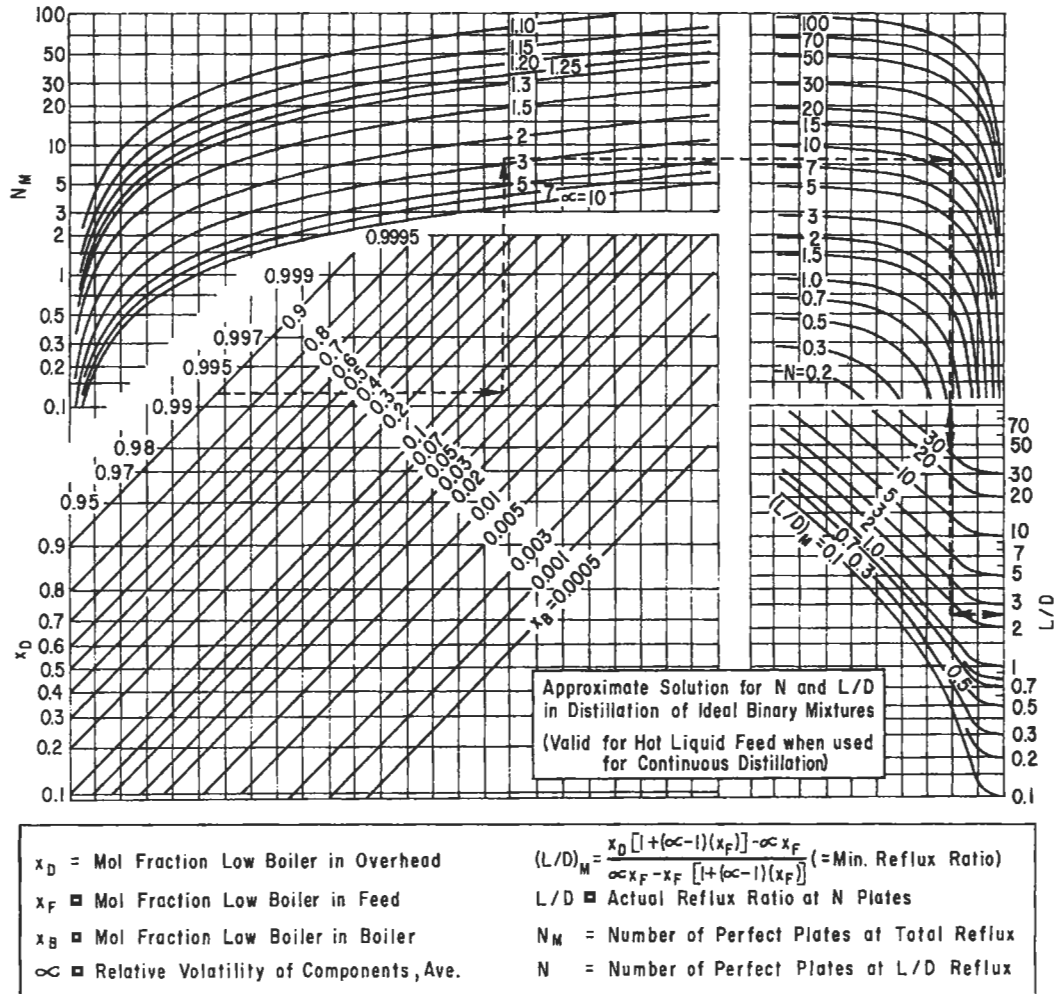


Figure 8-16. Approximate solution for N and L/D in distillation of ideal binary mixtures. Used by permission, Faasen, J.W., *Industrial & Eng. Chemistry*, V. 36 (1944), p. 248., The American Chemical Society, all rights reserved.

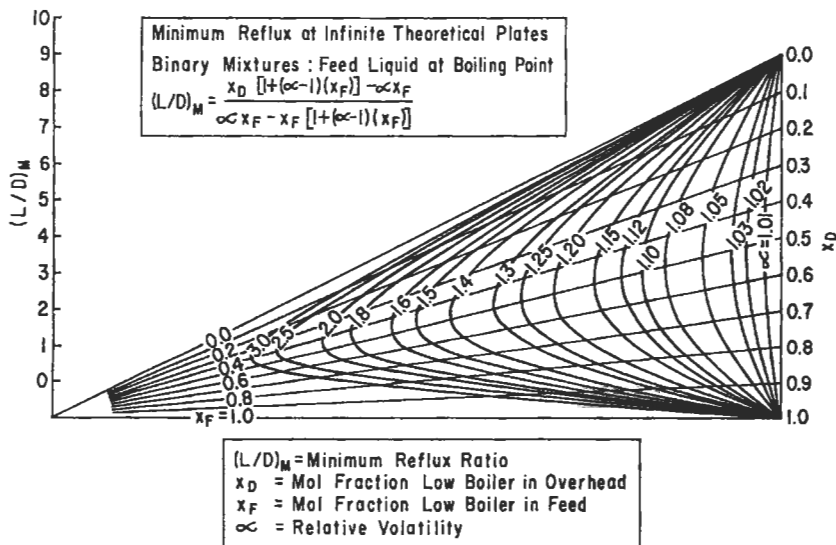


Figure 8-17. Minimum reflux at infinite theoretical plates. Used by permission, The American Chemical Society, Smoker, E. H., *Ind. Eng. Chem* V. 34 (1942), p. 510, all rights reserved.

x = liquid mol fraction of a component
 y = vapor mol fraction of a component
 π = system total pressure, absolute

Partial pressure:

$$P_a = \pi y_a \quad (8-3)$$

$$P_b = \pi y_b$$

When temperature is constant and at equilibrium for a homogeneous mixture (such as azeotrope), the composition of the liquid is identical with the composition of the vapor, thus $x_i = y_i$, and the relative volatility is equal to 1.0.

$$K_i = y_i / x_i, \text{ that is, } \frac{\text{mol fraction of } i \text{ in vapor phase}}{\text{mol fraction of } i \text{ in liquid phase}} \quad (8-9)$$

$$\alpha_{ab} = K_a / K_b = \text{relative volatility of components a to b} \quad (8-34)$$

where i = compound identification
 r = reference compound

As previously discussed, the charts of K values are available, but do apply primarily to hydrocarbon systems. Reference 79 presents important other data on K value relationships. See Figures 8-4A and 8-4B for charts with pressure effects included (not ideal, but practical charts).

$$\alpha_{1,2} = K_1 / K_2 = P_1 / \pi \quad (8-35)$$

For multicomponent mixtures [79, 59]:

$$y_2 = \frac{x_2}{\alpha_{1/2} x_1 + x_2 + \alpha_{3/2} x_3 + \alpha_{4/2} x_4 + \dots} = \frac{x_2}{\sum \alpha x} \quad (8-36)$$

where 1,2,3,4, . . . are components in a multicomponent mixture

$\alpha_{1/2}$ = relative volatility of component 1 with respect to component 2

$\alpha_{3/2}$ = relative volatility of component 3 with respect to component 2.

$$x_2 / y_2 = \alpha_{1/2} (x_1 / y_1) \quad (8-37)$$

$$y_1 = \alpha_{1/2} x_1 / (\sum \alpha x) \quad (8-38)$$

$$y_3 = \alpha_{3/2} x_3 / (\sum \alpha x), \text{ etc.} \quad (8-38A)$$

$$x_1 = \frac{y_1 / \alpha_{1/2}}{\sum (y / \alpha)}, \quad x_2 = \frac{y_2 / \alpha_{2/2}}{\sum (y / \alpha)}, \quad y_3 = \frac{y_3 / \alpha_{3/2}}{\sum (y / \alpha)}, \quad (8-39)$$

For a binary system with constant relative volatilities:

$$\alpha_{1,2} = \frac{y_1 / x_1}{(1 - y_1) / (1 - x_1)} \quad (8-40)$$

or,

$$y_1 = \frac{\alpha x_1}{1 + (\alpha - 1)x_1} \quad (8-41)$$

Winn [99] proposes a modification to recognize temperature variation effects on relative volatility. The method does not apply to mixtures forming azeotropes or at conditions near the critical. Kister [94] proposes:

$$K_1 = \alpha_{1,2} K_2$$

$$N_{min} = \frac{\ln \left[\frac{(x_{1k})_D (x_{hk})_B}{(x_{1k})_B (x_{hk})_D} \right]^{b_{1k}}}{\ln \beta_{1k/hk}} \quad (8-42)$$

α can vary with temperature, so some average α should be used between top and bottom temperature.

When b_{1k} and $\beta_{1k/hk}$ are constants at a fixed or constant pressure, but evaluated for the light (l) and heavy (h) keys at top and bottom temperatures, their relationship is [94]:

$$\beta_{1k/hk} = K_{lk} / (K_{hk})^{b_{1k}}, \text{ at fixed pressure} \quad (8-43)$$

Winn's equation reduced to Fenske's at $b_{1k} = 1.0$ and

$$\beta_{1k/hk} = \alpha_{lk/hk} \quad (8-44)$$

Example 8-4: Determine Minimum Number of Trays by Winn's Method (used by permission [99])

The minimum number of trays necessary to debutanize the effluent from an alkylation reactor will be calculated. The feed, products, and vapor-liquid equilibrium constants of the key components at conditions of temperature and pressure corresponding to the top tray and reboiler are shown in Table 8-1.

The constants β and b are evaluated using Equation 8-43 as follows:

$$0.94 = \beta (0.70)^b$$

$$3.55 = \beta (3.00)^b$$

Divide to solve for value of b . Then:

$$3.78 = (4.29)^b$$

$$b = 0.913$$

$$\beta = 1.301$$

By use of Winn's Method [99] for product rates:

$$\beta^{n+1} = \left(\frac{L_D}{W} \right) \left(\frac{W'}{L_D'} \right) \left(\frac{B}{D} \right)^{1-b}, \text{ for liquid overhead product} \quad (8-45)$$

Table 8-1
Data for Alkylation Deisobutanizer; Example 8-4 Using
Winn's Method

Component	Feed, moles	Overhead, moles	Bottoms, moles	Equilibrium K's Top tray	Reboiler
Ethylene	1	1
Ethane	2	2
Propane	48	48
Isobutane	863	848	15	0.94	3.55
n-Butane	132	71	61	0.70	3.00
Isopentane	33	33
n-Pentane	5	5
Alkylate	277	277
	1361	970	391

Used by permission, Winn, F. W., *Pet. Ref. V. 37, No. 5 (1958)*, p. 216, Gulf Pub. Co.

$$\beta^{n+2} = \left(\frac{V_D}{W}\right) \left(\frac{W'}{V_D'}\right)^b \left(\frac{B}{D}\right)^{1-b}, \text{ for vapor overhead product} \quad (8-46)$$

where B = mols of bottoms
 b = exponent in Equation 8-43
 D = total mols of overhead product
 n = minimum number of equilibrium trays in tower
 K = y/x = vapor-liquid equilibrium ratio for a component
 L = mols of a component in liquid phase
 P = vapor pressure, psia
 T = absolute temperature, °R
 V = mols of a component in vapor phase
 W = total mols of bottoms product
 x = mol fraction of a component in liquid phase
 y = mol fraction of a component in vapor phase
 α = relative volatility
 β = constant in Equation 8-43
 π = total pressure, psia
 L = total mols in liquid phase
 V = total mols in vapor phase

subscripts or superscripts:

D = distillate

B = bottoms

(') = heavy key component

1, 2 . . . = tray number

The minimum number of theoretical stages is calculated as follows:

$$(1.301)^{n+1} = (848/15) (61/71)^{0.913} (391/970)^{0.087}$$

$$= 45.5$$

$$n + 1 = 14.5$$

This is exactly the number of stages obtained by tray-to-tray calculations with the K correlation of Winn [236]. The

minimum number of stages by the Fenske equation, with a geometric average α of 1.261, is 16.8. The Fenske equation gives an answer that is too high by 2.3 stages or 16%.

For ideal systems following Raoult's Law; relative volatility $\alpha_{1h} = p_1/p_h$, ratio of partial pressures.

For a binary distillation, α is calculated at top and bottom conditions and a geometric mean used where the differences are relatively small.

$$\alpha_{avg} = \sqrt{\alpha_D (\alpha_B)} \quad (8-47)$$

Kister [94] recommends that the determination of α for calculation as:

- (1) $\alpha_{avg} = \alpha$ evaluated at $T_{avg} = (T_{top} + T_{Bot})/2$ where $T = ^\circ F$ (8-48)
- (2) $\alpha_{avg} = \alpha$ at feed tray temperature
- (3) Winn's [99] method previously discussed.

For hydrocarbon systems, the following is often used [65]

$$\alpha_{ir} = \frac{y_i x_r}{y_r x_i} = \frac{K_i}{K_r} \quad (8-36A)$$

where i = any component

r = component to which all the relative volatilities are referred

K_i = equilibrium distribution coefficient for component, i

K_r = equilibrium distribution coefficient for component to which relative volatilities are referred

For values of α near 1.0, extreme care must be used in establishing data, as a small change in the value of α_{avg} may double the number of trays.

The exact procedure is to estimate a temperature profile from top to bottom of the column and then calculate α for each theoretical tray or stage by assuming a temperature increment from tray to tray. For many systems this, or some variation, is recommended to achieve good separation calculations.

$$\alpha_{1h} = \frac{y_1 x_h}{x_1 y_h} \quad (8-35)$$

For non-ideal systems:

$$\alpha_{1h} = \frac{\gamma_1 K_1}{\gamma_h K_h} \quad (8-49)$$

The vapor-liquid equilibrium relationship may be determined from

$$y_1 = \frac{\alpha_{1h}(x_1)}{1 + (\alpha_{1h} - 1)x_1} \quad (8-50)$$

By assuming values of x_1 , the corresponding y_1 may be calculated.

For hydrocarbon systems, where $K_i = y_i/x_i$, then,

$$y_1/y_2 = (K_1/K_2)(x_1/x_2), \text{ and} \quad (8-51)$$

$$\alpha_{i,r} = K_i/K_r = \text{relative volatility} \quad (8-36A)$$

Example 8-5: Boiling Point Curve and Equilibrium Diagram for Benzene-Toluene Mixture

Using the vapor pressure data for benzene and toluene [59]:

1. Construct a boiling point diagram at a total pressure of 760 mm Hg, Figure 8-18.
2. From the boiling point diagram construct the equilibrium x-y curve for a total pressure of 760 mm Hg, Figure 8-19.

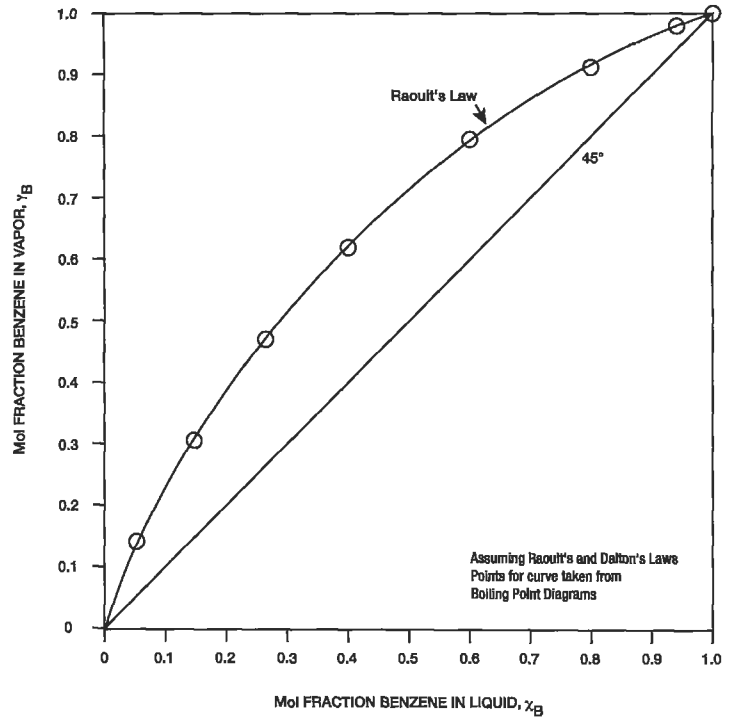


Figure 8-19. X-y diagram for benzene in benzene-toluene mixture at 760 mm Hg total pressure, Example 8-5.

Vapor pressure data as read from tables or graphs:

Temp, °C	Vapor Pressure- Benzene, mm Hg	Vapor Pressure- Toluene, mm Hg
80	760	280
90	1,000	410
100	1,320	550
110	1,740	740
111.5	1,760	760

Use Raoult's and Dalton's Laws:

$$P_B = P_T = \pi_{\text{Total}}$$

$$P_B = P_B x_B$$

$$P_T = P_T x_T$$

$$\text{Then: } x_B = \frac{\pi - P_T}{(P_B - P_T)}$$

$$x_T = 1 - x_B$$

$$y_T = 1 - y_B$$

$$y_B = P_B/\pi$$

where p_B = vapor pressure, benzene
 p_T = vapor pressure, toluene

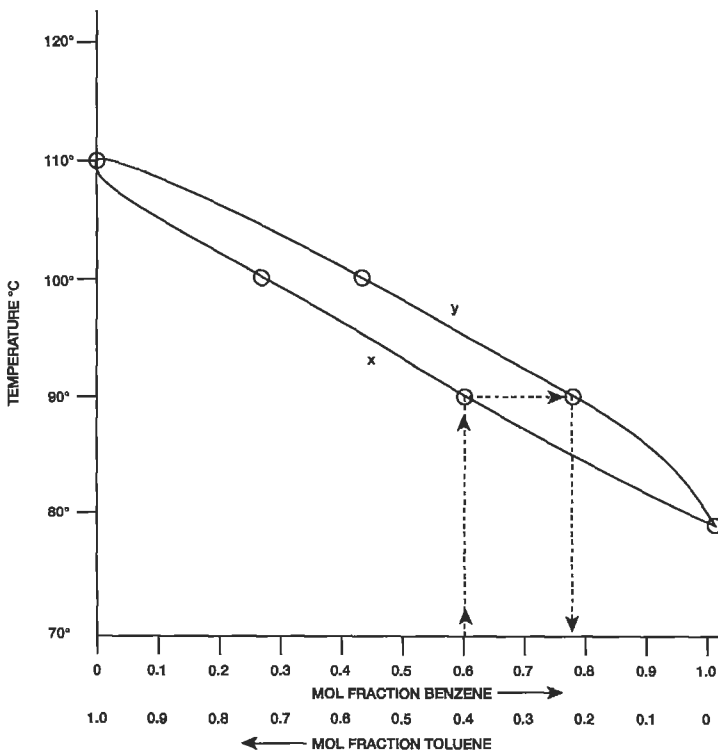


Figure 8-18. Boiling point diagram for Example 8-5. Benzene-toluene, total pressure = 760 mm Hg. Used by permission of Robinson & Gilliland.

Temp °C	$(P_B - P_T)$	$(\pi - P_T)$	x_B	x_T	$y_B = \frac{P_B x_B}{\pi}$	y_T
80	480	480	1.0	0	1.0	0
90	590	350	0.593	0.407	0.780	0.220
100	770	210	0.273	0.727	0.474	0.526
110	1,000	20	0.0	0.980	0.0457	0.954
111.5	1,000	0	0.0	1.0	0.0	1.0

Plot values of x_B , x_T , y_T , and y_B on Figure 8-18.

Example 8-6: Repeat Example 8-5 using K-values. Refer to basis of Example 8-4.

Using the data from Reference 59 (pp. 221, and 233):

Temp. °C	K_T	Rel. Vol., $\alpha_{B/T}^*$	$K_B = \alpha K_T$	$1 - K_T$	$(K_B - K_T)$
80	0.37	2.65	0.981	0.63	0.611
90	0.53	2.48	1.314	0.47	0.784
100	0.73	2.39	1.745	0.27	1.015
110	0.97	2.35	2.28	0.03	1.31
111.5	1.0	2.35	2.35	0.0	1.35

*Read from chart [59].

$X_B = \frac{1 - K_T}{(K_B - K_T)}$	$x_T = 1 - x_B$	$y_B = K_B x_B$	$y_T = K_T x_T$
*1.031	0.0	*0.981	0.0
0.60	0.40	0.789	0.212
0.266	0.734	0.464	0.535
0.0229	0.977	0.0523	0.946
0.0	1.0	0.0	1.0

*Note: If graphs could be read close, these values would be equal to 1.0.

Procedure

1. Read K value for toluene from tables or charts.
2. Read α values for benzene/toluene from Reference 59.
3. Calculate K (benzene) from: $\alpha_{B/T} = K_B/K_T$
4. Calculate $x_{benzene}$:

$$y_B = K_B x_B$$

$$y_T = K_T x_T$$

$$\Sigma 1.0 = K_B x_B + K_T x_T = K_B x_B + K_T (1 - x_B)$$

$$= x_B (K_B - K_T) + K_T$$

$$x_B = (1 - K_T) / (K_B - K_T)$$

5. Calculate $y_{benzene}$: $y_B = K_B x_B$
6. Plot boiling point diagram, see Figure 8-20.
7. Plot x-y diagram, see Figure 8-21.

Example 8-7: Flash Vaporization of a Hydrocarbon Liquid Mixture

What fraction of a liquid mixture containing 10 mole% propane, 65% n-butane and 25% n-pentane would be

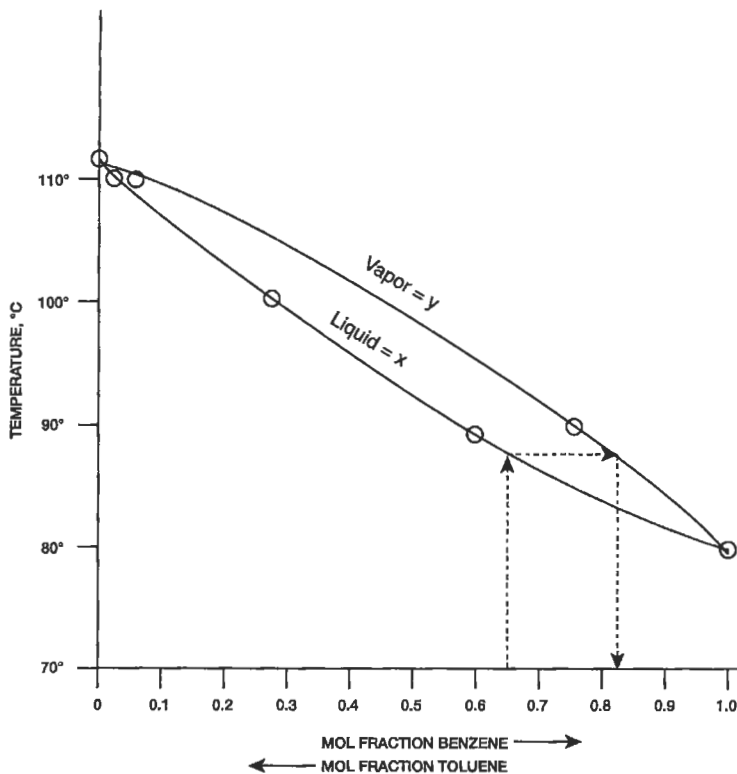


Figure 8-20. Boiling point diagram for benzene-toluene mixture using K values, total pressure 760 mm Hg; for Example 8-6.

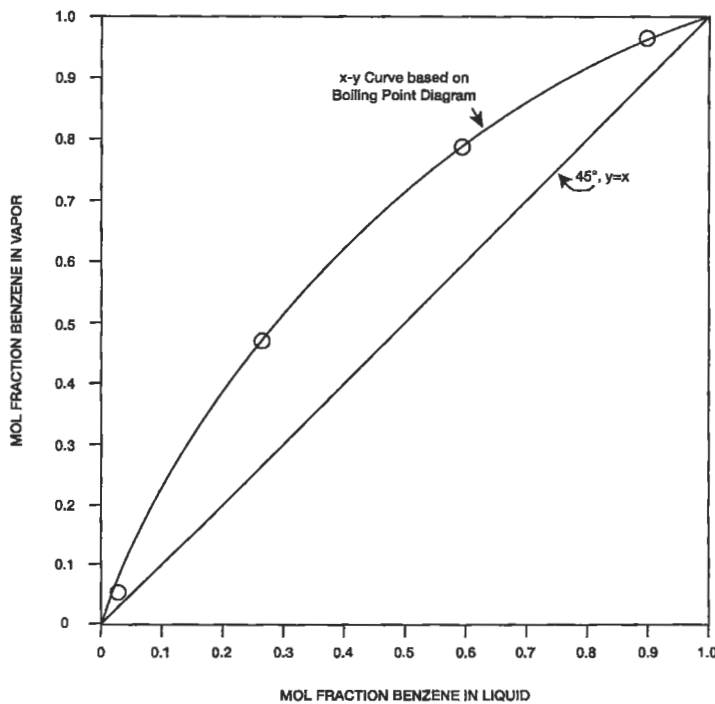


Figure 8-21. x-y diagram for benzene in benzene-toluene mixture, 760 mmHg total pressure, based on K-values, Example 8-6.

vaporized in a flash vaporization process at a temperature of 40°F and a pressure of 600 mm Hg abs?

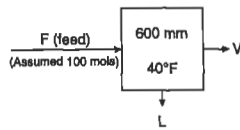
The following vapor pressure data for 40°F are available:

propane	3,800 mm Hg
n-butane	820 mm Hg
n-pentane	190 mm Hg

Assume Raoult's Law is applicable. At a total pressure, π , the temperature of flash must be between the dew point and bubble point.

Raoult's Law:

$$\begin{aligned}
 P_1 &= P_1 x_1 \\
 K_1 &= y_1/x_1 \\
 \pi y_1 &= P_1 x_1 \\
 y_1/x_1 &= P_1/\pi \\
 &= K_1
 \end{aligned}$$



	Mol%	Vapor Press. mm Hg = P_1	$K = \frac{P_1}{600}$	$\frac{FX}{V}$	$\frac{L}{V}$	$\frac{L}{KV}$	$1 + \frac{L}{KV}$
C ₃ H ₈	10	3,800	6.34	10	} 1.0	0.158	1.158
nC ₄ H ₁₀	65	820	1.37	65		0.73	1.73
nC ₅ H ₁₂	25	190	0.317	25		3.16	4.16

$$V = \frac{FX_i}{1 + L/(K_i V)}$$

$$\begin{array}{r}
 8.64 \\
 37.6 \\
 + 6.0 \\
 \hline
 \end{array}$$

V = 52.24 NOT a check, reassume

and recalculate. See Figure 8-22 for plot of results and the resultant extrapolation. Use this type chart as a guide to reduce the number of "guesses" to reach an acceptable solution. After several assumptions:

1. Assume feed = 100 mols
2. Assume L = 30
3. Then: V = 100 - 30 = 70 mols

X = mols of component i in vapor plus mols of component i in liquid divided by the total mols of feed (liquid + vapor)

F = mols of feed

Following the same headings as previous table it continues:

	Mol%	FX	Vapor Press.	$\frac{L}{V}$	$\frac{L}{KV}$	$1 + \frac{L}{KV}$
C ₃ H ₈	10	10	3,800	0.429	0.0677	1.067
nC ₄ H ₁₀	65	65	820	0.429	0.314	1.314
nC ₅ H ₁₂	25	25	190	0.429	1.352	2.352

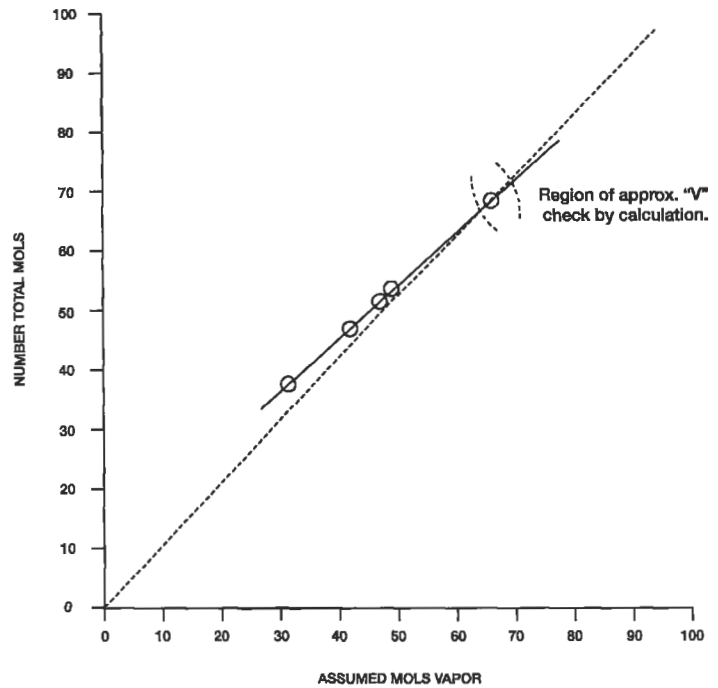


Figure 8-22. Extrapolation curve to determine approximate value of "V" for Example 8-7.

$V = \frac{FX}{1 + \frac{L}{KV}}$	* y; mol. frac.
9.38	0.135
49.4	0.711
<u>10.63</u>	<u>0.153</u>
69.41	0.999

These values are close enough for most calculations.

Therefore, after several trial-and error calculations these results indicate that after flashing, there would be 70% vapor (approximately) of above composition and 30% (mol) liquid.

Quick Estimate of Relative Volatility

Wagle [92] presents an estimate method for the average relative volatility of two components, related to the normal boiling points and the latent heats of vaporization of the two components, in the temperature range of their boiling points:

$$\alpha = \exp [0.25164 (1/T_{b1} - 1/T_{b2}) (L_1 + L_2)] \tag{8-52}$$

where α = relative volatility between the two components in the temperature range T_{b1} to T_{b2}

T_{b1} = normal boiling point of Component 1, °K

T_{b2} = normal boiling point of Component 2, °K

L_1 = latent heat of vaporization for Component 1 at T_{b1} , kcal/kmole

L_2 = latent heat of vaporization for Component 2 at T_{b2} , kcal/kmole

If a compound's latent heat is not known, it can be estimated from the normal boiling points and molecular weight.

Example 8-8: Relative Volatility Estimate by Wagle's Method [92] (used by permission)

The average relative volatility of benzene and toluene can be determined using the following data: $T_{bb} = 353.3$ K, $T_{bt} = 383.8$ K, $L_b = 7,352$ kcal/kmole, and $L_t = 7,930$ kcal/kmole (where the subscripts b and t denote benzene and toluene, respectively). Substituting these values into Equation 8-52 above, we find that:

$$\alpha_{bt} = \exp \left[0.25164 \times \left(\frac{1}{353.3} - \frac{1}{383.8} \right) \times (7,352 + 7,930) \right] = 2.375$$

This compares with a value of 2.421 for α determined using vapor-pressure/temperature charts.

Minimum Reflux Ratio: Infinite Plates

As the reflux ratio is decreased from infinity for the total reflux condition, more theoretical steps or trays are required to complete a given separation, until the limiting condition of Figure 8-23 is reached where the operating line touches the equilibrium line and the number of steps to go from the rectifying to stripping sections becomes infinite.

If the operating lines of Figure 8-23 intersect at x_c, y_c outside or above the equilibrium line when insufficient reflux is used, the separation is impossible.

This graphical representation is easier to use for non-ideal systems than the calculation method. This is another limiting condition for column operation, i.e., below this ratio the specified separation cannot be made even with infinite plates. This minimum reflux ratio can be determined graphically from Figure 8-23, as the line with smallest slope from x_D intersecting the equilibrium line at the same point as the "q" line for mixture following Raoult's Law.

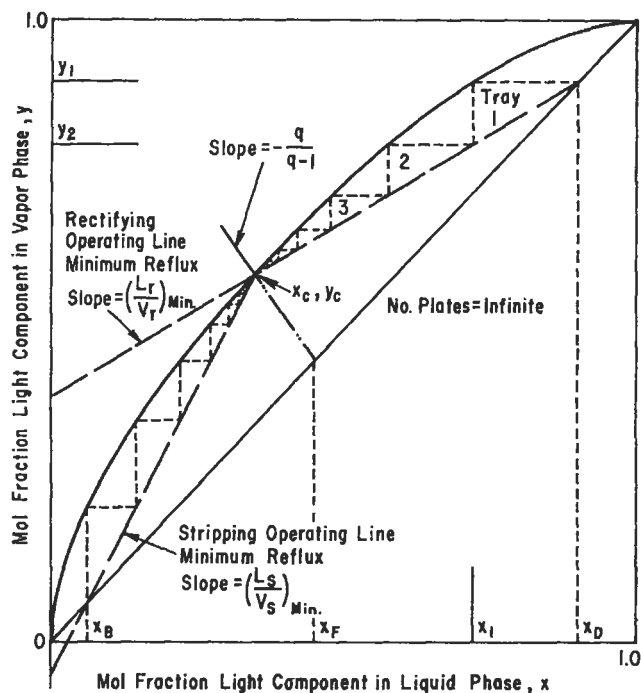


Figure 8-23. Fractionation of binary mixture at minimum reflux condition.

External reflux ratio = L/D

Slope of line from x_D :

$$\left(\frac{L}{V} \right)_{\min} = \frac{(L/D)_{\min}}{(L/D)_{\min} + 1} = \frac{x_D - y_c}{x_D - x_c} \quad (8-53)$$

L/V = internal reflux ratio

For non-ideal mixtures the minimum L/V may be as indicated in Figure 8-15, and hence not fixed as indicated above.

Figure 8-17 presents a convenient and acceptably accurate nomogram of Smoker's [66].

$$\left(\frac{L}{D} \right)_{\min} = \frac{x_D - y_c}{y_c - x_c} \quad (8-54)$$

where x_c and y_c are coordinates of intersection of minimum reflux "operating" line with equilibrium curve. At Boiling Point $x_c = x_F$.

Underwood's algebraic evaluation [73] for minimum reflux ratio is acceptable for handling ideal or near ideal systems:

Bubble Point Liquid, $q = 1.0$

$$(L/D)_{\min} = \frac{1}{\alpha - 1} \left[\frac{x_{1D}}{x_{1F}} - \frac{\alpha(1 - x_{1D})}{(1 - x_{1F})} \right] \quad (8-55)$$

All vapor feed, no superheating, $q = 0$

$$(L/D)_{\min} = \frac{1}{\alpha - 1} \left[\frac{\alpha x_{1D}}{x_{1F}} - \frac{(1 - x_{1D})}{(1 - x_{1F})} \right] - 1 \quad (8-56)$$

For the general case the relation is more complex in order to solve for $(L/D)_{\min}$.

$$\frac{(L/D)_{\min}(x_{1F}) + q x_{1D}}{(L/D)_{\min}(1 - x_{1F}) + q(1 - x_{1D})} = \frac{\alpha [(L/D)_{\min} + 1] y_{1F} + (q - 1) x_{1D}}{[(L/D)_{\min} + 1](1 - x_{1F}) + (q - 1)(1 - x_{1D})} \quad (8-57)$$

Short et al. [230] discuss minimum reflux for complex fractionators.

Theoretical Trays at Actual Reflux

The Gilliland correlation [23] of Figure 8-24A has proven satisfactory for many binary as well as multicomponent mixtures over a wide range of reflux ratios and number of plates.

Many systems appear to be economically designed for $\frac{(L/D) - (L/D)_{\min}}{(L/D) + 1} = 0.1$ to 0.33 and using actual reflux ratios

of 1.2 to 1.5 times the ratio at minimum reflux. For systems of greatly varying relative volatility this should not be used; instead, a Ponchon or enthalpy method must be followed.

Eduljee [84] suggests an equation to replace the Gilliland plot as easier to use. The data input must be the same. For tray towers:

$$Y_T = 0.75 - 0.75X^{0.5668} \quad (8-58)$$

$$Y_T = \frac{S_t - S_{\min}}{(S + 1)} \quad (8-59)$$

$$X = \frac{(L/D) - (L/D)_{\min}}{L/D + 1} \quad (8-60)$$

where S_t = theoretical actual trays at actual reflux, L/D , including overhead total condenser and reboiler
 Y_T = correlation expression similar to Gilliland's
 X = correlation expression similar to Gilliland's
 R = reflux ratio, L/D where L is liquid returned to the column in mols/hr
 D = distillate rate in mols/hr
 L = liquid returned to column, mols/hr
 NTU = total number of transfer units

$$\alpha = \frac{\ln \alpha}{(\alpha - 1)}, \text{ where } \alpha_h \text{ taken as } 1.0$$

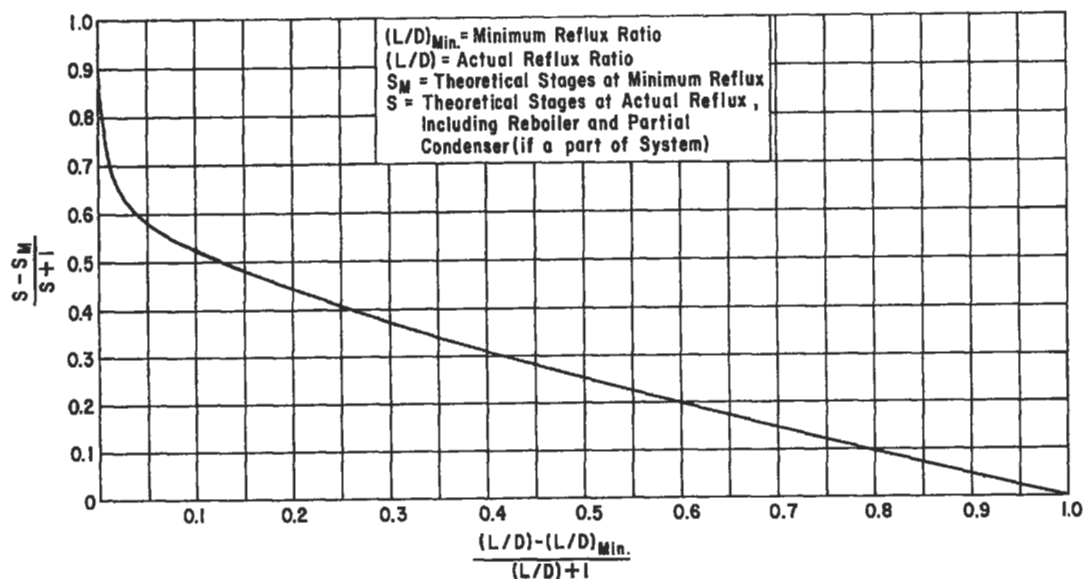


Figure 8-24A. Correlation of theoretical plates with reflux ratio.

subscripts:

- h = heavy
- min = minimum
- P = for packed towers
- T = for tray column

After calculating X, and solving for Y using Equation 8-58, then solve for the theoretical trays, S_t , at the *actual* selected reflux ratio (L/D) from the equation for Y. The equation appears to represent several reliable data references.

For packed towers, the corresponding relation for trays is [84]:

$$Y_P = 0.763 - 0.763 x^{0.5806} \quad (8-60A)$$

$$\text{and, } Y_P = \frac{NTU - NTU_{\min}}{NTU + 2a} \quad (8-60B)$$

Mapstone [122] and Zankers [123] developed the chart shown in Figure 8-24B to follow Figure 8-24A to allow for

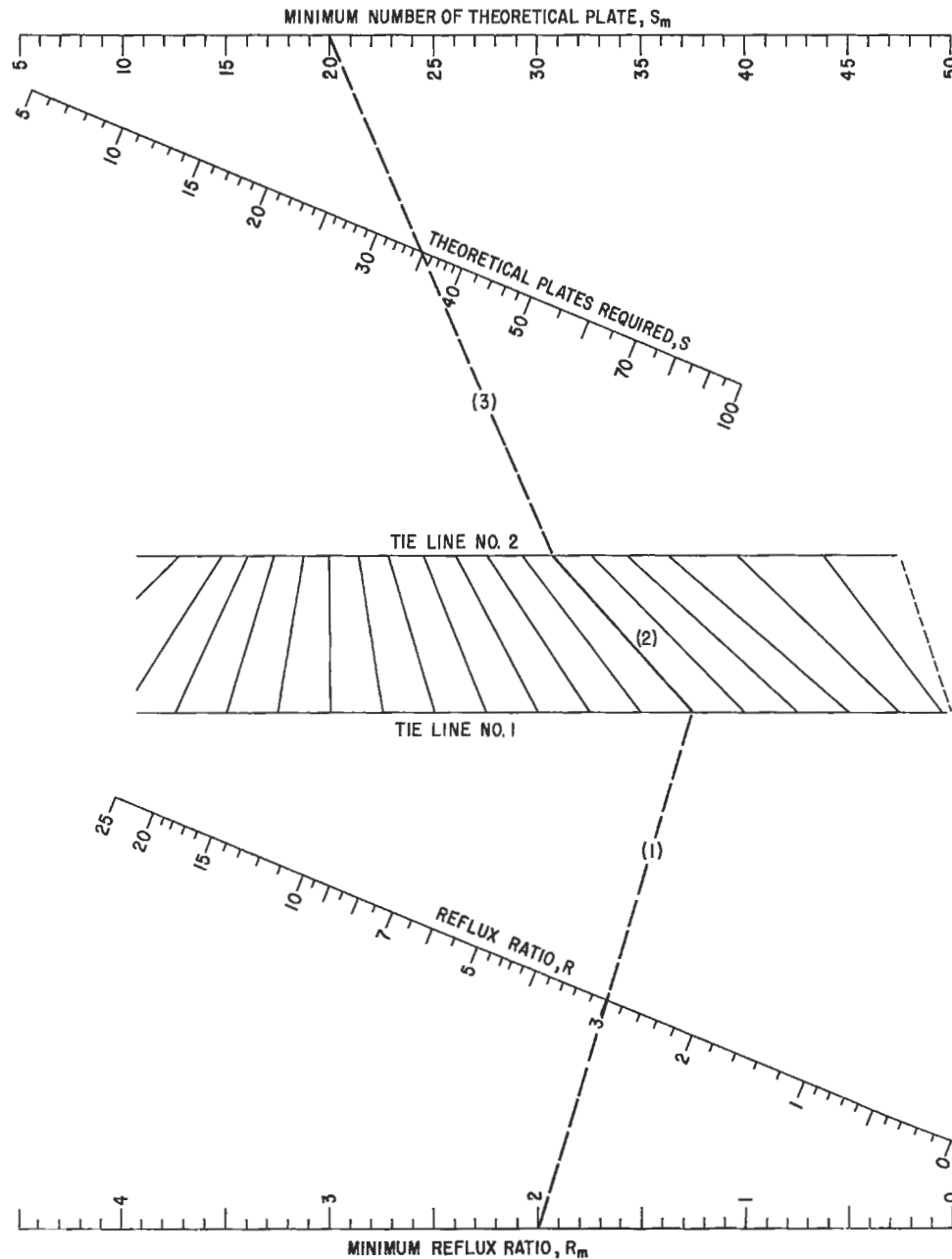


Figure 8-24B. Chart for reflux vs. trays. Use this nomogram for Gilliland's calculations for number of theoretical plates/trays. Used by permission, Mapstone, G.E., *Hydrocarbon Processing*, V. 47 No. 5 (1968), p. 169, Gulf Publishing Co., all rights reserved.

a quick evaluation of Gilliland's equation for theoretical plates at any reflux and minimum theoretical plates and minimum reflux ratio. The accuracy appears to satisfy industrial design needs, therefore it can be time saving when evaluating a range of values. For another interesting attempt to improve the Gilliland plot by use of equations, see Reference 136.

Example 8-9: Using Figure 8-24B to Solve Gilliland's Equation for Determining Minimum Theoretical Plates for Setting Actual Reflux (used by permission [122])

If the minimum reflux ratio is 2.0 and the minimum number of theoretical plates is 20, how many plates will be required if a reflux ratio 1.5 times the minimum is used?

Solution. The required reflux ratio, $R = 1.5 \times 2.0 = 3.0$

1. Connect 2.0 on left hand R_{\min} scale with 3.0 on left diagonal R scale and extend to cut Tie Line 1.
2. Transfer this value across the central maze to Tie Line 2.
3. Connect this point on Tie Line 2 with 20 on the right hand S_{\min} scale to cut the right diagonal S scale at 35 (calc. 34.9).

The number of theoretical plates required will be 35.

It will be noted that if any three of the four variables, S , S_{\min} , R , and R_{\min} are known, this chart can be used by an analogous procedure to give the fourth.

where S = theoretical plates at any reflux
 S_{\min} = minimum number of theoretical plates
 R = any reflux ratio
 R_{\min} = minimum reflux ratio

"Pinch Conditions" on x-y Diagram at High Pressure

Wichterle et al. [91] identify that near the critical pressure point of the more volatile component, all systems exhibit a "pinch" phenomenon at high pressure as shown in Figure 8-25 [91]. To obtain accurate separation performance, the K-value data used must be accurate in this narrow range of separation. For hydrocarbon systems, as well as systems involving hydrogen, nitrogen, and methane, the data must be accurate and not necessarily just a general equation for the particular compound. This is crucial to high accuracy computer performance analysis. Space does not allow inclusion of this method in this text.

McCormick [97] presents a correlation for Gilliland's chart relating reflux, minimum reflux, number of stages, and minimum stages for multicomponent distillation. Selecting a multiplier for actual reflux over minimum reflux is important for any design. Depending on the com-

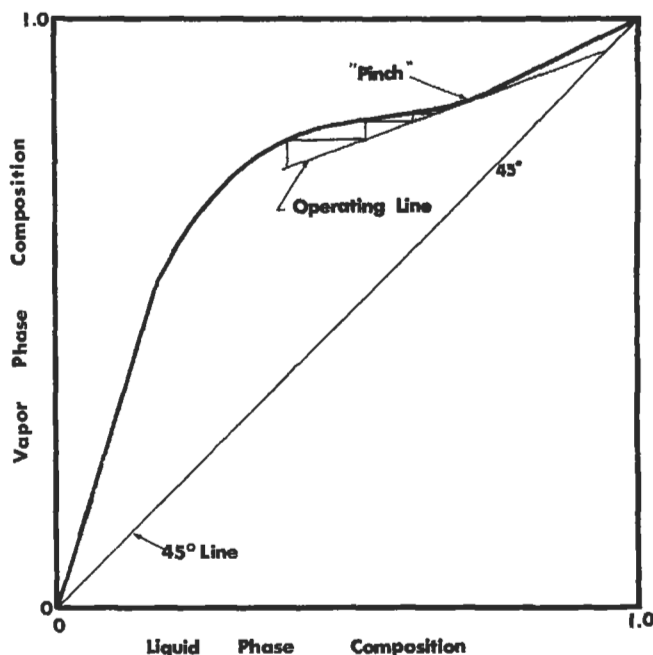


Figure 8-25. Example of typical "pinch point" for critical region for high-pressure distillation. Used by permission, Wichterle, I., Kobayashi, R., and Chappellear, P. S., *Hydrocarbon Processing*, Nov. (1971) p. 233, Gulf Publishing Co., all rights reserved.

plexity and analysis of the component's separation by the stages, the actual reflux can vary from 1.2 to 1.5 to 2.0, depending on the economics. The proposed equation agrees satisfactorily with other methods, and especially in the extreme ranges of Gilliland's plots [97], as well as the most used region.

$$R = A R_{\min}$$

$$X = \frac{R - R_{\min}}{R + 1} = \frac{(A - 1)(R_{\min})}{(A R_{\min} + 1)} = \frac{A - 1}{(A + 1/R_{\min})} \quad (8-61)$$

Representative values of X calculated with Equation 8-61 are given in the following table for values of R_{\min} and multiplier A . Reflux actual values can be assumed, and the system tested for R_{\min} , or used vice versa.

For actual versus minimum stages in a column,

$$Y = (N - N_{\min}) / (N + 1) \quad (8-62)$$

$$Y = 1 + \left[\frac{(R - R_{\min})}{(R + 1)} \right]^{(0.0456 \ln X + 0.44)} \quad (8-63)$$

$$X = (R - R_{\min}) / (R + 1) \quad (8-64)$$

Operational Values of X Calculated via Equation 8-61 for a Range of Reflux Ratios*

R_{min}	Multiplier A										
	0.02	1.05	1.07	1.10	1.12	1.15	1.17	1.20	1.30	1.40	1.50
1	0.010	0.024	0.034	0.048	0.063	0.070	0.092	0.091	0.130	0.167	0.200
3	0.015	0.036	0.050	0.070	0.092	0.101	0.132	0.130	0.184	0.231	0.273
5	0.016	0.040	0.055	0.077	0.102	0.111	0.145	0.143	0.200	0.250	0.294
10	0.018	0.043	0.060	0.083	0.110	0.120	0.157	0.154	0.214	0.267	0.313
Total reflux	0.020	0.048	0.065	0.091	0.120	0.130	0.170	0.167	0.231	0.286	0.393

*Used by permission, McCormick, J. E., *Chemical Engineering*, v. 95 no. 13 (1988), all rights reserved.

- where
- A = parameter in correlating equation or multiplier on R_{min}
 - B = parameter in correlating equation
 - ln = natural logarithm
 - log = logarithm to the base 10
 - N = actual theoretical stages required for a given separation
 - N_{min} = minimum theoretical stages required for a given separation
 - R = external reflux ratio for a given separation
 - R_{min} = minimum external ratio for a given separation
 - X = $(R - R_{min}) / (R + 1)$
 - Y = $(N - N_{min}) / (N + 1)$

The following is a short approximation method for minimum reflux ratios for multicomponent mixtures [98]:

$$R_{min} = \frac{1}{[(x_{FLK})_{eff} [(\alpha_{LK})_{avg} - 1]]} \quad (8-65)$$

- where $(x_{FLK})_{eff} = x_{FLK} / (x_{FLK} + x_{FHK})$
- n = number of components
 - R_{min} = minimum reflux ratio
 - x = liquid mol fraction
 - α_i = relative volatility of component i based on heavy key
 - α_{LK} = relative volatility of component, i, based on light key.

subscripts:

- avg = average
- eff = effective
- F = feed
- FHK = heavy key in feed
- FLK = light key in feed
- i = component
- LK = light key
- HK = heavy key

Kister [94, 95] examines binary distillation systems with multiple feeds, one or more side products, one or more points of heat removal or addition, and various combinations.

Example 8-10: Graphical Design for Binary Systems [59]

The benzene-toluene example of Robinson and Gilliland [59] has been elaborated on and expanded after the advanced distillation course of Holland [25], Figure 8-26.

It is desired to separate an equimolal mixture of benzene and toluene into a top product containing 95 mol % benzene and a bottom product containing 95 mol % toluene. The distillation is to be carried out at atmospheric pressure. Use a total condenser.

- A. Calculate the minimum reflux ratio if the feed is liquid at its boiling point.
- B. Calculate the theoretical plates required if a reflux ratio (L/D) of 1.5 times the minimum is employed.

Feed = 50 mols benzene + 50 mols toluene
 Overhead = 95% benzene
 Bottoms = 95% toluene

Material balance with respect to benzene:

$$\begin{aligned} 0.50(100) &= (0.95)(D) + 0.05B \\ 50 &= .95D + .05(100 - D) \\ 50 &= .95D + 5 - .05D \\ 45 &= .90D \\ D &= 45 / .90 = 50 \text{ mols overhead product} \\ D &= \text{overhead product, mols} \\ B &= \text{bottoms, mols} \end{aligned}$$

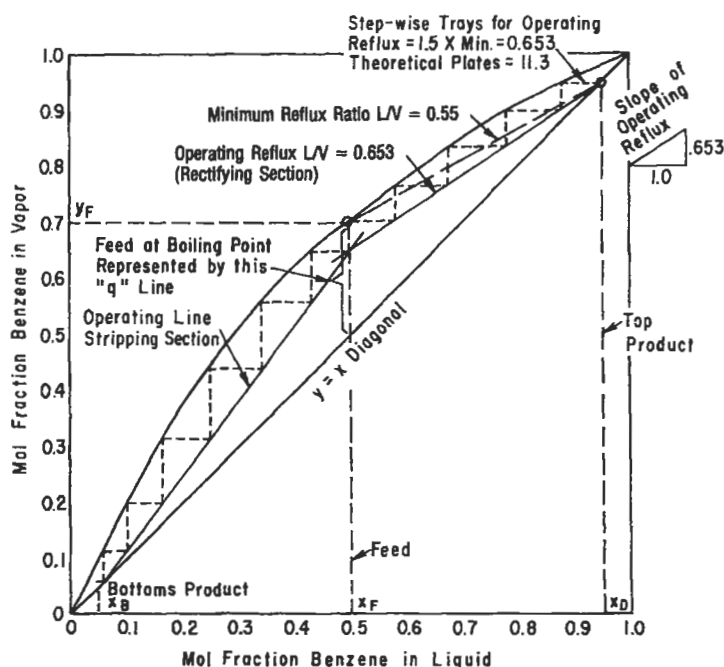


Figure 8-26. Equilibrium curve; benzene-toluene for Example 8-10 (curve data only). Used by permission, Robinson, C. S. R. and Gilliland, E. R., *Elements of Fractional Distillation*, 4th Ed. McGraw-Hill Book Co. (1950), all rights reserved.

A. For a Feed at its Boiling Point:

$$\frac{L_n}{V_n} = \frac{L/D}{L/D+1} \text{ or } \frac{L}{V} = \frac{x_D - y_F}{x_D - x_F}, y_F = 0.70 \text{ (from curve)}$$

$$= \frac{0.95 - 0.70}{0.95 - 0.50}$$

Minimum L/V = 0.55 mol reflux/mol vapor up

$$\text{substituting: } 0.55 = \frac{L/D}{L/D+1}$$

$$0.55 L/D + 0.55 = L/D$$

$$0.45 L/D = 0.55$$

$$\text{Reflux/Product} = L/D = 0.55/0.45 = 1.22$$

The value of L/D minimum should be equal to:

$$\frac{L_{12}}{D} = \frac{x_D - y_c}{y_c - x_c} = \frac{0.95 - 0.70}{0.70 - 0.50} = \frac{.25}{.20} = 1.25$$

The slight difference is probably due to inaccuracy in reading $y_c = 0.70$ from equilibrium curve.

B. Theoretical Plates at L/D = 1.5 Times Minimum:

$$\text{Operating Reflux Ratio} = (1.5) (1.25) = 1.878 = L/D$$

Slope of operating line at this reflux ratio:

$$\frac{L}{V} = \frac{L/D}{L/D+1}$$

$$\frac{L}{V} = \frac{1.878}{1.878+1} = 0.653$$

From Graph, L/V = 0.653 was plotted based on feed at its boiling point, No. of theoretical plates (step-wise graph) = 11.3

Now, to calculate theoretical plates:

Rectifying section:

$$y_n = \frac{L_n + 1}{V_n} x_{n+1} + \frac{D}{V_n} x_D \text{ operating line}$$

At: L/D = 1.878, D = 50 mols overhead

$$L = (1.878) (50) = 93.9 \text{ mols reflux to column}$$

$$V = L + D = 93.9 + 50 = 143.9 \text{ mols to vapor overhead}$$

$$y_n = \frac{93.9}{143.9} x_{n+1} + \frac{50}{143.9} (0.95) = 0.652 x_{n+1} + 0.331$$

For a total condenser: $y_{\text{top}} = x_D = x_R = 0.95$

From the equilibrium curve at $y_t = 0.95$

then: $x_t = 0.88$

$$y_{(t-1)} = 0.651 (x_t) + 0.331$$

$$y_{(t-1)} = 0.651 (0.88) + 0.331 = 0.903$$

$$y_{t-1} = 0.903, \text{ then } x_{t-1} \text{ from equilibrium curve} = 0.788$$

Now calculate y_{t-2}

$$y_{t-2} = 0.651 (.788) + 0.331 = 0.844$$

$$\text{At } y_{t-2} = 0.844, \text{ curve reads: } x_{t-2} = 0.69$$

$$\text{Then: } y_{t-2} = 0.651 (0.69) + .331 = 0.780$$

$$\text{At } y_{t-3}, \text{ curve reads: } x_{t-3} = 0.60$$

$$\text{Then: } y_{t-4} = 0.651 (0.60) + .331 = 0.722$$

$$\text{At } y_{t-4}, \text{ curve reads: } x_{t-4} = 0.52 \text{ (Feed Tray)}$$

$$\text{Then: } y_{t-5} = 0.651 (0.52) + .331 = 0.669 \text{ (too far below feed).}$$

Now go to *stripping section curve*:

$$y_m = \frac{L_{m+1} x_{m+1}}{V_m} - \frac{W}{V_m} x_B$$

The feed was at its boiling point:

$$V_n = V_m = 143.9$$

$$B = \text{Bottoms} = 50$$

$$L_m = B + V = 50 + 143.9 = 193.9$$

$$y_m = \left(\frac{193.9}{143.9} \right) x_{m+1} - \frac{50}{143.9} \quad (0.50)$$

$$= 1.35 x_{m+1} - .01736$$

Starting at $t - 4 = \text{feed tray}$:

$$x_{t-4} = 0.52$$

$$y \text{ (feed - 1)} = 1.35 x_f - 0.0176 (f - 1)$$

$$y_{(f-1)} = 1.35 (0.52) - 0.01736 + 0.685$$

$$\text{At } y_{t-1} = 0.685, x_{f-1} = 0.475,$$

Note: This is not too accurate due to switched operating line equations before the feed compositions were reached, yet, one more calculation on the stripping line would have placed us below the feed plate composition. Hence a change in reflux ratio is necessary in order to split right at the feed composition.

continuing:

$$y_{f-2} = 1.35 (0.475) - .01736 = 0.624$$

$$\text{From curve at } y_{f-2} = 0.624$$

$$x_{f-2} = 0.405$$

$$y_{f-3} = 1.35 (.405) - .01736 = 0.531$$

$$\text{From curve, } x_{f-3} = 0.32$$

$$y_{f-4} = 1.35 (.32) - .01736 = 0.416$$

$$x_{f-4} = 0.23$$

$$y_{f-5} = 1.35 (.23) - .01736 = 0.294$$

$$x_{f-5} = 0.15$$

$$y_{f-6} = 1.35 (.15) - .01736 = 0.186$$

$$x_{f-6} = 0.092$$

$$y_{f-7} = 1.35 (.092) - .01736 = 0.107$$

$$x_{f-7} = 0.05 \text{ (The desired bottoms composition)}$$

Total *theoretical* trays:

- rectifying section = 4
- feed tray = 1
- stripping section = 7
- total = 12 Trays

Example: 8-11 Thermal Condition of Feed

Using the same operating reflux (same fraction times the minimum) as was used in Example 8-10, calculate the theoretical plates required for feed of the following thermal conditions: Use Figure 8-27.

- (a) $q = 1.5$
- (b) $q = 0$
- (c) $q = -1.5$

A. For $q = 1.5$

Slope of "q" line = $-q/1 - q$

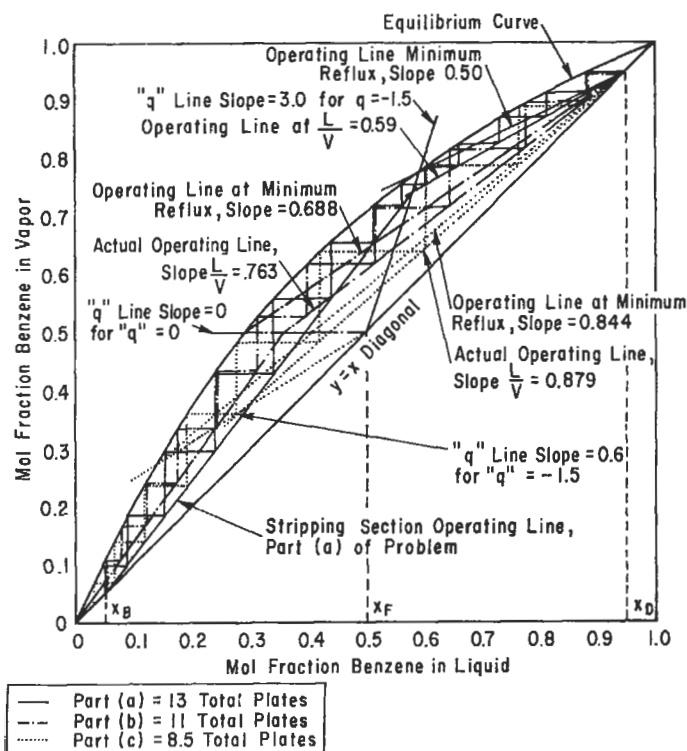


Figure 8-27. Equilibrium curve; benzene-toluene for Example 8-11 (curve data only). Used by permission, Robinson, C. S. R. and Gilliland, E. R., *Elements of Fractional Distillation*, 4th Ed. McGraw-Hill Book Co. (1950), all rights reserved.

Substituting, slope = $\frac{-1.5}{1-1.5} = \frac{-1.5}{-0.5} = +3$

Referring to calculations of Example 8-10, for an equimolar mixture of benzene and toluene in feed:

overhead product, $D = 50$ mols/100 mols feed

calculate $\left(\frac{L_R}{D}\right)_{\min} = \frac{x_D - y_c}{y_c - x_c}$

where $x_D = 0.95$
 $y_c = 0.774^*$
 $x_c = 0.59^*$

$$= \frac{0.95 - 0.774}{0.774 - 0.59}$$

$$= \frac{0.176}{0.184}$$

$(L/D)_{\min} = (L_R/D)_{\min} = 0.956$ min. reflux ratio, reflux/product

*Read from graph at intersection of "q" line for 1.5 and minimum reflux operating line.

Slope of Operating Line at Min. Reflux:

$$\left(\frac{L}{V}\right) = \left(\frac{L_R}{V}\right)_{\min} = \frac{L/D}{L/D + 1} = \frac{0.956}{0.956 + 1} = 0.49$$

(Graph reads 0.59 but this depends much on accuracy of plot.)

calculating

$$\left(\frac{L}{V}\right)_{\min} = \frac{x_D - y_c}{x_D - x_c}$$

$$= \frac{.95 - .774}{.95 - .59} = 0.49$$

Actual Operating Line:

Operating reflux ratio = $(1.5) (L/D) = 1.5 (0.956) = 1.432$ reflux/product

Slope of actual operating line:

$$\frac{L}{V} = \frac{L/D}{L/D + 1} = \frac{1.432}{1.432 + 1} = 0.59$$

Graphically, read 13 steps or *theoretical* plates from the top plate through bottom reboiler (assuming a total condenser).

rectifying section = 5
 feed plate = 1
 stripping section = 7 (includes reboiler)
 13 Plates including reboiler

To calculate this stepwise:

Operating line of rectifying section:

$$y_{n+1} = \frac{L_r}{V_r} x_n + \frac{D x_D}{V_r}$$

$$L/V = 0.59$$

$$L/D = 1.432, D = 50 \text{ mols product}$$

$$L = (50) 1.432 = 71.6 \text{ mols liquid reflux}$$

$$V_r = L_r + D = 71.6 + 50 = 121.6 \text{ mols}$$

$$\text{then: } y_{n+1} = 0.59 x_n + 50 (0.95)/121.6$$

$$y_{n+1} = 0.59 x_n + 0.39, \text{ operating line equation}$$

$$\text{At top: } y_{n+1} = x_D = 0.95$$

So: From equilibrium curve at $y_{n+1} = 0.95$, read the liquid in equilibrium, which is x_n (or top plate in this case) $x_n = x_{\text{top}} = 0.88$.

Now substitute this value $x = 0.88$ into the equation and calculate the vapor coming up from the first plate below the top ($t - 1$). Thus, if $x_n = \text{top plate}$, $y_{n+1} = \text{vapor from plate below top}$. Now, read equilibrium curve at $y_{(t-1)}$ and get $x_{(n+1)}$ or x_{t-1} which is liquid on plate below top. Then using x_{t-1} , calculate y_{t-2} (second plate below top, etc.). Then, read equilibrium curve to get corresponding liquid x_{t-2} . Continue until feed plate composition is reached, then switch to equation of stripping section and continue as before until desired bottoms composition is reached.

Operating line of stripping section:

$$y_m = \frac{L_s x_{m+1}}{V_s} - \frac{B x_B}{V_s}$$

Because the feed is a super cooled liquid, L_s/V_s is *not* equal to L_r/V_r . From definition of "q":

$$L_s = L_r + qF$$

$$L_s = 71.6 + (1.5) (100)$$

$$L_s = 221.6$$

$$\text{Also: } \frac{V_r - V_s}{F} = 1 - q$$

$$\frac{121.6 - V_s}{100} = 1 - 1.5$$

$$\frac{121.6 - V_s}{V_s} = -50$$

$$V_s = 171.6$$

$$\text{So: } \frac{L_s}{V_s} = \frac{221.6}{171.6} = 1.29$$

$$\frac{B}{V_s} = \frac{50}{171.6} = 0.291$$

Stripping section operating line:

$$y_m = 1.29 x_{m+1} - 0.291 x_B$$

$$x_B = 0.05$$

$$y_m = 1.29 x_{m+1} - 0.01455$$

Use this equation as described above following down from the feed plate cross-over from the rectifying equation to the stripping equation.

B. For $q = 0$

This represents feed as all vapor (not superheated).

Slope of "q" line:

$$= \frac{-q}{1-q} = \frac{-0}{1-0} = 0$$

This represents no change in overflow from the feed plate, and the increase in vapor flow is equal to the mols of feed.

$$\text{Minimum reflux: } \left(\frac{L}{D}\right)_{\min} = \frac{x_D - y_c}{y_c - x_c}$$

where: $x_D = 0.95$

$$\left. \begin{array}{l} y_c = 0.50 \\ x_c = 0.29 \end{array} \right\} \text{read from graph}$$

$$= \frac{0.95 - 0.50}{0.50 - 0.29}$$

$$= 2.14 \text{ min. reflux ratio, reflux/product}$$

Slope of operating line at minimum reflux:

$$\left(\frac{L}{V}\right)_{\min} = \frac{L/D}{L/D + 1} = \frac{2.14}{2.14 + 1} = 0.682$$

Slope from graph = 0.688

Operating reflux ratio = (1.5) (2.14) = 3.21, reflux/product, $(L/D)_{\text{op}}$

Slope of operating line = $(L/V)_{\text{op}} = 3.21/(3.21 + 1) = 0.763$

No. of theoretical plates from graph = 11

No. plates rectifying section = 5

feed plate = 1

stripping section = 5 (includes reboiler)

total = 11 (includes reboiler)

Rectifying Section Equation for Operating Line:

$$y_{n+1} = \frac{L_r}{V_r} x_n + \frac{D x_D}{V_r}$$

$$L/V = 0.763$$

$$L/D = 3.21$$

$$L = (3.21) (50 \text{ mol product, } D) = 160.6 \text{ mols (reflux liquid)}$$

$$V_r = L_r + D = 160.6 + 50$$

$$V_r = 210.6 \text{ mols vapor up column}$$

$$\text{then: } y_{n+1} = 0.763 x_n + \frac{50}{210.6} (0.95)$$

$$y_{n+1} = 0.763 x_n + 0.225$$

Liquid Down Stripping Section:

$$L_s = L_r + qF$$

$$L_s = 160.6 + (0) (100 \text{ mols feed})$$

$$L_s = 160.6 = L_r$$

Vapor Up Stripping Section:

$$\frac{V_r - V_s}{F} = 1 - q$$

$$\frac{210.6 - V_s}{100} = 1 - 0$$

$$210.6 - V_s = 100$$

$$V_s = 110.6 \text{ mols}$$

Stripping Section Equation for Operating Line

$$y_m = \frac{L_s}{V_s} x_{m+1} - \frac{B}{V_s} x_B$$

$$y_m = \frac{160.6}{110.6} x_{m+1} - \frac{50}{110.6} (0.05)$$

$$y_m = 1.452 x_{m+1} - 0.0226$$

Use these equations as described for the (a) part of problem in solving for number of theoretical plates stepwise.

C. For $q = -1.5$

This represents feed as a superheated vapor, and there is a decrease in liquid overflow from feed plate.

$$\text{Slope of "q" line} = \frac{-q}{1-q} = \frac{-(-1.5)}{1-(-1.5)} = 0.60$$

$$\text{Minimum reflux: } (L/D)_{\min} = \frac{x_D - y_c}{y_c - x_c}$$

where $x_D = 0.95$

$$\left. \begin{array}{l} y_c = 0.277 \\ x_c = 0.138 \end{array} \right\} \text{read from graph}$$

$$= \frac{.95 - .277}{.277 - .138}$$

$$(L/D)_{\min} = 4.84 \text{ reflux/product}$$

Slope of operating line at minimum reflux:

$$\begin{aligned} (L/V)_{\min} &= \frac{L/D}{L/D + 1} = \frac{4.84}{4.84 + 1} \\ &= 0.830 \text{ (graph reads 0.844)} \end{aligned}$$

Actual Operating Line:

$$\text{Operating reflux ratio} = (1.5) (4.84) = 7.26 \text{ reflux/product}$$

$$\text{Slope of actual operating line} = (L/V) = \frac{7.26}{7.26 + 1} = 0.879$$

Graphically we read 8.5 total plates thru bottom reboiler

rectifying section = 5

feed plate = 1

stripping section = 2.5 (includes reboiler)

total = 8.5 (includes reboiler)

Equations for Stepwise Tray to Tray Calculations Rectifying Section Operating Line

$$y_{n+1} = \frac{L_r}{V_r} x_n + \frac{D x_D}{V_r}$$

$$L_r/V_r = 0.879$$

$$L/D = 7.26$$

$$L_r = (7.26) (50) = 363 \text{ mols liquid reflux}$$

$$V_r = L_r + D = 363 + 50 = 413$$

$$y_{n+1} = 0.879 x_n + \frac{50}{413} (0.95)$$

$$y_{n+1} = 0.879 x_n + 0.115$$

Liquid Down Stripping Section:

$$L_s = L_r + qF$$

$$L_s = 363 + (-1.5) (100) = 213 \text{ mols liquid}$$

Vapor Up Stripping Section:

$$\frac{V_r - V_s}{F} = 1 - q$$

$$\frac{413 - V_s}{100} = 1 - (-1.5) = 2.5$$

$$-V_s = 250 - 413$$

$$V_s = 163 \text{ mols vapor}$$

Stripping Section Operating Line:

$$y_m = \frac{L_s}{V_s} x_{m+1} - \frac{B}{V_s} x_B$$

$$y_m = \frac{213}{163} x_{m+1} - \frac{50}{163} \quad (.05)$$

$$y_m = 1.307 x_{m+1} - 0.01535$$

Use these equations as described for Part (a) in solving for theoretical plates.

Example 8-12: Minimum Theoretical Trays/Plates/Stages at Total Reflux

A finishing column is required to produce 99.9% (vol.) trichlorethylene purity from 10,000 lb/hour of a feed of 40% (wt.) trichlorethylene and 60% (wt.) perchlorethylene. Only 1% (vol.) of the trichlorethylene can be accepted in the bottoms.

Because the process system that will receive vents from this condensing system is operating at 5 psig, allow 5 psi pressure drop to ensure positive venting and set top of tower pressure at 10 psig.

	(1)	(2)	(1) (2)	Mol
Feed (158°F)	Wt %	Mol Wt	Mols	Fraction
Trichlorethylene	40	131.4	0.00304	0.456
Perchlorethylene	60	165.9	0.00362	0.544
	100		0.00666	1.000

$$\text{Avg mol wt } 1.00/.00666 = 150.0$$

Overhead

Overhead temperature for essentially pure products at 10 psig = 223°F from vapor pressure curve.

Bottoms

Allow 10 psi tower pressure drop, this makes bottom pressure = 20 psig = 1,800 mm Hg.

Material Balance:

$$\text{Feed rate: mols/hr} = \frac{10,000 \text{ lb/hr}}{(150.0)} = 66.7$$

$$x_1 F = x_1 D + x_1 B$$

$$0.456 (66.7) = 0.999 D + 0.01 B$$

$$30.4 = .999 D + .01 (66.7 - D)$$

$$D = 30.05 \text{ mols/hr}$$

$$\text{bottoms: } B = F - D$$

$$B = 66.7 - 30.05 = 36.65 \text{ mols/hr}$$

Bottoms Composition:	Mol Fraction	Mols/hr	V. P. (316°F) mm Hg	V. P. Frac.
Trichlor	0.01	0.3665	4,200	42
Perchlor	0.99	36.2835	1,780	1,762
		1.00	36.65	1,804 mm

The 1,804 mm compares to the balance value of 1,800 mm = 20 psig.

Overhead Composition	Mol Fraction	Mols/Hr
Trichlor	0.999	30.02
	0.001	0.03
	1.000	

Relative Volatility: overhead conditions

$$\alpha_{\text{tri/per}} = \frac{\text{v.p. (tri)}}{\text{v.p. (per)}} = \frac{1,280 \text{ mm}}{385 \text{ mm}} = 3.32 \quad (223^\circ \text{F})$$

Bottom Conditions

$$\alpha_{\text{tri/per}} = \frac{\text{v.p. (tri)}}{\text{v.p. (per)}} = \frac{4,200 \text{ mm}}{1,780 \text{ mm}} = 2.36 \quad (316^\circ \text{F})$$

$$\text{mean } \alpha = \sqrt{(3.32)(2.36)} = 2.80$$

Thermal Condition of the Feed at 158°F

At conditions of feed tray, assume pressure is 15 psig = 1,533 mm Hg. Determine bubble point:

Component	X_{iF}	assume $t = 266^\circ \text{F}$ v.p. mm Hg	Partial Press. x (V.P.)
Trichlor	0.456	2,350	1,072
Perchlor	0.544	880	478
			1,550

This is close enough to 1,533 mm; actual temperature might be 265°F, although plotted data are probably not that accurate. Because the feed enters at 158°F and its bubble point is 266°F, the feed is considered sub-cooled.

Heat to vaporize one mol of feed,

Component	x_{IF}	Latent Ht. @ 266°F Btu/mol	$(x_F)(L_v)$	Btu/Mol (°F) C_p @ 158°F	$(x_F)(C_p)$ (266-158)
Trichlor	0.456	12,280	5,600	30.9	1,523
Perchlor	0.544	14,600	7,950	36.4	2,180
			13,550		3,703
			Btu/mol		Btu/mol

$$q = \frac{\text{heat required to vaporize one mol of feed}}{\text{latent heat of one mol of feed}}$$

$$q = \frac{13,550 - 3,703}{13,550} = \frac{17,253}{13,550} = 1.272$$

Minimum Number Tray at Total Reflux

$$\begin{aligned} x_{D1} &= 0.999 \\ x_{Dh} &= 0.001 \\ x_{B1} &= 0.01 \\ x_{Bh} &= 0.99 \\ \alpha_{\text{Avg}} &= 2.8 \end{aligned}$$

For a total condenser system:

$$\begin{aligned} (N_{\min} + 1) &= \frac{\log(x_{D1}/x_{Dh})(x_{Bh}/x_{B1})}{\log \alpha_{\text{avg}}} \\ &= \frac{\log(.999/.001)(.99/.01)}{\log 2.8} \end{aligned}$$

$$N_{\min} + 1 = 11.18$$

$$N_{\min} = 10.18 \text{ trays, not including reboiler}$$

Summary:

Min. total physical trays in column	= 10.18
Reboiler	1.0
For conservative design, add feed tray	1.0
Minimum total theoretical stages	12.18, say 12

Minimum Reflux Ratio

Because this is not feed at its boiling point, but sub-cooled liquid, the convenient charts cannot be used with accuracy. Using Underwood's general case:

$$\begin{aligned} & \frac{(L/D)(x_{IF}) + q x_{ID}}{(L/D)(1 - x_{IF}) + q(1 - x_{ID})} \\ &= \frac{\alpha \{[(L/D) + 1]y_{IF} + (q - 1)(x_{ID})\}}{[(L/D) + 1](1 - x_{IF}) + (q - 1)(1 - x_{ID})} \end{aligned}$$

Solve first for y_{IF} , assuming that the system follows the ideal (as it closely does in this instance).

$$y_{IF} = \frac{x_{IF}(\alpha_F)}{1 + (\alpha_F - 1)x_{IF}}$$

This takes the place of drawing the equilibrium curve and solving graphically, and is only necessary since the "q" is not 1.0 or zero.

The α should be for the feed tray. However, the value of $\alpha = 2.8$ should be accepted for *feed tray* conditions (not 158°F). It would not be if this were predominantly a rectifying or a stripping operation.

$$y_{IF} = \frac{0.456(2.8)}{1 + (2.8 - 1)(0.456)} = 0.70$$

Now, substituting to solve for $(L/D)_{\min}$.

$$\begin{aligned} & \frac{(L/D)(0.456) + 1.272(0.999)}{(L/D)(1 - 0.456) + 1.272(1 - 0.999)} \\ &= \frac{2.8\{[(L/D) + 1]0.70 + (1.272 - 1)(0.999)\}}{(L/D) + 1(1 - 0.456) + (1.272 - 1)(1 - 0.999)} \\ & \frac{(L/D)(0.456) + 1.271}{(L/D)(0.544) + 0.00127} = \frac{2.8\{[(L/D)(0.70) + 0.70 + 0.271]\}}{(L/D)(0.544) + 0.544 + 0.000271} \end{aligned}$$

Solving this quadratic:

$$(L/D)_{\min} = 0.644$$

Reading Figure 8-17 for $(L/D)_{\min}$ assuming a liquid feed at the boiling point, $(L/D)_{\min} = 1.2$. This demonstrates the value of taking the thermal condition of the feed into account.

Actually, any point on one of the curves represents a condition of reflux and number of trays that will perform the required separation.

Theoretical Trays at Actual Reflux

Assume actual reflux ratios of 1.2, 1.8, 2.25, 3.0 times the minimum and plot the effect on theoretical plates using Gilliland plot.

Actual Reflux Ratio	$\frac{(L/D) - (L/D)_{min}}{L/D + 1}$	(From Fig. 8-24A) $N - N_{min}$	N (Theo.)	Conservative Add 1 For Feed, Total N
0.772	0.0722	0.552	26.2	27
1.16	0.239	0.416	19.8	21
1.45	0.329	0.356	17.9	19
1.93	0.439	0.288	16.1	17

$$\frac{(L/D) - (L/D)_{min}}{(L/D) + 1} = \frac{0.772 - 0.644}{0.772 + 1} = 0.0722$$

Read value from curve Figure 8-24A.

$$\frac{N - N_{min}}{N + 1} = 0.552$$

$$\frac{N - 11.18}{N + 1} = 0.552$$

$$N = 26.2$$

Note that these values for theoretical trays *do not* contain corrections in overall efficiency, and hence *are not* the *actual* trays for the binary distillation column. Efficiencies generally run 50–60% for systems of this type which will yield a column of actual trays almost twice the theoretical at the operating reflux.

Figure 8-28 presents the usual determination of *optimum* or *near optimum* theoretical trays at actual reflux based on performance. It is not necessarily the point of least cost for all operating costs, fabrication costs or types of trays. A cost study should be made to determine the merits of moving to one side or other of the so-called optimum point. From the Figure 8-28:

First choice actual reflux ratio, $L/D = 1.33$
Corresponding theoretical trays or stages, $N = 18.6$

Note that the 18.6 includes the reboiler, so physical trays in column = 17.6. Do not round-off decimal or fractions of trays until after efficiency has been included.

Tray Efficiency

Base at average column temperature of $(158 + 266)/2 = 212^\circ\text{F}$.

Component	x_{iF}	Viscosity, cp	$(\mu) (x_i)$
Trichlor	0.456	0.27	0.123
Perchlor	0.544	0.36	<u>0.196</u>
			0.319 cp.

From Figure 8-29:

Efficiency = 47.5%

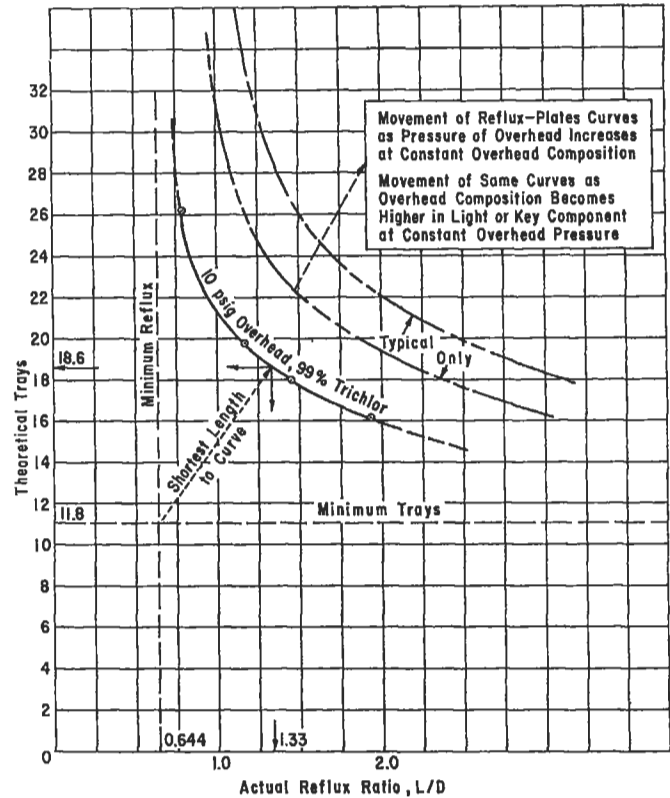


Figure 8-28. Relationship of reflux ratio and theoretical trays, for Example 8-12.

Actual Trays at Actual Reflux

Actual $L/D = 1.33$
Actual trays = $18.6/0.475 = 39.2$ (including reboiler)
Physical trays: $39.2 - 1$ (reboiler) + 1 (conservative, feed) = 39.2

Round-off to: 40 trays plus reboiler plus total condenser.

Note: If there is any reason to know that the efficiency of this system is usually lower (or in same chemical family), then either the efficiency should be reduced to account for this or the trays should have an additional allowance. In practice, this same column might be installed as 40 trays in one plant, 45 in another and 50 in another.

Tray Details

Tray details will be considered in a later example.

Tray Efficiency

Several empirical efficiency correlations have been developed from commercial equipment and some laboratory data and serve most of design problems for the average hydrocarbon and chemical systems. They are empirical correlations and the application in new systems is unpredictable. For this reason results for efficiencies are

evaluated by more than one method to obtain some idea of the possible spread. Even so, in light of the AIChE study discussed below, some of these empirical methods can be off by 15–50%. Comparisons indicate these deviations are usually on the safe or low side. The relation of Drickamer and Bradford [16] of Figure 8-29 has been found to agree quite well for hydrocarbon, chlorinated hydrocarbons, glycols, glycerine and related compounds, and some rich hydrocarbon absorbers and strippers.

The relation of O'Connell [49] (Figure 8-29) has generally also given good results for the same systems but generally the values are high. The absorber correlation of O'Connell (Figure 8-29) should be used as long as it generally gives lower values than the other two relations. It can be used for stripping of gases from rich oils provided care is exercised to not accept too high values.

The area of absorption and stripping is difficult to correlate for the wide range of peculiarities of such systems. The correlation of Gautreaux and O'Connell [22] allows

a qualitative handling of tray mixing to be considered with overall and local efficiencies. In general it agrees with the Drickamer correlation at least for towers to seven feet in diameter. Although the effect of liquid path apparently must be considered, the wide variety of tray and cap designs makes this only generally possible, and the overall correlations appear to serve adequately.

The American Institute of Chemical Engineer's Distillation Tray Efficiency Research [2] program has produced a method more detailed than the short-cut methods, and correspondingly is believed to produce reliable results. This method produces information on tray efficiencies of new systems without experimental data. At present there is not enough experience with the method and its results to evaluate its complete range of application.

Murphree [85] developed "point" and "overall" distillation tray efficiencies, which are examined in detail in Reference 2. The expressions are [59]:

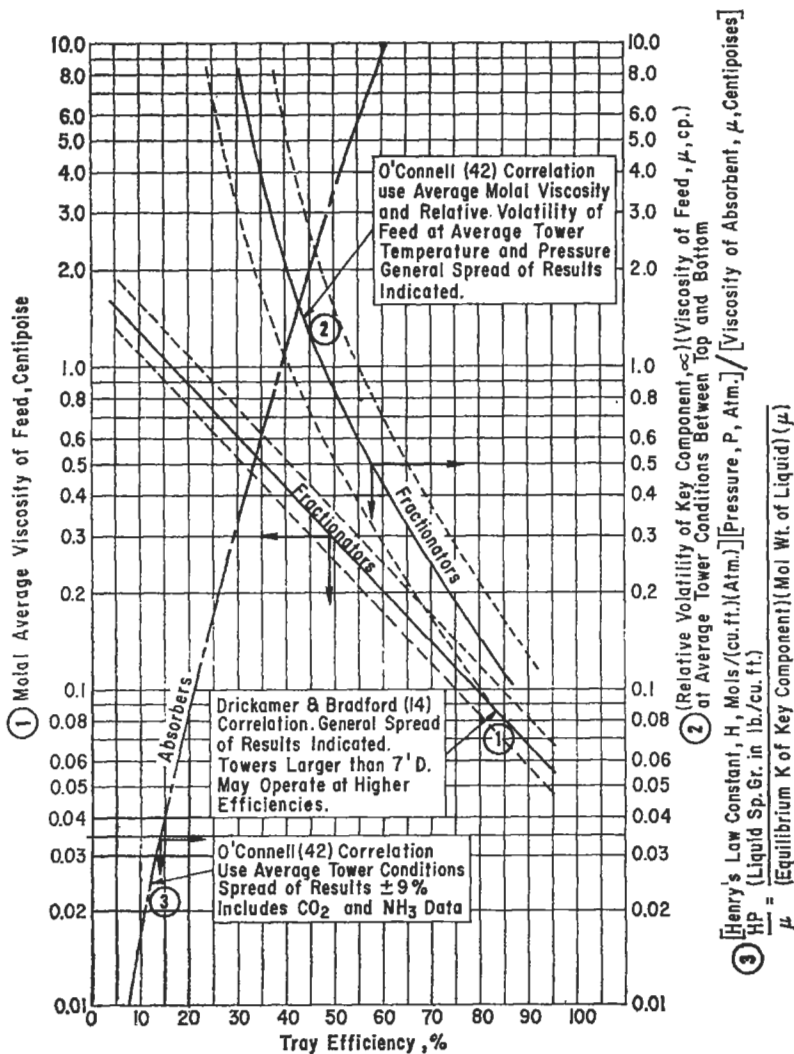


Figure 8-29. Empirical correlations of overall efficiencies for Fractionation and Absorption.

$$\text{Plate/Tray Efficiency: } E_{MV}^o = \frac{y_i - y_o}{y_i - y_e^*} \quad (8-66)$$

The plate/tray efficiency is the integrated effect of all the point efficiencies.

$$\text{Point Efficiency: } E_{MV}^* = \frac{y_i' - y_o'}{y_i' - y_e} \quad (8-67)$$

$$\text{Overall tray efficiency, } E_o = \frac{\text{No. Theoretical Trays}}{\text{No. of Actual Trays}} \quad (8-68)$$

where y_i = average composition of vapor entering tray
 y_o = average composition of vapor leaving tray
 y_e^* = composition of vapor in equilibrium with liquid flowing to plate below
 y_i' = vapor composition entering local region
 y_o' = vapor composition leaving local region
 y_e = vapor composition in equilibrium with the liquid in the local region

The proposal for calculating column vapor plate efficiencies by MacFarland, Sigmund, and Van Winkle [86] correlates with the Murphree vapor plate efficiencies in percent:

$$E_M = \frac{y_n - y_{n+1}, \%}{y^* - y_{n+1}} \quad (8-69)$$

where y_n = average light key mol fraction of vapor leaving plate n
 y_{n+1} = average light key mol fraction of vapor entering plate n
 y^* = light key mol fraction of vapor in perfect equilibrium with liquid leaving plate n

Data from bubble cap and perforated tray columns for the Murphree vapor plate efficiencies are correlated [86]:

$$E_M = 7.0 (N_{DG})^{0.14} (N_{SC})^{0.25} (N_{Re})^{0.08} \quad (8-70A)$$

or,

$$E_M = 6.8 (N_{Re} N_{SC})^{0.1} (N_{DG} N_{SC})^{0.115} \quad (8-70B)$$

Referenced to 806 data points for binary systems, Equation 8-70A gives absolute deviation of 13.2%, which is about as accurate, or perhaps more so, than other efficiency equations. Equation 8-70B uses the same data and has an absolute average deviation of 10.6%. See Example 8-13 for identification of dimensionless groups.

Example 8-13: Estimating Distillation Tray Efficiency by Equations 8-70A and 8-70B (used by permission of McFarland et al. [86])

Solving the problem defined in the following table will show the equations for estimating system physical properties and their relation to the calculation of Murphree vapor plate efficiencies:

System properties*	Acetone	Benzene
Molecular weight, M, lb/lb mole	58.08	78.11
Viscosity, μ lb/hr-ft	0.5082	0.8155
Parachor, [P]	162.1	207.1
API specific gravity coeff [240]:		
A	0.8726	0.9485
B	0.00053	0.00053
C	21.6	18.0
E	536.0	620.6
Operating data		
Acetone mole fraction, x_1	= 0.637	
Benzene mole fraction, x_2	= 0.363	
Temperature, T, °F	= 166	
Superficial vapor mass velocity, G, lb/hr-sq ft	= 3,820	
Vapor velocity, U _v , ft/hr	= 24,096	
Weir height, h _w , ft	= 0.2082	
Fraction free area, FA	= 0.063	

*Used by permission of McFarland et al. [86].

Liquid densities for pure hydrocarbon are calculated [240] as a function of temperature using the following equation for specific gravity:

$$sg_L = A - BT - C/(E - T)$$

The liquid density is then:

$$\rho_L = (62.32) (sg_L)$$

For acetone,

$$\rho_{L,1} = (62.32) [0.8726 - 0.00053(166) - 21.6/(536.0 - 166)] = 45.3 \text{ lb/ft}^3$$

For benzene,

$$\rho_{L,2} = (62.32) [0.9485 - 0.00053(166) - 18.0/(620.6 - 166)] = 51.2 \text{ lb/ft}^3$$

Vapor densities are calculated from the ideal gas relation:

$$\rho_V = MP_t/555(T + 460)$$

where total pressure P_t is given in millimeters of mercury.

Mixture densities of the binary mixtures require a knowledge of volume fraction for each component. The component molar volume is:

$$V_i = M_i/\rho_i$$

For acetone and benzene, respectively:

$$V_{L,1} = (58.08)/45.3 \\ = 1.282 \text{ ft}^3/\text{lb mole}$$

$$V_{L,2} = (78.11)/51.2 \\ = 1.526 \text{ ft}^3/\text{lb mole}$$

For the liquid mixture:

$$V_{L,\text{mix}} = x_1 V_{L,1} + x_2 V_{L,2} \\ = (0.637) (1.282) + (0.363) (1.526) \\ = 1.371 \text{ ft}^3/\text{lb mole}$$

Then the volume fraction of a component is calculated assuming an ideal mixture.

$$v_i = V_i/V_{\text{mix}}$$

For acetone and benzene, respectively:

$$v_{L,1} = 0.817/1.371 = 0.596$$

$$v_{L,2} = 0.554/1.371 = 0.404$$

The liquid density of the binary mixture is then:

$$\rho_{L,\text{mix}} = v_{L,1} \rho_{L,1} + v_{L,2} \rho_{L,2} \\ = (0.596) (45.3) + (0.404) (51.2) \\ = 47.6 \text{ lb/ft}^3$$

The vapor density can be found in an analogous manner.

$$\rho_{V,\text{mix}} = v_{V,1} \rho_{V,1} + v_{V,2} \rho_{V,2}$$

However, the example problem does not require a calculation for vapor density. Instead, the superficial vapor mass velocity G can be substituted into Equation 8-73 because:

$$G = U_V \rho_V$$

Liquid viscosity of the binary mixture, when not reported with the experimental efficiency results, is estimated using:

$$\mu_{L,\text{mix}} = (\sum x_i \mu_i^{1/3})^3$$

The pure component viscosities are given in the literature [240, 241] as a function of temperature.

For the example,

$$\mu_{L,\text{mix}} = [(0.637) (0.5082)^{1/3} + (0.363) (0.8155)^{1/3}]^3 \\ = 0.609 \text{ lb/hr-ft}$$

Liquid surface tension is calculated using the Sugden Parachor method [242]. Neglecting vapor density, surface tension for the liquid mixture is:

$$\sigma_{L,\text{mix}} = [(\rho_{\text{mix}}/M_{\text{mix}}) |P|_{\text{mix}}]^4$$

where σ is in dynes/cm, ρ is in gm/cm³ and the parachor,

$$[P]_{\text{mix}} = \sum x_i [P]_i$$

Values of the parachor are given in the literature [240]. Then the example gives:

$$M_{\text{mix}} = (0.637) (58.08) + (0.363) (78.11) \\ = 65.35 \text{ lb/lb mole}$$

$$[P]_{\text{mix}} = (0.637) (162.1) + (0.363) (207.1) \\ = 178.4$$

$$\rho_{\text{mix}} = 47.6/62.32 = 0.7638 \text{ gm/cu cm}$$

$$\sigma_{\text{mix}} = [(0.7638/65.35) (178.4)]^4 \\ = 18.96 \text{ dynes/cm}$$

Diffusivity of the liquid light key component is calculated by the dilute solution equation of Wilke-Chang [243].

$$D_{LK} = (3.24 \times 10^{-8}) (\psi M_{\text{mix}})^{1/2} (T + 460)/\mu_{\text{mix}} (V_{LK})^{0.6}$$

Wilke-Chang reported the recommended values for ψ as follows: water, 2.6; benzene, heptane and ether, 1.0; methanol, 1.9; ethanol, 1.5; unassociated solvents, 1.0. The mixture parameter for the example problem is considered unity.

Then,

$$D_{LK} = (3.24 \times 10^{-8}) (65.35)^{1/2} (166 + 460)/(0.609) (1.282)^{0.6} \\ = 2.32 \times 10^{-4} \text{ ft}^2/\text{hr}$$

Dimensionless groups for the example problem are:

$$N_{Dg} = \sigma_L/\mu_L U_V \quad (8-71) \\ = (5.417 \times 10^5)/(0.609) (2.4092 \times 10^4) \\ = 37$$

$$N_{Sc} = \mu_L/\rho_L D_{LK} \quad (8-72) \\ = (0.609)/(47.6) (2.32 \times 10^{-4}) \\ = 55$$

$$N_{Re} = h_w G/\mu_L (FA) \quad (8-73) \\ = (0.2082) (3.82 \times 10^3)/(0.609) (0.063) \\ = 2.07 \times 10^4$$

Murphree vapor plate efficiency is calculated two ways:

$$E_M = 7.0 (N_{Dg})^{0.14} (N_{Sc})^{0.25} (N_{Re})^{0.08} \quad (8-70A) \\ = 7.0 (37)^{0.14} (55)^{0.25} (2.07 \times 10^4)^{0.08} \\ = 7.0 (1.66) (2.72) (2.26) = 71\%$$

$$\begin{aligned}
 E_M &= 6.8 (N_{Re} N_{Sc})^{0.1} (N_{Dg} N_{Sc})^{0.115} & (8-70B) \\
 &= 6.8 [(2.07 \times 10^4) (35)]^{0.1} [(37) (55)]^{0.115} \\
 &= 6.8 (4.04) (2.40) = 66\%
 \end{aligned}$$

In this example, Equation 8-70B gives a more conservative design basis.

where A, B, C, E = constants in equation

- D = molecular diffusion coefficient, sq ft/hr
- E_M = Murphree vapor plate efficiency, %
- FA = fractional free area
- h_w = weir height, inches
- G = superficial mass vapor velocity based on the cross-sectional area of the column, lb/hr-sq ft
- M = molecular weight, lb/lb mole
- N = dimensionless number
- P = pressure, consistent units
- [P] = Sugden parachor
- sg = specific gravity
- T = temperature, °F
- U = superficial velocity, ft/hr
- V = molar volume, ft³/lb mole
- v = volume fraction
- x = mole fraction in the liquid
- y = mole fraction in the vapor
- μ = liquid viscosity, lb/hr-ft
- ρ = density, lb/ft³
- σ = surface tension, dynes/cm
- ψ = mixture parameter

Subscripts

- i = component
- L = liquid
- LK = liquid light key
- mix = binary mixture
- n = plate number
- t = total
- V = vapor

Biddulph [90] emphasizes the importance of using point efficiencies rather than tray efficiencies or overall column efficiencies, due to the wide fluctuations that often exist.

Kessler and Wankat [101] have examined several column performance parameters, and for O'Connell's [49] data presented in Figure 8-29 they propose equations that reportedly fit the data generally within about $\pm 10\%$ limits:

A. Distillation Trays

$$E_o = 0.54159 - 0.28531 \log_{10} \alpha \mu \quad (8-74)$$

B. Plate Absorbers (data fit $\pm 5\%$)

$$E_o = 0.37237 + 0.19339 \log_{10} (HP/\mu) + 0.024816 (\log_{10}(HP/\mu))^2 \quad (8-75)$$

- where E_o = overall efficiency
- H' = Henry's law constant, lb mole/(atm) (ft³)
- P = pressure, atmospheres
- α = relative volatility
- μ = viscosity, centipoise, cp

Gerster [176] presents the results of studies on the tray efficiencies of both tray and packing contacting devices. Note that Gerster compares his work to the AIChE Manual [2].

In terms of the change in gas composition [2]:

$$E_G = E_{OG} = \frac{y - y_{n+1}}{y^* - y_{n+1}} \quad (8-76)$$

- where E_G = overall column efficiency
- E_{OG} = overall point efficiency in vapor terms (see Ref. 2, page 38)
- y_{n+1} = component mol fraction in the gas to the point considered
- y = component mol fraction in the gas from the point considered
- y^* = composition the leaving gas would have if it left the point in equilibrium with the liquid

In Table 8-2 Proctor [178] compares efficiencies of sieve and bubble cap trays (plates). He concludes that the sieve design provides a 15% improvement in plate efficiencies. To fully evaluate the actual efficiencies in any particular system, the physical properties, mechanical details of the trays, and flow rates must be considered. See Reference 2 also.

Table 8-2
Comparative Efficiencies of Sieve and Bubble-Cap Trays/Plates [178]

Plate Type	Vapor Throughput, Lb Mole/Hr of Dry H ₂ S	Over-all Plate Efficiency, %	
		Cold Tower	Hot Tower
Sieve	18,200	69 \pm 5	75 \pm (8)*
Bubble-cap	16,200	60 \pm 5	69 \pm 5

*See the discussion of accuracy of the plate efficiency results in the text. Used by permission of the American Institute of Chemical Engineers; all rights reserved.

Strand [179] proposes a better agreement between experimental and predicted efficiencies when recognizing a liquid by-passing factor to correct predicted values determined by the AIChE method. The results suggest that for the representative systems studied recognition of a *liquid* by-passing factor for a tray can lower the AIChE method results by as much as 5 to 10% to be in better agreement with experimental results. A vapor by-passing effect was not required to correlate the data. Because the Murphree vapor efficiencies vary considerably for various systems, the data in Reference 179 can only be a guide for other systems not studied.

This suggests that caution must be exercised when establishing a tray efficiency for any type contacting device by (1) using actual test data if available for some similar system or (2) comparing several methods of predicting efficiency, and (3) possible use of a more conservative efficiency than calculated to avoid the possibility of ending up with a complete column with too few actual trays—a disastrous situation if not discovered prior to start-up operations.

Sakata [180] evaluates the degree of mixing of the liquid as it flows across a tray and its effect on the tray efficiency, Figure 8-30. For plug flow the liquid flows across the tray with no mixing, while for partial or “spot” mixing as it flows over the tray, an improved tray efficiency can be expected. For a completely mixed tray liquid, the point efficiency for a small element of the tray, E_{OG} , and tray efficiency, E_{MV} , are equal.

From Figure 8-31 the effect of mixed and unmixed “pools” of liquid can be noted. For a completely mixed tray, there is no concentration gradient from inlet to outlet, and therefore the entire tray has a uniform composition. The degree of mixing across the tray as determined by the number of discrete mixing pools on the tray has an effect on the relationship between E_{OG} and E_{MV} as a function of λ .

where $\lambda = mV/L$

m = slope of vapor-liquid equilibrium curve

V = vapor rate, lb mols/hr

L = liquid rate, lb mols/hr

Hughmark [181] has proposed empirical correlations for better fit of experimental data to transfer units and thus tray efficiency comparison with the AIChE method [2].

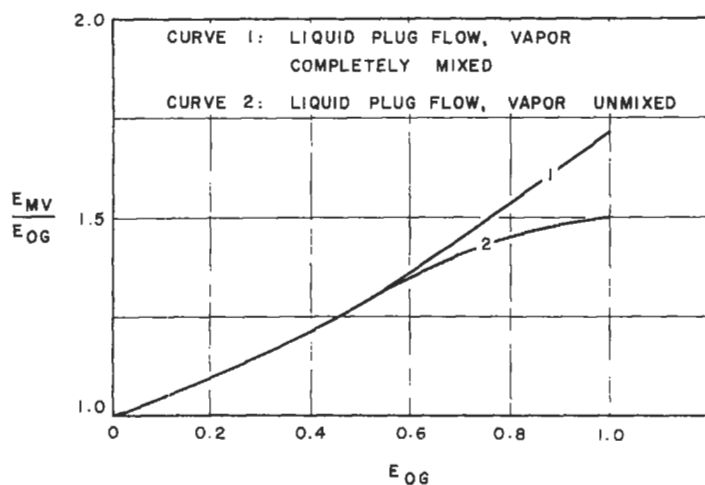


Figure 8-30. Effect of vapor mixing on tray efficiency. Reprinted by permission, Sakata, M., The American Institute of Chemical Engineers, *Chem. Eng. Prog.* V. 62, No. 11 (1966), p. 98, all rights reserved; reprinted by permission from Lewis, W. K., Jr., *Ind & Eng. Chem.* V. 28 (1936), and by special permission from Fractionation Research, Inc.

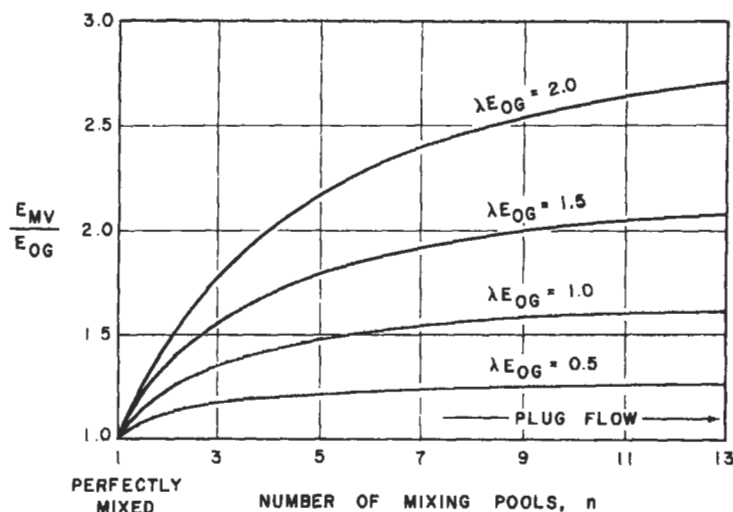


Figure 8-31. Typical effect of liquid mixing on tray efficiency. Reprinted by permission, Sakata, M., The American Institute of Chemical Engineers, *Chem. Eng. Prog.* V. 62., No. 11 (1966), p. 98, all rights reserved; reprinted by permission from Lewis, W. K., Jr., *Ind. & Eng. Chem.* V. 28. (1936), p. 399, and by special permission from Fractionation Research, Inc., all rights reserved.

Ryan et. al. [185] examined the prediction of misting and bubbling in towers, tray and packed, and assessed the impact.

Batch Distillation

Batch distillation [129, 130, 131, 133, 138, 140, 142, 170] as compared to continuous distillation is used for process requirements in which (1) feed composition may change from batch to batch; (2) batches are relatively small fixed volumes of a mixture wherein certain component(s) is/are to be separated into relatively pure components, leaving a heavier residue; (3) the process improvement requirement is on an irregular cycle; and (4) negligible holdup in the column (when used) and condenser relative to that in the receiver and kettle. The system operates on a fixed feed quantity, thereby yielding a fixed distillate and residue. See Figure 8-32. In the batch operation the vessel is charged with a fixed amount of liquid mixture that is to be separated by boiling in the charge vessel, allowing the vapors to rise either through an open, trayed column, or packed column contacting section above the “pot,” then condensing the vapors, and collecting the components according to their boiling points. Thus, the separation can be developed by the boilup to collect essentially only, or nearly only, the light boilers, then followed by the next higher boiling fraction and collecting it, etc., until the light ends and the heavies or residues are at the collection and concentration levels desired.

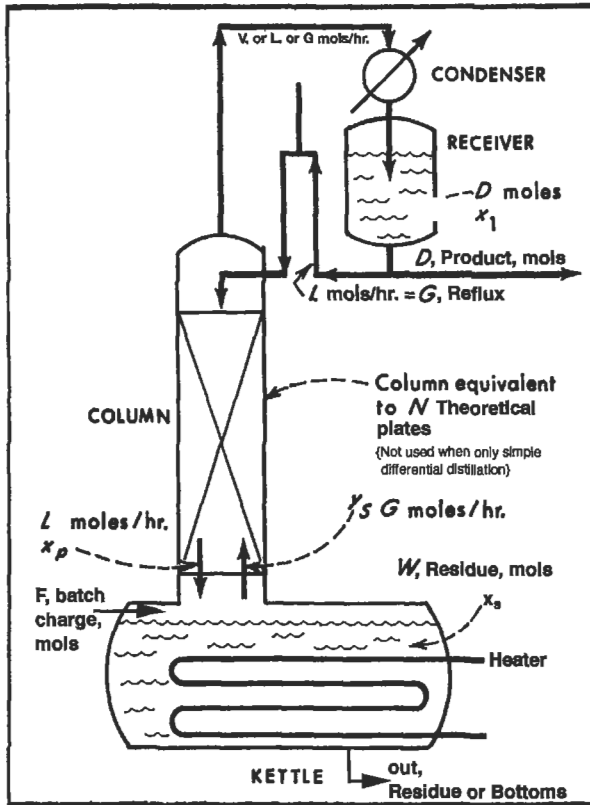


Figure 8-32. Batch operations: constant reflux ratio and variable overhead composition for fixed number of theoretical stages/trays. Used and modified by permission, Treyball, R. E., *Chem. Eng.* Oct. 5 (1970), p. 95.

Differential Distillation; Simple Batch, No Trays or Packing; Binary Mixtures, No Reflux

For systems of high (above approximately 3.0) constant relative volatility the Raleigh equation can be expressed:

$$\ln = \frac{B_{T1}}{B_{T0}} = \frac{1}{\alpha - 1} \ln \frac{(1 - x_0)x_1}{(1 - x_1)x_0} + \ln \frac{(1 - x_0)}{(1 - x_1)} \quad (8-77)$$

$$\text{or: } \ln \frac{B_{T1}}{B_{T0}} = \int_{x_0}^{x_1} \frac{dx}{y^* - x_1} \quad (8-78)$$

Equation requires graphical integration.

where B_{T0} = total moles liquid in bottom of still at start, T_0
 B_{T1} = total moles liquid in bottom of still at time, T_1
 x_0 = mol fraction of component, i , in bottoms B_{T0} at start, time T_0
 x_1 = mol fraction of component, i , bottoms B_T , at time, T

α = relative volatility of light to heavy components
 y^* = equilibrium value of x_i

The condensed vapor is removed as fast as it is formed.

The results of either relation allow the plotting of an instantaneous vapor composition for given percents of material taken overhead.

The outline of Teller [70, 133] suggests using the differential form above. Vapor is assumed to be in equilibrium with liquid.

1. Calculate or obtain an x - y equilibrium diagram for the light component.
2. Select values of x_i and read equilibrium values of y_i from Step 1 above.
3. Calculate values of $1/(y_i - x_i)$ and tabulate.
4. Plot curve of $1/(y_i - x_i)$ versus x_i ; see Figure 8-38, graphical integration by Simpson's rule.
5. From the plot of Step 4, determine the area under the curve from initial bottoms concentration of x_{i0} mol fraction at beginning of distillation down to the final lower concentration of x_{i1} in bottoms.
6. The area from Step 5 represents

$$\ln W/W_i \text{ or } \ln W_{i1}/W_{i0}, \text{ or } (B_{T0}/B_T)$$

where W_{i1} = the final kettle/still pot content, moles
 W_{i0} = the initial kettle/still pot content, moles

or, for constant relative volatility for a binary mixture for a simple still/kettle/bottoms pot with no internal packing or trays, a direct analytical solution is [133]:

$$\ln = \frac{W_1}{W_{i0}} = \frac{1}{\alpha - 1} \ln \left[\frac{x_w (1 - x_i)}{x_i (1 - x_w)} \right] + \ln \left[\frac{(1 - x_i)}{(1 - x_w)} \right] \quad (8-79)$$

where W_1 = content of kettle at any time, moles
 W_{i0} = initial content of kettle, moles
 W_0 = moles liquid initially in still or kettle
 α = relative volatility
 D = distillate rate, moles/hr
 L = liquid rate, moles/hr
 V = vapor rate, moles/hr
 x = mol fraction of a specific component in liquid
 y = mol fraction of a specific component in vapor
 θ = time, hours

Subscripts:

D = distillate related
 i , or o = initial
 1 = final or later
 w = relating to bottoms (kettle/still pot)

7. For each value of x , and the values of (B_{T0}/B_{T1}) found

above, calculate $\frac{B_{T0} - B_{T1}}{B_{T0}}$ (100), the percent of material taken overhead.

8. A plot of the distillate composition, y versus percent distilled (from Step 7) will show the value of the instantaneous vapor composition.

The usual Raleigh Equation form [130] is for the conditions of a binary simple differential distillation (no trays or packing), no reflux, but with constant boilup.

$$\ln \left(\frac{W_o}{W_i} \right) \int_{x_1}^{x_0} \frac{dx}{(y-x)} \quad (8-80)$$

For a binary mixture the values of x and y can be obtained from the equilibrium curve. Select values of x_1 and read the corresponding value of y from the equilibrium curve. Tabulate values of $1/(y-x)$, and plot versus x_1 , resulting in a graphical integration of the function $dx/(y-x)$ [130] between x_0 and x_1 . This system would have no column internals and no reflux.

Simple Batch Distillation: Constant α , with Trays or Packing, Constant Boilup, and with Reflux [129] Using x - y Diagram

The system material balance from Treybal [129] using a heated kettle and distillation column following a McCabe-Thiele diagram, using reflux, but having only a batch (kettle) charge:

$$F = D + W \quad (8-81)$$

$$Fx_F = Dx_D + Wx_W \quad (8-82)$$

$$D = F (x_F - x_W) / (x_D - x_W) \quad (8-83)$$

G = mol/hr boilup overhead

L = mols reflux in the column

D = overhead receiver contents, mols

Starting with an empty overhead receiver, the time θ_1 to condense D mols of vapor to fill the receiver, when the vapor boilup rate is G mols/hr.

$$\theta_1 = D/G$$

during which time the receiver is filling and there is no reflux and the kettle mixture follows a Raleigh distillation [129]. Under this condition, when the distillate receiver just becomes full, the composition of the kettle contents are x_{Si} , and [129],

$$\log \frac{Fx_F}{Wx_{Si}} = \alpha \log \left[\frac{F(1-x_F)}{W(1-x_{Si})} \right] \quad (8-84A)$$

$$\text{or, } \frac{(1-x_{Si})^\alpha}{x_{Si}} = \left(\frac{F}{W} \right)^{\alpha-1} \frac{(1-x_F)^\alpha}{x_F} \quad (8-84B)$$

Solve for x_{Si} by trial and error.

After this reflux runs down the column the desired lighter components leave, and a desired residual composition is left, following the Raleigh equation to express the material balance.

Most batch distillations/separations are assumed to follow the constant relative volatility vapor-liquid equilibrium curve of

$$y = \frac{\alpha x}{1 + x(\alpha - 1)} \quad (8-50)$$

After filling the receiver, reflux runs down the column at the same molar rate as the vapor back up ($L = G$). The operating line has a slope of 1.0. Then there are "n" plates/trays between composition x_p and x_1 (the mol fraction in distillate). As the distillation continues, the operating line moves closer to the 45° line of the diagram, and x_1 and x_p (and x_s) become richer and leaner, respectively, until at the end x_1 becomes x_D and x_s becomes x_w . The required time is θ_2 .

During a batch distillation at constant pressure, the temperature rises to accomplish the separation as the more volatile component's concentration is reduced in the bottoms (kettle) or residue.

For a batch differential distillation where no reflux is used, there is only boilup of a mixture of the desired lighter component, which leaves the kettle, and a desired residual bottoms composition is left in the kettle. This type of distillation follows the Raleigh equation to express the material balance. However, while simple, not having tower packing or trays or reflux does not offer many industrial applications due to the low purities and low yields involved. Repeated charges of the distillate back to the kettle and redistilling will improve overhead purity.

The minimum number of plates [129], for infinite time for separation:

$$N_{\min} + 1 = \frac{\log \left(\frac{x_D}{1-x_D} \right) \left(\frac{1-x_w}{x_w} \right)}{\log \alpha} \quad (8-85)$$

For operating line with slope of unity, from Smoker's equation:

$$N = \frac{\log \left\{ x_1' \left[1 - \frac{c(\alpha-1)x_p'}{\alpha-c^2} \right] / x_p' \left[1 - \frac{c(\alpha-1)x_1'}{\alpha-c^2} \right] \right\}}{\log (\alpha/c^2)} \quad (8-86)$$

Equilibrium curve:

$$y = \frac{\alpha x}{1 + (\alpha - 1)x} \quad (8-50)$$

Operating line: $y = x + b$ (see Reference 129 for diagram). They intersect at $x = k$.

$$\text{Then, } y = \frac{\alpha k}{1 + (\alpha - 1)k} = k + b, \text{ when } x = k \quad (8-87)$$

$$\text{where } b = (\alpha k/c) - k \\ c = 1 + (\alpha - 1)k$$

$$\text{Then, } x_p + b = \frac{\alpha x_s}{[1 + (\alpha - 1)x_s]}$$

Coordinates:

$$x_1' = x_1 - k$$

$$y' = y - (b + k)$$

$$x_p' = x_p - k$$

For the more volatile component at any time:

$$x_1 = (Fx_F - Wx_s)/D \quad (8-88)$$

$$b = y_s - x_p$$

$$\theta_2 = (W/G) \int_{x_w}^{x_{si}} (dx_s/b), \text{ time, hrs for refluxed distillation}$$

Fixed Number Theoretical Trays: Constant Reflux Ratio and Variable Overhead Compositions

Raleigh equation form [130]:

$$\ln(W_1/W_0) = \int_{x_{w0}}^{x_w} dx_w / (x_D - x_w) \quad (8-90)$$

where W_0 = mols liquid mixture originally charged to still
 W_1 = mols final content in still
 x_{w0} = Initial mol fraction of more volatile component in mixture
 x_w = composition of liquid in still, mol fraction
 x_i = mol fraction of component in liquid phase
 x = mol fraction of more volatile component in liquid
 x_D = instantaneous mol fraction of the component in the distillate that is leaving the condenser at time θ .
 x_{Di} = initial distillate composition, mol fraction
 x_i = mol fraction component in liquid phase
 y_i = mol fraction of component in the vapor phase
 D = mols of distillate per unit time, or mols of distillate at time θ , or distillate drawoff.
 K_A, K_B = equilibrium vaporization constants for A and B, respectively

L = mols of liquid per unit time, or liquid return to column

P = distillate drawoff percentage = $100/(R + 1)$

P_i = pure component vapor pressure, mm Hg

R = reflux ratio (liquid returned to column)/(distillate drawoff); subscripts indicate number of plates, R_{\min}

V = vapor rate up column, mols per unit time

θ = time

Batch with Constant Reflux Ratio, Fixed Number Theoretical Plates in Column, Overhead Composition Varies

At any time θ [131]:

$$\ln(W_1/W_0) = \ln \frac{S}{S_0} = \int_{x_{s0}}^{x_s} \frac{dx_s}{(x_D - x_s)} = \int_{x_{w0}}^{x_w} \frac{dx_w}{(x_D - x_w)} \quad (8-91)$$

where S_0 = mols originally charged to kettle

S = mols in mixture in still (kettle) at time θ

x_D = mol fraction of a more volatile component in the distillate entering the receiver at time θ

x_{s0} = mol fraction of a more volatile component in the initial kettle charge

x_s = mol fraction of a more volatile component in the kettle at time θ

D = mols of distillate at time θ

To solve the right side of the Raleigh-like equation, integrate graphically by plotting:

$1/(x_D - x_s)$ vs. x_s

The area under the curve between x_{s0} and x_s is the value of the integral. Plot the equilibrium curve for the more volatile component on $x - y$ diagram as shown in Figure 8-33. Then, select values of x_D from the operating line having the constant slope, L/V , from equation

$$L_{n+1} = L_n + D$$

are drawn from the intersection of x_D and the diagonal. Then from these L/V lines, draw steps to the equilibrium curve, the same for a binary McCabe-Thiele diagram [130]. The proper operating line is the one that requires the specified number of theoretical plates (stages) in moving stepwise down from the initial desired distillate composition to the composition of the mixture initially charged to the kettle (or pot or still). The kettle acts like and is counted as one theoretical stage or plate. The intersection of the last horizontal step (going down the column) from x_D with the equilibrium curve is the still or kettle bottoms composition, x_w , at the completion of this batch distillation. Using the system material balance and the constant reflux ratio used (L/V), calculate the total

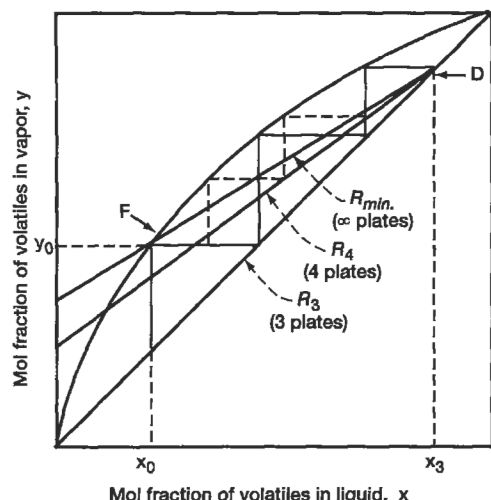


Figure 8-33. Variable reflux ratio at various theoretical plates to achieve a specified separation from x_0 kettle to x_3 distillate overhead. Note, all reflux ratios shown yield same separation, but with different numbers of theoretical plates/stages; D = Distillate; F = Kettle Conditions; x_0, y_0 at equilibrium. Used by permission, Ellerbee, R. W. *Chem. Eng.* May 28 (1973), p. 110.

thus a minimum reflux requirement. Minimum reflux is calculated [133]:

$$(L/V_{\min}) = (y_D - y_i)/(x_D - x_i); \text{ (see Figure 8-33)} \quad (8-92)$$

Note that $y_D = x_D$ on the diagonal of the equilibrium plot, and y_i and x_i are points of intersection with the equilibrium curve. For an abnormal equilibrium curve (as compared to regular or normal shape) see Figure 8-34.

Once a minimum reflux has been established (which is not an operating condition), then a realistic reflux ratio of from 1.5 to as much as 10 times the minimum can be selected. Of course, the larger the reflux value down the column the more vapor has to be boiled up, and the greater will be the required column diameter. So, some economic balance must be determined.

Solving the typical Raleigh equation:

$$\ln \frac{W_i}{W} = \int_{x_i}^{x_w} \frac{dx_w}{(x_D - x_w)} \quad (8-93)$$

The average distillate composition will be:

$$x_{D \text{ avg}} = \frac{W_i x_i - W x_w}{(W_i - W)}$$

vapor generated by the kettle. The heat duty of the kettle can be calculated using the appropriate latent and sensible heat of the mixture components.

For a constant reflux ratio, the value can be almost any ratio; however, this ratio affects the number of theoretical plates and, consequently, actual trays installed in the rectification section to achieve the desired separation. Control of batch distillation is examined in Reference 134.

The internal reflux ratio is L/V , and is the slope of the operating line. The external reflux is [133]:

$$R = L/D$$

$$\text{and } V = L + D$$

$$V/L = L/L + D/L = 1 + 1/R = (R + 1)/R$$

$$\text{Then } L/V = R/(R + 1)$$

$$\text{and, } R = (L/V)/[1 - (L/V)], \text{ see Figure 8-33.}$$

Point F on the figure represents conditions in the kettle or still with x_i, y_i , or x_0, y_0 . Line DF represents slope of the operating line at minimum reflux. The step-wise development from point D cannot cross the intersection, F, where the slope intersects the equilibrium line, and leads to an infinite condition, as point F is approached. Thus, an infinite number of theoretical trays/stages is required, and

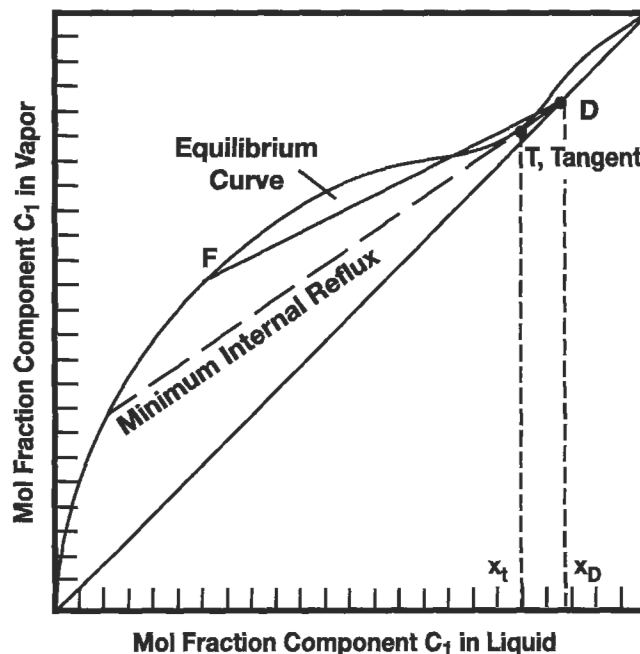


Figure 8-34. Minimum reflux for abnormal equilibrium curve for Batch Operation, constant reflux ratio.

A trial-and-error calculation is necessary to solve for W until a value is found from the $\ln W_i/W$ equation above that matches the $x_{D \text{ avg}}$ which represents the required overhead distillate composition. By material balance:

$$V = L + D, \text{ and } R = L/D$$

$$V/D = L/D + 1 = R + 1$$

$$D = V/(R + 1)$$

$$W = W_i - D\theta = W_i - V\theta/(R + 1) \quad (8-94)$$

$$e^Q = \frac{W_i}{W_i - \frac{V\theta}{R + 1}}$$

$$Q = \int_{x_i}^{x_w} \frac{dx_w}{(x_D - x_w)} \quad (8-95)$$

$$\theta = (R + 1) \left[\frac{W_i}{V} \left(\frac{e^Q - 1}{e^Q} \right) \right] \quad (8-96)$$

$$\theta = (W_i - W)/D = \frac{(R + 1)}{V} (W_i - W) \quad (8-97)$$

Referring to Figure 8-35 the constant internal reflux ratio, L/V is shown for several selected values of reflux ratios [131]. Only one at a time can be used for actual operation. Starting at the intersection of the diagonal line (distillate composition), step off the theoretical plates. For example, from Figure 8-35 at constant reflux, using operating line No. 1, starting at $x_D = 0.95$, for one theoretical plate, the bottoms composition in component A would be approximately $x_W = 0.885$; then going down one more plate at the same L/V , a second theoretical plate yields a bottoms of x_B or $x_W = 0.83$, still yielding $x_D = 0.95$. If the L/V for the operating line No. 4 is used (same slope as line No. 1), then the expected performance would be $x_D = 0.60$, and after one theoretical plate, the bottoms would be 0.41 at the same reflux ratio as the first case; and for $x_D = 0.60$ and two theoretical plates, $x_W = 0.31$.

where D = relates to distillate

i = relates to initial condition

W = relates to bottom or pot liquors

Batch with Variable Reflux Rate Rectification with Fixed Number Theoretical Plates in Column, Constant Overhead Composition

Overall material balance at time θ [130, 131]:

$$S = S_o \left(\frac{x_D - x_{so}}{x_D - x_s} \right) \quad (8-98)$$

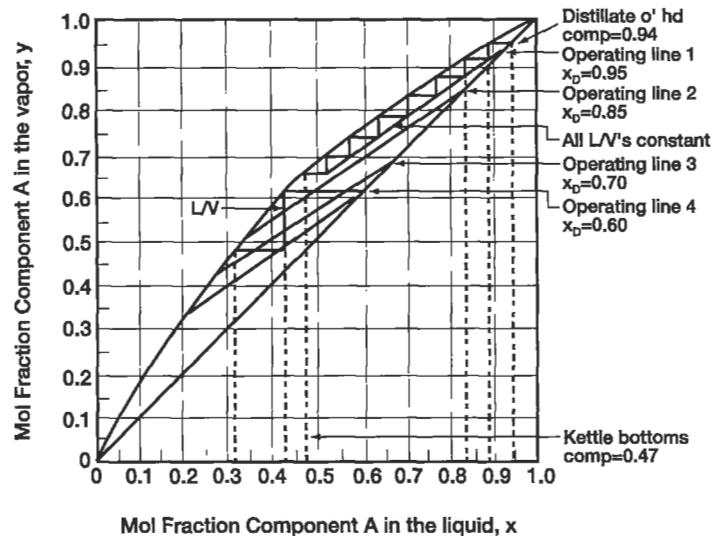


Figure 8-35. Batch distillation: constant reflux ratio after McCabe-Thiele diagram. Revised/adapted and used by permission, Schweitzer, P.A. *Handbook of Separation Techniques for Chemical Engineers*, McGraw-Hill Book Co. (1979); also reprinted by special permission, *Chem. Eng. Jan. 23 (1961)*, p. 134., © 1961 by McGraw-Hill, Inc., New York.

$$W = W_o \left(\frac{x_D - x_{wo}}{x_D - x_w} \right) \quad (8-99)$$

where W = mols in still/bottoms at any time

W_o = mols in still/bottoms at initial charge time

This mode of batch rectification requires the continuous adjustment of the reflux to the column in order to achieve a steady overhead distillate composition. Starting with a kettle obviously rich in the more volatile component, a relatively low reflux ratio will be required to achieve the specified overhead distillate composition. With time, the reflux ratio must be continuously increased to maintain a fixed overhead composition. Ultimately, a practical maximum reflux is reached and the operation normally would be stopped to avoid distillate contamination.

At constant molal overflow: The time required for the distillation only,

$$\theta = [W_o (x_D - x_w)/V] \int_{x_w}^{x_{wo}} \frac{dx_w}{\left(1 - \frac{L}{V}\right) (x_D - x_w)^2} \quad (8-100)$$

does not include charging the kettle, shutdown, cleaning, etc.

To determine the column (with trays) diameter, an approach [130] is to (1) assume θ hours; (2) solve for V , lb/hr vapor up the column at selected, calculated, or assumed temperature and pressure; (3) calculate column diameter using an assumed reasonable vapor velocity for the type of column internals (see section in this volume on "Mechanical Designs for Tray Performance").

Solve for the value of θ by graphically or otherwise plotting

$$1/[1 - (L/V)] (x_D - x_W)^2$$

versus x_W and determining the area under the curve between x_{W0} and x_W . Then substitute this value for the integral in the Equation 8-100 and solve for θ .

Figure 8-36 illustrates the variable reflux batch process with operating lines with different L/V slopes all passing through x_{Di} (distillate desired overhead composition for i). Establish the McCabe-Thiele-like steps down each operating line until the last horizontal step or stage intersecting the equilibrium line indicates the accepted bottoms composition, x_{Wi} . This must be done before the integral of the previous equation can be determined, because x_{Wi} is determined in this manner.

Using Figure 8-33 the separation from x_o , initial kettle volatile material to x_3 as the distillate of more volatile overhead requires three theoretical plates/stages at total reflux. Using finite reflux R_4 , and four theoretical plates the same separation can be achieved with infinite theoretical plates and the minimum reflux ratio, R_{min} . The values of reflux ratio, R , can be determined from the graph with the operating line equation as,

$$y \text{ (intercept)} = x_D / (R + 1)$$

where x_D = concentration of volatiles in the overhead distillate, mol fraction

R = reflux ratio (L/D), where L is the liquid returned as reflux to the column

D = quantity of liquid distillate withdrawn (see Figure 8-32)

The distillate percentage drawoff, P ,

$$P = 100 / (R + 1), \%$$

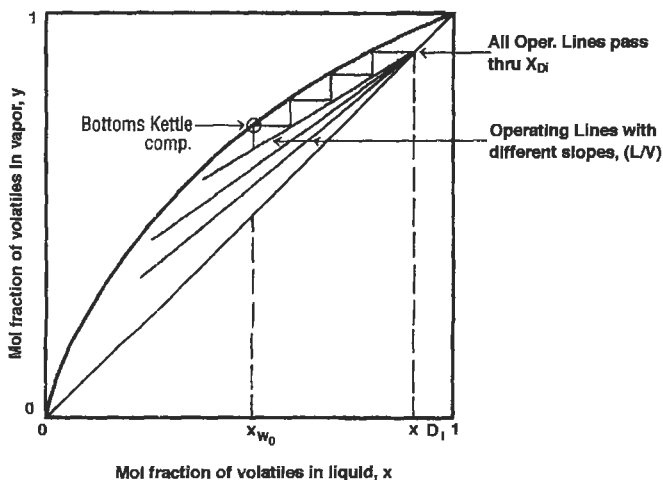


Figure 8-36. Variable-reflux batch process solution. Modified and used by permission, Ellerbee, R. W., *Chem. Eng.*, May 28 (1973), p. 110.

$$P = 100 (y/D_D), \%$$

The values of overhead composition can be varied from x_3 of Figure 8-33 to other values as the drawoff percentage changes. As the drawoff percentage decreases, the distillate specification can be better maintained as the distillation operation continues for a fixed number of plates. For further discussion see References 129, 130, 131, 133.

Example 8-14: Batch Distillation, Constant Reflux; Following the Procedure of Block [133]

Purify a mixture of ethanol and water; 11,500 lb

	<u>Lb</u>	<u>Mols</u>	<u>Mol Fraction</u>
Feed to kettle:			
ethanol, 35 wt%	4,025	95.42	0.187
water, 65 wt %	<u>7,475</u>	<u>415.27</u>	<u>0.803</u>
Totals	11,500	510.69	1.000

Overhead distillate product desired: 91.5 wt% ethanol.

Kettle bottoms residue: Not specified, as results from separation.

Vaporization rate: Assume 72 mols/hr

Average mol. weight of feed: = 11,500/510.69 = 22.51

Overhead Product:

	<u>Weight %</u>	<u>Lb</u>	<u>Mols</u>	<u>Mol Fraction</u>
Ethanol	91.5	91.5	1.99	0.808
Water	<u>8.5</u>	<u>8.5</u>	<u>0.472</u>	<u>0.192</u>
	100.0	100.0	2.465	1.000

Select L/V (internal reflux) = 0.75

Then: $L/V = R / (R + 1) = 0.7875 = R / (R + 1)$, see below;

$R = 3.705$ (external reflux, L/D)

Because $V = L + D$

$$72 \text{ mols/hr} = (0.7875 V) + D$$

Use the ethanol curve similar to Figure 8-37, or refer to the data of Reference 133; the point of tangency of the line from the distillate composition of the diagonal is $x_D = 0.80$ and $y_v = 0.80$. Thus the minimum internal reflux is set by this tangent line:

$$L/V = \frac{y_D - y_T}{x_D - x_T} = \frac{0.80 - 0.695}{0.80 - 0.60} = 0.525$$

For practical design, select $L/V = (1.5) (0.525) = 0.7875$.

Select L/V internal reflux lines and add to the equilibrium plot, similar to that shown for a "normal" curve of Figure 8-35, but unlike the abnormal ethanol curve shown.

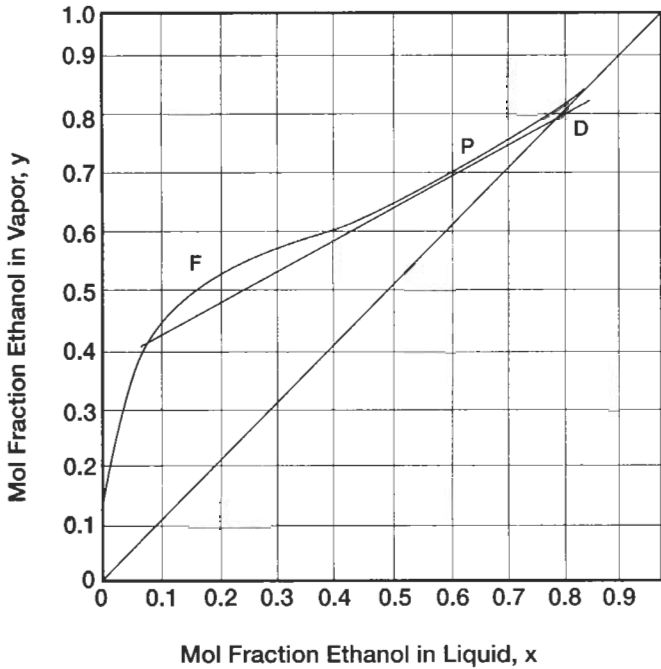


Figure 8-37. x-y diagram for ethanol-water mixture, showing minimum reflux. Used by permission, Block, B. *Chem. Eng.* Feb. 6 (1961), p. 87.

Tabulate:

Select x_D	x_W	$(x_D - x_W)$	$1/(x_D - x_W)$
0.808			
0.770			
0.750	read, 0.085	0.665	1.5037

For a plot of $x_D = 0.750$, slope = 0.7875, read x_W at the equilibrium line for each theoretical tray and plot similar to Figure 8-38. Then determine the area under the curve between the selected x_W and the product x_D . Then:

$$\ln W_i / W = \int_{x_i}^{x_w} \frac{dx_w}{(x_D - x_w)} = \text{area under the curve} \quad (8-100A)$$

For this example, $\ln (W_i/W) =$ approximately 0.210
Then, $W_i/W = 1.2336$

$$W = \frac{510.69}{1.2336} = 413.98 \text{ mols bottoms for } x_W = 0.085$$

$$\begin{aligned} \text{Average overhead composition, } x_{D \text{ avg}} &= \frac{W_i x_i - W x_W}{W_i - W} \\ &= \frac{[(510.69)(0.187) - (413.98)(0.085)]}{(510.69 - 413.98)} \end{aligned}$$

$$x_{D \text{ avg}} = 0.6236$$

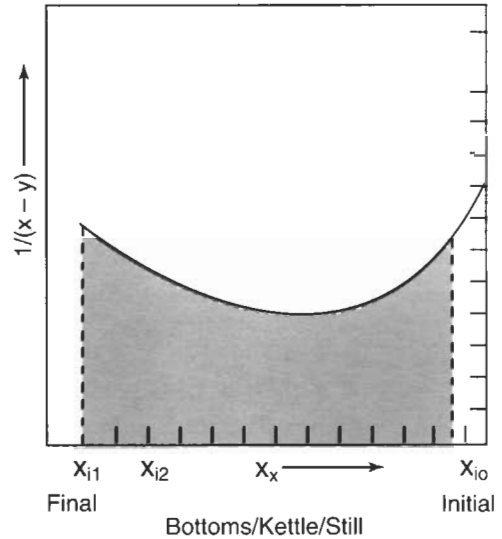


Figure 8-38. Graphical integration of Rayleigh or similar equation by Simpson's Rule, for Example 8-14.

Time required for distillation only (not set up, draining, cleaning, etc.):

$$\theta = (R + 1) [W_i/V] [(e^Q - 1)/e^Q]$$

$$Q = \int_{x_i}^{x_w} \frac{dx_w}{x_D - x_w} = \ln \frac{W_i}{W} \quad (\text{see right side of Equation 8-100A})$$

$$\theta = (3.705 + 1) \frac{(510.69) (e^{0.210} - 1)}{[72 (e^{0.210})]} = 6.32 \text{ hours}$$

$$\text{Distillation rate} = \frac{W_i - W_w}{\theta} = \frac{510.69 - 413.98}{6.32} = 15.30 \text{ mols/hr}$$

Checking:

$$\theta = (R + 1) (W_i - W) / V$$

$$\theta = (3.705 + 1) (510.69 - 413.98) / 72$$

$$\theta = 6.31 \text{ hours}$$

where D = distillate rate, moles/hr

L = liquid flow, moles/hr

V = vapor rate, moles/hr

\bar{V} = quantity of vapor, moles

W = contents of still pot, moles

x = mole fraction of substance in liquid

y = mole fraction of substance in vapor

a = relative volatility

θ = time, hr

Subscripts

D = relating to distillate

i = initial

w = relating to pot liquors

Example 8-15: Batch Distillation, Vapor Boil-up Rate for Fixed Trays (used by permission of Treybal [129]; clarification added by this author)

Distill a small quantity each day to obtain relatively pure o-xylene from a mixture of ortho and para xylene, having boiling points of 142.7°C and 138.4°C, respectively. The feed is 15 lb-mols (about 225 gallons) per batch, at 0.20 mol fraction para. The desired residue product is 0.020 in the kettle, while the distillate is to be 0.400 mol fraction para. A distillation column equivalent to 50 theoretical plate is to be used.

The time requirement is to complete the distillation/recovery in six hours, allowing an extra two hours for charging, emptying, and cleaning. What is the constant rate that the distillation must be carried out?

$$F = 15 \text{ lb-mols/hr}$$

$$x_f = 0.20$$

$$x_D = 0.400$$

$$x_w = 0.02$$

The material balance:

$$D = F(x_f - x_w)/(x_D - x_w)$$

$$D = 15(0.2 - 0.02)/(0.400 - 0.020) = 7.105 \text{ mols}$$

$$\text{Then, } F = D - W$$

$$W = 15 - 7.105 = 7.895 \text{ mols}$$

$$\theta_1 = D/G$$

$$\text{and, } \theta = 7.105/G$$

$$\frac{(1 - x_{si})^\alpha}{x_{si}} = \left(\frac{F}{W}\right)^{\alpha-1} \frac{(1 - x_f)^\alpha}{x_f}$$

$$\frac{(1 - 0.18530)^{1.152}}{0.18530} = \left(\frac{15}{7.895}\right)^{1.152-1} \frac{(1 - 0.2)^{1.152}}{0.2}$$

$$4.26 = 4.26$$

At 138.4°C, the vapor pressures of ortho and para are 660 and 760 mm Hg, respectively. Because Raoult's law applies:

$$\alpha = 760/660 = 1.152$$

Solving the equation by trial and error shows that $x_{si} = 0.18530$. Solving for the minimum number of plates required:

$$N_{\min} + 1 = \frac{\log\left(\frac{x_D}{1-x_D}\right)\left(\frac{1-x_W}{x_W}\right)}{\log \alpha}$$

$$N_{\min} + 1 = \frac{\log\left(\frac{0.40}{1-0.40}\right)\left(\frac{1-0.02}{0.02}\right)}{\log 1.152}$$

$$N_{\min} + 1 = \frac{1.514}{0.06145} = 24.6$$

$$N_{\min} \text{ (in column)} + 1 \text{ (kettle)} = 24.6$$

The results indicate that 25 theoretical plates are minimum; then by assuming an efficiency of 50%, total actual trays of 50 should be adequate. Choose values of k (see nomenclature) and solve for b and x_s by:

$$b = (\alpha k/c) - k$$

$$c = 1 + (\alpha - 1)k$$

$$Ax_s^2 + Bx_s + C = 0$$

The tabulated results are:

k	b	x_s
0.0200	0.00297	0.01899
0.0500	0.00716	0.04842
0.0750	0.01043	0.07301
0.1000	0.01347	0.09728
0.1250	0.01631	0.12109
0.1500	0.01895	0.14470
0.1750	0.02137	0.17145
0.2000	0.02360	0.18133

Graphical integration shows the area under the curve, Figure 8-38A, to be 15.764. Applying this to:

$$\theta_2 = (W/G) \int_{x_W}^{x_{si}} (dx_s/b)$$

$$\text{Then, } \theta_2 = 7.895(15.764)/G = 124.46/G$$

$$\theta_1 + \theta_2 = 6 \text{ hr} = 7.105/G + 124.46/G$$

$$G = 21.93 \text{ lb-mols vapor/hr}$$

This is the boilup rate, which is approximately 3.3 ft³ vapor/sec. An approximately 1 ft 0 in. diameter column can handle this rate; however, because it is in the usual size for a packed tower (or cartridge trays), the diameter must be checked using the packed tower calculations in Chapter 9 of this volume.

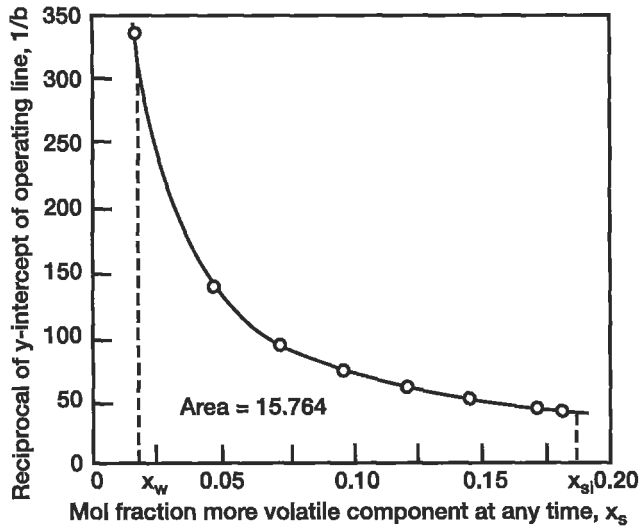


Figure 8-38A. Graphical integration for boil-up rate of batch distillation for Example 8-15. Used by permission, Treybal, R. E., *Chem. Eng. Oct. 5 (1970), p. 95.*

where A, B, C, E, H, J, K = constants developed in article [129]

b = y-intercept of operating line

c = constant

D = distillate, lb-moles

F = charge to batch distillation, lb-moles

G = vapor boilup rate, lb-moles/hr

k = value of x at intersection of operating line and equilibrium curve

L = liquid reflux rate, lb-moles/hr

N = number of ideal plates in column

N_{\min} = minimum value of N

W = residue, lb-moles

x = mole fraction more volatile component in liquid

x_D = mole fraction more volatile component in final distillate

x_f = mole fraction more volatile component in feed

x_p = mole fraction more volatile component in liquid leaving column at any time

x_s = mole fraction more volatile component in kettle at any time

x_{si} = value of x_s when distillate receiver is first filled

x_W = mole fraction more volatile component in final residue

x_1 = mole fraction more volatile component in distillate at any time

y = mole fraction more volatile component in vapor

y_s = mole fraction more volatile component in vapor entering column at any time

α = relative volatility

θ_1 = time for filling distillate receiver, hr

θ_2 = time for refluxed distillation, hr

Example 8-16: Binary Batch Differential Distillation

Dimethyl ether is to be separated from methanol. A batch type operation is to be tried to see if an existing coil-in-tank can be used. The pressure of the system will be about 55 psia. How many total mols will remain in the bottoms when the bottoms liquid composition contains 0.5 mol percent dimethyl ether? What is the composition of the total overhead collected?

Component	Initial Charge		At 104°F		
	Mols	Mol Fraction	Vap. Press. psia	$K = P/x$	$y^* = Kx$
Dimethyl ether	61	0.427	125.0	2.27	0.97
Methanol	82	0.573	5.1	0.093	0.05
	143	1.000			$\Sigma = 1.02$

Initial boiling point of mixture = 104°F.

$$\ln \frac{B_{T1}}{B_{T0}} = \frac{1}{\alpha - 1} \ln \frac{(1 - x_0)x_1}{(1 - x_1)(x_0)} + \ln \frac{(1 - x_0)}{(1 - x_1)} \quad (8-101)$$

$$B_{T0} = 143 \text{ mols}$$

$$x_0 = 0.427$$

$$x_1 = 0.005$$

$$\alpha = 125/5.1 = 24.5$$

$$\ln \frac{B_{T1}}{143} = \frac{1}{24.5 - 1} \ln \frac{(1 - 0.427)(0.005)}{(1 - .005)(.427)} + \ln \frac{(1 - 0.427)}{(1 - 0.005)}$$

$$= 0.0426 \ln \frac{.00286}{.425} + \ln \frac{0.573}{0.995}$$

$$= 0.0426 \ln 148.5 - \ln 1.73$$

$$= 0.0426 (\ln 1.485 + \ln 100) - \ln 1.73$$

$$= -0.0426 (0.395 + 4.605) - 0.548$$

$$\ln \frac{B_{T1}}{143} = -0.761$$

$$\ln \frac{143}{B_{T1}} = 0.761$$

$B_{T1} = 143/2.14 = 67$ mols remaining in bottom when dimethyl ether is 0.5 mol %.

Total vapor collected overhead = $143 - 67 = 76$ mols

Mols dimethyl ether in bottoms = $0.005 (67) = 0.335$

Mols dimethyl ether overhead = 76 - 0.335 = 75.665

Composition of total overhead collected:

$$\text{Dimethyl ether} = \frac{75.665}{76.0} (100) = 99.6\%$$

Methanol = 100.0 - 99.6 = 0.4%

Differential Distillation—Simple Batch, Without Trays, Multicomponent Mixture

For multicomponent systems, the relation of the system can be expressed using the relative volatility:

$$B_i = B_{i0} \left(\frac{B_b}{B_{b0}} \right)^{\alpha_i} \quad (8-102)$$

where B_i = mols of component, i, after a given time of distillation

B_{i0} = mols of component, i, at start of distillation

B_b = mols of component, b, used as reference for volatility after a given time of distillation

B_{b0} = mols of component, b, used as reference for volatility, at start of distillation.

Knowing the amount of components present at the beginning, the quantity remaining after the distillation can be calculated.

Example 8-17: Multicomponent Batch Distillation

A mixture of hydrocarbons at 80 psia is to be differentially distilled until the mols of propane is reduced to 10 mols per 100 mols of bottom feed material. A kettle with bottom coil is to be used, and no trays.

Material in kettle at start of distillation:

Component	Mol Fraction
C ₂ H ₆	0.10
C ₃ H ₈	0.25
N-C ₄ H ₁₀	0.35
i-C ₄ H ₁₀	<u>0.30</u>
	1.00

Basis: 100 mols of bottoms feed

Bubble Point of Initial Charge

Component	x _i Mol. @ 50°F		Assumed α _i 50°				
	Fract	K _i	y = k _x	105°, K _i	K _i /K _p	α 105° K _i /K _p	α Avg
C ₂ H ₆	0.10	4.5	0.45	7.2	3.81	3.28	3.54
C ₃ H ₈	0.25	1.18	0.295	2.2	1.0	1.0	1.0
n-C ₄ H ₁₀	0.35	0.33	0.115	0.75	0.28	0.341	0.310
i-C ₄ H ₁₀	<u>0.30</u>	0.48	<u>0.144</u>	1.0	0.407	0.454	0.430
		1.00	1.004				
			O.K.				

Note: K values at 80 psia from *Natural Gasoline Supply Man's Assoc. Data Book* [48].

Propane is reference material.

$$\alpha_{i,50^\circ} = \frac{K_i}{K_{\text{propane}}} = \frac{4.5}{1.18} = 3.81$$

$$\alpha_{i,105^\circ} = \frac{K_i}{K_{\text{propane}}} = \frac{7.2}{2.2} = 3.28$$

$$B(\text{Total}) = \Sigma B_i = \Sigma B_{i0} \left(\frac{B_b}{B_{b0}} \right)^{\alpha_i}$$

$$B(\text{ethane}) = (10) \left(\frac{10}{25} \right)^{3.54} = \frac{10}{25.6} = 0.39 \text{ mols in bottoms}$$

Component	B _i	Final Bottoms x _i	Vapor	
			Press. at 105°, P _i	p _i = P _i x _i
C ₂ H ₆	0.39	0.00686	840 psia	5.75
C ₃ H ₈	10.00	0.176	200	35.2
n-C ₄ H ₁₀	26.30	0.463	57	26.4
i-C ₄ H ₁₀	20.20	0.355	78	27.6
	56.89	1.000		94.9

(Too high, assume lower temperature and re-calculate)

$$x_i = 0.39/56.89 = 0.00686$$

Vapor pressure from N.K. Rector chart in Reference 48.

Second Try

Component	Initial x _i	α _i 50°	Assume 95°, K _i	α95° K _i /K _p	α Avg.
C ₂ H ₆	0.10	3.81	6.7	3.35	3.58
C ₃ H ₈	0.25	1.0	2.0	1.0	1.0
n-C ₄ H ₁₀	0.35	0.28	0.67	0.335	0.307
i-C ₄ H ₁₀	0.30	0.407	0.92	0.46	0.432

Component	Final B _i	Vapor Press. @95°F _i	Final x _i	Σp _i = P _i x _i
C ₂ H ₆	0.378	750	0.0066	4.8
C ₃ H ₈	10.0	174	0.175	30.4
n-C ₄ H ₁₀	26.4	47	0.464	21.8
i-C ₄ H ₁₀	<u>20.2</u>	67	0.354	<u>23.7</u>
	56.97			80.7
				psia

Therefore the final temperature should be close to 95°F, because 80.7 psia compares satisfactorily with the operating pressure of 80 psia.

Total mols of bottoms remaining at end: 56.9 mols liquid

Total mols vaporized = 100 - 56.9 = 43.1

Liquid composition mol fraction is given in column "Final x_i," and corresponds to the actual mols B_i, noting that there are the required 10 mols of propane in the bottoms under these conditions.

Batch Distillation With Fractionation Trays—Constant Overhead Product Composition, Multicomponent and Binary

The method of Bogart [4] is useful in this case. The basic relation is:

$$\theta = \frac{B_{T0} (x_{iD} - x_{iB})}{V} \int_{x_{iB}}^{x_{iF}} \frac{dx}{(1 - L/V) (x_{iD} - x_{iB})^2} \quad (8-103)$$

Application may be (1) to determine a column diameter and number of plates or (2) to take an existing column and assume an operating reflux for the fixed trays and determine the time to separate a desired cut or product.

where θ = time from start when given L/V will produce constant overhead composition, x_{iD}
 B_{T0} = mols total batch charge to still
 V = total mols per hour vapor overhead
 x_{iD} = mol fraction light key component in overhead product
 x_{iB} = mol fraction light key component in original charge

Suggested procedure for situation (2) above: using existing column

1. Calculate minimum number of plates and minimum reflux ratio
 - (a) For multicomponent mixture, select key components, light and heavy

- (b) Calculate relative volatility, α_i , referenced to heavy key component, at top and bottom temperatures, and determine geometric average α .
- (c) Calculate minimum theoretical plates at total reflux by Fenske's equation (8-32).
- (d) Use Gilliland correlation to determine actual reflux ratio, using an *estimated* number of actual plates, and a minimum reflux ratio from:

$$(L/D)_{\min} = \left(\frac{1}{\alpha - 1} \right) \left[\left(\frac{x_{iD}}{x_{iB}} \right) - \alpha \left(\frac{x_{hD}}{x_{hB}} \right) \right]$$

- (e) Calculate:

$$\text{Internal } (L/V) = \frac{L/D}{L/D + 1}$$

2. Set up table: Keep x_{iD} values constant

*Assumed "x ₁ " values	(L/V)	(1 - L/V)	(x _{iD} - x ₁ *)	A	B
x (Bottoms)	•	•	•	•	•
x ₂	•	•	•	•	•
x ₃	•	•	•	•	•
:	•	•	•	•	•
x (Feed)	•	•	•	•	•

$$A = (1 - L/V) (x_{iD} - x_1^*)^2$$

$$B = \frac{1}{(1 - L/V) (x_{iD} - x_1^*)^2}$$

*Assume "x₁" values of bottoms compositions of light key for approximate equal increments from final bottoms to initial feed charge. Calculate L/V values corresponding to the assumed "x₁" values by inserting the various "x₁" values in the Fenske equation for minimum reflux ratio of 1-(d). The "x₁" values replace the x_{iB} of this relation as the various assumptions are calculated. The actual (L/D) are calculated as in 1-(d) keeping the minimum number of trays constant. Complete the table values.

3. Plot $\frac{1}{(1 - L/V) (x_{iD} - x_1^*)^2}$ vs (x₁)*

The total area, ΣA, under the curve may be obtained in several ways; the rectangular or trapezoidal rules are generally quite satisfactory. The area concerned is between the original feed and the final bottoms composition for the particular component.

4. Time required for a batch

$$\theta = B_{T0} \frac{(x_{iD} - x_{iB})}{V} (\Sigma A) \quad (8-104)$$

V is an assumed or known value, based on reboiler capacity.

5. Plot of reflux quantity versus time.

From the L/D values of 1-(e), knowing the L/V, using V assumed as constant, calculate the necessary reflux fluid, L. Figure 8-39 indicates a plot of time to produce a constant product composition and the necessary external reflux returned to the tower.

The batch distillation of a binary is somewhat simplified, as L/V values can be assumed, and since there is only enrichment of the overhead involved, only one operating line is used per operating condition. Theoretical trays can be stepped off and x_{iB} values read to correspond. The plots involved are the same as previously described.

Steam Distillation

Live steam is in direct contact with fluids being distilled, either batch or continuous. Often, this process is called open steam distillation.

Ellerbe [127, 128] provides an excellent summary of steam distillation basics. The theory of *direct* steam distillation evolves around the partial pressures of the immiscible organics/petroleum/petroleum component and the presence of direct open steam in the system. The system may consist of the organic immiscible plus steam (vapor and/or liquid). Each liquid exerts its own vapor pressure independent of the other. Thus, the total pressure of the system is the *sum* of the individual vapor pressures of the two liquids (assuming the liquids do not dissolve in each other). An important use of this approach is to separate a volatile organic from non-organic impurities.

At constant temperature, the partial pressure for each component and the composition of the vapor phase are

independent of the mols of liquid water or organic compound present. For example, for a system held at 800 mm Hg, the mixture could boil at, say, 250°F, and both liquids present would boil over together. Should one evaporate (boiling away before the other), the system vapor pressure then would fall to the temperature corresponding to the remaining material.

For a system such as discussed here, the Gibb's Phase Rule [59] applies and establishes the "degrees of freedom" for control and operation of the system at equilibrium. The number of independent variables that can be defined for a system are:

$$\phi + F = C + 2 \tag{8-105}$$

- where ϕ = number of phases present
- F = degrees of freedom
- C = number of components present

For example, for steam (saturated vapor, no liquid) distillation with one organic compound (liquid), there are two phases, two components, and two degrees of freedom. These degrees of freedom that can be set for the system could be: (1) temperature and (2) pressure; or (1) temperature and/or (2) concentration of the system components, or either (1) pressure and (2) concentration. In steam distillation steam may be developed from water present, so there would be both a liquid water and a vapor phase water (steam) present. For such a case, the degrees of freedom are $F = 2 + 2 - 3 = 1$.

The basis laws of operation involve the partial pressures of the components as discussed earlier.

For batch steam distillation: stripping [127, 128]

$$y_s = p_s/\pi \tag{8-106}$$

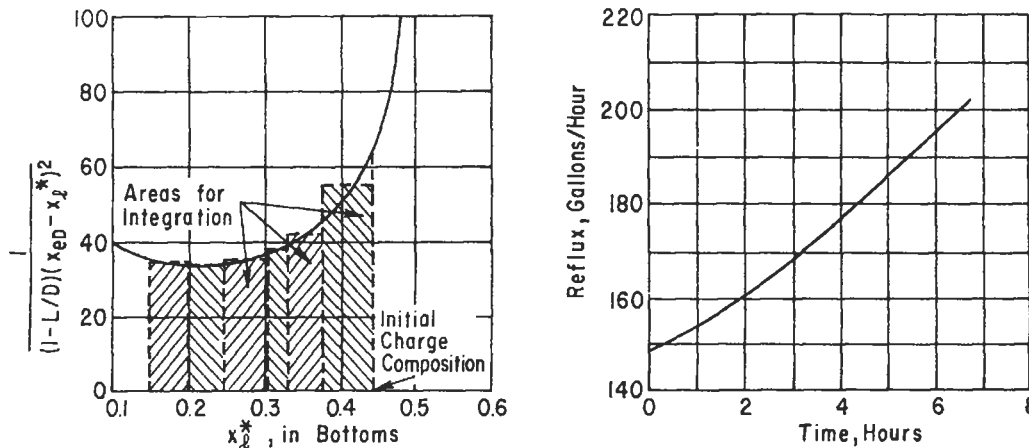


Figure 8-39. Batch distillation with trays; constant overhead product.

π = total system pressure (also see Equation 8-3)

$$y_{im} = p_{im}/\pi$$

The steam required for the distillation is

$$\pi = p_s + p_{im} \quad (8-107)$$

(also see Equation 8-4)

$$y_s = \frac{\pi - p_{im}}{\pi}$$

The steam required per mol of immiscible liquid vaporized is

$$\frac{y_s}{y_{im}} = \frac{\pi - p_{im}}{p_{im}} = \frac{p_s}{p_{im}} \quad (8-107A)$$

$$N_s = N_{im} (\pi - p_{im})/p_i$$

When the sum of the partial pressures of the steam and the material distilled reach the system pressure, boiling begins and both components go overhead in the mol ratio of their partial pressures. Upon condensation of the overhead mixture, the condensate receiver will contain two layers that can be separated by gravity.

The weight ratio of steam to the immiscible liquid in the vapor is

$$\frac{W_s}{W_{im}} = (p_s M_s)/(p_{im} M_{im}) \quad (8-108)$$

Any non-volatile material in the mixture will be left in the still bottoms.

The Hausbrand vapor-pressure diagram [127, 128] in Figure 8-40 is a useful approach for the steam distillation calculation. This particular diagram was prepared for six organic compounds and the corresponding water vapor pressure as $(\pi - p_s)$ for three system pressures of 760, 300, and 70 mm Hg versus temperature,

where M = molecular weight of material

p = partial pressure, mm Hg

W = weight of material in vapor

N = number of mols

N_o = number of mols of non-volatile material present

y = mol fraction of material in vapor

π = system pressure, mm Hg

p_{im} = pure component vapor pressure of the immiscible liquid being distilled

Subscripts:

im = immiscible liquid

s = steam

1 = initial

2 = remaining

The water curve intersects the particular organic compound and at that point the temperature is the one at which the steam distillation can take place, because the partial pressures are additive at this point. For example,

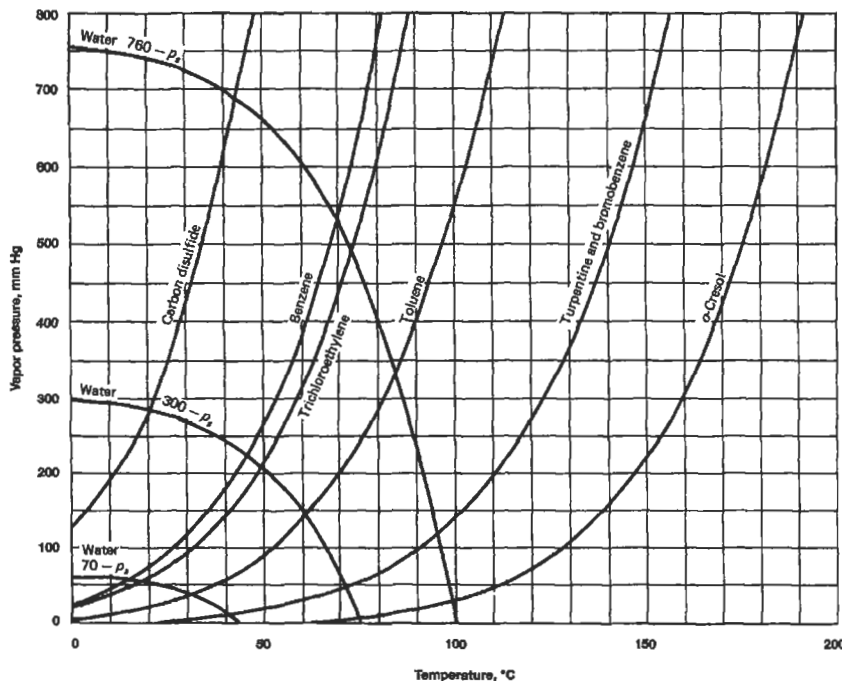


Figure 8-40. Hausbrand vapor-pressure diagram for various liquids and at three system steam pressures. A similar diagram can be constructed for other organic/hydrocarbon systems. Used by permission, Ellerbee, R. W., *Chem. Eng.* Mar. 4 (1974), p. 108.

for 300 mm Hg total pressure system, reading the intersection point for benzene and steam at 46°C, gives 220 mm Hg for benzene and (300 - 220) or 80 mm Hg. Then the mol ratio of benzene to water vapor 220/80 = 2.75; or 2.75 parts of benzene to 1 part of water.

When the composition of the compounds in the still or bottoms changes significantly as the batch distillation progresses, an unsteady state condition will exist as for differential distillation (see discussion of this subject later).

When nonvolatile material in the bottoms is significant, and no liquid water exists there—that is, p_s is below saturation of the steam pressure at the still temperature—then the Raoult's Law steam efficiency is [127]: Values of E are found to range from 60% to 70% for many organics, but values of 90% to 95% are reported [127] for good sparger design for steam injection, and molecular weight of organics < 100, and 50% for many lubricating oils.

$$E = \frac{p_{im}}{p_{im} \left(\frac{N_{im}}{N_{im} + N_o} \right)} \quad (8-109)$$

where E = vaporization efficiency of steam distillation

Note that for this discussion now, p_{im} , just above and in equations to follow, refers to the pure component vapor pressure of the immiscible liquid being distilled [127]. When steam is added to the still [127]:

$$\frac{p_s}{p_{im}} = \frac{\pi - p_{im}}{p_{im}} = \frac{\pi}{p_{im}} - 1 \quad (8-110)$$

and, for a constant distillation temperature, p_{im} is constant. Then for constant pressure:

$$N_s = \left(\frac{\pi}{E p_{im}} - 1 \right) (N_{im1} - N_{im2}) + \frac{\pi N_o}{E p_{im}} \ln \frac{N_{im1}}{N_{im2}} \quad (8-111)$$

As the organic or volatile material is reduced due to the batch distillation, the steam pressure rises during the progress of the operation due to the loss of the volatile material, and the decrease of p_{im} . When the volatile material is stripped down to a low residual concentration, then p_s approaches the total system pressure, π . When the steam saturation pressure and temperature is greater than π , no steam condensation will occur during the operation.

When the non-volatile concentration is low to insignificant in the still feed, then N_o is small relative to N_{im} . Then p_{im} is considered constant [127]:

$$p_{im} = E p_{im} \quad (8-112)$$

$$N_s = (p_s/p_{im}) (N_{im1} - N_{im2}) \quad (8-113)$$

Then, the distillate:

$$\frac{W_s}{W_{im}} = \frac{(\pi - p_{im}) M_s}{p_{im} M_{im}} \quad (8-114)$$

Operation of the open still with only a steam injection sparger to bring steam below the liquid level in the still may not be totally efficient as for the same condition operating the unit with internal trays as a stripping column. This should be examined for each situation, as the installation of trays can be expensive, particularly if they do not aid significantly in achieving the desired separation. Generally, when no liquid water is present, the best operations of an open still (with condenser) may be at the highest working temperature suitable for the effects on the fluids (i.e., no polymer formation, no breakdown, etc.). Often, direct steam injection can be reduced for any operation by careful heating of the still by an internal reboiler coil, or possibly a steam jacket. The heat sensitivity of the compounds involved must be recognized.

Steam Distillation—Continuous Flash, Multicomponent or Binary

This system requires direct steam injection into the still with the liquid, all the steam leaves overhead with the boiled-up vapors (no internal condensation) in a steady-state operation, and system at its dew point. Steam is assumed immiscible with the organics. Steam distillation is usually applied in systems of high boiling organics, or heat sensitive materials which require separation at vacuum conditions.

$$\frac{M_s}{B_{T0}} = \frac{\pi}{P_b B_{T0}} \left[\sum_{i \neq s} \frac{B_{i0}}{\alpha_i} \right] - 1 \quad (8-115)$$

b is more volatile reference component

$i \neq s$ = components, i , are not to include steam, s

M_s = total mols steam required

B_{T0} = total mols hydrocarbons at start (not including the steam)

B_{T1} = mols liquid in bottoms of still at time, T

B_{i0} = mols of component, i , at start

α_i = relative volatility of more volatile to each of other components

P_b = vapor pressure of reference more volatile component, b

π = total system pressure, absolute

B_b = mols of component, b , used as reference for volatility, after a given time of distillation

B_o = mols of component, b , used as reference for volatility, at start of distillation

Example 8-18: Multicomponent Steam Flash

A mixture of bottoms material of composition B_{i0} below has accumulated in the run-down tank. It is necessary to

separate the volatile organic heavies from the tarry polymerized residue (heavy liquid). Steam is to be injected into the insulated tank containing heating coils. The system is to operate at 200 mm Hg absolute pressure and 250°F with no condensation of the steam. The organic volatile heavies contain:

Component	Vapor Pressure @ 250°F	$\alpha = P_i/P_A$	Mols B_{io}	B_{io}/α_i
A	35 mm Hg	1.0	45	45
B	20	0.57	40	70
C	6	0.171	26	152
			111	267
			mols	

$$\frac{M_s}{B_{To}} = \frac{\pi}{P_b B_{To}} \left[\sum \frac{B_{io}}{\alpha_i} \right] - 1$$

$$\frac{M_s}{111} = \frac{200}{35 (111)} [267] - 1$$

$$= 13.75 - 1 = 12.75$$

$M_s = 1,417$ total mols steam required for 111 mols mixture
Mols steam/mol of mixture organic volatiles = $1,417/111 = 12.8$

Steam Distillation—Continuous Differential, Multicomponent or Binary

The results of the differential distillation end the same as the flash distillation, although the mechanism is somewhat different. This is a batch type operation distilling differentially. All sensible and latent heat are supplied separately from the steam or by superheat in the steam. Steam acts as an inert in the vapor phase, and quantity will vary as the distillation proceeds, while temperature and pressure are maintained.

$$\frac{M_s}{B_{T1} - B_{To}} = 1 - \frac{\pi}{P_b (B_{T1} - B_{To})} \left[\sum \frac{B_{io}}{\alpha_i} \left[\left(\frac{B_b}{B_{bo}} \right)^{\alpha_i} - 1 \right] \right] \quad (8-116)$$

If all the volatile materials are distilled: $\left(\frac{B_b}{B_{bo}} \right) = 0$
and $B_{T1} = 0$

This relation is handled very similar to the flash steam separation.

If all of the material is not to be removed as overhead vapors from the still, leave a percentage of a particular compound in the bottoms, then select the particular compound as the reference material "b" for α determinations.

$$B_b = (\text{Fraction retained}) (B_{bo})$$

$$\text{and } \left(\frac{B_b}{B_{bo}} \right) = (\text{Fraction retained})$$

substitute and solve for B_{T1} .

$$B_{T1} = \sum_{i=S} B_{io} \left(\frac{B_b}{B_{bo}} \right)^{\alpha_i} \quad (8-117)$$

Knowing B_{T1} , the relation for M_s can be solved to determine mols of steam to reduce initial material to percentage of a compound in the remaining bottoms. If steam condenses, the requirement for steam increases by this amount.

Steam Distillation—Continuous Flash, Two Liquid Phases, Multicomponent and Binary

Because water will be present in this system, and is assumed immiscible with the other components, it will exert its own vapor pressure. This situation is similar to many systems where the liquid to be flashed enters below its dew point, and hence requires the use of steam to heat (sensible + latent) as well as steam for the partial pressure effect.

Mols steam in vapor phase only:

$$M_s (\text{vapor}) = P_s \sum \frac{B_{io}}{P_i} \quad (\text{at assumed flash temperature})$$

where P_s = vapor pressure of steam

P_i = vapor pressure of each component at the flash temperature

Mols steam to heat is sum of sensible plus latent.

Total mols steam is sum of M_s (vapor) plus heating steam.

System total pressure:

$$\pi = \frac{M_s + B_{To}}{\sum_{i=S} \frac{B_{io}}{P_i}}, \text{ absolute} \quad (8-118)$$

B_{To} = mols (total) volatile material at start

Open Live Steam Distillation—With Fractionation Trays, Binary

Open or direct injection of steam into a distillation system at the bottom may be used to heat the mixture as well as to reduce the effective partial pressure of the other materials. In general, if steam is used to replace a reboiler, one tray is added to replace the reboiler stage, and from one-third to one or more trays may be needed to offset the

dilution of the system with water in the lower portion. Of course, where steam is acceptable, it replaces the cost of a reboiler and any cleaning associated with this equipment. For most columns, quite a few trays can be purchased to offset this cost.

When one of the components of the binary is water, and steam is used, the following equation is used for the operating stripping line (there is no rectifying section):

For component not including water:

$$V_s y_i (m) = L_s x_i (m+1) - B x_{iB}$$

$$\text{Slope of operating line } (L/V)_m = B/S$$

Operating line intersects the x-axis at x_{iB} .

The step-off of trays starts at x_{iB} on the x-axis, $y = 0$.

Open steam is used for stripping of dissolved or absorbed gases from an absorption oil, with all of the steam going overhead, and the stripped oil leaving at the bottom. This absorption coefficient of the oil for the component must be known to construct the equilibrium curve. The operating curve is constructed from several point material balances around the desired component, omitting the oil as long as its volatility is very low. The trays can be stepped off from a plot of y vs. x as in other binary distillations, again using only the stripping section.

Example 8-19: Continuous Steam Flash Separation Process: Separation of Non-Volatile Component from Organics

It is desired to separate a non-volatile material from an equimolal mixture of benzene, toluene, and xylene at 80°C. Vapor pressure data for these compounds are shown in several physical property sources. The following approximate values for the specific heats and latent heats of vaporization may be used:

$$\begin{aligned} \text{Benzene: } c_p &= 0.419 \text{ cal/gm}^\circ\text{C} \\ \Delta H_v &= 97.47 \text{ cal/gm} \end{aligned}$$

$$\begin{aligned} \text{Toluene: } c_p &= 0.44 \text{ cal/gm}^\circ\text{C} \\ \Delta H_v &= 86.53 \text{ cal/gm} \end{aligned}$$

$$\begin{aligned} \text{Xylene: } c_p &= 0.40 \text{ cal/gm}^\circ\text{C} \\ \Delta H_v &= 82.87 \text{ cal/gm} \end{aligned}$$

If the mixture is separated by a continuous flash process and the components are considered insoluble in water (check references) and the feed enters at the flash chamber at 20°C, calculate the mols of steam condensed, the total mols steam required per 100 mols of feed, and

the total pressure. Use steam at 212°F and atmospheric pressure.

1. This is to be done by a continuous flash process.
2. All the feed is to be flashed.
3. Steam does the heating.
4. Some steam condenses.
5. Water is immiscible with the materials.

Feed:

Benzene:	33.33 + mols
Toluene:	33.33 + mols
Xylene:	33.33 + mols
	100.00 mols feed

Because water will be present in liquid phase, it will only exert its vapor pressure. Temperature of flash = 80°C.

$$N_2 = P_s \sum L_i^\circ / P_i$$

where N_2 = mols steam in vapor only

P_s = vapor pressure of steam

L_i° = mols of each component at start

P_i = vapor pressure of each component at temperature

Component	Mols at start L_i°	P_i at 80°C, mm Hg	L_i° / P_i	Mol Wt
Benzene	33.33	760	0.043	78
Toluene	33.33	280	0.1190	92
Xylene	33.33	120	0.277	106
			0.4397	

$$P_s \text{ at } 80^\circ\text{C} (176^\circ\text{F}) = 6.868 \text{ lb/sq in. abs (from steam tables)}$$

$$= \frac{760}{14.7} (6.868) = 354 \text{ mm Hg abs}$$

$$\begin{aligned} N_2 &= P_s \sum L_i^\circ / P_i \\ &= 354 (0.4397) = 155.7 \text{ mols steam in vapor per 100 mols of} \\ &\quad \text{feed (volatile) material} \end{aligned}$$

Steam required to heat feed to 80°C:

$$\begin{aligned} \text{Benzene: Sensible heat} \\ (78) (33.33) [(0.419 \text{ cal/gm}^\circ\text{C}) (1.8)] (80^\circ - 20^\circ) \\ = 117,800 \text{ Btu} \end{aligned}$$

$$\begin{aligned} \text{Latent heat} \\ (78) (33.33) (97.46 \times 1.8) = 454,000 \end{aligned}$$

$$\begin{aligned} \text{Toluene: Sensible heat} \\ (92) (33.33) [0.44 \times 1.8] (80^\circ - 20^\circ) = 145,600 \end{aligned}$$

$$\begin{aligned} \text{Latent heat} \\ (92) (33.33) (86.53 \times 1.8) = 477,000 \end{aligned}$$

Xylene: Sensible heat
 (106) (33.33) [0.40 × 1.8] (80°–20°) = 153,000

Latent heat
 (106) (33.33) (82.87 × 1.8) = 525,000

Total heat load: 1,872,400 Btu

$$\text{Lbs steam required for heat load} = \frac{1,872,400 \text{ Btu}/100 \text{ mols}}{970 \text{ Btu}/\text{lb at } 212^\circ\text{F}}$$

$$= 1,932 \text{ lbs steam}/100 \text{ mols volatile}$$

$$\text{Mols steam required for heat load} = \frac{1,932}{18}$$

$$= 107.2 \text{ mols steam}/100 \text{ mols volatile material}$$

$$\text{Total mols steam}/100 \text{ mols volatile feed} = 155.7 + 107.2$$

$$= 262.9$$

Total pressure of system:

$$\pi = \frac{N_2 + L^{\circ}_T}{\sum_{i=1}^s L_i/P_i}$$

$$L_T = \text{Total mols volatile material at start} = 100$$

$$\pi = \frac{155.7 + 100}{0.4397} = 580 \text{ mm Hg abs}$$

Example 8-20: Open Steam Stripping of Heavy Absorber Rich Oil of Light Hydrocarbon Content (used by permission following the method of R. W. Ellerbee, *Chemical Engineering* [127])

A gas processing plant selectively extracts ethylene and ethane from an incoming natural gas mixture stream. These two light hydrocarbons are absorbed in a heavy gasoline type absorber "oil," and then stripped with open steam in an open tower. The system data are (see Figure 8-41):

Rich oil rate to tower:	8,500 mol/hr
Overhead product of ethylene and ethane:	775 mol/hr
Overhead product from accumulator:	55% vapor and 45% liquid
Accumulator conditions:	48 psia and 135°F
Reflux hydrocarbon in top vapor @ 175°F:	850 mol/hr
Steam (superheated) enter bottoms below tray:	14,000 lb/hr
Water partial pressure in the mixed vapor at bottoms:	20 psi
Hydrocarbons mix partial pressure:	50 psi – 20 psi = 30 psi

Neglect pressure drops through the system.

Determine: How much water is removed from the overhead accumulator and the intermediate dehydrator or water removal tray? No water is removed from the bottoms due to the use of superheated steam.

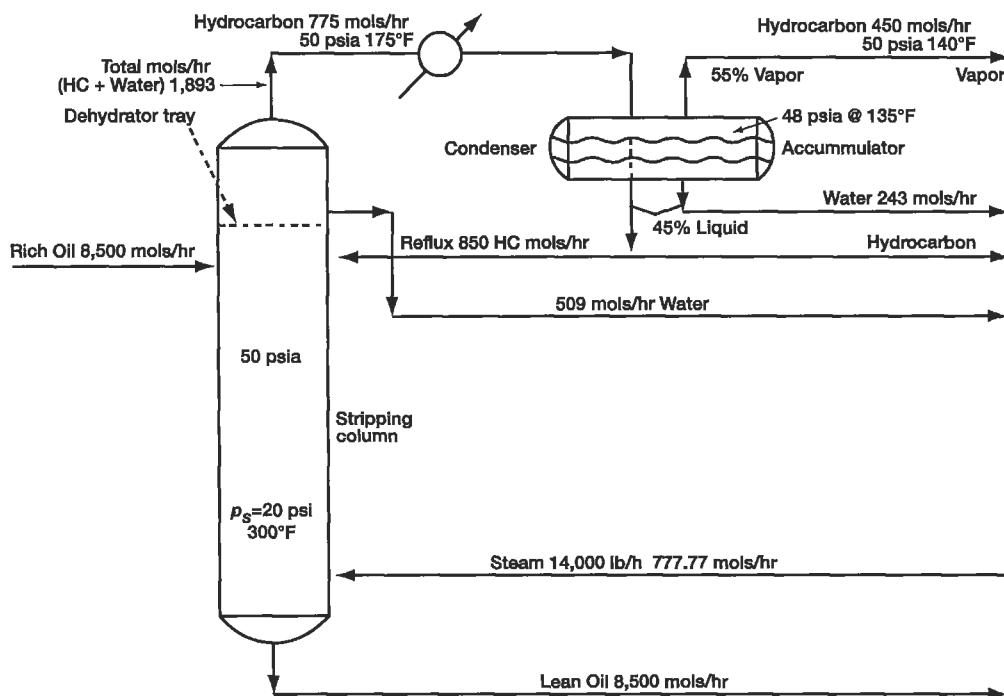


Figure 8-41. Open steam stripping light hydrocarbons from a rich oil. Modified for Example 8-20 and used by permission, Ellerbee, R. W., *Chem. Eng.* Mar. 4 (1974), p. 108.

From steam tables (saturated) at:

Top of tower, 175°F, vapor pressure water, psia = 6.8
 Mol fraction water vapor at top of tower: 6.8/48 psia = 0.1416
 Mol fraction hydrocarbon at top of tower: 1 - 0.1416 = 0.8584
 Total mols mix HC vapor and water vapor

at tower overhead: $\frac{775 + 850}{0.8584} = 1,893.0$

Mols of water vapor in tower overhead:
 1,893 - (775 + 850) = 268

Accumulator @ 48 psia & 135°F, water
 vapor pressure: = 2.6 psia

Mol fraction water in accumulator vapor: = 2.6/48 = 0.0541

Mol fraction HC in accumulator vapor: = 1 - 0.0541 = 0.9459

Total mols vapor leaving accumulator: = $\left[\frac{(775)(0.55)}{0.9459} \right] = 450.6$

Mols water vapor leaving accumulator: = 450.6 - (775)(0.55)
 = 24.35

Mols liquid water withdrawn from
 accumulator: = 268 - 24.35 = 243.65

Mols liquid water collected on dehydrator
 tray and removed at that point up tower
 above where reflux returns below this tray: = 777.7 - 268
 (water vapor in tower overhead) = 509.7 mols/hr

Mols steam entering tower: = 14,000/18 = 777.7 mols/hr

Distillation With Heat Balance

This type of evaluation of a distillation system involves a material and heat balance around each tray. It is extremely tedious to do by conventional means, and is now handled with computers. But even with this untiring worker, the volume of calculations is large and requires a relatively long time. Only those special systems that defy a reasonable and apparently economical solution by other approaches are even considered for this type of solution.

The detailed method involves trial and error assumptions on both the material balance as well as the heat balance.

Unequal Molal Overflow

This is another way of expressing that the heat load from tray to tray is varying in the column to such an extent as to make the usual simplifying assumption of equal molal overflow invalid. The relations to follow do not include heats of mixing. In general they apply to most hydrocarbon systems.

1. Equation of operating line in rectifying section, light component [59]

$$L_{n+1} = V_n - D$$

$$y_n = \left(\frac{M_D - H_n}{M_D - h_{n+1}} \right) x_{n+1} + \left(\frac{H_n - h_{n+1}}{M_D - h_{n+1}} \right) x_D$$

$$\frac{L_{n+1}}{V_n} = \frac{M_D - H_n}{M_D - h_{n+1}} = 1 - \frac{H_n - h_{n+1}}{M_D - h_{n+1}} \quad (8-119)$$

2. Equation of operating line in stripping section, light component

$$L_{m+1} = V_m + B$$

$$y_m = \left(\frac{M_B - H_m}{M_B - h_{m+1}} \right) x_{m+1} + \left(\frac{H_m - h_{m+1}}{M_B - h_{m+1}} \right) x_B$$

$$\frac{L_{m+1}}{V_m} = 1 - \frac{H_m - h_{m+1}}{M_B - h_{m+1}} \quad (8-120)$$

$$\frac{D}{V_m} = \frac{H_m - h_{m+1}}{M_m - h_{n+1}}$$

where $M_B = h_B - Q_B/B$

$$M_D = Q_c/D + h_D$$

$$M_B = h_w - \frac{Q_s}{W}$$

H_n = total molal enthalpy of vapor at conditions of plate n, $H_n = \sum H_{ni} (y_{ni})$

h_n = total molal enthalpy of liquid at conditions of plate n, $h_n = \sum h_{ni} (x_{ni})$

s = lb (or mols) steam per lb (or mol) bottoms

H_m = total molal enthalpy of vapor at plate m (below feed)

N = mols residue or bottoms per unit time

Q_B = heat added in still or bottoms

Ponchon-Savarit Method—Binary Mixtures

This graphical method allows solution of many distillation systems which would require considerable work if attempted by rigorous methods. Robinson and Gilliland have technical and descriptive details substantiating the method [8, 59]. Figure 8-42 presents a summary of the use of this method and appropriate interpretations. Scheiman [104] uses the Ponchon-Savarit diagrams to determine minimum reflux by heat balances. Campagne [216, 217] suggests a detailed technique for using the Ponchon-Savarit method with a computer simulation, which leads to designs not possible before. Many illustrations given in the reference aid in understanding the technique.

The basic method allows the non-ideal heat effects of the system to be considered as they affect the plate-to-plate

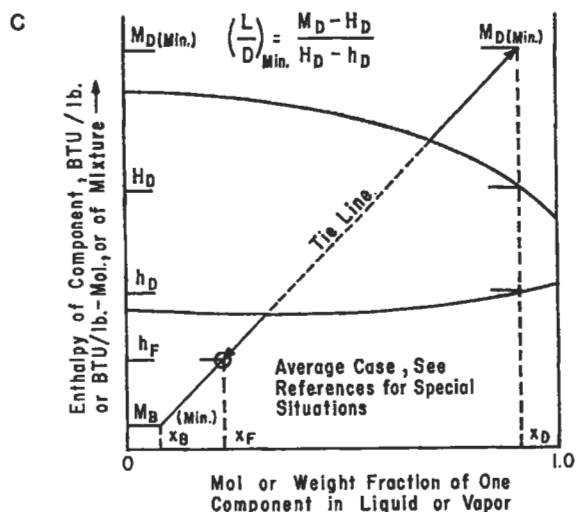
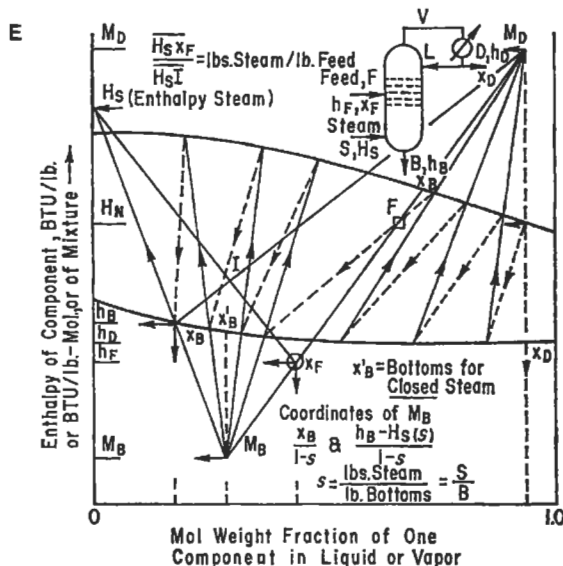
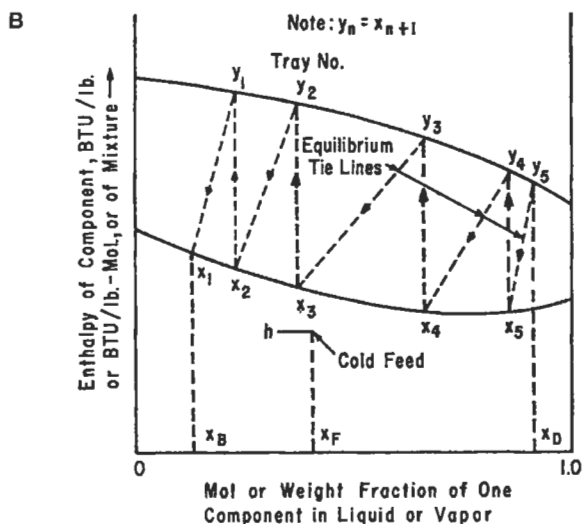
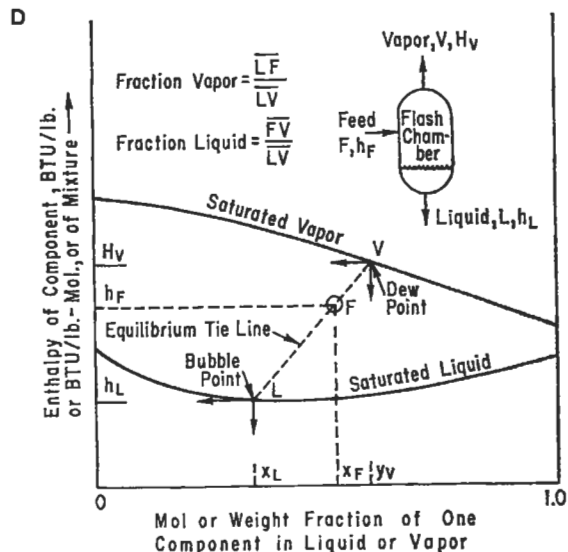
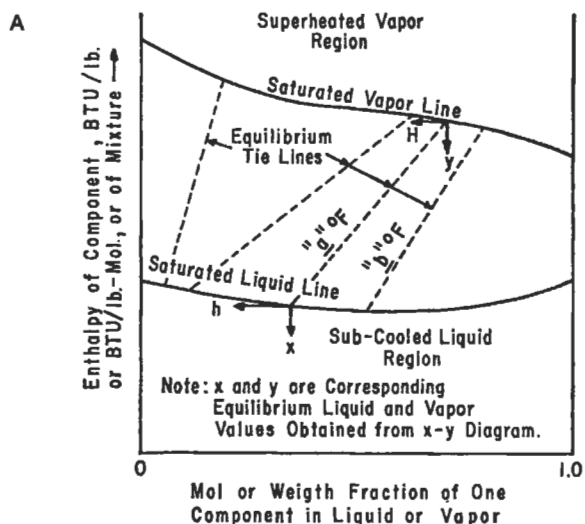


Figure 8-42A-E. Performance analysis of unequal molal overflow for binary systems using Ponchon-Savarit Method.

performance. The systems as represented in the diagrams are usually at constant pressure, but this is not necessarily the case. The equilibrium tie lines connect points fixed by the x - y values to corresponding saturated liquid and saturated vapor conditions at a constant temperature, such as "a" °F or "b" °F. The mol fractions are obtained from the usual x - y diagram for the system, and the enthalpy values are relative to a fixed datum for the available heat data of the particular components. For such systems as ammonia-water and ethanol-water the data are readily available. The saturated liquid line represents the enthalpies of liquid mixtures at the various compositions all at a constant pressure. This is the bubble point curve. The dew point curve is produced by plotting the enthalpies of the various vapor

mixtures at the saturation temperature at a constant pressure.

An effort has been made to present the basic understanding of the method as it applies to systems involving unequal molal overflow, open steam distillation and single flash vaporization in Figures 8-42 and 8-43.

To obtain extreme or even necessary accuracy for some design conditions, the end portions of the graphical representation may require enlargement from the usual size for graphical plotting. In most cases a size of 11 x 17 inches is suggested.

Example 8-21: Ponchon Unequal Molal Overflow

An ammonia-water recirculating solution of 62 wt % is to be stripped of the ammonia for recovery by condensa-

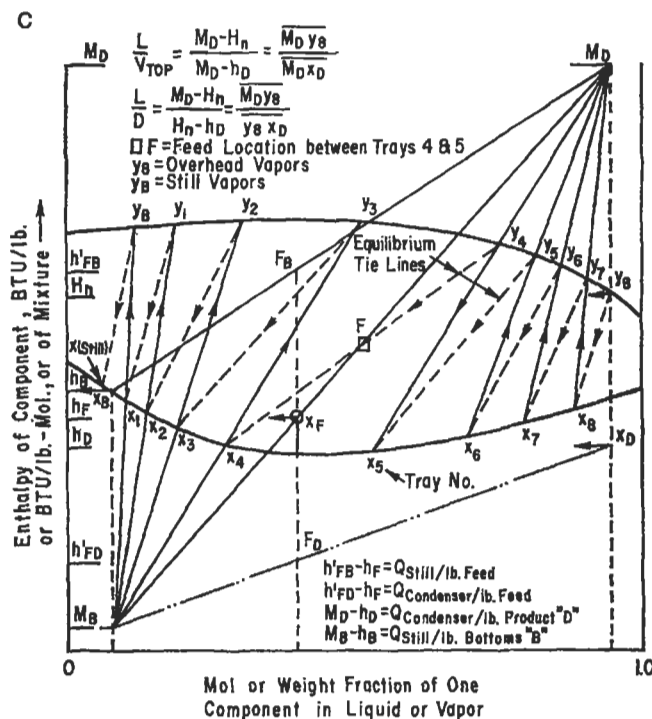
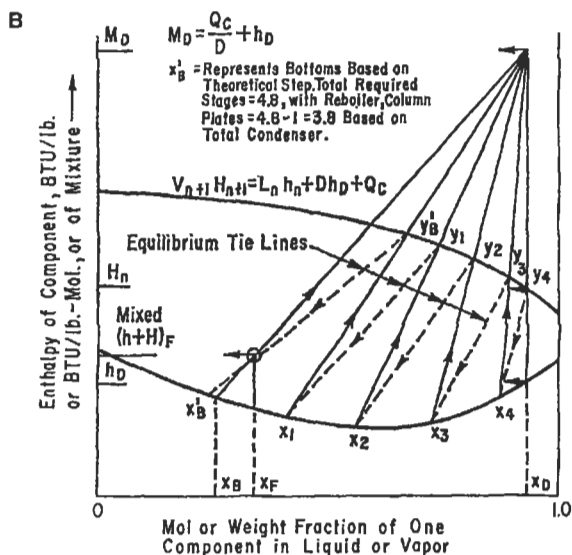
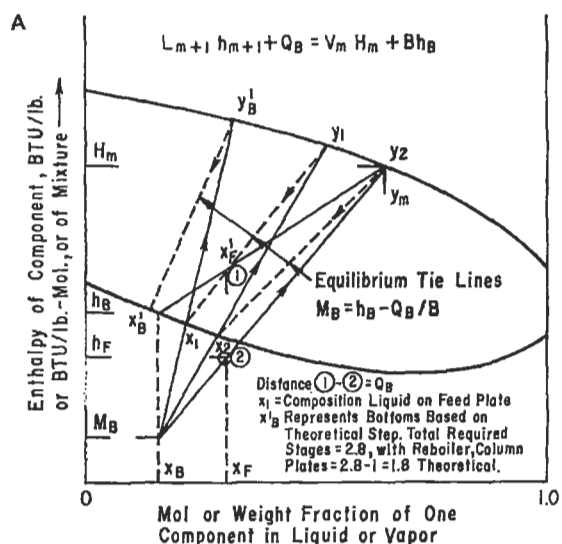


Figure 8-43A-C. Graphical solution of unequal molal overflow, binary systems.

tion at 260 psia with river water cooling. The overhead ammonia product is to be at least 99.5 wt % and the bottoms should approach 0.05 wt % ammonia. The feed enters as a liquid at its boiling point, with an enthalpy of 42 Btu/lb.

Enthalpy Diagram

Prepared by reading the h and H values from the Jennings and Shannon Aqua-Ammonia Tables [35] at 260 psia and various wt %'s of ammonia in the liquid. The tie lines connect the vapor compositions with the equilibrium liquid values, Figure 8-44.

Vapor-Liquid Equilibrium Diagram

Prepared from corresponding x and y values in Reference 35 at 260 psia, Figure 8-45.

Number of Trays

- $x_F = 0.62$ weight fraction ammonia
- $x_D = 0.995$ weight fraction ammonia
- $x_B = 0.0005$ weight fraction ammonia

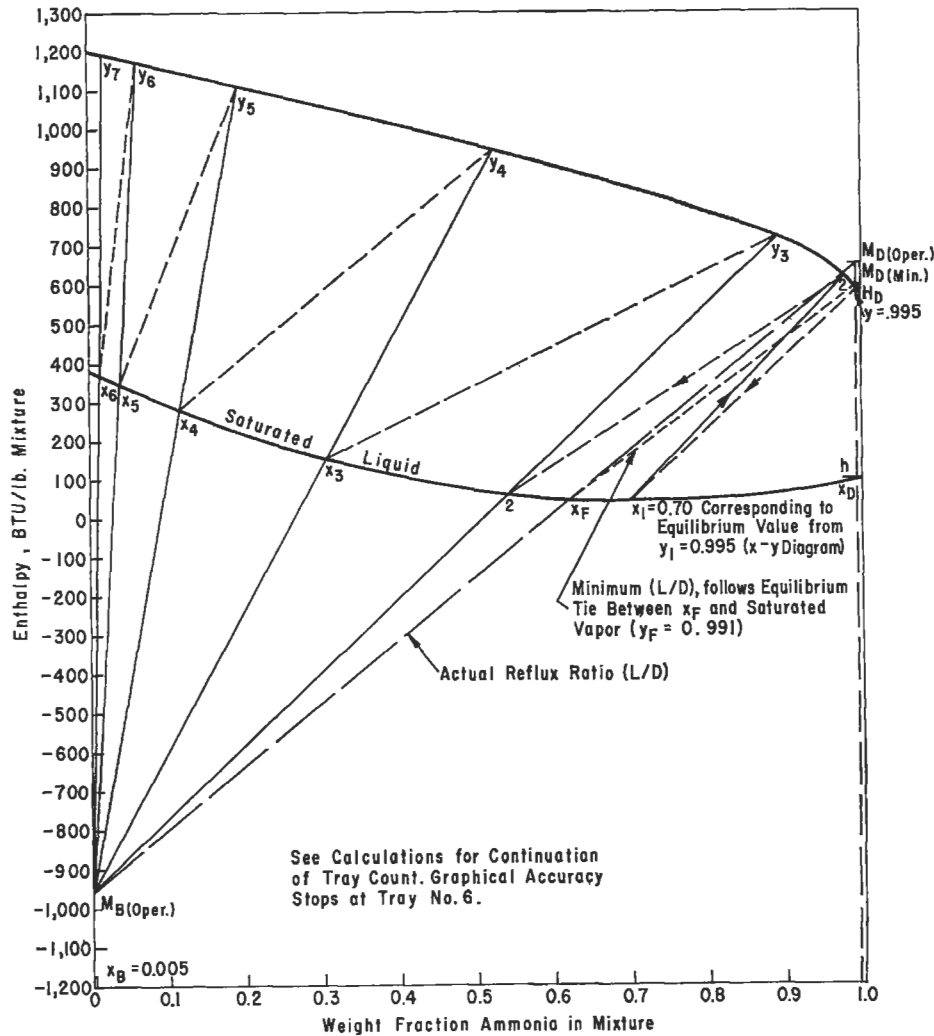


Figure 8-44. Ponchon type diagram for ammonia-water distillation.

1. Minimum Reflux

$$\left(\frac{L}{D}\right)_{\min} = \frac{(M_D)_{\min} - H_D}{H_D - h_D} \quad (8-121)$$

From enthalpy-composition diagram:

$$H_D = 590 \text{ Btu/lb}$$

$$h_D = 92 \text{ Btu/lb (assuming no subcooling)}$$

$$(M_D)_{\min} = 596 \text{ Btu/lb}$$

$(M_D)_{\min}$ is determined by reading the equilibrium y value corresponding to the feed composition 0.62 from the x - y diagram, noting it on the enthalpy diagram on the saturated vapor curve, and connecting the tie line, then extending it on to intersect with the x_D ordinate 0.995, reading $(M_D)_{\min} = 596 \text{ Btu/lb}$

$$\left(\frac{L}{D}\right)_{\min} = \frac{596 - 590}{590 - 92} = 0.012$$

2. Operating reflux ratio, L/D

$$\text{Select } (L/D)_{\text{actual}} = 10 (L/D)_{\min} = 10 (0.012) = 0.12$$

This is not unusual to select an operating reflux ratio ten, or even fifty times such a low minimum. Selecting a higher reflux can reduce the number of trays required, and this becomes a balance of the reduction in trays versus operating and capital expense in handling the increased liquid both external to the column and internally.

3. Operating M_D

$$(L/D)_{\text{act}} = 0.12 = \frac{M_D - 590}{590 - 92}$$

$$M_D = 649.8 \text{ Btu/lb}$$

Locate this value on the diagram and connect it to the feed point, x_F . Extend this line to intersect the bottoms condition ordinate (extended), x_B . In this case, it is impos-

sible to represent the value, $x = 0.005$, accurately, but construct it as close as possible to the required condition. M_B is now located. Improvement of this accuracy will be shown later in the problem.

Following the procedures shown in Figures 8-43, 8-44, and 8-45, the trays are constructed from the top or overhead down toward the bottom. The x values are read to correspond to the y values constructed. This establishes the tie line. When the x value tie line points (representing the trays) cross the feed ordinate, the construction is shifted from using the point M_D to the point M_B . Note that only $1\frac{1}{2}$ theoretical trays are required above the feed, since this is predominantly a stripping type operation. The number of theoretical trays or stages which can be easily plotted is six to seven counting down from the top. The sixth tray is too inaccurate to use graphically. Instead of calculating the balance of the trays assuming a straight line equilibrium curve from tray seven to the end, the plot could be enlarged in this area and the trays stepped off. By reference to the x - y diagram it can be seen that the equilibrium line from $x = 0.02$ to $x = 0$ is straight.

For the condition of straight operating and equilibrium curves, the number of plates can be calculated including the "reference" plate (number seven in this case) [59].

$$N_B = \frac{\ln \left[\frac{[(VK/L) - 1][(x_m/x_{1B}) - 1] + 1}{(V/L)(K - 1)} \right]}{\ln VK/L} \tag{8-122}$$

where N_B = number of trays from tray m to bottom tray, but not including the still or reboiler

x_m = tray liquid mol fraction for start of calculations (most volatile component)

x_{1B} = mol fraction most volatile component in bottoms

For the lower end of the equilibrium curve,

$$y_m = 5.0 x_m \text{ (by slope calculation of } x\text{-}y \text{ diagram)}$$

For the stripping section: consider top seven trays, vapor entering tray No. 6, $y_7 = 0.02$, $m = \text{tray } 7$, $m + 1 = \text{tray } 6$, reading from diagram,

$$(L/V)_m = 1 - \frac{H_m - h_{m+1}}{M_B - h_{m+1}} = 1 - \frac{(1,190 - 369)}{-960 - 369} = 1.618$$

use $H_m = 1,190$

$h_{m+1} = 369$

$M_B = -960$

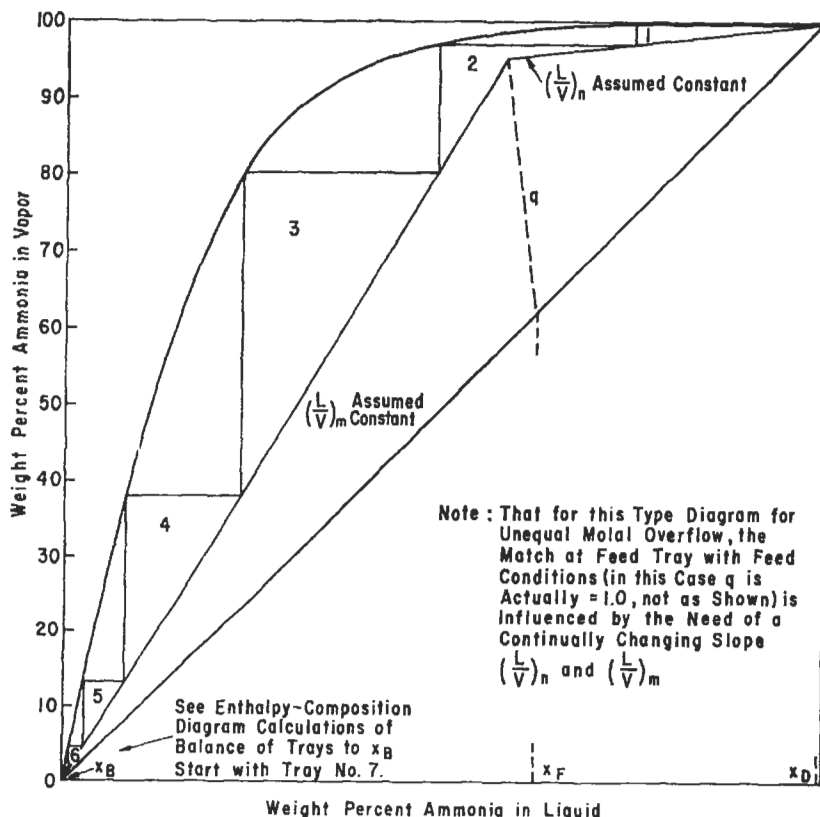


Figure 8-45. McCabe-Thiele diagram for ammonia-water system.

$$x_7 = \frac{y_7}{5.0} = \frac{0.02 \text{ (from graph)}}{5.0} = 0.004$$

$$N_B = \frac{\ln \left[\frac{(5.0/1.618 - 1) 0.004 / 0.0005 - 1}{(1/1.618)(5.0 - 1)} + 1 \right]}{\ln 5/1.618}$$

$N_B = 1.71$ trays (theoretical) not including reboiler, but including tray number 7, the one used as reference.

Total trays = 7 (from diagram plus $(1.71 - 1) = 7.7$ theoretical, plus a reboiler or 8.7 including a reboiler.

Tray efficiency is calculated as previously demonstrated and will not be repeated, except that normally stripping tray efficiencies run lower than rectification efficiencies. For ammonia-water stripping such as this example most over-all efficiencies run 50–60%.

Note that if the problem of accurate graphical representation occurs in the rectification end of the diagram, the corresponding relation to use to calculate the balance of the trays, assuming straight line operating and equilibrium lines in the region is [59]:

Rectifying section:

$$N_n = \frac{\ln \left[\frac{(1 - L/V) + x'_n / y'_D (L/V - K')}{1 - K'} \right]}{\ln L/K'V} - 1 \quad (8-123)$$

where K' = equilibrium constant for the *least* volatile component, $K' = y/x$

N_n = number of plates above (but not including) reference plate n

y', x' = mol fractions *least* volatile component

Multicomponent Distillation

The basic background and understanding of binary distillation applies to a large measure in multicomponent problems. Reference should be made to Figure 8-1 for the symbols.

Multicomponent distillations are more complicated than binary systems due primarily to the actual or potential involvement or interaction of one or more components of the multicomponent system on other components of the mixture. These interactions may be in the form of vapor-liquid equilibria such as azeotrope formation, or chemical reaction, etc., any of which may affect the activity relations, and hence deviations from ideal relationships. For example, some systems are known to have two azeotrope combinations in the distillation column. Sometimes these, one or all, can be "broken" or changed in the vapor pressure relationships by addition of a third chemical or hydrocarbon.

To properly handle the changing composition relationships it is almost essential to utilize some electronic computer techniques if good accuracy is to be achieved. Even three component systems become tedious using desk size electronic calculators without significant internal memory. Computers can be well programmed to handle the complexities of trial and check for convergence to a pre-set acceptable limit.

Techniques for convergence of the digital computer program are often the heart of an efficient multicomponent calculation. There are several techniques incorporated into many programs [27, 76, 112, 135, 139, 168].

Key Components

The two components in a feed mixture whose separations will be specified.

1. Adjacent keys: key components that are adjacent with respect to their volatilities.
2. Split keys: key components that are separated in volatilities by a non-key component, i.e., the system of components contains one or more whose volatilities fall between the volatilities of the designated keys.
3. Light key: the designation of the key component with the highest volatility of the two key components.
4. Heavy key: the designation of the key component with the lowest volatility of the two key components.
5. Example: component designations

Component	Relative Volatility		Designation
	$\alpha_{1/h}$	7°F. and 550 psia	
Hydrogen	11.7		Lighter than Key
Methane	3.7, α_1		<i>Light Key</i> , l
Ethylene	1.0, α_h		<i>Heavy Key</i> , h
Ethane	0.72		Heavier than Key
Propylene	0.23		Heavier than Key
Propane	0.19		Heavier than Key

Hengstebeck [137] presents a simplified procedure for reducing a multicomponent system to an equivalent binary using the "key" components. From this the number of stages or theoretical plates and reflux can be determined using conventional binary procedures and involving the McCabe-Thiele method.

Liddle [136] presents a shortcut technique for multicomponent calculations based on improving the Fenske and Gilliland correlations.

Minimum Reflux Ratio—Infinite Plates

This is the smallest value of external reflux ratio (L/D) which can be used to obtain a specified separation. This is

not an operable condition. Knowledge of the minimum reflux ratio aids considerably in establishing an economical and practical operating ratio. Ratios of 1.2 to 2.0 times the minimum are often in the economical range for hydrocarbon chemical systems. However, it is well to recognize that high reflux rates increase column size (but reduce number of trays required), reboiler size, steam rate, condenser size and coolant rate.

For adjacent key systems, all components lighter than the light key appear only in the overhead, and all components heavier than the heavy key appear only in the bottoms, and the keys each appear in the overhead and bottoms in accordance with specifications.

For a split key system the lights and heavies distribute the same as for adjacent key systems. However, the component(s) between the keys also distribute to overhead and bottoms.

At minimum reflux, the regions in which the number of trays approaches infinity (called the pinch zones and region of constant compositions) are:

1. Binary system: pinch zone adjacent to feed plate
2. Multicomponent:
 - a. Three components with no component lighter than light key: pinch zone in stripping section adjacent to feed plate.
 - b. Three components with no component heavier than heavy key: pinch zone in rectifying section adjacent to feed plate.
 - c. Three components mixture: pinch zones may be above and below feed plate.
 - d. Greater than four components: pinch zones appear in rectifying and stripping sections.

For systems with one sidestream drawoff, either above or below the feed, Tsuo et al. [102] propose a method for recognizing that the minimum reflux ratio is greater for a column with sidestream drawoff. At the sidestream the operating line has an inflection. For multifeed distillation systems, the minimum reflux is determined by factoring together the separate effect of each feed [103].

Lesi [105] proposes a detailed graphical procedure for figuring multicomponent minimum reflux by a graphical extension of a McCabe-Thiele diagram, assuming infinite plates or equilibrium stages. In this traditional model the concentration in the distillate of the components heavier than the heavy key component are assumed to be zero, and the heavy key component reaches its maximum concentration at the upper pinch point (see Figures 8-23 and 8-25). Therefore, this assumption is that only the heavy and light keys are present at the upper pinch point, similar in concept to the handling of a binary mixture [106]. The method assumes (a) only the key components are dis-

tributed, (b) no split key components exist, (c) total molal overflow rates and relative volatilities are constant. This method provides good agreement with the detailed method of Underwood.

Yaws [124] et al. provide an estimating technique for recovery of each component in the distillate and bottoms from multicomponent distillation using short-cut equations and involving the specification of the recovery of each component in the distillate, the recovery of the heavy key component in the bottoms, and the relative volatility of the light key component. The results compare very well with plate-to-plate calculations, Figure 8-46, for a wide range of recoveries of 0.05 to 99.93% in the distillate.

The distribution of components for the distillate and the bottoms is given by the Hengstebeck-Geddes equation [124, 125, 126]:

$$\log (d_i/b_i) = A + B \log \alpha_i \quad (8-124)$$

where d_i = mols of component i in distillate
 b_i = mols of component i in bottoms
 α_i = relative volatility of component i
 A, B = correlation constants

A material balance for the i component in the feed is:

$$f_i = d_i + b_i \quad (8-125)$$

Then the quantity of component i in the distillate can be expressed as a mol fraction recovered, or d_i/f_i . Likewise, the mol fraction of component i recovered in the bottoms is b_i/f_i , or $1 - d_i/f_i$. Substituting into Equation 8-124:

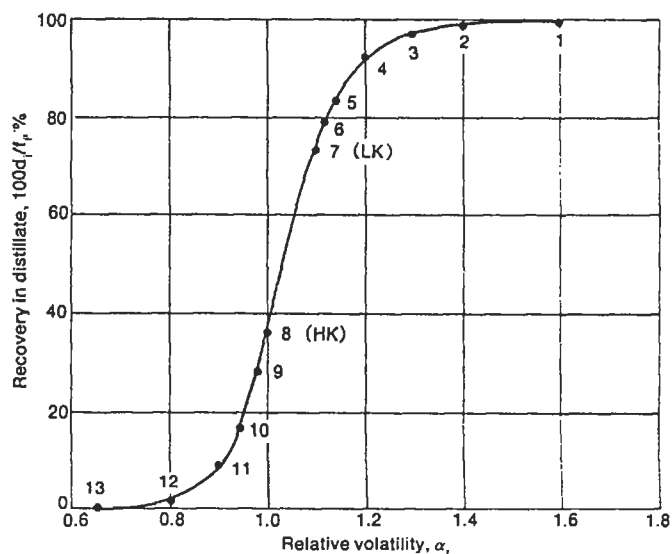


Figure 8-46. Yaws short-cut method compared to plate-to-plate calculations. Used by permission, Yaws, C. L. et al. *Hydrocarbon Processing*, V. 58, No. 2 (1979) p. 99. Gulf Publishing Co., all rights reserved.

$$\log \left[\frac{(d_i/f_i)}{1 - (d_i/f_i)} \right] = A + B \log \alpha_i \quad (8-126)$$

Solving for recovery of component *i* in the distillate gives

$$d_i/f_i = (10^A \alpha_i^B) / (1 + 10^A \alpha_i^B) \quad (8-127)$$

From a material balance, recovery of component *i* in the bottoms is

$$b_i/f_i = 1 / (1 + 10^A \alpha_i^B) \quad (8-128)$$

The correlation constants required for Equations 8-127 and 8-128 are obtained by specifying a desired recovery of the light key component LK in the distillate and the recovery of the heavy key component HK in the bottoms. Then the constants are calculated as follows:

$$A = -\log \left[\frac{(b_{HK}/f_{HK})}{1 - (b_{HK}/f_{HK})} \right] \quad (8-129)$$

$$B = \frac{\log \left[\left(\frac{d_{LK}/f_{LK}}{1 - (d_{LK}/f_{LK})} \right) \left(\frac{b_{HK}/f_{HK}}{1 - (b_{HK}/f_{HK})} \right) \right]}{\log \alpha_{LK}} \quad (8-130)$$

Example 8-22: Multicomponent Distillation by Yaw's Method [124] (used by permission)

Assume a multicomponent distillation operation has a feed whose component concentration and component relative volatilities (at the average column conditions) are as shown in Table 8-3. The desired *recovery* of the light key component O in the distillate is to be 94.84%. The recovery of the heavy key component P in the bottoms is to be 95.39%.

Table 8-3

Yaws' Method for Selected Distillation Recovery from a Specific Feed for Example 8-22

Component	f_i	α_i
M	0.10	2.30
N	0.13	1.75
O (LK)	0.25	1.45
P (HK)	0.23	1.00
Q	0.15	0.90
R	0.08	0.83
S	0.06	0.65

Used by permission, *Hydrocarbon Processing*, Yaws, C. L., et al V. 58 No. 2 (1979), p. 99, Gulf Pub. Co., all rights reserved.

The recoveries of the non-key components are estimated by first calculating the correlation constants:

$$b_{HK}/f_{HK} = 0.9539, \text{ given}$$

$$A = -\log \left(\frac{0.9539}{1 - 0.9539} \right)$$

$$= -\log 20.69 = -1.3158$$

$$d_{LK}/f_{LK} = 0.9484, \text{ given}$$

$$\alpha_{LK} = 1.45, \text{ from Table 8-3}$$

$$B = \frac{\log \left[\left(\frac{0.9484}{1 - 0.9484} \right) \left(\frac{0.9539}{1 - 0.9539} \right) \right]}{\log 1.45}$$

$$= (\log 380.3) / (\log 1.45) = 15.988$$

The recovery of component M in the distillate is then

$$d_M/f_M = (10^{-1.3158} 2.30^{15.988}) / (1 + 10^{-1.3158} 2.30^{15.988}) = 0.99997, \text{ from Equation 8-127}$$

The recovery of component M in the bottoms is

$$b_M/f_M = 1 / (1 + 10^{-1.3158} 2.30^{15.988}) = 0.00003, \text{ from Equation 8-128}$$

Repeating Equations 8-126 and 8-127 for each of the other non-key components in the feed mixture gives the results shown in Table 8-4. Good agreement was demonstrated.

Algebraic Plate-to-Plate Method

Like any plate-to-plate calculation this is tedious, and in most instances does not justify the time because shorter

Table 8-4
Results for Example 8-22 for Multicomponent Distillation

Component	Percent recovery	
	In dist. (100 d_i/f_i)	In btms. (100 b_i/f_i)
M	99.997	0.003
N	97.731	2.269
O (LK)	94.840	5.160
P (HK)	4.610	95.390
Q	0.889	99.111
R	0.245	99.755
S	0.005	99.995

Used by permission, *Hydrocarbon Processing*, Yaws, C. L., et al V. 58 No. 2 (1979), Gulf Pub. Co., all rights reserved.

methods give reasonably acceptable results. VanWinkle [75] outlines the steps necessary for such calculations.

With current computer technology there are several commercial programs available (as well as personal and private) that perform tray-to-tray stepwise calculations up or down a column, using the latest vapor pressure, K-values, and heat data for the components. This then provides an accurate analysis at each tray (liquid and vapor analysis) and also the heat duty of the bottoms reboiler and overhead total or partial condenser.

Torres-Marchal [110] and [111] present a detailed graphical solution for multicomponent ternary systems that can be useful to establish the important parameters prior to undertaking a more rigorous solution with a computer program. This technique can be used for azeotropic mixtures, close-boiling mixtures and similar situations.

An alternate improved solution for Underwood's method is given by Erbar, Joyner, and Maddox [113] with an example, which is not repeated here.

Underwood Algebraic Method: Adjacent Key Systems [72]

This system for evaluating multicomponent adjacent key systems, assuming constant relative volatility and constant molal overflow, has proven generally satisfactory for many chemical and hydrocarbon applications. It gives a rigorous solution for constant molal overflow and volatility, and acceptable results for most cases which deviate from these limitations.

Overall Column—Constant α

$$(L/D)_{\min} + 1 = \frac{(\alpha_a x_a)_D}{\alpha_a - \theta} + \frac{(\alpha_b x_b)_D}{\alpha_b - \theta} + \dots + \frac{(\alpha_i x_i)_D}{\alpha_i - \theta} \quad (8-131)$$

In arriving at $(L/D)_{\min}$ the correct value of θ is obtained from:

$$1 - q = \frac{(\alpha_a x_a)_F}{\alpha_a - \theta} + \frac{(\alpha_b x_b)_F}{\alpha_b - \theta} + \dots + \frac{(\alpha_i x_i)_F}{\alpha_i - \theta} = \sum \frac{x_{Fi}}{1 - \theta/\alpha_i} \quad (8-132)$$

The "q" value is the same as previously described for the thermal condition of the feed.

Rectifying section only:

$$V_r = \sum_{i=1,h,L} \frac{Dx_{Di}}{1 - \theta/\alpha_i} \quad (8-133)$$

Stripping section only:

$$V_s = \sum_{i=1,h,H} \frac{Bx_{Bi}}{1 - \theta/\alpha_i} \quad (8-134)$$

At the minimum reflux condition all the θ values are equal, and generally related:

$$\alpha_h < \theta < \alpha_l$$

Suggested Procedure

1. From Equation 8-131 expressing θ and q evaluate θ by trial and error, noting that θ will have a value between the α of the heavy key and the α of the light key evaluated at or near pinch temperatures, or at α avg. Suggested tabulation, starting with an assumed θ value, θ_a :

Component	x_{Fi}	$\alpha_i x_{Fi}$	$\alpha_i - \theta$	$\frac{\alpha_i x_{Fi}}{\alpha_i - \theta}$	$\frac{\alpha_i x_{Fi}}{(\alpha_i - \theta)^2}$
a	x_{Fa}	$\alpha_a x_{Fa}$	$\alpha_a - \theta_a$	$\frac{\alpha_a x_{Fa}}{\alpha_a - \theta_a}$	$\frac{\alpha_a x_{Fa}}{(\alpha_a - \theta_a)^2}$
b	x_{Fb}	$\alpha_b x_{Fb}$	$\alpha_b - \theta_a$	$\frac{\alpha_b x_{Fb}}{\alpha_b - \theta_a}$	$\frac{\alpha_b x_{Fb}}{(\alpha_b - \theta_a)^2}$
•	•	•	•	•	•
•	•	•	•	•	•
				$\Sigma \Psi (\theta_a)$	$\Sigma \Psi' (\theta_a)$

Ψ, Ψ' , represents function.

Corrected θ by Newton's approximation method:

$$\theta_c = \theta (\text{assumed}) - \frac{\Psi (\theta_a)}{\Psi' (\theta_a)} \quad (8-135)$$

Repeat the same type of tabular computation, substituting the corrected θ_c for the θ_a . If the second corrected θ'_c checks closely with θ_c , the value of θ has been obtained, if not, a third recalculation should be made using the θ'_c value as the new assumed value.

Note that average α values should be used (constant) for each component unless the values vary considerably through the column. In this latter case follow the discussion given elsewhere in this section.

2. Calculate $(L/D)_{\min}$ by substituting the final θ value in Equation 8-130 solving for $(L/D)_{\min}$. Note that this requires evaluating the functions associated with θ at the composition of the distillate product. The α values are the constant values previously used above.

Underwood Algebraic Method: Adjacent Key Systems; Variable α

For varying α systems, the following procedure is suggested:

1. Assume $(L/D)_{\min}$ and determine the pinch temperature by Colburn's method.
2. At this temperature, evaluate α at pinch and α at overhead temperature, obtaining a geometric average α . As an alternate, Shiras [63] indicates a t_{avg} value which gives acceptable results when compared to pinch and stepwise calculations. This suggestion calculates,

$$t_{\text{avg}} = (Dt_o + Bt_B)/F$$

- Determine Underwood's θ value as previously described, using the average α value.
- Calculate $(L/D)_{\min}$ and compare with assumed value of (1) above. If check is satisfactory, $(L/D)_{\min}$ is complete; if not, reassume new $(L/D)_{\min}$ using calculated value as basis, and repeat (1) through (4) until satisfactory check is obtained.

where t_o = overhead temp °F
 t_B = bottoms temp °F
 t_{avg} = avg temp, °F

To aid in solving the tedious Underwood equation to ultimately arrive at $(L/D)_{\min}$, Frank [100] has developed Figure 8-47, which applies for liquid feed at its bubble point and whether the system is binary or multicomponent, but does require that the key components are adjacent. Otherwise, the system must be solved for two values of θ [74]. To obtain the necessary parameters for Figure 8-47, Frank recommends using the same overhead con-

centrations that were used in or calculated by the Fenske equation for the Underwood solution. (θ = Underwood constant.)

Underwood Algebraic Method: Split Key Systems: Constant Volatility [72]

Although this method appears tedious, it is not so unwieldy as to be impractical. It does require close attention to detail. However, a value of $(L/D)_{\min}$ can be obtained with one trial that may be satisfactory for "order of magnitude" use, which is quite often what is desired before proceeding with detailed column design and establishment of operating L/D

- Assume θ_f values and check by

$$\sum \frac{\alpha_i x_{Fi}}{\alpha_i - \theta_f} = 1 - q \quad (8-136)$$

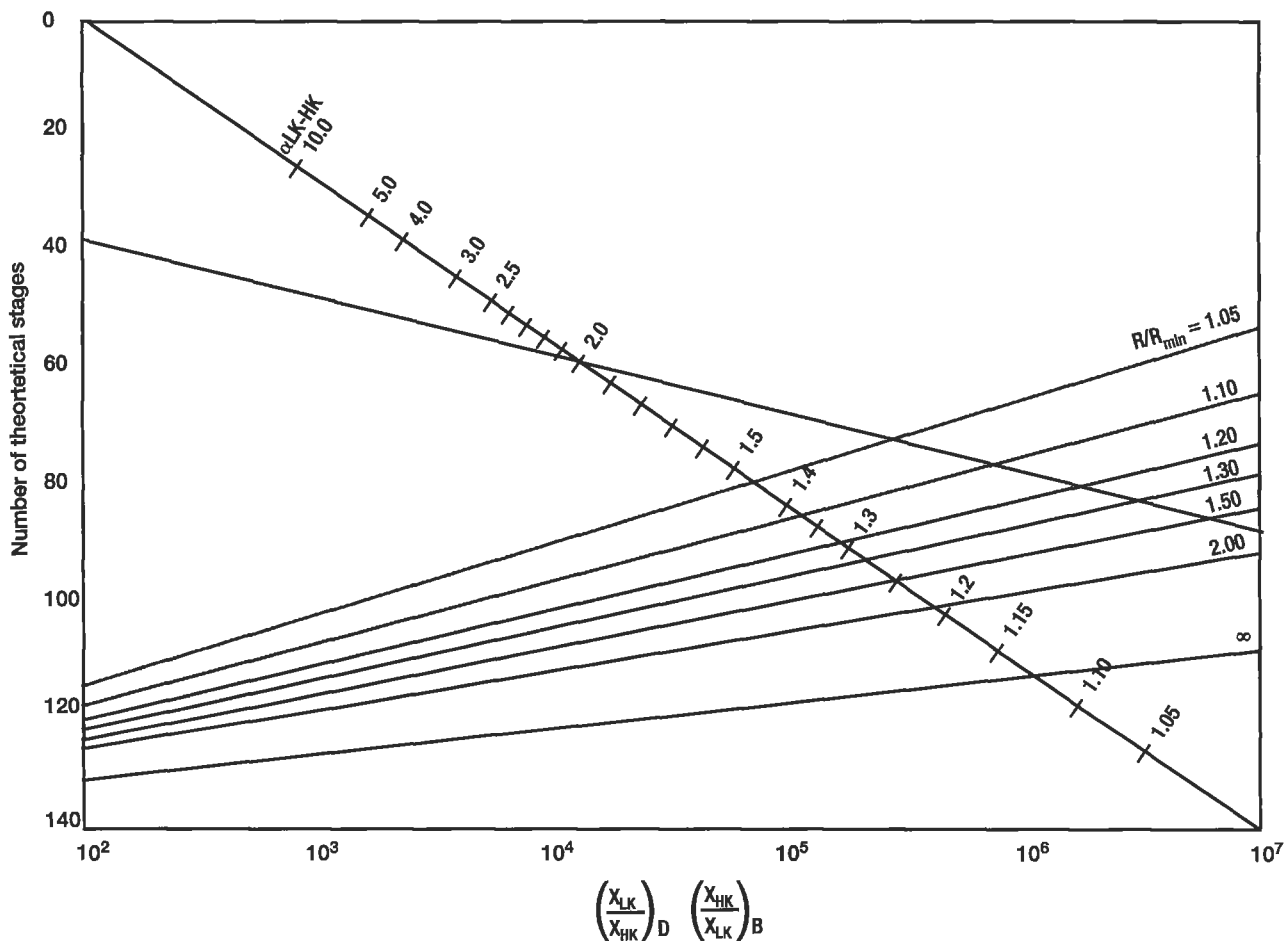


Figure 8-47. Short-cut solution of Fenske-Underwood-Gilliland theoretical trays for multicomponent distillation. Used by permission, Frank, O., *Chem. Eng.* Mar. 14 (1977), p. 109.

There are a total solutions of θ_{fi} equal to one more than the number of split components between the keys. The θ_f values will be spaced:

$$\alpha_{13} \theta_{f3} \alpha_4 \theta_{f4} \alpha_5 \theta_{f5} \alpha_{h6}$$

where α_1 is the light key and component number 3, and correspondingly for the heavy key, component number 6. Determine θ values as for constant volatility case of adjacent keys.

For some systems, the θ values can be assumed without further solution of the above relation, but using these assumed values as below.

2. Calculate,

$$v = \frac{\frac{1}{(P)(\theta_{fi})}}{\frac{1}{(P)(\alpha_i)}} \quad (8-137)$$

which represents (for the hypothetical system set up in (1)) the product of $(\theta_{f5}) (\theta_{f4}) (\theta_{f3})$ divided by the product of $(\alpha_5) (\alpha_4)$, based upon the lightest component being numbered one, the next two, etc., the heaviest components having the higher numbered subscripts. P means product, and $i = h - 1, i = 1 + 1$ are limits for evaluation referring to components between the keys, and the light and heavy keys.

3. Calculate,

$$\omega_j = \frac{\frac{1}{(P)} \left(1 - \frac{\alpha_i}{\alpha_j} \right)}{\frac{1}{(P)} \left(1 - \frac{\theta_{fi}}{\alpha_j} \right)} \quad (8-138)$$

For the θ example shown in (1) above:

$$\omega_3 \text{ (light key)} = \frac{(1 - \alpha_5/\alpha_3)(1 - \alpha_4/\alpha_3)}{(1 - \theta_{f5}/\alpha_3)(1 - \theta_{f4}/\alpha_3)(1 - \theta_{f3}/\alpha_3)}$$

Also calculate ω for all components lighter than light key.

$$\omega_6 \text{ (heavy key)} = \frac{(1 - \alpha_5/\alpha_6)(1 - \alpha_4/\alpha_6)}{(1 - \theta_{f5}/\alpha_6)(1 - \theta_{f4}/\alpha_6)(1 - \theta_{f3}/\alpha_6)}$$

Component, j	ω_j	α_j	$\frac{\omega_j}{\alpha_j} x_{Dj}$	$\omega_j x_{Dj}$	$\frac{\omega_j}{\alpha_j} (x_{Dj})$
1 (light key)	•	•	•	•	•
h (heavy key)	•	•	•	•	•
L_{i+1}	} lighter than light key, etc.	•	•	•	•
L_{i+2}					
L_{i+3}					
				$\Sigma \omega_j x_{Dj}$	$\Sigma \frac{\omega_j}{\alpha_j} (x_{Dj})$

4. Calculate $(L/V)_{min}$: (internal)

$$(L/V)_{min} = (v) \frac{\sum_{j=h,1,L} D \left(\frac{\omega_j}{\alpha_j} \right) (x_{Dj})}{\sum_{j=h,1,L} D (\omega_j) x_{Dj}} \quad (8-139)$$

5. Calculate External $(L/D)_{min}$:

$$(L/D)_{min} = \frac{1}{(V/L)_{min} - 1} \quad (8-140)$$

For variable α conditions, the pinch temperature can be used for α determinations as previously described.

Example 8-23: Minimum Reflux Ratio Using Underwood Equation; Calculate the Minimum Reflux Ratio

Use $\phi_{fi} = 0.584$ to begin, (assumed).

Expanding to determine more exact value of ϕ_{fi} .

$$\Omega \phi = \Omega \phi_a + \phi - \phi_a \Omega' \phi_a$$

$$\Omega \phi = \sum \frac{\alpha_i x_{fi}}{(\alpha_i - \phi)} - (1 - q)$$

$$\phi_{fi} = \frac{\phi_a - \Omega \phi_a}{\Omega' \phi_a}$$

$$\Omega' \phi = \sum \frac{\alpha_i x_{fi}}{(\alpha_i - \phi)^2}$$

Component	X_{fi}	$\alpha_i X_{fi}$	$\alpha_i - \phi_a$	$\left[\frac{\alpha_i X_{fi}}{\alpha_i - \phi_a} \right]$	$\left[\frac{\alpha_i X_{fi}}{(\alpha_i - \phi_a)^2} \right]$
1	0.10	0.025	-0.334	-0.0749	+0.224
2	0.225	0.1125	-0.084	-1.34	+15.9
3	0.450	0.450	+0.416	+1.08	+2.6
4	0.225	0.450	+1.416	+0.318	+0.224
				$\Sigma = -0.016$	$+18.948 = \Omega' \phi_a$

$$\Omega \phi_a = -0.016 - (1 - q)$$

$$\phi_a = -0.016 - (1 - 1)$$

$$\phi_a = -0.016$$

$$\phi_{f1\text{-corrected}} = 0.584 - (-0.016)/(18.948) = 0.584 + 0.00084 = 0.58484$$

Now use this new value of ϕ_{f1} in Underwood's equations;

$$\sum_{i=h,L} \frac{Dx_{Di}}{1 - \frac{\phi_r}{\alpha_i}} - V_r = 0$$

For minimum reflux: $\phi_{f1} = \phi_r = \phi_s$

From calculations of related problem* the value of Dx_{Di} has been calculated:

$$Dx_{Di} = 0.01072 \text{ for heavy key}$$

$$Dx_{Di} = 0.428 \text{ for light key}$$

$$Dx_{Di} = 0.225 \text{ for lighter than light key.}$$

$$\left[\frac{0.01072}{1 - \frac{0.5848}{0.50}} + \frac{0.428}{1 - \frac{0.5848}{1.0}} + \frac{0.225}{1 - \frac{0.5848}{2.0}} \right] - V_r = 0$$

$$[-0.638 + 1.03 + 0.318] - V_r = 0$$

From related problem, D has been determined to be = 0.6657 mols/mol feed.

$$-V_r = -1.285$$

$$V_r = 1.285$$

$$(V_r)_{\min} = (L_r)_{\min} + D$$

$$(L_r)_{\min} = 1.285 - 0.6637 = 0.622$$

$$\left(\frac{L_r}{D} \right)_{\min} = \frac{0.6622}{0.6637} = 0.94, \text{ Minimum Reflux Ratio}$$

Minimum Reflux Colburn Method: Pinch Temperatures [12]

This method has also found wide usage and might be considered less tedious by some designers. It also yields an approximation of the rectifying and stripping section pinch temperatures. For adjacent keys,

Rectifying:

$$\left(\frac{L}{D} \right)_{\min} = \frac{1}{\alpha - 1} \left(\frac{x_D}{x_n} - \alpha \frac{x_{hD}}{x_{hn}} \right) \quad (8-141)$$

where α = relative volatility of any component referenced to the heavy key component

x_{hD} = overhead composition of heavy key component, mol frac

x_{hn} = pinch composition of heavy key component, mol frac

x_D = overhead composition of any light component, mol frac

x_n = pinch composition of any light component, mol frac

1. Calculate D, B, Dx_{Di} and Bx_{Bi} from problem specification.
2. Assume or set the operating pressure and overhead temperature (may be calculated).
3. Calculate the liquid and vapor quantities and their respective compositions in the feed to the column.
4. Calculate estimated ratio of key components on feed plate based on the liquid portion of the feed.

$$r_f = \frac{\text{Mol fraction light key}}{\text{Mol fraction heavy key}}$$

- (a) For all liquid feed at feed tray temperature (boiling point)

r_f = mol fraction ratios in feed.

- (b) For a part or all vapor feed just at its dew point,

r_f = ratio of key components in the equilibrium liquid phase of feed.

- (c) For all liquid feed below feed plate temperature

r_f = ratio of key components at intersection point of operating line (from a McCabe-Thiele diagram).

5. Determine approximate pinch zone liquid composition for light key component

$$x_{In} = \frac{r_f}{(1 + r_f)(1 + \sum \alpha_i x_{Fi})_H} \quad (8-142)$$

$\sum \alpha_i x_{Fi}$ = sum of $\alpha_{h+1} x_{Fh+1} + \alpha_{h+2} x_{Fh+2} + \dots$ for

all components in liquid portion of feed *heavier* than heavy key. Note that x_{Fi} values are the mol fractions of the component in the liquid portion of feed only and the $\sum x_{Fi}$ equal to 1.0.

6. Calculate approximate value for $(L/D)_{\min}$.

$$\left(\frac{L}{D} \right)_{\min} = \frac{1}{\alpha_i - 1} \left(\frac{x_{iD}}{x_{in}} - \alpha \frac{x_{hD}}{x_{hn}} \right)$$

The second term in the right hand parentheses can be omitted unless the mol fraction of the heavy key in the distillate, x_{hD} , is 0.1 or greater. Use $x_{hn} = x_{in}/r_f$.

7. Estimate stripping and rectifying pinch temperatures at values one-third and two-thirds of the interval between the column bottoms and overhead, respectively.

8. Calculate internal vapor and liquid flows.

$(L_r/D)_{\min}$ = assumed

Solve for $(L_r/V_r)_{\min}$

$$(L_r/V_r)_{\min} = \frac{1}{1 + (D/L_r)_{\min}} \quad (8-143)$$

$L_r = (\text{number}) (V_r) = (L_r/D)_{\min}(D)$

D is known

Calculate V_r and L_r from above.

In stripping section:

Solve directly for L_s

$$L_s = L_r + qF$$

Solve for V_s :

$$\frac{V_r - V_s}{F} = 1 - q \quad (8-144)$$

Calculate L_s/B

9. Evaluate pinch compositions at the assumed temperatures of Step 7. If this temperature does not give a balance, other temperatures should be assumed and a balance sought as indicated below. Either of the following balances can be used, depending upon the convenience of the designer:

Rectifying:

$$\sum x_{Dri} = \sum x_n = \sum_{i=h,l,L'} \left(\frac{Dx_{Di}/V_r}{\alpha_i K_h - L_r/V_r} \right) = 1 \quad (8-145)$$

$$\text{or } \sum x_n = \sum_{i=h,l,L'} \left(\frac{Dx_{Di}/V_r}{K_i - L_r/V_r} \right) = 1$$

$$\text{or } \sum x_n = \sum_{i=h,l,L'} \left(\frac{x_{Di}}{(\alpha_i - 1)(L_r/D)_{\min} + \alpha_i x_{hDi}/x_{hn}} \right) = 1$$

When the heavy key in the overhead is very small, less than 0.1 mol fraction, the last term of the denominator can be omitted.

$$\text{or } \sum x_n = \sum_{i=h,l,L'} \frac{x_{Di}}{K_i + (K_i - 1)(L_r/V_r/D)_{\min}} = 1$$

Note that the calculations are only made for the heavy key, h; light key, l; and all components lighter than it, L' . If there are split keys, the calculation is to include all components lighter than the heavy key.

Stripping pinch compositions:

$$\sum x_{Dsi} = \sum x_m = \sum_{i=H,h,l} \frac{Bx_{Bi}/V_s}{L_s - \alpha_i K_h} = 1 \quad (8-146)$$

$$\text{or } \sum x_m = \sum_{i=H,h,l} \frac{Bx_{Bi}/V_s}{L_s - K_i} = 1$$

$$\text{or } \sum x_m = \sum_{i=H,h,l} \frac{\alpha_i x_{Bi}}{(\alpha_1 - \alpha_i)(L_s/B)_{\min} + \alpha_i x_{iB}/x_{iD}} = 1$$

Because the second term of the denominator is usually negligible when the light key in the bottoms is very small; less than 0.1 mol fraction, this term is often omitted.

$$\text{or } \sum x_m = \sum_{i=H,h,l} \frac{x_{Bi}}{K_i + (1 - K_i)(L_s/B)_{\min}} = 1$$

Note that these calculations are made for the light key, l; heavy key, h; and all components heavier than the heavy key, H. For split key systems, the calculations are made for all components heavier than the light key.

10. Calculate mol fraction ratio:

(a) Stripping pinch

$$r_{ps} = \frac{\text{light key}}{\text{heavy key}}$$

(b) Rectifying pinch

$$r_{pr} = \frac{\text{light key}}{\text{heavy key}}$$

(c) $p = r_{ps}/r_{pr}$

11. Calculate for each component in pinch.

Rectifying: apply only to components lighter than light key, $i = L'$

$$\frac{(\alpha_i - 1)\alpha_i}{\alpha_i}$$

Read from Figure 8-48 value of C_{ni} for each component.

Calculate for each component:

$$(C_{ni})(x_{i,pr})$$

Sum these values:

$$\sum_{i=L'} C_{ni} x_{ip}$$

Stripping: apply only to components heavier than heavy key, $i = H$.

$$(\alpha_1 - 1) (\alpha_1)$$

Read from Figure 8-48 value of C_{mi} for each component.

Calculate for each component:

$$C_{mi} \alpha_i x_{i,ps}$$

Sum these values:

$$\sum_{i=H} C_{mi} \alpha_i x_{i,ps}$$

12. Calculate:

$$p' = \frac{1}{[1 - \sum C_n x_{i,pr}] [1 - \sum C_m \alpha_i x_{i,ps}]} \quad (8-147)$$

If the two values of p are not very nearly equal, this requires a retrial with a new $(L/D)_{\min}$, and a follow through of the steps above.

When $r_{ps}/r_{pr} > p'$, the assumed $(L/D)_{\min}$ is too high. Note that r_{ps}/r_{pr} changes rapidly with small changes in $(L/D)_{\min}$, p' changes slightly. When $p = p'$, the proper $(L/D)_{\min}$ has been found. Colburn reports the method accurate to 1%. It is convenient to graph the assumed $(L/D)_{\min}$ versus p and p' in order to facilitate the selection of the correct $(L/D)_{\min}$.

Example 8-24: Using the Colburn Equation Calculate the Minimum Reflux Ratio

The mixture of four components is as listed below, using n-butane as the base component.

Component	Relative Vol.	x_f	$(S_r)_i = D x_D / B x_B$
1	0.25	0.10	—
Hvy Key	0.50	0.225	0.05
n-butane	1.0	0.450	20.00
4	2.0	0.225	—

$$D x_{Di} = \frac{(S_r)_i F x_{Fi}}{1 + (S_r)_i}$$

$$S_r = \text{separation ratio} = \frac{D x_{Di}}{B x_{Bi}}$$

If all at top, $S_r = 1$

If all at bottom, $S_r = 0$

For component No. 3; Basis; 1 mol feed,

$$D x_{D3} = \frac{(20) [(1) (0.450)]}{1 + 20} = 0.428$$

For component No. 2,

$$D x_{D2} = \frac{(0.05) (1 + 0.225)}{1 + 0.05} = 0.01072$$

Because this is at minimum reflux, and adjacent keys system,

$$F x_{FL} = D x_{DL}$$

$$F x_{FH} = B x_{BH}$$

Therefore, for component No. 4, lighter than light key,

$$F x_{F4} = (1) (0.225) = 0.225$$

$$\text{Then, } D x_{D4} = 0.225$$

For component No. 1, heavier than heavy key, this component will not appear in the overhead.

Bottoms:

$$F x_{Fi} = D x_{Di} + B x_{Bi}$$

$$F \frac{F x_{Fi}}{B x_{Bi}} = \frac{D x_{Di}}{B x_{Bi}} + 1$$

$$\frac{F x_{Fi}}{B x_{Bi}} = (S_r)_i + 1$$

$$(S_r)_i = \frac{D x_{Di}}{B x_{Bi}}, \text{ by definition}$$

$$\text{Then, } B x_{Bi} = \frac{F x_{Fi}}{(S_r)_i + 1}$$

Component No. 1:

$$F x_{F1} = B x_{B1} = (1) (0.1) = 0.10$$

Component No. 2:

$$(S_r)_i = \frac{D x_{D2}}{B x_{B2}} = 0.05$$

Substituting in equation previously established,

$$B x_{B2} = \frac{(1) (0.225)}{(0.05) + 1} = 0.214$$

or, because $D x_{D2}$ has been calculated,

$$B x_{B2} = \frac{D x_{D2}}{(S_r)_i} = \frac{0.01072}{0.05} = 0.214$$

Component No. 3:

$$Bx_{B3} = \frac{Dx_{D2}}{(S_r)_i} = \frac{0.428}{20} = 0.0214$$

Component No. 4: This component will not be in the bottoms because it is lighter than the light key Overhead:

$$Dx_{D1} + Dx_{D2} + Dx_{D3} + Dx_{D4} = D$$

$$0 + 0.01072 + 0.428 + 0.225 = D$$

$$D = 0.66372 \text{ mols overhead product/mol feed}$$

Composition of Overhead:

Component	Dx_{Di}	Mol%
1	0	0
2	0.01072	1.6
3	0.428	64.6
4	0.225	33.9
	0.66372	100.1%

Composition of Bottoms:

Component	Bx_{Bi}	Mol %
1	0.10	29.9
2	0.214	63.8
3	0.0214	6.3
4	0	0
	0.3354	100.0%

To have some idea of what value to use in Colburn's "exact" method for minimum reflux, use Colburn's "approximate" method to establish the order-of-magnitude of the minimum reflux:

$$\left(\frac{L}{D}\right)_{\min} = \frac{1}{\alpha - 1} \left(\frac{x_D}{x_n} - \alpha \frac{x_{hD}}{x_{hn}} \right)$$

where x_D and x_n = top and pinch composition of a given light component

x_{hD} and x_{hn} = top and pinch composition of the heavy key component

α = relative volatility of the given component with reference to the heavy key

Estimating Pinch Composition:

$$x_n \text{ (approx)} = \frac{r_f}{(1 + r_f)(1 + \sum \alpha x_z)}$$

where r_f = ratio of liquid composition of light to heavy key component on feed plate

x_n = mol fraction of a component in the liquid in the rectifying column pinch

x_z = mol fraction of a component in the liquid part of the feed where the feed is part vapor

$$r_f = 0.450/0.225 = 2.0$$

$$\sum \alpha x_z = (0.5)(0.10) = 0.05$$

$$\alpha_{\text{light/heavy key}} = \frac{1}{0.5} = 2.0$$

$$x_n \text{ (approx)} = \frac{2.0}{(1 + 2.0)(1 + 0.05)} = \frac{2}{3.15} = 0.635$$

In terms of heavy key:

$$\alpha_{l/h} = 2.0$$

$$\alpha_{1/1} = 0.25$$

$$\alpha_{l/h} = (\alpha_{l/h})(\alpha_{1/1}) = (2.0)(0.25) = 0.5$$

$$\text{approx} \left(\frac{L}{D}\right)_{\min} = \frac{1}{(2.0 - 1)} \left(\frac{0.645}{0.635} \right)$$

$$x_{D3} = 0.646$$

$$\left(\frac{L}{D}\right)_{\min} = 1.017 \text{ approx.}$$

Now: Use Colburn's more detailed method:

$$\text{Assume} \left(\frac{L}{D}\right)_{\min} = 1.017$$

$$\left(\frac{L}{V}\right)_{\min} = \frac{1}{1 + \left(\frac{D}{L}\right)_{\min}} = \frac{1}{1 + \frac{1}{1.017}}$$

$$\left(\frac{L}{V}\right)_{\min} = \frac{1}{1.017 + 1} = 0.506$$

$$V = L + D$$

$$\frac{V}{L} = 1 + \frac{D}{L}$$

$$\frac{L}{V} = \frac{1}{1 + \frac{D}{L}}$$

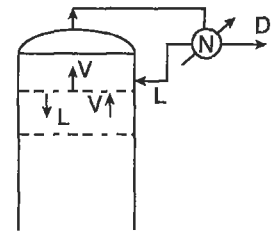
$$L_r = (0.506)(V_r)$$

$$\text{And: } L_r = (1.017)(D_r)$$

$$\text{Then: } (0.506)V_r = (1.017)(D_r) = (1.017)(0.66372)$$

$$V_r = \frac{(1.017)(0.66372)}{0.506} = 1.332 \text{ mols/mol feed}$$

$$L_r = (1.017)(0.66372) = 0.674 \text{ mols/mol feed.}$$



The feed is a boiling point liquid from statement of problem:

$$q = 1.0$$

$$L_s = L_r + qF$$

Basis: 1 mol feed:

$$L_s = 0.674 + (1)(1) = 1.674$$

(min)

$$\frac{L_r - V_s}{F} = 1 - q$$

$$\frac{1.332 - V_s}{1} = 1 - 1 = 0$$

$$V_s = 1.332$$

$$\frac{L_s}{V_s} = \frac{1.674}{1.332} = 1.255$$

Determine temperature of rectifying section pinch.

$$1 = \sum_{i=h,l,L} \frac{Dx_{Di}/V_r}{K_i - \frac{L_r}{V_r}}$$

Compo- nents	$\frac{Dx_{Di}}{V_r}$	$\frac{K_B @ 118^\circ F}{V_r}$	α_i	$\alpha_i K_B$	$\frac{L_r}{V_r}$	$K_i - \frac{L_r}{V_r}$	$\frac{Dx_{Di}/V_r}{K_i - (L_r/V_r)}$	
h	0.01072	0.00805	1.06	0.50	0.506	0.024	0.333	
l	0.428	0.321		1.0		1.06	0.554	0.580
L	0.225	0.169		2.0		2.12	1.614	0.104
							$\Sigma = 1.017$	

Note: $0.225/1.332 = 0.169$

$$K_i = \alpha_i K_B$$

B = reference

Assume temperature at rectifying pinch. If the components were known, then the overhead dew point and bot-

tom bubble point could be determined, and from this an approximation could have been made of the pinch temperature. Because these cannot be calculated, one must use trial-and-error to get correct pinch temperature.

Because the 1.017 is reasonably close to 1.0, continue calculations composition of rectifying pinch:

$$x_{pri} = \frac{Dx_{Di}/V_r}{K_i - L_r/V_r} = \frac{Dx_{Di}/V_r}{\alpha_i K_B - L_r/V_r}$$

Compo- nents	$\frac{Dx_{Di}/V_r}{(K_i - L_r/V_r)}$	Revised Mol Fraction
2 = h	0.333	$0.333/1.017 = 0.328$
3 = l	0.580	0.572
4 = L	0.104	0.102
	1.017	1.002

Determine temperature of stripping section pinch:

$$1 = \sum_{i=H,h,l} \frac{Bx_{Bi}/V_s}{\frac{L_s}{V_s} - K_i} = \frac{Bx_{Bi}/V_s}{\frac{L_s}{V_s} - \alpha_i K_B}$$

Compo- nents	Bx_{Bi}	$\frac{Bx_{Bi}/V_s}{L_s/V_s}$	$\frac{K_B @ 130^\circ F}{L_s/V_s}$	α_i	$\alpha_i K_B$	$\frac{L_s/V_s - \alpha_i K_B}{(L_s/V_s) - \alpha_i K_B}$	$\frac{Bx_{Bi}/V_s}{(L_s/V_s) - \alpha_i K_B}$	
1 = H	0.10	$\frac{0.10}{1.332} = 0.0752$	1.255	1.23	0.25	0.308	0.947	0.0794
2 = h	0.214	0.1605			0.50	0.615	0.640	0.252
3 = l	0.0214	0.0160			1.00	1.23	0.025	0.640

Exact K_B must lie between 1.23 and 1.24. Because there is a difference involved in calculation, the result is very sensitive to small changes in K .

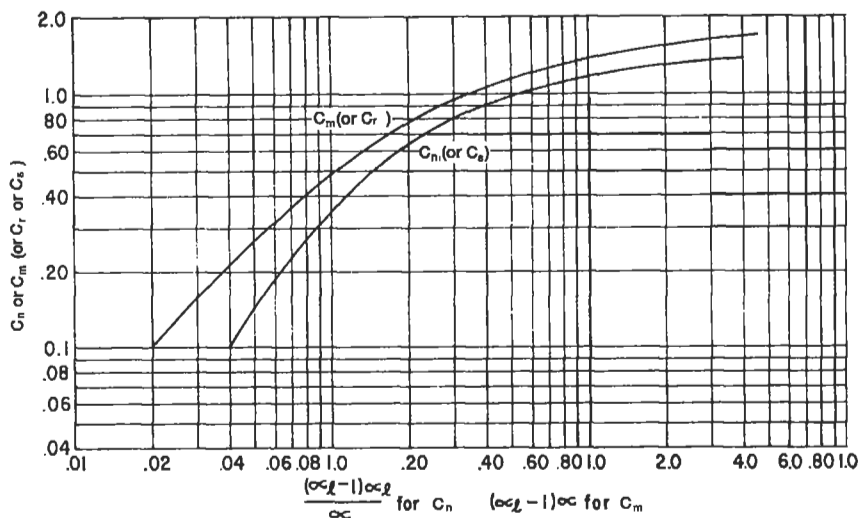


Figure 8-48. Colburn minimum reflux factors, above (C_n) and below (C_m) feed point. Used by permission, Colburn, A. P. The American Institute of Chemical Engineers, *Trans. Amer. Inst. Chem. Engr.* V. 37 (1941), p. 805, all rights reserved.

Composition of Stripping Pinch:

Components	See Last Col. Above	Revised Mol Fraction
1 = H	0.0794	0.0794/0.9714 = 0.0817
2 = h	0.252	0.2585
3 = l	<u>0.64</u>	<u>0.659</u>
	0.9714	0.9992

Calculate C_r for each component lighter than light key.
There is only one component lighter than light key in this example, #4

$$\left[\left(\frac{\alpha_1}{\alpha_h} - 1 \right) \left(\frac{\alpha_l}{\alpha_L} \right) \right] = \left[\left(\frac{1}{0.50} - 1 \right) \left(\frac{1}{2} \right) \right] = (2 - 1) \left(\frac{1}{2} \right) = 0.50$$

Reading curve, $C_r = 1.0 = C_n$ (see Figure 8-48)

Evaluate C_s for No. 1:

$$\left[\left(\frac{\alpha_1}{\alpha_h} - 1 \right) \alpha_H \right] = \left[\left(\frac{1.0}{0.5} - 1 \right) (0.25) \right] = (2 - 1) (0.25) = 0.25$$

Reading curve, $C_s = 0.875$ (see Figure 8-48)

Now, substitute into Colburn correlation, for check,

$$\frac{x_{prl} x_{psh}}{x_{prh} x_{psl}} = \left(1 - \sum_L C_r x_{prl} \right) \left(1 - \sum_H \frac{\alpha_{psH}}{\alpha_{psh}} C_s x_{psH} \right)$$

$$\frac{(0.572)(0.2585)}{(0.328)(0.659)} = (1 - ((1)(0.102))) \left(1 - \left(\frac{0.25}{0.50} \right) (0.875) (0.0817) \right)$$

$$0.684 = (1 - 0.102) (1 - 0.0318) = (0.898) (0.9682)$$

$$0.684 \approx 0.868$$

Because left side of equation is smaller than right side, $\left(\frac{L}{D} \right)_{min}$ assumed was too large. Try a smaller value around 0.95.
Right side of equation is not so sensitive to change.

- where L = all components lighter than light key
- Σ = sum of all components lighter than light key,
L does not include light key
- Σ = sum of all components heavier than heavy key,
H does not include heavy key
- p = pinch
- r = rectifying
- s = stripping
- l = light key
- h = heavy key
- H = all components heavier than heavy key, not including the heavy key

L = all components lighter than light key, not including the light key
 C_r, C_s = empirical constants

Scheibel-Montross Empirical: Adjacent Key Systems: Constant or Variable Volatility [61]

Although this method has not found as much wide acceptance when referenced to use by designers or controversial discussion in the literature, it nevertheless allows a direct approximate solution of the average multicomponent system with accuracy of 1-8% average. If the key components are less than 10% of the feed, the accuracy is probably considerably less than indicated. If a split key system is considered, Scheibel reports fair accuracy when the split components going overhead are estimated and combined with the light key, the balance considered with the heavy key in the L/D relation.

$$\left(\frac{L}{D} \right)_{min} = \frac{1}{x_{IF} + \Sigma x_{FL}} \left[x_{IF} R' + (x_{hF} + \Sigma x_{FH}) \sum \frac{x_{FH}}{\alpha_1 - 1} + \sum \frac{x_{FL}}{\alpha_L} \left(1 + \frac{\alpha_1}{\alpha_L} \right) \right] \quad (8-148)$$

- where x_{IF} = mol fraction of light key in feed
- Σx_{FL} = sum of all mol fractions lighter than light key in feed
- R' = pseudo minimum reflux
- Σx_{FH} = sum of all mol fractions heavier than heavy key in feed
- x_{hF} = mol fraction heavy key in feed
- α_1 = relative volatility of light key to heavy key at feed tray temperature
- α_H = relative volatility of components heavier than heavy key at feed tray temperature
- α_L = relative volatility of components lighter than light key at feed tray temperatures
- x_{it} = mol fraction liquid at intersection of operating lines at minimum reflux. (Calculated or from graph.)
- x_{io} = mol fraction light key in overhead expressed as fraction of total keys in overhead.

Pseudo minimum reflux:

$$R' = \frac{x_{io}}{(\alpha_1 - 1) x_i} - \frac{(1 - x_i) (\alpha_i - 1)}{(1 - x_{io}) \alpha_i} \quad (8-149)$$

When the overhead contains only a very small amount of heavy key, the second term in the equation may be neglected.

Intersection of operating lines at Equilibrium Curve:

$$x_{it} = \pm \sqrt{\frac{(\alpha_1 - 1)(1 + m) \left(\frac{x_{iF}}{x_{iF} + x_{hF}} \right) - \alpha_1 - m}{2m(\alpha_1 - 1)} \left[\left[(\alpha_1 - 1)(1 + m) \left(\frac{x_{iF}}{x_{iF} + x_{hF}} \right) - \alpha_1 - m \right]^2 + 4m(\alpha_1 - 1)(1 + m) \left(\frac{x_{iF}}{x_{iF} + x_{hF}} \right) \right]} \quad (8-150)$$

The proper value for x_{it} is positive and between zero and one. Actually this is fairly straightforward and looks more difficult to handle than is actually the case.

Pseudo ratio of liquid to vapor in feed:

$$m = \frac{x_L - \Sigma x_{FH}}{x_v - \Sigma x_{FL}} = \frac{F_L - \Sigma F_H}{F_v - \Sigma F_L} \quad (8-151)$$

where x_L = mol fraction of feed as liquid

x_v = mol fraction of feed as vapor

F_L = mols of liquid feed

F_v = mols of vapor feed

ΣF_H = total mols of components heavier than heavy key in feed

ΣF_L = total mol of components lighter than light key in feed.

Example 8-25: Scheibel-Montross Minimum Reflux [61]

A tower has the following all liquid feed composition:

Component	Feed Mols/hr	Overhead Mols/hr	Bottoms Mols/hr
A	30	30.0	—
B (light key)	20	19.5	0.5
C (heavy key)	20	0.5	19.5
D	30	—	30.0
	100	50.0	50.0

Relative volatilities referenced to the heavy key, C:

$$\alpha_A = 4.0$$

$$\alpha_B = 2.0 = \alpha_1$$

$$\alpha_C = 1.0 = \alpha_h$$

$$\alpha_D = 0.5$$

$$\text{Calculate: } m = \frac{x_L - \Sigma x_{FH}}{x_v - \Sigma x_{FL}} = \frac{1.0 - 0.30}{0 - 0.30} = -2.33$$

Intersection of Operating Lines:

$$x_{it} = \sqrt{\frac{(2-1)(1-2.33) \left(\frac{0.2}{0.2+0.2} \right) - 2 - (-2.33) \pm \left[\left[(2-1)(1-2.33) \left(\frac{0.2}{0.2+0.2} \right) - 2 - (-2.33) \right]^2 + 4(-2.33)(2-1)(1-2.33) \left(\frac{0.2}{0.2+0.2} \right) \right]}{2(-2.33)(2-1)}}$$

$$x_{it} = 0.610, \text{ or } -0.459 \text{ (not acceptable)}$$

Pseudo minimum reflux ratio:

$$x_{lo} = \frac{19.5}{19.5 + 0.5} = 0.975$$

$$R' = \frac{0.975}{(2-1)(0.610)} - \frac{(1.0 - 0.975)(2)}{(1-0.610)(2-1)}$$

$$R' = 1.472$$

Minimum reflux ratio:

$$(L/D)_{\min} = \frac{1}{0.2 + 0.3}$$

$$\times \left[0.2(1.472) + (0.2 + 0.3) \left(\frac{0.3}{\frac{2}{0.5} - 1} \right) + \frac{0.3}{4} \left(1 + \frac{2}{4} \right) \right]$$

$$(L/D)_{\min} = 0.912$$

Minimum Number of Trays: Total Reflux—Constant Volatility

The minimum theoretical trays at total reflux can be determined by the Fenske relation as previously given

$$S_m = N_{\min} + 1 = \frac{\log \left(\frac{x_{Dl}}{x_{Dh}} \right) \left(\frac{x_{Bh}}{x_{Bl}} \right)}{\log \alpha_{\text{avg}}} \quad (8-152)$$

Note that N_{\min} is the number of trays in the column and does not include the reboiler. When α varies considerably through the column, the results will not be accurate using

the α_{avg} as algebraic average, and the geometric means is used in these cases.

$$\alpha_{avg} = [(\alpha_t) (\alpha_b)]^{1/2}$$

For extreme cases it may be necessary to calculate down from the top and up from the bottom until each section shows a fairly uniform temperature gradient from tray to tray. Then the Fenske relation is used for the remaining trays, using the conditions at the trays calculated as the terminal conditions instead of the actual overhead and bottoms.

Chou and Yaws Method [96]

This method for multicomponent distillation involving more than one feed and more than one side stream requires a reliable minimum reflux.

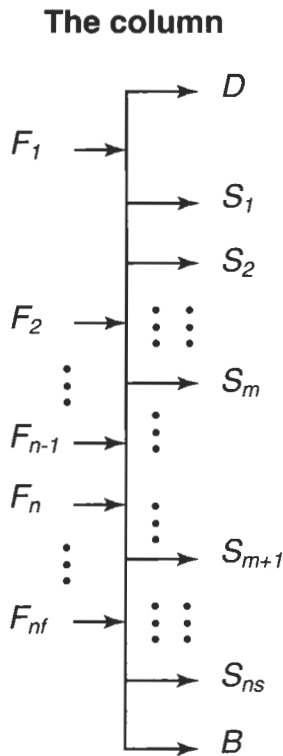
In summary, the calculation procedure is as presented by the authors:

For the systems rated above, the minimum reflux ratio is [96]:

$$R_{min} = R_F + R_{OF} + R_S \tag{8-153}$$

$$R_{min} = R_F + \sum F_{FR,j} F_j + \sum F_{SR,k} S_k \tag{8-154}$$

This includes recognizing the contribution from the feed (R_F), "other feeds" (R_{OF}), and sidestreams (R_S). The R_F portion is determined assuming no other feeds or side-streams are present. The R_{OF} and R_S parts represent the summation of the contributions of other feeds and side-streams to the overall column minimum reflux ratio. The calculation sequence consists basically of three steps, here reproduced by permission of Chemical Engineering, Chou and Yaws, April 25, 1988, all rights reserved [96]:



1. Determine Underwood θ for each feed, using equation involving feed concentration:
 $\theta_1, \theta_2, \dots, \theta_{nf}$

$$1 - q_{Fn} = \sum_{i=1}^c \frac{\alpha_i Z_i F_n}{\alpha_i - \theta_n} \tag{8-155}$$

2. Determine the "minimum reflux ratio" candidate for each feed:
 $R_{min,1}, R_{min,2}, \dots, R_{min,nf}$

$$R_{min,n} = R_F + R_{OF} + R_S = R_{F,n} + \sum_{j=1}^{n-1} F_{FR,j} F_j + \sum_{k=1}^m F_{SR,k} S_k \tag{8-156}$$

where: $R_{F,n} = \sum_{i=1}^c \frac{\alpha_i x_{i,D}}{\alpha_i - \theta_n} - 1$

$$F_{FR,j} = -\frac{1}{D} \left(\sum_{i=1}^c \frac{\alpha_i Z_i F_j}{\alpha_i - \theta_n} + q_{Fj} - 1 \right)$$

$$F_{SR,k} = \frac{1}{D} \left(\sum_{i=1}^c \frac{\alpha_i Z_{i,Sk}}{\alpha_i - \theta_n} + q_{Sk} - 1 \right)$$

3. Compare the candidates for minimum reflux ratio. The candidate having the largest (maximum) numerical value is the minimum reflux ratio for the column.
 $R_{min} = \text{Max} (R_{min,1}, R_{min,2}, \dots, R_{min,nf})$

Example 8-26: Distillation With Two Sidestream Feeds

Data for Example 8-26, which includes two sidestreams

Component	Relative Volatility α	Mole Fraction				
		Feed		Distillate	Sidestream	
		z_i, F_1	z_i, F_2	x_D	z_i, S_1	z_i, S_2
1 (LK)	2.0	.58	.45	.999	.975	.900
2 (HK)	1.0	.20	.30	.001	.025	.099
3 (HK + 1)	0.5	.22	.25	0	0	.001

Feeds: $F_1 = 50$ mol/hr, $q_{F1} = 1$ (saturated liquid)
 $F_2 = 100$ mol/h, $q_{F2} = 0$ (saturated vapor)

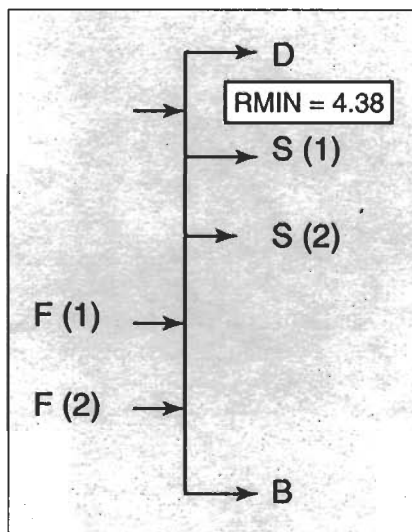
Sidestreams: $S_1 = 20$ mol/h, $q_{S1} = 1$ (saturated liquid)
 $S_2 = 20$ mol/h, $q_{S2} = 1$ (saturated liquid)

Distillate: $D = 36$ mol/h

Minimum reflux and other results for Example 8-26

1. UNDERWOOD THETAS:
 FOR FEED 1 THETA (1) = 1.164
 FOR FEED 2 THETA (2) = 1.485
2. MINIMUM REFLUX CANDIDATES:
 FOR FEED 1 RMIN (1) = 3.450271
 FOR FEED 2 RMIN (2) = 4.375502
3. TRUE MINIMUM REFLUX RATIO:
 RMIN = 4.38

Column representation of results of Example 8-26



where B = bottoms flowrate, mol/h
 c = number of components
 D = distillate flowrate, mol/h
 F = flowrate of feed, mol/h
 F_j = flowrate of feed j , mol/h
 F_{FR} = factor for contribution of other feed flow to minimum reflux
 F_{FRj} = factor for contribution of feed j flow to minimum reflux
 F_{SR} = factor for contribution of sidestream flow to minimum reflux
 $F_{SR,k}$ = factor for contribution of sidestream k flow to minimum reflux
 HK = heavy key component
 L = liquid flowrate, mol/h
 LK = light key component
 nf = number of feeds
 ns = number of sidestreams
 m = number of sidestreams above feed n
 q_F = thermal condition of feed
 q_S = thermal condition of sidestream
 R = reflux ratio
 R_F = feed component of minimum reflux
 $R_{F,n}$ = feed component of minimum reflux for feed n
 R_{OF} = other-feeds component of minimum reflux
 R_{min} = minimum reflux ratio
 R_S = sidestream component of minimum reflux
 S = flowrate of sidestream, mol/h
 S_k = flowrate of sidestream k , mol/h
 V = vapor flowrate, mol/h
 x_i = mole fraction of component i in liquid
 y_i = mole fraction of component i in vapor
 $z_{i,F}$ = mole fraction of component i in feed
 $z_{i,Fj}$ = mole fraction of component i in feed j
 $z_{i,S}$ = mole fraction of component i in sidestream
 $z_{i,Sk}$ = mole fraction of component i in sidestream k
 α = relative volatility
 θ = underwood parameter

Subscripts

B = bottoms
 D = distillate
 F = feed
 F_j = feed j
 F_n = intermediate feed

Theoretical Trays at Operating Reflux

The method of Gilliland [23] (Figure 8-24) is also used for multicomponent mixtures to determine theoretical trays at a particular operating reflux ratio, or at various ratios.

The Brown and Martin [9] curve of Figure 8-49 is also used in about the same manner, and produces essentially the same results, but is based on internal vapor and liquid flows.

The values needed to use the graph include:

$$(L/V)_r = \frac{1}{1 + (D/L)} \quad (8-158)$$

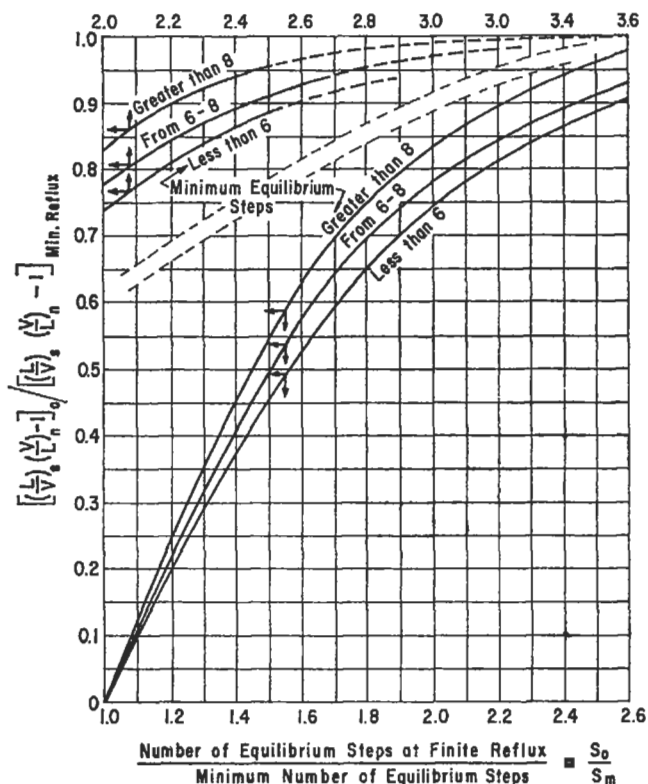


Figure 8-49. Brown and Martin: operating reflux and stages correlated with minimum reflux and stages. Used and adapted by permission, Van Winkle, M., *Oil and Gas Jour.* V. 182, Mar. 23 (1953).

where $(D/L) = 1/(L/D)$

$$L_s = L_r + qF \quad (8-159)$$

$$L_r = (L/D) (D_r) \quad (8-160)$$

$$V_s = V_r - F(1 - q) \quad (8-161)$$

Note that when $(L/D)_{min}$ is used as the starting basis, the L_r , L_s , V_r , V_s and their ratios will be for the minimum condition, and correspondingly so when the operating reflux is used.

The combined Fenske-Underwood-Gilliland method developed by Frank [100] is shown in Figure 8-47. This relates product purity, actual reflux ratio, and relative volatility (average) for the column to the number of equilibrium stages required. Note that this does not consider tray efficiency, as discussed elsewhere. It is perhaps more convenient for designing new columns than reworking existing columns, and should be used only on adjacent-key systems.

Eduljee [107] evaluated published data and corrected relationships for determining the number of actual trays versus actual reflux with reasonably good agreement:

First Trial:

when $1.1 < R/R_m \leq 2.0$

$$(S/S_m) (R/R_m) = 2.82$$

when $R/R_m > 2.0$

$$(S/S_m) (R/R_m) = 0.7 + 1.06 (R/R_m) \quad (8-162)$$

If the number of actual trays, S , calculates to be 27 or greater, then revert to the following for better accuracy:

Second Trial:

when $1.1 < R/R_m \leq 2.0$

$$S = 2.71 (R_m/R) (S_m) + 0.38 \quad (8-163)$$

when $R/R_m > 2.0$

$$S = [0.67 (R_m/R) + 1.02] (S_m) + 0.38 \quad (8-164)$$

where n = number of theoretical trays in the rectifying section

R = reflux ratio (O/D)

S = number theoretical trays in the column, including reboiler

Subscript

m = minimum

The feed plate location, for either rectifying or stripping sections:

For R/R_m from 1.2 to 3.6:

$$(n/n_m) (R/R_m) = 1.1 + 0.9 (R/R_m) \quad (8-165)$$

Hengstebeck [224] presents a technique for locating the feed tray by plotting.

Example 8-27: Operating Reflux Ratio

The minimum reflux ratio $(L/D)_{\min}$ has been determined to be 1.017. Using the Brown and Martin graph [9], evaluate the theoretical number of trays at an operating reflux of 1.5 times the minimum. The minimum number of stages was determined to be 22.1 including the reboiler. See Figure 8-49.

The column will have a total condenser. Product rate D is 0.664 mols/mol feed, and the feed is a boiling point liquid.

Minimum values:

$$\left(\frac{L}{V}\right)_{\min} = \frac{1}{1 + (D/L)_{\min}} = \frac{1}{1 + 1/1.017} = 0.506$$

$$0.506 V_r = 1.017 (D_r) = 1.017 (0.664)$$

$$V_r = 1.332 \text{ mols per mol of feed}$$

$$L_r = 1.017 (0.664) = 0.674 \text{ mols/mol feed}$$

$$q = 1.0$$

$$L_s = (0.674) + (1) (1) = 1.674 \text{ mols/mol feed}$$

$$V_s = 1.332 - (1) (1 - 1) = 1.332 \text{ mols/mol feed}$$

$$\left(\frac{L}{V}\right)_s = \frac{1.674}{1.332} = 1.255$$

Operating values:

$$\text{Operating } (L/D)_o = (1.5) (1.017) = 1.525$$

$$\left(\frac{L}{V}\right)_o = \frac{1}{1 + 1/1.525} = 0.603$$

$$V_r = \frac{(1.525)(0.664)}{0.603} = 1.68 \text{ mols/mol feed}$$

$$L_r = (1.525) (0.664) = 1.013 \text{ mols/mol feed}$$

$$q = 1.0$$

$$L_s = 1.013 + (1) (1) = 2.013$$

$$V_s = 1.68 - (1) (1 - 1) = 1.68$$

$$(L/V)_s = 2.013/1.68 = 1.198$$

For graph:

$$\left[\left(\frac{L}{V}\right)_s \left(\frac{V}{L}\right)_r - 1\right]_o = 1.198 \left(\frac{1}{0.603}\right) - 1 = 0.985$$

$$\left[\left(\frac{L}{V}\right)_s \left(\frac{V}{L}\right)_r - 1\right]_{\min} = (1.255) \left(\frac{1}{0.506}\right) - 1 = 1.48$$

Read curve for "greater than 8" minimum equilibrium steps:

$$\text{at } 0.985/1.48 = 0.666$$

$$\text{Curve reads: } S_o/S_M = 1.64$$

$$\text{Theoretical stages at reflux } (L/D) = 1.525$$

$$S_o = S_M (1.64) = 22.1 (1.64)$$

$$S_o = 36.2 \text{ stages}$$

$$\text{Theoretical trays at the operating reflux } (L/D) = 1.525$$

$$N_o = 36.2 - 1 \text{ (for reboiler)} = 35.2 \text{ trays in column}$$

Actual Number of Trays

From the theoretical trays at operating reflux the actual trays for installation are determined:

$$N_{\text{act}} = N_o/E_o \quad (8-166)$$

The reboiler is considered 100% efficient, and likewise any partial condenser, if used. Therefore the value N_o represents the *theoretical* trays or stages in the column proper, excluding the reboiler and partial condenser. E_o represents the overall tray efficiency for the system based upon actual test data of the same or similar systems, or from the plot of Figure 8-29, giving operating information preference (if reliable).

Feed Tray Location

The approximate location can be determined by the ratio of the total number of theoretical stages above and below the feed plate from the Fenske total reflux relation:

$$\frac{S_r}{S_s} = \frac{n+1}{m+1} = \frac{\log(x_1/x_h)_D (x_h/x_1)_F}{\log(x_1/x_h)_F (x_h/x_1)_B} \quad (8-167)$$

The relation is solved for S_r/S_s . The results are not exact, because the feed tray composition is very seldom the same as the feed; which is the assumption in this relation. Actually, the feed point or correct location for the feed may be off by two or three theoretical trays. This will vary with the system. It does mean, however, that when this approach is used for feed plate location, alternate feed nozzles should be installed on the column to allow for experimental location of the best feed point. These extra nozzles are usually placed on alternate trays (or more) both above and below the calculated location. A minimum of three alternate nozzles should be available.

When the feed point is located by a match from tray-by-tray calculation, the correct point can be established with greater confidence, but still alternate nozzles are suggested since even these detailed calculations can be off to a certain extent.

The actual number of trays in the rectifying section $(N_{\text{act}})_r$ can be determined by:

$$S_M = S_r + S_s \quad (8-168)$$

$$S_M = S_s (S_r/S_s) + S_s$$

Solve for S_s , because S_M and S_r/S_s are known.

Obtain S_r by difference.

$$(N_{\text{act}})_r = \frac{S_r}{E_o} \quad (\text{for total condenser; if partial condenser use } (S_r - 1)/E_o)$$

$$(N_{\text{act}})_s = (S_s - 1)/E_o \quad (\text{for columns with reboilers}) \quad (8-169)$$

For systems with wide variation in relative volatility, the suggestion of Cicalese, et al. [9] is often used to evaluate the theoretical total equilibrium stages in the rectifying and stripping sections:

$$S_r = \frac{\log \frac{(x_1/x_h)_D}{(x_1/h_h)_F}}{\log \alpha \text{ (average above feed)}} \quad (8-170)$$

$$S_s = \frac{\log \frac{(x_1/h_h)_F}{(x_1/x_h)_B}}{\log \alpha \text{ (average below feed)}} \quad (8-171)$$

where S_r = number theoretical trays/plates in rectifying section

S_s = number theoretical trays/plates in stripping section

Maas [108] presents a useful analysis for selecting the feed tray in a multicomponent column. For accuracy it involves the use of a tray-by-tray computer calculation.

Kirkbride's [174] method for estimating the ratio of theoretical trays above and below the feed tray allows estimation of the feed tray location:

$$\log \frac{(N_n)}{(N_m)} = 0.206 \log \left[\frac{W}{D} \left(\frac{x_{hF}}{x_{lF}} \right) \left(\frac{x_{lW}}{x_{hD}} \right)^2 \right] \quad (8-172)$$

where N_n = number of trays above feed tray

N_m = number of trays below feed tray

D = mols per hour of overhead product

W = mols per hour of bottoms product

Subscripts

h = heavy key

l = light key

F = feed

W = bottoms

D = overhead

Estimating Multicomponent Recoveries

Yaws et al. [141] present a useful technique for estimating overhead and bottoms recoveries with a very good comparison with tray-to-tray computer calculations. The procedure suggested uses an example from the reference with permission:

1. Plot relative volatility (α_i) and % desired recovery for LK and HK. Draw a straight line through these two points. The non-key component points will also be on this straight line.

2. Using α_i and the component distribution line, estimate % recovery of non-key components in distillate and bottoms.

From the references [124, 141]:

$$\log (d_i/b_i) = a + b \log \alpha_i \quad (8-173)$$

where d_i = mols of component i in distillate
 b_i = moles of component i in bottoms
 α_i = relative volatility of component i
 a, b = correlation constants

$\log (d_i/b_i)$ vs. $\log \alpha_i$ gives a straight line (Figure 8-50). By superimposing a Y_{iD} scale over the d_i/b_i scale,

$$d_i/b_i = Y_{iD}/Y_{iB}$$

where Y_{iD} = % recovery of i in distillate

Y_{iB} = % recovery of i in bottoms

f_i = total mols of component i in distillate and bottoms

$$\text{Then } Y_{iB} = 100 - Y_{iD} \quad (8-174)$$

$$\text{and } d_i/b_i = Y_{iD}/(100 - Y_{iD}) \quad (8-175)$$

From Equation 8-174, Table 8-5 is constructed for selected values of d_i/b_i at various values of Y_{iD} from 99.9% to 0.1%.

Component Recovery Nomograph (Figure 8-50)

A nomograph is constructed by plotting d_i/b_i vs. α_i on log-log graph paper and then superimposing a Y_{iD} scale over the d_i/b_i scale, according to the values given in Table

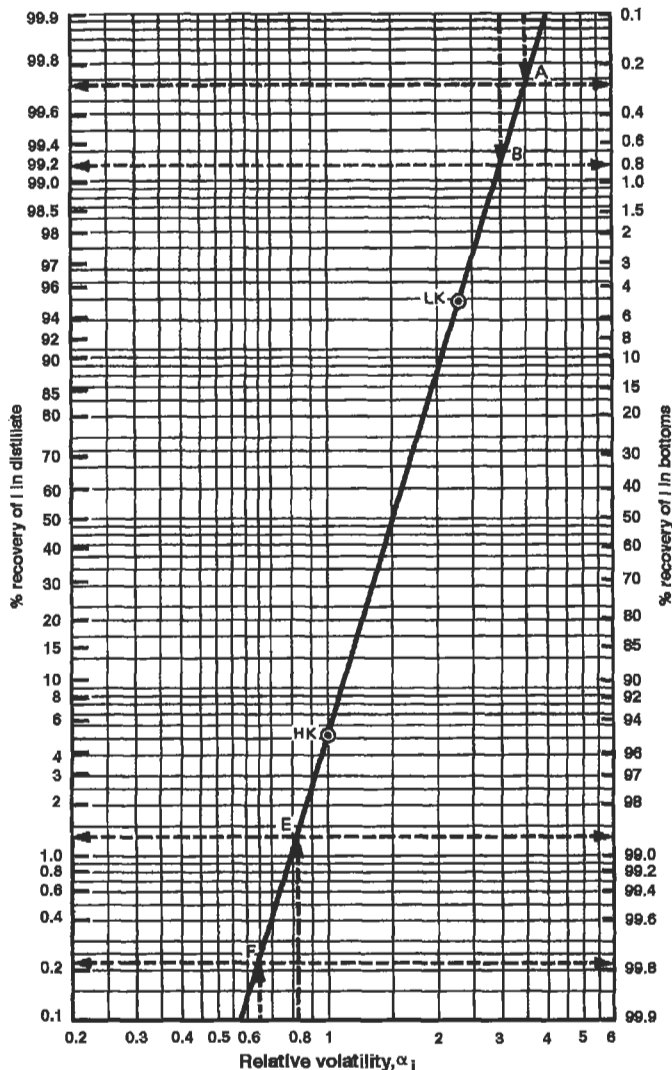


Figure 8-50. Estimation of recovery of non-key components using short-cut method of Yaws, et al. Used by permission, Yaws, C. L. et al., *Chem. Eng.*, Jan. 29 (1979), p. 101.

Table 8-5
Material Balance for Estimated Multicomponent Distillation Recoveries for Example 8-28 Using Method of Yaws, Fang, and Patel

Feed Component	Composition, Mol. Fr.	Relative Volatility	Keys
A	0.05	3.5	
B	0.20	3.0	
C	0.30	2.3	Light
D	0.25	1.0	Heavy
E	0.15	0.83	
F	0.05	0.65	

Distillate Component	Recovery Desired, %	Recovery Derived, %*
A		99.72**
B		99.20**
C	95	—
D	5	—
E		1.30**
F		0.22*

Bottoms Component	Recovery Desired, %	Recovery Derived, %*
A		0.28**
B		0.80**
C	5	—
D	95	—
E		98.70**
F		99.78**

*See calculations

**From Figure 8-50

Used by permission, Yaws, C. L., et al., *Chem. Eng.*, Jan. 29 (1979), p. 101, all rights reserved.

8-6. The resulting nomograph, relating component recovery and component relative volatility, is given in Figure 8-51. This may be used to estimate component recovery in distillate and bottoms, as follows:

Example 8-28: Estimated Multicomponent Recoveries by Yaws' Method [141] (used with permission)

Component C is to be separated from Component D by distillation. A 95% recovery of both key components (LK, HK) is desired. Saturated-liquid feed composition and relative volatilities (at average column conditions) are given in Table 8-5.

Using the graphical short-cut method for component distribution, estimate the recovery of non-key components in distillate and bottoms.

Solution:

- α_i and % desired recovery are plotted for LK and HK ($\alpha_C = 2.3$, 95% recovery of C in distillate and $\alpha_D = 1$, 95% recovery of D in bottoms), as shown in Figure 8-50. See Figure 8-51 for working chart. A straight line is then drawn through the two points.
- Using $\alpha_A = 3.5$, $\alpha_B = 3.0$, $\alpha_E = 0.83$, $\alpha_F = 0.65$, and the component distribution line, the recovery of non-key components is estimated. The results are shown in Table 8-6.

Component	Recovery in distillate, %	Recovery in bottoms, %	Remarks
A	99.72	0.28	Graph
B	99.20	0.80	Graph
C (LK)	95	5	Specified
D (HK)	5	95	Specified
E	1.3	98.7	Graph
F	0.22	99.78	Graph

Table 8-6
Table of Y_{iD} Values for Solving Yaws, Fang, and Patel Short Cut Recoveries Estimate

Y_{iD}	d_i/b_i	Y_{iD}	d_i/b_i	Y_{iD}	d_i/b_i	Y_{iD}	d_i/b_i
99.9	999	96	24.0	40	0.6670	2	0.02040
99.8	499	94	15.7	30	0.4290	1.0	0.01010
99.6	249	92	11.5	20	0.2500	0.8	0.00806
99.4	166	90	9.00	15	0.1760	0.6	0.00604
99.2	124	85	5.67	10	0.1110	0.4	0.00402
99.0	99.0	80	4.00	8	0.0870	0.2	0.00200
98.5	65.7	70	2.33	6	0.0638	0.1	0.00100
98.0	49.0	60	1.50	4	0.0417		
97.0	32.3	50	1.00	3	0.0309		

Used by permission, Chem. Eng., Yaws, C. L., et al Jan. 29 (1979), p. 101, all rights reserved.

Table 8-7 [141] illustrates the good agreement between the proposed method with the tray-to-tray calculations for Case I-High Recovery: 95% LK recovery in distillate, 94% HK in bottoms; Case II, Intermediate Recovery: 90% LK recovery in distillate, 85% HK recovery in bottoms; and Case III Low Recovery: 85% LK recovery in distillate, 81% HK recovery in bottoms.

Tray-by-Tray

Rigorous tray-by-tray computations for multicomponent mixtures of more than three components can be very tedious, even when made omitting a heat balance. Computers are quite adaptable to this detail and several computation methods are in use.

The direct-solution method of Akers and Wade [1] is among several which attempt to reduce the amount of trial-and-error solutions. This has been accomplished and has proven quite versatile in application. The adaptation outlined modifies the symbols and rearranges some terms for convenient use by the designer [3]. Dew point and bubble point compositions and the plate temperatures can be determined directly. Constant molal overflow is assumed, and relative volatility is held constant over sections of the column.

Rectifying section: reference component is heavy key, x_{h1}

Table 8-7
Comparison of Yaws, et al. Short Cut Nomograph Results vs. Plate-to-Plate Calculations

	Component	Nomograph	Composition X_i		
			Plate to plate	Distillate	Bottoms
Case I	A	0.0901	0.0901	0.0002	0.0002
High	B	0.3588	0.3591	0.0026	0.0023
recovery	C (LK)	0.5197	0.5190	0.0269	0.0278
(16 trays)	D (HK)	0.0271	0.0271	0.5271	0.5271
	E	0.0041	0.0045	0.3314	0.3308
	F	0.0002	0.0002	0.1118	0.1118
Case II	A	0.0879	0.0880	0.0016	0.0012
Inter-	B	0.3466	0.3464	0.0128	0.0120
mediate	C (LK)	0.4814	0.4770	0.0683	0.0726
recovery	D (HK)	0.0668	0.0682	0.4839	0.4835
(13 trays)	E	0.0155	0.0187	0.3218	0.3187
	F	0.0018	0.0018	0.1116	0.1120
Case III	A	0.0866	0.0872	0.0034	0.0028
Low	B	0.3376	0.3395	0.0250	0.0227
recovery	C (LK)	0.4561	0.4552	0.1015	0.1027
(9 trays)	D (HK)	0.0844	0.0839	0.4606	0.4610
	E	0.0308	0.0295	0.3016	0.3031
	F	0.0045	0.0046	0.1079	0.1077

Used by permission, Chem. Eng., Yaws, C. L., et al Jan. 29 (1979), p. 101, all rights reserved.

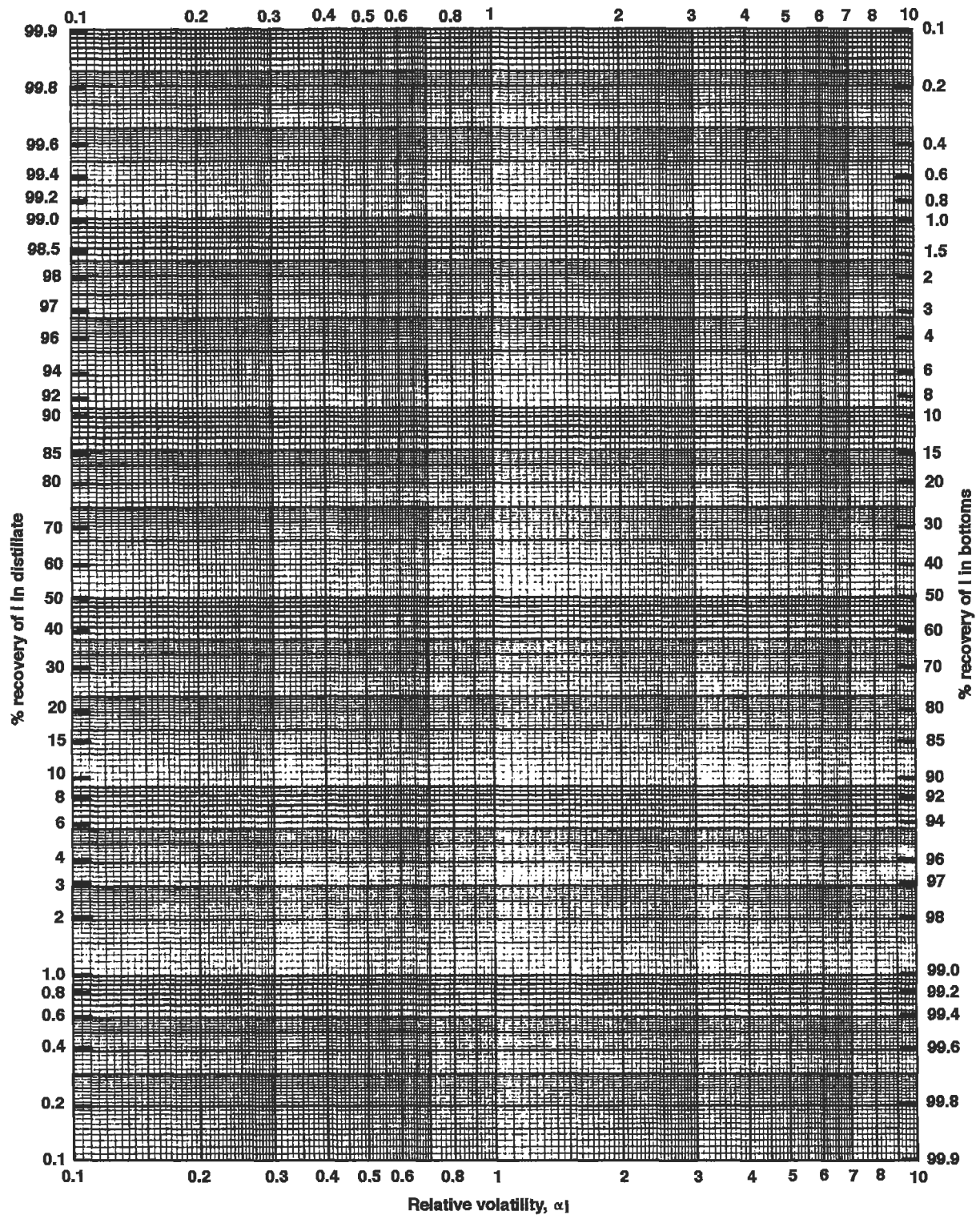


Figure 8-51. Working chart for Yaws, et. al short-cut method for multicomponent distillation for estimating component recovery in distillate and bottoms. Used by permission, Yaws, C. L. et al., *Chem. Eng.*, Jan. 29 (1979), p. 101.

$$\left(\frac{x_i}{x_h}\right)_n = \frac{1}{\alpha_i} \left[\frac{(L/D)(x_i)_{n+1} + x_{Di}}{(L/D)(x_h)_{n+1} + x_{Dh}} \right] \quad (8-176)$$

$\Sigma x_i = 1.0$ (Including x_h)

$$\Sigma \left(\frac{x_i}{x_h}\right)_n = \left(\frac{1}{x_h}\right)_n$$

The compositions of each component are obtained from the $(x_i/x_h)_n$ ratio.

The tray temperature is obtained from:

$$K_h = \frac{1}{\Sigma \alpha_i x_i} \quad (8-177)$$

K_h is evaluated at the column pressure by use of suitable K charts.

Stripping section: reference component is heavy key, x_h, y_h .

$$\left(\frac{y_i}{y_h}\right)_m = \alpha_i \left[\frac{(V_s/B)(y_i)_{m-1} + x_{Bi}}{(V_s/B)(y_h)_{m-1} + x_{Bh}} \right] \quad (8-178)$$

$\Sigma (y_i/y_h)_m = 1.0$ (including y_b)

The composition of each component on a tray is obtained from $(y_i/y_h)_m$.

The tray temperature is obtained from:

$$K_h = \Sigma y_i / \alpha_i \quad (8-179)$$

at the column pressure using K charts for the heavy key or reference component.

Procedure:

A. Rectifying Section

- Determine material balance around column, including reflux L, distillate product D, bottoms product B.
 - With total condenser, the reflux composition is equal to the condensed distillate product composition.
 - With a partial condenser, the product D is a vapor, so a dew point must be run on its composition to obtain the liquid reflux composition.
- Determine top tray temperature for use in relative volatility calculations by running a dew point on the overhead vapor. For total condenser its composition is same as distillate product. For a partial condenser, run a dew point on the column overhead vapor composition as determined by a material balance around the partial condenser, reflux, and product.

- Determine $(x_i/x_h)_2$, for tray No. 2 (second from top), for each component, using the x values for the reflux as the initial x_i ($n + 1$).
- Total this column to yield $\Sigma(x_i/x_h)$. This equals $1/x_h$.
- Determine x_i for each component by:

$$x_i = \frac{(x_i/x_h)}{\Sigma (x_i/x_h)} \quad (8-180)$$

This is liquid composition on tray.

- Continue down column using the composition calculated for tray above to substitute in Equation 8-176 to obtain the (x_i/x_h) for the tray below.
- Test to determine if α is varying to any great extent by calculating $\alpha_i x_i$ for a test tray. $\Sigma \alpha_i x_i = 1/K_h$. Determine temperature and evaluate corresponding values. Use new α_i if significantly different.
- Continue step-wise calculations until the ratio of light to heavy key on a tray equals (or nearly so) that ratio in the liquid portion of the feed. This is then considered the feed tray.
- If there are components in the feed and bottoms which do not appear in the overhead product, they must gradually be introduced into the calculations. The estimated position above the feed tray to start introducing these components is determined by:

$$\frac{x_{Fi}}{x_a} = \left[\frac{1}{(1 + D/L) K_i} \right]^{p''} \quad (8-181)$$

where x_{Fi} = mol fraction of a component in feed that does not appear in overhead

x_a = small arbitrary mol fraction in the liquid p'' plates above the feed plate

p'' = number of plates above the feed where introduction of components should begin

B. Stripping Section:

- Determine bubble point temperature of bottoms and composition of vapor, y_{Bi} , up from liquid. Calculate relative volatility of light to heavy component at this temperature.
- From these calculate vapor compositions, using Equation 8-178 calculate the ratio (y_i/y_h) for the first tray at the bottom.
- Total $\Sigma (y_i/y_h)$ to obtain $1/y_h$
- Calculate y_i for tray one

$$y_i = \frac{(y_i/y_h)}{\Sigma y_i/y_h}, \quad \Sigma y_i/y_h = 1/y_h \quad (8-182)$$

$\Sigma y_i = 1.0$

5. Calculate (y_i/y_h) for next tray, using the y_i values of tray one $(m - 1)$ in the equation to solve for $(y_i/y_h)_m$.
6. Test to determine if α is varying significantly by $K_h = \Sigma (y_i/\alpha_i)$. Evaluate temperature of heavy component at the column bottoms pressure (estimated) using K charts or the equivalent. If necessary, calculate new α_i values for each component at the new temperature. Recheck every two or three trays if indicated.
7. Introduce components lighter than the light key which are not found in the bottoms in the same general manner as discussed for the rectifying section.

$$x_{Fi}/x_a = [(1 + D/L)K_i]^{p'} \quad (8-183)$$

where p' is the number of trays below the feed tray where the component, i , is introduced in an assumed amount (usually small) x_a . Then x_{Fi} is the mol fraction of the component in the feed.

8. Continue step-wise calculations until ratio of light to heavy keys in the liquid portion of the feed essentially matches the same component ratio in the liquid on one of the trays.
9. The total of theoretical trays in the column is the sum of those obtained from the rectifying calculations, plus those of the stripping calculations, plus one for the feed tray. This does not include the reboiler or partial condenser as trays in the column.

Tray-by-Tray: Using a Digital Computer

Multicomponent distillation is by far the common requirement for process plants and refineries, rather than the simpler binary systems. There are many computer programs which have been developed to aid in accurately handling the many iterative calculations required when the system involves three to possibly ten individual components. In order to properly solve a multicomponent design, there should be both heat and material balance at every theoretical tray throughout the calculation.

To accommodate the step-by-step, recycling and checking for convergences requires input of vapor pressure relationships (such as Wilson's, Renon's, etc.) through the previously determined constants, latent heat of vaporization data (equations) for each component (or enthalpy of liquid and vapor), specific heat data per component, and possibly special solubility or Henry's Law deviations when the system indicates.

There are several valuable references to developing and applying a multicomponent distillation program, including Holland [26, 27, 169], Prausnitz [52, 53], Wang and Henke [76], Thurston [167], Boston and Sullivan [6], Maddox and Erbar [115], and the pseudo-K method of Maddox and Fling [116]. Convergence of the iterative trials to reach a criterion requires careful evaluation [114]. There are sever-

al convergence techniques with some requiring considerably less computer running time than others.

Example 8-29: Tray-to-Tray Design Multicomponent Mixture

A column is to be designed to separate the feed given below into an overhead of 99.9 mol % trichloroethylene. The top of the column will operate at 10 psig. Feed temperature is 158°F.

Feed	Mol Fraction	Overhead		Bottoms	
		Mols	Mol Fraction	Mols	Mol Fraction
(A) Trichloroethylene	0.456	0.451	0.999	0.00549	0.010
(B) β Trichloroethane	0.0555	0.00045	0.001	0.05505	0.101
(C) Perchloroethylene	0.3625	0.36250	0.661
(D) Tetras (1)	0.0625	0.0625	0.114
(E) Tetras (2)	<u>0.0635</u>	<u>0.0625</u>	<u>0.114</u>
	1.0000	0.45145	1.000	0.54804	1.000

Note: the material balance for overhead and bottoms is based on:

- (a) 99.9 mol % trichlor in overhead
- (b) 1.0 mol % trichlor in bottoms
- (c) 1.0 mol feed total
- (d) Light key = trichloroethylene
Heavy key = β trichloroethane

Determine Overhead Temperature

Because trichlor is 99.9% overhead, use it only to select boiling point from vapor pressure curves at 10 psig overhead pressure = 223°F (1,280 mm Hg abs).

Determine Bottoms Temperature (Bubble Point)

Allowing 10 psig column pressure drop, bottoms pressure = 20 psig (1,800 mm Hg abs)

Component	x_{iB}	Try $t = 320^\circ\text{F}$ Vapor Press.		
		mm Hg	x_i (vp.)	$(y_i)_B$
A	0.01	4,500	45	0.0249
B	0.101	2,475	250	0.1382
C	0.661	1,825	1,210	0.67
D	0.114	1,600	183	0.1012
E	0.114	1,050	<u>120</u>	<u>0.0664</u>
			1,808	1.0007
			mm Hg abs.	

This compares quite well with the selected 1,800 mm bottoms pressure. Bottoms temperature is 320°F.

Relative Volatilities: Light to Heavy key

$$\text{At top: } \alpha = \frac{\text{v.p. Tri}}{\text{v.p. } \beta \text{ Tri}} = \frac{1280}{600} = 2.13$$

$$\text{At bottoms: } \alpha = \frac{\text{v.p. Tri}}{\text{v.p. } \beta \text{ Tri}} = \frac{4500}{2275} = 1.98$$

$$\alpha \text{ (average)} = [(2.13)(1.98)]^{1/2} = 2.06$$

Minimum Stages at Total Reflux

$$\begin{aligned} S_M = N_{\min} + 1 &= \frac{\log(x_{Dl}/x_{Dh})(x_{Bh}/x_{Bl})}{\log \alpha_{\text{avg}}} \\ &= \frac{\log(0.999/0.001)(0.101/0.01)}{\log 2.06} \\ &= \frac{4.003}{0.318} = 12.6 \text{ theoretical stages} \end{aligned}$$

Minimum Stages Above Feed:

$$\begin{aligned} S_r &= \frac{\log(0.999/0.001)(0.0555/0.456)}{\log 2.13} \\ &= \frac{2.082}{0.328} = 6.35 \text{ theoretical stages} \end{aligned}$$

Thermal Condition of Feed

Feed temperature = 158°F

Calculated bubble point of feed = 266°F at assumed feed tray pressure of 15 psig.

$$q = \frac{\text{Heat to bring feed to boiling point} + \text{Heat to vaporize feed}}{\text{Latent Heat of one mol of feed}}$$

q = 1.298 (Calculations not shown, but handled in same manner as for example given in binary section, however all feed components considered, not just keys.)

Minimum Reflux—Underwood Method, Determination of α Avg.

Assume pinch temperatures (usually satisfactory because α does not vary greatly) at $1/2$ and $3/4$ of over-all column temperature differences.

Lower pinch = $320 - 1/2(320 - 223) = 288^\circ\text{F}$

Upper pinch = $320 - 3/4(320 - 223) = 255^\circ\text{F}$

Component	@255°F		@288°F		α_i (avg)
	v.p.	α	v.p.	α	
A	2050	2.00	3050	1.91	1.955
B	1025	1.00	1600	1.00	1.00
C	750	0.732	1180	0.737	0.735
D	650	0.634	1035	0.647	0.641
E	390	0.380	650	0.406	0.393

To start, assume $\theta = 1.113$ (it must lie between 1.00 and 1.955).

Component	x_{Fi}	$\alpha_i x_{Fi}$	$(\alpha_i - \theta)$	$\frac{\alpha_i x_{Fi}}{(\alpha_i - \theta)}$	$\frac{\alpha_i x_{Fi}}{(\alpha_i - \theta)^2}$
A	0.456	0.891	0.842	1.058	1.252
B	0.0555	0.0555	-0.113	-0.491	4.33
C	0.3625	0.266	-0.378	-0.704	1.86
D	0.0625	0.0401	-0.472	-0.085	0.18
E	0.0625	0.0246	-0.720	-0.0342	0.0472
			$\Sigma = -0.2562$		$\Sigma 7.669$

$$\theta_c = 1.113 - (-0.2562/7.669) = 1.113 + 0.0334$$

$\theta_c = 1.146$ (this is close enough check to original, to not require recalculation.)

The correct value of 1.146 should be used.

Check for balance:

$$1 - q = \sum \frac{x_{Fi}}{1 - \theta/\alpha_i} = \sum \frac{\alpha_i x_{Fi}}{\alpha_i - \theta} = -0.256$$

$$1 - 1.298 = -0.298 = -0.256$$

This could be corrected closer if a greater accuracy were needed. This is not as good a match as ordinarily desired.

$$(L/D)_{\min} + 1 = \frac{(\alpha_a x_a)_D}{\alpha_a - \theta} + \frac{(\alpha_b x_b)_D}{\alpha_b - \theta}$$

(for all distillate components)

$$(L/D)_{\min} + 1 = \frac{(1.955)(0.999)}{(1.955 - 1.146)} + \frac{1.00(0.001)}{(1.00 - 1.146)}$$

$$= 2.41 + (-0.00685)$$

$$= 2.404$$

$$(L/D)_{\min} = 2.404 - 1.0 = 1.40$$

Operating Reflux and Theoretical Trays—Gilliland Plot

Min trays = $S_M = 12.6$

$$(L/D)_{\min} = 1.4$$

Assume $(L/D)_o$	$\frac{(L/D)_o - (L/D)_M}{(L/D)_o + 1}$	Read: $S - S_M/(S + 1)$	Theo Stages S
1.4	0	∞	∞
1.6	0.0768	0.546	29
2.0	0.20	0.445	23.5
3.0	0.40	0.312	18.8
4.0	0.52	0.245	17
∞	—	—	12.6

These values are plotted in Figure 8-52. From the curve, the operating $(L/D)_o$ was selected, and the theoretical stages corresponding are 19.

Tray-by-Tray Calculation—Ackers and Wade Method

Rectifying Section, $(L/D)_o = 3:1$

Light key = Trichlor; Heavy key = β Tri

Relative Volatilities to start: Use average of top and feed

	α_{avg}
A	2.05
B	1.00
C	0.734

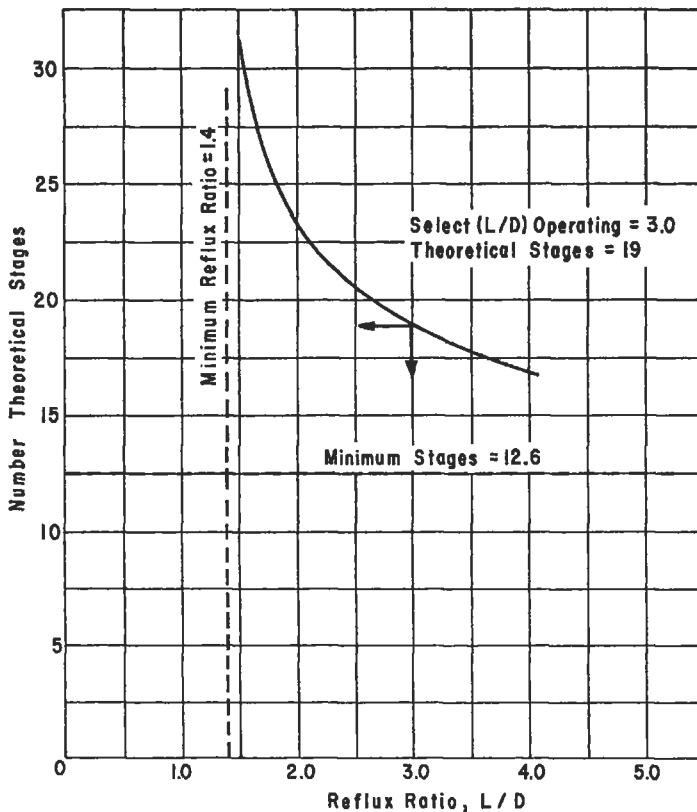


Figure 8-52. Gilliland Plot for multicomponent Example 8-28.

Neglect the heavier than perchlor components in the rectifying section.

In order to carry the perchlor it is assumed at 0.0001 mol fraction in overhead and reflux, the β -Tri is reduced to 0.0005 mol fraction for these calculations being tighter specifications than the initial calculated balance. The overall effect will be small.

Component	$x_{iD} = x_i$ (Reflux)	$(x_i/x_h)_1$	$(x_i)_1$	$(x_i/x_h)_2$	$(x_i)_2$
A	0.9994	975.02	0.9984	545.5	0.9971
B	0.0005	1.00	0.001024	1.0	0.001828
C	0.0001	0.273	0.000280	0.359	0.000656
		$\Sigma = 976.293$	0.999704	546.859	
			(close enough)		

Typical calculations:

$$\left(\frac{x_i}{x_h}\right)_1 = \frac{1}{\alpha_i} \left[\frac{(L/D)(x_i)_{n+1} + x_{Di}}{(L/D)(x_h)_{n+1} + x_{Dh}} \right]$$

For component A: Tray 1

$$\left(\frac{x_i}{x_h}\right)_1 = \frac{1}{2.05} \left[\frac{(3)(0.9994) + 0.9994}{(3)(0.0005) + 0.0005} \right] = 975.02$$

Component B:

$$\left(\frac{x_i}{x_h}\right)_1 = \frac{1}{1.00} \left[\frac{3(0.0005) + 0.0005}{3(0.0005) + 0.0005} \right] = 1.00$$

Component C:

$$\left(\frac{x_i}{x_h}\right)_1 = \frac{1}{0.734} \left[\frac{3(0.0001) + 0.0001}{3(0.0005) + 0.0005} \right] = 0.272$$

$$(x_A)_1 = 975.02/976.293 = 0.9984$$

$$(x_B)_1 = 1.00/976.293 = 0.001024$$

$$(x_C)_1 = 0.273/976.293 = 0.000280$$

Tray 2: Component A

$$\left(\frac{x_i}{x_h}\right)_2 = \frac{1}{2.05} \left[\frac{3(0.9984) + 0.9994}{3(0.00102) + 0.0005} \right] = 545.5$$

Component B

$$\left(\frac{x_i}{x_h}\right)_2 = \frac{1}{1.00} \left[\frac{3(0.00102) + 0.0005}{3(0.00102) + 0.0005} \right] = 1.00$$

Component C

$$\left(\frac{x_i}{x_h}\right)_2 = \frac{1}{0.734} \left[\frac{3(0.00028) + 0.0001}{3(0.0005) + 0.0005} \right] = 0.359$$

	$(x_i/x_h)_3$	$(x_i)_3$	$(x_i/x_h)_4$	$(x_i)_4$	$(x_i/x_h)_5$	$(x_i)_5$
A	325.24	0.9952	200.81	0.9916	126.61	0.9851
B	1.0	0.00306	1.0	0.004938	1.0	0.007781
C	<u>0.514</u>	0.001573	<u>0.682</u>	0.00337	<u>0.908</u>	0.007065
	326.754		202.492		128.518	

	$(x_i/x_h)_6$	$(x_i)_6$	$(x_i/x_h)_7$	$(x_i)_7$	$(x_i/x_h)_8$	$(x_i)_8$
A	80.60	0.9736	52.05	0.9520	33.97	0.9138
B	1.0	0.01208	1.0	0.01829	1.0	0.0269
C	<u>1.213</u>	0.01465	<u>1.633</u>	0.02987	<u>2.21</u>	0.05945
	82.813		54.683		37.18	

	$(x_i/x_h)_9$	$(x_i)_9$	$(x_i/x_h)_{10}$	$(x_i)_{10}$	$(x_i/x_h)_{11}$	$(x_i)_{11}$
A	22.47	0.8491	15.196	0.7501	7.716	0.5421
B	1.0	0.03779	1.0	0.04936	1.0	0.07026
C	<u>2.994</u>	0.1131	<u>4.061</u>	0.2005	<u>5.516</u>	0.3876
	26.464		20.257		14.232	

Ratio of keys in feed = $0.456/0.0555 = 8.2$
 Ratio of keys on Tray No. 10 = $0.7501/0.04936 = 15.2$
 Ratio of keys on Tray No. 11 = $0.5421/0.07026 = 7.7$

Tray No. 11 should be used as feed tray (counting down from the top). Note that since the relative volatility did not change much from top to feed, the same value was satisfactory for the range.

Stripping Section

Determine V_s : per mol of feed

$$(L/V)_r = \frac{1}{1 + D/L} = \frac{1}{1 + \frac{1}{3}} = 0.75$$

$$V_r = \frac{(L/D)D}{(L/V)} = \frac{3(0.45145)}{0.75} = 1.806$$

$$L_r = (L/D)(D) = 3(0.45145) = 1.35 \text{ mols/mol feed}$$

$$L_s = L_r + qF = 1.35 + 1.298(1.0) = 2.648$$

$$V_s = V_r - F(1 - q) = 1.806 - (1.0)(1 - 1.298) = 2.104$$

$$V_s/B = 2.104/0.54804 = 3.84$$

Relative volatilities, α_i , determined at average temperature between bottom and feed of column. Usually the pinch temperature gives just as satisfactory results.

Component	x_{iB}	y_{iB}	$(\alpha_i)_{avg}$	$(y_i/y_h)_1$	$(y_i)_1$	$(y_i/y_h)_2$	$(y_i)_2$
A	0.010	0.0249	1.905	0.319	0.0543	0.552	0.107
B	0.101	0.1382	1.00	1.000	0.170	1.00	0.194
C	0.660	0.6700	0.740	3.800	0.647	3.08	0.597
D	0.114	0.1012	0.648	0.517	0.088	0.389	0.0754
E	0.114	0.0664	0.411	<u>0.241</u>	0.0411	<u>0.1476</u>	0.0286
				5.877		5.1686	

Typical calculations: starting at bottom and working up the column.

Tray 1: Component A

$$(y_i/y_h)_1 = \alpha_i \left[\frac{(V_s/B)(y_i)_{m-1} + x_{Bi}}{(V_s/B)(y_h)_{m-1} + x_{Bh}} \right]$$

$$= 1.905 \left[\frac{(3.84)(0.0249) + 0.010}{3.84(0.1382) + 0.101} \right]$$

$$(y_i/y_h)_1 = 0.319$$

$$(y_i)_1 = 0.319/5.877 = 0.0543$$

Tray 2: Component A

$$(y_i/y_h)_2 = 1.905 \left[\frac{(3.84)(0.0543) + 0.010}{3.84(0.170) + 0.101} \right]$$

$$= 0.552$$

Continuation of the calculations gives an approximate match of ratio of keys in feed to those on plate 10. Then feed tray is number 10 from bottom and this is also number 11 from top.

Liquid mol fraction ratio from vapor mol fraction ratio:

$$(x_i/x_h) = \frac{(y_i/y_h)}{\alpha_{i/h}}$$

$$\text{Ratio on tray no. 9} = 15.018/1.905 = (x_i/x_h) = 7.9$$

$$\text{Ratio on tray no. 10} = 19.16/1.905 = 10.05$$

$$\text{Ratio in feed} = 8.2$$

$$\text{Total theoretical trays} = 11 + 10 - 1 \text{ (common feed tray count)}$$

$$= 20 \text{ not including reboiler}$$

$$\text{Total theoretical stages} = 20 + 1 \text{ (reboiler)} = 21$$

This compares with 19 theoretical stages from Gilliland Plot.

Tray Efficiency

Use average column temperature of 271°F and feed analysis.

Component	x_{iF}	μ, cp	μx_{iF}	vp.	$\alpha_{i/h}$
A	0.456	0.28	0.128	2500	1.94
B	0.0555	0.36	0.020	1290	
C	0.362	0.37	0.134		
D	0.0625	0.40	0.025		
E	0.0625	0.48	<u>0.030</u>		
$\Sigma = 0.337 \text{ cp}$					
$\alpha \Sigma (\mu)(x_{iF}) = 1.94(0.337) = 0.654$					

Using Figure 8-29

Drickamer and Bradford curve, $E_o = 46\%$
 O'Connell curve, $E_o = 53.8\%$

In this case, recommend using:

$$E_o = (46 + 53.8)/2 = 49.6\%$$

Actual trays in column:

$$N_{act} = 20/0.496 = 40.3 \text{ trays}$$

From tray-by-tray calculations, feed tray is $10/0.496 = 20.1$ trays from bottom, use 20.

Generally, practice would be to select a column allowing a few extra trays, making column total trays = 45.

	No.
Rectifying trays	= 22
Feed	= 1
Stripping	= 22
	45

Feed nozzles should be located on trays Nos. 21, 23, and 25 counting up from the bottom tray as No. 1.

Heat Balance—Adjacent Key Systems with Sharp Separations, Constant Molal Overflow

Total Condenser Duty

Refer to Figure 8-53 (System (1)).

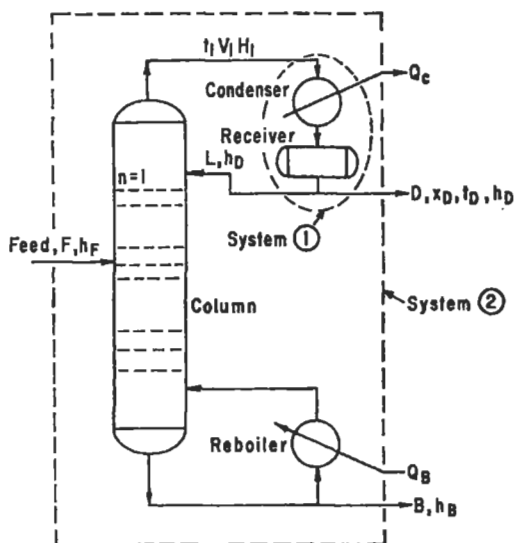


Figure 8-53. Heat balance diagram.

1. Assume or set condenser liquid product temperature, t_D .
2. Calculate condensing pressure, with t_D as bubble point (if subcooling exists, and t_D is below bubble point, use bubble point temperature for pressure calculation only).

$$3. V_1 = L + D$$

$$H_1 V_1 = [L h_D + D h_D] + Q_c \quad (8-184)$$

$$H_1 = \sum_1^I H_{li} y_{li} \text{ at } t_1 \quad (8-185)$$

$$h_D = \sum_1^i h_{Di} x_{Di}$$

$$Q_c = V_1 (H_1 - h_D) \quad (8-186)$$

4. Calculate t_1 and x_1 by dew point on vapor V_1 . Then determine H_1 , referring to top tray as number one in this case.

where H_1 = total vapor enthalpy above reference datum for sum of all contributing percentages of individual components, i , in stream, Btu/lb, or Btu/mol

h_D = total liquid enthalpy above reference datum for sum of all contributing percentages of individual components, i , in product stream. (Also same as reflux), Btu/lb or Btu/mol.

5. For partial condenser: replace Dh_D by DH_D in Step 3. A dew point on compositions of y_D (vapor) give t_D or total pressure. Also get liquid composition x_D (liquid reflux in equilibrium with product vapor y_D . Overhead vapor is sum of compositions of y_D and x_P . A dew point on this vapor (overhead from tray one top)) gives top tray temperature, t_1 .

$$V_1 H_1 + Q_c = L h_D + D H_D$$

Reboiler Duty

Refer to Figure 8-53 (System (2))

1. Determine bottoms temperature by bubble point on liquid x_B .
2. From feed condition determine enthalpy.

$$h_F = \frac{\sum V_F (H_i y_i)_F + \sum L_F (h_i x_i)_F}{F} \quad (8-187)$$

3. Solve for Q_B , reboiler duty, Btu/hr

$$F h_F + Q_B = D h_D + B h_B + Q_c \quad (8-188)$$

where h_D = total enthalpy of distillate product, Btu/mol or Btu/lb

h_B = total enthalpy of bottoms product, Btu/mol or Btu/lb
 h_F = total enthalpy of feed, Btu/mol or Btu/lb

Example 8-30: Tray-By-Tray Multicomponent Mixture Using Digital Computer

This example summarizes a typical short multicomponent distillation using the techniques previously cited (see Computer Printout).

The problem was to separate component 4 from component 5 while keeping component 5 losses into the overhead at less than 5 weight % of the total overhead or to recover in the bottoms better than 90% (weight) of the component 5 entering in the feed.

The feed composition is:

Component	Mols	Pounds	Boil Point, °F
1	0.623	53.68	155.7
2	7.234	130.36	313.0
3	80.223	7423.03	244.2
4	1.717	127.20	332.6
5	9.678	1395.28	380.3
6	0.525	85.37	476.6
	100.000	9214.91	

Enthalpy, Btu/unit flow 2,901.076; lb = 31.48

Feed temperature: 90°F, liquid at stage 5 from top, Equimolal overflow not assumed

Column Pressure: 0.39 (top) to 0.86 (bottom) psia, distributed uniformly to each tray

Reflux Ratio: 0.50 (assumed)
 Assumed No. Theoretical Stages: 8 including condenser and reboiler

Summary of input data to computer:

1. Molecular weights
2. Boiling points
3. "K" value equations for each component as a function of pressure
4. Equations for calculating enthalpy of liquid of each component as a function of temperature
5. Equations for calculating enthalpy of vapor of each component as a function of temperature
6. Initial values for stages to start calculations
 - a. linear temperature gradient
 - b. linear pressure gradient

The results of the computer calculation are as summarized by copies of the printouts. Note that Stage *one* is the product from an overhead condenser and is liquid, as is the bottoms or reboiler outlet product. The results show that the initial criteria have been met for recovery of component 5; however, this does not reflect any optimization of reflux or final number of stages (theoretical trays) that might be required to accomplish the separation in a final design.

As an example, if this were the final column selection, then the column trays = 8-condenser-reboiler = 6 theoret-

(text continued on page 99)

Computer Printout for Multicomponent Distillation

```

NUMBER OF STAGES =      8      (INCLUDING CONDENSER AND REBOILER)
NUMBER OF COMPONENTS =    6
COMPONENTS              MOLECULAR WEIGHT    NORMAL BOILING POINT, DEG.F.
  1                      96.170           155.70
  2                      18.020           212.00
  3                      92.530           244.20
  4                      74.080           332.60
  5                      144.170          380.30
  6                      162.610          476.60
COLUMN PRESSURE =      0.39    TO      0.86 PSIA
REFLUX RATIO =      0.5000
EQUIMOLAL OVERFLOW NOT ASSUMED

FEED STREAMS

STAGE 5 (LIQUID FEED STREAM), TEMP. =  90.00 DEG.F.
COMPONENT              MOLS              LBS.
  1                      0.623              53.66
  2                      7.234             130.36
  3                      80.223            7423.03
  4                      1.717             127.20
  5                      9.678            1395.28
  6                      0.525              85.37
TOTAL                  100.000           9214.91
ENTHALPY, BTU/ UNIT FLOW  2901.076           31.48
    
```

PRODUCT STREAMS

OVERHEAD RATE = 89.797 MOLS LIQUID
 0.0 MOLS VAPOR

BOTTOMS RATE = 10.203 MOLS LIQUID

SUM OF PRODUCTS = 100.000 MOLS

INITIAL VALUES FOR STAGE VARIABLES (LINEAR TEMP. GRADIENT, LINEAR PRESSURE GRADIENT, EQUIMOLAL OVERFLOW,
 SPECIFIED HEAT LOSSES NOT INCLUDING OVERHEAD CONDENSER AND BOTTOMS REBOILER)

STAGE	TEMP. DEG. F.	PRESS. PSIA	L (MOLS)	V (MOLS)	Q (BTU)
1	85.00	0.39	44.898	0.0	0.0
2	102.86	0.46	44.898	134.695	0.0
3	120.71	0.52	44.898	134.695	0.0
4	138.57	0.59	44.898	134.695	0.0
5	156.43	0.66	144.898	134.695	0.0
6	174.29	0.73	144.898	134.695	0.0
7	192.14	0.79	144.898	134.695	0.0
8	210.00	0.86	10.203	134.695	0.0

STAGE NO. 1 OVERHEAD CONDENSER

TEMPERATURE = 81.75 DEG. F
 PRESSURE = 0.39 PSIA

	-----MOL FRACTIONS-----		K	-----LIQUID PRODUCT-----		-----VAPOR PRODUCT-----	
	X	Y		81.75 DEG. F.	LBS	81.75 DEG. F.	LBS
1	0.693787E-02	0.579909E-01	0.835864E+01	0.62300	53.684	0.0	0.0
2	0.805591E-01	0.111028E+00	0.137823E+01	7.23397	130.356	0.0	0.0
3	0.893344E+00	0.829924E+00	0.929014E+00	80.21964	7422.723	0.0	0.0
4	0.180887E-01	0.101670E-02	0.562068E-01	1.62431	120.329	0.0	0.0
5	0.106980E-02	0.384860E-04	0.359752E-01	0.09607	13.850	0.0	0.0
6	0.608310E-07	0.566875E-09	0.931235E-02	0.00001	0.001	0.0	0.0
	1.000000	0.999998		89.79700	7740.937	0.0	0.0
ENTHALPY, BTU/UNIT FLOW =				2318.02881	26.890	20467.7891	244.037
CONDENSER HEAT DUTY =				2499393.0 BTU			

-----LIQUID REFLUX----- (R = 0.500000)
 81.75 DEG. F.
 -----MOLS----- -----LBS-----

1 N-HEXANE	0.31150	26.842
2 WATER	3.61698	65.178
3 EPICHLOROHYDRIN	40.10982	3711.361
4 GLYCIDOL	0.81216	60.165
5 GMA	0.04803	6.925
6 MCM	0.00000	0.000
	44.89850	3870.471
ENTHALPY, BTU/UNIT FLOW = 2318.02881 26.890		

STAGE NO. 2

TEMPERATURE = 95.98 DEG. F
 PRESSURE = 0.46 PSIA

	-----MOL FRACTIONS-----		K	-----LIQUID-----		-----VAPOR-----	
	X	Y		MOLS	LBS	MOLS	LBS
INTERNAL STREAMS LEAVING STAGE							
1	0.702365E-03	0.693785E-02	0.987776E+01	0.03030	2.611	0.93450	80.526
2	0.438818E-01	0.805594E-01	0.183580E+01	1.89314	38.114	10.85099	195.535
3	0.738175E+00	0.893351E+00	0.121019E+01	31.84622	2946.731	120.33041	1138.172
4	0.196187E+00	0.106980E-01	0.922004E-01	8.46386	627.003	2.43651	180.496
5	0.210494E-01	0.106981E-02	0.508229E-01	0.90811	130.922	0.14410	20.775
6	0.462302E-05	0.608316E-07	0.131582E-01	0.00020	0.032	0.00001	0.001
	1.000000	1.000007		43.14185	3741.413	134.69550	11611.500
ENTHALPY, BTU/UNIT FLOW =				2958.33154	34.112	20873.9062	242.141

STAGE NO. 3

TEMPERATURE = 115.04 DEG. F
 PRESSURE = 0.52 PSIA

	-----MOL FRACTIONS-----		K	-----LIQUID-----		-----VAPOR-----	
	X	Y		MOLS	LBS	MOLS	LBS
INTERNAL STREAMS LEAVING STAGE							
1	0.379421E-03	0.491427E-02	0.129519E+02	0.01563	1.347	0.65330	56.295
2	0.245430E-01	0.686564E-01	0.279735E+01	1.01098	18.218	9.12711	164.471
3	0.470701E+00	0.842987E+00	0.179089E+01	19.38924	1794.086	112.06575	10369.441
4	0.414043E+00	0.758873E-01	0.183279E+00	17.05534	1263.460	10.08837	747.346
5	0.902625E-01	0.755377E-02	0.836849E-01	3.71812	536.041	1.00419	144.774
6	0.711249E-04	0.154139E-05	0.216712E-01	0.00293	0.476	0.00020	0.033
	1.000000	1.000000		41.19226	3613.627	132.93884	11482.352
ENTHALPY, BTU/UNIT FLOW =				4063.29980	46.318	21326.8906	246.916

Distillation

STAGE NO. 4
 TEMPERATURE = 131.91 DEG. F
 PRESSURE = 0.59 PSIA

	-----MOL FRACTIONS-----			K	-----LIQUID-----		-----VAPOR-----	
	X	Y			MOLS	LBS	MOLS	LBS
INTERNAL STREAMS LEAVING STAGE								
1	0.403078E-03	0.487530E-02	0.160854E+02	0.01203	1.037	0.63861	55.029	
2	0.159964E-01	0.629432E-01	0.393465E+01	0.63502	11.443	8.24489	148.573	
3	0.309609E+00	0.760431E+00	0.245599E+01	12.29079	1137.266	99.60825	9216.750	
4	0.442138E+00	0.142611E+00	0.322527E+00	17.55190	1300.244	18.68048	1383.850	
5	0.231266E+00	0.291193E-01	0.125906E+00	9.18075	1323.588	3.81431	549.909	
6	0.687129E-01	0.264091E-04	0.326110E-01	0.02728	4.436	0.00294	0.477	
	1.000000	1.000000		39.69777	3778.014	130.98926	11354.582	
ENTHALPY, BTU/UNIT FLOW =				5421.28906	56.965	21947.7500	253.195	

STAGE NO. 5
 TEMPERATURE = 144.67 DEG. F
 PRESSURE = 0.66 PSIA

	-----MOL FRACTIONS-----			K	-----LIQUID-----		-----VAPOR-----	
	X	Y			MOLS	LBS	MOLS	LBS
TOTAL FEEDS TO STAGE								
1				0.62300	53.684	0.0	0.0	
2				7.23400	130.357	0.0	0.0	
3				80.22301	7423.031	0.0	0.0	
4				1.71700	127.195	0.0	0.0	
5				0.67800	1395.277	0.0	0.0	
6				0.22000	85.370	0.0	0.0	
				99.99998	9214.906	0.0	0.0	
ENTHALPY, BTU/UNIT FLOW =				2901.07593	0.0	0.0	0.0	

	-----MOL FRACTIONS-----			K	-----LIQUID-----		-----VAPOR-----	
	X	Y			MOLS	LBS	MOLS	LBS
INTERNAL STREAMS LEAVING STAGE								
1	0.266697E-03	0.490374E-02	0.183858E+02	0.03452	2.975	0.63501	54.719	
2	0.123573E-01	0.607659E-01	0.491730E+01	1.59954	28.824	7.86887	141.797	
3	0.237150E+00	0.714384E+00	0.301213E+01	30.69696	2840.390	92.50896	8559.852	
4	0.312228E+00	0.148094E+00	0.474257E+00	40.41512	2993.952	19.17737	1420.659	
5	0.433081E+00	0.716411E-01	0.165407E+00	56.05843	8081.941	9.27715	1337.486	
6	0.491682E-02	0.210695E-03	0.428481E-01	0.63644	103.491	0.02728	4.437	
	1.000000	0.999999		129.44102	14051.566	129.49477	11518.941	
ENTHALPY, BTU/UNIT FLOW =				6947.83984	64.003	22570.4453	253.735	

STAGE NO. 6
 TEMPERATURE = 188.49 DEG. F
 PRESSURE = 0.73 PSIA

	-----MOL FRACTIONS-----			K	-----LIQUID-----		-----VAPOR-----	
	X	Y			MOLS	LBS	MOLS	LBS
INTERNAL STREAMS LEAVING STAGE								
1	0.820382E-05	0.289519E-03	0.352913E+02	0.00105	0.091	0.03452	2.975	
2	0.107639E-02	0.134144E-01	0.124627E+02	0.13827	2.492	1.59951	28.823	
3	0.358612E-01	0.257415E+00	0.717825E+01	4.60658	426.246	30.69373	2840.090	
4	0.167536E+00	0.338161E+00	0.201852E+01	21.52092	1594.270	40.32170	2987.031	
5	0.788222E+00	0.389783E+00	0.494524E+00	101.25171	14597.457	46.47696	6700.582	
6	0.729625E-02	0.935050E-03	0.128159E+00	0.93725	152.405	0.11149	18.130	
	1.000000	0.999998		128.45580	16772.957	119.23819	12577.629	
ENTHALPY, BTU/UNIT FLOW =				11524.1094	88.257	27816.3281	263.704	

STAGE NO. 7
 TEMPERATURE = 213.25 DEG. F
 PRESSURE = 0.79 PSIA

	-----MOL FRACTIONS-----			K	-----LIQUID-----		-----VAPOR-----	
	X	Y			MOLS	LBS	MOLS	LBS
INTERNAL STREAMS LEAVING STAGE								
1	0.189382E-06	0.891154E-05	0.470578E+02	0.00003	0.002	0.00105	0.091	
2	0.611520E-04	0.116901E-02	0.191176E+02	0.00808	0.146	0.13824	2.491	
3	0.365365E-02	0.389279E-01	0.106551E+02	0.48272	44.666	4.60334	425.947	
4	0.447734E-01	0.181203E+00	0.404748E+01	5.91546	438.217	21.42773	1587.366	
5	0.935284E+00	0.775205E+00	0.828903E+00	123.56973	17815.047	91.67026	13216.098	
6	0.162279E-01	0.348651E-02	0.214863E+00	2.14403	388.640	0.41229	67.043	
	1.000000	1.000000		132.12006	18646.711	118.25296	15299.031	
ENTHALPY, BTU/UNIT FLOW =				14190.3711	100.545	32961.2969	254.772	

Applied Process Design for Chemical and Petrochemical Plants

STAGE NO. 8 (REBOILER ----- LIQUID STREAM IS BOTTOMS PRODUCT)

TEMPERATURE = 224.68 DEG. F
 PRESSURE = 0.86 PSIA

INTERNAL STREAMS LEAVING STAGE	-----MOL FRACTIONS-----		K	-----LIQUID-----		-----VAPOR-----	
	X	Y		-----MOLS-----	-----LBS-----	-----MOLS-----	-----LBS-----
1	0.400988E-08	0.204898E-06	0.510988E+02	0.00000	0.000	0.00002	0.002
2	0.299190E-05	0.660195E-04	0.220665E+02	0.03003	0.001	0.00805	0.145
3	0.324473E-03	0.393227E-02	0.121192E+02	0.00331	0.306	0.47941	44.360
4	0.908419E-02	0.477594E-01	0.525762E+01	0.09269	6.866	5.82269	431.344
5	0.939133E+00	0.934957E+00	0.995584E+00	9.58198	1381.433	113.98735	16433.555
6	0.514552E-01	0.132798E-01	0.258093E+00	0.52500	65.370	1.61904	263.271
	1.000000	0.999995		10.20300	1473.976	121.91722	17172.676

ENTHALPY, BTU/UNIT FLOW = 15248.2773 105.550 35206.3750 249.947

REBOILER HEAT DUTY = 2573009.0 BTU
 CONDENSER HEAT DUTY = 2499393.0 BTU

OVERALL COMPONENT BALANCES (MOLS) ---- BEFORE FINAL FORCING ----

	IN	OUT	IN/OUT
1	0.62300	0.62300	1.00000000
2	7.23400	7.23400	1.00000000
3	80.22301	80.22293	1.00000000
4	1.71700	1.71700	1.00000000
5	9.67800	9.67804	0.99999583
6	0.52500	0.52500	0.99999529
	99.99998	99.99995	1.00000000

NORMALIZED PRODUCT STREAMS ---- AFTER COMPONENT BALANCES FORCED ----

STAGE NO. 1 ----- OVERHEAD CONDENSER

TEMPERATURE = 81.75 DEG. F
 PRESSURE = 0.39 PSIA

COMPONENT	-----LIQUID PRODUCT-----				-----VAPOR PRODUCT-----			
	MOLS	MOL FRACTION	LBS	MASS FRACTION	MOLS	MOL FRACTION	LBS	MASS FRACTION
1	0.62300	0.693787E-02	53.684	0.693506E-02	0.0	0.0	0.0	0.0
2	7.23397	0.805591E-01	130.356	0.168398E-01	0.0	0.0	0.0	0.0
3	80.21964	0.893345E+00	7422.723	0.958892E+00	0.0	0.0	0.0	0.0
4	1.62431	0.180887E-01	120.329	0.155445E-01	0.0	0.0	0.0	0.0
5	0.09636	0.106980E-02	13.850	0.178914E-02	0.0	0.0	0.0	0.0
6	0.00001	0.608307E-07	0.001	0.114746E-06	0.0	0.0	0.0	0.0
	89.79697		7740.937		0.0		0.0	

STAGE NO. 8 (REBOILER)

TEMPERATURE = 224.68 DEG.
 PRESSURE = 0.86 PSIA

COMPONENT	-----LIQUID PRODUCT-----				-----VAPOR PRODUCT-----			
	MOLS	MOL FRACTION	LBS	MASS FRACTION	MOLS	MOL FRACTION	LBS	MASS FRACTION
1	0.00000	0.400989E-08	0.000	0.239181E-08	0.0	0.0	0.0	0.0
2	0.00003	0.299191E-05	0.001	0.373200E-06	0.0	0.0	0.0	0.0
3	0.00331	0.324474E-03	0.306	0.207826E-03	0.0	0.0	0.0	0.0
4	0.09269	0.908423E-02	6.866	0.465829E-02	0.0	0.0	0.0	0.0
5	9.58194	0.939133E+00	1381.427	0.937216E+00	0.0	0.0	0.0	0.0
6	0.52499	0.514551E-01	85.369	0.579180E-01	0.0	0.0	0.0	0.0
	10.20296		1473.969		0.0		0.0	

(text continued from page 95)

ical. Actual trays at an estimated 65% tray efficiency = $6/0.65 = 9.23$ or use 10 *actual* trays in the column itself.

Example 8-31: Multicomponent Examination of Reflux Ratio and Distillate to Feed Ratio

The detailed calculations of Figure 8-54 present an example of the excellent performance analysis information that can be developed by an orderly or systematic study of the variables in a multicomponent system. There are other variables to be studied as well.

This design is targeted to produce 99.5 weight % propylene overhead while not allowing more than 1 weight % in the bottoms.

Note that in a high purity condition as is represented in this example, the system is quite sensitive to the overhead withdrawal rate (product from the system). This system is for the purification of propylene from a feed high in propylene, with lesser amounts of propane, butane, and ethane.

Without a digital computer the detail of Figure 8-54 would be practically impossible and cost prohibitive in terms of time involved.

Stripping Volatile Organic Chemicals (VOC) from Water with Air

Li and Hsiao [143] provide a useful approach to the environmental problem of removing (by stripping) volatile organics from solution in a contaminated water stream by using fresh air as the stripping medium. It should be noted that a number of industrial firms perform this stripping with steam. The mass balance on the VOC component around the column (trayed or packed) as shown in Figure 8-55 uses the symbols of Reference 143.

$$\frac{L}{V} = \frac{y_i - y_{n+1}}{x_o - x_N} \text{ (slope of operating line)} \quad (8-189)$$

- where x_o = VOC mol fraction (ratio of number of mols of a specific VOC component in water solution to the total mols of all contaminants contained in the water)
- x_N = mol fraction of VOC component in the stripped water
- N = number of trays (theoretical) or transfer units for a packed tower
- y_i = mol fraction VOC component in exiting VOC contaminated air

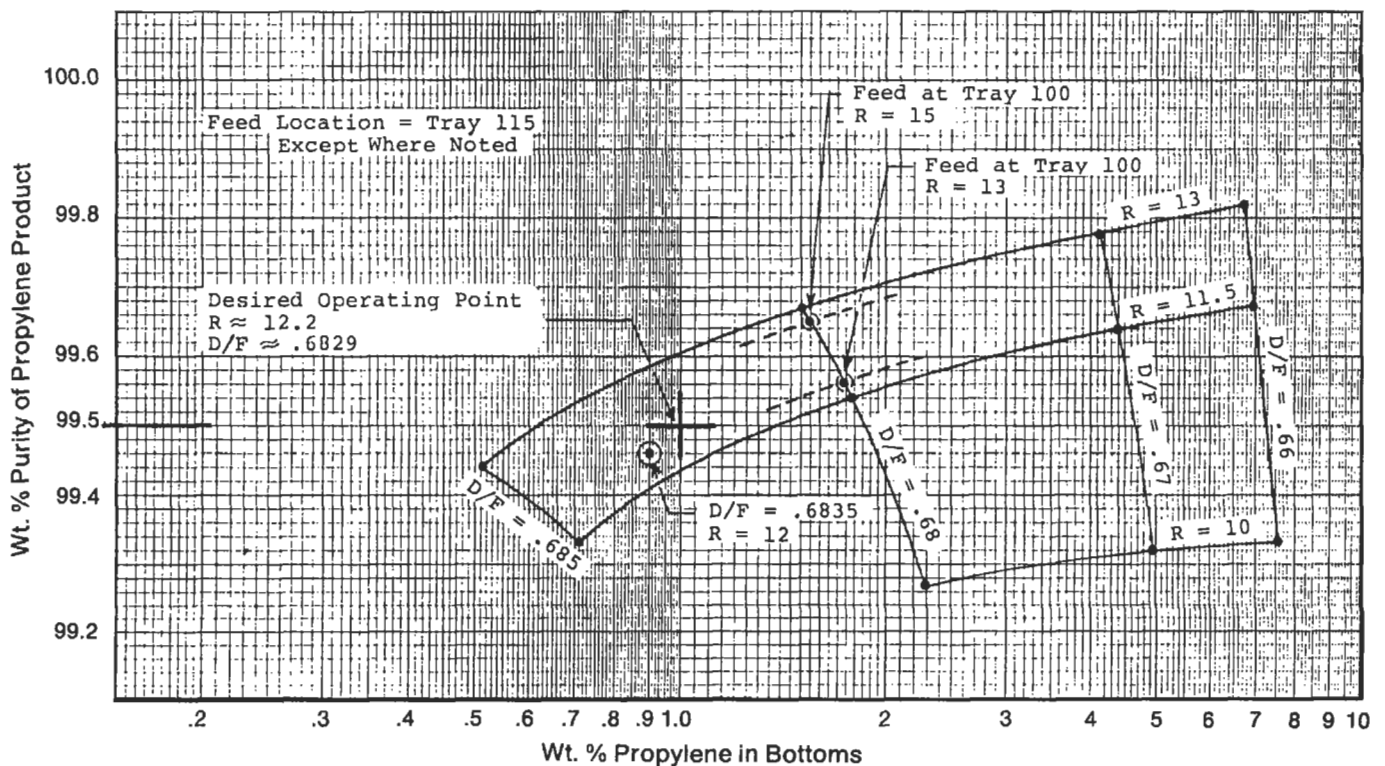


Figure 8-54. Effect of reflux ratio and distillate feed ratios on propylene content of product and bottoms for Example 8-29.

- y_{N+1} = mol fraction VOC component in the incoming fresh air, equals zero for fresh air
 L = volumetric flow rate for incoming contaminated water
 V = volumetric flow rate for incoming fresh air
 V_{\min} = minimum fresh air flow required based on slope of operating line L/V on x - y diagram
 x_N = mol fraction VOC contaminant in exiting water stream, usually aimed at meeting the environmental regulations
 S_{\min} = minimum stripping factor at minimum flow rate for air
 S_{opt} = optimum stripping factor, where treatment costs are a minimum, referenced to costs of utilities, maintenance, depreciation, labor. As economic conditions change one may need to adjust S_{opt} , see Reference 143.

The concentrations of most of the VOC compounds in the contaminated water are usually expressed in ppm as are the remainder residue compounds in the water exiting the tower. These are usually small values. As an approximation:

$$(L/V_{\min}) = K$$

where K = equilibrium constant (varies for each component)

$$K = y^*/x^*$$

y^* = equilibrium molar fraction of VOC components in air

x^* = equilibrium molar fractions of VOC components in water

Minimum stripping factor at corresponding minimum air flowrate:

$$S_{\min} = K/(L/V_{\min}) = 1.0 \quad (8-190)$$

$$V_{\min} = L/K$$

The component with the lowest equilibrium constant is called the key component in the stripping process, because it yields the largest value of V_{\min} . This largest value is the "true" minimum air flowrate, whereas the actual air flowrate should be selected at 1.20 to 2.0 times the minimum. This becomes a balance between fewer theoretical stages at actual air flowrate, yet requires a larger diameter column to carry out the operation.

It can be important to examine the problem and evaluate the optimum stripping factor based on related costs, thus:

$$S_{\text{opt}} = K (L/V_{\text{opt}}) \quad (8-191)$$

$$V_{\text{opt}} = S_{\text{opt}} (V_{\min}) \quad (8-192)$$

The Henry's Law constant, H , can be substituted for the equilibrium constant, K , when the system operates at or very close to atmospheric pressure:

$$H = p^*/x^* \quad (8-193)$$

where p^* = the partial pressure, atm, of the contaminant in equilibrium with x^*

Tables 8-8 and 8-9 provide values for selected Henry's Law Constants respectively [143].

The optimum stripping factor, S_{opt} , is expressed as a percent of residue, (100) (x_N/x_o) , for water rates of 30 gpm, 300 gpm, and 3,000 gpm.

$$S_{\text{opt}} = 1 + aH^b$$

Constants a and b were determined from a linear regression for $x_N/x_o = 4.75\%$ and x_N and $x_o = 0.05\%$ for the packed and tray towers. The optimum stripping factor decreases as the Henry's Law constant decreases. Due to the complex relationship between cost and performance, the authors [143] recommend caution in attempting to extrapolate from the water flowrate ranges shown.

Example 8-32: Stripping Dissolved Organics from Water in a Packed Tower Using Method of Li and Hsiao [143]

Using a packed tower, remove hexachloroethane (HCE) concentration of 110 ppm in water to 0.05 ppm using fresh air operating at essentially atmospheric pressure using a fan/blower putting up $1\frac{1}{2}$ in. water pressure. The concentration of propylene dichloride (PDC) in the contaminated water is 90 ppm, and is to be reduced to 0.05 ppm in the exiting water. The water flowrate = 300 gpm. The required packing (or trays) must be determined by using a vapor-liquid equilibrium plot, setting slope L/V and stepping off the number of stages or transfer units. See Figure 8-55.

From Table 8-9 (Packed Tower):

Hexachloroethane: Henry's Law constant = 547.7 atm

Propylene dichloride: Henry's Law constant = 156.8 atm

1. For hexachloroethane: $x_N/x_o = 0.05$ ppm/100 ppm = 0.05%

For propylene dichloride: $x_N/x_o = 0.05$ ppm/100 ppm = 0.05%

2. $S_{\text{opt}} = 6.0$ for HCE, and 3.9 for PDC.
3. For HCE:

$$V_{\min} = L/K = (300) (8.33) (359 \text{ scf/mol}) / (18 \text{ lb/mol}) (547.7) = 91.1 \text{ scf/minute}$$

Table 8-8
Henry's Law Constants and Optimum Stripping Factors for Selected Organic Compounds for Use With Tray Towers
@ 25°C (77°F)

Chemicals	Henry's Law constant	x_N/x_o %	L = 30 gpm	L = 300 gpm	L = 3,000 gpm
1,1,2,2-tetrachloroethane	24.02	4.75	1.7	1.65	1.35
		0.05	2.3	2.1	1.6
1,1,2-trichloroethane	47.0	4.75	1.98	1.98	1.56
		0.05	3.10	3.00	2.18
1,2-dichloroethane	61.2	4.75	2.09	2.14	1.67
		0.05	3.34	3.31	2.40
propylene dichloride	156.8	4.75	3.1	3.3	2.5
		0.05	5.1	5.5	4.0
methylene chloride	177.4	4.75	2.96	3.38	2.57
		0.05	5.38	5.84	4.1
chloroform	188.5	4.75	3.15	3.6	2.72
		0.05	5.8	6.3	4.37
1,1,1-trichloroethane	273.56	4.75	4.1	4.6	3.2
		0.05	7.1	7.2	5.5
1,2-dichloroethene	295.8	4.75	3.7	4.7	3.4
		0.05	7.59	8.6	5.84
1,1-dichloroethane	303.0	4.75	3.81	4.84	3.5
		0.05	7.8	8.9	6.0
hexachloroethane	547.7	4.75	6.3	7.5	5.1
		0.05	10.5	14.5	8.4
hexachlorobutadiene	572.7	4.75	6.5	7.8	5.3
		0.05	11.0	15.2	9.1
trichloroethylene	651.0	4.75	6.6	8.3	5.8
		0.05	13.9	16.9	10.9
1,1-dichloroethene	834.03	4.75	7.2	10.5	6.9
		0.05	12.0	19.2	12.0
perchloroethane	1,596.0	4.75	9.8	13.3	11.8
		0.05	16.1	36.1	22.4
carbon tetrachloride	1,679.17	4.75	9.2	11.7	12.1
		0.05	15.4	33.0	21.0

Used by permission, *Chem. Eng. Li, K. Y. and Hsiao, K. J., V. 98, No. 7 (1991), p. 114; all rights reserved.*

For PDC:

$$V_{\min} = L/K = (300 \text{ gpm}) (8.33) (359)/(18) (156.8) \\ = 317.8 \text{ scf/min}$$

4. Use the larger air rate as control required, which is the 317.8 scf/minute required for PDC, to calculate the optimum flowrate.

$$5. V_{\text{opt}} = (3.9) (317.8) = 1,239.4 \text{ scf/min}$$

$$S_{\text{opt}} = K/(L/V_{\text{opt}})$$

$$V_{\text{opt}} = S_{\text{opt}} (V_{\min})$$

6. Therefore, the operating conditions would be:

$$L = 300 \text{ gpm}$$

$V = 1,239 \text{ scf/min}$ (minimum, may want to consider actually using 10–15% more for some assurance that the required conditions will be met.

7. Determine the tower diameter based on the flows of (6) above. See Chapter 9, this volume for packed tower design.

Troubleshooting, Predictive Maintenance and Controls for Distillation Columns

Troubleshooting currently is much more sophisticated due to the technical tools available for investigating and analyzing performance than several years ago. The gamma radiation scanning technique of several distillation specialist companies [158, 182] provides one type of data gathering that can significantly aid in determining whether a column is having liquid/vapor flow and or distribution problems. Figure 8-56 is one case study of a problem column. This system provides an accurate density pro-

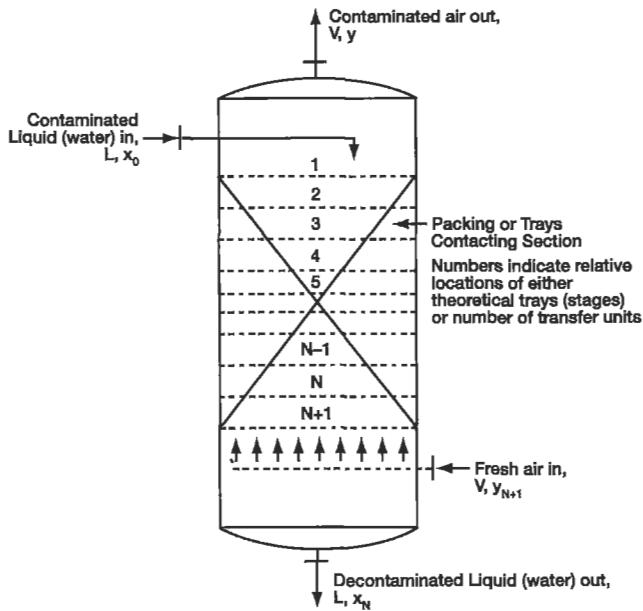


Figure 8-55. Schematic stripping tower using air to strip organics from water solution. Adapted and used by permission, Li, K. Y. and Hsiao, K. J., *Chem. Eng.*, V. 98, No. 7 (1991) p. 114.

file of the operating fluids on each tray or through the packing of a packed column.

Other troubleshooting techniques can include computer modeling, checking the reliability of instrumentation, measuring quality of product streams with varying reflux rates, measuring column tray temperatures at close intervals, stabilizing the feed rate, bottoms withdrawal and overhead condensing rates. Surprising results can be obtained, including:

1. Trays may have damage to caps, valves, distributors, sieve holes, or packing for packed towers.
2. The contacting devices of (1) above may actually be missing, i.e., blown off one or more trays, so all that is existing is a "rain-deck" tray with no liquid-vapor contacting.
3. Crud, polymer, gunk and other processing residues, plus maintenance tools, rags, or overalls may be plugging or corroding the liquid flow paths.
4. Entrainment.
5. Weeping of trays, or flooding of packing or trays.
6. Foaming limitations.
7. Unusual feed conditions, unexpected or uncontrolled.
8. Many other situations, almost too odd to imagine. References on this topic include 159–166, 182, 238.

The topic of control of distillation columns has been discussed by many authorities with a wide variety of experience [117–120, 237], and is too specialized to be covered in this text.

Nomenclature for Part 1: Distillation Process Performance

- A, B thru K = Constants developed in original article
 a, b, c = Correlation constants (distillation recoveries [141])
 a = Activity of component
 a_i = Activity of component, i
 av or avg = Average
 B, C, D = Virial coefficients, Equation 8-11
 B = Bottoms product or waste, lb mols/hr, also = W
 B_b = Mols of component, b, used as reference for volatility, after a given time of distillation
 B_{bo} = Mols of component, b, used as reference for volatility, at start of distillation
 B_i = Mols of component, i, after a given time of distillation
 B_{io} = Mols of component, i, at start of distillation
 B_{Ti} = Total mols of liquid in bottoms of still at time, T_1
 B_{To} = Total mols liquid (not including any steam) in bottom of still at start time T_o (batch charge)
 b = y intercept of operating line; or constant at fixed pressure for Winn's relative volatility
 b_i = Mols of component, i, in bottoms
 C = No. components present, phase rule; or no. components, or constant
 C_{mi} = Factor in Colburn Minimum Reflux method, pinch conditions, stripping
 C_{ni} = Factor in Colburn Minimum Reflux method, pinch conditions, rectifying
 C_p = Specific heat, Btu/lb ($^{\circ}$ F)
 D = Mols of distillate or overhead product, lb mols/hr; or batch distillation, mols
 d_i = Mols component, i, in distillate
 E = Vaporization efficiency of steam distillation
 E_G = Overall column efficiency
 E_o = Overall tray efficiency
 E_{MV}^* = E_{OG} = Murphree point efficiency, fraction
 E_{MV}^o = Murphree plate/tray efficiency, = E_M
 F = Degrees of Freedom, phase rule; or, charge to batch still, mols
 F = Feed rate to tower, lb mols/hr; or, mols of feed, (batch distillation) entering flash zone/time all components except non-condensable gases
 F_{FR} = Factor for contribution of other feed flow to minimum reflux
 F_L = Mols of liquid feed
 F_V = Mols of vapor feed
 F_t = $F + V_s$ = mols feed plus mols of non-condensable gases
 F_R = $F_{SR,k}$ = Factor for contribution of sidestream, k, flow to minimum reflux
 F_{SR} = Factor for contribution of sidestream flow to minimum reflux
 F_{FRj} = Factor for contribution of feed, j, flow to minimum reflux
 f = Fugacity at a specific condition

Table 8-9
Henry's Law Constant and Optimum Stripping Factors for Selected Organic Compounds for Use With Packed Towers
@ 25°C (77°F)

Chemicals	Henry's Law constant	x_N/x_0 %	L = 30 gpm	L = 300 gpm	L = 3,000 gpm
1,1,2,2-tetrachloroethane	24.02	4.75	1.39	1.66	1.84
		0.05	1.88	2.30	2.59
1,1,2-trichloroethane	47.0	4.75	1.45	1.89	2.32
		0.05	2.00	2.79	3.37
1,2-dichloroethane	61.2	4.75	1.46	1.97	2.54
		0.05	2.03	2.95	3.73
propylene dichloride	156.8	4.75	1.6	2.43	3.9
		0.05	2.3	3.9	6.13
methylene chloride	177.4	4.75	1.57	2.37	3.90
		0.05	2.23	3.87	6.20
chloroform	188.5	4.75	1.59	2.46	4.10
		0.05	2.28	4.05	6.61
1,1,1-trichloroethane	273.56	4.75	1.67	2.7	5.08
		0.05	2.43	4.62	8.37
1,2-dichloroethene	295.8	4.75	1.65	2.68	5.08
		0.05	2.40	4.50	8.40
1,1-dichloroethane	303.0	4.75	1.67	2.72	5.20
		0.05	2.40	4.63	8.66
hexachloroethane	547.7	4.75	1.85	3.27	7.74
		0.05	2.7	6.0	13.6
hexachlorobutadiene	572.7	4.75	1.88	3.48	8.1
		0.05	2.78	6.20	14.27
trichloroethylene	651.0	4.75	1.82	3.27	7.78
		0.05	2.68	5.87	14.0
1,1-dichloroethene	834.03	4.75	1.84	3.37	8.50
		0.05	2.70	6.10	15.9
perchloroethane	1,596.0	4.75	2.10	4.20	13.2
		0.05	3.10	7.90	26.1
carbon tetrachloride	1,679.17	4.75	2.06	4.2	13.2
		0.05	3.1	7.9	26.45

Used by permission, *Chem. Eng.* Li, K. Y. and Hsiao, K. J., V. 98, No. 7 (1991), p. 114; all rights reserved.

- f° = Fugacity at reference standard condition
 f_i = Feed composition, i ; or, = total mols of component, i , in distillate and bottoms
 G = Boilup rate, mols/hr
 H = Total enthalpy, above reference datum, of vapor mixture at tray or specified conditions, Btu/lb mol, or Btu/lb
 $H' = H_{ij} =$ Henry's Law constant, lb mols/(cu ft) (atm)
 H_n = Total molal enthalpy of vapor at conditions of tray, n , entering tray; $H_n = \sum H_{ni} (y_{ni})$
 H_s = Total enthalpy of steam, Btu/lb mol, or Btu/lb
 HK = Heavy key component in volatile mixture
 h = Enthalpy of liquid mixture or pure compound at tray conditions of temperature and pressure, or specified point or condition, Btu/lb mol, or Btu/lb
 h_n = Total molal enthalpy of liquid at conditions of tray, n ; $h'_n = h_{ni}(x_{ni})$
 h_D = Molal enthalpy of product or total liquid enthalpy above reference datum for sum of all contributing percentages of individual components
 h_{n+1} = Molal enthalpy of liquid leaving plate $n + 1$
 h_a = Total molal enthalpy of liquid at conditions of tray, n ; $h_n = \sum h_{ni}(x_{ni})$
 K = Equilibrium constant for a particular system ($= y/x$)
 K' = Equilibrium constant for least volatile component, $K' = y/x$
 K_i = Equilibrium distribution coefficient for component, i , in system
 k = Experimentally determined Henry's Law constant, also can be K
 k = Value of x at intersection of operating line and equilibrium curve on x - y diagram (batch operation)
 kpa = Metric pressure



TRAY DAMAGE AND FLOODING
03/21/88 10:27:15
SCALES: 70 - 7000

PROCESS DIAGNOSTICS
1-800-288-8970

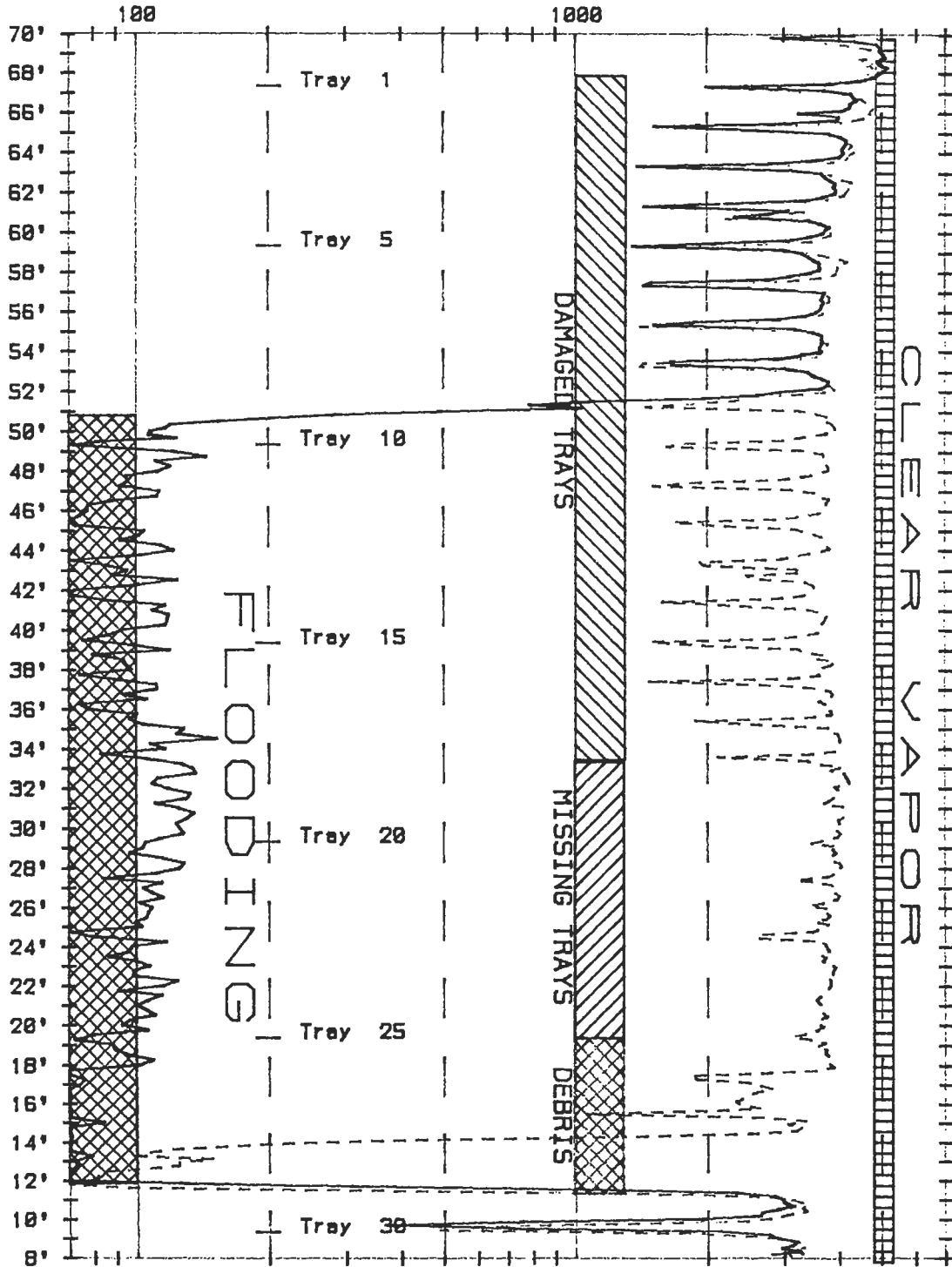


Figure 8-56. Examples of gamma ray scanning "diagnostic diagnosis" of depropanizer column to evaluate performance. Used by permission, Tru-Tec Division, Koch Engineering Co., Inc.

- L = Liquid flowrate return to tower as reflux, lb mols/hr, mols component in liquid phase; or, L_1 , L_2 = Latent heat of vaporization; or, volumetric flowrate for incoming contaminated water (stripping VOC with air); or mols liquid produced from F per unit time, leaving flash zone
 L_r = Liquid flowrate down rectifying section of distillation tower, lb mols/hr
 L_s = Liquid flowrate down stripping section of distillation tower, lb mols/hr
 LK = Light key component in volatile mixture
 L/V = Internal reflux ratio
 L/D = Actual external reflux ratio
 $(L/D)_{\min}$ = Minimum external reflux ratio
 M = Molecular weight of compound
 M_s = Total mols steam required
 m = Number of sidestreams above feed, n
 N = Number of theoretical trays in distillation tower (not including reboiler) at operating finite reflux. For partial condenser system N includes condenser; or number theoretical trays or transfer units for a packed tower (VOC calculations)
 N_B = Number of trays from tray, m , to bottom tray, but not including still or reboiler
 N_{\min} = Minimum number of theoretical trays in distillation tower (not including reboiler) at total or infinite reflux. For partial condenser system, N_{\min} includes condenser; also, minimum value of N
 N_n = Number of theoretical trays above feed, or reference plate, n , but not including n
 N_m = Number of theoretical trays before feed tray
 N_{im} = Mols of immiscible liquid
 N_o = Mols of non-volatile material present; or, number of theoretical trays/stages in column only, not reboiler or condenser
 N_s = Mols of steam
 n = Number of theoretical trays in rectifying section or number of components, or minimum number of equilibrium trays
 n_f = Number of feeds
 n_s = Number of sidestreams
 P = Pressure, atmospheres; or, vapor pressure of component, atm.; or, P = number of phases; or, P = for batch operations, percentage draw-off
 P_i = Vapor pressure of each component
 P_s = Vapor pressure of steam, absolute
 P_b = Vapor pressure of reference more volatile component, b
 p = p_i = Partial pressure of one compound in liquid, absolute units, or, ratio r_{ps}/r_{pr} ; also, p_i = partial pressure of solute (Henry's Law)
 p = Total pressure of system = π
 p' = Number of trays below feed where introduction of light components should begin, Akers-Wade calculation method
 p_i^* = Vapor pressure component, i , in pure state at temperature
 p_{ii}^* = Similar to above by analogy
 p'' = Number of trays above feed where introduction of heavy components should begin. Akers-Wade calculation
 p_{im} = Pure component vapor pressure of immiscible liquid, mm Hg
 p_s = Partial pressure of steam, mm Hg
 Q_B = Net heat in through reboiler, reboiler duty, Btu/hr; or heat added in still or bottoms
 Q_c = Net heat out of overhead condenser, Btu/hr, = $w c_p (t_i - t_o)$
 q = q_F = Thermal condition of feed, approximately amount of heat to vaporize one mol of feed at feed tray conditions divided by latent heat of vaporization of feed
 q_s = Thermal condition of sidestream(s)
 R = Reflux ratio = External reflux ratio for a given separation, = L/D , L = liquid rectifying column
 R = Actual reflux ratio, O/D
 R_m = Minimum reflux ratio, O/D
 R' = Pseudo minimum reflux ratio
 R_{\min} = Minimum external reflux ratio for a given separation
 R_F = Feed component of minimum reflux
 $R_{F, n}$ = Feed component of minimum reflux for feed, n
 R_{OF} = Other feed components of minimum reflux
 R_S = Sidestream component of minimum reflux
 r_{ps} = Ratio of light to heavy keys, stripping pinch
 r_{pr} = Ratio of light to heavy keys, rectifying pinch
 r_f = Ratio mol fraction light key to heavy key in feed
 S = Steam flowrate, lb/hr or lb mols/hr; or theoretical stages at actual reflux (Figure 8-24) including reboiler and partial condenser, if any; or batch, mols in mixture in still kettle at time θ
 S_n = Theoretical stages at minimum reflux
 S_M = Minimum theoretical stages at total reflux from bottoms composition through overhead product composition, including reboiler and any partial condenser (if used); or minimum stripping factor at minimum flowrate of air
 S_k = Flowrate of sidestream, k , mols/hr
 S_o = Theoretical stages at a finite operating reflux; or batch, mols originally charged to kettle
 S_r = Theoretical stages in total rectifying section, including partial condenser, if used
 S_s = Theoretical stages in total stripping section, including reboiler
 S_t = Theoretical trays/stages at actual reflux, L/D , including reboiler and total condenser
 S_{opt} = Optimum stripping factor
 $(SR)_i$ = Separation factor
 s = Pounds (or mols) steam per pound (or mol) of bottoms; or flowrate of sidestream, mols/hr
 T = Temperature, °Abs R
 t_B = Bottoms temperature, °F
 t_i = Temperature in, °F
 t_o = Temperature out, °F; or overhead temperature, °F
 V = V_t = Total vapor leaving flash zone/unit time at specific temperature and pressure; or total overhead vapor from tower, mols/hr; or mols of component in vapor phase; or volumetric flowrate for incoming fresh air
 \bar{V} = Quantity of vapor, mols
 V_r = Vapor flowrate up rectifying section of tower, lb mols/hr
 V_s = Vapor flowrate up stripping section of tower, lb mols/hr; or mols non-condensable gases entering with feed, F , and leaving with vapor, V /time

V_{\min} = Minimum fresh air flow based on slope of operating line, L/V, on x-y diagram
 v = Vapor flowrate, mols/hr; or molar volume
 W = Bottoms product, or still bottoms, or kettle bottoms, mols; also see B; or mols/hr bottoms product; or mols of residue or bottoms/unit time (Ponchon heat balance)
 W = Weight of material in vapor (steam distillation)
 W_1 = Mols final content in still
 W_{i1} = Contents of still pot or kettle at any point, 1, after start for components, i, mols
 W_{i0} = Initial contents of kettle or still pot, mols, for component, i
 W_o = Mols liquid mixture originally charged to still pot
 w = Pounds coolant per hour
 $x_i = x$ = Mol fraction of component in liquid phase; or mol fraction solute in solution (Henry's Law)
 $x_f = x_{1F}$ = Mol fraction of any component in feed, vapor + liquid, F_i ; $x_f = F_{x_f}/F_t$
 x' = Mol fraction of least volatile component
 $x'_1 = x_1 - k$
 $x'_p = x_p - k$
 x = Mol fraction more volatile component in liquid
 x_1 = Mol fraction of component, i, in liquid mixtures as may be feed distillate or bottoms, B_T , at any time, T_1 ; or mol fraction more volatile in vapor entering column at any time (or in distillate)
 x_{it} = Mol fraction liquid at intersection of operating lines at minimum reflux, Scheibel-Montross equation
 x_{hf} = Mol fraction heavy key in feed
 x_n = Pinch composition any light component mol fraction
 x_N = Mol fraction VOC component in the stripped water exiting, usually targeted at meeting environmental regulations
 x_{iD} = Mol fraction light key component in overhead product; or, any light component (Colburn)
 x_{iB} = Mol fraction light key component in keys in original charge
 x_{io} = Mol fraction light key in overhead expressed as fraction of total keys in overhead
 x_{1B} = Mol fraction most volatile component in bottoms
 x_{hD} = Overhead composition of heavy key component, mol fraction
 x_{hn} = Pinch composition of heavy key component, mol fraction
 x_1 = Mol fraction of component in liquid phase; or mol fraction more volatile component in vapor entering column at any time
 x_s = Mol fraction of a more volatile in kettle at time θ
 x_{si} = Value of x_s when distillate receiver is first filled
 x_{so} = Mol fraction more volatile in kettle at time θ
 x_w = Mol fraction more volatile component in bottoms residue (final); or, composition of liquid in still, mol fraction
 x_{wo} = Initial mol fraction of more volatile component in liquid mixture
 X_F = Mol fraction more volatile component in feed
 x_D = Mol fraction more volatile component in final distillate = mol fraction in distillate leaving condenser at time θ
 x_p = Mol fraction of more volatile component in liquid leaving column at any time

x_L = Mol fraction of feed as liquid, Scheibel-Montross
 x_{1o} = Mol fraction light key in overhead expressed as fraction of total keys in overhead, Scheibel-Montross equation
 x_m = Tray liquid mol fraction for start of calculations (most volatile component)
 x_o = Mol fraction of component, i, in bottoms B_{T0} at start time, T_o ; or VOC mol fraction
 x_v = Mol fraction of feed as vapor, Scheibel-Montross equation
 $y = y_i$ = Mol fraction of component in vapor phase, as may be feed, distillate, or bottoms; or Henry's Law, y_i = mol fraction solute in vapor
 y_i = Mol fraction VOC component in the exiting VOC contaminated air
 y' = Mol fraction of least volatile component
 y^* = Equilibrium value corresponding to x_i
 y_n = Average light key mol fraction vapor leaving plate, n
 y_{n+1} = Average light key mol fraction vapor entering plate, n + 1
 Y_{N+1} = Mol fraction VOC component in the incoming fresh air (equals zero for fresh air)
 y_j = Mol fraction solvent component in vapor
 y_s = Mol fraction steam in vapor
 Y_{iB} = Percent recovery of, i, in the bottoms
 Y_{iD} = Percent recovery of, i, in the distillate
 Z = Compressibility factor
 $z_{i,F}$ = Mol fraction component, i, in feed
 $z_{i,Fj}$ = Mol fraction component, i, in feed, j
 $z_{i,S}$ = Mol fraction component, i, in sidestream
 $z_{i,Sk}$ = Mol fraction component, i, in sidestream, k

Greek Symbols

α, α_1 = Relative volatility of light key to heavy key component, or any component related to the heavy key component, except Equation 8-65, α_1 is based on heavy key
 α_{avg} = Average relative volatility between top and bottom sections of distillation tower/column
 α_i = Relative volatility of more volatile to each of other components (steam distillation)
 α_i = Relative volatility of component, i
 α_H = Relative volatility of components heavier than heavy key, at feed tray temperature
 α_i = Relative volatility of more volatile to each of other components
 α_L = Relative volatility of components lighter than light key at feed tray temperature
 β = Constant of fixed pressure in Winn's relative volatility, Equation 8-43
 θ = Time from start of distillation to fill receiver, or value of relative volatility (Underwood Parameter) to satisfy Underwood Algebraic Method
 θ_1 = Time for filling distillate receiver, hrs
 θ_2 = Time for refluxed distillation (batch), hrs
 μ = Viscosity, centipoise
 ν = Activity, coefficient
 π = total system pressure, absolute; atm, mm Hg, psia
 $\pi = 3.14159$
 Σ = Sum
 ψ = First derivative function

ψ' = Second derivative function
 ω_j = Function in Underwood's Algebraic method for minimum reflux ratio
 Ω = Fugacity coefficient
 ϕ = No. phases from phase rule

Subscripts

a, b, c, etc. = Specific components in a system or mixture
 Avg, Av = Average
 B = Any consistent component in bottoms product
 B = b = Bottoms
 b = Exponent in Winn's relative volatility equation
 D = Any consistent component in condensed overhead product or distillate
 eff = Effective
 F = Feed
 F_j = Feed, j
 F_r = Intermediate feed, Scheibel-Montross method
 FL = FH = All mol fractions lighter than light key in feed, Scheibel-Montross method
 FHK = Heavy key in feed
 FLK = Light key in feed
 HK = h = hk = Heavy key component
 H = Components heavier than heavy key
 h = Heavy, or heavy or high boiling component in mixture; also heavy key component
 i = Any component identified by subscripts 1, 2, 3, etc., or by a, b, c, etc.; or initial condition, i
 im = Immiscible liquid
 j = Specific components in a system or mixture
 l = lk = Light key component; or light or low boiling component in mixture
 lh = Refers to light component referenced to heavy component
 LK = Light key component
 L = Liquid, Scheibel-Montross method only; or components lighter than light key
 M = min = Minimum
 m = No. trays in stripping section; or tray number
 n = No. trays in rectifying section; or tray number
 o = Initial conditions; or i; or operating condition
 p_r = Pinch condition in rectifying section
 p_s = Pinch condition in stripping section
 P = For packed towers
 w = Relates to bottoms or pot liquor, or kettle bottoms
 r = Rectifying section; or component to which all the relative volatilities are referred
 s = Steam, or stripping section of column
 t = Top, or total
 T = For tray towers
 v = Vapor
 1 = Initial, steam distillation
 2 = Remaining, steam distillation
 1, 2, 3, etc. = Tray numbers; or specific components in a system or mixture
 (') = Superscript, heavy key component or least volatile

Part 2: Hydrocarbon Absorption and Stripping

(With Contributions by Dr. P. A. Bryant)

Many operations in petrochemical plants require the absorption of components from gas streams into "lean" oils or solvents. The resultant "rich" oil is then stripped or denuded of the absorbed materials. The greatest use of this operation utilizes hydrocarbon materials, but the basic principles are applicable to other systems provided adequate equilibrium data are available.

Several methods [17, 18, 29, 40, 62, 67, 223] for handling this design have been offered and each has introduced a concept to improve some feature. An approximation method combination of Kremser-Brown [40, 67] and a more complete method of Edmister [18] will be summarized. Figure 8-57 summarizes the system and terminology. The accepted nomenclature for absorption and stripping is located on page 121.

Kremser-Brown-Sherwood Method— No Heat of Absorption [18]

This method gives reasonably good results for systems involving relatively lean gas and small quantities being absorbed. For rich gases the error can be considerable (more than 50% for some components). It has given generally good results on natural gas and related systems.

Absorption—Determine Component Absorption in Fixed Tray Tower (Adapted in part from Ref. 18).

1. Calculate the total mols of gas inlet to the absorber identifying the quantities of individual components.
2. Assuming the tower pressure as set and an average of top and bottom temperatures can be selected (these may become variables for study), read equilibrium K_i values from charts for each component in gas.
3. Assume or fix a lean oil rate.
4. Calculate

$$\frac{L_o}{V_{N+1}} = \frac{\text{Mols/hr lean oil in}}{\text{Mols/hr rich gas in}} \quad (8-194)$$

Assume this value constant for tower design.

5. Calculate absorption factor, $A_i = L_o/(V_{N+1})(K_i)$, using values of (2) and (4) above for each component.
6. Calculate fraction absorbed for each component, assuming a fixed overall tray efficiency for an

assumed number of actual trays (or an existing column with trays).

- (a) Theoretical trays, $N = (\text{tray efficiency, } E_o) \times (\text{no. actual trays})$
- (b) Fraction absorbed

$$E_{ai} = \frac{Y_{N+1} - Y_1}{Y_{N+1} - Y_o^*} = \frac{A_i^{N+1} - A_i}{A_i^{N+1} - 1} \quad (8-195)$$

where Y_o^* is often considered zero or very small. Solve using A_i values.

7. Mols each component absorbed/hr.
= $(V_o Y_{(n+1)i})(E_{ai})$
8. Mols each component absorbed/(mol inlet lean oil) (hr) = X_{iR}
9. Mols of each component in gas out top of absorber: = (mols component in inlet gas)—(mols component absorbed)
10. Mols of component in gas out top of absorber/mol of inlet rich gas:

$$E_{ai} = \frac{Y_{N+1} - Y_1}{Y_{N+1} - Y_o^*}$$

Solve for Y_1

11. Correct values from first calculation, Steps 1 through 10, using the ΣX_{iR} values of Step 8, as follows.
12. Calculate A_i :

$$A_i = \frac{L_o}{V_{N+1} K_i} (1 + \Sigma X_{iR}) \quad (8-196)$$

13. Calculate absorption efficiency, E_{ai} , using new A_i value

$$E_{ai} = \frac{A_i^{N+1} - A_i}{A_i^{N+1} - 1}, \text{ read Figure 8-58}$$

14. Calculate mols absorbed/hr:
= (E_{ai}) (mols component in inlet rich gas)
15. Mols of each component in gas out top of absorber/hr = (mols component in)—(mols component absorbed)

16. Mols of component in outlet gas/mol inlet rich gas
Solve for Y_{1i}

$$E_{ai} = \frac{Y_{N+1} - Y_{1i}}{Y_{N+1} - Y_o}$$

If the X_1 in equilibrium with Y_1 is desired:

$$X_1 = \frac{Y_1 (1 + \sum X_{ir})}{K \sum Y_i} \quad (8-197)$$

17. Improved values can be obtained by recalculation from Step 11 if there is too great a difference between the “ Σ mols absorbed” from trial no. 1 and trial no. 2.

First Trial

Component	Inlet $Y_{(N+1)i}$	Mols/Hr In	K_i	$A = \frac{L}{VK_i}$
•	•	•	•	•
•	•	•	•	•
•	•	•	•	•
	1.00	Σ •		

Component	Fraction Absorbed, E_{ai}	Mols Absorbed	X_{iR}	Mol/Hr Off Gas	$Y_{1i(out)}$
•	•	•	•	•	•
•	•	•	•	•	•
•	•	•	•	•	•
		Σ •	Σ •	Σ •	

For second trial, see Step 11.

18. A graphical stepwise procedure offered by Sherwood [62] also summarized by Reference 18. Y and X are plotted and handled stepwise as in distillation. The equilibrium line equation is for any single component:

$$\frac{Y_i}{X_i} = K_i \left(\frac{\sum Y_i}{1 + \sum X_i} \right) \quad (8-198)$$

For a complete denuded inlet solvent at the top $\Sigma X = 0$, using K at top column conditions. The slope of the operating line = L_o/V_{N+1} = mols lean oil entering/mols wet gas entering.

Absorption—Determine Number Trays For Specified Product Absorption

- For fixed tower temperature, pressure, gas feed rate, specified or assumed operating (L_o/V_{N+1}) times minimum value, specified component recovery out of inlet gas.
- Calculate:
 - Mols component in inlet gas/hr
 - Mols in outlet gas

$$= \frac{100 - (\% \text{ recovery}) (\text{total mols in})}{100}$$

(c) Mols component absorbed = inlet – outlet

3. Calculate: E_{ai} for specified component (specified in 1.)

$$E_{ai} = \frac{\text{mols component in} - \text{mols component out}}{\text{mols component in}} = \text{specified fraction recovery}$$

4. Minimum (L/V) for specified component:

$$(L_o/V_{N+1})_{min} = KE_a \left[\frac{\sum Y}{1 + \sum X} \right]$$

Assuming equilibrium at bottom, $\Sigma Y = 1$. Ignoring ΣX gives slightly conservative value,

$$\left(\frac{L_o}{V_{N+1}} \right)_{min} = K_i E_{ai}$$

5. Operating $(L_o/V_{N+1})_o$

$$= (\text{specified unit}) (L_o/V_{N+1})_{min}$$

6. Operating

$$A_{io} = \left(\frac{L_o}{V_{N+1}} \right)_o \left(\frac{1}{K_i} \right) \quad (8-199)$$

7. Theoretical plates at operating (L_o/V_{N+1}) : solve for N .

$$E_{ai} = \frac{A_{io}^{N+1} - A_{io}}{A_{io}^{N+1} - 1} \quad (8-200)$$

$$(N + 1) \log (A_{io}) = \log \left[\frac{(A_{io} - E_{ai})}{(1 - E_{ai})} \right]$$

8. Actual trays at operating (L_o/V_{N+1}) :

$$N_o = N/E_o$$

E_o values may be calculated from Figure 8-29 or assumed at 20 to 50% as an estimating value for hydrocarbon oil and vapors, pressures atmospheric to 800 psig, and temperatures of 40°F to 130°F (see Table 8-11).

9. Lean oil rate:

$$L_o = (A_i) (K_i) (V_{N+1})_o, \text{ mols/hr} \quad (8-201)$$

10. For other components: E_{ai} is estimated by

$$E_{ai} = (E_{ai}) \left(\frac{K_1}{K_2} \right), \text{ with} \quad (8-202)$$

a limiting value of unity.

Stripping—Determine Theoretical Trays and Stripping Steam or Gas Rate For a Component Recovery [18]

The rich gas from the absorption operation is usually stripped of the desirable components and recycled back to the absorber (Figure 8-57). The stripping medium may be steam or a dry or inert gas (methane, nitrogen, carbon oxides—hydrogen, etc.). This depends upon the process application of the various components.

1. The rich oil flow rate and absorbed component compositions (this is the only composition of concern, not the oil composition, unless reaction or change takes place under the system conditions) are known. From the temperature levels of the available condensing fluids (water, refrigerant, etc.), determine a column operating pressure which will allow proper condensation of the desirable components at the selected temperature, allowing for proper Δt for efficient heat transfer. The condensing pressure (and column operating pressure) may be dictated by the available steam pressure used in stripping or the pressure on the inert stripping gas.
2. From K charts, determine K_i values for each component at the column temperature and pressure.

3. From a fixed percentage of recovery for key component ($= E_{si}$ for key component), mols component stripped/hr $= G_{mi} = (L_{m+1}) (X_{m+1}) (E_{si})$
4. Estimate stripping efficiency for components other than the key by:

$$E_{s2} = E_{skey} \left(\frac{K_{key}}{K_2} \right) \quad (8-203)$$

Assume Known		$\Sigma X_i =$		$E_{s, key} (1 + \Sigma X_i)$
V_o	L_o	V_o/L_o	$(LX_i)_{m+1}/L_o$	
—	Same	—	—	—
—	for	—	—	—
—	all	—	—	—
—	trials	—	—	—

$\Sigma Y_i =$	$E_{s, key} (1 +$		
$\Sigma X_i)$	$1 + \Sigma Y_i$	$K_{key} (1 + \Sigma Y_i)$	$\frac{K_{key} (1 + \Sigma Y_i)}{K_{key} (1 + \Sigma Y_i)}$
$\Sigma G_{mi} (\text{Step 3})/V_o$	—	—	—
—	—	—	—
—	—	—	—

Note that no recovery can be greater than 1.00, so any value so calculated is recorded as 1.00, indicating that the component is completely stripped from the rich oil. Calculate mols stripped per hour for each component as in Step 2.

5. The minimum stripping medium (steam or gas) lean oil ratio is estimated by a trial and error procedure based on key component:

By assuming several values of V_o , plot V_o/L_o versus $E_{s, Key} (1 + \Sigma X_i) / K_{Key} (1 + \Sigma Y_i)$. The point where they are equal gives the minimum value for V_o/L_o . This calculation can be thought of as assuming equilibrium at the gas outlet end and being slightly conservative by including the $(1 + \Sigma X_i)$ term. Operation at this point requires infinite plates; therefore, values larger than the minimum should be used. For economical as well as reasonable operation several values of $(V_o/L_o)_{oper}$ should be tried and corresponding plates evaluated.

$$V_o (\text{operating}) = (\text{assumed } (V_o/L_o)_{oper}) (L_o \text{ inlet}), \text{ mols/hr}$$

6. Calculate S_i for the key component, using the value of $(1 + \Sigma X_i)$ calculated in Step 5. Calculate

$$(1 + \Sigma Y_i) = 1 + \Sigma \frac{Y_{mi} (\text{Step 3})}{V_o (\text{oper})}$$

$$\text{then, } S_{io} = K_i \left(\frac{V_o}{L_o} \right)_{oper} \left(\frac{1 + \Sigma Y_i}{1 + \Sigma X_i} \right) \quad (8-204)$$

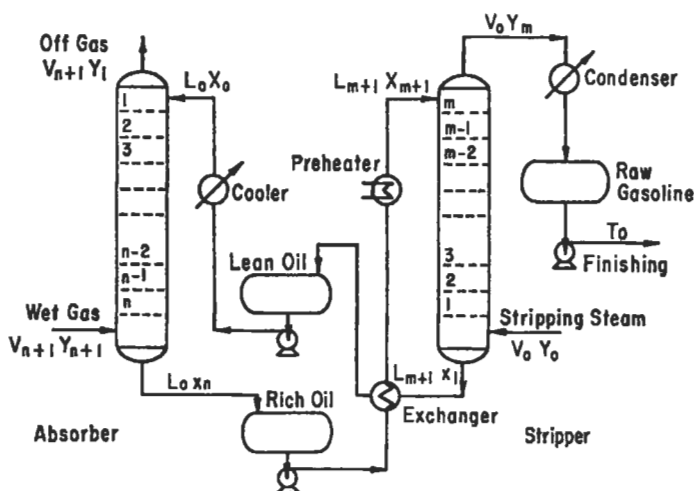


Figure 8-57. Flow diagram of absorption-stripping for hydrocarbon recovery from gaseous mixture. Used by permission, Edmister, W. C., *Petroleum Engr.*, Sept. (1947) to January (1948).

Sometimes the last term on right can be neglected.
 7. Calculate number of theoretical trays, M.

$$E_{si} = \frac{S_{io}^{M+1} - S_{io}}{S_{io}^{M+1} - 1} \quad (8-205)$$

$$(M_o + 1) \log S_{io} = \log \left[\frac{S_{io} - E_{si}}{1 - E_{si}} \right] \quad (8-206)$$

8. Actual trays at operating reflux:

$$M_{act} = \frac{M_o}{E_o} \quad (8-207)$$

9. Calculate for each component corrected amount stripped:

For each component:

$$S_i = K_i \left[\left(\frac{V_o}{L_o} \right)_{oper} \left(\frac{1 + \sum Y_i}{1 + \sum X_i} \right) \right] \quad (8-208)$$

$(V_o/L_o)_{oper}$ = fixed in Step 5.

$(1 + \sum Y_i)$ and $(1 + \sum X_i)$ come from Step 6.

10. From Figure 8-58, read $(S^{M+1} - S)/S^{M+1} - 1 = E_{si}$ for each component at the fixed *theoretical* required trays and at individual S_i values.

11. For final detail, recalculate mols stripped per hour from new E_{si} values and the total quantities of each component in the incoming rich oil. If values do not check exactly, adjustments can be made in steam rate and $\sum Y_i$ to give exact values. In many cases this accuracy is not justified since the method is subject to some deviation from theoretically correct values.

12. A graphical solution is presented by Edmister [18] and handled like step-wise distillation.

Equilibrium line: starts at origin of X-Y plot.

For assumed X values, calculate Y corresponding for key component from

$$\frac{X_i}{Y_i} = \frac{1}{K_i} \left(\frac{1 + \sum X_i}{1 + \sum Y_i} \right)$$

At lean oil end of tower: $\sum Z_i = 0$ and $\sum Y_i = 0$.

Slope of equilibrium line is $Y/X = K_i$

At rich oil end of tower:

$$Y_i = K_i X_i \left(\frac{1 + \sum Y_i}{1 + \sum X_i} \right)_R \quad (8-209)$$

Where X_i , $\sum X_i$ and $\sum Y_i$ are known. R = rich end.

Operating line:

$$\text{Slope} = L_o/V_o = \frac{\text{Mols lean oil leaving stripper}}{\text{Mols stripping steam (or gas) entering}}$$

At lean end, $Y_i = 0$ (or nearly so in most cases); if not, plot accordingly.

Stripping—Determine Stripping-Medium Rate For Fixed Recovery [18]

1. The composition and quantity of rich oil, and percent recovery of a specified key component are known, also column pressure and temperature.
2. Using Figure 8-58, assume a value for theoretical plates, read S_e corresponding to specified value of recovery E_{si} for key component, since:

$$E_s = (S^{M+1} - S)/(S^{M+1} - 1)$$

Note that with this procedure, the effect of the number of theoretical plates available can be determined. In an existing column where the number of trays are fixed, the theoretical trays can be obtained by evaluating an efficiency for the system.

3. The value of $S_e = S_i$ for key component obtained in Step 2 is equal to

$$S_i = K_i \frac{V_o}{L_o} = \left(\frac{1 + \sum Y_i}{1 + \sum X_i} \right)$$

Using key component:

$$\frac{V_o}{L_o} \left(\frac{1 + \sum Y_i}{1 + \sum X_i} \right) \left(\frac{S_i}{K_i} \right), \text{ known}$$

Set up table: use K_i for each component to calculate Column 4.

Component	Mols/hr in Rich Oil	K_i at Col. Cond.	$K_i \left\{ \frac{V_o (1 + \sum Y_i)}{L_o (1 + \sum X_i)} \right\}$	E_{si}	Mols/hr Stripped
—	—	—	—	—	—
—	—	—	—	—	—
—	—	—	—	—	—
	Σ				Σ

From values of S_i calculated ($=S_e$), read E_{si} values from Figure 8-58 at the number of theoretical trays assumed in Step 2. Note that the S_e corresponds to the number of trays selected, hence will give a value for performance of the system under these particular conditions.

4. Calculate the mols of each component stripped/hr
 $= (L_{M+1} X_{M+1})_R (E_{si})$
5. Calculate, V_o , mols/hr. of stripping medium required (steam or gas)

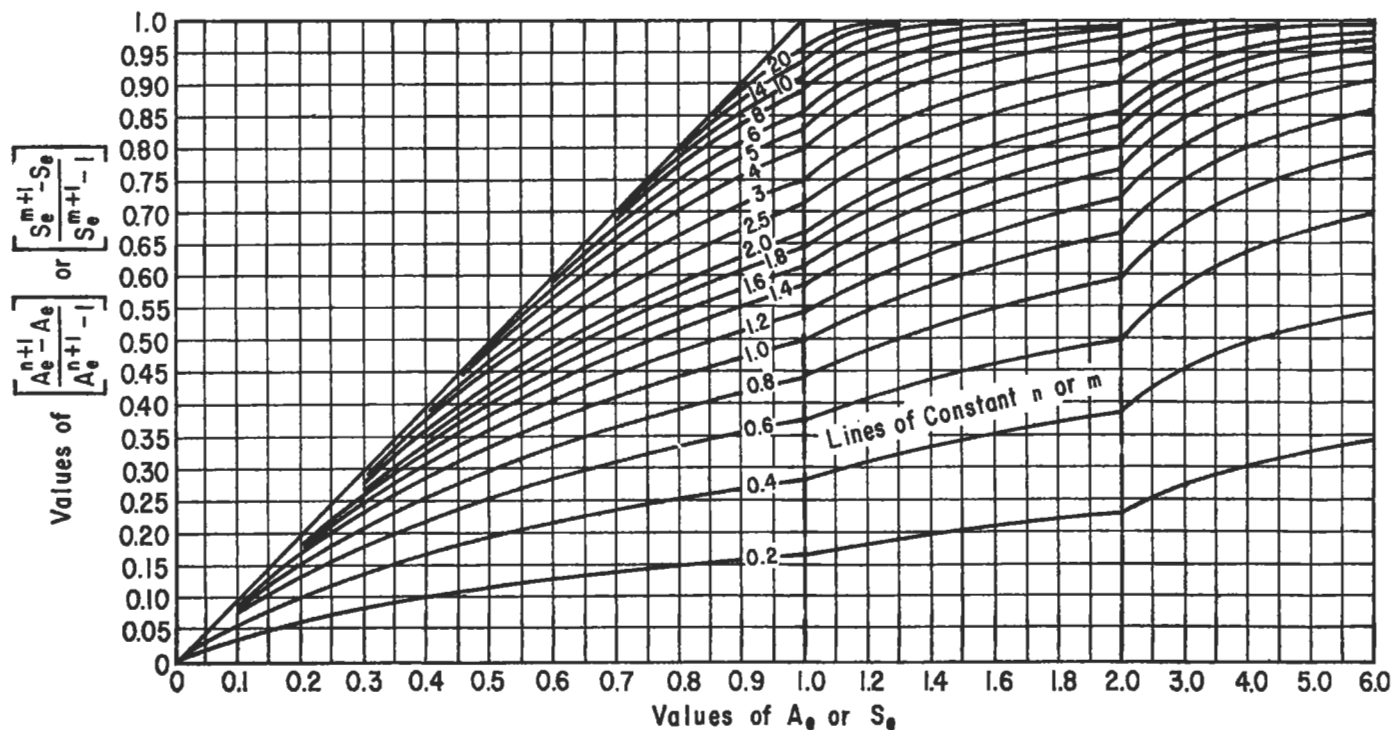


Figure 8-58. Absorption and stripping factors, E_a or E_s vs. effective values A_e or S_e (efficiency functions). Used by permission, Edmister, W. C., *Petroleum Engr.*, Sept. (1947) to Jan. (1948).

From Step 3, $\frac{V_o}{L_o} \left(\frac{1 + \Sigma Y}{1 + \Sigma X} \right)$ is known (equals S_i / K_i)

for key component.

Multiply by L_o .

Then, multiply result by $\frac{(1 + \Sigma \text{mols/hr in rich oil}/L_o)}{(1 + \Sigma \text{mols/hr stripped (Step 3)}/V_o)}$

This is equal to V_o . Note that V_o also is in the right hand side of the denominator, so fractions must be cleared.

Absorption—Edmister Method

This method [18] is well suited to handling the details of a complicated problem, yet utilizing the concept of average absorption and stripping factors. It also allows for the presence of solute components in the solvent and the loss of lean oil into the off gas. Reference 18 presents more details than are included here. Reference 18 is Edmister's original publication of the basic method for absorbers and strippers. Reference 18 also generates the

treatment to include distillation towers and presents the same graphical relationships in a slightly modified form.

Absorption: Lean Oil Requirement for Fixed Component Recovery in Fixed Tower [18]

1. The rich gas is known, the theoretical trays are fixed (or assumed and corresponding result obtained), the operating pressure and temperature can be fixed.
2. For key component and its fixed recovery, E_a , read A_e from Figure 8-58 at the fixed theoretical trays, N .

$$E_a = \frac{A_e^{N+1} - A_e}{A_e^{N+1} - 1}$$

3. Assume: (a) Total mols absorbed
(b) Temperature rise of lean oil (Normally 20–40°F)
(c) Lean oil rate, mols/hr, L_o
4. Using Horton and Franklin's [29] distribution relation for amount absorbed (or vapor shrinkage), per tray:

$$= \left(\frac{V_1}{V_{N+1}} \right)^{1/N}$$

or: $\left(\frac{V_1}{V_{N+1}} \right)^{1/N} = \frac{V_i}{V_{i+1}}$ (8-210)

Mols off gas leaving top tray

$$= V_1 = V_{N+1} - \text{Mols absorbed (assumed)}$$

Mols gas leaving bottom tray No. N

$$= V_N = V_{N+1} (V_1/V_{N+1})^{1/N}$$

$$\text{Mols gas leaving Tray No. 2 (from top)} = V_2 = \frac{V_1}{\left(\frac{V_1}{V_{N+1}} \right)^{1/N}}$$

$$\text{Liquid leaving top tray No. 1} = L_1 = L_0 + V_2 - V_1$$

where V_2 = vapor leaving tray No. 2 from top, mols/hr

L_0 = lean oil entering (assumed completely free of rich gas components), mols/hr

L_N = liquid leaving bottom tray, mols/hr

V_N = vapor leaving bottom tray, mols/hr

Liquid leaving bottom tray

$$= L_4 = L_0 + \text{Mols absorbed (assumed)}$$

5. Calculate: At top, L_1/V_1

At bottom, L_N/V_N

6. Use Horton-Franklin method to estimate temperatures at tower trays:

$$\frac{T_N - T_i}{T_N - T_o} = \frac{V_{N+1} - V_{i+1}}{V_{N+1} - V_1}$$
 (8-211)

where T_o = lean oil temperature, °F

T_N = bottom tray temperature, °F

T_i = tray, i, temperature, °F

T_{N+1} = inlet rich gas temperature, °F

These relations assume constant percent absorption per tray, and temperature change proportioned to the vapor contraction per tray. For estimating use only.

Temperature bottom tray = $T_N = T_{N+1} +$ (assumed rise)

Temperature top tray

$$= T_N - (\text{assume rise}) \left(\frac{V_{N+1} - V_{\text{Tray2}}}{V_{N+1} - V_1} \right)$$

7. Read K values from equilibrium charts for components in feed at temperatures of (a) top tray and (b) bottom tray.

8. Calculate A_{Ti} and A_{Bi} for each component.

$$A_{Ti} \text{ (for top conditions)} = L_1 / (K_i V_1)$$

$$A_{Bi} \text{ (for bottom conditions)} = L_N / (K_i V_N)$$

where A_{Ti} = absorption factor for each component at conditions of top tray

A_{Bi} = absorption factor for each component at conditions of bottom tray.

9. Read A_e values corresponding to A_{Ti} and A_{Bi} values from Figure 8-59.

10. Read E_{ai} values for fraction absorbed from Figure 8-58 using the A_e values of Step 9 and the fixed or assumed theoretical trays.

11. Calculate the mols of each component absorbed by: (Mol component in inlet rich gas) (E_{ai})

Suggested tabulation:

Com- ponent	Mols Rich Gas In	Absorption Factors			E_{ai} , Frac. Absorbed	Mols Absorbed
		K Top	K Bottom	A_T A_B A_e		
—	—	—	—	—	—	—
—	—	—	—	—	—	—
—	—	—	—	—	—	—

12. If the result does not yield the desired amount of the key component absorbed, then reassume the lean oil quantity, L_o , and recalculate. Adjustments may have to be made separately or simultaneously in the assumed absorption quantity until an acceptable result is obtained. After two or three trials a plot of the key variables will assist in the proper assumptions.

Absorption: Number of Trays for Fixed Recovery of Key Component

Here we also consider the more general case when the lean oil contains some of the components to be absorbed from the entering gas. The relationships are most conveniently written as follows [18], for a given component:

$$v_1 = f_s l_o + (1 - f_a) v_{n+1}$$
 (8-212)

$$f_s = \frac{S_e^{n+1} - S_e}{S_e^{n+1} - 1}$$
 (8-213)

$$f_a = \frac{A_e^{n+1} - A_e}{A_e^{n+1} - 1}$$
 (8-214)

Rearranging 8-213 yields

$$1 - f_a = \frac{A_e - 1}{A_e^{n+1} - 1}$$
 (8-215)

Combining Equations 8-211, 8-212 and 8-214 results in

$$v_1 = \left(\frac{S_e^{n+1} - S_e}{S_e^{n+1} - 1} \right) l_o + \left[1 - \left(\frac{A_e^{n+1} - A_e}{A_e^{n+1} - 1} \right) \right] v_{n+1}$$
 (8-216)

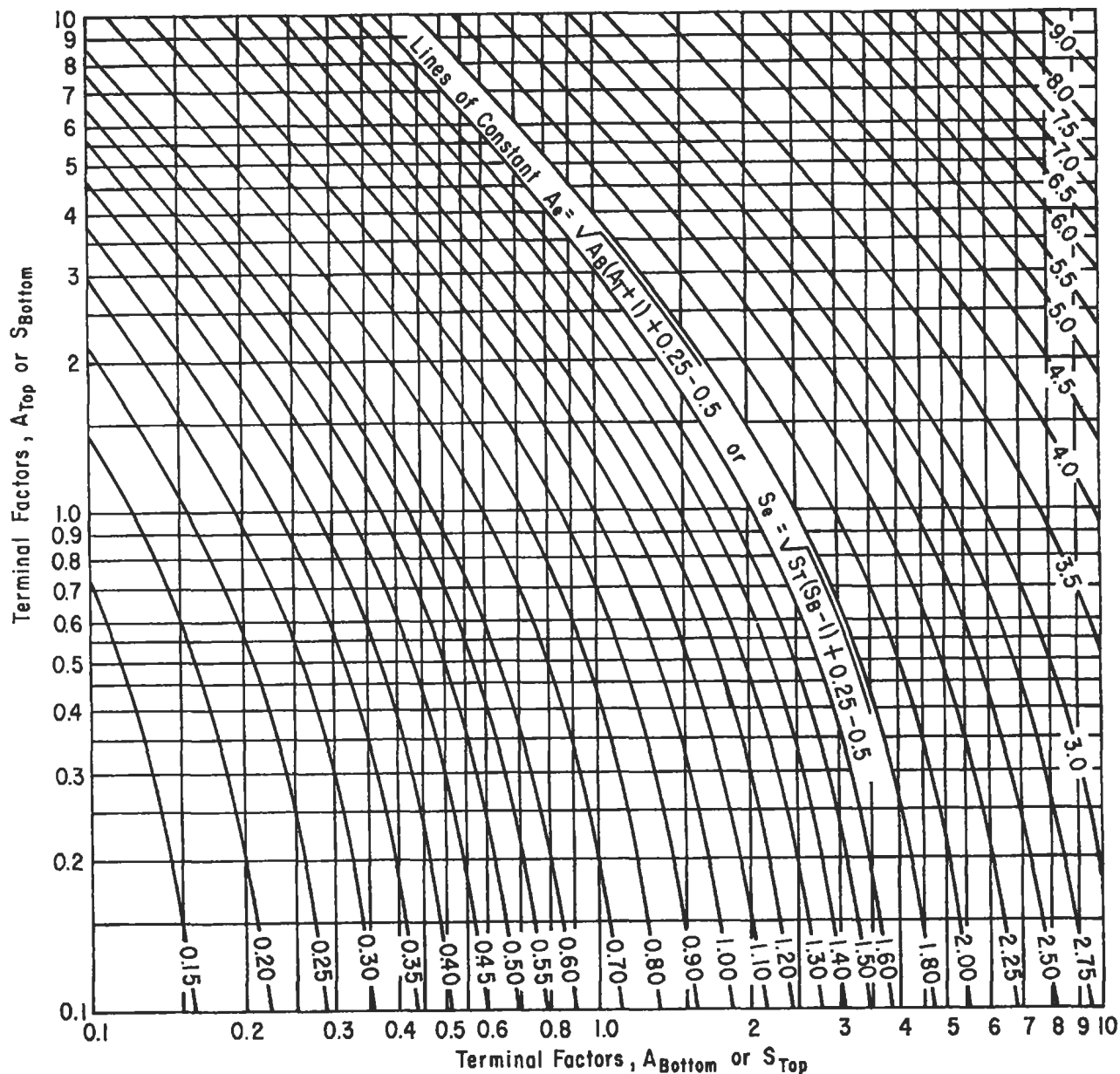


Figure 8-59. Effective absorption and stripping factors used in absorption, stripping and fractionation as functions of effective factors. Used by permission, Edmister, W. C., *Petroleum Engr.* Sept. (1947) to Jan. (1948).

which can be written as

$$v_1 = \left[1 - \left(\frac{S_e - 1}{S_e^{n+1} - 1} \right) \right] l_o + \left(\frac{A_e - 1}{A_e^{n+1} - 1} \right) v_{n+1} \quad (8-217)$$

- where
- v_{1i} = molar gas flow rate of component "i" leaving plate 1 in absorber
 - l_{oi} = molar flow of component "i" in entering liquid to absorber
 - v_{n+1i} = molar gas flow rate of component "i" in entering gas to absorber

- f_{si} = the fraction of V_{n+1i} that is absorbed by the liquid phase
- f_{ai} = the fraction of V_{n+1i} that is absorbed by the liquid
- n = absorber theoretical trays, also = N
- m = stripper theoretical trays, also = M

A material balance on the key component fixes v_1 , l_o and v_{n+1} for the key. A_e is estimated after A_T and A_B are calculated using approximate conditions at the top and bottom, with a multiple of the minimum solvent rate,

which is estimated by assuming equilibrium at the bottom of the tower. S_e is estimated from S_T and S_B . Note that $S_T = 1/A_T$ and $S_B = 1/A_B$. A trial and error solution for the number of theoretical stages is effected by using Equation 8-217 (or 8-216 and Figure 8-58). Values of v_1 for the non-keys can be calculated by using these relationships directly with the calculated value of n . If necessary, the entire procedure can be repeated, using the better estimates of the component flowrates in the leaving streams that were estimated in the first iteration.

Example 8-33: Absorption of Hydrocarbons with Lean Oil

The gas stream shown in Table 8-10 is fed to an isothermal absorber operating at 90°F and 75 psia. 90% of the n-butane is to be removed by contact with a lean oil stream consisting of 98.7 mol% non-volatile oil and the light components shown in Column 2 of Table 8-10. Estimate the composition of the product streams and the required number of theoretical stages if an inlet rate of 1.8 times the minimum is used.

Solution:

1. Initial estimates of extent of absorption of non-keys.

As a rough approximation, assume the fraction absorbed of a given component is inversely proportional to its K value (Equation 8-202). For example:

$$n-C_4, \text{ in off gas} = 33.6 - (0.9) (33.6) = 3.36$$

$$C_1, \text{ in off gas} = 1,639 - (0.9) \left(\frac{0.65}{42.5} \right) (1,639.2) = 1,616.6$$

$$C_2, \text{ in off gas} = 165.8 - (0.9) \left(\frac{0.65}{7.3} \right) 165.8 = 152.5$$

The other estimates in column 5 of Table 8-10 are calculated in a similar manner. Note that the C_5 s are assumed to be completely absorbed for this first iteration.

2. Inlet rate of rich oil.

The maximum mol fraction $n-C_4$ in the leaving liquid is taken as that in equilibrium with the incoming gases. Thus, for $n-C_4$,

$$\frac{l_n}{(L_n)_{\min}} = \frac{0.017}{0.65} = 0.02617$$

A material balance of $n-C_4$ yields

$$l_n = 0.002 L_o + (0.9) 33.6$$

With the absorption efficiencies assumed above,

$$L_n = L_o + 126.34$$

Combining the above equations yields the estimate of the minimum lean oil rate:

$$\frac{0.002 (L_o)_{\min} + (0.9) 33.6}{(L_o)_{\min} + 126.38} = 0.02617$$

$$\text{or } (L_o)_{\min} = 1,114.3 \text{ mols/hr}$$

$$\text{Thus, } L_o = 1.8 (1,114.3) = 2,005.7 \text{ mols/hr}$$

3. Effective Absorption Factor for $n-C_4$.

The total rich oil out is estimated as

$$L_n = 1,975 + 2,005.7 - 1,848.66 = 2,132.04$$

The absorption factors are calculated by

$$A_T = 2,005.7 / (.65) (1,848.66) = 1.669$$

$$A_B = 2,132.04 / (.65) (1,975) = 1.661$$

Table 8-10
Calculation Summaries for Example 8-33

Component	90°F K 75 psia	Feed Gas In (mols/hr)	Lean Oil in (Mol. Fraction)	Initial Estimate Of Net Amount Absorbed (mols/hr)	Off-Gas				Lean Oil In (mols/hr)	Rich Oil Out (mols/hr)
					Initial Estimate (mols/hr)	After First Iteration (mols/hr)	After Second Iteration (mols/hr)	After Third Iteration (mols/hr)		
Methane	42.5	1,639.2	—	22.6	1,616.6	1,597.5	1,598.4	1,598.4	—	40.8
Ethane	7.3	165.8	—	13.3	152.5	141.2	141.8	141.8	—	24.0
Propane	2.25	94.9	—	24.67	70.23	49.84	50.76	50.76	—	44.14
i-Butane	0.88	17.8	0.001	11.83	5.97	3.10	3.13	3.13	1.91	16.58
n-Butane	0.65	33.6	0.002	30.24	3.36	3.36	3.36	3.36	3.83	34.07
i-Pentane	0.28	7.9	0.004	7.9	0	2.08	2.03	2.03	7.66	13.53
n-Pentane	0.225	15.8	0.006	15.8	0	2.51	2.44	2.44	11.49	24.85
Heavy Oil	0	—	0.987	0	0	0	0	0	1,889.83	1,889.83
		1,975.0	1.000	126.34	1,848.66	1,799.57	1,801.92	1,801.92	1,914.72	2,087.78

$$A_e = \sqrt{1.661(2.669) + .25} - 0.5 = 1.664$$

The stripping factor, S_e , is taken as $1/A_e = 0.6010$

4. Calculation of required number of theoretical stages.
Using Equation 8-216 for n-butane,

$$3.36 = \left(\frac{0.601^{n+1} - 0.601}{0.601^{n+1} - 1} \right) 4.0 + \left[1 - \left(\frac{1.664^{n+1} - 1.664}{1.664^{n+1} - 1} \right) \right] 33$$

which is equivalent to

$$3.36 = \left[1 - \left(\frac{0.601 - 1}{0.601^{n+1} - 1} \right) \right] 4.0 + \left(\frac{1.664 - 1}{1.664^{n+1} - 1} \right) 33.6$$

Solving for n by trial and error yields, $n = 5.12$

5. Calculation of absorption of non-keys.

Equation 8-217 is used with $n = 5.12$ to calculate v_1 , as for example, for i-butane,

$$A_T = 1.233$$

$$A_B = 1.227$$

$$A_e = \sqrt{1.227(2.333) + 0.25} - 0.5 = 1.229$$

$$S_e = \frac{1}{1.229} = 0.8137$$

$$v_o = 17.8$$

$$l_o = (0.001)(2,005.7) = 2.01$$

$$v_1 = \left[1 - \left(\frac{0.8137 - 1}{0.8137^{6.12} - 1} \right) \right] 2.01 + \left(\frac{1.229 - 1}{1.229^{6.12} - 1} \right) 17.8 = 3.10$$

$$l_n = 17.8 + 2.01 - 3.10 = 16.71$$

The remaining non-keys in the off-gas are calculated in a similar manner and are tabulated in Column 6 of Table 8-10. Note that the calculated values are somewhat different from the assumed values in Column 5.

6. Second Iteration.

Using the previous calculated values, the net amount absorbed is $1,975 - 1,799.59 = 175.41$ mols/hr. The minimum rate of lean oil is calculated from

$$\frac{(0.002)(L_o)_{\min} + 0.9(33.6)}{(L_o)_{\min} + 175.41} = 0.02617$$

from which $(L_o)_{\min} = 1,061.2$ mols/hr and

$$L_o = 1.8(1,061.2) = 1,910.2 \text{ mols/hr}$$

An overall material balance gives $L_n = 2,085.6$. The effective absorption factor for n-C₄ is $A_e = 1.627$, and $S_e = 0.6145$, n is calculated from

$$3.36 = \left[1 - \left(\frac{0.6145 - 1}{0.6145^{n+1} - 1} \right) \right] 3.82 + \left(\frac{1.627 - 1}{1.627^{n+1} - 1} \right) 33.6$$

from which $n = 5.20$ theoretical stages.

The non-key components are computed and tabulated in Column 7 of Table 8-10.

7. Third Iteration.

A third iteration gave $(L_o)_{\min} = 1,063.73$, $L_o = 1,914.72$, $L_n = 2,087.8$, and $V_1 = 1,801.92$, with no change in the calculated off gas component flows.

The stripping calculations are handled in a manner similar to the steps above, and using the figures indicated.

Intercooling for Absorbers

Most absorbers require some intercooling between some stages or trays to remove heat of absorption and to provide internal conditions compatible with proper or required absorption. Some temperature rise (10–30°F) is usually designed into the initial conditions. The rise above this must be handled with intercoolers.

The total intercooler duty is the difference between the total heat in of the rich gas and lean oil and the total heat out of the off gas and rich oil all at the terminal calculated or design conditions. The total duty is often divided between several coolers placed to re-cool the oil as it passes down the column. If intercoolers are not used, then the absorption cannot meet the design terminal outlet conditions and the quantity of material absorbed will be reduced. If the intercooling is too great so as to sub-cool, then greater absorption may be achieved, but this can be controlled by the intercooler operation.

A second approach to the same result involves the same requirements as for a balanced "heat" design; the heat of absorption of the actual components absorbed must equal the sum of the heat added to the lean oil and to the lean

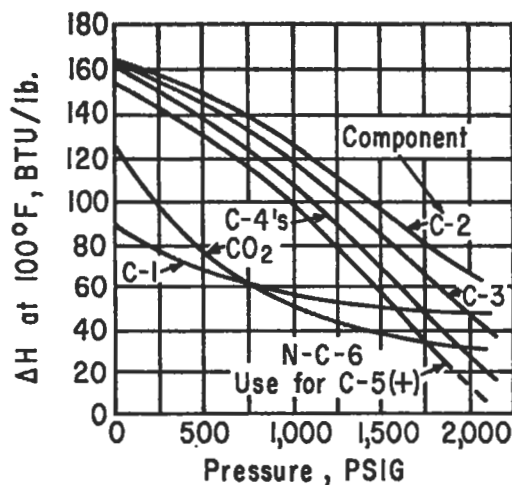


Figure 8-60. Component heats of absorption. Used by permission, Hall, R. J., and Raymond, K., *Oil and Gas Jour.*, Nov. 9 (1953) thru Mar. 15 (1954).

gas. For hydrocarbon materials these factors can be developed by using total heats.

The relation of Hull and Raymond [32] considers heat loss through the column wall, and indicates that either the

total heat of absorption or the rich oil outlet temperature for system balance can be calculated. Thus, if a reasonable temperature balance is not obtained, the heat load for the intercoolers can be set.

$$W_{Lo} C_{pLo} (T_{Ro} - T_{Lo}) + W_{DG} C_{pDG} (T_{DG} - T_{IG}) + W_s C_{ps} (T_{Ro} - T_{IG} = \Delta H_s - 0.024 U A'' (T_{AV} - A_{AMB})) \quad (8-218)$$

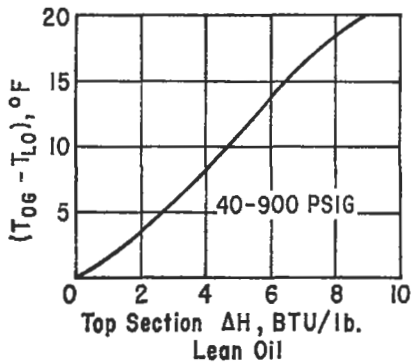


Figure 8-61. Hydrocarbon systems; overhead gas minus lean oil temperature for components absorbed in top "theoretical" tray (or top actual three trays). Used by permission, Hull, R. J., and Raymond, K., *Oil and Gas Jour.*, Nov. 9 (1953) thru Mar. 15 (1954).

Figure 8-60 presents actual total heats of absorption based on experimental studies [32]. As long as the hydrocarbon absorption is in the range of 80–120°F, the values read from the graph should apply.

Estimation of discharge gas temperature may be made from Figure 8-61 based on test data.

The design of absorbers has not received the empirical design guidelines study so prevalent in distillation problems. The graph of Hutchinson [34], Figure 8-62, is convenient to examine a problem to determine preliminarily the effects of design. This curve is compatible with the conventional absorption factor graphs. The percent extraction gives a quick evaluation of the possibilities of

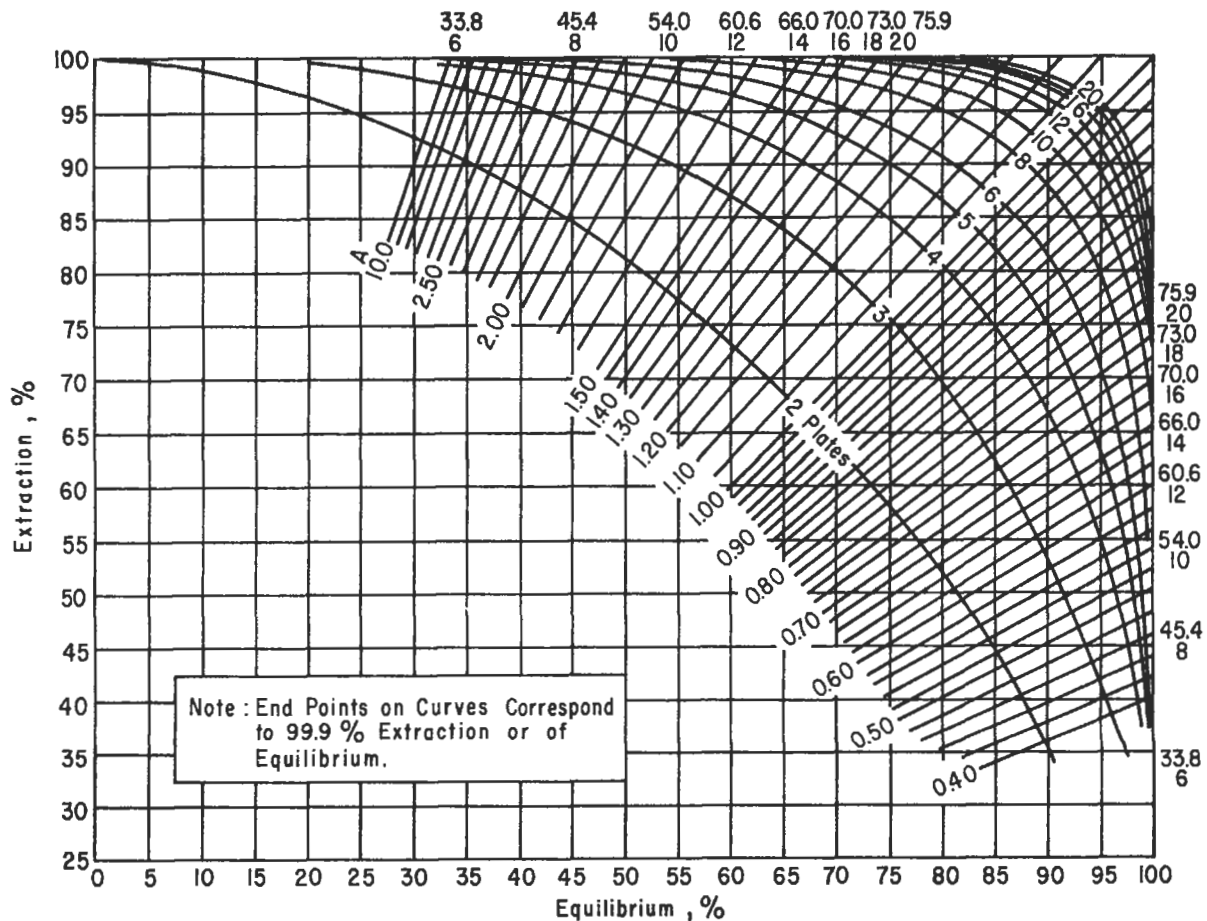


Figure 8-62. Absorption equilibrium curve. Used by permission, Hutchison, A. J. L., *Petroleum Refiner*, V. 29 (1950), p. 100, Gulf Pub. Co., all rights reserved.

accomplishing the desired absorption. As the number of trays in the absorber is increased, the amount of heavier material (larger A values) absorbed increases greater than the lighter components (lower A values). More heavier materials are also absorbed as the temperature of absorption is lowered. Thus, a cold lean oil has more capacity per gallon than a warm oil. This requires a study of the entire process and not just the one unit. Heat economy, oil flows, and tower costs all enter into a full evaluation of the absorber as it fits into the plant system.

Many designs are set up by assuming the number of theoretical trays, using best available information for tray efficiencies and then calculating the expected performance. A series of such studies might be made.

Absorption and Stripping Efficiency

Unfortunately, the efficiencies for tray and overall column operation are incomplete and nullify to a certain extent some very high quality theoretical performance design. Tray efficiencies may be estimated by Figure 8-29 or Table 8-11.

Table 8-11
Absorption-Stripping Approximate Tray Efficiencies**

Type	Pressure Range, psig	Temp., °F	Range Efficiency %
Absorption			
Hydrocarbon Oils & Vapors	0-800	30-130	35-50
Propane-key	100-2,100	—	30-37*-38
Butane-key	100-2,100	—	28-33*-36
Stripping			
Hydrocarbon Oils with Steam	0-130	300-550	50-80
Unsaturates in Oil with closed reboiler	0-50	—	25-35

*Average value

**Hull, R. J. and K. Raymond, *Oil and Gas Journal*, Nov. 9, 1953-March 15, 1954 [32], used by permission.

Example 8-34: Determine Number of Trays for Specified Product Absorption

A gas stream is to have the ethylene removed by absorption in a lean oil of molecular weight 160, sp. gr. 0.825. The inlet gas is at 70 psig and 100°F and the oil is at 80°F. The gas rate is 16,000,000 scf/day (60°F). Examine the tower performance for 98% ethylene recovery at 1.25 times the minimum L_o/V_N .

Feed Gas

Component	Mol or Volume %
H ₂	18.5
CH ₄	22.3
C ₂ H ₄	20.5
C ₂ H ₆	0.5
C ₃ H ₆	22.0
C ₃ H ₈	0.7
n, C ₄ H ₁₀	2.5
n, C ₅ H ₁₂	13.0
	100.0

Determine the oil rate and the number of theoretical and actual trays required. (Note: this example illustrates that unreasonable results must be examined, not just accepted.)

$$1. \text{ Inlet rich gas rate} = \frac{16,000,000}{359 \left(\frac{14.7}{14.7} \right) \left(\frac{460 + 60}{460 + 32} \right)} \quad (24)$$

$$= 1,756 \text{ mols/hr}$$

$$\text{Mols ethylene in} = (20.5/100) (1,756) = 360 \text{ mols/hr}$$

$$\text{Mols ethylene in outlet gas} = (100 - 98/100) (360)$$

$$= 7.20 \text{ mols/hr}$$

$$\text{Mols ethylene absorbed in oil} = 360 - 7.2 = 352.8 \text{ mols/hr}$$

$$2. \text{ Specified ethylene separation} = 0.98 = E_{ai}$$

$$= \frac{\text{Mols in} - \text{Mols out}}{\text{Mols in}}$$

3. Minimum L/V for ethylene:

$$\left(\frac{L_o}{V_{N+1}} \right)_{\min} = K_i E_{ai}$$

Average tower conditions for K:

$$\text{Temperature} = (100 + 80)/2 = 90^\circ\text{F}$$

Pressure: allow 20 psi pressure drop, then top pressure would be 70 - 20 = 50 psig

$$\text{Average: } (50 + 70)/2 = 60 \text{ psig}$$

K (ethylene) at 60 psig and 90°F = 11.5 (from equilibrium charts).

$$\left(\frac{L_o}{V_{N+1}} \right)_{\min} = (11.5) (0.98) = 11.28$$

$$4. \text{ Operating } (L_o/V_{N+1})_o = (1.25) (11.28) = 14.1$$

$$5. \text{ Operating } A_{iO} = \left(\frac{L_o}{V_{N+1}} \right)_o \left(\frac{1}{K_i} \right) = \frac{14.1}{11.5} = 1.227$$

6. Theoretical trays at operating (L_o/V_{N+1}) :

$$E_{ai} = \frac{A^{N+1} - A_i}{A^{N+1} - 1} = \frac{(1.227)^{N+1} - 1.227}{(1.227)^{N+1} - 1} = 0.98$$

$$(N+1) \log 1.227 = \log \left[\frac{1.227 - 0.98}{1 - 0.98} \right]$$

$$N = 11.22$$

7. Actual plates at operating (L_o/V_{N+1}):

Efficiency of oil at 90°F, and sp. gr. of 0.825 corresponding to API of 40.

Viscosity = 0.81 centipoises

For O'Connell's efficiency correlation, Figure 8-29.

$$\frac{0.825 (62.3 \text{ lb/ft}^3)}{(11.5) (160) (0.81)} = 0.0345$$

Reading curve (3), Eff. = 14%

This value is low, but agrees generally with the specific data in O'Connell's [49] report.

Although Drickamer's data are not so specific for absorption, the graph of this correlation gives Eff. = 20% for the 0.81 cp. Because no better information is available, use Eff. = 15%.

$$\text{Actual trays, } N_o = N/E_o = 11.22/0.15 = 74.8$$

Use $N_o = 75$ trays

8. Lean oil rate = $L_o = A_i (K_i) (V_{N+1})_o = (1.227) (11.25) (1,756)$

$$L_o = 24,200 \text{ mols/hr}$$

$$\text{GPM oil} = \frac{24,200 (160)}{(8.33) (0.825) (60)} = 9,400$$

This is unreasonable, and is due to the effect of

- Operating pressure being too low, thus giving a high K value
 - Ethylene being light component and difficult to absorb
 - Temperature too high.
9. Recalculation of Steps 3 thru 8.

Assume operating pressure is 700 psig, $K = 1.35$. Note that this same K value could have been achieved by lowering the operating temperature to -90°F. This is also not practical from the oil standpoint or even from the economics of operating the entire system and refrigeration system at this level, unless (1) the refrigeration is available and (2) a suitable oil is available.

$$\text{Min } (L/V) = (1.35) (0.98) = 1.32$$

$$\text{Operating } (L/V_{N+1})_o = (1.25) (1.32) = 1.65$$

$$\text{Operation } A_{io} = 1.65/1.35 = 1.222$$

Theoretical trays at operating (L_o/V_{N+1}):

$$(N+1) \log 1.222 = \log \left[\frac{1.222 - 0.98}{1 - 0.98} \right]$$

$$N = 11.2 \text{ trays}$$

$$\text{Efficiency} = \frac{(0.825) (62.3)}{(1.35) (160) (0.81)} = 0.294$$

Reading curve 3, Eff. = 29%

Actual trays = 11.1/0.29 = 38.6. Say 40 trays.

Lean oil rate = (1.222) (1.35) (1,756) = 2,900 mols/hr

$$\text{GPM} = \frac{(2,900) (160)}{(8.33) (0.825) (60)} = 1,122$$

This is still a large quantity of oil to absorb the ethylene. Under some circumstances it might be less expensive to separate the ethylene by low-temperature fractionation.

Example 8-35: Determine Component Absorption in Fixed-Tray Tower

An existing 40-tray tower is to be examined to determine the absorption of a rich gas of the following analysis:

Component	Mols/hr	Mol wt	104° K _i 176 psia
H ₂	500.0	2	59.0
CH ₄	20.9	16	56.0
C ₂ H ₄	131.5	26	8.1
CO	230.0	28	12.3
C ₃ H ₄	3.5	40	0.07
C ₄ H ₂	4.1	50	0.009
	890.0		

- The key component is methyl acetylene, C₃H₄. Recovery will be based on 96.5% of this material.

The tower average temperature will be assumed = 104°F.

The operating average pressure will be = 161 psig.

- The K_i values are tabulated for the conditions of (1), and were determined from laboratory test data for the special solvent oil being considered.

$K_i = 14.7 (H_i)/176$, where H_i is Henry's constant expressed as atm/mol fraction for each component. Note that conventional K charts are only applicable to hydrocarbon oil systems, and do not apply for any special solvents.

3. Calculate tray efficiency for C_3H_4 .

Using O'Connell's correlation:

(solvent) at $104^\circ F = 2.3$ cp

Sp. gr. = 1.0

Mol. wt. solvent = 180

 $K = 0.07$

$$HP = \frac{\text{Sp. Gr. solvent}}{(K_{C_3H_4}) (\text{M. W. solvent})} = \frac{(1.0) (62.3)}{(0.07) (180)} = 4.94$$

$$\frac{HP}{\mu} = \frac{4.9}{2.3} = 2.13$$

Efficiency = 46.5% (From Figure 8-29)

Use: 45%

Actual number trays in column = 40

Theoretical trays based on 45% efficiency = (40) (.45) = 18

4. Using $E_{ai} = 96.5\%$ for C_3H_4 , read A_i from Figure 8-58.At $n = 18$

$$A_c = A_i = 1.04$$

$$A_i = L_o / KV_{N+1}$$

$$V_{N+1} = 890 \text{ mols/hr}$$

$$L_o = (1.04) (0.07) (890) = 64.8 \text{ mols/hr}$$

$$L_o / V_{N+1} = 64.8 / 890.0 = 0.0728$$

5.

Component	Inlet		$A_i = \frac{L_o}{V_{N+1} K_i}$	E_{ai}
	$Y_{(N+1)i}$	Mols/Hr		
H ₂	0.562	500.0	0.001235	0.001235
CH ₄	0.0235	20.9	0.00130	0.00130
C ₂ H ₂	0.1478	131.5	0.009	0.009
CO	0.258	230.0	0.00592	0.00592
C ₃ H ₄	0.00393	3.5	1.04	0.965
C ₄ H ₂	0.00462	4.1	8.1	1.000
	0.99985	890.0		

Component	Mols/Hr		Mols/Hr Off Gas	Y_{li} (out)
	Absorbed	X_{iR}		
H ₂	0.617	0.00953	*499.383	0.561
CH ₄	0.0272	0.00042	20.8728	0.02348
C ₂ H ₂	1.185	0.0183	130.315	0.14647
CO	1.36	0.021	228.64	0.2565
C ₃ H ₄	3.37	0.052	0.13	0.00014
C ₄ H ₂	4.1	0.0633	0	0
	10.659	0.1645		

*These are subtraction differences and do not infer that the results are this accurate.

Typical calculations: for hydrogen

$$A_i = 0.0728 / 59.0 = 0.001235$$

From Figure 8-58 at $n = 18$ trays theoretical, and $A_i = 0.001235$ read E_{ai} , except that in this low region some values cannot be read accurately. When A_i is considerably less than 1.0, use $E_{ai} = A_i$ (very little light material recovered), and when A_i is quite a bit larger than 1.0, use $E_{ai} = 1.0$ (heavy material mostly recovered).

$$\begin{aligned} \text{Mols component absorbed/hr} &= (V_{N+1}) (Y_{(N+1)i}) E_{ai} \\ &= (890) (0.562) (0.001235) \\ &= 0.617 \end{aligned}$$

$$\begin{aligned} \text{Mols component absorbed/mol lean oil} &= X_{iR} = 0.0617 / 64.8 \\ &= 0.00953 \end{aligned}$$

Mols of component in off gas out top of absorber:

$$= 500.0 - 0.617 = 499.383 \text{ mols/hr}$$

Mols component in, out top of absorber/mol inlet rich gas

$$E_{ai} = \frac{Y_{N+1} - Y_{li}}{Y_{N+1} - Y_o^*} \quad \text{let } Y_o^* = 0$$

$$0.001235 = \frac{0.562 - Y_{li}}{0.562}$$

$$Y_{li} = 0.5614$$

6. Correcting values and recalculating

Component	Inlet		$A_i = \frac{L_o}{V_{N+1} K_i} (1 + \sum X_{iR})$	E_{ai}
	$Y_{(N+1)i}$	Mols/Hr		
H ₂	0.562	500.0	0.00144	0.00144
CH ₄	0.0235	20.9	0.001513	0.001513
C ₂ H ₂	0.1478	131.5	0.01048	0.01048
CO	0.258	230.0	0.00689	0.00689
C ₃ H ₄	0.00393	3.5	1.21	0.98
C ₄ H ₂	0.00462	4.1	9.43	1.00

Component	Mols/Hr		Off Gas	
	Absorbed	X_{iR}	Mols/Hr	Y_{li}
H ₂	0.72	0.0111	499.28	0.561
CH ₄	0.0317	0.000488	20.869	0.0232
C ₂ H ₂	1.38	0.0213	130.12	0.1463
CO	1.585	0.0244	228.415	0.257
C ₃ H ₄	3.43	0.0529	0.07	0.00008
C ₄ H ₂	4.1	0.0633	0	0
	11.246	0.1734	878.754	0.9775

Typical calculations, using hydrogen:

$$A_i = \frac{L_o}{V_{N+1} (K_i)} (1 + \sum X_{iR}) = \frac{0.0728}{59.0} (1 + 0.1645) = 0.00144$$

$$\text{Mols component absorbed/hr} = (0.00144) (500) = 0.72$$

Mols component absorbed/mol lean oil = $0.72/64.8 = 0.0111$

Mols of component in off gas out top of absorber:

$$= 500.0 - 0.72 = 499.28$$

These results do not justify recalculation for greater accuracy. Note that 98% of the C_3H_4 is absorbed instead of 96.5% as initially specified. This could be revised by reassuming a lower (slightly) oil rate, but this is not considered necessary.

The off gas analysis Y_1 represents mols gas out per mol entering rich gas.

For a new design a study should be made of number of trays against required lean oil for a given absorption.

Nomenclature For Part 2, Absorption and Stripping

(Special notations, all others same as for Distillation Performance Nomenclature, Part 1)

- A' = Edmister's effective absorption factor
- A'' = Outside surface area of absorber, ft^2
- A = Absorption factor, average
- A_e = Effective absorptive factor
- A_{Bi} = Absorption factor for each component at conditions of bottom tray
- A_{Ti} = Absorption factor for each component at conditions of top tray
- $C_p = c_p$ = Specific heat, Btu/lb ($^{\circ}F$)
- E_a = Absorption Efficiency, or fraction absorbed
- E_o = Overall tray efficiency, fraction
- E_s = Stripping efficiency, or fraction stripped
- f_{ai} = Fraction of v_{n+1i} absorbed by the liquid
- f_{si} = Fraction of l_{oi} stripped out of the liquid
- G_{mi} = Mols individual components stripped per hour
- ΔH = Total heat of absorption of absorbed components, thousand Btu/day
- K = Equilibrium constant, equals y/x , at average tower conditions
- L_{M+1} = Mols/hour rich oil entering stripper
- L_N = Liquid leaving bottom absorber tray, mols/hr
- L_o = Mols/hr lean oil entering absorber, or leaving stripper
- l_{oi} = Molar flow of component "i" in entering liquid to absorber
- M = Number theoretical stages in stripper
- $m = M$ (see above)
- N = Number theoretical stages in absorber
- $n = N$ (see above)
- S, S_e = Stripping factor, average and effective, respectively
- S' = Edmister's effective stripping factor
- T_i = Tray i, temperature, $^{\circ}F$
- T_N = Bottom tray temperature, $^{\circ}F$
- T_{N+1} = Inlet rich gas temperature, $^{\circ}F$

- T_o = Lean oil temperature, $^{\circ}F$
- U = Overall heat transfer coefficient between absorber outside surface and atmosphere, Btu/(ft^2) ($^{\circ}F$) (hr); usual value = 3.0
- V_1 = Mols/hr lean gas leaving absorber
- V_i = Gas leaving tray i, mols/hr
- V_{i+1} = Gas leaving tray, $i + 1$, mols/hr
- V_N = Vapor leaving bottom absorber tray, mols/hr
- V_{N+1} = Mols/hr rich gas entering absorber
- V_o = Mols/hr stripping medium (steam or gas) entering stripper
- v_{1i} = Molar gas flowrate of component "i" leaving plate 1 in absorber
- v_{n+1i} = Molar gas flowrate of component "i" in entering gas to absorber
- W = Rate of flow, thousand lb/day
- X = Number mols absorbed component or stripped per mol lean oil entering column
- X_1 = Number mols liquid phase component in equilibrium with Y_1
- X_{iR} = Mols of a component in liquid absorbed per mol of lean oil entering column
- ΣX_i = Total mols of all liquid phase components absorbed per mol of lean oil (omitting lean oil present in liquid phase, considered = 1.0)
- X_{M+1} = Number liquid phase mols of component entering stripper per mol of lean oil
- X_{oi} = Number liquid phase mols of component entering absorber with lean oil per mol of lean oil
- Y_1 = Number vapor phase mols of component leaving top plate of absorber per mol rich gas entering absorber
- Y_i = Mols component in vapor phase from tray "i"/mol rich gas entering absorber
- ΣY_i = Total mols of all vapor phase components stripped per mol of stripping medium
- Y_{N+1} = Number vapor phase mols of component entering absorber per mol rich gas entering
- Y_o^* = Number vapor phase mols of component in equilibrium with lean oil per mol of rich gas entering

Subscripts

- 1, 2, etc. = Components in a system
- Amb = Ambient
- A_{vg}, A_v = Arithmetic average
- DG = Discharge gas
- e = Effective
- i = Individual components in mixture
- IG = Intake gas
- Key = Key component
- L = Lean concentration end of column
- LO = Lean oil
- Min = Minimum condition
- o = Operating condition
- R = Rich concentration end of column
- RO = Rich oil
- S = Absorbed components

Part 3: Mechanical Designs for Tray Performance

Determining the number of theoretical and actual trays in a distillation column is only part of the design necessary to ensure system performance. The interpretation of distillation, absorption, or stripping requirements into a mechanical vessel with internal components (trays or packing, see Chapter 9) to carry out the function requires use of theoretical and empirical data. The costs of this equipment are markedly influenced by the column diameter and the intricacies of the trays, such as caps, risers, weirs, downcomers, perforations, etc. Calculated tray efficiencies for determination of actual trays can be lost by any unbalanced and improperly designed tray.

Contacting Trays

The particular tray selection and its design can materially affect the performance of a given distillation, absorption, or stripping system. Each tray should be designed so as to give as efficient a contact between the vapor and liquid as possible, within reasonable economic limits. It is not practical in most cases to change the design of each tray to fit calculated conditions. Therefore, the same tray design is usually used throughout the column, or the top section may be of one design (or type) while the lower section is of another design. The more individual tray designs included in a column, the greater the cost.

This concept has not gained commercial popularity due to the proprietary nature of the Fractionation Research, Inc. (FRI) data being limited to member organizations, and the public literature does not contain much independent research and application data. General industrial and commercial proprietary designs available are listed in Table 8-12, but may not be all-inclusive:

Tray Types and Distinguishing Application Features

Bubble Cap

Vapor rises up through “risers” or “up-takes” into bubble cap, out through slots as bubbles into surrounding liquid on tray. Bubbling action effects contact. Liquid flows over caps, outlet weir and downcomer to tray below, Figures 8-63–67, 79, and 81.

Capacity: moderately high, maintains efficiency.

Efficiency: most data are for this type, as high as other tray designs.

Entrainment: about three times that of perforated type plate or sieve tray. Jet-action accompanies bubbling.

Flexibility: most flexible of tray designs for high and low vapor and liquid rates. Allows positive drain of liquid from tray. Liquid heads maintained by weirs.

Application: all services except extremely coking, polymer formation or other high fouling conditions. Use for extremely low flow conditions where tray must remain wet and maintain a vapor seal.

Tray Spacing: 18-in. average, 24- to 36-in. for vacuum conditions.

Sieve Tray or Perforated Tray With Downcomers

Vapor rises through small holes ($\frac{1}{8}$ to 1-in.) in tray floor, bubbles through liquid in fairly uniform manner. Liquid flows across tray floor over weir (if used), through downcomer to tray below. Figures 8-67A–C, and 8-68B.

Capacity: As high or higher than bubble cap at design or down to 60% of design rates with good efficiency. At lower throughputs performance drops as efficiency falls off rapidly.

Efficiency: As high as bubble caps in region of design, but falls to unacceptable values when capacity reduces below 60% (approximately)

Entrainment: Only about one-third that of bubble cap trays.

Flexibility: Not generally suitable for columns operating under variable load, falling below 60% of design. Tray weeps liquid at low vapor rates.

Application: Systems where high capacity near-design rates to be maintained in continuous service. Handles suspended solid particles flushing them down from tray to tray. Holes become plugged in salting-out systems where trays run hot and dry (as underside of bottom tray).

Tray Spacing: Can be closer than bubble cap due to improved entrainment. Fifteen inches is average, 9-in., 10-in. and 12-in. are acceptable, with 20- to 30-in. for vacuum.

Perforated Plate Without Downcomers: (Dual-Flow, from FRI)

Vapor rises through holes ($\frac{3}{16}$ to 1-in.) in tray floor and bubbles through liquid. At the same time liquid head forces liquid countercurrent through these holes and onto tray below. Liquid flow forms random patterns in draining and does not form continuous streamlets from each hole. See Figures 8-67D and 8-68A.

Table 8-12
General Listing and Comparison of the Major Contacting Trays⁺

Type Tray	Manufacturer	Efficiency Capacity	Turn-down	Pressure Drop	Operating Flexibility
Bubble Cap Figures 8-63, 64, 66	Several	Med. to 60%	Good low flows, exceeds Valve Tray	High	Good
Sieve Figures 8-67A, 67C, 68B	Several	High	High/Limited	Medium	Medium
Sieve	Linde	High	High/Medium	Low	Good/Medium
Dual Flow* Figure 8-68A	Shell Dev.	High	High/Medium	Low	Low
Float Valve Figures 8-69A, 69B	Nutter	High	High/High	Medium	Good
Fixed V-Grid Figure 8-70	Nutter	Out performs Sieve Tray	High/High	Medium	Good
MVG Tray Figures 8-71A, 71B	Nutter	High	High/4:1 > by 15-/ratio 30%	Medium	Good
Flexitray Type A Figure 8-72 valve lift w/srp edge orifice, round	Koch	Higher than Sieve Tray. Lower entrain than Sieve	Wide range	Low	Good
Flexitray Type A w/ contoured hole Figure 8-73B	Koch	Ditto above	Ditto above		Ditto above
Flexitray Type T, rnd. Figure 8-73A retained by fixed hold down, srp edge hole	Koch	Ditto above	Ditto above		Ditto above
Flexitray Type T _o lift, con- toured hole Figure 8-72	Koch	Higher than Sieve, w/ lower entr.	Wide range	Low	Good
Flexitray Type S, fixed triangular valve Figure 8-72	Koch	Medium	Good, fixed by design	Medium	Good to Medium
Ballast, Valve V-Series V-1 thru V-5 valves Figure 8-74 and 8-77	Glitsch	Higher than Sieve	High/High	Medium Similar to Sieve	Good
Ballast Valve Figures 8-75 and 8-76 A-Series lift, A-1 A-5 w/cages Figure 8-75	Glitsch	Higher than Bubble Cap or Sieve	High/High	Medium to low	Good

Table 8-12 (Cont'd)
General Listing and Comparison of the Major Contacting Trays

Type Tray	Manufacturer	Efficiency Capacity	Turn-down	Pressure Drop	Operating Flexibility
Nye Tray Figure 8-78 **	Glitsch	Same or better than Sieve/Valve	Similar to Sieve or Valve	Low	Good
Bubble Cap (FRI plain 3 in. and 4 in.) Figure 8-79	Norton	Good	High/High	Medium	Good
Valves, MR2L Figure 8-80	Norton	Good	Medium/Good	Medium	Good
Valve, L	Norton	Good	Medium/Good	Medium	Good
Caged, MR2	Norton	Good	Medium/Good	Medium	Good
Valve, M	Norton	Good	Medium/Good	Medium	Good
Caged, MR7	Norton	Good	Medium/Good	Medium	Good
Caged, G	Norton	Good	Medium/Good	Medium	Good

*Not in wide usage.

**Nye Tray, 10–20% increased tray (over sieve or valve) capacity and good efficiency. More capacity from existing column. Improved inlet area for sieve or valve tray with greater area for vapor-liquid disengagement.

*Not offered as all inclusive analysis, but as somewhat general guidelines based on the respective manufacturer's literature description and best interpretation by this author. This Table is not intended to be a decision-making guide, and the author recommends that the engineer discuss and present separation requirements to the respective manufacturers. There is no intention to suggest a negative performance by any manufacturer's designs or fabricated equipment.

This specialized Sieve Tray design is of high efficiency and operates with exceptional short tray spacings, sometimes as low as 6 in. between trays. Compiled from recent manufacturer's literature. Credit is acknowledged for the use of this material, which is not all-inclusive in this table.

Capacity: Quite similar to sieve tray, as high or higher than bubble cap tray from 50% up to 100% design rate (varies with system and design criteria). Performance at specification quality falls off at lower rates.

Efficiency: Usually not quite as high as bubble caps in region of design, but falls to unacceptable values below 60% design rate.

Entrainment: Only about one-third that of bubble cap tray.

Application: Systems where high capacity near-design rates to be maintained in continuous service. Handles suspended crystal and small solid materials, as well as polymer forming materials. Holes become plugged in salting-out systems where trays run hot and dry (as underside of bottom tray). Good in vacuum or low-pressure-drop design.

Tray Spacing: Can be closer than bubble cap due to improved entrainment. Twelve-inch is average; 9 to 18-in. acceptable; 18 to 30 in. for vacuum.

Proprietary Trays

There are many special tray designs which solve special problems and exceed the capabilities of the conventional trays. The comments regarding performance are those claimed by the manufacturer, see Table 8-12.

Not all tray designs solve special problems, even though some may have unique performance features. Most of

these trays have the bubbling contact action from valves, either moveable (liftable) or fixed (usually stamped or cut from the tray floor itself). In addition to the valve trays above, there are sieve trays (with multiple downcomers) of Union Carbide Corp., Linde Div., and the Turbogrid tray of Shell Development Co., and Ripple Tray (sieve type) of Stone and Webster Engineering Corp.

Bubble Cap Tray Design

The bubble cap has been studied extensively and several design recommendations have been presented over the years. The most complete and generally applicable is that of Bolles [5]. It should be stressed that proper mechanical interpretation of process requirements is essential in design for efficient and economic operation. There is not just one result, but a multiplicity of results, each unique to a particular set of conditions, and some more economical than others. Yet at the same time, many of the mechanical design and fabrication features can be identical for these various designs.

The tray and caps operate as a unit or system; therefore they must be so considered in design (Figures 8-63 and 8-66).

Due to the public nature of so many design techniques, the individual engineer has sufficient information to prepare a design that can be expected to perform satisfactorily.

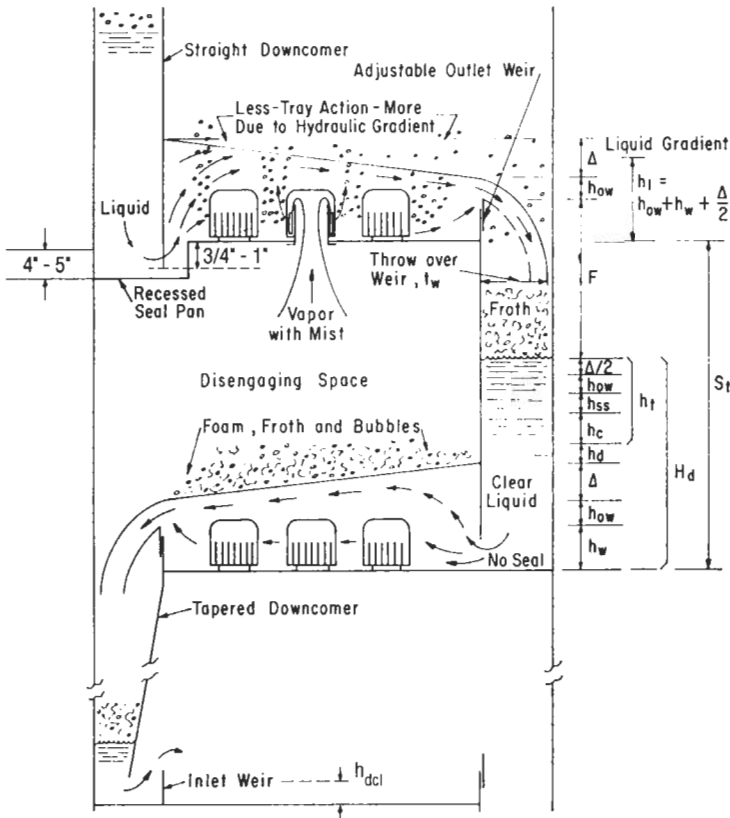


Figure 8-63. Bubble cap tray schematic—dynamic operation.



Figure 8-65. Slip-type cartridge assembly for bubble cap trays in small column, 1-ft-10¹/₆-in. I.D. Used by permission, Glitsch, Inc.

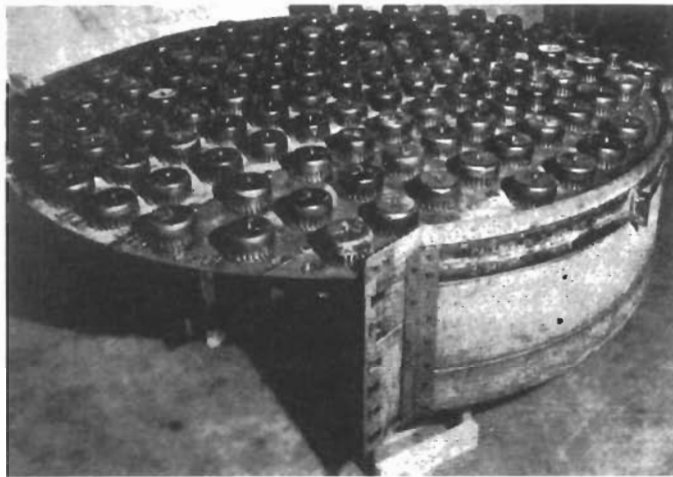


Figure 8-64. Bubble cap tray in large column. Used by permission, Glitsch, Inc.

In addition nearly all of the major tray manufacturers can and do design bubble cap trays as well as the other types on request for comparison with competitive types of trays.

The Fractionation Research, Inc. design procedures are proprietary for the financial participants in this extensive test program.

Standardization

The custom design of the trays for each application is usually unnecessary and uneconomical. Instead most designers use a standard reference tray layout and cap size to check each system. If the results of the tray hydraulics study indicate operation unsatisfactory for the standard operation, then alterations of those features controlling the out-of-line performance is in order, using the same method as will be outlined for the initial design of a custom tray. It is understood that such a standard tray cannot be optimum for every application but experience has demonstrated that many applications fit. The economic advantages of using a limited number of bubble cap sizes and designs are reflected in warehouse stocks. The standardization of layouts, downcomer areas, weir lengths and many other features are reflected in savings in engineering mechanical design time.

At the same time, systems that do not adapt themselves to this standardization should be recognized and handled as special designs.

Design Objectives

Each tray design should ultimately resolve and achieve the following:

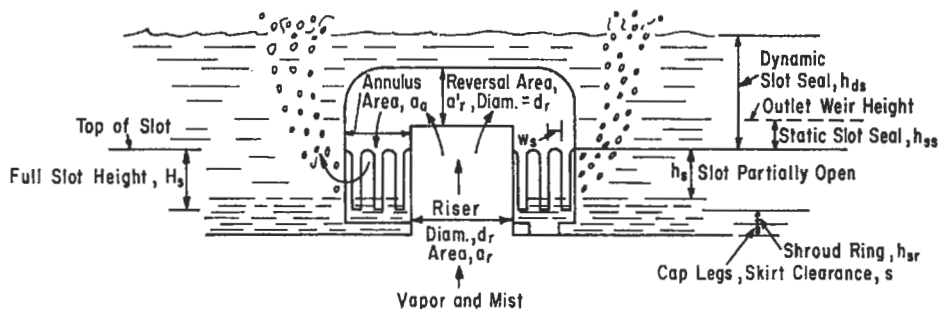


Figure 8-66. Bubble cap performance.

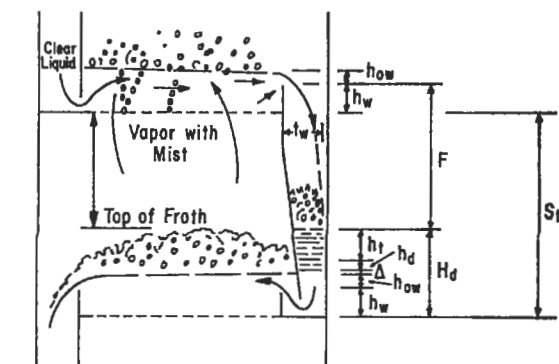
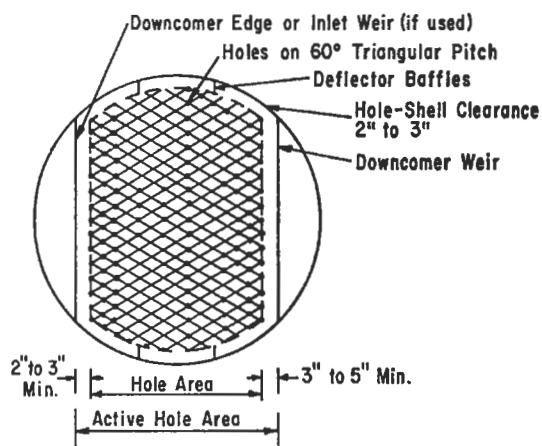


Figure 8-67A. Sieve or perforated tray with downcomers.

1. Capacity: high for vapor and/or liquid as required. This yields the smallest column diameter for a given throughput. Flexibility or adaptability to high and low fluctuations in vapor and liquid rates.
2. Pressure Drop: low pressure drop is necessary to reduce temperature gradients between top and bottom of the column. High pressure drop is usually (but not always) associated with uneconomical

design. In some systems pressure drop is not a controlling feature, within reasonable limitations.

3. Efficiency: high efficiency is the objective of each tray performance. The better the contact over a wide range of capacities, the higher will be the efficiency throughout this range.
4. Fabrication and Installation Costs: details should be simple to maintain low costs.
5. Operating and Maintenance Costs: mechanical details must account for the peculiarities of the system fluids (coking, suspended particles, immiscible fluids, etc.) and accommodate the requirements for drainage, cleaning (chemical or mechanical), corrosion, etc., in order to keep the daily costs of operation and downtime to a minimum.

Bubble-Cap-Tray Tower Diameter

Column diameter for a particular service is a function of the physical properties of the vapor and liquid at the tray conditions, efficiency and capacity characteristics of the contacting mechanism (bubble trays, sieve trays, etc.) as represented by velocity effects including entrainment, and the pressure of the operation. Unfortunately the interrelationship of these is not clearly understood. Therefore, diameters are determined by relations correlated by empirical factors. The factors influencing bubble cap and similar devices, sieve tray and perforated plate columns are somewhat different.

The Souders-Brown [67] empirically correlated maximum allowable mass velocity is represented in Figure 8-82 for "C" Factor determination, and in Figure 8-83 for solution of the relation:

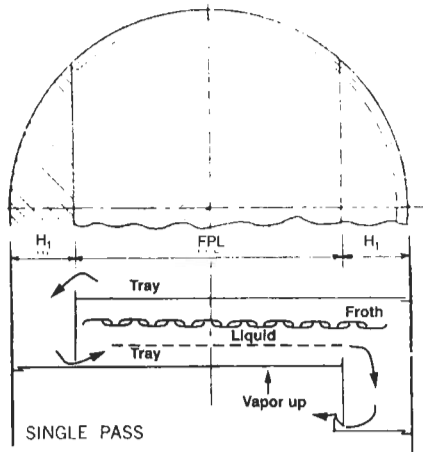
$$W = C [\rho_v (\rho_L - \rho_v)]^{1/2} \quad (8-219)$$

where W = maximum allowable mass velocity through column using bubble cap trays, lb/ft² cross-section) (hour)

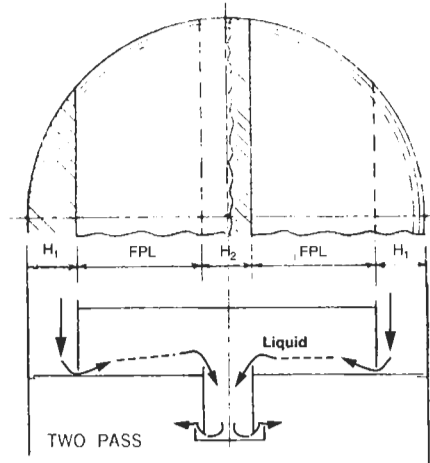
C = factor from Figure 8-82 related to entrainment

ρ_v = vapor density, lbs/ft³

ρ_L = liquid density, lbs/ft³



A.



B.

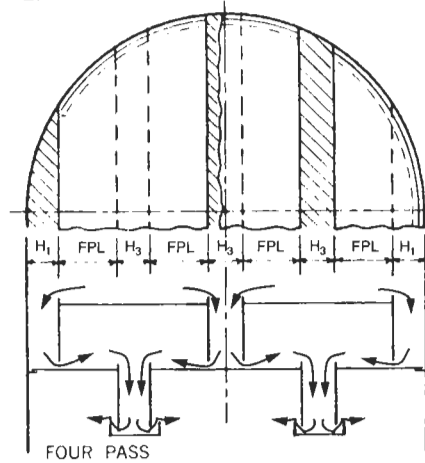


Figure 8-67B. For sieve tray layout arrangements; typical one-, two-, and four-pass tray flow patterns with clarifying flow markings by this author. Used by permission, Glitsch, Inc., Bul. 4900-5th Ed.

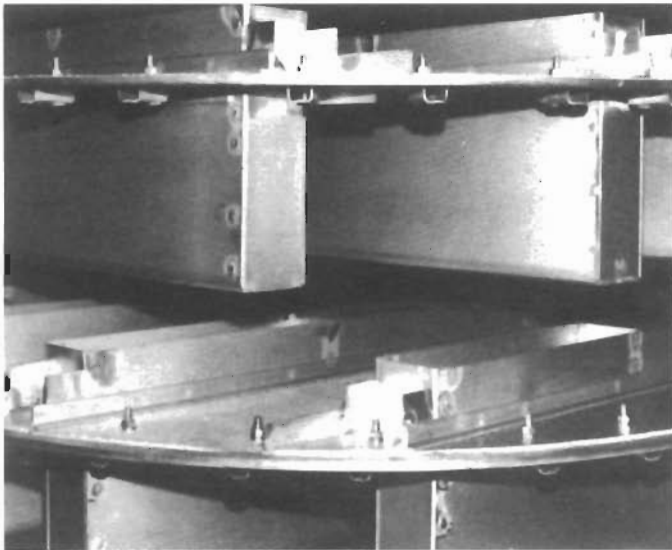


Figure 8-67C. Linde multiple-downcomer tray. Used by permission, Union Carbide Corp., Linde Division.

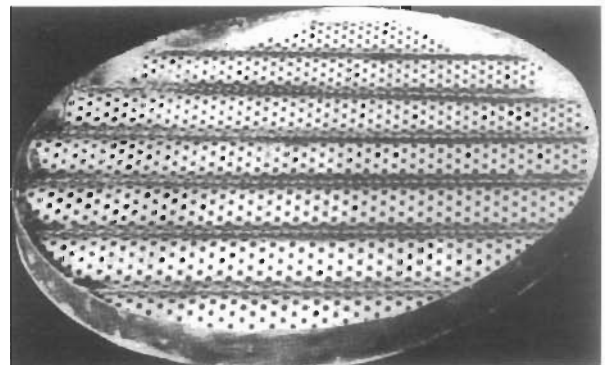


Figure 8-67D. Ripple tray (no downcomers). Used by permission, Stone and Webster Engineering Corp., Boston, Mass.

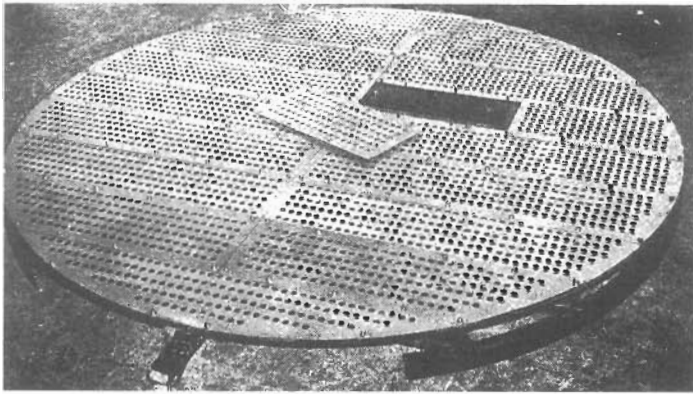


Figure 8-68A. Perforated tray without downcomer. Used by permission, Hendrick Mfg. Co., Carbondale, Pa.

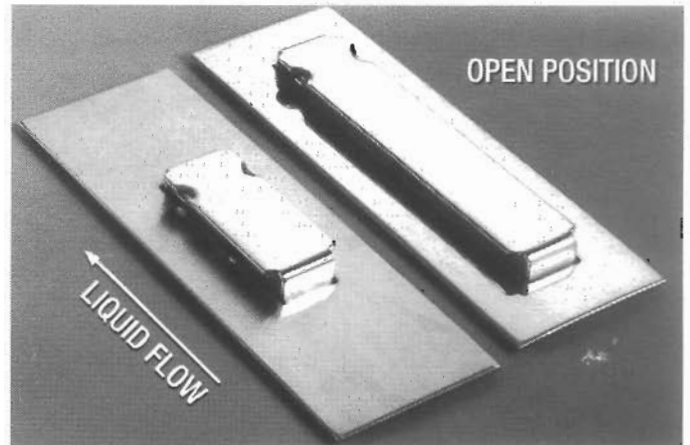


Figure 8-69B. Nutter float valves™ in open and closed positions for use on distillation trays. Used by permission, Nutter Engineering, Harsco Corp., Bul. N-2.

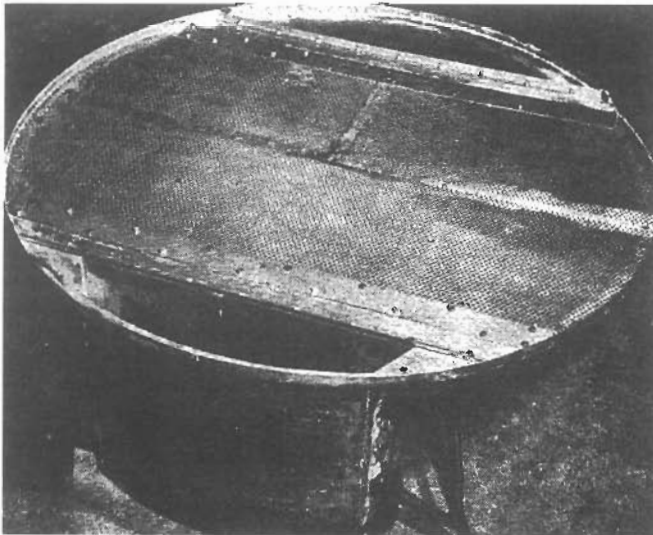


Figure 8-68B. Sieve tray with integral downcomer. Used by permission, Hendrick Mfg. Co., Carbondale, Pa.

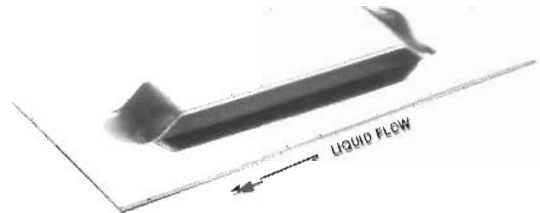


Figure 8-70. Nutter V-Grid™ fixed valve for trays. Used by permission, Nutter Engineering, Harsco Corp., Bul. N-2.

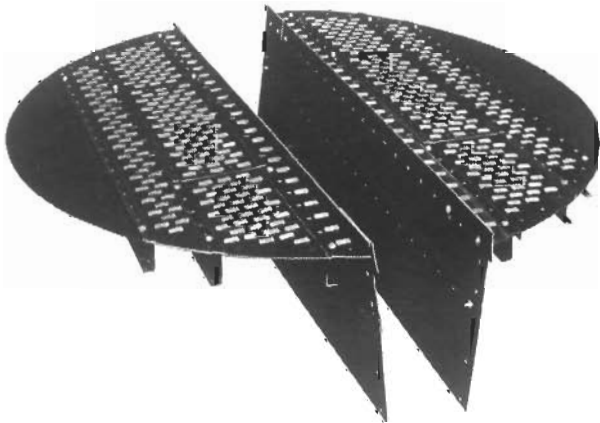


Figure 8-69A. Nutter BDH™ Float valve tray with downcomer. Used by permission, Nutter Engineering, Harsco Corp.

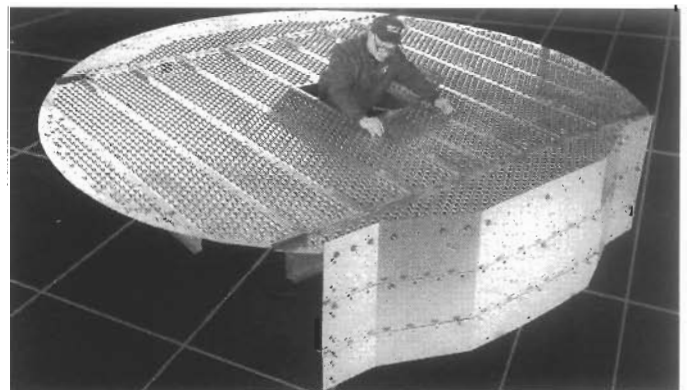


Figure 8-71A. Nutter MVG™ high performance fixed valve tray with 4:1 turndown ratio. Used in new installations and to replace sieve trays. Used by permission, Nutter Engineering, Harsco Corp., Bul. CN-4.

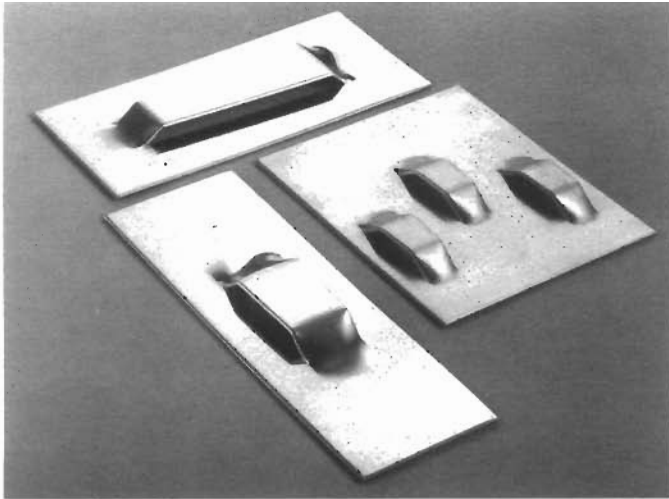


Figure 8-71B. Nutter LVG™ long, SVG™ short, and MVG™ tray slots. MVG™ tray slots are always placed in a triangular pattern. Used by permission, Nutter Engineering, Harsco Corp.

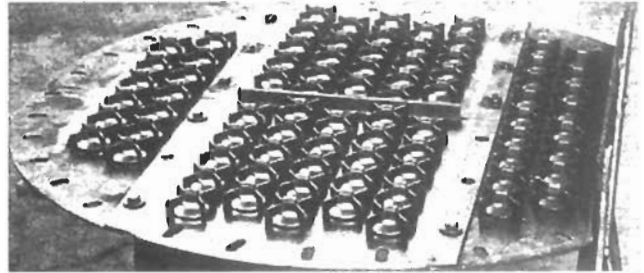


Figure 8-73A. Type "T" Flexitray®. Used by permission, Koch Engineering Co. Inc.

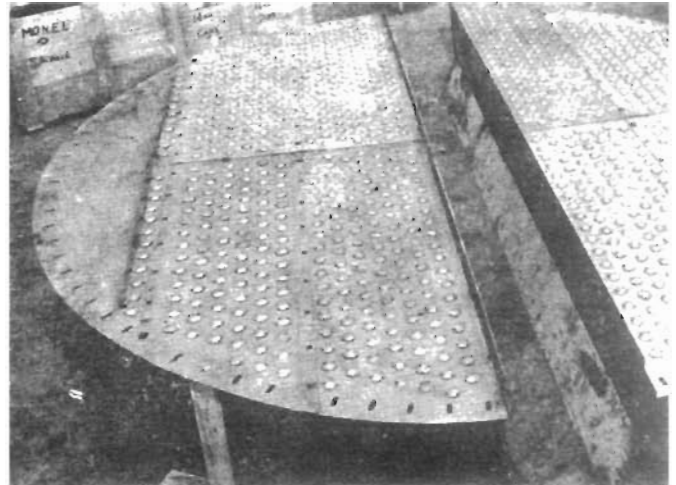


Figure 8-73B. Type "A" Flexitray® with double pass. Used by permission, Koch Engineering Co., Inc.

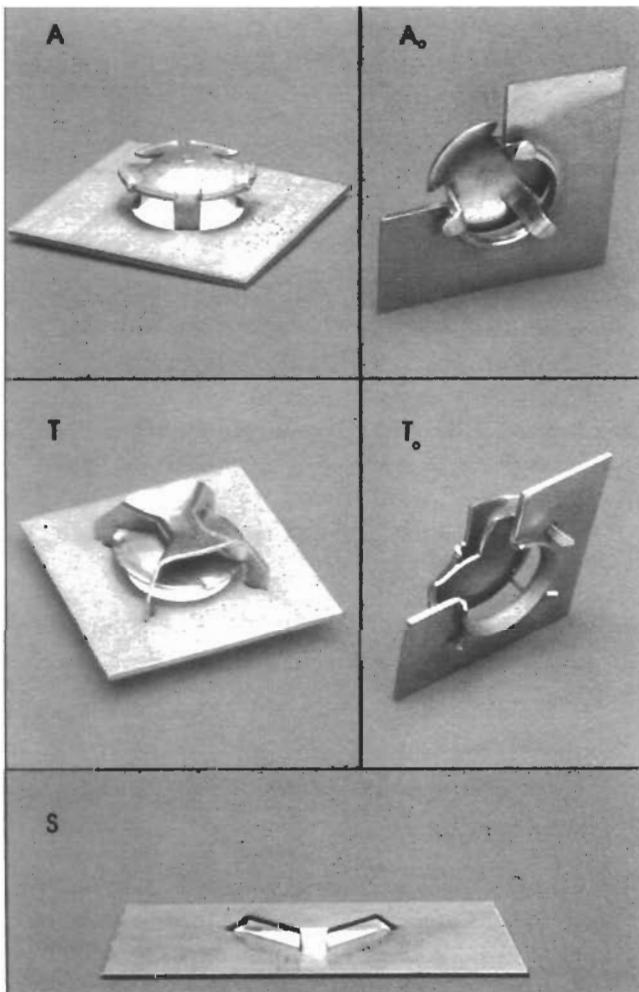
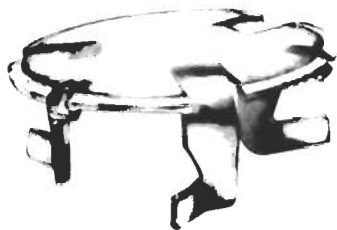


Figure 8-72. Types of standard Koch valves. Used by permission, Koch Engineering Co., Inc., Bul. KT-6A.

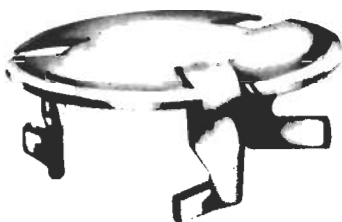
- A** Standard valve with integral legs used for most services, utilizing a sharp-edged orifice in the tray floor.
- A₀** Same "A" valve, but with a contoured hole in the tray floor for lower operating pressure drop.
- T** Round valve retained by a fixed holddown and a sharp-edged hole in the tray floor for all services, including fouling, slurry and corrosive applications.
- T₀** The same "T" valve and holddown with a contoured, low-pressure drop hole in the tray floor.
- S** Stationary valve punched up from the tray floor.

The A, A₀, T and T₀ valves can be supplied either with a flat periphery for tightest shutoff against liquid weepage at turndown rates or with a three-dimpled periphery to minimize contact with the tray deck for fouling or corrosive conditions.



Standard Dimensions:
Diameter: 17/8"
Initial Opening: 0.10"
V-1, V-4, GV-1, and V-1H

Figure 8-74a.



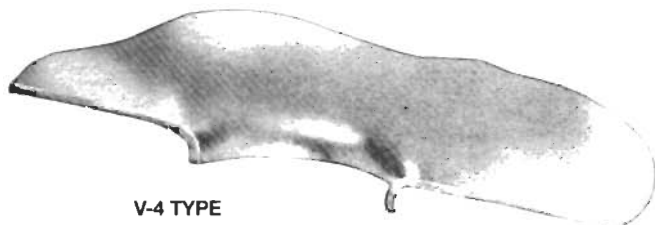
Standard Dimensions:
Diameter: 17/8"
Initial Opening: none (flush seating)
V-1X, V-4X, GV-1X, and V-1HX

Figure 8-74b.



V-1 TYPE
(Flat Orifice)
Figure 8-74c.

Diameter of Orifice Opening: 1 17/32"



V-4 TYPE
(Extruded Orifice)

Figure 8-74d.

Figures 8-74a–d. Glitsch Ballast® Valves, V-series. Used by permission, Glitsch, Inc., Bul. BU-69 (Rev.).

The “C” factor is determined at the top and bottom (or intermediate) positions of the column in order to evaluate the point of maximum required diameter. The “W” rate obtained in this solution is the maximum allowable, and hence corresponds to the minimum acceptable diameter for operation with essentially no entrainment carryover from plate to plate. Normally a factor of “safety” or “ignorance” of 1.10 to 1.25 would be applied (W divided by 1.10 to 1.25) if irregularities in capacity, system pressure or other significant variables can be anticipated. Recent experience indicates that the relation is somewhat conservative for pressure (5 to 250 psig) operated distillation systems, and the maximum allowable rate can be increased by 5–15% (W times 1.05 to 1.15) exercising judgment and caution. Basically this reflects the satisfactory operation at conditions tolerating some entrainment with no noticeable loss in fractionating efficiency. In any case the shell diameter should be rounded to the nearest inches on the diameter for fabrication standardization. Diameters such as 3 ft, 8 5/8 in. inside diameter are to be avoided, but can be used if conditions warrant. Standard tray layouts for caps, weirs, etc. are usually set at 6-in. intervals of diameter starting about 24 to 30 in.

The diameter based on vapor flowrate, V' , in the region of greatest flow:

$$D = \left[\frac{4}{\pi} \left(\frac{V'}{W} \right) \right]^{1/2} \quad (8-220)$$

Entrainment may not be the controlling factor in proper design. In cases of high liquid load or with extremely foamy or frothy fluids the tendency to flood is generally increased by close tray spacing. The hydraulics of the tray operation must be evaluated and the liquid height in the downcomer reviewed for approach to flooding. If liquid height in the downcomer exceeds one-half the tray spacing, the spacing should be increased and the column rechecked. In such cases entrainment is of no worry as the allowable entrainment vapor capacity will be greater than needed to satisfy the increased tray spacing.

Tray Layouts

Flow Paths

The simplest tray arrangement considering fluid flow and mechanical details is the cross-flow shown in Figure 8-84 (page 137). It fits the majority of designs. When liquid flows become small with respect to vapor flows the

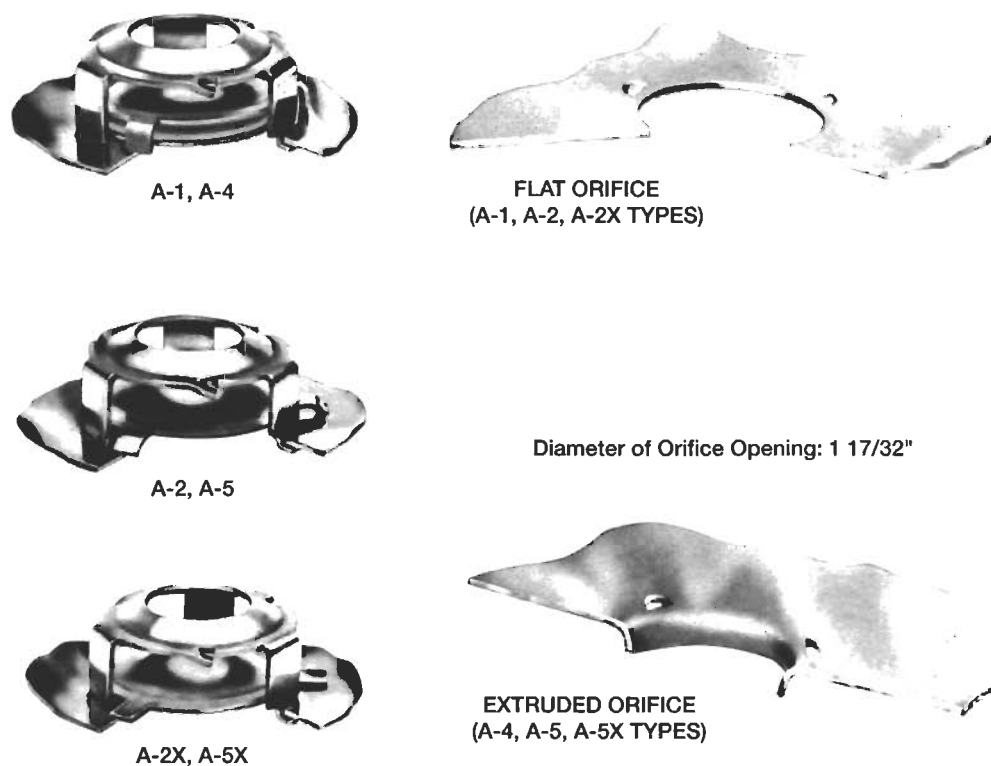


Figure 8-75. Glitsch Ballast® Valves, A-Series. Used by permission, Glitsch, Inc., Bul. BU-69 (Rev.).

reverse flow tray is recommended; when liquid load is high with respect to vapor, the double pass tray is suggested, as the path is cut in half and the liquid gradient reduced; and for the extremely high liquid loads the double-pass cascade is suggested. These last two are usually encountered only in large-diameter towers.

The liquid flow paths across the tray are important, as channeling to one area or another prevents efficient vapor contact. Short tray baffles are often installed to prevent short circuiting, particularly near the column shell wall. The segmental downcomer with straight chordal type weirs provides an efficient initial distribution pattern for liquid. Circular or pipe-type downcomers with corresponding shaped weirs require careful attention to the liquid path as it leaves or enters such a downcomer. For small liquid flows they serve very well. A guide for tentative selection of the tray type for a given capacity is given in Table 8-13 [5] (page 137).

Figure 8-85 (page 138) and Table 8-14 (page 138) identify the distribution of areas of a tray by the action of the tray area.

A tray design guide is given in Table 8-15 (page 138) and is as presented by Bolles [5] except with modifications where noted.

Figure 8-86 (page 139) is a 3-ft 0-in. diameter tray, and is representative of details associated with tray design. A typical 4-in. pressed cap is shown in Figures 8-79 and 81.

The details of these figures are only one set of many which will adequately serve as a general purpose tray. Because such a tray is adaptable to many services, it cannot be as specific for optimum design, as the designer of a particular system might prefer. Table 8-16 (page 154) gives bubble cap and riser layout data and weir lengths for other sizes of general purpose trays.

Caps suitable for particular tray designs are shown in Figures 8-87, 88 and 89. The rectangular caps require layouts differing from the bell caps, but similar in design principles of flow path evaluation.

Liquid Distribution: Feed, Side Streams, Reflux

For tray columns, bubble caps, valves or sieve, the feed liquid usually enters the column either in between functioning trays or at the top (reflux). The liquid or liquid/vapor mixture for flashing liquids must be dispersed uniformly across the tray. Such an arrangement often requires a special tray designed for the purpose to allow

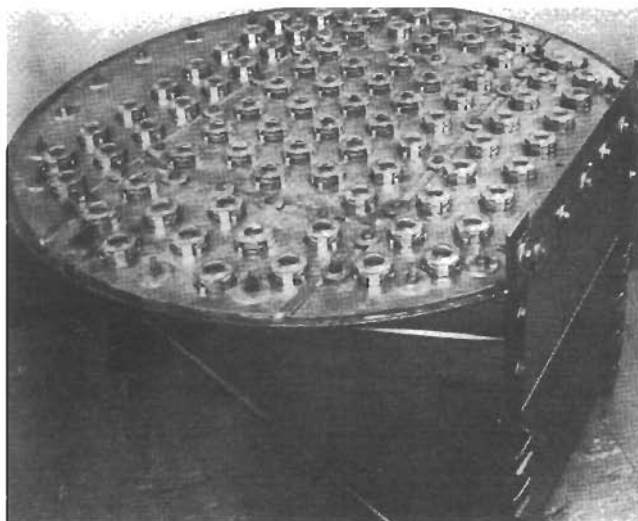


Figure 8-76. Type A-1 Ballast[®] Tray. Used by permission, Glitsch, Inc.



Figure 8-77. Type V-1 Ballast[®] Tray. Used by permission, Glitsch, Inc.

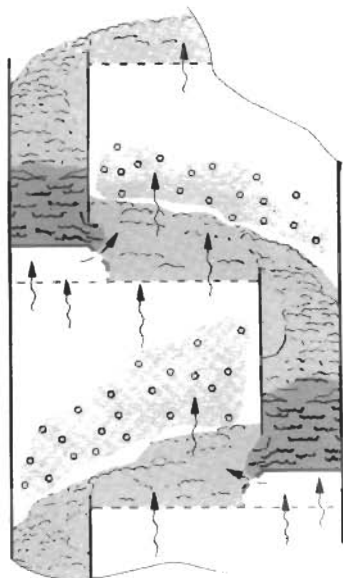


Figure 8-78. Glitsch Nye[™] Tray action to improve conventional sieve and valve tray performance by 10–20%. Used by permission, Glitsch, Inc., Bul. GLI-5138.

The Nye Tray increases the area available for disengagement of this light froth. In addition to the normal perforated section, vapor can now flow into the inlet area below the downcomer. Vapor enters the contact zone of the Nye Tray through the perforated face of the inlet panel, under the liquid coming out of the downcomer.

Specifically, the Nye Tray achieves this improvement by using a patented inlet area on a sieve or valve tray, which increases the area available for vapor-liquid disengagement.

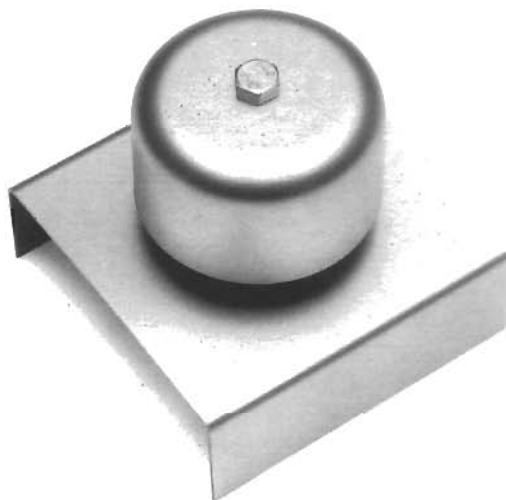


Figure 8-79. Norton FRI Plain Bubble Cap (3 in. and 4 in.), slotted skirt caps available. Used by permission, Norton Chemical Process Products Corp., Stow, Ohio.

The Norton standard bubble cap is the Fractionation Research Inc. (FRI) plain cap. It is available in 3-in. and 4-in. OD and custom sizes as well.

The FRI cap has a plain skirt; however, we also manufacture caps with various cap slot designs. Caps and risers can also be offered to our clients' specific requirements.



Figure 8-80. Typical Norton Valve Tray Valves. Used by permission, Norton Chemical Process Products Corp., Stow, Ohio., Bul. FT-2.

liquid to flow downward to the next active separation tray, and at the same time allow vapors to rise uniformly to the underside (entering) of the vapor flow devices on the next active (working) tray above. This requires attention to the respective flow to avoid upsetting the separation performance of the working trays. An allowance should be made for upset separation performance at this location in the column by adding two actual trays or minimum of one theoretical tray divided by the estimated tray efficiency to the total actual trays in the column, and locating accordingly.

Feintuch [221] presents calculations for a pipe distributor with tray and downcomers to disperse the reflux or feed liquid uniformly across the tray (which should not be counted as a "working tray," but a distribution device) and

allow the liquid flow from the downcomer to the tray below to be the first "working" tray. The same concept applies to intermediate feed trays. Designs may vary depending on diameter of the column (see Figure 8-84) and requirements for liquid and vapor flow. Some designs direct the incoming liquid into the downcomer of the top tray of a column with only some adjustments for weir heights.

Layout Helps

The scheme for arranging caps and downcomers as proposed by Bolles [5] is one of several. Plain drafting using the suggested guides is a bit longer than the short cuts. The layout sheet of Figures 8-90 and 8-91 is convenient

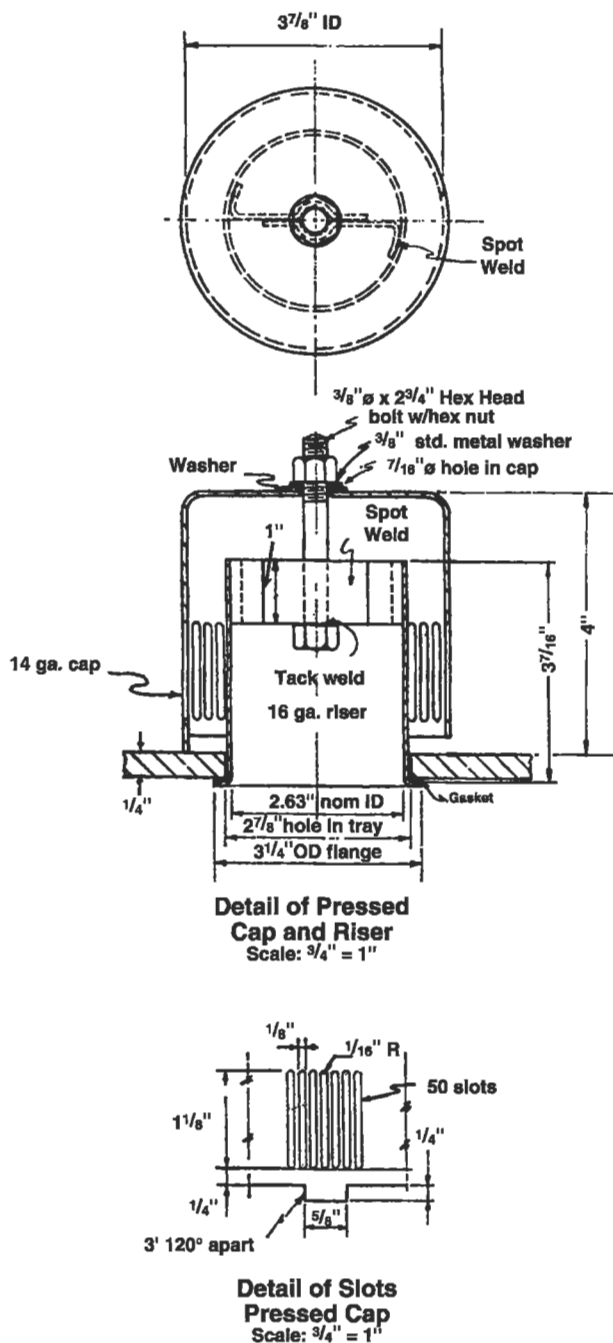


Figure 8-81. Typical $\frac{3}{8}$ -in. I.D. (nominal 4 in.) pressed bell bubble cap.

once cap-pitch master layouts are made for the sizes normally used. Figures 8-92–8-99 and 8-86 present tray layouts to match the data given in Table 8-16. These have successfully fitted many different processing situations.

Cap Layout

Caps should be arranged on the plate in 60° equilateral layout, with the liquid flowing into the apex of the triangle rather than parallel to the base. The liquid flows normal to each row of caps.

Cap Pitch Center to Center

Cap sizes 2-in., 3-in., and 4-in.: recommended cap lane distance of $1\frac{1}{2}$ in. (with $\frac{1}{4}$ -in. minimum, $1\frac{1}{4}$ -inch maximum) plus cap outside diameter.

For cap sizes of 6 and 8 in.: recommended cap lane distance of $1\frac{1}{2}$ in. ($\frac{1}{4}$ -in. minimum, $2\frac{1}{2}$ -in. maximum) plus cap outside diameter.

Weirs

Figure 8-100 is convenient for arriving at weir lengths relative to their effect on segmental downcomers.

(a) Inlet

These contribute to the uniform distribution of liquid as it enters the tray from the downcomer. There are about as many tray designs without weirs as with them. The downcomer without inlet weir tends to maintain uniform liquid distribution itself. The tray design with recessed seal pan ensures against vapor backflow into the downcomer, but this is seldom necessary. It is not recommended for fluids that are dirty or tend to foul surfaces. The inlet weir is objectionable for the same reason.

The first row of caps next to the weir or inlet downcomer must be set back far enough to prevent bubbling into the downcomer. The inlet weir prevents this, although it can be properly handled by leaving about 3 in. between inlet downcomer and the nearest face of the first row of caps.

The height of an inlet weir, if used, should be 1 to $1\frac{1}{2}$ in. above the top of the slots of the bubble caps when installed on the tray.

If inlet weirs are used they should have at least two slots $\frac{3}{8}$ -in. by 1-in. flush with the tray floor to aid in flushing out any trapped sediment or other material. There should also be weep or drain holes below the downcomer to drain the weir seal area. The size should be set by the type of service, but a minimum of $\frac{3}{8}$ -in. is recommended.

(b) Outlet

These are necessary to maintain seal on the tray, thus ensuring bubbling of vapors through liquid. The lower the submergence, i.e., the distance between top of slots of bubble caps and liquid flowing on the tray, the lower the tray pressure drops. However, this submergence must be some reasonable minimum value ($\frac{1}{4}$ to $\frac{3}{8}$ -in.) to avoid excessive by-passing of vapor through void spots in the surging, moving liquid body as it travels across the tray from inlet to outlet.

The adjustable weir feature of many tray designs allows a standard tray to be utilized in different services by readjusting the weir height as needed. The fixed portion of the weir should never be lower than the top of the slots of the bubble caps. Depending upon service, the adjustable weir

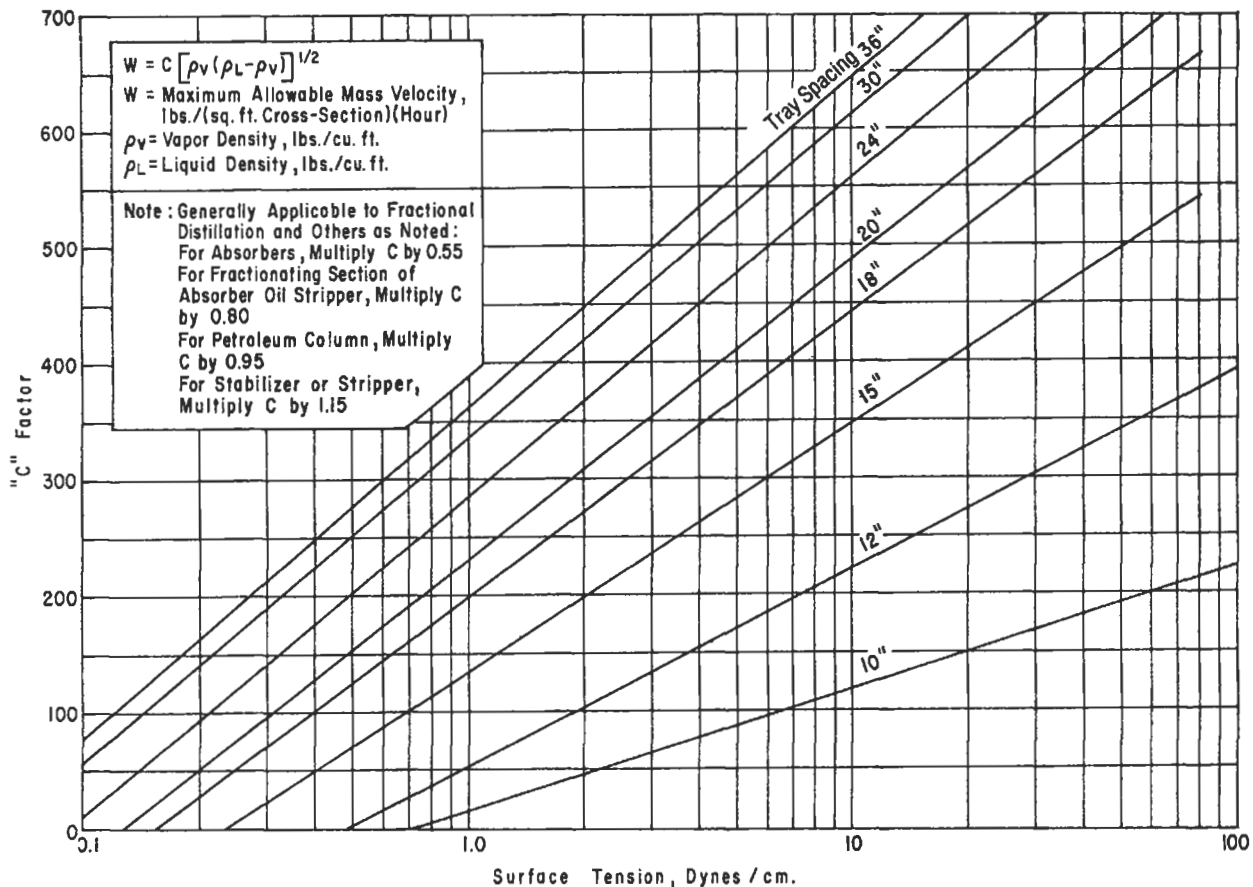


Figure 8-82. "C" factors for column diameter using bubble cap trays. Adapted by permission, The American Chemical Society, Souders, M., Jr., and Brown, G. G. *Ind. and Eng. Chem.* V. 26 (1934), p. 98, all rights reserved.

should be capable of traveling a minimum of 2 in., with designs for some trays being 4 to 6 in.

Downcomer

Figure 8-100 is convenient for determining the downcomer area and width for a given weir length (see Table 8-16 also).

The downcomer from a tray must be adequate to carry the liquid flow plus entrained foam and froth. This foamy material is disengaged in the downcomer as only clear liquid flows onto the tray below. The vertical and straight segmental downcomer is recommended, although the segmental tapered design has been used quite successfully (Figures 8-67a and 8-86). In the latter design the wide mouth of the inlet as compared to the outlet is considered to provide better foam disengagement conditions.

The consensus seems to be that a ratio of the upper area to the outlet area (lower) be in the range of 1.5 to 2.0 [190].

Circular or pipe downcomers are also used, usually for low liquid flow and small diameter columns, generally below 18 in. diameter. The pipe projects above the tray to

serve as the overflow weir. (Note: Calculate flow down on this circular basis, assuming the pipe can be surrounded by liquid on the tray.)

The downcomer seal on the tray is recommended [5] based on the liquid flow path:

Liquid Path, Downcomer to Outlet

Weir, ft	Downcomer Seal, in.
Below 5	0.5
5-10	1.0
Above 10	1.5

Liquid By-Pass Baffles

Also known as redistribution baffles, these short stub baffles guide the liquid flow path to prevent excessive by-passing of the bubble cap field or active tray area. Unfortunately this action is overlooked by many designers with

(text continued on page 154)

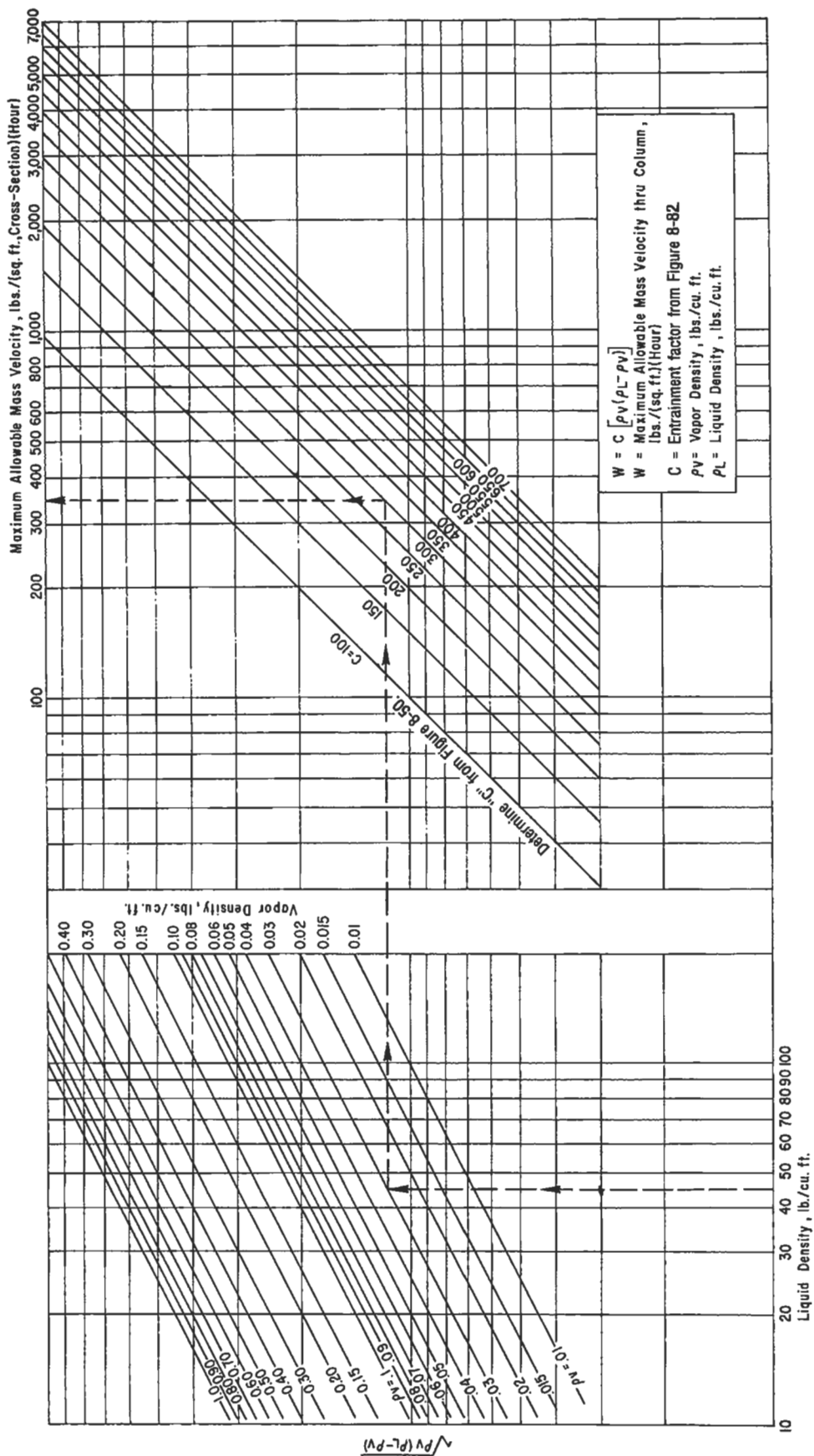


Figure 8-83. Allowable mass velocity for fractionation, absorption, and stripping columns.

Distillation

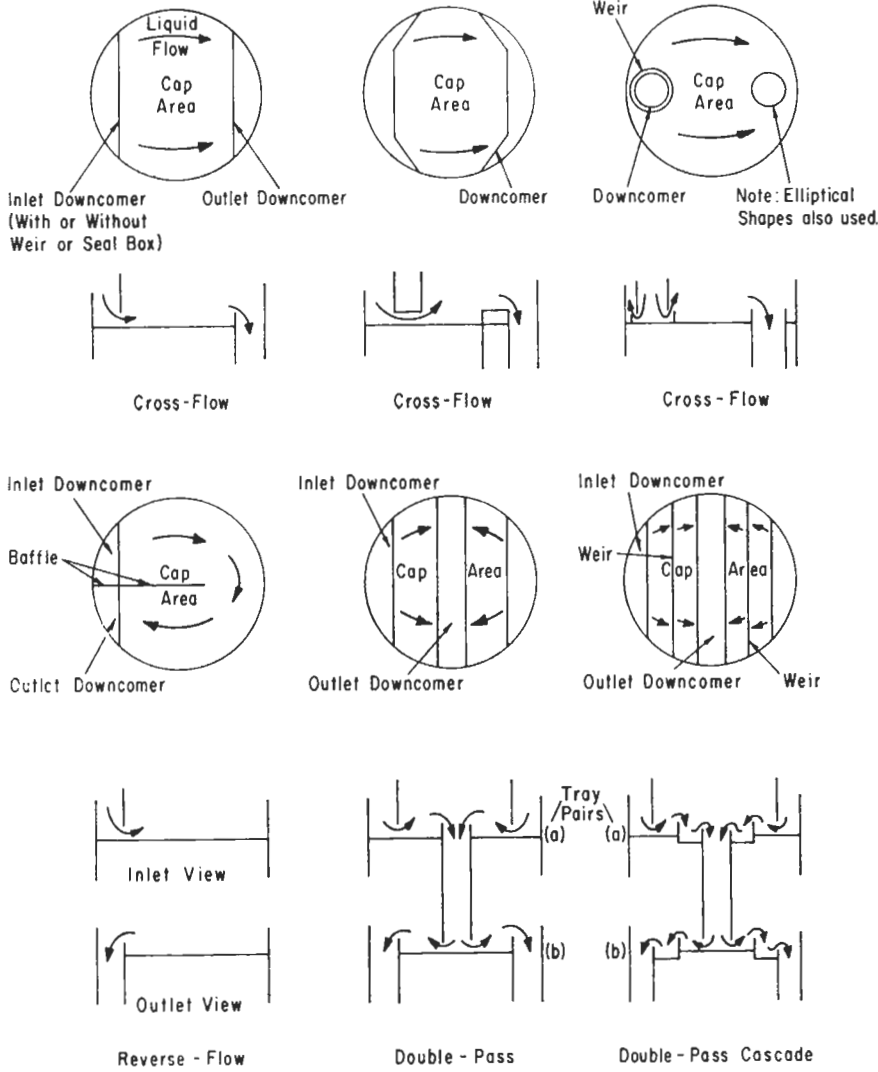


Figure 8-84. Tray types by liquid paths.

Table 8-13
Guide for Tentative Selection of Tray Type

Estimated Tower Dia. ft.	Range of Liquid Capacity, GPM			
	Reverse Flow	Cross Flow	Double Pass	Cascade Double-Pass
3	0-30	30-200
4	0-40	40-300
6	0-50	50-400	400-700
8	0-50	50-500	500-800
10	0-50	50-500	500-900	900-1,400
12	0-50	50-500	500-1,000	1,000-1,600
15	0-50	50-500	500-1,100	1,100-1,800
20	0-50	50-500	500-1,100	1,100-2,000

Used by permission, Bolles, W. L., *Petroleum Processing*, Feb. thru May (1956).

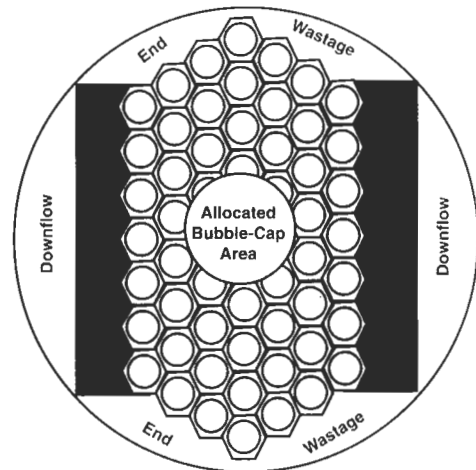


Figure 8-85. Classification of tray area. Used by permission, Bolles, W. L., *Petroleum Processing*, Feb. thru May (1956).

Table 8-14
Approximate Distribution of Areas as Percent
of Tower Area
 (Allocated cap area is determined by difference)

Tower Diam- eter ft.	Downflow Area		Liquid Distribution Area			
	Cross Flow	Double Pass	Cross Flow	Double Pass	Cascade Double	End Wastage
3	10-20	10-25	10-30
4	10-20	8-20	7-22
6	10-20	20-30	5-12	15-20	5-18
8	10-20	18-27	4-10	12-16	4-15
10	10-20	16-24	3-8	9-13	20-30	3-12
12	10-20	14-21	3-6	8-11	15-25	3-10
15	10-20	12-18	2-5	6-9	12-20	2-8
20	10-15	5-7	9-15	2-6

Used by permission, Bolles, W. L., *Petroleum Processing*, Feb. thru May (1956).

Table 8-15
Tray Design Guide for Bubble Caps*

Materials of Construction	
Type	Light gage metal [†]
Material	Determined by corrosion conditions
Tray Type	
General use	Cross-flow
Low L/V ratio	Reverse-flow
High L/V or large towers	Double-pass
Very high L/V or very large towers	Double-pass, cascade
Downcomers and Weirs	
Downcomer type	Segmental
Downflow baffle	Vertical
Weirs for normal loads	Straight
Weirs for low loads	Notched
Weir adjustment	1-3 in. [†]
Length: Cross-flow trays, % Tower Dia.	60-70% [†]
Length: Double pass trays, % Tower Dia.	50-60% [†]
Downcomer width for double-pass trays	8-12 in. [†]
Bubble-Caps	
Nominal size for:	
2.5-3 ft. towers	4 in. [†]
4-10 ft. towers	4 in.
10-20 ft. towers	6 in.
Design	Use suggested standards [†]
Pitch	Equil. triangular, rows normal to flow
Spacing	1-3 in.
Skirt height	0.25-1.5 in. [†]
Fastening	Removable design

Bubble-Caps (Cont.)

Clearances

Cap to tower wall	1.5 in. minimum
Cap to weir	3 in. minimum
Cap to downcomer or downflow baffle	3 in. minimum [†]

Tray Dynamics

Mean slot opening

Maximum	100% slot height
Minimum	0.5 in.

Mean dynamic slot submergence

Vacuum operation	0.25-1.5 in. [†]
Atmospheric	0.50-2.0 in. [†]
50-100 psig	1.0-3.0 in. [†]
200-500 psig	1.5-4.0 in. [†]

Vapor distribution ratio (Δ/h_c)

0.5 maximum

Height clear liquid

in downcomers

50% downflow height, maximum

Downflow residence time

5 seconds, minimum

Liquid throw over weir

60% downflow width, maximum

Entrainment

As mol/mol dry vapor

0.10 maximum

Pressure drop

As limited by process

Tray Spacing

For towers 2.5-10 ft.[†]

18 in.

For towers 4-20 ft.[†]

24 in.

Miscellaneous Design Factors

Inlet weirs

Use as required for liquid distribution[†]

Intermediate weirs:

.....

Minimum height > height liquid downstream

Reverse-flow baffles:

.....

Minimum height twice clear liquid

Redistribution baffles

Location:

All rows where end space is 1-in. >

cap spacing

Clearance to caps

Same as cap spacing

Height

Twice height clear liquid

Downflow baffle seal

Weir to baffle < 5 ft.

0.5 in.

Weir to baffle 5-10 ft.

1.0 in.

Weir to baffle > 10 ft.

1.5 in.

Tray design deflection (structural)

1/8 in.

Drain holes

Size

3/8-5/8 in.

Area

4 sq. in./100 sq. ft. tray area

Leakage

Max. fall 1.0 in. from top of weir in

20 min. with drain holes plugged

Construction Tolerances

Tray levelness[†]

1/8-inch Max. under 36-inch dia.[†]

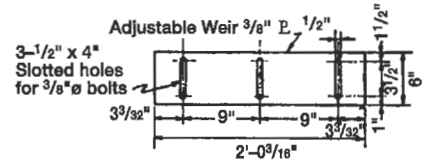
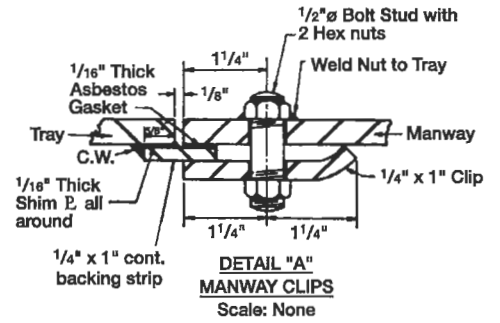
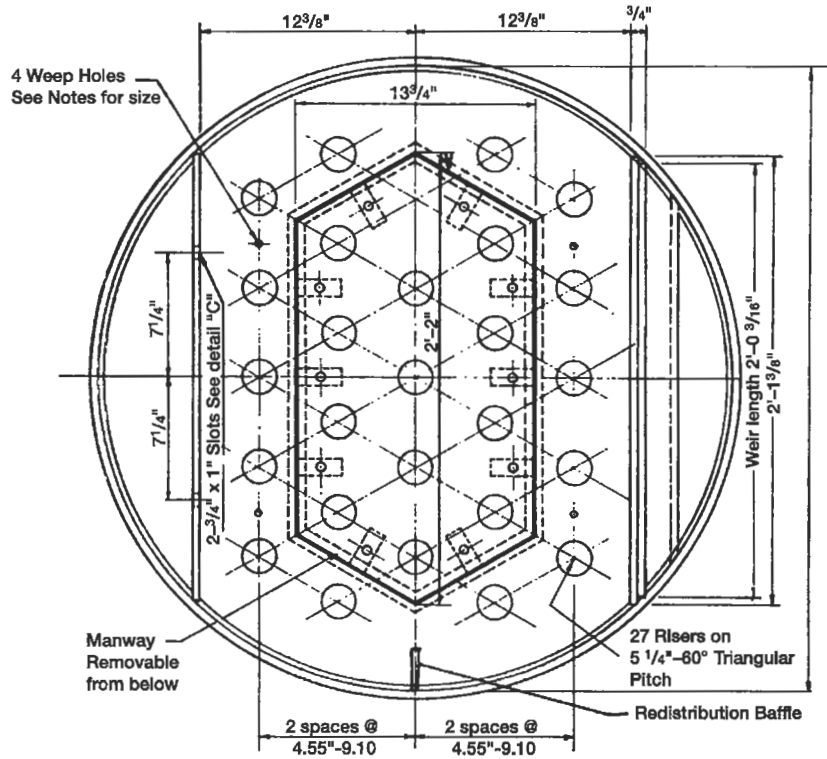
1/16-inch Max. 36-60-inch dia.[†]

1/8-inch Max. over 60-inch dia.[†]

Weir levelness

±1/16 in.[†]

*Used by permission, Bolles, W. L., *Petroleum Processing*, Feb. thru May (1956); [†] indicates modification by Ludwig.



WEIR DETAIL "B"
Scale: 1 1/2" = 1'-0"
Fabricator shall furnish 3-3/8" Ø Machine bolts with Hex Nuts & Washers for each tray.

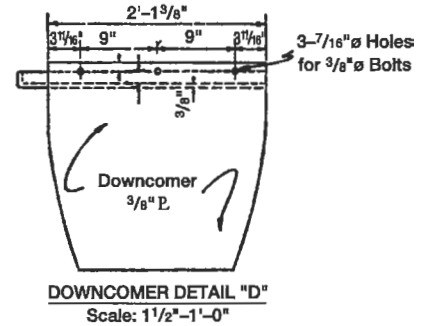
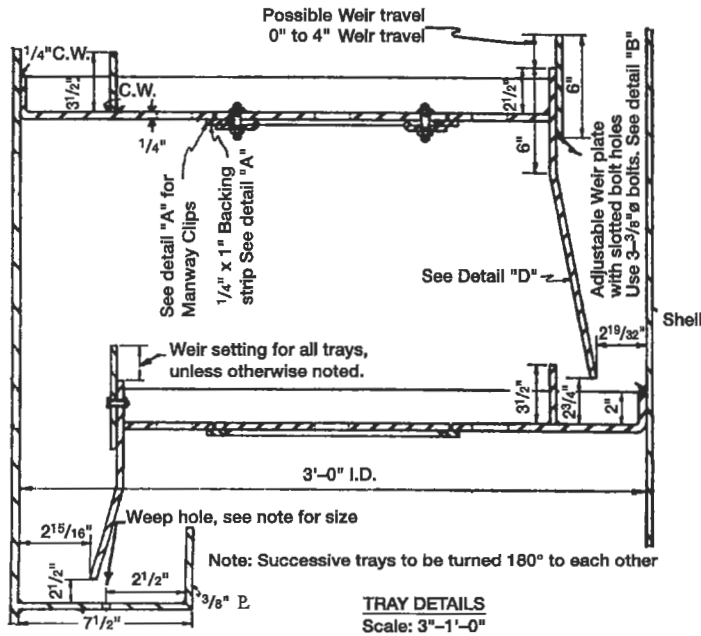
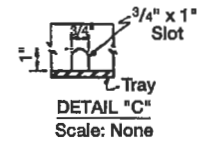


Figure 8-86. Typical bubble cap tray details: 3-ft-0-in. diameter column, 4-in. caps.

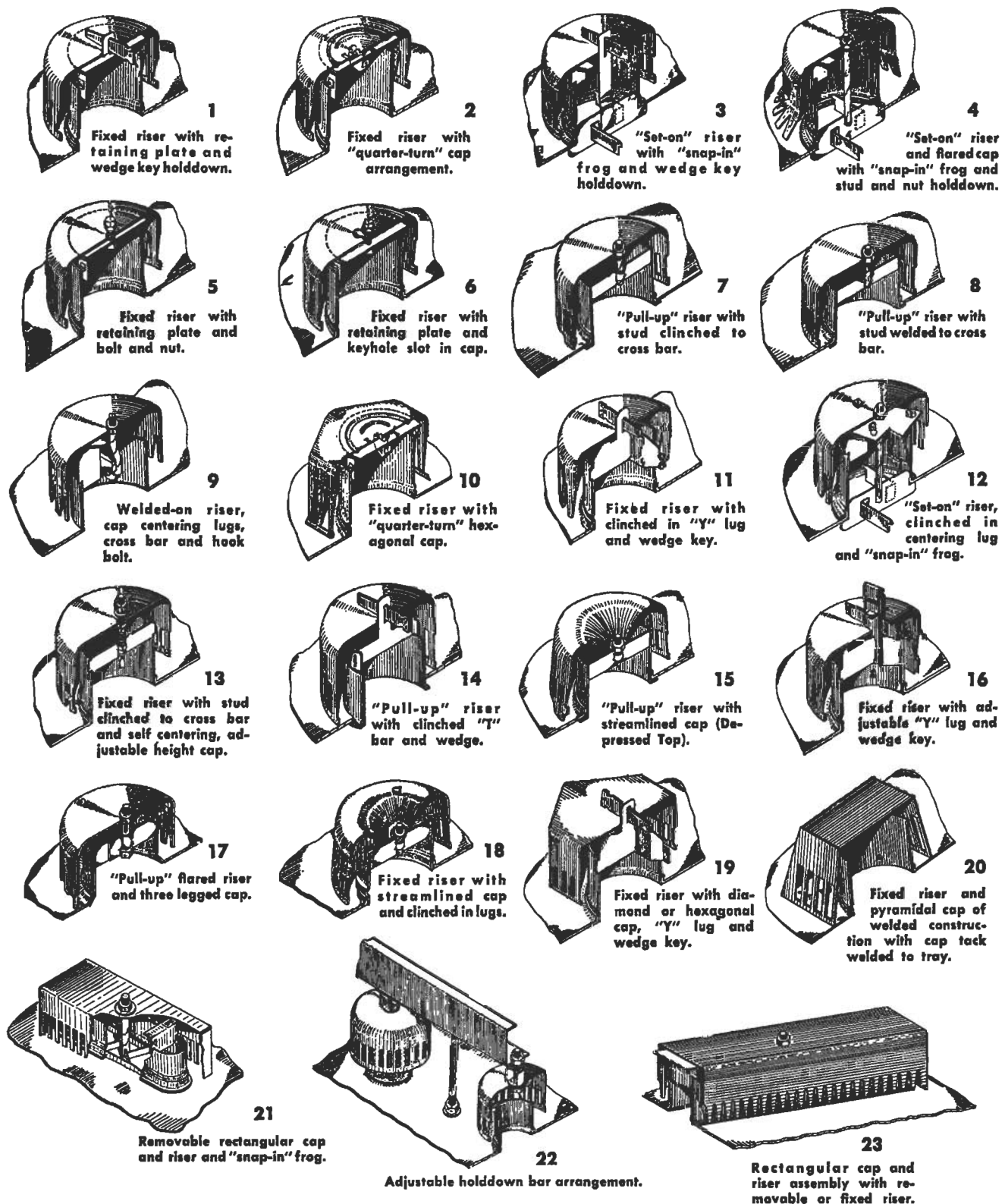


Figure 8-87. Bubble cap and riser design. Used by permission, Glitsch, Inc.

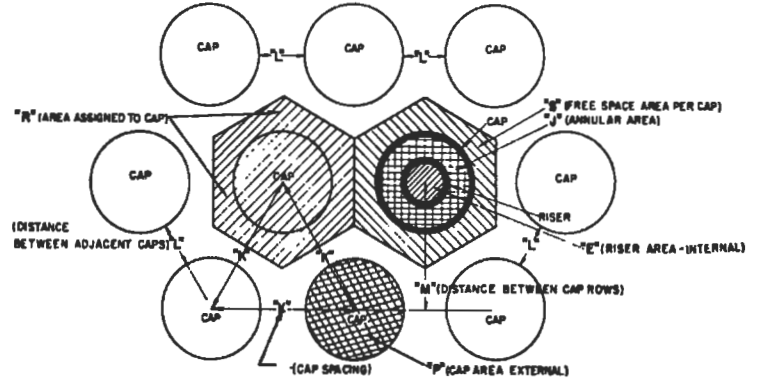
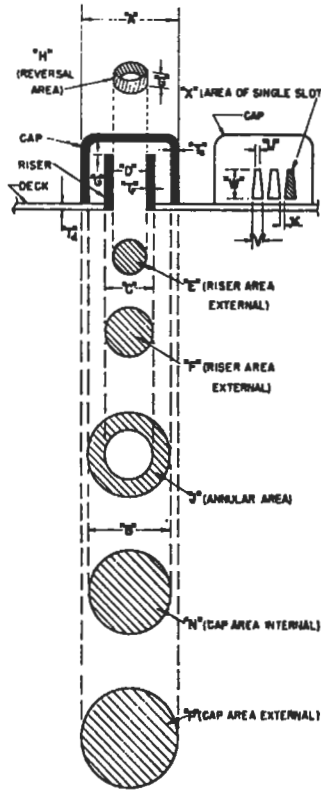
GENERAL NOTES

- (1) "a" dimension should not be less than metal thickness on closed tooth slots, and preferable 1.5 times metal thickness. (Does not apply on open tooth slots if slots are tapering to a top tooth width of 2 times metal thickness.)
- (2) Bubble cap I.D. has been set as a fixed dimension with the O.D. of the cap a minor variable. This permits the use of a standard slotting mandrel for various gauges of material used on a cap with a fixed I.D. dimension. Fixing the cap I.D. will also maintain a constant inside area and its relationship to annular area.
- (3) Riser O.D. has been set as a fixed dimension to prevent disturbing balance between riser area and annular area and allow ease of fitting of risers to deck sections irrespective of metal thickness used on risers. This is important principally on "pull-up" riser inserted through the deck from beneath the tray.
- (4) Columns "U", "V" and "W" are assumed and established to give a cap slot area of approximately 1.7 to 1.85 times the riser area. The size and shape of the slots have been arbitrarily selected so that column "Z" could be calculated. These columns are of academic interest and may be of value as a comparison in selecting a slot shape or area of greater desirability.
- (5) Formula to find riser I.D. "D" (with a wall thickness = t_r) when annular area = ϕ . Vapor uptake area. ϕ = any desired ratio of vapor uptake area to annular area. ($J = \phi E$)

$$D = \frac{2}{\phi + 1} \sqrt{\frac{N(\phi + 1)}{\pi} - \phi t_r^2} - \frac{2 t_r}{\phi + 1}$$

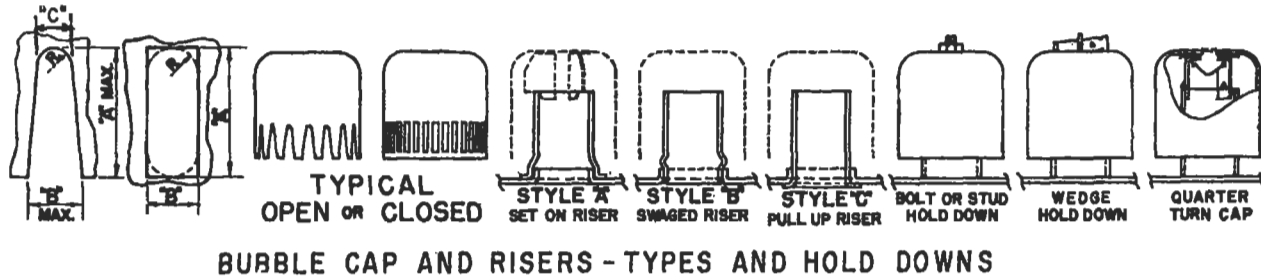
BUBBLE CAP FIXED I.D.		RISER #1 VAPOR RISER SIZE FOR AN APPROXIMATE VALUE OF ANNULAR (OR REVERSAL) AREA = RISER (VAPOR UPTAKE) AREA. J (or M) = E +								RISER #2 VAPOR RISER SIZE FOR AN APPROXIMATE VALUE OF ANNULAR (OR REVERSAL) AREA = 1.25 RISER (VAPOR UPTAKE) AREA. J ₁ (or H ₁) = 1.25 E ₁						CAP SPACING (Δ) FOR AN APPROXIMATE VALUE OF FREE SPACE AREA = 2.0 : AREA RISER #1 OR 2.4 : AREA RISER #2				
A	B	C	D	E	F	G	H	J	C ₁	D ₁	E ₁	F ₁	G ₁	H ₁	J ₁	K	L	M	N	P
O.D.	I.D.	O.D.	I.D.	INTERNAL RISER AREA	EXTERNAL RISER AREA	VERTICAL SPACE RISER TO CAP	REVERSAL AREA	ANNULAR AREA	O.D.	I.D.	INTERNAL RISER AREA	EXTERNAL RISER AREA	VERTICAL SPACE RISER TO CAP	REVERSAL AREA	ANNULAR AREA	CAP SPACING	DISTANCE BETWEEN ADJACENT CAPS	DISTANCE BETWEEN CAP BOWS	INTERNAL AREA OF CAP (FIXED)	EXTERNAL AREA OF CAP (16 GA)
FOR 16 ga. (0.63)	FIXED FOR ALL GAUGES	FIXED FOR ALL GAUGES	FOR 16 ga. (0.63)	$\frac{\pi D^2}{4}$	$\frac{\pi C^2}{4}$	FOR H: 1 = 1 MIN.	$\pi D G$	N - F	FIXED FOR ALL GAUGES	FOR 16 ga. (0.63)	$\frac{\pi D_1^2}{4}$	$\frac{\pi C_1^2}{4}$	FOR H: 1 = 1.33 MIN.	$\pi D_1 G_1$	N - F ₁	FOR E: 1 = 2 MIN.	K - A	.866 K	$\frac{\pi B^2}{4}$	$\frac{\pi A^2}{4}$
9.00	8%	6%	6.187	30.069	31.296	1%	31.588	30.366	6	5.875	27.109	28.274	1%	34.607	33.588	12%	3%	10.5	61.862	63.617
8.50	8%	5%	5.812	26.535	27.688	1%	27.39	27.40	5%	5.50	23.758	24.85	1%	30.238	30.238	11%	3	9.96	55.088	56.745
8.00	7%	5%	5.50	23.758	24.850	1%	24.83	23.857	5%	5.187	21.135	22.164	1%	26.482	26.541	10%	2%	9.36	48.707	50.265
7.50	7%	5%	5.125	20.629	21.648	1%	21.12	21.07	5	4.875	18.665	19.635	1%	22.973	23.083	10%	2%	8.822	42.718	44.179
7.00	6%	4%	4.750	17.721	18.665	1%	18.65	18.457	4%	4.50	15.904	16.80	1%	21.21	20.322	9%	2%	8.23	37.122	38.485
6.50	6%	4%	4.437	15.466	16.349	1%	15.68	15.571	4%	4.187	13.772	14.607	1%	17.26	17.313	8%	2%	7.63	31.92	33.183
6.25	6%	4%	4.250	14.186	15.033	1%	15.02	14.432	4%	4.00	12.566	13.364	1%	16.487	16.101	8%	2%	7.31	29.465	30.68
6.00	5%	4%	4.062	12.962	13.772	1%	13.55	13.338	4	3.875	11.793	12.566	1%	15.218	14.544	8%	2%	7.03	27.11	28.274
5.75	5%	4	3.875	11.793	12.566	1	12.174	12.284	3%	3.687	10.680	11.416	1%	13.75	13.434	7%	2	6.72	24.85	25.967
5.50	5%	3%	3.687	10.68	11.416	1	11.585	11.275	3%	3.50	9.621	10.321	1%	12.371	12.37	7%	1%	6.44	22.691	23.758
5.25	5%	3%	3.50	9.621	10.321	1%	10.30	10.308	3%	3.375	8.946	9.621	1%	11.26	11.008	7%	1%	6.17	20.629	21.648
5.00	4%	3%	3.375	8.946	9.621	1%	9.278	9.044	3%	3.187	7.9798	8.6179	1	10.014	10.047	6%	1%	5.84	18.665	19.635
4.75	4%	3%	3.187	7.98	8.618	1%	8.234	8.182	3%	3.00	7.069	7.67	1	9.425	9.13	6%	1%	5.58	16.8	17.721
4.50	4%	3%	3.00	7.069	7.67	1%	7.65	7.363	3	2.875	6.492	7.069	1%	8.463	7.964	6%	1%	5.31	15.033	15.904
4.25	4%	2%	2.812	6.213	6.777	1%	6.63	6.587	2%	2.687	5.673	6.213	1%	7.388	7.151	5%	1%	4.98	13.364	14.186
4.00	3%	2%	2.625	5.412	5.94	1%	6.185	5.853	2%	2.50	4.909	5.412	1%	6.381	6.381	5%	1%	4.71	11.793	12.566
3.75	3%	2%	2.50	4.909	5.412	1%	4.909	4.909	2%	2.375	4.430	4.909	1%	5.596	5.412	5%	1%	4.45	10.321	11.05
3.50	3%	2%	2.312	4.20	4.667	1%	4.54	4.279	2%	2.187	3.76	4.20	1%	4.721	4.746	4%	1%	4.12	8.967	9.6211
3.25	3%	2%	2.125	3.547	3.976	1%	4.172	3.694	2%	2.00	3.1416	3.547	1%	4.316	4.123	4%	1%	3.84	7.6699	8.2958
3.00	2%	2%	1.968	3.042	3.44	1%	3.092	3.052	2	1.875	2.761	3.1416	1%	3.68	3.35	4%	1%	3.57	6.4918	7.0686
2.75	2%	1%	1.781	2.491	2.853	1%	2.798	2.559	1%	1.687	2.236	2.580	1%	2.979	2.832	3%	1%	3.5	5.4319	5.9396
2.50	2%	1%	1.5937	1.995	2.32	1%	2.19	2.11	1%	1.531	1.841	2.153	1%	2.41	2.277	3%	1	3.15	4.4301	4.9087
2.25	2%	1%	1.437	1.623	1.917	1%	1.694	1.6296	1%	1.3437	1.418	1.694	1%	1.845	1.853	3%	1%	2.71	3.5466	3.9761
2.00	1%	1%	1.250	1.227	1.485	1%	1.473	1.2762	1%	1.187	1.108	1.353	1%	1.40	1.408	2%	1%	2.38	2.7612	3.1416
1.75	1%	1%	1.062	.887	1.108	1%	1.04	.966	1%	1.00	.785	.994	1%	1.19	1.080	2%	1%	2.11	2.0739	2.4053
1.50	1%	1%	.906	.645	.835	1%	.71	.650	1%	.8434	.559	.7371	1%	.827	.748	2%	1%	1.788	1.4849	1.7671
1.25	1%	1%	.730	.418	.576	1%	.429	.418	1%	.6875	.371	.5185	1%	.540	.4753	1%	1%	1.52	.994	1.2272
1.00	1%	1%	.553	.2401	.361	1%	.271	.2403	1%	.525	.2164	.3318	1%	.309	.2695	1%	1%	1.19	.6013	.7854

Figure 8-88. Bubble cap and riser comparison data. Used by permission, Glitsch, Inc.



R	S	FREE SPACE AREA RATIO TO #1 RISER AREA	FREE SPACE AREA RATIO TO #2 RISER AREA	TOTAL CAP SLOT AREA (Z) FOR AN APPROXIMATE VALUE OF CAP SLOT AREA = 1.7 AREA RISER #1 OR 1.85 AREA RISER #2 ⁽¹⁾ (a = SLOT LIGAMENT)							CAP SLOT AREA RATIO TO #1 RISER AREA	CAP SLOT AREA RATIO TO #2 RISER AREA	POR 16 ga. RISERS		CIRCUMFERENCE OF RISER D = INSIDE DIAM.	CIRCUMFERENCE OF RISER D ₁ = INSIDE DIAM.	ACTUAL G	ACTUAL G ₁	
				T	U ⁽⁴⁾	V ⁽⁴⁾	W ⁽⁴⁾	X	Y	Z ⁽⁴⁾			ACTUAL D = $\sqrt{.538R - .008 - .002}$	ACTUAL D ₁ = $\sqrt{.889/316R - .005 - .055}$					
.866 K ²	R - P			OUTSIDE CIRCUM OF CAP	SLOT WIDTH AT TOP	SLOT WIDTH AT BOTTOM	SLOT LENGTH	AREA OF SINGLE SLOT	NUMBER OF SLOTS PER CAP	TOTAL SLOT AREA			(5)	(5)					
				T A	AS-SHOWN	AS-SHOWN	CALCULATED	$W(U+V)/2$	(T) a	$T/(a+V)$	XY								
127.31	63.693	2.118	2.350	28.274	1/2	1/2	2 1/2	1.875	1/2	28	52.6	1.749	1.940	6.213	5.865	19.439	18.457	1.572	1.82
114.53	57.785	2.178	2.432	26.703	1/2	1/2	3 1/2	1.751	1/2	26	45.6	1.718	1.919	5.865	5.532	18.360	17.279	1.50	1.73
101.2	50.935	2.144	2.410	25.133	1/2	1/2	3 1/2	1.625	1/2	25	40.6	1.709	1.921	5.50	5.190	17.28	16.297	1.38	1.629
89.87	45.691	2.215	2.448	23.562	1/2	1/2	3	1.50	1/2	23	34.5	1.672	1.848	5.148	4.861	16.10	15.315	1.31	1.51
78.16	39.672	2.239	2.494	21.991	1/2	1/2	2 1/2	1.375	1/2	22	31.3	1.746	1.968	4.798	4.523	14.923	14.137	1.24	1.44
67.25	34.167	2.209	2.481	20.42	1/2	1/2	2 1/2	.882	1/2	30	26.75	1.730	1.942	4.458	4.194	13.941	13.155	1.12	1.32
61.7	31.02	2.187	2.469	19.835	1/2	1/2	2 1/2	.882	1/2	28	24.75	1.745	1.970	4.268	4.025	13.382	12.556	1.08	1.28
57.2	28.926	2.232	2.453	18.85	1/2	1/2	1 1/2	.588	1/2	38	22.20	1.713	1.882	4.088	3.861	12.763	12.174	1.05	1.20
52.0	26.033	2.207	2.438	18.064	1/2	1/2	1 1/2	.546	1/2	36	19.70	1.670	1.845	3.913	3.697	12.174	11.583	1.01	1.16
47.9	24.142	2.260	2.509	17.279	1/2	1/2	1 1/2	.546	1/2	34	18.55	1.737	1.928	3.738	3.528	11.585	10.996	.973	1.13
44.2	22.552	2.344	2.521	16.494	1/2	1/2	1 1/2	.437	1/2	38	16.62	1.727	1.838	3.548	3.359	10.996	10.403	.937	1.04
39.5	19.865	2.221	2.489	15.708	1/2	1/2	1 1/2	.425	1/2	36	15.20	1.699	1.905	3.383	3.195	10.403	10.014	.85	1.00
35.9	18.179	2.278	2.572	14.923	1/2	1/2	1 1/2	.407	1/2	34	13.82	1.732	1.955	3.208	3.03	10.14	9.425	.81	.969
33.5	17.594	2.489	2.710	14.137	1/2	1/2	1 1/2	.375	1/2	32	12.00	1.698	1.848	3.028	2.861	9.425	9.032	.78	.882
28.62	14.434	2.323	2.544	13.352	1/2	1/2	1 1/2	.359	1/2	30	10.78	1.735	1.900	2.833	2.697	8.836	8.443	.745	.847
25.53	12.984	2.399	2.645	12.566	1/2	1/2	1 1/2	.3285	1/2	28	9.2	1.700	1.874	2.676	2.528	8.247	7.854	.710	.812
22.75	11.70	2.383	2.641	11.781	1/2	1/2	1 1/2	.313	1/2	27	8.44	1.719	1.905	2.50	2.362	7.854	7.461	.625	.725
18.57	9.949	2.369	2.646	10.996	1/2	1/2	1 1/2	.2825	1/2	25	7.04	1.676	1.872	2.32	2.196	7.265	6.872	.589	.691
17.04	8.744	2.465	2.783	10.21	1/2	1/2	1 1/2	.246	1/2	23	6.13	1.728	1.931	2.15	2.025	6.676	6.283	.563	.656
14.72	7.651	2.515	2.771	9.4248	1/2	1/2	1	.250	1/2	21	5.25	1.726	1.901	1.968	1.861	6.183	5.890	.494	.569
12.62	6.680	2.482	2.987	8.6394	1/2	1/2	1	.187	1/2	23	4.3	1.726	1.923	1.793	1.692	5.595	5.301	.457	.534
10.6	5.691	2.853	3.091	7.854	1/2	1/2	1/2	.164	1/2	21	3.45	1.729	1.874	1.618	1.527	5.007	4.81	.421	.473
8.46	4.484	2.763	3.162	7.0686	1/2	1/2	1/2	.152	1/2	18	2.74	1.688	1.922	1.44	1.359	4.516	4.22	.361	.439
6.56	3.418	2.786	3.085	6.2832	1/2	1/2	1/2	.141	1/2	15	2.11	1.720	1.904	1.263	1.192	3.927	3.731	.325	.377
5.13	2.72	3.067	3.465	5.4978	1/2	1/2	1/2	.0862	1/2	18	1.55	1.747	1.975	1.086	1.03	3.338	3.1416	.259	.344
3.682	1.915	2.969	3.426	4.7124	1/2	1/2	1/2	.078	1/2	15	1.17	1.814	2.093	.908	.849	2.846	2.65	.228	.282
2.65	1.42	3.397	3.827	3.927	1/2	1/2	1/2	.0585	1/2	12	.703	1.682	1.895	.730	.693	2.293	2.16	.182	.220
1.64	.854	3.557	3.946	3.1416	1/2	1/2	1/2	.039	1/2	10	.390	1.624	1.802	.553	.525	1.737	1.65	.138	.163

Figure 8-88. Cont'd.



EXPLANATION

The slots shown below for various cap diameters may be furnished in any of the riser styles and hold-down styles shown above with either open or closed slot arrangement as limited in the chart.

Cap I.D.	NO. SLOTS	A CLOSED	A OPEN	B	C	R	Cap I.D.	NO. SLOTS	A CLOSED	A OPEN	B	C	R	Cap I.D.	NO. SLOTS	A CLOSED	A OPEN	B	C	R
1 7/8	30	3/4	1 1/4	3/4	3/4	—	3 3/4	40	3/4	3/4	3/4	3/4	3/4	4 3/8	18	1 1/4	1 1/4	3/4	3/4	3/4
	30	1 1/4	1 1/4	3/4	3/4	—		12	3/4	3/4	3/4	3/4	3/4		32	1	3/4	3/4	3/4	—
2 1/16	12	1/2	3/4	3/4	1/4	1/4	3 3/4	18	1	1 1/4	3/4	3/4	3/4	4 3/8	36	1 1/4	1 1/4	3/4	3/4	—
2 3/16	28	3/4	1 1/4	3/4	0	0		18	1 3/4	1 3/4	3/4	3/4	3/4		25	1 1/2	1 1/4	3/4	3/4	3/4
2 3/4	38	3/4	1 1/4	3/4	3/4	—	3 3/4	19	1 1/2	1 1/4	3/4	3/4	3/4	4 3/8	20	1 3/4	1 1/2	3/4	3/4	3/4
	38	3/4	1 1/4	3/4	3/4	—		21	1 1/2	1 3/4	3/4	3/4	3/4		27	1 3/4	1 1/2	3/4	3/4	3/4
2 3/4	18	3/4	1 1/4	3/4	3/4	—	3 3/4	19	1 3/4	1 1/2	3/4	3/4	3/4	4 3/8	30	2 1/4	2	3/4	3/4	3/4
	25	1/2	3/4	3/4	3/4	—		21	1 3/4	1 3/4	3/4	3/4	3/4		18	1 1/2	1 3/4	3/4	3/4	3/4
2 7/8	38	3/4	1 1/4	3/4	3/4	—	3 3/4	34	1	3/4	3/4	3/4	—	5 1/8	20	1 3/4	1 3/4	3/4	3/4	3/4
	48	3/4	1 1/4	3/4	3/4	—		21	1	3/4	3/4	3/4	—		5 3/8	20	1 1/2	1 3/4	3/4	3/4
2 7/8	50	3/4	1 1/4	3/4	3/4	—	3 3/4	34	1 1/4	1 3/4	3/4	3/4	—	5 3/8	30	1 1/2	1 3/4	3/4	3/4	3/4
	18	3/4	1 1/4	3/4	3/4	—		32	1 3/4	1 3/4	3/4	3/4	—		5 3/8	20	1 3/4	1 3/4	3/4	3/4
2 7/8	21	1	1 3/4	3/4	3/4	—	3 3/4	24	1 1/2	1 3/4	3/4	3/4	—	5 3/8	48	1 3/4	1 3/4	3/4	3/4	3/4
	38	3/4	1 1/4	3/4	3/4	3/4		30	1 1/4	1 3/4	3/4	3/4	3/4		5 7/8	26	3/4	3/4	3/4	3/4
2 7/8	25	1 1/4	1 3/4	3/4	3/4	—	3 3/4	18	1 1/4	1 3/4	3/4	3/4	3/4	5 7/8		48	3/4	3/4	3/4	3/4
	18	1 3/4	1	3/4	3/4	3/4		20	1 1/4	1 3/4	3/4	3/4	3/4		32	1	3/4	3/4	3/4	—
2 7/8	14	1 1/4	1 3/4	3/4	3/4	3/4	3 3/4	52	3/4	3/4	3/4	3/4	3/4	5 7/8	33	1 3/4	1 3/4	3/4	3/4	3/4
	18	1	1 3/4	3/4	3/4	3/4		50	1	3/4	3/4	3/4	3/4		30	1 3/4	1 3/4	3/4	3/4	3/4
2 7/8	21	1	1 3/4	3/4	3/4	3/4	3 3/4	51	1 1/2	1 3/4	3/4	3/4	3/4	5 7/8	60	1 1/2	1 3/4	3/4	3/4	3/4
	38	1/2	3/4	3/4	3/4	—		40	3/4	3/4	3/4	3/4	3/4		25	1 1/2	1 3/4	3/4	3/4	3/4
2 7/8	25	3/4	1 1/4	3/4	3/4	—	3 3/4	32	1 1/2	1 3/4	3/4	3/4	3/4	5 7/8	48	1 3/4	1 3/4	3/4	3/4	3/4
	48	1 3/4	1 1/4	3/4	3/4	—		38	1 1/2	1 3/4	3/4	3/4	3/4		20	2 1/4	2 1/4	3/4	3/4	3/4
2 7/8	18	1 1/4	1 3/4	3/4	3/4	3/4	3 3/4	40	3/4	3/4	3/4	3/4	—	5 7/8	38	2 1/4	2 1/4	3/4	3/4	3/4
	40	3/4	3/4	3/4	3/4	—		28	1 1/2	1 3/4	3/4	3/4	—		48	3/4	3/4	3/4	3/4	—
2 7/8	18	1 1/4	1 3/4	3/4	3/4	3/4	3 3/4	16	1 1/2	1 3/4	3/4	3/4	3/4	5 7/8	30	1 3/4	1 3/4	3/4	3/4	—
	38	1/2	3/4	3/4	3/4	—		28	1 3/4	1 3/4	3/4	3/4	—		50	1 3/4	1 3/4	3/4	3/4	—
3	16	1	1 3/4	3/4	3/4	3/4	3 3/4	66	3/4	3/4	3/4	3/4	3/4	6	28	1 1/2	1 3/4	3/4	3/4	3/4
	24	1	1 3/4	3/4	3/4	3/4		28	1	3/4	3/4	3/4	—		32	1 1/2	1 3/4	3/4	3/4	3/4
3	32	1	1 3/4	3/4	3/4	3/4	4 1/8	32	1	3/4	3/4	3/4	—	6 1/8	40	1 3/4	1 3/4	3/4	3/4	—
	18	1	1 3/4	3/4	3/4	—		26	1 1/2	1 3/4	3/4	3/4	—		32	1 1/2	1 3/4	3/4	3/4	3/4
3	21	1	1 3/4	3/4	3/4	—	4 1/8	32	1 1/4	1 3/4	3/4	3/4	—	6 1/8	32	2	1 3/4	3/4	3/4	3/4
	28	1 1/4	1 3/4	3/4	3/4	—		26	1	3/4	3/4	3/4	—		32	1 3/4	1 1/2	3/4	3/4	3/4
3	40	1 3/4	1 3/4	3/4	3/4	—	4 1/8	32	1 1/2	1 3/4	3/4	3/4	—	6 1/8	32	1 3/4	1 1/2	3/4	3/4	3/4
	25	1 3/4	1 1/4	3/4	3/4	—		24	1 3/4	1 1/2	3/4	3/4	3/4		6 1/2	40	1 3/4	1 3/4	3/4	3/4
3 1/16	24	1	1 3/4	3/4	3/4	—	4 1/4	24	1 1/4	1 3/4	3/4	3/4	3/4	6 3/8	28	1 3/4	1 1/2	3/4	3/4	3/4
3 3/8	45	1 1/4	1 3/4	3/4	3/4	3/4		4 3/8	32	1	3/4	3/4	3/4		—	7	22	3	2 3/4	3/4
3 3/8	18	1 3/4	1 3/4	3/4	3/4	3/4	4 3/8	40	1	3/4	3/4	3/4	—	7 1/8	24	1 3/4	1 1/2	3/4	3/4	3/4

Figure 8-89. Bubble cap and risers—types and hold-downs. Used by permission, Glitsch, Inc.

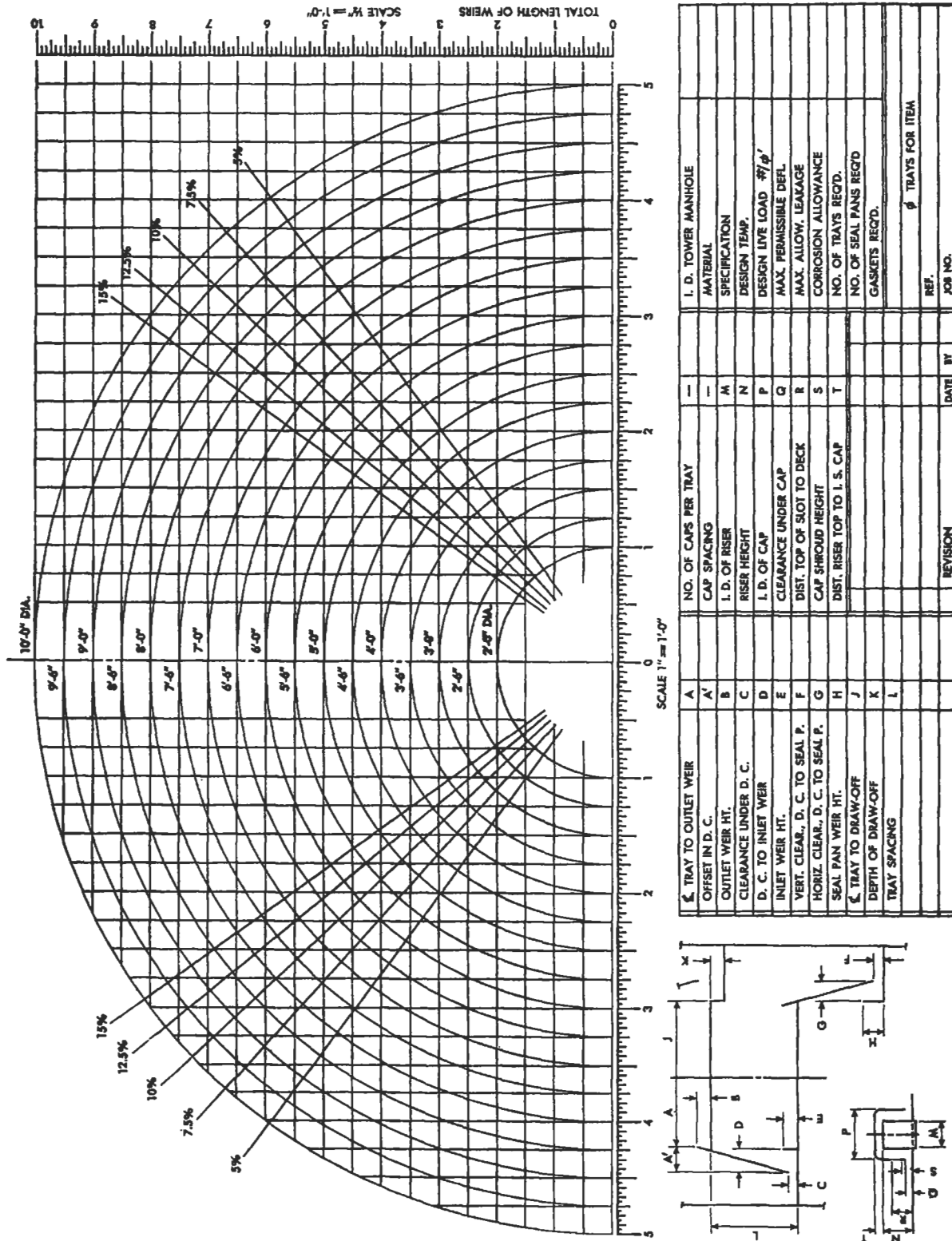


Figure 8-90. Distillation tray layout form. (Use with Figure 8-91, not reproduced to scale.) Used by permission, Wyatt Metal and Boiler Works, Inc. © (1956).

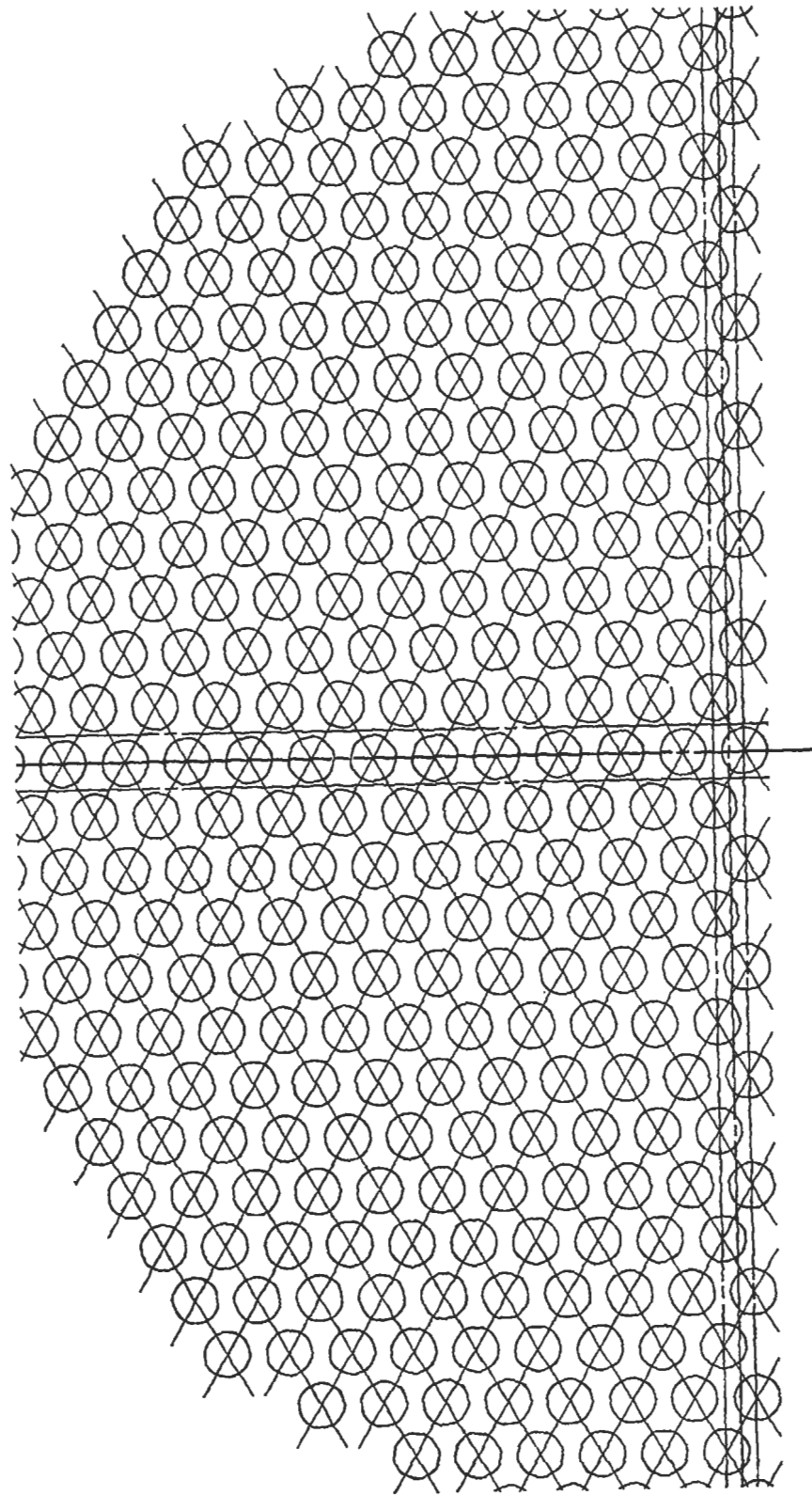


Figure 8-91. 4-in. diameter bubble caps on 5.5-in. Δ pitch. Used by permission, Wyatt Metal and Boiler Works, Inc., © (1956).

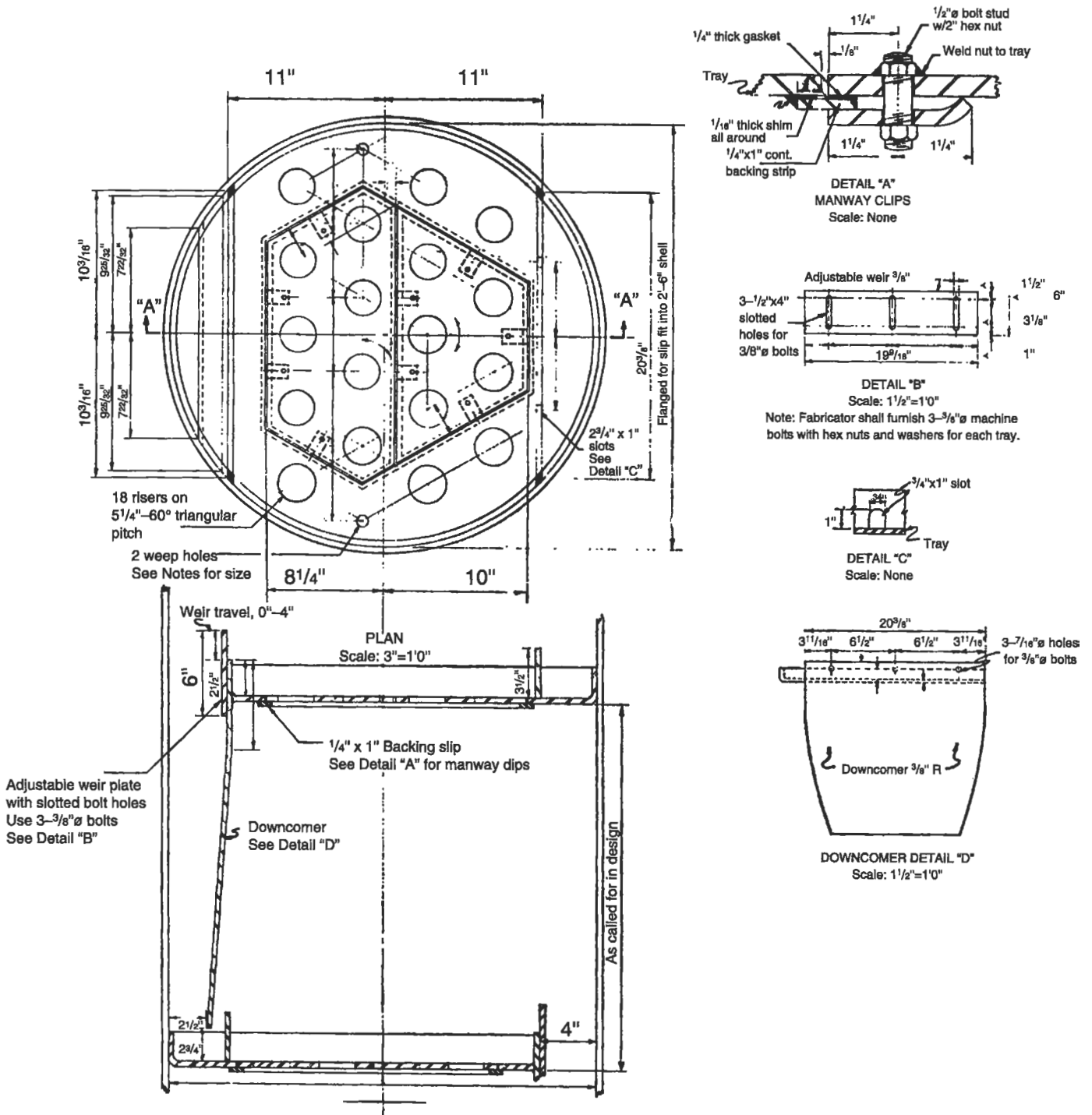


Figure 8-92. 2-ft-6-in. dia. column—4-in. caps.

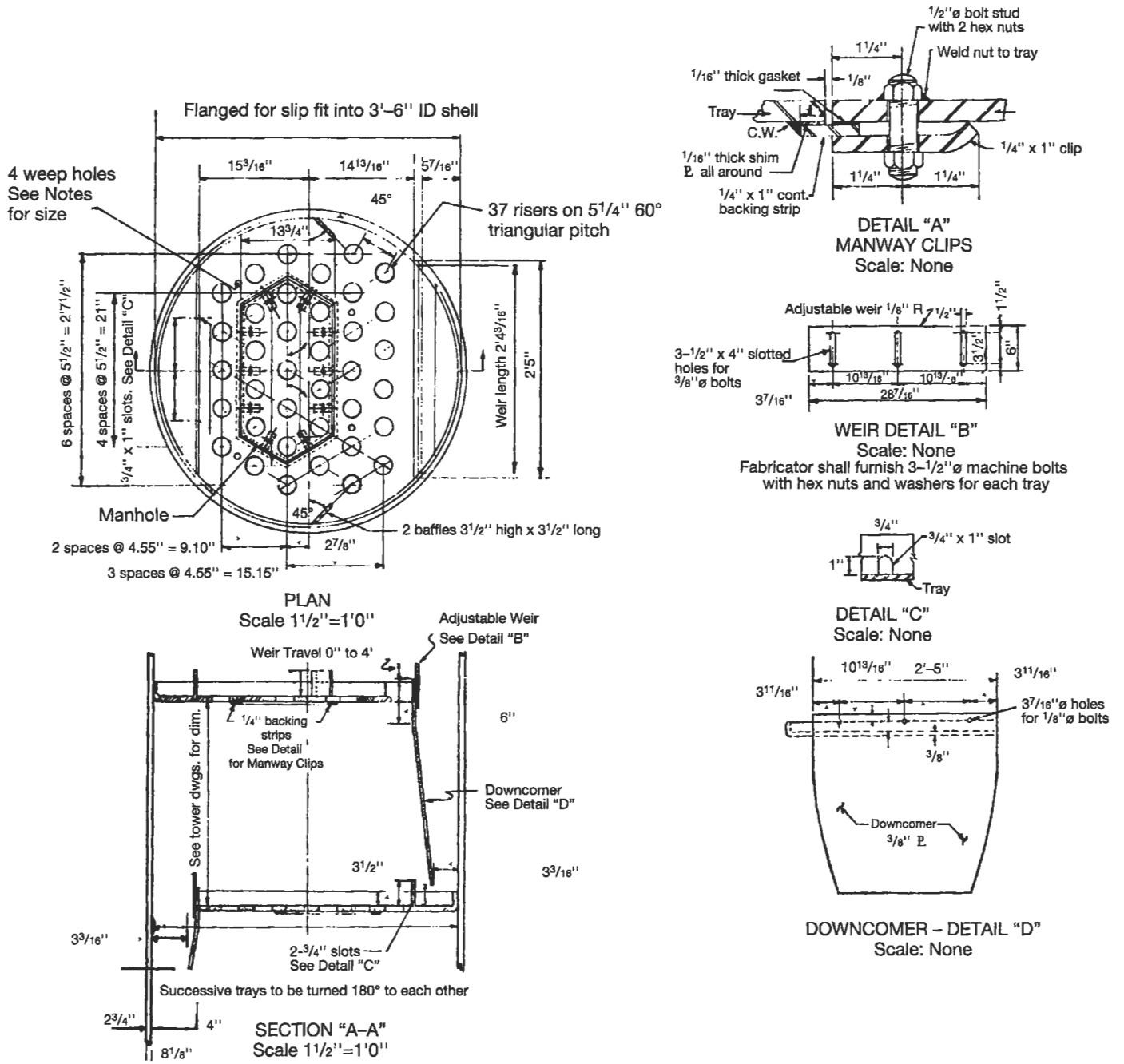
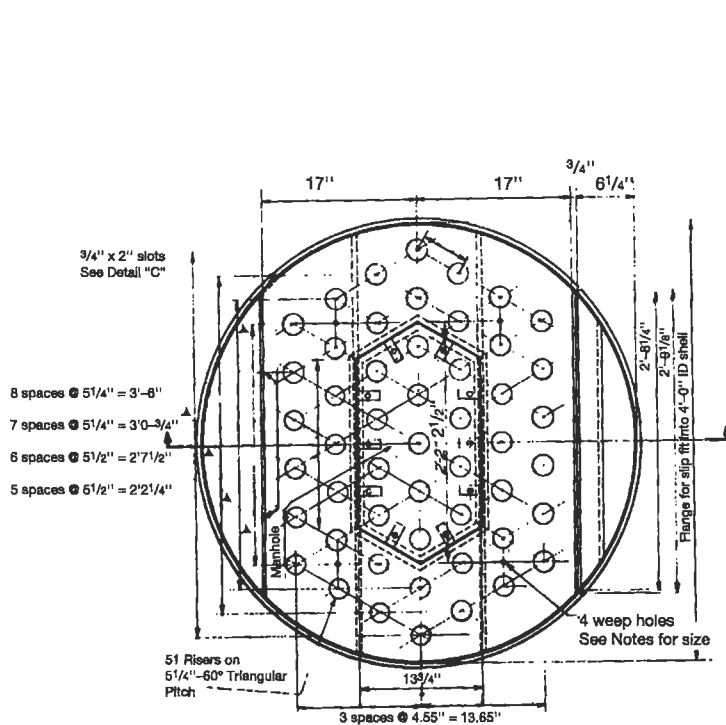
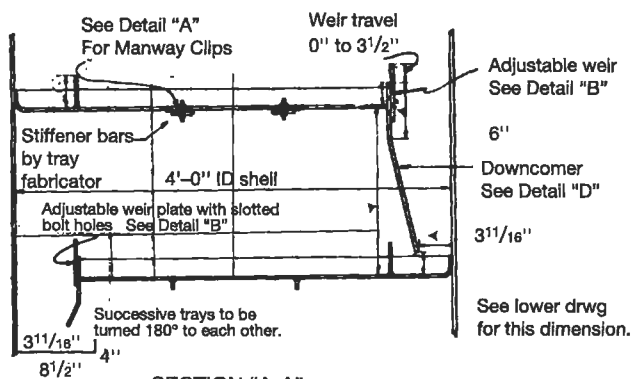


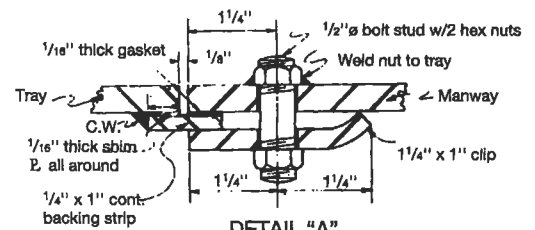
Figure 8-93. 3-ft-6-in. dia. column—4-in. caps.



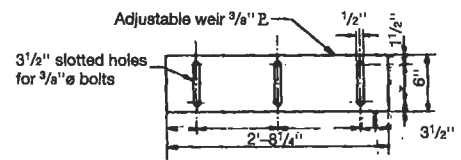
PLAN
Scale 1 1/2" = 1'0"



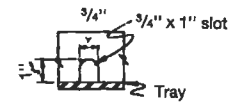
SECTION "A-A"
Scale 1 1/2" = 1'0"



DETAIL "A"
MANWAY CLIPS
Scale: None

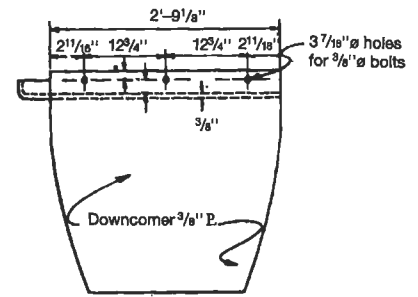


WEIR DETAIL "B"
Scale: None
Fabricator shall furnish 3-3/8" ø machine bolts
with hex nuts and washers for each tray.



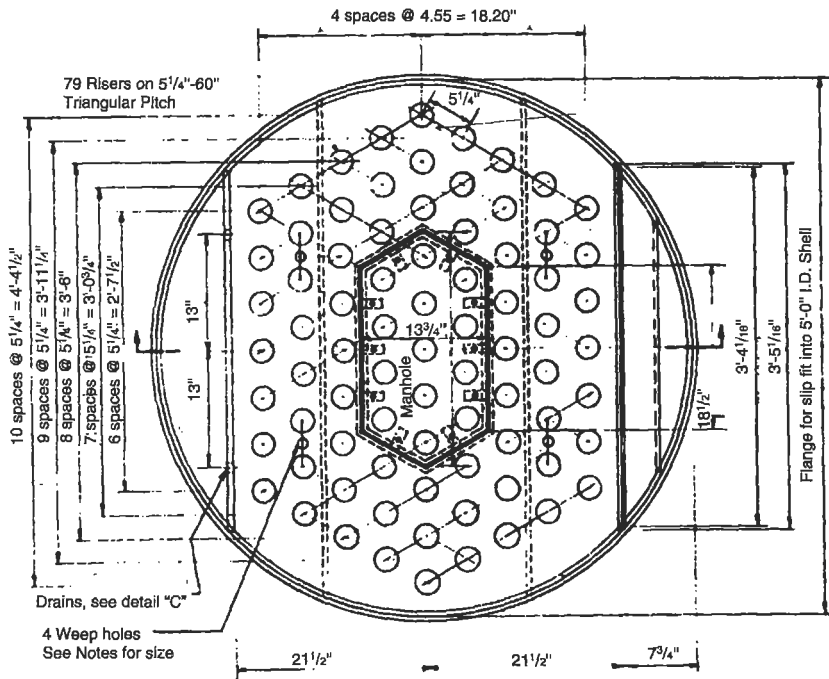
DETAIL "C"
Scale: None

12 9/4" 3/4"

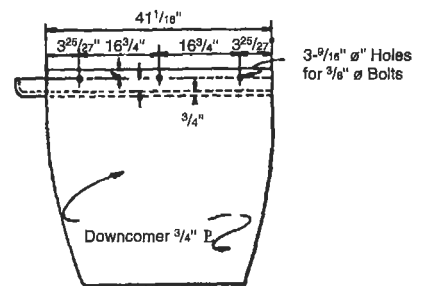
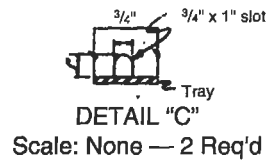
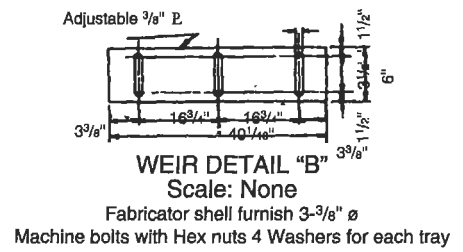
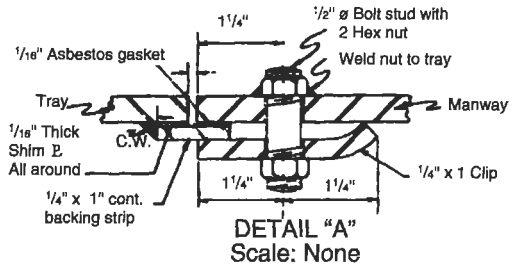
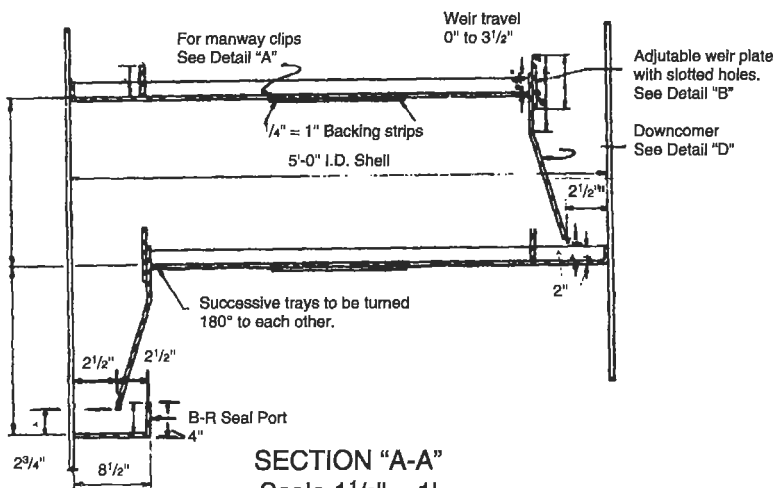


DOWNCOMER DETAIL "D"
Scale: None

Figure 8-94. 4-ft-0-in. dia. column—4-in. caps.



PLAN
Scale 1 1/2" = 1'-0"



DOWNCOMER DETAIL "D"
Scale None

Figure 8-95. 5-ft-0-in. dia. column—4-in. caps.

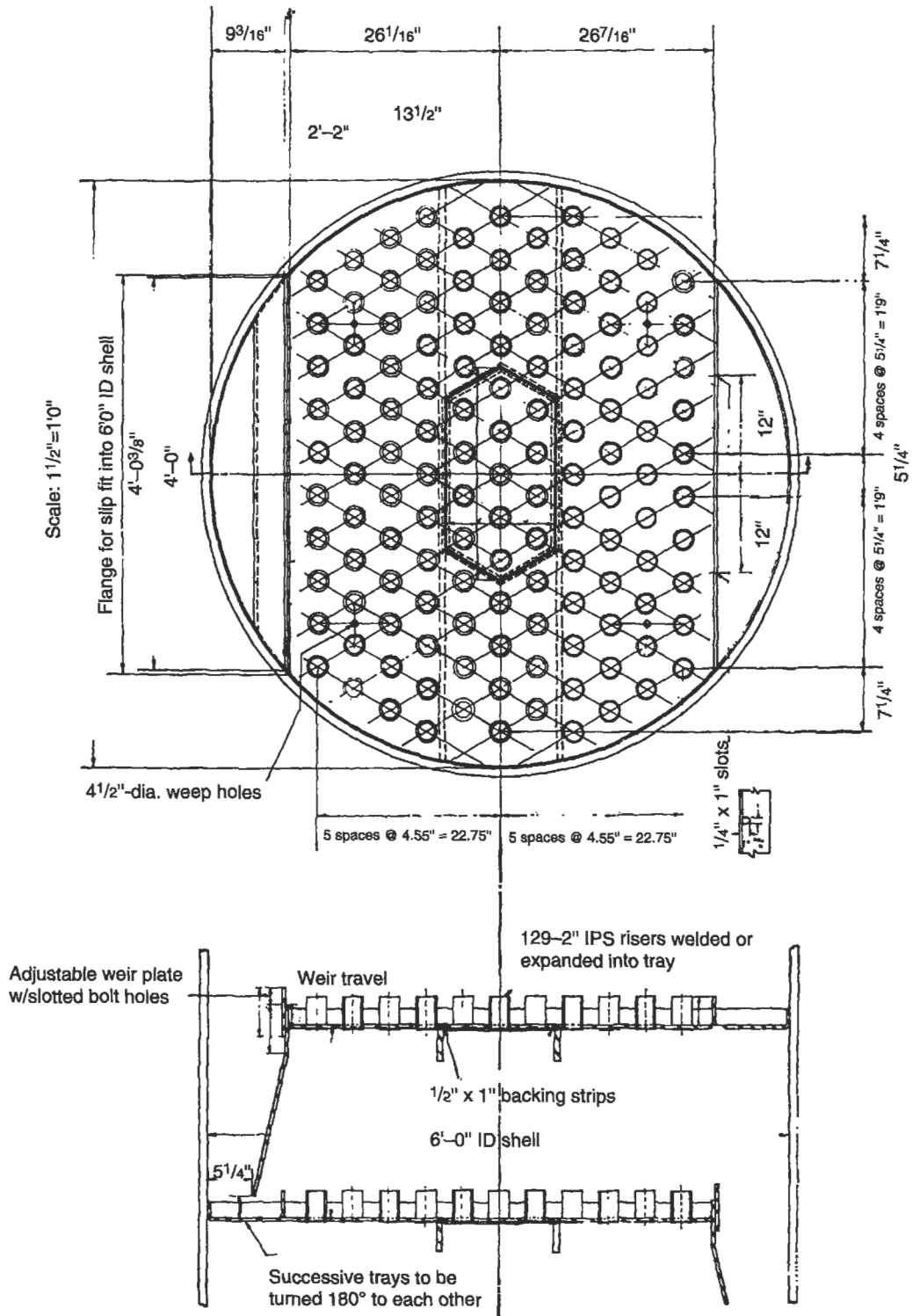


Figure 8-96. 6-ft-0-in. dia. column—4-in. caps.

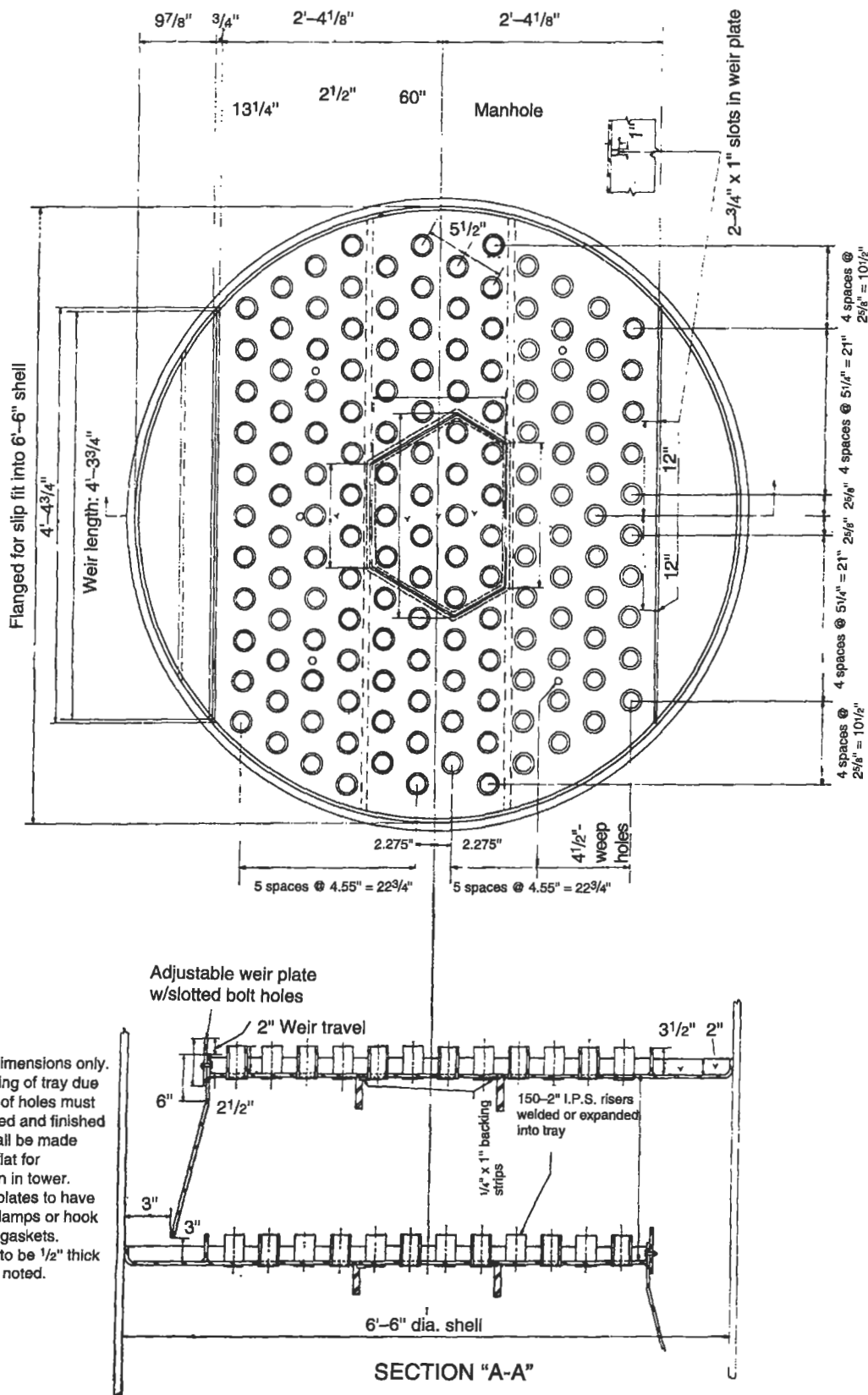


Figure 8-97. 6-ft-6-in. dia. column—4-in. caps.

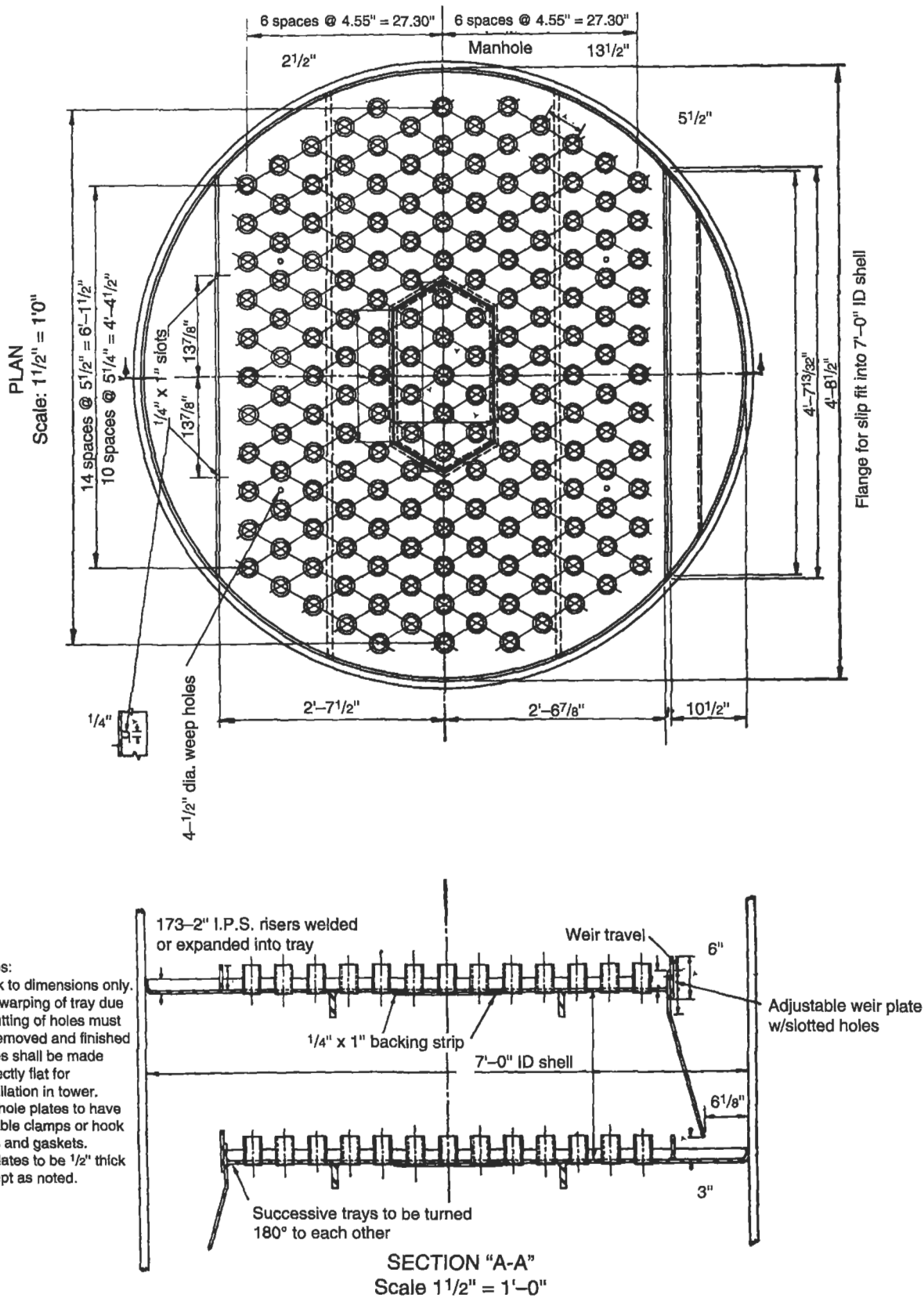
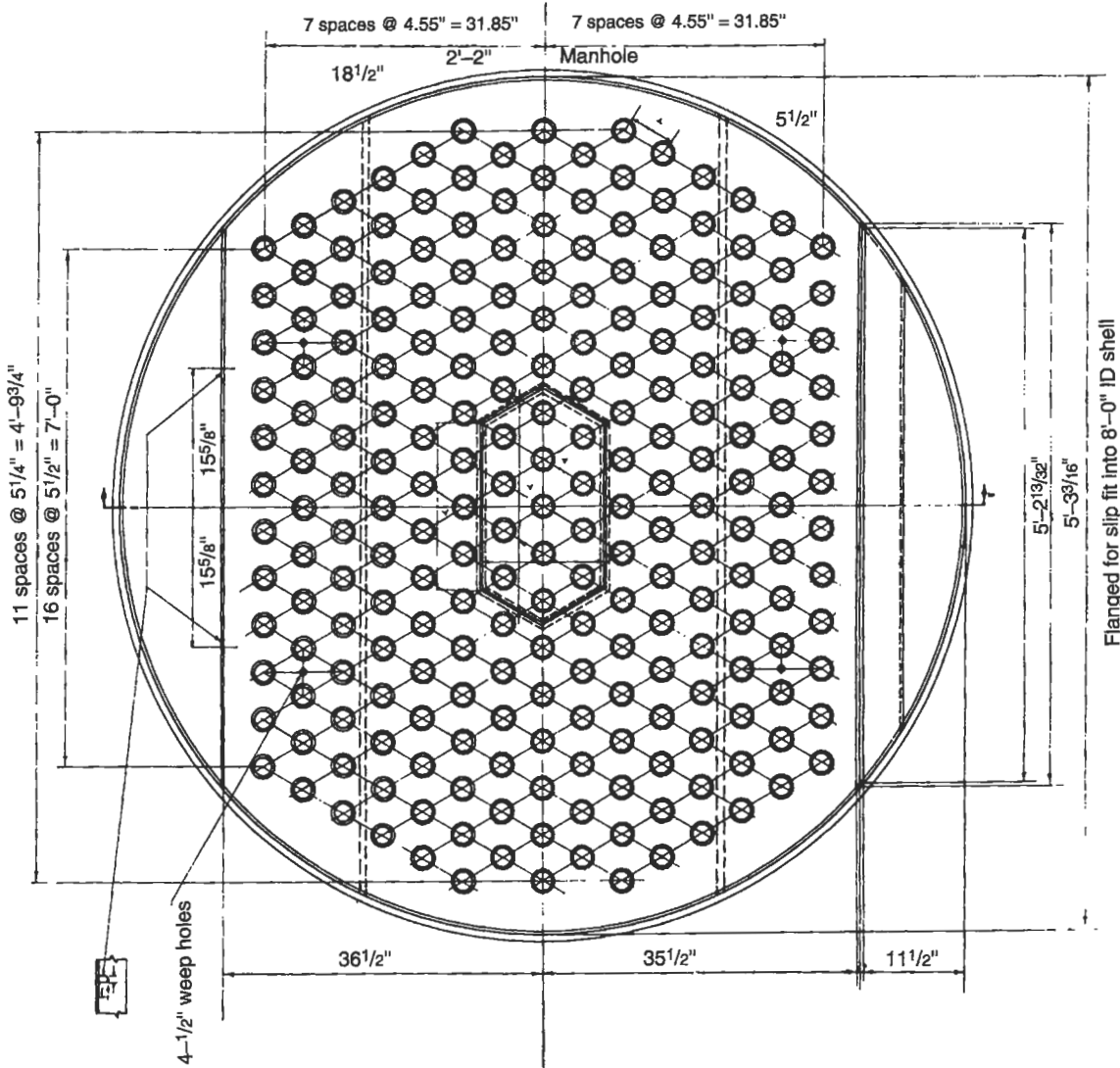
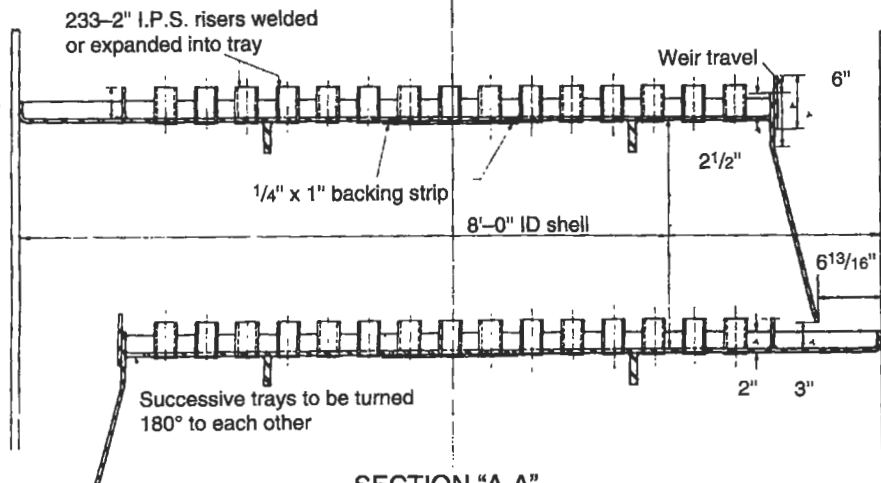


Figure 8-98. 7-ft-0-in. dia. column—4-in. caps.



Notes:
 Work to dimensions only.
 Any warping of tray due to cutting of holes must be removed and finished plates shall be made perfectly flat for installation in tower.
 Manhole plates to have suitable clamps or hook bolts and gaskets.
 All plates to be 1/2" thick except as noted.



SECTION "A-A"
 Scale 1 1/2" = 1'-0"

Figure 8-99. 8-ft-0-in. dia. column—4-in. caps.

Table 8-16
General Purpose Distillation Trays Using 3/8-in. I.D. Pressed Metal Bell Caps on 5/8-in. Centers

Inside Diameter	2 ft-6 in.	3 ft-0 in.	3 ft-6 in.	4 ft-0 in.	5 ft-0 in.	6 ft-0 in.	6 ft-6 in.	7 ft-0 in.	8 ft-0 in.
Total Area, ft ²	4.91	7.07	9.62	12.56	19.63	28.28	33.18	38.48	50.26
Liquid Flow	Cross	Cross	Cross	Cross	Cross	Cross	Cross	Cross	Cross
No. Downflow Weirs (1)	One	One	One	One	One	One	One	One	One
No. Downflow Seals (2)	One	One	One	One	One	One	One	One	One
No. Caps & Risers/Tray	18	27	37	51	79	129	150	173	223
No. Rows/Tray	4	5	6	7	9	11	12	13	15
Total Slot Area, ft ² (3)	1.15	1.73	2.38	3.27	5.08	8.29	9.64	11.1	14.29
Percent of Tower Area	23.4	24.5	24.8	26.0	25.9	29.3	29.1	28.9	28.50
Total Riser Area, ft ² (4)	0.683	1.04	1.42	1.96	3.00	4.95	5.56	6.64	8.57
Percent of Tower Area	13.9	14.7	14.8	15.6	15.3	17.5	16.75	17.25	17.05
Overflow Weir Length, ft (1)	1.625	2.05	2.35	2.686	3.35	4.0	4.31	4.62	5.21
Percent of Tower Diameter	65.0	68.0	67.1	67.0	67.0	66.7	66.0	66.05	65.1
Downflow Segment Area (5)									
Maximum Area, ft ²	0.338	0.642	0.80	0.96	1.41	2.12	2.39	2.85	3.50
Minimum Area, ft ²	0.167	0.225	0.33	0.45	0.69	0.886	1.027	1.14	1.47
Under Flow Clearance, in.	2½	2¾	2¾	2¾	2¾	2¾	3	3	3
Under Flow Area, ft ²	0.274	0.354	0.426	0.473	0.604	0.710	0.750	0.887	1.01
Up Flow Area,									
Minimum ft ² (6)	0.137	0.365	0.335	0.552	0.795	0.740	0.882	1.000	1.21

(1) 2½ in. minimum height above tray floor, with adjustable weir 0 to 3½ in. additional.

(2) 3½ in. high above tray floor.

(3) Slots are 50-½ in. × 1½ in. per cap. Caps on triangular pitch.

(4) Riser inside diameter = 2.68 in.

(5) Design uses tapered segmental downcomer and inlet weir.

(6) Area between downcomer and inlet weir for up-flow of inlet liquid. All trays included access manway.

(text continued from page 135)

resulting low tray efficiencies. Table 8-15 gives recommendations for layout.

Liquid Drainage or Weep Holes

Holes for drainage must be adequate to drain the column in a reasonable time, yet not too large to interfere with tray action. Draining of the column through the trays is necessary before any internal maintenance can be started or before fluid services can be changed, when mixing is not desirable. The majority of holes are placed adjacent to the outlet or downcomer weir of the tray. However, some holes are placed in the downcomer inlet area or any suspected low point in the mechanical layout of the column.

The study of Broaddus et al. [7] can be used to develop the following drainage time relation, and is based on fluids of several different densities and viscosities:

$$\theta = \frac{(0.18N + 0.15)(\mu)^{0.12}(A_n)}{(\rho)^{1/4}(d_h/h')^{1.2}} \quad (8-221)$$

where θ = time to drain tower, minutes

A_n = net open liquid area of one tray, equal to total tower cross section minus area occupied by caps

and minus area of segmental or other downcomer at outlet of tray, ft²

ρ = liquid density, grams/cc at liquid temperature in tower

μ = viscosity of liquid at tower temperature, centipoise
 d_h = weep hole diameter, in. Note that this is the diameter equivalent to the area of all the weep holes/tray
 h' = height of overflow weir or bubble cap riser, whichever is smaller, in.

N = total number of actual trays in tower

The accuracy of this relation is given as 14% maximum, 6% average.

A general recommendation [5] is to provide four square inches of weep hole area per 100 ft² of net open liquid tray area in the tower. This latter refers to the total of all trays in the tower.

Bottom Tray Seal Pan

The bottom tray of a tower must have its downcomer sealed to prevent upflow of reboiled vapors. The downcomer of this tray is usually equal to or 6 in. longer than the other downcomers to ensure against bottom vapor surges or pulses in pressure breaking the seal. The seal pan is designed to avoid liquid back pressure and minimum restrictions to liquid flow.

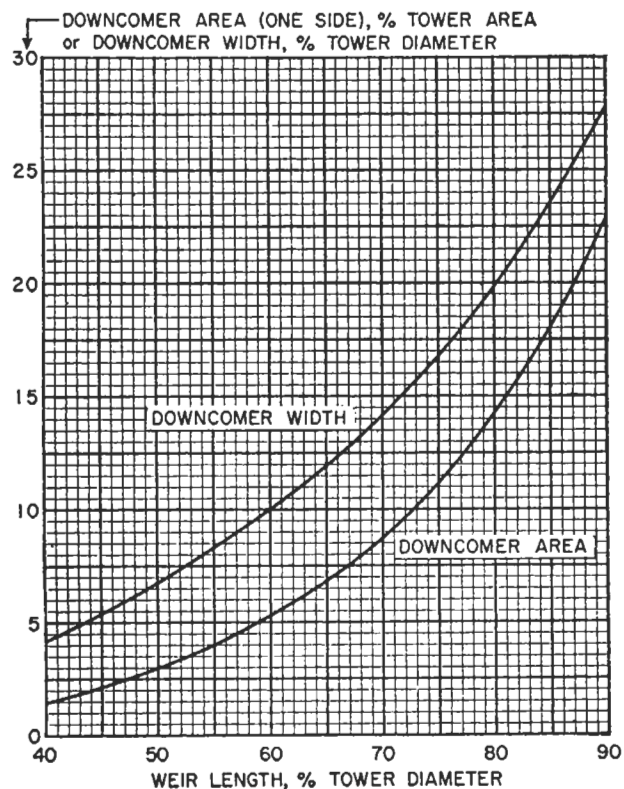


Figure 8-100. Segmental downcomer design chart. Used by permission, Bolles, W. L. *Pet. Processing*; Feb. thru May (1956).

Turndown Ratio

Turndown can be applied to all types/styles of tray columns; however, it is more relevant to sieve and valve trays. The generally accepted explanation of turndown is as follows [199] (also see Figure 8-101):

Turndown ratio is the ratio of the maximum allowable vapor rate at or near flooding conditions (rates) to the minimum vapor rate when weeping or liquid leakage becomes significant; it may be termed the minimum allowable vapor velocity [193, 199, 200].

1. For bubble cap trays, this ratio is approximately 10:1.
2. For sieve trays, this ratio is approximately 2-3:1.
3. For valve trays, this ratio is approximately 4-5:1.

Bubble Caps

Although there are many styles and dimensions of caps in use, the round bell shaped bubble cap is quite practical and efficient. It is recommended as a good basis for the contacting requirements. This selection does not infer that other contacting caps are not acceptable, in fact many are in use in the chemical and petroleum industry. Their design criteria is limited to the proprietary knowledge of the manufacturer and not available to the designer.

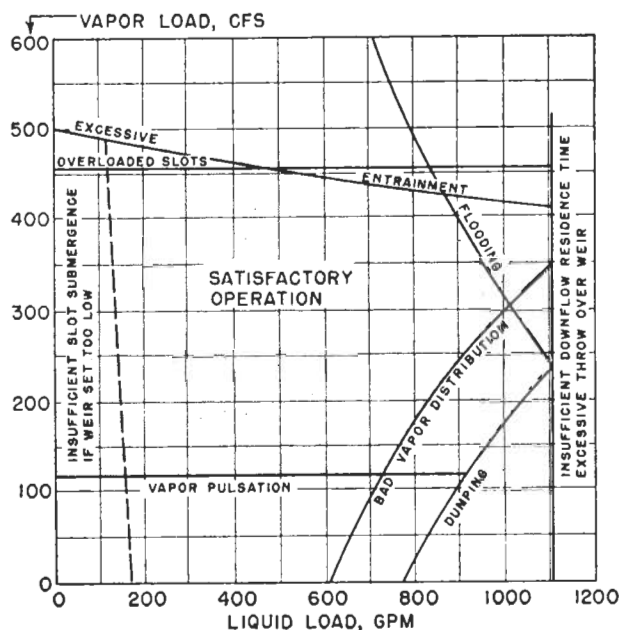


Figure 8-101. Qualitative effect of liquid and vapor loads on bubble cap tray performance. Used by permission, Bolles, W. L., *Pet. Processing*, Feb. thru May (1956).

Dimensions

The most popular and perhaps most adaptable size is about 4 in. O.D. (3 3/8 in. I.D.). The 3-in. and 6-in. are also in common use for the smaller and larger diameter towers, although it is not necessary to change cap size with change in tower diameter. For a given active cap area the cost of installing the smaller diameter caps is 10-15% greater than the 4-in., while the larger (and fewer number) 6-in. caps are about 15% cheaper. There is usually less waste tray area with the 3-in. caps than the 4-in. or 6-in. caps. Table 8-17.

For the sake of standardization and developing a feel on the part of the designer for the effect of various design variables on tray performance, the 4-in. cap (or 3 3/8-in. or 4 1/8-in.) caps are recommended as good general purpose units. This means that any application from a 2.5-ft dia. to 10-ft dia. tower is first evaluated using the 4-in. cap. If there are points of poor performance, cap sizes can be

Table 8-17
General Purpose Guide for Pressed Cap Size Selection

Tower Diameter, Ft	General Purpose Size, I.D., In.	Possible Alternate, In.
2.5, 3	3 3/8	2 1/2; 3; 3 1/2
3.5, 4	3 3/8	3; 5 1/2
5, 6, 7, 8, 9, 10	3 3/8	6
11, 12, 13, 14	6	3 3/8

changed and the performance re-evaluated to adjust in the direction of optimum performance.

Pressed steel caps of 12 to 14 U.S. Standard gage are the most frequently used, although cast iron caps are used in some services such as corrosive chlorinated hydrocarbons, drying with sulfuric acid, etc. Alloy pressed caps maintain the light weight desirable for tray construction, yet frequently serve quite well in corrosive conditions. Special caps of porcelain, glass, and plastic are also available to fill specific applications. The heavier caps require heavier trays or more supports in the lighter trays. The use of hold-down bars on caps is not recommended for the average installation; instead, individual bolts and nuts are preferred. Some wedge type holding mechanisms are satisfactory as long as they will not vibrate loose.

Slots

The slots are the working part of the cap, i.e., the point where the bubbling action is initiated. Slots are usually rectangular or trapezoidal in shape, either one giving good performance. A single comparison [5] indicates the rectangular slots give slightly greater capacity than the trapezoidal, while the trapezoidal slots give slightly better performance at low vapor rates (flexibility). This study shows that triangular slots are too limited in capacity, although they would be the better performers at low vapor rate. Generally, the capacity range offered by the rectangular and trapezoidal slots is preferred.

Slot Sizes

Width: $\frac{1}{8}$ - $\frac{1}{2}$ -in., $\frac{1}{8}$ -in. recommended rectangular $\frac{1}{8}$ -in. \times $\frac{1}{4}$ -in. to $\frac{1}{2}$ -in. \times $\frac{3}{8}$ -in., $\frac{3}{16}$ -in. \times $\frac{5}{16}$ -in. recommended trapezoidal

Height: $\frac{3}{4}$ -in. to $1\frac{1}{2}$ -in., $1\frac{1}{4}$ -in. to $1\frac{1}{2}$ -in. recommended

Shroud Ring

This is recommended to give structural strength to the prongs or ends of the cap. The face of the ring may rest directly on the tray floor or it is recommended to have three short legs of $\frac{1}{4}$ -in. for clean service. For all materials the skirt clearance is often used at $\frac{1}{2}$ to 1-in., and for dirty service with suspended tarry materials it is used as high as $1\frac{1}{2}$ in. These legs allow fouling or sediment to be washed out of the tray, and also allow emergency cap action under extremely overloaded conditions—at lower efficiencies.

Tray Performance—Bubble Caps

A bubble cap tray must operate in dynamic balance, and the closer all conditions are to optimum, the better the performance for a given capacity. Evaluation of perfor-

mance requires a mechanical interpretation of the relationship of the tray components as they operate under a given set of conditions. This evaluation includes the determination of:

1. Tray pressure drop
 - a. Slot opening
 - b. Static and dynamic slot seals
 - c. Liquid height over weir
 - d. Liquid gradient across tray
2. Downcomer conditions
 - a. Liquid height
 - b. Liquid residence time
 - c. Liquid throw over weir into downcomer
3. Vapor distribution
4. Entrainment
5. Tray efficiency

The evaluation is made in terms of pressure drops (static and friction) through the tray system. Figures 8-63 and 8-66 diagrammatically present the tray action.

An understanding of the action of the bubble cap tray is important to good design judgment in deciding upon the acceptance of a particular design. The passage of vapor through the caps and liquid across the tray is complicated by fluid actions associated with the mechanical configuration and with the relative velocities of the fluids at various points on the tray. The quantitative considerations will be given in more detail in later paragraphs. However, the qualitative interpretation is extremely valuable. The following descriptions are presented for this purpose.

Tray Capacity Related to Vapor-Liquid Loads

Figure 8-101 presents a generalized representation of the form useful for specific tray capacity analysis. Instead of plotting actual vapor load versus liquid load, a similar form of plot will result if actual vapor load per cap (here the cap row relative to inlet or outlet of tray is significant) versus the liquid load per inch or foot of outlet weir length.

Although each plot must be for a specific system of conditions, Figures 8-102 and 8-103 are extremely valuable in analyzing the action of a bubble tray.

For Figure 8-103 Bolles points out that the cap loads for inlet and outlet rows will be essentially balanced or "lined out" when the shaded areas are equal.

From Figure 8-101, the region of satisfactory tray operation is bounded by performance irregularities. Here all the caps are flowing vapor; the bubbling action is acceptable from an efficiency standpoint; entrainment is within design limits; there is no dumping (or back flow) of liquid down the risers, and no undesirable vapor jetting around the caps.

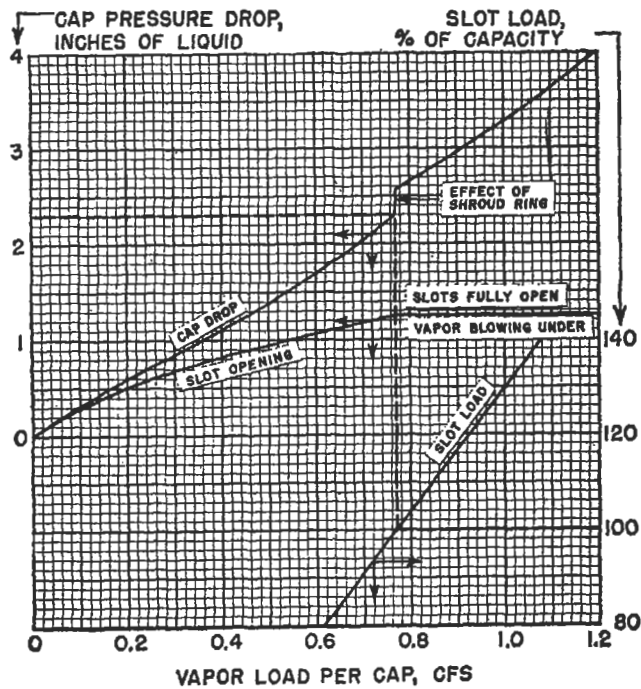


Figure 8-102. Effect of vapor load on slot opening, slot load, and pressure drop. Used by permission, Bolles, W. L., *Pet. Processing*, Feb. thru May (1956).

Tray Balance

A tray is in balance when it operates with acceptable efficiency under conditions at or very near those of design.

Tray Flexibility

A tray is flexible when it operates with acceptable efficiency under conditions which deviate significantly from those established for design. The usual changes affecting flexibility are vapor and/or liquid loading. A tray may operate down to 50% and up to 120% of vapor load, and down to 15% and up to 130% of liquid load and still be efficient. Beyond these points its efficiency may fall off, and the flexible limits of the tray would be established.

Tray Stability

A tray is stable when it can operate with acceptable efficiencies under conditions that fluctuate, pulse, or surge, developing unsteady conditions. This type of operation is difficult to anticipate in design, and most trays will not operate long without showing loss in efficiency.

Flooding

A bubble tray tower floods when the froth and foam in the downcomer back up to the tray above and begin accumulating on this tray. The downcomer then contains a mixture of lower density than the clear liquid, its capacity becomes limited, disengagement is reduced, and the level rises in the downcomer. This level finally extends onto the tray above, and will progress to the point of filling the column, if not detected and if the liquid and vapor loads are not reduced. Flooding is generally associated with high liquid load over a rather wide range of vapor rates. The foaming tendencies of the liquid influence this action on the tray. The design condition for height of clear liquid in the downcomer for flooding is usually set at 0.60 to 0.80 of $(S_t + h_w)$. See Figure 8-63.

Pulsing

A bubble tray pulses when the vapor rate is low and unsteady, when the slot opening is low (usually less than 1/2 in.), and when the liquid dynamic seal is low. With irregular vapor flow entering the caps, the liquid pulses or surges, even to the point of dumping or back-flowing liquid down the risers. The best cure is a steady vapor rate and good slot opening to allow for reasonable upsets.

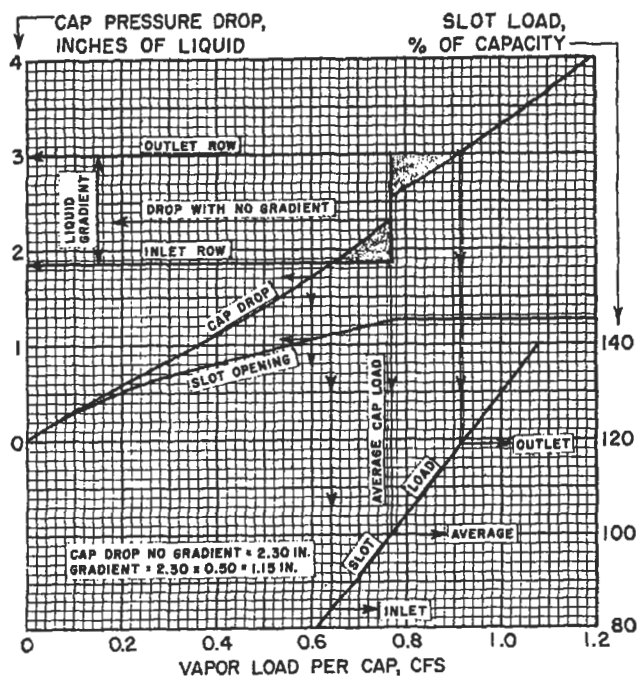


Figure 8-103. Effect of liquid gradient on vapor distribution with 0.5 vapor distribution ratio. Used by permission, Bolles, W. L., *Pet. Processing*, Feb. thru May (1956).

Blowing

A bubble tray blows when the vapor rate is extremely high, regardless of the liquid rate, causing large vapor streams or continuous bubbles to be blown through the liquid. The efficiency and contact is low and entrainment is usually high. Here also low slot seals contribute to the sensitivity of the tray to such action.

Coning

A bubble tray cones when the liquid seal over the slot is low and the vapor rate is so high as to force the liquid completely away from the cap, thus bypassing the liquid entirely. Obviously, efficiency is unsatisfactory. The dynamic slot seals recommended in Table 8-18 normally will prevent such action.

Entrainment

A bubble tray has high entrainment when mist and liquid particles carry up in the vapor from the liquid on one tray through the riser and cap on to the tray above. Bubble caps tend to entrain by jetting liquid-vapor mixtures high above the tray. Sufficient tray spacing must be available to prevent the quantity of material from significantly affecting the efficiency of the system. The quantitative presentation of entrainment in later paragraphs is designed to work to this end.

Overdesign

Overdesign is often necessary in designing a tray, although caution must be exercised to prevent a piling-up or accumulation of safety factors resulting in numbers which are totally unrealistic for performance. In other words, the magnitude, effect, and significance of overcapacity figures must be continuously monitored as each factor is calculated. A factor of 10–15% on liquid and vapor rates is usually acceptable. However, each should be

checked relative to the effect on maximum cap vapor capacity and entrainment, and on liquid gradient and buildup in the downcomer.

Total Tray Pressure Drop

This is normally taken as the wet bubble cap pressure drop plus the "mean dynamic slot seal" in inches of clear or unaerated liquid on the tray.

Guide values for normal operations, drop per tray.

Pressure	Vacuum (500 mm Hg and below)
2–4 in. water	2–4 mm Hg

Liquid Height Over Outlet Weir

For a straight (non-circular) weir, the head of liquid over its flat top is given by the modified Francis Weir relation (Figure 8-104; also see Figure 8-63):

$$h_{ow} = 0.092 F_w (L_g/l_w)^{2/3} \quad (8-222)$$

The modifying factor F_w developed by Bolles [5] for restriction at the shell due to segmental downcomer application is determined from Figure 8-105.

When h_{ow} values exceed $1\frac{3}{4}$ to 2 in., consider special downcomers or down pipes to conserve cap area for high vapor loads.

Notched outlet weirs (usually 60° V-notch) are only used for low liquid flow rates, and the head over this type of weir with notches running full [13].

$$L_g = 14.3 (l_w/n) [h_{ow}^{5/2} - (h_{ow} - h_n)^{5/2}] \quad (8-223)$$

For notches not running full

$$L_g = 13.3 (l_w/n) (h_{ow})^{5/2} \quad (8-223A)$$

where h_{ow} = height of liquid crest over flat weir, in.

l_w = length of weir (straight), feet

L_g = liquid flow rate, gallons per minute, tray or tray section

n = depth of notches in weir, in.

h_{ow}' = height of liquid above bottom of notch in weir, in.

h_n = depth of notches in weir, in.

$$\text{For circular weirs (pipes) } h_{ow} = L_g/10 d_w \quad (8-224)$$

where d_w = diameter of circular weir, in.

Slot Opening

The slot opening is the vertical opening available for vapor flow during operation of the cap under a given set of conditions. It has been found to be essentially independent of surface tension, viscosity and depth of liquid over

Table 8-18
Suggested Slot Seals

Tower Operating Pressure	Static Slot Seal [15], In.	Dynamic Slot Seal [5], In.
Vacuum, 30–200 mm Hg. abs	0–0.25	0.5–1.5
Atmospheric	0.5	1.0–2.0
50–100 psig	1.0	1.5–3.0
300 psig	1.5	2.0–4.0
500 psig	1.5	2.0–4.0

Used by permission, Bolles, W. L., *Petroleum Processing*, Feb. thru May (1956), and Davies, J. A., *Pet. Refiner* V. 29, No. 93 (1950), Gulf Pub. Co.

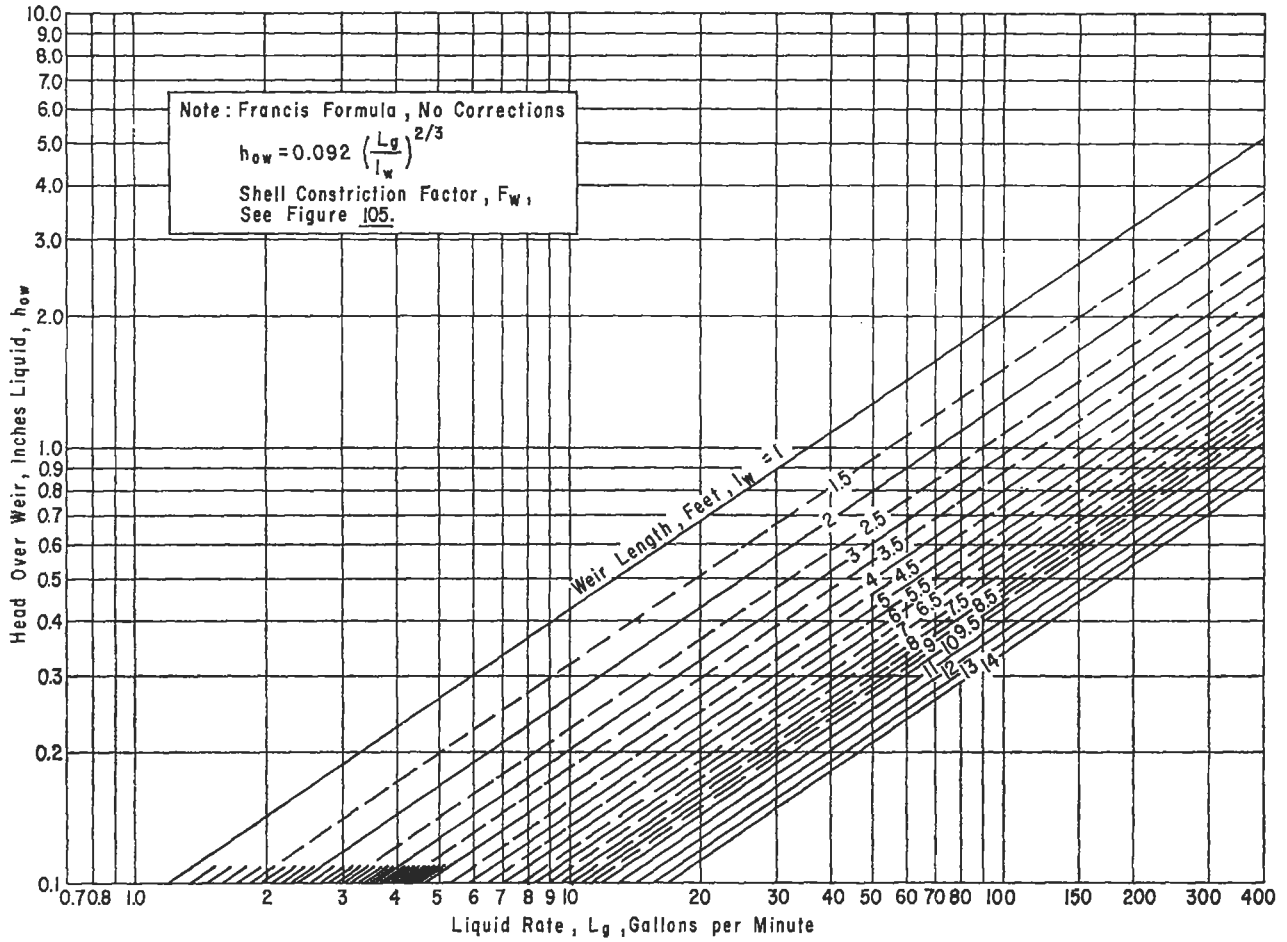


Figure 8-104. Liquid height over straight weir.

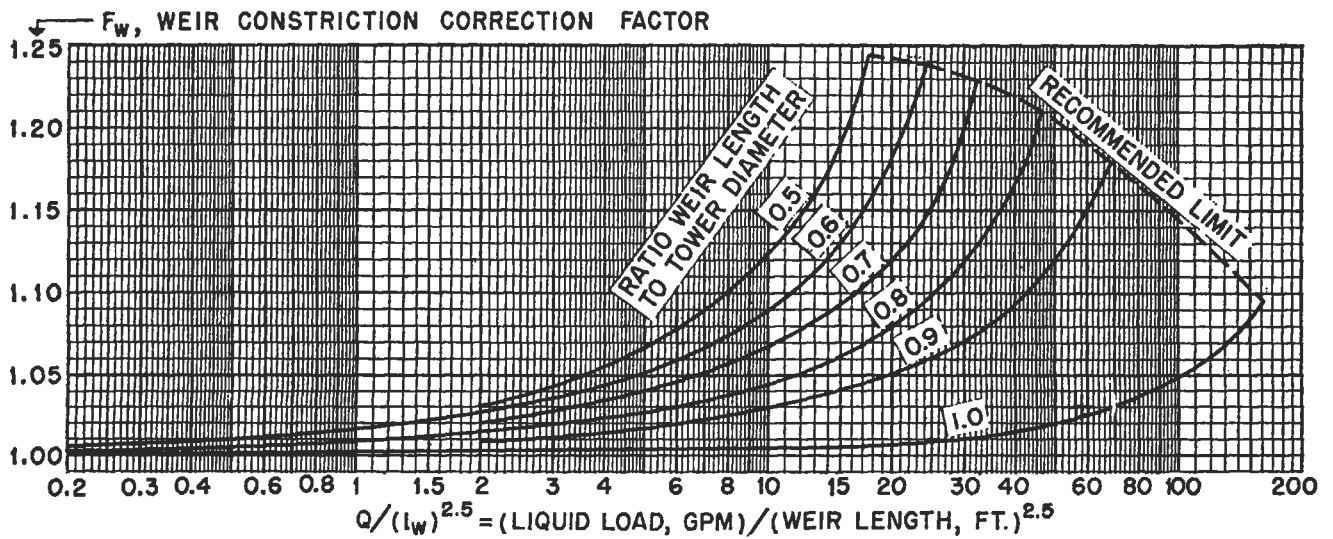


Figure 8-105. Weir formula correction factor for segmental type weirs. Used by permission, Bolles, W. L., *Pet. Processing*, Feb. thru May (1956).

the cap. When the required opening exceeds the available, the vapor will either flow under the cap, create greater pressure drop or both.

A. Caps with Rectangular Slots [60]

$$h_s = 32 \left(\frac{\rho_v}{\rho_L - \rho_v} \right)^{1/3} \left(\frac{V}{N_c (N_s) (w_s)} \right)^{2/3} \quad (8-225)$$

where h_s = slot opening, or pressure drop through slot, in. liquid

V = total vapor flow through tray, ft^3/sec

N_c = number of caps per tray

N_s = number of slots per cap

w_s = width of slot (rectangular), in.

Figure 8-106 presents a quick solution of this relation. Maximum slot capacity [5]:

$$V_m = 0.79 (A_s) \left[H_s \left(\frac{\rho_L - \rho_v}{\rho_v} \right) \right]^{1/2} \quad (8-226)$$

where A_s = total slot area per tray, ft^2

H_s = slot height, in.

V_m = maximum allowable vapor load per tray, ft^3/sec

B. Caps with Trapezoidal Slots

A trial solution is involved in determining the slot opening for trapezoidal slots [5]. The relation for maximum capacity at full slot opening is:

$$V_m = 2.36 (A_s) \times \left[\frac{2}{3} \left(\frac{R_s}{1+R_s} \right) + \frac{4}{15} \left(\frac{1-R_s}{1+R_s} \right) \right] \times \left[H_s \left(\frac{\rho_L - \rho_v}{\rho_v} \right) \right]^{1/2} \quad (8-227)$$

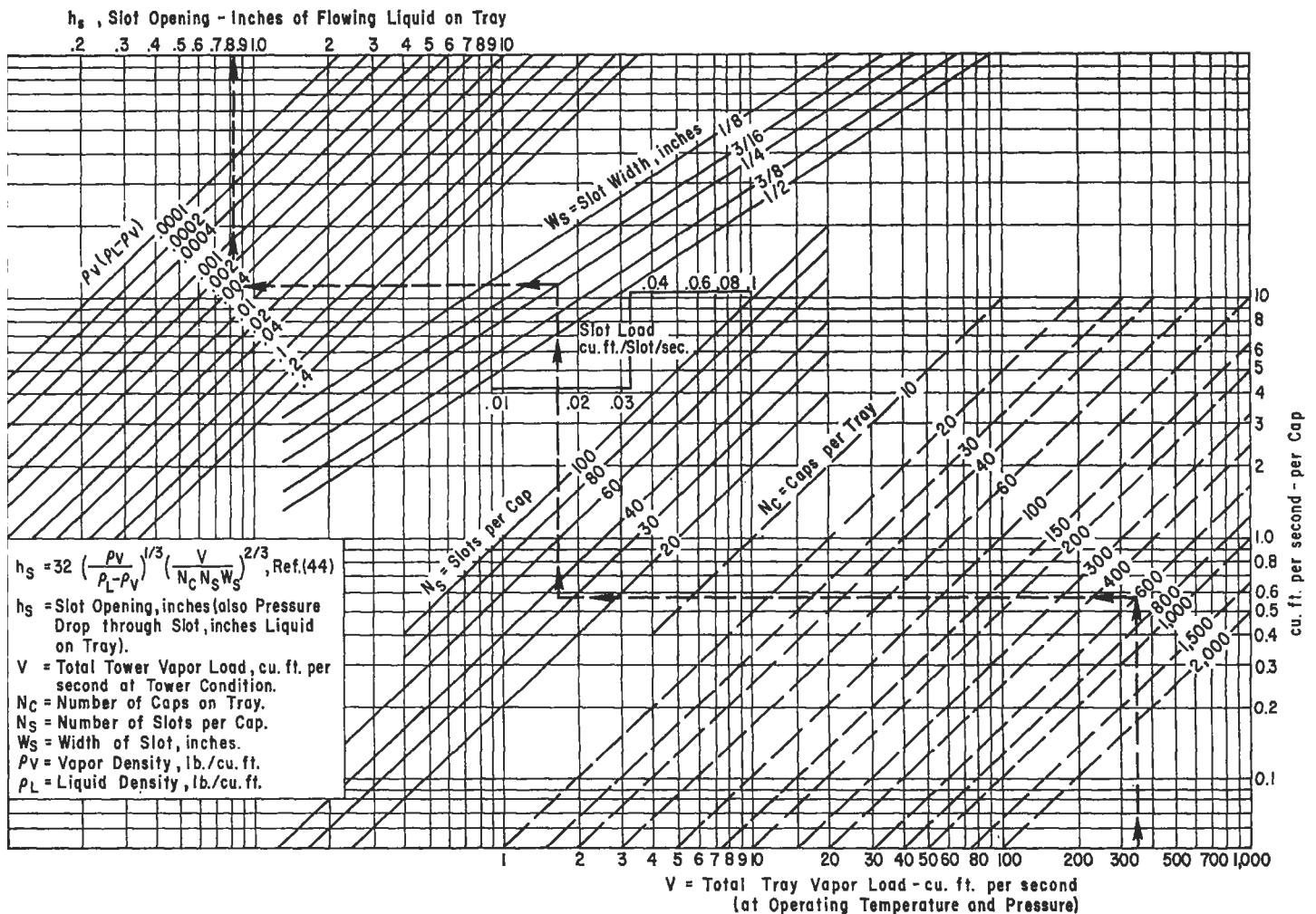


Figure 8-106. Opening of rectangular-vertical slots for bell type bubble cap. Used by permission, Stone and Webster Engineering Corp., Boston, Mass.

where R_s = ratio of top to bottom widths of trapezoid slot.

Figure 8-107 is useful in solving for the slot height as a percentage of the vapor capacity and of full opening.

Whenever possible, the slots should be designed to be 50–60% open to allow for pulses and surges in vapor flow.

Liquid Gradient Across Tray

The difference in height of liquid between the liquid inlet and liquid outlet sides of a tray is the liquid gradient. This is the result of frictional drag on the caps and internals plus resistance created by the bubbling action. A tray with high liquid gradient may be operating inefficiently and at reduced capacity if the rows of caps covered by high liquid are not bubbling, thus forcing all the vapor through the rows of caps nearer the tray outlet where the liquid head is lower. Liquid gradient is one of the criteria which must be checked to assure proper understanding of a tray design and its performance.

The recommendation of Bolles [5] is based on the work of Davies [14, 15] and serves the average design adequately. It assumes an I.D. of bubble cap to I.D. of riser of 1.42 and this is close to the range for 85% of the installations. Small deviations will be negligible. It must be remembered that the agreement between the several investigators is good [24, 38, 44] but still lacks a final solution to all situations. In general, calculated values should not be considered better than ± 0.2 -in.

The relation:

$$\left(\frac{L_g/l_{fw}}{C_d}\right) = 25.8 \left(\frac{\gamma}{1+\gamma}\right) (\Delta'_r)^{1/2} \left[1.6 \Delta'_r + 3 \left(h_1 + \frac{0.3s}{\gamma}\right)\right] \quad (8-228)$$

Solve for left side expression, and determine (Q/L_w) from Figure 8-108, or use Figures 8-109–112

- where L_g = total liquid load in tray or tray section, gpm
- $L_w = l_{fw}$ = total flow width across tray normal to flow, ft
- C_d = liquid gradient factor (Ref. 5, Figure 7, not needed to solve)
- γ = ratio of distance between caps to cap diameter
- Δ'_r = liquid gradient per row of caps, uncorrected, in.
- h_1 = depth of clear liquid on tray, in.
- s = cap skirt clearance, in.
- $L_w = l_{fw}$
- $Q = L_g$
- $h_1 = h_w + h_{ow} + \Delta/2$ (8-229)

Some designers use $\Delta/5$ to $\Delta/3$ in place of $\Delta/2$.

The charts of Figures 8-109–112 were developed [5] from the modified Davies equation to simplify the solution of a tedious problem. The mean tray width is usually taken as average of weir length and column diameter. Special tray patterns may indicate another mean value.

The values of liquid gradient read from these charts are uncorrected for vapor flow. This correction is a multiplier read from Figure 8-113.

Corrected $\Delta = \Delta' C_v$ (8-230)

$V_o = V =$ vapor load for tray, ft³/sec

Although this method appears to be conservative for the average case, it is not strictly correct for towers with liq-

(text continued on page 166)

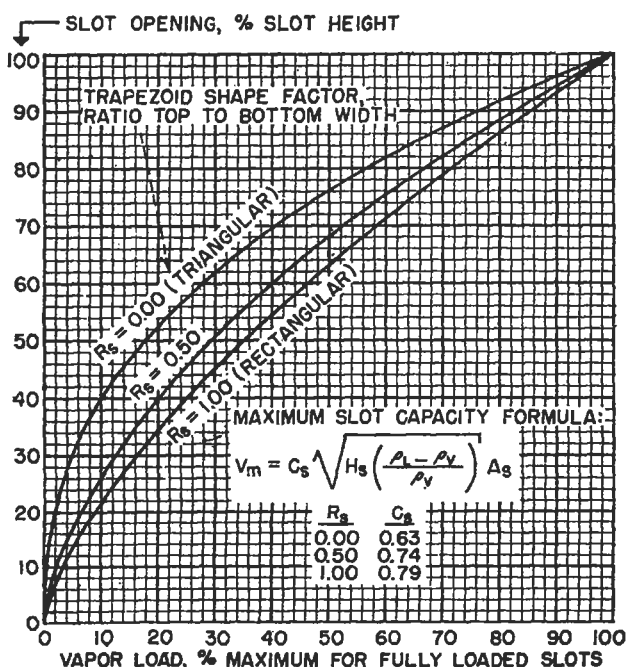


Figure 8-107. Trapezoidal slot generalized correlation. Used by permission, Bolles, W. L., *Pet. Processing*, Feb. thru May (1956).

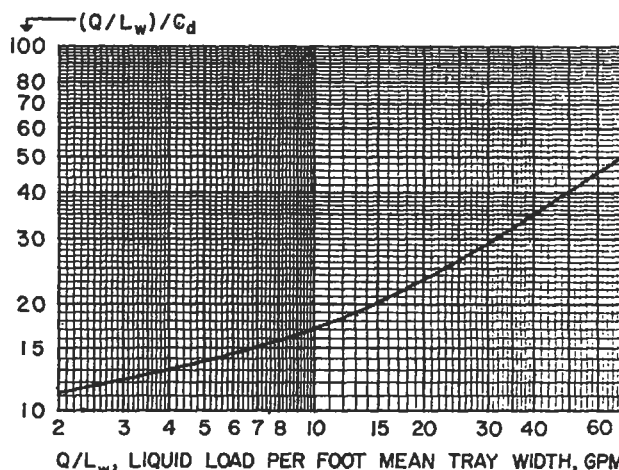


Figure 8-108. Modified liquid gradient factor chart for no hold-down bars. Used by permission, Bolles, W. L. *Pet. Processing*, Feb. thru May (1956).

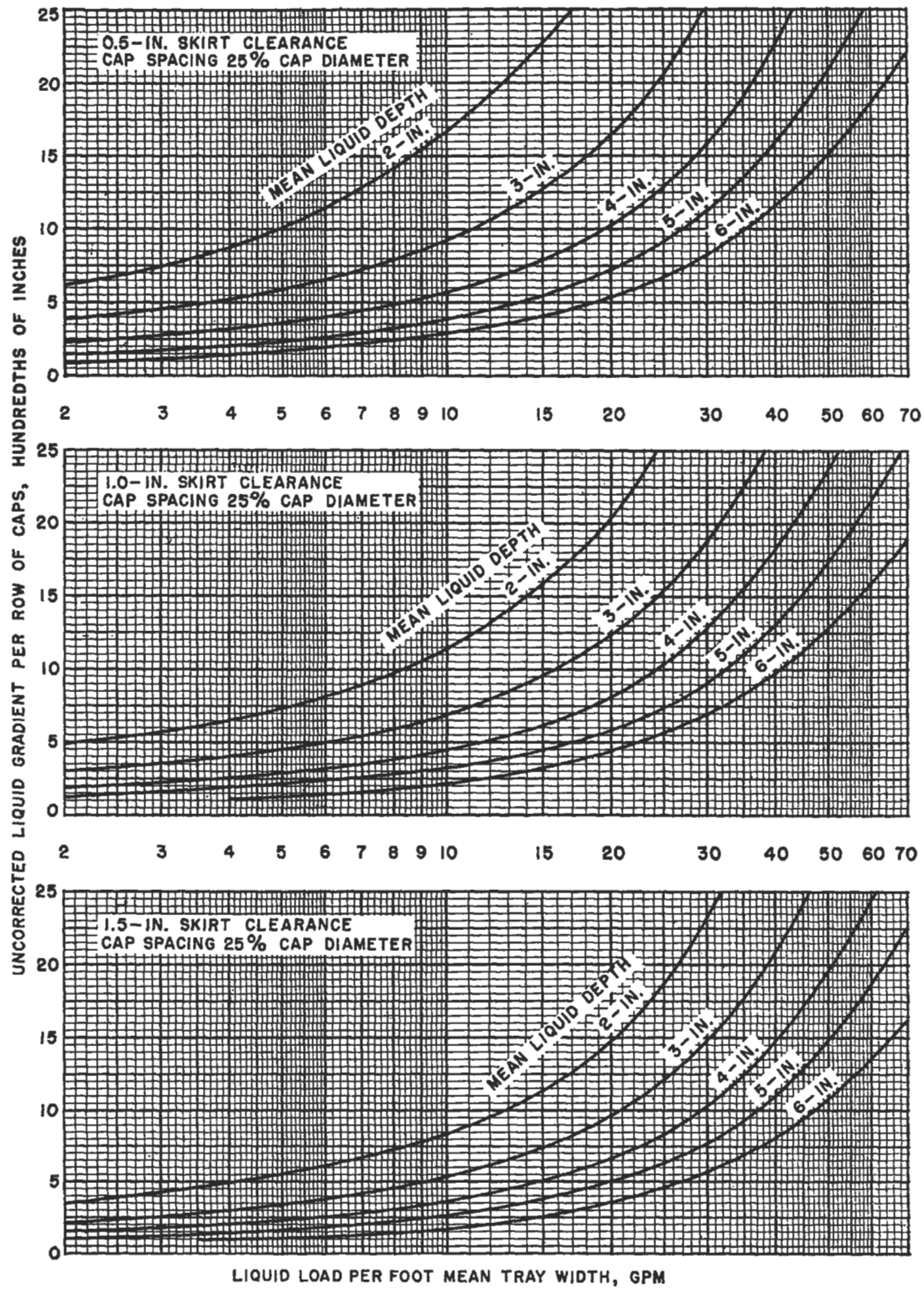


Figure 8-109. Liquid gradient chart—cap spacing 25% cap diameter. Used by permission, Bolles, W. L., *Pet. Processing*, Feb. thru May (1956).

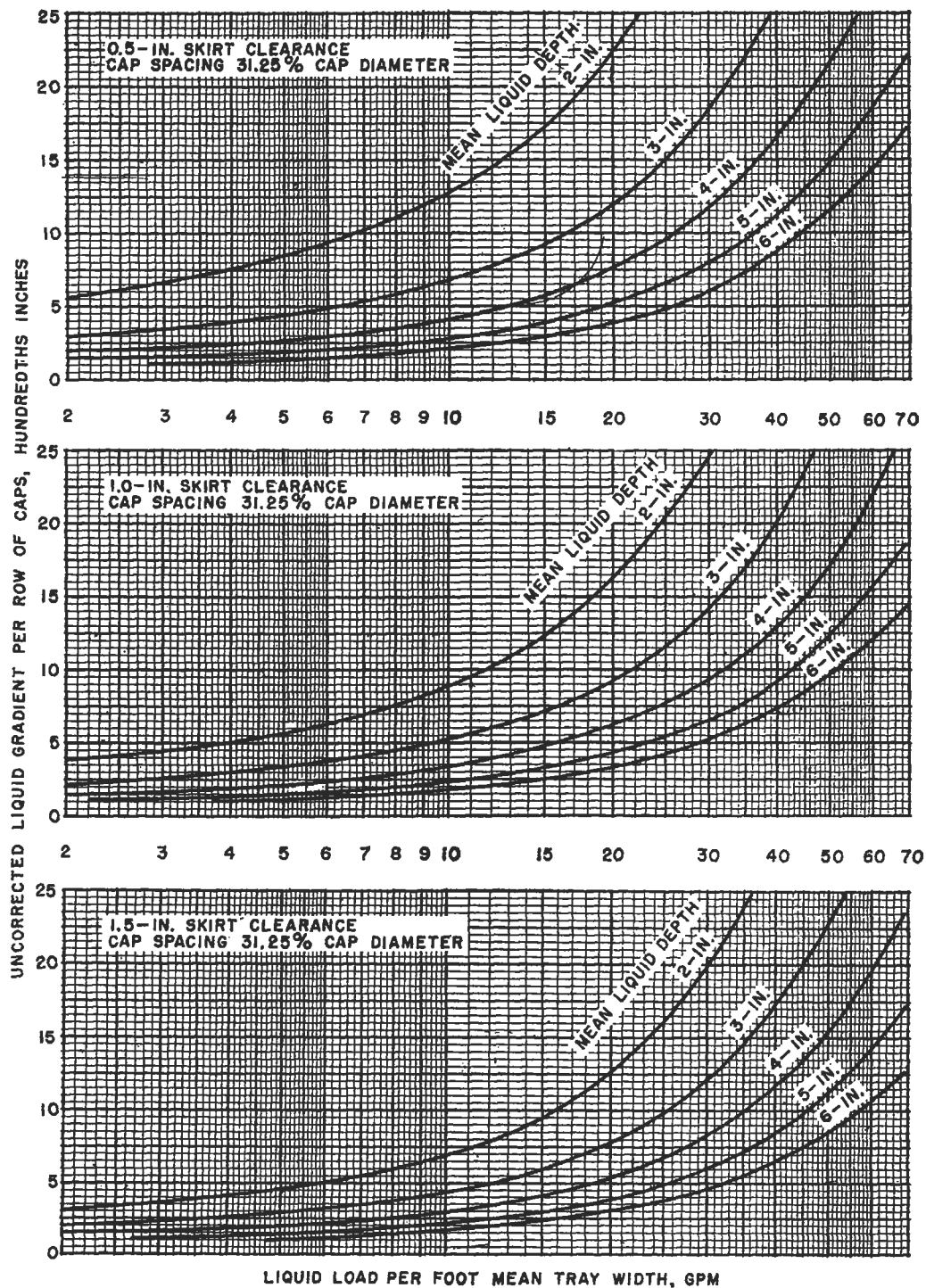


Figure 8-110. Liquid gradient chart—cap spacing 31.25% cap diameter. Used by permission, Bolles, W. L., *Pet. Processing*, Feb. thru May (1956).

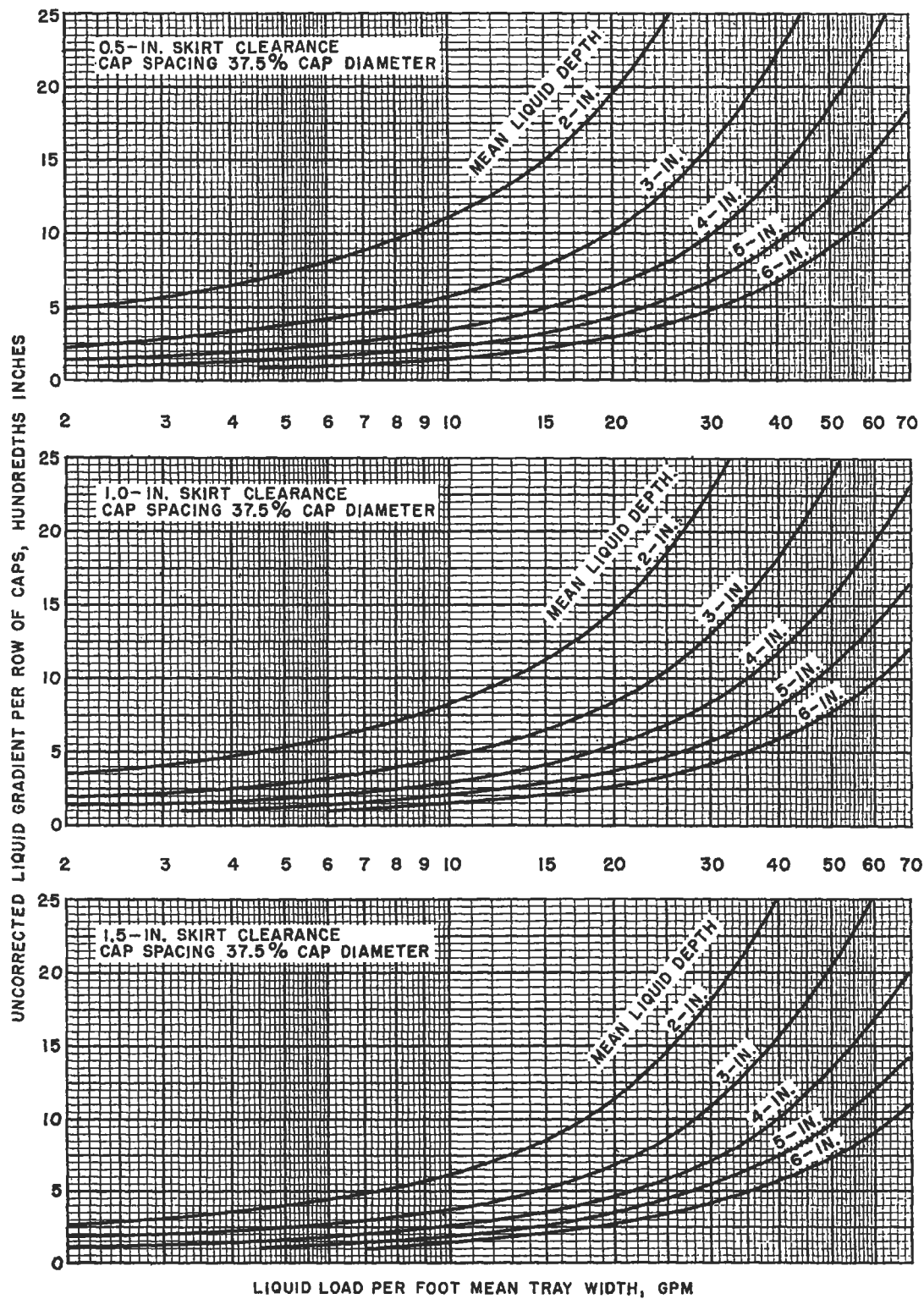


Figure 8-111. Liquid gradient chart—cap spacing 37.5% cap diameter. Used by permission, Bolles, W. L., *Pet. Processing*, Feb. thru May (1956).

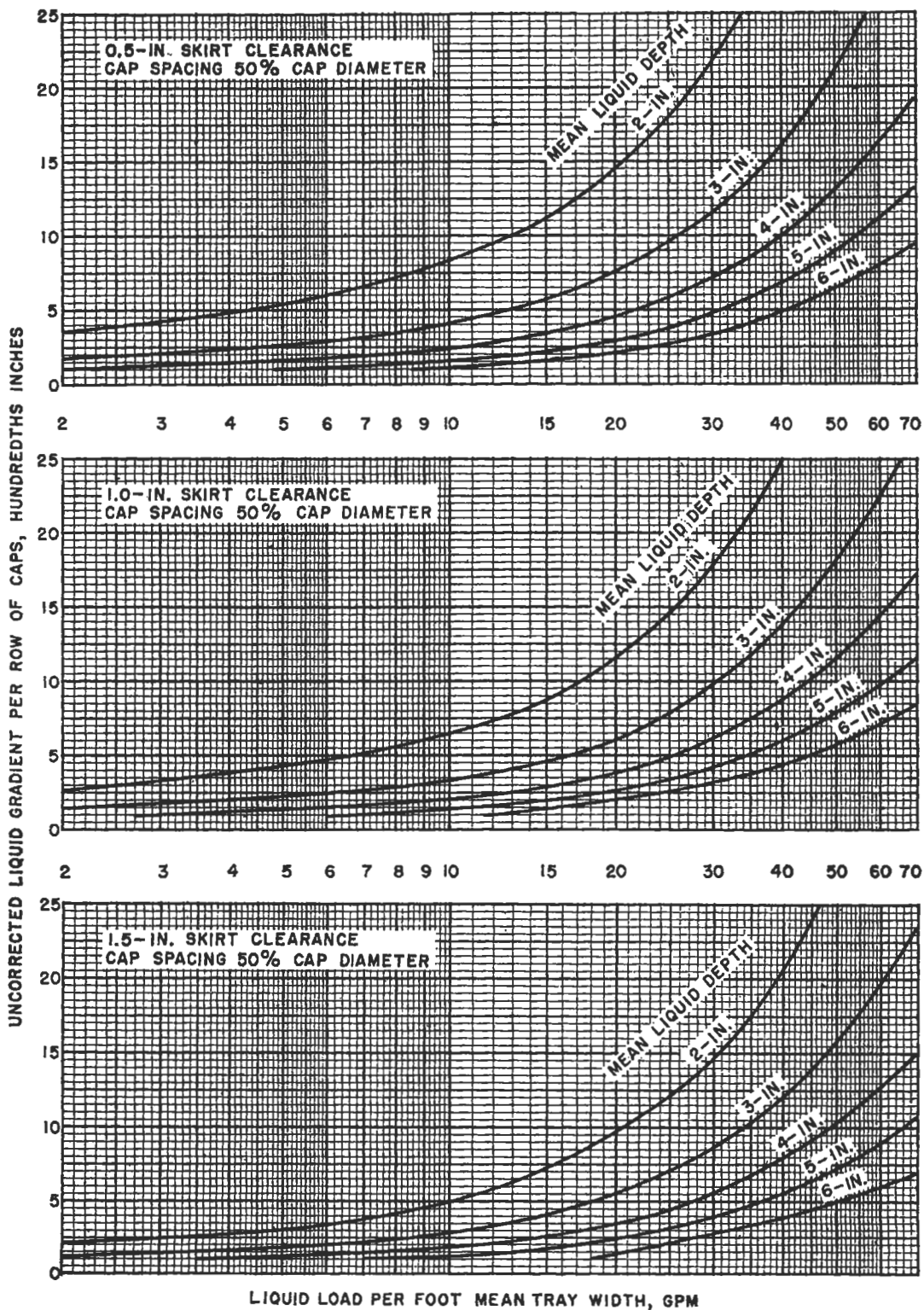


Figure 8-112. Liquid gradient chart—cap spacing 50% cap diameter. Used by permission, Bolles, W. L., *Pet. Processing*, Feb. thru May (1956).

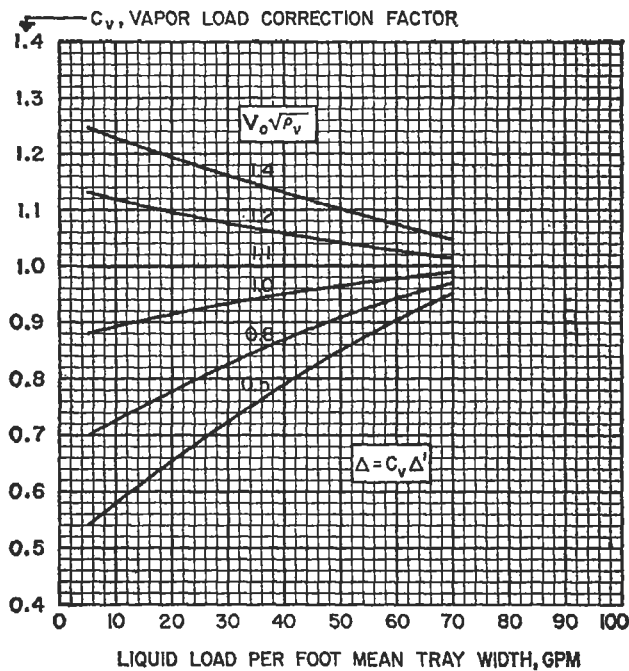


Figure 8-113. Correction of liquid gradient for vapor load. Used by permission, © The American Chemical Society, Davies, J. A., *Ind. and Eng. Chem*, V. 39, (1947) p. 774.

(text continued from page 161)

liquid flowing over the cap. Therefore it would be well to check the results of gradients over 1.0 in. by comparing with some of the other methods and with the tabulation of data of Reference 38.

Adjustments to the tray or caps is usually not considered unless the calculated gradient exceeds $\frac{1}{2}$ to 1 in. liquid. Several schemes are in use:

1. Raise cap in inlet half of tower by one-fourth to one-half the calculated gradient, but not exceeding 1 in.
2. For large towers (usually over 8 ft in diameter) check the hydraulic gradient for sections of the tray normal to liquid flow, adjusting each section by not more than one-half the gradient.
3. Slope the trays downward from liquid inlet to outlet, with the total drop from inlet to outlet weir not exceeding one-half the calculated gradient.
4. Cascading the tray by using weirs as dams to divide the tray in steps, each step or section of the tray having no significant gradient from its inlet to outlet. This is usually only considered for trays 10 ft in dia. and larger, as it adds considerably to the cost of each tray.
5. More elaborate tests and adjustments can be made [5]. However, they are usually unnecessary except in unusual cases of very high liquid loads and/or large columns.

In any case, the average head over the cap slots for the section should approximately equal the average head over the adjoining sections, and the inlet and outlets of the section should not be extreme, even though the average is acceptable. The object of fairly uniform head over the slots should be kept in mind when reviewing the gradient adjustments.

Riser and Reversal Pressure Drop

The method proposed by Bolles fits the average design problem quite satisfactorily. However, for low pressure drop designs as in vacuum towers, it may well require checking by the more detailed method of Dauphine [13].

A. Bolles' Design Method [5]:

Solve for the combined riser, reversal, annulus, and slot pressure drop by:

$$h_{pc} = K_c \left(\frac{\rho_v}{\rho_L - \rho_v} \right) \left(\frac{V}{A_r} \right)^2 \quad (8-231)$$

The constant, K_c , is obtained from Figure 8-114, noting that the annular area between riser and cap must always be larger than the riser area for K_c to be valid.

where h_{pc} = cap assembly pressure drop, including drop through riser, reversal, annulus, slots, in. liquid

A_r = total riser area per tray, ft²

K_c = constant for Bolles bubble cap pressure drop equation, Figure 8-114

B. Modified Dauphine Relations [5, 11]:

1. Riser pressure drop

(1) Reversal Area Greater than Riser Area

$$h_r = 0.111 \frac{d_r}{\rho_L} \left[(\rho_v)^{1/2} \left(\frac{V}{A_r} \right) \right]^{2.09} \quad (8-232)$$

(2) Reversal Area Less than Riser Area

$$h_r = 0.099 \frac{d_r}{\rho_L} (a_r/a_r')^{1/2} \left[(\rho_v)^{1/2} \left(\frac{V}{A_r} \right) \right]^{2.1} \quad (8-233)$$

2. Reversal and annulus pressure drop

The reversal area is the area of the cylindrical vertical plane between the top of the riser and the underside of the bubble cap through which the incoming vapor must pass. The vapor then moves into the annulus area between the inside diameter of the cap and the outside diameter of the riser before entering the slots in the cap.

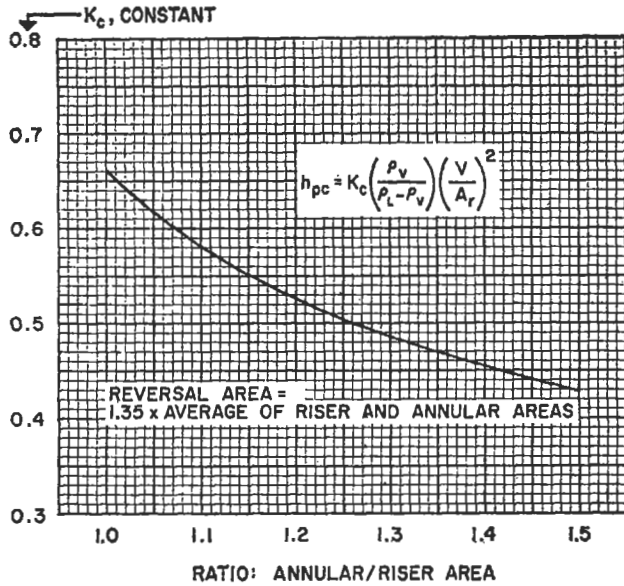


Figure 8-114. Bubble cap pressure drop constant (Bolles' Method). Used by permission, Bolles, W. L., *Pet. Processing*, Feb. thru May (1956).

The pressure drop due to reversal is independent of slot height and riser height as long as riser height is greater than 2 in. and the cap slot height does not exceed the riser height [13]. When riser height is less than 2 in., the reversal pressure drop increases as long as the slot height is less than the riser height.

For riser height greater than 2.5 in.:

$$h_{ra} = \frac{0.68}{\rho_L} \left[\left(\frac{2a_r^2}{a_x a_c} \right) (\rho_v)^{1/2} \left(\frac{V}{A_r} \right) \right]^{1.71} \quad (8-234)$$

3. Dry cap pressure drop: rectangular slots.

The slot pressure drop through the dry cap increases nearly linearly with cap diameter.

$$h'_s = \frac{0.163}{\rho_L} \left[(d_c \rho_v)^{1/2} \left(\frac{V}{A_r} \right) \right]^{1.73} \quad (8-235)$$

4. Total dry cap pressure drop

$$h'_c = h_r + h_{ra} + h'_s \quad (8-236)$$

5. Wet cap pressure drop

$$h_c = h'_c / C_w \quad (8-237)$$

The correction factor, C_w , is obtained from Figure 8-115. Figure 8-115 applies to cap slots 1 in. through 2 in., and if slots are smaller (around 1/2 in.) the C_w factor increases about 25% average (10-50%). The relation applies only to the pressure drop attributable to the conditions of liquid on the tray up to the top of the slots.

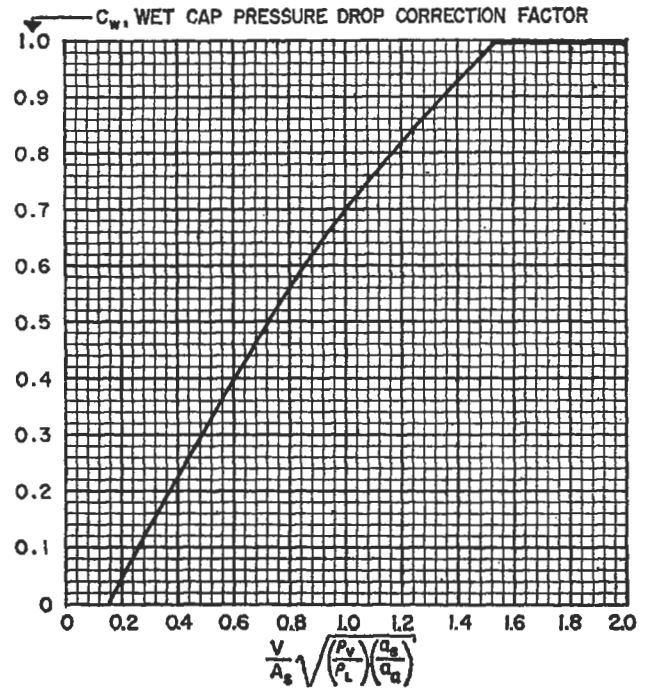


Figure 8-115. Correction for wet pressure drop, C_w , (after Dauphine); used by permission, Bolles, W. L., *Pet. Processing*, Feb. thru May (1956), using data of Dauphine [13].

6. Total bubble cap pressure drop

$$h_c = h_{pc} + h_s \quad (8-238)$$

h_s from Equation 8-225 and Figure 8-106

Total Pressure Drop Through Tray

A. Bolles' Method

$$h_t = (h_{pc} + h_s) + h_{ss} + h_{ow} + \Delta/2 \quad (8-239)$$

B. Dauphine Method

$$h_t = h_c + h_{ss} + h_{ow} + \Delta/2 \quad (8-240)$$

Downcomer Pressure Drop

The head loss in liquid flowing down the downcomer, under its underflow edge (and up over an inlet weir, if used) and onto the tray is important in determining the back up of liquid in the downcomer. There are many suggested relations representing this head loss.

A. Segmental Type Downcomer

1. Downcomer friction loss plus underflow loss

$$h_{du} = 0.56 \left[\frac{L_g}{449 (A_d)} \right]^2 \quad (8-241)$$

or, (alternate)

$$h_{du} = 0.03 \left[\frac{L_g}{100 (A_d)} \right]^2, \text{ in. liquid} \quad (8-242)$$

2. Loss through inlet weir

When an inlet weir is used, the additional resistance to flow may be approximated by:

$$h'_d = 0.3 v_{du}^2 \quad (8-243)$$

B. Circular or Pipe-Type Downcomer

These downcomers are suggested only where liquid flow is relatively small for the required tower diameter, allowing a maximum of space for bubble caps.

$$h_{dc} = 0.06 (L_g/a_d)^2 \quad (8-244)$$

Liquid Height in Downcomer

The backup of clear liquid during flowing conditions must be determined in order to set the proper tray spacing. Tray spacing is usually set at twice the liquid height in the downcomer. This can be adjusted to suit the particular system conditions.

$$H_d = h_w + h_{ow} + \Delta + h_d + h_t \quad (8-245)$$

Downcomer Seal

The importance of the downcomer seal is to prevent vapor from the tray from bubbling into the downcomer (see Figure 8-63), whether the trays are bubble cap, valve or sieve types. If a seal weir is not included in the tray design, then operation problems to avoid flooding, weeping and unstable performance, including pressure drop, are increased, particularly during the start-up phase.

The major factors governing the proper *design for clearance* under the downcomer (see Figure 8-63), and the distance between the bottom of the downcomer and the tray it is emptying onto are [190]: (a) downcomer sealing, (b) downcomer pressure drop, and (c) fouling and/or corrosive nature of the fluids. The smaller the clearance, the more stable will be the tray start-up due to the greater restriction to vapor flow into and up the empty liquid downcomer.

Referring to Figure 8-63, the weir height, h_w , must always be greater than the clearance under the downcomer, i.e., between bottom of downcomer and tray floor, h_{dc1} . Always avoid too low clearance as this can cause flooding of liquid in the downcomer. There are flow conditions

where this condition may not be valid, therefore, the tray flow range from start-up to overload should be examined by the designer before finalizing the physical details.

Some authors recommend clearance of $\frac{1}{4}$ in. to $\frac{1}{2}$ in. less than the tray weir height, but always greater than $\frac{1}{8}$ in. [190].

The bottom of the downcomer must be sealed below the operating liquid level on the tray. Due to tolerance in fabrication and tray level, it is customary to set the downcomer seal referenced to the weir height on the outlet side of the tray. Recommended seals, based on no inlet weir adjacent to the downcomer, and referenced as mentioned are given in Table 8-19.

For trays with inlet weirs, seal values may be reduced if necessary for high flow conditions. A good tray design is centered about a 1.5-in. clearance distance between tray floor and bottom of downcomer edge.

Tray Spacing

Adequate tray spacing is important to proper tray operation during normal as well as surging, foaming, and pulsing conditions. Because the downcomer is the area of direct connection to the tray above, the flooding of a tray carries to the tray above. To dampen the response, the tray must be adequately sealed at the downcomer and the spacing between trays must be approximately twice the backup height of liquid in the downcomer. Thus for normal design:

$$S_t \geq 2 H_d$$

where S_t = tray spacing, in.

H_d = height of liquid in downcomer, in.

Once foam or froth in the downcomer backs up to the tray above, it tends to be re-entrained in the overflowing liquid, making it apparently lighter, and accentuating this height of liquid-foam mixture in the downcomer. The downcomer must be adequate to separate and disengage this mixture, allowing clear liquid (fairly free of bubbles) to flow under the downcomer seal.

A tray inlet weir tends to ensure sealing of the downcomer, preventing the bubbling caps from discharging a mixture into the downcomer.

Table 8-19
Downcomer Liquid Seal [15]

Tower Diameter, Ft	Seal, Outlet Weir Height minus Distance Downcomer Off Tray Floor, In.
6 and below	0.5
7-12	1
13 and above	1.5

Used by permission, Davies, J. A., *Pet. Refiner*, V. 29 (1950) p. 121. Gulf Publishing Co., all rights reserved.

The residence time in the downcomers is another criterion of adequate tray spacing.

Residence Time in Downcomers

To provide reasonably adequate time for disengagement of foam and froth from the liquid in the downcomer, the total downcomer volume is checked against a minimum allowable average residence time of 5 seconds.

For various foaming characteristics of the liquid of the system, Kister [190] reports a recommendation of W. L. Bolles based on course lectures at the University of New South Wales and the University of Sydney as follows:

Foaming Tendency	Example	Residence Time, Seconds
Low	Low MW hydrocarbons, and alcohols	3
Medium	Medium MW hydrocarbons	4
High	Mineral oil absorbers	5
Very High	Amines, glycols	7

Table 8-20 gives suggested downcomer clear liquid velocities based on relative foaming characteristics of the fluid on the tray at tray conditions.

Liquid Entrainment from Bubble Cap Trays

The work of Simkin, Strand, and Olney [64] correlates most of the work of other investigators, and can be used for estimation of probable entrainment from bubble cap trays as shown in Figure 8-116. It is recommended that the liquid entrainment for design be limited to 0.10 mols/mol dry vapor.

Eduljee's [19] correlation of literature data appears to offer a route to evaluating the effect of entrainment on tray spacing and efficiency. It is suggested as another check on other methods. Figure 8-117 may be used as recommended:

Table 8-20
Suggested Downcomer Velocities

Approximate Tray Spacing, In.	System Foaming Characteristics		
	Allowable Clear Liquid Velocities, ft/sec		
	High	Medium	Low
18	0.15-0.2	0.35-0.42	0.45-0.52
24	0.25-0.32	0.48-0.52	0.55-0.60
30	0.30-0.35	0.48-0.52	0.65-0.70
Typical Representative System	Amine, Glycerine	Oil systems	Gasoline, Light Hydrocarbons

Used by permission, *Pet. Processing*, Bolles, W. L., Feb. thru May (1956).

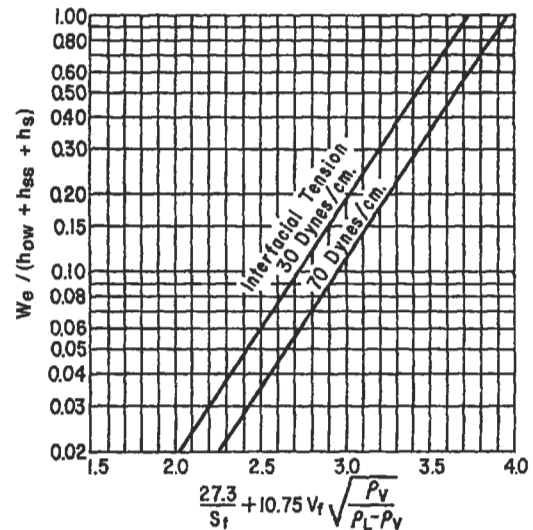


Figure 8-116. Correlation of entrainment for bubble caps. Used by permission, Bolles, W. L., *Pet. Processing*, Feb. thru May (1956), using data of Simkin et al. [64].

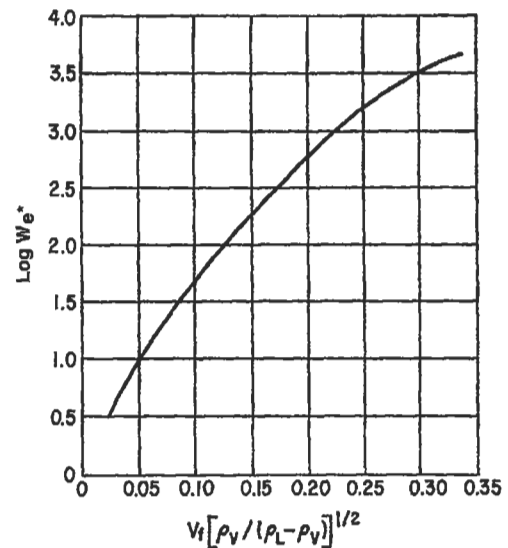


Figure 8-117. Eduljee's entrainment correlation for bubble caps. Used by permission, Eduljee, H. E., *British Chemical Engineer*, Sept. (1958).

1. Assume or establish a level of acceptable entrainment, such as 10 mols liquid/100 mols vapor.
2. Determine effect on efficiency by Colburn's relation (see Efficiency section).
3. Calculate total entrainment as pounds of liquid per hour, based on total vapor flow in tower.
4. Determine area of tray above caps (equals tower area minus area of two downcomers for cross-flow tower).

5. Calculate liquid entrainment, W'_e , as pounds of liquid per square foot of net tray area, equals (Step 3)/(Step 4), lbs/hr (ft²)
6. Calculate vapor velocity, v_f , based on area of (Step 4), ft/sec
7. Calculate density factor, $[\rho_v/\rho_L - \rho_v]^{1/2}$
8. Calculate $v_f [\rho_v/(\rho_L - \rho_v)]^{1/2}$
9. From Figure 8-117, read $\text{Log } W_e^*$
10. Calculate S'' from

$$\text{Log } W_e^* = \text{Log } W'_e + 2.59 \text{Log } S'' + \text{Log } \mu + 0.4 \text{Log } \sigma$$
11. Assume a foam height, h_f , of approximately twice the height of the dynamic tray seal, in. This agrees with several investigators for *medium* foaming systems.
12. Minimum tray spacing $S_t = h_f + S'$, in.

where v_f = vapor velocity based on free area above caps (not including two downcomers), ft/sec

W_e^* = entrainment corrected for liquid properties and plate spacing

W_e = liquid entrainment mass velocity, lbs entrainment per minute per/ft², based on *net* tray area.

S' = effective tray spacing, distance between top of foam, froth, or bubbles, and tray above, in.

S'' = clear height above foam or froth (equals tray spacing minus foam height above tray floor), ft

μ = viscosity of liquid, centipoise

σ = surface tension of liquid, dynes/cm

W_e' = entrainment (based on assumed allowance) lbs liquid/(ft² free plate area) (hr)

h_f = height of top of foam above tray floor, in.

Free Height in Downcomer

$$F = S_t + h_w - H_d \quad (8-246)$$

Slot Seal

The static slot seal is the fixed distance between the top of the outlet weir and top of the bubble cap slots.

The actual operating or dynamic slot seal is more indicative of conditions pertaining to the tray in operation and is [5]:

$$h_{ds} = h_{ss} + h_{ow} + \Delta/2 \quad (8-247)$$

Note that this seal varies across the tray, although the tray design must be such as to make the value of h_{ds} nearly the same for each row of caps.

In order to ensure good efficiencies and yet a definite seal consistent with allowable pressure drops, suggested values for h_{ds} are modified from the references and shown in Table 8-18.

Bolles [5] recommends dynamic slot seals on bubble caps to check against calculated values. See Table 8-18.

Inlet Weir

The inlet weir, see Figure 8-92, for any tray, i.e., bubble cap, valve or sieve, is important in ensuring a seal on the inlet downcomer as well as maintaining a more uniform liquid level across the flowing tray. The recessed seal pan, Figure 8-63, provides the same benefits plus it reduces sieve tray leakage on the inlet side of the tray due to lower immediate liquid head increase usually occurring at the tray weir. It is necessary to drill weep holes for drainage of the tray at shut-down in the blocked-off inlet weir area, but limit the number and size of holes to avoid excessive weep-drainage during tray operation.

Bottom Tray Seal Pan

This seal acts like a typical downcomer seal from the tray above, and should be dimensioned approximately the same, except:

1. To avoid liquid backup in the downcomer, provide a downcomer height that is about 1.5 times the selected tray spacing in the column.
2. To ensure non-surfing liquid flow under the downcomer, use a clearance, h_{dc1} , of at least 3 times the design for the other trays, or a minimum of 2 in. to 4 in.
3. Enlarge the clearance between the downcomer face and the inlet weir (or equivalent), (see Figure 8-92 or 63) to 1.5 to 2 times the dimensions used for the other trays.
4. Provide drainage holes in seal pan to allow adequate drainage, flushing and cleaning, but not too large (number) to prevent liquid backup sufficient to maintain a seal on the tray.

Throw Over Outlet Segmental Weir

To ensure unobstructed vapor passage above the froth and liquid in the downcomer from a tray, the liquid mixture must not throw against the shell wall. The distance of throw over the weir is given by Reference 5. See Figure 8-63.

$$t_w = 0.8 [h_{ow} (F)]^{1/2}, \text{ in.} \quad (8-248)$$

$$h_f' = S_t + h_w - H_d, \text{ in.} \quad (8-249)$$

For center downcomers as in a two-pass design, the throw must be conservatively less than a distance that would cause the opposing streams entering the same downcomer to interfere with each other. Sometimes the installation of a splash baffle will help avoid conditions leading to flooding and loss of tray efficiency.

Vapor Distribution

The vapor distribution approximation

$$R_v = \Delta/h_c$$

is an indication of the uniformity of vapor flow through the caps on the inlet side of the tray to those on the outlet side and the tendency of inlet caps to stop bubbling. Davies [14, 15] recommends values for the ratio of 0.4, not to exceed 0.6; Bolles recommends 0.5. Only at values around 0.1 is essentially uniform vapor flow maintained through all the caps. As the R_v ratio increases, a smaller percentage of the vapor flows through the inlet tray caps and a larger percentage is shifted to the outlet caps. This cross-flow of vapor increases the effect of Δ on the tray and accentuates the problem. Unfortunately it is often overlooked in many tray examinations. When the ratio reaches the value equal to the cap drop at full slot capacity (usually 1.75 to 2.5 in.) liquid will flow or dump back down the risers at the inlet row of caps. This is definitely improper tray operation, providing markedly reduced tray efficiencies.

For stepped caps (tray level, risers of different heights) or cascade tray (tray consisting of two or more levels) care must be taken to analyze all the conditions associated with level changes on the tray. Reference 5 discusses this in some detail.

Bubble Cap Tray Design and Evaluation

Example 8-36: Bubble Cap Tray Design

Check the trays for a finishing tower operating under vacuum of 75 mm Hg at the top. The estimated pressure drop for the twenty trays should not exceed 50–60 mm Hg. Fifteen trays are in the rectifying section, five in the stripping section.

Following the suggested form, and starting with the standard tray design existing in the unit, the calculations will be made to check this tray, making modifications if necessary. The 6-ft 0-in. diameter tower was designed originally for a significantly different load, but is to be considered for the new service. The tray features are outlined in Table 8-16. It becomes obvious that the tray is too large for the requirements, but should perform reasonably well. The weakest point in performance is the low slot velocity.

Tray Design*

Tower application or service: *Product Finishing*

Tower Inside Diameter: 6 ft, 0 in.

Tray Type: *Cross Flow*

Tray Spacing, 24 in.; Type outlet weir: *End*
Note: Tray spacing was set when the 6-ft, 0-in. diameter was determined.

No. downcomers/tray 1; Located: *End*

Cap Data:

- (1) Cap I.D., ID, $3\frac{3}{8}$ in., Spacing: $5\frac{1}{2}$ in. Δ 60° centers
- (2) Total height, $3\frac{15}{16}$ in.
- (3) No./tray, N_c , 129
- (4) Slots: No., N_s , 50
- (5) Height, H_s , $1\frac{1}{2}$ in.
- (6) Width, w_s , $\frac{1}{8}$ in.
- (7) Skirt Height, s , $\frac{1}{4}$ in.
- (8) Shroud Ring height, h_{sr} , $\frac{1}{4}$ in.
- (9) Height of inside surface of cap above tray, 3.94 in.
- (10) Riser I.D., 2.68 in.
- (11) Riser height above tray floor, 3 in.

Areas:

- (12) Riser inside cross-sectional, a_r , 5.43 in.² per riser
- (13) Total riser inside cross-sect. area/tray, A_r , 4.95 ft²
- (14) Riser outside cross-sectional area a_{ro} , 5.94 in² per riser. Riser is $2\frac{3}{4}$ -in O.D.; $\pi(2.75)^2/4 = 5.94$
- (15) Cap inside cross-sectional area a_c , 11.79 in² per cap. Cap is $3\frac{3}{8}$ -in. I.D.; $\pi(3\frac{3}{8})^2/4 = 11.79$
- (16) Total cap inside cross-sectional area, A_c , 10.53 ft²
- (17) Annular area per cap, a_a , in.², $(11.79 - 5.94) = 5.85$
- (18) Total annular area per tray, A_a , 5.24 ft²
- (19) Reversal area per cap, a_r' , in.² = $\pi(2.69)(3.94 - 3.0) = 7.95$. $d = (2.75 + 2.63)/2 = 2.69$ in.
- (20) Total reversal area, per tray, A_r' , ft² $(129/144)(7.95) = 7.12$
- (21) Slot area per cap, a_s , (50) ($\frac{1}{8}$) (1.5) = 9.39 in.²
- (22) Total slot area per tray, A_s , 8.40 ft²

Tray Details

- (23) Length of outlet overflow weir, l_w , 4.0 ft
- (24) Height of weir (weir setting) above tray floor, h_w , 2.5 in.
- (25) Inlet weir (downcomer side) length (if used), 4.0 ft
- (26) Inlet weir height above tray floor, 3 in.
- (27) Height of top of cap slots above tray floor, 2 in.
- (28) Static slot submergence or static slot seal (2.5–2.0), h_{ss} , 0.5 in.
- (29) Height of bottom of downcomer above tray floor, $2\frac{3}{4}$ in.
- (30) Downcomer flow areas: (a) Between downcomer and tower shell, 0.886 ft²
- (31) (b) Between bottom downcomer and tray floor, 0.710 ft²
- (32) (c) Between downcomer and inlet weir, 0.740 ft²
- (33) Riser slot seal, (3.0 – 2), 1.0 in.

*Adapted by permission from Ref. 15, modified to suit recommendations offered in this presentation.

Tray Operations Summary and

Pressure Drop	Top	Bottom			
A. Tray number	20	1	Read $F_w = 1.018$ from Figure 8-105		
B. Operating pressure, mm. Hg	75	100	$h_{ow} = 0.092 (1.018) (3.74/4)^{2/3}$	0.0989	0.0989
C. Operating temperature, °F	60	100	Use $\frac{1}{4}$ in.-V-notched weir, 2.5 in. from tray floor to bottom of notch. This is necessary because of low liquid flow.		
D. Vapor flow, lbs/hr	6,565	6,565	b. Static submergence, h_{ss} , in.	0.5	0.5
E. Vapor volume, ft^3/sec @ operating conditions, V	132.2	105	c. Caps		
F. Vapor density, lbs/ft^3 operating conditions	0.0138	0.01735	Modified Dauphine and Cicalese, [11, 13] dry cap basis.		
G. Liquid flow, gallons/minute, L_g	3.74	3.74	1. Riser pressure drop, reversal area greater than riser area.		
H. Liquid flow, $\text{lbs}/\text{hr.}$, L'	1,515	1,515			
I. Liquid flow, ft^3/sec @ operating conditions	0.00834	0.00776	$h_r = 0.111 \left(\frac{2.63}{50.5} \right) \left[(0.0138)^{1/2} \left(\frac{132.2}{4.95} \right) \right]^{2.09}$		
J. Liquid density, lbs/ft^3 @ operating conditions	50.5	54.2	$= 0.06333$	0.0633	0.0462
K. Superficial vapor velocity, based on Tower I.D., ft/sec , $132.2/28.28$	4.67	3.7	2. Reversal and annulus pressure drop		
L. Vapor velocity based on cap area between inlet and outlet weirs, ft/sec $132/[28.28 - 2(2.12)]$	5.49	4.37	Riser height > 2.5 in.		
M. Volume of downcomer: Area top segment, <i>Perry's Hdbk.</i> 3rd Ed. pg. 32. $h/D = 9\frac{5}{16}$ in./72 = 0.1276, $A = 0.05799(6)^2 = 2.08 \text{ ft}^2$	4.04	4.04	$h_{ra} = \frac{0.68}{50.5} \left[\frac{2(5.43)^2}{(7.95)(11.79)} (0.0138)^{1/2} \left(\frac{132.2}{4.95} \right) \right]^{1.71}$		
Lower taper, use h @ % of vert. taper for estimate. $8/72 = 0.111$, $A = 0.04763(6)^2 = 1.71 \text{ ft}^2$ Volume = $(2.08)(0.5) + (1.71)(21/12) = 4.04 \text{ ft}^3$			$= 0.045$	0.045	0.0322
N. Liquid residence time in downcomer, seconds, $(4.04)/0.00834 = 485$	485	520	3. Rectangular slot dry pressure drop		
O. Throw over downcomer weir (sideflow), inches	1.17	1.17	$h'_s = \frac{0.163}{50.5} \left[[3.875(0.0138)]^{1/2} \left(\frac{132.2}{8.40} \right) \right]^{1.73}$		
P. Throw over downcomer weir (center flow), min. =	—	—	$= 0.0308$	0.0308	0.0231
Q. Tray layout, actual downcomer width, in.	$9\frac{5}{16}$	$9\frac{5}{16}$	4. Total dry cap pressure drop		
Taper downcomer has 6 in. vertical dimension at $9\frac{5}{16}$ in. wide. Tapers to $5\frac{1}{2}$ in., 24 in. below tray.	$5\frac{1}{2}$	$5\frac{1}{2}$	$h'_c = h_r + h_{ra} + h'_s = 0.0633 + 0.045 + 0.0308 = 0.139$	0.1391	0.1015
R. Slot velocity: minimum $3.4 / (\rho_G)^{1/2}$ ft/sec	29	25.9	5. Wet cap pressure drop		
S. Slot velocity: maximum = $12.1 / (\rho_G)^{1/2} = 12.1 / (0.0138)^{1/2}$ and $12.1 / (0.01735)^{1/2}$, ft/sec	103.1	92	$\frac{V}{A_s} \left[\frac{\rho_v}{\rho_L} \left(\frac{a_s}{a_a} \right) \right]^{1/2}$		
T. Slot velocity: Superficial, $u_o = V/A_s = 132.2/8.40$ and $105/8.4$ ft/sec	15.7	12.5	$= \frac{132.2}{8.40} \left[\frac{0.0138}{50.5} \left(\frac{9.39}{5.85} \right) \right]^{1/2} = 0.33$		
Pressure Drop, Inches Liquid on Tray	Top	Bottom	From Figure 8-115, $C_w = 0.16$		
a. Height of liquid over weir (straight weir) $L_g/(l_w)^{2.5} = 3.74/(48/12)^{2.5} = 0.1168$			$h_c = h'_c/C_w = 0.1391/0.16 = 0.87$	0.87	0.847
$l_w/D = 4/6 = 0.667$			6. Check maximum pressure drop through wet caps:		
			$h_c \text{ max.} = 0.0633 + 0.045 + (1.5 + 0.25)$, in.	1.8	1.3
			Since h_c is less than $h_c \text{ max.}$, cap is O.K. and not blowing under shroud ring		
			Bolles' recommendation		
			7. Riser, reversal, annulus pressure drop		
			$a_a/a_r = 5.85/5.43 = 1.075$		
			From Figure 8-114, $K_c = 0.598$		

$$h_{pc} = 0.598 \left(\frac{0.0138}{50.5 - 0.0138} \right) \left(\frac{132.2}{4.95} \right)^2 = 0.118 \quad 0.0861$$

$$h_{du} = 0.56 \left(\frac{3.74}{449 (0.710)} \right)^2$$

8. Slot pressure drop, Rectangular slots

$$h_s = 32 \left(\frac{0.0138}{50.5 - 0.0138} \right)^{1/3} \left(\frac{132.2}{129 (50) \left(\frac{1}{8} \right)} \right)^{2/3} = 0.626 \quad 0.626 \quad 0.566$$

d. Liquid Gradient

Mean tray width = $(4 + 6)/2 = 5$ ft
 GPM/ft mean tray width = $3.74/5 = 0.75$
 Assumed mean liquid depth, $h_1 = 2.5 + 0.0989 + 0.1$

Uncorrected Δ' /row caps = approx. 0.02 in.

$$v_o (\rho_v)^{1/2} = 4.67 (0.0138)^{1/2} = 0.548$$

C_v , from Figure 8-113 = estimated 0.55 (off chart)

No. cap rows = 11

$$\text{Corrected } \Delta = (0.02) (0.548) (11) = 0.1206 \text{ inches} \quad 0.12 \quad 0.12$$

$$\Delta/2, \text{ inches (essentially negligible in this case)} \quad 0.06 \quad 0.06$$

e. Total pressure drop per tray, in. liquid

1. Modified Dauphine

$$h_t = h_c + h_{ss} + h_{ow} + \Delta/2 = 0.87 + 0.5 + 0.0989 + 0.06 = 1.528 \quad 1.505$$

2. Bolles

$$h_t = h_{pc} + h_s + h_{ss} + h_{ow} + \Delta/2 = 0.118 + 0.626 + 0.5 + 0.0989 + 0.06 = 1.502 \quad 1.310$$

f. Pressure drop for 15 trays in rectifying section

1. Modified Dauphine, 15 (1.528) = 22.9 in. liquid = 34.2 mm Hg 34.2 mm

2. Bolles, 15 (1.502) = 22.4 inches liquid = 33.4 mm Hg 33.4 mm

Pressure drop for 5 trays in stripping section

1. Modified Dauphine, 5 (1.505) = 7.52 in. liquid = 11.1 mm

2. Bolles, 5 (1.42) = 6.56 in. liquid = 9.7 mm

Total pressure drop for 20 trays
 1. Modified Dauphine 45.3 mm
 2. Bolles 43.1 mm

g. Height liquid in downcomer

1. Segmental, underflow plus friction 0.000077 \quad 0.000077

2. Segmental, upflow when inlet weir used Neg. \quad Neg.

$$h_d' = 0.3 v_{du}^2$$

3. Total segmental loss, h_d 0.000077 \quad 0.000077

4. Circular downspout

5. Liquid height in downcomer
 $H_d = h_w + h_{ow} + h_d + h_t + \Delta = 2.5 + 0.0989 + 0.000077 + 1.638 + 0.35 = 4.58 \quad 4.56$

6. Free height in downcomer
 $F = S_t + h_w - H_d = 24 + 2.5 - 4.58 = 21.69 \quad 21.71$

7. Throw over weir
 $t_w = 0.8 [h_{ow} (F)]^{1/2} = 0.8 [0.0989 (21.69)]^{1/2} = 1.17 \quad 1.17$

h. Vapor distribution ratio
 $R_v = \Delta/h_c = 0.12/0.87 = 0.138 \quad 0.141$

i. Slot seal
 Dynamic, $h_{ds} = h_{ss} + h_{ow} + \Delta/2 = 0.5 + 0.0989 + 0.06 = 0.65 \quad 0.65$

Liquid Velocity in Downcomer

Minimum cross-section area of downcomer = 0.886 ft²

Liquid rate = 0.00834 ft³/sec

Velocity = 0.00834/0.886 = 0.00942 ft/sec

This is very low and confirms that there should be ample disengaging capacity in the downcomers. The downcomers are too large for good design.

Slot Velocity

The results of lines R, S, and T indicate that the vapor velocity through the cap slots is lower than desirable for good bubbling.

Slot Opening

The slot opening, h_s , given in line c8 is only slightly lower than the normal design of 50–60% of H_s , or 0.75 in. to 0.90 in.

Vapor Distribution Ratio

The values of line (h) are quite in line with good vapor flow through all the caps. This is as would be expected,

since the hydraulic gradient is low; too low to require any compensation.

Liquid Entrainment

$$v_f = 132.2 / [28.28 - 2(2.12)] = 5.5 \text{ ft/sec}$$

$$\frac{27.3}{s_t} + 10.75 v_f \left(\frac{\rho_v}{\rho_L - \rho_v} \right)^{1/2}$$

$$= \frac{27.3}{24} + 10.75 (5.5) \left(\frac{0.0138}{50.5 - 0.0138} \right)^{1/2}$$

$$= 1.13 + 0.978 = 2.108$$

Reading Figure 8-116

For 27 dynes/cm surface tension

$$W_e / h_{ow} + h_{ss} + h_s = 0.026$$

$$W_e = (0.026)(0.098 + 0.5 + 0.626) = 0.0317 \text{ lbs/min ft}^2$$

$$\text{Entrainment} = (0.0317) [28.28 - 2(2.12)] = 0.764 \text{ lbs/min}$$

$$\text{Entrainment ratio} = 0.764 / (6565/60) = .00698$$

This value of entrainment is negligible. For a new column design, this would indicate that the tower was too large, and a smaller shell should be considered.

Conclusion

This is not a good tray design, but it should operate. However, a reduced efficiency is to be expected due to low vapor velocities.

Because the liquid flow is low also, 1/4-in. v-notched weirs should be used to ensure uniform flow and level across the tray. The bottom of the notches should be 2.5 in. above the tray floor.

Sieve Trays with Downcomers

The performance analysis of these trays is quite similar to bubble caps, but more so to valve trays, because the tray has the same basic mechanical features. The difference being that bubble caps and valves are replaced by perforations or holes in the tray for entrance of the gas to the liquid on the tray. Figures 8-67A and 8-118 and 119 represent the general construction of a sieve tray.

Sieve trays have been used in both clean and fouling service, including solutions of suspended particles. The bubbling action seems to wash the solids down from tray to tray provided there are no corners or "dead" spots on the tray. Sieve trays are preferably selected for applications which can be operated at from 50–100% of capacity without too sudden a surge from one rate to another significantly different. When operating within the design range, the efficiency of these trays for many systems is better than

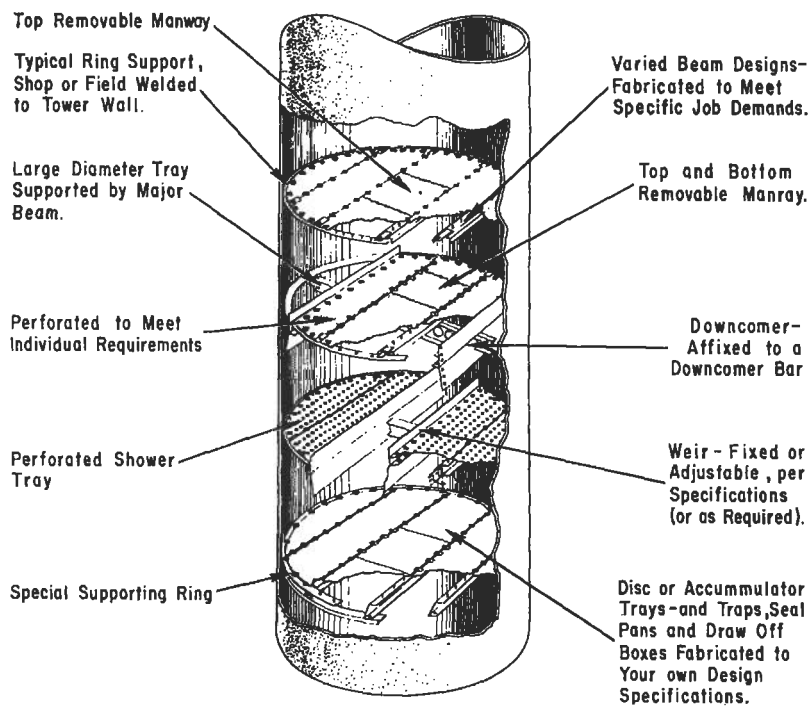


Figure 8-118. Sieve tray with downcomers, tower assembly. Used by permission, Hendrick Mfg. Co.

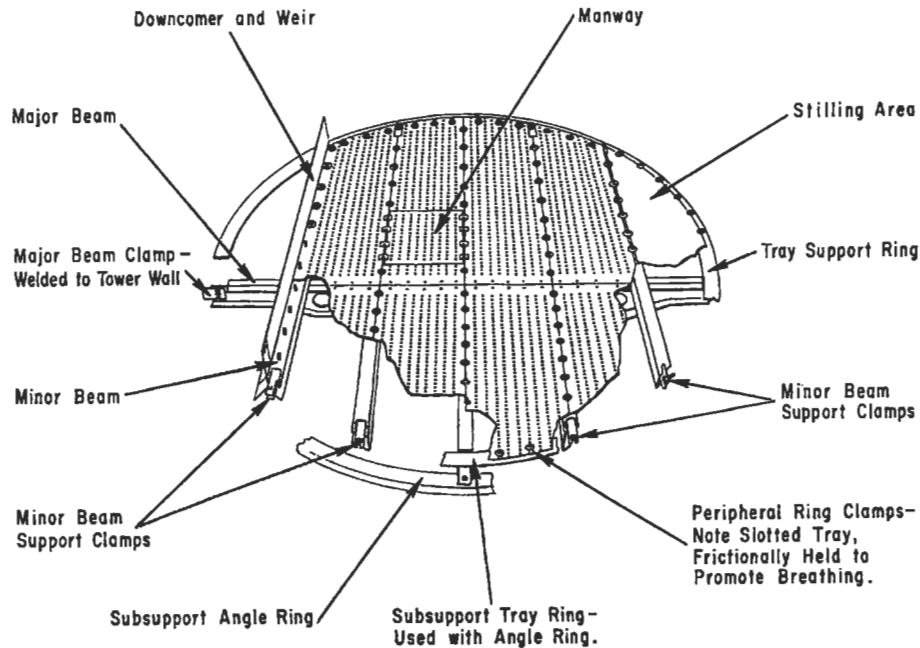


Figure 8-119. Sieve tray with downcomers, tray components. Used by permission, Hendrick Mfg. Co.

for bubble cap trays, although without specific test data it is still impossible to safely take advantage of this feature of performance.

In some sieves the capacity is 1.5 to as much as 3 times that of a bubble cap tray provided careful consideration has been given to all design features.

The "type tray" guide proposed by Huang and Hodson [30] serves to identify the major breaks in type of tray design (Figure 8-120). In the region between types, the selection is not sharp and the design should be evaluated based on other criteria.

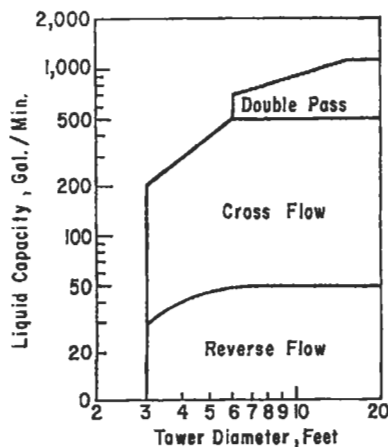


Figure 8-120. Selection guide, perforated trays with downcomers. Used by permission, Chen-Jung and Hodson, J. R. *Petroleum Refiner*, V. 37 (1958) p. 104, Gulf Publishing Co., all rights reserved.

Various aspects of sieve tray performance have been studied [30, 31, 33, 36, 41, 42, 45, 71, 78] and several design methods have been recommended [30, 31, 41, 42, 189, 197]. The following composite method has given good performance in operating towers, and is based on satisfying the three critical capacity features, i.e., entrainment, flooding, and weeping.

The action on this type of tray seems to produce fewer jets of liquid froth than a bubble cap tray. The entrainment from the surface of the bubbling liquid-froth mixture is less (about $\frac{1}{2}$) than a bubble cap tray for the same superficial tower velocity and tray spacing. Generally the trays will flood before capacity reaches a limitation set by entrainment.

The proprietary "Linde Tray," Figure 8-67C, is a proven tray design used for new installations [198], and also often for improving the performance of existing distillation columns by replacing the older and possibly less efficient trays. One of the advantages of this type tray is its capability of being installed at tray spacings as low as 9 to 10 in. and frequently at 12 in. The tray efficiency varies with the distillation system, but as a general guide, will be equal to that of a multipass tray.

A definition of terms, some more related to sieve trays than other types, are provided by Chase [192] (used by permission, *Chem. Eng.*, July 31, 1967):

Cross flow: Liquid flowing across a plate (rather than straight down through the holes) so that it falls to the plate below through a channel at one side of the plate.

Liquid throw: The horizontal distance traveled by the liquid after flowing over a weir.

Dual flow: Both liquid and vapor pass through the perforations on the tray; there are no downcomers.

Radial flow: Liquid flowing radially from, or to, an inlet (or outlet) located at the center of the tray, to (or from) downcomers (or inlets) at the tray periphery.

Reverse flow: Liquid flowing from the inlet on one side of the tray (around a center baffle) reverses its direction at the other side of the tray, and flows back to the downcomer on the same side of the tray where the inlet is.

Split flow: Liquid flow across the tray is split into two or more flow paths.

Double pass: A split-flow tray with two liquid flowpaths on each tray. Each path handles half of the total liquid flow.

Blowing: A condition where the rising vapor punches holes through the liquid layer on a tray and usually carries large drops and slugs of liquid to the next tray.

Coning: A condition where the rising vapor pushes the liquid back from the top of the hole, and passes upward with poor liquid contact.

Dumping: A condition caused by low vapor rates where all of the liquid falls through some holes (rather than over the weir) to the tray below, and vapor rises through the remaining holes.

Raining: A condition similar to dumping (no liquid goes over the weir) except that, because of higher vapor rates, the liquid fall through the holes is more uniform.

Weeping: A condition occurring when the vapor rate is not large enough to hold all the liquid on the tray, so that part of the liquid flows over the outlet weir while the rest falls through the holes.

Flooding: A condition that gives rise to a sharp decline in tray efficiency and a sharp increase in pressure drop. Flooding is commonly due to either an excessive carryover of liquid to the next tray, or to an inability of the system to convey the liquid flow to the tray below.

Oscillation: A wave-type motion of the liquid on the tray, perpendicular to the normal direction of flow.

Seal point: The point at which a weeping condition changes to raining.

Injection regime: A condition in which the liquid above the plate is in the form of individual drops dispersed in the vapor; thus, there is virtually no mixing in the main bulk of the liquid.

Stable regime: The preferable hydrodynamic condition of the aerated liquid on a sieve tray. The aerated material exists as a stable froth; gas-liquid contact is good.

Turndown ratio: A term used by designers to denote ratio of minimum-allowable to operating throughput.

Segmental downcomer: The channel for liquid flow formed by an enclosed segmental tray section.

F factor: The vapor kinetic-energy parameter, often used as a correlating term for flooding velocity, foam density, etc.

Souder and Brown equation: $G/A = K[d_v (d_L - d_v)]^{1/2}$, where G/A = superficial vapor flow, lb/(hr) (ft²), and d_v and d_L = vapor and liquid densities, lb/ft³. See Equation 8-219.

Tower Diameter

The tower diameter may be calculated for first approximation by the Souders-Brown method; however, this has been found to be conservative, since it is based on no liquid entrainment between trays. Actually, some entrainment can be tolerated at negligible loss in efficiency or capacity.

There are several approaches to column diameter design [65, 74] as well as the proprietary techniques of major industrial and engineering designers. Some of these use the proprietary Fractionation Research Institute methods which are only available on a membership basis and do not appear in the technical literature.

In general, a better first approximation and often a more economical tower diameter is determined using Figure 8-121 [33].

$$e_w = 0.22 \left(\frac{73}{\sigma} \right) \left(\frac{v_c}{S'} \right)^{3.2} \quad (8-250)$$

$$S' = S_t - 2.5 h_c \quad (8-251)$$

where e_w = weight of liquid entrained/unit weight of vapor flowing in sieve tray column

σ = liquid surface tension, dynes/cm

v_c = vapor velocity based on column cross-section, ft/sec

S' = effective tray spacing, distance between top of foam and next plate above, in.

h_c = height of clear liquid in bubbling zone, in.

This is based on a frothed mixture density of 0.4 that of the clear liquid on the tray, and has been found to be a reasonable average for several mixtures.

Entrainment values of 0.05 lbs liquid/lb vapor are usually acceptable, with 0.001 and 0.5 lb/lb being the extremes. The specific design dictates the tolerance on entrainment. From the calculated vapor velocity, v_c , the diameter of the column can be calculated using:

$$D = \left[\frac{4}{\pi} \left(\frac{V}{v_c} \right) \right]^{1/2}, \text{ feet} \quad (8-252)$$

Entrainment does not usually become a problem until the tray is operating at 85–100% of the flooding condition. Figure 8-121 is convenient for solving for e_w .

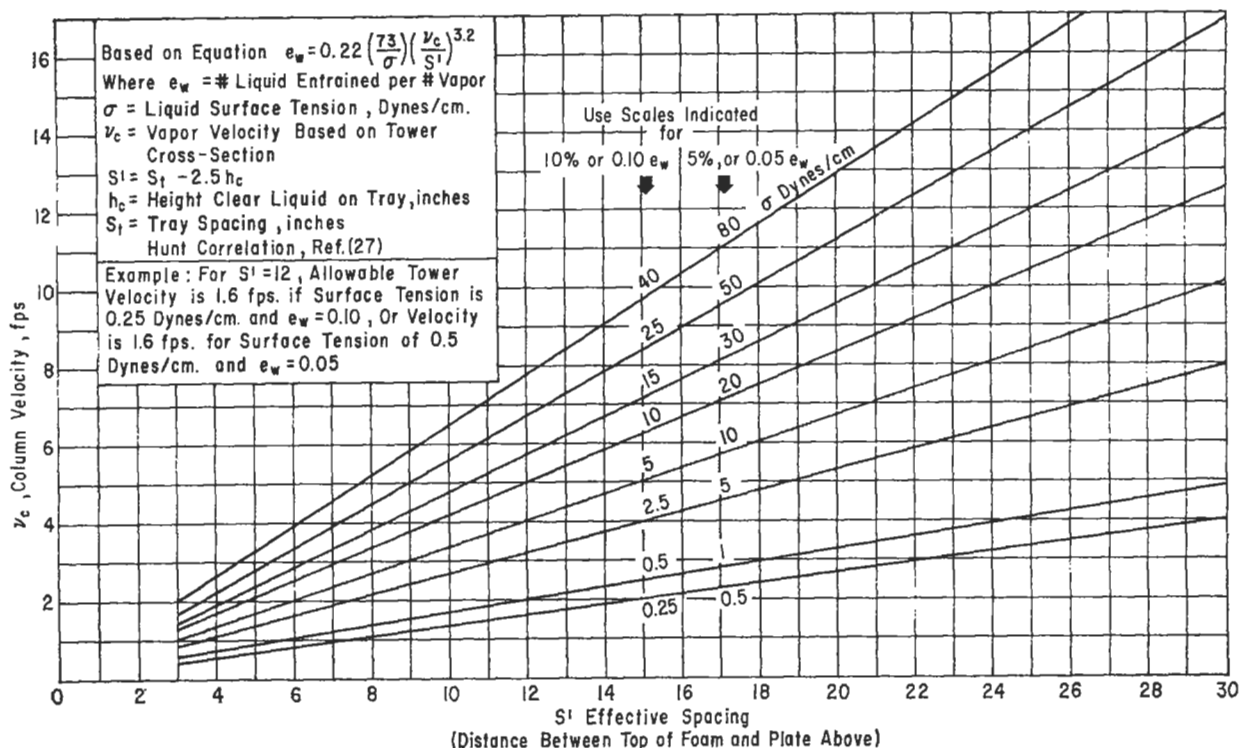


Figure 8-121. Sieve tray entrainment correction. Used by permission, Hunt, C. D'A., Hanson, D. N., and Wilke, C. R., The American Institute of Chemical Engineers, *Chemical Engineers Journal*, V. 1 (1955), p. 441, all rights reserved.

Tray Spacing

Tray spacing can usually be about 6 in. less than for a corresponding bubble tray. Sieve trays are operating on spacings of 9 in. and up to 30 in., the latter being necessary for high vacuum service. Spacing of 12–16 in. is common.

Minimum spacing is the same as recommended for bubble cap trays, i.e., $S_t = 2 H_d$.

Downcomer

Downcomers are designed for the same conditions as bubble tray towers.

Biddulph, Thomas, and Burton [209] studied the effects of downcomer designs, i.e., chordal or segmental, circular downpipe, low liquid flows, sloped downcomer (good for disengaging foam/bubbles, etc.) and envelope type, for use with sieve trays and then developed a modification of the segmental style by installing a downcomer weir on the tray floor inside the weir outlet (see Figures 8-122A and B). This replaces the usual weir, which is placed outside of the outlet of the downcomer. Note that it runs for only about 75% of the chordal length of the downcomer width. The authors state that this still provides a liquid seal all along the inlet, but does provide space at

the ends to exert a positive influence on the tray liquid flow pattern. For the segmental downcomer:

1. Mechanism 1 of Figure 8-122B [209] is dominant when the underflow clearance at a given liquid rate is increased, the underflow velocity decreases and the severity of recirculation decreases.
2. Mechanism 2 of Figure 8-122B becomes apparent when the flow recirculation on the tray increases with increasing underflow clearance. The curvature of the column wall influences the movement of the liquid toward the center. High underflow clearance does not even out maldistribution due to backup where the irregular flow pattern enters into the tray below. This allows flow separation to occur on the downcomer floor, and leads to enhanced retrograde flow.

Biddulph [209] et al. summarize “rules of thumb” that have been expressed elsewhere in the literature for downcomer sizing (used by permission of *Chem. Eng. Prog.* V. 89, No. 12, 1993).

“Rules of thumb that have developed out of many years of industrial experience relating to downcomer sizing include:

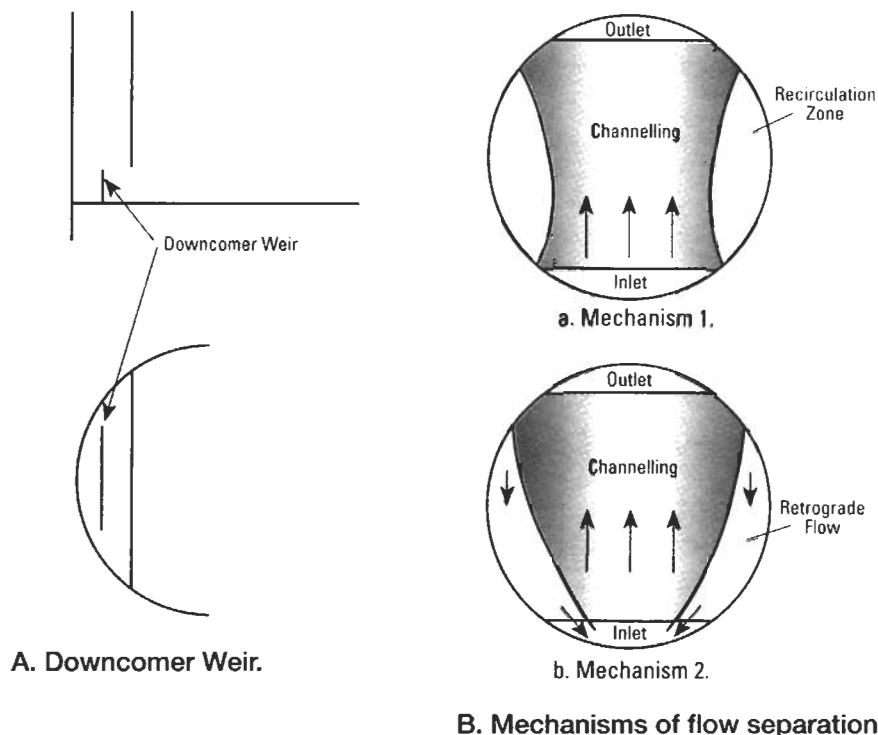


Figure 8-122. Modification of downcomer weir at tray floor outlet; (A) downcomer weir; (B) mechanism of flow separation. Used by permission, Biddulph, M. W. et al. The American Institute of Chemical Engineers, *Chem. Eng. Prog.* V 89. No. 12 (1993), p. 56, all rights reserved.

1. Set the velocity of the unaerated liquid under the downcomer to 1.6 ft/sec (0.5 m/sec).
2. Let the liquid velocity under the downcomer equal the liquid velocity on the tray to give a smooth entry [237].
3. Hold the head loss due to the underflow clearance, h_{udc} , to no more than 1.0–1.5 in. of hot liquid [117].
4. Allow at least 3 sec residence time in the downcomer for disengagement of vapor for a nonfoaming system, and 6 sec for a foaming system [238].”

Figure 8-123 illustrates a typical sieve tray capacity chart. Entrainment by jet flooding or limitation by downcomer flooding are two of the main capacity limiting factors. The liquid backup in the downcomer must balance the pressure drop across the tray, with the process balance [209].

$$\alpha_d h_{fd} = h_{WT} + h_{li} + h_{udc} - h_n \quad (8-253)$$

where h_{fd} = downcomer backup, in.

h_{WT} = wet tray head loss, in.

h_{li} = clear liquid head at the inlet to tray, in.

h_{udc} = head loss due to underflow clearance, in.

h_n = head in the back of downcomer, in. (usually negligible except at high liquid load)

α_d = mean aeration factor of froth, dimensionless (see Figure 8-126)

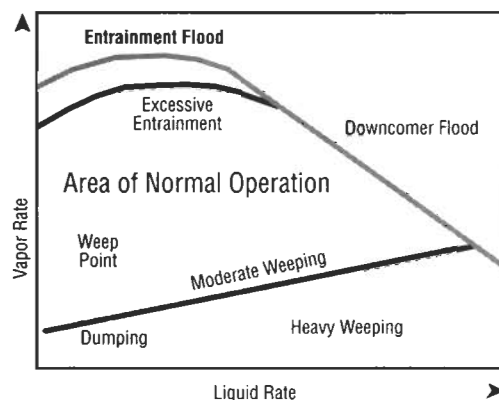


Figure 8-123. Sieve tray capacity chart. Used by permission, Biddulph, M. W., et al. The American Institute of Chemical Engineers, *Chem. Eng. Prog.* V. 89 No. 12 (1993), p. 56, all rights reserved.

Hole Size and Spacing

Most of the literature has presented data for trays with holes of $\frac{1}{8}$ -in. through $\frac{1}{4}$ -in. diameter. The work of Hunt et al. [33] includes $\frac{1}{2}$ -in. holes. Some commercial units have used $\frac{3}{8}$ - and 1-in. holes, although these sizes should be used with caution when adequate data are not available. The recommended hole size for the average clean service is $\frac{3}{16}$ -in. based on present published data. Holes of $\frac{1}{2}$ -in.

may be used for any service including fouling and fluids containing solids with no loss in efficiency. Holes of 1/8-in. dia. are often used in vacuum service.

Holes spaced closer than twice the hole diameter lead to unstable operation. The recommended spacing is 2.5 d_o to 5 d_o with 3.8 d_o being preferable [42]. Holes are usually placed on 60° equilateral triangular pitch with the liquid flowing normally to the rows. Holes should not be greater than 2.5–3 in. apart for effective tray action.

The percentage hole area in a tray varies according to the needs of the design; the usual range is 4–15% of the total tower cross-section. Experience has indicated that this is a questionable basis, and it is clearer to refer areas to the active bubbling section of the tray, provided liquid cannot by-pass this area. Thus, rather arbitrarily, but referenced to test literature, the effective tray action area might be the area enclosed by encircling the perforated hole area a distance 2–3 in. from the periphery holes. On this basis, the hole area would be 6–25% with a usual value range of 7–16% with about 10% being preferred.

Tray Hydraulics

Figure 8-124 illustrates a typical pressure drop diagram for a sieve tray. Note that the figure is for liquid flowing

with gas countercurrent. For dry tray only gas is flowing and no liquid, and the pressure drop is a function of the orifice coefficient. For wet tray pressure drop, gas and liquid are both flowing, and the pressure drop is a function of clear liquid head, head over the weir, and hydraulic gradient, residual pressure drop, foam density and height, aeration and two-phase regime factors, bubbling frequency [192]. The pressure drop associated with the downcomer is a function of liquid backup, foam density and aeration factor, and liquid throw at the outlet weir [192]. See Figure 8-101, which relates similar factors for bubble cap trays, as well as valve trays.

Figure 8-125 [192] presents a typical performance diagram of the operating features of a sieve tray.

Height of Liquid Over Outlet Weir, h_{ow}

This may be calculated as recommended for bubble cap trays. Minimum weir height is 0.5-in., with 1–3 in. preferred. See Figure 8-67A.

Hydraulic Gradient, Δ

Tests have indicated that the hydraulic gradient is negligible or very small for most tray designs. Usual design practice is to omit its effect unless the value of Δ is expected to be greater than 0.75 in. If hydraulic gradient is appreciable, then the holes nearer to the tray inlet (liquid) will tend to weep before those nearer the tray outlet.

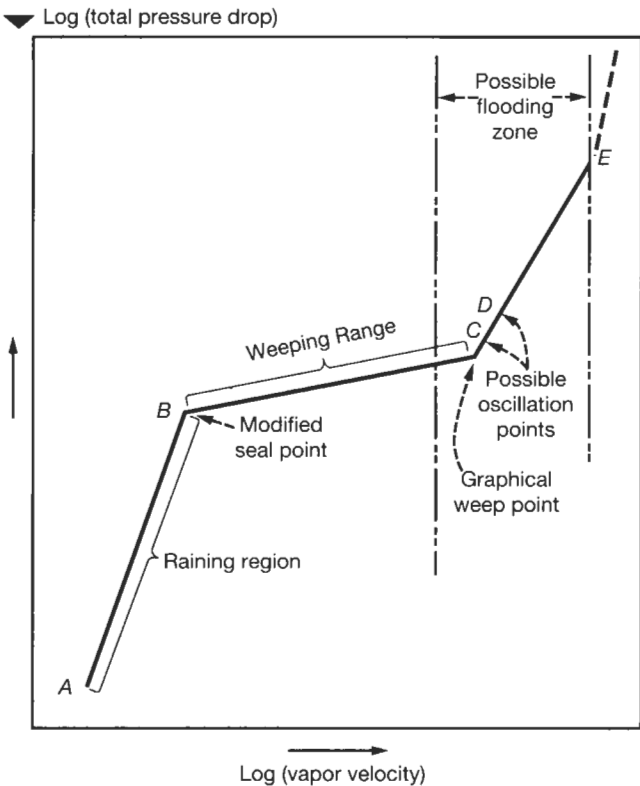


Figure 8-124. Typical operating curve of sieve trays with downcomers. Note modes of operation; used by permission, *Chem. Eng.*, Chase, J. D., July 31 (1969), p. 105. Also see Klein [201], Figure 8-148.

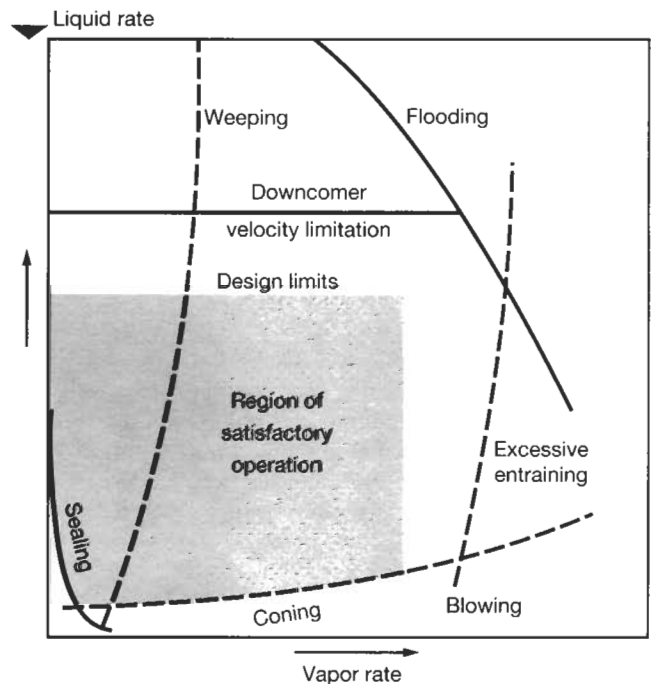


Figure 8-125. Performance diagram of sieve trays (note article reference No. 18); used by permission, Chase, J. D., *Chem. Eng.*, July 31 (1969), p. 105.

This creates the same type of cross-flow and improper distribution as was discussed for bubble cap tray operation. The recommendation of Hughmark and O'Connell [31] includes corrections to the friction factor of Klein [39].

For stable tray operation, the hydraulic gradient should be less than one half the dry tray pressure drop. For conditions of high weir height and high v_o (ρ_v)^{1/2} the greater the friction factor affecting the hydraulic gradient [25]. Also, the greater the liquid flow the higher the pressure drop and gradient.

For the tray liquid to move from inlet to outlet of tray, there must be a liquid flow gradient on the tray in that direction. See Figure 8-67A. The sieve tray usually has less problems with liquid gradient than bubble cap or valve trays, the general guide to avoid gradient problems (good tray stability) is similar to bubble cap design [193]:

$$\text{Hydraulic Gradient, } \Delta = (h_{li} - h_{lo}), < 0.5 h_h \quad (8-254)$$

$$\Delta = \frac{f (v_f)^2 l_w}{12 g R_h}, \text{ in. (f from Figure 8-127)} \quad (8-255)$$

v_f = velocity of froth, cross-flow, ft/sec

Use velocity of aerated mass same as for clear liquid.

R_h = hydraulic radius of the aerated mass for cross-flow, ft

$$R_h = \frac{\text{cross section}}{\text{wetted perimeter}}, \text{ ft} \quad (8-256)$$

$$= \frac{h'_f l_{fw}}{2h'_f + 12 l_{fw}}, \text{ ft} \quad (8-257)$$

where l_{fw} = total flow width across tray, normal to flow, ft. For this equation, use arithmetic average between tower diameter, D , and weir length, l_w

h'_f = height of froth (aerated mass) above tray floor, in., estimated from discussion under "Total Wet Tray Pressure Drop" (see Figure 8-126)

f = friction factor for froth cross-flow

l_w' = length of flow path, ft

g = acceleration of gravity, ft/sec²

h_i = equivalent height of clear liquid on tray, in

h_{lo} = height of clear liquid at overflow weir, in

h_{li} = height of clear liquid on inlet side of tray, in

h_w = height of weir above tray floor, in

h_h = head loss due to vapor flow through perforations, in. liquid

ρ_l = density of clear liquid, lb/ft³

μ_l = viscosity of liquid, lb/ft sec

q = liquid flow rate, ft³/sec

v_f = velocity of froth cross-flow, ft/sec

Figure 8-127 [193] is used to determine friction factor, f .

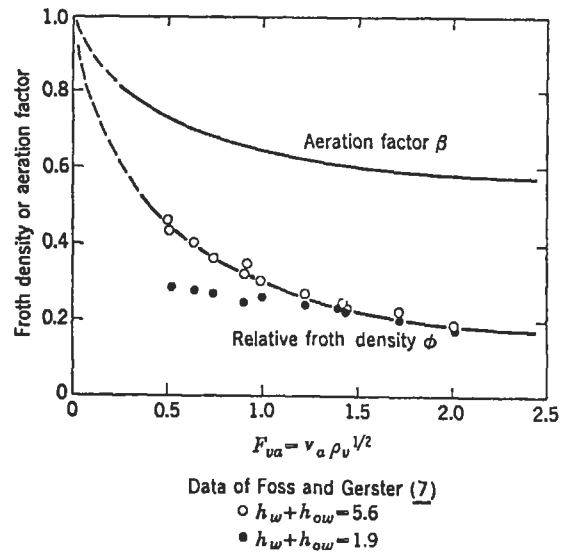


Figure 8-126. Aeration factor, sieve trays. Used by permission, Smith, B. D. *Design of Equilibrium Stage Processes*, Chapter 15, by J. R. Fair, McGraw-Hill Book Co. (1963), all rights reserved.

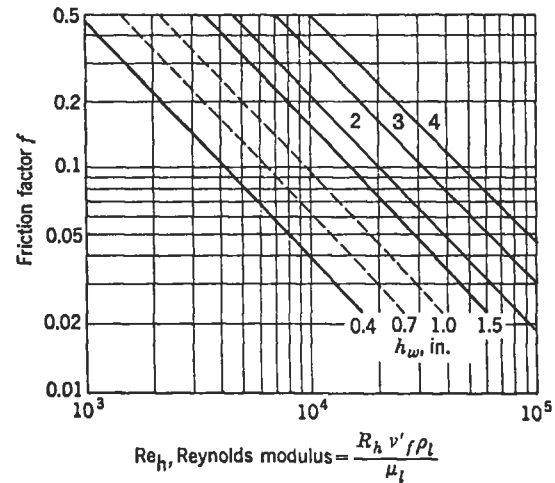


Figure 8-127. Friction factor for froth crossflow, sieve trays. (Note extrapolation by this author). Used by permission, Smith, B. D., *Design of Equilibrium Stage Processes*, Chapter 15, by J. R. Fair, McGraw-Hill Book Co. (1963), all rights reserved.

Reynolds No. Modulus:

$$Re_h = \frac{R_h v_f \rho_l}{\mu_l} \quad (8-258)$$

The relationship between f and Re_h is given in Figure 8-127 and is recommended for design purposes. The velocity of the aerated mass is the same as for the clear liquid.

$$v_f = 12 q / (h_i l_{fw}) \quad (8-259)$$

Dry Tray Pressure Drop

This is the drop occurring when the vapor passes through the holes on the tray. The relation below [25] correlates the data of several of the major investigators with a maximum deviation of less than 20% and an average deviation of 10%.

$$h_{dt} = 0.003 [v_o^2 \rho_v] \left(\frac{\rho_{water}}{\rho_L} \right) (1 - \beta^2) / C_o^2 \quad (8-260)$$

$$F_s = v_o (\rho)^{1/2}, F^2 = v_o^2 (\rho_v) \quad (8-261)$$

where h_{dt} = pressure drop through dry perforated tray, inches liquid on tray

v_o = vapor velocity through perforated holes, ft/sec

β = fraction perforated hole area in perforated tray area only

C_o = orifice coefficient from Figure 8-128

Note that β is not the fraction of hole area in the active tray region, but is limited to the perforated section only.

Fair's Method [193]

This method calculates the dry tray pressure drop and allows for correcting the two-phase flow effects at various entrainment ratios.

$$h_h = \frac{6 v_o^2 \rho_v}{g C_o^2 \rho_1} = 0.186 [\rho_v (v_o / C_o)^2] / \rho_1 \quad (8-262)$$

C_o is a function of the velocity of approach, hole diameter/tray-thickness ratio, Reynold's number through the

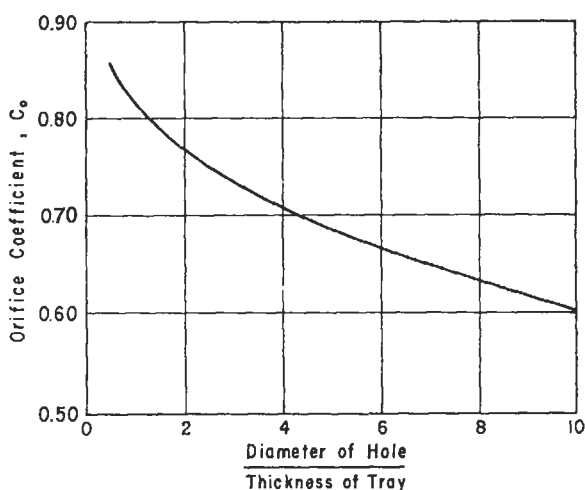


Figure 8-128. Orifice coefficient for perforated trays. Used by permission, Hughmark, G. A., and O'Connell, H. E., The American Institute of Chemical Engineers, *Chem. Eng. Prog.*, V. 53, (1957), p. 127M, all rights reserved.

hole, condition or design of the "lip" of the hole, and some other less prominent variables. The correlation for this concept for the orifice discharge coefficient is from Liebson, et al. [42], see Figure 8-129. Use C_o from this figure in Equation 8-262,

where A_h = net perforated area of tray, ft^2

A_a = active or "bubbling" area of tray, generally, $(A_t - 2A_d)$, ft^2

A_d = downcomer area, cross-sectional area for total liquid down-flow, ft^2

A_t = total tower cross-sections, area, ft^2

C_o = vapor discharge coefficient for dry tray

g = acceleration of gravity, 32.2 ft/sec^2

h_h = head loss due to vapor flow through perforations, in. liquid

v_o = vapor velocity through perforations, ft/sec

ρ_1 = clear liquid density, lb/ft^3

ρ_v = vapor density, lb/ft^3

Static Liquid Seal on Tray, or Submergence

Aeration of the liquid by gas bubbles reduces density. The usual and somewhat conservative approach recommends that this aeration effect be neglected. Many successful towers have trays operating on this design basis [45].

$$A. \quad h_{sl} = (f)h_w + h_{ow} \quad (8-263)$$

$f = 1.0$

where f = aeration factor

h_{sl} = static liquid seal on sieve tray, in. liquid

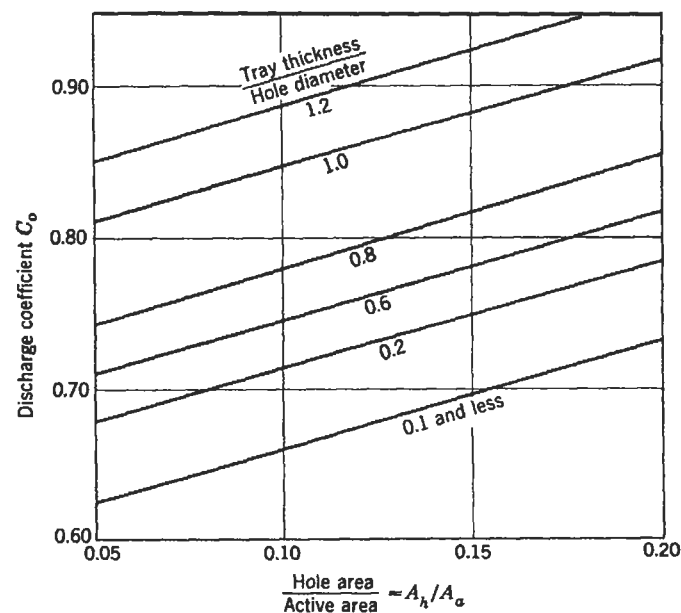


Figure 8-129. Discharge coefficients for vapor flow, sieve trays. Used by permission, Smith, B. D., *Design of Equilibrium Stage Processes*, Chapter 15, by J. R. Fair, McGraw-Hill Book Co. (1963); data from I. Liebson, R. E. Kelley, and L. A. Bullington, *Petroleum Refiner*, V. 36 (2), Feb. (1957) p. 127; V. 36 (3), (1957) pp. 288, all rights reserved.

B. A second and also successful method accounts to a certain extent for the aeration effect, based on test data from many references. This method is not quite as conservative when estimating total tower pressure. This follows the effective head concept of Hughmark et al. [31]. Effective head, h_e , is the sum of the hydrostatic head plus the head to form the bubbles and to force them through the aerated mixture. Figure 8-130 is the correlation for h_e plotted against submergence, h_{s1} [31]. See "Dynamic Liquid Seal."

Dynamic Liquid Seal

When hydraulic gradient is a factor in the tray design, the dynamic liquid seal should be used in place of h_{s1} for the determination of effective head.

$$h_{dl} = (f)h_w + h_{ow} + \Delta/2 \quad (8-264)$$

where h_{dl} = dynamic liquid seal for sieve tray, in. liquid
 h_e = effective liquid head taking aeration of liquid into account, in. liquid, from Figure 8-130

The aerated liquid pressure drop includes that generated by forming bubbles [193] due to surface tension effects. The equivalent height of clear liquid on the tray is given [193]:

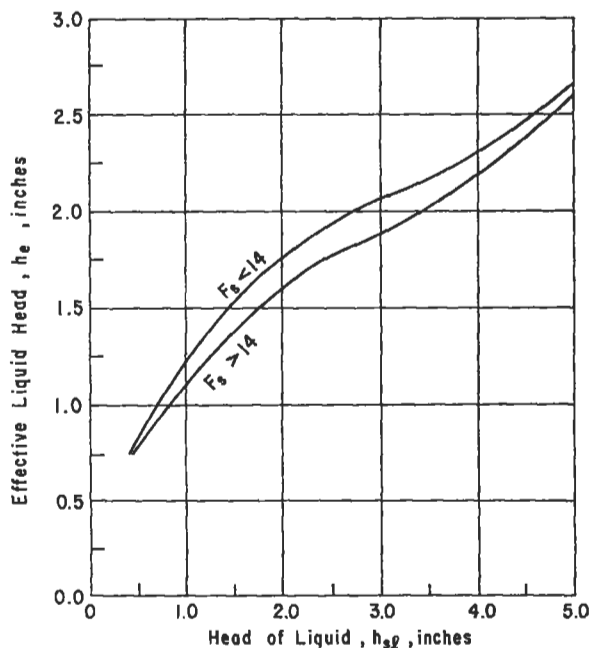


Figure 8-130. Effective liquid head for sieve trays with downcomers. Used by permission, Hughmark, G. A. and O'Connell, H. E., The American Institute of Chemical Engineers, *Chem. Eng. Prog.* V. 53, (1957), p. 127M, all rights reserved.

$$h_l = \beta (h_w + h_{ow}) \quad (8-265)$$

The term, h_l , represents the hydrostatic head on the tray, while $(h_w + h_{ow})$ is the liquid seal at the tray outlet weir, expressed as clear liquid. The factor, β , can be obtained from the upper curve in Figure 8-126 [193].

$$\phi = \frac{h_l}{h_f} = \frac{\text{Equivalent height of clear liquid on tray, in.}}{\text{Height of froth (aerated mass) on tray, in.}}$$

ϕ = relative froth density, ratio of froth density to clear liquid density

$$\beta = (\phi + 1)/2 = \text{aeration factor*}, \text{ see Figure 8-126} \quad (8-266)$$

(*From Hutchison, et al, Ref. 11 in Ref. 193)

Use β for design pressure drop calculations [193].

where F_{va} = vapor flow parameter based on active area, defined by $F_{va} = v_a \rho_v^{0.5}$ (8-267)

h_l = equivalent height of clear liquid on tray, in.

h_f = height of froth (aerated mass) on tray, in.

h_{ow} = height of liquid crest over weir, measured from top of weir (straight or circular), or from bottom of notches (v-notch weirs), in.

h_w = height of weir above tray floor, in.

v_a = vapor velocity based on active area, ft/sec

β = aeration factor, dimensionless, Figure 8-126

Total Wet Tray Pressure Drop

A. Conservative

$$h_t = h_w + h_{ow} + h_{dt} + \Delta/2$$

This will give a higher pressure drop per tray than the method (B).

B. Hughmark and O'Connell Method

The results of this approach agree with a considerable number of tests reported over a wide range of operation.

$$h_t = h_{dt} + h_e \quad (8-268)$$

C. Fair Method from Reference 193 (used by permission)

Total pressure drop across the tray:

$$h_t = h_h + \beta(h_w + h_{ow}) \text{ (see aeration factor above)}$$

For weeping sieve trays, see Figures 8-131 and 8-132, and example in later paragraph.

h_h = head loss due to vapor flow through perforations, in. liquid. See Equation 8-262.

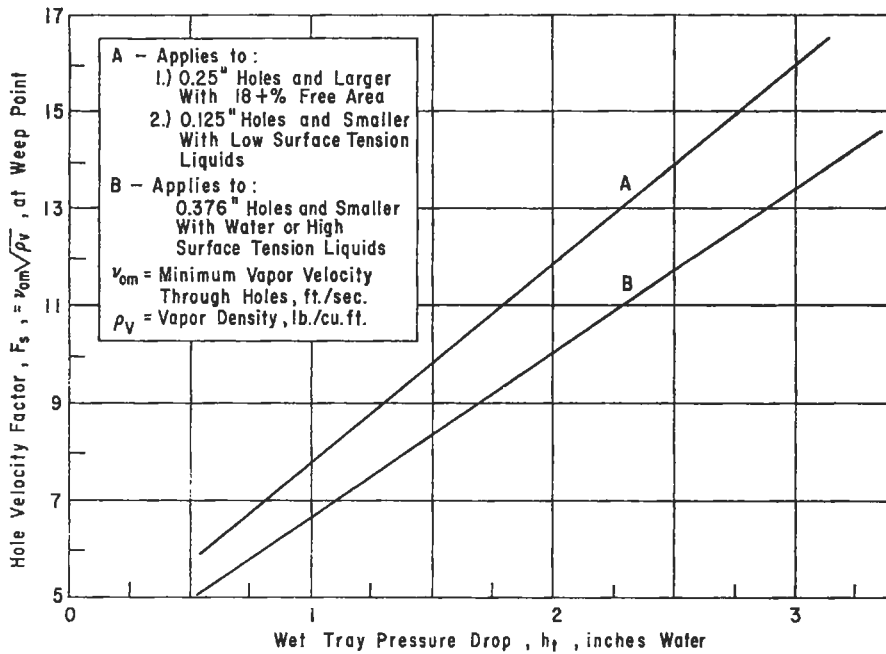


Figure 8-131. Weeping correlation for sieve trays with downcomers. Used by permission, Hughmark, G. A. and O'Connell, H. E., The American Institute of Chemical Engineers, *Chem. Eng. Prog.* V. 53. (1957), p. 127M, all rights reserved.

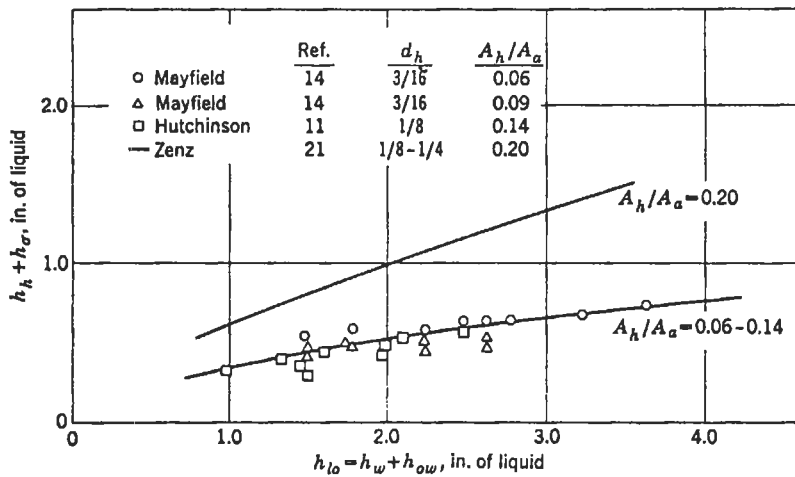


Figure 8-132. Weeping sieve trays. Used by permission, Smith, B. D., *Design of Equilibrium Stage Processes*, Chapter 15 by J. R. Fair, McGraw-Hill Book Co. (1963), all rights reserved.

Determine C_o from Figure 8-129 [193]. Note that determining froth density is by experiment and/or best judgment based on similar or related systems. Usually $\phi \approx 1.0$ to 0.50. The method checks literature and industrial tests about $\pm 15\%$.

Pressure Drop through Downcomer, h_d

Calculate as for bubble cap tray.

Liquid Backup or Height in Downcomer

$$H_d = h_t + h_w + h_{ow} + \Delta + h_d \tag{8-269}$$

Note that if an inlet tray weir is used, the $(h_w + h_{ow})$ group is replaced by the corresponding $(h_w' + h_{ow}')$ calculated for the inlet weir using the same algebraic relations.

Free Height in Downcomer

$$F = S_t + h_w - H_d \tag{8-270}$$

Minimum Vapor Velocity: Weep Point

The "weep point" is considered to be the minimum vapor velocity that will provide a stable tray operation, pre-

venting liquid from passing through the holes and bypassing the overflow weir and downcomer.

This point is generally considered the lower point of operation for the tray while maintaining acceptable efficiency. Some systems are known to operate at only slight reduction in efficiency while vapor velocities are well below the weep point values. It is impossible to predict this behavior at present. Weeping is usually the limiting condition in design for low vapor rate, high liquid rate systems. Some factors affecting the weep point of any system are described in the following sections.

Weeping and dumping are types of drainage that occur during tray operation, and are more sensitive in the operation/control of sieve trays than for valve or bubble cap trays. Lessi [194] presents an analysis of these conditions. Weeping simply means that the gas/vapor volume passing upward through the tray is not sufficient to prevent liquid on the tray from running back down to the tray below, thereby affecting the tray efficiencies. Dumping is a term more associated with sieve trays than the others; however, in concept it represents a large or excessive amount of liquid draining off the tray, greater than weeping, and could be considered a type or forerunner of flooding of the column.

Hsieh and McNulty [210] developed a new correlation for weeping of sieve and valve trays based on experimental research and published data. For sieve trays the estimation of the weeping rate and weep point is recommended using a two-phase countercurrent flow limitation model, CCFL.

The procedure [210] for weeping calculation and determination of vapor rate that will result in a certain weeping rate (used by permission, Reference 210 *Chemical Engr. Progress*, all rights reserved):

- (a) Calculate Z

$$Z = h_c^{1.5} / 12 D_H^{0.5} \quad (8-271)$$

- (b) Use values of m and C as determined by Reference 210

For sieve trays

$$m = 2.01$$

$$C = 0.74$$

For type T-valve style (Koch)

$$m = 2.87$$

$$C = 0.74$$

For type A-valve style (Koch)

$$m = 2.01$$

$$C = 0.74$$

- (c) Calculate J^*_L

$$J^*_L = V_L \left[\frac{\rho_L}{g Z (\rho_L - \rho_G)} \right]^{1/2} \quad (8-272)$$

using the given volumetric weeping liquid rate, and total hole area.

- (d) Calculate J^*_G

$$J^*_G^{1/2} + m J^*_L^{1/2} = C \quad (8-273)$$

$$J^*_G = C$$

- (e) Calculate vapor rate, V_G , based on value of J^*_G in (d) above using:

$$J^*_G = V_G \left[\frac{\rho_G}{g Z (\rho_L - \rho_G)} \right]^{1/2}, \text{ solve for } V_G \quad (8-274)$$

- (f) Using V_G from (e) above based on superficial gas rate calculate $V_{G, \text{weep}}$ based on total perforated hole area only, ft/sec. That is:

$$\text{ft}^3/\text{sec vapor} - (V_G, \text{ft/sec}) (A_H, \text{ft}^2)$$

The weep point for sieve or valve trays is the vapor rate at which the liquid weeping rate is diminished to zero. Thus, J^*_L approaches zero as J^*_G is increased [210]. For a vapor rate that leads to J^*_G higher than the weep point value, then there should be no weeping.

$$W_{\text{index}} > 0, \text{ for no weeping}$$

$$W_{\text{index}} = J^*_G - J^*_G(\text{weep pt.})$$

The higher the value of W_{index} , the more confidence that there will be no weeping [210]. At a constant weep point, J^*_G then, the higher the percentage opening of the tray, and the higher will be the vapor volumetric flow required to satisfy the weep point criteria.

To calculate the weep point, use $J^*_G = 0.74$ and calculate Z from (a) above, then calculate V_G from (e) above.

The author's [210] report that the test results show that below the weep point for the Type-T and Type-A valve trays, a consistently low weeping rate can be maintained, while for sieve trays the weeping rate increases rapidly at low gas flow. For similar operating conditions, the weeping rate for a valve tray can be an order of magnitude lower than the corresponding weeping rate for a sieve tray with the same open area. The tests assume uniform weeping across the entire tray deck; however, recent tests [210] indicate that for a larger 8-ft diameter (versus 3-ft) tray, weeping occurs preferentially along the periphery of the bubbling area, indicating that for the larger diameter the actual weeping rate can be lower by more than 30% when referenced to the present models prediction.

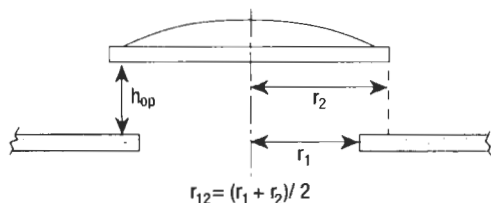
The equivalent hole diameter for use in the equation for Z when considering the two types of valve trays studied here is given by:

$$D_{\text{HE}} = 2 [1 / (2.581) (F_2 + F_3) (R_V)]^{1/2}, \quad (8-275)$$

(equivalent hole diameter, in.), see Equation 8-277

For Type-T valves: $R_V = 1.0$

For Type-A valves: $R_V = 0.8$



For the valve tray equivalent hole diameter, see illustration.

$$F_0 = \frac{1}{h_{op}} - \frac{1}{r_{12} h_{op} - r_1} + \frac{2(r_{12} + h_{op})}{3 \left[h_{op} + \sqrt{225 - r_1^2} - \sqrt{225 - r_{12}^2} \right]^2} \quad (8-276)$$

$$F_1 = \ln \frac{r_{12} (r_{12} + h_{op} - r_1)}{r_1 h_{op}} + (r_{12} + h_{op}) F_0 \quad (8-277)$$

$$F_2 = \left(1 - 2 \ln \frac{r_2}{r_{12}} - \left(\frac{h_{op}}{r_{12} + h_{op}} \right)^2 \right) F_1 / 8h_{op}^2 \quad (8-278)$$

$$F_3 = \frac{r_2 - \frac{r_1}{\sqrt{2}}}{r_1^2 \left[\left(r_2 - \frac{r_1}{\sqrt{2}} \right)^2 + \left(\frac{h_{op}}{2} \right)^2 \right]^{1/2}} \quad (8-279)$$

$$D_{HE} = 2 \left(\frac{1}{2.581 (F_2 + F_3) R_V} \right)^{1/2} \quad (8-280)$$

Note: all dimensions in inches

- where A_H = total hole area, ft^2
- A_{OP} = open area of tray, ft^2
- A_{VM} = maximum valve open area, ft^2
- C = empirical constant in CCFL correlation
- C_L = liquid phase loading factor defined in Equation 8-282, ft/s
- C_{LW} = measured rate of weeping from Equation 8-277
- C_V = gas phase loading factor defined in Equation 8-281, ft/s
- D_H = hole diameter, in.
- D_{HE} = equivalent hole diameter, in., Equation 8-280
- D_V = valve diameter, in.
- F_V = valve tray F-factor, $ft^3/min/valve$
- F_{VM} = valve tray F-factor at the beginning of the valve open region, $ft^3/min/valve$
- g = gravitational constant, ft/s^2
- h_c = clear liquid height, in.
- h_D = dry tray pressure drop, in.

H_{GAP} = maximum lift of a valve, in.

H_{OP} = valve lift, that is, the distance between the bottom of a valve and the top of the tray deck, in.

J_G^* = dimensionless gas velocity

J_L^* = dimensionless weeping liquid velocity

m = empirical constant in CCFL correlation

N_V = valve density, number of valves/ ft^2

Q_{GV} = volumetric gas flow rate to a valve, $ft^3/min/valve$

R_V = fractional opening in the circumference of a valve

V_G = superficial gas velocity in channel (not tower), ft/s

V_{GH} = gas phase superficial hole velocity, ft/s

V_L = superficial liquid velocity in channel (not tower), ft/s^* , for sieve trays, divide total vapor volume by total perforated hole area

V_{LH} = liquid phase superficial hole velocity, ft/s^* , for sieve trays, divide total liquid flow by total perforated hole area

z' = Laplace capillary constant

Z = characteristic length in CCFL model

* for valve trays, see calculation analysis in text

Greek letters

ρ_G = gas density, lbm/ft^3

ρ_L = liquid density, lbm/ft^3

σ = surface tension, $dyne/cm$

Figures 8-133–136 illustrate the correlation of the data with the proposed model and resulting design procedure. Additional illustrations accompany the reference. For Figure 8-133 the C_V and C_L parameters are plotted. For sieve trays, the actual hole velocities are used; where for the Type-T valve tray the “hole” velocities are calculated based on the maximum open area, A_{VM} .

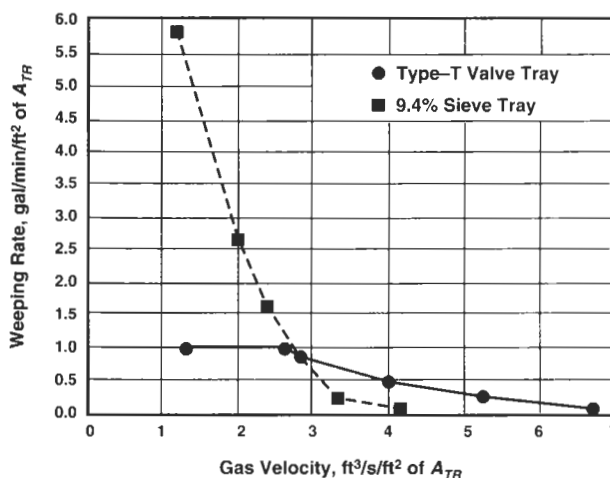


Figure 8-133. Weeping performance comparison. (Valve tray also gives a lower weep rate at a liquid flow rate of 50 gal/min/ft of weir.) Used by permission, The American Institute of Chemical Engineers; Hsieh, C-Li. and McNulty, K. J., *Chem. Eng. Prog.* V. 89, No. 7 (1993), p. 71, all rights reserved.

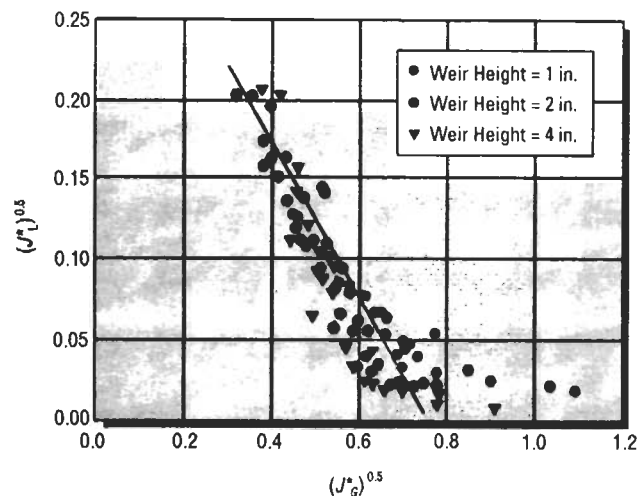


Figure 8-134. Weeping data for 9.4% open area sieve tray. Used by permission, The American Institute of Chemical Engineers; Hsieh, C.-Li. and McNulty, K. J., *Chem. Eng. Prog.* V. 89, No. 7 (1993), p. 71, all rights reserved.

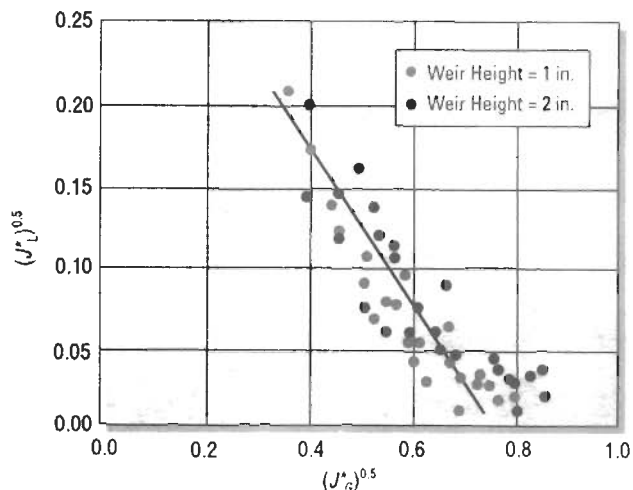


Figure 8-136. Weeping correlation for Type-A valve (Koch) tray. Used by permission, Hsieh, C. Li. and McNulty, K. J., The American Institute of Chemical Engineers, *Chem. Eng. Prog.* V. 89, No. 7 (1993), p. 71, all rights reserved.

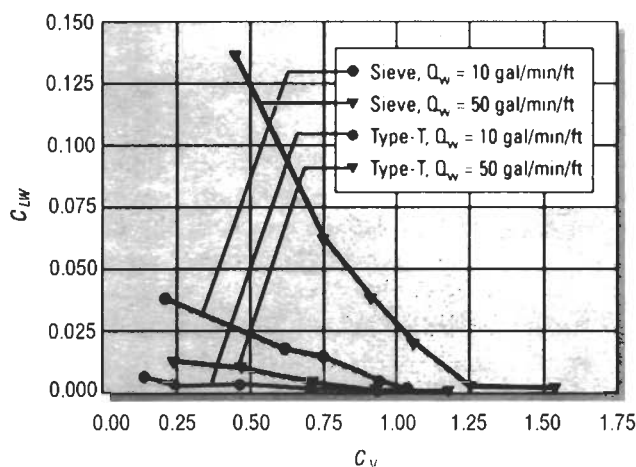


Figure 8-135. Weeping rate of Type-T valve (Koch) vs. sieve tray. Used by permission, Hsieh, C. Li. and McNulty, K. J., The American Institute of Chemical Engineers, *Chem. Eng. Prog.*, V. 89, No. 7 (1993), p. 71, all rights reserved.

$$A_{VM} = (\pi D_V H_{GAP} R_V N_V) / 144$$

$$C_v = V_{GH} [\rho_G / (\rho_L - \rho_G)]^{1/2} \quad (8-281)$$

$$C_L = V_{LH} [\rho_L / (\rho_L - \rho_G)]^{1/2} \quad (8-282)$$

$$C_v = m C_L^{1/2} = C \quad (8-283)$$

Hsieh and McNulty [210] (also see section on Sieve Trays) show that the weeping rate for 14.3% open area valve Koch Type-T (Figure 8-72) is nearly an order of mag-

nitude less than a corresponding sieve tray with the same percent open area. The typical valve tray tends to throttle the liquid as well as vapor flow as flows change. As an example of tests, Figure 8-133 [210] compares sieve and valve tray weeping at 50 gpm/min/ft weir with the gas and liquid rates based on the total bubbling area of the tray, A_{TR} . Note that the action of the Type-T valve closes down as the gas flow rate drops, but maintains a low weeping rate within its entire weeping region [210]. This also allows the efficiency of the tray to stay relatively constant over the weeping region.

The weeping rate of the sieve tray is strongly influenced by the gas flow rate, that is, the weeping rate will increase as the gas flow rate reduces below the weep point, i.e., where the weeping starts. Note the comparison of sieve and valve trays during weeping, Figure 8-135 [210].

Figure 8-136 [210] correlates weeping for the Type-A (Koch) valve trays, discussed earlier. For more details on the estimated design, see reference cited. The correlation developed with sieve trays still is used, and Equations 8-271–274 cover valve trays for rate of weeping and weep point. For columns larger than about 3-ft diameter the actual weeping rate can be more than 30% lower than the current calculations indicate. This is largely due to a non-uniform weeping along the periphery of the bubbling area of the tray.

Weep Point (Velocity)

1. Increases as the liquid surface tension decreases
2. Decreases as the hole size decreases

- Increases as the plate thickness decreases
- Increases as the percentage free area increases
- Increases for hole spacing close to $2d_o$ and smaller. Spacing of $3d_o$ and $4d_o$ give better operation. Only the $\frac{1}{8}$ -in. holes of Hunt [33] indicate that $2d_o$ spacing may be acceptable if the holes are very small.
- Decreases with increasing wettability of liquid on plate surface. Kerosene, hexane, carbon tetrachloride, butyl alcohol, glycerine-water mixtures all wet the test plates better than pure water. The critical tray stability data of Hunt et al., [33] is given in Table 8-21 for air-water, and hence the velocities for other systems that wet the tray better than water should be somewhat lower than those tabulated. The data of Zenz [78] are somewhat higher than these tabulated values by 10–60%.

These values are to be used in guides in establishing first estimates of lower limiting vapor velocities. Actual values should be calculated as outlined in the following.

The two approaches to determining the weep point are:

A. Conservative Design

- Assume a minimum vapor velocity through the holes.
- Calculate h_{dt} , Equation 8-260
- Compare calculated h_{dt} with value of dry tray pressure drop as given:

$$h_{dt}(\text{weep}) = 0.2 + 0.067(h_w + h_{ow})$$

This is based on the correlation of Mayfield [45] where: $h_{dt}(\text{weep})$ = dry tray pressure drop at tray weep point, in. liquid.

- Set minimum design dry tray pressure drop 30% above the value of $h_{dt}(\text{weep})$.

B. Normal Design [31]

- Assume a minimum vapor velocity through the holes. Calculate $v_{om}(\rho_v)^{1/2}$ (minimum)

- Calculate wet tray pressure drop, determine effective head from Figure 8-130.
- Read weep point velocity factor, $v_{om}(\rho_v)^{1/2}$, from Figure 8-131.

The assumed value of v_{om} must be greater than the value read from the curve for $v_{om}(\rho_v)^{1/2}$.

- Minimum design vapor velocity through the holes may be used as calculated, or if additional safety is required increase the value by 20%.

Entrainment Flooding

The increasing use of sieve trays in industrial process distillation and absorption-stripping situations has caused the development of important performance and design information. Flooding is caused by back-up (build-up) in the downcomer and/or entrainment [183, 184]. When the tray downcomers are sized to carry the liquid load and vapor disengagement in the downcomer (bubbles), the entrainment (jet) flooding is more likely to be the controlling mechanism. If the process application generates froth, this will further complicate the flooding condition.

Most studies have used the Souders-Brown [67] droplet settling velocity concept to relate entrainment flooding. In this mechanism, flooding develops due to a sufficiently high upward vapor velocity through the cross-section of the net area of the column to suspend droplets, and is expressed as the Souders-Brown flooding constant, C_{SB} , [94, 183, 184].

$$v_{N,\text{flood}} = C_{SB} [(\rho_L - \rho_V)/\rho_V]^{1/2} \quad (8-284)$$

C_{SB} = flooding constant = C-Factor

$$C_{SB} = v_{\text{flood}} [\rho_G/(\rho_L - \rho_G)]^{1/2}, \text{ ft/sec} \quad (8-285)$$

The entrainment increases as vapor velocity through the column increases to a power of 2 to 5, or as small as a 10% change in vapor rate results in tenfold change in entrainment [94]. Low pressure applications usually require lower powers, while higher pressure requires higher powers [94]. Entrainment quantities are sensitive to the vapor velocity. Often, low pressure and vacuum applications develop significant entrainment problems, even when operating below the flood point. Medium to high pressure systems are not often bothered except when operating at the flood point.

Generally, when spray entrainment changes to more froth on the tray or in the tray vapor space, then entrainment has been found to increase with liquid rate [94].

As tray spacing increases, entrainment reduces in quantity, but does increase with the sieve tray hole diameter [183, 184], but generally increases with reduction in hole

Table 8-21

Tray Stability with Varying Liquid Head, Air-Water System

Hole Diam., In. Spacing, In.	Calculated Critical Gas Velocity in Holes Ft/Sec			
	$h_{di} = h_w + h_{ow} + \Delta/2$			
	1.0 In.	1.8 In.	2.8 In.	3.8 In.
$\frac{1}{8} \times 4d_o$	5	25	32	35
$\frac{1}{4} \times 4d_o$	20	30	45	55
$\frac{1}{2} \times 3d_o$	27	40	55	70
$\frac{1}{2} \times 4d_o$	25	27	27	30
$\frac{1}{2} \times 6d_o$	30	35	40	45

Used by permission, The American Institute of Chemical Engineers, *A.I.Ch.E. Jour.* Hunt, C.D'A et al., V. 1, (1955), p. 441. All rights reserved.

diameter. Kister [94] discusses the effects of hardware relationships on spray and froth entrainment.

For sieve trays Kister's [94, 184] final correlation is for the Souder-Brown flooding coefficient and is essentially independent of pressure. The Kister and Haas correlation: [94][184]

$$C_{SB} = 0.144 \left[\frac{d_H^2 \sigma}{\rho_L} \right]^{0.125} (\rho_G / \rho_L)^{0.1} (S/h_{ct})^{0.5} \quad (8-286)$$

Correcting for the froth-to-spray regime transition [94]:

$$h_{ct} = (h_{ct})_{water} (62.3/\rho_L)^{0.5(1-n)} \quad (8-287)$$

$$n = 0.0231 d_H/A_f \quad (8-288)$$

where [94]

$$(h_{ct})_{water} = \frac{0.29 A_f^{-0.791} d_H^{0.833}}{(1 + 0.0036 Q_L^{-0.59} A_f^{-1.79})} \quad (8-289)$$

C_{SB} = C-factor at flood, ft/sec

v_{flood} = superficial vapor velocity at flood, ft/sec, based on net area, A_N , ft²

A_f = fractional hole area, A_H/A_B

A_h = hole area, ft² (net)

A_B = bubbling area, column cross-section area less total of downcomer areas, downcomer seal areas and areas of any other non-perforated region, ft²

A_N = net area (column cross-section area less downcomer top area) ft²

h_{ct} = clear liquid height at transition from froth to spray regime, in. liquid.

d_H = hole diameter, in.

S = tray spacing, in.

n = a parameter in the spray regime, in.

σ = surface tension, dynes/cm

ρ_L = liquid density, lb/ft³

ρ_G or ρ_V = vapor density, lb/ft³

Q_L = liquid load, gpm/in. of outlet weir length

Kister and Haas [184] recommend using 25 dynes/cm in Equation 8-286 when the actual surface tension is ≥ 25 dynes/cm. This correlation is reported [94, 184] to give better effects of physical properties, and predicts most sieve and valve tray entrainment flood data to ± 15 to 20%, respectively.

Kister and Haas [184] analyzed sieve and tray data as earlier described [94] and then related their results to the application for sieve and valve trays.

Recommended Range of Application. The Kister and Haas [184] Flood Correlation (used by permission, Kister, H. Z., Distillation Design, McGraw-Hill, Inc., 1992)

Flooding mechanism: Entrainment (jet) flood only

Tray types: Sieve or valve trays only

Pressure: 1.5–500 psia (Note 1)

Gas velocity: 1.5–13 ft/s

Liquid load: 0.5–12 gpm/in of outlet weir (Notes 2, 3, 5)

Gas density: 0.03–10 lb/ft³ (Note 1)

Liquid density: 20–75 lb/ft³

Surface tension: 5–80 dyne/cm

Liquid viscosity: 0.05–2.0 cp

Tray spacing: 14–36 in. (Notes 4, 5)

Hole diameter: $\frac{1}{8}$ in.

Fractional hole area: 0.06–0.20 (Note 5)

Weir height: 0–3 in.

NOTES:

1. At pressures above 150 psia, downcomer flood is often the capacity limitation. This limitation is not predicted by the correlation. Caution is required.
2. At high liquid loads (above 7–10 gpm/in.), downcomer flood is often the capacity limitation. This limitation is not predicted by the correlation. Caution is required.
3. Equation 8-289 does not apply for liquid loads lower than 0.5 gpm/in. of weir (35)*. For this reason, this correlation must not be extended to lower liquid rates.
4. At lower tray spacing, entrainment flooding may be related to lifting of the froth envelope and to froth rather than spray height. This correlation must not be extended to lower tray spacing.
5. The correlation does not apply when the following three conditions occur simultaneously. (a) Ratio of flow path length to tray spacing is high (> 3); (b) liquid rate is high (> 6 gpm/in of weir); and (c) fractional hole area is high ($> 11\%$). Under these conditions, entrainment flooding is related to vapor channeling and vapor cross flow rather than spray height.

Fair's [183] design procedure to establish an entrainment flooding condition or "point" is as follows: Design Procedure (From Fair, Reference 183, by permission)

The design method presented in this article is best summarized by a stepwise procedure:

1. Establish liquid and vapor flow rates and densities. Obtain or estimate liquid surface tension. If conditions vary significantly across the tower, apply this method to each section of interest wherein conditions can be considered constant.
2. Calculate the flow parameter, $FP = L/G \sqrt{\rho_V/\rho_L}$
3. Estimate the flood point from Figure 8-137, which accounts for liquid flow effects and is a ratio of liquid/vapor kinetic effects [79]. Flooding velocity is obtained from

*References in () are from the original source.

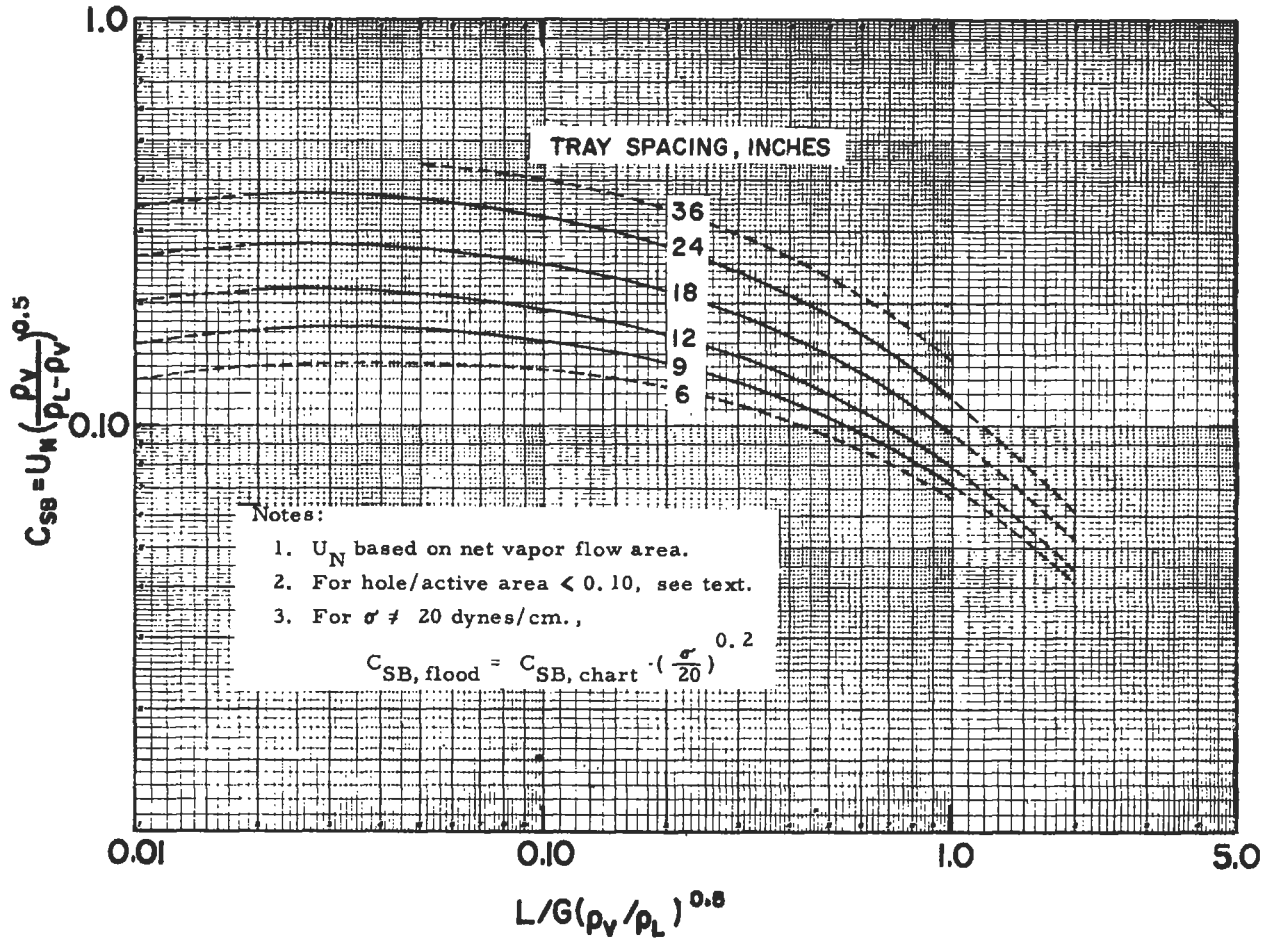


Figure 8-137. Flooding capacity, sieve trays; weir height is less than 15% of tray spacing; low- to non-foaming system; hole area at least 10%; hole sizes 1/8-in. to 1/4-in. dia.; surface tension = 20 dynes/cm. Used by permission, Fair, J. R., *Petro/Chem. Engineer*, Sept (1961), p. 46, reproduced courtesy of Petroleum Engineer International, Dallas, Texas.

$$U_{N, flood} = \frac{C_{SB, flood}}{[\rho_v / (\rho_L - \rho_v)]^{1/2}} \quad (8-284)$$

$$C_{SB, design} = C_{SB, chart} \left(\frac{\sigma}{20}\right)^{0.2}$$

Note that the values taken directly from Figure 8-137 apply to sieve trays having a hole area of 10% or more of active area; holes no larger than 1/4 in., and liquid surface tension of 20 dynes/cm. Corrections are as follows:

a. Hole area

Hole/Active Area	$C_{SB, design} / C_{SB, chart}$
0.10	1.00
0.08	0.90
0.06	0.80

b. Hole size

No correction for hole diameter < 1/4 in. Correction factors for larger diameters not known.

c. Surface tension

4. Choose tower diameter that will give the desired approach to flooding. Or, if dealing with an existing tower, calculate the approach to flooding.
5. Estimate the fractional entrainment ψ from Figure 8-138 or 8-139.

Using Figure 8-138:

$$\text{Percent flood} = \left[\frac{C_{SB, operating} \times 100}{C_{SB, flood}} \right] \frac{L}{G} = \text{Constant} \quad (8-290)$$

Use with Figure 8-137 to estimate both flood point and entrainment.

$$\text{The wet efficiency is: } E_W / E_D = \frac{1}{1 + E_D (\psi / (1 - \psi))} \quad (8-291)$$

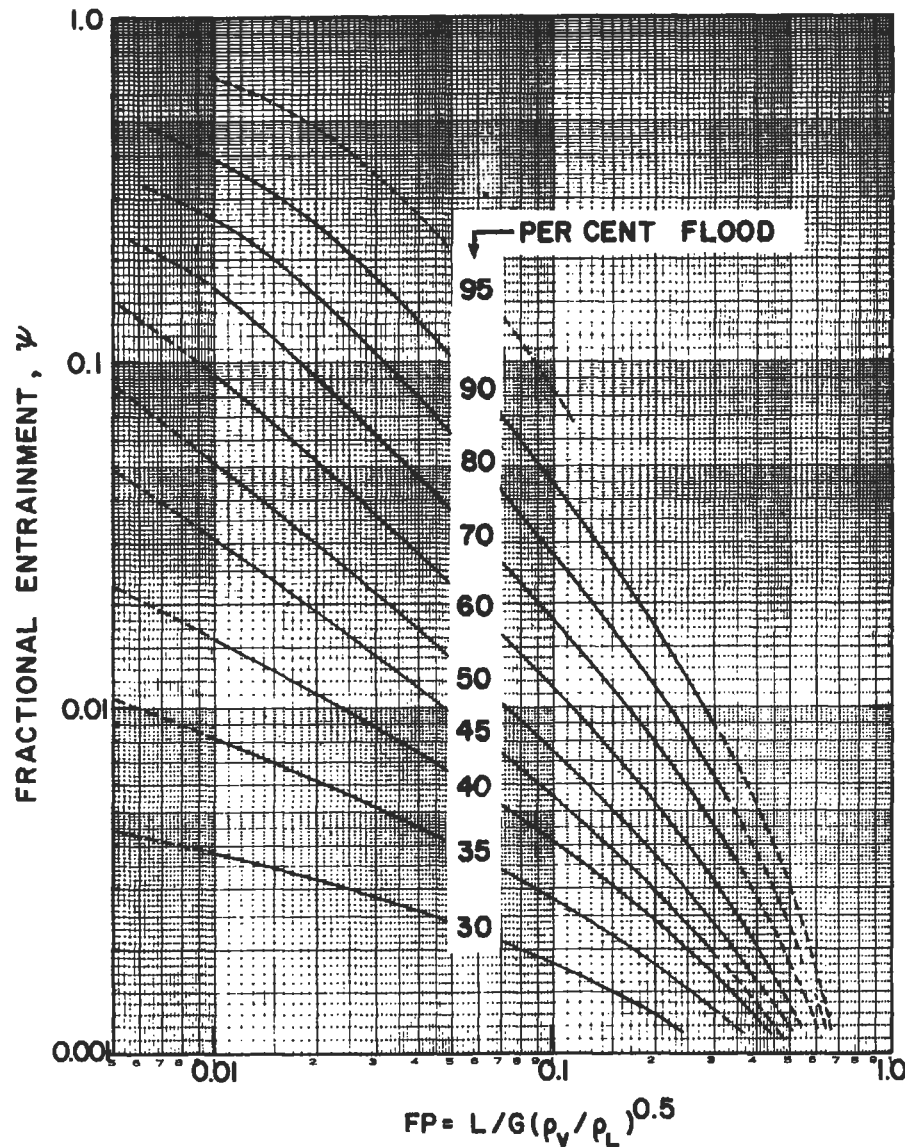


Figure 8-138. Fractional entrainment, sieve trays. Used by permission, Fair, J. R., *Petro/Chem. Engineer*, Sept. (1961), p. 45, reproduced by courtesy of Petroleum Engineer International, Dallas, Texas.

where C_{SB} = Souders-Brown capacity coefficient, ft/sec
 e = entrainment rate, lb mols/sec
 \bar{e} = entrainment rate, lb/lb dry vapor
 E_D = dry tray efficiency, fractional
 E_W = wet tray efficiency, fractional
 FP = flow parameter, dimensionless
 G = vapor mass rate, lb/sec or lb/hr
 h_f = froth height, in.
 h_L = clear liquid height, in.
 L = liquid mass rate, lb/sec or lb/hr
 L_{MD} = liquid molar rate (without entrainment) lb mols/sec
 T = tray spacing, in.
 U_N = vapor linear velocity based on area for de-entrainment (usually tower cross-section minus one downcomer), ft/sec

ρ_L = Liquid density, lb/ft³
 ρ_v = Vapor density, lb/ft³
 σ = Surface tension, dynes per cm
 σ_w = Surface tension of water, dynes/cm
 $\phi = C_{SB}/U_N = [\rho_v/(\rho_L - \rho_v)]^{0.5}$
 ψ = Entrainment expressed as fraction of gross down-flow

Fair [183] relates sieve trays and includes valve tray remarks to the extensive work done for bubble cap trays. Figure 8-137 and 8-139 show flooding data for 24-in. spacing of bubble cap trays from [81] and represents data well for 36-in. diameter columns, and is conservative for smaller columns. Fair's work has been corrected to 20 dynes/cm surface tension by:

$$C_{SB(20)}/C_{SB} = (20/\sigma)^{0.2} \quad (8-292)$$

for similar systems, where $\phi_1 = \phi_2$. Because the flow parameter is related to C_{SB} and ϕ , it is affected also:

$$(FP)\sigma = 20/(FP) = (\sigma/20)^{0.2} \quad (8-293)$$

$$(FP) = L/G\sqrt{\rho_v/\rho_L} \quad (8-294)$$

$$C_{SB} = U_N [\rho_v/(\rho_L - \rho_v)]^{1/2} \quad (8-295)$$

Figure 8-138 [183] is useful for data correlation, but is not necessary for design purposes [183]. It shows that at high values of parameter FP, sieve trays can be operated very close to the flood point without significant entrainment. Actually, bubble cap trays show the same characteristics [183]. In the low flow parameter region, such trays have a definite advantage, see Figure 8-139. For sieve tray flooding see data in Figures 8-140 A, B, C, D, E. For reference the bubble cap entrainment for the 24-in. spacing of trays is in Figure 8-139. Figure 8-140 E is for 18 in.-24 in. tray spacings. All sieve tray charts represent holes $< \frac{1}{4}$ in. and approximately 10% hole area referred to plate area between weirs, or active area [183].

When the hole area is much less than 10% of the active tray area, the flooding limit should be reduced. Fair [183]

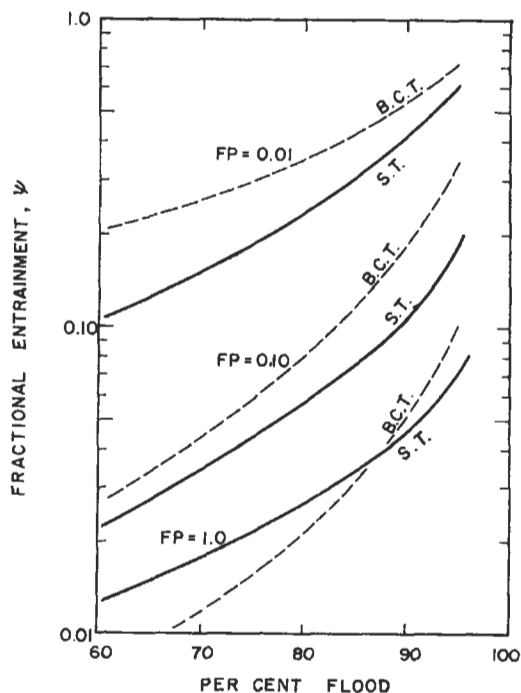


Figure 8-139. Entrainment comparison: sieve trays vs. bubble caps for 24-in. tray spacing. Note: B.C.T. = Bubble Cap Tray; S.T. = Sieve Tray; FP = Flow Parameter. Used by permission, Fair, J. R., *Petro-Chem Engineer*, Sept. (1961), p. 45, reproduced courtesy of Petroleum Engineer International, Dallas, Texas.

suggests the following factors to reduce the $C_{SB}/C_{SB,chart}$. See paragraph 3(a) above.

Figure 8-137 is used for estimating the entrainment-flood point. Liquid particle entrainment is generally considered as reducing tray efficiency (performance).

Figure 8-138 [183] represents the final entrainment correlation used for estimating, thus, based on published data:

$$\text{Percent Flood} = [C_{SB,oper}(100)/C_{SB,flood}] [L/G] \\ = \text{Constant}$$

The calculated entrainment values may be as good or better than measured values [183]. Figure 8-139 illustrates comparison of entrainment between bubble cap and sieve trays. Fair [183] concludes that for vacuum to moderate pressure applications, sieve trays are advantageous from an entrainment-flooding stand-point.

Example: 8-37: Sieve Tray Splitter Design for Entrainment Flooding Using Fair's Method; (used by permission [183])

For a sieve tray xylene splitter, the following flow conditions are specified:

Liquid rate	200,000 lb/hr
Vapor rate	220,000 lb/hr
Liquid density	46.8 lb/ft ³
Vapor density	0.266 lb/ft ³
Surface tension	16 dynes/cm

From a consideration of contacting requirements, a tower 9.5 ft in diameter is selected. Other pertinent details are: 24-in. tray spacing, 1-in. weir height, $\frac{3}{8}$ -in. dia. holes, 10% hole area (referred to active area) and 8.3 ft² down-comer area.

The available vapor flow area is $70.8 - 8.3 = 62.5$ ft.²

Hence,

$$U_N = \frac{220,000}{(3,600)(0.266)(62.5)} = 3.68 \text{ ft/sec}$$

$$C_{SB} = 3.68 \left[\frac{0.266}{46.8 - 0.27} \right]^{1/2} = 0.278$$

$$\frac{L}{G} \sqrt{\frac{\rho_v}{\rho_L}} = \frac{200,000}{220,000} \left[\frac{0.266}{46.8} \right]^{1/2} = 0.069$$

From Figure 8-137 C_{SB} for flooding is 0.340. This value is for 20 dynes/cm, 10% hole area and small holes. The only correction required is for surface tension:

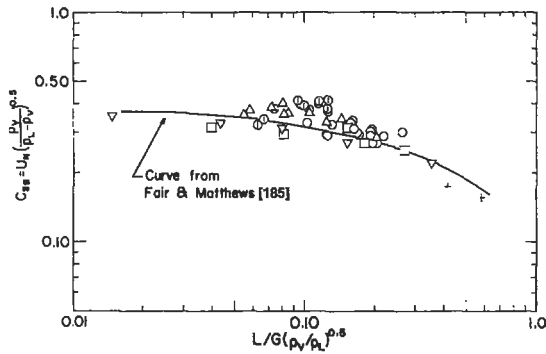


Figure 8-140A. Bubble cap tray flooding; 24-in. tray spacing.

Studies of Bubble-Cap Tray Flooding.
(24-in. Tray Spacing)

Symbol (Fig. 1)	Investigator	System	Tower diameter (in.)	Surface tension (Dynes/cm)
▽	Manning et al ²²	Toluene/Iso-octane	60	20
□	Muller & Othmer ²⁴	Nitrogen/Absorption Oil	66	28
△	Fractionation research ²	Cyclohexane/n-Heptane	48	12
○	Gerster et al ²	Acetone-Benzene	24	13-20
○	Clay et al ⁵	Isobutane/n-Butane	36	8-10
●	Kelley et al ¹⁹	Cracked gas fractionation	192	17
+	Kelly ¹⁸	Refinery gas absorption	90	22

Note: All holes < 1/4-in. dia and about 10% of tray active hole area referred to plate area between weirs.

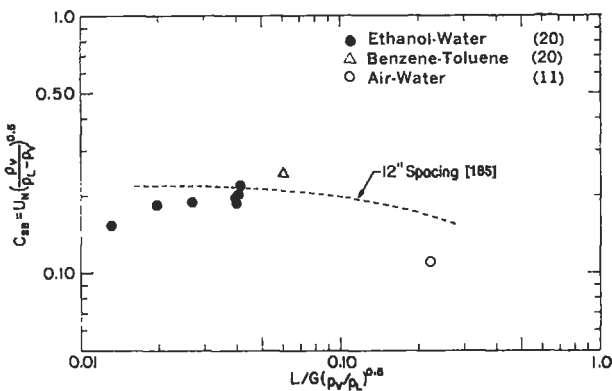


Figure 8-140B. Sieve tray flooding, 6-in. tray spacing.

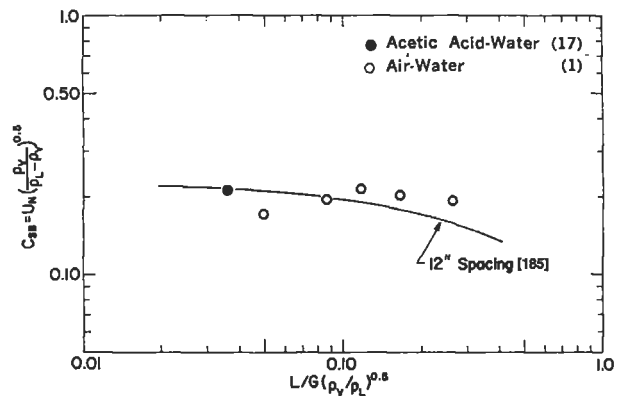


Figure 8-140D. Sieve tray flooding, 12-in. tray spacing.

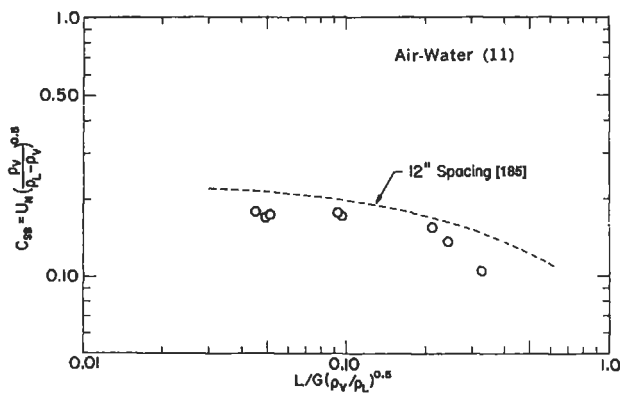


Figure 8-140C. Sieve tray flooding, 9-in. tray spacing.

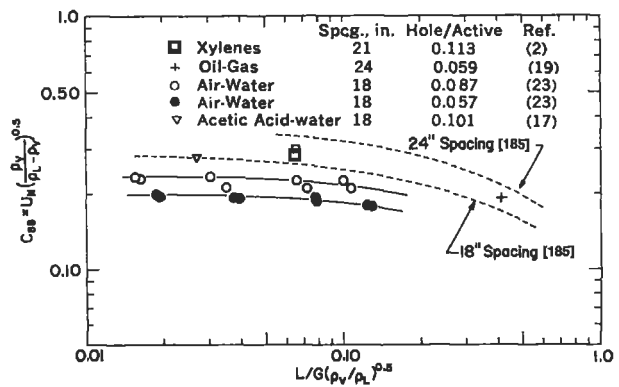


Figure 8-140E. Sieve tray flooding, 18-in.-24-in. tray spacing.

Figure 8-140. Studies of sieve tray and bubble cap tray flooding (24-in. tray spacing). (Note that the references listed on the illustrations in Figure 8-140 are from the original source, while Ref. 185 is from this text.) Used by permission, Fair, J. R., *Petro/Chem Engineer*, Sept. (1961) p. 45, reproduced courtesy Petroleum Engineer International Dallas, Texas.

$$C_{SB, \text{ flood}} = 0.340 \left(\frac{16}{20} \right)^{0.2} = 0.328$$

$$\text{Thus, percent flood} = \frac{0.278}{0.328} \times 100 = 85\%$$

From Figure 8-138, $\psi = 0.055$

$$\begin{aligned} \text{Finally, entrainment} &= \frac{0.055}{0.945} (200,000) = 11,600 \text{ lb/hr} \\ &= 11,600 \text{ lb/hr} \end{aligned}$$

If the dry efficiency at this point in the column is 90%, the wet efficiency is calculated by means of Equation 291:

$$E_w = \frac{0.90}{1 + 0.90 \left(\frac{0.055}{0.945} \right)} = 0.855 = 85.5\%$$

Experimental flooding and entrainment data for sieve trays are not plentiful, and measurements are not precise. Accordingly, it has been necessary to relate correlations of flooding and entrainment to those of the well-known device, the bubble-cap tray. It appears that the two devices have about the same flooding limits, so long as usual design practice is followed. However, the sieve tray shows entrainment advantages, especially when used in vacuum and atmospheric service.

The flooding capacity for sieve trays has been set into mathematical equation by Ward [187] using Fair's equation [183] and Figure 8-137. This in turn allows for the determination of the column diameter, assuming that an allowance is made in the flooding velocity so as not to design for flooding, but perhaps 25% below. I have not personally verified the equation of Ward [187], but Ward does show comparison curves, i.e., his with Fair's. Ward's equation for sieve tray flooding capacity factor:

$$C_F = \frac{0.26S_{ts} - 0.029S_{ts}^2}{[1 + 6F_{lv}^2 S_{ts}^{0.7498}]^{0.5}}, \text{ ft/sec} \quad (8-296)$$

$$FP = F_{lv} = \text{Flow Parameter} = (L'/V') (\rho_v/\rho_l)^{0.5} \quad (8-297)$$

where S_{ts} = tray spacing, ft

L' = liquid mass flow, lb/sec

V' = vapor mass flow, lb/sec

ρ_v = vapor density, lb/ft³ at flowing conditions

ρ_l = liquid density, lb/ft

Ward [187] reports the best fits for the curves at tray (or plate) spacing in the range of 0.5 to 3.0 feet, and at the ends of the curves.

By analogy to Fair's [183] work,

$$U_{\text{flood}} = C_{SB, \text{ flood}} [(\rho_L - \rho_v)/\rho_v]^{0.5}, \text{ ft/sec} \quad (8-298)$$

Calculate column diameter using U_{flood} reduced by 15–25%, or increase the calculated column area by about 25% and convert to a working diameter.

Maximum Hole Velocity: Flooding

The maximum hole velocity will give a liquid build up in the downcomer of 50% of the tray spacing.

To determine the maximum velocity:

1. Assume a hole velocity.
2. Calculate liquid height in downcomer, H_d by Equation 8-269.
3. If $H_d = \frac{1}{2} S_t$, the assume hole velocity is satisfactory; if not, repeat until a close balance is obtained.

Design Hole Velocity

The design velocity for selection of the holes also sets the minimum tower diameter. To take advantage of as much flexibility in operation as possible throughout the expected operating range, the following points should be considered in setting this velocity.

A. Select a design velocity near the weep point if:

1. The design vapor rate is, or is very close to, the minimum rate.
2. All change in capacity is to be as an increase over design rate.
3. Reduction in efficiency can be tolerated if vapor rate falls to weep point minimum or below.
4. Low tray pressure drop is required, as for vacuum systems. Design with extra caution under vacuum, since data correlations have not been checked in this region.

B. Select a design velocity near the maximum velocity if:

1. The design vapor rate is the maximum expected. All change will be to lower rates.
2. High efficiency is required.
3. High pressure drops are acceptable.

Tray Stability

Figure 8-141A of Huang and Hodson [30] and Figure 8-141B can be prepared from an evaluation of limits of tray performance using the relations set forth herein, or as presented in the original reference using slightly different analysis.

Unstable liquid oscillations on a tray have received only limited examination when compared to perhaps tray weeping, flooding and froth build-up. Biddulph [87] pro-

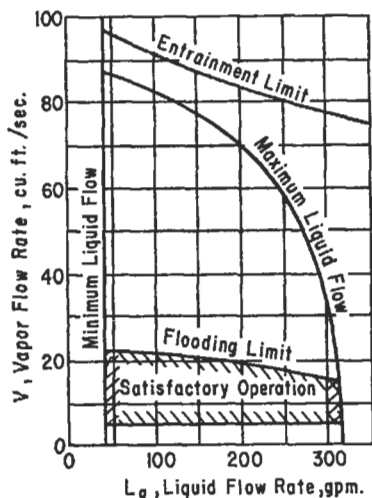


Figure 8-141A. Typical performance chart; perforated tray with downcomer. Used by permission, Huang, Chen-Jung and Hodson, J. R., *Pet. Refiner*, V. 37 (1958) p. 104, Gulf Publishing Co., all rights reserved.

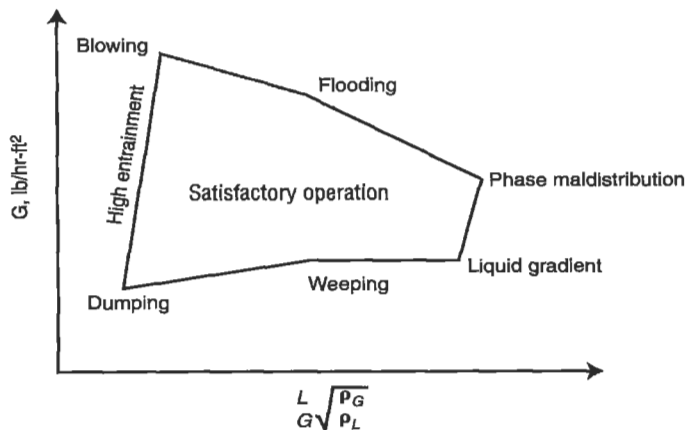


Figure 8-141B. Effects of vapor and liquid loadings on sieve tray performance. Used by permission, King, C. J. *Separation Processes*, McGraw-Hill Book Co., Inc. (1971), all rights reserved.

poses a dimensionless number to predict when biphasic liquid-gas oscillations will occur on distillation trays; this predicts the onset of oscillation:

$$B_s = \frac{U \epsilon h_f \rho_g}{g d^3 \rho_L \bar{\alpha}} \quad (8-299)$$

where B_s = dimensionless group identifier
 U = superficial vapor velocity, m/sec
 ϵ = eddy kinematic viscosity, m²/sec
 h_f = froth height, m
 ρ_g = gas density, kg/m³

g = gravitational constant, m/sec²
 d = column diameter, m
 ρ_L = liquid density, kg/m³
 $\bar{\alpha}$ = relative froth density, = h_L/h_f
 h_L = clear liquid head, m

The interpretation of criterion for the use of B_s is that:

1. Full-wave oscillations will not occur for values below $B_s = 0.5 \times 10^{-5}$
2. Half-wave oscillations will not occur for values below $B_s = 2.5 \times 10^{-5}$

To counter the oscillation effects, Biddulph [87] recommends use of two vertical baffles made of expanded metal with approximately 1-cm openings (0.394-in.) and installing them parallel to the flow path from the inlet weir to the outlet weir, and located at the $\frac{1}{2}$ and $\frac{3}{4}$ dimensions across the tray diameter. This oscillation phenomenon exhibits itself as the vapor rate increases and then the generally "even" layer of liquid changes by making violent lateral movements at right angles to the liquid flow. The two primary forms show a peak of liquid at one wall and a trough at the opposite wall (called half-wave oscillation). This condition then reverses.

With increasing vapor rate, the oscillations become more violent, and liquid entrainment increases up to 70%, decreasing the tray efficiency. On sieve trays, extra weeping occurs up to 150% compared to a stable tray. Full-wave oscillation is represented by a peak wave forming along the center of the tray with a trough at each wall. This position then reverses itself, and is called "full-wave" oscillation. The full-wave occurs at lower vapor rates than half-wave oscillation. Increases in entrainment and weeping also occur, and are most likely to be characteristic of medium- to small-sized columns, particularly those operating at reduced pressure.

To determine the likely possibility of oscillations occurring in a new or an existing column, or even sections of a column, the original article is recommended.

Vapor Cross-Flow Channeling on Sieve Trays

Kister et al. [213] have concluded from examining reported cases of cross-flow channeling related to poor sieve tray column performance that under specific conditions the cross-flow channeling does occur. See Figure 8-142 [213] for diagram of the postulated vapor flow across a tray. It is known to occur for valve trays and bubble cap trays. This condition has not been studied very much in the open literature; however, several investigators including myself have observed in industrial practice the

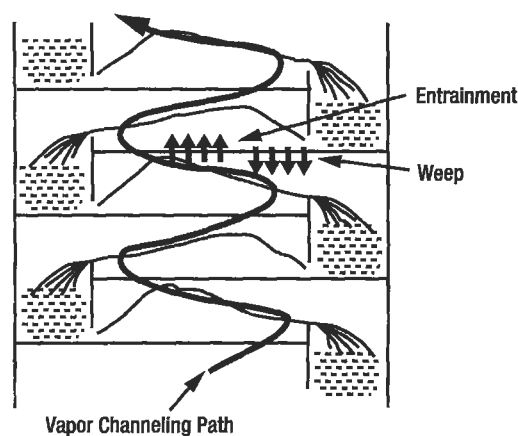


Figure 8-142. Vapor cross-flow channeling. Note entrainment near tray middle and outlet, and weep near tray inlet. Used by permission, Kister, H. Z., Larson, K. F. and Madsen, P. E., *The American Institute of Chemical Engineers, Chem Eng. Prog.* V. 88, No. 11 (1992), p. 86, all rights reserved.

selective weeping of sieve trays. Referring to Figure 8-142 [213] the situation is for sieve and valve trays at low pressure below 72.5 psig when all three listed conditions occur simultaneously [213]:

1. A fractional hole area (or valve slot) greater than 11% of the bubbling area.
2. A ratio of liquid flow path length to tray spacing greater than 2–2.5:1.
3. A liquid flow rate exceeding 50–60 m³/hr-m of outlet weir (537.9–645.5 ft³/hr-ft of outlet weir length)

Vapor cross-flow channeling:

1. Intensifies as the fractional hole area increases.
2. Intensifies as outlet weir height increases and as the liquid flow rate increases.
3. For valve trays the effects observed only for the venturi (low dry pressure drop) valve.
4. For bubble cap trays the phenomenon is believed to be induced by excessive hydraulic gradient; it is recommended to keep hydraulic gradient to less than 40% of the dry pressure drop.
5. For sieve and valve trays vapor cross-flow channeling is believed to occur when dry pressure drop is low (low vapor velocities, high fractional hole area and smooth openings) and with a significant hydraulic gradient (i.e., long flow path, high liquid velocities) [213].
6. Is believed to be a froth regime (liquid in continuous phase above the tray and gas present as bubbles in the liquid) phenomenon rather than a spray regime (gas in continuous phase above the tray and liquid present

as drops dispersed in the gas), which is usually in vacuum and low liquid-rate service [213].

Large fractional hole area, long flow path relative to tray spacing and high liquid flow rate are the key factors leading to the formation or intensification of vapor cross-flow channeling on sieve and valve trays.

Tray Layout

Some of the details of tray layout are given in Figure 8-67A. The working details can be set by the required performance.

1. A tower diameter is selected based on Souders-Brown (20–50 percent conservative, usually) or Hunt's relation, Equation 8-250.
2. Assume a tray layout: downcomer areas, non-perforated area; perforated area. Base downcomer requirements on bubble cap tray information of Figure 8-100.
3. Determine the percent hole area in the active tray portion for pressure drop calculation. Note that hole size does not have to be set at this point. (Figure 8-143.)
4. Calculate the expected tray performance.
5. From the selected design hole velocity and the total vapor rate corresponding, the total number of holes can be determined for a given assumed hole diameter.

$$\text{No. holes} = \frac{V(144)}{v_d (a_o)} \quad (\text{ft}^2/\text{hole}) \quad (8-300)$$

From Figure 8-144 or by calculation determine the plate area required for the holes on the pitch selected. Several selections may be tried to be used with the tray layout. These should be checked to agree with the assumed per cent hole area of Step 3.

6. If the tray does not balance area-wise, assume a new area arrangement or even diameter, if indicated, and recheck the procedure.

Example 8-38: Sieve Tray Design (Perforated) with Downcomer

The conditions for tray design in a chlorinated hydrocarbon finishing tower are:

1. Clean service, no fouling or suspended material
2.

	Top	Bottom
Vapor rate, ft ³ /sec	5.23	5.58
Liquid rate, gpm	9.57	22.1
Vapor Density, lb/ft ³	0.582	0.674
Liquid Density, lb/ft ³	83	85
Surface tension, dynes/cm	20	20+
3. Tray spacing is to be close as possible, because vertical installation space is a premium.

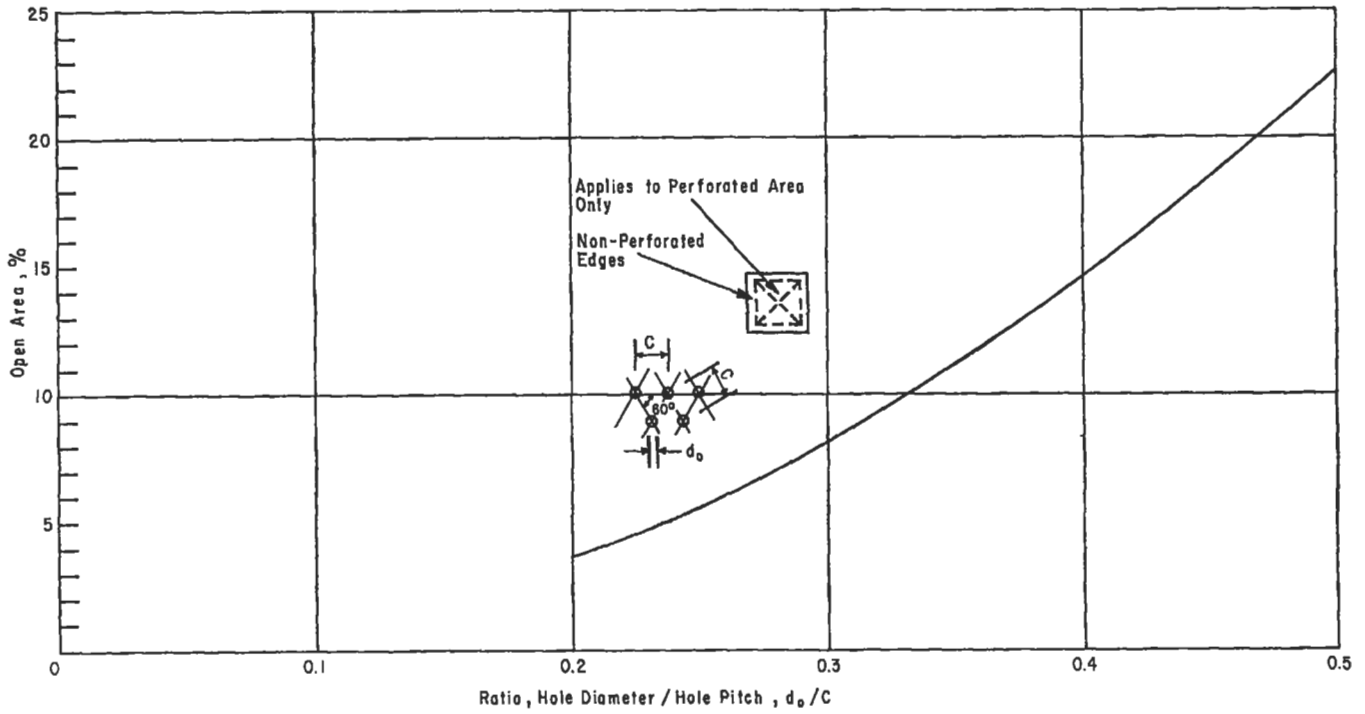


Figure 8-143. Percent open hole area for perforated and sieve trays.

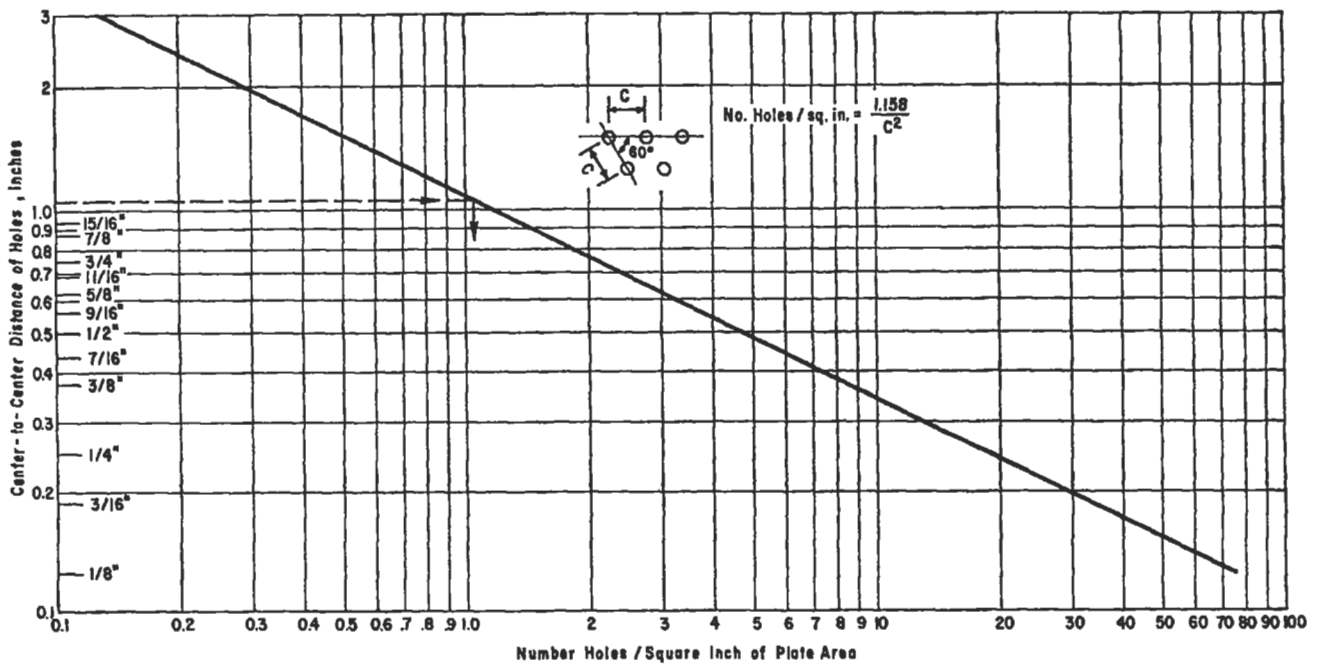


Figure 8-144. Number of holes in perforated plates.

Estimated Tower Diameter

Souders-Brown method

$$W = C [\rho_v (\rho_L - \rho_v)]^{1/2}$$

From Figure 8-82 $C = 100$ for 9-in. tray spacingIn this case rates are close and ρ_v does not change much from bottom to top of tower.

$$W = 100 [0.674 (85 - 0.674)]^{1/2} = 753 \text{ lbs/hr (ft}^2\text{)}$$

$$= \frac{753}{(3600)(0.582)} = 0.36 \text{ ft}^3/\text{sec (ft}^2\text{)}$$

$$\text{Tower cross-section area} = 5.23/0.36 = 14.5 \text{ ft}^2$$

$$\text{Diameter} = [(4/\pi)(14.5)]^{1/2} = 4.28 \text{ ft}$$

Using Hunt equation:

$$\text{Assume: } h_w + h_{ow} = 1.5 \text{ in.}$$

$$S' = S_t - 2.5 h_c = 9 - 2.5 (1.5) = 5.25 \text{ in.}$$

$$\text{At surface tension} = 20 \text{ dynes/cm,}$$

$$\text{For } e_w = 5\% = 0.05$$

$$\text{Figure 8-121 reads: allowable tower velocity} = 2.2 \text{ ft/sec}$$

$$\text{Required tower area} = 5.58/2.2 = 2.54 \text{ ft}^2 \text{ (bottom, largest)}$$

$$\text{Diameter} = [(4/\pi)(2.54)]^{1/2} = 1.8 \text{ ft}$$

$$\text{Select: tower diameter} = 2.5 \text{ ft}$$

A 2-ft tower would be expected to perform satisfactorily with properly designed trays. However, a 2.5-ft tower is the minimum diameter suitable for internal inspection and maintenance. The cost of a tray tower of 2.5-ft has been found to be no more, and from some bids 5 percent less, than the smaller 2-ft. tower. A 2-ft. tower would either be used with packing or with trays inserted from the top on rods with spacers. This would allow removal of the trays for inspection and maintenance.

Tray Layout Based on 2.5-ft Diameter Tower

Use a segmental downcomer on a cross-flow tray.

From the residence time in downcomers for bubble cap trays, and at the very low tray spacing of 9 inches, select an allowable liquid velocity of 0.1 ft/sec.

$$\text{Downcomer area} = \frac{22.1 \text{ gpm}}{7.48 (60) (0.1)} = 0.492 \text{ ft}^2$$

$$\text{Total tower area} = \pi (2.5)^2/4 = 4.91 \text{ ft}^2$$

$$\text{Percent of tower area} = 0.492 (100)/4.91 = 10.01\%$$

Using Figure 8-100 for segmental downcomers, at 10% downcomer area, the weir length is 72.8% of tower diameter.

$$\text{Weir length} = 72.8 (30)/100 = 21.8 \text{ in.}$$

Since standard details for fabrication are already available for a tray with a 19.5-in. weir in a 30-in. tower (65% of dia.), try this as first tray examined. This is 6.8% of tower cross-sectional area. Downcomer area = 0.068 (4.91) = 0.334 ft².

*Hole Size*Try $\frac{3}{16}$ -in. dia. on $\frac{1}{2}$ -in. pitch

This is spacing of 2.66 d_o , and is as close as good design would suggest. Use $\frac{1}{8}$ -in. tray thickness.

$$\text{Ratio } d_o/c = \frac{3/16}{1/2} = \frac{3}{8} = 0.375$$

Percent hole area = 12.8% (of perforation area only) as shown in Figure 8-143.

Minimum Hole Velocity: Weeping

$$\text{Assume: } v_o (\rho_v)^{1/2} = 13$$

$$\text{Assume: Submergence} = 1.5 \text{ in.} = h_{s1} = h_{d1} \text{ (neglecting } \Delta/2\text{)}$$

Dry Tray Pressure drop, h_{dt}

$$= 0.003 (v_o^2 \rho_v) \left(\frac{\rho_{\text{water}}}{\rho_L} \right) (1 - \beta^2) / C_o^2$$

$$\text{The hole diam./tray thickness ratio} = \frac{3/16}{1/8} = 1.5$$

$$\text{From Figure 8-128, orifice coefficient, } C_o = 0.78, \beta = 0.128$$

$$h_{dt} = \frac{0.003 (13)^2 (62.3/85) (1 - (0.128)^2)}{(0.78)^2} = 0.608 \text{ in. liquid}$$

Effective head

$$\text{For } h_{s1} = 1.5, F_s < 14$$

$$\text{Read Figure 8-130; effective head} = 1.58 \text{ in. liquid}$$

Total Wet Tray Pressure Drop

$$h_t = 0.608 + 1.58 = 2.188 \text{ in. liquid}$$

*Weep Point*Using Figure 8-131 Curve A, and $h_t = 2.19$ in. liquid

$$\text{Read weep point velocity} = 12.5 = v_{om} (\rho_v)^{1/2}$$

Curve A is used when in doubt, and it gives a higher minimum v_{om} , which is on safer side for design.

Because $v_{om} (\rho_v)^{1/2} = 12.5$ is less than the assumed value of 13, the 13 will be used.

Maximum Hole Velocity at Flood Conditions

Assume $F_s = v_o (\rho v)^{1/2} = 20$ max.

Dry tray pressure drop

$$= 0.003 F_s^2 \left(\frac{\rho_{water}}{\rho_L} \right) (1 - \beta^2) / C_o^2$$

$$= 0.003 (20)^2 (62.3/85) (1 - (0.128)^2) / (0.78)^2$$

$$= 1.44 \text{ in. liquid}$$

Effective head, h_e

= 1.4 in. liquid, for $F_s > 14$ and $h_{sl} = 1.5$

Total wet tray pressure drop, $h_t = 1.44 + 1.4 = 2.84$ inches liquid

Liquid Back-up or Height in Downcomer

$$H_d = h_t + (h_w + h_{ow}) + \Delta + h_d$$

$$H_d = 2.84 + 1.5 + 0 + 0 \text{ (assumed, to be confirmed)}$$

$$H_d = 4.34 \text{ in. liquid}$$

The limit on H_d for flooding is $S_t/2 = 9/2 = 4.5$ in. Therefore $F_s = 20$ appears to be close to minimum.

Design Hole Velocity

Select a velocity represented by F_s factor between minimum and maximum limits.

20 > Design > 13

Select a median value of $F_s = 17$, because freedom to operate above and below the design value is preferred in this case.

Design Basis

$F_s = 17$

1. Weir Height selected = $h_w = 1.0$ inch
2. Height of liquid over weir, $h_{ow} = 0.52$ in.
From Figure 8-104 at 22.1 gpm and $l_w = 1.62$ ft
3. Submergence, $h_{sl} = (f) (h_w) + h_{ow} = (1) (1.0) + 0.52 = 1.52$ in. liquid
4. Downcomer pressure loss. Clearance between bottom of downcomer and plate = 1-in. max. Underflow area = (9.5 in.) (1 in.)/144 = 0.065 ft². Because this is less than the downflow area (of 0.334 ft²), it must be used for pressure drop determination. No inlet weir used on this design.

$$h_{du} = 0.56 \left[\frac{L_g}{449 (A_d)} \right]^2 = 0.56 \left[\frac{22.1}{449 (0.065)} \right]^2 = 0.312 \text{ in liquid across restriction}$$

5. Dry tray pressure drop

$$h_{dt} = 0.003 (17)^2 (62.3/85) (1 - (0.128)^2 / (0.78)^2) = 1.04 \text{ in. liquid}$$

6. Effective head

$$h_{sl} = 1.52 \text{ in.}$$

$$h_e = 1.4 \text{ in. liquid for } F_s > 14, \text{ Figure 8-130}$$

7. Total wet tray pressure drop

$$h_t = 1.04 + 1.4 = 2.44 \text{ in. liquid}$$

8. Total tower pressure drop for 45 trays:

$$\Delta P \text{ (tower)} = \frac{(2.44) (45)}{1728 \text{ cu. in./cu. ft.}} \left(\frac{83 + 85}{2} \right) = 5.33 \text{ psi}$$

An actual operating tower measured 5 psi ±. It is satisfactory to average the conditions for top and bottom of tower when flows do not vary significantly. Otherwise, parallel determinations must be carried through for top and bottom (and even feed in some cases) conditions.

9. Number of holes required

Hole size selected = 3/16-in.
Hole spacing or pitch = 1/2-in.
From Figure 8-144, Holes/in.² plate area = 4.62
Area of a 3/16-in. hole = 0.0276 in.²

Calculation Summary

Maximum Velocity	Design Velocity	Weep Point
$F_s = 20$	17	13
$v_o \text{ top} = 20 / (0.582)^{1/2} = 26.2 \text{ ft./sec.}$	$= 17 / (0.582)^{1/2} = 22.3$	$= 13 / (0.582)^{1/2} = 17$
$v_o \text{ Bot.} = 20 / (0.674)^{1/2} = 24.4 \text{ ft./sec.}$	$= 17 / (0.674)^{1/2} = 20.7$	$= 13 / (0.674)^{1/2} = 15.8$
No. Holes required: CFS at top = 5.23 No. holes =		
$\frac{5.23 (144)}{26.2 (0.0276)} = 1040$	$= \frac{5.23 (144)}{22.3 (0.0276)} = 1223$	$= \frac{5.23 (144)}{17 (0.0276)} = 1605$
CFS at bottom = 5.58 No. holes =		
$\frac{5.58 (144)}{24.4 (0.0276)} = 1195$	$= \frac{5.58 (144)}{20.7 (0.0276)} = 1410$	$= \frac{5.58 (144)}{15.8 (0.0276)} = 1845$

The selected design $F_s = 17$ gives the number of holes to operate at these conditions. Note that the values of 1223 and 1410 holes for the top and bottom respectively indicated operations somewhat closer to the tower maximum than to the weep point. This usually insures as good an efficiency as is obtainable for a given system. It may limit the flexibility of the tower, since there will not be enough holes to operate down to the weep point at the given design flow rates.

On the other hand the tower should be able to operate at changing vapor and liquid loads without serious upset. In this type of tray the designer has a selection of holes, in this case: For the top select 1,100 to 1,500; for the bottoms, select 1,300 to 1,750, and still expect acceptable performance.

The fabrication of all trays may be punched or drilled (more expensive) with 1410 holes, and those in the lower section have blank strips placed over the inlet and outlet edge rows until approximately 1223 holes are left open in the top section above the feed tray.

For close examination of systems having varying latent heats and flow rates, it is wise to examine several points in the tower, even tray by tray in some cases, to be certain that the number of holes in that tray does not place its performance too close to the weep or flood conditions. Towers have been built and operated at rated peak loads with every tray having a significantly different number of holes.

10. Mechanical tray layout details. Allow a total of $3\frac{1}{2}$ -in. on diameter for extension of tray ring-type support into the tower. This reduces available tray area. Other support details might make more area available. Each must be examined.

Allow 5-in. clearance (no holes) between inlet downcomer and first row of holes. The 5 in. could be reduced to 3 in. minimum if an inlet weir were used.

Allow 3-in. clearance (no holes) between outlet weir and adjacent row of holes.

Downcomer width = 3.6 in. (From Figures 8-100 and 8-145 at 65% weir length).

Area determinations: Figure 8-145.

Area of segment of circle (2) with chord AD:

Diameter circle (2) = $30 - 3.5 = 26.5$ in.

Height of chord = $13.25 - (15 - 3.6 - 5) = 6.85$ in.

Chord height/circle dia. = $6.85/26.5 = 0.258$

Referring to *Perry's Handbook*, (pg. 32, 3rd Ed.)

Area = $0.161 (26.5)^2 = 113.2$ in.²

Area of segment of circle (2) width chord BC:

Height of chord = $13.25 - (15 - 3.6 - 3) = 4.85$

$h/D = 4.85/26.5 = 0.183$

Area = $0.0984 (26.5)^2 = 69.1$ in.²

Area of circle (2) = $\pi (26.5)^2 = 552$ in.²

Area available for holes = $552 - 113.2 - 69.1 = 369.7$ in.²

Area required for holes = $(1410)/4.62$ holes/in.² = 305 in.²

Actually not all of the tray needs to be drilled. However, the location of "dead" or unperforated areas must be carefully selected, preferable next to weirs. A special punching (or drilling) arrangement for the holes can run the cost of the trays quite high. It will probably be preferable to check effect of punching holes in entire area A B C D of Figure 8-145.

Area = 369.7

No. holes = $369.7 (4.62) = 1,710$ holes

This number is in the range of acceptable performance for bottom section and should be punched. If performance indicates fewer holes are preferable, blanking strips can be added (or even added before the trays are installed). The top trays definitely require blanking of holes.

Example 8-39: Tower Diameter Following Fair's Recommendation in Smith [193] (used by permission)

Following the example of Fair [193], the technique is summarized (used by permission, as paraphrase, not copied directly, with a different example):

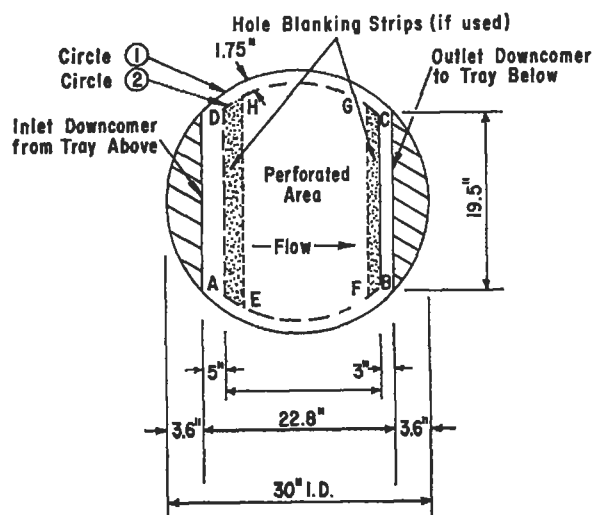


Figure 8-145. Sieve tray with downcomer layout for Example 8-38.

Design a sieve tray column to separate benzene and toluene to produce 35,000 lb/hr of benzene as overhead product at atmospheric pressure and use a reflux ratio of 5:1 (reflux returned to net overhead). Using the top tray as the first design basis, which can be followed by other points in the column, determine by the material balance:

Top tray data:

Material: 95%+ benzene

Molecular Weight: 78.1

Operating pressure: 14.7 psia

Operating temperature: 176°F

Liquid Density: 43.3 lb/ft³

Vapor Density: 0.168 lb/ft³

Liquid Surface Tension: 21 dynes/cm

Maximum liquid load: 5(35,000) = 175,000 lb/hr (504 gpm)

Maximum Vapor load: 210,000 lb/hr \cong (347 ft³/sec)

System: Non-foaming, non-corrosive, non-fouling

Tower Diameter

Flow Parameter:

$$F_{lv} = \frac{L'}{V'} (\rho_v / \rho_L)^{0.5} \quad (8-297A)$$

$$= \frac{175,000}{210,000} (0.168 / 43.3)^{0.5} = 0.0519$$

Tray Spacing and Design

Select as quite common; $\frac{3}{8}$ -in. dia. holes, with hole area/tower area = 0.10, 14 U S Std. gauge stainless steel tray material, which is 0.078 in. thick, 2-in. weir height, and 24-in. tray spacing.

Select single cross-flow tray, segmental downcomers, and straight weirs, with weir length equaling 77% of tower diameter. The downflow segment is 12.4% of the tower area.

Diameter

From Figure 8-137 read,

$C_{SB} = 0.36$, at F_{lv} at 0.0519 (previous calculation)

The system surface tension is approximately 20 dynes/cm, therefore no correction is necessary.

In this system, use 85% of flooding condition for design:

Vapor flooding velocity = $v_f = U_{N,flood} = C_{SB} / (\rho_v / (\rho_L - \rho_v))^{1/2}$

At 85% flood:

$U_{N,flood} = v_f = (0.36) (0.85) / [(0.168) / (43.30 - 0.168)]^{0.5} = 4.90$ ft/sec, vapor velocity based on net cross-sectional area for vapor flow above tray, usually, $(A_t - A_d)$, ft²

$V = 347$ cfs

At 88% total tower area, $A_d = 0.12 (A_t)$, ft²; downcomer area

$$A_t = 347 / [(1 - 0.12) (4.90)] = 80.47 \text{ ft}^2$$

Tower diameter, $D = [(80.47) (4) / \pi]^{0.5} = 10.12$ ft for 85% flooding.

For fabrication convenience and practicality, select, $D = 10.5$ ft

Actual A_t at 10.5 ft = 86.59 ft²

Mechanical Features

$$A_t = 86.59 \text{ ft}^2$$

$$A_d = 0.12 (86.59) = 10.39 \text{ ft}^2$$

A_n = Net cross-section area for vapor flow above tray,

$$(A_t - A_d) = 86.59 - 10.39 = 76.2 \text{ ft}^2 \text{ (usual situation)}$$

A_a = active or bubble area of tray,

$$(A_t - 2A_d) = [86.59 - 2 (10.5)] = 65.59 \text{ ft}^2$$

$$A_h = \text{net perforated area of tray, ft}^2 = (0.10) (86.59) = 8.66 \text{ ft}^2$$

Actual Flow Conditions

Vapor velocity based on net area = 347 cfs/ A_n

$$U_n = 347 / 76.2 = 4.55 \text{ fps}$$

$$\text{Approach to flooding} = [U_{n,\text{design}} / U_{n,\text{flood}}] [100] \\ = [4.55 / 4.90] (85) = 78.99\%$$

Entrainment

Refer to Figure 8-138, Fractional Entrainment, Sieve Trays [183] and for $F_{lv} = FP = 0.0519$, and 77.4% of flooding.

Fractional Entrainment $\psi = 0.06$

$$\psi = \frac{\epsilon}{(L' + \epsilon)}$$

ϵ = Liquid entrainment, lb mols/hr

$$\epsilon = [0.06 / (1 - .06)] (175,000 / 78.1) = 143 \text{ mols/hr} \\ = 11,168 \text{ lb/hr}$$

Pressure Drop

With a hole/active area ratio = 8.66/65.59 = 0.132

$$\text{With a tray thickness/hole diameter ratio} = 0.078 / (3/16) \\ = 0.416$$

Orifice coefficient, Figure 8-129, read at 0.41 tray/hole gives C_o orifice coefficient = 0.75

Hole velocity = 347/8.66 = 40.06 fps

Dry Tray pressure drop

$$h_h = 0.186 \rho_v / \rho_L (v_o / C_o)^2$$

$$= 0.186 (0.168 / 43.3) [40.06 / 0.75]^2 = 2.06 \text{ in. liquid}$$

Weir flow = 0.77 (10.5) (12 in/ft) = 97.02 in. weir length

$$= 8.085 \text{ ft}$$

Weir crest @ 504 gpm, L_g (see Figure 8-104):

$$\begin{aligned} h_{ow} &= 0.092 (L_g/l_w)^{2/3} = \\ &= 0.092 (504/8.08)^{2/3} \\ &= 1.45 \text{ in. liquid} \end{aligned}$$

In such a large column, the weir constriction factor (Figure 8-105) is not significant and is not applied to the above h_{ow} .

Aeration:

From Figure 8-126:

$$F_{va} = v_a (\rho_v)^{0.5} \text{ for active area}$$

$$F_{va} = (347/65.59) (0.168)^{0.5} = 2.168$$

Read figure; aeration factor, $\beta = 0.58$

Then, the wet-tray pressure drop is:

1. Operating liquid seal loss, clear liquid on tray

$$\begin{aligned} h_l &= \beta (h_w + h_{ow}) = 0.58 (2 \text{ in.} + 1.45 \text{ in.}) \\ &= 2.00 \text{ in. liquid} \end{aligned}$$

2. Total tray pressure drop:

$$\begin{aligned} h_t &= h_h + \beta (h_w + h_{ow}) \\ h_t &= 1.98 + 2.00 = 3.98 \text{ in. liquid} \end{aligned}$$

Weep Point

Surface Tension Head:

$$\begin{aligned} h_\sigma &= \frac{0.0405}{\rho_l d_h} = \frac{0.0405 (21)}{43.3 (0.1875)} \\ &= 0.1034 \text{ in. liquid} \end{aligned}$$

$$\text{Then: } A_h/A_a = 8.82/65.59 = 0.134$$

Referring to Figure 8-132:

$h_{l0} = h_w + h_{ow}$, in. liquid, height of clear liquid at overflow weir

$$h_{l0} = 2 \text{ in.} + 1.45 = 3.45 \text{ in.}$$

$$h_h + h_\sigma = 1.98 + 0.103 = 2.08 \text{ in. liquid}$$

Reading the intersection of 3.45 vs. 2.08 shows that for either weep point curve, the weep point is well below the values for operation, so this design not near the weep point.

Turndown Ratio

By trial and error the tray can be examined to determine the rates that will coincide with the weep point. Thus, the entrainment can establish the upper limit of operation, and the liquid weeping through the perforations represents the lower limit of stable operations; that is, turndown is generally used to represent the ratio of the

maximum allowable liquid rate (at flooding) to the minimum allowable operating throughput.

Downcomer liquid handling:

Based on clear liquid, downcomer velocity:

$$\begin{aligned} v_d &= \frac{\text{gpm}}{(7.48) (60) (A_d)} = \frac{504}{(7.48) (60) (10.5)} \\ &= 0.106 \text{ ft/sec} \end{aligned}$$

Referring to Table 8-20 for low foaming hydrocarbons on 24-in. tray spacing, this velocity of 0.106 fps is quite "safe" compared to a suggested range of 0.55–0.60 fps.

Based on tray spacing of 24 in., assume 50% downcomer full, then:

$$\begin{aligned} \text{height of liquid} &= 12 \text{ in.} = 1 \text{ ft} - 0 \text{ in. then,} \\ \text{residence time} &= 1 \text{ ft}/0.106 \text{ fps} = 9.43 \text{ sec} \end{aligned}$$

This is compared to about 3 sec reported by Bolles [190]. This should be checked, and the tray spacing may have to be increased, depending on the recalculation for the entire tray.

Liquid Gradient

Referring to equations for aerated liquid pressure drop,

$$h_f = \frac{h_l}{2\beta - 1} = \frac{2.001}{[2(0.58) - 1]} = 12.5 \text{ in.}$$

Velocity of froth:

$$l_f = 504 / (7.48 \text{ gal/ft}^3) (60 \text{ sec/min}) = 1.12 \text{ cfs}$$

$$v_f' = \frac{12 l_f}{h_l l_{fw}} = \frac{12 (1.12)}{(2.00) (9.1)} = 0.729 \text{ fps}$$

Note Tower diameter = 10.5 ft

$$\text{Weir length} = \frac{8.085}{18.58 \text{ ft}}$$

$$\text{Average length for } l_{fw} = 18.58/2 = 9.29 \text{ ft}$$

Hydraulic radius of aerated mass, $R_H = \frac{(\text{cross section})}{(\text{wetted perimeter})}$, ft

$$R_H = \frac{h_f D_f}{2h_f + 12D_f} = \frac{(12.5) (9.29)}{(2) (12.65) + (12) (9.29)} = 0.859 \text{ ft}$$

Reynold's Modulus:

$$\begin{aligned} R_{eh} &= \frac{R_H v_f' \rho_l}{\mu_l} = \frac{(0.859) (0.729) (43.3)}{[(0.32) (6.72 \times 10^{-4})]} \\ &= 1.260 \times 10^5 \end{aligned}$$

From Figure 8-127 read friction factor:
 $f = 0.018$ approximate extrapolation
 Area of downcomer flow segment:

$$\text{From Appendix Tables: } A = d^2(\text{coef}) \quad (8-301)$$

From Figure 8-100:

At 77% weir times tower diameter, then downcomer area = 12.4% of tower area, or 18% of tower diameter is downcomer width (depth, i.e. weir to wall = 0.18 (10.5) = 1.89 ft for one downcomer). Then, net free area between weirs = 10.5 - 1.89 - 1.89 = 6.72 ft

$$\begin{aligned} \text{Gradient, } \Delta', &= \frac{f (v_f')^2 l_{fp}}{g R_H} \\ &= \frac{(0.018) (0.729)^2 [(6.72) (12)]}{(32.2) (0.859)} = 0.0278 \text{ in.} \end{aligned}$$

This is low and should not be a problem across the tray.

Downcomer backup: Assume 1/2-in. clearance between bottom edge of downcomer and tray floor (or equivalent depending on design of downcomer-tray relationship.) See Figure 8-63.

$$A_d = h_{dcl} W_i / 144 \quad (8-302)$$

$$A_d = (1.5) [(8.085) (12)] / 144 = 1.01 \text{ ft}^2$$

Head loss through downcomer underflow:

$$h_{du} = (0.03) \left[\frac{L_g}{100 A_d} \right]^2 \quad (8-303)$$

$$h_{du} = (0.03) \left[\frac{504}{100 (1.01)} \right]^2 = 0.747 \text{ in. liquid}$$

Downcomer backup : See Equation 8-245;

$$\begin{aligned} H_d &= h_w + h_{ow} + \Delta + h_{du} + h_t \text{ in.} \\ &= 2 + 1.45 + 0.0278 + 0.747 + 3.98 \\ &= 8.20 \text{ in. liquid backup} \end{aligned} \quad (8-304)$$

This is satisfactory, because it is less than 50% of the tray spacing of 24-in. Therefore, the tray appears to have adequate liquid handling capacity. No hole blanking strips required.

Perforated Plates Without Downcomers

Perforated plates without downcomers have only recently been included in commercial equipment. The data for rating the performance is not adequately covered in the literature, since the present developments in industrial equipment have not been released. The information included here is based only on available data and experience, yet it may serve as a basis for rating, because the basic nature of the contact is quite analogous to the sieve tray. The limits of performance are not well defined; therefore the methods outlined cannot be considered firm. However, they are adequate for many applications and as the basis for further study.

The action of the perforated tray (Figure 8-146) is one of simultaneous flow of vapor and liquid through different holes on a tray; they do not flow countercurrently and simultaneously through the same holes. For a tray in its operating range, the liquid-vapor bubble mixture is in constant agitation. There is usually a level of relatively clear liquid on the tray followed on top by a bubbling, agitated mass, part of which becomes frothy and/or foamy in appearance depending upon the tray operation and the fluid system properties. There are wavelets of froth-liquid mixture moving from one place to another over the tray. As the head builds up sufficient to overcome the tray hole pressure drop, the vapor stops flowing in the region and liquid drips and drains through. As soon as the head is reduced, the draining stops and bubbling starts. This action is taking place randomly over the tray. Sutherland [69] observed that vapor was flowing through 70–90% of the holes, well distributed over the plate. Liquid flowed through the 30–10% of the holes.

The only available data for correlation is that of Sutherland on air-water [69] and of Myers [47] on two hydrocarbon systems. The latter data being at close tray spacings for laboratory columns.

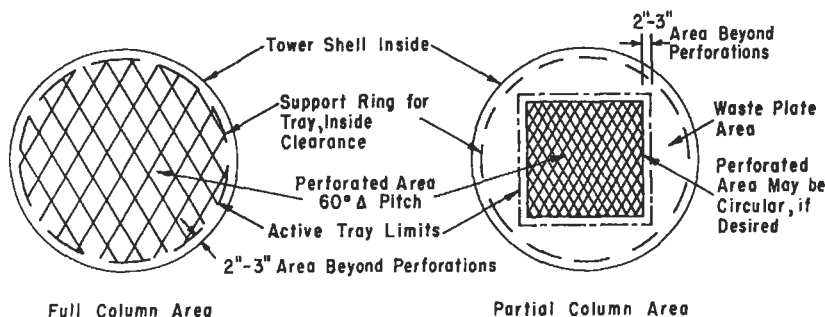


Figure 8-146. Perforated trays without downcomers.

These trays are somewhat sensitive to rapid changes in tower conditions. Towers over 40 trays must be controlled within fine limits.

The perforated plate, punched plate, or Dual-Flow plate are terms used to refer to a tray operating without downcomers, with vapor and liquid passing countercurrent through perforations in the tray. The Dual-Flow term has been coined by Fractionation Research, Inc., and its design know-how is restricted to contributing members, and cannot be presented in this book.

Diameter

There is essentially no published work on specific tests with these trays as relates to entrainment, etc. However, the very close similarity between a perforated plate without downcomers and one with downcomers is sufficient to justify using some data for one in the design of the second.

This is the case with diameter determination. The relation of Equation 8-250 for the perforated tray or sieve tray with downcomers can be used for the plate without downcomers. Generally, the liquid level and foam-froth height will be higher on this tray, hence the value of h_c , clear liquid on the tray, may range from 1-in. to 6-in. depending on the service.

Capacity

In general, the vapor capacity for a given tray diameter is 10–35% greater than bubble cap trays and somewhat greater than sieve trays with downcomers. The flexibility or range is limited because reasonable efficiencies fall-off near the dump point for most systems. Usual designs limit the lower operating point to 60–70 of the flood point, unless particular data is available to safely allow reduction in lower limits without the accompanying loss in tray efficiency.

Pressure Drop

The pressure drop of these trays is usually quite low. They can be operated at an effective bubbling condition with acceptable efficiencies and low pressure drops. For more efficient operation the clear liquid height on the tray appears to be similar to the sieve tray, i.e., 1.5–2-in. minimum. This is peculiar to each system, and some operate at 1 in. with as good an efficiency as when a 2-in. is used. When data is not available, 2 in. is recommended as a median design point.

Dry Tray Pressure Drop

As should be expected, the relation of Hughmark [31] correlated the data of Sutherland [69] quite well.

$$\text{thus: } h_{dt} = 0.003 (v_o^2 \rho_v) \left(\frac{\rho_{\text{water}}}{\rho_L} \right) (1 - \beta^2) / C_o^2$$

$$F_h^2 = v_o^2 \rho_v \quad (8-305)$$

The orifice coefficient can be read from Figure 8-128. Sutherland used $C_o = 0.85$ and 0.73 for $\frac{3}{16}$ -in. and $\frac{1}{4}$ -in. holes respectively, in $\frac{1}{4}$ -in. plate.

Effective Head, h_e

Although Sutherland did not obtain an equation for total tray pressure drop, correlation at this time indicates that it follows the effective head concept of Hughmark. This is a limited evaluation because the data available did not indicate any clear liquid heights over about 0.75 in.

When “head of liquid” is considered “clear liquid on the tray,” Figure 8-130 may be used to read the effective head, h_e . Values of h_{cl} beyond 1 in. have not been checked for lack of data, but do agree generally with the plotted results of Sutherland [69].

Total Wet Tray Pressure Drop

For the data checked,

$$h_t = h_{dt} + h_e, \text{ (also see Equation 8-268)} \quad (8-306)$$

These results cannot be expected to correlate for a tray just becoming active (very low liquid on tray, 0.1 in. \pm), but have been satisfactory at 0.2-in. for clear liquid height, h_{cl} .

To determine a tray operation with respect to pressure drop, the value of h_{cl} must be assumed at a reasonable value,—the larger the better the contact, and higher the pressure drop. Values of h_{cl} should be limited to about 4 in., following sieve tray practice.

Hole Size, Spacing, Percent Open Area

Hole size is as important in perforated plates without downcomers as far the sieve tray. Published data limits a full analysis of the relationships; however, the smaller holes, $\frac{1}{8}$ -in., $\frac{3}{16}$ -in., $\frac{1}{4}$ -in. appear to give slightly higher efficiencies for the same tray spacing [47]. Unfortunately the data [69] for the larger $\frac{3}{8}$ -in. holes was not evaluated for efficiencies. Experience has indicated efficiencies equal to or only slightly, 10–15%, less for $\frac{3}{8}$ -in. holes when compared to $\frac{3}{16}$ -in. holes for some systems. Holes as small as $\frac{1}{16}$ -in., $\frac{3}{32}$ -in. and $\frac{1}{8}$ -in. were considered unsatisfactory for high surface tension materials such as water [47].

Sutherland reports frothy type contact for $\frac{3}{16}$ -in. holes and jetting spray bubbly action for $\frac{3}{8}$ -in. holes.

Percent open tray areas of 20–30% appear to be optimum for hydrocarbon systems [47].

The larger holes are recommended for high surface tension liquids.

Holes are usually spaced a minimum of $2 d_o$, with $3 d_o$ to $4 d_o$ being preferable. The distance between holes should never exceed 3 in. Thin plates appear to be preferable to thick.

Tray Spacing

The height of the liquid-froth mixture on the tray is important in determining tray spacing, as tray flooding moves up the column as the liquid mixture of one tray approaches the underside of the tray above. Tray spacing is recommended as twice the maximum design height of liquid-froth mixture on the tray h_{al} . Spacing of 9, 12, 15, 18 and 24 in. have been used with good success. The closer the spacing, the less the tray flexibility. The 15-in. spacing is usually a good design value.

The height of aerated liquid-froth mixture on the tray, h_{al} , (in.) was determined to agree with the following relation [69] for air-water for 23% and 40% open trays.

$$h_{al} = 1.25 F_c + 0.0005 L + (0.54/\beta) - 2.45 \quad (8-307)$$

$$F_c = v_c \rho_v^{1/2} \quad (8-308)$$

L = Liquid rate, lb/(hr) (ft² of active plate)

This relation does not hold for plates having 10% open hole area, as the heights are several times the corresponding heights for 23% and 40% trays at the same vapor rate, F_c .

For water, the total height of aerated mixture relative to the height of clear liquid on the tray, h_{al}/h_{cl} , had values of 10 to 3. The higher values being obtained from the $\frac{3}{16}$ -in. (smaller) holes. Liquid flow rate does not appear to influence these values to any extent.

Higher open tray areas tend to produce a spray rather than a froth. High vapor rates produce a spray, while the higher liquid rates produce a froth [69].

If these trays are used in systems with exceedingly high foaming tendencies, tray action may be impaired to the extent of improper performance. In such cases, the foaming tendency should be examined experimentally. Antifoam agents have proven quite helpful in some problem cases using these trays.

Entrainment

Data are not available to distinguish between the entrainment of sieve and perforated trays without downcomers. The relation of Hunt et al. [33] given for sieve trays is recommended, and should apply quite well.

Sutherland [69] reports for air-water entrainment of 0.0001 to 0.1 lb liquid/lb vapor, averaging 0.01 for 15-in. tray spacing at hole velocity F_s values of 3 to 15. $F_h = v_o \rho_v^{1/2}$. These values are 1–10% of bubble cap plates. Simkin et al., [64] reports a comparison with the Turbo-grid tray giving only 3–60% of the entrainment of bubble caps over a wide range of operation.

Sutherland's [69] relation for air-water on 15-in. tray spacing correlating $\frac{3}{16}$ -in. holes on 40% and 23% open area, and $\frac{3}{16}$ -in. holes with 23% open area is:

$$e_w = 6.31 (10^{-7}) (F_s)^{4.57} \quad (8-309)$$

where e_w = entrainment, lb liquid/lb vapor

The correlation of $\frac{3}{16}$ -in. holes in 40% open trays is

$$e_w = 2.37 (10^{-4}) (F_s)^{1.73} \quad (8-310)$$

Why this deviates from the previous correlation is not understood.

Dump Point, Plate Activation Point, or Load Point

These trays will dump liquid excessively through the perforations giving exceedingly low efficiencies [47] unless a minimum vapor rate is maintained for a given liquid capacity. The smaller the holes the lower the dump point (vapor velocity).

Figure 8-147 indicates minimum values of F_h to initiate acceptable bubbling tray action. Efficiency at this activation or load point might be expected to be low; however Myers results indicate good values at this rate.

It is recommended that trays be designed for a minimum of 10% above the lower plate activation values. Below these values the tray will dump liquid and become inoperable.

Efficiency

Tray efficiency is as high as for bubble caps and almost as high as sieve trays. It is higher than bubble caps in some systems. Performance indicates a close similarity to sieve trays, since the mechanism of bubble formation is almost identical. The real point of concern is that the efficiency falls off quickly as the flow rate of vapor through the holes is reduced close to the minimum values represented by the dump point, or point of plate initial activation. Efficiency increases as the tray spacing increases for a given throughput.

Myers found only a slight decrease in efficiency with an increase in hole size. Industrial experience indicates that large holes of $\frac{1}{2}$ -in. and $\frac{3}{8}$ -in. can be designed to operate as efficiently as a small hole, say $\frac{3}{16}$ -in.

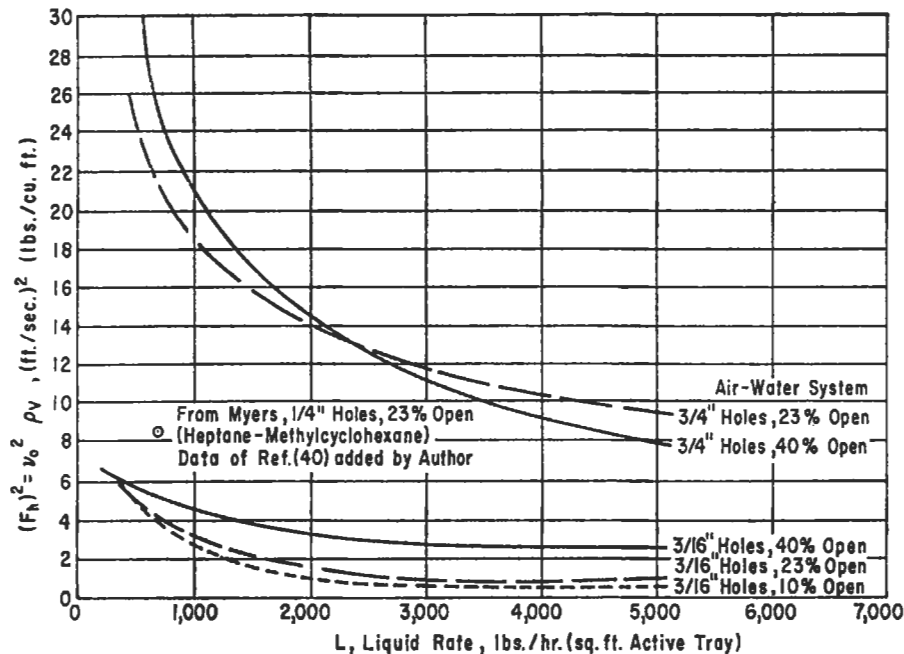


Figure 8-147. Vapor and liquid rates for tray activation; perforated trays, no downcomers. Compiled from data of Sutherland [69] and Myers [47].

Efficiency appears to fall off significantly for open tray areas above 30%. The higher efficiencies are usually obtained in the 20–25% range of open hole area [47].

Higher efficiencies are obtained for operating conditions within 85–95% of the tray flood point.

Flood Point

At the flood point, liquid continues to flow down the column, but builds up at a greater rate from tray to tray. Sutherland [69] demonstrated that flooding moves up the column from the point of origin. For this reason it is important to design perforated trays without downcomers with extra care, as changing internal rates are quickly reflected in performance if the proper hole requirements are not met. They are a useful tray for steady state operations.

Tray Designs and Layout

1. Establish a tower design diameter using the Souders-Brown method or the relation of Hunt, both given previously.
2. Determining the vapor and liquid rates in the tower at all possible critical points of change. The anticipated maximum and minimum values must be defined.
3. Determine the values of the plate activation velocities (or load points), F_h^2 , for the minimum as well as maximum liquid loads at top and bottom of the tower and any intermediate points exhibiting significant change in flow rates. For partial column area

trays of Figure 8-146 the v_c refers to the area of active tray limits. If the minimum rates are more than 20% below the maximum, the smaller hole sizes and open areas should be selected.

4. Select a design hole vapor rate, v_o , of 1.25 to 1.5 times the minimum values of the plate activation point, or about 25% below the hole velocity at flood conditions.
5. Check the number of holes required at each maximum rate to determine if the required holes can be placed in the tower area.

Use Figure 8-144 to aid in the determination. If more plate area is required than is available, back-calculate the necessary maximum hole velocity. Check if this is reasonable (say not over twice the minimum). If so, the diameter is still acceptable; or change the hole spacing to allow more or fewer holes to be placed in the given diameter of the tower. Use limiting values previously given on hole spacing.

6. Calculate the total wet tray pressure drop, using an assumed height of clear liquid on the tray of 0.5-in. minimum to 4-in. maximum (1 to 2-in. are usual values).
7. Determine height of aerated liquid on the tray, h_{a1} .

If foaming characteristics of the system are less than air-water, results will be conservative. For systems tending to greater foam and bubbles than the air-water system, approximate a value of h_{a1} by multiplying calculated value by 2, or 3 or known relative relationship.

8. Set tray spacing at twice the selected value of h_{a1} .
9. Check entrainment at maximum vapor rate.
10. Physical arrangement: refer to Figure 8-146.

For new towers, the designs will usually develop to utilize the entire tower cross-section. However, for existing towers with perforated trays being installed to replace bubble caps or packing, the optimum active tray area may not utilize the entire cross-section. If the number of holes required is small compared to available area, it is better to group the holes on $2.5 d_o$ to $3.5 d_o$ than to exceed these limits. Holes separated by more than 3 in. are not considered effective in tray action so necessary for good efficiency. Blanking strips may be used to cover some holes when more than required have been perforated in the tray.

If trays are punched, the sharp hole edge side should face the entering vapor.

Example 8-40: Design of Perforated Trays Without Downcomers

A tower separates a weak ammonia solution. Design trays using perforated plates without downcomers for the following conditions as determined from the column performance calculations.

	<u>Top Tray</u>	<u>Bottom Tray</u>
Liquid, gpm	40.8	17.8
Lb/ft ³	38.8	54.2
Dynes/cm	<13	59
Vapor, ft ³ /sec	5.22	4.3
Lb/ft ³	0.593	0.408

Estimated Tower Diameter

$$e_w = 0.22 (73/\sigma) (v_c/S')^{3.2}$$

Allowable velocity: assume $S' = 15$ in. - 2.5 (1.5 in.) = 11.25 in.

From Figure 8-121 for $e_w = 0.05$ and assumed 15-in. tray spacing at top, tower velocity $v_c = 4$ ft/sec

at bottom, $v_c = 6.4$ ft/sec

Tower area at 4 ft/sec limiting: = $5.22/4 = 1.30$ ft²

Diameter = $[(4/\pi) 1.30]^{1/2} = 1.29$ ft. Say 1 ft 6 in.

Comparison:

Souders-Brown, Figure 8-83 at top tray conditions, which are limiting.

$W = 2000$ lbs/hr (ft²) Max. allowable vapor velocity

Top vapor rate = $5.22 (0.593) (3600) = 11,130$ lb/vapor/hr

Required area = $11,130/2000 = 5.5$ ft²

Diameter = 2.64 ft, Say 2 ft, 8 in.

Because it is known that the entrainment from perforated trays is considerably less than for bubble caps, the 2-ft, 8-in. diameter would be very conservative and perhaps excessively large.

Tower diameters in the 1-ft, 6-in. to 2-ft range are not usually economical as tray installations. A packed tower might prove the best economically. Trays can be installed on a central rod and spacer arrangement, with seals between trays and tower shell. Such an arrangement usually brings the cost of the installation up to that of a 2-ft, 6-in. tower. This is the smallest practical size that a man can crawl through.

For the purpose of this design, assume that a cost study has verified the above remarks, and a 2-ft, 6-in. tower will be used. This means that entrainment will be very low on a 15-in. tray spacing. Therefore, a smaller spacing should be considered. From usual fabrication costs, 12-inch spacing is about the closest spacing to consider.

The allowable velocity by Hunt for this spacing, $S' = 8.25$, $v_c = 4$
 $(8.25/11.25) = 2.94$ ft/sec

Tower area = $\pi (2.5)^2/4 = 4.9$ ft²

Actual tower velocity = $5.22/4.9 = 1.06$ ft/sec

Therefore 12-in. spacing should be O.K. entrainment-wise, check aeration later.

Plate Activation Velocities (Minimum)

Top:

Liquid rate, $L = (40.8 \text{ gpm}/7.48) (38.8) (60)$
 $= 12,200$ lb/hr (ft²)

From Figure 8-147, read $F_h^2 = 1.0$ @ $\frac{3}{16}$ -in. holes, 23% open area.

$$(v_o \rho_v^{1/2})^2 = 1.0 = v_h^2 \rho_v$$

$$v_o = (1/\rho_v)^{1/2} = (1/0.593)^{1/2} = 1.298 \text{ ft/sec}$$

Bottom:

$L = 17.8 (54.2) (60)/7.48 = 7,730$ lb/hr (ft²)

From Figure 8-147 read $F_h^2 = 1.0$ @ $\frac{3}{16}$ -in. holes, 23% open area
 $v_h = (1/0.408)^{1/2} = 1.56$ ft/sec

Note that Figure 8-147 indicates the operating liquid minimum range is quite stable in the region of design for these trays. The vapor rate must never fall below the above values or instability will immediately set in and dumping will result.

Design Hole Velocity

Set at 1.5 times the activation velocity, or 2.34 ft/sec at the top and 1.95 ft/sec at the bottom.

Hole Arrangement

$\frac{3}{16}$ -in. dia. on $60^\circ\Delta$ pitch, spaced on $\frac{3}{8}$ -in. centers

This gives 22.6% open area (Figure 8-143), close enough to the 23% selected.

No. holes/in² = 8.3

Area required for holes:

Top: $5.22/2.34 = 2.23$ ft²

No. holes = $2.23 (144) (8.3) = 2670$

Bottom: $4.3/1.95 = 2.2$

No. holes = $2.2 (144) (8.3) = 2640$

Since these are so close the same number of holes can be perforated in all plates. These should be drilled (punched) in a 1-ft, 6-in. \times 1 ft, 6-in. square area as per Figure 8-145. This will reduce costs of trays slightly as compared to custom perforating to different number of holes.

The tower area is 4.9 ft²; therefore the entire tray will not be perforated for the conditions of design.

If there is the possibility of vapor and liquid rates being reduced to 50% of the indicated values, this would place the trays as selected above at the dumping point, or activation point, which is not a good operating condition. In this situation the number of holes should be reduced in order to maintain a velocity of vapor through the holes greater by at least 15% than the activation velocity.

Wet Tray Pressure Drop

(a) Dry Tray Pressure Drop

$$h_{dt} = 0.003 (v_o^2 \rho_v) \left(\frac{\rho_{\text{water}}}{\rho_L} \right) (1 - \beta^2) / C_o^2$$

Top appears to be region of greatest pressure drop $h_{dt} = 0.003 [(2.34)^2 (0.593)] (62.3/38.8) (1 - (0.226)^2) (0.82)^2$

$C_o = 0.82$ for $\frac{3}{16}$ -in. hole in $\frac{3}{8}$ -in. tray (Figure 8-128)

$h_{dt} = 0.0222$ in. liquid

(b) Effective Head

Assume clear liquid height on tray = 1 in. (note, 1 in. may be a slightly better value than the 1.5 in. assumed when determining e_w).

From Figure 8-130, effective head, $h_e = 1.1$ in. liquid at $F_s = 2.34 (0.593)^{1/2} = 1.81$

(c) Total wet tray pressure drop

$$h_t = 0.022 + 1.1 = 1.12 \text{ in. liquid}$$

Total Tower Tray Pressure Drop

For 15 trays, the maximum expected drop using the expected tray drop at the top:

$$= 15 (1.12) = 16.8 \text{ in. liquid}$$

$$= \left(\frac{16.8}{12} \right) \frac{(38.8)}{2.31 (62.3)} = 0.38 \text{ psi}$$

A more precise approach requires evaluation of the wet tray drop for the bottom condition also. However, since it will give a lower value (by inspection), the higher result is preferred as long as a vacuum tower is not being designed. Here, the careful approach is justified.

It must also be remembered that the data used in establishing the design criteria are not accurate to better than ± 10 –20%.

Height of Aerated Liquid on Tray

$$h_{al} = 1.25 F_e + .0005L + (0.54/\beta) - 2.45$$

At top:

$$= 1.25 [(1.06) (0.593)^{1/2}] + .0005 (12,200) + 0.54/0.226 - 2.45$$

$$= 1.002 + 6.1 + 2.39 - 2.45$$

$$h_{al} = 7.06 \text{ in. (evaluated as air-water)}$$

Tray Spacing

From this value of h_{al} it is essential that the trays be spaced no closer than 2 (7.06), say 15 in. If lab tests indicate these mixtures foam more than water-air, the value of 15 in. should be increased in relative proportion.

Proprietary Valve Trays Design and Selection

For proper design of proprietary valve trays (see previous illustrations), the design operating data, basic thermodynamics, and physical properties of the fluids must be submitted to the appropriate manufacturer's technical department for evaluation and final design recommendation. Often the designer for the operating company has established sufficient computer programs to essentially make the equivalent studies as the tray manufacturer, for example see Figure 8-54. To examine the variations in expected tray(s) performance, several select studies must be made, and results plotted, to analyze the variables and their effects on performance. Billet [208] has reviewed the progress in the design and performance of valve trays.

Klein [201] has evaluated from the literature including manufacturer's, i.e., Glitsch [202], Koch [203], and Nutter [204], design procedures for their respective valve type tray

and has developed an approximation procedure suitable for *estimating* designs. This procedure then can be confirmed by the respective manufacturers' examining for the unique application of their valve trays. Note that Klein's [201] references to the manufacturers design manuals are somewhat earlier versions, but are not anticipated to significantly change the estimating value by the design engineer. Klein's design method summary follows (by permission):

Dry Tray Pressure Drop

For an operating tray the pressure drop profile is shown in Figure 8-148 [201]. The valves are "closed" at low hole vapor velocities, although, due to the design of the valves (see Figures 8-72 and 8-74), the metal tabs keep some styles of valves open sufficiently to allow some vapor and some liquid through, even at low flow rates.

In the Figure 8-148 point "A" is where the valves on the tray are still "closed" but are just beginning to open. The pressure drop increases as the velocity increases from "0" to point "A."

The vapor hole velocity at "A" is [201]:

$$v_{pt, A} = \sqrt{T_v R_{vw} (C_{vw} / K_c) (\rho_{vm} / \rho_v)}, \text{ ft/sec} \quad (8-311)$$

where $v_{pt, A}$ = vapor velocity through holes, closed balance point, ft/sec

T_v = metal thickness of valve, in.

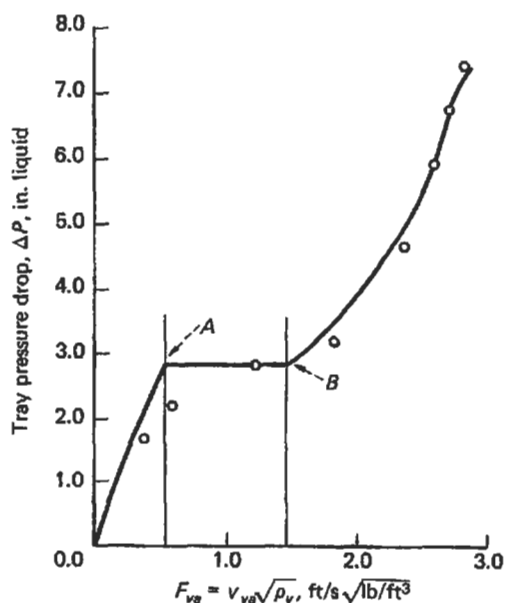


Figure 8-148. Typical operating valve tray pressure drop profile. Valves start to open at A, the closed balance point. Used by permission, Klein, G. F. *Chem. Eng.* V. 89, No. 9 (1982) p. 81; all rights reserved.

R_{vw} = ratio, valve weight with legs/valve weight without legs, dimensionless, Table 8-22.

C_{vw} = eddy loss coefficient, dimensionless, Table 8-22

K_c = loss coefficient, valves closed (sec)² (in.)/ft², see Table 8-23

$v_a = v_{va}$ = vapor velocity through tray active bubbling area, ft/sec

F_{va} = tray factor based on active bubbling area
= $v_{va} = v_h \sqrt{\rho_v}$, (ft/sec) ($\sqrt{lb/ft^3}$)

ρ_{vm} = valve metal density, lb/ft³, Table 8-24

ρ_v = vapor density, lb/ft³

g = acceleration of gravity, 32 ft/(sec-sec)

v_h = vapor velocity through valve holes, ft/sec

β = tray aeration factor, dimensionless

ΔP = tray pressure drop, in. liquid

ρ_{vm} = valve metal density,

t_d = tray deck thickness, in.

ϕ = relative froth density, dimensionless

Note: In Table 8-22 for R_{vw} , the flat orifice refers to a rectangular design valve and the venturi refers to a circular style valve.

The pressure drop remains essentially constant as long as the liquid flow on tray remains steady during the period point A to point B on the diagram (the open balance point) [201]. At point B all valves are completely open off their seats, but are on the verge of closing and may be oscillating from open to closed. At point B the vapor velocity through the holes, opened balance point is:

$$v_{pt, B} = \sqrt{T_v R_{vw} (C_{vw} / K_o) (\rho_{vm} / \rho_v)}, \text{ ft/sec} \quad (8-312)$$

$$v_{pt, A} / v_{pt, B} = \sqrt{K_c / K_o} \quad (8-313)$$

where K_o = loss coefficient, valves opened, (sec)² (in.)/ft², Table 8-23

$v_{pt, B}$ = vapor velocity through holes, open balance point, ft/sec

Values of R_{vw} , and C_{vw} are given in Table 8-22 and ρ_{vm} in Table 8-24. The closed and open loss coefficients for the dry tray pressure drop are given in Table 8-23.

Table 8-22
Coefficients for the Closed and Open Balance Point
Equations: Equations 8-311 and 8-312

Valve type	Flat orifice, R_{vw}	Venturi orifice, R_{vw}
3 legs	1.23	1.29
4 legs	1.34	1.45
Caged (no legs)	1.00	1.00

(Note: Obtained from measurements on valves)

$C_{vw} = 1.3$ for flat and venturi valves

Used by permission, *Chem. Eng.* Klein, G., May 3 (1982), p. 81; all rights reserved.

Table 8-23
Closed and Open Loss Coefficients for Dry Tray
Pressure Drop Equations 8-314 and 8-315

Orifice type	Tray deck thicknesses of:		
	0.134 in. (10 gage)	0.104 in. (12 gage)	0.074 in. (14 gage)
K_c			
Flat	6.154	6.154	6.154
Venturi	3.077	3.077	3.077
K_o			
Flat	0.821	0.931	1.104
Venturi	0.448	0.448	0.448

Used by permission, *Chem. Eng.*, Klein, G., May 3, (1982), p. 81; all rights reserved.

Table 8-24
Common Materials Used for Distillation Valves

Metals	Weight, lb/ft ³
Carbon steel	490
Type 304 Stainless Steel	501
Type 316 Stainless Steel	501
Type 310 Stainless Steel	501
Chrome Stainless Steel, 400 series	484
Monel, 400	551
Nickel	555
Aluminum	170

Turndown: It is proposed by Klein [201] that the oscillatory motion of the valve accounts for the greater turn-down of a valve compared to other tray-valve designs. The turn-down can be controlled by the number of "working" or oscillating valves on the tray, or by changing the uniformity of weight of the valves per tray or the valve design to obtain different velocities through different valves on the same tray.

Beyond point B on the diagram, the pressure drop for the tray increases as the vapor rate increases. Use Equation 8-314 or 8-315 to determine the dry tray pressure drop, ΔP , in. liquid, Bolles [205] per Klein [201]:

For closed valves: $h_h = K_c (\rho_v/\rho_l) v_h^2$, in. liquid (8-314)

For open valves: $h_h = K_o (\rho_v/\rho_l) v_h^2$, in. liquid (8-315)

where v_h = vapor velocity through holes, ft/sec

h_h = dry tray pressure drop, in. tray liquid

ρ_l = liquid density, lb/ft³

ρ_v = vapor density, lb/ft³

Aerated-Tray Liquid Pressure Drop

Klein [201] has developed the correlation based on published data of others (his citations) as shown in Figure 8-149. Because the method of aeration between sieve trays [205] and valve trays is different [201], the same aeration correlation cannot be used, because valve trays have lower

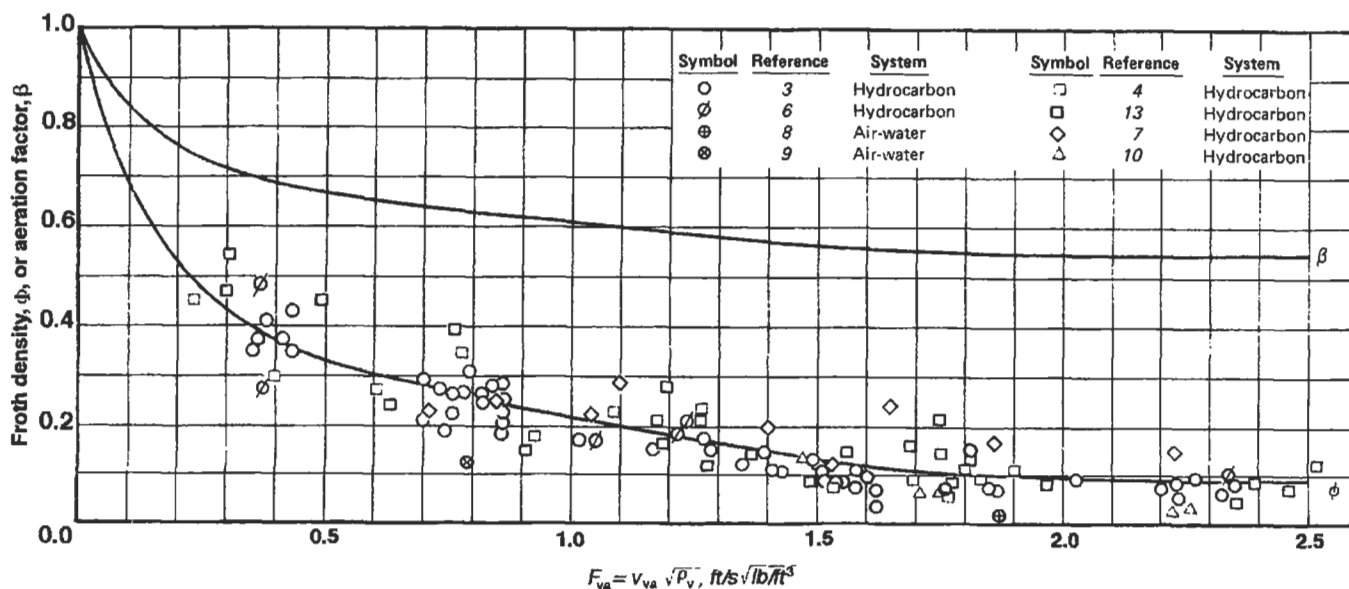


Figure 8-149. Correlation for aerated-tray-liquid pressure drop developed from published data for various valves. Note: ϕ = relative froth density. Reference numbers are from original article [201]. Used by permission, Klein, G. F., *Chem. Eng.* V. 89, No. 9 (1982), p. 81; all rights reserved.

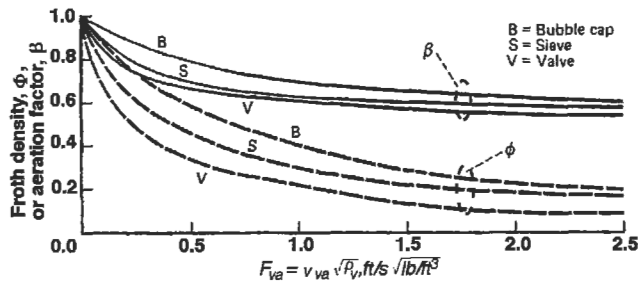


Figure 8-150. Valve trays have the lowest liquid pressure drop of all three types of trays employed (also see Ref. 88, 183, 193 for additional interpretation). Used by permission, Klein, G. F., *Chem. Eng. V.* 89, No. 9 (1992), p. 81; all rights reserved.

liquid ΔP . Figure 8-150 [201] compares the aeration factor for valve, sieve, and bubble cap trays. Figure 8-149 also presents a curve for the relative froth density, ϕ , used for determining froth height as:

$$h_f = h_l / \phi \quad (8-316)$$

$$h_l = \beta (h_w + h_{ow}) \quad (8-317)$$

$$h_{ow} = 0.48 (Q_l / L_{wi})^{2/3}$$

Hutchinson cited by Klein [201] developed the relation between β and ϕ ;

$$\beta = (\phi + 1) / 2$$

with this equation, the aeration factor curve β can be developed from the relative froth density curve of Figure 8-149.

Overall tray pressure drop: [201]

$$h_t = h_h + h_l \quad (8-318)$$

$$\text{or, } h_t = h_h + \beta (h_w + h_{ow}) \quad (8-319)$$

where h_t = total tray pressure drop, in. tray liquid
 h_l = aerated tray liquid pressure drop or equivalent clear liquid on a tray, in. tray liquid
 h_f = froth height on tray, in.
 h_h = dry tray pressure drop, in. tray liquid
 h_w = weir height, in.
 h_{ow} = crest of liquid over tray weir, in. liquid
 β = tray aeration factor, dimensionless
 ΔP = tray pressure drop, in. liquid
 ϕ = relative froth density, dimensionless
 Q_l = liquid flow on tray, gal/min
 L_{wi} = weir length, in.
 F_{va} = tray F Factor, based on active bubbling area

$$= v_{va} \sqrt{\rho_v}, (\text{ft/sec}) \left(\sqrt{\text{lb/ft}^3} \right)$$

 G = vapor rate through all valves, lb/hr

Example: 8-41: Procedure for Calculating Valve Tray Pressure Drop (after Klein [201])

For a venturi type tray, assume the following conditions:

Vapor flow: = 50,000 lb/hr = G
 Liquid flow: = 205 gpm = Q_l
 $\rho_v = 1.91 \text{ lb/ft}^3$
 $\rho_l = 31.0 \text{ lb/ft}^3$
 $L_{wi} = 55 \text{ in.}$
 $h_w = 3 \text{ in.}$
 $F_{va} = 1.1$

Tray froth height: Assume: 12 in.

Per cent of jet flood: 65%

Valve thickness: 16 gage (0.060 in.), 4-legs

Valve material: carbon steel, see Table 8-24.

Valve hole area: 1.65 sq. ft. (separate calculation) = h_o

Tray pressure drop and froth height:

1. Determine $v_{pt, A}$ and $v_{pt, B}$, from Equations 8-311, 312, or 313.

$$v_{pt, A} = \frac{\sqrt{T_v R_{vw} (C_{va} / K_c) (\rho_{vm} / \rho_v)}}{\sqrt{(0.06) (1.45) [(1.3 / 3.077) (490 / 1.91)]}}, \text{ft/sec}$$

Closed:

$$v_{pt, A} = 3.06 \text{ ft/sec}$$

Open:

$$\frac{v_{pt, B}}{v_{pt, A}} = \sqrt{K_c / K_o}$$

$$v_{pt, B} = 3.06 \sqrt{3.077 / 0.448} = 8.01 \text{ ft/sec}$$

2. Determine actual hole velocity, v_h :

$$v_h = \frac{G}{(3,600) (\rho_v) (a_h)} = \frac{50,000}{3600 (1.91) (1.65)} = 4.40 \text{ ft/sec}$$

Because the actual velocity is operating between the point A and point B, ($v_{pt, A}$ and $v_{pt, B}$):

$$h_h = K_c (\rho_v / \rho_l) (v_h)^2, \text{ for closed valve} = 3.077 (1.91 / 31.0) (3.06)^2 = 2.08 \text{ in. liquid}$$

$$h_h = K_o (\rho_v / \rho_l) (v_h)^2 = 0.448 (1.91 / 31) (8.01)^2 = 1.77 \text{ in. liquid, open valve}$$

Because the tray is not near jet flooding, referring to Figure 8-149,

$$F_{va} = 1.04, \text{ then } \beta = 0.61$$

$$h_{ow} = 0.48 (Q_l / L_{wi})^{2/3} = 0.48 (205 / 55)^{2/3} = 1.15 \text{ in. liquid}$$

$$h_l = \beta (h_w + h_{ow}) = 0.61 (3 + 1.15) = 2.53 \text{ in. liquid}$$

Overall Tray Pressure Drop:

$$h_t = h_h + h_l = 1.77 + 2.53 = 4.3 \text{ in. liquid}$$

Froth Height:

$$h_{ow} = 1.15 \text{ in. liquid, (see calculation above)}$$

Using F-Factor, determine β and ϕ from Figure 8-149.

$$\text{at } F_{va} = 1.04, \text{ then: } \beta = 0.61 \text{ and } \phi = 0.22$$

$$h_l = 2.53 \text{ in. liquid. (see calculation above)}$$

Calculate froth height, h_f :

$$h_f = h_l/\phi = 2.53/0.22 = 11.5 \text{ in.}$$

Klein [201] refers to Thorngren [206, 207] but suggests that this proposed valve tray flooding is reasonably involved, although considered useful.

Proprietary Designs

The design engineer cannot adequately design a valve tray that includes the operating valves and expect to have reliable performance. The proper approach is to assemble all of the required system/column operating performance requirements and then turn the problem over to a manufacturer who has tested its own valve designs and is capable of predicting reliable performance. The manufacturer can then provide a hydraulic design for the tray, as well as the expected performance of the entire column/tray system. The major manufacturer/designs are Nutter Engineering, Harsco Corporation, [204]; Koch Engineering Co., Inc. [203]; Glitsch, Inc. [202], and Norton Chemical Process Products Corporation [233].

There are other manufacturers and engineering companies that are capable through good computer programs of designing competitive distillation designs, and it is not the intent of the above listing to omit any reliable organization, but to simply list the generally considered major suppliers in the U.S.

One important point to consider is whether or not the organization has obtained commercial sized data on equipment designed and fabricated to their designs, and how the two results compare. The respective design procedure as set forth in each company's design manual will not be outlined in this text, as there is too much detail necessary to produce a reliable tray performance design, and this is included in the manuals. The overall purpose of the information presented in this text is to allow the designer to (1) become knowledgeable in the component details necessary for a proper design and be able to com-

municate with the final designer/manufacturer and interpret the significance of the final results, and (2) be capable of preparing approximate designs for preliminary information and to develop calculated results to compare with the final designs of others. The designs developed by the methods/procedures presented here are considered reliable for these purposes, and even as final designs, provided there are actual process data and experience to compare with.

Capps [188] compares valve and sieve tray performance as related to capacity and flooding. Also see sieve tray section presented earlier in this chapter.

Capps [188] examines sieve and valve tray capacity performance and Figure 8-151 [188] is offered for preliminary column sizing or for determining whether a debottlenecking study is justified. The correlation for flooding, tray rating, and design of a tray are all based on the capacity factor, C_T , equation (Souders and Brown [68] by Capps [188]).

At total reflux ($L/V = 1$) Capps found several points in the FRI data that corresponded with this [241] definition of ultimate capacity, i.e., the liquid and vapor load at which any increase in either liquid or vapor would induce flooding by at least one of the following mechanisms:

1. Figure 8-151 shows capacity factor (Souders-Brown velocity) versus system factor (pressure, in this case for hydrocarbons) with L/V as a parameter. In Figure 8-151 the predicted ultimate capacity for a hydrocarbon is obtained by reading the capacity factor at incipient flood for a given pressure at a given reflux ratio, L/V . This Souders-Brown velocity then can be used to predict the maximum load achievable for a given column diameter, or, the minimum tower area required for a given load [188, 241].
2. Flood factor is the usual design safety factor (e.g., 80% of flood, $F_{\text{flood}} = 0.80$)

$$C_T = m_{\text{vap}} (24/S)^{0.5} / [A_T (\rho_{\text{vap}} (\rho_{\text{liq}} - \rho_{\text{vap}}))^{0.5}] \quad (8-320)$$

$$V_{\text{load}} = m_{\text{vap}} / [(\rho_{\text{vap}} (\rho_{\text{liq}} - \rho_{\text{vap}}))^{0.5}]^{0.5}, \text{ ft}^3/\text{sec} \quad (8-321)$$

$$\text{or, } C_T = V_{\text{load}} / (A_T) (24/S)^{0.5}, \text{ ft/sec}$$

$$\text{or, } D_T = [6.238 m_{\text{vap, flood}} / (F_{\text{flood}}) (C_{T, \text{flood}}) (\rho_{\text{vap}} (\rho_{\text{liq}} - \rho_{\text{vap}}) S)^{0.5}]^{0.5} \quad (8-322)$$

$$\text{Capacity factor, } C_T = V_{\text{load}} / A_T$$

$$V_{\text{load}} = m_{\text{vap}} / [(\rho_{\text{vap}} (\rho_{\text{liq}} - \rho_{\text{vap}}))^{0.5}]^{0.5}, \text{ ft}^3/\text{sec} \quad (8-323)$$

Using the Souders-Brown factor:

$$C_T = m_{\text{vap}} (24/S)^{0.5} / [A_T (\rho_{\text{vap}} (\rho_{\text{liq}} - \rho_v))]^{0.5} \quad (8-324)$$

or,

$$C_T = V_{\text{load}} / (A_T) (24/S)^{0.5}, \text{ ft/sec} \quad (8-325)$$

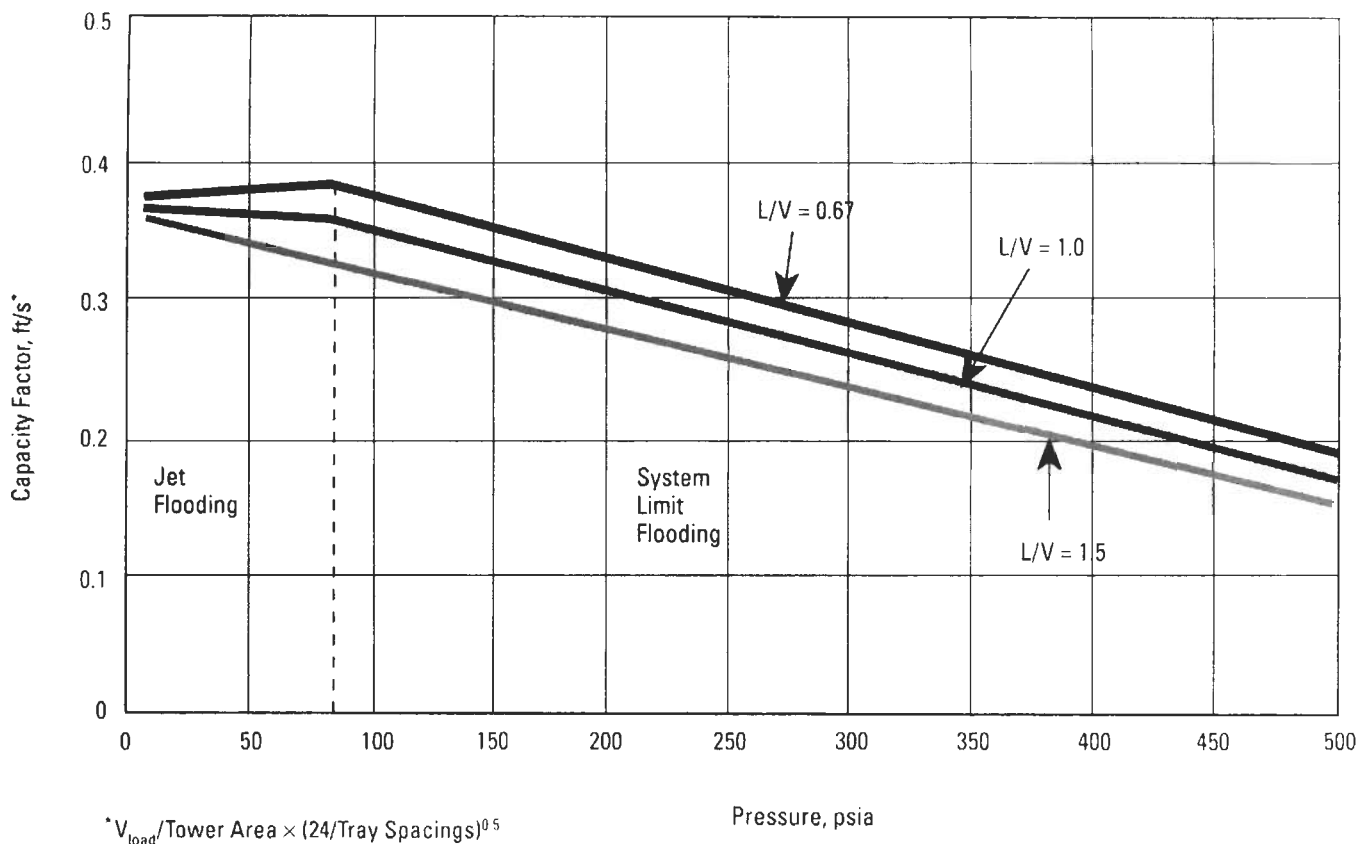


Figure 8-151. Graphical correlation of sieve tray ultimate capacity for hydrocarbons. Used by permission, Capps, R. W., The American Institute of Chemical Engineers, *Chem. Eng. Prog.* V. 89, No. 3 (1993), p. 35, all rights reserved.

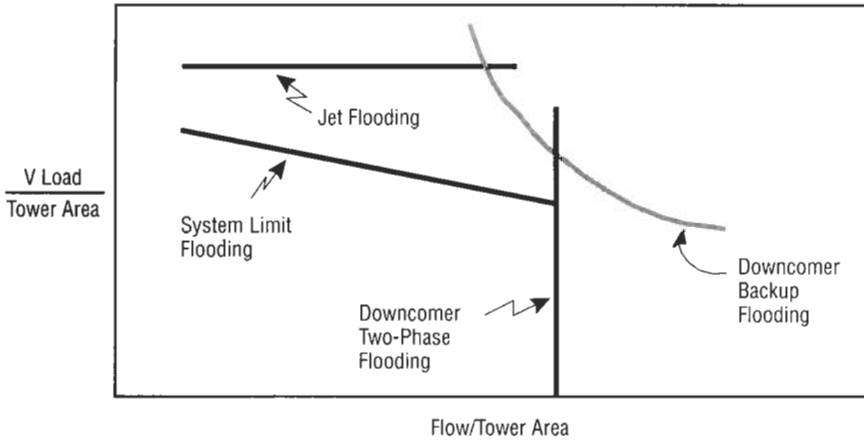
Capps analyzes that from Figure 8-151 [188], which was derived from data of Fractionation Research, Inc. in commercial scale tests, a 450-psig deethanizer operating at a capacity factor of 0.18 in the rectifying section may not be worth retraying to debottleneck a process, while a 30-psig crude column at a capacity factor of 0.25 may provide a good economic rate of return for retraying operation/or revamp. These generalized decisions are established by spotting the capacity factors on the chart and noting the potential improvement possible to reach the appropriate L/V curve.

Note that “jet flooding” capacity is fairly insensitive to system physical properties, but that the “system limit” capacity is strongly dependent on physical properties.

Generalized mechanical performance of high pressure and vacuum tray hydrocarbon distillation are shown in Figures 8-152A and 8-152B. The representations are for concepts only and do not represent any published data per se. The charts illustrate the effects of physical properties and pressure on flooding situations. Because flooding is an important condition that limits the performance and capacity of a column, it deserves attention and understanding. The four mechanisms of flooding are [188]:

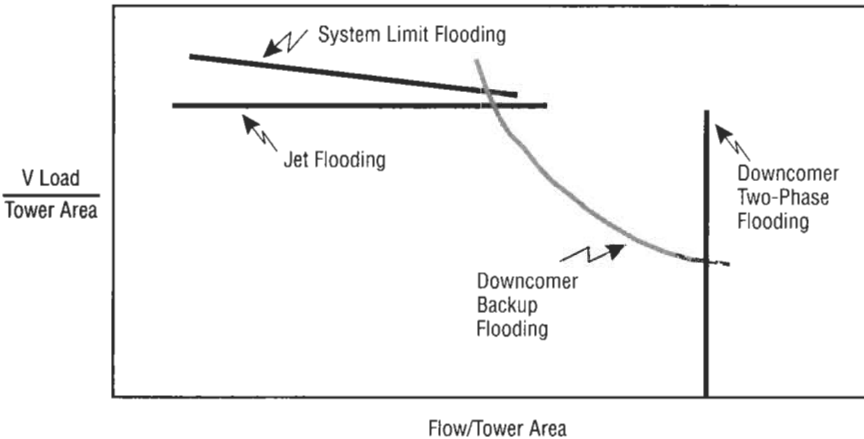
1. *Jet flooding* occurs due to liquid entrainment induced by vapor jets passing through the liquid flowing on the tray. The entrained droplet may carry into the tray area above and reduce tray efficiency and capacity.
2. *System limit flooding* is similar to jet flooding, due to low surface tension and low density difference between liquid and vapor. Terminal velocity of some entrainment droplets is less than the upward vapor velocity, and hence they are carried up into the tray above, thus reducing tray efficiency and capacity.
3. *Downcomer backup flooding* results from pressure drop at bottom outlet of downcomer, causes liquid to back-up in the downcomer and flood the tray above. Generally the cause is due to excessive tray pressure drop.
4. *Downcomer two-phase flooding* results from vapor failing to disengage from downcomer liquid, and causing two-phase flow to pass through the downcomer bottom outlet, causing backup in the downcomer to the tray above. Generally, this occurs in high pressure systems with low surface tension and low density differences.

where A_B = bubbling area of tray, ft²
 A_{DCT} = downcomer top area, ft²



Note: Drawing not to scale.

Figure 8-152A. Mechanical performance correlations for high-pressure fractionation trays. Used by permission, Capps, R. W., The American Institute of Chemical Engineers, *Chem. Eng. Prog.* V. 89, No. 3, (1993), p. 35, all rights reserved.



Note: Drawing not to scale.

Figure 8-152B. Mechanical performance correlations for vacuum fractionation trays. Used by permission, Capps, R. W., The American Institute of Chemical Engineers, *Chem. Eng. Prog.*, V. 89, No. 3, (1993), p. 35, all rights reserved.

- A_T = tower area, ft²
- C_T = capacity factor, based on tower area, ft/s
- C_{Tflood} = capacity factor at flood, ft/s
- D_T = tower diameter, ft
- F_{flood} = flood factor, dimensionless
- L/V = internal reflux ratio, dimensionless
- m_{vap} = vapor rate, lb/s
- $m_{vapflood}$ = vapor rate at flood, lb/s
- ρ_{vap} = vapor density, lb/ft³
- ρ_{liq} = liquid density, lb/ft³
- S = tray spacing, in.
- V_{load} = vapor load, corrected for density, ft³/s

Baffle Tray Columns

Fair [211] has presented and reviewed many studies of baffle tray, or “splash/shower deck” distillation columns. Figures 8-153 and Figure 8-154 illustrate a simple tray arrangement. The performance of the column is based on

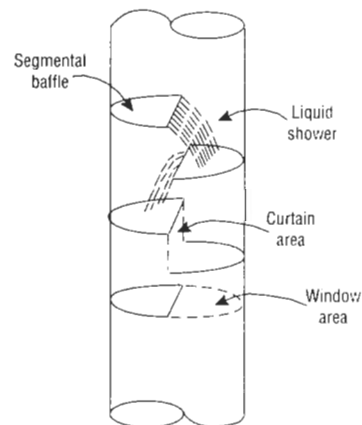


Figure 8-153. Simple side-to-side baffle arrangement, with liquid flow cascades, for baffle tray column. Used by permission, Fair, J. R., *Hydrocarbon Processing*, V. 72, No. 5 (1993) p. 75, Gulf Pub. Co., all rights reserved.

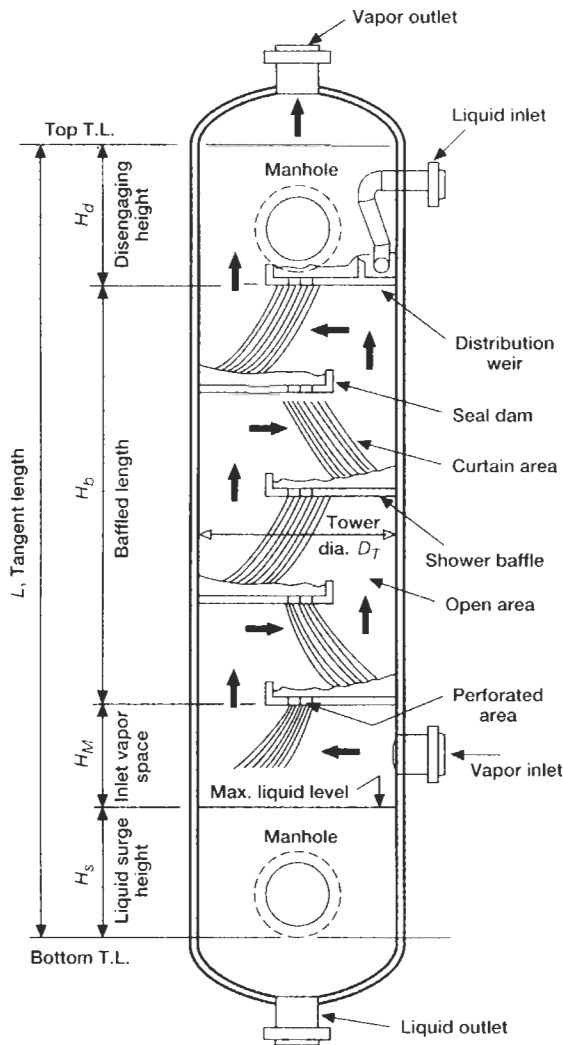


Figure 8-154. Baffle column showing possible enhancements. Used by permission, Fair, J. R., *Hydrocarbon Processing*, V. 72, No. 5 (1993), p. 75, Gulf. Pub. Co., all rights reserved.

the contacting of the up-coming gas/vapor with the liquid cascading from one tray to the one below. The gas must flow through the liquid curtain, and in so doing contacts the liquid for mass and heat transfer.

The baffle patterns in the column can be segmental (simple) up to about 4-ft diameter column, and larger columns can use a disk and donut design as in heat exchangers, or the double segmented or even multi-segmented as in the layouts discussed under bubble caps earlier in this text.

Pressure drop for 50% cut baffles [211]: (see Figures 8-154 and 8-155)

$$\Delta P_{dry} = 0.186 (v_w/C_v)^2 (\rho_g/\rho_l), \text{ in. liquid/baffle} \quad (8-326)$$

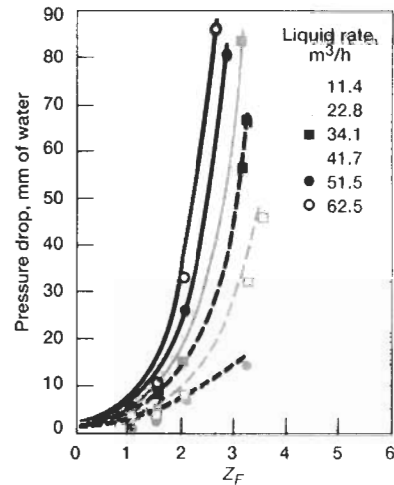


Figure 8-155. Pressure drop for 50% cut baffles at 2.0-ft spacing. The abscissa parameter Z_F is defined as $Z_F = v_w/0.0692 (\rho_g/\rho_l)^{0.5}$. Used by permission Fair, J. R., *Hydrocarbon Processing*, V. 72, No. 5 (1993) p. 75, Gulf Pub. Co., all rights reserved.

The pressure will be affected by flow rate.

The discharge coefficient, C_v , is often used as 0.6 to 0.7. These are noted to be high. For 32% and 20% windows (see Figure 8-153 [211]) and curtains, respectively, a coefficient of 0.27 has been determined. The values of C_v from Lemieux's data [212] as presented by Fair [211]:

L, lb/hr-sq ²	C_v
0	0.55
3000	0.41
6000	0.30
10,000	0.20
12,000	0.15
15,000	0.15

L , is based on the superficial cross-section of the column, lb/hr-ft², and v_w is the linear gas velocity based on the window area, ft/sec,

$$v_w a = C_1 G^m L^n \quad (8-327)$$

The pressure drop data of Lemieux [212] are shown by Fair [211] in Figure 8-155, although there is limited mass transfer data available, Fair [211] has offered this approximate design equation:

$$(HTU)_{og} = (C_g/C_l L_{bc}^{0.41}) (Sc_g/Pr_g)^{2/3} \quad (8-328)$$

Then, converting to HETP:

$$HETP = (HTU)_{og} [(\ln \lambda)/(\lambda - 1)] \quad (8-329)$$

where a = interfacial area, ft^2/ft^3
 C_1 = constant in heat transfer equation = 0.0025
 (English units)
 C_g = specific heat, $\text{Btu}/\text{lb}\cdot^\circ\text{F}$
 C_v = orifice coefficient, Equation 8-326
 G = gas mass velocity, $\text{lb}/\text{hr}\cdot\text{ft}^2$
 h_g = gas phase heat transfer coefficient, $\text{Btu}/\text{hr}\cdot\text{ft}^2\cdot^\circ\text{F}$
 h_L = liquid phase heat transfer coefficient, $\text{Btu}/\text{hr}\cdot\text{ft}^2\cdot^\circ\text{F}$
 HETP = height equivalent to a theoretical plate, ft
 HTU = height of a transfer unit, ft
 L = liquid mass velocity, $\text{lb}/\text{hr}\cdot\text{ft}^2$
 m = exponent ≈ 1.0
 n = exponent 0.44
 Pr = Prandtl number, dimensionless
 Sc = Schmidt number dimensionless
 U_s = linear velocity of gas based on total column
 cross-sectional area, ft/sec
 v_w = linear velocity of gas based on window area, ft/sec

Subscripts

g = gas
 L = liquid
 og = overall (gas concentration basis)

Greek Letters

ΔP = pressure drop, in. liquid
 λ = slope ratio, slope equilibrium line/slope
 operating line, Equation 8-329
 ρ = density, lb/ft^3

Example 8-42: Mass Transfer Efficiency Calculation for Baffle Tray Column (used by permission [211])**Data for example calculation**

System	
Mixture	50–50 molar cyclohexane/ n-heptane
Total reflux operation	
Operating pressure	24 psia
Temperature	238°F
Relative volatility	1.57
Slope of equilibrium line	1.21
Flow Rates	
Vapor F-factor	1.0 ft/sec (lb/ft^3) ^{0.5}
Gas mass velocity	2,100 $\text{lb}/\text{hr}\cdot\text{ft}^2$
Liquid mass velocity	2,100 $\text{lb}/\text{hr}\cdot\text{ft}^2$
Properties	
Liquid density	38.0 lb/ft^3
Liquid viscosity	0.56 $\text{lb}/\text{ft}\cdot\text{hr}$
Liquid diffusion coefficient	2.40×10^{-4} ft^2/hr
Gas density	0.34 lb/ft^3
Gas viscosity	0.020 $\text{lb}/\text{ft}\cdot\text{hr}$
Gas diffusion coefficient	0.114 ft^2/hr
Gas Schmidt number	0.516
Gas specific heat	0.294 $\text{Btu}/\text{lb}\cdot^\circ\text{F}$

Gas thermal conductivity 0.012 $\text{Btu}/\text{hr}\cdot\text{ft}\cdot^\circ\text{F}$
 Gas Prandtl number 0.490

For an F-factor of 1.0 ft/s (lb/ft^3)^{0.5}, $L = G = 2,100$ $\text{lb}/\text{hr}\cdot\text{ft}^2$. For Equation 8-328 a value of C_1 is taken as 0.0025. Then, by Equation 8-329 and assuming that most, if not all, of the resistance is in the gas phase,

$$(\text{HTU})_{og} = \frac{0.294}{(0.0025)(2,100)^{0.44}} \left(\frac{0.516}{0.490} \right)^{2/3} = 4.20 \text{ ft}$$

and

$$\text{HETP} = 4.20 (\ln 1.21/0.21) = 3.81 \text{ ft}$$

Thus, a 20-foot baffle tray section, with 50% cut baffles on 24-in. spacing can contain 10 elements and produce 5.2 theoretical stages of separation. A corresponding crossflow sieve tray section, with 10 trays at 90% efficiency (16)*, can produce 9 theoretical stages. This ratio is about as expected.

The pressure drop per baffle is:

$$\Delta P_{\text{wet}} = 0.186 (3.43/0.42)^2 (0.34/38.0) = 0.11 \text{ in. liquid}$$

For the 20-ft section, total $\Delta P = 10 \times 0.11 = 1.10$ in. liquid. The crossflow sieve tray would have a significantly higher pressure drop.

Tower Specifications

Performance calculations must be interpreted for mechanical construction and for summary review by others concerned with the operation and selection of equipment. Typical specification sheets are given in Figures 8-156A and B for the tower and internal trays, respectively. Suggested manufacturing tolerances are given in Figure 8-157. A composite cut-a-way view of tower trays assembled is shown in Figure 8-158. A Fractionation Research, Inc. (FRI) suggested distillation tray data sheet is shown in Figures 8-159.

The calculation of nozzle connections has not been demonstrated, but normally follows line sizing practice, or some special velocity limitation, depending upon nozzle purpose.

Tower shells may be ferrous, non-ferrous, stainless alloys or clad (such as monel-clad-steel). The trays are usually light gage metal consistent with the corrosion and erosion problems of the system. The velocity action of vapors flowing through holes and slots accentuates the erosion-corrosion problems, and often a carbon steel tower will use

*Note: References in () are from original article.

(text continued on page 218)

Job No. _____ Page _____ of _____ Pages

B/M No. _____ TOWER SPECIFICATIONS No. Units One Item No. T-3

Service Methanol Finishing Size 4'-0" I.D. x 45 Trays

No. Trays 45 Type Bubble Caps 4" Pressed Steel Foot Packing _____ Size _____ Sprays _____

Tower Internals Spec. Dwg. No. A

OPERATING AND MECHANICAL CONDITIONS

Oper. Press. 1.0 to 5.0 PSIG. Oper. Temp. 220 °F
 Des. Press. 30.0 PSIG. Des. Temp. 350 °F
 Code ASME Stamp. Req'd. Yes Density of Contents 47 lbs./cu. ft.
 Lethal Construction No Self Supporting Yes
 Materials: Shell Carbon Steel Heads C.S. Skirt C.S.
 Lining: Metal None Rubber or Plastic None
 Brick None Cement None
 Internal Corrosion Allowance 1/32" to 1/16" max.
 Insulation? Yes No Class Standard for 200°F

NOZZLES

SERVICE	NO. REQ'D.	SIZE	PRESS. CL.	FACING	MARK NO.
Feed*	3	2"	150	Raised F.	A
Reflux	1	2"	150	RF	B
Vapor Out	1	6"	150	RF	C
Liquid Out	1	2"	150	RF	D
Reboiler Vapor	1	6"	150	RF	E
Reboiler Liquid	1	3"	150	RF	F
Drain	<u>on piping</u>				
Safety Valve	1	4"	150	R.F.	G
Manhole	4	18"	150	R.F.	H
Gage Glass	2	3/4"	6000*	Coupling	J
Level Control	2	2"	150	RF	K
Thermowell Pts.	9	1"	6000*	Coupling	L
Pressure Taps	2	3/4"	6000*	Coupling	M
Sample Conn.	4	3/4"	6000*	Coupling	N

* Feed Points to be located in: Vapor Space Downcomer to tray

REMARKS

1. TW Points in Vapor Located- Tray # 1, 21, 23, 25, 27, 44
 2. TW Points in Liquid Located- Tray # 1, 21, 44
 3. Sample Points in Vapor Located-
 4. Sample Points in Liquid Located- Tray # 20, 22, 24, 44
 5. Pressure Taps Located in Vapor Space as Follows: Below tray #1, above tray #45

Locate nozzle (C) 3' below tray #1.
 Seal paper for tray #1 to be 2" high downcomer with 1 extra seal depth over normal.

By: _____ Chk'd. _____ App. _____ Rev. _____ Rev. _____ Rev. _____

Date _____

P.O. To: _____

Figure 8-156A. Tower specification form.

Job No. _____

B/M No. _____

**TOWER INTERNALS SPECIFICATIONS
TRAY TYPE COLUMNS**

Page _____ of _____ Pages
No. Units <u>one</u>
Item No. <u>T-3</u>

Contacting Device - - Bubble Cap, Sieve, Dualflow Bubble Cap

No. of Trays 45 Type: Fixed, ~~Removable~~ (From Top, Bottom) Welded (Bolted, Clamped)

Tray Spacing 18" except as noted, Manway (Yes,) (Removable from Top, Bottom) X

Bubble Cap: Number/Tray 51, Size 3 3/8" E.D., ~~6.0"~~ Spacing 5/4 C to C, Gauge 14

Riser: Diameter 2 3/4 O.D., Gauge 16

Holes: Number _____, Size _____ Diam., Spacing _____ C to C

Clearance Between Holes and Tower Wall _____

Clearance Between Holes and Weirs _____

Tray Thickness (Not Required for Bubble Caps) _____

Type of Flow: Split, Cross

Inlet Weirs: (Yes, No): _____ Height Above Tray Floor 3 1/2 Inches

Outlet Weirs: Length 2'-9 1/8"

(a). Fixed Weir Height Above Tray Floor 2 1/2 Inches

(b). Weir Adjustable From 2 1/2 To 4 Inches Above Tray Floor

(c). Weir Set 3 Inches Above Tray Floor; Weir Slots Covered (Yes,)(No)

Downcomer: (Yes, No) Type: _____ Pipe, Segmental (Straight, Tapered)

Downcomers (Fixed, Removable): _____ Clearance Above Tray Floor 2 3/4 Inches

Seal Pan Distance Below Bottom Tray 24" Seal 4 1/2 Inches

Weep Holes: No./Tray 4 Size 2/8"

Hydraulic Gradient Provision: None required, all caps same height above tray

Standards:

(a). Bubble Cap Drawing No. A - XYZ

(b). Tray Layout Drawing No. B - XYZ

(c). Tower Tolerances Drawing No. C - XYZ

MATERIALS OF CONSTRUCTION

Bubble Cap and Riser: Carbon steel Gaskets: asbestos

(a). Bolts, Nuts and Washers: carbon steel

Trays: Carbon steel Gaskets asbestos Bolting: carbon steel

Tray Supports, Downcomers and Seal Pan: carbon steel

REMARKS

Trays to be standard design and layout with removable center section for access through tower from above.

Caps to be assembled and mounted on trays in fabricator's shop.

By _____	Chk'd _____	App. _____	Rev. _____	Rev. _____	Rev. _____
Date _____					

P.O. To: _____

Figure 8-156B. Tower internals specifications form, tray type columns.

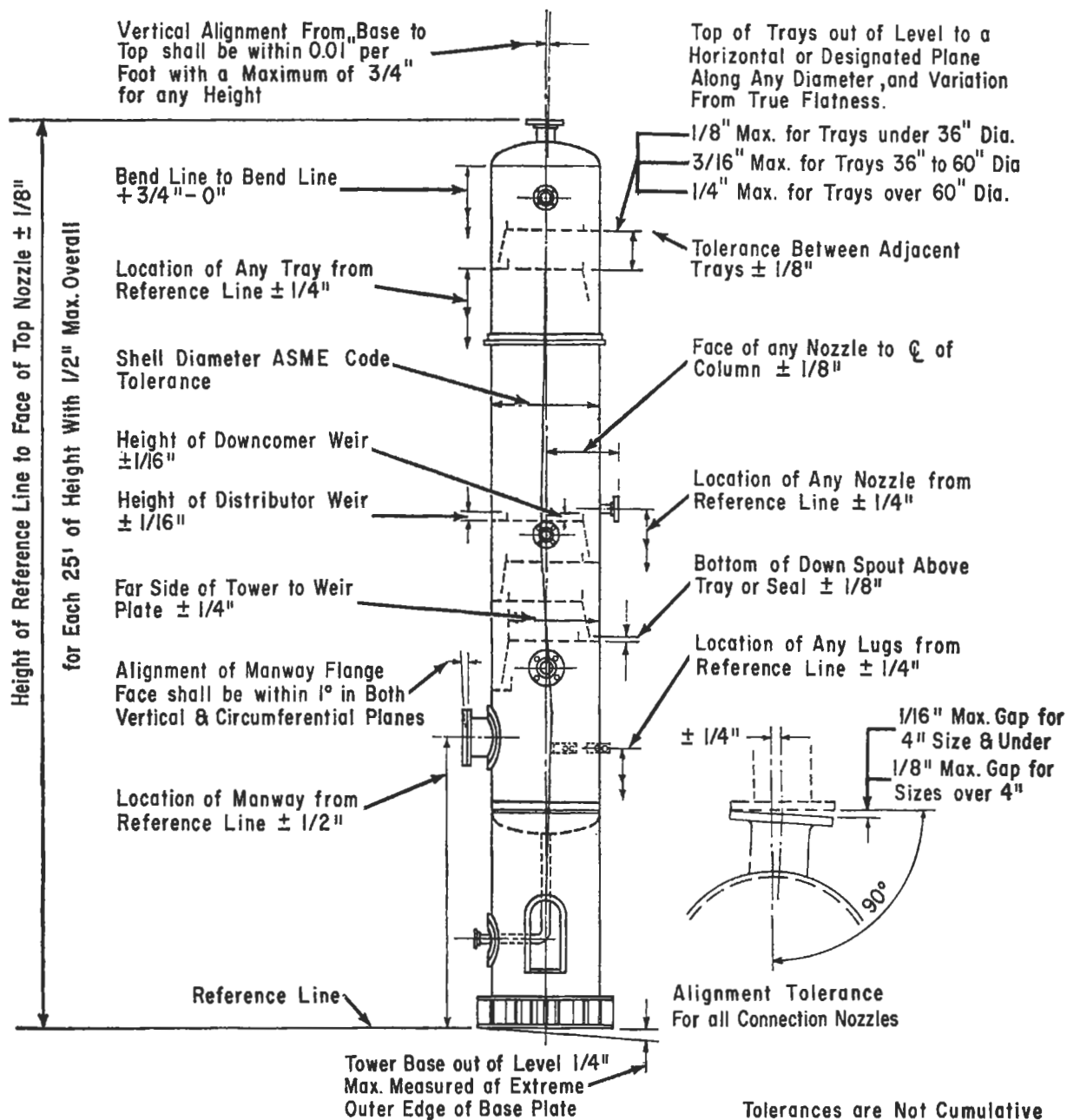


Figure 8-157. Suggested tolerances for distillation type towers.

(text continued from page 215)

stainless, alloy steel, monel or nickel trays, caps and all internal parts. Sometimes just the cap or hole portion of the trays are of expensive construction.

When clad metal is used, it is often specified as 1/8-in. or 1/4-in. minimum clad thickness. This is usually sufficient to allow proper weld connections. Care must be used in sealing all internal joints of clad material to prevent exposure of the base metal.

The towers are designed in accordance with the particular code (such as ASME Unfired Pressure Vessel) used by the company or required by law. To provide stiffness and bending strength in high winds, design normally figures a wind load recommended for the area. It is not unusual to design for 75 to 100 mph winds, taking into account the external insulation, piping, ladders and platforms in computing the effective force areas. Foundations must be adequate to carry the total dead weight of the erected tower, platforms, etc. plus the weight of water

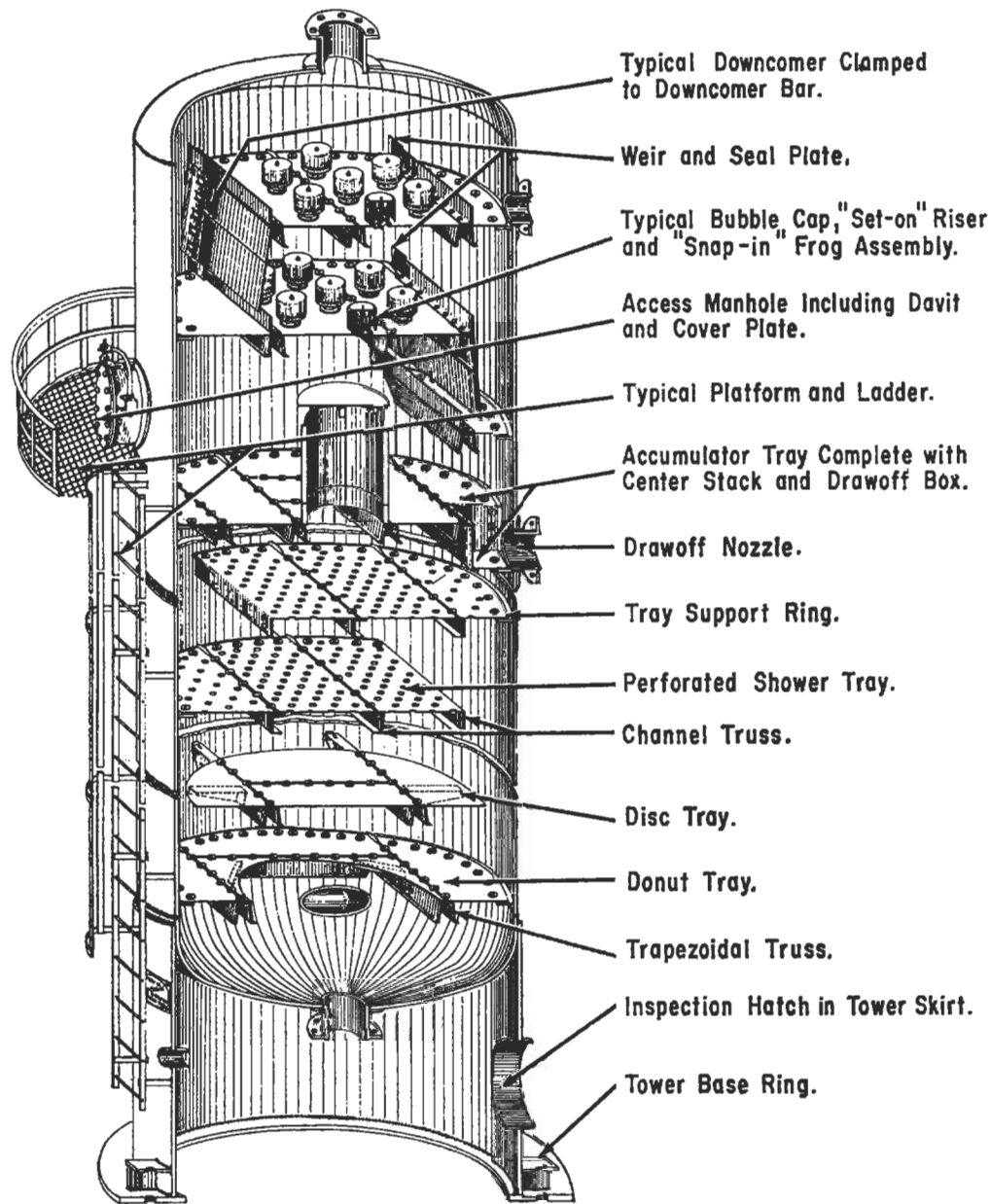


Figure 8-158. Composite tower-tray assembly illustrating special trays with corresponding nozzles. Used by permission, Glitsch, Inc.

(or perhaps other fluid) to allow for in-place testing, or complete tower flooding.

Tray types are selected for performance. However, when a particular type is not specifically required, it is well to consider that, in carbon steel, the trays installed (not including tower shell) cost approximately:

Bubble Caps, 25% > Sieve, 10% > Perforated without downcomers.

When specifying the mechanical arrangement details, it is important for the designer to take on the role of plant operator to analyze what information is needed and how

it is to be obtained. For example, once a column is in operation, it is often necessary to determine what may be preventing the system from meeting design specifications as to through-put or quality of top, bottom, or side-draw products. To determine such information it is essential to provide at least the following minimum mechanical features to allow extracting needed samples, temperatures, variations in feed entries, etc. (see Figures 8-156A and B), for example:

1. Thermocouple entry points on about every other tray measure either liquid or vapor temperature.

TRAY DATA SHEET		Sheet 1 of 2
Client _____	Plant Location _____	Engineer _____
Job No. _____	Inquiry No. _____	Date _____
Item No. _____	Service _____	
Tray No. 1 = Top/Btm		
Section (Name/Description)	_____	_____
Tray Numbers Included	_____	_____
Loading at Actual Tray No.	_____	_____
Number of Trays Required	_____	_____
NORMAL VAPOR TO:		
Weight Rate, kg/h	_____	_____
Density, kg/m ³	_____	_____
Volume Rate, Actual m ³ /s	_____	_____
Molecular Weight	_____	_____
Viscosity, mPa-s	_____	_____
Pressure, kPa (bar a)	_____	_____
Temperature, °C	_____	_____
Design Range, % of Normal	_____	_____
NORMAL LIQUID FROM:		
Weight Rate, kg/h	_____	_____
Density, kg/m ³	_____	_____
Volume Rate, Actual m ³ /s	_____	_____
Molecular Weight	_____	_____
Surface Tension, mN/m	_____	_____
Viscosity, mPa-s	_____	_____
Temperature, °C	_____	_____
Design Range, % of Normal	_____	_____

TRAY DATA SHEET		Sheet 2 of 2
Item No. _____	Service _____	
Section (Name/Description)		
Tray Numbers Included		
PERFORMANCE REQUIREMENTS:		
Max. ΔP per Tray, mmHg (mbar)	_____	_____
Max. % Jet Flood	_____	_____
Max. DC Liq. Velocity, m/s	_____	_____
Max. DC Backup, Clear Liq., mm	_____	_____
Derating Factor	_____	_____
Purpose for Derating (Foaming, System, Safety)	_____	_____
MECHANICAL REQUIREMENTS:		
Tower Inside Diameter, mm	_____	_____
Number of Passes	_____	_____
Tray Spacing, mm	_____	_____
Type of Tray	_____	_____
Hole/B Cap Diameter, mm	_____	_____
Deck Material/Thickness, mm	_____	_____
Valve/B Cap Material	_____	_____
Hardware Material	_____	_____
Support Material/Thickness, mm	_____	_____
Total Corrosion Allowance, mm	_____	_____
Vessel Manhole I.D., mm	_____	_____
MISCELLANEOUS:		
Solids Present: Yes / No	Flashing Feed: Yes / No	
Anti-Jump Baffles: Yes / No / Vendor Preference		
Recessed Seal Pans: Yes / No / Vendor Preference		
Specify Equal Bubbling Areas / Flow Path Lengths per pass		
Design Load:		
_____ kPa (mbar) with _____ mm deflection at _____ C. or		
_____ Standard: 1.4 kPa with 3 mm at 150° C.		

Figure 8-159. Data specification sheets suggested by Fractionation Research, Inc. (FRI) for distillation trays. Used by permission, Yeoman, N. The American Institute of Chemical Engineers, *Chem. Eng. Prog.*, V. 85, No. 10 (1989), p. 15, all rights reserved.

- Provide at least three, and perhaps four feed nozzles in addition to the one "theoretically" calculated to be the optimum location. Select these feed locations approximately two and four trays above and below the design basis or theoretical location. These extra nozzles must be oriented on the column so they have proper feed entry spargers or distributors (entry can be onto the tray or into the downcomer) and can be valved from a feed manifold to select the alternate desired location for testing purposes.
- Reflux nozzles must be arranged to enter the tray with proper designed internal pipe to the tray downcomer or distributor.
- Pressure tap (couplings) to take several pressure readings in the vapor space above a specific tray up the column. It is better to have too many entries available for testing than to be short and not be able to properly examine the column.
- Sample draw-off connections, usually for liquid from the trays, but some top (overhead) and reboiler vapor as well as liquid can be very useful.

Mechanical Problems in Tray Distillation Columns

Although it appears that a fabricated column with welded internal components, supports, trays, etc. should be free from mechanical problems, actual experience proves this is not the case. Most trays are bolted onto supports, and for large columns, tray sections are assembled inside by bolting together. Actual experience has found that poor column performance can often be attributed to bubble caps and valves knocked (or blown) off position on the trays and often blown to one corner of a tray. Sometimes this condition is found for several trays in a section of the column, thereby preventing any vapor-liquid contacting and creating a significant loss of distillation efficiency.

Some of this condition can be attributed to surging or "burping" inside and creating pressure surges under increased pressure. Other conditions of mechanical damage include nuts coming off bolts, and tray metal and welds cracking at or near supports, corrosion of tray sections and welds is often caused by pressure pulsations from the tray action creating vibration and "auto-pulsations" of the trays producing resonant or near resonant conditions at or near the tray's first or second natural frequencies [214]. Winter [214] presents rough estimating correlations for predicting natural frequencies and deflection of trays.

Troubleshooting Distillation Columns

To respond to difficulties during operation of distillation columns a very careful and itemized analysis must be made of (a) the process, (b) the mechanical details of the column, and (c) the instrumentation for operation and control. A good column performance designer is generally in an excellent position to examine the operating performance and diagnose the nature and specific location of the conditions that may be preventing or contributing to good column performance. This often may involve detailed computer studies of data compared to tray-by-tray performance.

It is beyond the scope of this text to thoroughly examine this subject; however, there are several good references (but not all inclusive) including Hasbrouck, et al. [215] and Kister [117].

Nomenclature for Part 3: Tray Hydraulics Design

$A = A_T$ = Total cross-sectional area of tower diameter, ft^2
 A_a = Total annular cap area per tray, ft^2 ; or
 = Active or "bubbling" area of tray, generally $(A_t - 2A_d)$, ft^2 see Figures 8-119 and 8-129
 A_B = Bubbling area; column area minus total of downcomer and downcomer seal areas, ft^2 or m^2
 A_c = Total cap area inside cross section area per tray, ft^2
 A_d = Downcomer area, cross-sectional area for total liquid down-flow, ft^2 ; or,
 = Minimum flow area at bottom (under) of downcomer per tray, ft^2
 A_f = Fractional hole area (actual hole area/bubbling area, A_B)
 A_h = Net perforated area of tray, ft^2
 A_H = Total hole area, ft^2
 A_n = Net open liquid area of one tray, equal to total tower section minus area occupied by caps and risers and minus area of segmental or other downcomer at outlet of tray, ft^2 ; or
 = Net area, column area minus area at top of the downcomers, m^2
 A_{op} = Open area of tray, ft^2
 A_s = Total slot area per tray, ft^2
 A_t = Total tower cross-section area, ft^2
 A_r = Total riser inside area per tray, ft^2

A'_r = Total reversal area per tray, ft^2
 a_a = Annular area per cap, in.^2
 a_c = Inside cross-section area of cap, in.^2
 a_d = Cross-section flow area, minimum, of down-pipe clearance area between tray floor and down-pipe bottom edge, or up-flow area between outer circumference down-pipe and any inlet tray weir, in.^2
 a_o = Individual hole area per hole on sieve tray, in.^2
 a_r = Riser inside cross-section area per riser, in.^2
 a'_r = Reversal area per cap assembly, in.^2
 a_{ro} = Riser outside cross-section area, based on O.D., in.^2 per riser
 a_s = Slot area per cap, in.^2
 A_t = Total tower cross-sectional area, ft^2
 A_{VM} = Maximum valve open area, ft^2
 a_x = Smaller area value, a_a or a_r , for use in Equation 8-231 or 8-233
 B_s = Dimensionless group identifier
 C = Factor for Souders-Brown maximum entrainment relation; or
 = Empirical constant in CCFL correlation
 C_d = Liquid gradient factor
 C_g = Specific heat, $\text{Btu/lb}\cdot^\circ\text{F}$
 C_F = Flooding capacity factor, ft/sec
 C_1 = Constant in heat transfer Equation 8-328 = 0.0025
 C_L = Liquid phase loading factor, ft/sec , Equation 8-282
 C_o = Orifice (vapor discharge) coefficient for dry tray, Figure 8-128, or 8-129, respectively
 C_{SB} = C-Factor at flood (Souders-Brown coefficient), ft/sec (or, m/sec); or
 = Souders-Brown flooding constant defined by Equation 8-286
 C_T = Capacity factor based on tower area, ft/sec
 $C_{T,\text{flood}}$ = Capacity factor at flood, ft/sec
 C_v = Liquid gradient vapor load correction factor; or
 = Discharge coefficient (see accompanying table); or
 = Gas phase loading factor, ft/sec , Equation 8-281
 C_{vw} = Eddy loss coefficient, dimensionless, Table 8-22
 C_w = Wet cap pressure drop correction factor, Figure 8-115
 c = Hole spacing center to center, in.
 $D = D_T$ = Tower inside diameter, ft
 D_f = Total flow width across tray, normal to flow, ft
 D_H = Hole diameter, in.
 D_{HE} = Equivalent hole diameter, in.
 D_V = Valve diameter, in.
 d = Column diameter, (m)
 d_c = Inside diameter of cap, in.
 d_h = Diameter of weep hole, in. Note that this is the diameter equivalent to area of all weep holes per tray; or
 = Hole diameter, in. (or mm)
 d_o = Hole diameter, in.
 d_r = Inside diameter of riser, in.
 d_v = Diameter of valve unit at narrowest opening, mm
 d_w = Diameter of circular weir, in.
 E_d = Dry tray efficiency, fraction
 E_w = Wet tray efficiency, fraction
 e_w = Weight of liquid entrained per unit weight of vapor flowing, lb/lb
 f = Aeration factor (usually = 1.0); or
 = Friction factor for froth cross flow, Equation 8-255
 f_{hg} = Friction factor for liquid gradient, cross-flow for sieve trays

- F = Free height in downcomer above clear liquid level (not froth level)
 F_c = Tower velocity factor
 F_{flood} = Flood factor, dimensionless
 $F_h = v_o \sqrt{\rho_v}$ for perforated trays, no downcomers
 $FP = F_{1v}$ = Flow parameter, dimensionless
 F_s = Hole factor = $v_{om} (\rho_v)^{1/2}$
 F_{va} = Vapor flow parameter based on active area, defined by $F_{va} = v_a \rho_v^{1/2}$, or
 = Tray F factor based on active (bubbling) area = $v_{va} \rho_v^{1/2}$ (ft/sec) (lb/ft³)^{1/2}
 F_w = Modification factor to weir formula
 F_W = Flow parameter, dimensionless
 $G = V$ = Vapor or gas flow, lb/hr (see Figures 8-82 or 83, or Equations 8-219 or 290); or
 = Gas mass velocity, lb/hr-ft²
 g = Acceleration of gravity, 32.2 ft/sec-sec
 H_{GAP} = Maximum lift of a valve, in.
 H_d = Height of clear liquid in downcomer, in.
 H_s = Slot height of bubble cap, in.
 $(HTU)_{OC}$ = Height of transfer unit, ft
 $HETP$ = Height equivalent to a theoretical plate/tray/stage, in. or ft, or possibly mm
 h_{σ} = Head loss due to bubble formation, in. liquid; or
 = Head loss due to vapor flow through perforations, in. liquid
 h' = Height of overflow weir or bubble cap riser, whichever is smaller, in.
 h_{al} = Height of aerated liquid on tray, in.
 h_{cw} = Wet cap pressure drop (riser, reversal, annulus, slots), in. liquid
 h_c = Head of liquid in bubbling zone; wet cap pressure drop; or taken as in. clear liquid on tray
 h'_c = Total dry cap pressure drop, in. liquid
 $h_{cl} = h_c$ = Height of clear liquid on tray, in. (or mm)
 $h_{cl,i}$ = Clear liquid at the inlet, in.
 h_{ct} = Clear liquid height at froth-to-spray transition, in. liquid (or mm)
 h_d = Total head loss under downcomer, in. liquid
 h'_d = Head loss between segmental downcomer and tray inlet weir, in. liquid
 h_{dc} = Head loss of circular down-pipe at point of greatest restriction, in. liquid
 h_{dcl} = Downcomer height clearance between bottom of downcomer and tray floor, in.
 h_{dl} = Dynamic liquid seal on sieve or perforated tray, in. liquid
 h_{ds} = Dynamic slot seal, in. liquid
 h_{dt} = Pressure drop through dry perforated or sieve tray, in. liquid
 h_{du} = Downcomer head loss due to friction and underflow, in. liquid
 h_e = Effective liquid head taking aeration of liquid into account, in. liquid, Figure 8-130
 h_f = Height of top of foam above tray floor, in. (or mm)
 h'_f = Height of free fall of liquid in downcomer; in. or
 = Height of froth on tray (aerated mass), in.
 h_{fd} = Downcomer backup, in.
 h_h = Head loss due to vapor flow through perforations, in. liquid; or
 = Dry tray pressure drop, in. liquid
 h_L = Clear liquid head, m
 h_1 = Depth of clear liquid on tray, inches; (or m); or
 = Aerated tray, liquid pressure drop or equivalent clear liquid on tray, in. tray liquid
 h_{li} = Height of clear liquid on inlet side of tray, in.
 h_{lo} = Height of clear liquid at overflow weir, in.
 h_n = Depth of notch in weir, in.; or
 = Head in the back of downcomer, in. (usually negligible)
 h_{ow} = Height of liquid crest over flat weir; or measured from weir (straight or circular); or from bottom of notches (v-notch weir), in.
 h_{ow}' = Height of liquid above bottom of notch in notched weir, in.
 $h_{op} = H_{op}$ = Valve lift, i.e., distance between bottom of a valve and top of the tray deck, in.
 h_{pc} = Cap assembly partial pressure drop, including drop through riser, reversal, annulus, slots, in. liquid
 h_r = Pressure drop through risers, in. liquid
 h_{ra} = Pressure drop through reversal and annulus, in. liquid
 h_s = Slot opening, or pressure drop through slot, in. liquid
 h'_s = Pressure drop through dry slots, in. liquid
 h_{sl} = Static liquid seal on sieve tray, in. liquid
 h_{ss} = Static slot seal, in.
 h_{sr} = Height of cap shroud ring, in.
 h_t = Total vapor pressure drop per tray, in. liquid (wet tray)
 h_{udc} = Head loss due to the underflow clearance, in.
 h_v = Maximum vertical travel of a valve on a valve tray, metric
 h_w = Height of weir above tray floor (to top of flat weir, or bottom of notch in notched weir), in.
 h_{WT} = Wet tray head loss, in. liquid
 K_c = Constant for Bolles' partial bubble cap pressure drop equation, Figure 8-114; or
 = Loss coefficient, valve closed, (sec)²(in.)/(ft²)
 $L = L'$ = Liquid flow, lb/hr or lb/sec (or m³/hr/m weir length); or
 = Liquid rate, lb/hr (ft² active plate/tray)
 L_{bc} = Liquid mass velocity, lb/hr-ft² based on superficial cross section of column
 L/V = Internal reflux ratio, dimensionless
 L_{wi} = Weir length, in.
 L_g = Liquid flow rate, gpm = Q
 l_f = Liquid flow rate, ft³/sec
 $l_{fw} = L_w$ = Total flow width across tray normal to flow, ft
 l_w = Length of straight weir, ft
 $l_w' = l_{fp}$ = Length of liquid flow path, ft
 m_{vap} = Vapor rate, lb/sec
 m = Exponent in CCFL correlation, or Equation 8-327, equals approx. 1.0
 N = Total number of actual trays in tower
 N_c = Number of caps per tray
 N_s = Number of slots per bubble cap
 N_v = Valve density, number of valves per ft²; or
 = Number of valve units on a valve tray
 n = Depth of notches in weir, in; or
 = Exponent defined by Equations 8-288 and 327
 ΔP = Dry tray pressure drop for 50% cut baffles, in. liquid per baffle; or
 = Actual tray pressure drop, in. liquid
 P_r = Prandtl number dimensionless
 P_v = Fractional opening in the circumference of a valve; or, P_1

Q = Liquid load, gpm = L_g
 R_h = Hydraulic radius for froth cross flow, ft
 R_s = Ratio of top to bottom widths of trapezoidal slot, bubble cap dimensions
 R_v = Vapor distribution ratio, dimensionless
 R_{vw} = Ratio valve weight with legs/valve weight without legs, dimensionless, see Table 8-22
 Re_h = Reynolds Number modulus
 Re_{ch} = Reynolds modulus for friction cross-flow
 Δ'_r = Liquid gradient per row of caps, uncorrected, in.
 S' = Effective tray spacing, distance between top of foam, froth, or bubbles and tray above, in. Note: for Hunt's relation, S' = tray spacing minus 2.5 h_c
 Sc = Schmidt number, dimensionless
 S'' = Same as S' , except unit, ft
 $S_t = S$ = Tray spacing (actual), in. ft, m
 S_{ts} = Tray spacing, ft
 s = Cap skirt clearance between cap and tray floor, in.
 T_v = Metal thickness of valve, in.
 t_w = Liquid throw over weir, in.
 U = Superficial vapor velocity, m/sec
 U_N = Vapor linear velocity based on net area for de-entrainment usually tower cross-section minus one downcomer, ft/sec
 $U_a = v_a$ = Vapor velocity based on active area, A_a , ft/sec
 V = Total vapor flow through tray or tower, ft³/sec
 V' = Internal vapor flow, lb/hr or lbs/sec, Equation 8-297
 V_G = Superficial gas velocity in channel (not tower), ft/sec
 V_{load} = Vapor load corrected for density, ft/sec
 V_m = Maximum allowable vapor load per tray, ft³/sec
 v_c = Superficial vapor velocity in tower, ft/sec (based on tower cross-section)
 v_d = Design hole vapor velocity, ft/sec; or
 = Downcomer velocity, ft/sec
 v_{du} = Velocity of liquid flowing between segmental downcomer and inlet weir, ft/sec
 v_f = Vapor velocity through equivalent net tray area, based on tower area minus twice downcomer area, ft/sec; also
 = Velocity of froth cross flow, ft/sec
 v'_f = Velocity of froth, ft/sec
 V_{flood} = Gas superficial velocity based on tray net area, A_n , ft/sec
 v_h = Vapor velocity through valve hole, ft/sec
 $v_{pt} = v_o$ = Vapor velocity through holes, ft/sec
 $v_w = U_w$ = Linear velocity of gas based on window area, ft/sec
 v_{om} = Minimum velocity through holes at weep point, ft/sec
 W = Maximum allowable mass velocity through column using bubble cap trays, lb/(hr) (ft² tower cross section)
 W_e = Liquid entrainment mass velocity, lb entrainment/(min) (ft²), based on net tray area of tower minus twice downcomer area
 W'_e = Assumed allowable liquid entrainment mass velocity derived from assumed allowable loss mols liquid/mol vapor, lb/hr (ft²), based on net tray areas same as for W_e
 W^*_e = Liquid entrainment mass velocity corrected for liquid properties and plate spacing, lb entrainment/(hr) (ft²), based on net tray area as for W_e

w_1 = Weir length, in.
 w_s = Width of slot (rectangular), in.
 z = Characteristic length in CCFL model, ft

Greek Symbols

α = Relative volatility, dimensionless
 α_d = Mean aeration factor of froth (dimensionless)
 $\bar{\alpha}$ = Relative froth density, h_l/h_f
 β = Fraction perforated or open hole area in perforated area of tray (not fraction hole area in tower area); or
 = Aeration factor, f , dimensionless
 λ = Slope of equilibrium line/slope of operating line
 Δ = Liquid gradient (corrected) for tray or tray section, in.
 Δ' = Uncorrected liquid gradient for tray or tray section, in.
 Δ'_r = Liquid gradient per row of caps, uncorrected, in.
 ϕ = Relative froth density, ratio of froth density to clear liquid density
 ϵ = Eddy kinematic viscosity, m²/sec (assumed equal to eddy diffusivity; see Ref. 2)
 θ = Time to drain tower, min
 μ = Viscosity of liquid at tower temperature, centipoise, cp
 μ_l = Viscosity of liquid, lb/ft-sec
 π = Pi = 3.14
 ψ = Entrainment expressed as fraction of gross down-flow
 ρ = Liquid density at temperature of tower, gm/cc
 ρ_L = Liquid density, lbs/ft³, or kg/m³
 ρ_v = Vapor density, lbs/ft³, or kg/m³
 ρ_{vm} = Valve metal density, lb/ft³
 σ = Surface tension of liquid, dynes/cm

Subscripts

F = Flood = At flood point
 $g = G$ = Gas
 $H_2O = H = h$ = Water
 $L = l$ = Liquid
 $OG = og$ = Overall (gas concentration basis)
 $Vap = vap$ = Vapor

References

1. Akers, W. W. and D. E. Wade, "New Plate-to-Plate Method," *Pet. Ref.* V. 36, p. 199 (1954).
2. American Institute of Chemical Engineers, "Bubble Tray Design Manual, Prediction of Fractionation Efficiency," Amer. Inst. Chem. Engrs. (1958).
3. Biggers, M. W., private communication.
4. Bogart, M. J. P., "The Design of Equipment for Fractional Batch Distillations," *Trans. A.I.Ch.E.* V. 33, p. 139 (1937).
5. Bolles, W. L., "Optimum Bubble-Cay Tray Design," *Pet. Processing*; Feb. through May 1956.
6. Boston and Sullivan, *Canadian Jour. of Chem. Engr.* V. 50, Oct. (1972).
7. Broadus, J. E., A. J. Moose, R. L. Huntington, "How to Drain Bubble Cap Columns" *Pet. Ref.*, Feb. (1955).

8. Brown, G. G. and Associates, *Unit Operations*, 4th Ed. John Wiley and Sons, New York, N.Y., (1953).
9. Brown, G. G. and H. Z. Martin, "An Empirical Relationship Between Reflux Ratio and the Number of Equilibrium Plates in Fractionating Columns," *Trans. A.I.Ch.E. V. 38*, No. 5 (1939).
10. Chueh, P. L. and J. M. Prausnitz, I.&E.C. Fundamentals V. 6, p. 492, Amer. Chem. Society (1967).
11. Cicalese, J. J., J. J. Davis, P. J. Harrington, G. S. Houghland, A. J. L. Hutchinson, and T. J. Walsh, *Pet. Ref. V. 26*, May, p. 127 (1947).
12. Colburn, A. P., "Calculation of Minimum Reflux Ratio in Distillation of Multicomponent Mixtures," *Trans. A.I.Ch.E. V. 37*, p. 805 (1941).
13. Dauphine, T. C. "Pressure Drops in Bubble Trays," Sc. D. Thesis, Mass. Inst. Technology (1939).
14. Davies, J. A., "Bubble Tray Hydraulics," *Ind. Eng. Chem. V. 39*, p. 774, Amer. Chem. Society (1947).
15. Davies, J. A., "Bubble Trays—Design and Layout," *Pet. Ref. V. 29*, 93, p. 121 (1950).
16. Drickhamer, H. G. and J. B. Bradford, "Overall Plate Efficiency of Commercial Hydrocarbon Fractionating Columns," *Trans. A.I.Ch.E. V. 39*, p. 319 (1943).
17. Edmister, W. C., "Design for Hydrocarbon Absorption and Stripping," *Ind. Eng. Chem. V. 35*, p. 837 (1943).
18. Edmister, W. C., "Hydrocarbon Absorption and Fractionation Process Design Methods," *Pet. Engr. May 1947–March 1949* and, "Absorption and Stripping—Factor Functions for Distillation Calculations by Manual and Digital—Computer Methods," *A.I.Ch.E. Journal*, V. 3, No. 2 p. 165 (1957).
19. Eduljee, H. E. "Entrainment From Bubble-Cap Distillation Plates," *British Chem. Engr.*, p. 474, Sept. (1958).
20. Ewell, R. H., J. M. Harrison, and Lloyd Berg, "Hydrocarbon Azeotropes," *Pet. Engr.*, (installment, Oct., Nov., Dec. (1944))
21. Faassen, J. W., "Chart for Distillation of Binary Mixtures," *Ind. Eng. Chem. V. 36*, p. 248, (1944).
22. Gautreaux, M. F., H. E. O'Connell, "Effect of Length of Liquid Path on Plate Efficiency," *Chem. Eng. Prog. V. 51*, p. 232 (1955).
23. Gilliland, E. R., "Multicomponent Rectification," *Ind. Eng. Chem. V. 32*, pp. 1101 and 1220 (1940).
24. Good, A. J., M. H. Hutchinson, W. C. Rousseau, "Liquid Capacity of Bubble Cap Plates," *Ind. Eng. Chem., V. 34*, p. 1445 (1942).
25. Holland, C. D., Advanced Distillation Course in Extension, Texas A&M College (1954).
26. Holland, C. D., *Multicomponent Distillation*, Prentice-Hall (1963).
27. Holland, C. D., *Unsteady State Processes with Applications in Multicomponent Distillation*, Prentice-Hall.
28. Horsley, L. H., "Azeotropic Data," *Advances in Chemistry Series*, American Chemical Society, Washington, D.C.
29. Horton, G., W. B. Franklin, "Calculation of Absorber Performance and Design," *Ind. Eng. Chem. V. 32*, p. 1384 (1940).
30. Huang, Chen-Jung, and J. R. Hodson, "Perforated Trays Designed This Way," *Pet. Ref. V. 37*, p. 104 (1958).
31. Hughmark, G. A., and H. E. O'Connell, "Design of Perforated Plate Fractionating Towers," *Chem. Eng. Prog. V. 53*, p. 127-M (1957).
32. Hull, R. J. and K. Raymond, "How To Design and Evaluate Absorbers," *Oil and Gas Jour.*, Nov. 9, 1953 through Mar. 15, 1954.
33. Hunt, C. D'A., D. N. Hanson and C. R. Wilke, "Capacity Factors in the Performance of Perforated Plate Columns," *A.I.Ch.E. Jour. V. 1*, p. 441 (1955).
34. Hutchinson, A. J. L., "A System of Calculations for Light Hydrocarbons," *Pet. Ref. Oct. 1950–April 1951*.
35. Jennings, B. H. and F. P. Shannon, "Aqua-Ammonia Tables," Lehigh University, Part 1, Science and Technology Series No. 1, Bethlehem, Pa.
36. Jones, J. B. and C. Pyle, "Relative Performance of Sieve and Bubble Cap Plates," *Chem. Eng. Progress*, V. 51, p. 424 (1955).
37. Kelly, R. G., *Oil and Gas Journal*, April 18, p. 128, (1955).
38. Kemp, H. S. and C. Pyle, "Hydraulic Gradient Across Various Bubble Cap Plates," *Chem. Eng. Prog. V. 45*, p. 435 (1949).
39. Klein, J. H., D. Sc. Thesis, Mass. Inst. Technology, (1950).
40. Kremser, A., "Theoretical Analysis of Absorption Process," *Nat. Pet. News*, V. 22, p. 48 (1930).
41. Lee, D. C., Jr., "Sieve Trays," *Chem. Eng.* p. 179, May 1954.
42. Leibson, I., R. E. Kelley and L. A. Bullington, "How to Design Perforated Trays," *Pet. Ref. V. 36*, p. 127 (1957).
43. Martin, G. Q., "Guide To Predicting Azeotropes," *Hydrocarbon Processing*, No. 1, p. 241 (1975).
44. May, J. A. and J. C. Frank, "Compensation for Hydraulic Gradient in Large Fractionator," *Chem. Eng. Prog. V. 51*, p. 189 (1955).
45. Mayfield, F. D., W. L. Church, Jr., A. C. Green, D. C. Lee, Jr. and R. W. Rasmussen, "Perforated-Plate Distillation Columns," *Ind. Eng. Chem. V. 44*, p. 2238 (1952).
46. Munk, Paul, "Design of Bubble Cap Trays," *Pet. Ref. V. 34*, p. 104 (1955).
47. Myers, H. S., "A Versatile Fractionating Column," *Ind. Eng. Chem. V. 50*, p. 1671 (1958).
48. *Natural Gasoline Supply Men's Association, Engineering Data Book*, 7th Ed. 1957, Tulsa, Oklahoma.
49. O'Connell, H. E., "Plate Efficiency of Fractionating Columns and Absorbers," *Trans. A.I.Ch.E. V. 42*, p. 741 (1946).
50. Orye, R. V. and J. M. Prausnitz, *Ind. Eng. Chem. 57*, 5, p. 19 (1965).
51. Palmer, D. A., "Predicting Equilibrium Relationships for Maverick Mixtures," *Chem. Eng.*, June 9, (1975) p. 80.
52. Prausnitz, J. M. and P. L. Cheuh, *Computer Calculations for High Pressure Vapor-Liquid Equilibrium*, Prentice-Hall Inc. (1968).
53. Prausnitz, J. M., C. A. Eckert, R. V. Orye and J. P. O'Connell, *Computer Calculations for Multicomponent V-L Equilibria*, Prentice-Hall (1967).
54. Prausnitz, J. M., *Molecular Thermodynamics of Fluid Phase Equilibria*, Prentice-Hall (1969).
55. Redlich, O., and A. T. Kister, *Ind. Eng. Chem., V. 40*, p. 345 (1948).
56. Redlich, O., and J. N. S. Kwong, *Chem. Rev. V. 44* (1949), p. 233.
57. Redlich, O., T. Kister, and C. E. Turnquist, *Chem. Engr. Progr. Sym. Ser. 48*, 2, (1952) p. 49.
58. Renon, H. and J. M. Prausnitz, *A.I.Ch.E. Jour.*, V. 14, (1968) p. 135.
59. Robinson, C. S. R. and E. R. Gilliland, *Elements of Fractional Distillation*, McGraw-Hill, 4th Ed., (1950).
60. Rogers, M. C. and E. W. Thiele, "Pressure Drop in Bubble-Cap Columns," *Ind. Eng. Chem. V. 26*, p. 524 (1934).
61. Scheibel, E. G. and C. F. Montross, "Empirical Equation for Theoretical Minimum Reflux," *Ind. Eng. Chem. V. 38*, p. 268 (1946).

62. Sherwood, T. K., *Absorption and Extraction*, McGraw-Hill Book Co., Inc., New York, N.Y. (1937).
63. Shiras, R. N., D. N. Hansen, C. H. Gibson, "Calculation of Minimum Reflux in Distillation Columns," *Ind. Eng. Chem. V. 42*, p. 871 (1950).
64. Simkin, D. J., C. P. Strand and R. B. Olney, "Entrainment from Bubble Caps," *Chem. Eng. Prog.*, V. 50, p. 565 (1954).
65. Smith, B. D., *Design of Equilibrium Stage Processes*, McGraw-Hill (1963).
66. Smoker, E. H., "Nomographs for Minimum Reflux Ratio and Theoretical Plates for Separation of Binary Mixtures," *Ind. Eng. Chem. V. 34*, p. 509 (1942).
67. Souders, M., Jr., G. G. Brown, "Fundamental Design of Absorbing and Stripping Columns for Complex Vapors," *Ind. Eng. Chem. V. 24*, p. 519 (1932).
68. Souders, M., Jr., G. G. Brown, "Design of Fractionating Columns," *Ind. Eng. Chem. V. 26*, p. 98 (1934).
69. Sutherland, S., Jr., "Characteristics of Countercurrent Vapor Liquid Flow at a Perforated Plate. M. S. Thesis, Jan. 1958. Texas A&M College.
70. Teller, A. J., "Binary Distillation," *Chem. Eng.* p. 168, Sept. (1954).
71. Umholtz, C. L. and M. Van Winkle, "Effect of Hole Free Area, Hole Diameter, Hole Spacing Weir Height, and Downcomer Area," *Pet. Ref. V. 34*, p. 114 (1955).
72. Underwood, A. J. V., "Fractional Distillation of Multicomponent Mixtures," *Chem. Eng. Prog. V. 44*, p. 603 (1948).
73. Underwood, A. J. V., *Trans. Inst. Ch. E. (London) V. 10* p. 112 (1932).
74. Van Winkle, M., *Distillation*, McGraw-Hill, Inc. (1967).
75. Van Winkle, M., "Multicomponent Distillation," *Oil and Gas Journal*, p. 182, Mar. 23, (1953).
76. Wang, J. C. and G. E. Henke, "Tridiagonal Matrix for Distillation," *Hydrocarbon Processing. V. 45*, No. 8, (1966) p. 155.
77. Wilson, G. M., *J. Am. Chem. Soc.*, V. 86, (1964) p. 127.
78. Zenz, F. A., "Calculate Capacity of Perforated Plates," *Pet Ref. V. 33*, p. 99 (1954).
79. Gas Processors Suppliers Association; *Engineering Data Book*, V. 1 and 2, 3rd, Rev., 9th Ed. (1977), produced in cooperation with the Gas Processors Association.
80. DePriester, C. L., The American Institute of Chemical Engineers; *Chem. Eng. Prog. Sym. Ser. V. 49*, No. 7 (1953) p. 1.
81. Nelson, W. L., "*Petroleum Refinery Engineering*" 1st Ed McGraw-Hill Co., Inc. (1936), p. 244.
82. Carroll, J. J., "What Is Henry's Law?" *Chem. Eng. Prog. V. 87*, Sept. (1991), p. 48.
83. Carroll, J. J., "Use Henry's Law for Multicomponent Mixtures," *Chem. Eng. Prog. V. 88*, No. 8 (1992) p. 53.
84. Eduljee, H. E., "Equations Replace Gilliland Plot," *Hydro. Proc. V. 54*, No. 9 (1975), p. 120.
85. Murphree, E. V., *Ind. Eng. Chem. V. 17*, (1925), p. 747.
86. MacFarland, S. A., P. M., Sigmund, and M. Van Winkle, "Predict Distillation Efficiency," *Hydro. Proc. V. 51*, No. 7 (1972), p. 111.
87. Biddulph, M. W., "When Distillation Can Be Unstable," *Hydro. Proc. V. 54*, No. 9 (1975), p. 123.
88. Fair, J. R., "Tray Hydraulics-Perforated Trays," Chap. 15 in *Design of Equilibrium Stage Processes*, Smith, B. D., McGraw-Hill, New York, (1963), p. 552.
89. Leva, M., "Film Tray Equipment for Vacuum Distillation," *Chem. Eng. Prog. V. 67*, No. 3 (1971), p. 65.
90. Biddulph, M. W., "Tray Efficiency Is Not Constant," *Hydro. Proc. Oct. (1977)*, p. 145.
91. Wichterle, I., R., Kobayashi, and P. S. Chappelaar, "Caution! Pinch Point in Y-X Curve" *Hydro. Proc. Nov. (1971)*, p. 233.
92. Wagle, M. P., "Estimate Relative Volatility Quickly," *Chem. Eng. V. 92*, No. 9 (1985), p. 85.
93. Reid, R. C., J. M. Prausnitz, and T. K. Sherwood, "*The Properties of Gases and Liquids*," 3rd Ed., McGraw-Hill, New York, (1977), p. 214.
94. Kister, H. Z., "*Distillation Design*," McGraw-Hill, Inc. (1992).
95. Kister, H. Z., "Complex Binary Distillation," *Chem. Eng. V. 92*, No. 2 (1985), p. 97.
96. Chou, S-M. and C. L. Yaws, "Minimum Reflux for Complex Distillations," *Chem. Eng. V. 95*, No. 6 (1988), p. 79.
97. McCormick, J. E., "A Correlation for Distillation Stages and Reflux," *Chem. Eng. V. 95*, No. 13 (1988) p. 75.
98. Venkateswara, Rao K., and A. Raviprasad, "Quickly Determine Multicomponent Minimum Reflux Rates," *Chem. Eng. V. 14* (1987), p. 137.
99. Winn, F. W., "New Relative Volatility Method for Distillation Calculations," *Pet. Refiner (now Hydro. Proc.) V. 37*, No. 5 (1958), p. 216.
100. Frank, O., "Shortcuts for Distillation Design," *Chem. Eng. Mar. 14, (1977)*, p. 109.
101. Kessler, D. P. and P. C. Wankat, "Correlations for Column Parameters," *Chem. Eng. V. 95*, No. 13 (1988) p. 71.
102. Tsuo, Fu-Ming, C. L. Yaws and J-S. Cheng, "Minimum Reflux for Sidestream Columns," *Chem. Eng. July 21, (1986)*, p. 49.
103. Chou, S-M. and C. L. Yaws, "Reflux for Multifeed Distillation," *Hydro. Proc. Dec. (1986)*, p. 41.
104. Scheiman, A. D., "Find Minimum Reflux by Heat Balance," *Hydro. Proc. Sept. (1969)*, p. 187.
105. Lessi, A., "New Way to Figure Minimum Reflux," *Hydro. Proc. V. 45*, No. 3 (1966), p. 173.
106. Hengstebeck, R. J., "*Distillation—Principles and Design Procedures*," Reinhold. Pub. Co. New York, (1961), p. 120.
107. Eduljee, H. E., "Easy Way to Remember Reflux vs. Trays," *Hydro. Proc. V. 42*, No. 5 (1963), p. 185.
108. Maas, J. H., "Optimum-Feed Stage Locations in Multicomponent Distillations," *Chem. Eng. Apr. 16 (1973)*, p. 96.
109. Dechman, D. A., "Correcting the McCabe-Thiele Method for Unequal Molal Overflow," *Chem. Eng. Dec. 21 (1964)* p. 79.
110. Torres-Marchal, C., "Graphical Design for Ternary Distillation Systems," *Chem. Eng. V. 88*, No. 21 (1981) p. 134.
111. Torres-Marchal, C., "Calculating Vapor-Liquid Equilibria for Ternary Systems," *Chem. Eng. V. 88*, No. 21 (1981), p. 141.
112. Maddox, R. N., "Calculations for Multicomponent Distillation," *Chem. Eng. Dec. 11 (1961)*, p. 127.
113. Erbar, R. C., R. S. Joyner, and R. N. Maddox, "For Multicomponent Columns, How to Calculate Minimum Reflux," *Petro/Chem Engr. Mar. (1961)*, p. C-19.
114. Lyster, W. N., S. L. Sullivan, D. S. Billingsley, and C. D. Holland, "Digital Computer Used to Figure Distillation This New Way," *Pet. Ref. (now, Hydro. Proc.)*, June (1959), p. 221.
115. Maddox, R. N., and J. H. Erbar, "Programming Plate to Plate Distillation Calculations," *Refining Engr. Sept. (1959)*, p. C-35.
116. Maddox, R. N., and W. A., Jr., Fling, "Try the Pseudo-K Method for Short-cut Multicomponent Distillation Columns," *Petro/Chem Engr. Mar. (1961)* p. C-37.
117. Kister, H. Z., "*Distillation Operation*," McGraw-Hill, Inc. (1990).
118. Forman, E. R., "Control Systems for Distillation," *Chem. Eng. Nov. 8 (1965)*, p. 213.
119. Hoffman, H. L., "HP/PR Special Report, Automatic Control for Distillation," *Hydro. Proc. and Pet. Ref. V. 42*, No. 2 (1963), p. 107.

120. Shinskey, F. G. "Process-Control Systems," McGraw-Hill Book Co., 2nd Ed. (1979).
121. Trigueros, D., Coronado-Velasco, C. and A. Gornez-Munoz, "Synthesize Simple Distillation the Thermodynamic Way," *Chem. Eng.* V. 96, No. 8 (1989), p. 129.
122. Mapstone, G. E., "Reflux versus Trays By Chart," *Hydro-Proc.* V. 47, No. 5 (1968), p. 169.
123. Zanker, A., "Nomograph Replaces Gilliland Plot," *Hydro. Proc.* May (1977), p. 263.
124. Yaws, C. L., P. M. Patel, F. H. Pitts, and C. S. Fang, "Estimate Multicomponent Recovery," *Hydro. Proc.* V. 58, No. 2 (1979), p. 99.
125. Hengstebeck, R. J. *Trans. A.I.Ch.E.* V. 42 (1946) p. 309.
126. Geddes, R. L., *A.I.Ch.E. Jour.* V. 4 (1958), p. 389.
127. Ellerbee, R. W., "Steam-Distillation Basics," *Chem. Eng. Mar.* 4 (1974), p. 105.
128. Ellerbee, R. W., Section 1.4 in Schweitzer, P. A. (editor), *Handbook of Separation Techniques for Chemical Engineers*, McGraw-Hill Book Co. (1979).
129. Treybal, R. E., "A Simple Method for Batch Distillation," *Chem. Eng.* Oct. 5 (1970), p. 95.
130. Ellerbee, R. W., "Batch Distillation Basics," *Chem. Eng.* May 28 (1973), p. 110.
131. Schweitzer, P. A. "Handbook of Separation for Chemical Engineers," McGraw-Hill Book Co. (1979).
132. Perry, R. H., and Green, D. "Perry's Chemical Engineers Handbook," 6th Ed. McGraw-Hill Book Co. (1984).
133. Block, B., "Batch Distillation of Binary Mixtures Provides Versatile Process Operations," *Chem. Eng.* Feb. 6 (1961) p. 87.
134. Block, B., "Control of Batch Distillations," *Chem. Eng.* Jan. 16 (1967) p. 147.
135. Brasens, J. R., "For Quicker Distillation Estimates," *Hydro. Proc.* Oct. (1969), p. 102.
136. Liddle, C. J., "Improved Short-cut Method for Distillation Calculations," *Chem. Eng.* Oct. 21 (1968), p. 137.
137. Hengstebeck, R. J., "An Improved Shortcut for Calculating Difficult Multicomponent Distillations," *Chem. Eng.* Jan. 13 (1969), p. 115.
138. Guy, J. L., "Modeling Batch Distillation in Multitray Columns," *Chem. Eng.* Jan. 10 (1983), p. 99.
139. Van Winkle, M. and W. G. Todd, "Optimum Fractionation Design by Simple Graphical Methods," *Chem. Eng.* Sept 20 (1971), p. 136.
140. Koppel, P. M., "Fast Way to Solve Problems for Batch Distillation," *Chem. Eng.* Oct. 16 (1972), p. 109.
141. Yaws, C. L., C-S. Fang, and P. M. Patel, "Estimating Recoveries in Multicomponent Distillation," *Chem. Eng.* Jan. 29 (1979), p. 101.
142. Kumana, J. D., "Run Batch Distillation Processes with Spreadsheet Software," *Chem. Eng. Prog.* Dec. (1990), p. 53.
143. Li, K. Y. and K. J. Hsiao, "How to Optimize an Air Stripper," *Chem. Eng.* V. 98, No. 7 (1991), p. 114.
144. Salmon, R., "New Method for V/L Flash Calculations," *Pet. Ref.* (now *Hydro. Proc.*) V. 36, No. 12 (1957), p. 133.
145. Lockhart, F. J., and R. J., McHenry, "Figure Flash Equilibria Quicker This Way," *Pet. Ref.* V. 37, No. 3 (1958), p. 209.
146. Gallagher, J. L., "New Short-cut for Flash Calculations," *Hydro. Proc.* V. 42, No. 2 (1963), p. 157.
147. Holland, C. D. and P. R., Davidson, "Simplify Flash Distillation Calculations," *Pet. Ref.* V. 36, No. 3 (1957), p. 183.
148. Deam, J. R. and R. N., Maddox, "How to Figure Three-Phase Flash," *Hydro. Proc.* V. 51, No. 10 (1969), p. 163.
149. Henly, E. J. and L. D., Seader, "Equilibrium-Stage Separation Operations in Chemical Engineering," J. Wiley and Sons, Inc. (1981).
150. Eckles, A., P., Benz, and S., Fine, "When to Use High Vacuum Distillation," *Chem. Eng.* V. 98, No. 5 (1991), p. 201.
151. Elsby, K., et al., "Packing Performance in Vacuum Distillation," *A.I.Ch.E. Symposium Series No. 104 Distillation and Adsorption*, (1987), pp. 143-148.
152. "Vacuum Technology for Chemical Engineering," Leybold, AG., p. 11.
153. Holland, C. D., S. E., Gallun, and M. J., Lockett, "Modelling Azeotropic and Extractive Distillation," *Chem. Eng.* Mar. 23 (1981), p. 185.
154. Luyben, W. L., "Azeotropic Tower Design by Graph," *Hydro. Proc.* Jan. (1973), p. 109.
155. Stichlmair, J., J. R., Fair, and J. L., Bravo, "Separation of Azeotropic Mixtures via Enhanced Distillation," *Chem. Eng. Prog.* V. 85, No. 1 (1989), p. 63.
156. Gerster, J. A., "Azeotropic and Extractive Distillation," *Chem. Eng.* Prog. V. 65, No. 9 (1969), p. 43.
157. Holland, C. D., et al., "Solve More Distillation Problems," 13 Parts; *Hydrocarbon Processing*, Part 1, V. 53, No. 7 (1974); Part 2, V. 53, No. 11 (1974); Part 3, V. 54, No. 1 (1975); Part 4, V. 54, No. 7 (1975); Part 5, V. 55, 0.1 (1976); Part 6, V. 55, No. 6 (1976); Part 7, V. 56 No. 5 (1977); Part 8, V. 56, No. 6 (1977); Part 9, V. 59, No. 4 No. (1980); Part 10, V. 59, No. 7 (1980); Part 11, V. 60, No. 1 (1981); Part 12, V. 60, No. 7 (1981), Part 13, V. 83, No. 11, (1983).
158. Tru-Tec Division of Koch Engineering Co. Inc. *Bulletin TPD-1 and TCS-1*; Koch Engineering Co. Inc. Wichita, Kn. 67208-0127.
159. Harrison, M. E., and J. J. Frana, "Trouble-Shooting Distillation Columns," *Chem. Eng.* V. 96, No. 3 (1989) p. 116.
160. Kister, H. Z., K. F., Larson and P. E., Madsen, "Vapor Cross-Flow Channeling on Sieve Trays: Fact or Myth?" *Chem. Eng. Prog.* V. 88, No. 11 (1992), p. 86.
161. Niesenfeld, A. E., "Reflux or Distillate: Which to Control?" *Chem. Eng.* Oct. 6 (1969), p. 169.
162. Ludwig, E. E., "Applied Project Engineering and Management," 2nd Ed., Gulf Publishing Co. (1988), p. 453.
163. Rys, R. A., "Advanced Control Techniques for Distillation Columns," *Chem. Eng.* Dec. 10 (1984), p. 75.
164. Kister, H. Z., "Distillation Operation," McGraw-Hill Publishing Co., Inc. (1990).
165. Kister, H. Z., "How to Prepare and Test Columns Before Start-Up," *Chem. Eng.* Apr. 6 (1981) p. 97.
166. Chin, T. G., "Guide to Distillation Pressure Control Methods," *Hydro. Proc.* V. 59, No. 10 (1979), p. 145.
167. Thurston, C. W., "Computer Aided Design of Distillation Column Controls," *Hydro. Proc.* V. 60, No. 8 (1981), p. 135.
168. Holland, C. D., "Fundamentals of Multicomponent Distillation," McGraw-Hill Book Co. Inc. (1981).
169. Holland, C. D. and A. I., Liapis, "Computer Methods for Solving Dynamic Separation Problems," McGraw-Hill, Inc. (1983).
170. Haring, H. G., B. J., Grootenhuis, and H. W., Knol, "Programming Batch Distillation," *Chem. Eng.* Mar. 16 (1964), p. 159.
171. Nisenfeld, A. E. and C. A., Stravinski, "Feed Forward Control for Azeotropic Distillation," *Chem. Eng.* Sept. 23 (1968), p. 227.
172. Othmer, D. F., "Azeotropic Separation," *Chem. Eng. Prog.* V. 59, No. 6 (1963), p. 67.
173. Fair, J. R. and W. L., Bolles, "Modern Design of Distillation Columns," *Chem. Eng.* Apr. 22 (1968) p. 156.
174. Kirkbride, C. G., *Petro. Refiner*, V. 23, No. 9 (1944) p. 87.

175. Winn, F. W., "Equilibrium K's by Nomograph," *Petro. Refiner*, V. 33, No. 6 (1954) p. 131.
176. Gerster, J. A., "A New Look at Distillation Tray Efficiencies," *Chem. Eng. Prog.*, V. 59, No. 3 (1963) p. 35.
177. Williamson, W. R. and H. L. W. Pierson, senior thesis, University of Delaware, (June, 1961).
178. Proctor, J. F., "A New Look at Distillation-2: Sieve and Bubble Plates Comparative Performance," *Chem. Eng. Prog.*, V. 59, No. 3 (1963), p. 47.
179. Strand, C. P., "A New Look at Distillation-3: Bubble Cap Tray Efficiencies," *Chem. Eng. Prog.*, V. 59, No. 4 (1963), p. 58.
180. Sakata, M., "Liquid Mixing in Distillation Columns," *Chem. Eng. Prog.*, V. 62, No. 11 (1966), p. 98.
181. Hughmark, G. A., "Point Efficiencies for Tray Distillations," *Chem. Eng. Prog.*, V. 61, No. 7 (1965) p. 97.
182. Bowman, J. D., "Use Column Scanning Predictive Maintenance," *Chem. Eng. Prog.*, V. 87, No. 2 (1991), p. 25.
183. Fair, J. R., "How to Predict Sieve Tray Entrainment and Flooding," *Petro/Chem Engr.* Sept. (1961), p. 45.
184. Kister, H. Z. and J. R., Haas, "Predict Entrainment Flooding on Sieve and Valve Trays," American Institute of Chemical Engineers, *Chem. Eng. Prog.*, V. 86, No. 9 (1990), p. 63.
185. Fair, J. R. and R. L. Matthews, *Petro. Ref.*, V. 37, No. 4 (1958), p. 153.
186. Kister, H. Z. and J. R., Haas, *I. Chem. Eng. Symp. Series*, V. 104 (1987), p. A483.
187. Ward, T. J., "A New Correlation for Sieve Trays," *Chem Eng*, V. 96, No. 6 (1989), p. 177.
188. Capps, R. W., "Consider the Ultimate Capacity of Fractionation Trays," *Chem. Eng. Prog.*, V. 89, No. 3 (1993), p. 37.
189. Barnicki, S. D. and J. F., Davis, "Designing Sieve Tray Columns-Part 1," *Chem. Eng.*, V. 96, No. 10 (1989) p. 140; and Part 2, *ibid* No. 11 (1989), p. 202.
190. Kister, H. Z., "Downcomer Design for Distillation Tray Columns," *Chem. Eng.*, Dec. 29 (1980), p. 55.
191. Yeoman, N., "The FRI Tray Data Sheet," *Chem Eng. Prog.*, V. 85, No. 12 (1989), p. 14.
192. Chase, J. D., "Sieve Tray Design, Part 1," *Chem Eng.*, July 31 (1967), p. 105.
193. Fair, J. R., Chapter 15 in *Design of Equilibrium Stage Processes*, B. D. Smith, McGraw-Hill, (1963).
194. Lessi, A., "How Weeping Affects Distillation," *Hydro. Proc.*, V. 51, No. 3 (1972) p. 109.
195. Jamison, R. H., "Internal Design Techniques," *Chem Eng. Prog.*, V. 65, No. 3 (1969) p. 46.
196. Kister, H. Z., "Design and Layout for Sieve and Valve Trays," *Chem. Eng.*, V. 87, No. 18 (1980).
197. Economopoulos, A. P., "Computer Design of Sieve Trays and Tray Columns," *Chem. Eng.*, V. 85, No. 27 (1978) p. 109.
198. Frank, J. C., G. R. Geyer, and H., Kehde, "Styrene-Ethyl-Benzene Separation with Sieve Trays," *Chem. Eng. Prog.*, V. 65, No. 2 (1969), p. 79.
199. King, C. J., *Separation Processes*, McGraw-Hill Book Co. (1971), p. 555.
200. Henley, E. J. and J. D., Seader, "Equilibrium Stage Separations in Chemical Engineering," John Wiley and Sons (1981), p. 507.
201. Klein, G. F., "Simplified Model Calculates Valve-Tray Pressure Drop," *Chem. Eng.*, V. 89, No. 9 (1982), p. 81.
202. Glitsch, Inc. "Ballast Tray Design Manual," Bul. 4900, 5th Ed. Glitsch, Inc. (1974, 1989), Dallas, Texas.
203. Koch Engineering, Inc. "Flexitray Design Manual," Bul. 960-1 (1982), Koch Engineering Co. Inc, Wichita, KN.
204. Nutter Engineering, "Nutter Float Valve Tray Design Manual," and "Electronic Design Manual Version 2.0," Nutter Engineering, a Harsco Corp. (1990), Tulsa, Okla.
205. Bolles, W. L., *Chem Eng Prog.*, V. 72, No. 9 (1976), p. 43.
206. Thorngren, J. T., *Ind. Eng. Chem. Proc. Des.*, V. 11, No. 3 (1972), p. 428.
207. Thorngren, J. T., "Valve Tray Flooding Generalized," *Hydro. Proc.*, V. 57, No. 8 (1978) p. 111.
208. Billet, R., "Development of Progress in the Design and Performance of Valve Trays," *British Chem. Eng. Apr.* (1969).
209. Biddulph, M. W., C. P., Thomas, and A. C., Burton, "Don't Downplay Downcomer Design," *Chem. Eng. Prog.*, V. 89, No. 12, (1993), p. 56.
210. Hsieh, C-Li., and K. J., McNulty, "Predict Weeping of Sieve and Valve Trays," *Chem. Eng. Prog.*, V. 89, No. 7, (1993), p. 71.
211. Fair, J. R., "How to Design Baffle Tray Columns," *Hydro. Proc.*, V. 72, No. 5 (1993), p. 75.
212. Lemieux, E. J., "Data for Tower Baffle Design," *Hydro. Proc.*, V. 62, No. 9 (1983), p. 106.
213. Kister, H. Z., K. F., Larsen, and P. E., Madsen, "Vapor Cross-flow Channeling on Sieve Trays, Fact or Myth?" *Chem. Eng. Prog.*, V. 88, No. 11 (1992), p. 86.
214. Winter, J. R., "Avoid Vibration Damage to Distillation Trays," *Chem. Eng. Prog.*, V. 89, No. 5 (1993), p. 42.
215. Hasbrouck, J. F., J. G., Kunesh, and V. C., Smith, "Successfully Troubleshoot Distillation Towers," *Chem Eng. Prog.*, Mar. (1993), p. 63.
216. Campagne, W. V. L., "Use Ponchon-Savarit in Your Process Simulation, Part 1," *Hydro. Proc.*, V. 72, No. 9 (1993), p. 41.
217. *Ibid*, V. 72, No. 10 (1993), p. 63.
218. Liebert, T., "Distillation Feed Preheat—Is It Energy Efficient?" *Hydro. Proc.*, V. 72, No. 10, (1993) p. 37.
219. Kister, H. Z., K. F., Larsen, and T., Yanagi, "How Do Trays and Packings Stack Up?" *Chem. Eng. Prog.*, V. 90, No. 2 (1994), p. 23.
220. Kister, H. Z., K. F., Larsen, and T., Yanagi, "Capacity and Efficiency: How Trays and Packings Compare?" presented at A.I.Ch.E Spring Meeting, Houston, Tex. Mar.-April (1993).
221. Feintuch, H. M., "Distillation Distributor Design," *Hydro. Proc.*, Oct. (1977), p. 150.
222. Cassata, J. R., S., Dasgupta, and S. L., Gandhi, "Modeling of Tower Relief Dynamics," *Hydro. Proc.*, V. 72, No. 10 (1993), p. 71.
223. Maddox, R. N., "Absorber Performance," *Oil and Gas Journal*, May 25 (1964), p. 146.
224. Hengstebeck, R. J., "Finding Feed Plates from Plots," *Chem. Eng.*, July 29 (1968), p. 143.
225. McCabe, W. L. and Thiele, E. W. "Graphical Design of Fractionating Columns," *Ind. and Eng. Chem.*, June (1925) p. 605.
226. Hengstebeck, R. J., "A Simplified Method for Solving Multi-component Distillation Problems," presented at A.I.Ch.E. meeting, Chicago, Ill., Dec. 16 (1945); published in *Trans. A.I.Ch.E.*, (1946), p. 309.
227. Edmister, W. C., "Multicomponent Fractionation Design Method," presented A.I.Ch.E. meeting, Houston, Tex. Mar. 31 (1946); published, *Trans. A.I.Ch.E.*, V. 42, No. 4 (1946), p. 15.
228. Lewis, W. K. and G. L., Matheson, "Studies in Distillation," received by A.I.Ch.E. (1932), publication date not known.
229. Graves, R. G., "Rigorous Distillation Method," *Pet. Ref.*, V. 38, No. 5 (1959), p. 209.
230. Short, T. E. and J. H., Erbar, "Minimum Reflux for Complex Fractionators," *Petro/Chem. Engr.*, Nov. (1963), p. 30.

231. Kister, H. Z., and I. D., Doig, "Distillation Pressure Ups Thruput," *Hydro. Proc.* July (1977), p. 132.
232. Billet, R. and L., Raichle, "Optimizing Method for Vacuum Rectification, Part I," *Chem. Eng.* Feb. 13 (1967), p. 145 and Part II, Feb. 27 (1967), p. 149.
233. Norton Chemical Process Products Corp., Akron, Ohio.
234. Starling, K. E., *Fluid Thermodynamic Properties for Light Petroleum Systems*, Gulf Pub. Co. (1973).
235. Winn, F. W., "Equilibrium K's by Nomograph," *Pet. Ref. V.* 33 (1954).
236. Nutter, D. E., private communication.
237. Lockett, M. J., "Distillation Try Fundamentals," Cambridge University Press, Cambridge, U.K. (1986).
238. Urva, I. J. and M. C. G., del Cerro, "Liquid Residence Time in Downcomers for Foaming and Non-Foaming System," in *Gas Separation and Purification*, V. 6, No. 2 (1992) p. 71.
239. Nutter, D. E. and D., Perry, "Sieve Tray Upgrade 2.0-The MVG (TM) Tray," presented at the AIChE Spring National Meeting, Houston, Texas, March 22, 1995, unpublished, copyright by Nutter Engineering, Harsco Corporation.
240. American Petroleum Institute, Technical Data Book—Petroleum Refining, Port City Press Inc., Baltimore, Md (1966).
241. Gallant, R. W., *Hydrocarbon Processing*, V. 47, No. 8 (1968), p. 127.
242. Perry, J. H. (editor), *Chemical Engineers' Handbook*, McGraw-Hill Book Co., New York, (1963).
243. Wilke, C. R., Chang, P., *AIChE J.*, V. 1 (1955), p. 264.
- Coulter, K. E., "Part I: Applied Distillation—Fundamentals," *Pet. Ref. V.* 31, No. 8 (1952) p. 95.
- Coulter, K. E., "Part II: Applied Distillation—Bubble Cap and Packed Distillation Columns," *Pet. Ref. V.* 31, No. 10 (1952).
- Coulter, K. E., "Part III: Applied Distillation—Dehydration Columns and Steam Distillation," *Pet. Ref. V.* 31, No. 11 (1952).
- Coulter, K. E., "Part IV: Applied Distillation—Column Control," *Pet. Ref. V.* 31, No. 12 (1952).
- Davidson, J. W. and G. E. Hayes, "Ethylene Purification, Process Design of Ethylene-Ethane Fractionator," *Chem. Eng. Prog. V.* 54, No. 12 (1958), p. 52.
- Eckhart, R. A., and A. Rose, "New Method for Distillation Prediction," *Hydro. Proc. V.* 47, No. 5 (1968), p. 165.
- Economopoulos, A. P., "A First Computer Method for Distillation Calculations," *Chem. Eng.* April 24 (1978), p. 91.
- Eichel, F. G., "Efficiency Calculations for Binary Batch Rectification with Holdup," *Chem. Eng.* July 18 (1966), p. 159.
- English, G. E. and M. Van Winkle, "Efficiency of Fractionating Columns," *Chem. Eng.* No. 11 (1963), p. 241.
- Fair, J. R., W. L., Bolles, and W. R. Nisbet, "Ethylene Purification-Demethanization," *Chem. Eng. Prog. V.* 54, No. 12 (1958), p. 39.
- Finelt, S., "Better C₃ Distillation Pressure," *Hydro. Proc.*, V. 58, No. 2 (1979) p. 95.
- Golden, S. W., N. P. Lieberman, and E. T. Lieberman, "Troubleshoot Vacuum Columns with Low Capital Methods," *Hydro. Proc. V.* 72, No. 7 (1993), p. 81.
- Gordon, K. F., J. A. Davies, "Distillation," *Refining Engr.* Feb. (1960) p. C-31.
- Graven, R. G., "For Multicomponent Rigorous Distillation Method," *Pet. Ref.* May (1959), p. 209.
- Grosberg, J. A. and G. E. Mapstone, "Short-Cut to V-L Equilibria Solutions," *Pet. Ref.* Mar. (1955), p. 193.
- Guerreri, G., "Short Cut Distillation Design: Beware," *Hydro Proc. V.* 48, No. 8 (1969), p. 137.
- Guerreri, G., "Graphs Show Methane-Ethylene Split," *Hydro. Proc. V.* 48, No. 8 (1967), p. 108.
- Huan-Yang Chang, "Gilliland Plot in One Equation," *Hydro. Proc.*, V. 60, No. 10 (1981), p. 146.
- Humphrey, J. L. and A. F. Siebert, "New Horizons in Distillation," *Chem. Eng.* Dec. (1992), p. 86.
- Ibid.*, "Separation Technologies: An Opportunity for Energy Savings," *Chem. Eng. Prog. V.* 88, No. 3 (1992), p. 31.
- Hunting, R. D., and J. W. Robinson, "Predict Composition of Binary Mixtures," *Chem. Eng.*, July 9 (1984), p. 91.
- Kesler, M., "Shortcut Program for Multicomponent Distillation," *Chem. Eng. V.* 88, No. 9 (1981), p. 85.
- Lanz, W. T., "Absorption Factor to Keep Lean-Oil Rate Down," *Oil and Gas Jour.* July 15 (1957) p. 88.
- Lenoir, J. M., "Predict Flash Points Accurately," *Hydro. Proc.* Jan. (1975), p. 95.
- Lieberman, N. P., "Checklist Is Key to Dealing with Distillation Troubles," *Oil and Gas Jour.* Sept. 10 (1979) p. 121.
- Ibid.*, "Processes Show Signs of Fouled Trays," Feb. 2 (1981), p. 98.
- Maddox, R. N. and J. H. Erbar, "Equilibrium Calculations by Equations of State," *Oil and Gas Jour.* Feb. 2 (1981), p. 74.
- Madsen, N., "Finding the Right Reflux Ratio," *Chem. Eng.*, V. 78, No. 25 (1971), p. 73.
- Mankey, D. B., "A Better Method for Calculating Relative Volatility," *Hydro. Proc.* Jan. (1972), p. 113.
- McWilliams, M. L., "An Equation to Relate K-Factors to Pressure and Temperature," *Chem. Eng.* Oct. 29 (1973) p. 138.
- Meili, A., "Heat Pumps for Distillation Columns," *Chem. Eng. Prog. V.* 86, No. 6 (1990), p. 60.

Bibliography

- Alleva, R. Q., "Improving McCabe-Thiele Diagrams," *Chem. Eng.* Aug. 6 (1962) p. 111.
- Barna, B. A. and R. F. Ginn, "Tray Estimates for Low Reflux," *Hydro. Proc. V.* 64, No. 5 (1985), p. 115.
- Berg, L., S. V. Buckland, W. B. Robinson, R. L. Nelson, T. K. Wilkinson, and J. W. Petrin, "More on Azeotropic Distillation," *Hydro Proc. V.* 45, No. 2 (1966), p. 103.
- Billet, R. and L. Raichle, "Optimizing Method for Vacuum Rectification—Part I," *Chem. Eng.* Feb. 13 (1967), p. 145.
- Ibid.*, "Operating Method for Vacuum Rectification—Part II," *Chem. Eng.* Feb. 27 (1967) p. 149.
- Boynton, G. W., "Iteration Solves Distillation," *Hydro. Proc.* Jan. (1970), p. 153.
- Brinkley, M. J., "New Developments in Petrochemicals Distillation Equipment Technology," Seminar No. 34, Dec. 10 (1987) New York, by Glitsch, Inc., Bulletin No. 379.
- Burningham, D. W. and F. D. Otto, "Which Computer Design for Absorbers?" *Hydrocarbon Processing*, 46, Oct. (1967), p. 163.
- Buthod, P., N. Perez, and R. Thompson, "Program Constants Developed for SRK Equation," *Oil and Gas Jour.* Nov. 27 (1978) p. 60.
- Chou, A., A. M. Fayon, and B. M. Bauman, "Simulations Provide Blueprint for Distillation Operation," *Chem. Eng.* June 7 (1976), p. 131.
- Chou, Yung-ho, "Understand the Potential of Sub-Cooled Distillate Condensate," *Chem. Eng. Prog. V.* 88, No. 6 (1992), p. 5.
- Coates, Jesse and B. S. Pressburg, "Analyze Absorption in Gas Separations," *Chem. Engr.* Oct. 3 (1960) p. 99.
- Coates, J. and B. S. Pressburg, "Adsorption Theory Guides Process Design," *Chem. Eng.* Feb. 19 (1962), p. 129.

- Murdoch and C. D. Holland, "Multicomponent Distillation," *Chem. Eng. Prog.* May (1952), p. 254.
- Nemunaitis, R. R., "Sieve Trays? Consider Viscosity," *Hydro. Proc.* Nov. (1971) p. 235.
- Parekh, R. H., "Absorption and Stripping Design," *Pet. Ref.* V. 34, No. 8 (1955) (Part 3; see earlier issues for Parts 1 and 2) p. 123.
- Prater, N. H., "Designing Stripping Columns," *Pet. Ref.* V. 33, No. 2 (1954) p. 96.
- Ripps, D. L., "Minimum Reflux Figured an Easier Way," *Hydro. Proc.* V. 47, No. 12 (1968), p. 84.
- Rooney, J. M., "Simulating Batch Distillation," *Chem. Eng.* V. 91, No. 10 (1984) p. 61.
- Shih, Y-P., T-C. Chou, and C-T. Chen, "Best Distillation Feed Points," *Hydro. Proc.* V. 50, No. 7 (1971), p. 93.
- Smith, R. B., T. Dresser, and S. Ohlswager, "Tower Capacity Rating Ignores Trays," *Hydro. Proc. and Pet. Refiner*, V. 40, No. 5 (1963) p. 183.
- Sofer, S. S., and R. G. Anthony, "Distillation, Real vs. Theory," *Hydro. Proc.* V. 52, No. 3 (1973), p. 93.
- Surowies, A. J., "A New Approach to Multicomponent Distillation—Part 1," *Petro/Chem. Engr.* Aug. (1963), p. 29.
- Tassoney, J. P., "Fast Analysis for Multistage Distillation," *Chem. Eng.* V. 96, No. 10 (1989), p. 191.
- Thompson, R. B. and E. D. Frigar, "Take this Shortcut in Computing Absorbers Material Balance," *Pet. Ref.*, V. 32, No. 4 (1953), p. 145.
- Toor, H. L. and J. K. Burchard, "Plate Efficiencies in Multicomponent Distillation," *A.I.Ch.E. Jour.* June (1960), p. 202.
- Van Winkle, M. and W. G. Todd, "Minimizing Distillation Costs via Graphical Techniques," *Chem. Eng.* Mar. 6 (1972), p. 105.
- Waterman, W. W., J. P. Frazier, and G. M. Brown, "Compute Best Distillation Feed Point," *Hydro. Proc.* V. 47, No. 6 (1968), p. 155.
- Zenz, F. A., "Designing Gas-Absorption Towers," *Chem. Engr.* Nov. 13 (1972), p. 120.
- Zomosa, A., "Quick Design of Distillation Columns for Binary Mixtures," *Chem. Eng.* Jan. 24 (1983), p. 95.

Packed Towers

Packed towers are used as contacting equipment for gas-liquid and liquid-liquid systems. Figures 9-1A and B present a cross-section of a typical unit. The shell is usually cylindrical, although square wooden, light metal, or reinforced plastic towers are used. The basic unit consists of:

1. Shell
2. Packing (one or more sections)
3. Packing support(s)
4. Liquid distributor(s)

(text continued on page 234)

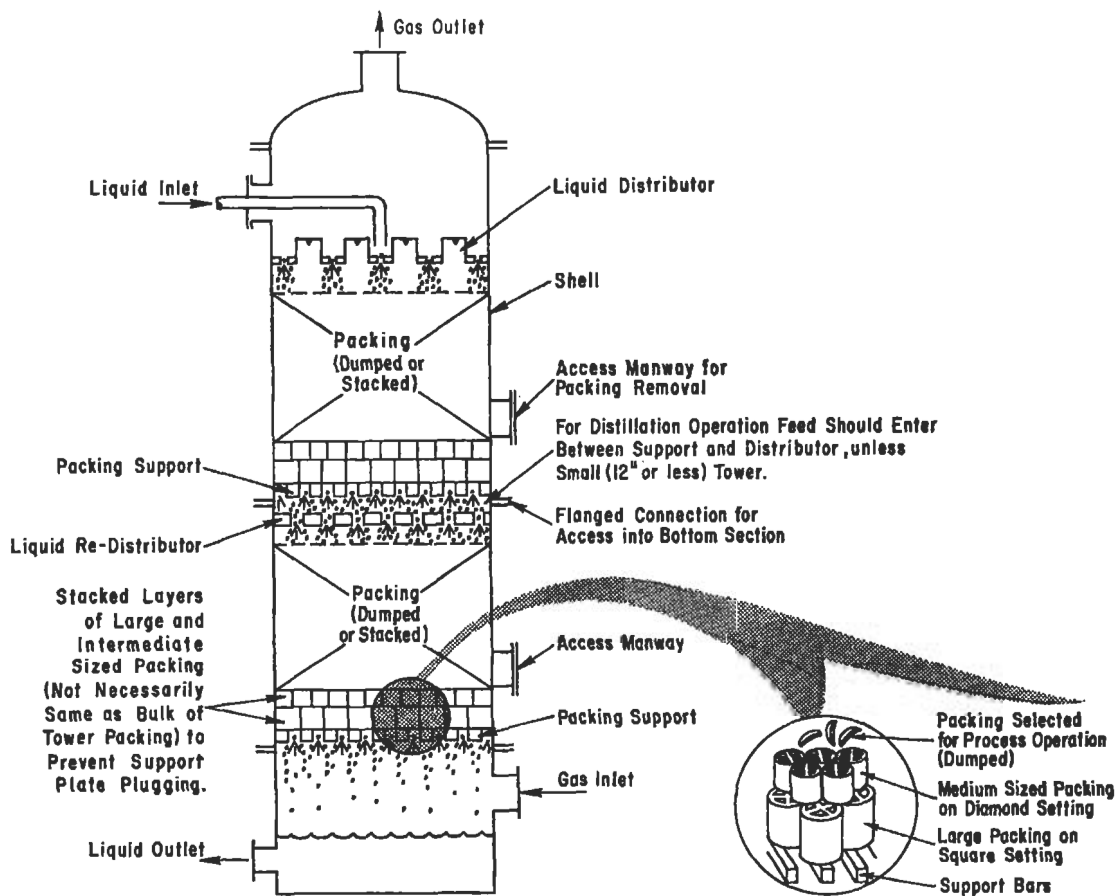


Figure 9-1A. Cross-section of typical packed tower.

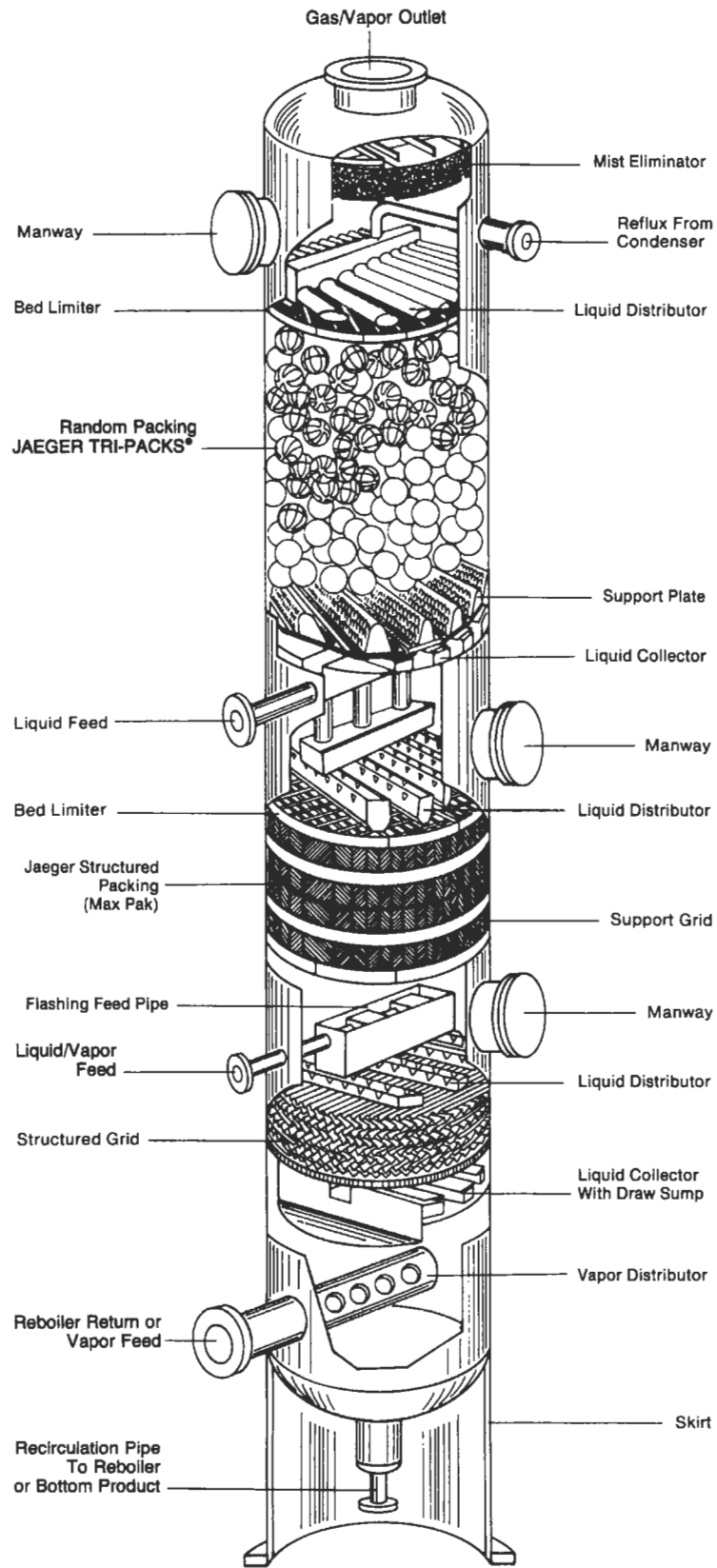


Figure 9-1B. Typical packed tower with internals for improved distillation. Used by permission of Jaeger Products Inc., Bull. 1100.

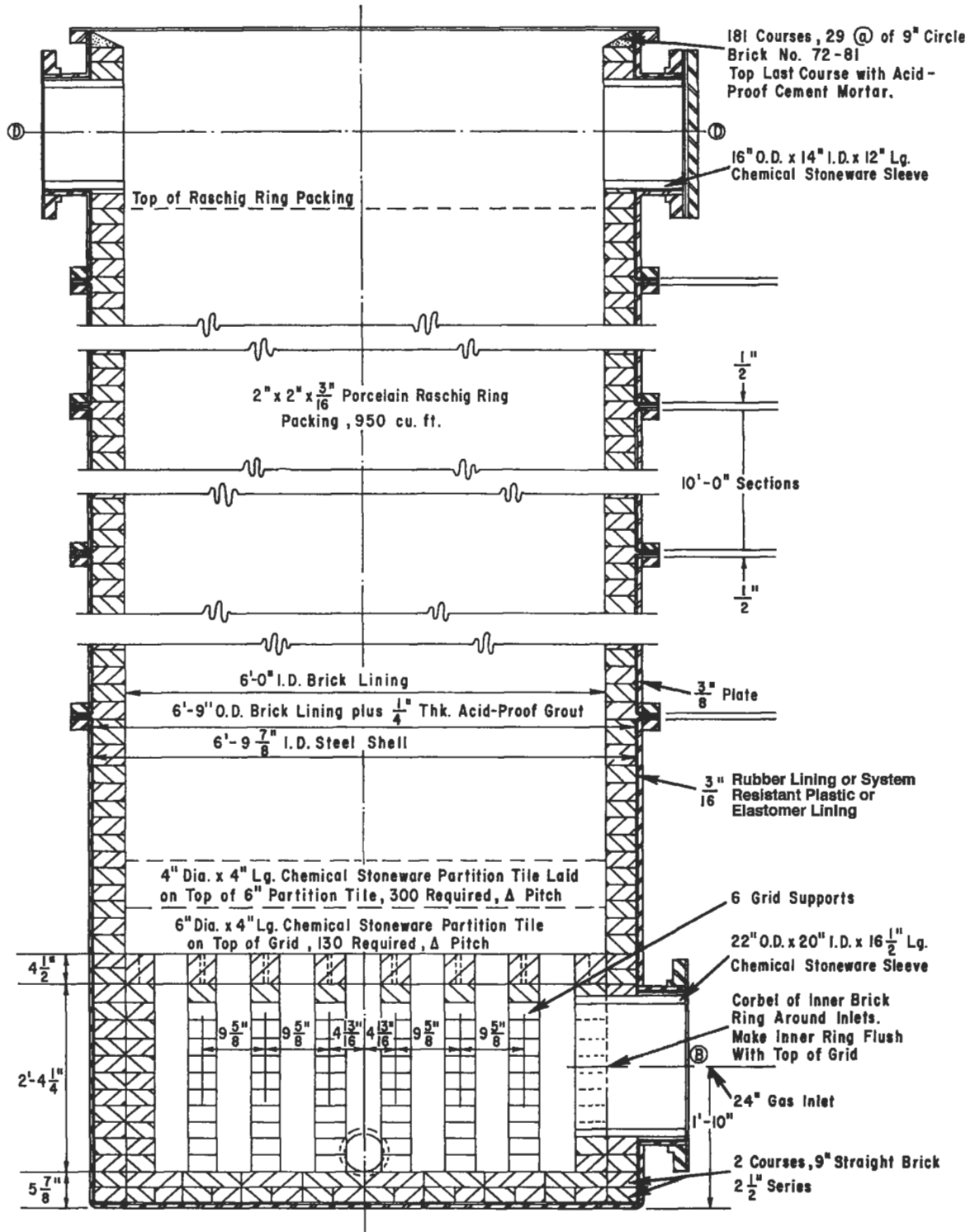


Figure 9-2A. Cross-section of membrane and brick-lined packed tower. Depending on tower diameter, certain dimensions should be modified, particularly packing. Also see Figures 9-2B and 9-2C.

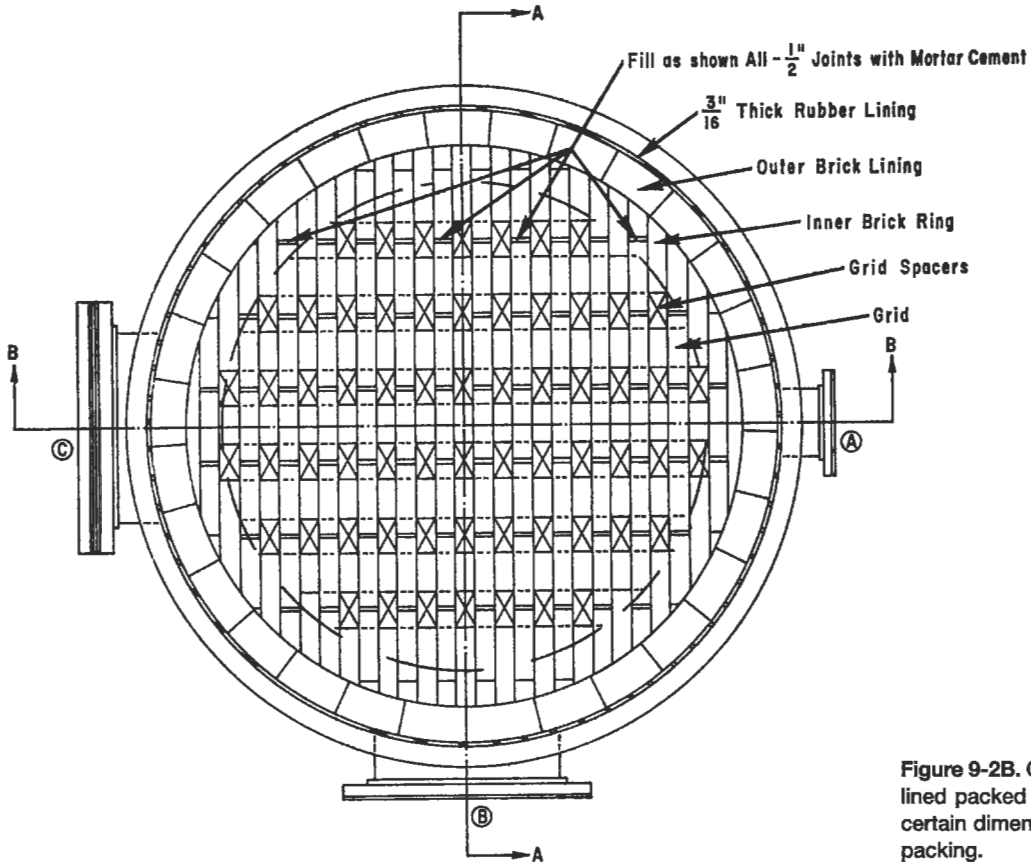


Figure 9-2B. Cross-section of membrane and brick-lined packed tower. Depending on tower diameter, certain dimensions should be modified, particularly packing.

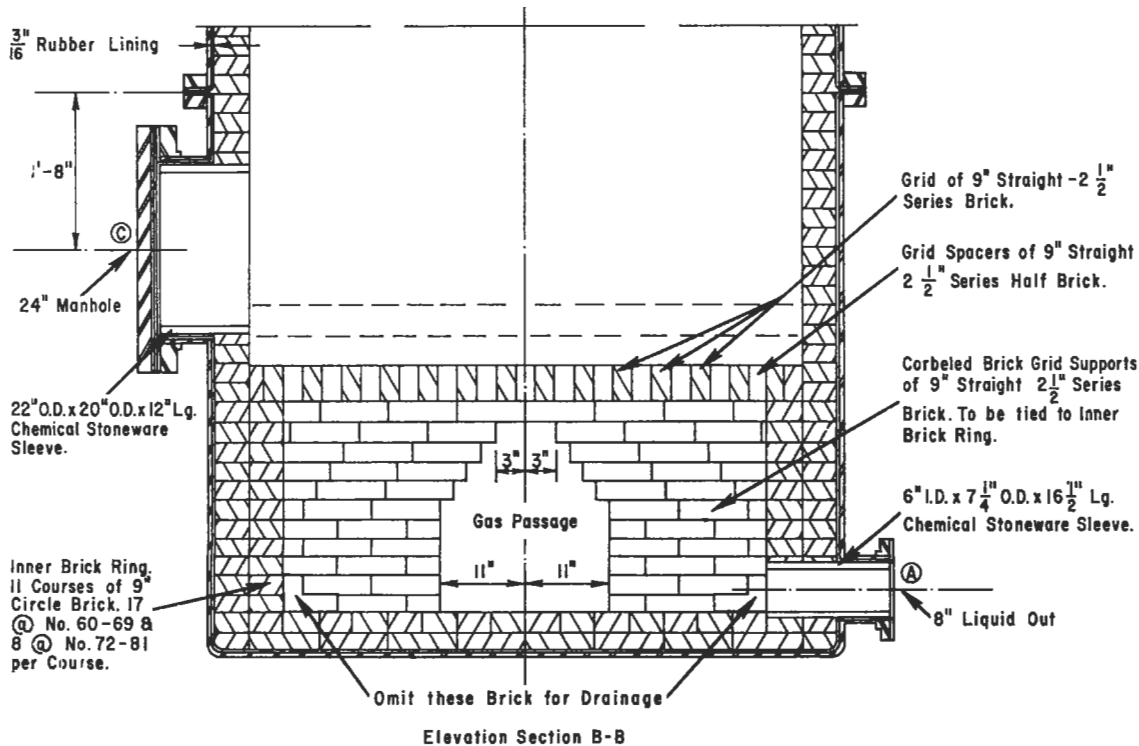


Figure 9-2C. Cross-section of membrane and brick-lined packed tower. Depending on tower diameter, certain dimensions should be modified, particularly packing.

(text continued from page 230)

5. Intermediate supports and redistributors
6. Gas and liquid entrance and exit nozzles

Many of the mechanical aspects of tower construction and assembly have an influence upon the design and interpretation of tower performance. Every effort should be made to increase the effectiveness of contact between the process streams and to reduce losses by entrainment or wall effects at a minimum expenditure of pressure drop. At the same time the design must be consistent with the economics dictated by the process and type of construction.

Shell

The shell may be of metal (steel, alloy, or non-ferrous), plastic, wood or some combination which may require the addition of liners or inner layers of rubber, plastic or brick. The mechanical problems of attaching inner nozzles, supports and brick require considerable attention that is not an integral part of sizing the equipment. Figures 9-2A-C show a typical large steel brick-lined-membrane lined tower with corbeled brick support locations. In these towers, temperature and/or corrosive conditions usually dictate the internal lining, and the selection of the proper acid- (or alkali-) proof cements.

Ceramic, plastic and other non-metal tower shells are used quite often (Figures 9-3, 4, and 5). It is important to consider in ceramic construction that the main inlet or outlet nozzles or any other large connections should be oriented 90° to each other to reduce the possibility of cracking the walls, as most cracks go one-half diameter. Preferably there should only be one nozzle at any one horizontal plane. The nozzles should never carry any piping or other stress load.

The bell and spigot type tower, Figures 9-3 and 9-4, is satisfactory for 2 to 2.5 psi in 12-in. dia. to 30-in. dia. towers when the joints are packed with chevron-type caulking compound. For operating pressures of 5 psi in 18-in. through 48-in. dia., use non-asbestos and silicate cement. Special hold-down packing gland-type rings will allow operation at slightly higher pressure. The porcelain towers should be used for the higher pressures rather than the weaker stoneware.

The rate of heating or cooling a stoneware or porcelain tower should not exceed 15°F/min.

Random Packing

The distributor and packing are the heart of the performance of this equipment. Their proper selection entails an understanding of packing operational characteristics and the effect on performance of the points of significant physical difference between the various types.

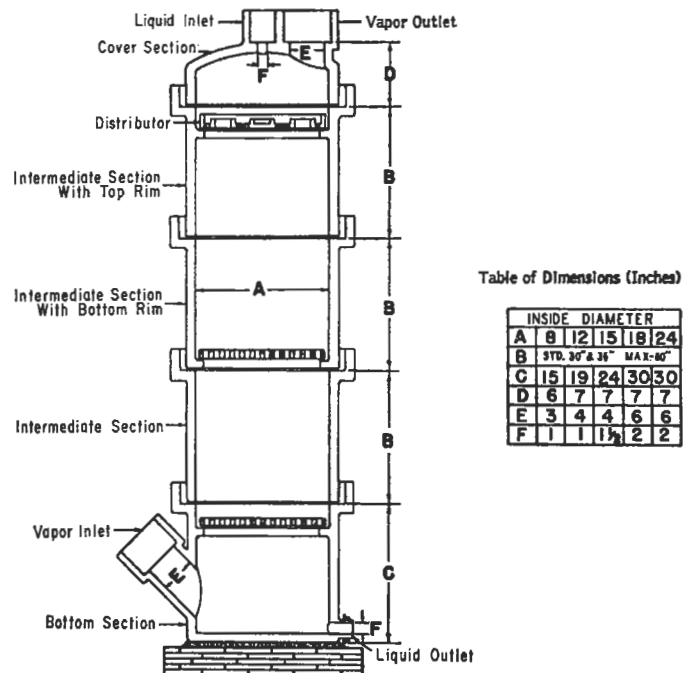


Figure 9-3. Bell and spigot ceramic tower. Used by permission of General Ceramics and Steatite Corp.

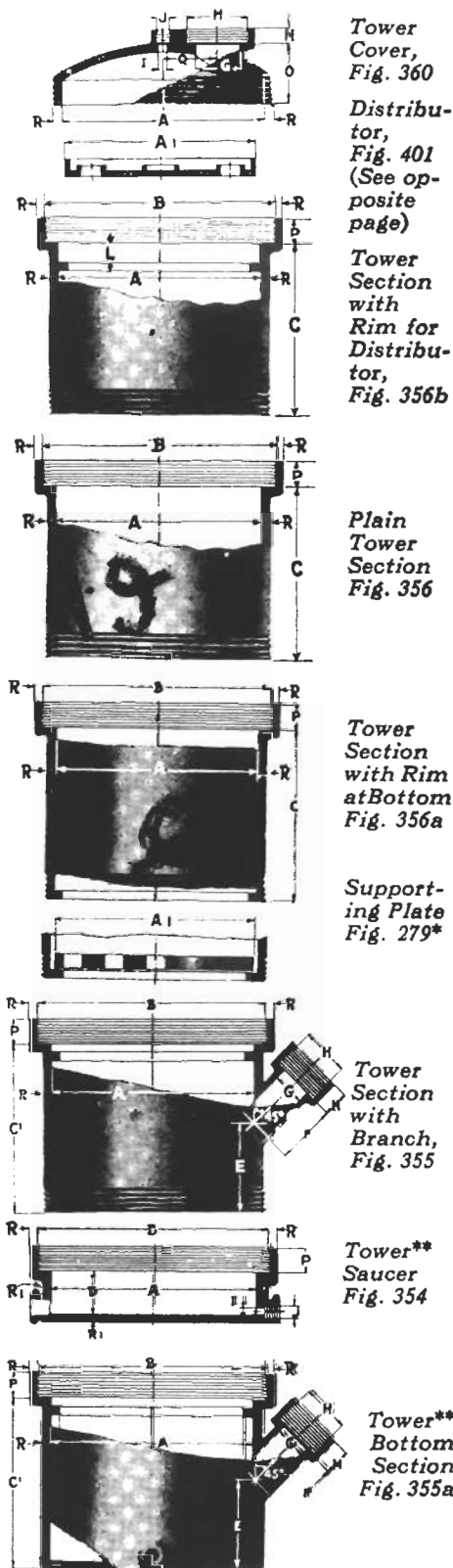
Good progress has been made in the past decade in the development of packing for difficult and wide ranging process applications. These types include:

1. *Random particle* packings are discrete, individually shaped particles designed to provide contacting surfaces between normally down-flowing liquid and up-flowing vapor/gas. The degree of effectiveness of the various shapes varies along with the mass pressure drop through the packed bed. Usually these particles are "dumped" into the column (tower) and allowed to gently float to their free-fall resting position in a column full of water. Some shapes and sizes are not installed using water, but dumped in using a special "sock" that allows the particles to be lowered without a damaging free fall. Sometimes large particles are hand set "dry" into position to tightly fill the tower. See Figure 9-1A. The vapor-liquid performance is different between the different methods of loading, and appropriate data must be available to properly size the tower. The random "dumped" (wet or dry) method is the technique usually used for most published data. See Figures 9-6A-9-6X.
2. *Structured packing*, which is offered by several manufacturers, is usually composed of pack "pads" fabricated by shaping/crimping, bending, rolling, etc. sheets of thin gauge metal or wire. (See Figures 9-6Y to 9-6OO.) Some "pads" or packs are formed using various plastic material, selected to be resistant to the fluid services involved.

DIMENSIONS OF STANDARD TOWERS						
Inside Diameter of Tower A	24 in.	30 in.	36 in.	40 in.	48 in.	60 in.
A	24	30	36	40	48	60
A'	23 1/4	29 1/4	35	39	47 1/2	58
B	27 1/2	34	41 1/2	45	54 1/2	67 1/2
C	36	36	36	36	36	36
C'	30	30	36	36	40	40
D	6	6	6	6	6	6
E	15	15	15	15	15	15
F	10	12	14	14	18	18
G	6	8	12	12	18	18
H	8	10 1/2	14 3/4	14 3/4	21	21
I	1	1	1	1 1/2	1 1/2	1 1/2
J	2 1/2	2 1/2	2 1/2	3	3	3
L	4	4	4	4	4	4
M	3	3	3	3	3	3
O	7	9 3/8	11 1/2	11 5/8	13 3/4	18
P	3	3	3	3	3	3
Q	7	8	11	11	14	16
R	1 1/2	1 1/4	1 3/8	1 1/2	1 3/4	2
R'	1 1/2	1 3/8	1 1/4	1 3/4	2	2
S	3/4	3/4	1	1	1 1/4	1 1/4

S is inside diameter of ground in faucet.

	WEIGHTS					
	Diameter					
	24 in.	30 in.	36 in.	40 in.	48 in.	60 in.
Tower Cover, Fig. 360 Weight, lbs.	80	130	215	300	500	700
Tower Distributor, Fig. 401 and 401a Weight, lbs.	36	60	100	120	170	250
Plain Tower section, Fig. 356 Weight, lbs.	220	300	430	520	700	1000
Tower Section with Rim Fig. 356a and 356b Weight, lbs.	225	310	445	540	750	1100
Supporting Plate, Fig. 279 Weight, lbs.	30	80	140	160	250	400
Tower Section with branch, Fig. 355 Weight, lbs.	230	320	530	630	900	1800
Tower Saucer, Fig. 354 Weight, lbs.	120	200	250	340	500	800
Tower Bottom Section, Fig. 355a Weight, lbs.	260	370	610	730	1000	1500



Tower Cover, Fig. 360

Distributor, Fig. 401 (See opposite page)

Tower Section with Rim for Distributor, Fig. 356b

Plain Tower Section Fig. 356

Tower Section with Rim at Bottom Fig. 356a

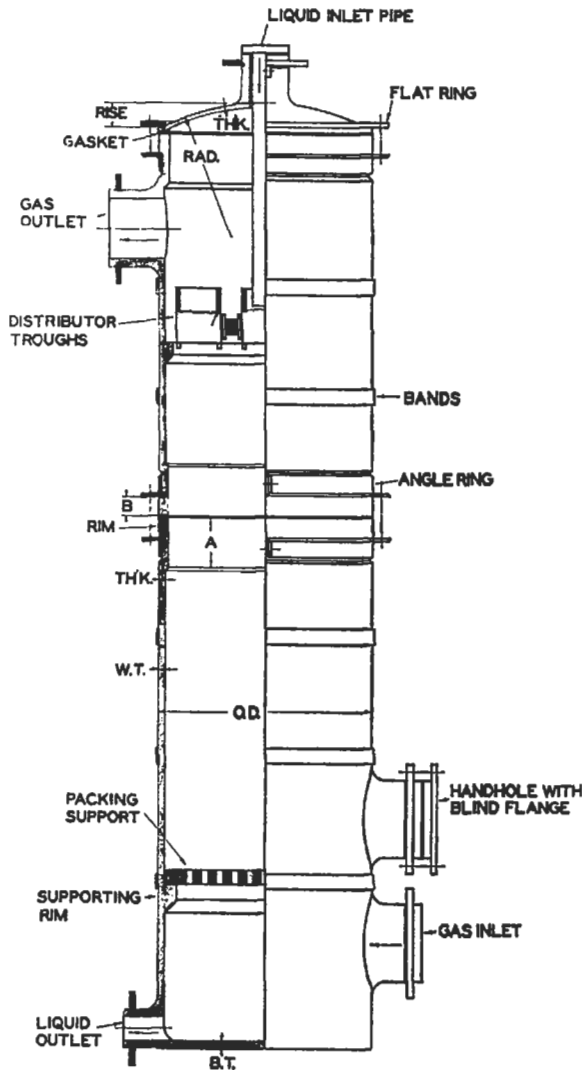
Supporting Plate Fig. 279*

Tower Section with Branch, Fig. 355

Tower** Saucer Fig. 354

Tower** Bottom Section Fig. 355a

Figure 9-4. Physical dimensions of stoneware tower sections, bell and spigot. Used by permission of General Ceramics and Steatite Corp.



3. Grid packing is probably the newest type packing. It is lower in pressure drop, and has higher capacity, and lower efficiency than the other types. (See Figures 9-6PP-9-6UU.)

The types and corresponding physical data for packing are given in Figure(s) 9-6 and Tables 9-1 through 9-15. The evaluation of these materials for various conditions of service is given later. However, Table 9-16 outlines packing service applications and Table 9-17 summarizes usual packing type applications.

Packing Supports

The packing support may be anything from cross-grid bars spaced to prevent fall-through of packing to more refined speciality units designed to direct the flow of gas and liquid. (See Figures 9-7A-9-7F.) Good tower performance is definitely linked to proper packing support. The net free flow cross-sectional area of the support should be 65% (or larger) of the tower area, and greater than the free area of the packing itself. In addition, the effect of the free area "blocking" by the positioning of the packing on the support must be considered. To allow for this, every effort should be made to obtain as large a support-free area as possible and yet remain consistent with the structural strength of the material being used. If this area is too restricted, liquid build-up will occur at the plate, reducing efficiency and increasing pressure drop of the tower, and leading to a flooding condition. A lot depends on the material of construction that the system requires; for example, carbon or graphite bar grids, brick grid piers, some steel grating grids and most rubber or plastic cov-

DESIGN INFORMATION FOR SINGLE OR MULTIPLE SECTION CYLINDRICAL HAVEG TOWERS

Size	O.D.	Max. Height of Section	Wall & Bottom Thickness		Support Rim I.D. x Tk.	Joint for Section Towers										COVER						Staves and Hoops		
			W.T.	B.T.		Rim			Angle Ring			Gasket		Bolts		Head			Flat Ring			Bolts	No. of Hoops	No. of Staves
			A	B		Thk.	Size	I.D.	B.C.	I.D.	O.D.	No.	Size	Rad.	Rise	Thk.	I.D.	O.D.	Thk.	Size				
12"	13½"	15'-0"	¾"	¾"	4	1	1½"	2 x2 x¾"	12¾"	15½"	11¾"	13½"	12	½x3½"	8¾"	2¼"	½"	11¼"	16¾"	¾"	½x3"
15"	16½"	15'-0"	¾"	¾"	11¾x1	4	1	1½"	2 x2 x¾"	15¾"	17¾"	14	16½"	12	½x3½"	12¾"	2¼"	½"	14	19½"	¾"	½x3"
18"	18½"	15'-0"	¾"	¾"	14 x1	4½"	1½"	1½"	2 x2 x¾"	18¾"	20¾"	17	19½"	12	½x4½"	18½"	2	½"	17½"	23	½"	½x3½"
20"	21½"	15'-0"	¾"	¾"	16¼x1¼"	4½"	1½"	1½"	2 x2 x¾"	20¾"	23¾"	19½"	21½"	16	½x4½"	18	2¾"	½"	19½"	24¾"	½"	½x3½"
2'	25½"	15'-0"	¾"	¾"	20 x1¼"	4½"	1½"	1½"	2 x2 x¾"	24¾"	26¾"	23	25½"	18	½x4½"	25	2¾"	¾"	23½"	28½"	½"	½x3½"
2'-6"	31½"	15'-0"	¾"	1"	24 x1½"	5	1½"	1½"	2½x2½x¾"	30¾"	33¾"	28	31½"	20	½x5"	32¾"	3¾"	¾"	29	36	¾"	½x4"
3'	37½"	14'-6"	¾"	1"	28¾x1½"	5	1½"	1½"	2½x2½x¾"	36¾"	39¾"	34¾"	37¾"	28	½x5"	38	3¾"	¾"	34¾"	41¾"	¾"	½x4"
3'-6"	43½"	14'-6"	¾"	1"	36 x1½"	6½"	3	1½"	2½x2½x¾"	42¾"	45¾"	41	43½"	28	½x8"	47¾"	4¾"	¾"	41	48	¾"	½x5½"	¾"	25
4'	49½"	14'-6"	1"	1½"	40¾x2	7	3	1½"	3 x3 x½"	48¾"	51¾"	48¾"	49½"	32	¾x8"	48¾"	8	¾"	47	54	¾"	¾x8"	¾"	28
5'	61½"	14'-0"	1"	1½"	53½x2	7	3	1½"	3 x3 x½"	60¾"	63¾"	58¾"	61¾"	40	¾x8"	58¾"	7¾"	1	59	66	¾"	¾x8½"	¾"	35
6'	74	14'-0"	1"	1½"	65 x2½"	7½"	3	1½"	3½x3½x½"	73	76½"	70¾"	74	48	¾x8"	75	8¾"	1	71½"	79½"	¾"	¾x8½"	¾"	42
7'	86¾"	13'-6"	1½"	1¾"	7½"	3	2	3½x3½x½"	85¾"	88¾"	82¾"	86¾"	52	¾x8"	87½"	10	1	83¾"	91¾"	¾"	¾x8½"	¾"	49
8'	98¾"	13'-0"	1½"	1¾"	8	3	2	4 x4 x¾"	97¾"	100¾"	94¾"	98¾"	60	¾x8½"	91¾"	12¾"	1¼"	95¾"	104¾"	¾"	¾x7"	¾"	58
8'	110¾"	12'-6"	1½"	1¾"	8	3	2	5 x5 x¾"	109¾"	112¾"	106¾"	110¾"	72	¾x8½"	108½"	13¾"	1¼"	107¾"	117¾"	¾"	¾x7"	¾"	68
10'	120	12'-0"	1½"	1¾"	9	3	2½"	5 x5 x¾"	118¾"	122½"	115½"	120	80	¾x8½"	119½"	15	1¼"	116¾"	126¾"	¾"	¾x7"	¾"	69

All dimensions are in inches unless otherwise noted.

Figure 9-5. Typical reinforced plastic packed tower construction; with dimensions used by permission of Havg Corp., Bull. F-7.

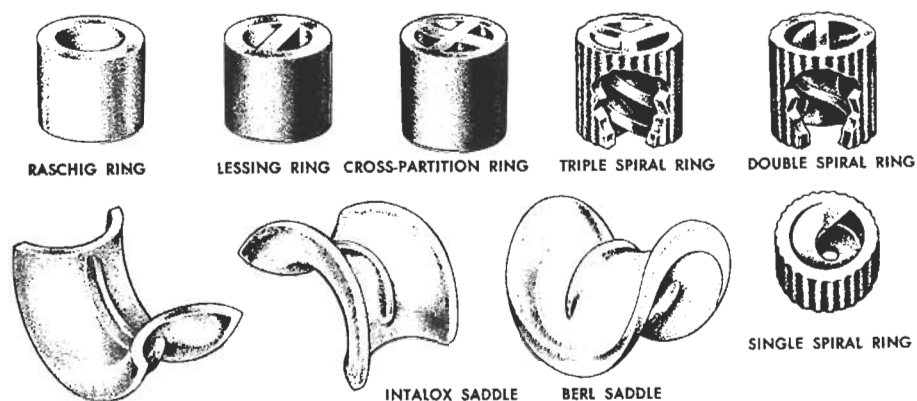


Figure 9-6A. Various packing shapes (ceramic).

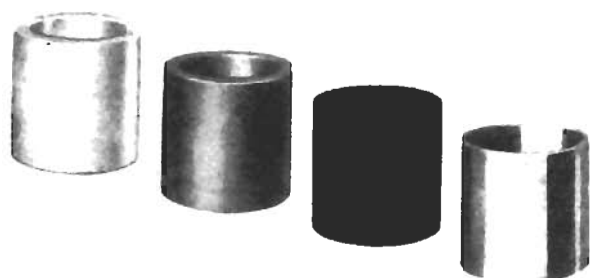


Figure 9-6B. Raschig rings (ceramic, carbon, metal).



Figure 9-6D. Berl saddles (ceramic), dumped.



Figure 9-6C. Intalox® saddles (ceramic), dumped. Used by permission of Norton Chemical Process Products Corp.

ered metal grids have inherently low free cross-sectional areas. These may be less than 65% free area. Pressure drops through support plates, such as shown in Figure 9-7D, are reported [82] not to exceed 0.3 in. water for most applications. Also see Figures 9-7A-C, E, F. Fouling service can create pressure drop problems.

(text continued on page 243)



Figure 9-6E. Pall rings (metal), dumped.

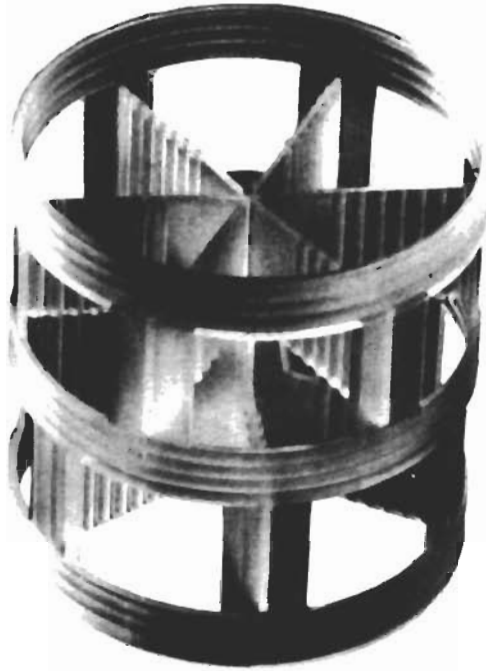


Figure 9-6F. Koch Flexiring (plastic). Used by permission of Koch Engineering Co., Inc., Bull. PFR-1.



Figure 9-6H. Plastic pall ring. Note: Glitsch Ballast Ring[®] and others are quite similar. Used by permission of Norton Chemical Process Products Corp., Bull. DC-11 and PTP-1 (11/87).



Figure 9-6I. Metal pall ring. Note: Glitsch Ballast Ring[®] and Koch Engineering Flexiring[®] are quite similar. Used by permission of Norton Chemical Process Products Corp., Bull. N-60D and Bull. MTP-1 (4/94).



Figure 9-6G. Norton Hy-Pak[®] (metal). Used by permission of Norton Chemical Process Products Co., Inc., Bull. DC-11 and MTP-1 (4/94).



Figure 9-6J. Metal Intalox (IMTP[®]). Used by permission of Norton Chemical Process Products Corp., Bull. IHP-1 (12/91).

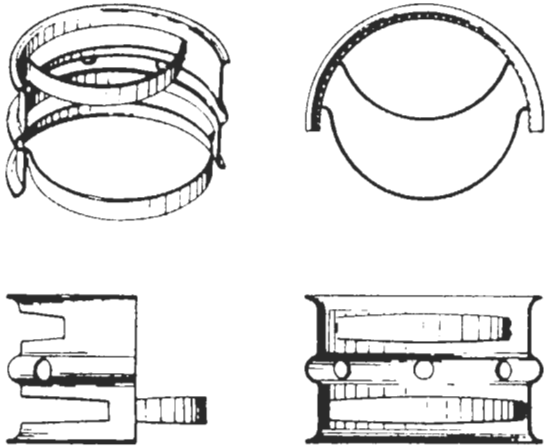


Figure 9-6L. Metal Top-Pak® low liquid/high gas flow and high heat transfer packing. Used by permission of Vereinigte Füllkörper-Fabriken GmbH & Co. Ransbach Baumbach, Germany.

MECHANICAL SPECIFICATIONS						
	No. 0.7	No. 1.0	No. 1.5	No. 2.0	No. 2.5	No. 3.0
Pieces/ft ³	4740	1900	760	385	250	120
ft ² /ft ³	69	51	38	29	25	20
lb/ft ³	11.0	11.1	11.3	10.8	9.0	8.3
% Void	97.8	97.8	97.8	97.9	98.2	98.4
Relative HETP Values	0.64	0.78	0.92	1.00	1.17	1.40

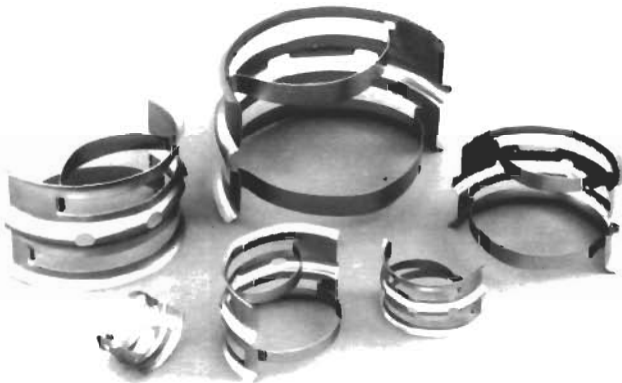


Figure 9-6K. Nutter Ring™ (metal random packing). Used by permission of Nutter Engineering, Harsco Corp., Bull. NR-2.

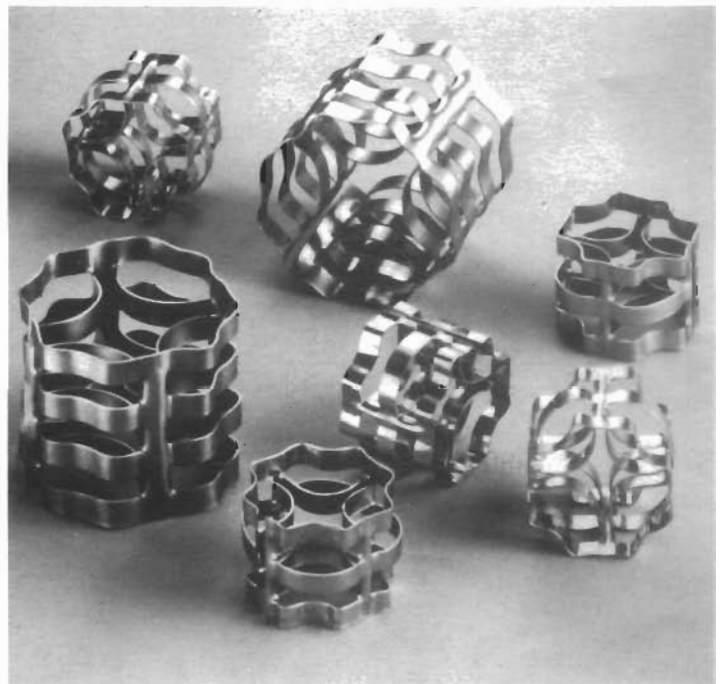


Figure 9-6M. Metal VSP® high capacity packing. Used by permission of Vereinigte Füllkörper-Fabriken GmbH & Co. Ransbach Baumbach, Germany.

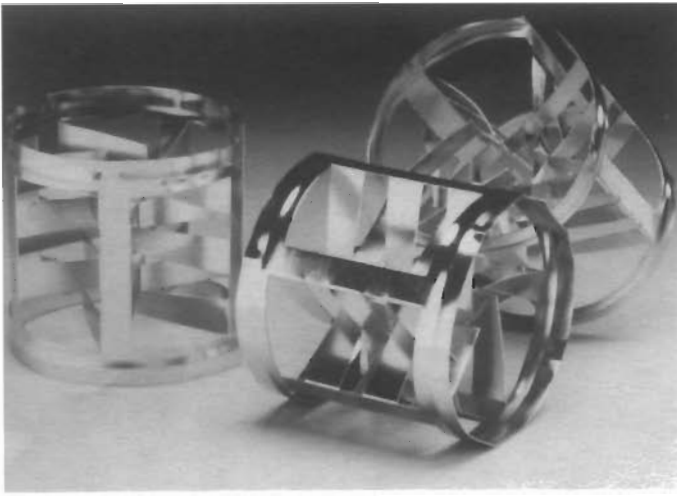


Figure 9-6N(a). Koch Metal HcKp™ random packing. Used by permission of Koch Engineering Co., Inc., Bull. KRP-2.

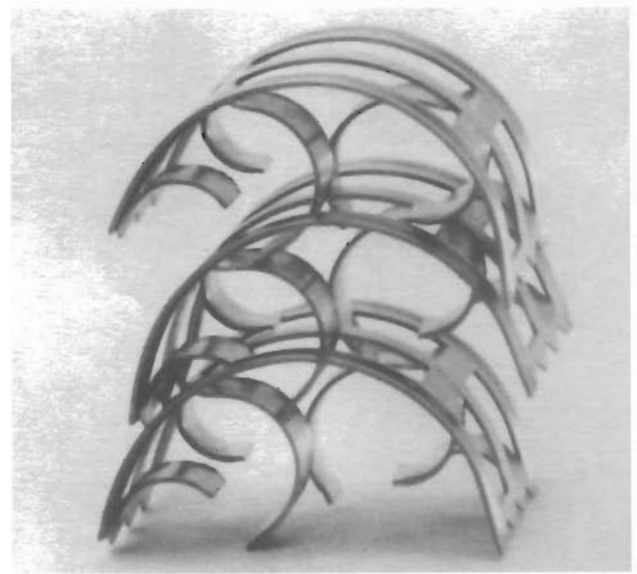


Figure 9-6P. Metal Chempak® packing. Used by permission of Chem-Pro Equipment Corp., licensed from Dr. Max Leva.

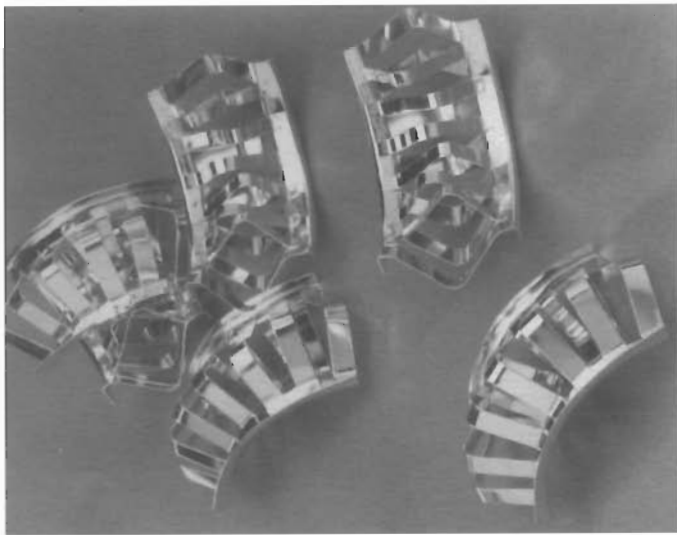


Figure 9-6N(b). Fleximax™ high performance random metal packing; available in two sizes and reported by manufacturer to be a fourth generation random packing. Used by permission of Koch Engineering Co., Inc., Bull. KFM-1.

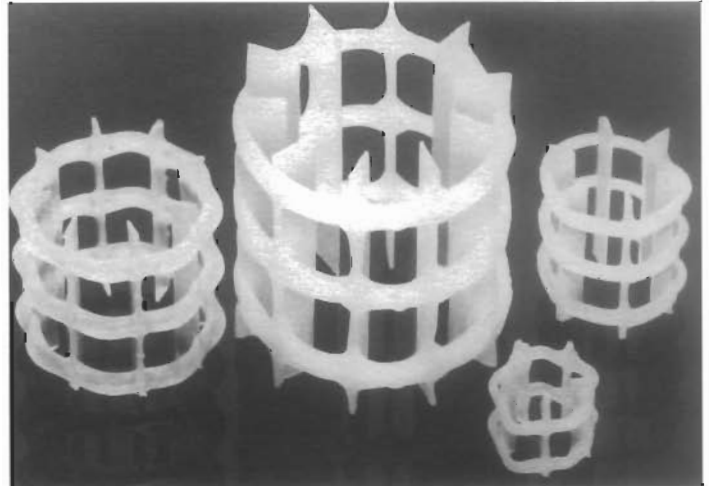


Figure 9-6Q. Plastic Nor-Pac® packing; fabricated of most corrosion resistant plastics. Used by permission: NSW Corporation.

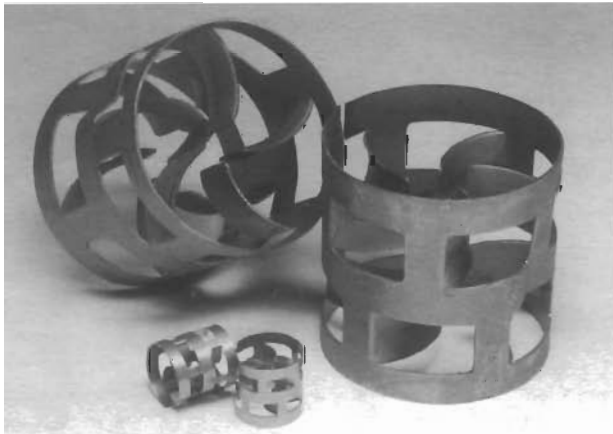


Figure 9-6O. Koch Metal Flexiring®, available in 1/2-in.-3 1/2-in. diameter. Used by permission of Koch Engineering Co., Inc., Bull. KRP-2.

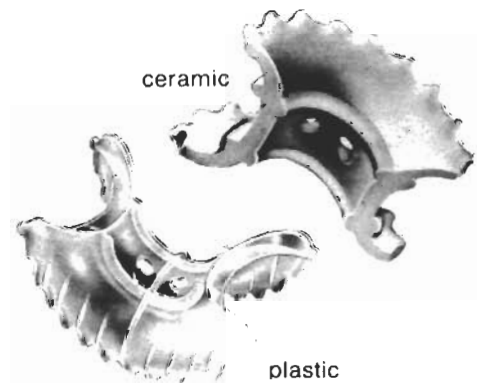


Figure 9-6R. Super Intalox® Saddles. Note: Glitsch Ballast Saddle® and Koch Engineering Flexisaddle® are quite similar. Used by permission of Norton Chemical Process Products Corp., Bull. N-60D.

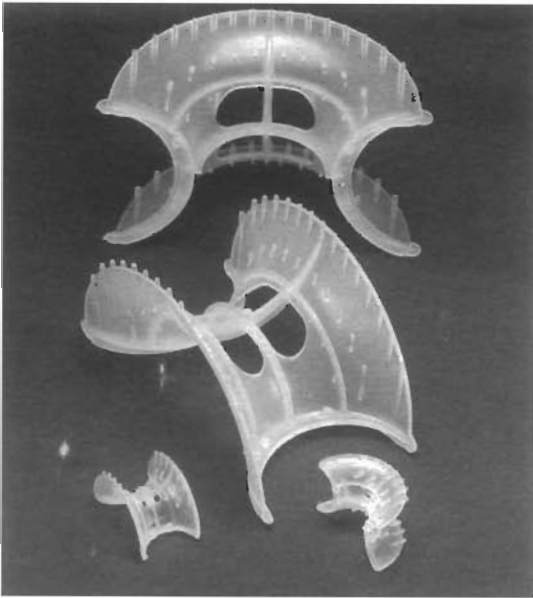


Figure 9-6S. Koch Flexisaddles™ (plastic); available in 1-in.-3-in. Used by permission of Koch Engineering Co., Inc., Bull. KRP-2.

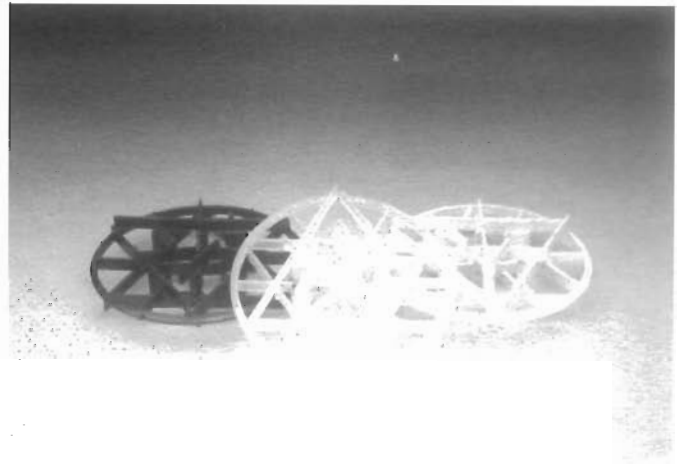


Figure 9-6U. Norton Intalox® high-performance Snowflake® packing (plastic). Used by permission of Norton Chemical Process Products Corp., Bull. 1SPP-1R.

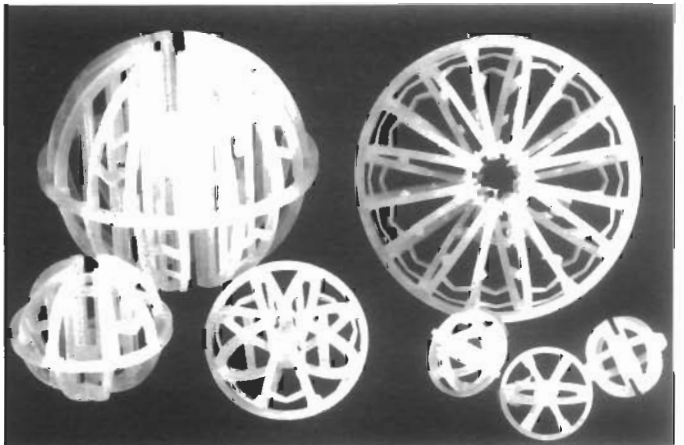
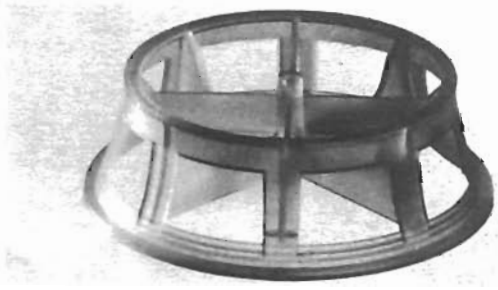


Figure 9-6V. Jaeger Tri-Packs® high-performance packing fabricated of corrosion resistant plastic. Used by permission of Jaeger Products, Inc.

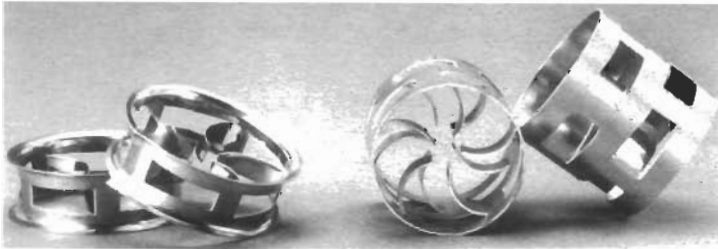


Figure 9-6W. Rauschert Hiflow® high-performance rings and saddles packing (plastic and metal). Used by permission of Rauschert Industries, Inc., div. of Rauschert GmbH & Co. KG; Paul-Rauschert-Str. 6; D-96349 Steinwiesen, Germany.



Figure 9-6T. (Top) Cascade® Mini-Ring, (metal and plastic). Originally used by permission of Mass Transfer, Inc., now, Glitsch, Inc. (middle and bottom) Elevation and plan views of Ballast® rings (right) and Cascade Mini-Rings (left). Note how high aspect ratio of former permits occlusion of interior surfaces. Low aspect ratio of Cascade Mini-Rings, on the other hand, favors orientation that exposes internal surfaces for excellent film formation, intimate mixing, and gas-liquid contact. Used by permission of Glitsch, Inc. Bull. 345.

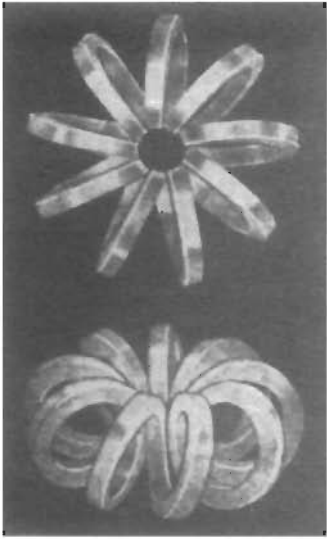


Figure 9-6X. Teller rosette packing (plastic). Used by permission of Hawshaw Chemical Co. and Dr. A. J. Teller.



Figure 9-6Y. Panapak formed/structured packing for a 6-ft diameter column (original design). Used by permission of Packed Column Corp.

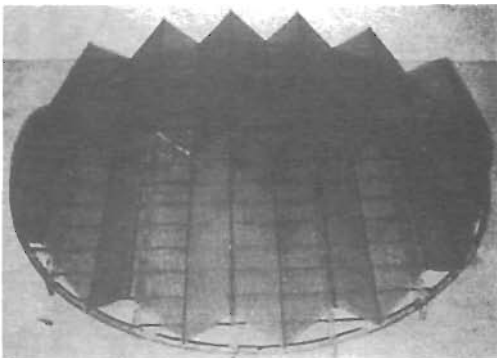


Figure 9-6Z. Panapak packing for a 6-ft diameter column, latest design. Used by permission of Packed Column Corp.

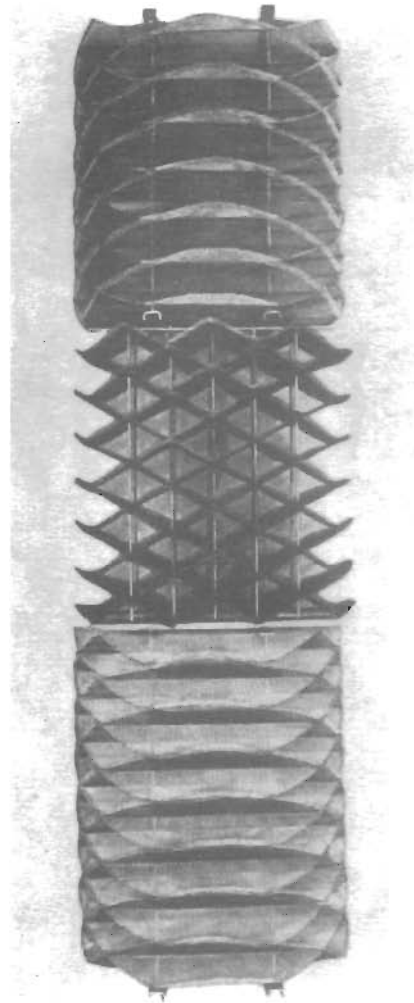


Figure 9-6AA. Cartridges 8½ ft high of 32-in. I.D. Spraypak Packing. Used by permission of Denholme, Inc., Bull. No. 8.

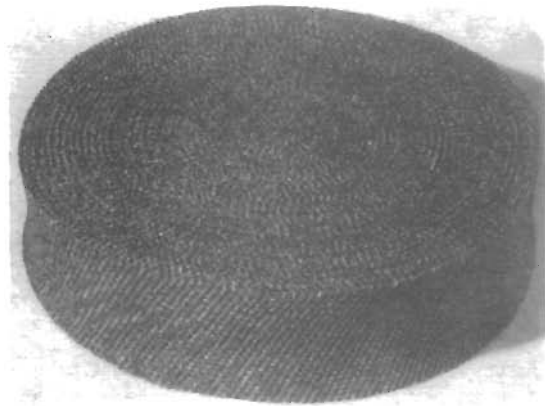


Figure 9-6BB. Goodloe packing. Used by permission originally of Packed Column Corp., now under license to Glitsch, Inc.

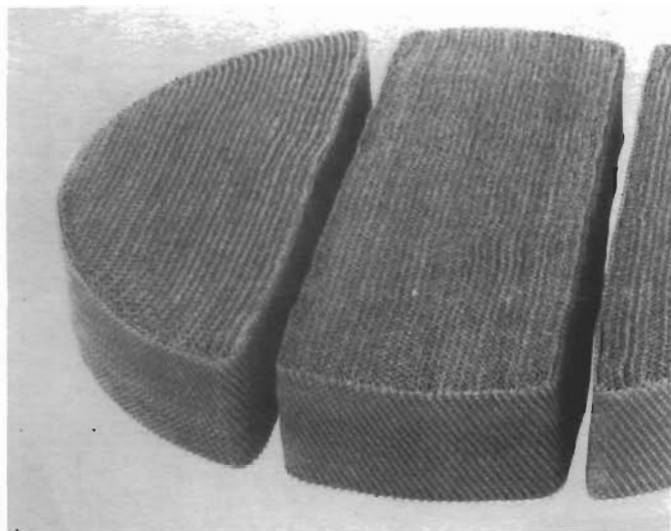


Figure 9-6CC. York-Twist™ structured tower packing. Note insert showing weave and sections fabricated to fit through manway for larger towers. Used by permission of Otto H. York Co., Inc., a division of Glitsch, Inc.

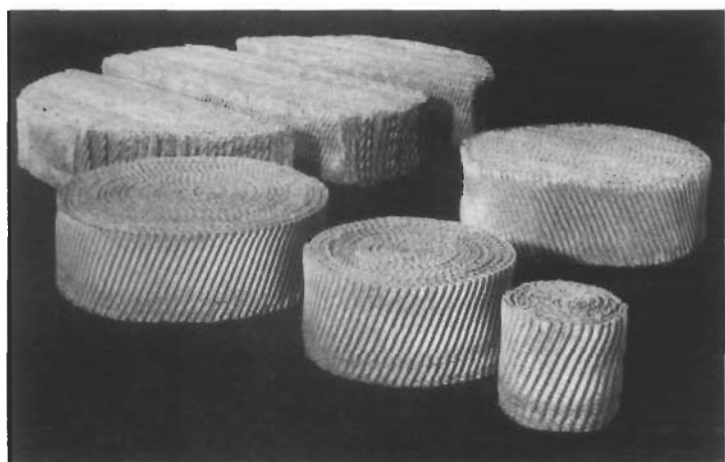
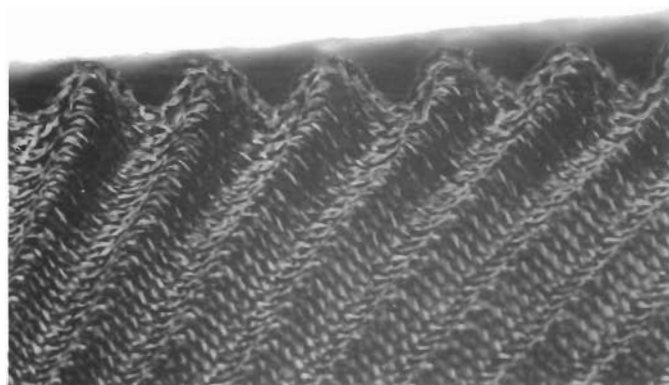


Figure 9-6DD. ACS knitted mesh structured packing. Used by permission of ACS Industries, Inc., Separations Technology Group, Bull. B-129 (1992).



Multistrand wire, close-knit in two layers, holds stable liquid film by surface tension. Falling films of liquid form expansive contact surface with rising vapor layers.

(text continued from page 237)

In some large towers the support grid is built up from supporting brick arches coming from the bottom (see Figures 9-2A, B, and C). Quite often in large towers, drip point grid tile is used as the supporting first layer, either as a support "plate" itself, or as the support for other packing stacked on it (Table 9-15). This initial stacking of the first and perhaps second courses of packing prevents the blocking of free area usually associated with dumping packing on support plates. The resultant net free area "balance" around the support grid or plate and its first two courses of packing (whether dumped or stacked) should be calcu-

lated to evaluate the effect on tower performance. Figures 9-1A, 9-1B, and 9-3 show a typical arrangement of several support plates.

The weight to be carried by the support plate is the sum of the weight of the packing plus the weight of the flooded liquid volume of the packing voids plus any pressure surges that might be imposed on the system. The effect of side thrust of the packing in reducing the dead packing load on the support should be ignored, as it is an indeterminate figure. Normally each support is required to support only the weights of the packed section directly above it and not

(text continued on page 246)

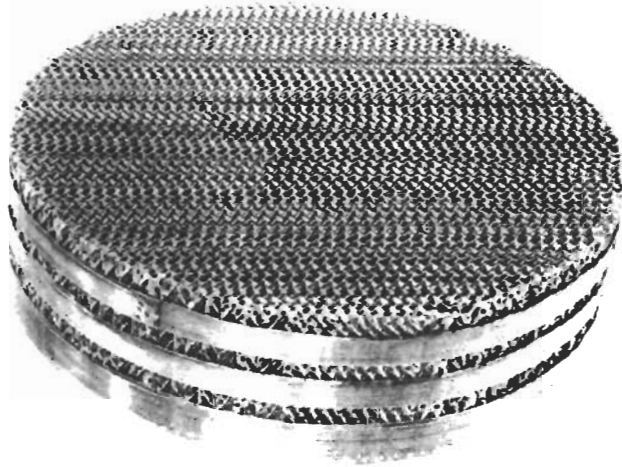


Figure 9-6EE. Koch/Sulzer® packing. Used by permission of Koch Engineering Co., Inc., Bull. KS-2.

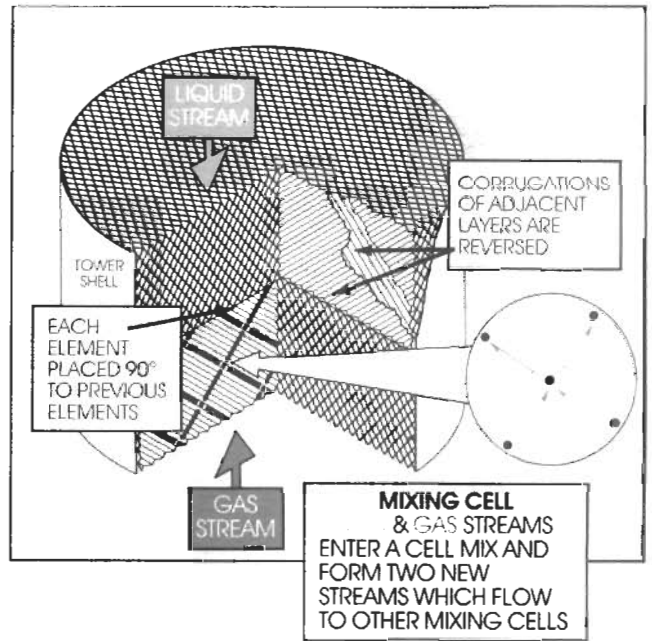


Figure 9-6FF. Liquid and gas mixing in Koch/Sulzer® packing elements. Used by permission of Koch Engineering Co., Inc., Bull. KS-2.

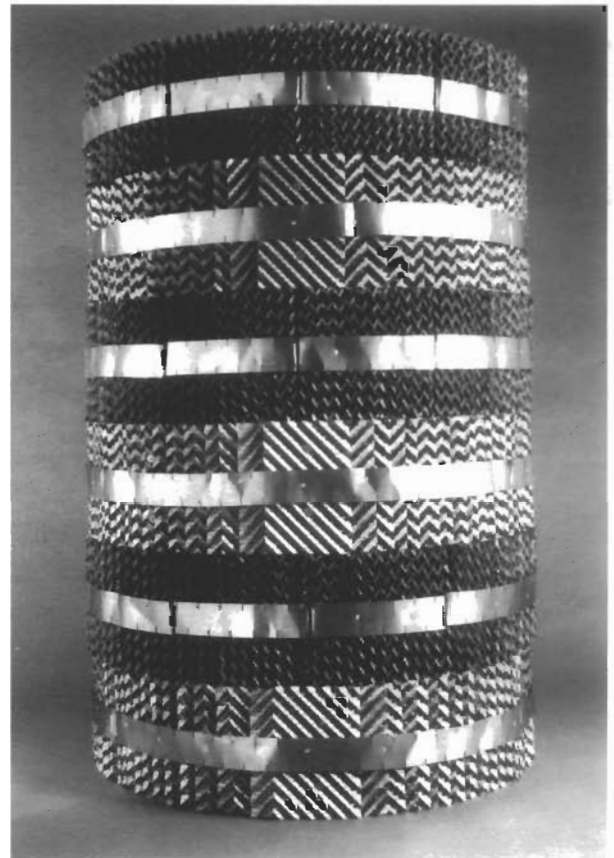


Figure 9-6GG. Koch Flexipac® structured packing. Used by permission of Koch Engineering Co., Inc., Bull. KFP-4.

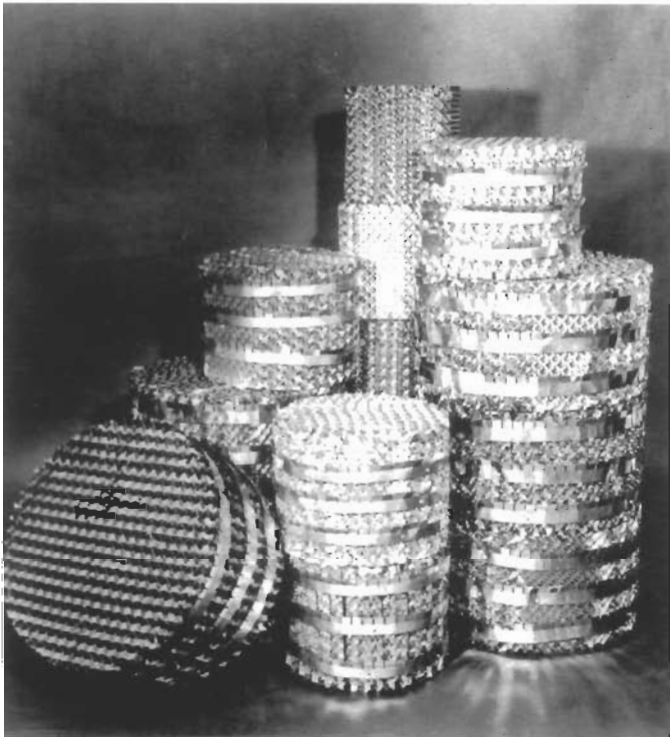


Figure 9-6HH. Metal Max-Pak™ structured packing fabricated from corrugated sheets. Used by permission of Jaeger Products, Inc., Bull. 500.

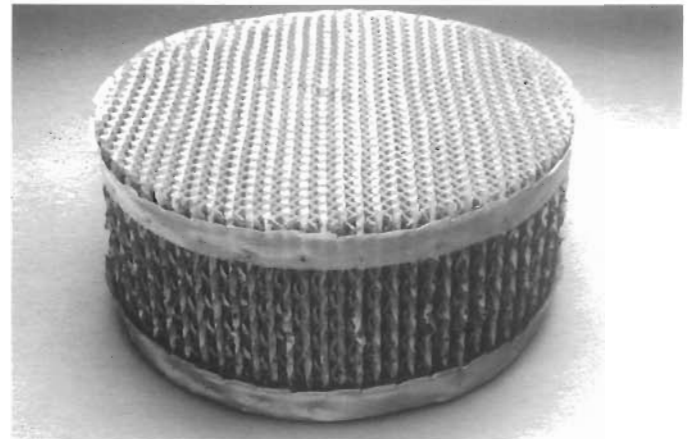


Figure 9-6JJ. Intalox® high performance wire gauze structured packing. Used by permission of Norton Chemical Process Products Corp., Bull. WG-1.

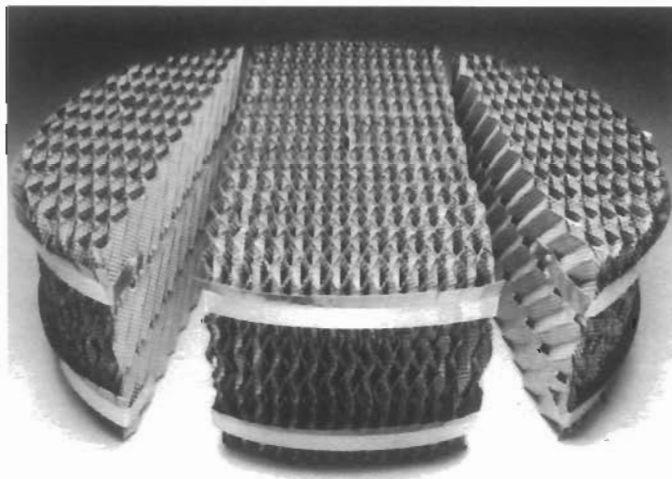


Figure 9-6II. Intalox® high-performance structured packing. Used by permission of Norton Chemical Process Products Corp., Bull. IS-2T.

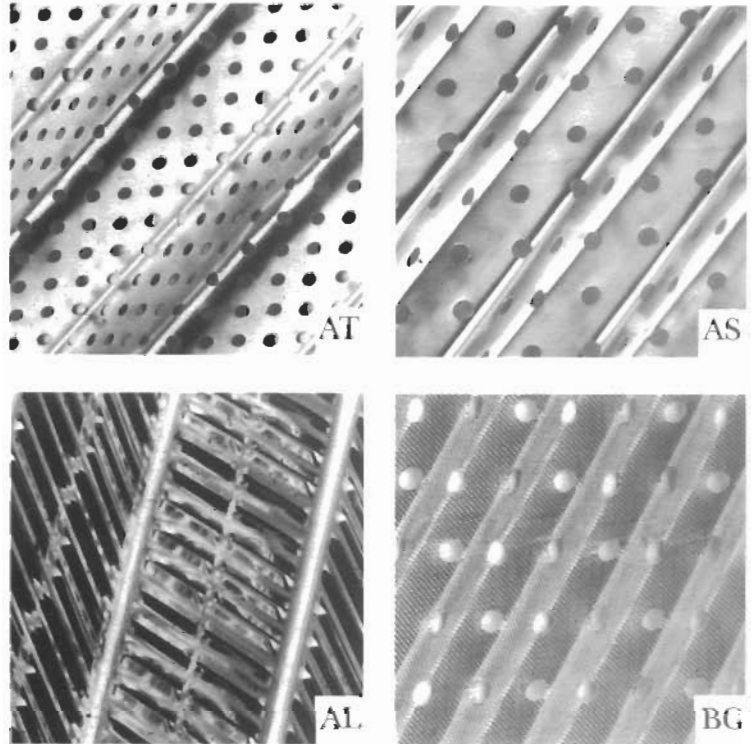


Figure 9-6KK. Glitsch Gempak® structured packing series designs. *Series AT*—Smooth surface with small crossover points on narrow rectangular pitch. A general purpose style, especially suitable for low wetting rates and high vacuum applications. *Series AS*—A general purpose style suited for high wetting and heat transfer applications. Both AT and AS series are particularly suited for refinery applications and can be used in the wash zones of atmospheric and vacuum crude towers, or FCCU main fractionators. *Series AL*—Metal surface with louvres in a repetitive pattern. Especially suited for low wetting rates and chemical applications. *Series BG*—A wire gauze packing, crimped to 60° from the horizontal. Recommended for high efficiency applications at very low wetting rates (clean service). Used by permission of Glitsch, Inc. Bull. 5140 (1993).

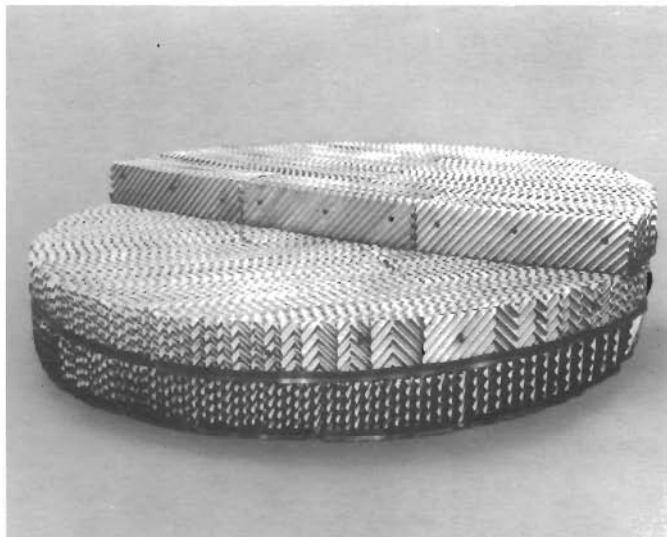


Figure 9-6LL. Montz-Nutter high-efficiency structured packing assembly (Type B-1™ with wiper bands and seal strip). Used by permission of Nutter Engineering, Harsco Corp., Bull. B-1.

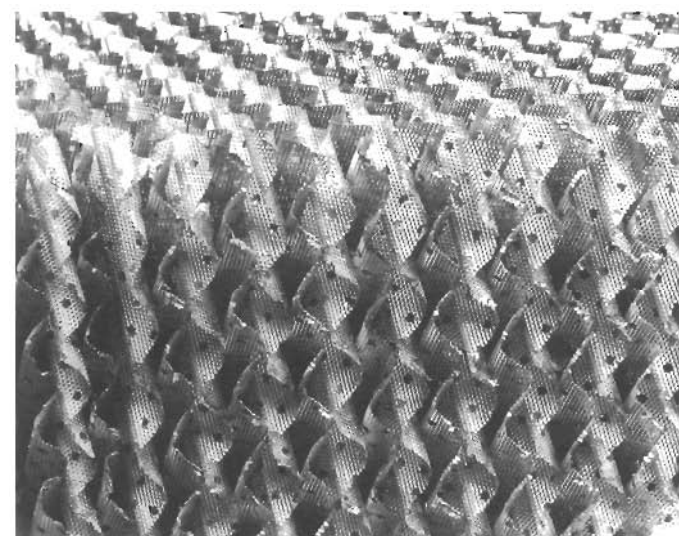


Figure 9-6MM. Nutter BHS™ structured packing with expanded metal texture, which maintains high mass transfer efficiency across all operating conditions. Nutter Engineering designs and manufactures BSH in North America under exclusive license from Julius Montz GmbH of Germany. Used by permission of Nutter Engineering, Harsco Corp.

(text continued from page 243)

those separately supported above or below it. If any intermediate supports or redistributors are not separately supported on the tower wall but rest on the packing itself, the bottom support would carry the entire tower load of packing as mentioned, plus the weights of intermediate support and redistribution plates. This is not good practice as it complicates the packing and repacking of the tower in addition to possibly imposing heavy loads on the bottom supports.

As a general rule packing heights per support plate should not exceed 12 ft for Raschig rings or 15–20 ft for most other packing shapes. Other types fit within these limits. The mechanical, vibrational and thermal shock loads become important and sometimes affect the tower operation beyond these limits.

Liquid Distribution

Liquid distribution probably plays the most important part in the efficient operation of a packed tower. A good packing from the process viewpoint can be reduced in effectiveness by poor liquid distribution across the top of its upper surface or the packing sections below any feed inlet(s) or reflux inlets.

(text continued on page 254)

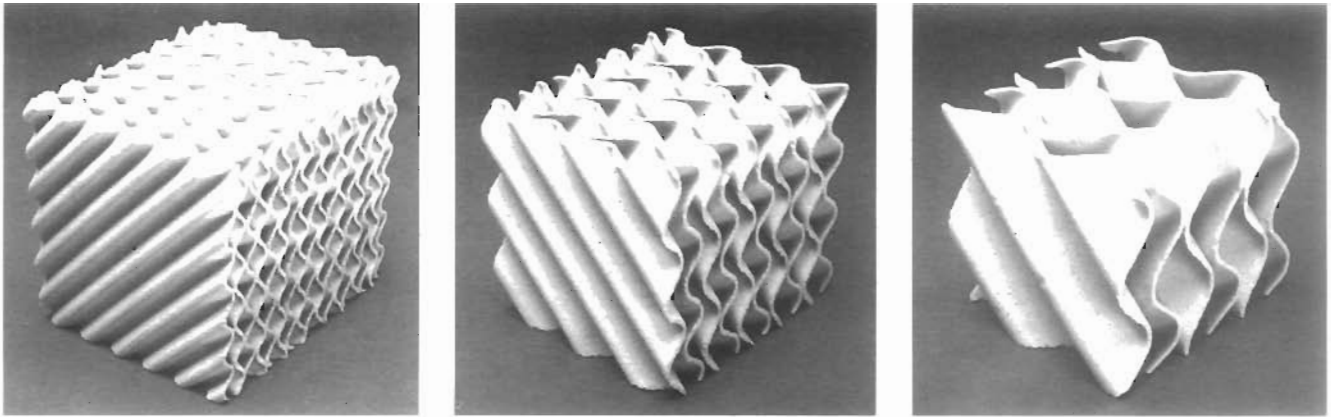


Figure 9-6NN. Koch Ceramic Flexeramic® structured packing of stoneware or ceramic fabrication. Used by permission of Koch Engineering Co., Inc., Bull. KCP-2.

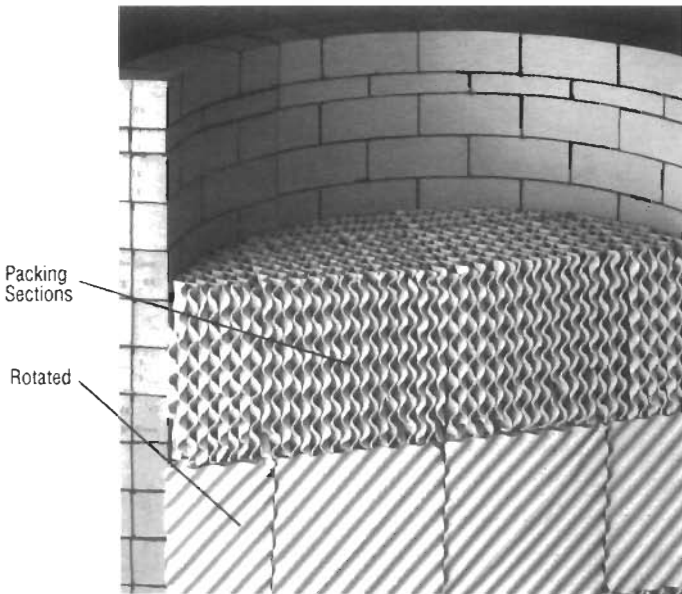


Figure 9-6OO. Installation of Ceramic Flexeramic® structured packing of stoneware or ceramic. Used by permission of Koch Engineering Co., Inc., Bull. KCP-2.

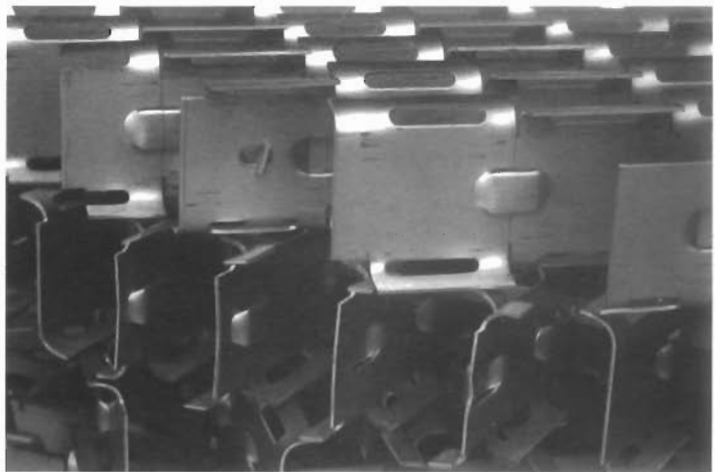


Figure 9-6QQ. Nutter Snap-Grid™ high-capacity grid packing with good structural integrity (interlocking) and reduced fouling. Used by permission of Nutter Engineering, Harsco Corp., Bull. CSG-2.

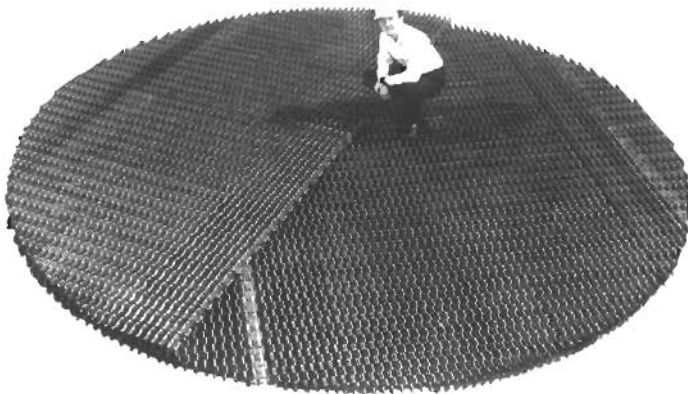


Figure 9-6PP. Nutter Snap-Grid™ grid packing as assembled. Used by permission of Nutter Engineering, Harsco Corp., Bull. CSG-1.

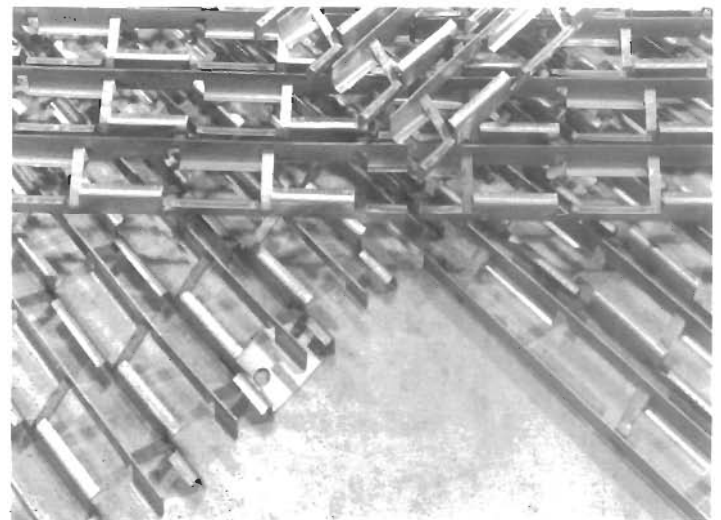


Figure 9-6RR. Intalox® Grid-type packing; useful for fouling, solids and heat transfer; high-strength, low-pressure drop, high capacity, better efficiency than most structured and random packing. Used by permission of Norton Chemical Process Products Corp., Bull. IG-1.

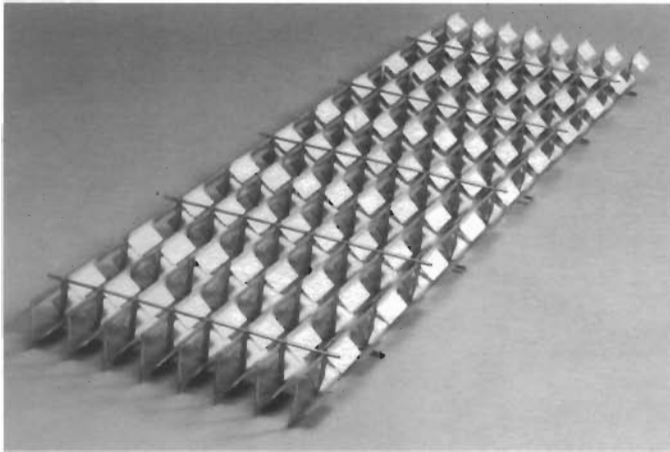


Figure 9-6SS. Flexigrid® Style 3 high-efficiency structured packing. Used by permission of Koch Engineering Co., Inc., Bull. KFG-2.

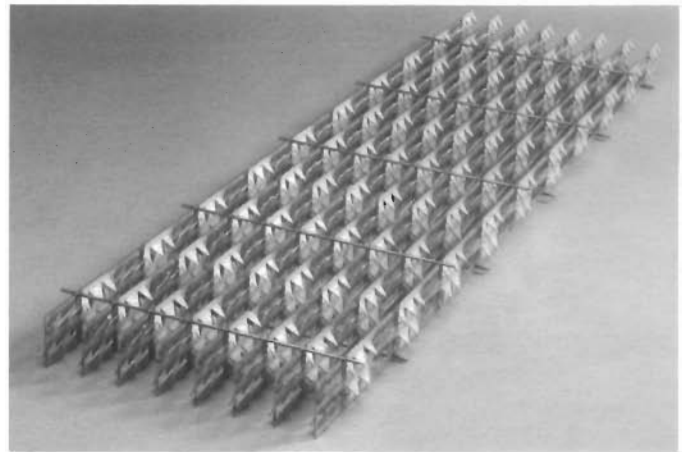
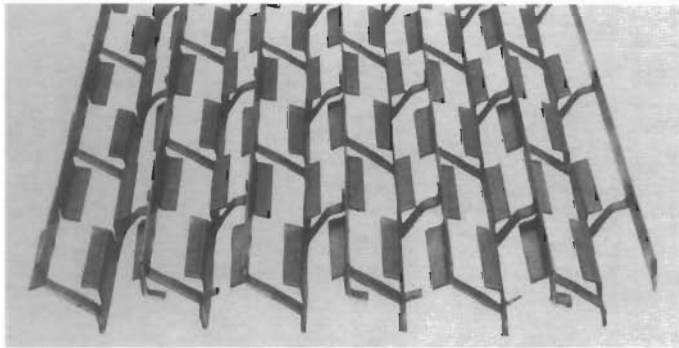
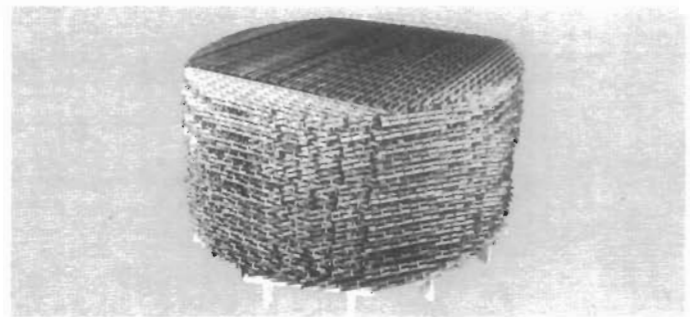


Figure 9-6TT. Flexigrid® Style 2 high-capacity structured packing. Used by permission of Koch Engineering Co., Inc., Bull. KFG-2.



EF-25A Grid is used to process coking-prone feeds and up to 40% solids slurries



Because Grid is free to expand and contract without damage under thermal stress, Grid can maintain its structural integrity in turbulent vapor streams as hot as 1000°F.

Figure 9-6UU. Glitsch-grid™ packing, Style EF-25A. Used by permission of Glitsch, Inc., Bull. 163L84B.

Table 9-1
Chemical Stoneware and Chemical Porcelain Raschig Rings

Normal Size, In.	Wall Thickness, In.	O.D. and Length, In.	Approx. Avg. Number per Ft ³	Approx. Avg. Weight per Ft ³ , Lb**	Approx. Avg. Surface Area, F ² /Ft ³	Percent Free Gas Space	Equivalent Spher. Diam. Dp, In.
½	⅜	½	10,700	52	124	65	0.48
¾	⅜	¾	5,600	48-52	100	68	0.57
1	⅜	1	3,100	46	78	69	0.65
1¼	⅜	1¼	1,350	42	58	72	0.87
1½	⅜	1½	670	46	44	71	1.10
2	⅜	2	390	40	36	73	1.40
3	⅜	3	165	39	28	74	1.75
4	⅜	4	50	35	19	77	2.65
+3(D)	⅜	3	74	67	29	60	2.65
+3(S)	⅜	3	64	58	25	66	2.65
4	½	4	25	40			

¾, 2½, 4, and 6 in. available on special order. The 3-in., 4-in., and 6-in. O.D. sizes are also made with ribbed or corrugated outside surfaces. The 3-in., 4-in., and 6-in. sizes can be made in lengths up to 12 in., on special order.

**Porcelain Rings are about 5% heavier than Stoneware. These weights are the average for both.

+Data for stacked arrangement. "D" indicates diamond pattern. "S" indicates square pattern.

Original by permission, M. Leva, Ref. 40 and Bulletin TP-54, U.S. Stoneware Co., Akron, OH.; updated CTP-1 dated 9/88, by permission of Norton Chemical Process Products Corp.

Table 9-2
Carbon Raschig Rings

Nominal Size, In.	Wall Thickness, In.	O.D. and Length, In.	Approx. Avg. Number per Ft ³	Approx. Avg. Weight per Ft ³ , Lb	Approx. Avg. Surface Area, F ² /Ft ³	Percent Free Gas Space	Equivalent Spher. Diam. Dp, In.
¼	⅙	¼	85,000	46	212	55	0.27
½	⅙	½	10,600	27	114	74	0.42
¾	⅙	¾	3,150	34	74	67	0.72
1	⅙	1	1,330	27	57	74	0.87
1¼	⅙	1¼	678	31	45	69	1.10
1½	¼	1½	390	34	37.5	67	1.40
2	¼	2	166-157*	27	28.5	74	1.75
3	⅙	3	50-44*	23	19	78	2.50
3(D)	⅙	3	74	49.5	29	66	2.50
3(S)	⅙	3	64	43	25	71	2.50

S = Square pattern }
D = Diamond pattern } Stacked

From: M. Leva, U.S. Stoneware Co., Akron, Ohio, Ref. 40, and Bulletin CP-2512, National Carbon Co., New York, N.Y.; updated 12/93 by permission Norton Chemical Process Products Corp., Bull. CTP-1.

*Varies with supplier

Table 9-3
Metal Raschig Rings

Nominal Size, In.	Wall Thickness, In.	O.D. and Length, In.	Approx. Avg. Number per Ft ³	Approx. Avg. Weight per Ft ³ , Lb*	Approx. Avg. Surface Area F ² /Ft ³	Percent Free Gas Space	Equivalent Spher. Diam. Dp, In.
¼	⅙	¼	88,000	133	236	72	0.22
⅜**	⅙	⅜	27,000	94	—	81	—
½**	⅙	½	11,400	75	123	85	0.34
⅝**	⅙	⅝	11,200	132	118	73	0.44
¾**	—	¾	5,800	—	—	86	—
19/32	⅙	19/32	7,300	66	112	86	0.40
19/32	⅙	19/32	7,000	120	106.5	75	0.50
¾**	⅙	¾	3,340	52	81.7	89	0.46
¾**	⅙	¾	3,140	94	70.6	80	0.58
1**	⅙	1	1,430	39	62.2	92	0.56
1**	⅙	1	1,310	71	55.2	86	0.70
1¼**	⅙	1¼	730	62	49.3	87	0.75
1½**	⅙	1½	375	49	39.2	90	0.90
2**	⅙	2	165	37	29.3	92	1.15
3**	⅙	3	55	25	19.8	95	—
3(D)	⅙	3	74	35	29	93	—
3(S)	⅙	3	64	30	25	94	—

*Based upon Carbon Steel Rings; other weights are: Stainless Steel 105%; Copper 120%; Aluminum 37%; Monel and Nickel 115%.

Usually metal Raschig rings are made with fitted butted-joints.

Original by permission, M. Leva, [40] and U.S. Stoneware Co., Akron, OH.; updated 9/88 by permission of Norton Chemical Process Products Corp., Bull. MTP-1 and TP-78.

Note: Sizes availability varies with manufacturers.

**Usual commercial sizes

S = Square pattern }
D = Diamond pattern } Stacked

Table 9-4
Metal Lessing Rings

Size, In.	Wall Thickness, In.	O.D. and Length, In.	Approximate Number per Ft ³	Approximate Weight per Ft ³ , Lb*	Approximate Surface Area Ft ² /Ft ³	Percent Free Gas Space	Equivalent Spherical Dia., Dp, In.
¼	½	¼	81,840	195	306.8	60	0.24
⅜	½	⅜	25,110	114	217.1	76	0.31
½	½	½	10,974	100	166.4	81	0.38
½	⅙	¼	10,230	172	153.4	66	0.46
⅝	½	⅝	6,789	86	145.6	82	0.45
⅝	⅙	⅝	6,510	150	138.4	68	0.57
¾	½	¾	3,171	71	108.5	85	0.52
¾	⅙	¾	2,967	130	93.3	71	0.63
1	½	1	1,339	52	81.5	90	0.62
1	⅙	1	1,251	95	73.7	80	0.77
1¼	⅙	1¼	674	81	64.1	82	0.99
1½	⅙	1½	391	65	53.6	87	1.02
1¾	⅙	1¾	246	58	46.0	89	1.13
2	⅙	2	167	49	40.8	90	1.24

All figures are on a dumped basis. Metal Lessing Rings are also made in stainless steel, copper, and aluminum.

*Weights shown are for carbon steel. By permission: U.S. Stoneware Co. Bul. TP54, now, Norton Chemical Process Products Corp., Stow, OH. [5] except column 8, [40].

Table 9-5
Ceramic Lessing Rings

O.D. and Length, In.	Wall Thickness, In.	Approx. No. of Rings per Ft ³ , Dumped	Approx. Wt. Per Ft ³ , Dumped	Percent Free Gas Space	Approx. Surface Area per Ft ³	Equiv. Spher. Diameter Dp, In.
1	¼	1,300	50	66	69	0.95
1¼	⅙	650	56	62	53	1.20
1½	¼	350	58	60	40	1.55
2	⅝	150	49	68	32	1.90

From M. Leva, U.S. Stoneware Co., [40], by permission, now, Norton Chemical Process Products Corp., Stow, OH.

Table 9-6A
Chemical Stoneware and Ceramic Berl Saddle Packings

Nominal Size	Approx. Average Number/Ft ³	Approx. Wt./Ft ³ , lb	Approx. Average Surface Area Ft ² /Ft ³	Percent Free Gas Space*	Equivalent Spher. Diam. Dp, In.
¼	113,000	56	274	60-67	0.23
½	16,200	54	142	63	0.42
¾	5,000	48	82	66	0.58
1	2,200	45	76	69-70	0.76
1½	580	38	44	73-75	1.10
2	250	40	32	72-75	1.55

From M. Leva, U.S. Stoneware Co., [40], by permission.

*Updated by permission Jaeger Products, Inc.

Table 9-6B
Steel* Berl Saddles

1	2,500	87	85	83
1½	825	60	58	88

* Other metals available.

Courtesy Maurice A. Knight Co., Bulletin No. 11, now, by permission Koch Engineering Co., Inc.

Table 9-7
Ceramic Intalox®* Saddles

Nominal Size, In.	Approximate Number per Ft ³	Approximate Weight per Ft ³ , Lb	Approximate Surface Area Ft ² /Ft ³	Percent Free Gas Space	Equivalent Spherical Diameter Dp, In.
¼	117,500	54	300	64	0.20
⅜	50,000	50	—	67	—
½	17,000	46	190	69	0.32
¾	6,200	44	102	71	0.48
1	2,100	42	78	72	0.68
1½	660	39	59.5	74	0.96
2	240	37	36	75	1.38
3	52	37	—	75	—

Data shown applies to Intalox Saddle made either from chemical stoneware or chemical porcelain. Weights per cubic foot are based on chemical porcelain. Chemical stoneware Intalox Saddles will weigh approximately 5% less.

*Trade name Norton Co.

Orig. By permission: U.S. Stoneware Co., Akron, Ohio, Ref. 5, except column 6, from Ref. 40; updated 9/88 by permission of Norton Chemical Process Products Corp., Inc., Bull. CTP-1, 9/88.

Table 9-8
Ceramic Cross-Partition Rings

Outside Diameter In.	Outside Length In.	Wall Thickness, In.	Number of Ringers per Ft ³		Weight of Ringers per Ft ³ , Lb		Percent Free Gas Space		Ft ² of Surface Area per Ft ³ of Packing		Net Cross-Section Area of Packing in Ft ² /Ft ²	
			D Setting	S Setting	D Setting	S Setting	D Setting	S Setting	D Setting	S Setting	D Setting	S Setting
3*	3	⅜	74	50*-64	73	47*-63	47-48	54-55	41-43	35-37	.53	.46
4	3	½	41	36	81-72	71-63	46-49	52-55	31-33	27-29	.54	.47
4	4	⅝	31	27	81-62	71-54	45-56	52-61	30-32	26-29	.54	.47
6	4	¾	14	12	73-70	62-60	51-50	58-57	22	19	.49	.42
6	6	¾	9	8	70	62	53-50	58-56	20	18	.49	.42

Also made with outer surfaces ribbed or corrugated, and in lengths up to 12 in. Rings with different wall thicknesses than above can be made on special order. Porcelain rings weigh about 5% more than above. For D and S patterns, see Figure 9-16. Compiled from Ref. 40, U.S. Stoneware Bull. TP-54, and Maurice A. Knight Co. (now, Koch Engineering Co., Inc.) Chemical Equipment Bulletin, by permission; updated 2/89 by permission of Norton Chemical Process Products Corp. Bull. WG-1.

For 3-in. size only; * indicates dumped rings only; all others stacked diamond (D) or square pattern stacked (S).

Table 9-9
Ceramic Spiral Packing Rings*

	Out- side Diam. In.	Out- side Length In.	Wall Thick- ness In.	Number of Rings per Ft ³		Weight of Rings per Ft ³		Percent Free Gas Space		Ft ² of Surface Area per Ft ³ of Packing		Net Cross- Section Area of Packing in Ft ² /Ft ²	
				D	S	D	S	D	S	D	S	D	S
				Setting	Setting	Setting	Setting	Setting	Setting	Setting	Setting	Setting	Setting
Single	3¼-3	3	⅙	63-74	54-64	60-67	52-58	58-52	66-59	40-41	34-36	.32	.27
	4	4	⅙	31	27	61-60	55-52	60-57	67-64	32	28	.33	.28
Spiral	6	6	¼	9	8	59-54	51-48	66-61	70-66	21	19	.28	.25
Double	3¼	3	⅙	63	54	67	58	56	63	44	37	.37	.32
	4	4	⅙	31	27	64	58	59	64	35	31	.38	.33
	Spiral	6	6	¼	9	8	65	58	64	68	23	21	.32
Triple	3¼	3	⅙	63	54	69	60	50	57	50	42	.51	.44
	4	4	⅙	31	27	65	59	53	58	40	35	.46	.40
	Spiral	6	6	¼	9	8	68	60	60	64	24	21	.32

*Basic data in table for U.S. Stoneware "Cyclohelix" spiral packing, Bul. TP 54, Ref. 5. Data for other spiral packings shown set to right from Maurice A. Knight Co. (now, Koch Engineering Co., Inc.) Bulletin No. 11, by permission. For D and S patterns, Figure 9-16.

Table 9-10
Pall Rings—Metal

Size O.D. & Length, In.	Wall † Thickness, In.	Approx. Number Ft ³	Approx.* Weight, Lb/Ft ³	Surface Area Ft ² /Ft ³	Percent Free Gas Space
¾	0.018	5,800	37	104	93
1	0.024	1,400	30	63	94
1½	0.030	375	24	39	95
2	0.036	165	22	31	96
3½	0.048	33	17	20	97
Plastic‡					
¾	—	6,060	5.95	—	87
1	—	1,430	4.4	—	90
1½	—	420	4.35	—	91
2	—	175	3.85	—	92
3½	—	33	3.45	—	92

By permission, Norton Chemical Process Products Corp., TP-78 and PR-16 and MTP-1(9/88); other manufacturer's data are equivalent

†Standard gauge carbon steel, approximate

‡Weights referenced to polypropylene; other plastics available, high density polyethylene, glass reinforced polypropylene and fluorinated vinyls

Table 9-11
Teller Rosette (Tellerette) Plastic*

Nominal Size, In.	No. Units per Ft ³	Weight per Ft ³ , Lb	Surface Area Ft ² /Ft ³	Percent Free Gas Space
1	1125	10	76	83

*Harshaw Chemical Co. "Tellerette" bulletin, and Dr. A. J. Teller.

Table 9-12
Super Intalox® Saddles: Ceramic†

Size No. Designation	Approximate Number/Ft ³	Weight‡ Lbs/Ft ³	Surface Area Ft ² /Ft ³	Percent Free Gas Space
1	1,500	35	76	77
2	180	38	32	75
Plastic				
1	1,500	5.85	63	90
2	180	3.75	33	93
3	42	3.00	27	94

By permission, Norton Chemical Process Products Corp., Bull. SI-72 and Bull. PTP-1; other manufacturer's data are equivalent.

†Also available in polypropylene (including glass reinforced); high density polyethylene, rigid PVC, fluorinated vinyls.

‡Weights for polypropylene; others are times PP: 1.03 for high density polyethylene; 1.54 for PVC; 1.87 to 1.95 for fluorinated vinyls.

Table 9-13
Hy-Pak™* Metal Packing

Size No. Designation	Approximate Number/Ft ³	Weight, ** Lb/Ft ³	Percent Free Gas Space
1	850	19	97
1½	270	—	97
2	105	14	98
3	30	13	98

*By permission, Norton Chemical Products Corp., Bull. HY-30®, dated 9/88 reg. trademark.

**Weight for standard gauge carbon steel, available in most other common metals.

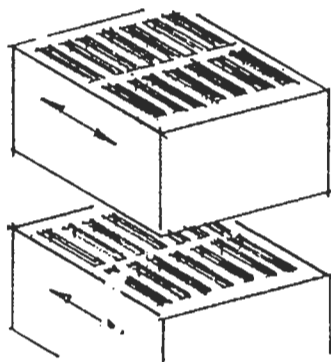
Table 9-14
Chempak® Metal Packing*

1	950	19	96
---	-----	----	----

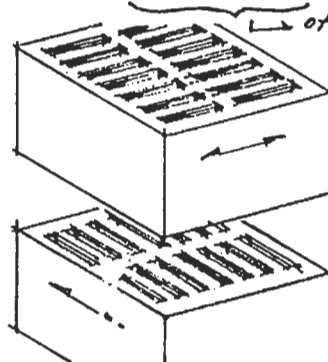
*By permission Chem-Pro Equipment Corp., Licensed from Dr. Max Levo, Bull. 702. Weight is for carbon steel.

Table 9-15
Grid Tile (Drip Point)*

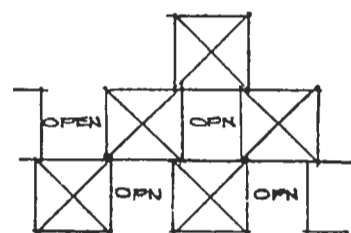
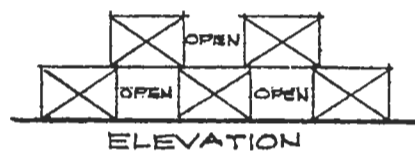
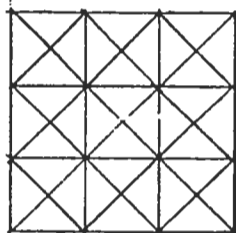
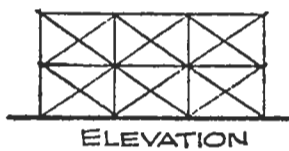
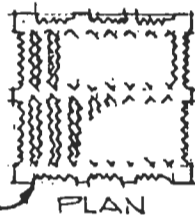
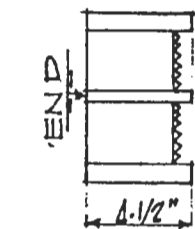
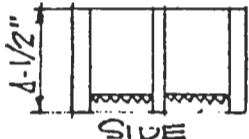
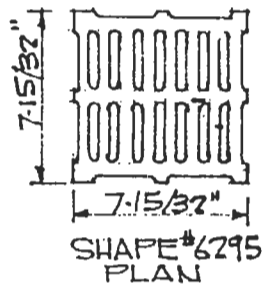
ARRANGEMENT OF TILE IN STACKED PACKING		SURFACE CONTACT PER CU. FT.		FREE AREA PER SQ. FT. HOR SURFACE		NUMBER PCS. PER CU. FT.		WEIGHT PER CU. FT.		PRESSURE DROP	
		TILE SHAPE		TILE SHAPE		TILE SHAPE		TILE SHAPE		TILE SHAPE	
		6295	6897	6295	6897	6295	6897	6295	6897	6295	6897
		SQ. FT.	SQ. FT.	SQ. FT.	SQ. FT.	PCS	PCS	LBS	LBS	GAL/MIN/SQ. FT.	GAL/MIN/SQ. FT.
CONTINUOUS FLUE	GRID	24.01	34.09	.435	.420	6.88	6.88	79.12	79.12	SEE MFG'S LITERATURE FOR CHARTS SHOWING PRESSURE DROP IN INCHES OF WATER PER FT. OF HEIGHT	
	CHECKER'D	14.5	22.0	.67	.67	3.36	3.36	38.64	38.64		
CROSS FLUE	GRID	24.01	34.09			6.88	6.88	79.12	79.12		
	CHECK'R'D	14.5	22.0			3.36	3.36	38.64	38.64		
DUMPED											



CONTINUOUS
FLUE
ARRANGEMENT



CROSS
FLUE
ARRANGEMENT



CRUSHING
STRENGTH
ALLOWABLE
LBS/FT²

SPRAY
CHAMBERS =
41% OF
TOTAL VOL

* By permission, General Refractories Co.

Table 9-16
Packing Service Application

Packing Material	General Service Application	Remarks
Glazed and unglazed, Porcelain or Chemical Stoneware	Neutral and acid conditions except hydrofluoric, solvents. Not good in hot caustic (above 70°F)	Unglazed usual type specified except special requirement of low adsorption on surface. Special ceramics available for mild caustic. Porcelain stronger and more resistant than stoneware.
Carbon	Hot alkali, all acids except nitric, no oxidizing atmospheres.	Stand thermal shock, low cubic weight
Plastic	Alkali, salts, aqueous and acids depending on resin	Light weight
Steel and other light gauge metals	Hot alkali for steel, other service to suit metals	May be heavier than ceramic, more expensive

(text continued from page 246)

Poor distribution reduces the effective wetted packing area and promotes liquid channeling.

The final selection of the mechanism of distributing the liquid across the packing depends upon the size of the tower, type of packing (exposed surface, configuration), tendency of packing to divert liquid to tower walls, and materials of construction for distribution. Figures 9-8A–9-8L illustrates a few distribution types. Spray nozzles are used, but care must be taken in evaluating the percent of the total liquid that hits the walls and never enters the packing. Full cone nozzles with spray angles which will keep most of the liquid on the center portion of the packing for initial contact will perform quite well.

Spray nozzle manufacturers have spray angle data for various pressures at the nozzle inlet (pipe), see Figure 9-8L. This should be considered carefully in the distributor design, and the volume discharge per square foot of flat tower cross-section must be as uniform as possible. Careful layouts of nozzle arrangements are usually required, Figure 9-8K. Maximum rate variation of ± 5 to 6% of average flow is necessary in design [82].

There are many other types and variations in addition to those listed, although they are usually special-purpose trays and not necessarily generally adaptable.

Good design generally considers that the streams of liquid should enter onto the top of the packing on 3- to 6-in.

square centers for small towers less than 36 in. in diameter, and should number $(D/6)^2$ streams for 36-in. and larger, where D is the tower inside diameter in inches [22]. When the liquid stream spacings exceed 6-in. square pitch, consideration should lean to this figure. Most manufacturers make some type of distributor giving one stream every 6 in.² of tower area.

The number of irrigation or “drip-points” or entrance points per square foot of flat surface of the tower should be uniform for orifice, weir-type gravity, or pressure distributors, and need not exceed 10 points/ft² [82]. This uniformity must not be disturbed by support rings for supporting the distributor itself. The distribution must include the area adjacent to the wall, and the design must not “force” more liquid at the wall where it contacts the packing. Uniformity of points of distribution to the packing surface is extremely important. The volume flow per point must be carefully calculated.

Bonilla [131] presents an excellent examination of liquid distributors in packed towers. Packed towers with random packing or structured packing are more sensitive to poor or non-uniform distribution of liquid than tray towers. This requires that liquid and vapor enter the packing evenly distributed. Often, only the liquid distributor at the top of the packing is considered, but vapor distribution at the bottom or intermediate in the tower is quite important. The ultimate performance of a packing depends significantly on the initial distribution [131], with non-uniform distribution resulting in reduced packing efficiency, which can be expressed as a higher HETP, height equivalent to a theoretical plate/stage/tray. A higher surface area structured packing is more sensitive to the initial liquid non-uniform distribution than a lower surface area packing.

It is important to recognize that each packing has a natural liquid distribution [131] that will develop if sufficient bed depth is available. If the distribution is poorer than the natural distribution, the system will end up with concentration gradients and higher HETP values. When/if an improvement from a poor to natural distribution occurs slowly over many feet of packing, Bonilla [131] states that adding extra packing to a bed to compensate for the initial maldistribution does not work because the return to the natural distribution is not fast enough to compensate for the concentration gradients that have already formed.

Most liquid distributors feed onto the packing by gravity, rather than being pressurized. For any given tower design the distributor design and installation is an important component for assisting in aiding the packing to do its job. For best performance for the average distillation the distributor should be installed level to a tolerance of $\pm 1/8$ to $1/16$ in. and should be able to be leveled once it is in the tower. Table 9-18 [131] presents a comparison of many of the factors necessary to the selection and design

Table 9-17
Packing Type Application

Packing	Application Features	Packing	Application Features
Raschig Rings	Earliest type, usually cheaper per unit cost, but sometimes less efficient than others. Available in widest variety of materials to fit service. Very sound structurally. Usually packed by dumping wet or dry, with larger 4–6 in. sizes sometimes hand stacked. Wall thickness varies between manufacturers, also some dimensions; available surface changes with wall thickness. Produce considerable side thrust on tower. Usually has more internal liquid channeling, and directs more liquid to walls of tower. Low efficiency.	Grid Tile	Available with plain side and bottom or serrated sides and drip-point bottom. Used stacked only. Also used as support layer for dumped packings. Self supporting, no side thrust. Pressure drop lower than most dumped packings and some stacked, lower than some ½-in. × 1-in. and ½-in. × 2-in. wood grids, but greater than larger wood grids. Some HTU values compare with those using 1-inch Raschig rings.
Berl Saddles	More efficient than Raschig Rings in most applications, but more costly. Packing nests together and creates "tight" spots in bed which promotes channeling but not as much as Raschig rings. Do not produce as much side thrust; has lower HTU and unit pressure drops with higher flooding point than Raschig rings. Easier to break in bed than Raschig rings.	Teller Rosette (Tellerette)	Available in plastic, lower pressure drop and HTU values, higher flooding limits than Raschig rings or Berl saddles. Very low unit weight, low side thrust.
Intalox Saddles ¹ And Other Saddle-Designs	One of most efficient packings, but more costly. Very little tendency or ability to nest and block areas of bed. Gives fairly uniform bed. Higher flooding limits and lower pressure drop than Raschig rings or Berl saddles; lower HTU values for most common systems. Easier to break in bed than Raschig rings, as ceramic.	Spraypak ³	Compared more with tray type performance than other packing materials. Usually used in large diameter towers, above about 24-in. dia., but smaller to 10-in. dia. available. Metal only.
Pall Rings ²	Lower pressure drop (less than half) than Raschig rings, also lower HTU (in some systems also lower than Berl saddles), higher flooding limit. Good liquid distribution, high capacity. Considerable side thrust on column wall. Available in metal, plastic and ceramic.	Panapak ⁴	Available in metal only, compared more with tray type performance than other packing materials. About same HETP as Spraypak for available data. Used in towers 24 in. and larger. Shows some performance advantage over bubble cap trays up to 75 psia in fractionation service, but reduced advantages above this pressure or in vacuum service.
Metal Intalox ³ Hy-Pak ⁴ Chempak ⁷	High efficiency, low pressure drop, reportedly good for distillations.	Stedman Packing	Available in metal only, usually used in batch and continuous distillation in small diameter columns not exceeding 24-in. dia. High fractionation ability per unit height, best suited for laboratory work. Conical and triangular types available. Not much industrial data available.
Spiral Rings	Usually installed as stacked, taking advantage of internal whirl of gas-liquid and offering extra contact surface over Raschig ring, Lessing rings or cross partition rings. Available in single, double and triple internal spiral designs. Higher pressure drop. Wide variety of performance data not available.	Sulzer, Flexipac, and similar	High efficiency, generally low pressure drop, well suited for distillation of clean systems, very low HETP.
Lessing Rings	Not much performance data available, but in general slightly better than Raschig ring, pressure drop slightly higher. High side wall thrust.	Goodloe Packing ⁵ and Wire Mesh Packing	Available in metal and plastic, used in large and small towers for distillation, absorption, scrubbing, liquid extraction. High efficiency, low HETP, low pressure drop. Limited data available.
Cross-Partition Rings	Usually used stacked, and as first layers on support grids for smaller packing above. Pressure drop relatively low, channeling reduced for comparative stacked packings. No side wall thrust.	Cannon Packing	Available in metal only, low pressure drop, low HETP, flooding limit probably higher than Raschig rings. Not much literature data available. Used mostly in small laboratory or semi-plant studies.
		Wood Grids	Very low pressure drop, low efficiency of contact, high HETP or HTU, best used in atmospheric towers of square or rectangular shape. Very low cost.
		Poly Grid ⁶	Plastic packing of very low pressure drop, developed for water-air cooling tower applications.

Compiled from literature:

- 1 Trade name of Norton Chemical Process Products Corp.
- 2 Introduced by Badische Anilin and Sodafabrik, Ludwigshafen am Rhein
- 3 Trade name of Denholme Inc., Licensed by British Government
- 4 Trade name of Packed Column Corp.
- 5 Trade name of Packed Column Corp.
- 6 Trade name of The Fluor Products Co.
- 7 Trade name of Chem-Pro Equip. Corp.

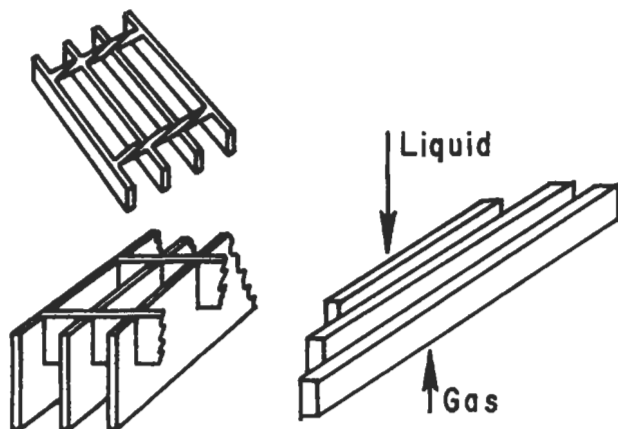
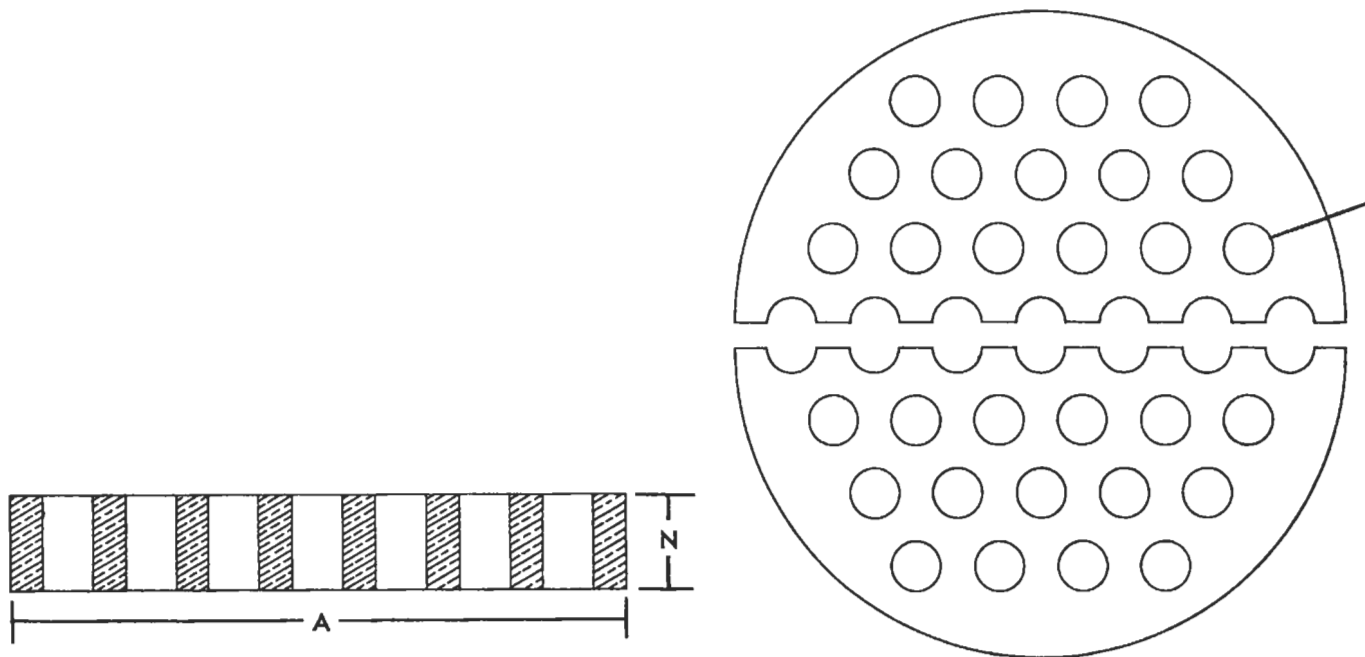


Figure 9-7A. Bar-grid support. Used by permission of U.S. Stoneware Co. (now, Norton Chemical Process Products Corp.).



DIMENSIONS PERFORATED SUPPORT PLATE

Tower Diameter in Inches.....	12	15	18	20	24	30	36	42	48	60
Diameter of Plate "A".....	11	14	17	19	23	29	35	40	45½	57½
Height of Plate "N".....	1	1	1	1	1	1½	2	2½	3	4
Diameter of Holes "C".....	1	1¼	1¼	1½	2	2	2½	3	3½	3½
Number of Holes.....	22	31	31	38	37	61	61	55	61	101
Approximate Weight (lbs.).....	16	19	23	28	35	85	150	185	260	425

Figure 9-7B. Perforated support plates. Used by permission of U.S. Stoneware Co. (now, Norton Chemical Process Products Corp.).

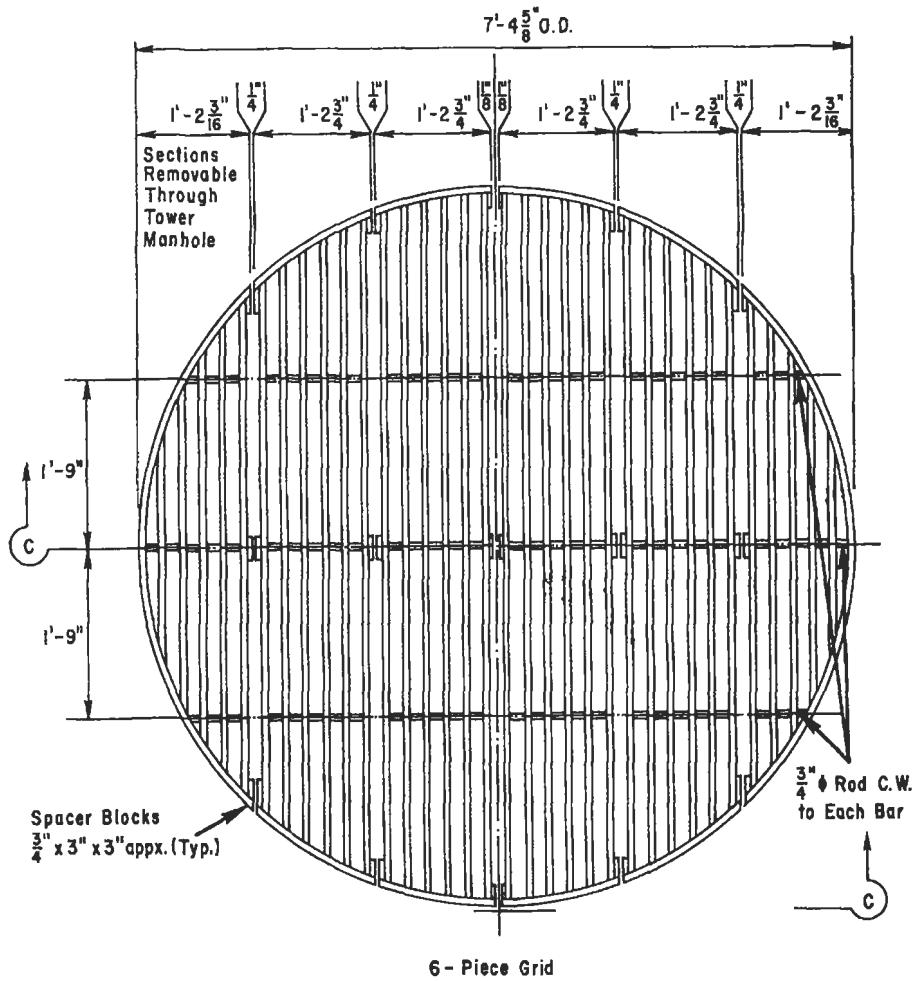
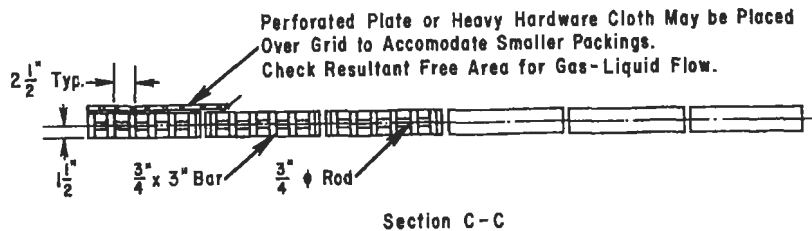


Figure 9-7C. Bar-grid support plate, typical details.



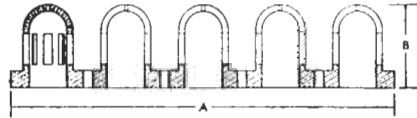
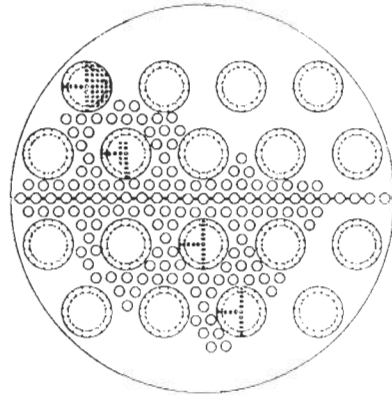
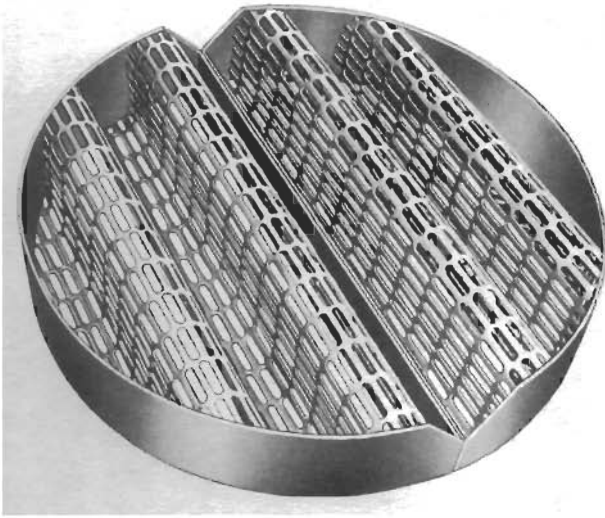
of types and styles of distributors. Selection of types depends on liquid rate, turndown requirements, plugging or fouling tendencies, feed flow, and many other considerations [131]. The abbreviations in Table 9-18 are for four basic types of distributors described as follows:

Pan Distributors (PAN)

Also known as riser tube distributors (RTD) [131], these consist of a flat tray with orifices uniformly spaced to allow liquid to flow onto the packing below. This tray has vapor risers, uniformly spaced, but not interfering with

the liquid orifice holes. These are used for clean liquids in towers of 2 ft–10 ft diameter [131]. It can be installed between flanges in towers smaller than 2 ft. It is good for low to high liquid rates to the tray. With 2-1/4 in. diameter risers, about 20 uniformly spaced drip points/ft² can be achieved, and useful for high purity fractionation. When flow of vapor and liquid are high, the separation efficiency of the system may not be good when only 4 to 6 drip-points/ft² are able to be installed due to space occupied on the tray by the larger vapor risers. For high vapor flows

(text continued on page 264)

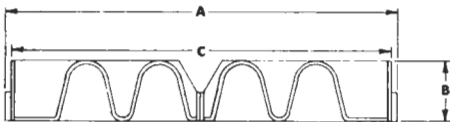
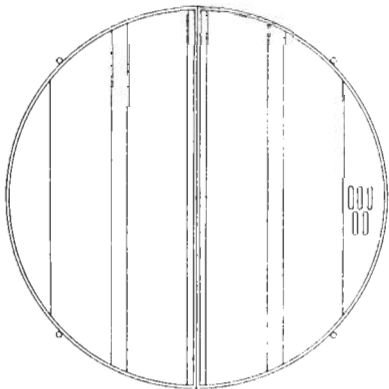


DIMENSIONS FOR SUPPORT PLATE (CHEMICAL PORCELAIN)

Tower Diam. (Inside)	Plate Diam. "A"	No. of Risers	Overall Height "B"	Per Cent of Free Area	Packing Size (Min.)	Support Ledge (Min.) ‡	Approx. Net Wt. (lbs.)
12"	11-1/4"	4	5-3/4"	52.5	1/2"	3/4"	10
14"	13-1/4"	4	6-7/8"	58.0	1/2"	3/4"	14
15"	14-1/4"	4	6-7/8"	54.6	1/2"	3/4"	16
16"	15-1/4"	4	7"	56.8	1/2"	3/4"	18
18"	17-1/4"	4	7-9/16"	53.0	1/2"	3/4"	28
20"	19"	4	7-9/16"	51.4	3/4"	1"	30
24"	23"	6	7-11/16"	54.6	3/4"	1"	38
30"	29"	10	7-7/8"	55.2	3/4"	1"	76
*36"	35"	18	8"	64.2	1"	1"	98
*42"	40-1/2"	20	8-1/4"	60.2	1"	1-1/2"	180
*48"	46-1/2"	24	8-1/2"	52.9	1-1/2"	1-1/2"	292
*60"	58"	40	9"	60.6	1-1/2"	2"	400

*For these sizes use no more than 10 feet of packed depth unless designed for specific load requirement

‡In order to avoid blocking any free area of the support plate the maximum width of the support ledge should not be appreciably greater than the minimum width shown. In pre-fabricated ceramic towers, 24" and 30" towers have a 1 1/2" support ledge, the 36" tower a 1 1/2" ledge and the 42" and 48" towers a 2" support ledge

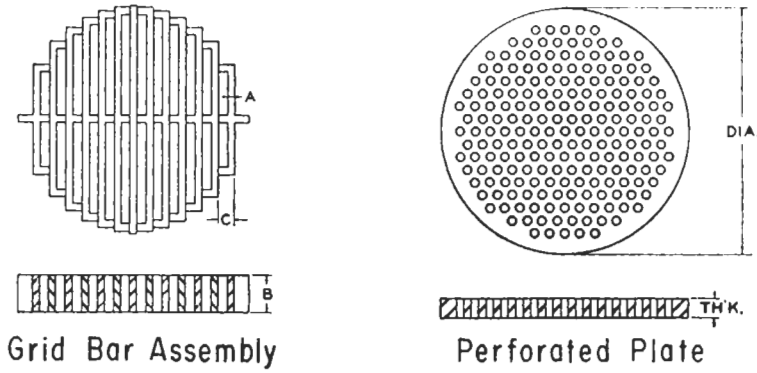


MODEL 818 "GAS - INJECTION" METAL SUPPORT PLATE

TOWER I.D.		DIA. OVER SPACERS A	HEIGHT B	PLATE DIA. C	SUPPORT LEDGE (MIN.)	MIN. DIA. OF ACCESS	APPROX. NET WEIGHT (LBS.)*
INCHES	MM						
12	305	-----	4 1/2"	11 3/4"	3/4"	8"	7
13 1/4	337	-----	4 1/2"	12 3/4"	3/4"	9"	8
14 1/4	362	-----	4 1/2"	13 3/4"	3/4"	9"	9
15 1/4	388	-----	4 1/2"	14 3/4"	3/4"	10"	10
17 1/4	438	-----	4 1/2"	16 3/4"	3/4"	10"	11
19 1/4	489	-----	4 1/2"	18 3/4"	1"	11"	12
21 1/4	540	-----	4 1/2"	20 3/4"	1"	12"	17
23 1/4	591	-----	4 1/2"	22 3/4"	1"	13"	19
29 1/4	743	-----	4 1/2"	28 3/4"	1"	16"	25
36	914	35 1/2"	4 1/2"	34 3/4"	1"	14"	40
42	1067	41 1/2"	4 1/2"	40 3/4"	1 1/2"	16"	52

*Weights shown are for standard construction and material thickness, carbon steel.

Figure 9-7D. Typical efficient metal and porcelain support plate designs for gas injection into packing. Designs also available in plastic-FRP, polypropylene, PVC, etc. (Also see Figure 9-7F.) Used by permission of Norton Chemical Process Products Corp.



Haveg Packing Supports

Tower Dia.	GRID BARS				PERFORATED PLATE					
	No.	Size			% Free Area	Dia.	Th'k.	Holes No.	Dia.	% Free Area
		A	B	C						
12"	7	1/2	2 1/2	1 1/2	48	13 1/2	1	33	3/4	6
15"	9	3/4	2 1/2	1 1/2	30	13 3/8	1 1/4	55	3/4	10
18"	9	3/4	2 1/2	1 1/2	34	16 1/2	1 1/2	65	3/4	8
20"	9	3/4	2 1/2	1 1/2	37	19 1/2	1 5/8	95	3/4	9
2'	13	3/4	3 1/2	1 1/2	39	23 1/4	1 3/4	134	3/4	9
2'-6"	15	3/4	3 1/2	1 1/2	36	29 1/4	2	188	3/4	7
3'	19	3/4	3 1/2	1 1/2	38	35	2	299	3/4	9
3'-6"	21	3/4	3 1/2	1 3/4	41	41 1/4	2	402	3/4	9
4'	27	3/4	5	1 3/4	41	47	2 1/4	544	3/4	10
5'	31	3/4	5	1 3/4	45	58 1/2	2 1/2	843	1	19
6'	37	3/4	5	1 3/4	46	71	3	1277	1	20
7'	43	3/4	6	1 3/4	46
8'	51	3/4	6	1 3/4	47
9'	57	3/4	6	1 3/4	48
10'	61	3/4	6	1 3/4	50

Note: All Dimensions are in inches unless Otherwise Noted.
Perforated Plate Free Area Should Be increased when Possible

Figure 9-7E. Reinforced plastic support plate. Used by permission of Haveg Corp., Bull. F-7.

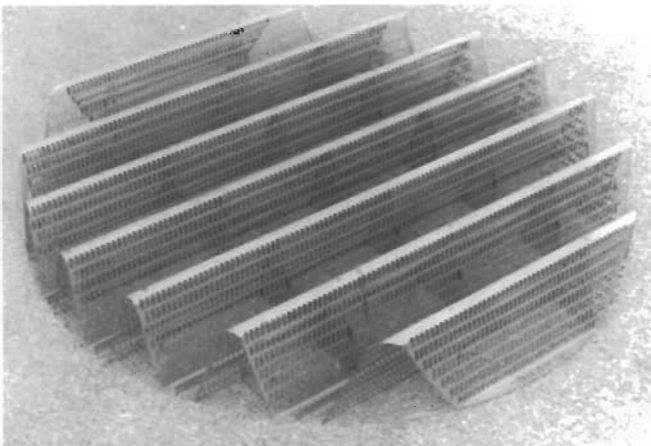


Figure 9-7F. Support plate for high gas/vapor flow. (Also see Figure 9-7D.) Used by permission of Jaeger Products, Inc.

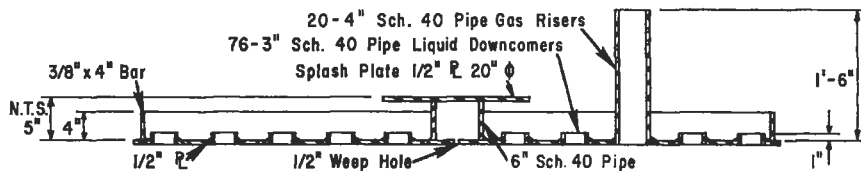
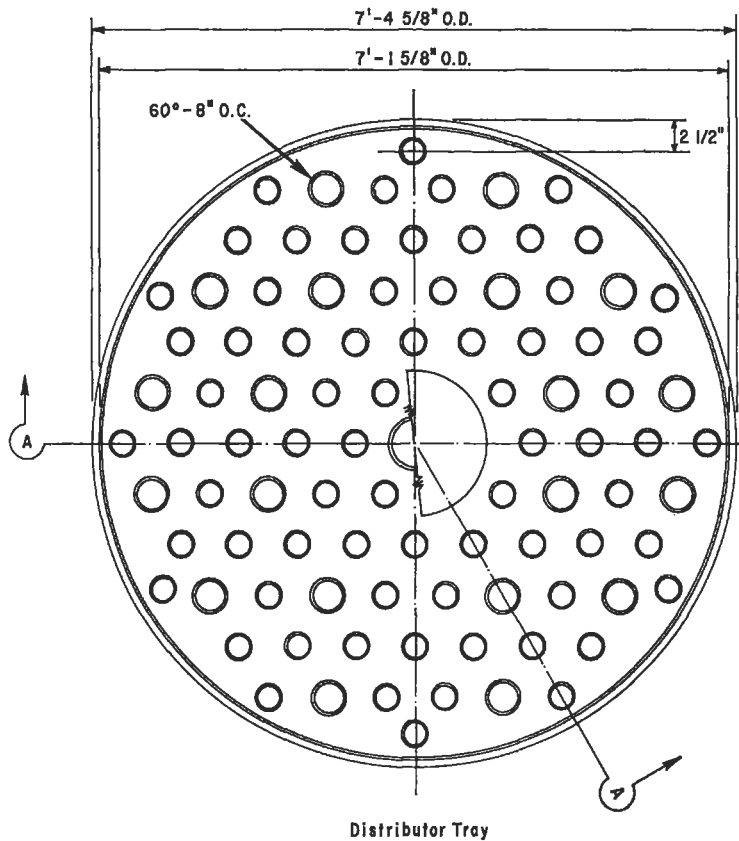


Figure 9-8A. Multilevel distributor with splash plate.

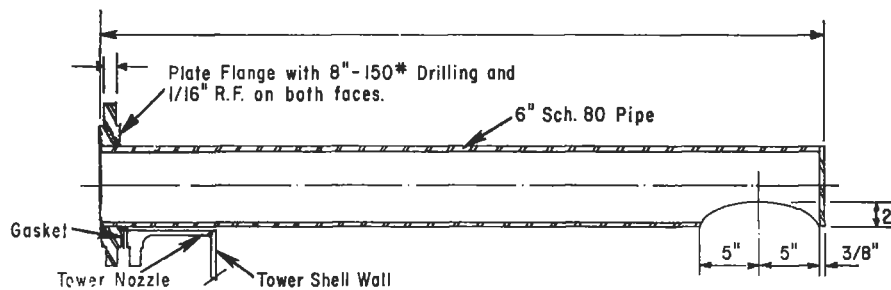


Figure 9-8B. Inlet pipe for distributor, Figure 9-8A.

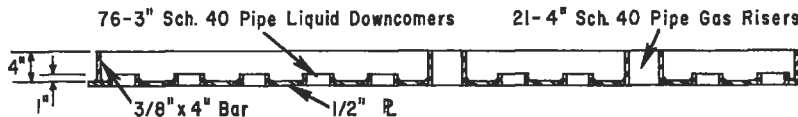
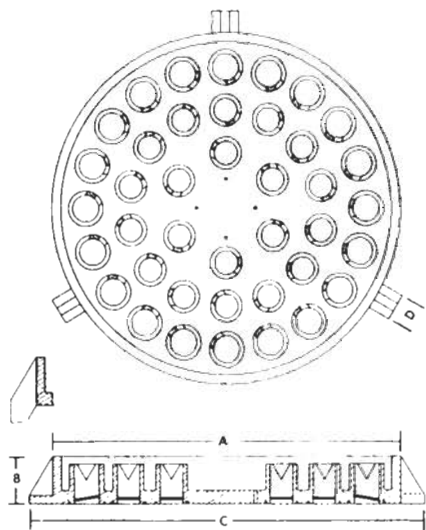


Figure 9-8C. Distributor for intermediate level distribution.



DIMENSIONS FOR "WEIR FLOW" DISTRIBUTOR (CERAMIC)

Tower Dia.	Plate Dia. "A"	Overall Dia. "B"	Overall Dia. "C"	Width of Lugs "D"	No. of Weirs	Flow (Gallons Per Minute)	Approx. Net Weight
24"	20"	23"	5 3/4"	3"	8	16	55
30"	25"	29"	5 1/4"	3"	18	36	70
36"	30"	35"	5 1/4"	3"	18	36	120
42"	35"	41"	5 1/2"	3"	36	72	150
48"	40"	46"	5 1/2"	3"	40	80	190
60"	50"	58"	6"	4"	48	96	270

*Raised lugs standard on this size only

Figure 9-8D. Weir-flow distributor. Used by permission of U.S. Stoneware Co., Bull. TA-40 (now, Norton Chemical Process Products Corp.).

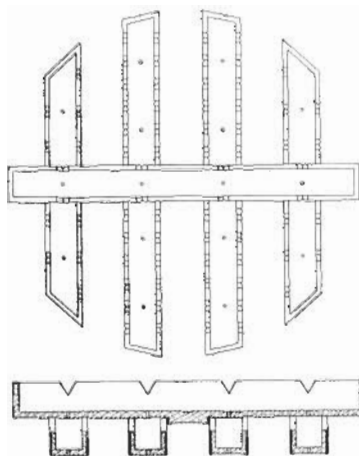


Figure 9-8E. Trough liquid distributor. Used by permission of U.S. Stoneware Co. (now, Norton Chemical Process Products Corp.).

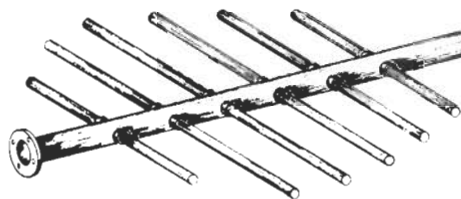
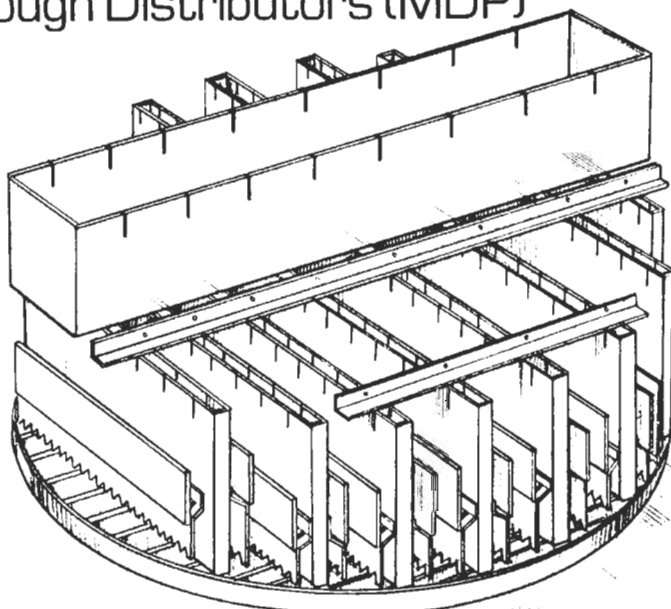


Figure 9-8F. Typical design inlet liquid distributor using holes (orifices) on underside of distribution pipes. Note: Number of side pipes adjusted to provide uniform entry per square foot of tower cross-section area. Holes at wall should be spaced on same basis.

Koch/Sulzer[®] Trough Distributors (MDP)



This distributor is widely used for structured packing applications in medium-to-large-diameter columns. The header above the lateral arrangement provides for cost-effective sectionalized designs without the need for gaskets. Elevated holes in both the header and laterals provide superb fouling resistance. As a result of multiple drip points (MDP), a curtain of liquid falls perpendicular to the top of the packing.

In a typical design, the header box may have holes in the floor or, for fouling services, holes in metering boxes that are welded inside the header. The header is leveled independently by lugs attached to the laterals. Laterals have holes punched in the sides above the floor of the lateral. The MDP baffle arrangement directs the liquid onto the packing with a typical lateral hole density of 10 points/ft². Turn-down capabilities: typically 2.5:1. A two-stage design can be provided for higher turn-down requirements.

Overall distributor height is approximately 24". The distributor is leveled from a supporting grid, which normally rests on the top of the packed bed. The vessel manway is usually located at or above the header elevation.

*U.S. Patent: 4,816,191
Canadian Patent: 1,261,249

**See note

NOTE: "SULZER" is the registered trademark of Sulzer Brothers Ltd., Winterthur, Switzerland. Koch Engineering Company, Inc. is the exclusive licensee and distributor of packing, internals, static mixers, mist eliminators and other quality process equipment for the chemical, petrochemical and petroleum industries, bearing the SULZER[®] trademark in the U.S., Canada and Mexico.

Figure 9-8G. Koch/Sulzer[®] trough distributor (MDP), for medium to large diameter columns for structured packing (patented), one of several designs available. Used by permission of Koch Engineering Co., Inc., Bull. KS-6.

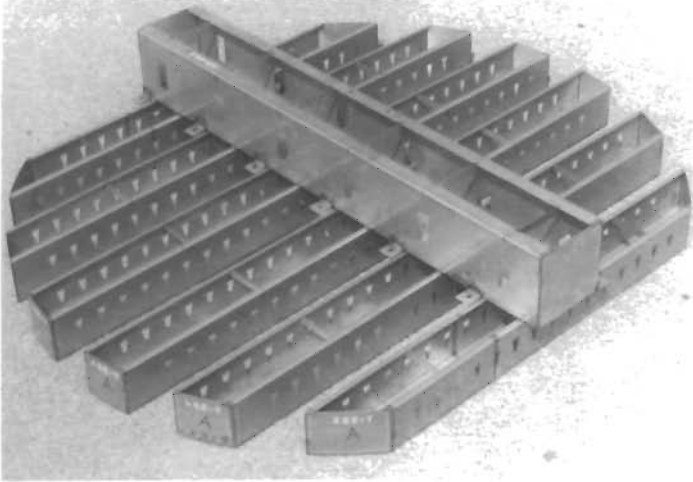


Figure 9-8H. Orifice pan liquid distributor with round or rectangular chimneys and a flat floor sealed to vessel support ring. For a large vessel, it can be sectioned to pass through a manway. Used by permission of Jaeger Products, Inc., Bull.-1100.

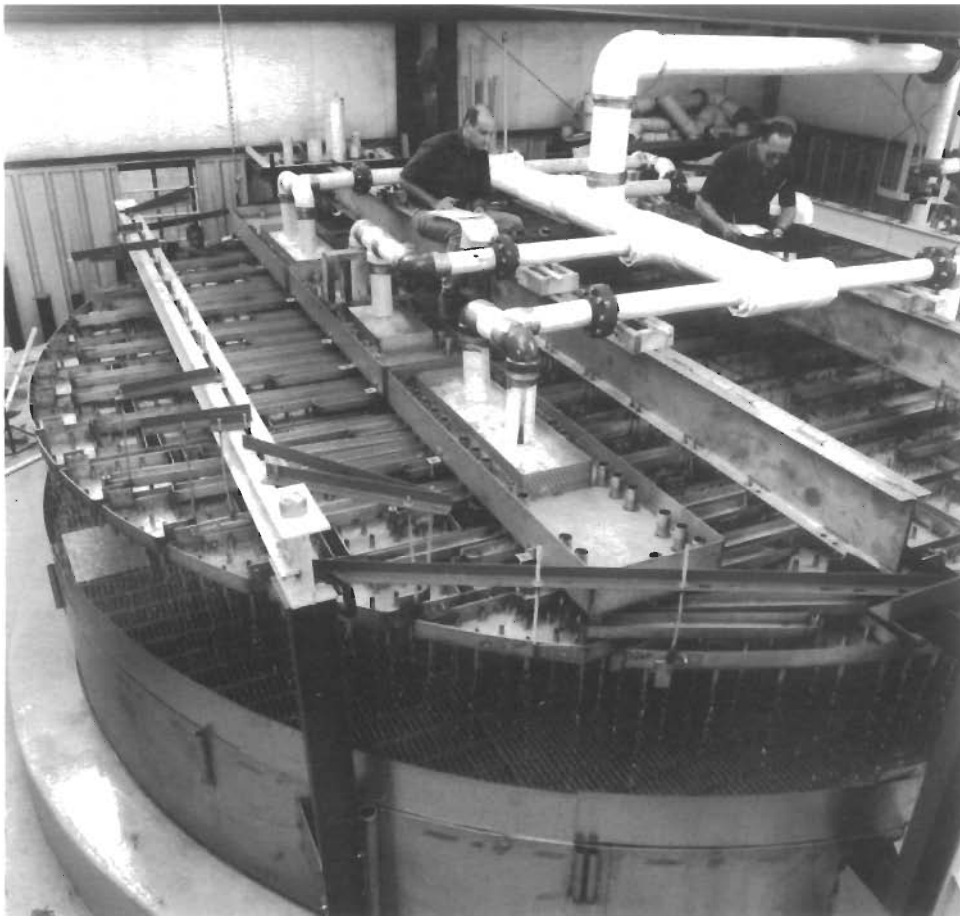


Figure 9-8I. Multipan MTS-109 two-stage liquid distributor. Used by permission of Nutter Engineering, Harsco Corp., Bull. CN-4.

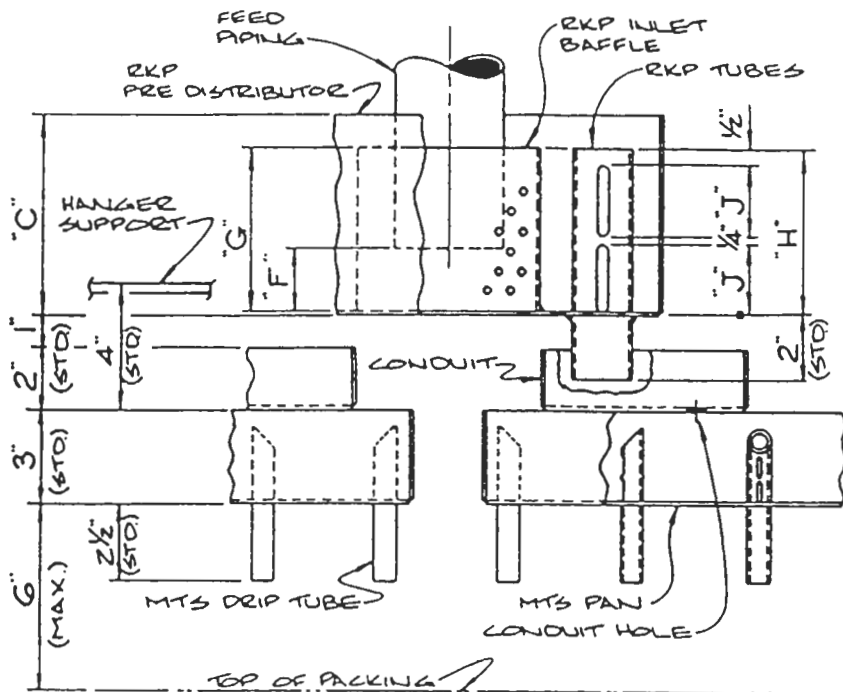
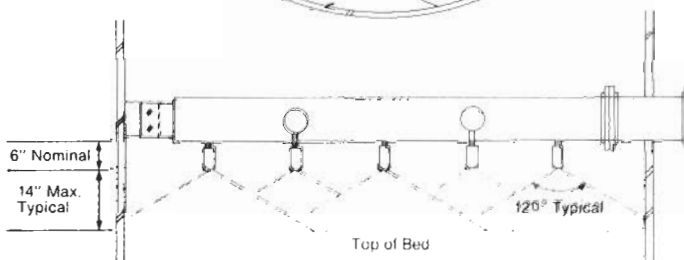
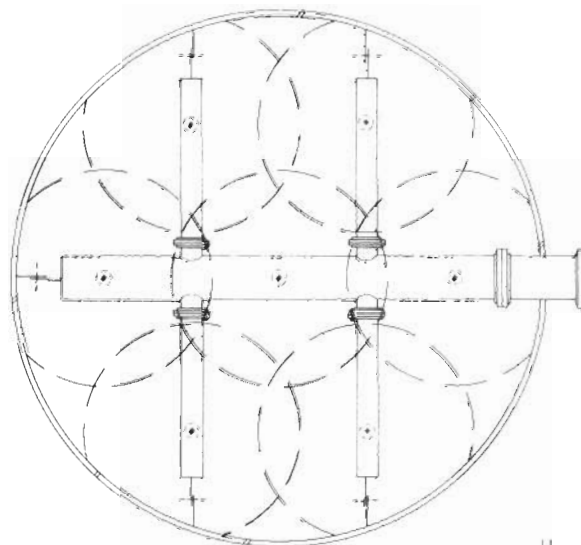


Figure 9-8J. MTS-109 Multipan two-stage liquid distributor for optimum liquid distribution for uniform flow; for random and structured packings for low to moderate liquid rates, less than 5 gpm/ft². Also used for redistributor. Used by permission of Nutter Engineering, Harsco Corp., Bull. TI-1, under license from The Dow Chemical Co., protected by U.S. Patents No. 4,472,325; 4,808,350; 5,013,491.



312" diameter spray distributor for refinery vacuum tower

Figure 9-8K. Spray nozzle distributor using full-cone wide-angle spray nozzles (depends on tower diameter). Not recommended for distillation applications, where the point-type distributors provide higher packing efficiency. Used by permission of Nutter Engineering, Harsco Corp., Bull. TI-1.



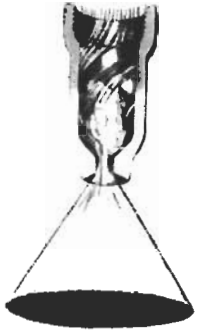


Figure 9-8L. Full cone spray nozzle as used for liquid distribution. Used by permission of Spraying Systems, Co., Cat. 55.

(text continued from page 257)

the design must be carefully evaluated [131]. For uniform hole performance all holes must be punched in the same direction, i.e., top down or bottom up.

Equation 9-1 can be used to correlate the number of holes to the liquid head for a specific hole diameter, d :

$$n = Q / [4 d^2 (h - h_d)^{0.5}] \quad (9 - 1)$$

$$Q = 5.10 (n) (a) (h - h_d)^{0.5} \quad (9 - 2)$$

$$Q = K (n) (a) (h - h_d)^{0.5} \quad (9 - 3)$$

This is considered the basis design for the distributor [131]. $K = 0.16$ for average. The hole punch direction has a strong influence on the value of K . $K = 0.6$ if holes are punched down [131].

For distributors of any design, including the PAN, it is important to filter the feed or reflux liquid entering the distributor to reduce the possibilities of plugging of the orifice holes. Otherwise, the random plugging will cause non-uniform distribution onto the packing below. It is important to avoid leakage around the risers because this can destroy the liquid distribution pattern [131].

Symbols are used by permission of Bonilla, [131]:

A = distributor quality factor

B = distributor quality factor

C_T = vapor capacity factor

Table 9-18
Guidelines for Selection of Liquid Distributors

Factor	Type of Distributor					
	PAN (RTD)	POH (Gravity)	POH (Pressure)	NTD	SNH	VND
Uniformity	VG	VG	F	VG	P	P
Solids handling	P	P	F	G	G	VG
Turndown	G	G	G	G	P	P
Ease of installation	F	F	G	F	VG	G
Ease of leveling	F	G	VG	F	VG	F
As redistributor	G ^{1,2}	No ²	No	No ²	No	No ²
Height requirement	M	L	VL	H	M	H
Cost	H	M	L	H	L	M
Residence time	H	L	L	M	L	M
Suitable for large diameters (>10 ft)	P	G	G	G	VG	G
Leakage potential	H ³	No	No	No	No	No
At high vapor rates	P	G	G	G	VG	G
At high liquid rates	G	G	G	G	VG	G
At low liquid rates	G	VG	G	VG	P	P
For high-purity fractionation	VG	VG	P	VG	P	P
Heat transfer	G	G	F	G	VG	G
Liquid feed handling	Yes ¹	No	No	Yes	No	Yes
Flashing feed handling	Yes ^{1,2}	No ²	No	No ²	No	No ²

Key: VG = very good; G = good; F = fair; P = poor; H = high; M = moderate; L = low; and VL = very low. "No" means that the distributor cannot be used for the particular factor.

¹No significant liquid mixing provided, however.

²Very good if used in conjunction with a chimney tray.

³Leakfree if seal-welded.

Reproduced by permission of The American Institute of Chemical Engineers; Bonilla, J. A., *Chem Eng. Prog.* Vol. 89, No. 3 (1993) © p. 47; all rights reserved.

$$= [(\text{vapor velocity}) (\text{vapor density}) / (\text{liquid} - \text{vapor densities})]^{0.5}$$

DQ = distributor quality

a = surface area of an orifice hole, in.²

d = diameter of hole, in.

h = liquid height over orifice, in.

h_d = vapor pressure drop across distributor, in. (Calculate h_d by the vapor flow equation through distributor open area.)

n = number of holes

Q = liquid volumetric flow rate, gpm

K = flow coefficient

V = horizontal liquid velocity, ft/sec (in distributor)

The use of narrow trough PAN distributors is a better choice to prevent leakage from towers above 3–9 ft diameter and larger [131].

Turndown on a PAN type tray should be limited to 2:1 (ratio of high to low flow rates), which results in a reasonable design. Bonilla [131] points out that it is costly to design for short-term high turndown rates such as start-up, shutdown, or for other short term periods, because it is better to increase reflux ratio to increase internal loads for such periods rather than design the distributor for large turndown.

Trough Distributors (NTD)

These consist of multiple troughs 3–4 in. wide [131], and are fed by feed or parting boxes mounted above, or by multiple pipes mounted 90° to the direction of the troughs. The parting boxes distribute the liquid to troughs through calibrated orifices in the bottom or wall. The feed points out of the troughs to the packing are usually in the bottom or at the wall of the troughs. Locating the holes in the trough sidewalls allows for collection of rust and any other sediment in the trough bottoms and avoids plugging the orifice holes. This style has a capability of handling large vapor loads and the distributor design allows for good liquid distribution. These troughs can be readily leveled across a tower, and can still handle low to medium liquid rates, and can handle turndown of up to 5:1 by special and careful design [131]. This should not be used for slurry systems; rather, a V-notch version is better suited, but may not be as accurate for liquid distribution.

The NTD's are quite often used with structured packing where it may be desired to have an overflow sheet of liquid onto the packing and (rather than through holes) oriented at 90° to the top structured layer [131].

With a trough distributor it is often more difficult to obtain uniform distribution next to the tower wall than with a PAN or orifice pipe distributor. Bonilla [131] recommends the rule of thumb: Any 10% of the outer surface area of packing in the tower should not receive more or less liquid than the average 10% of the surface area.

The use of V-notches in a trough wall for overflow is more sensitive to leveling problems than the other designs, and for the same $\pm\frac{1}{8}$ - to $\frac{1}{16}$ -in. level tolerance produces a more severe non-uniform flow distribution. The quality of distribution from a V-notch is poor compared to the other types of trough distributor, but does have advantages in slurry systems [131]. It should not be used for critical distillation applications, but is good for heat transfer and where solids are in the system.

Pipe Orifice Headers (POH)

These distributors are fabricated of pipe lengths tied to a central distribution header (usually) with orifice holes drilled in the bottom of the various pipe laterals off the header. This style of distributor can be fed by pressure or gravity for clean fluids. The gravity feed is considered better for critical distillation application when uniformity of the flow of the drip points (or flow points) through out the cross-section of the tower is extremely important, and is excellent for low flow requirements such as below 10 gpm/ft² [131].

This design is restricted to a 2:1 turndown and is not practical for large liquid rates compared to the NTD or RTD styles [131].

Spray Nozzle Headers (SNH)

These are similar in design to the pipe orifice distributor using small angles (<90°) spray nozzles instead of orifices. Because the sprays can be selected to cover varying cross-sections per spray, the total number can be small compared to the orifice holes that would be required. The spray from the nozzle should be "full cone" and not "hollow cone" to provide a uniform liquid circle that should overlap to avoid dry-spots. The spray nozzles operate under pressure, with the manufacturer providing flow rates and patterns for variations in system pressure. A careful layout is required to evaluate how much liquid flows through each square foot of tower and therefore the packing. This style of distributor is good for heat transfer and vapor washing, with little or no fractionation, although they have been used successfully for distillation operations.

Turndown is usually limited to 0.5:1, and liquid distribution can be poor if the sprays are not carefully laid out and the system flow tested for uniformity. Another problem is misting of the liquid from the sprays and the resulting entrainment out of the tower or up to overhead mist eliminators.

Number of Flow or Drip Points Required [131]

1. For low purity hydrocarbon fraction, the number of drip or separate flow points should be 6–10 drip points/ft² of tower cross-section surface area.

- For high purity hydrocarbon fractionation, the number of drip points recommended for good irrigation is 10–20 drip points/ft². Increasing the number of drip points much beyond 20 may not help improve the packing performance. Table 9-19 suggests the approximate number of useful drip points/ft² for various sizes of random packing. Experience and design judgment may indicate more or less should be used. From Table 9-19 Bonilla points out that at the lower liquid rates into the distributor a larger number of holes are required to effectively wet the packing due to the lower spreading rates from the lower flows.
- Minimum recommended hole diameters [131]—
 - Carbon steel system: $\frac{3}{8}$ -in. (use filter on entering liquid)
 - Stainless steel: $\frac{1}{8}$ -in. (experience suggests $\frac{3}{16}$ -in. minimum) (use filter on entering liquid)
- Recommended [131] rule of thumb to avoid liquid entrainment from the entering liquid by the vapor out of the tower: Limit the vapor capacity factor C_f to about 0.4 ft/sec,

$$\text{where } C_f = V [(\rho_v)/(\rho_L - \rho_v)]^{0.5} \quad (9-4)$$

A value of C_f greater than 0.8 ft/sec in the distributor openings is likely to flood the distributor, or result in heavy entrainment.

Table 9-19
Suggested Number of Drip Points/Ft² for Random Packings

Regular Fractionation	High Liquid Loads		Low Liquid Loads	
	High Liquid Rates	Low Liquid Rates	High Liquid Rates	Low Liquid Rates
Small packings	8	10	8	10
Midsized packings	6	8	6	8
Large packings	6	6	6	6

High Purity Fractionation	High Liquid Rates		Low Liquid Rates	
	High Liquid Rates	Low Liquid Rates	High Liquid Rates	Low Liquid Rates
Small packings	12	14	12	14
Midsized packings	10	12	10	12
Large packings	10	10	10	10

Note:

Small packings include Pall rings 1 in. and smaller, CMR No. 2 and smaller, IMTP 40 or smaller, and Nutter ring No. 1 or smaller; structured packings with $\frac{1}{4}$ in. crimp and smaller.

Medium packings include Pall rings 1- $\frac{1}{2}$ in. to 2 in., CMR No. 2.5 to 3, IMTP 50, and Nutter ring No. 1.5 and 2.0; structured packings with $\frac{1}{4}$ in. to $\frac{1}{2}$ in. crimps.

Large packings include Pall rings 2- $\frac{1}{2}$ in. and larger, CMR No. 4 and 5 and larger, IMTP 70 or larger, and Nutter ring No. 2.5 or larger; structured packings with crimps larger than $\frac{1}{2}$ in.

Reproduced by permission: The American Institute of Chemical Engineers; Bonilla, V. A. *Chem. Eng. Prog.*, V. 89, No. 3 (1993), p. 47; all rights reserved.

Uniform distribution is essential for efficient use and performance of the packing. The distribution of drip points onto the packing should ensure the same amount of liquid wetting of the packing for each square foot of tower cross-sectional area. The area near the wall must also receive its same uniform share of the liquid by ensuring the same drip points per square foot right out to the vessel wall, i.e., to within one pitch of the orifice holes from the trough or PAN distributor. Bonilla [131] suggests the following rule of thumb for distributor design: The outer 10% of the surface area of the tower cross section should have 10% of the total liquid rate; this means 10% of the uniform number of holes. For some situations a separate liquid line from a point on the distributor over to a void layout area may be necessary to move liquid to that location. Despite earlier thinking, Bonilla [131] emphasizes that the vessel wall should receive the same liquid unit quantity as the rest of the packing. The general performance on separation HETP for poor liquid flow in the wall area of the packing is lower compared to the other regions of the column cross section.

For flashing feeds entering between packed sections it is best to enter on a chimney type tray, allowing the liquid to mix, and then allow this to flow onto a NTD or PDH style tray.

For orifice trays a minimum level of 2 in. of liquid should be held on the tray. This varies with the size and

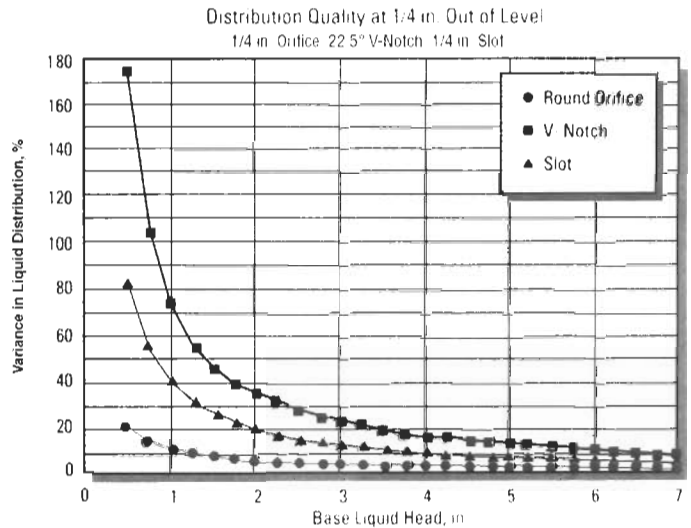


Figure 9-9. Liquid maldistribution is a function of opening, shape, and liquid head over the opening for a $\frac{1}{4}$ -in. out-of-level distributor. The openings were $\frac{1}{4}$ -in. dia. orifice, $\frac{1}{4}$ -in. slot, and 22.5° V-notch. Used by permission of The American Institute of Chemical Engineers, Bonilla, J. A., *Chemical Engineering Progress*, V. 89, No. 3 (1993) p. 47, and with special permission from Fractionation Research, Inc., all rights reserved.

shape of the drain holes. Figure 9-9 illustrates the effects of different base liquid heights over the hole and the resulting variation in liquid distribution for a tray or trough that is $\frac{1}{2}$ -in. out of level, comparing the round and slot orifices and the V-notch.

Parting boxes and troughs are so special to the system flows that after the engineer has established these, the services of a competent manufacturer should be consulted. Therefore, due to the detail required, design calculations are not presented in this text.

Redistribution of the down-flowing liquid from an upper packed bed onto the bed below is recollected onto a collection and redistribution tray and should be treated as a distribution problem like the entry of the liquid on to the top bed. Generally, the height of a bed of packing before collection of down-flowing liquid varies with the packing size, style, and the total bed height. As a guide, redistribution should occur after 10 to 20 ft of packing for random style; but is better recommended by the manufacturer for the structured packing.

Overall, the careful design of a distributor for liquid in the top of a packed tower, and for the redistribution of liquid flowing down multi-section packing in the tower, is essential to good consistent tower performance. However, the liquid flow is not alone, the uniformity of vapor distribution is likewise essential, because non-uniform vapor distribution can cause non-uniform liquid downflow. Then, there is the selection of the packing itself and its characteristics and requirements/sensitivity to the uniform distribution of the liquid and vapor. As earlier emphasized, the level of the distributor tray or trough can be critical to the consistent uniform liquid distribution.

For stacked packing the liquid usually has little tendency to cross-distribute, and thus moves down the tower in the cross-sectional area that it enters. In the dumped condition most packings follow a conical distribution down the tower, with the apex of the cone at the liquid impingement point. After about 12 ft vertical height, the liquid flows vertically downward unless redistributed. For uniform liquid flow and reduced channeling of gas and liquid with as efficient use of the packing bed as possible, the impingement of the liquid onto the bed must be as uniform as possible.

Because the liquid tends to flow to the wall, and any that reaches it is reduced in effective contact possibilities, no large percentage (not over 10%) of the total liquid should enter the packing at the top packing-wall circumference, or within 5–10% of the tower diameter from the tower wall. With this approach the bulk of the liquid starts down the tower somewhat away from the wall.

When using plate-type distributors, an out-of-level condition can cause serious channeling of liquid down one part of the column and gas up the other. Provision should be

made for self-adjusting levels of liquid, such as V-notches, which will allow for shifting of tower alignment, brick walls, etc. Gas velocities through the tower at the point of leaving the packing and/or through the distributor plate gas risers should be low to reduce liquid carry-through. This can be calculated by using liquid entrainment limitations. From limited tests it appears that there is essentially no entrainment off a packing until the flooding point is reached.

The various packings have different characteristics for distributing the liquid throughout the bed. Leva [40] shows the results of Baker, et al. [3] which illustrates the effect of various types of distribution on the liquid pattern inside the packing. A general summary is given in Table 9-20.

Strigle [82] has established that the necessity for uniformity of liquid rate increases as the number of theoretical stages per packed bed increases. Below five theoretical stages the column of packing is not so sensitive to the uniformity of liquid distribution. With more than five stages per bed the liquid distribution has a significant effect on the packing efficiency. Larger packing sizes are

Table 9-20*
Liquid Distribution Patterns in Packed Columns
(Data in 6-in., 12-in., and 24-in. Dia. Towers)

Packing	Tower Dia. In.	Type Liquid Feed	Percent Liquid Distribution in Inner $\frac{1}{4}$ Tower Area	
			2 Ft from Top	8 Ft from Top
$\frac{1}{2}$ -In. Raschig Rings	6	Center Point	40	40
	12	Center Point	90	78 (4 ft down)
	12	4 Point	70	65 (4 ft down)
1-In. Raschig Rings	2	Center Point	95	70 (4 ft down)
	2	4 Point	70	60 (4 ft down)
$\frac{1}{2}$ -In. Berl Saddles	6	Center Point	60	50
	12	Center Point	95	88 (4 ft down)
	12	4 Point	70	60 (4 ft down)
1-In. Berl Saddles	12	Center Point	85	65 (4 ft down)
	12	4 Point	75	55 (4 ft down)
1-In. Lessing Rings	12	Center Point	90	55
	12	4 Point	70	55
	12	19 Point	70	50
	24	Center Point	100	90
	24	12 Point	80	70
$\frac{1}{2}$ -In. Glass Rings	6	Center Point	90	70 (7 ft down)
	6	Center Point	83	75 (7 ft down) 3 ft/sec, air
	6	4 Point	75	70 (7 ft down)
	6	4 Point	75	75 (7 ft down) 3 ft/sec, air
	6	4 Point	75	75 (7 ft down) 3 ft/sec, air
$\frac{1}{2}$ -In. Spheres	6	Center Point	83	85 (4 ft down)
	6	Center Point	90	90 (4 ft down, 2.5 ft/sec, air

*Compiled from M. Leva. *Tower Packings and Packed Tower Design*, 2nd Ed., U.S. Stoneware Co. (now, Norton Chemical Process Products Corp.) (1953), Ref. 40, by permission.

less sensitive to the uniformity of liquid distribution than the smaller sizes.

Norton [83] classifies liquid distributors as:

1. High performance Intalox®: 90–100% quality
2. Intermediate performance: 75–90% quality
3. Historic standard: generally 30–65%

The quality grading system relates to uniformity of distribution across the tower cross-section, where 100% quality indicates ideal uniform distribution. Distributors are designed to suit the system, particularly the packing type and size.

The type of distribution to select depends on the sensitivity of the tower performance to the liquid distribution as discussed earlier. Norton's [83] data indicate that the sensitivity of tower performance to liquid distribution quality depends only on the number of theoretical stages in each bed of packing achievable at its "System Base HETP" [83]. Tower beds of high efficiency packing are more sensitive to liquid distribution quality than shorter beds of medium efficiency packing [83]. It is important to extend the uniformity of the distributor all the way to within one packing particle diameter of the tower wall [85].

Good liquid distribution starting right out of the distributor and onto the top layer of packing is essential to develop the full usefulness of the packing bed [85]. In principle this applies to all types and sizes of packing. Kunesh, et al. [84, 85] present FRI (Fractionation Research, Inc.) studies on distribution that reflect the importance of maintaining level distributor trays (devices), and eliminating discontinuities or zonal flow (Figure 9-10). Their results further show that a "packed

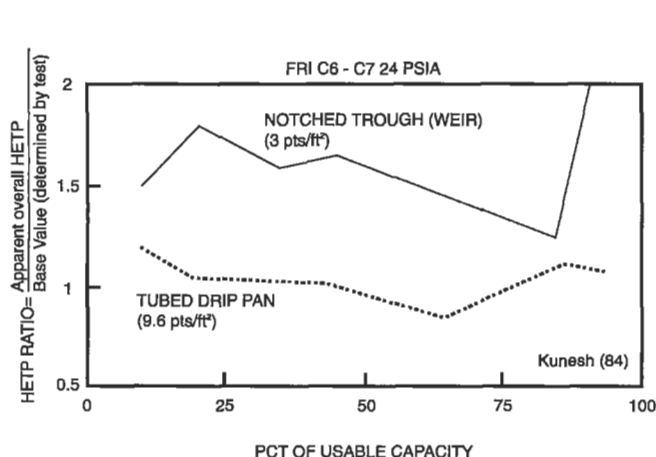


Figure 9-10. Effect of liquid maldistribution on efficiency; FRI data for 25-mm Pall rings in cyclohexane/n-heptane distillation with two different quality distributors. Used by permission of the American Institute of Chemical Engineers, *Chemical Engineering Progress*, Perry, D. and Nutter, D., Jan. (1990) p. 30, and by special permission of Fractionation Research, Inc., all rights reserved.

bed has a reasonable tolerance for both a uniform or smooth variation in liquid distribution and for one that is totally random." Once a system has become maldistributed, the recovery to natural and constant HETP is a very complex problem.

Perry et al. [85] point out that packed columns are more dependent on liquid distribution than trayed columns, as can be appreciated by the differences in the way the liquid must flow down the two types of columns. Liquid distribution quality is measured or described as [85]:

1. Number of distribution points (distribution density).
2. Geometric uniformity of distribution points across the cross-section of the tower.
3. Uniformity of liquid flow from the distributor points.

Currently, most designs use 4 to 10 distribution points per square foot of tower cross-section, with 9 points being generally considered useful for a wide variety of random and structured packings [85]. The distribution demands of small random packings are greater than for the large sizes due to the lower radial spreading coefficients, i.e., the larger the radial spreading coefficient the more quickly the initial liquid distribution will reach an equilibrium with the "normal" or "natural frequency" of distribution (see Figure 9-11).

Hoek [86] proposed a radial spreading coefficient to characterize the liquid distribution. This coefficient is a measure of how quickly a packing can spread a vertical liquid stream radially as the liquid progresses down the column [86]. Radial mixing tends to reduce the effects of

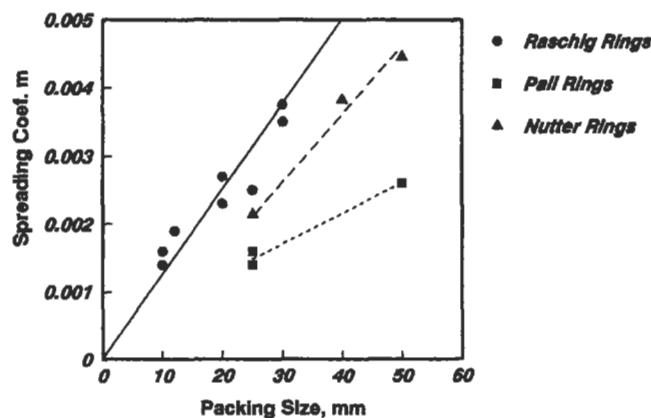


Figure 9-11. Radial spreading coefficients for several types and sizes of packings. Small packings require better initial distribution. The larger the radial spreading coefficient, the more rapid the initial distribution will reach its natural equilibrium of flow distribution. After Hoek, P. J., Wesselingh, J. A., and Zuiderweg, [86], and Nutter, D. [88]; reproduced with permission of the American Institute of Chemical Engineers; Perry, D., Nutter, D. E., and Hale, A., *Chemical Engineering Progress*, Jan. (1990), p. 30; all rights reserved.

poor efficiency due to concentration gradients brought about by liquid maldistribution. The “spreading coefficients” of structured packing are larger than for random packing. The spreading for structured packing occurs in a somewhat different manner due to the layering of the structured packing.

The entrance of a liquid-flashing vapor mixture into the distillation column feed location requires a specially designed distribution tray to separate the vapors from the liquid, which must drop onto the packing bed for that section in a uniform pattern and rate.

Structured packing requires specially designed distributors recommended by the respective manufacturers to ensure the same important uniform liquid distribution across any bed of this type of packing.

Redistributors

The liquid coming down through the packing and on the wall of the tower should be redistributed after a bed depth of approximately 3 tower diameters for Raschig rings and 5–10 tower diameters for saddle packings. As a guide, Raschig rings usually have a maximum of 10–15 ft of packing per section, while saddle packing can use 12–20 ft. This redistribution brings the liquid off the wall and outer portions of the tower and directs it toward the center area of the tower for a new start at distribution and contact in the next lower section.

The redistributor must be sealed against the tower wall to collect all of the liquid coming down the tower from the packed section above (Figure 9-11). Then it must be capable either singly or in conjunction with a distributor placed below it of redistributing the collected liquid from an upper packed section to the top of the next lower section in an efficient manner. (See discussion in previous paragraph on distributors.) The gas/vapor riser opening must be so covered by design as to avoid liquid dropping directly through the gas risers and onto the packed section below. This vapor flow area must be relatively large to avoid localized development of high pressure drop and up-setting the performance.

The height of packing before redistribution is a function of the liquid flow pattern through the packing, and this is a function of the size and type of packing. Some towers have 20–30 ft of packing with no redistribution; however, the reasons may be economic as well as operational. The exact amount of performance efficiency sacrificed is subject to question, although with 20–35% of the liquid flowing down the walls after 10 ft of ring packing depth, it appears reasonable to consider that performance is lost for most of this liquid. Redistribution is usually not necessary for stacked bed packings because the liquid flows

essentially in vertical streams. However, most packed tower services do not use stacked packing.

Physically the redistributions may be a simple and relatively inefficient side wiper as in Figure 9-12 or 9-13; a conventional support grid or plate plus regular distribution plate as used at the top; a combination unit similar to Prym support and distributor; or a support plate as shown in Figures 9-14 and 9-7D and 7E, a circular plate with holes.

The possibility of causing flooding in the tower at the redistribution point must not be overlooked, as too much restriction by a wall wiper, or by packing on a plate can be the focal point for poor tower performance. The velocity conditions should be checked for the smallest cross-section.

Wall Wipers or Side Wipers

The wall wiper liquid collector/redistributor, Figure 9-12, is most useful in reducing the by-passing effects of liquid running down the walls of small towers. They do not truly take the place of a redistributor system placed periodically in the tower. For larger towers of 4 ft diameter and greater, they are not as useful because they collect a smaller portion of the total tower liquid, and cannot effectively redistribute it throughout the tower cross-section as discussed in the paragraphs under “Distributors.” They do serve a useful purpose for the smaller towers, through about 18 in.–20 in.–30 in. They can restrict vapor flow up, as well as inhibit redistributing the collected liquid uniformly across the tower.

Hold-down Grids

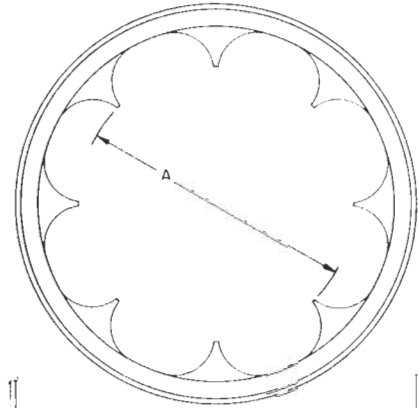
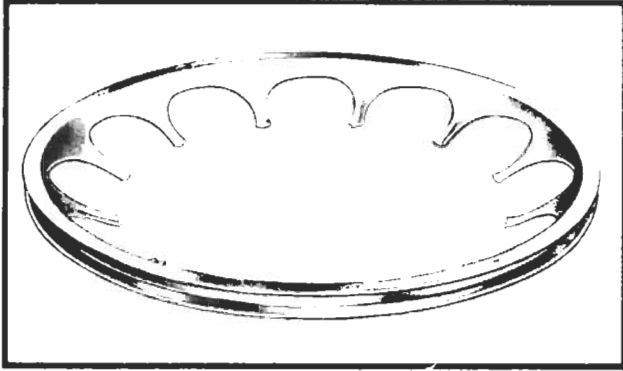
To reduce ceramic or carbon packing breakage and blowing out of light weight plastic packing when a tower surges due to gas pockets, uneven loading, etc., it is sometimes helpful to have heavy hardware cloth or other stiff but open grid resting (floating) at the top of the tower and on the top of the packing (Figures 9-15A and 15B).

This grating or grid must be heavy enough to hold down about the top five feet of packing, yet must be able to move down as the packing settles, always resting at the top of the packing. If the packing is restricted in upward movement, it usually will not be crushed. If the packing does break and crush, the bed settles and its characteristics change considerably.

Bed-limiters are usually lighter weight and must be bolted in place, not resting on the packing.

They are used with metal and plastic packings to prevent the bed lifting, or the entrainment of individual pieces of packing from being carried out of the tower. These packings usually do not break, and as long as the bed temperature is below the softening or deflection point

Metal "Rosette" Redistributor



TOWER I.D.		PLATE DIA.	DIAMETER A	HEIGHT B
INCHES	MM			
4	102	OUTSIDE DIAMETER OF SEALING STRIP WILL BE 1/16 INCH GREATER THAN TOWER I.D.	2 ¹³ / ₁₆ "	1/4"
6 ¹ / ₁₆	154		4 ⁷ / ₁₆ "	1/4"
7 ¹⁵ / ₁₆	202		5 ⁷ / ₈ "	7/16"
10	254		7 ⁵ / ₈ "	3/8"
11 ¹⁵ / ₁₆	303		8 ¹ / ₂ "	9/16"
13 ¹ / ₈ "	333		9 ¹ / ₂ "	5/8"
15	381		11 ¹ / ₄ "	11/16"
16 ⁷ / ₈ "	429		12 ³ / ₈ "	13/16"
18 ¹³ / ₁₆	478		13 ³ / ₈ "	1"
21 ¹ / ₄ "	540		15 ⁷ / ₈ "	1"
22 ⁵ / ₈ "	575		16 ¹ / ₂ "	1 1/4"

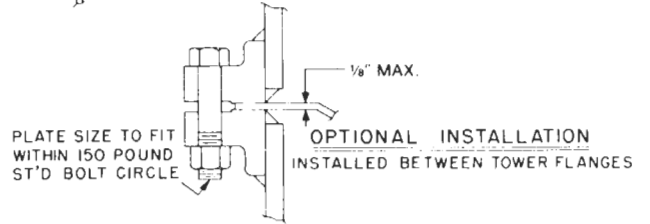


Figure 9-12. Metal rosette style redistributor. Used by permission of Norton Chemical Process Products Corp., Bull. TA-80.

for plastic packing, the bed should not compress or consolidate to create operational limitations.

Packing Installation

Stacked

Stacked packing is a hand operation and rather costly. It is avoided where possible except for the initial layers on supports. Liquid distributed on a stacked packing usually flows straight down through the packing immediately adjacent to the point of contact. There is very little horizontal liquid flow. Packing patterns perform differently, and are illustrated in Figure 9-16A-C.

Dumped

Dumping is the most common method of packing installation. If possible, the tower should be filled with

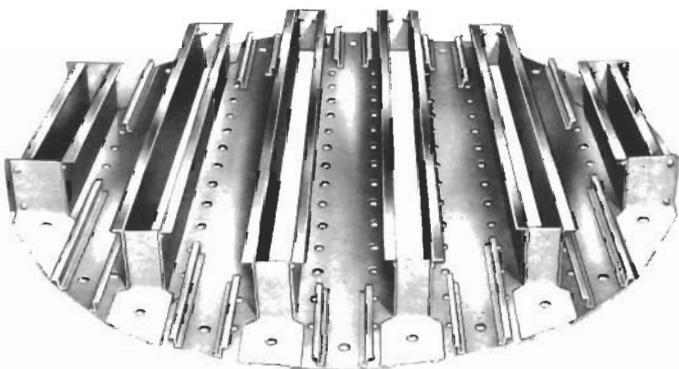


Figure 9-13. Typical metal full cross-section redistributor. Used by permission of Norton Chemical Process Products Corp., Bull. TA-80.

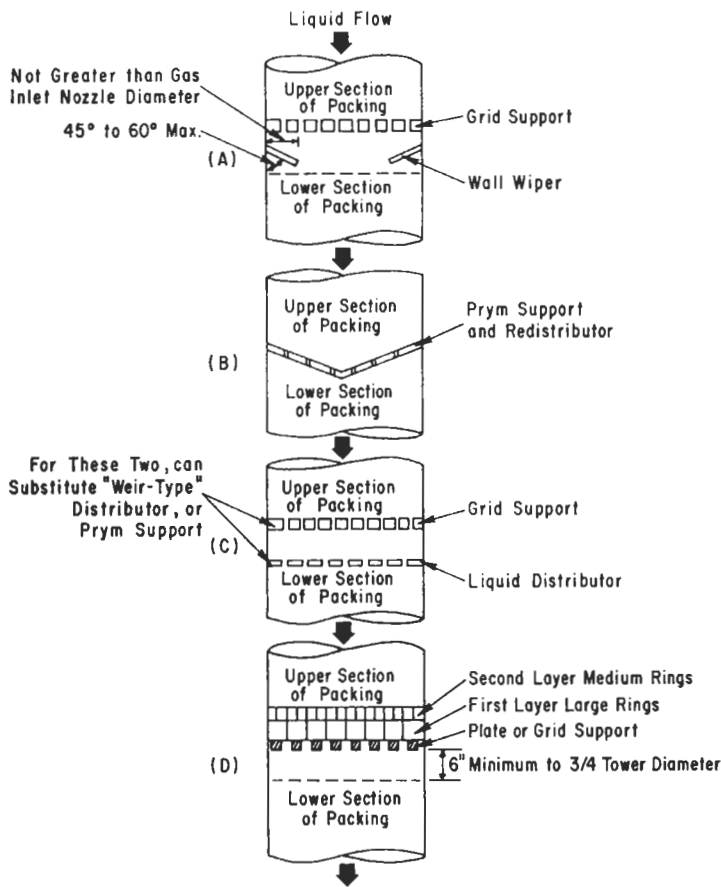


Figure 9-14. Liquid redistribution in packed towers. Used by permission of Norton Chemical Process Products Corp.

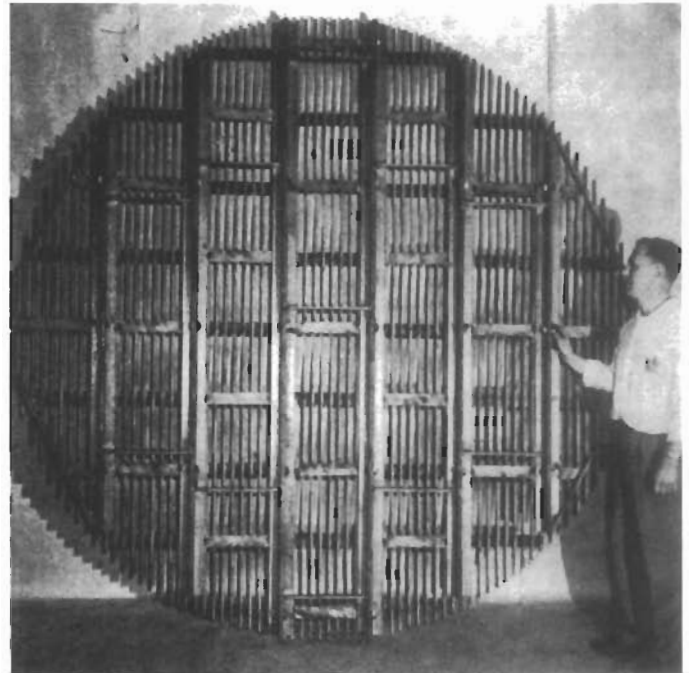
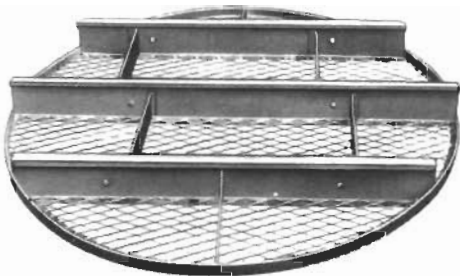


Figure 9-15A. Hold-down plate for packed tower. Used by permission of U.S. Stoneware Co. (now, Norton Chemical Process Products Corp.).



TOWER I.D.		DIA OVER SPACERS A	HEIGHT B	PLATE DIA C	NUMBER OF PIECES	MIN. DIA. OF ACCESS	APPROX NET WEIGHT (LBS)*
INCHES	MM						
17 ¹ / ₂	438	17"	4"	16 ¹ / ₂ "	2	10"	36
19 ¹ / ₂	489	19"	4"	18 ¹ / ₂ "	2	11"	45
21 ¹ / ₂	540	21"	4"	20 ¹ / ₂ "	2	12"	52
23 ¹ / ₂	591	23"	4"	22 ¹ / ₂ "	2	13"	59
29 ¹ / ₂	743	28 ¹ / ₂ "	4"	27 ¹ / ₂ "	2	16"	98
36	914	35 ¹ / ₂ "	4"	35 ¹ / ₂ "	3	14"	140
42	1067	41 ¹ / ₂ "	4"	41 ¹ / ₂ "	3	16"	188

*Weights shown are for standard construction and material thickness.

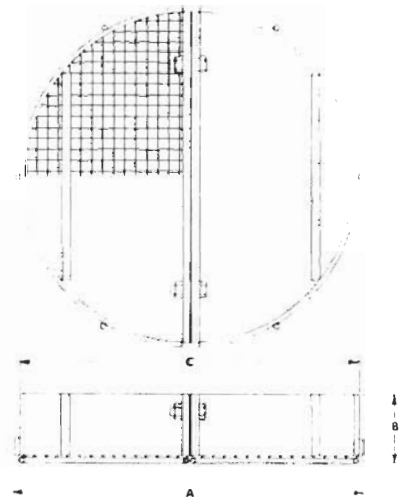


Figure 9-15B. Typical metal hold-down plate for use with ceramic or carbon packing. Note: It rests directly on top of the packing; bed-limiters are similar in design in metal or plastic, bolted to column wall above packing. Used by permission; Norton Chemical Process Products Corp., Bull. TA-80.



Figure 9-16A. Stacked packing: square pattern (S). Used by permission of U.S. Stoneware Co. (now, Norton Chemical Process Products Corp.).

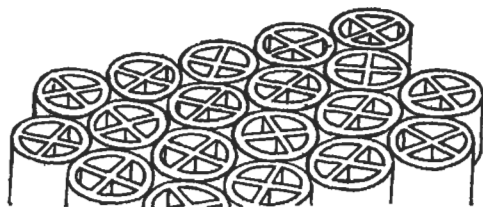


Figure 9-16B. Stacked packing: diamond pattern (D). Used by permission of U.S. Stoneware Co. (now, Norton Chemical Process Products Corp.).

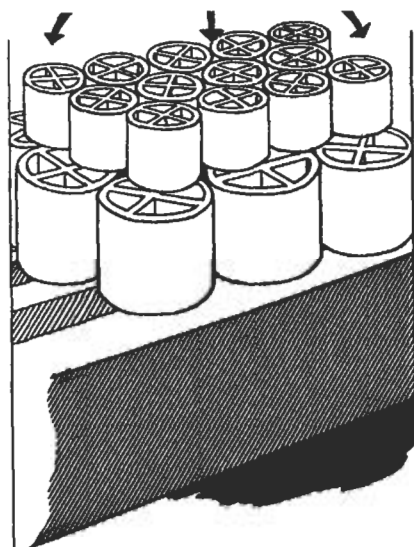


Figure 9-16C. Stacked packing: packing assembly. Used by permission of U.S. Stoneware Co. (now, Norton Chemical Process Products Corp.).

water for ceramic packings after installation of the bottom support arrangement, including any stacked rings, and the loose packing floated down to rest on top of the support. The fall should be as gentle as possible since broken packing tightens the bed and increases pressure drop.

One manufacturer [22] suggests loading ceramic ring type packing using a sheet metal cone in the tower thereby causing the rings to slide off the cone and fill to the edges first. The cone is lifted as the rings are floated or dropped in. This technique is believed to reduce the ten-

dency for rings to channel liquid to the tower wall. Saddle-type packing does not require the use of the cone.

In packing a tower dry, high hydrostatic heads are thus avoided on joint connections; however, extra care must be taken to avoid ceramic breakage. The packing will probably settle after installation, but it should not be pressed or tamped in place. This will cause extra breakage. The packing should not be allowed to fall more than two feet to the bed surface. It should be dumped at random to avoid developing any pattern. The dry packed tower will be more dense than the wet packed and should not be pressed or tamped in place. The pressure drop for dry packed beds can be as much as 50–60% greater than for wet packed. Dry packing is not the preferred method due to significant settling that will occur.

Metal and plastic packing can be dumped dry into the tower; however, reasonable care must be exercised, and the drop should not be more than 10–15 ft, using a chute with a cloth sock (open) on the end to cushion the impact.

Repacking a tower will usually show a variation in pressure drop. For small 8-in. dia. units the variation may be as much as 100%. In larger columns 24-in. dia. and up, this variation is noticed, but only to about 50% or less.

Packing Selection and Performance

Guide Lines: Trays versus Packings

Kister et al. [136] prepared one of the few comprehensive distillation studies for the application selection of valve and sieve trays compared to random or structured packing. This reference is based on a more comprehensive evaluation of accumulated data by the same authors [137]. Many separate studies have been conducted for trays [138] including bubble caps as well as various packings, but few, if any attempt to establish similar conditions to make a viable comparison as is attempted in References 136, 137. There are four main differences related to capacity and separation [136] when considering:

1. An optimal tray design, one that balances tray and downcomer area so that neither prematurely restricts capacity, and set weir height, weir geometry, clearance under the downcomer, and fractional hole area so as to maximize efficiency and capacity.
2. Optimal packing design, which configures distributors, supports, and bed heights to avoid loss of efficiency to maldistribution and no premature capacity restriction occurs [136].

The four main differences are [136]:

1. Differences between the capacity and efficiency of an optimal tray and an optimal packed tower design.

2. Deviations from optimal design of trays, packings and other tower internals, e.g., distributors and baffles.
3. Unique system characteristics and special design features, e.g., corrosion, foaming, chemical reaction, and fouling, and designs to overcome such problems.
4. Capacity and separation gains due to lower pressure drop of packing. Pressure drop of packing is typically 3 to 5 times lower than that of trays.

Due to the need to use case-by-case analysis the Kister studies [136, 137] focused on item 1. The data evaluated came from published reports by Fractionation Research (FRI) and Separation Research Program (SRP) at the University of Texas, taken from commercial size equipment rather than laboratory research columns. The FRI data includes No. 2 and No. 2.5 Nutter random rings packing, and Norton's Intalox® 2T structured packing, each considered currently state-of-the-art or close to it, while the sieve and valve trays were of FRI's latest designs, plus Nutter's proprietary valve trays, all using 24-in. tray spacing.

To allow for the vertical height required for packed tower distributors and redistributors—and in tray towers the vertical height used by additional trays—typically using 10%–20% of the vertical packed height (10% for 2-in. random packing and 20% for structured packing) [136] the analysis indicated:

$$\text{Practical packing HETP, HETP}_{\text{Packing, Practical}} = (m) (\text{HETP})_{(\text{Test packing})} \quad (9-5)$$

$$\text{For, practical trays HETP, } (\text{HETP})_{\text{Tray, practical}} = 97.5 (S/E) \quad (9-5A)$$

where m = factor higher than test HETP; = 1.1 for 2-in. random packing
 = 1.2 for structured packing used
 S = tray spacing, in.
 E = overall column efficiency, %

Capacity factor:

$$C_s = U_G \sqrt{\rho_G / (\rho_L - \rho_G)} \quad (9-6)$$

Tray spacing [136]:

$$C_{s,\text{flood}} \propto S^{0.5} \quad (9-7)$$

Correlating liquid rate and pressure, see Figure 9-17.

$$FP = L/V \sqrt{\rho_G / \rho_L} \quad (9-8)$$

$$\text{Capacity parameter} = C_s F_p^{0.5} v^{0.05} \quad (9-8A)$$

where C_s = capacity factor, ft/sec, based on tower superficial area

- E = overall column efficiency, trayed column, %
- FP = flow parameter, dimensionless
- HETP = height equivalent of a theoretical plate, in.
- L = liquid flow rate, lb/hr-ft² of cross-sectional area
- m = constant, allowing for vertical tower height consumed by distribution/redistribution equipment
- S = tray spacing, in.
- U = velocity, ft/sec based on tower superficial area
- or, U_G = superficial velocity based on cross-section area of empty column, ft/sec
- V = vapor flow rate, lb/hr-ft² of cross-sectional area
- ρ = density, lb/ft³
- F_p = packing factor, empirical
- ν = kinematic viscosity, liquid, centistokes (kinematic viscosity = viscosity, centipoise/specific gravity (not density))

subscripts:

- G = gas
- L = liquid

Figure 9-17 plots flood capacity versus flow parameter. The FP values of 0.4–0.7 are estimated by Kister, et al. [136] in absence of data. The plots show that for low and moderate pressures the flood capacity factor versus FP correlates the effects of liquid rate and pressure on the optimized tray capacity [136]. At higher pressures an additional effect of pressure on capacity shows a decline of optimized tray capacity.

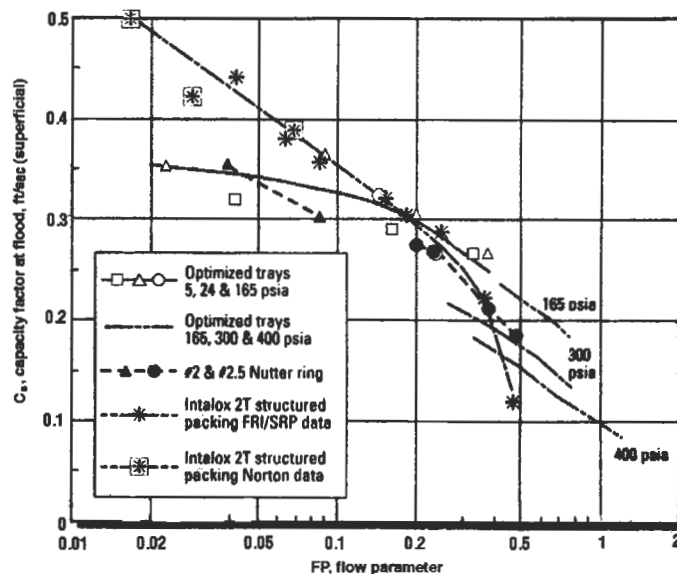


Figure 9-17. Overall comparison of capacity at flood for 24-in. tray spacing with random packing. Reproduced with permission of the American Institute of Chemical Engineers, Kister, H. Z., Larson, K. F., Yanagi, T., *Chemical Engineering Progress*, V. 90., No. 2 (1994) p. 23; all rights reserved.

Figure 9-18 plots HETP versus FP for optimized trays at 24-in. spacing, and No. 2 and No. 2.5 Nutter Rings and Intalox® 2T structured packing.

In summary, Kister, et al. [136] are quoted in their conclusions:

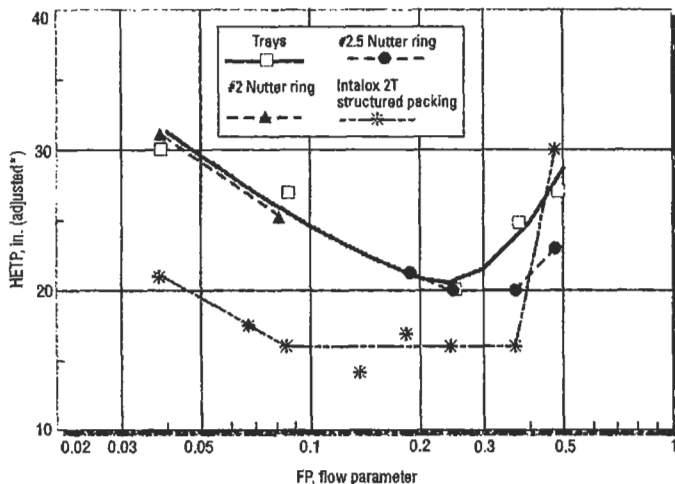
“Comparing trays at 24-in. tray spacing with a state-of-the-art 2–2.5-in. (nominal) random packing, and with a state-of-the-art structured packing of 67 ft²/ft³ specific surface area, all optimally designed, we found that:

At FPs of $\approx 0.02 - \approx 0.1$:

- The trays and the random packing have much the same efficiency and capacity.
- The structured packing efficiency is about 50% higher than either the trays or the random packing.
- As FP increases from 0.02 to 0.1, the capacity advantage of the structured packing (over the trays or over the random packing) declines to 0 from 30–40%.

At FPs of 0.1–0.3:

- The trays and the random packing have much the same efficiency and capacity.
- The structured packing has much the same capacity as the trays and the random packing.
- As FP increases from 0.1 to 0.3, the efficiency advantage of the structured packing over the random packing and over the trays declines to about 20% from about 50%.



*Adjusted for vertical height consumed by distributor, redistributor and end tray; see equations 1 to 3

Figure 9-18. Overall comparison of efficiency for “state-of-the-art” random and structured packing with trays at 24-in. spacing. Reproduced with permission of the American Institute of Chemical Engineers; Kister, H. Z., Larson, K. F., Yanagi, T. *Chemical Engineering Progress*, V. 90, No. 2 (1994) p. 23; all rights reserved.

At FPs of 0.3–0.5:

- Efficiency and capacity for the trays, the random packing, and the structured packing decline with a rise in flow parameter.
- The capacity and efficiency decline is steepest in the structured packing, shallowest in the random packing.
- At an FP of 0.5 and 400 psia, the random packing appears to have the highest capacity and efficiency, and the structured packing the least.

The above results are based on data obtained for optimized designs and under ideal test conditions. To translate our findings to the real world, one must factor in liquid and vapor maldistribution, which is far more detrimental to the efficiency of packings than trays. In addition one also must account for poor optimization or restrictive internals, which are far more detrimental to the capacity of trays than packings.”

Chen [133] highlights the long-term growth of the technically popular use of bubble cap trays, valve and sieve trays, followed by the increased popularity of packed columns accompanied by the development of random and structured packings. There are some applications in chemical/petrochemical/petroleum/gas treating processes where one type of contacting device performs better and is more economical than others. Chen [133] points out:

1. A typical tray has opening area ranging 8% to 15% of the tower cross-section area.
2. A typical packed tower design has more than 50% of open tower cross-section, with the void fraction of a packed tower being higher at around 90% of tower volume, resulting in the following:
 - (a) Pressure drop per theoretical stage—Packed towers usually result in lower pressure drop per theoretical stage than trays. Trays often are 3 to 8 mm Hg per theoretical stage, with packing having about 1 to 2 mm Hg for random packing and 0.01 to 0.8 mm Hg for structured packing. For high pressure systems, the difference may not be significant, while for atmospheric and below atmospheric pressures, the difference can be quite significant.
 - (b) Liquid hold-up—Trays usually hold-up 8 to 12% of tower volume, compared to 1 to 6% for packed towers. This can be significant for systems involving thermal degradation and requiring very short residence times, which also aids in sharp separations.
 - (c) Liquid/vapor ratios—Trays are designed for low liquid/vapor ratios, while packed towers are operated from low to high liquid/vapor ratios (often

in absorbers and scrubbers). Low L/V ratios are usually associated with distillation, with \approx (approx.) less than 10 gallons of process liquid/(min) (ft²) of tower cross-section area)

- (d) Liquid cooling—This is usually better handled in tray towers, and it is easier to draw-off liquid from trays for removal from the system, or for external recirculation.
- (e) Foaming systems—The contact surfaces of packings promote film action compared to droplets from trays for mass and heat transfer. The packings tend to be more resistant to entrainment and induce less foaming.
- (f) Corrosion—Corrosion problems with some fluid systems are easier and less costly dealt with by corrosion resistant packings than fabricated trays.
- (g) Solids and slurries—Trays will handle solids and slurry systems better than packings; and if solids build-up does occur washing/flushing treatment will usually “wash” or dissolve the solids attached to the trays easier than attempting a thorough cleaning of packing.
- (h) Costs—Other than special needs requiring one contacting mechanism or another, small-diameter columns of 18-in. diameter or less can be assembled less expensively as packed towers. For some applications of larger diameter columns, the packed tower may still provide the less expensive choice. This should undergo a cost analysis comparison.

Chen [133] recommends the following guidelines for the design of the important distributors of liquid (still must pass vapor):

Pan-type distributor: Plate with drilled/punched holes for liquid downflow and vapor risers.

Vapor riser: 15 to 45% of tower cross-section area, round risers usually 4 in. or 6 in. diameter, although the round design usually has less free area than a rectangular design. Usual standard height is 6 in., however, any height can be used as long as it is well above the liquid height on the tray. The pressure drop through the vapor riser should be low:

$$\Delta P = 0.46 [D_v/D_1] [V/A]^2, \text{ in. of liquid} \quad (9 - 9)$$

Liquid orifices on tray pan: usually at least 10 or more orifices per square foot of tower area. The orifice diameter can be determined [133]:

$$d = 0.23 [Q/(K)(H)^{0.5}]^{0.5} \quad (9 - 10)$$

where ΔP = pressure drop through risers, in. of liquid

V = vapor rate, ft³/second

A = riser area, ft²

D_v = vapor density, lb/ft³

D_1 = liquid density, lb/ft³

d = orifice diameter, in.

Q = liquid flow rate, gal/min

H = differential head at orifice, ft of liquid

K = discharge coefficient, for punched holes = 0.707

Liquid design height is usually one-half of the riser height. At minimum rates the depth on the tray can vary from 1/2 in. to about 1 in. below top of riser height for maximum rates. The minimum orifice diameter is recommended at 1/4 in. diameter to overcome miscellaneous plugging of the holes [133]. Experience indicates the holes really should be 3/8 in. to avoid industrial plugging problems.

Other useful distributor types have been referred to and previously illustrated. For redistribution, the vapor risers may be 12 in.–18 in. tall, and with protective “hats” to prevent liquid dropping from the tray/section above. The space between the cover “hat” on the riser and the bed above should be 18 in. to 12 in. minimum to allow for proper vapor redistribution entering the packed section above. The importance of a level distributor cannot be overemphasized.

Any of the available packings will usually perform the operation of another; the differences being in efficiency of contact, expressed as HTU, HETP or Kga, and pressure drop for the *particular* packing-fluid system. Therefore, system data is very important and helpful in selecting a packing. When it is not available, an effort should be made to find any analogous system as far as process type, fluids, physical properties, pressure and temperature conditions, etc. If this is not possible, then the best judgment of the designer must be used.

Eckert [125] provides some basic guidelines to good packing selection for various system performance requirements. Kunesh [126] illustrates the often-determined pressure drop advantage of random packed towers over the usual valve tray. See Figure 9-19 [126].

For a preliminary reference and guide to the broad comparison of packings versus various distillation tray types Table 9-21 is helpful. Although the table includes the listing for more prominent manufacturers of trays and packing materials, it is not all inclusive as far as reliable manufacturers of either trays or packing. Table 9-22 [123] compares trays, random and structured packing, and HETP, where

C-Factor

$$C = V_s [D_v/(D_1 - D_v)]^{0.5}, \text{ ft/sec} \quad (9 - 11)$$

Souders-Brown C-Factor

$$= V_s [\rho_v/(\rho_1 - \rho_v)]^{0.5} \quad (9 - 12)$$

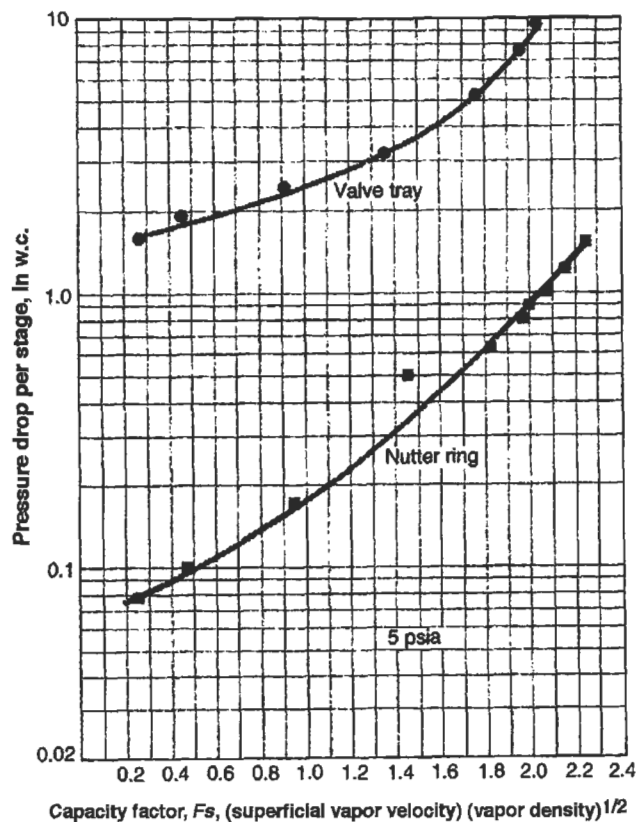


Figure 9-19. Comparison of typical valve tray and random packing showing that packing reduces pressure drop significantly. Used by permission of Kunesh, J. G., *Chemical Engineering*, V. 94, No. 18 (1987) p. 101, all rights reserved.

and F-Factor

$$F = V_s (D_v)^{0.5} = V_s (\rho_v)^{0.5}, (\text{ft}/\text{sec}) (\text{lb}/\text{ft}^3)^{0.5} \quad (9-13)$$

where V_s = superficial vapor velocity, ft/sec (across tower cross-section)

$$D_v = \text{vapor density, lb}/\text{ft}^3 = \rho_v$$

$$D_l = \text{liquid density, lb}/\text{ft}^3 = \rho_l$$

Trays are usually designed with F-factor from 0.25 to 2.0 for a turndown of 8:1. Pressure drop per theoretical stage falls between 3 and 8 mm Hg. Note that bubble cap trays are on the high side and sieve trays are on the lower end of the range. Varying tray spacing and system efficiency, the HETP for trays are usually between 24 in. and 48 in. [133]. The C-factor is the familiar Souders and Brown capacity equation.

The number of packing sizes, types (designs), and materials of construction currently available to the designer has increased considerably. To select a packing for a process application requires a weighing of information and an evaluation of the closest comparable data.

Overview

Kunesh [126] presents an overview of the basis for selecting random packing for a column application. In first deciding between a trayed tower or a packed one, a comparative performance design and its mechanical interpretation should be completed, considering pressure drop, capacity limitations, performance efficiencies (HETP), material/heat balances for each alternate. For one example relating to differences in liquid distribution performance, see Reference 126.

For a packed tower selection, the larger packing size generally provides the greater capacity, with less pressure drop, but at the expense of lower efficiency (higher HETP) than a somewhat smaller size. Some of the ultimate performance depends on the column diameter, the length devoted to packing, the primary variable determined to be packing size, with packing type an important secondary consideration. Obviously, there is a close balance here, particularly between the various design shapes (types) of the different manufacturers.

For quite accurate performance data on a specific packing type/size, consult the respective manufacturers and do not rely only on the generalization charts of the published literature. Because these charts are continuously being improved, they are quite useful for a good approximate design (and even final in some instances). Some competitive manufacturer's packing is so close in design to another's that there is little real difference in performance, particularly because a reasonable "factor of safety" should be applied more specifically to packing height (when separation of components is more important) than to tower diameter (volume/mass capacity).

Fractionation Research, Inc. (FRI) [126] has found that these parameters plus a few others affect efficiency (HETP): system to be separated, concentration of components, absolute pressure level, column diameter, and bed length, depth, or height (the latter two primarily related to the quality of liquid/gas distribution). Kunesh [126] cautions regarding selecting an efficiency prediction (HETP) that is "close to the operating conditions for an accurate/final design." Experience suggests it may be necessary to select a final design HETP from the best available data (family of compounds, pressure of operation and specific packing type and size) and add a factor of "safety" to suit the situation, perhaps 15–30%.

Contacting Efficiency, Expressed as Kg_a , HTU, HETP

When specific data on system are not available, and often they will not be, then close comparisons should be sought. If nothing more can be done, tabulate the relative

Table 9-21
Relative Performance Characteristics of Tower Packing and Column Trays¹

Company	Configuration	Material of Const. ²	Relative Cost ³	Mass Transfer ⁴	Pressure Drop	Capacity	Comments
GLITSCH, INC.							
Trays							
P-K Trays TM	Trays w/baffles	M	Mod	Med	Lo	V.Hi	
Screen Trays [®]	Venturi effect	M	Mod	Med	Lo	V.Hi	
Ballast [®]	Valve trays	M	Mod	Med	Med	Med	
Bubble Cap	Bubble cap	M	Hi	Med	Hi	Med	
Random Packing							
Ballast [®]	Pall rings	M, P	Lo	Med	Med	Med	
Cascade Mini-Rings [®]	Low aspect ratio	M, P, C	Mod	V.Hi	Lo	Hi	Atmospheric-high pressure service
Structured Packing							
Gempak [®] A	Corrugated, perforated, lanced	M, P	Mod	V.Hi	V.Lo	V.Hi	Gempak [®] packings designed for high to moderate vacuum service
Gempak [®] AT	Corrugated, perforated, lanced	M	Mod	V.Hi	V.Lo	V.Hi	high heat transfer service
Glitsch Grid [®] EF-25A, EF-25AP	Lattice grid	M, P	Lo	Lo	Lo	Hi	
York Product							
Structured Packing							
Goodloe [®]	Knit mesh	M, P	Hi	E.Hi	Hi	Hi	
Goodloe [®]	Bicomponent knit mesh	P + M	Lo	E.Hi	Med	Hi	
JAEGER PRODUCTS INC.							
TRI-PACKS [®] (Hacketten [®] in Germany)	Hollow spherical	P	Hi	E.Hi	Lo	V.Hi	New scrubbing and stripping applications
NOR-PAC [®]	Cylindrical rings/ ribs	P	Lo	Hi	E.Lo	V.Hi	Replacement scrubbing & stripping applications
METAL VSP [®]	Hollow slotted ring	M	Mod	E.Hi	Lo	V.Hi	Used in new service. Resists damage by flow upset
TOP-PAK [®]	Semi-spherical	M	Lo	V.Hi	Lo	V.Hi	Large diameter packing for large columns
NOVALOX [®] SADDLES	Smooth, beveled, longitud. ribs	C	Mod	Med	Med	Lo	Traditional shape. Excellent mechanical strength
BERYL [®] SADDLES	Smooth, beveled longitud. ribs	C	Hi	Med	Med	Lo	and resistance to thermal shock and chemical attack
Structured Packing NOR-PAC [®] KOMPAKT [®]	Multi-layers screen cylinder	P	Hi	Hi	Lo	Hi	Ideal packing for horizontal scrubbers
Metal structural packing	Vertical sheets (New design)	M	Hi	E.Hi	E.Lo	E.Hi	

(table continued)

Table 9-21 (Continued)
Relative Performance Characteristics of Tower Packing and Column Trays¹

Company	Configuration	Material of Const. ²	Relative Cost ³	Mass Transfer ⁴	Pressure Drop	Capacity	Comments
KOCH ENGINEERING							
Trays							
FLEXITRAY® 4 variations	Circular slotted valve	M	Lo	Med	Med	Med	
Random Packing							
FLEXIRING®	Slotted cylinder	M	Mod	Hi	Lo	Med	
	Internal tongues	P	Lo	Hi	Lo	Med	
K-PAC®	Modif FLEXIRING®	M	Mod	Hi	V.Lo	Hi	
	increased voids						
FLEXISADDLE®	Saddle	P, C	Lo	Med	Med	Med	
Structured Packing							
FLEXIPAC® (Mellpak® in Europe)	Geomtr. arrngd. corrug. sheets	M, P	Hi	V.Hi	V.Lo	Hi	
SULZER (KS)		M, P	V.Hi	E.Hi	V.Lo	V.Hi	
NORTON CHEMICAL PROCESS PRODUCTS							
Trays							
Valve tray	Valve	M	Mod	Med	Med	Med	
Sieve tray	Slotted cylinder	M	Mod	Med	Med	Med	
Bubblecap	Bubblecap	M	Mod	Med	Hi	Med	
Random Packing							
IMTP®	Rib finger type	M	Mod	Hi	Lo	Hi	
HY-PAK®	Slotted cylinder	P	Mod	Med	Lo	Hi	
SNOWFLAKE™	Short cylinder ribbed	P	Lo	Hi	Lo	Hi	
Pall rings	Slotted cylinders	M	Mod	Med	Med	Med	
Pall rings	Slotted cylinders	P	Lo	Med	Med	Med	
Super INTALOX®	saddle	P	Lo	Med	Med	Med	
Saddles							
Super INTALOX®	saddle	C	Mod	Med	Med	Med	
Saddles							
Structured Packing							
INTALOX®	corrugated	M	Hi	Hi	Lo	Hi	
structured packing							
INTALOX® wire	woven	M	Hi	E.Hi	E.Lo	Hi	
NUTTER ENGINEERING							
Trays							
FLOAT VALVE® tray	Rectangular valve	M	Mod	Med	Med	Med	Lateral release of vapor Unopposed liquid flow
V-GRID® tray	Tapered slot	M	Mod	Med	Med	Med	Fixed open, high strength Resistant to fouling

Table 9-21 (Continued)
Relative Performance Characteristics of Tower Packing and Column Trays¹

Company	Configuration	Material of Const. ²	Relative Cost ³	Mass Transfer ⁴	Pressure Drop	Capacity	Comments
Random Packing							
Nutter Rings	Crimped, curved slotted strips	M	Mod/Lo	Hi	V.Lo	Hi	Superior liquid spreading F.R.I. tested efficiency
Structured Packing							
SNAP-GRID TM	Slotted, snaplock shape	M	Hi	Med	E.Lo	E.Hi	"I" beam configuration High capacity, non-fouling
Montz A3 TM	Wire-weave corrugated	M	V.Hi	V.Hi	Lo	Hi	Highest efficiency
Montz B1 TM	Embossed sheet metal	M	Hi	V.Hi	V.Lo	Hi	Sinusoidal corrugations Maximum surface utilized

GENERAL COMMENTS

- Comparisons of relative cost and performance are applicable only within same manufacturer.
 - M = Metal (Generally 304 SS. Other alloys available); P = Plastic (Wide selection); C = Ceramic
 - Costs: Mod = Moderate or = conventional packing; Lo = conventional packing; Hi = conventional packing
 - Mass Transfer efficiency
 - Structured packings frequently used for high vacuum service
 - Carbon steel and other metals sometimes available.
 - Wide range of plastics generally available
 - Packing efficiency and capacity vary with specific application. Contact vendor for assistance in making final decision.
 - There is no intention to reflect negatively on any manufacturer's packing or trays (author note).
- Used by permission; W.P. Stadig, *Chemical Processing*[®], Feb. (1989), Ritman Publishing Co.

Table 9-22
Typical Performance Characteristics Comparison of Tower Packings and Trays

Characteristic	Type of Internal		
	Trays	Random Packing	Structured Packing
Capacity			
F-factor, (ft/s) (lb/ft ³) ^{1/2}	0.25–2.0	0.25–2.4	0.1–3.6
C-factor, ft/s	0.03–0.25	0.03–0.3	0.01–0.45
Pressure drop, mm Hg/ theoretical stage	3–8	0.9–1.8	0.01–0.8
Mass transfer efficiency, HETP, in.	24–48	18–60	4–30

Reproduced by permission: Chen, G. K., *Chem. Eng.*, Mar. 5 (1984) p. 40, all rights reserved.

efficiency for other systems and apply judgement to select a value.

The HETP (Height Equivalent to a Theoretical Plate (stage or plate)) is the tray spacing divided by the fractional overall tray efficiency [82]. The transfer unit concept has been useful for generalized correlations [89]. Because packed towers operate with continuously changing compositions through the packed height, the concept

of HETP has been to determine the number of theoretical stages (plates) required for a given separation by the usual discrete tray-by-tray method (stepwise) and then using the height of packing equivalent to one theoretical plate, multiply to obtain the total height of packing. This requires the use of experimentally or industrially determined HETP values for the same system or one quite close in terms of pressure, types, or families of fluids and packing size and family type (see Figure 9-18 and Table 9-22 and later discussion). Table 9-23 [133] compares several process systems and the corresponding average HETP for 2-in. diameter slotted packing rings.

Packing Size

This affects contact efficiency; usually, the smaller packing is more efficient; however, pressure drop increases.

As a general guide, use:

Random Packing Size, Nominal, in.	Column Diam., in.
$\frac{1}{2}$ – $\frac{3}{4}$	6–12
$\frac{3}{4}$ –1	12–18
1–1 $\frac{1}{2}$	18–24
1 $\frac{1}{2}$ –2	24–48
2–3	36–larger

Table 9-23
HETP Comparison of 2-in.-Dia. Slotted Rings

System	Top pressure, mm Hg	Bed depth, ft	Averaged HETP, in.
Acetone/water	740	5	18
		10	20
Iso-octane/toluene	740	5	24
		10	30
		20	32
	100	5	24
		10	26
Methanol/water	740	10	21
		20	28
Iso-propanol/water	740	10	24
Para/ortho xylene	100	10	33
		50	31
		16	28
Ethylbenzene/styrene	100	10	22
		20	26

Basis: Test-column diameter: 24–42 in.

Used by permission: Chen, G. K., *Chem. Eng. Mar.* 5 (1984), p. 40, all rights reserved.

The packing sizes listed relate to ceramic (where available), metal, and plastics. The plastic random packing must be used well under its softening temperature. Due to packing weight of the bed, the packing can compress as the temperature increases and thereby become less effective and increase the system pressure drop to the point of causing flooding. Therefore, the manufacturer should be consulted for upper limits of operating temperatures for design selection of the particular plastic suited for performance requirements and corrosion resistance. Under these conditions it is important that the plastic packing surface be "wetted" to allow film formation.

Pressure Drop

This is important to most column designs. Recognize that pressure drop will increase due to:

1. Unsteady column operations
2. Increased liquid/vapor loads
3. Breakage of ceramic packings (this can be serious)
4. Compaction/deflection of plastic packings

Materials of Construction

Give careful consideration to fluids, temperatures of systems, aeration. Plastic materials may be quite good for the application; however, carefully determine the recommended *long-term heat deflection* characteristics. With time,

many plastics will deform, thereby changing the packing bed characteristics, and the column pressure drop. As a general rule, do not select a plastic to operate at any time within 50°F of the softening or deflection temperature of the plastic.

Particle versus Compact Preformed Structured Packings

Particle packings (random) are usually (not always) less efficient than the pre-packaged/preformed assemblies; however, particle types are generally more flexible in loading and the ability to handle "dirty" fluids.

Cost of the packing and its effect on the system costs must be considered, as some packings are much more expensive than others, yet produce very little improved performance. Table 9-17 presents some comparative information. The most common packings and hence the ones with the most available data are Raschig rings, Berl saddles, several saddle types and Pall Rings® (Norton Co.) or equivalent.

As a guide with only rough experimental backing, the ratio of maximum random packing size to tower diameter is

Raschig rings:	1:20 (Reference 5)
	1:8 (Reference 52)
Berl saddles:	1:10
Intalox saddles:	1:8 to 1:10 (Reference 6)

The 1:8 ratio is in more common use for most packings; however recent data indicated that Raschig rings require a larger ratio approaching 1:20.

These ratios are useful in dealing with small towers, and serve as guides for the borderline cases of others. There are no guides to the smallest sized packing to place in a tower. However, ½-in. is about the smallest ceramic used with ¾-in. and 1-in. being the most popular. Operating and pressure drop factors will usually control this selection.

Packed towers are not limited to small units; in fact the largest processing towers for absorption and stripping operations are probably in these towers. Some units are 40 and 50 ft in diameter using 2-in. and larger packings to heights of 20–30 ft. Other units are 5–6 ft in diameter with 60 ft of packing. Towers with a 24-in. dia. and smaller are most often used with packing rather than trays due to mechanical limitations of trays in small towers.

Fouling of Packing

Random and structured packings are susceptible to surface fouling due to process conditions and/or the presence of oxygen as may be related to bacterial growth. Some systems will precipitate solids or crystals from solution usually due to the temperature and concentration effects. Bravo [135] discusses air-water stripping and illus-

trates the effects of iron present in these systems on packing and fouling of distributors.

Fouled packing can significantly reduce the performance of the system and is one condition that should be examined when packed tower systems deteriorate. For some systems, an acid or solvent flush (or wash) will accomplish the needed thorough cleaning. The need for such a supplemental maintenance during various stages should be recognized at the time of initial system design. Also for water soluble systems, the use of pH adjustment, pretreating with sequestering agents or biocides, ozone treatment and other steps specific to the system's problems [135] may be necessary or helpful.

Minimum Liquid Wetting Rates

To feed enough liquid into the tower to effectively place a wet film of liquid over all the packing, a minimum wetting rate (MWR) has been evaluated for guidance in operation and design. Morris and Jackson [52] recommended the MWR shown in Table 9-24.

A minimum liquid rate for any tower packing is used by some designers as 1,500 lb liquid/(hr) (ft² tower) referring to liquid of properties of water.

$$L_{\min} = (\text{MWR}) (a_t) \tag{9-14}$$

where L_{\min} = liquid rate, ft³/(hr) (ft² cross-section)
 MWR = value of minimum wetting rate from Table 9-24

The minimum wetting rate is a function of the packing material surface (Table 9-25) and the physical properties of the liquid involved, particularly the viscosity and the

**Table 9-24
 Minimum Wetting Rate***

Packing	MWR Rate, Liquid, ft ³ /(hr) (ft ² cross sect.)	Packing Surface area per tower volume, ft ² /ft ³
Rings (Raschig, Lessing, etc.), thru 3-in. dia.	0.85	
Grid type (wooden, etc.) (pitch 2 in.)	0.85	
All packings larger than 3 in.	1.3	
Polished metal packings and poor wetting surfaces (some plastics, glazed porcelain, etc.)	1.3, estimate to 2.5	Preferably etch surfaces to reduce problem.

*Compiled by permission from Morris and Jackson, *Absorption Towers*, Butterworth Scientific Pub. (1953) London and Imperial Chemical Industries, Ltd., Ref. 52.

**Table 9-25
 Packing Wetting Rates Related to Packing Material Surface**

Surface	MWR _T Gpm/ ft ²	Reasonable Minimum Wetting rate		Materials
		ft ³ /ft ² hr	m ³ /m ² h	
Unglazed ceramic	0.187	1.5	0.5	Chemical stoneware
Oxidized metal	0.27	2.2	0.7	Carbon steel, copper
Surface treated metal	0.40	3.2	1.0	Etched stainless steel
Glazed ceramic	0.80	6.4	2.0	
Glass	1.00	8.0	2.5	
Bright metal	1.20	9.6	3.0	Stainless steel, tantalum
PVC-CPVC	1.45	11.6	3.5	**
Polypropylene	1.60	12.8	4.0	**
PTFE/FEP	2.00	16.0	5.0	**

*Modified by author from Glitsch literature.

**Requires proper surface wetting treatment. Important that surface wetting be tested and treatment applied if necessary.

Values based on > 43 ft²/ft³ specific area of packing. By permission of Mass Transfer, Inc., Bull. TP/US/BI (1978) and Glitsch Bull. No. 345.

surface tension. Most plastic and some metal packings require surface treatment before the packing particle will wet uniformly, or even will wet at all. Without film forming characteristics on the surface area, the contact of the liquid-vapor will be poor and the tower performance efficiency can be expected to fall off. The packing should be tested for wettability in the service before completing the tower design and packing selection.

Kister [90] has evaluated Schmidt's [92] somewhat complicated equation for minimum wetting rate and proposes:

$$\text{MWR}_G = (\text{MWR}_T \text{ using Table 9-25 in gpm/ft}^2) (60/a_t)^{0.5} \tag{9-15}$$

where MWR_G = minimum wetting rate, gpm/ft², generalized for other packings using Kister's evaluation
 MWR_T = minimum wetting rate, gpm/ft² from Table 9-25
 a_t = specific surface area of packing, ft²/ft³

Another expression of "reasonable minimum wetting rate" [48] is given in Table 9-25. The surface characteristics of the packing material are important in the type of liquid film (or droplets) that flow across, around, and drip off of the surface. The better the specific liquid wets the packing surface and forms a moving film the more efficient will be the packing for distillation, absorption, etc. In general, from the table it can be noted that the surfaces that tend to wet easily have the lower minimum wetting rates. The data given in Table 9-25 do not agree too well

with the recommendations of Table 9-24. Although there is no validation, it is believed that the information in Table 9-25 is more current and represents a more recent evaluation of available data. However, the fact that the results are not identified by packing design types, suggests there probably still needs to be more evaluation of this factor.

Note that when packing is changed from one material of construction to another, it is important to recognize the effect on minimum wetting rate for the new condition.

Loading Point—Loading Region

Examination of Figure 9-20 shows the pressure drop of the packed bed with gas flow and no liquid flow as the dry curve. As liquid is added to the top of the packing the effect on pressure drop is immediately noticeable. Note that the lower part of all the liquid rate curves parallel the slope of the "dry" bed curve; however, at a point a noticeable change in the slope of the pressure drop curve occurs. This is attributed to the transition of liquid hold-up in the bed from being only a function of liquid rate to a condition of liquid hold-up also being a function of gas rate. Although the change seems to occur for some packings at a point, it is difficult to determine accurately for all packings, and is perhaps better considered a region—from the first point of inflection of the curve to its second. Towers are usually designed to operate with gas-liquid rates in the loading region or within about 60–80% of its upper point. As will be discussed later, it is necessary to operate farther from the loading point for some situations than others due to the relative proximity of the loading to the flooding point.

For Figure 9-21A the loading region is centered about the 0.75 in./ft pressure drop curve; the preferred design range being 0.35 to a maximum of 1.0 in. of water/ft.

Figure 9-21D indicates the loading region as centered about line B, which is a reasonable upper design condition.

Figures 9-21B and -21C are the earliest generalized pressure drop correlations (GPDC) proposed and have been used for many industrial plant design. Progressively, Figures 9-21E–H are more recent correlations. These charts will be discussed in a later section.

Figure 9-21F is the most current updated version of the GPDC as presented by Strigle [139] to facilitate interpolation of the ordinate and pressure drop curves on the chart. The flooding and loading regions are not identified. For this chart:

$$1. \text{ Flow parameter (FP), abscissa} = \frac{L_h}{G_h} \left[\frac{\rho_G}{\rho_L} \right]^{0.5} \quad (9-16)$$

$$2. \text{ Capacity parameter (CP), ordinate} = C_s F^{0.5} \nu^{0.5} \quad (9-17)$$

$$C_s = V_g \sqrt{\rho_G / (\rho_L - \rho_G)}, \text{ ft sec}$$

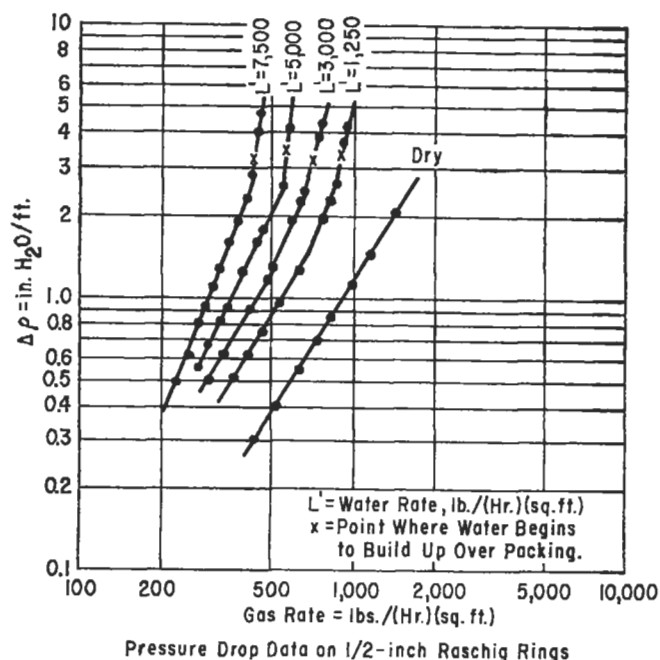
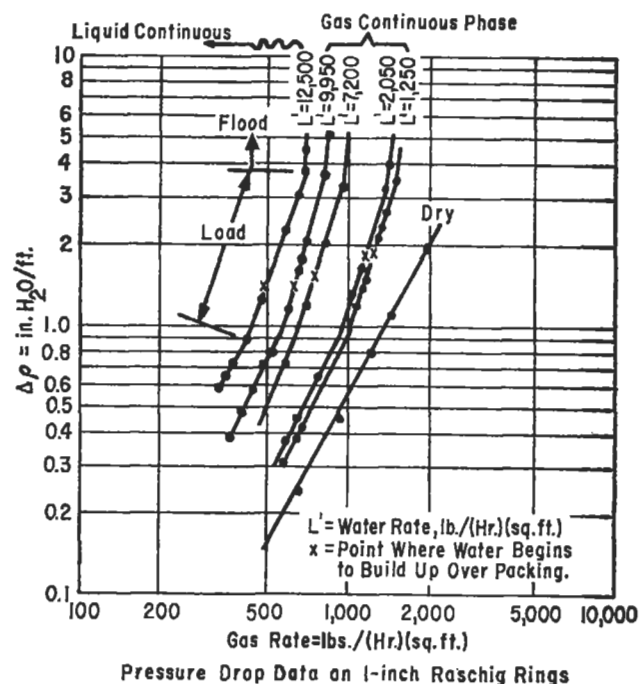


Figure 9-20. Pressure drop flow characteristics in conventional packed towers. Reproduced by permission of the American Institute of Chemical Engineers, Sarchet, B. R., *Trans. Amer. Institute of Chemical Engineers*, V. 38, No. 2 (1942) p. 293; all rights reserved.

where C_s = capacity factor, ft/sec

V_g = superficial gas velocity corrected for densities, ft/sec

F = packing factor from Table 9-26A–E

L_h = liquid mass velocity, lb/(ft²) (hr)

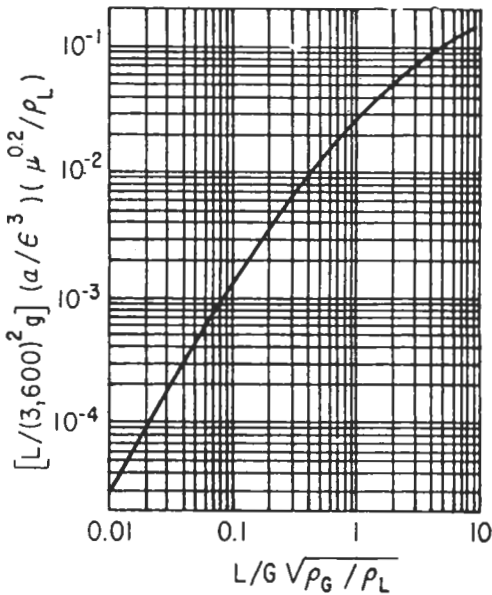
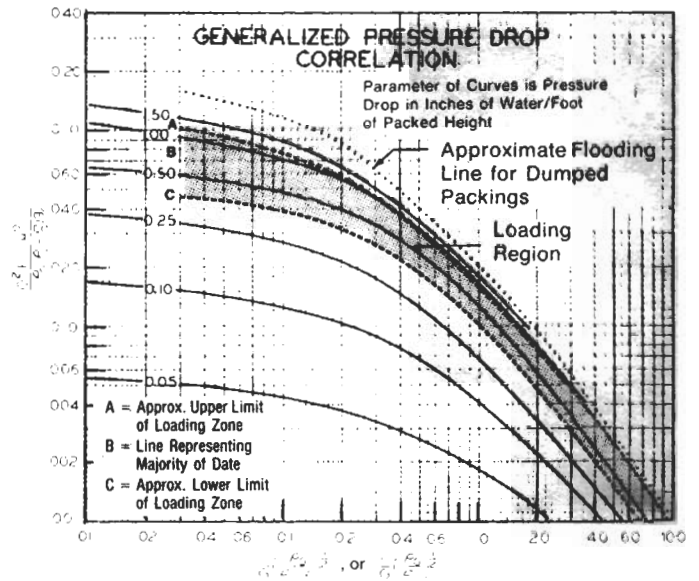


Figure 9-21A. Sherwood-type correlation for flooding gas rate at a given liquid rate. Used by permission of Zenz, F. A., *Chemical Engineering*, Aug. (1953), p. 181; all rights reserved.



L = LIQUID RATE, LBS./SEC., SQ. FT. μ = VISCOSITY OF LIQUID, CENTIPOISE.
 G = GAS RATE, LBS./SEC., SQ. FT. g_r = GRAVITATIONAL CONSTANT = 32.2 FT./SEC.²/SEC.
 ρ_L = LIQUID DENSITY, LBS./CU. FT. L' = LIQUID RATE, LBS./HR.
 ρ_G = GAS DENSITY, LBS./CU. FT. G' = GAS RATE, LBS./HR.
 F = PACKING FACTOR = 3/ε'

Figure 9-21C. Generalized pressure drop correlation essentially equivalent to Figure 9-21B. Used by permission of Norton Chemical Process Products Corp.

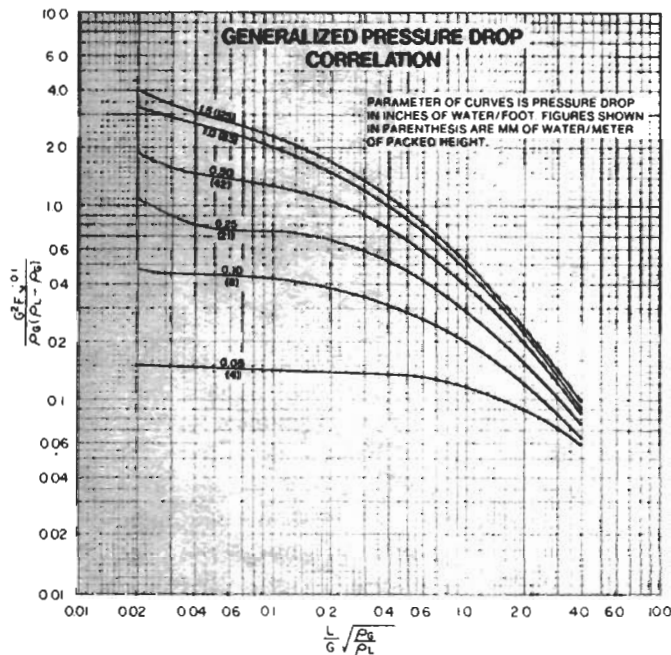


Figure 9-21B. Recent generalized pressure drop correlation. Note: v = viscosity of liquid in centipoise. Used by permission of Norton Chemical Process Products Corp.

G_h = gas mass velocity, lb/(ft²) (hr)
 ρ_G = gas mass density, lb/ft³
 ρ_L = liquid density, lb/ft³
 v = kinematic liquid viscosity, centistokes, note: centistokes = centipoise/(ρ_L/62.4)

Note differences in some symbol units for various GPDC charts.

For tower sizing:

1. Calculate using ordinate value = C_sF^{0.5}v^{0.05}
2. Calculate allowable gas mass velocity (ft/sec), C_s

Flow parameter at maximum flow location:

$$FP = \frac{L}{G} [\rho_G / \rho_L]^{0.5} \tag{9-18}$$

Strigle [139] reports that the correlation of Figure 9-21-F (and probably Figure 9-21C, because it is from the same data) predicts pressure drops to an accuracy of ±11%, and suggests that this is probably the best attainable with available data for the many different sizes and shapes of packing. Better accuracy can be attained only when using data specific to a particular packing family of sizes, such as the Nutter, Norton, and Glitsch respective packings noted hereafter. For Figures 9-21-B through H, at high liquid rates, pressure drop may become somewhat greater than obtained from the charts (GPDC), particularly for the smaller packing sizes. For the higher liquid rates, use the particular charts of the manufacturer of the packing for the type and size, rather than the GPDC.

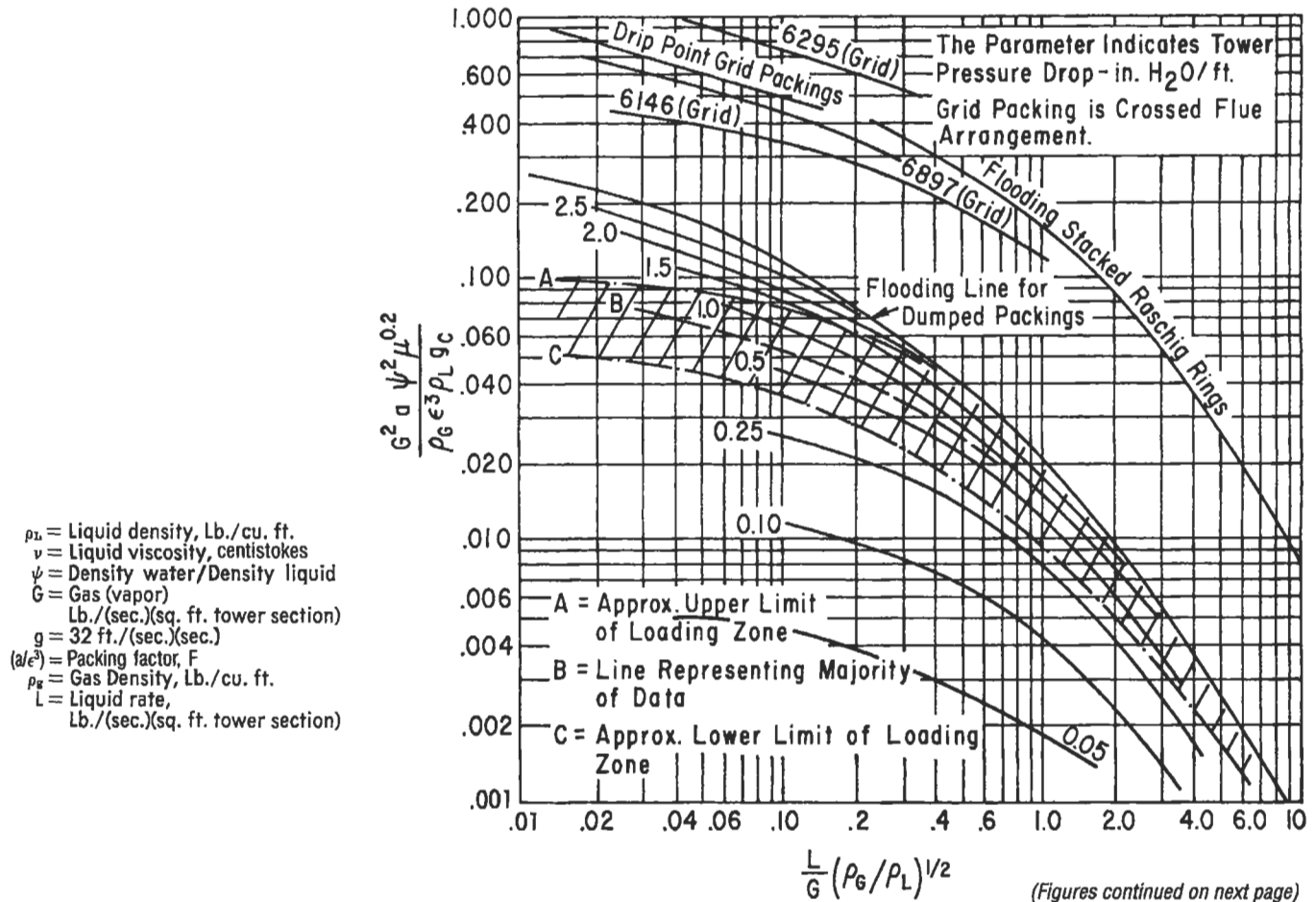


Figure 9-21D. Loading, flooding and pressure drop correlation (one of earlier versions). Adapted by permission from Leva, M. *Tower Packing and Packed Tower Design*, 2nd ed. U.S. Stoneware Co.

Strigle [139] reports that Kister and Gill's [93] tests indicate that from over 3,000 pressure drop measurements the results fit Figure 9-21-G for 80% (excellent) and another 15% (reasonable) fit.

Strigle [82, 94] describes the hydraulics and HETP performance of a packed column by referring to Figure 9-22. As noted, the HETP values are essentially constant over a wide range of C_s values shown as B-C on the figure. Note that C_s can be expressed:

$$C_s = V_g [\rho_g / (\rho_1 - \rho_g)]^{0.5} \quad (9-19)$$

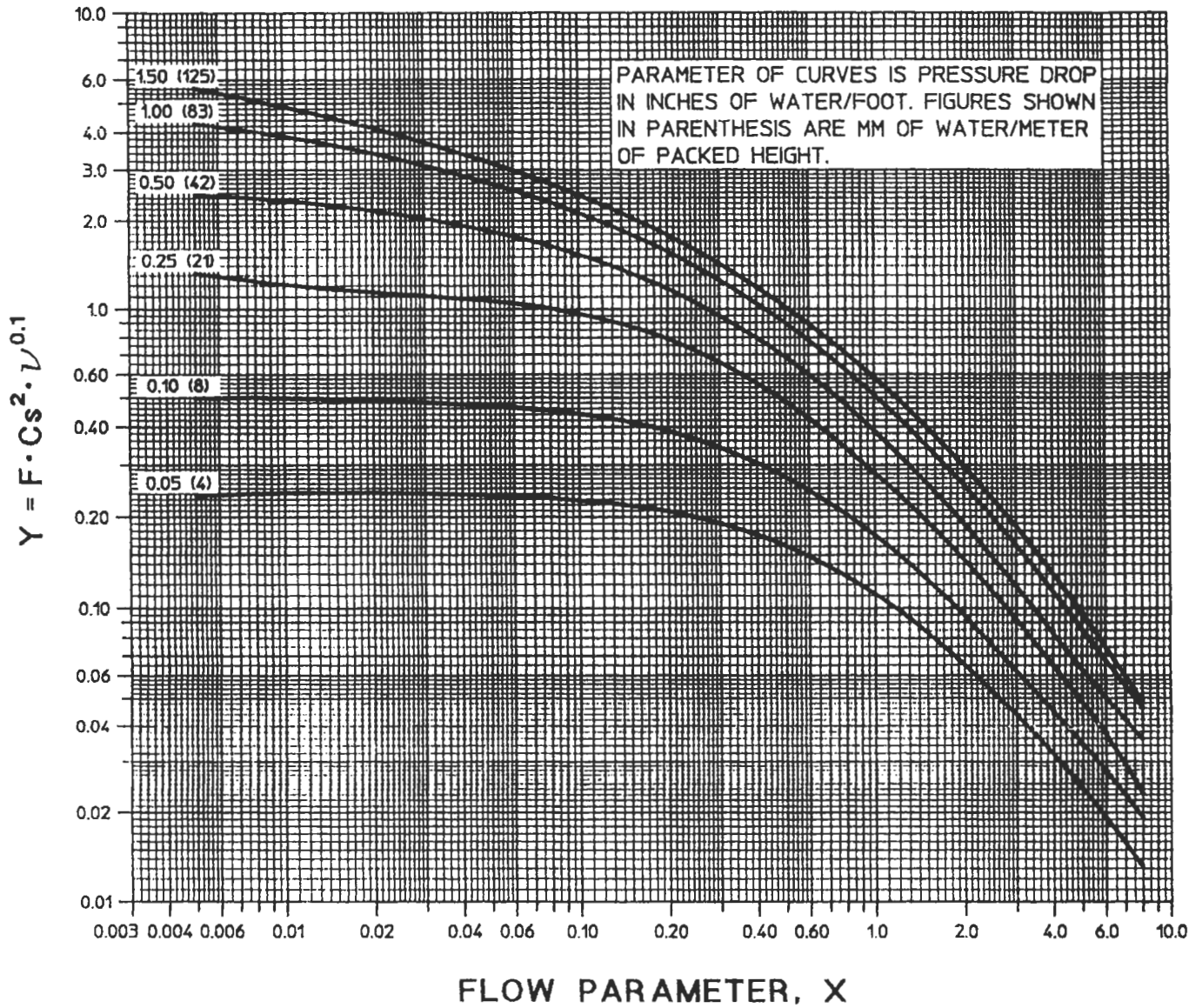
$$\text{or, } G / [\rho_g (\rho_1 - \rho_g)]^{0.5}$$

With increasing vapor rate, the contact between liquid and vapor increases to increase the rate of mass transfer and the HETP value will improve in efficiency of contact and drop from point C to E to point D. With increasing vapor rate, liquid entrainment will occur into the vapor phase and lower the efficiency (and raise the HETP) to

the "maximum operating efficiency" [94] at point F where the C_s value rises above the efficiency used for design. Thus, the "maximum operating capacity" is well below any physical flooding point. In fact, the term "maximum operating capacity" is considered as a much more meaningful term to establish performance than "loading point" where earlier this was referred to as about point C [82]. The value of C_s at point D for atmospheric distillations has been found to occur at about 91% of the "maximum operating capacity" [94] at point F. The capacity factor C_s for design at point E has been set at the "maximum operating capacity," point F. The value of C_s for point E is approximately 87% of C_s at the maximum efficiency, point D. By setting the design capacity, C_s , as previously noted, the system should then be capable of operating up to 125% of design capacity and remain stable, and be conservative for mass transfer efficiency for vapor boil-up rates from point E to point F.

(text continued on page 288)

GENERALIZED PRESSURE DROP CORRELATION



NOMENCLATURE

PROPERTY	SYMBOL	BRITISH UNITS	METRIC UNITS	DEFINITIONS
Gas Rate	G	Lbs/ft ² sec	KG/M ² sec	$X = \frac{L}{G} \frac{\sqrt{\rho_g}}{\sqrt{\rho_L}}$
Liquid Rate	L	Lbs/ft ² sec	KG/M ² sec	
Gas Density	ρ_g	Lbs/ft ³	KG/M ³	$C_s = \frac{G}{\sqrt{\rho_g} \sqrt{\rho_L - \rho_g}} = \frac{F_s}{\sqrt{\rho_L - \rho_g}}$
Liquid Density	ρ_L	Lbs/ft ³	KG/M ³	
Liquid Viscosity	ν	Centistokes	Centistokes	$F_s = \frac{G}{\sqrt{\rho_g}}$
Coefficient F	F	Packing Factor, dimensionless		

Figure 9-21E. Latest version, generalized pressure drop correlation (GPDC). Used by permission of Norton Chemical Process Products Corp. (rev. 1985).

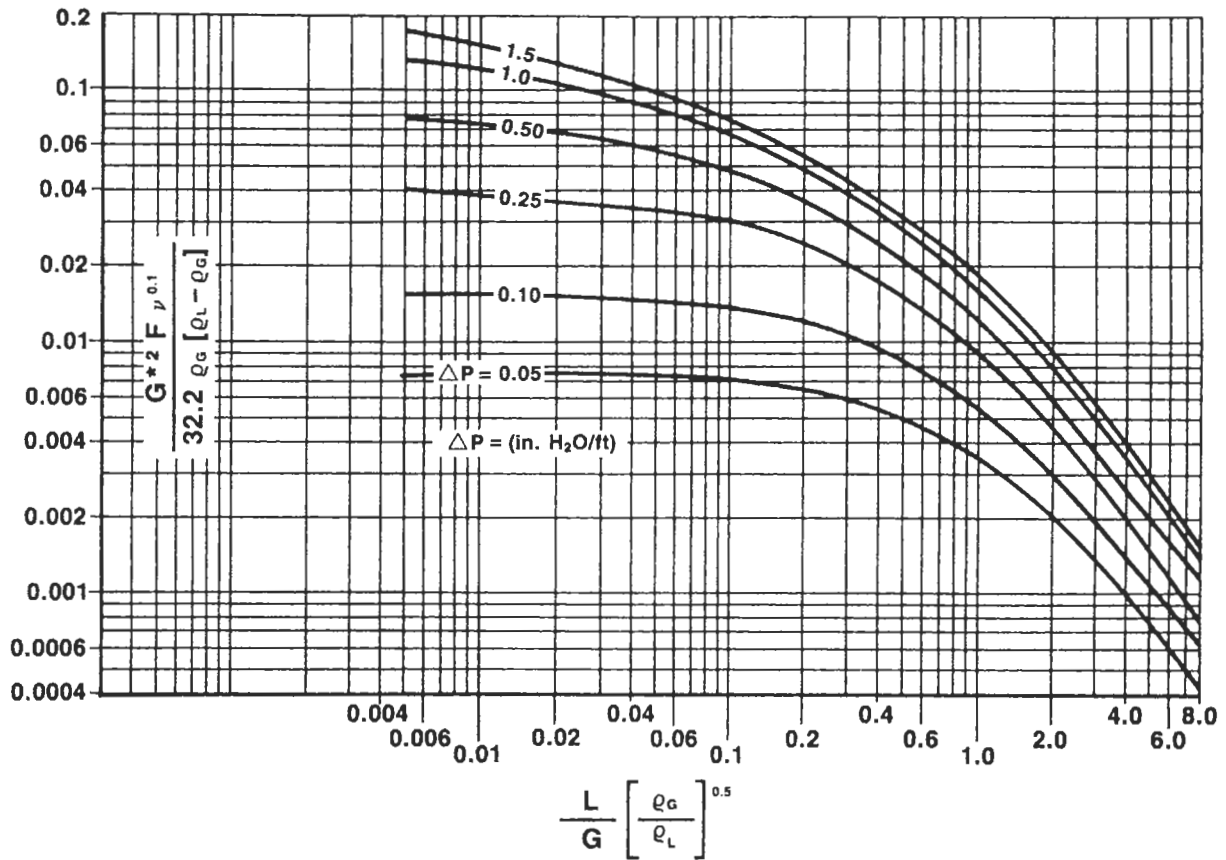
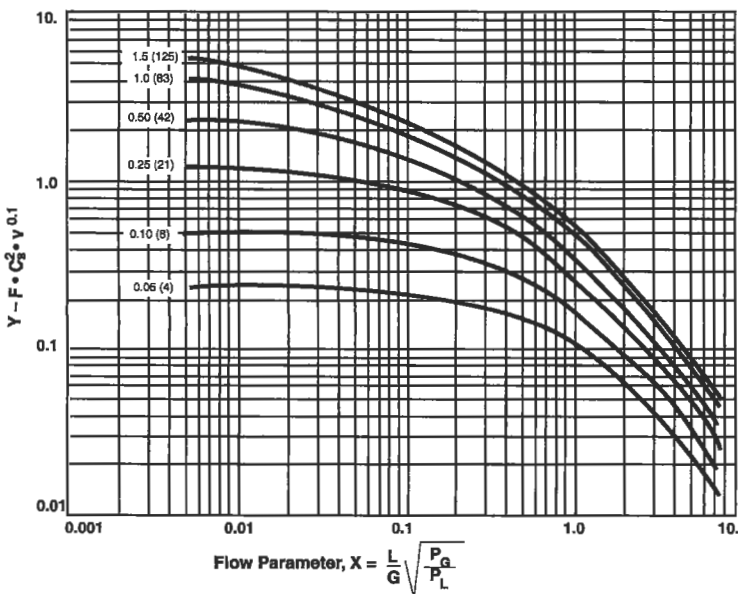


Figure 9-21F. Strigle's latest generalized pressure drop correlation. Note G^* = gas mass velocity, lb/ft²-sec. Used by permission of Strigle, R. F. Jr., *Packed Tower Design and Applications; Random and Structured Packings*, 2nd ed. Gulf Publishing Co., © (1994) p. 19.



Value for Coefficient F (Packing Factor)

IMTP Size	No. 15	No. 25	No. 40	No. 50	No. 70
F when C_s in m/s	549	441	258	194	129
F when C_s in ft/s	51	41	24	18	12

Symbols:

- $c_s = V \sqrt{P_G / (P_L - P_G)}$, ft/sec, or m/sec.
- V = Superficial gas velocity, ft/sec, or m/sec.
- P_G = Gas or vapor density, lb/ft³, or kg/m³
- P_L = Liquid density, lb/ft³, or kg/m³
- L = Liquid mass rate, lb/hr, or kg/hr
- G = Gas mass rate, lb/hr, or kg/hr
- σ = Surface tension, dyne/cm
- μ = Liquid viscosity, centipoise
- ν = Liquid kinematic viscosity, centistokes

Figure 9-21G. Generalized pressure drop correlation for non-foaming systems for IMTP metal random packing. Parameter of curves is pressure drop in inches of water/foot packed height. Numbers in parentheses are mm of water/meter of packed height. Used by permission of Norton Chemical Process Products Corp., Bull-IHP-1, 12/91 (1987).

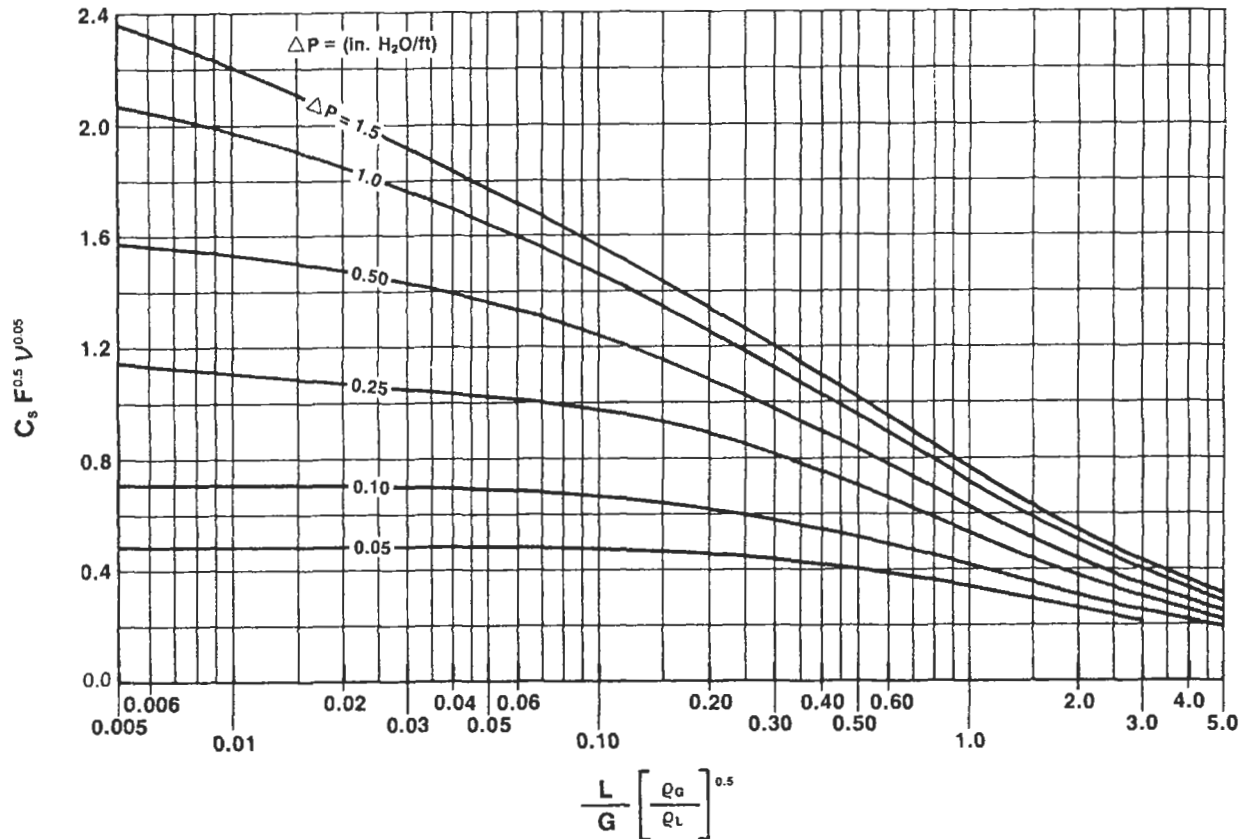


Figure 9-21H. Updated generalized pressure-drop correlation rearranged version of earlier Eckert and Leva, using linear scale for the ordinate and use of capacity factor, C_s . Used by permission of Strigle, R. F., Jr., *Packed Tower Design and Applications; Random and Structured Packings*, 2nd ed. © Gulf Publishing Co. p. 21 (1994). Note: G = gas, lb/ft²-hr, L = liquid, lb/ft²-hr.

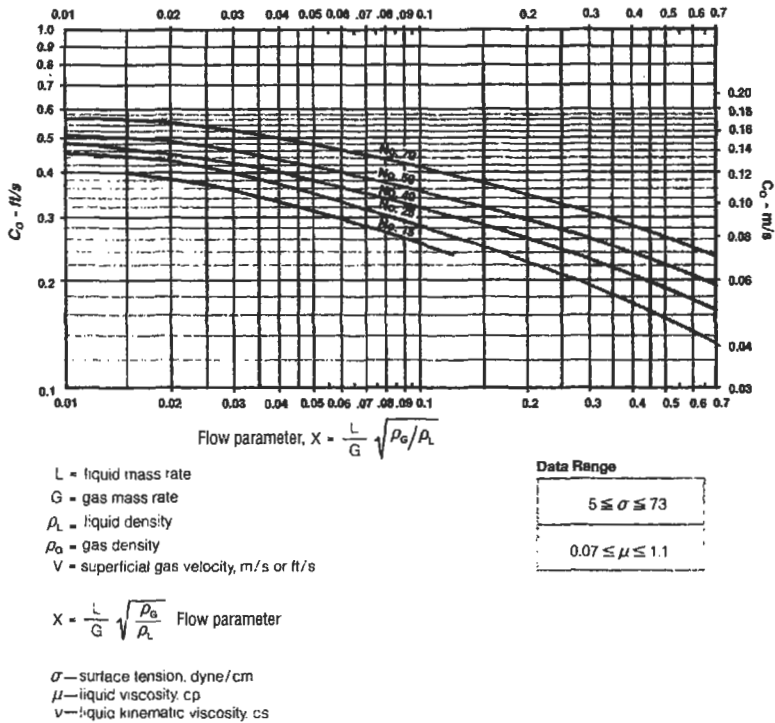


Figure 9-21I. Norton IMTP Packing, Efficient Capacity Correlation for random metal packing only for non-foaming systems. Norton recommends designing up to 90% of efficient capacity:

$$\text{Efficient Capacity, } C_{SC} = C_o \left[\frac{\sigma}{20} \right]^{0.16} \left[\frac{\mu}{0.2} \right]^{-0.11}, \text{ ft/sec.}$$

Used by permission of Norton Chemical Process Products Corp., Bull. IHP-1 (9/87).

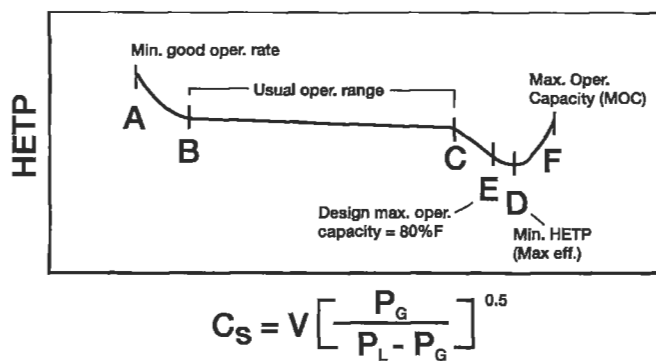


Figure 9-22. Typical HETP curve illustrating operating and design relationships. Normally reasonably constant over wide range of vapor flows. Note: C_s = capacity factor; V = gas mass velocity = lb/ft²/sec. Adapted by permission from Strigle, R. F. Jr. and Rukovena, F., and reproduced with permission of the American Institute of Chemical Engineers, *Chemical Engineering Progress*, Mar. (1979); all rights reserved.

(text continued from page 284)

Thus, for mass transfer performance design a specific design HETP value should be established, which in effect represents the range from point B through E for C_s values above point F, the HETP values will be greater (and thus less efficient contact).

Some recent evaluations of data by other investigators indicate that a so-called loading region does not exist as clearly as may be suggested by some data, and therefore they suggest operations essentially up to the flooding point. For a good, reliable design that must allow for fluctuations in feed, and possibly column back-pressure up sets, designing to the flood region cannot be recommended. Design limits are discussed later.

Flooding Point

At the second sharp change in the slope of the pressure drop curve, Figure 9-20, the packing tends to hold up more and more liquid as the gas flow increases. This creates a rapid increase in pressure drop. The flooding point of the system is said to be the point of the second inflection of the pressure drop curve. Here the liquid build-up on top of the packing becomes increasing higher and the pressure drop essentially goes to infinity for a finite increase in gas rate. In many actual cases operation can be maintained at the flooding point, but it will be erratic, the performance (efficiency) of operation poor, and the entrainment carry-over excessively high. It is obvious that towers are not designed for flood point operations, but at 40–60% of gas and liquid rates associated with this point. Figure 9-21D indicates that the flooding region usually is above 2.5 in. water/ft, but note how cramped and much

more sensitive this condition becomes as the extreme right hand side of the graph is approached.

Kister's [93] study indicates that flooding with the current newer-designed packings occurs just below 2 in. water/ft of packing, somewhat below the prediction given by the earlier Eckert chart, Figure 9-21C or D. The data plotted by Kister indicate that for larger packings (2 in. and 3 in., for example) the flooding point is noted at much lower pressure drops than suggested by Figure 9-21C. The pressure drop at flood point has been found to be independent of the Flow Parameter on the charts, but does vary with the packing family and packing types [93, 95].

Kister [93] has developed a new approach at establishing the flood point that appears to suit the available data and is obviously more accurate than reading the upper curve on Figure 9-21C.

$$\Delta P_{\text{flood}} = 0.115 F_p^{0.7} \quad (\text{do not extrapolate below } F_p = 14) \quad (9-20)$$

where ΔP_{flood} = pressure drop at flood point for all random packings, in. water/ft of packing

F_p = packing factor, empirical, based on packing size and shape, 1/ft, see Tables 9-26A–E.

By calculating the ΔP_{flood} , the capacity parameter can be determined using the calculated flow parameter and Figure 9-21E, and, if available, the SLE (Sherwood, Leva, Eckert) charts of Reference 93. For $F_p > 60$, the calculated ΔP_{flood} using the equation coincides with Eckert's Figure 9-21C flood line. Figure 9-23 illustrates the relationship of packing factors to flooding pressure drop and is represented by the ΔP_{flood} equation. The predicted results of the equation are ± 10 to 15% based on the plotted data [93].

Foaming Liquid Systems

For an accurate design, the effects of foaming of the liquid as it flows through the random packed/structured bed should be known, estimated, or determined by experimentation. There is little published data on the subject except Eckert [24] and Strigle [82]. Generally, foaming systems produce higher pressure drops than non-foaming, most probably due to the blocking of packing voids by the foam. Therefore, it is wise to determine the foaming related nature of the specific system, and because there are no numerical data published, the designer must use judgment and make allowances for a pressure drop greater than read from any of the charts, perhaps even 2 to 3 times greater.

Hsu [124] presents equations for directly calculating random packings based on published data and which are adaptable for computer programming and thereby studying the effects of variables. The basic data are essentially a match with Figure 9-21D.

Table 9-26A
Packing Factors,* ft⁻¹
Wet and Dumped Packing

Packing Type	Material	Nominal Packing Size, In.										
		¼	⅜	½	⅝	¾	1 or #1	1¼	1½	2 or #2	3	3½ or #3
Intalox® IMTP®	Metal				51 (#15)		41 (#25)		24 (#40)	18 (#50)		12 (#70)
Hy-Pak™	Metal						45		29	26		16
Super Intalox® Saddles	Ceramic						60			30		
Super Intalox Saddles	Plastic						40			28		18
Pall Rings	Plastic				95-102*		52*-55		31*-40	26	18*	17
Pall Rings	Metal		76*-81		76*		48*-56		33*-40	23*-27		18
Intalox® Saddles	Ceramic	725	330	200		145	92		52	40		22
Raschig Rings	Ceramic	1600	1000	580	380	255	179	125	93	65		37
Raschig Rings	½" Metal	700	390	300	170	155	115					
Raschig Rings	⅙" Metal			410	300	220	144	110	83	57		32
Berl Saddles	Ceramic	259		240		170	110		65	45		
Snowflake™	Plastic							13 (#38)		13 (#50)		13 (#90)

*By permission Norton Co., from data compiled in Norton Co. Laboratories, Copyright 1977.

Packing factors determined with an air-water system in 30" I.D. Tower.

Updated by permission from R.F. Strigle, Jr., *Random Packings and Packed Towers*, Gulf Publishing Co. (1987), added Snowflake™ data by permission Norton Chemical Process Products Corp., Bull. ISPP-IR, E/90; * by permission Jaegar Products Co.

Table 9-26B
Koch Packing Factors*

Packing Type	Material	Nominal Packing Size, In.										
		¼	⅜	½	⅝	¾	1 or #1	1¼	1½	2 or #2	3	3½ or #3
Flexisaddles	Plastic						30			20		15
Flexirings	Plastic†				78		45		28	22		18
Flexisaddles	Ceramic	600		200		145	98		52	40	22	

*By permission, Koch Engineering Co. Inc.

†Use for plastic or metal.

Table 9-26C
Glitsch Packing Factors*

Packing Type	Material	Nominal Packing Size, In.										
		¼	⅜	½	⅝	¾	1 or #1	1¼	1½	2 or #2	3	3½ or #3
Ballast™ Ring	Metal						48		28	20		15
Ballast™ Ring	Plastic				97		52		32	25		16
Ballast™ Saddle	Plastic						30			20		15

*By permission, Glitsch Inc.

Surface Tension Effects

Strigle [82] reports that there is no broadly documented agreement of the surface tension effects on the capacity of packed beds. Eckert [24, 82] concluded that surface tension of a non-foaming liquid had no effect on capacity.

These results were later confirmed. For absorption systems these results also hold [82].

For hydrocarbons in high-pressure fractionators Strigle [82] reports there is aeration of the rather low surface tension liquid phase. This effect increases with the lower surface tension and as the vapor density increases, thus

Table 9-26D
Glitsch Packing Factors for Cascade® Mini-Rings

Size	Plastic	Ceramic	Metal
0	—	—	55
0A	60	—	—
1	29	—	40
1A	30	—	—
1.5	—	—	29
2	15	38	22
2A	30	—	—
2B	18	—	—
2C	19	—	—
2.5	—	—	19
3	11	24	14
3A	12	—	—
4	—	—	10
5	—	18	8
7	—	15	—

Used by permission: Glitsch, Inc., Bull. 345

Table 9-26E*
Nutter Ring™ Random Packing

Size No.	Pieces/Ft ³	Ft ² /Ft ³	Lb/Ft ³	% Void	Packing Factor**	Relative HETP Values
0.7	4,740	69	11.0	97.8	xx	0.72
1.0	1,900	51	11.1	97.8	30	0.83
1.5	760	38	11.3	97.8	24	0.94
2.0	385	29	10.8	97.9	18	1.00
2.5	250	25	9.0	98.2	xx	1.18
3.0	120	20	8.3	98.4	xx	1.40

*Nutter uses their own proprietary computer program and not the conventional GPDC Chart shown in Figures 9-21B-E.

**Values shown developed by Kister [90] from data supplied by Nutter Engineering Co., a Harsco Corp.

Used by permission of Nutter Engineering Co., a Harsco Corp.; Bull. NR-2

reducing the effective liquid density, and increasing the volume occupied by a given mass of liquid is increased. This aeration effect can vary from 0.9 at atmospheric pressure for non-foaming liquids to 0.7 for hydrocarbon systems (not absorbers operating at 35% of critical pressure).

Kaiser [140] presents a correlation analysis for flooding in packed towers that is more analytical in the performance approach. It is based on single phase hydraulics. It would have been helpful for the article to present a comparison of results with the other more conventional techniques.

Packing Factors

The use of "packing factors" is established in the design concepts of evaluating packed tower performance. Essentially all of the manufacturer's published data are for "wet and dumped" packing factors, F. Robbins proposes using

"dry" factors only. (See later write-up.) This factor is a unique characteristic of each packing size and experimentally determined style/design. These factors cannot be determined by calculation from the physical dimensions, they are more accurately determined experimentally.

Packing factor selection significantly affects the performance of a packed tower system. These factors are only suitable for discreet particle type packing, and their values vary depending on how the packing is installed in the tower. For example, the factors for a ceramic packing are different for packing floated (dumped) into a tower full of water and the particles allowed to float down when compared to the same packing dumped into a dry empty tower where significant breakage can occur and consolidate the packing, or even to packing "hand-placed" or stacked dry.

Often it is only necessary to change a packing size or type to modify the capacity and/or contacting efficiency

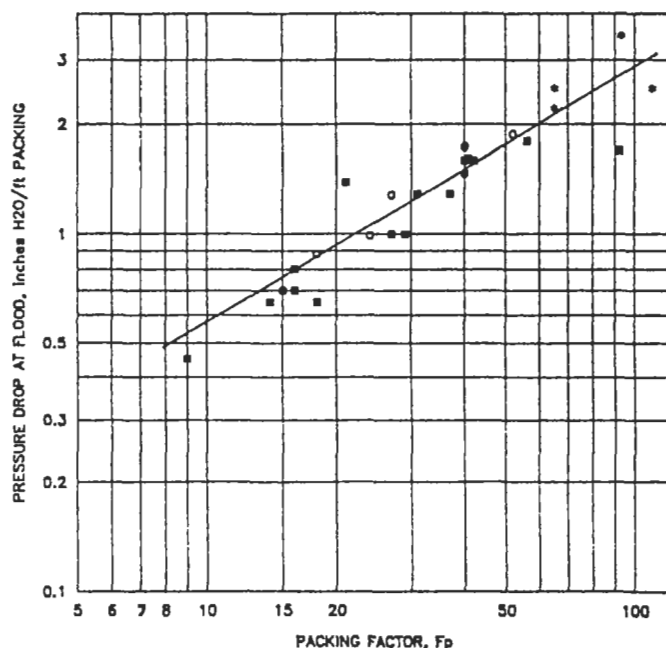


Figure 9-23. Flood pressure drop vs. packing factor for random packings. Reproduced with permission of the American Institute of Chemical Engineers, Kister, H. Z. and Gill, D. R., *Chemical Engineering Progress*, V. 87, No. 2 © (1991); all rights reserved.

of an existing tower, because this change affects the packing factor. Tables 26A–E present specific packing factors from the manufacturers.

Many of the packings of the various manufacturers are essentially identical in shape, size, and performance factors. Some packing manufacturers suggest adjusting packing factors for vacuum and pressure distillations; however, this should only be done after consultation.

The experimentally determined packing factors are the only reliable values to use for design calculations; although estimates can be made for packing shapes when no data are available. The packing characteristic is expressed as:

$$F = a/\epsilon^3 \quad (9-21)$$

where a_t = specific surface of packing, ft^2/ft^3
 a = effective interfacial area for contacting, ft^2/ft^3
 ϵ = fractional voids

The values of a/ϵ^3 determined experimentally by Lobo et al. are indicated [47]. These are the values in the development of the basic relation expressed in Figure 9-21A with correction of ψ^2 suggested by Leva [41]. These a/ϵ^3 values were found to correlate a considerable amount of the literature data within 12%. This would mean about a 6% error in tower diameter determined at flooding conditions.

Lobo et al. [47] proposed the packing factor, F , and experimentally determined that it better represented the data than the calculated a/ϵ^3 term. Values calculated using surface area per cubic foot and percent free gas space from manufacturer's tables can be as much as 40% off. The values are dependent upon the method of packing the tower, i.e., dry dumped, wet dumped, or wet dumped and shaken. The latter condition may approximate the situation after a tower has been running a while and the packing settled.

Experience definitely indicates that the packing factor, F , increases with hours of operation for ceramic materials up to some limit. This is due to settling, breakage, plugging, etc. For design of commercial towers, values of F should be increased from 15 to 75% for ceramic materials, over values read from Tables 9-26A–E. The percent increase depends upon the tendency of the shape to disintegrate into smaller pieces during operations—flooding, gas surging, etc. In general, circular shapes exhibit the least tendency to break up. As a reasonable value where data are available, the average of the wet dumped, and wet-dumped-and-shaken values for tower voidages is recommended.

Leva [40] has correlated the data of Lubin into correction factors to apply to a non-irrigated bed pressure drop to end up with pressure drop for a liquid-gas system in the loading to flooding range. In general this does not appear any more convenient to use than Figure 9-21D.

Relations expressing the fractional voids in a ring packed bed are useful in estimated the “ ϵ ” values for a/ϵ^3 determinations [47]. The average deviation is $\pm 2.6\%$.

Dry packed tower:

$$\epsilon = 1.046 - 0.658 \phi \quad (9-22)$$

Wet packed, unshaken tower:

$$\epsilon = 1.029 - 0.591 \phi \quad (9-23)$$

Wet packed and shaken tower:

$$\epsilon = 1.009 - 0.626 \phi \quad (9-24)$$

where

$$\phi = \frac{1 - (d_i/d_o)^2}{(ld_o^2)^{0.0170}}, \text{ not valid if } \phi < 0.20 \text{ or for extra thick walls or solids}$$

l = ring height, in.
 d_o = outside diameter of ring, in.
 d_i = inside diameter of ring, in.

The generalized correlations of Sakiadis and Johnson [59] are reported to satisfy a wide variety of systems.

Manufacturers of commercial packings provide packing factors for their products. Many of the commonly used (not

necessarily all) packing factors are presented in Table 9-26A. These values are to be used with the application of Figures 9-21B and 9-21F. Factors presented in Figures 9-24A and 9-24B can also be used where the design requires them.

Recommended Design Capacity and Pressure Drop

The relationships in packed tower performance which are concerned specifically with the gas and liquid flows through a bed are expressed as a function of pressure drop. Pressure drop may be created by poor packing arrangements, i.e., tight and open sections in the bed, breakage of packing and settling of the bed, or plugging of void spaces by solids or reaction products. All of these are in addition to the inherent characteristic resistance of a *particular* packing to flow of fluids. This resistance will be different if the system is single phase as contrasted to two phase for most distillation, adsorption, scrubbing, or desorption operations. The basic pressure drop performance pattern of nearly all packings can be shown as in Figure 9-20.

Below the loading region, the pressure drop can be read from appropriate system curves if they are available, as Figure 9-20. However, for general use the data have been well correlated, Figures 9-21B–9-21F. The slope of most of the curves for pressure drop indicate a proportionality of 1.8 to 2.8 power of the superficial gas mass

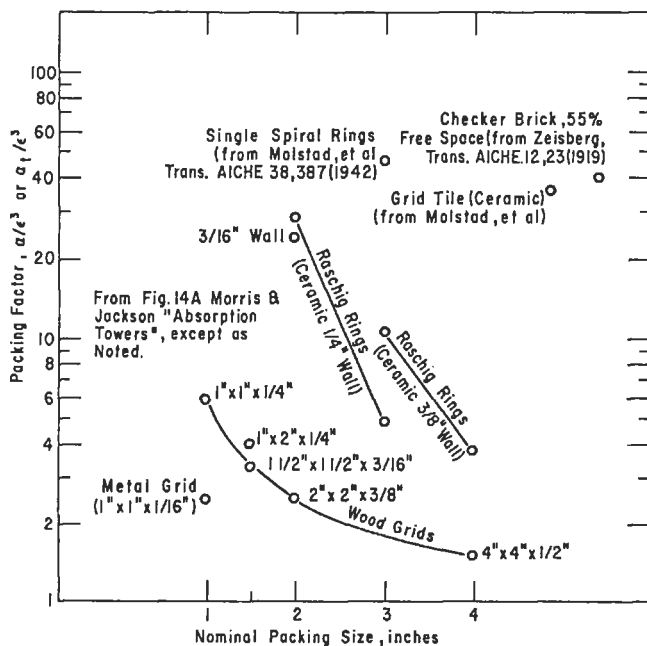


Figure 9-24A. Packing factors (stacked packing selected grids). Used by permission of Morris and Jackson, *Absorption Towers* Butterworth Scientific Publications, and Imperial Chemical Industries, Ltd., and adapted by U.S. Stoneware Co. (now, Norton Chemical Process Products Corp.).

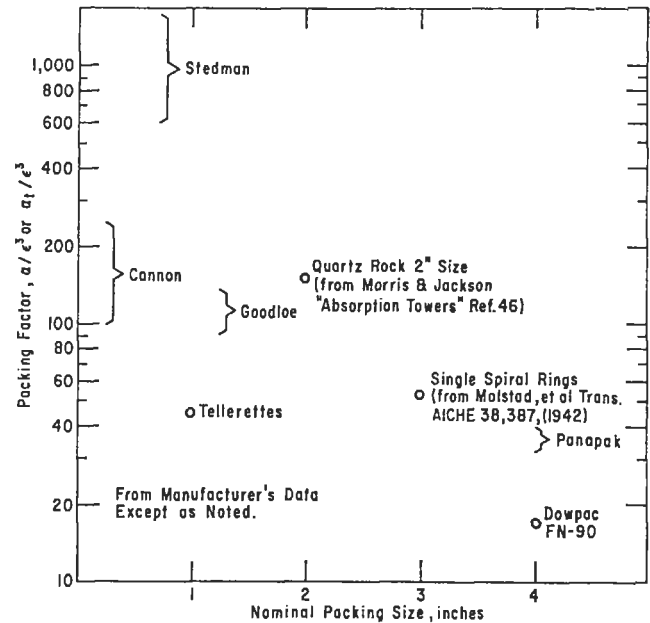


Figure 9-24B. Packing factors (screen packing and random dumped packing). Used by permission of U.S. Stoneware Co. (now, Norton Chemical Process Products Corp.).

velocity up the tower. This performance is typical of the gas-continuous range of packed tower operation. In Figure 9-20 the curves for performance at water rates of $L' = 1,250$ through $L' = 9,950$ all seem to be a part of the same family. The curve $L' = 12,500$ will be discussed later. The pressure drop information to follow is valid only for the gas-continuous type of operation. Fortunately the majority of packed towers operate in this condition; however, the liquid-continuous will be considered later.

Pressure drop data for several styles and arrangements of drip point grid tile are given in Figures 9-25A–9-25E. These are not included in the general GPDC correlations for random packings.

Figures 9-21E, F, and H are about the latest general purpose correlations presented by several manufacturers of packing materials. The relative differences between the various correlations appear to be minor, thereby allowing any packing performance to be evaluated on any chart, as long as the packing factors, F , have been determined on the same basis. Packing factors are presented in Tables 9-26A and B and are identified for the discrete particle packings similar to those illustrated in Figures 9-6A–6X because the compacted, structured, or grid packing materials such as shown in Figures 9-6Y–6UU do not use the same packing factor concept for design evaluation. Therefore, because each proprietary material such as those in Figures 9-6Y–6UU has its own design/rating technique, the respective manufacturer should be consulted, because they cannot be rated using Figures 9-21A–21I.

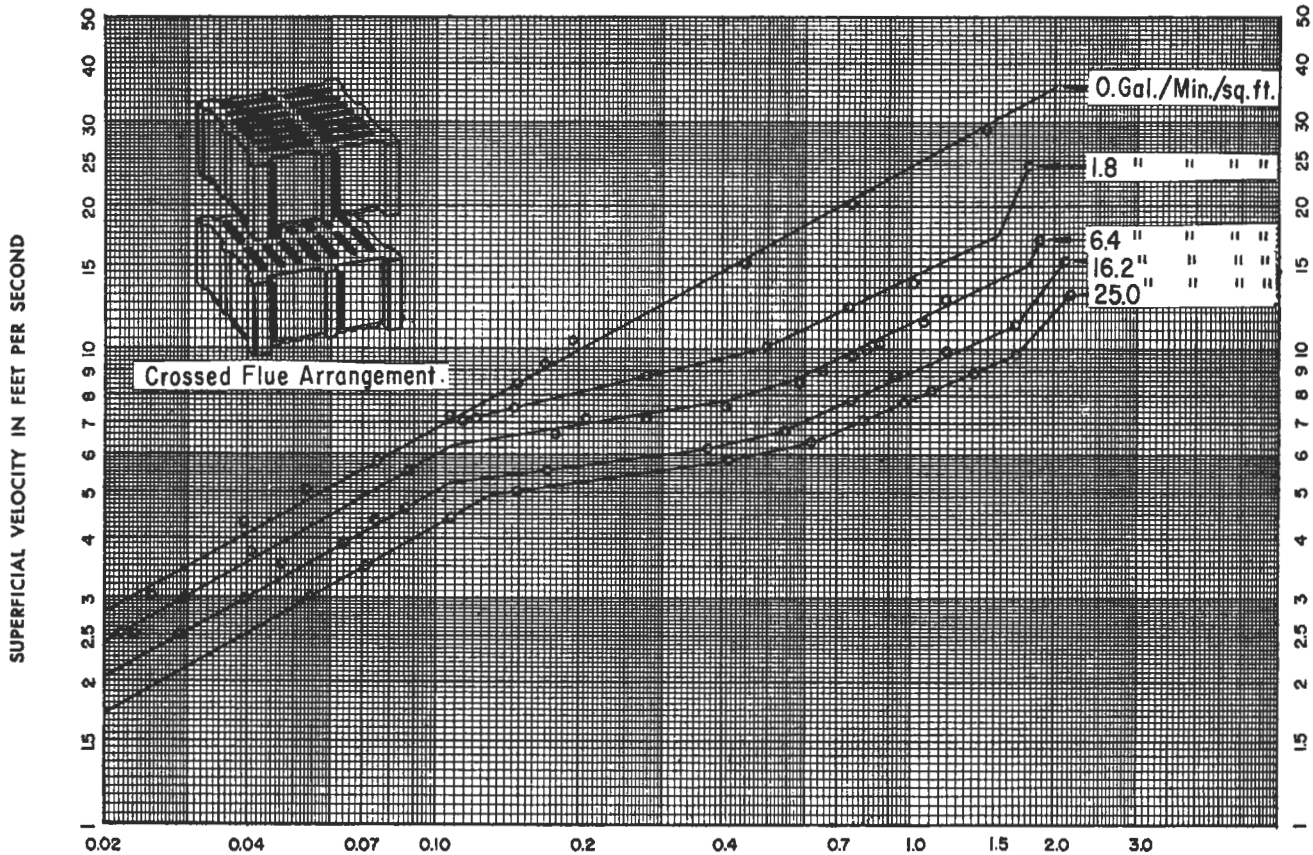


Figure 9-25A. Pressure drop in inches of water per foot of height, drip point tile, shape 6295 with crossed flue arrangement. Used by permission of General Refractories Co.

Pressure Drop Design Criteria and Guide: Random Packings Only

- A. Determine the height of packing required (not a function of diameter) from HETP in distillation section and K_{ga} in absorption section. This provides the total height of packing required, considering the packing efficiencies and minimum wetting requirements, previously discussed. From this total height, the expected total column pressure drop can be established, recognizing the pressure loss through support plates, distribution devices, etc.
- B. Calculate the abscissa of Figure 9-21F; for example, $L/G\sqrt{\rho_G/\rho_L}$, or other abscissa values.
- C. Select a design/operating pressure drop, as shown on the curves of Figure 9-21F. Suggested selection basis is as follows:
 1. Low to medium pressure column operation, select design pressure drop of 0.40 to 0.60 in. water/ft of packing height, although some towers will operate at 1.5 to 2.0 in. water/ft. Select a design C_s above point C and below point D, Figure 9-22.
 2. Absorption and similar systems; select pressure drop of 0.1 to 0.4 in. water/ft of packing, or 0.25 to 0.4 for non-foaming systems. For "median" foaming systems use a maximum of 0.25 in. water/ft for the highest loading rate [82], see Table 9-27. The values in the table should be reduced for high viscosity fluids. At rates above 20, limit the gas rate to 85% of the rate which would give a pressure drop of 1.5 in. water/ft referring to the GPDC, Figure 9-21F.
 3. Atmospheric or pressure distillation, select pressure drop of 0.50–1.0 in. water/ft.
 4. Vacuum distillation varies with the system and particularly with the absolute pressure required at the bottom of the column; normally select low pressure drop in the range of 0.1 to 0.2 in. water/ft of packing. For in vacuum service of 75 mm Hg and lower, the pressure drop obtained from the GPDC,

(text continued on page 296)

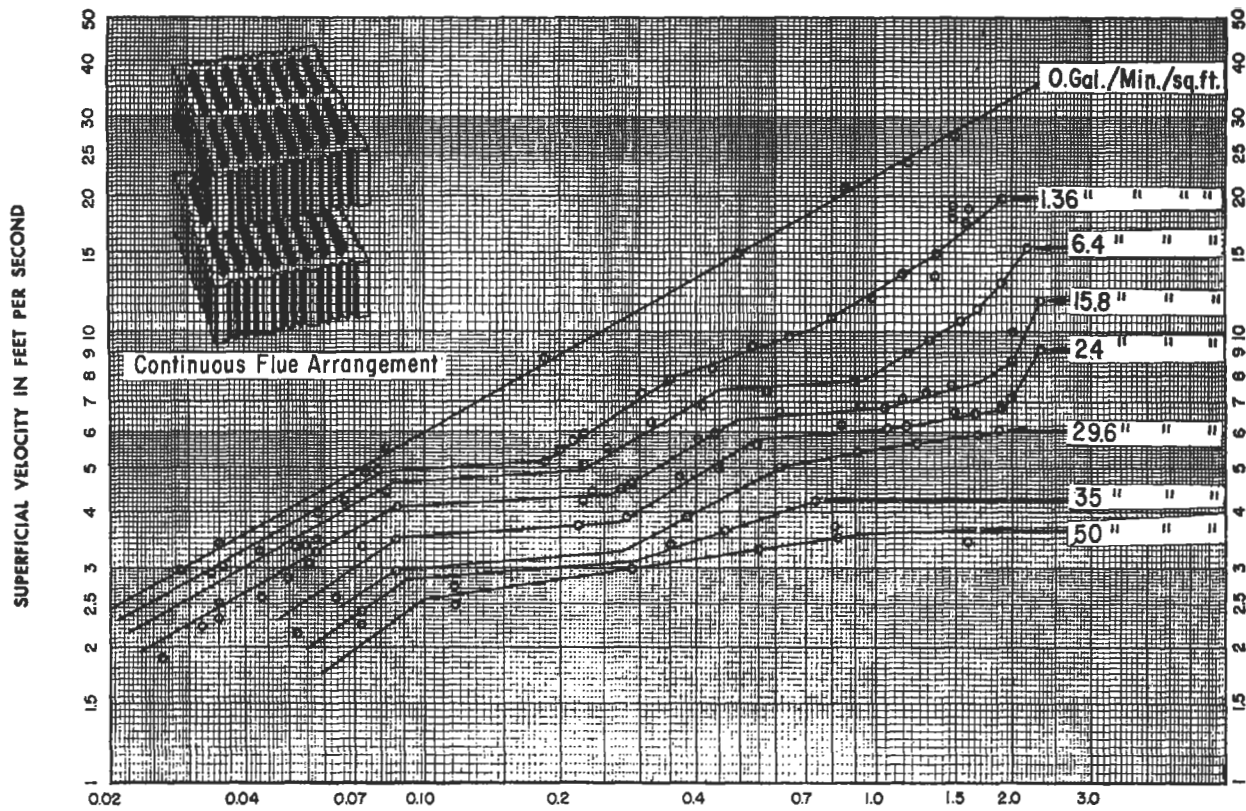


Figure 9-25B. Pressure drop in inches of water per foot of height, drip point tile shape 6897 with continuous flue arrangement. Used by permission of General Refractories Co.

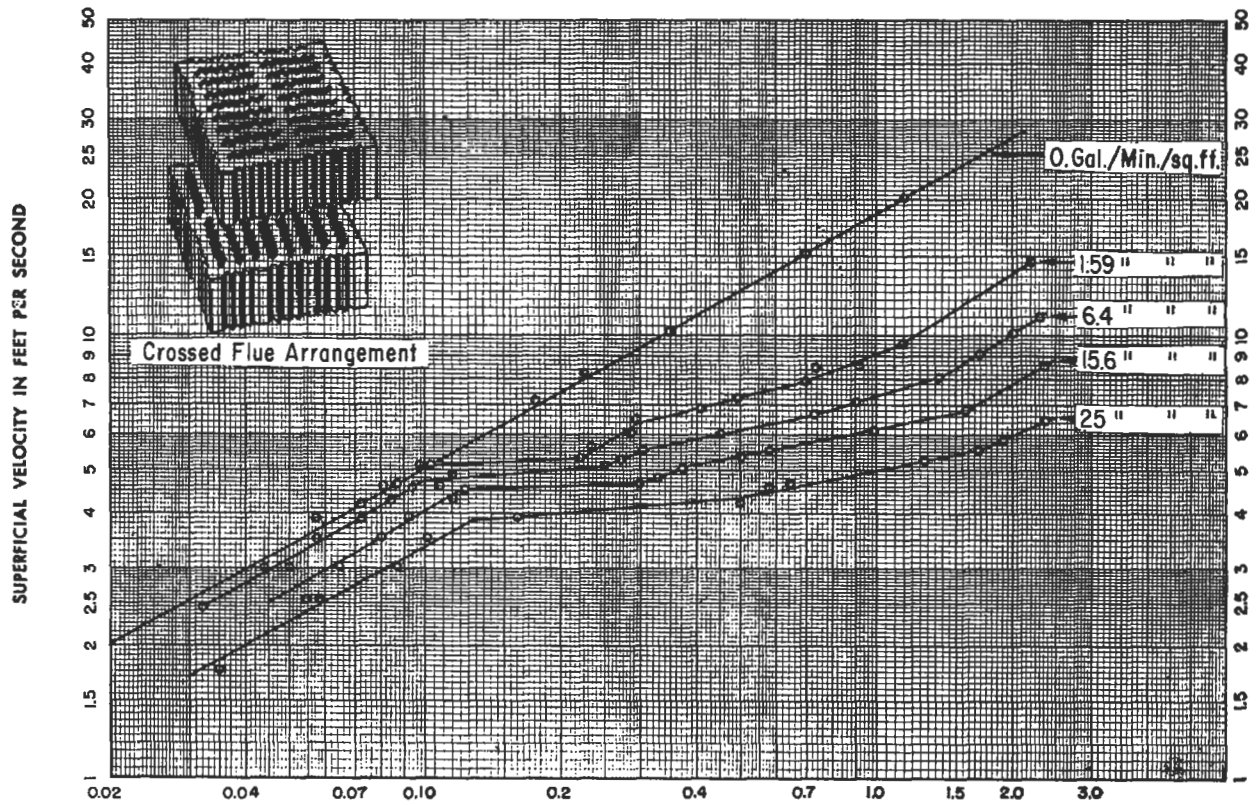


Figure 9-25C. Pressure drop in inches of water per foot of height, drip point tile shape 6897 with crossed-flue arrangement. Used by permission of General Refractories Co.

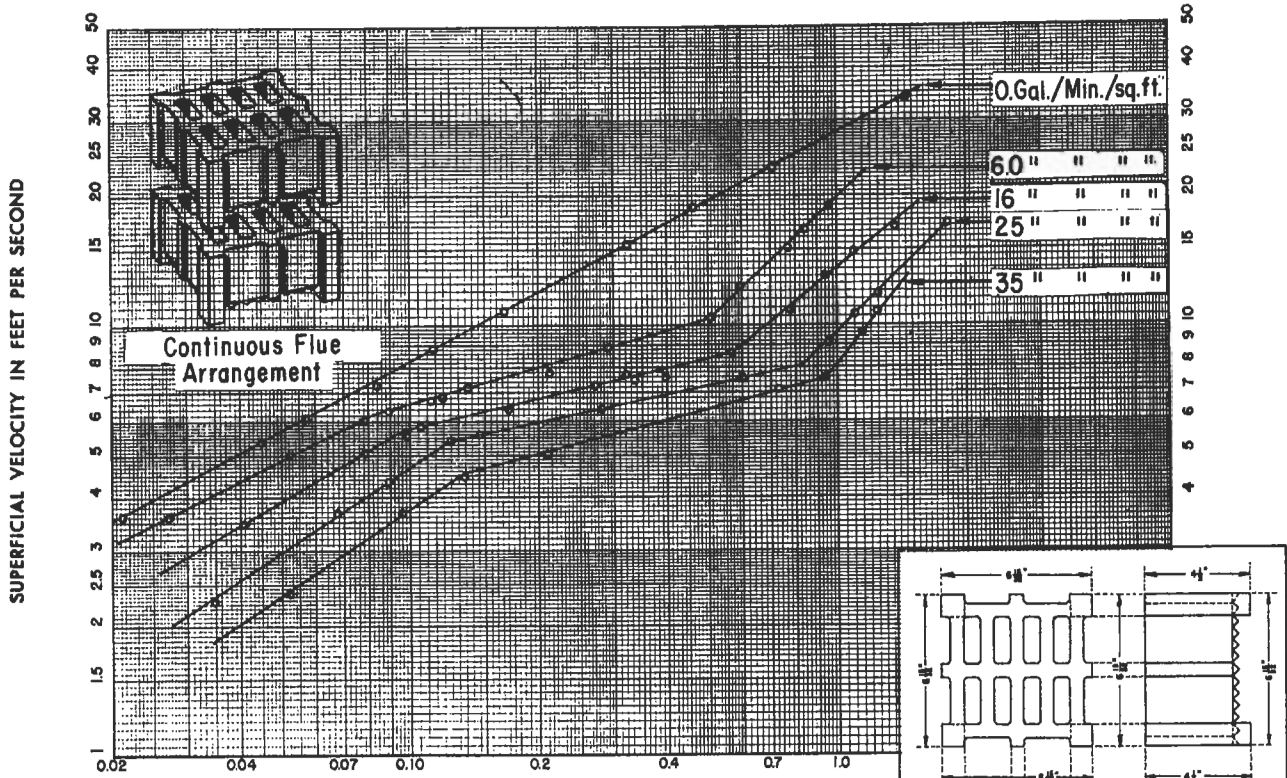


Figure 9-25D. Pressure drop in inches of water per foot of height; drip point tile shape 6146 with continuous flue arrangement. Used by permission: General Refractories Co.

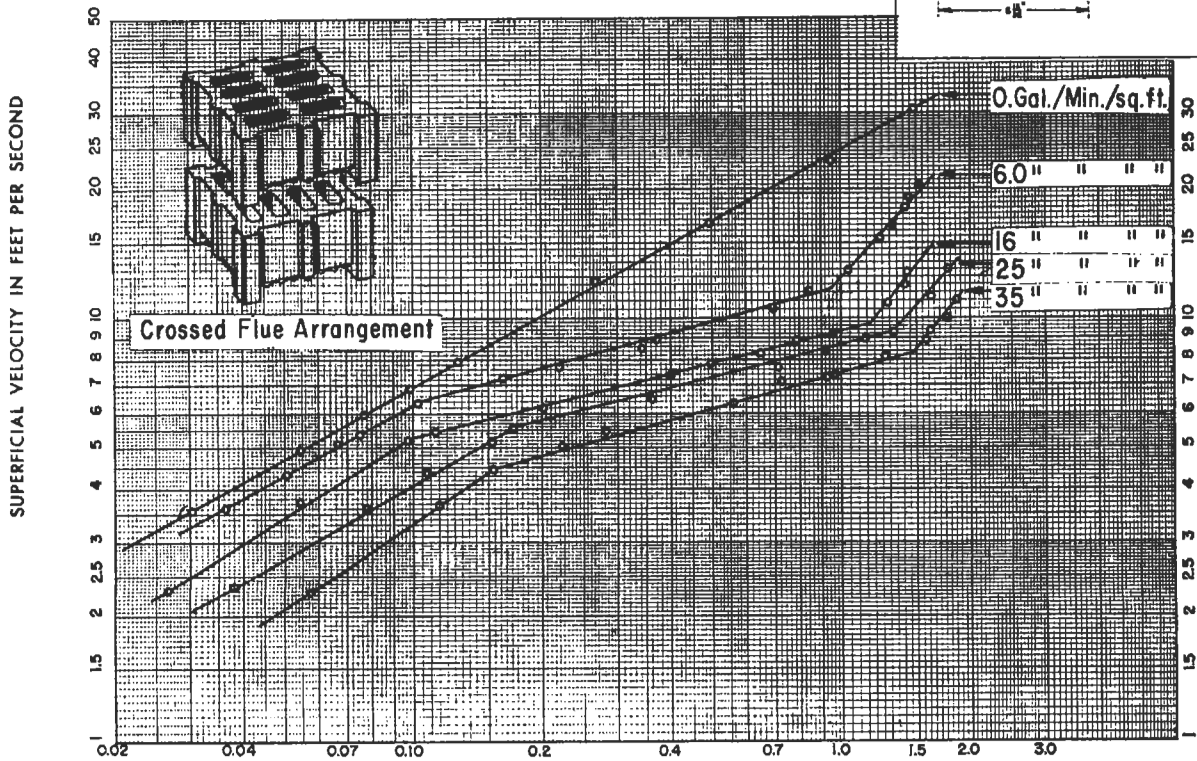


Figure 9-25E. Pressure drop in inches of water per foot of height, drip point tile shape 6146 with cross flue arrangement. Used by permission of General Refractories Co.

Table 9-27
Maximum Recommended Liquid Loading

Packing Size (in.)	Liquid Rate (gpm/ft ²)
¾	25
1	40
1½	55
2	70
3½	125

Used by permission of Strigle, R. F., Jr., "Random Packing and Packed Towers" © (1987), Gulf Publishing Co., all rights reserved.

(text continued from page 293)

Figures 9-21F and 21G (for Norton's IMTP packing only) can be up to 20% higher than industrial experience for the same C_s values at a flow parameter (FP) of 0.01 [82]. At an absolute column pressure of 10 mm Hg or less, the pressure drop actual can be up to 30% lower than that read from the Figure 9-21F at the FP of 0.01 and the same C_s value [82]. The conclusion is that the generalized correlation, Figures 9-21F and -21G always give a conservative design ΔP at operating pressures less than 70 mm Hg abs. Several other factors must be considered, such as variability of gas and liquid rates and densities or specific volumes.

5. Foaming materials should be operated at 0.1–0.25 in. water/ft, or better, obtain data. Actual ΔP /ft may run 2–5 times chart values.
6. Vacuum service requires recognition of minimum liquid flow; refer to section on minimum wetting rate. Pressure drops are designed to be low, but normally not lower than 0.10 in. water/ft.
7. Stripping gas from a liquid phase; pressure drop is usually set to be 0.15 to 50 in. water/ft packing at the flow rates for maximum loading, or maximum operating capacity. For foaming systems set pressure drop at ≤ 0.25 in. water/ft using inert gas. But for steam use, set pressure drop ≤ 0.3 maximum in. water/ft for medium foaming conditions [82].
8. For high pressure distillation of light hydrocarbons, industrial performance indicates that the pressure drop actually obtained is about two times that predicted by the use of the GPDC charts, Figure 9-21F and 9-21G (for Norton's IMTP packing only). When the vapor density is at least 6% of the liquid density, the actual pressure drop is expressed [82]:

$$\Delta P = \frac{33 F^{0.5} (C_s)^{2.4}}{\sigma} \text{ in. water/ft packing} \quad (9-25)$$

where C_s = capacity factor, ft/sec
 σ = surface tension, dynes/cm
 F = packing factor

For non-hydrocarbon systems Strigle [82] recommends the general outline to follow, but more detail for a specific design may be obtained from the reference as well as the manufacturer:

1. Select a design C_s vapor rate as a percent of the MOC (maximum operating capacity) of the packing.
2. Adjust maximum C_s required; adjusting for:
 - (a) Effect of liquid viscosity: The maximum operating capacity varies as the 0.2 to 0.25 power of surface tension of the liquid phase.
 - (b) Packing capacity increases as the reciprocal of liquid viscosity to the 0.1 to 0.13 power. This effect is limited to liquid viscosities not < 0.09 cps.
 - (c) Select design C_s at 80 to 87% of the MOC C_s for the packing.
 - (d) When the gas density exceeds 6% of the liquid density, the pressure drop should be examined by Equation 9-25.

Pressure drop should not exceed at maximum operating capacity [94] [139]:

$$\Delta P_{\max} \leq (0.019) (F)^{0.7}, \text{ in. water/ft packing} \quad (9-26)$$

or, from Kister and Gill [93, 139], pressure drop at flood for random dumped packing:

$$\Delta P_{\text{flood}} = 0.115F^{0.7}, \text{ in. water/ft packing} \quad (9-20)$$

- (e) For pressures approaching the critical, contact the packing manufacturer for performance guidance.
 - (f) Select a design C_s that provides allowances for operational and capacity fluctuation and/or surges. A suggested 15–25% above the design rate is usually adequate [82], making the design C_s from 80–87% of the maximum operational C_s for the specific packing. The maximum operational capacity, MOC, $C_{s,\max}$, is the point, C (Figure 9-22), where the vapor rate has increased to a point where it begins to interact with the liquid. In previous publications this point was termed "loading point." Actually for rates slightly greater than point C, the efficiency of the packing increases (HETP becomes smaller).
- D. Select a packing and determine its packing factor from Tables 9-26A–E. Packing is selected for its expected process HETP or K_{ga} performance, pressure drop and materials of construction for the system. Table 9-17 presents summary comments for applications. Selection guides are as follows:

1. As packing factor, F , becomes larger by selection of smaller sized packing; gas capacity for the column is reduced; and pressure drop will increase for a fixed gas flow.
2. Some packings are sized by general dimensions in inches, while some shapes are identified by numbers, #1, #2, #3 for increasing size.
3. Not all packings are manufactured in all materials of construction, i.e. ceramic, various plastics, various metals.
4. Packing size versus tower diameter recommendations; general guides not mandatory, base selection on performance.

Tower Diam., ft	Nominal Packing Size, in.
<1.0	<1
1.0–3.0	1–1½
>3.0	2–3

Table 9-27 shows what Strigle [82] recommends for the maximum liquid loading as related to packing size.

- E. Referring to Figure 9-21B or 21C, read up from the abscissa to the pressure drop line selected, and read across to the ordinate (note differences):

$$\text{Ordinate No.} = \frac{G^2 F \mu^{0.1}}{\rho_G (\rho_L - \rho_G) g_c}, \text{ (Figure 9-21C)} \quad (9-27)$$

$$\text{or, } \frac{G^2 F \nu^{0.1}}{(\rho_G [\rho_L - \rho_G])}, \text{ (Figure 9-21B)} \quad (9-28)$$

$$\text{or, } C_s F^{0.5} \nu^{0.05}, \text{ (Figure 9-21H)} \quad (9-29)$$

Note units change for Figure 9-21G,

$$\text{where } C_s = V_g [\rho_g / (\rho_L - \rho_G)]^{0.5}, \text{ ft/sec} \\ \nu = \text{kinematic liquid viscosity, centistokes} \quad (9-30)$$

Substitute F and the other knowns into the equation and solve for G , the gas mass flow rate, lbs/ft² sec, or G_g , lb/hr-ft², as applicable.

Then, determine the required tower cross-section area and diameter:

$$\text{Diameter, ft} = 1.1283 \left[\frac{\text{Gas rate, lb/sec, } G''}{G, \text{ lb/sec-ft}^2} \right]^{1/2}$$

Effects of Physical Properties

For nonfoaming liquids, capacity of packing is independent of surface tension. Foaming conditions reduce capacity significantly and design should recognize by selecting operating pressure drop at only 50% of normal non-foaming liquid.

For liquids of viscosity of 30 centipoise and lower, effect on capacity is small. For high viscosity select larger packing to reduce pressure drop, and also consult packing manufacturer.

Robbins' [96] correlation for pressure drop in random particle packed towers is based on a "dry packing factor," F_{pd} , whereas most of manufacturer's published values have determined F (packing factor) from wet and dumped data, and is that used in Figures 9-21A–F, 9-21H. Referenced to the tables in Robbins' presentation indicates that the differences may be small between the dry, F_{pd} , and the wet and dumped, F (such as Table 9-26A), being from 0 to 10 points, averaging about 2–3 points lower. The packing manufacturer should be consulted for dry packing factors to use in Robbins' method. The "dry" data simply means that there is no liquid (but gas) flowing. Robbins [96] lists values of F_{pd} for metal, plastic and ceramic packings. Dry bed pressure-drop [96]:

$$\Delta P = C_o \rho_g V_s^2 = C_o F_s^2 = C_o G^2 / \rho_g \quad (9-31A)$$

Values of C_o come from Leva [41].

Robbins' new equation for generalized pressure drop for random tower packings:

$$\Delta P = C_3 G_f^2 (10^{2.7} \times 10^{-5} [L_f]) + 0.4 [L_f / 20,000]^{0.01} \\ \times [C_3 G_f^2 (10^{2.7} \times 10^{-5} [L_f])]^4 \quad (9-31B)$$

$$G_f = G [0.075 / \rho_g]^{0.5} [F_{pd} / 20]^{0.5} = 986 F_s [F_{pd} / 20]^{0.5} \quad (9-31C)$$

$$L_f = L [62.4 / \rho_L] [F_{pd} / 20]^{0.5} \mu^{0.1} \quad (9-31D)$$

The method as described by Robbins [96]:

1. For operating pressures above 1 atm, multiply G_f (Equation 9-31C) by $(10^{0.3}) (\rho_g)$.
2. For small packings with F_{pd} of 200 or greater, substitute $\mu^{0.2}$ in previous equation for $\mu^{0.1}$.
3. For large packings with F_{pd} below 15, use $(20/F_{pd})^{0.5}$ in place of $[F_{pd}/20]^{0.5}$ in previous equation for L_f , Equation 9-31D.
4. Dry bed pressure-drop:

$$F_{pd} = 278 (\Delta P_{db}) / F_s^2 \quad (9-31E)$$

Dry bed pressure drop values usually run 0.1 to 0.5 in. water/ft of packing [96]. Use Equation 9-31B when L_f is below 20,000. Packings operate essentially dry when L_f is below 1,500 (about 3 gpm/ft²) at $F_p = 20$. Pressure drop at flooding is suggested to be predicted by Kister and Gill's relationship [93] presented in this text.

Robbins [96] suggested random packed column design is similar to others presented in this text, but high-lighted to determine diameter of packed column:

1. Establish liquid and vapor rates.
2. Determine fluids physical properties.
3. Select design pressure drop for operations. Suggested values of below 1.0 in. water/ft. Low-pressure, atmospheric, and pressure columns usually require 0.5 to 0.7 in. water/ft, with absorbers and strippers around 0.2–0.6 in. water/ft. For vacuum distillation low values of 0.05–0.6 in. water/ft are often necessary, usually depending on the required boiling point of the bottoms.
4. Calculate L_f/G_f , values of F_{pd} cancel out.
5. Using Equation 9-31B trial and error, calculate using G_f for given L_f/G_f until the desired ΔP is obtained. L_f must be below 20,000. For higher L_f use chart in the original article not included here.
6. Select packing for column, and establish packing factor, F_{pd} .
7. Calculate column cross-section area using the operational gas rate, G , and the calculated value of G_f (gas loading factor):

$$G = G_f / [(0.075/\rho_g)^{0.5} (F_{pd}/20)^{0.5}], \text{ lb/hr/ft}^2 \quad (9-31F)$$
8. Establish tower diameter; Robbins [96] recommends that the tower diameter should be at least 8 times the packing size; if not, repeat the calculations with different packing.

where

- A = tower cross-sectional area, ft²
- C₀ = constant specific to a particular packing
- C₁ = constant specific to a particular packing
- C₃ = 7.4 × 10⁻⁸
- C₄ = 2.7 × 10⁻⁵
- D = tower diameter, ft
- F_p = packing factor, dimensionless
- F_{pd} = dry-bed packing factor, dimensionless
- F_s = V_s (ρ_g)^{0.5}, (ft/sec) (lb/ft³)^{0.5}
- G = gas loading, lb/hr-ft²
- GA = design vapor flow rate, lb/hr
- G_f = gas loading factor
- L = liquid loading, lb/hr-ft²
- L_f = liquid loading factor
- ΔP = specific pressure drop, in. water/ft of packing
- ΔP_{pb} = specific pressure drop through dry bed, in. water/ft of packing
- V_s = superficial gas velocity, ft/sec
- ρ_g = gas density, lb/ft³
- ρ_L = liquid density, lb/ft³
- μ = liquid viscosity, centipoise

Strigle [82] and Kister [93] point out the importance of evaluating data where available to reduce the need for interpolating the GPDC charts. The question of reasonably accurate (±10 to 15%) flooding pressure drop data has been studied by Kister [93], and the results suggest that the establishment of flooding pressure drop curves

such as in Figure 9-21C may not be consistently accurate due to the variations in data used for correlation, i.e., data just as flooding begins, and then at full flooding. The data presented is for gas-liquid systems and not liquid-liquid extraction as Strigle [82] recognizes in his Chapter 11.

Strigle [82] identifies a regime 20% above point F on Figure 9-22 as the maximum hydraulic capacity and is termed the flooding point for atmospheric operations.

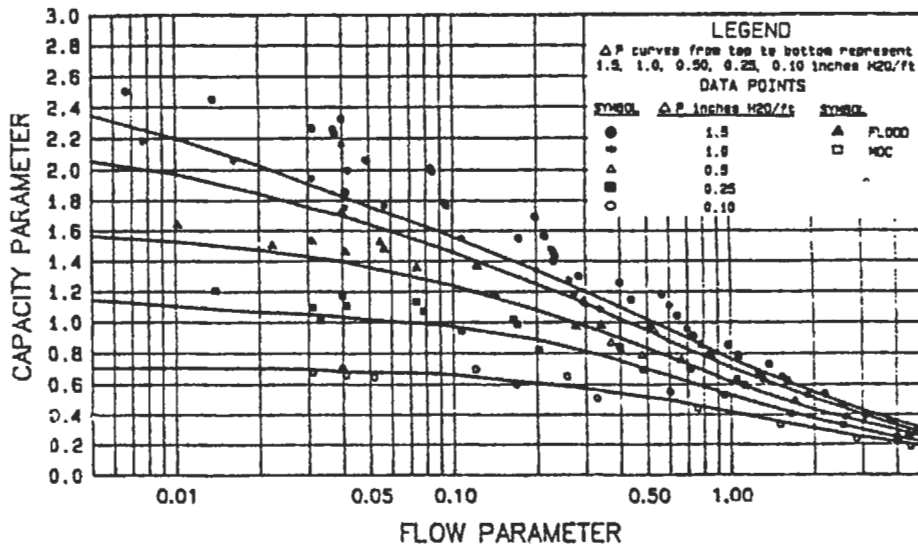
Kister [93] has correlated large quantities of available data for flooding and offers a new correlation based on the same GPDC correlation, which is, as Kister refers to it, the Sherwood-Leva-Eckert (SLE) correlation chart as developed by Strigle [82], Figure 9-21H, for semi-log plot. Kister [90, 93] has presented plots showing the plotted data points on the Strigle or SLE charts for a wide selection of packing. In effect this illustrates how the data fit the generalized charts.

For example, Figures 9-26 and 9-27 from Kister [93] illustrate the collected data superimposed on the SLE chart for the specified pressure drops, specific packing and column size, and packing heights at designated packing factors. Kister [93] recommends using the specific SLE chart (also see Kister [90] for a wide selection of charts) and interpolating and extrapolating the curves when the design/operating requirements fall close to the data points on the selected chart. Extrapolating too far can ruin the validity of the pressure drop results.

When the design/operating requirements are far from the chart's data points, contact the manufacturer of the packing for data and also consider selecting another type and/or size of packing to provide a better fit. In selecting a chart to use, do not overlook the nature of the physical process system, i.e., whether predominantly aqueous or non-aqueous, and whether there are foaming characteristics as well as high or low viscosity fluids. Kister's assessment is that both the study in Reference 93 and Strigle [82] show that the large volume of published data does fit the Strigle [82] charts (Figure 9-21E, F) quite well and gives "good pressure drop predictions." A significant variation is that the curves predict an optimistic (too low) value for non-aqueous systems at high flow parameters of the chart. Also, similar optimistic values are noted for non-aqueous systems at low flow parameters, such as for vacuum distillation, for example. Unfortunately, most data from the data banks were obtained on small scale as compared to industrial size equipment, and so the statistical fit is still not adequate for industrial design with confidence and reliability [93].

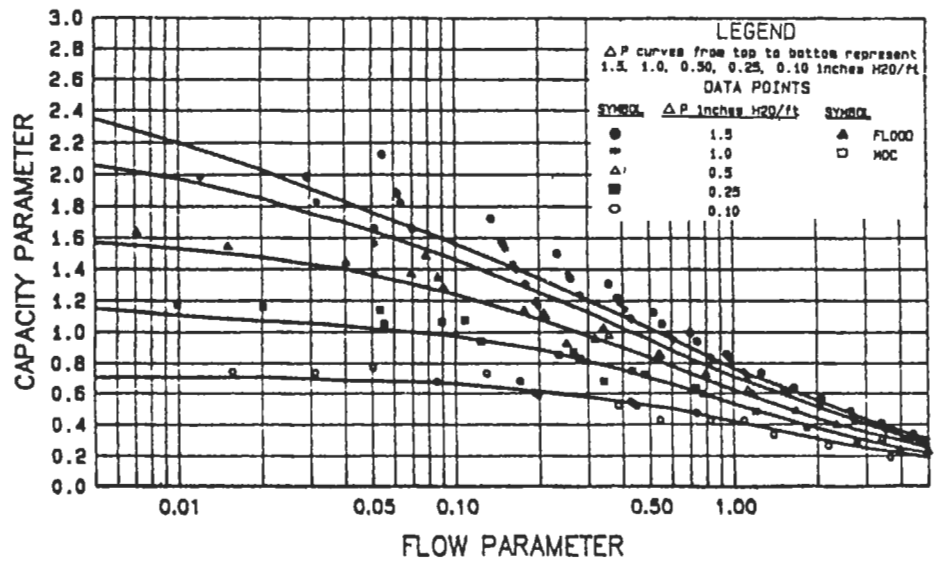
Performance Comparisons

Strigle [94] presents some helpful comparisons referring to Figure 9-22, and Tables 9-28–31 from [94] present



Basis: $F_p=56$
Pressure drop measured in Inches H₂O/ft

Figure 9-26. SLE Data Chart for 1-in. metal Pall rings, aqueous systems, pressure drop only. Data from 15-84 in. dia. test columns with packed heights of 2-10 ft. Reproduced with permission of the American Institute of Chemical Engineers, Kister, H. Z. and Gill, D. R., *Chemical Engineering Progress*, V. 87, No. 2 © (1991) p. 32; all rights reserved.



Basis: $F_p=27$
Pressure drop measured in Inches H₂O/ft

Figure 9-27. SLE Data Chart for 2-in. metal Pall rings, aqueous systems, pressure drop only. Data from 30-84 in. dia. test columns with packed heights of 2-18 ft. Reproduced with permission of the American Institute of Chemical Engineers, Kister, H. Z. and Gill, D. R., *Chemical Engineering Progress*, V. 87, No. 2 © (1991), p. 32; all rights reserved.

valuable key design and operational points related to Figure 9-22.

For design, select C_s above the loading point C (on Figure 9-22) and below the maximum efficiency rate, point D. Usually, the flow at point C is 70 to 75% of that at maximum point F [94]. The design C_s (point E) should allow at least 15% increase in rates before reaching the maximum operating capacity of the packing. This allows for usual variation in operations [94]. The design C_s value should be at least 80 to 85% of the maximum operational C_s (MOC) for the best turn-down condition during operation.

Prediction of Maximum Operating Capacity (MOC)

Strigle [94] proposed this term to better describe the performance of a packed column at or near the previously described "loading point." Kister [93] evaluated the limited published data and proposed using the MOC at 95% of the flood point. The flood point can be estimated by Equation 9-20 or from the plots in References 90 and 93. The data are reported to be within 15-20% of the prediction [93]. See Figure 9-22 for the identification of MOC on the HETP vs. C_s chart. For more accurate information

Table 9-28
Maximum Capacities of Various Packings

Packings	C_s at Maximum Efficiency, ft/sec	ΔP at Maximum Efficiency, H ₂ O/ft	C_s at Maximum Capacity, ft/sec	ΔP at Maximum Capacity, H ₂ O/ft
2 in. Pall Rings	0.295	0.81	0.315	1.29
2 in. Intalox Saddles	0.248	0.96	0.279	1.74
#50 Intalox Metal Packing	0.327	0.52	0.345	0.88
#40 Intalox Metal Packing	0.290	0.60	0.310	0.99
1-½-in. Pall Rings	0.269	0.95	0.287	1.48
1-½ in. Intalox Saddles	0.211	1.09	0.237	1.88
#40 Intalox Metal Packing	0.290	0.60	0.310	0.99
#25 Intalox Metal Packing	0.260	0.96	0.278	1.62

Note: #25 Intalox[®], Norton = app. 1-in. size

#40 Intalox[®], Norton = app. 1½-in. size

#50 Intalox[®], Norton = app. 2-in. size

Reproduced by permission of The American Institute of Chemical Engineers, Strigle, R. F., Jr. and Rukovena, F. *Chem. Eng. Prog.* Vol. 75, Mar. © (1979) p. 86, all rights reserved.

Table 9-29

Design Efficiency and Capacity for Selected Packings

Packing	Design C_s , ft/sec	Design HETP, ft
2 in. Pall Rings	0.256	2.32
2 in. Intalox Saddles	0.216	2.50
#50 Intalox Metal Packing	0.284	2.12
#40 Intalox Metal Packing	0.252	1.74
1-½-in. Pall Rings	0.234	1.78
1-½ in. Intalox Saddles	0.183	1.87
#40 Intalox Metal Packing	0.252	1.74
#25 Intalox Metal Packing	0.226	1.38

Note: #25 Intalox[®], Norton = app. 1-in. size

#40 Intalox[®], Norton = app. 1½-in. size

#50 Intalox[®], Norton = app. 2-in. size

See Figure 9-22 for C_s vs. tower internals.

Used by permission of The American Institute of Chemical Engineers, Strigle, R. F., Jr. and Rukovena, F. *Chem. Eng. Prog.*, Vol. 75, Mar. © (1979) p. 86, all rights reserved.

Table 9-30

Comparison of Maximum Capacity Designs

Packing	Relative Tower Diameter	Relative Packed Height	Relative Packing Volume
2 in. Pall Rings	1.00	1.00	1.00
2 in. Intalox Saddles	1.09	1.08	1.28
#50 Intalox Metal Packing	0.95	0.91	0.82
#40 Intalox Metal Packing	1.01	0.75	0.76
1-½-in. Pall Rings	1.00	1.00	1.00
1-½ in. Intalox Saddles	1.13	1.05	1.34
#40 Intalox Metal Packing	0.96	0.98	0.91
#25 Intalox Metal Packing	1.02	0.78	0.80

Reproduced by permission: The American Institute of Chemical Engineers, Strigle, R. F., Jr., and Rukovena, F., *Chem. Eng. Prog.* Vol. 75, Mar. © (1979) p. 86, all rights reserved.

Table 9-31

Comparison of Constant Pressure Drop Designs

$\Delta P = 0.5$ in Water Per Theoretical Plate

Packing	Relative Diameter	Relative Height	Relative Volume
2 in. Pall Rings	1.00	1.00	1.00
2 in. Intalox Saddles	1.10	1.08	1.31
#50 Intalox Metal Packing	0.85	0.91	0.66
#40 Intalox Metal Packing	0.89	0.75	0.59
1-½ in. Pall Rings	1.00	1.00	1.00
1-½ in. Intalox Saddles	1.13	1.05	1.34
#40 Intalox Metal Packing	0.87	0.98	0.74
#25 Intalox Metal Packing	0.97	0.78	0.73

Reproduced by permission: The American Institute of Chemical Engineers, Strigle, R. F., Jr., and Rukovena, F., *Chem. Eng. Prog.* Vol. 75, Mar. © (1979) p. 86, all rights reserved.

contact the respective packing manufacturers as most of their data is yet unpublished.

Capacity Basis for Design

Whether for a distillation, absorption, or stripping system the material balance should be established around the top, bottom, and feed sections of the column. Then, using these liquid and vapor rates at actual flowing conditions, determine the flooding and maximum operating points or conditions. Then, using Figures 9-21B, -21E, or -21F, establish pressure drop, or assume a pressure drop and back-calculate a vapor flow rate, and from this a column diam-

eter. Even though the column diameter may show a difference between the requirements at the top, bottom and/or middle of the column, do not be too quick to try to create a column design with diameter variations as the results vary up the column. Sometimes for vacuum columns the calculations show that a larger diameter in the upper section would perform better, so check out using the same diameter throughout the column, because this is the least expensive, and somewhat easier to fit all the parts together. Even though the pressure drop or HETP may not be the same throughout [154, 156, 157], adjustments can be made, if warranted, to even changing the packing size or style/type in various segments of the column. This requires some careful calculations for the effective HETP and the total height of the individual sections and then the total column/tower. But, it is often worth the effort, particularly for tall towers, say above 20–30 ft of packing. For low pressures as well as other columns, determine the pressure drop for each packed section of the column, plus the pressure drop through the internal components.

Proprietary Random Packing Design Guides

Norton Intalox Metal Tower Packing (IMTP®)

Norton offers a new high performance system centered around an improved Intalox® metal tower packing, including effective internals to provide the distribution and pressure drop consistent with the higher performance of the packing itself.

Figures 9-6J and -6U illustrate the IMTP packing. The manufacturer's key performance descriptions are [83]:

1. Greater capacity and efficiency than fractionation trays and other dumped packings.
2. Pressure drop approximately 40% lower than equivalent size Pall rings.
3. Low liquid hold-up.
4. Structural strength allows packing depths to 50 ft or more
5. Easy to use in distillation, from deep vacuum where low pressure drop is beneficial, to high pressure where capacity surpasses many trays.
6. HETP values nearly independent of flow rate.
7. Packing properties related to a performance curve:
 - (a) The system base HETP of a packing, which is the flat HETP value produced by uniform distribution.
 - (b) The efficient capacity (not the same as hydraulic capacity or flood point) of a packing, which is the greatest vapor rate at which the packing still maintains the system base HETP. Norton [96] rates packings by percent of efficient capacity rather than percent of flood.

Capacity Correlation [83]

Figures 9-21G and 9-21I present the proprietary estimating capacity charts for the various sizes of the Intalox® packing for a non-foaming system. The system base HETP of a packing is the flat HETP value produced by uniform distribution, see Figure 9-22.

The terminology for the chart referenced to Norton's [83] Intalox® random packing of various sizes designated as:

Size No.	Dimensions, in.
15	-
25	1
40	-
50	2
70	-

Design information used by permission of Norton Chemical Process Products Co.

$$\text{Flow parameter, } X = L/G \sqrt{\rho_G / \rho_L}, \text{ chart} \quad (9-32)$$

$$\text{Capacity parameter, } C_s = V \sqrt{\rho_G / (\rho_L - \rho_G)}, \text{ ft/sec or m/sec} \quad (9-33)$$

Capacity rating, C_o = feet/sec., or m/sec, from chart

$$\text{Efficient capacity, } C_{sc} = C_o \left[\frac{\sigma}{20} \right]^{0.16} \left[\frac{\mu}{0.2} \right]^{-0.11} \text{ ft./sec./or meters/sec.} \quad (9-34)$$

This is the greatest vapor rate at which the packing still maintains the system base HETP [83].

$$\text{Capacity rating} = [C_s/C_{sc}] (100) = \% \text{ capacity [83]}$$

Pressure drop equation: For IMTP packing, non-foaming system, use: Figure 9-21G or I.

where flow parameter, X = as previously noted, Equation 9-32.

$$\text{Capacity parameter, } Y = F C_s^2 v^{0.1}$$

Value for F coefficient (used by permission Norton [83])

IMTP size	No. 15	No. 25	No. 40	No. 50	No. 70
F when C_s in m/sec	549	441	258	194	129
F when C_s in ft/sec	51	41	24	18	12

where ν = liquid kinematic viscosity, centistokes

= μ / (sp.gr) centistokes

μ = liquid viscosity, centipoise

σ = surface tension, dynes/cm

L = liquid mass rate, lb/hr

G = gas mass rate, lb/hr

ρ_L = liquid density, lb/ft³

ρ_G = gas density, lb/ft³

$V_g = V$ = superficial gas velocity, ft/sec or m/sec

Note: 1 in. water/ft = 1.87 mmHg/ft = 6.15 mmHg/m

Superficial vapor velocity, $V_s = G/(\rho_G A)$ (9-35)

where $A = (\pi/4) D^2$, ft²

Packing Efficiency/Performance for IMTP Packing [96]

This is usually expressed as HETP, and for the IMTP packing when a high performance (uniform) liquid distributor is used in a column, the HETP is independent of the tower diameter and packing depth. Norton [83] has developed a concept for evaluating HETP for fluids (a) non-aqueous, (b) non-reacting and non-ionizing, and (c) low relative volatility (less than three) [83], as follows:

System base HETP of IMTP packing for distillation and reboiled stripping:

(A) System Base HETP = $A \left[\frac{\sigma}{20} \right]^{-0.16} (1.78)^\mu$, For $\mu \leq 0.4$ cp (9-36)

(B) System Base HETP = $B \left[\frac{\sigma}{20} \right]^{-0.19} \left[\frac{\mu}{0.2} \right]^{0.21}$ (9-37)
for $\mu > 0.4$ cp

expressed as millimeters or inches, depending on constants used for A and B in the previous equations. If $\sigma > 27$, use $\sigma = 27$, dynes/cm; μ = liquid viscosity, cp. Use the values of A and B as follows [Reference 83 by permission]:

Values of A and B for Equations 9-36 and 37

IMTP Size	No. 15	No. 25	No. 40	No. 50	No. 70
A-mm	271.3	331.4	400.7	524.9	759.9
A-in	10.68	13.05	15.78	20.67	29.92
B-mm	296.7	366.1	438.3	579.9	831.2
B-in	11.68	14.41	17.25	22.83	32.72

For commercial towers with good liquid/vapor distribution Norton [96] recommends standard designs use HETP values 13% above the system base HETP. If the system under consideration does not meet the physical properties limit, either use a conservative estimate or use actual plant or published data for the system. For comparison of HETP values for selected packings see Strigle and Rukovena [94], Figure 9-28.

Example 9-1, Hydrocarbon Stripper Design (Figure 9-29)

Design a packed tower splitter for a light hydrocarbon plant. The conditions of operation as determined from material balance are:

Operate at 430 psig, feed from ethylene tower at purification unit.

Feed: Volume: 55% ethylene
45% ethane

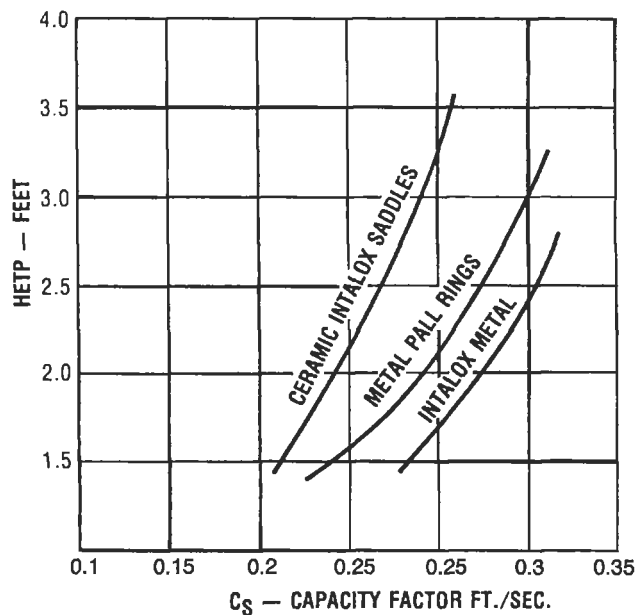


Figure 9-28. Packing comparison at design point for Intalox® ceramic saddles, metal pall rings, and metal Intalox®. Reproduced by permission of American Institute of Chemical Engineers, Strigle, R. F., Jr. and Rukovena, F., *Chemical Engineering Progress*, Mar. © (1979) p. 86; all rights reserved.

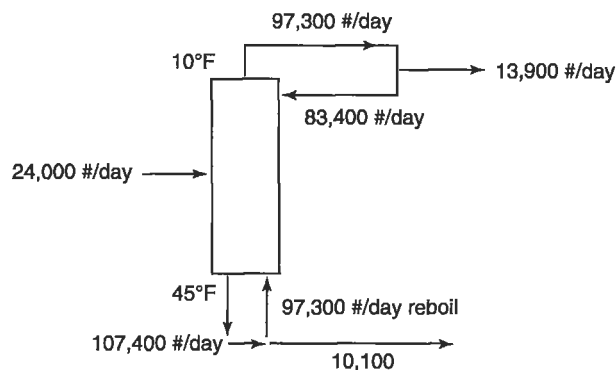


Figure 9-29. LHC plant stripper using packed tower; for Example 9-1.

Specifications to be:

- Overhead: 90% ethylene
- Bottoms: 95% ethane
- Feed: 13,000 lb/day ethylene
11,000 lb/day ethane

Determine feed temperature from ethylene tower.

- Bottoms: 25°F, Boiling point feed
- Bubble point of bottoms: At 445 psia

Composition x_B		$K@47^\circ F$	K_x	$K@45^\circ F$	K_x
Ethylene	0.05	1.36	0.068	1.35	0.067
Ethane	0.95	1.0	0.95	0.97	0.921
	1.00			1.018	0.988

Therefore, bubble point = 46°F

$$\alpha_{\text{bottoms}} = 1.35/0.98 = 1.38$$

Dew point on overhead: at 445 psia

Composition	y_{OH}	$K@15^\circ F$	y/K
Ethylene	0.90	1.05	0.857
Ethane	0.10	0.75	0.138
	1.00		0.995

Dew point on overhead: 15°F

Bubble point on overhead: Try 10°F at 445 psia

Composition	x_D	K	Kx
Ethylene	0.90	1.00	0.90
Ethane	0.10	0.80	0.08
	1.00		0.98

Bubble point > 10°F < 15°F = 12°F

$$\alpha_{\text{Top}} = 1.05/0.73 = 1.44$$

$$\alpha_{\text{avg}} = \sqrt{\alpha_{\text{top}} \alpha_{\text{bottom}}} = \sqrt{(1.38)(1.44)} = 1.41$$

Minimum Trays at Total Reflux

Fenske Equation:

$$N + 1 = \frac{\log(x_{1k}/x_{hk})_D (x_{hk}/x_{1k})_B}{\log \alpha_{\text{avg}}}$$

$$= \frac{\log(0.90/0.10)(0.95/0.05)}{\log 1.41}$$

$$= 14.8 \text{ theoretical trays}$$

Minimum Reflux

Gilliland Plot:

$$(L/D)_{\text{Min}} = \frac{X_D [1 + (\alpha - 1) x_F] - \alpha x_F}{(\alpha - 1) (x_F) (1 - x_F)}$$

$$= \frac{0.90 [1 + 0.41 (0.55)] - 0.775}{(6.41) (0.55) (0.45)} = 3.23$$

Use actual L/D = 6 : 1

Theoretical Plates vs. Reflux

Gilliland Plot

(L/D)	Theoretical Plates
3.25	Infinity
4.0	28.4
5.0	22.4
6.0	20.0
7.0	18.6
8.0	17.8
Infinity	14.2

Refer to Figure 9-30 for plot for this example.

Refer to Figure 9-29 for diagram of loading. From a material balance using (L/D) = 6.0; theoretical trays = 20

- (a) Feed = 24,000 lb/day
- (b) Distillate product: 13,900 lb/day
- (c) Reflux into column: 83,400 lb/day @ 6:1 reflux, L/D
- (d) Total gross overhead: 97,300 lb/day
- (e) Total bottoms out: 10,100 lb/day

Top of Column

$$\rho_v = \frac{(28)(445)(492)}{(359)(14.7)(470)} = 2.47 \text{ lb/ft}^3 \text{ @ } 430 \text{ psig \& } 10^\circ F$$

$$\rho_L = 0.39 (62.4) = 24.3 \text{ lb/ft}^3$$

Liquid viscosity = 0.07 cp

From Figure 9-21C:

$$L/G = \sqrt{\rho_v / \rho_l} = 83,400 / 97,300 \sqrt{2.47 / 24.3} = 0.27$$

Read:

$$\frac{G^2 F \mu^{0.1}}{\rho_G (\rho_L - \rho_G) g_c} = 0.067 \text{ (flooding, avg.)}$$

For average loading condition, read ordinate = 0.030

For average flooding: (from chart) using 1-in. metal Pall rings, with F = 56.

$$0.067 = G^2 (56) (0.07)^{0.1} / (32.2) (24.3 - 2.47) (2.47)$$

$$G = 1.648, \text{ ft/sec/ft}^2 \text{ for average flooding}$$

$$V_{\text{loading}} = 1.648 / 2.47 = 0.667 \text{ ft/sec}$$

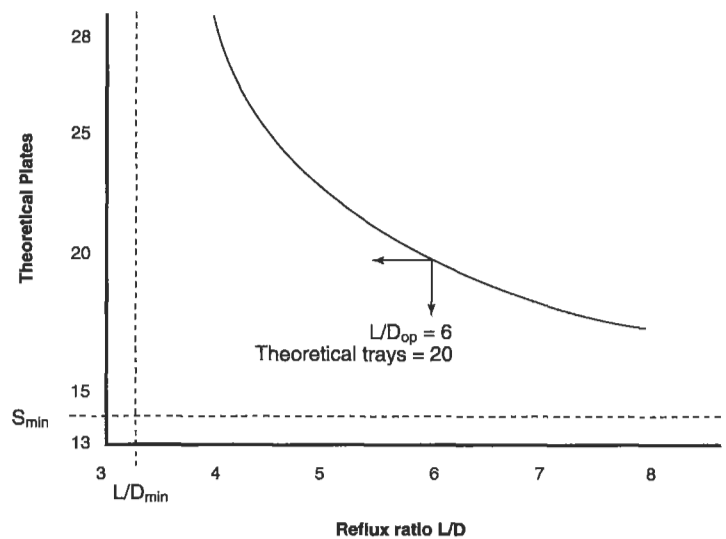


Figure 9-30. Gilliland Plot for Example 9-1.

Volume flow = $97,300 / (24) (3,600) (2.47) = 0.4559 \text{ ft}^3/\text{sec}$

Area required: $= .4559 / 0.667 = 0.6835 \text{ ft}^2 (= 98.4 \text{ in}^2)$

Column diameter = 11.19 in.

Use = 16-in. I.D. column

Bottom of Column:

$\mu_v = 0.0095 \text{ cp}$

$\mu_L = 0.07 \text{ cp}$

$$\rho_v = \frac{30 (445) (492)}{359 (14.7) (505)} = 2.47 \text{ lb/ft}^3$$

$$\rho_L = 0.4 (62.4) = 25 \text{ lb/ft}^3$$

$$L/G = \sqrt{\rho_v / \rho_L} = (107,400 / 97,300) \sqrt{2.47 / 25} = 0.346$$

Using packing factor, $F = 56$ for 1-in. Pall metal rings

Reading chart:

$$G^2 F \mu^{0.1} / (\rho_G) (\rho_L - \rho_G) (g_c) = 0.057, \text{ flooding, for reference, loading reads} = 0.036$$

$$G^2 (56) (0.07)^{0.1} / (2.47) (25 - 2.47) (32.2) = G^2 (0.02394)$$

$$\text{Area Req'd.} = 0.4559 / 0.4048 = 1.126 \text{ ft}^2 = 162.17 \text{ in}^2$$

Diameter = 14½-in. Use 16-in. diameter, See Appendix A-18

It is better to use smaller packing (less than 1 in.) in this diameter column (16-in. I.D.), such as ¾ in. if recalculated above. Packing of ½ in. or ¾ in. are better in this size column; however the effects of packing factor should be calculated if changed from ¾ in. packing.

HETP: Use HETP = 18 in. based on on-site column data and manufacturer's confirmation that for ¾ in. Pall rings in this system, the 18 in. HETP should perform satisfactorily. Note: For each design verify expected HETP through the manufacturer.

Redistribute the liquid every 10 ft and allow 2 ft additional for redistribution = 36 ft. Then use 4–10 ft sections of packing. For 20 theoretical plates, total performance packed height 20 (18 in./12 in.) = 30 ft. Allow for loss of equilibrium at (1) reflux entrance = 1 HETP and (2) feed entrance = 2 HETP and (3) redistribution (2) = 2 HETP; totals 5 HETP.

$5 \times 1.5 \text{ ft} = 7.5 \text{ ft}$ extra packing.

Total packing to install = $30 \text{ ft} + 7.5 \text{ ft} = 37.5 \text{ ft}$; Use 40 ft. Feed point, based on Kirkbride (See Chapter 8):

$$\log \frac{N_N}{N_M} = 0.206 \log \left[\left(\frac{B}{D} \right) \left(\frac{x_{hF}}{x_{IF}} \right) \left(\frac{x_{1B}}{x_{hD}} \right)^2 \right] \quad (9-38)$$

$$\begin{aligned} \log \frac{N_N}{N_M} &= 0.206 \log \left(\frac{10,100}{13,900} \right) \left(\frac{0.45}{0.55} \right) \left(\frac{0.05}{0.10} \right)^2 \\ &= 0.206 \log 0.149 \\ &= -0.206 (0.837) \\ &= -0.1725 \end{aligned}$$

$$\log \frac{N_M}{N_N} = 0.1725$$

$$N_M / N_N = 1.487$$

$$N_M + N_N = 40 \text{ ft}$$

$$1.487 (N_N) + N_N = 40$$

Then: $N_N = 16.08 \text{ ft}$, rectifying section; use 1 16.5-ft section
 $N_M = 23.92 \text{ ft}$, stripping section; use 2 12-ft sections

Allow 2 ft space between support of top section and redistributor of section 2 (from top).

Estimated pressure drop of loading from Figure 9-21C: = 0.40 in water/ft of packing. For total *packed* height, $\Delta P \approx (0.40) (16.5 + 24) = 16.2 \text{ in. water total (packing only)}$.

Preliminary evaluation of condenser requirements:

Condense: 97,300 lb/day

$$L_v = 115 \text{ Btu/lb}$$

$$q = 97,300 (115) / 24 = 466,229 \text{ Btu/hr}$$

For *approximate* estimate: assume overall heat transfer coefficient,

$$U = 100 \text{ Btu/hr (ft}^2 \text{) (}^\circ\text{F)}$$

$$\Delta T = 35^\circ\text{F for } (-25^\circ\text{F propylene)}$$

$$\text{Area Estimated} = 466,229 / (100) (35) = 133 \text{ ft}^2 \text{ (outside tubes)}$$

Recommend kettle type condenser (boiling propylene) (see chapter on Heat Transfer, Volume 3).

Nutter Ring [97]

Nutter offers an improved high performance random packing identified as Nutter Ring™, see Figure 9-6K. To achieve the best performance from any random packing, the liquid distributor must be level and the distributor points of the discharging liquid to the packing must be uniformly distributed, see earlier discussion on this topic.

The manufacturer's key performance descriptions and claims are:

1. Comparative tests at Fractionation Research, Inc. (FRI) [154] showed the No. 2 Nutter ring™ to have greater usable efficiency-capacity profile, with substantially lower pressure drop than is achieved with slotted rings. Usable capacity is comparable to 3½-in. Pall rings (see Figures 9-31A-C).
2. Ring form provides multiple circular crimped strips to encourage liquid surface renewal.

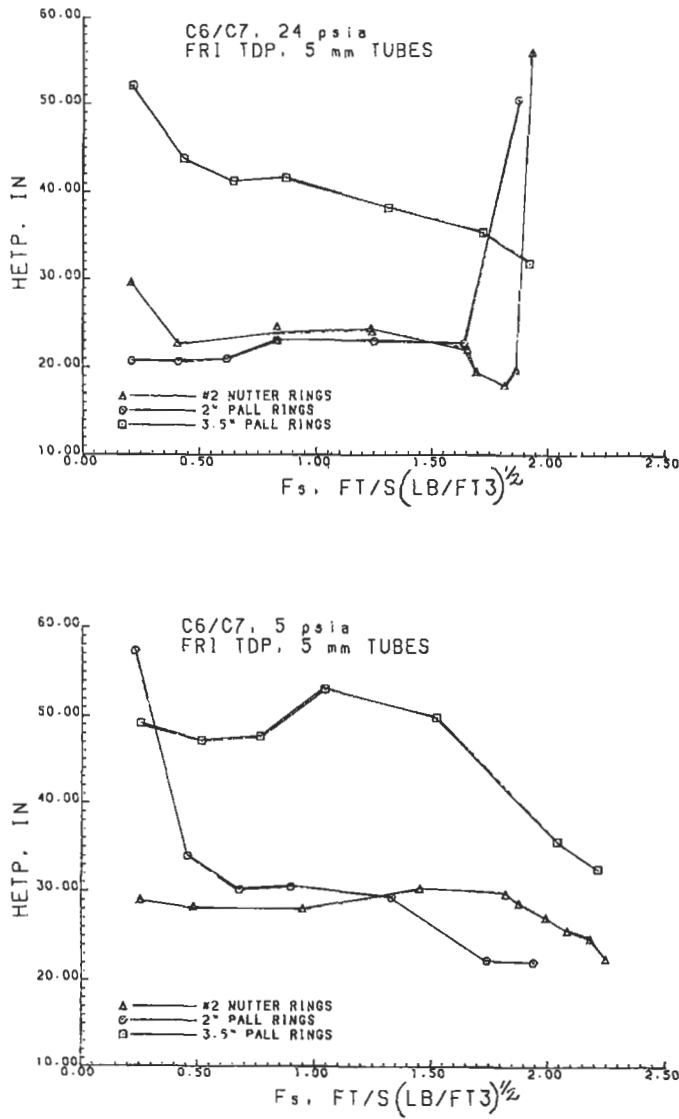


Figure 9-31A. Comparison of HETP for No. 2 Nutter Rings™ and Pall rings in a C₆/C₇ system at 24 psia and 5 psia using the FRI tubed drip pan distributor. Data prepared and used by permission of Nutter Engineering, Harsco Corp. and by special permission of Fractionation Research, Inc.; all rights reserved.

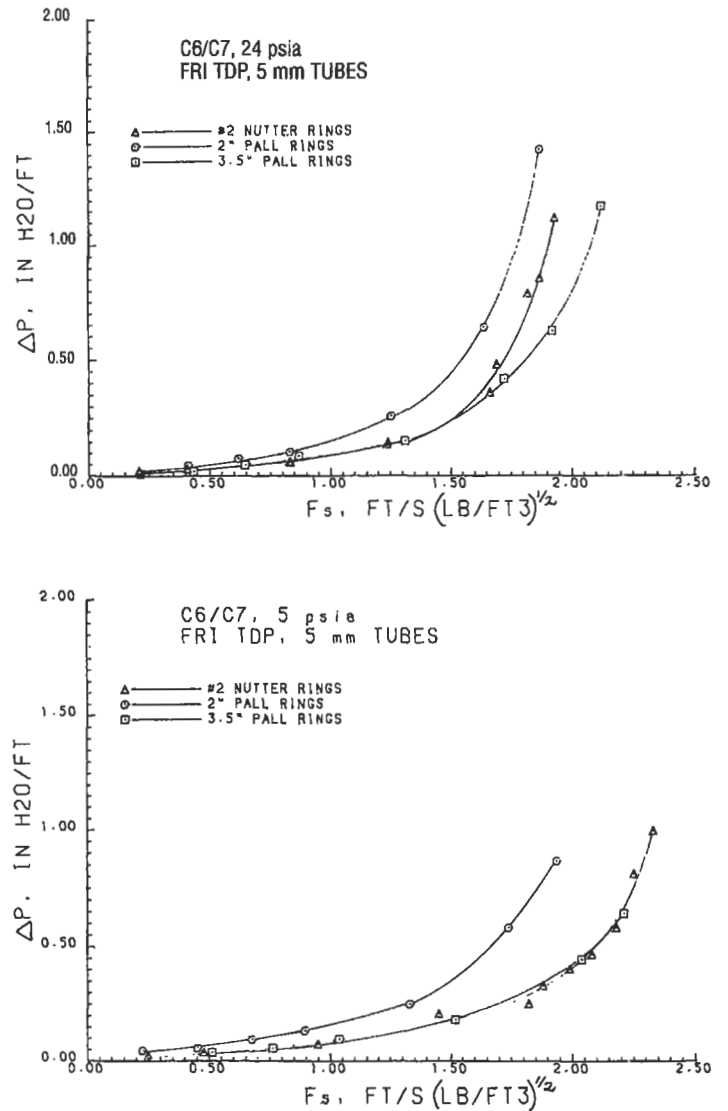


Figure 9-31B. Comparison of pressure drop for No. 2 Nutter Rings™ and Pall rings in a C₆/C₇ system at 24 psia and 5 psia using the FRI tubed drip pan distributor. Data prepared and used by permission of Nutter Engineering, Harsco Corp. and by special permission of Fractionation Research, Inc.; all rights reserved.

3. Perforated central trough enhances lateral liquid spreading and effectively wets the outside surface facing vapor flow.
4. Heavily ribbed main element for a high strength-to-weight ratio.
5. A pair of tapered slots and hoops provide maximum randomness with minimal nesting.
6. Efficiency enhanced by item (2) above, and the No. 2 Nutter Ring is better than 2-in. Pall rings [155, 157].
7. Superior surface utilization in mass and heat transfer, allowing shorter packed bed heights. Turn-down performance is superior over 2-in. and 3½-in. Pall rings.

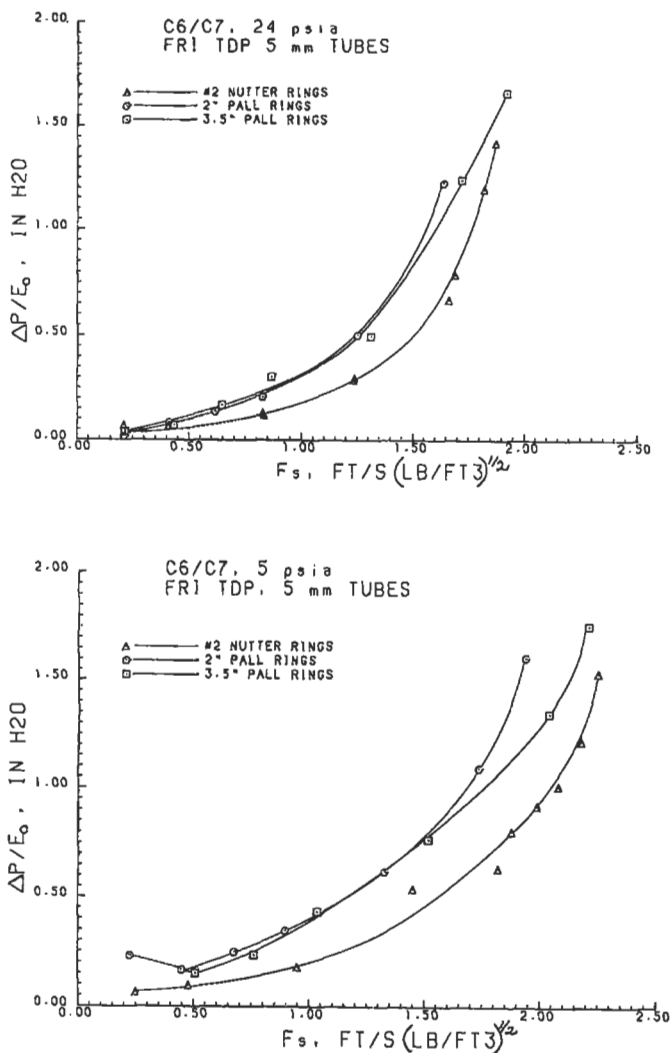


Figure 9-31C. Comparison of P/E_0 for No. 2 Nutter Rings™ and Pall rings in a C_6/C_7 system at 24 psia and 5 psia using the FRI tubed drip pan distributor. Data prepared and used by permission of Nutter Engineering, Harsco Corp. and by special permission of Fractionation Research, Inc.; all rights reserved.

8. Strength to weight ratio allows bed heights of 50 ft.
9. Lower pressure drop and greater usable capacity allow use of smaller diameter columns. Pressure drop per stage is 30–50% less than either size Pall ring.
10. Reproducible performance assured through uniform randomness [156].
11. All rings in sizes No. 0.7 to No. 3 diameter are proportional on all dimensions for accuracy in scale-up of pressure drop, capacity, and efficiency. See Figure 9-6K.
12. Plastic Nutter Rings™ are rigid and energy efficient, and permit applications to produce pressure drops per theoretical stage and bed heights, not attainable with other random particle packing.

Capacity Correlation [98]

This design presentation is proprietary to Nutter Engineering and is definitely more accurate than applying the Nutter Ring™ to the generalized pressure drop correlations (Figure 9-21B to -21F). Figures 9-21G and 9-21I do not apply because they are proprietary to another manufacturer. The procedures to follow supercede the equations in Nutter and Perry [99, 98], and are used by permission of Nutter Engineering, a Harsco Corp.

1. Determine % useful capacity; Assume a column diameter, or calculate using an existing column under study. Usable capacity is defined as the maximum loading condition where efficiency does not deteriorate significantly from that achieved over a lower range of loadings [99]. For the Nutter ring, the limiting pressure drop for usable capacity is 1 in. of hot liquid for low pressure systems. Designs should not exceed this value. This has been shown to hold for C_6 – C_7 system at 5 psia and for hydrocarbons at atmospheric to 24 psia. (See Figures 9-31A and 9-31B) [98].

$$\% \text{ Useful capacity} = (100) (C_s) (F_c/C_2) \quad (9-39)$$

where

$$C_s = \text{vapor rate} = V_s [\rho_v / (\rho_1 - \rho_v)]^{0.5}, \text{ ft/sec} \quad (9-40)$$

$$\rho_v = \text{vapor/gas phase density, lb/ft}^3$$

$$\rho_1 = \text{liquid phase density, lb/ft}^3$$

$$V_s = \text{vapor superficial velocity, ft/sec}$$

$$C_2 = \text{wet pressure drop intercept coefficient}$$

$$= (F_{Q1}) (F_{\text{size}}) (F_{\text{system}}) \quad (9-41)$$

$$F_{Q1} = \text{liquid rate factor for } C_2$$

$$F_{\text{size}} = \text{size factor for } C_2$$

$$F_{\text{system}} = \text{physical properties factor for } C_2$$

$$F_c = \text{useful system capacity factor}$$

$$= (0.535) ((\rho_1 - \rho_v) / \rho_v)^{0.12} \quad (9-42)$$

$$\text{Limits: } 0.728 \leq F_c \leq 1.04$$

$$F_{Q1} = 0.428 - 0.0141 Q_1 + 0.000326 Q_1^2 - 3.7 \times 10^{-6} Q_1^3 + 1.47 \times 10^{-8} Q_1^4 \quad (9-43)$$

$$Q_1 = \text{liquid superficial velocity, gpm/ft}^2$$

$$F_s = \text{vapor rate, } V_s (\rho_v)^{0.5}, \text{ (ft/sec) (lb/ft}^3)^{0.5} \quad (9-44)$$

$$F_{\text{size}} = X_1 + X_2 (Q_1) \quad (9-45)$$

$$X_1, X_2 = \text{constants from Table 9-32}$$

$$F_{\text{system}} = 1.130 (\sigma / \rho_1)^{0.179} \quad (9-46)$$

$$\sigma = \text{surface tension, liquid, dynes/cm}$$

$$\% \text{ System limit vapor velocity} = 100 V_s / [(0.760) (\sigma / \rho_v)^{0.461}] \quad (9-47)$$

(not applicable when $((\rho_1 - \rho_v) / \rho_v)^{0.5} > 4.5$)

Pressure drop: dry bed:

$$\Delta P_d = C_1 (F_s)^2 = \text{dry bed pressure drop, in. water/ft} \quad (9-48)$$

Table 9-32
Nutter Ring Hydraulic Coefficients

Nutter Ring ^(TM) Size	C1	X ₁	X ₂	X ₃	X ₄
0.7	0.141	0.735	-0.00646	1.0	0.05
1	0.095	0.870	-0.00562	1.10	0.08
1.5	0.070	0.969	-0.00230	1.12	0.08
2	0.059	1.000	0.0	1.15	0.08
2.5	0.051	1.0394	0.000653	1.15	0.08
3	0.037	1.124	0.002076	1.15	0.10

Used by permission of Nutter Engineering, a Harsco Corp.

where C₁ = coefficient from Table 9-32.

Operating pressure drop:

$$\Delta P = e^{[(C_s - C_2)/C_3]}, \text{ in. liquid/ft} \quad (9-49)$$

where C₃ = max. value of [(Z_{Q1}) (X₃)], or [X₄ itself] (9-50)

C₃ = wet pressure drop slope coefficient

$$Z_{Q1} = 0.1084 - 0.00350 Q_1 + 0.0000438 Q_1^2 + 7.67 \times 10^{-7} Q_1^3 - 1.4 \times 10^{-8} Q_1^4 \quad (9-51)$$

Z_{Q1} = liquid rate factor for C₃, in. water/ft

X₃, X₄ = constants from Table 9-32.

ΔP_d = dry bed pressure drop, in. water/ft

ΔP = operating pressure drop, in. liquid/ft

e = base of natural logarithms

X₁, X₂ = curve fit coefficients for C₂, Table 9-32.

X₃, X₄ = curve fit coefficients for C₃, Table 9-32.

μ = viscosity, centipoise, cp

Subscripts

g, v = gas or vapor phase

l = liquid phase

s = based on tower cross-sectional area

Figures 9-32A and B [98] illustrate the correlation of wet pressure drop and system vapor rate at various liquid rates for No. 2 Nutter rings; however, other available data indicate that other sizes of Nutter rings, Pall rings, and selected other packing shapes correlate in the same manner.

Figures 9-33A and B illustrate the fit of data taken by FRI on a commercial size column for hydrocarbon systems, using No. 2.5 Nutter rings at three different pressures, and comparing the latest Nutter proprietary correlation previously presented.

When considering pressure drop models based only on water, hydrocarbons system capacity can be significantly overstated. For Nutter random ring packings the pressure drop/capacity models fit the data within ±10% over the range of commercial interest, i.e., 0.1 to 1.0 in. water/ft of packing. Pressure drop values for design operation should

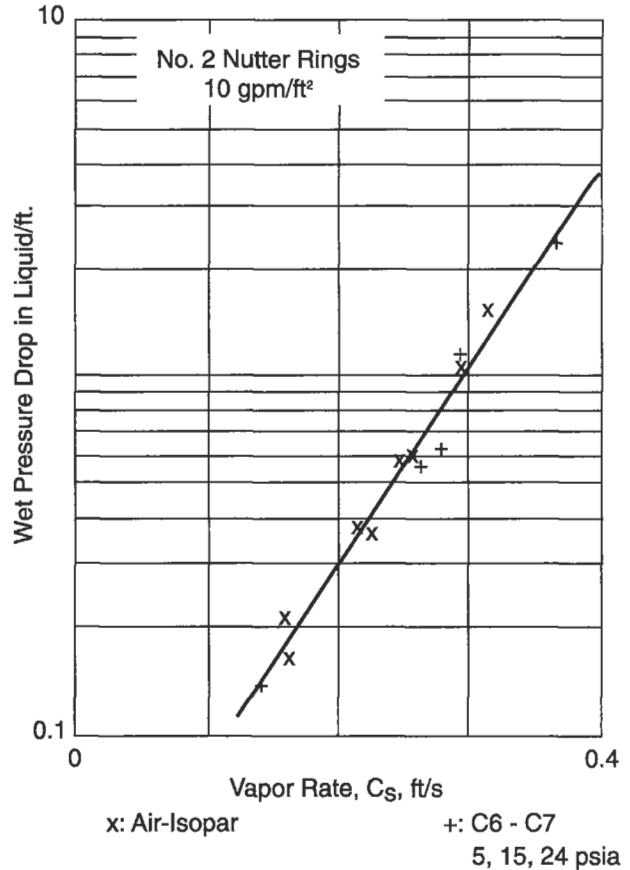


Figure 9-32A. Correlation of No. 2 Nutter RingsTM superficial capacity vs. wet pressure drop for 4 data sets and 3 separate tests. Note the 10:1 pressure drop range. Reproduced by permission from Nutter, D. E. and Perry, D., presented at New Orleans, La. meeting of American Institute of Chemical Engineers, March (1988), and by special permission of Fractionation Research, Inc.; all rights reserved.

not exceed 1.0 in. water/ft. This is generally 80% of flood capacity or 90% of useful capacity.

Tests by FRI and Nutter [132] emphasize that distribution of liquid must be uniform and at minimum values to achieve good HETP values over a range of system pressures for hydrocarbons distillation.

Glitsch performance data for their Cascade Mini-Ring[®] are shown in Figures 9-34A, B, and C for HETP with other published data and pressure drop for comparison with Pall rings and sieve trays. Note the abbreviation CMR stands for Cascade Mini-Rings.

Generally, it is not recommended to specify any packed section in a random packed tower to be greater than 20 ft in height. However, some packing manufacturers state that their packings will physically sustain greater heights and continue to produce good HETP values by maintaining a good uniform liquid flow internally, and that the liq-

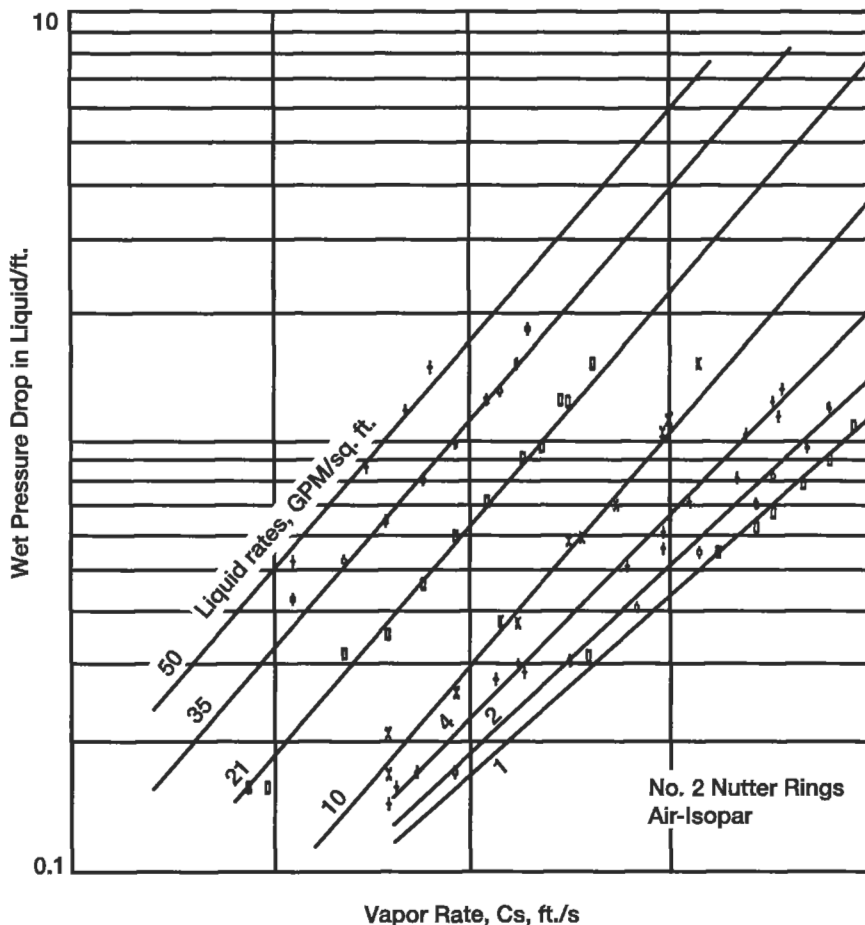


Figure 9-32B. Correlation of No. 2 Nutter Ring™ for 7 liquid rates versus wet pressure drop. Reproduced by permission from Nutter, D. E. and Perry, D., presented at New Orleans, La. meeting of American Institute of Chemical Engineers, March (1988), and by special permission of Fractional Research, Inc.; all rights reserved.

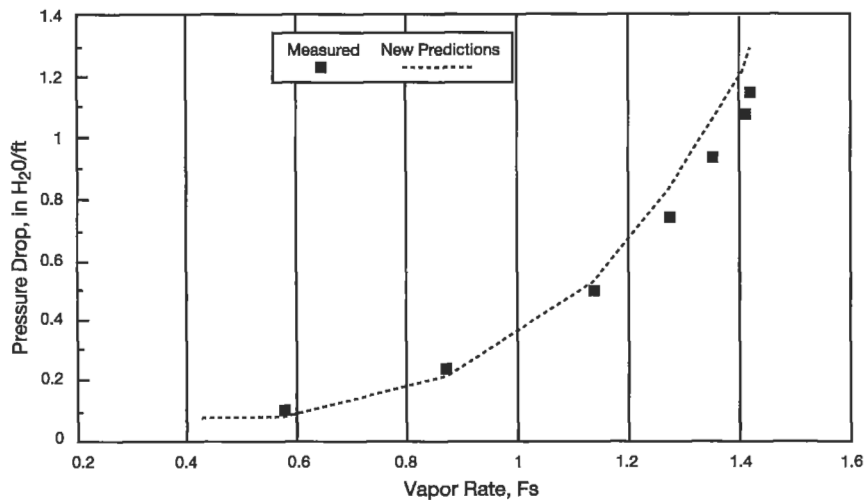


Figure 9-33A. Comparison of hydrocarbon systems fit to Nutter Correlation at 165 psia (No. 2.5 Nutter Ring™). Used by permission of Nutter Engineering Co., Harsco Corp. and by special permission of Fractionation Research, Inc.; all rights reserved.

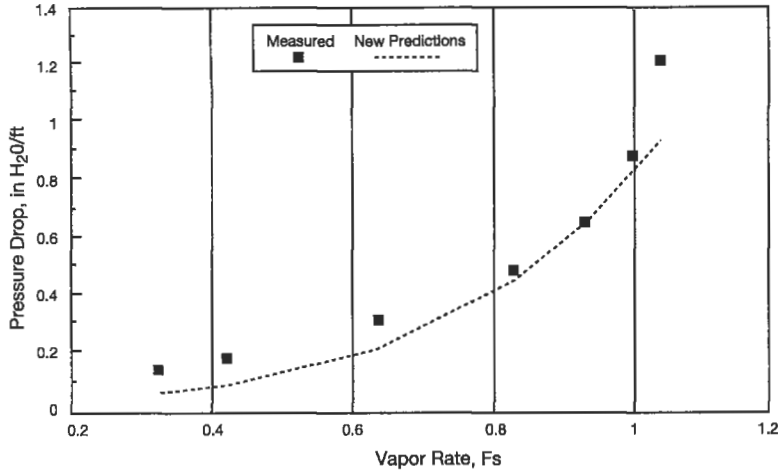


Figure 9-33B. Comparison of hydrocarbon systems fit to Nutter Correlation at 300 psia (No. 2.5 Nutter Ring™). Used by permission Nutter Engineering Co., Harsco Corp. and by special permission of Fractionation Research, Inc.; all rights reserved.

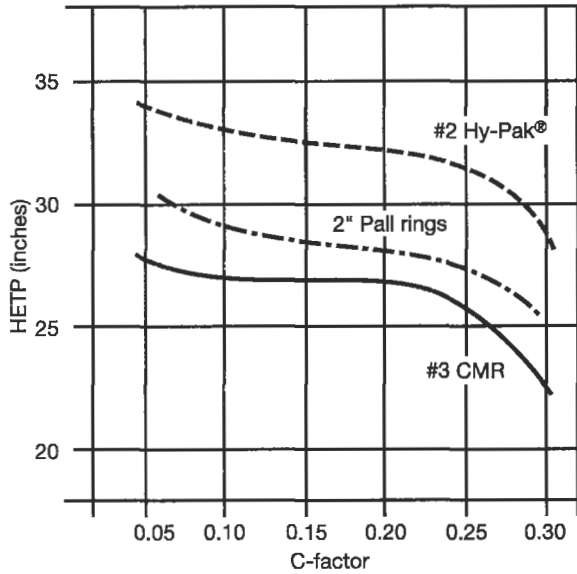


Figure 9-34A. Efficiency versus C-factor for various metal packings. Iso-octane/toluene, 740 mm Hg, reflux ratio 14:1, 15-in. I.D. column, 10-ft bed height. Not Glitsch test data. Note: CMR = Cascade Mini-ring®. Used by permission of Glitsch, Inc., Bull. 345.

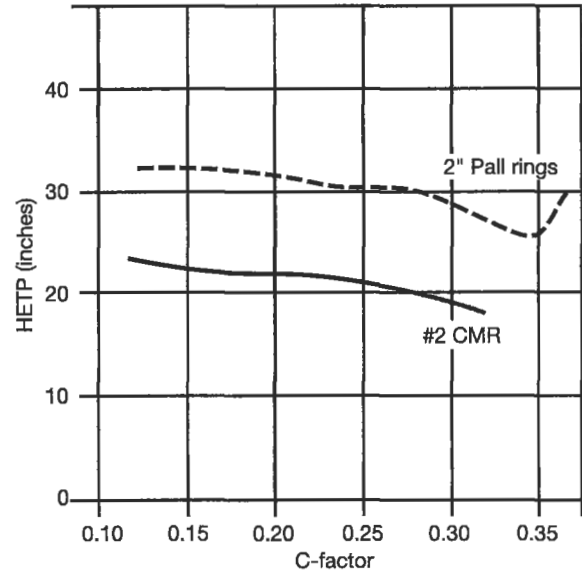


Figure 9-34B. Efficiency versus C-factor for metal rings. Data from Billet (Symposium Series 32, Institution of Chemical Engineers), London (1969). Used by permission of Glitsch, Inc., Bull. 345.

liquid/vapor internal contacting does not create significant channeling that will reduce the contact efficiency. The base for the initial statement above includes the distribution of liquid, redistribution of liquid, gas or vapor channeling, and process surging, plus many other situations unique to the process conditions. Structured packing heights should be determined by the manufacturer for the design conditions.

When trying to “balance” the several packed section heights as may be required for the process, it is complete-

ly acceptable to vary the individual heights to fit such requirements as location of return of reflux, multiple feed positions, and factors of safety on design. Thus one section may be 20 ft, another 17 ft, and another 25 ft as long as the process function has been thought out, i.e., the locations of the “breaks” in the packing sections do not interrupt an important control function by locating the temperature sensor too close to the top or bottom of section, unless that location is determined to be the proper sensing location. For this, along with other reasons, it is good to pre-

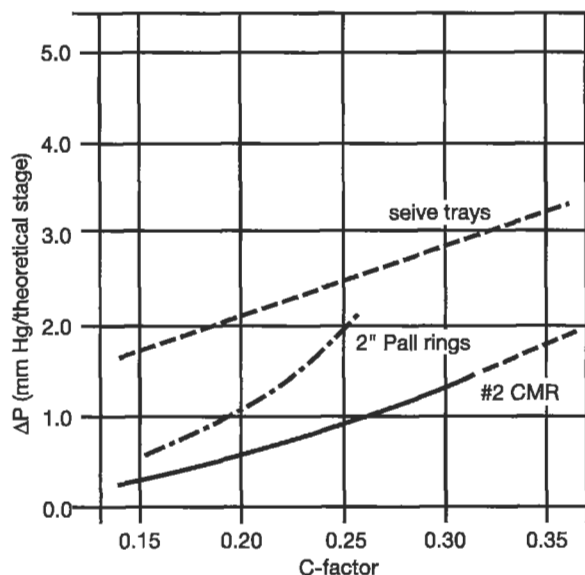


Figure 9-34C. Pressure drop versus C-factor for metal rings and sieve trays. Operating data from ethylbenzene/xylene service. 50 mm Hg top pressure. Naarden International test data. Used by permission of Glitsch, Inc., Bull. 345.

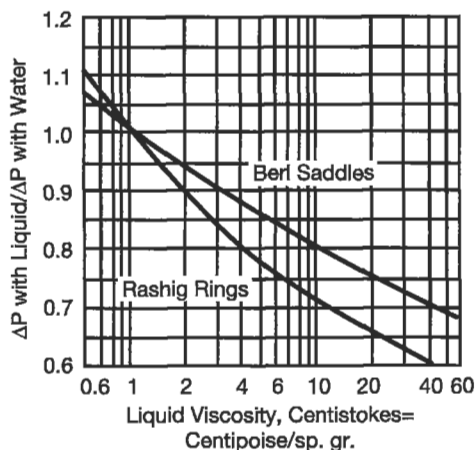


Figure 9-34D. Pressure drop correlation at flood point for use with Table 9-33. Used by permission of Zenz, F. A., *Chemical Engineering*, Aug. (1953) p. 176; all rights reserved.

pare a profile of the column and spot the controls and "interruptions" to packing continuity.

One extremely valuable concern is that at least three feed injection nozzle should be placed in the column during packing (installation) and then piped-up externally to allow alternate choices to test the column's best performance, and to allow for needed changes in feed location dictated by changes in the feed composition. In summary, everything that can be done mechanically including piping should be built into the column arrangement to be

able to accommodate both changing process requirements and errors or lack of agreement between calculations and actual operations performance.

Dumped Packing: Gas-Liquid System Below Loading

Figures 9-21B–H can be used effectively to determine the performance for new designs or for existing operating columns.

Dumped Packing: Loading and Flooding Regions, General Design Correlations

Figure 9-21B, -21F, or -21H may be used for any system to obtain a good estimate of pressure drop for practically any random packing material. The relative state of liquid position of the point on the graph, and the approximate pressure drops per foot of packing depth may be read as parameters. It is important to recognize that the load upper limit, line A, is essentially coincident with the flooding condition. It is also apparent that the relative relation of the operating point to the flooding and loading conditions is quite different at the extreme right of the figure for large values of the abscissa than for low values to the left.

The rearranged form of the same Sherwood [61, 62] equation allows the curve for flooding of dumped packings to be conveniently presented to facilitate calculation of the flooding gas rate, G_f , corresponding to a given liquid flow L [81], Figure 9-21A.

The packing factors to use with Figures 9-21B–F and -21H are given in Tables 9-26A–E.

Ward and Sommerfeld [130] present an equation based on the curves shown in Figure 9-21C, D and referenced to Eckert [125] and Leva [43] for calculating the gas and liquid flooding rates. There have been numerous other equations targeted for this purpose, but many are too awkward for easy general use. The proposed equations have been tested by the authors.

Gas flow rate at flooding:

$$G = B \exp [-3.845186 + 4.044306 (-0.4982244 \ln_e (AB^2) - 1)^{0.5}] \quad (9-52)$$

Liquid flow rate, L , at flooding:

$$L = \left[\frac{G}{(\rho_G / \rho_L)^{0.5}} \right] \exp [-4.303976 + 3.552134 (-0.645854 \ln_e (AG^2 - 1))^{0.5}] \quad (9-53)$$

where $A = F \psi \mu_L^{0.2} / \rho_G \rho_L g_c$
 $B = L (\rho_G / \rho_L)^{0.5}$
 A = correlating parameter
 B = correlating parameter
 F = packing factor, 1/ft, or, (ft)⁻¹

- G = gas flow rate, lb/(hr) (ft²)
 g_c = Newton's Law, proportionality factor
 = (4.17×10^8) , (ft-lb_m) (lb_F-hr²)
 L = liquid flow rate, lb/(hr-ft²)
 X = abscissa in the generalized pressure drop correlation,
 = $(L/G) (\rho_G/\rho_L)^{0.5}$
 Y = ordinate in the generalized pressure drop correlation,
 = $G^2 F \psi \mu_L^{0.2} / \rho_G \rho_L G_c$
 μ = viscosity, centipoise
 ρ = density, lb/ft³
 ψ = ratio of water density to liquid density

Subscripts

- G = gas phase
 L = liquid phase

The solution of the previous equations require careful attention to the sequence of the arithmetic. Perhaps one difficult requirement is the need to establish the L or G in lb/hr/ft² of tower cross-section, requiring an assumption of tower diameter. The equations are quite sensitive to the values of A and B .

Dumped Packing: Pressure Drop at Flooding

As a comparison or alternate procedure, the pressure drop at the flooding point as indicated by the upper break in the pressure drop curve can be estimated from Table 9-33 and Figure 9-34D for rings and saddles [81]. The values in the table multiplied by the correction ratio gives the pressure drop for the liquid in question, expressed as inches of water.

Dumped Packing: Pressure Drop Below and at Flood Point, Liquid Continuous Range

For a particular liquid-gas system and tower packing, performance indicates a region where the *liquid phase becomes*

Table 9-33

Pressure Drop at Upper Break Point (Flood) With Water As the Flowing Liquid [81]

Raschig Rings, In.	ΔP_f , In. H ₂ O/ft of Packed Bed	Berl Saddles, In.	ΔP_f , In. H ₂ O/ft of Packed Bed
2	2.5	1½	2.2
1½	2.5	1	2.5
1¼	4.0	¾	2.5
1 (ribbed)	3.0	½	2.0
1	4.0	¼	1.25
¾	3.0		
¾	2.5		
½	3.5		
¼	4.0		
¼	4.0		

By permission, F. A. Zenz, *Chem. Eng.*, Aug., 176 (1953), Ref. 81

continuous and the gas phase discontinuous. This is obviously at relatively high liquor rates, but not beyond the range of satisfactory performance for the equipment. This region is characterized by proportionally higher pressure drops than the gas-continuous region, and the existence of a critical liquid rate as this pressure drop deviation occurs.

Referring to Figure 9-20 the curve for L' -12,500 shows the beginning of the "move to the left," swinging away from the uniform slope of the curves for lower L' values.

This probably is not the L_c value for the system. The study of Zenz suggests that the critical liquid rate, L_c , is the minimum liquid rate that *completely* wets the packing thus having essentially all packing surface effective for gas contact. Rates above this value should be determined by allowable pressure drop and the limitation that the tower often begins to approach the flooding conditions more rapidly than in the gas-continuous region. Figure 9-35 correlates this L_c for Raschig rings and Berl saddles as a function of liquid viscosity.

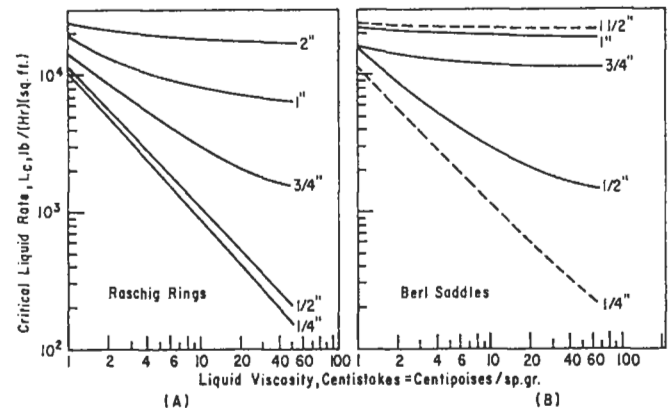


Figure 9-35. Values of liquid rate when the system becomes liquid continuous, L_c . Used by permission of Zenz, F. A., *Chemical Engineering*, Aug. (1953) p. 176; all rights reserved.

More work is needed to fully understand this feature of tower performance and extend the information to other common packings. Determination of L_c from the figures will indicate whether the tower is operating under gas-continuous (values of L lower than L_c) or liquid-continuous (values equal to or larger than L_c). The approximate degree of wetting of the packing can be evaluated as the ratio of L/L_c [73]. The pressure drop is evaluated using Figure 9-21B-F or H to determine the flooding liquid rate, L_f . Then calculate the ratio of L_f to actual L . Read Figure 9-36 to obtain ΔP actual/ ΔP_f . Thus, ΔP actual is the ratio value times ΔP_f calculated using Figure 9-34D and Tables 9-33 and -33A.

Table 9-33A
Revised Packed Tower Pressure Drop Correlation Constants for Towers Operating Below Flooding Region

Type of Packing	Mat'l	Nominal Packing Size (In.)												
		¼	⅜	½	⅝	¾	1	1¼	1½	1¾	2	3		
Intalox Saddles	Ceramic	α			1.04		0.52	0.52				0.13	0.14	
		β			0.37		0.25	0.16				0.15	0.10	
Raschig Rings	Ceramic	α			1.96	1.31	0.82	0.53				0.31	0.23	0.18
		β			0.56	0.39	0.38	0.22				0.21	0.17	0.15
Berl Saddles	Ceramic	α			1.16		0.56	0.53				0.21	0.16	
		β			0.47		0.25	0.18				0.16	0.12	
Pall Rings	Plastic	α						0.22		0.14			0.10	
		β						0.14		0.13			0.12	
Pall Rings	Metal	α				0.43		0.15				0.08	0.06	
		β				0.17		0.15				0.16	0.12	
Raschig Rings ½ in. Wall	Metal	α				1.20								
		β				0.28								
Raschig Rings ⅝-in. Wall	Metal	α			1.59	1.01	0.80	0.53				0.29	0.23	
		β			0.29	0.39	0.30	0.19				0.20	0.14	

By permission J. Eckert, U.S. Stoneware Co. (now, Norton Chemical Process Equipment Corp.) (1958).

Equation

$$\Delta p = \alpha \times 10^{\beta L} \left(\frac{G^2}{\rho_G} \right) \text{ (Limited to Region Below Flooding).}$$

Δp = Pressure Drop—in. H₂O/ft of packing

G = Gas Mass Velocity—lb/sec ft²

L = Liquid Mass Velocity—lb/sec ft²

ρ_G = Gas Density—lb/ft³

α and β = Constants.

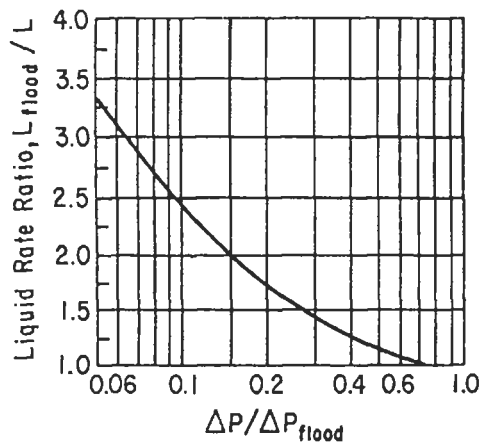


Figure 9-36. Pressure drop correlation at flooding. Used by permission of Zenz, F. A., *Chemical Engineering*, Aug. (1953) p. 181.

Pressure Drop Across Packing Supports and Redistribution Plates

Useful correlated information on pressure drop across packing supports and redistribution plates is practically not available. Some order of magnitude guide data is given in Figures 9-37–41.

Because these data are peculiar to the supports studied, it can serve only as a good estimate for other situations. It is important to remember that the results obtained with a bare plate, and one holding a layer of packing, can be quite different, the latter being the more realistic condition.

The only available test data [44] indicate that the plain flat plate (26–45% free area) has a decided detrimental effect on the allowable flooding conditions of the tower; whereas the wire screen, weir-type, and fused Raschig ring designs have very little effect when using Intalox saddles for packing.

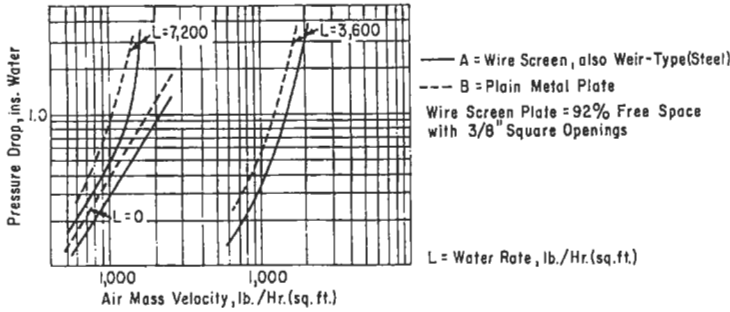
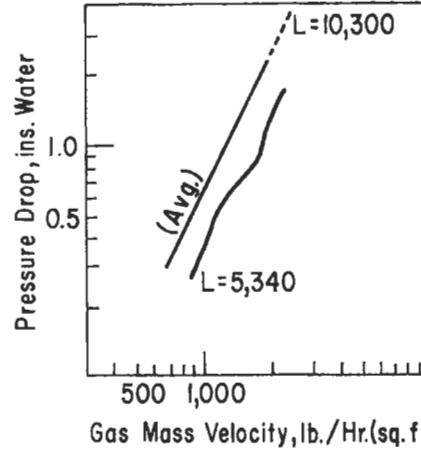


Figure 9-37. Comparison effect of pressure drop across support plate and bed of 1½ in. Intalox® saddles. Used by permission of Leva, M., Lucas, J. M., and Frahme, H. H., *Ind. Eng Chem.* V. 46, No. 6 (1954); all rights reserved.



Pressure Drop Through Fused Raschig Ring Plate, with Plate Covered with One inch of 1" Size Intalox Saddles (L=Liquid Mass Rate Parameter)

Plate = 58 % Free Area

Figure 9-39. Pressure drop through fused ceramic Raschig ring plate with plate covered with 1 in. of 1-in.-size Intalox® saddles. Used by permission of Leva, M., Lucas, J. M., and Frahme, H. H., *Ind. Eng. Chem.*, V. 46, No. 6 (1954); all rights reserved.

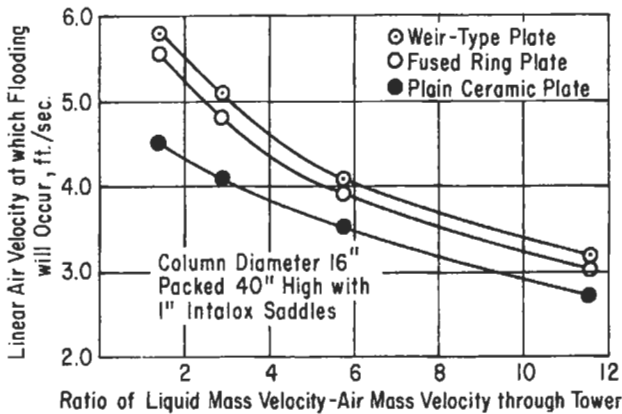


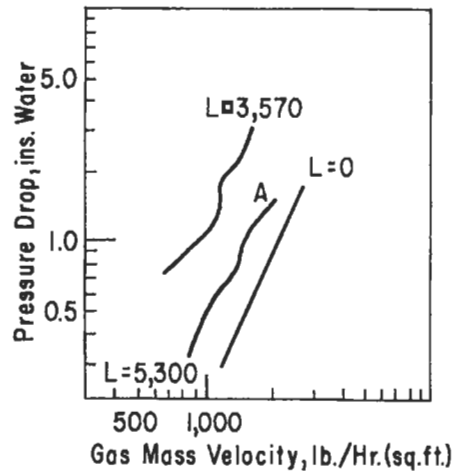
Figure 9-38. Effect of choice of support plate on flooding rate. Used by permission of U.S. Stoneware Co. (now, Norton Chemical Process Equipment Corp.).

In general the dumped saddle type packing should give less blocking to support openings than ring type.

Example 9-2: Evaluation of Tower Condition and Pressure Drop

Check the design of a 4-ft, 6-in. I.D. tower packed with 45 ft of 1-in. x 1/8-in. thick steel Raschig rings if the service requires a liquid rate of 2,250 lb/hr (ft²) of 10% caustic solution (sp. gr. = 1.22) and 4,540 lb/hr (ft²) of 110°F air containing CO₂ to be scrubbed at 365 psia.

1. Determine the operating range for the tower by referencing to Figure 9-21B or 9-21C. Use 9-21C for this example.



Pressure Drop through Plain Ceramic Plate

(L=Liquid Mass Rate Parameter)
Curve A also Represents Weir-Type Plate Covered With One inch of 1" Intalox Saddles
Plate = 20 % Free Area Plain Ceramic
= 60 % Free Area Weir-Type

Figure 9-40. Pressure drop through plain ceramic plate. Used by permission of Leva, M., Lucas, J. M., and Frahme, H. H., *Ind. Eng. Chem.*, V. 46, No. 6 (1954); all rights reserved.

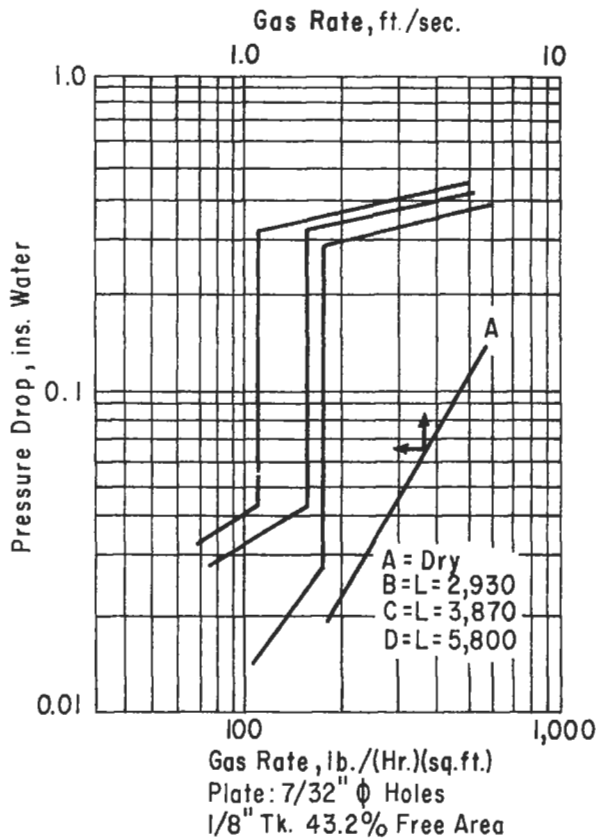


Figure 9-41. Flooding on perforated support plate. Used by permission of Lerner, B. J. and Grove, C. S., Jr., *Ind. Eng. Chem.*, V. 43, No. 1 (1951), p. 216; all rights reserved.

$$\rho_G = \left(\frac{29}{379}\right) \left(\frac{520}{570}\right) \left(\frac{365}{14.7}\right) = 1.732 \text{ lb/ft}^3$$

$$\rho_L = (62.3) (1.22) = 76.1 \text{ lb/ft}^3$$

$$\mu = 2 \text{ cp at } 104^\circ\text{F for liquid}$$

$$F = \frac{a}{\varepsilon^3} = 137 \text{ Table 9-26A note range.}$$

$$\frac{L}{G} [\rho_G / (\rho_L - \rho_G)]^{1/2} = \frac{2250}{4540} \left(\frac{1.732}{76.1 - 1.732}\right)^{1/2} = 0.07563$$

$$\frac{G^2}{\rho_G} \left(\frac{a}{\varepsilon^3}\right) \frac{\mu^{0.1}}{(\rho_L - \rho_G) g_c} = \frac{(4540/3600)^2 (1.07)^{0.1} (137)}{1.732 (76.1 - 1.732) (32.2)}$$

$$= 0.0563$$

2. Locating 0.0756 and 0.0563 on Figure 9-21C reading the intersection indicates a condition in the *lower loading region*, and a pressure drop of approximately 0.60 in. water/ft of packing.

3. Expected pressure drop through bed:

$$= (45 \text{ ft}) (0.60) = 27 \text{ in. water, total}$$

4. This bed should be in three sections (two might be acceptable under some circumstances, or if different packing were used) thereby requiring two intermediate combined packing supports and redistribution plates and one bottom support plate.

Estimate pressure drop per redistribution set-up or support

$$= 1.0 \text{ in.}$$

For two redistributors plus one support plate:

$$\text{Total estimated pressure drop} = (3) (1.0)$$

$$= 3 \text{ in. water}$$

5. Total estimated pressure drop through packed portion of tower:

$$\text{Bed } \Delta P = 27.0$$

$$\text{Internals} = \frac{3.0}{30.0} \text{ in. water}$$

Say, 30 to 35 in. water (this should be $30.0 \pm 15\text{--}20\%$)

6. Estimated percent of flooding

Reading the abscissa of Figure 9-21C at value 0.0756 for ordinate at flooding line for dumped packing:

$$= 0.13$$

Then, actual value of 0.0563 is:

$$\text{Percent of liquid flooding} = \frac{0.0563}{0.13} (100) = 43.3\%$$

Note that this rather low value will usually occur when operating at the low L/G values due to the greater operating spread between flooding and loading (see Figure 9-21C).

7. Estimated percent of loading (average)

Reading abscissa at 0.0756 for ordinate of line B gives ordinate = 0.078

$$\text{Percent of flooding} = \frac{0.0563}{0.078} (100) = 72.1\% \text{ (not very precise)}$$

This is an acceptable value and should not be exceeded except in known systems. It is preferable to operate reasonably close to the loading condition for best efficiency of contact.

As an alternate consideration, assume various pressure drops/foot of packing (same) and determine effect on calculated column diameter. Use the same input information as original stated conditions, then:

Assumed Pressure Drop, in. H ₂ O/ft	Calculated Column Diameter, ft
0.25	5.22
0.50	4.61
0.75	4.35

Example 9-3: Alternate Evaluation of Tower Condition and Pressure Drop

Using Example 9-2 as reference, the tower will be examined for critical liquor rate, L_c , using Figure 9-35.

$$\text{Centistokes} = \left(\frac{\text{centipoise}}{\text{sp gr}} \right) \text{ for caustic sol'n.} = \frac{2}{1.22} = 1.64$$

reading: $L_c = 16,000 \text{ lb}/(\text{hr}) (\text{ft}^2)$

Because actual $L' = 2250$ is less than 16,000 this tower operates in the gas continuous region.

Pressure drop at flooding from Table 9-33 and Figure 9-34D

$\Delta P_f = 4 \text{ in. water}/\text{ft}$ (not exact figure, because table is for ceramic rings)

Correction = 0.94

Then actual expected pressure drop at flooding:

$$\Delta P_f = (0.94) (4) = 3.76 \text{ in. water}/\text{ft}$$

For 45 ft of packing:

$$\Delta P_f \text{ total} = (45) (3.76) = 169 \text{ in. water}$$

Comparison with Figure 9-21C gives 3 in. water/ft (parameter) or a total of (3) (45) = 135 in. water. Neither of these values represents a condition (flooding) that should be considered for tower operation, except under known experience studies. Distillation operations sometimes operate above flooding, but other types of contacting normally require operations in the loading region (or below) for stable performance.

Example 9-4: Change of Performance with Change in Packing in Existing Tower

A tower is packed with 1-in. ceramic Raschig rings. It presently floods while drying water from a product at a production feed rate of 1,800,000 lbs/month with 0.25 mol% being water. Flooding does not start at the bottom, but at some intermediate point up the tower. What can be done to eliminate the flooding? Is it possible to increase production rate to 2,000,000 lbs/month?

1. Examine packing characteristics.

Size	a/ϵ^3	Surface area, ft^2/ft^3
1 In. Rashig Rings	158	58
1 In. Intalox	124	78
1 In. Berl Saddles	125	76
1 In. Pall Ring*	45	66.3
1½ In. Intalox	69	59.5
1½ In. Berl Saddle	79	44

*Metal, all others ceramic.

2. Percent of flooding for various packings, holding tower flow rates (including reflux) constant.

Refer to Flooding, Loading and Pressure Drop Chart, Figure 9-21D.

$\frac{L}{G} (\rho_G / \rho_L)^{0.5}$ remains constant for same separation at increased production rate

$\frac{G^2 \psi^2 \mu^{0.2}}{\rho_G \rho_{Lgc}} \left(\frac{a}{\epsilon^3} \right)$ increases as G^2 at increased production rate for a fixed a/ϵ^3 .

Percent of Flooding at 2,000,000 lb/mo. rate referenced to flooding at 1 in. ceramic Raschig rings

Packing	Percent of Flooding
1 In. R. R.	= 100%
1 In. Intalox	$\left(\frac{2}{1.8} \right)^2 \left(\frac{124}{158} \right) (100) = 96.9\%$
1 In. Pall Rings (metal)	$\left(\frac{2}{1.8} \right)^2 \left(\frac{45}{158} \right) (100) = 35.2\%$
1½ In. Intalox	$\left(\frac{2}{1.8} \right)^2 \left(\frac{69}{158} \right) (100) = 53.9\%$
1½ In. Berl Saddles	$\left(\frac{2}{1.8} \right)^2 \left(\frac{79}{158} \right) (100) = 61.8\%$

The flooding of the packing is a direct function of the a/ϵ^3 , therefore it is valid at constant separation to examine the performance as shown. The metal Pall rings appear to allow for a considerable increase in capacity. In fact the condition at 35.2% of flood might not be good from a contact efficiency standpoint.

3. Selection

The 1½-in. Intalox or Berl ceramic saddles would be the preferred choice because: (1) the flooding point is sufficiently low and yet probably not too far from the load point (only flood data available, but would estimate 70–85% of load); (2) the surface area per cubic foot is essentially the same as for the existing 1-inch Raschig rings. By reference to the effective interfacial area graphs, and by using the Berl saddle data instead of Intalox as an estimate because it is not

available, the separation performance would be expected to be essentially identical to the existing tower (for the Intalox); (3) the production rate can be increased; (4) the flooding can be removed from present operations using the 1½-in. Intalox or any of the other packings, but note that the a/ϵ^3 of the Berl saddles is not as high as the 1-in. R. R. This might mean less efficient contact, requiring more packing. However, from Figure 9-42 note that for a given L'/G' the Berl saddles are from 15–30% better wetted in any given packing volume. From Figures 9-43 and 9-44 the comparative effective areas, a , indicate that the Berl saddles have about the same area/ft³ as the existing rings. Therefore, it appears that the flooding can be stopped (lower a/ϵ^3) and yet the contact can be as good, or maybe a little better than it was originally.

4. Check support grid voidage

The packing support consists of a floor grating material with bar openings spaced to give 57.5% free void area of cross-section.

To avoid the possibility of local flooding at the support, it would be well to place a heavy hardware cloth

over this grid to keep the saddles from nesting at the first layer in the opening slots. It is preferable to have them resting on a surface that cannot be blanked easily.

Select a 1-in. × 1-in. (center line) × 0.063-in. wire cloth with voidage of 87.8%.

Combined voidage, support grid plus cloth:

$$= (0.575) (0.878) = 50.5\%$$

This should be satisfactory, but a value much lower than this could not be tolerated.

Dump Intalox (or Berl) saddles into tower while tower is filled with water.

Example 9-5: Stacked Packing Pressure Drop

Consider the problem of drying air with sulfuric acid, Example 9-6. If the mass transfer relations are evaluated, a reasonably good estimate of the new packed height can be determined for using 2-in. stacked ceramic Raschig rings in place of Intalox saddles. For the present, assume the new required stacked height is 25 ft. Although the pres-

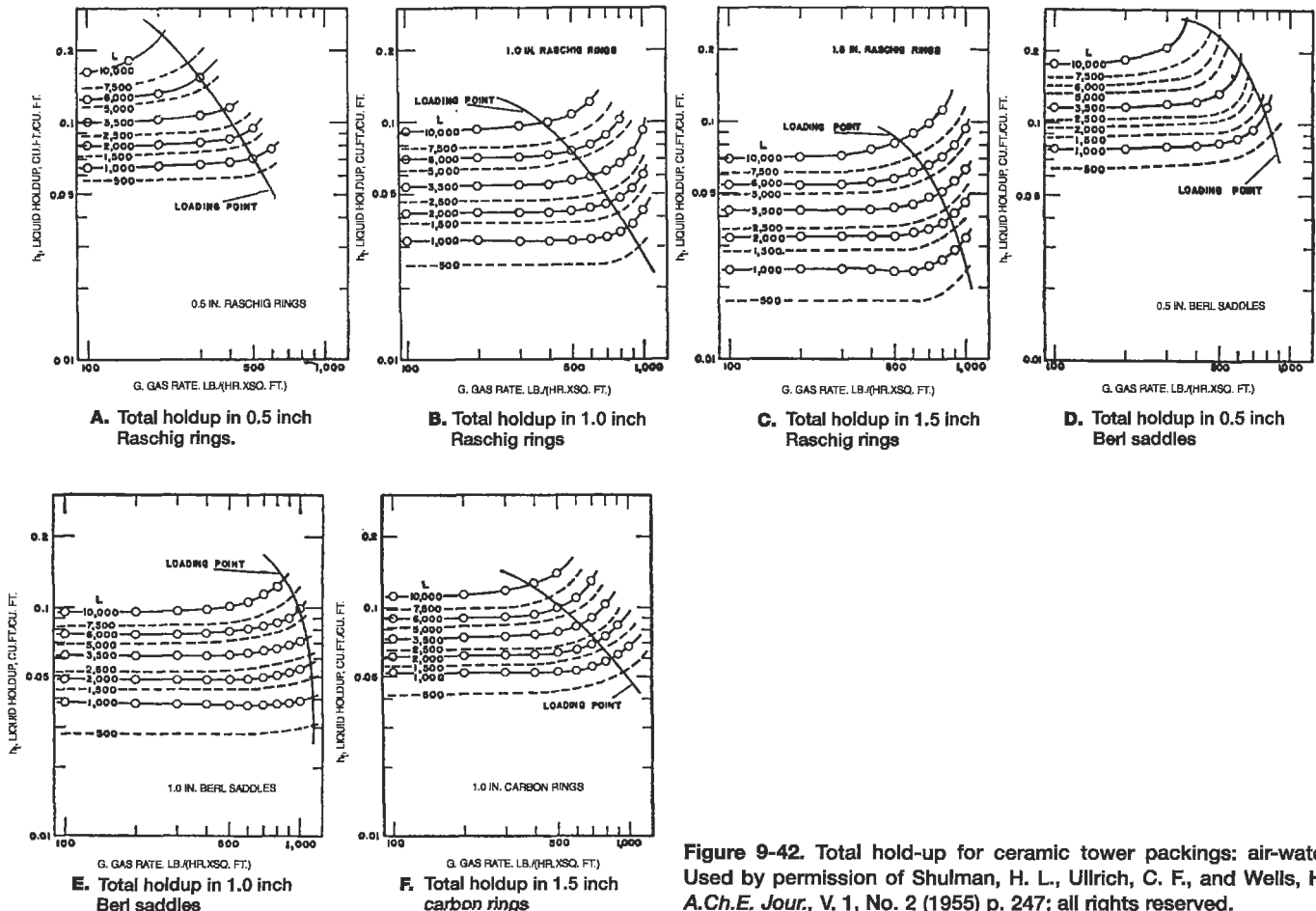


Figure 9-42. Total hold-up for ceramic tower packings: air-water. Used by permission of Shulman, H. L., Ullrich, C. F., and Wells, H.; *A.Ch.E. Jour.*, V. 1, No. 2 (1955) p. 247; all rights reserved.

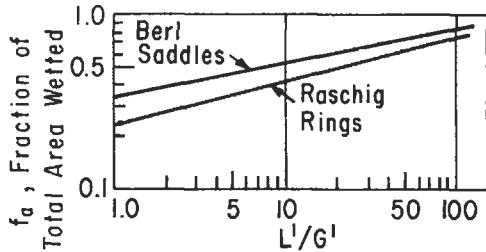


Figure 9-43. Fraction packing wetted. Used by permission of Shulman, H. L., Ullrich, C. F., Proulx, A. Z., and Zimmerman, J. O., *A.I.Ch.E. Jour.*, V. 1, No. 2 (1955) p. 253; all rights reserved.

sure drop per foot will be less and the flooding point higher than the dumped packing, it is inadvisable to go to a smaller diameter tower because of the high superficial gas velocity.

Using the 15-in. I.D. ceramic tower, the expected pressure drop will be:

$$\Delta P = (\alpha) (10^{\beta L}) \left(\frac{G^2}{\rho_G} \right)$$

From Reference 40 for 2-in. ceramic stacked Raschig rings:

$$\alpha = 0.06$$

$$\beta = 0.012$$

Liquor range checks satisfactory

$$G = 0.593 \text{ lb}/(\text{sec}) (\text{ft}^2)$$

Leva [40] has shown that for liquids other than water, the L must be corrected by the ratio of the density of water to that of the fluid in the system.

$$L = 0.378 \text{ lb}/(\text{sec}) (\text{ft}^2) \left(\frac{62.3}{112.6} \right) = 0.209$$

$$\rho_G = 0.087 \text{ lb}/\text{ft}^3$$

$$\Delta P = (0.06) (10^{(0.012)(.209)}) \left(\frac{(0.593)^2}{0.087} \right)$$

$$\Delta P = 0.00258 \text{ in. water}/\text{ft packed height (estimated)}$$

Total tower drop:

$$\text{Packing} = (0.00258) (25) = 0.064 \text{ in. water (approximate)}$$

$$\text{Support (estimated)} = 1.5 \text{ in. water}$$

$$\text{Total (approximate)} = 1.56 \text{ in. water}$$

Note that the weight of liquid will be greater in this arrangement at flooding, and the operating hold-up will be almost the same as the dumped Intalox. The total

weight of packing will be approximately 50% greater than if the same 2-in. rings had been dumped in place. Two-inch rings are not usually stacked. In this small tower made up of 3-ft ceramic sections, the stacking is not too difficult a job if there are conditions which justify the extra effort and expense.

Liquid Hold-up

Liquid hold up in a tower represents the liquid held in the void spaces of the packing during operating conditions. At flooding, essentially all of the voids are filled with liquid.

Usually low hold-up is desired but reasonable hold-up is necessary for efficient tower operation. The weight of liquid held in the packing must be considered when determining the support loads at the bottom of the packing, as well as the tower itself. The higher the hold-up for any particular packing the greater will be the gas pressure drop, and the longer the tower drainage time when shut down. Smaller size packing tends to have greater hold-up than larger packing.

Figure 9-44 presents water hold-up data that are correlated by [40]:

$$h_{tw} = 0.0004 \left(\frac{L'}{d_p} \right)^{0.6} \tag{9-54}$$

where h_{tw} = water hold-up, $\text{ft}^3 \text{ liquid}/\text{ft}^3 \text{ volume tower}$

L' = Liquid rate, $\text{lb}/(\text{hr}) (\text{ft}^2)$

d_p = Equivalent spherical packing diameter, inches (diameter of packing equivalent to sphere of same surface area as the packing piece). Values given for

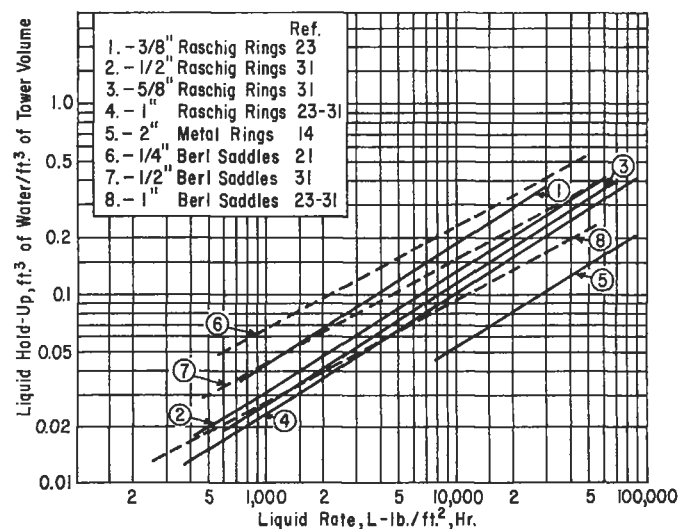


Figure 9-44. Gas-liquid hold-up data for ceramic rings and saddles. Used by permission of Leva, M. *Tower Packings and Packed Tower Design*, 2nd ed., U.S. Stoneware Co. (now, Norton Chemical Process Equipment Corp.) (1953).

some packings with physical data Tables 9-1 through 9-14 Area of sphere = π (diameter)².

For liquids other than water [36, 40]:

$$h_1 = h_{tw} (\mu_L)^{0.1} \left(\frac{62.3}{\rho_L} \right)^{0.78} \left(\frac{73}{\sigma} \right)^n \quad (9-55)$$

where h_1 = liquid hold-up, ft³/ft³ packed tower volume

μ_L = liquid viscosity, centipoise

ρ_L = liquid density, lb/ft³

σ = surface tension, dynes/cm

Values of exponent n are given in Figure 9-45.

Total liquid hold-up in packed bed, h_t = static hold-up, h_s , plus operating hold-up, h_o [64, 66].

The static hold-up is independent of liquid and gas rates, since it represents the liquid held in the packing after a period of drainage time, usually until constant weight of material is received. This requires approximately 1 hour for a 10-in. dia. \times 36-in. packed height tower. Table 9-34 adequately summarizes the data.

Total hold-up, h_t , of water is represented for Raschig rings and Berl saddles [66].

$$h_t = \alpha L' \beta / D_p^2 \quad (9-56)$$

$$\beta = \gamma D_p \theta$$

Constants are given in Table 9-35.

Figures 9-42 A, B, C, D, E, F present the graphical interpretation of the total hold-up equation. These are more

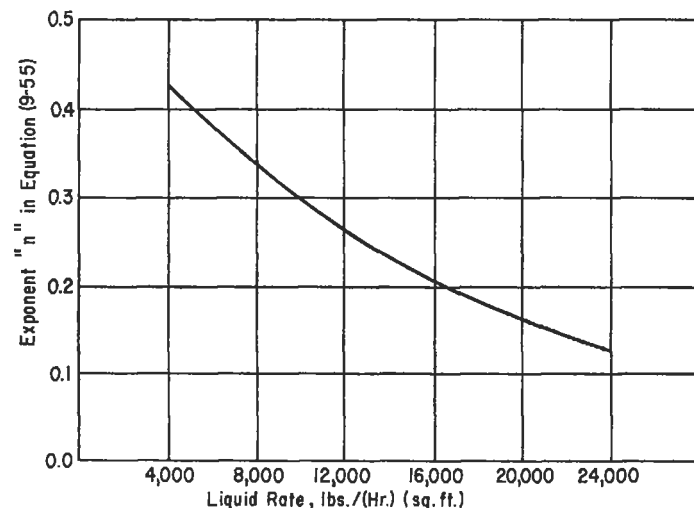


Figure 9-45. Liquid hold-up variation of surface tension exponent with liquid rate. Reproduced by permission of the American Institute of Chemical Engineers; Jesser, B. W., and Elgin, J. C. *Trans. A.I.Ch.E.* V. 39, No. 3 (1943) p. 295; all rights reserved.

Table 9-34
Static Hold-up in Random Packings

Packing Nominal Size, In.	Static Water Hold-up, h_s , Ft ³ /Ft ³ Packing
Raschig rings (unglazed porcelain)	
½	0.0325
1	0.0150
1½	0.0089
2	0.0058
Berl saddles (unglazed porcelain)	
½	0.0317
1	0.0110
1½	0.0052
Raschig rings (carbon)	
1	0.0358
1½	0.0200
2	0.0150

By permission of The American Institute of Chemical Engineers, Shulman, H. L. et al., *Chem. Engr. Jour.* Vol. 1, No. 2, 247 (1955) and *ibid.*, p. 259 (1955), Ref. 64 and 66, all rights reserved.

Table 9-35
Total Hold-up Constants

Packing	α	γ	θ
Porcelain Raschig ring	2.25×10^{-5}	0.965	0.376
Carbon Raschig ring	7.90×10^{-5}	0.706	0.376
Porcelain Berl saddles	2.50×10^{-5}	0.965	0.376
Porcelain, In.	Equivalent Spherical Dia., Ft		
½ R. R.	0.0582		
1 R. R.	0.1167		
1½ R. R.	0.1740		
2 R. R.	0.238		
½ Berl saddle	0.0532		
1 Berl saddle	0.1050		
1½ Berl saddle	0.155		
Carbon, In.			
1 R. R.	0.1167		
1½ R. R.	0.178		
2 R. R.	0.235		

By permission of The American Institute of Chemical Engineers, Shulman, H. L. et al., *Chem. Engr. Jour.* Vol. 1, No. 2, 247 (1955) and *ibid.*, p. 259 (1955), Ref. 64 and 66, all rights reserved.

convenient to apply where the system fits (or nearly fits) the curves.

These data are valuable for determining the total weight of liquid held in the packing, and also the void fraction, in an operating column. ϵ is the void fraction of the dry packing minus the total hold-up, h_t .

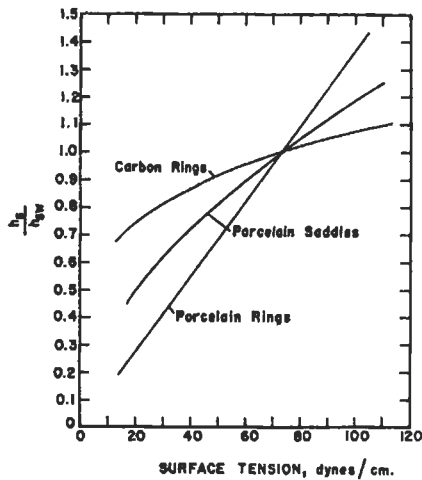
Correction Factors for Liquids Other Than Water

In order to use the data in systems handling liquids other than water correction equations and charts are used [66]. The charts are more convenient to use and are presented in Figures 9-46 A, B, C, D. First, determine the total or static hold-ups for water at 20°C; second, determine separately the correction for viscosity, density, and surface tension; third, multiply the water hold-up by each

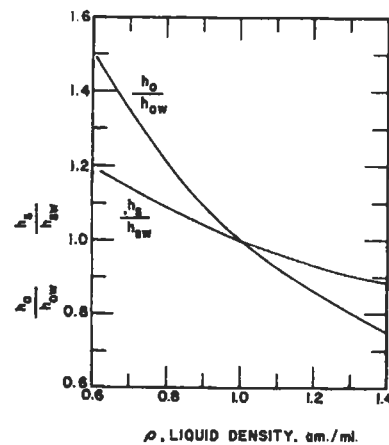
of the corrections to obtain hold-up for liquid of the specific system.

A second hold-up correlation reported by T. Otake and K. Okada [55] represents a survey of considerable literature, and is applicable to aqueous and non-aqueous systems for Reynolds numbers from 10, - 20,000 [40].

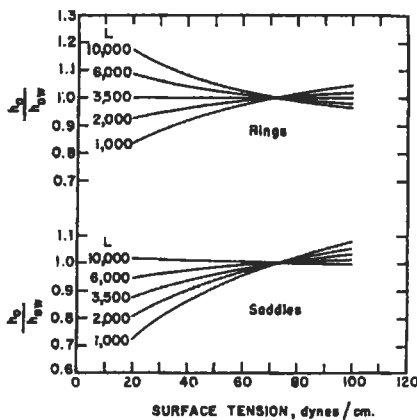
$$h_o = 1.295 \left(\frac{D'_p L}{\mu'} \right)^{0.676} \left[\frac{(D'_p)^3 g_c \rho^2}{\mu'^2} \right]^{-0.44} (aD'_p) \quad (9-57)$$



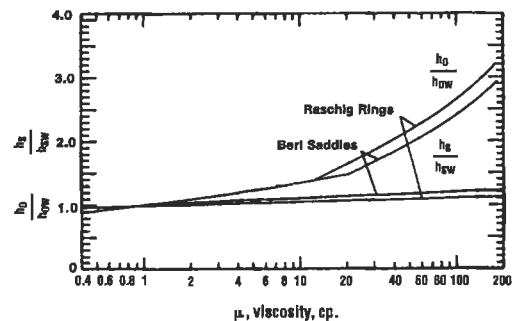
A. Factors to be applied to water static hold-ups to determine the effect of surface tension. Used by permission of American Institute of Chemical Engineers, *A.I.Ch.E. Jour.*, Shulman, H. L., Wells, N., Ullrich, C. F., and Proulx, A. Z., V. 1, No. 2 (1955) p. 259; all rights reserved.



C. Factors to be applied to water hold-ups to determine effect of liquid density. Used by permission of the American Institute of Chemical Engineers, *A.I.Ch.E. Jour.*, Shulman, H. L., Wells, N., Ullrich, C. F., and Proulx, A. Z., V. 1, No. 2 (1955) p. 259; all rights reserved.



B. Factors to be applied to water operating hold-ups to determine effect of surface tension. Reproduced by permission of the American Institute of Chemical Engineers, *A.I.Ch.E. Jour.*, Shulman, H. L., Wells, N., Ullrich, C. F., and Proulx, A. Z., V. 1, No. 2 (1955) p. 259; all rights reserved.



D. Factors to be applied to water hold-ups to estimate the effect of liquid viscosity. Used by permission of the American Institute of Chemical Engineers, *A.I.Ch.E. Jour.*, Shulman, H. L., Wells, N., Ullrich, C. F., and Proulx, A. Z., V. 1, No. 2 (1955) p. 259; all rights reserved.

Figure 9-46. Physical property corrections for liquid hold-up for ceramic packing and carbon packing (as noted). Reproduced by permission of *A.I.Ch.E. Jour.*, Shulman, H. L., Wells, N., Ullrich, C. F., and Proulx, A. Z., V. 1, No. 2 (1955) p. 259; all rights reserved.

Packing Wetted Area

Wetted packing area may differ considerably from the physical area of a packing. This is of particular importance in comparing the effectiveness of different packings.

It is only recently that a coordinated group of data became available for wetted areas in Raschig ring and Berl saddle packing [65].

Figure 9-43 represents the water-air and ammonia-water data for Berl saddles by [65, 67]:

$$f_a = \frac{a'}{a_t} = 0.35 \left[\frac{L'}{G'} \right]^{0.20} \quad (9-58)$$

and for Raschig rings by

$$f_a = \frac{a'}{a_t} = 0.24 \left[\frac{L'}{G'} \right]^{0.25} \quad (9-59)$$

where f_a = fraction of total packing area, a_t , that is wetted

a' = wetted packing surface not necessarily same as effective interfacial surface area for contact, ft^2/ft^3

a_t = total packing surface, ft^2/ft^3

L' = superficial liquid rate, $\text{lb}/\text{hr} (\text{ft}^2)$

G' = superficial gas rate, $\text{lb}/\text{hr} (\text{ft}^2)$

The fraction wetted area immediately indicates the effectiveness of contact for the liquid system in the packing. This packing area contact efficiency must be considered in some design problems.

Effective Interfacial Area

The effective interfacial area is used in mass transfer studies as an undivided part of individual and overall coefficients when it is difficult to separate and determine the effective area. The work of Shulman et.al., 65 presents a well organized evaluation of other work in addition to their own. One of the difficulties in correlating tower packing performance lies in obtaining the correct values for the effective interfacial areas of the packing on which the actual absorption, desorption, chemical reaction, etc. are completed. Figures 9-47 A, B, C, D, E, F, G present a correlation for water flow based on the ammonia-water data of Feller [27] and are valid for absorption work.

There are differences between wetted and effective area as discussed by Shulman [65]: (1) wetted-areas increase as packing size decreases; (2) effective area is smallest for the smallest packings; (3) the effective area seems to go through a maximum for the 1-inch size packing although the larger packings have almost as much area. This is better understood in terms of the hold-up data for these packings.

For vaporization in packed beds of Raschig rings and Berl saddles [66]:

$$a_{\text{vap}} = 0.85 (a_{\text{abs}}) \left(\frac{h_t}{h_o} \right) \quad (9-60)$$

$$a_{\text{vap}} = 0.85 (a_{\text{abs}})_w \left(\frac{h_t}{h_{ow}} \right) \quad (9-61)$$

where the subscripts *vap* and *abs* represent conditions of vaporization and absorption respectively, and subscript *w* represents a water system.

Entrainment From Packing Surface

There is not much data available on this point. Operational experience plus qualitative tests indicate that entrainment is negligible until the packing reaches the flooding condition. See discussion under distillation section.

Example 9-6: Operation at Low Rate, Liquid Hold-up

A sulfuric acid drying tower uses 98% acid for drying an incoming air stream. The pilot plant tests show that 15 ft of 1-in. ceramic Intalox packing will do this job. The plant scale rates are:

Air = 500 scfm at 90°F and 2 psig
Acid = 6 gpm at 90°F and sp gr = 1.81

Determine (1) the tower diameter (2) pressure drop (3) liquid hold-up

$$\begin{aligned} \text{air rate} &= \frac{500}{359} \left(\frac{29}{60} \right) \left(\frac{460 + 60}{460 + 90} \right) \left(\frac{14.7 + 2}{14.7} \right) \\ &= 0.725 \text{ lbs}/(\text{sec}) \end{aligned}$$

$$\text{liquid rate} = \left(\frac{18}{60} \right) \frac{(8.33)}{1.81} = 0.461 \text{ lb}/\text{sec}$$

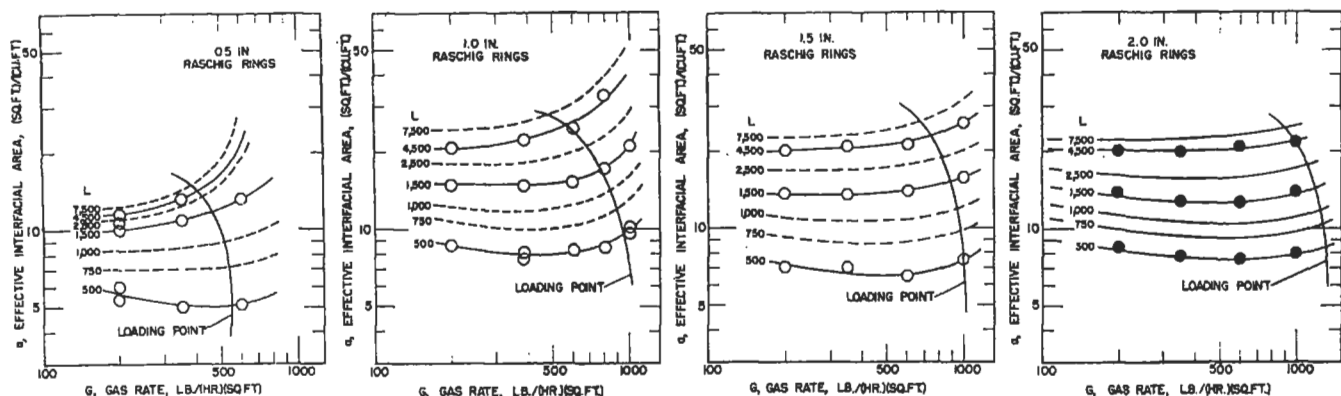
Assume for first trial:

Inside tower diameter = 12 in.

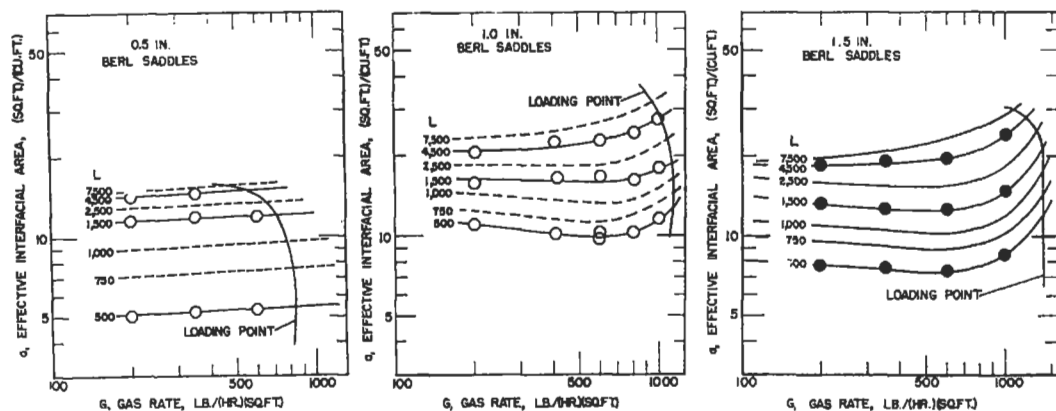
$$\text{Cross-section area} = \frac{\pi (1)^2}{4} = 0.785 \text{ ft}^2$$

$$\begin{aligned} \text{then : air rate, } G &= \frac{0.725}{0.785} = 0.925 \text{ lb}/(\text{sec}) (\text{ft}^2) \\ &= 3340 \text{ lb}/(\text{hr}) (\text{ft}^2) \end{aligned}$$

$$\begin{aligned} \text{liquid rate, } L &= \frac{0.461}{0.785} = 0.588 \text{ lb}/(\text{sec}) (\text{ft}^2) \\ &= 2120 \text{ lb}/(\text{hr}) (\text{ft}^2) \end{aligned}$$



A. Effective interfacial area for 0.5 in. Raschig rings. B. Effective interfacial area for 1-in. Raschig rings. C. Effective interfacial area for 1.5-in. Raschig rings. D. Effective interfacial area for 2.0-in. Raschig rings, using estimated hold-ups.



E. Effective interfacial area for 0.5-in. Berl saddles. F. Effective interfacial area for 1.0-in. Berl saddles. G. Effective interfacial area for 1.5-in. Berl saddles, using estimated hold-ups.

Figure 9-47. Effective interfacial areas for random ceramic tower packings. Note for gases or vapors other than air, use abscissa, G , as $G/(\rho_{\text{gas}}/0.075)^{0.8}$. Based on the data of Fellingner [27]. Used by permission of the American Institute of Chemical Engineers; *A.I.Ch.E. Jour.*, Shulman, H. L., Ullrich, C. F., Proulx, A. Z., and Zimmerman, J. O., V. 1, No. 2, (1955) p. 253. All rights reserved.

$$\rho_L = (1.81)(62.3) = 112.6 \text{ lb/ft}^3$$

$$\rho_G = \frac{29}{359} \left(\frac{460 + 60}{460 + 90} \right) \left(\frac{14.7 + 2}{14.7} \right) = 0.087 \text{ lb/ft}^3$$

$$\frac{L}{G} (\rho_G / \rho_L)^{1/2} = \frac{0.588}{0.925} \left(\frac{0.087}{112.6} \right)^{1/2} = 0.01975, \text{ (abscissa)}$$

$$\left(\frac{a}{\epsilon^3} \right) \text{ for 1-in. Intalox saddles} = 92 \text{ (Table 9-26A)}$$

(original value)

$$\psi^2 = \left(\frac{1}{1.81} \right)^2 = 0.305$$

$$g_c = 32.2 \text{ (lb) (ft) / (lb) (sec)}^2$$

$$\mu^{0.2} = (17.0)^{0.2} = 1.762 \text{ cp at } 90^\circ\text{F}$$

$$\frac{G^2}{\rho_G} \left(\frac{a}{\epsilon^3} \right) \frac{\psi^2 \mu^{0.2}}{\rho_L g_c} = \frac{(0.925)^2 (92) (0.305) (1.762)}{(0.087) (112.6) (32.2)} = 0.13411 \text{ (ordinate)}$$

Reading Figure 9-21D at the calculated ordinate and abscissa, we obtain:

- (a) An indicated operating condition above the upper loading limit
- (b) A condition of high pressure drop, approximately 1.5 in./ft of packing height
- (c) A situation too close to flooding, thus requiring a larger tower diameter

Second Assumption: Try 15-inch Dia. Ceramic Tower

Inspection of Figures 9-21B, C or D shows that the increase on tower diameter is not reflected in the value of the abscissa. By changing the tower diameter to 15-in. cross-section area = 1.22 ft².

$$G = \frac{0.725}{1.22} = 0.593 \text{ lb}/(\text{sec}) (\text{ft}^2)$$

$$L = 0.461/1.22 = 0.378 \text{ lb}/(\text{sec}) (\text{ft}^2)$$

$$\frac{G^2}{\rho_G} \left(\frac{a}{\varepsilon^3} \right) \frac{\psi^2 \mu^{0.2}}{\rho_L g_c} = (0.1535) \left(\frac{0.593}{0.925} \right)^2 = 0.063$$

This indicates operation in the loading region. The expected pressure drop is 0.5 in. water/ft.

Total expected pressure drop:

Packing = (0.5) (15) = 7.5 in. water

Support = 1.5 in. (estimated from Figures 9-37 and -38, -39, and -40 for a 58% open grid).

Total drop = 9.0 in. water (approximate)

Superficial gas velocity through tower:

$$= \frac{0.593 \text{ lb}/(\text{sec}) (\text{ft}^2)}{0.087 \text{ lb}/\text{ft}^3}$$

Entrainment

This velocity is slightly high and an entrainment knock-out or separator should be installed in the air stream following the tower, or in the top of the tower itself.

Liquid Hold-up in the Tower:

For water, the hold-up would be, from Equation 9-54.

$$h_{tw} = 0.0004 \left(\frac{L'}{d_p} \right)^{0.6}$$

$$d_p = 0.68 \text{ (from Table 9-7)}$$

$$h_{tw} = 0.0004 \frac{[(0.378)(3600)]^{0.6}}{(0.68)} = 0.0384 \text{ ft}^3/\text{cu ft} \text{ for water.}$$

For sulfuric acid:

From Figure 9-46C, h_o/h_{ow} , for density correction multiplier = 0.6.

From Figure 9-46B, correction for surface tension = 1.0 (at 70 dynes/cm)

From Figure 9-46D, correction for viscosity = 1.1 (at 18 cp)
 h_o , for acid = h_{ow} (0.6) (1.0) (1.1) = (0.0384) (0.66)
 = 0.0254 ft³ acid/ft tower volume

For a packed volume of 15 ft in a 15-in. I.D. tower, the total acid hold-up:

$$= [(15) (1.22)] (0.0254) (112.6 \text{ lb}/\text{ft}^3)$$

Total hold-up = 52.3 lb acid

Weights

Weight of dry packing in tower:

$$= (42 \text{ lb}/\text{ft}^3) [(15) (1.22)]$$

= 770 lb

Total weight on bottom support plate when operating (not flooded)

$$= 52.3 + 770 = 822.3 \text{ lb}$$

Some allowance should be made for surging or uneven operation.

The maximum expected weight of liquid would be at flooding conditions:

Using percent free gas space = 77.5

$$\text{Volume of liquid space} = (15) (1.22) (0.775)$$

= 14.2 ft³

$$\text{Weight of acid in this space} = (14.2) (112.6)$$

= 1,600 lb

$$\text{Maximum support load} = 770 + 1,600 = 2,370 \text{ lb}$$

This is the load that should be considered for the support design and selection. To allow for unusual conditions, specify support load = (1.1) (2,370) = 2,600-lb minimum.

Structured Packing

Structured packings as in use at the present time are composed of:

1. Wire-mesh weavings (Figures 9-6Y, 9-6Z, 9-6AA–FF).
2. Corrugated sheet, or crimped sheet (usually somewhat thin) (Figures 9-6GG–NN).
3. Grid-type, open, heavy (usually metal) bar-grid shapes stacked together (Figures 9-6 OO–TT).

Structured packings vary as to the preferred process application depending on the geometric arrangement of the components and:

1. High cost/ft³ of space
2. Easy plugging by solid particles
3. Importance of uniform liquid distribution across the packing
4. System operating under pressure [153] or vacuum

For most efficient performance, the fabricated sections of the structured packing usually are placed in a specific rotated pattern in the column to ensure uniform liquid flow, and vapor cross-mixing.

The materials of construction are usually stainless steel as well as specific other metals that will draw into wire, or crimp without cracking. The wire mesh types have been fabricated of some plastics such as Teflon[®], polypropylene, etc.; however, the surface must be wettable by the liquid, or the efficiency will be poor, and performance data are needed to complete a good design.

Nutter [99] reports that most, if not all structured packing (Figures 9-6LL and 9-6MM) follow the linear relationship of vapor rate vs. pressure drop at fixed liquid rates as exhibited by random packings.

Structured packing ACS ST-100 (Figure 9-6DD) is reported by the manufacturer to be equivalent in all respects to the original Sulzer packing, i.e., extremely low pressure drop and high efficiency (low HETP) over a wide range of liquid load, and high-vacuum applications. The design rating procedure by this manufacturer is confidential (as is also the best and final procedure for most other structured and grid packings) and design application data should be submitted for recommendations.

Preliminary Sizing for ACS Industries Series Woven X/S Knitted Wire Mesh Structured Packing

The following is extracted by permission from ACS Bulletin B-129 (Apr. 1992). Typical HETP is 3 in. compared to ACS product ST-100 of 7 in. Approximate comparison data are: ΔP as low as 0.1-in. water/theoretical tray; turn-down ratio about 20:1. Special series S construction recommended for smaller columns, and transverse Series X for larger ones. The suggested preliminary sizing procedure is:

1. Determine the number of theoretical plates/trays/stages using standardized methods.
2. Calculate minimum allowable superficial vapor velocity (flooding) for equal vapor and liquid loads, for the X-100 and S-100 packings.

$$u_{\max IE} = [0.0942/\mu^{0.33}] [(\rho_L - \rho_V)/\rho_V]^{0.57}, \text{ ft/sec} \quad (9-62)$$

where μ = liquid viscosity, cp
 ρ_L = liquid density, lb/cu ft³
 ρ_V = vapor density, lb/ft³

If liquid viscosity is less than 0.15 cp, use constant 0.53 in place of the $\mu^{0.33}$ term.

$u_{\max IE}$ = calculated or estimated maximum superficial vapor velocity

Calculate: L/G

L = total liquid load, lb/hr

G = total vapor load, lb/hr

Enter Figure 9-48 with this L/G and find the load ratio correction factor. Multiply $u_{\max IE}$ by this factor to determine the corrected maximum superficial vapor velocity, $u_{\max I}$, for X-100 and S-100 packings.

Correct the maximum vapor velocity again for the packing type, if other than X-100 or S-100.

$$u_{\max} = u_{\max I} (SS_1 PV_A / SS_A PV_1)^{0.5} \quad (9-63)$$

where u_{\max} = maximum vapor velocity for actual packing, ft/sec

$u_{\max I}$ = maximum superficial vapor velocity for X-100 and S-100 packing

SS_A = specific surface for the actual packing* (see Table 9-36-A-C)

SS_1 = specific surface for X-100 and S-100 packings (see Table 9-36)

PV_A = percent void volume for the actual packing*, (see Table 9-36)

PV_1 = percent void volume for the X-100 and S-100 packings

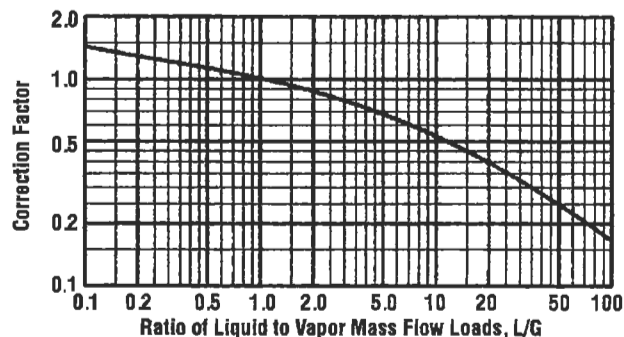


Figure 9-48. ACS maximum vapor velocity correction for L/G for woven/knitted wire mesh structured packing. Used by permission of ACS Industries, Inc., Separation Technology Division, Bull. B-129 (1992).

*For other series X and S packings consult manufacturer.

Table 9-36A
Mechanical Characteristics of Common Standard Packing
Styles (ACS Wire Mesh)

ACS Packing Style	Number of Strands	Strand Diam., In.	Density, lb/ft ³ (stainless)	Pct. Void Vol.	Sp. Surf., Ft ² /Ft ³
X-100, S-100*	12	0.0045	27.5	94.5	585
X-200,* S-200	8	0.0045	20.1	96.0	426

*For Series X, standard style is X-200 (8 strands)

For Series S, standard style is S-100 (12 strands)

By permission of ACS Industries, Separations Technology Group, Bul. B-129 (1992).

Table 9-36B
Experimental HETP Values from Various Sources for
Packings Equivalent to Stainless Steel X-200

System	Diam., In.	Absolute mm Hg	HETP, In.
Methylcyclohexane & toluene	1.25	760	1.25–2.00
	1.25	200	1.75–2.50
Methylcyclohexane & toluene	6	200–760	2–3
	18	200–760	4–6
Improved liquid distribution→	18	200–760	3.5
Methylcyclohexane & heptane	3	760	1.25–2
Ethylene dichloride & benzene	12	760	4–9
	1.25	50	1.25
Orthodichlorobenzene & orthodiethylbenzene	1.25	10	1.65
Phenol & orthocresol (no distributor used)	4	7–25	2.5–4
	4	85–100	2–3.5
	4	760	2–3.5
n-Hexanol & aniline	1.25	50–300	2.5–2.75
Nitrobenzene & aniline	1.25	5	3.5–4
n-Decanol & methyl naphthalene (no distributor used)	4	3	5
n-Decanol & methyl naphthalene	4	3	4
Methanol & water	1.25	760	9

By permission of ACS Industries, Separations Technology Group, Bul. B-129 (1992).

Table 9-36C
Rough HETP Correction Factor for Diameter

Column Diameter	HETP Proportional to:
Below 2 in.	1.0
2 to 6 in.	1.5
6 to 18 in.	2.0
Over 18 in.	2.5 to 3.0

By permission of ACS Industries, Separations Technology Group, Bul. B-129 (1992).

Calculate required column area and diameter using the maximum superficial vapor velocity, $u_{\max 1}$, and the actual vapor load.

Convert the mass vapor load, G , (lb/hr) to the actual vapor volumetric flow, V , in ft³/sec. Divide by u_{\max} to obtain the minimum cross-sectional column area, A , ft².

Correct this area by dividing the fraction of capacity at which the designer intends for the column to operate. A value of 0.7 is recommended, unless some other consideration suggests a different percentage.

$$A = V/u_{\max} = \text{column area, ft}^2$$

$$\text{Final Column inside net area} = A_F = A/0.70 \text{ capacity factor}$$

Calculate the column net inside diameter from the area values. Round to the nearest practical commercial column diameter such as 12 in., 15 in., 18 in., 24 in., 30 in., 36 in., and in increments of 6 in. Then recalculate the actual resulting vapor velocity.

$$\text{or, } A_o = A/0.7, \text{ ft}^2 \text{ required} \quad (9-64A)$$

$$\text{Column diameter} = \sqrt{4 A_o / \pi}, \text{ ft} \quad (9-64B)$$

Commercial size columns using Series X or Series S packing will operate at full efficiency with liquid loads as low as 5 gal/hr/ft² column area, and sometimes less liquid rate. They can operate satisfactorily exceeding liquid rates of 2,650 gal/hr/ft². See Figure 9-49.

HETP for ACS Series X-200 Structured Packing:

1. If plant or pilot plant data are available, use it.
2. Table 9-36B presents references for packings equivalent to the X-200 for the systems and conditions noted. See Figure 9-50.

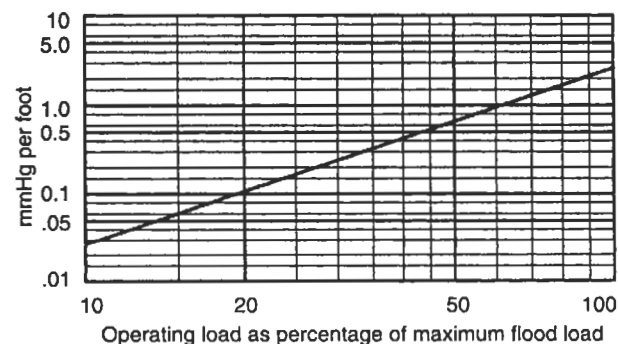
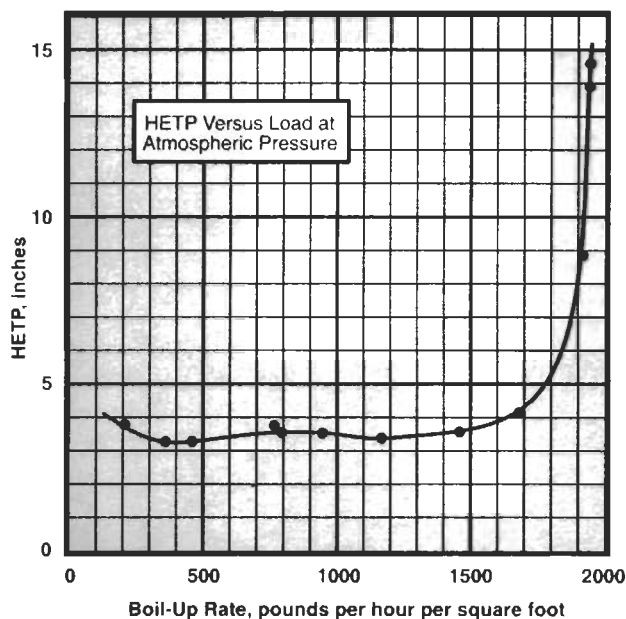
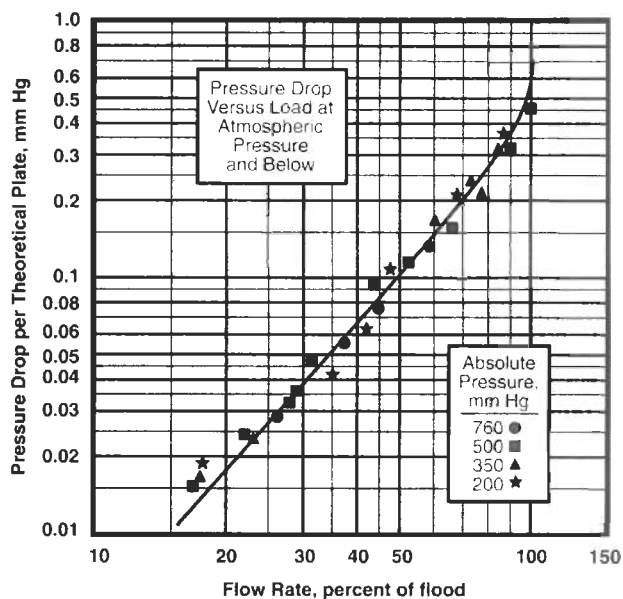


Figure 9-49. Estimated pressure drop referenced to percentage of maximum flood load for structured woven/knitted wire mesh X-100 and S-100. Referenced to liquid of 60 lb/ft³. To correct other liquids, multiply ΔP from figure by ratio of actual liquid density to 60. Used by permission of ACS Industries, Inc., Separation Technology Division, Bul. B-129 (1992).



A



B

Figure 9-50. HETP and pressure drop data for a typical distillation system. Packing: equivalent to X-200 (8 strands), stainless steel. System: methylcyclohexane and toluene. Reflux Ratio: 100%. Column Diameter: 18 inches. Packed Height: 5 feet. Used by permission: ACS Industries, Inc., Separation Technology Division, Bull. B-129 (1992).

3. Using an available HETP value for a specific Type X or S packing to convert to a column of different diameter, use the “rough” correction factors in Table 9-36C. These factors recognize that larger diameter columns have more uneven liquid distribution. When no HETP values or data are available, it is suggested to use the approximation developed for S-100 packing. Estimating HETP:

$$\text{HETP} = [0.18 + \mu^{0.55}] / [1.23 + (3.15/R^{0.27})] \quad (9-65)$$

where: HETP = height equivalent to a theoretical plate/tray/stage, ft
 μ = liquid viscosity, CP
 R = liquid rate, gal/hr/ft²

If μ is less than 0.30 cp, use 0.52 in place of the $\mu^{0.55}$ term.

To convert an available HETP value for a given system and column diameter to a different packing in the same series (X or S), assume HETP is inversely proportional to the specific surface (consult manufacturer for this detail).

$$\text{HETP}_2 = \text{HETP}_1 (SS_1/SS_2) \quad (9-66)$$

where 1 and 2 = two different wire mesh packings

For highly varying vapor loads through the column, pressure drop may be estimated for differences in latent heats from one point in the column to another; the pres-

sure drop should be calculated for each foot of packing, or less, adjusting the load. This particularly applies to vacuum columns or tall columns at high pressures. Maximum heights of a packed section in a column should be determined after consultation with the manufacturer.

Pressure Drop (Estimated):

Use Figure 9-49 to estimate column pressure per foot of packing height referenced to liquid load as percentage of maximum flood load. For varying load, perhaps $\pm 20\%$ -vacuum systems and varying latent heats in the column, calculate the pressure drop for each foot of packing or less; this requires adjusting the percentage load in each calculation.

Koch Sulzer Structured Packing [100]

This packing is woven wire mesh with the following characteristics as reported by the manufacturer/licensee [100]:

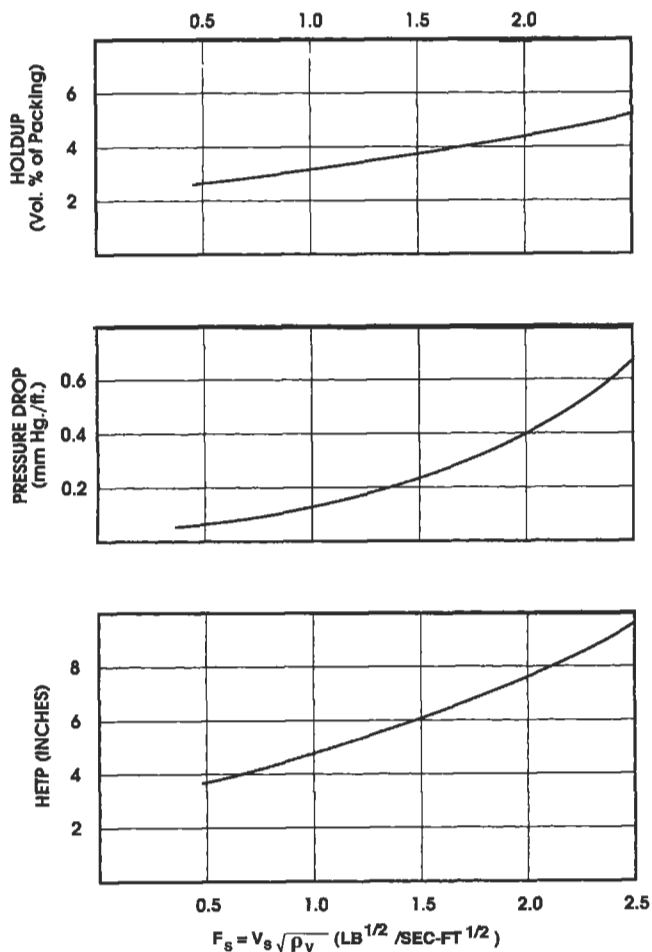
1. HETP of about 7 in., even at low liquid and vapor loads.
2. Efficiency essentially independent of column diameter.
3. Capacity and pressure drop characteristics superior to the best commercially available mass transfer devices.
4. Specific pressure drop of 0.2 mm Hg per theoretical tray

This packing is a woven wire fabric of parallel corrugated elements and is completely self-wetting. It does not require pre-flooding to attain the wetted condition. This packing has a flat surface of approximately 150 ft²/ft³, and a free area > 90%.

In operation, the liquid flows downwards in a zig-zag pattern. See Figure 9-6EE.

Example 9-7: Koch-Sulzer Packing Tower Sizing (used by permission, Bulletin KS-1, Koch Engineering Co. Inc.)

The following typical design problem illustrates the calculation procedure for Koch Sulzer Packing. A comparison of a KS Packing design and a Flexiring design will result in (for 2-in. metal Pall rings) top = 7.5-ft D and bottom = 8.5-ft D. See Figures 9-51-54.



Column Diameter 20 inches
 System cis-trans-decalin
 Top Pressure 20 mm Hg.
 Reflux Ratio Infinite

Figure 9-51. Characteristics of Koch/Sulzer packing, Gas loading factor, F_s versus HETP, pressure drop, and packing hold-up. Note: V_s = superficial gas velocity, ft/sec and ρ_v = vapor density, lb/ft³. Used by permission of Koch Engineering Co., Inc., Bull. KS-1 and KS-2.

Distill a diethanolamine-triethanolamine mixture to produce a 99.0 wt% DEA distillate product and a 95.0 wt% TEA bottoms product. The design material balance is as follows:

	Feed		Distillate		Bottoms	
	lb/hr	mol/hr	lb/hr	mol/hr	lb/hr	mol/hr
DEA	5,000	47.6	4,740	45.1	260	2.5
TEA	5,000	33.5	50	0.3	4,950	33.2
Totals	10,000	81.1	4,790	45.4	5,210	35.7

To preclude thermal degradation of the amine solution, the reboiler pressure must be limited to 10 mm Hg absolute pressure. Total allowable pressure drop is 3 mm Hg.

Solution

Distillation calculations result in a reflux ratio $L/D = 0.8$, with 4 theoretical trays for rectification and 4 theoretical trays for stripping, or a total of 8 trays. The design heat balance (neglecting heat losses) is as follows:

Heat Out	lb/hr	State	°F	Btu/lb	Btu/hr
Distillate	4,790	Liquid	296	160	766,000
Bottoms	5,210	Liquid	381	240	1,250,000
Ovhd. Cond.	—	—	—	—	2,470,000
	10,000				4,486,000
Heat In					
Feed	10,000	Liquid	314	180	1,800,000
Reboiler (Q_R)	—	By Difference			2,686,000
	10,000				4,486,000

Column Sizing for Koch Sulzer Packing

Bottom Section

The bottom section vapor loading is controlled by the reboiler vapor where:

$$V_r = Q_r / i_v \text{ TEA} = 2,686,000 / 192 = 14,000 \text{ lb/hr}$$

The design mass velocity at 10 mm Hg (Figure 9-52) is 460 lb/hr-ft². Applying the "f" factor correction for six carbon atoms (Figure 9-53) results in

$$f = 1.12$$

$$A = 14,000 (1.12) / 460 = 34.1 \text{ ft}^2$$

$$D = 6.6 \text{ ft, use 6 ft 9 in.}$$

$$V_s = V_r / 3600 (35.8) \rho_v$$

$$= 14,000 / 3,600 (35.8) (0.0031) = 35 \text{ ft/sec}$$

$$F_s = V_s (\rho_v)^{1/2} = 35 (0.0557) = 1.95 \text{ lb}^{1/2} / \text{ft}^{1/2} \text{ sec}$$

Considering the reboiler as a theoretical tray, for 3 theoretical trays the packing height for an HETP of 7 in. is 7 (3)/12 = 1.75 ft. This requires 4 standard elements which are 6.7 in. deep, or 80 ft³ of packing.

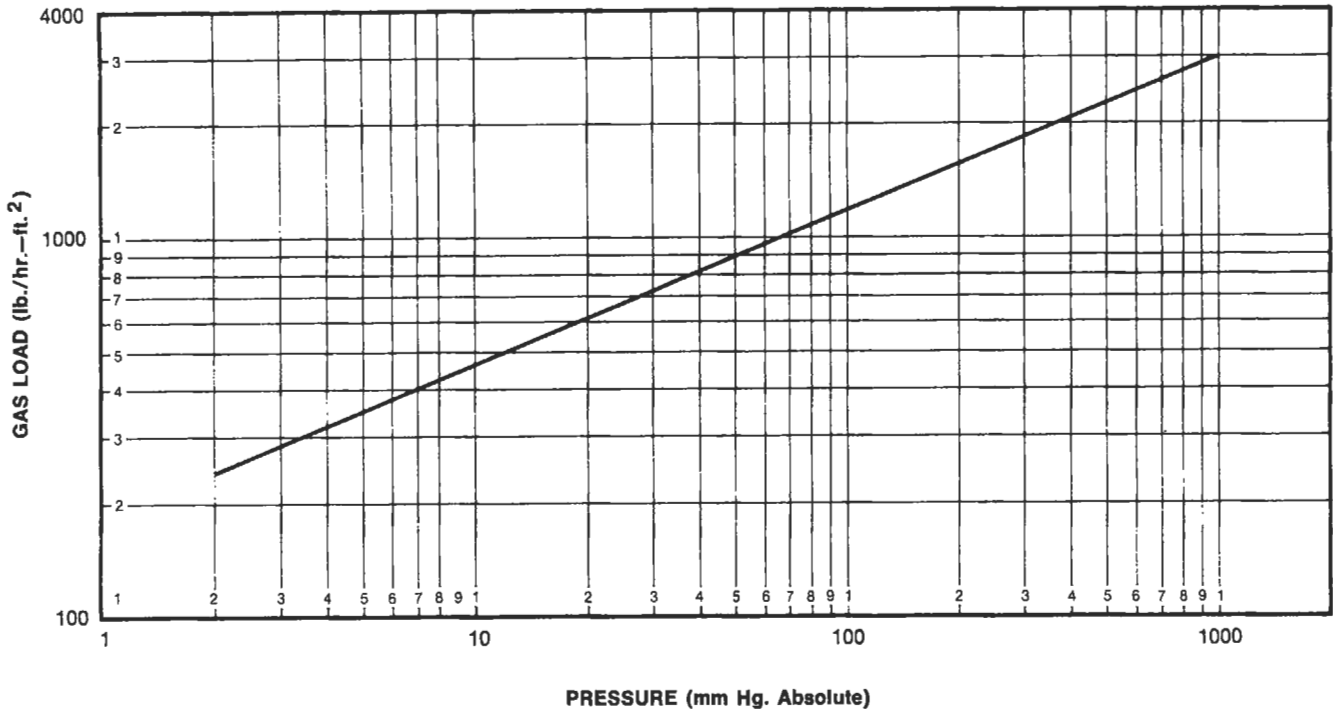


Figure 9-52. Koch/Sulzer packing. Design mass velocity (lb/hr-ft²) for HETP of 7 in. System cis-trans-decalin; molecular weight = 138. Used by permission of Koch Engineering Co., Inc., Bull. KS-1.

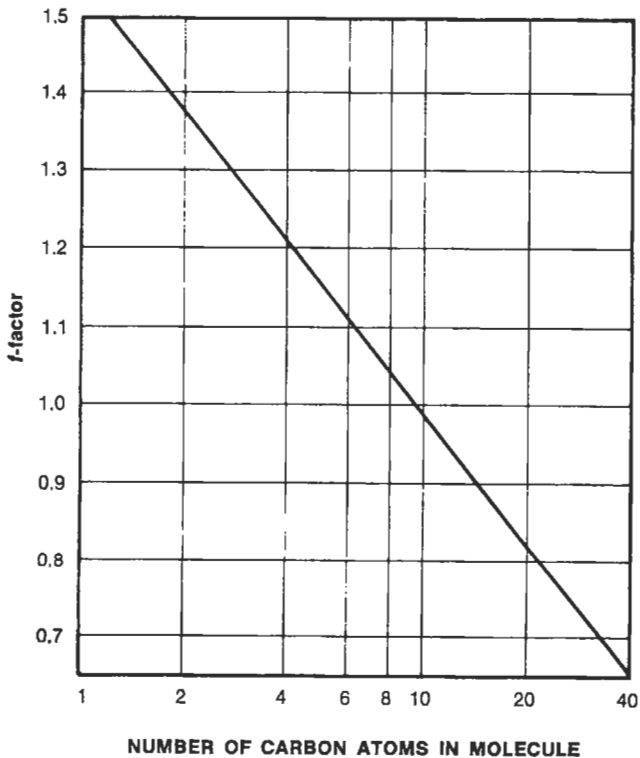


Figure 9-53. Koch/Sulzer packing. Design mass velocities for systems other than cis-trans-decalin are obtained by dividing the values from Figure 9-52 by the "f" factor. For the following groups corrections should be applied to the number of carbons in the molecule:

Paraffins, olefins acids, aldehydes, ketones	0
Benzene ring, alcohols, phenol	-1.0
Saturated ring	-0.5
Nitro	+1.0
Ether	+1.5
Ester, secondary amine	+2.0
Chlorine	+3.0
Bromine	+8.0

Used by permission of Koch Engineering Co., Inc., Bull. KS-1.

From Figure 9-51 the pressure drop is 0.38 mm Hg/ft or 0.85 mm Hg total.

Top Section

The top vapor load at an L/D of 0.8 is 8,620 lb/hr. The total pressure drop for 7 theoretical trays is slightly less than 2 mm Hg and ρ_v is 0.002 lb/ft³ at 8 mm Hg top pressure. Duplicating the calculations made for the bottom section results in

D = 5 ft 9 in.

Packing height = 2.8 ft

Pressure drop = 1.06 mm Hg

Therefore, use column diameter = 6 ft 9 in.

Nomenclature

A = cross-sectional area, ft²

D = diameter, ft

$F_s = V_s (\rho_v)^{1/2}$

G = vapor rate, lb/sec-ft²

$g_c = 32.2$ (lb mass) (ft)/(lb force) (sec)²

L = liquid rate, lb/sec-ft²

L/D = reflux ratio

P_f = packing factor

Q_c = condenser duty, Btu/hr

Q_r = reboiler duty, Btu/hr

V_r = reboiler vapor rate, lb/hr

V_s = superficial vapor velocity, ft/sec

ρ_l = liquid density, lb/ft³

ρ_v = vapor density, lb/ft³

l_v = latent heat of vaporization, Btu/lb

Koch Flexipac® Structured Packing

This type comes in four sizes, Types 1 through 4, and is constructed of corrugated metal sheets (See Figure 9-6GG). The types vary by corrugation size; the larger the type number, the greater is the depth of corrugation. The deeper corrugations give higher capacity and lower pressure drop. According to Koch reference [101], at the same efficiency, in countercurrent gas-liquid operation, this packing has a higher capacity and lower pressure drop than any available dumped or structured packing. The terminology for Figure 9-54 is:

$$F_s = V\sqrt{\rho_v} = [G/3,600(\rho_v)(A)](\sqrt{\rho_v}), \text{ ft/sec} \quad (9-67)$$

where G = vapor rate, lb/hr

V = vapor rate, ft/sec

ρ_v = vapor density, lb/ft³

A = cross-sectional area, ft²

ΔP = pressure drop, in. water/ft height

Chart parameter lines are gpm/ft^2 cross-section.

The Flexipac® structural packing have better efficiency than available random packing, particularly at low liquid rates, per Reference 101.

Intalox High Performance Metal Structured Packing [102]

According to the manufacturer's literature [102], this packing surpasses the best of other sheet-metal structured packings in terms of efficiency and capacity. See Figure 9-6II. The unique surface-texturing feature provides for greater use of the packing surface to achieve enhanced levels of mass transfer, and the overall geometry allows greater capacities and efficiencies to be obtained. Tests have been conducted on this and other packings at the University of Texas at Austin's "Separation Research Program, Center for Energy Studies" for distillation capacity and efficiency, and published in Reference 103.

For good and uniform performance of any structured packing it is essential to have uniform, consistent vapor and liquid distribution; therefore, much care must be given to the design details. See earlier discussion in this chapter.

For specific final performance sizing of a distillation column using Norton's Intalox® structured packing the designer is referred to the manufacturer's technical representatives, and should not assume the preliminary results obtained from any manufacturer's bulletin included here will necessarily serve as a final design. As a preliminary examination of a design problem (used by permission of Norton Chemical Process Products):

1. Calculate flow parameter, X

$$X = (L/G)\sqrt{\rho_g/\rho_L} \quad (9-68)$$

L = liquid mass rate, lb/sec

G = vapor or gas mass rate, lb/sec

ρ_g = gas density, lb/ft³ at conditions

ρ_L = liquid density, lb/ft³ at conditions

A = area, ft² tower cross-section area

2. Read chart, Figure 9-55, and obtain C_o , ft/sec, at packing type shown.

3. Calculate efficient capacity, C_{SC} :

$$C_{SC} = C_o [\sigma/20]^{0.16} [\mu/0.2]^{-0.11} \quad (9-69)$$

σ = surface tension, dynes/cm

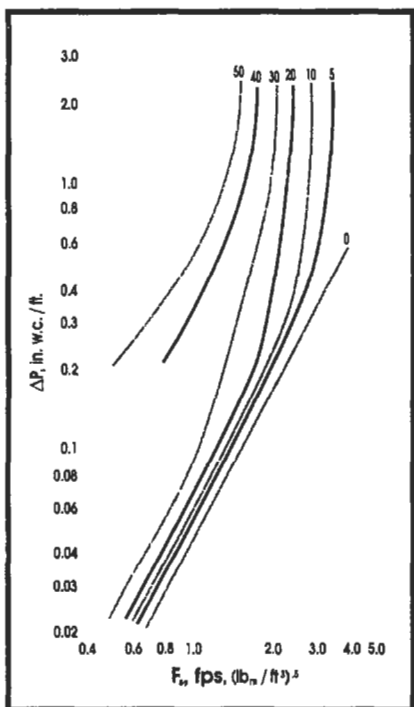
μ = liquid viscosity, cp

4. Calculate:

$$C_S = V\sqrt{\rho_G / (\rho_L - \rho_G)}, \text{ ft/sec}$$

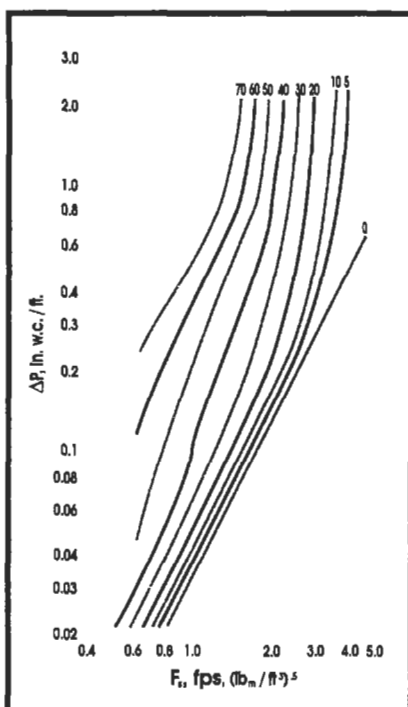
V = superficial gas velocity, ft/sec, or m/sec depending on the units used

V = $G/(\rho_G A)$, ft/sec



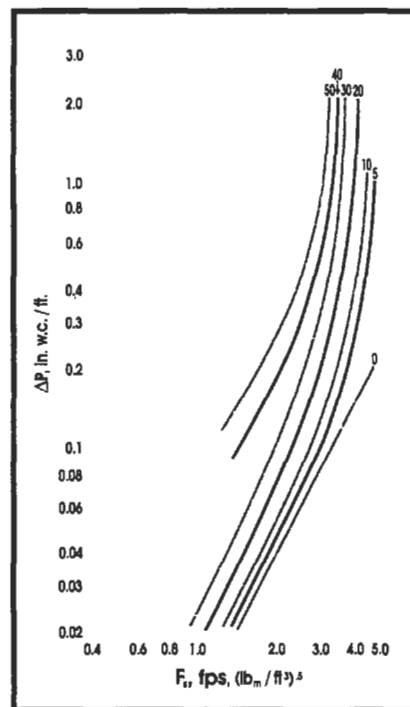
Pressure drop for Type 2Y FLEXIPAC®

A



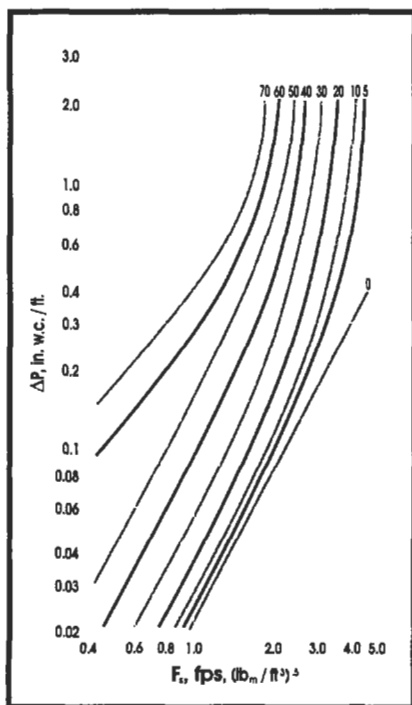
Pressure drop for Type 2.5Y FLEXIPAC®

B



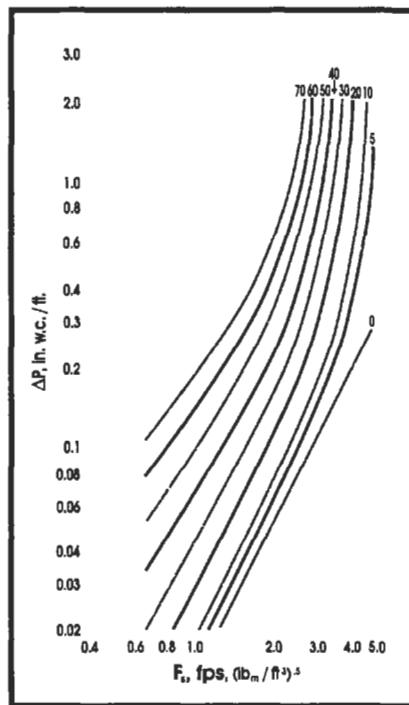
Pressure drop for Type 3X FLEXIPAC®

C



Pressure drop for Type 3Y FLEXIPAC®

D



Pressure drop for Type 4Y FLEXIPAC®

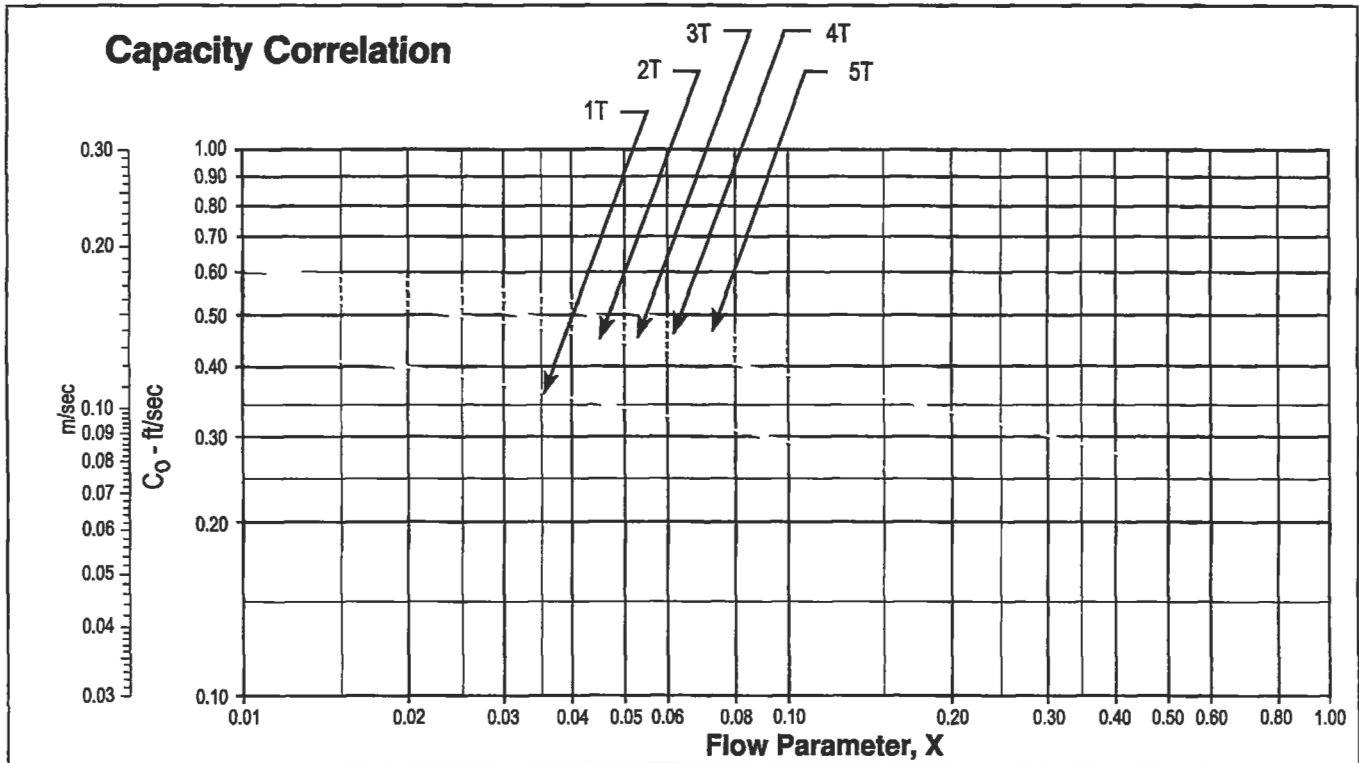
E

Figure 9-54. Typical pressure drop—capacity curves for countercurrent gas-liquid operation, for Koch Flexipac®. Used by permission of Koch Engineering Co., Inc., Bull. KFP-4. Parameter lines on charts are gpm/ft².

Packing Capacity

The Efficient Capacity of the packing in a non-foaming system can be estimated as:

$$\text{Efficient Capacity, } C_{SC} = C_o \left[\frac{\sigma}{20} \right]^{0.16} \left[\frac{\mu}{0.2} \right]^{-0.11}$$



Nomenclature and Definitions

- L — Liquid mass rate
- G — Gas mass rate
- ρ_L — Liquid density
- ρ_G — Gas density
- V — Superficial gas velocity, m/s or ft/s

$$X = \frac{L}{G} \sqrt{\frac{\rho_G}{\rho_L}} \quad \text{Flow parameter}$$

$$C_s = V \sqrt{\frac{\rho_G}{\rho_L - \rho_G}} \quad \text{m/s or ft/s}$$

$$F_s = V \sqrt{\rho_G} \quad \text{ft/sec } \sqrt{\text{lb/ft}^3}; \quad \text{or} \quad \text{m/s } \sqrt{\text{kg/m}^3}$$

$$\sigma = \text{Surface tension, dyne/cm} \quad \mu = \text{Liquid viscosity, cp}$$

Norton routinely designs towers up to 90% of Efficient Capacity. The limit of 90% of Efficient Capacity leaves an estimated 11% turn-up before the packing loses its design efficiency.

Figure 9-55. Capacity correlation for two types of Intalox® structured packing. Data range: $5 \leq \sigma \leq 73$ and $0.07 \leq \mu \leq 1.1$. Used by permission of Norton Chemical Process Products Corp., Bull. ISP-2 (1994).

5. Read pressure drop coefficient, F
 Read, F, for the approximate calculated C_s , ft/sec from Table 9-37 at calculated liquid rate, lb/hr-ft². Then read Y from IMTP Packing Pressure Drop chart, Figure 9-21G and then read curves showing pressure drop, (may require interpolation).
6. Typical HETP data are shown in Figure 9-56A-C.

Gempack® Structured Packing; Glitsch, Inc.

These packings are represented in part by Glitsch, Inc.'s bulletin [104] (Figure 9-6KK) and they cite the performance of the packing as:

1. High efficiency: 5-25 in. HETP (7.9-1.6 theoretical plates per meter.)
2. Low pressure drop: 0.5-0.7 mm Hg/theoretical plate
3. High vapor loadings: up to 0.5 C-Factor (up to 4.0 F-Factor)
4. High liquid capacity: 0.5-55 U.S. gpm/ft² (1.22-134 m³/m²/hr)
5. Wide turndown ratio: limited only by distributors
6. Availability: diameters from 4 in. to over 45 ft (10 cm to 13.7 meters)
7. Series available:
 - (a) Series AT: General purpose, suitable for low wetting rates and high vacuum applications.
 - (b) Series AS: General purpose, suitable for high wetting and heat transfer applications.
 - (c) Series AW: Latest generation of Gempack®, better efficiency with same hydraulic capacity as other series listed.
 - (d) Series AL: Especially suited for low wetting rates and chemical applications.
 - (e) Series BG: Wire gauze packing, crimped to 60° from horizontal, for high efficiency applications and very low wetting rates in clean service.

The performance and design information in Glitsch reference [104], as for all the other manufacturers with respect to their data and charts, is proprietary, but not necessarily warranted to be suitable for the designer's service/applications unless verified by the manufacturer's representatives.

Example 9-8: Heavy Gas-Oil Fractionation of a Crude Tower Using Glitsch's Gempack® (used by permission of Glitsch, Inc. Bulletin 5140)

The heavy naphtha-light gas oil fractionation zone of a crude tower has to be revamped to handle 25% more capacity. Because trays would be working at high percent flooding, Gempak structured packing is condensed (Figures 9-56A-D).

The loads are as follows:

- Vapor rate: 688,000 lb/hr, density: 0.355 lb/ft³ (ρ_v)
- Liquid rate: 381,000 lb/hr
 - specific gravity hot: 0.68 (42.42 lb/ft³) (ρ_l)
 - viscosity: 0.281 cp
- Non-Foaming System
- Tower diameter: 15 ft-0 in. (176.715 ft² cross sectional area)
- Height available for packed bed: 6.5' (78 in.) (excluding height for distributor)

1. Calculate the vapor load:

$$\begin{aligned} \text{Vapor, cfs} &= 688,000 / (3,600) (.355) = 538.3 \\ \text{Vapor velocity} = V_s &= (538.2) / (176.715) = 3.046 \text{ ft/sec} \\ \text{C-factor} = V_s [(\rho_v) / (\rho_l - \rho_v)]^{1/2} &= \\ 3.046 [(.355) / (42.42 - .355)]^{1/2} &= 0.28 \end{aligned}$$

(text continued on page 335)

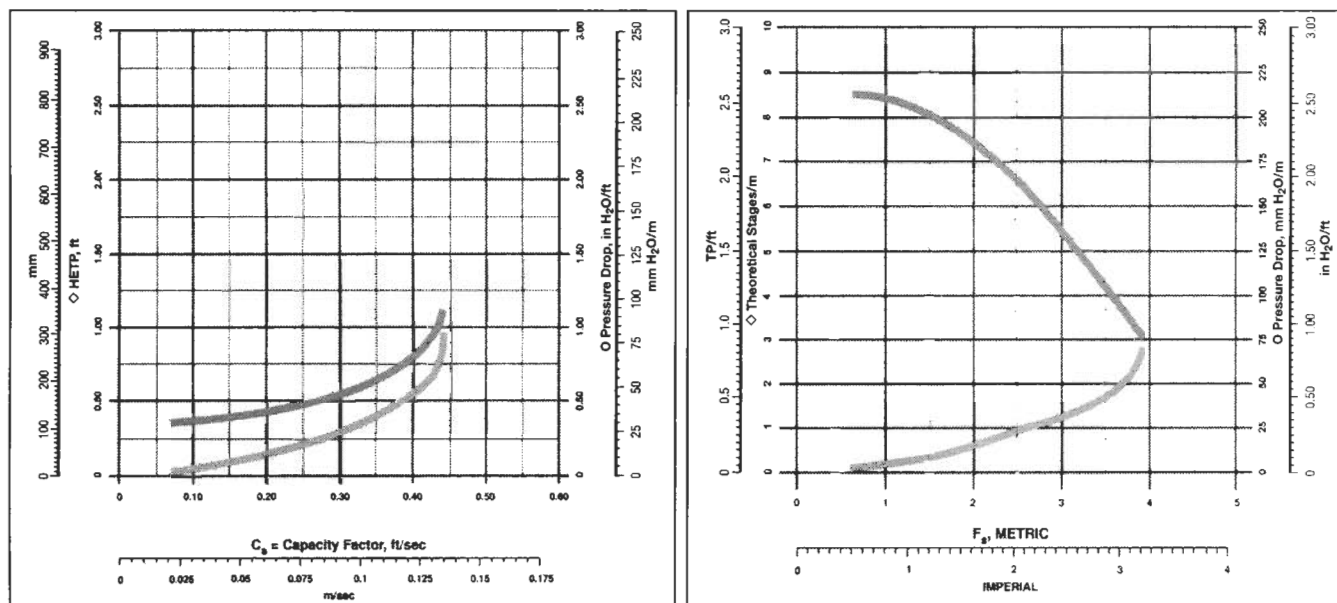
Table 9-37
Norton Intalox® Structured Packing Pressure Drop Coefficient F* for Type 2T Packing

Air/Water	Liquid, Kg/h • m ²	9,760	24,400	48,800	73,200	97,600	122,000
	Liquid, lb/h • ft ²	2,000	5,000	10,000	15,000	20,000	25,000
Intalox Structured Packing 2T							
F when C_s in m/s	205	215	250	300	325	365	
F when C_s in ft/s	19	20	23	28	30	34	

These packing factors can be used to predict the pressure drop of Intalox Structured Packing 2T when used with the Generalized Pressure Drop Correlation as illustrated in Norton's Intalox High-Performance Separation Systems; Figure 9-21G this text. Used by permission of Norton Chemical Process Products Corp., Bull. I-S-I-R.

Intalox® Wire Gauze Packing

System: Para/ortho Xylene at 16 mm Hg abs and total reflux



Intalox Structured Packing 1T

System: Iso-octane/Toluene at 100 mm Hg abs and total reflux

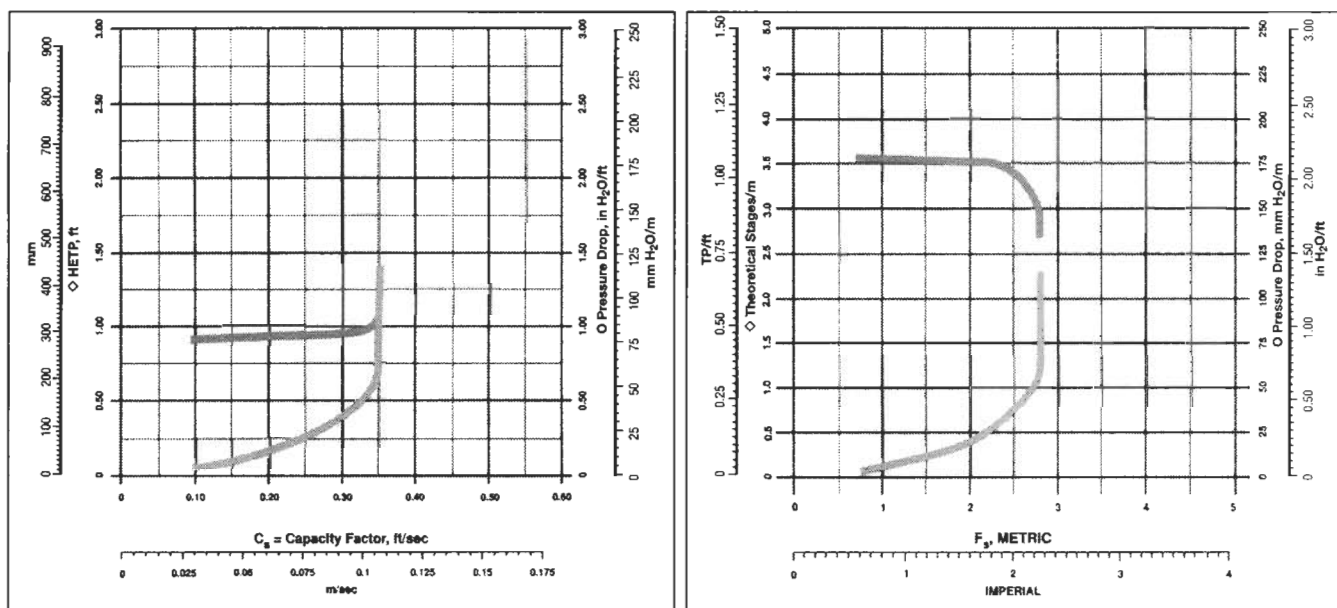
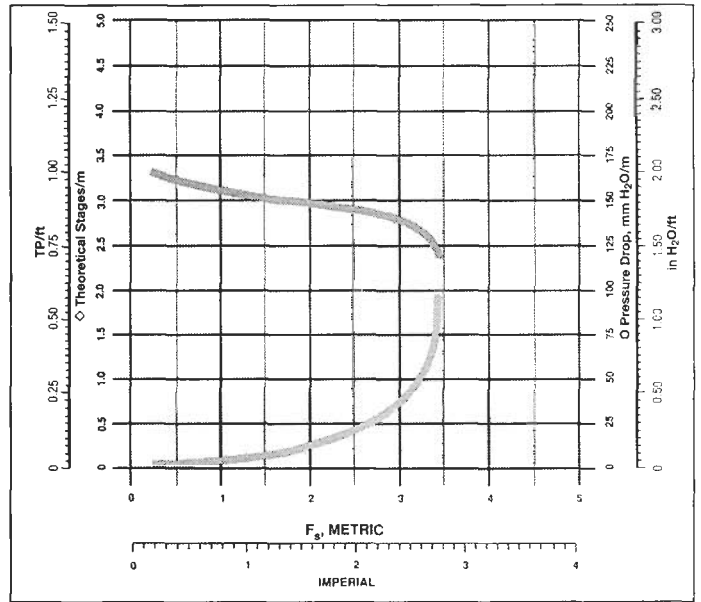
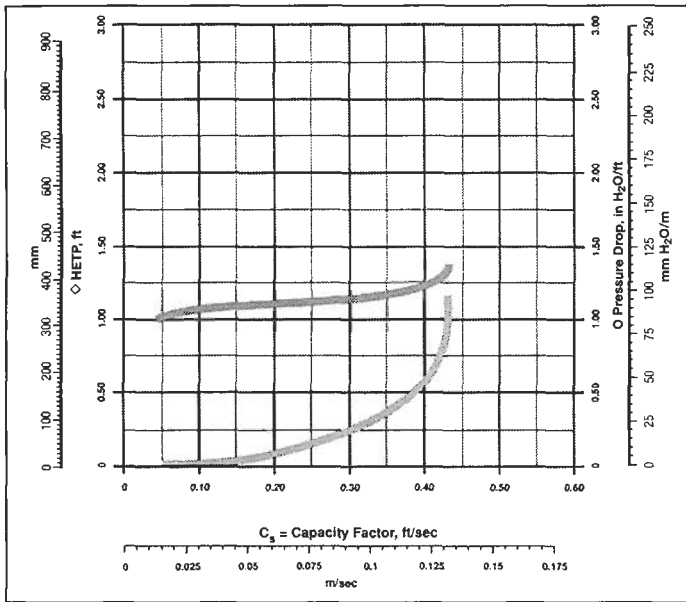


Figure 9-56A. Performance test results using Norton's Intalox® structured packing. Used by permission of Norton Chemical Process Products Corp., Bull. ISP-2.

Intalox Structured Packing 2T

System: Iso-octane/Toluene at 100 mm Hg abs and total reflux



Intalox Structured Packing 3T

System: Iso-octane/Toluene at 100 mm Hg abs and total reflux

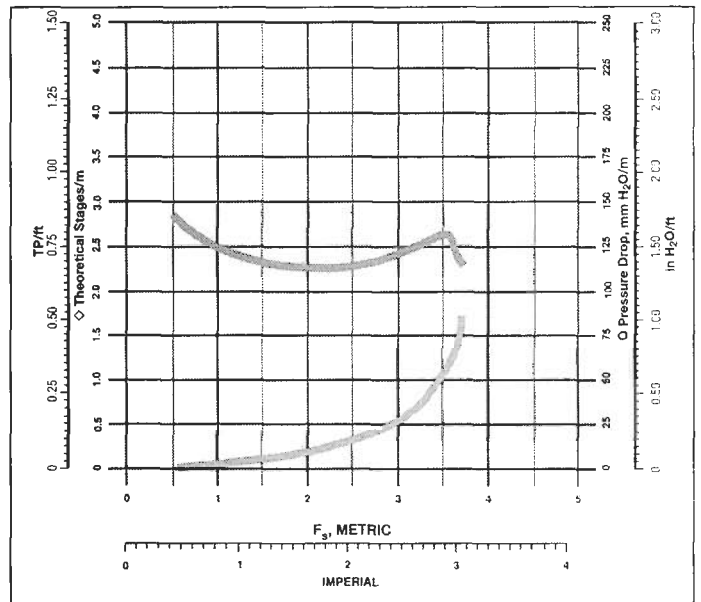
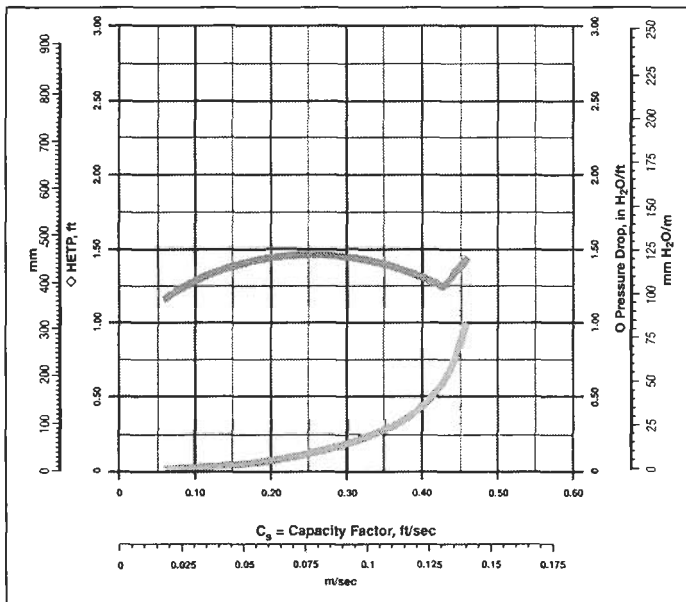
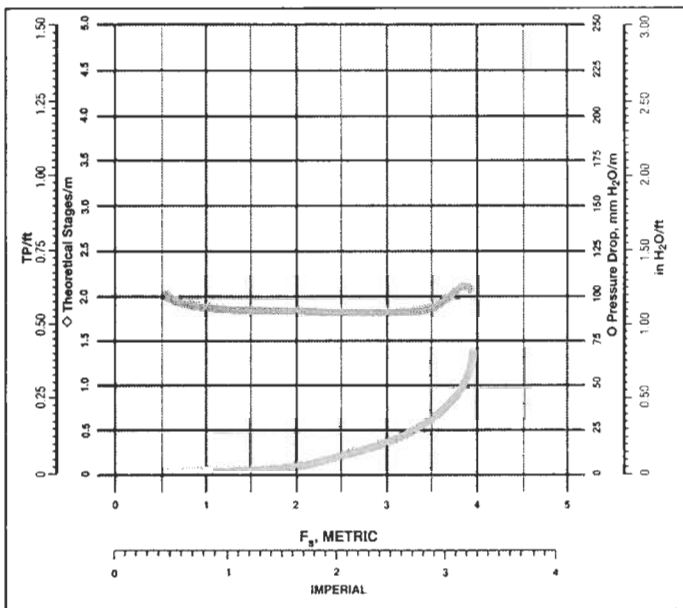
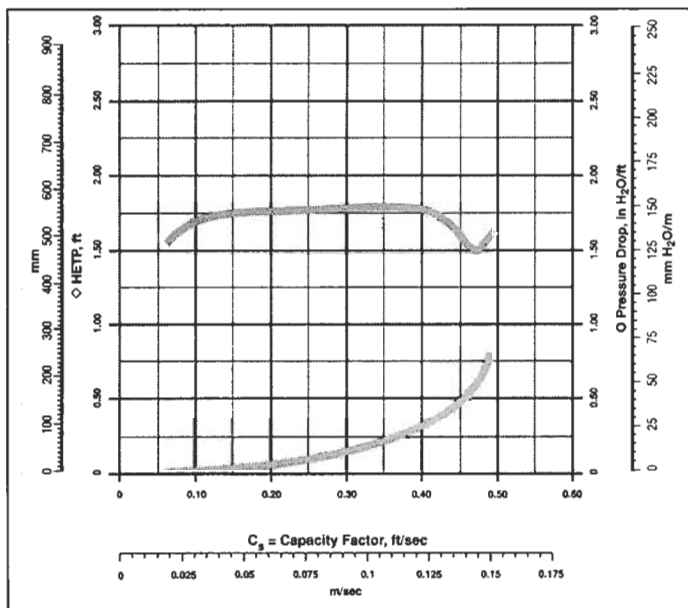


Figure 9-56B. Performance test results using Norton's Intalox[®] structured packing. Used by permission of Norton[®] Chemical Process Products Corp., Bull. ISP-2.

Intalox Structured Packing 4T

System: Iso-octane/Toluene at 100 mm Hg abs and total reflux



Intalox Structured Packing 5T

System: Iso-octane/Toluene at 100 mm Hg abs and total reflux

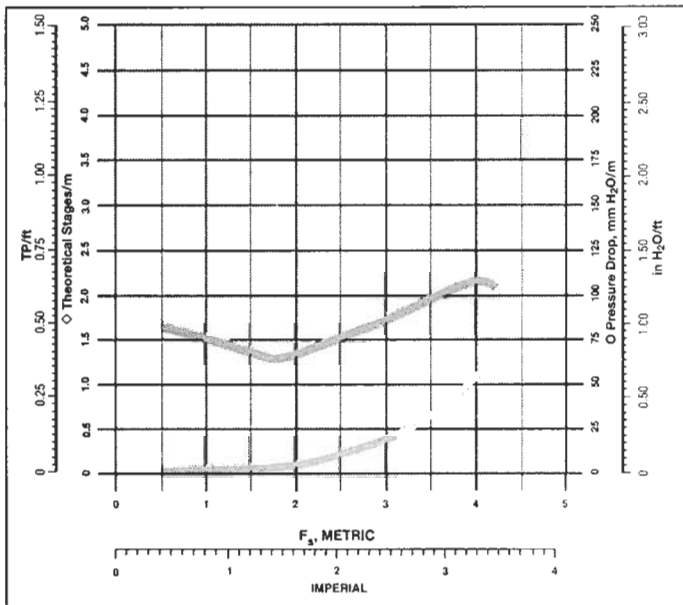
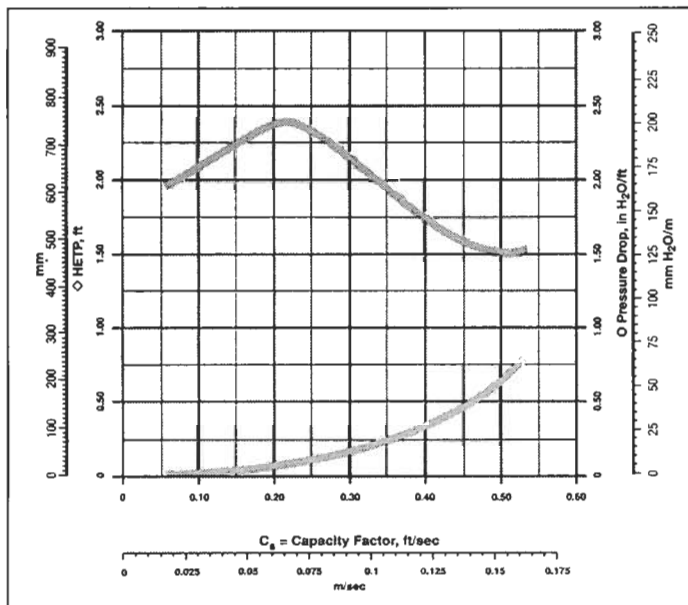


Figure 9-56C. Performance test results using Norton's Intalox® structured packing. Used by permission of Norton Chemical Process Products Corp., Bull. ISP-2.

(text continued from page 331)

2. Calculate the liquid load:

$$\begin{aligned} \text{gpm} &= (381,000)/(8.33) (60) (.68) = 1,120 \\ \text{gpm/ft}^2 &= (1,120)/(176.715) = 6.3 \end{aligned}$$

3. Select the Gempak size:

On plot of C-factor vs. liquid load as shown in Figure 9-57A mark the operating point (A) using 6.3 gpm/ft² and C-factor = 0.28. The point on the figure is above the Gempak AS (0.25-in. crimp height) packing flooding line. All other packing sizes would be operating below flooding. For example, if Gempak AS (0.375-in. crimp height) is to be used, the percent flooding at design loads will be:

- At constant L/V ratio—(OA/OD) × 100 = 75.2%
- At constant liquid rate—(100) (BA/BE) = 70.0%

Normally in distillation, flooding at constant L/V ratio is more representative of actual plant operations (constant liquid loads may also be representative in cases like absorbers). In general, percent flooding up to 75–80% is acceptable for continuous operation. Gempak AS (0.375-in. crimp height) would be a good selection for this example. Gempak AS (0.5-in. crimp height) would also be a good selection, with flooding of 70% at constant L/V ratio and 65% at constant liquid rate. Gempak AS (0.25-in. crimp height) would not be a good selection in this case since flooding would be over 100%.

4. Pressure Drop

On pressure drop plots, mark a C-factor of 0.28 and 6.3 gpm/ft² as shown in Figures 9-57B and 9-57C.

For Gempak AS (0.5-in. crimp height), ΔP = 0.31 in. liq/ft
For Gempak AS (0.375-in. crimp height), ΔP = 0.55 in. liq/ft

For a bed of 6.5 ft, the pressure drop for the bed is:

For Gempak AS (0.5-in. crimp height) = 0.31 × 6.5 = 2.0 inches of liquid
For Gempak AS (0.375-in. crimp height) = 0.55 × 6.5 = 3.6 inches of liquid

Pressure drop for both AS (0.5-in. crimp height) and AS (0.375-in. crimp height) packings is acceptable for the crude tower operation.

5. Efficiency, Figure 9-57D

On efficiency plot, mark C-factor at 0.28.

For Gempak AS (0.5-in. crimp height): HETP = 13.5 in.
(0.89 NTS/ft)

For Gempak AS (0.375-in. crimp height): HETP = 10.2 in.
(1.18 NTS/ft)

Note: The HETP's noted are valid only for o-/p-xylene at the test conditions. Nevertheless, the ratio of HETP's should remain approximately constant.

Grid Packing: Nutter Engineering (Figure 6-PP)

For applications and design details refer to the manufacturer concerning these types of packings.

Figure 9-58 illustrates performance of No. 3 Snap-Grid™. For mass transfer for distillation HETP, use:

$$\text{HETP} = H_{og} (\ln \lambda) / (\lambda - 1) \quad (9-70)$$

$$\text{where } \lambda = m (G_m / L_m) \quad (9-71)$$

HETP = height equivalent to a theoretical plate, inches

H_{og} = height of an overall gas phase transfer unit, inches

U_a = volumetric overall heat transfer coefficient, Btu/(hr) (ft³) (°F)

m = slope of equilibrium line expressed in mole fraction

G_m, L_m = gas, liquid molar rate based on superficial tower area, mol/(hr) (ft²)

H_g, H_l = height of gas, liquid phase transfer unit, inches

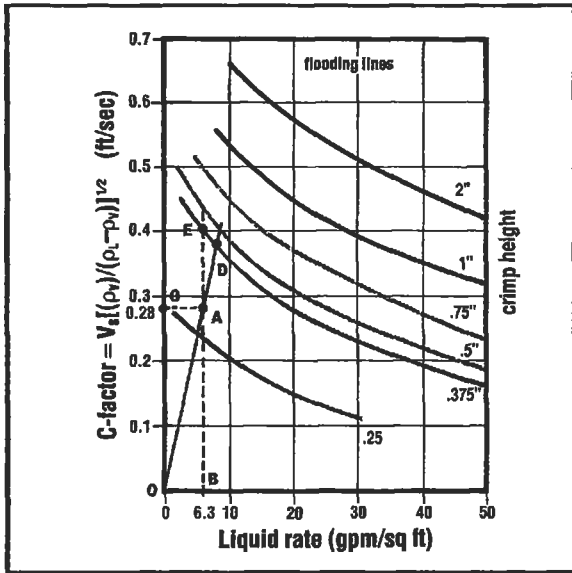
Re = Reynolds number of gas phase

Koch Flexigrid® Packing: Koch Engineering Co.

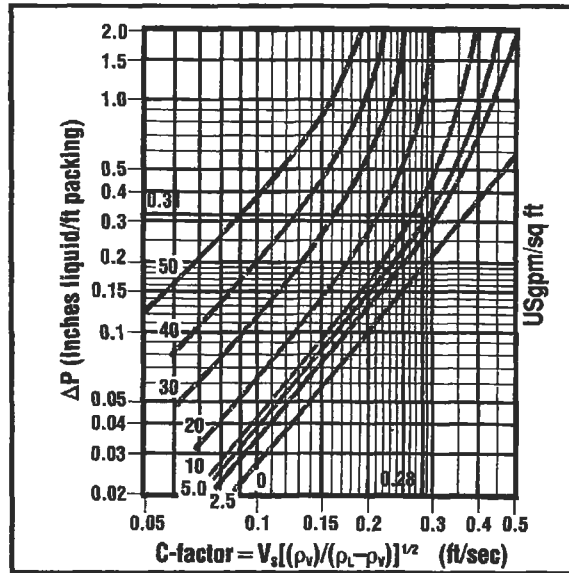
Koch Flexigrid® packing bulletin [106] states that the packing (Figures 9-6SS, -TT) has a fixed, ordered orientation and is supplied as layers that stack in a prescribed fashion within the bed. Features include [106]:

1. High capacity; constructed in 60 in. × 16 in. × 2¼ in. high modules.
2. High efficiency: constructed in 60 in. × 16 in. × 2¼ in. high modules.
3. Each successive layer of the grid is rotated 45° during installation.
4. Lower pressure drop.
5. Tendency to coke or foul far less than other grids, due to elimination of horizontal planes where liquids or solids can stagnate.
6. Low liquid holdup.
7. Fabricated of most metals, such as carbon steel, stainless steel, aluminum and others as required.

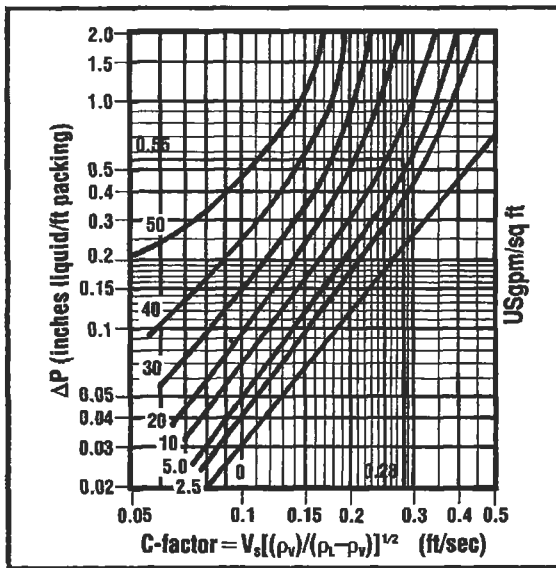
Capacity comparison at flooding is shown on Figure 9-59 as a function of the vapor and liquid capacity factors C_v and C_L. Koch developed correlations, used by permission [106]:



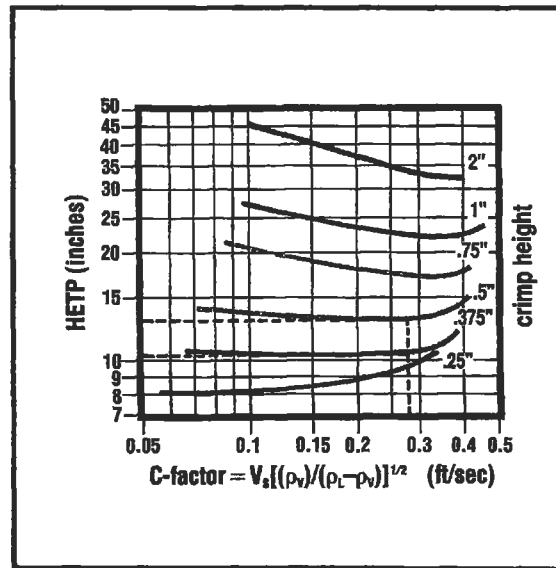
A. Gempak® flooding lines for Series AS. Used by permission of Glitsch, Inc., Bull. 5140.



B. Gempak® pressure drop, Series AS, with 0.50-in. crimp height. Used by permission of Glitsch, Inc., Bull. 5140.



C. Gempak® pressure drop, Series AS, with 0.375-in. crimp height. Used by permission of Glitsch, Inc., Bull. 5140.



D. Gempak® relative HETP. Used by permission of Glitsch, Inc., Bull. 5140.

Figure 9-57. For Example 9-8 typical Glitsch Gempak® preliminary design charts for structured packing. Note: These plots are to be used in carrying out the calculations described in the Glitsch bulletin. Graphic data presented here have been obtained in tests whose conditions may differ materially from your own. Curves on these pages are for Gempak with crimp angles of 45° from the horizontal, and should be sufficient for a preliminary review. The actual surface texture, which determines the final design, should be chosen in consultation with the Glitsch process engineering staff. Used by permission of Glitsch, Inc., Bul. 5140.

Flexigrid® Style 2 High Capacity

$$\% \text{ flood@const } L/V = 119 \times (C_v + .074 \sqrt{C_v C_L} + .00136 C_L) \quad (9-72)$$

$$\% \text{ flood@const } L = \frac{100 C_v}{.84 - .0676 \sqrt{C_L} + .00136 C_L} \quad (9-72A)$$

Flexigrid® Style 3 High Efficiency

$$\% \text{ flood@const } L/V = 165.34 \times (C_v + .06 \sqrt{C_v C_L} + .0009 C_L) \quad (9-73)$$

$$\% \text{ flood@const } L = \frac{100 C_v}{.605 - .0464 \sqrt{C_L} + .0009 C_L} \quad (9-73A)$$

const = constant

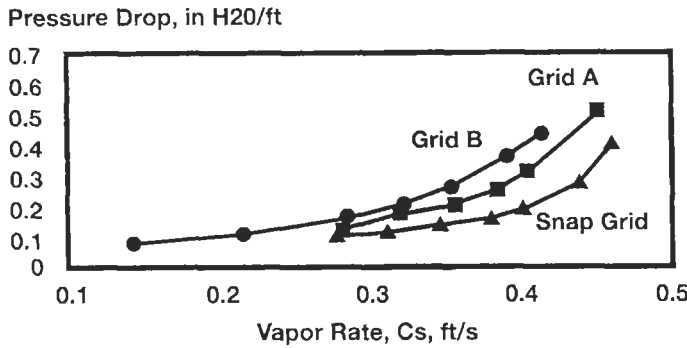


Figure 9-58. Nutter Snap-Grid™ typical performance charts for pressure drop. Used by permission of Nutter Engineering, Harsco Corp., Bull. CSG-2, for Air-Isopar @ 10gpm/ft².

$$C_L = \frac{V_L}{A} \left(\frac{\rho_L}{\rho_L - \rho_v} \right), \text{ gpm / ft}^2$$

where V_v = vapor rate, ft³/sec
 V_L = liquid rate, U.S. gpm
 A = tower area (πr^2) ft²
 ρ_v = vapor density, lbs/ft³
 ρ_L = liquid density, lbs/ft³

Typical pressure drops are shown in Figure 9-60. Mass transfer and heat transfer evaluations should be referred to the manufacturer.

Glitsch-Grid™ [107] (Figure 9-6UU)

This is an open area packing with multiple layers of lattice-type panels. This grid, as described by the manufacturer's bulletin, consists of vertical, slanted, and horizontal planes of metal. The vertical strips have horizontal flanges oriented alternately right and left. Due to the random overlap, the vapor path must zig-zag through the bed.

Per the manufacturer, this grid has extremely low pressure drop (0.5 mm Hg/ft) at capacities higher than is possible with any other mass transfer device. Grid capacity is approximately 50% greater than conventional trays, and about 35% greater than 3½-in. ballast rings. The grid is highly resistant to fouling, plugging, or coking by tars or solids. See Figures 9-61A and 9-61B for pressure drop and capacity performance comparison. HETP is available from the manufacturer and final design performance must be obtained from the same source.

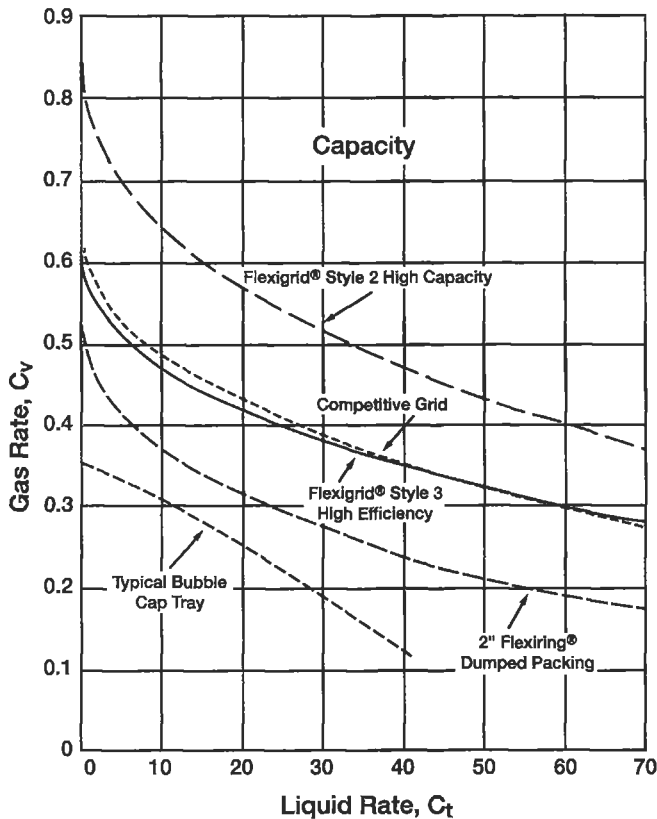


Figure 9-59. Comparison of capacities of Flexigridd® Styles 2 and 3 at flooding with 2-in. Flexiring® random packing, and a competitive grid. Used by permission of Koch Engineering Co., Inc., Bull. KFG-2.

Structured Packing: Technical Performance Features

Fair and Bravo [108] have performed extensive studies on structured packing and have developed general models for flooding, pressure drop, and mass transfer. Structured packing is now generally considered cost effective for moderate pressure and vacuum distillations when compared to trays and random packings [108]. The test work of the authors considered the trade-named structured packings of Intalox®, Gempac®, Flexipac®, Mellapak®, Sulzer, and Montz in their studies. See earlier figures for installations of these packings, many of which are quite similar. All of the cited packings are corrugated sheet type designs, except the Sulzer, which is a fabricated wire gauze construction. Table 9-38 summarizes the characteristics of the selected packings. Refer to the respective manufacturers for confirming details and design application techniques.

A "viscosity correction" should be made if $\mu_L > 10.0$ cp by multiplying the "% flood" obtained from Equations 9-72 through 9-73A by the term " $\mu_L^{.06}$ " in cp.

$$C_v = \frac{V_v}{A} \left(\frac{\rho_v}{\rho_L - \rho_v} \right)^{1/2}, \text{ ft / sec}$$

Flooding

At flooding or near flooding conditions [108]:

1. A rapidly increasing pressure drop with a relatively slight increase in gas rate (hydraulic flood) develops.

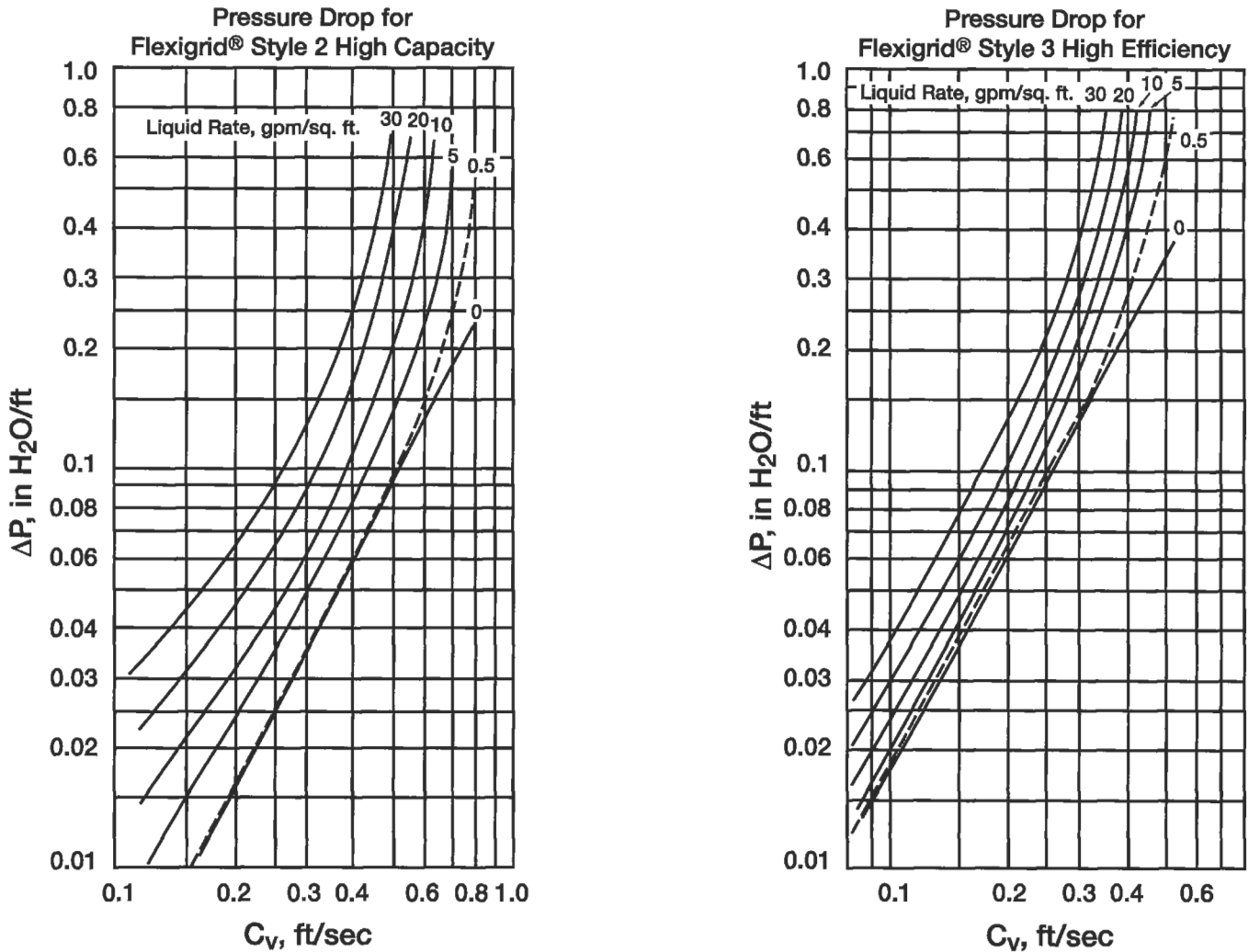


Figure 9-60. Pressure drop for Styles 2 and 3 Flexigrid® at selected liquid rates. Used by permission of Koch Engineering Co., Inc., Bull. KFG-2.

2. A rapidly decreasing efficiency with a relatively slight increase in gas rate (mass-transfer limitation) develops.
3. A general lack of column stability develops.

All of these conditions do not necessarily occur at the same liquid-gas loading. Generally, the mass-transfer limitation develops before the hydraulic flood condition as loadings are increased. Fair and Bravo [108] used the mass-transfer limitation as the limiting case for reasonable design of mass-transfer efficiencies. Figure 9-62 is based on hydraulic flood for several structured packings. The capacity limit is related to the corrugated elements as reflected in specific surface area. The capacity parameter, C_s in m/sec, = U_o.

$$C_s = V \sqrt{\rho_G / (\rho_L - \rho_G)}, \text{ m/sec}$$

V = superficial velocity, m/sec

ρ_G and ρ_L = gas and liquid density, respectively, kg/m³

Figures 9-63A and -63B illustrate for a specific packing the hydraulic flood and mass-transfer efficiency limitations. The differences in crimp height can influence the results. Figure 9-63B shows the effect of a higher flow parameter taken using larger columns; the system apparently was approaching its critical, but the cause of the performance is not yet known.

Pressure Drop

Structured packings maintain mass-transfer performance with minimum penalty for pressure drop [108]. Two models are presented for calculating pressure drop: (1) Bravo-Rocha-Fair [111] and (2) Stichlmair-Bravo-Fair [112]. Each method is quite involved with rather complex equations to calculate the factor to ultimately calculate a pressure drop. The authors [108] recommend for design using

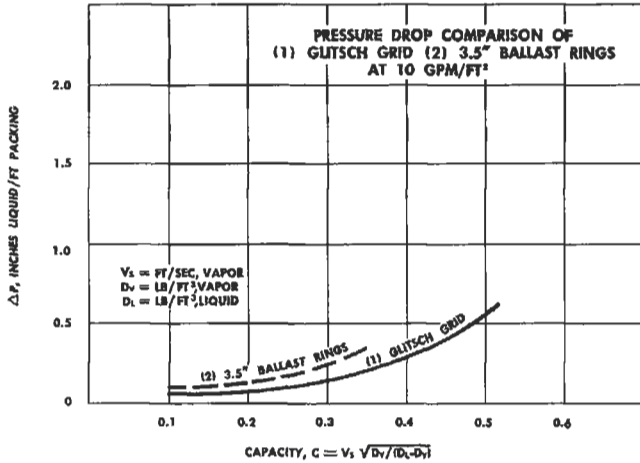


Figure 9-61A. Pressure drop comparison of Glitsch Grid™ and Ballast® rings at 10 gpm/ft². Used by permission of Glitsch, Inc. Bull. 9-72.

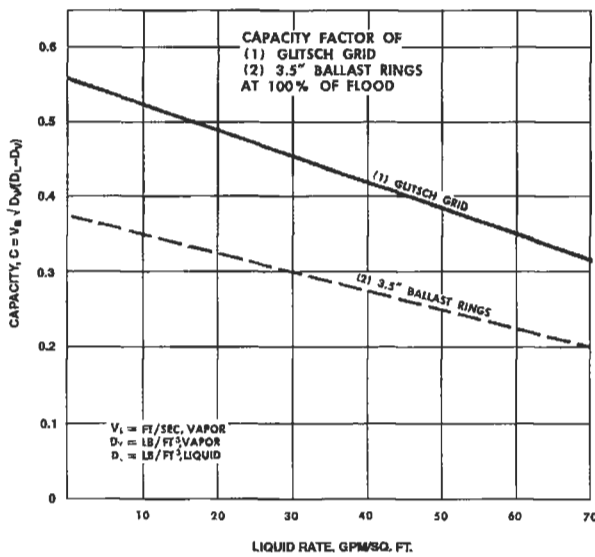


Figure 9-61B. Capacity performance comparison for Glitsch-Grid™ and Ballast® rings. Used by permission of Glitsch, Inc. Bull. 9-72.

1. Flooding: Empirical plots of data, as shown in Figures 9-62, 9-63A, 9-63B, and 9-64.
2. Pressure drop: Generalized model of Bravo, et al. [111], in combination with Stichlman [112]. Pressure drop at the flood point as a function of the flow parameter at the flood point is given in Figure 9-62 [108] for several packings using the Stichlman model equations for various system pressures [108].
3. Mass transfer: Generalized model of Bravo, et al. [113], with discount factors for wetted surfaces.

Hatfield [114] describes the improvements in commercial performance when Pall rings were replaced with Goodloe® packing.

Pressure drop through gauze and sheet metal structured packings [115] applies for the region below the loading point and cannot predict the flood point because liquid holdup vs. gas velocity is not included. The latest version of the equation is in Reference 108:

$$\Delta P = \left[0.171 + \frac{(92.7)}{(Re_g)} \right] \left((\rho_g) \frac{(U_{ge}^2)}{S} \right) \left[\frac{1}{1 + C_o Fr_1^{0.05}} \right]^5 \quad (9-74)$$

$$Re_g = \frac{S U_{ge} \rho_g}{\mu_g} \quad (9-75)$$

$$U_{ge} = U_g / \epsilon \sin \theta \quad (9-76)$$

$$Fr_1 = U_1^2 / (Sg) \quad (9-77)$$

where C_o = constant, value of 3.08 in Equation 9-74 recommended for all structured packings similar to such types as Flexipac 2® and Gempak 2®. Note: Reference 108 provides values for other structured packing sizes and styles and wire gauze. Refer to manufacturer for confirmation.

where c, C_o, C_1, C_2, C_3 = correlation constants

Fr_1 = liquid Froude number

g = gravitational constant

Re_g = Reynolds number for gas

S = length of corrugation side

U_{ge} = effective velocity of gas

U_g = superficial velocity of gas

U_1 = superficial velocity of liquid

Δp = pressure drop per unit packed height

ϵ = packing void fraction

θ = angle of flow channel (from horizontal)

μ = viscosity

ρ = density

f (subscript) = flooding conditions

g (subscript) = gas

l (subscript) = liquid

Billet [123] reports that metal gauze-type packing (such as Goodloe®) give better performance and lower costs for high vacuum distillations, particularly for thermally unstable mixtures. This comparison was made against Pall rings. For the performance information referenced here, see Figure 9-65 [123].

For general references during vacuum operations:

1. Due to the rapid decrease in specific efficiency with increasing load, the optimum load factor is equal to a

(text continued on page 342)

Table 9-38
 Characteristics of Representative Structured Tower Packings*

	Flexipac-2	Gempak 2A	Intalox 2T	Montz B1-200	Mellapak 250Y	**Sulzer BX
Specific Area (m^{-1})	223	223	220	200	250	500
Void Fraction	0.93	0.95	0.97	0.94	0.95	0.90
Corrugation Angle (degrees)	45	45	45	45	45	60
Crimp Height (m)	0.0125	0.0122	0.0104	0.0149	0.0119	0.0064
Corrugation Side (m)	0.0177	0.0180	0.0223	0.0250	0.0171	0.0088
Corrugation Base (m)	0.0250	0.0268	0.0390	0.0399	0.0241	0.0128

*All packing types listed are available in several different sizes. The corrugation angle is measured from the horizontal. Confirm details with manufacturer.

**Wire gauze for comparison.

Used by permission of The American Institute of Chemical Engineers; Fair, J. R. and Bravo, J. L., *Chem. Eng. Prog.* Vol. 89, No. 1 (1990), p. 19; all rights reserved.

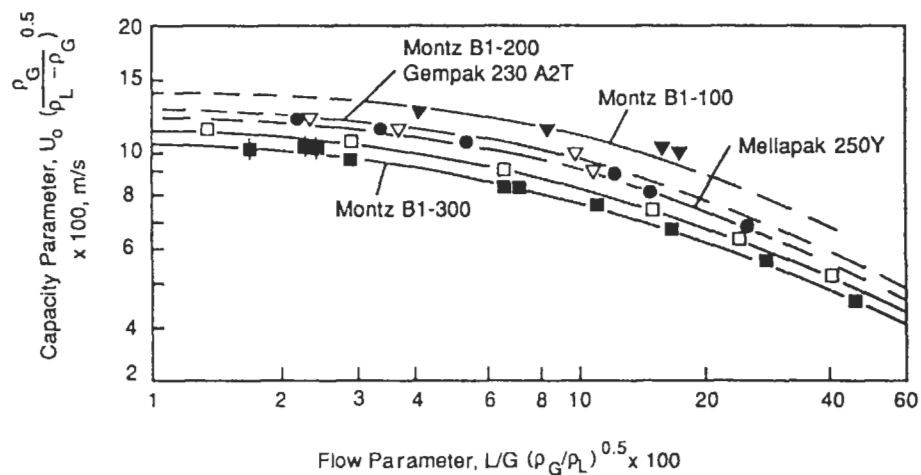


Figure 9-62. Flooding data for structured packings as reported by Billet [109]. Numbers following packing type indicate specific surface area in m^2/m^3 . Reproduced by permission of the American Institute of Chemical Engineers, Fair, J. R. and Bravo, J. L., *Chemical Engineering Progress*, V. 86, No. 1 (1990) p. 19; all rights reserved. Note, U_0 = vapor velocity, meters/sec.

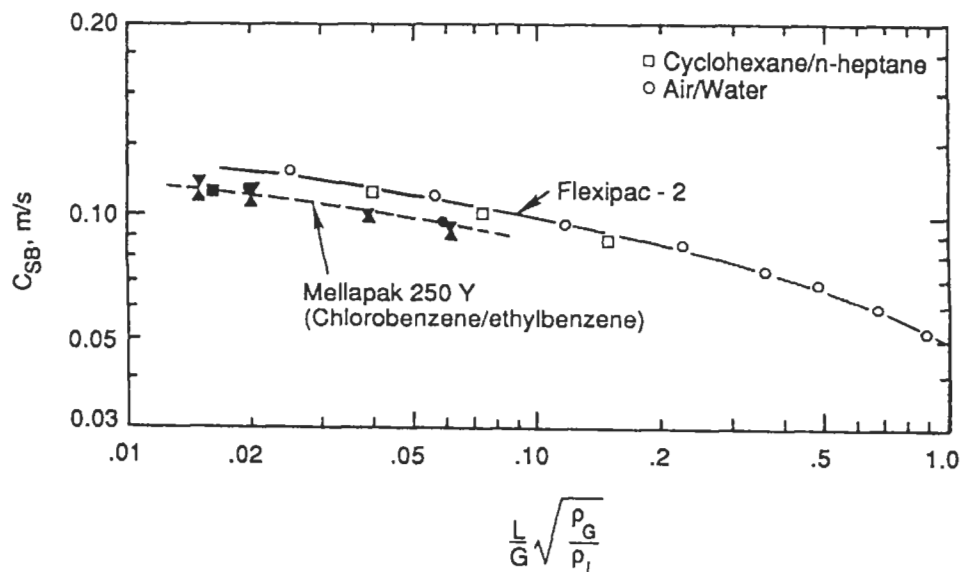


Figure 9-63A. Flooding data for structured packings obtained by pressure drop measurements as well as by efficiency measurements (see Ref. 108 for sources). Reproduced by permission of the American Institute of Chemical Engineers, Fair, J. R. and Bravo, J. L., *Chemical Engineering Progress*, V. 86, No. 1 (1990) p. 19; all rights reserved.

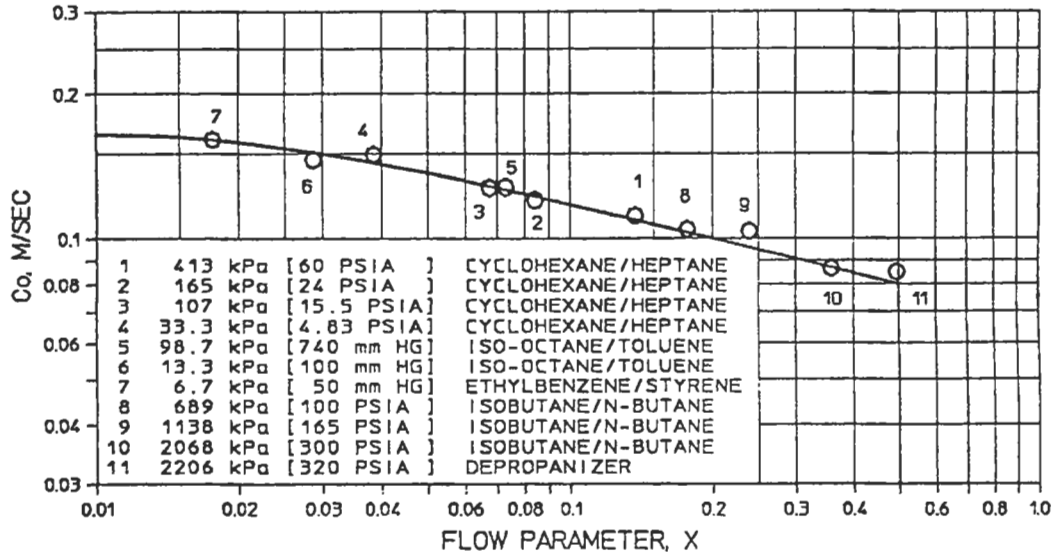


Figure 9-63B. Capacity correlation of structured Intalox® 2T. The capacity parameter is at the maximum efficient capacity (MEC) point defined by Rukovena and Koshy [151]. The MEC point is lower than the flood point and located where the packing will maintain its desired efficiency. Used by permission of Rukovena, E. and Koshy, T. D., private communication, and *Ind. and Eng. Chem. Res.* V. 32, No. 10 (1993) p. 2400; all rights reserved.

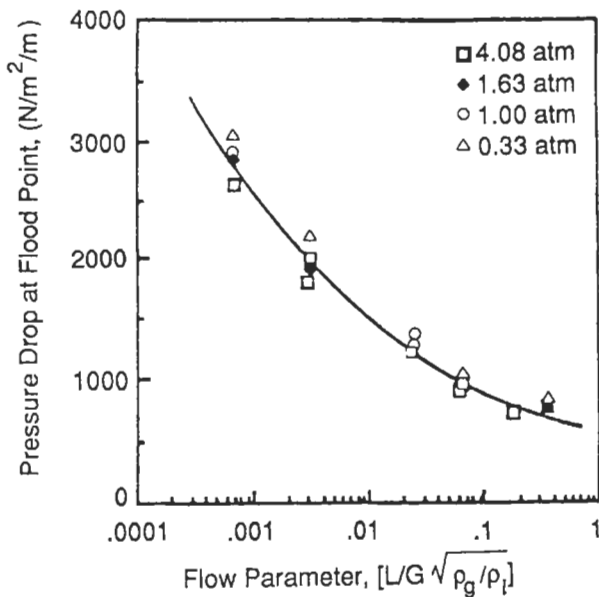


Figure 9-64. Pressure drop at the flood point as a function of loading. Values are calculated using the Stichlmair et al. model and distillation conditions using cyclohexane/n-heptane and Gempak® 2A packing. Note: ordinate $(N/m^2/m)/3.385^3 = \text{in. Hg/m}$. Reproduced by permission of the American Institute of Chemical Engineers, Fair, J. R. and Bravo, J. L., *Chemical Engineering Progress*, V. 86, No. 1 (1990) p. 19; all rights reserved.

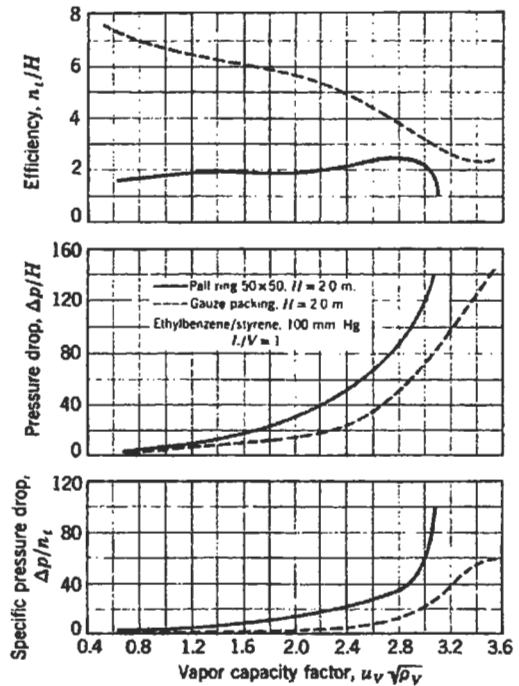


Figure 9-65. Performance of structured gauze packing vs. Pall rings. Used by permission of Billet, R., *Chemical Engineering*, V. 79, No. 4 (1972) p. 68; all rights reserved.

(text continued from page 339)

vapor capacity factor that in the vacuum systems is less than 60%–70% of the corresponding flood point (the actual decrease depending on the mixture). The average optimum load factor is given [123]:

$$\left(u_v \sqrt{\rho_v}\right)_{\text{opt}} = 2.4 \left(\text{m}^{-1/2} \text{sec}^{-1} \text{kg}^{1/2}\right) \quad (9-78)$$

2. Specific efficiency of packing:

$$n_t/H = 5, \text{ theoretical trays/meter}$$

3. Average pressure drop per theoretical tray:

$$(\Delta p/n_t)_{\text{opt}} = 5 \text{ mm water column}$$

where H = height of packing, m

n_t = number of theoretical trays

Δp = pressure drop, mm water column

u_v = vapor velocity per unit of free column cross-section, m/sec

ρ_v = density of vapor, kg/m^3

Guidelines for Structured Packings

1. Pressure drop: Range *usually* 0.3–0.5 in. water/ft, or, 30–40 mm water/m of packed height [116].
2. Lower holdup of liquid: Less than other packings, may require special attention to operational controls.
3. More difficult to purge: Operating vapors more difficult to purge from the system than random packings and trays. This poses potential fire, explosion, and toxic hazard.
4. Lower pressure drop for vacuum systems: Allows for better low pressure and vacuum system operation and lower bottoms temperature, with less degradation of bottoms product.
5. Internal uniform distribution: Properly designed devices to distribute and redistribute liquid entering the column is critical to obtain best performance of these types of packings.
6. Material of construction: The materials of fabrication for this type of packing are more critical to long life due to pad size, wall thickness of metal or plastic components, and actual selection based on the system corrosion, hydrogen attack, and oxygen attack in the column environment.
7. HETP values: Small packing with narrow corrugations gives low HETP values, but usually higher pressure drops. Plastic and some metal packing sheets, wires or corrugations may require special surface treatment to ensure good wettability.
8. Preliminary designs: These can usually be made from the generalized literature references; however, they are not a substitute for direct design of the specific

system in question by the packing manufacturer, referencing to a specific packing size and style. Several competitive designs are often helpful for a final design selection.

The test studies of several different structured packings of Dean et al. [117] indicated that structured packing performs well in water removed by triethylene glycol (TEG) from natural gas from field wells, giving a design point of $F_s = 3$ (where $F_s = V_s \sqrt{\rho_g}$, V_s = superficial velocity, ρ_g = gas density) for sizing. A high efficiency drip-point distributor is recommended, because it was far superior to a notched trough or spray nozzle distributor. Excellent turn-down to 12:1 was shown, still meeting outlet gas low water vapor specifications. HETP values ranged from 44 in. to 102 in., in this application. The number of theoretical trays was 2.8 to 4.6, varying with liquid and gas rates and packing style/size. Flooding occurred at 2.28 to 3.98 F_s value at 0.7 gpm/ft^2 at 650 psig.

A commercial 4-ft diameter refinery depropanizer unit's performance after replacement of the lower half of a trayed tower with Intalox-2T (R) structured packing is described in Reference 118.

Nutter [141] Montz B-1 structured packing, licensed from Julius Montz GmbH of Hilden, Germany, Figures 9-6LL and 9-6MM, is of uniform sinusoidal corrugations, which avoids sharp corners. The embossing on both sides of the sheet metal is closely spaced projections in a dot-matrix pattern, which spreads the liquid in a uniform film [141], without holes or slots. The design allows for an effective liquid-vapor seal at the tower wall by means of a metal wiper band. A representative performance is shown for pressure drop, Figure 9-66, and HETP, Figure 9-67. This packing is effectively used in low pressure (or vacuum) columns where large theoretical stages and low pressure drop are required, producing the lowest possible pressure drop per stage. Style B-1 is embossed sheet metal; Style BSH, is expanded textured sheet metal, high efficiency with maximum surface area; and Style A-3 is wire gauze construction.

Structured Packing Scale-up

Applications of structured packing into ethylene plant's various column systems [119] have been successfully achieved, but the individual manufacturers must be consulted to use their most directly applicable pilot and commercial data, which are generally not published. The use of published general correlations should only be used for a "first" or approximation design, while the delicate or important final design must be performed in cooperation with the manufacturer.

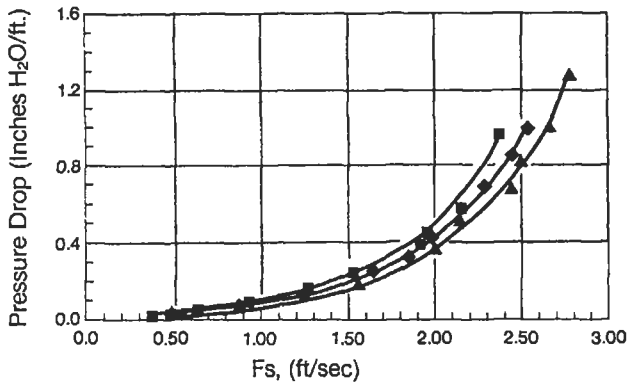


Figure 9-66. Representative pressure drop for Montz high-efficiency structured packings (several designs/styles) for a sheet metal packing. Performance can be accurately calculated by the manufacturer (See Figures 9-6LL and 9-6MM). Used by permission of Nutter Engineering Co., Harsco Corp., Bull. B-1. Specifications and descriptions used were in effect when this publication was approved for printing. Nutter Engineering reserves the right to discontinue models or options at any time, or change specifications, equipment or designs without notice and without incurring obligation. Using any of this information for specific applications should be done in consultation with Nutter Engineering personnel.

Huften et al. [120] tested gauze type packing for large commercial units, which resulted in a scale-up procedure that is too involved to reproduce here.

1. Estimate required packing height from Bravo, et al. [113] or manufacturer's information.
2. Calculate commercial scale HETP from Fair, et al. [108] and/or Huften, et al. [120].

Mass and Heat Transfer in Packed Towers

Most packed towers are used for mass transfer operations such as absorption, distillation, and stripping; however, there are other uses such as heat transfer quenching and entrainment knockout.

The usual packings and auxiliary features associated with these towers have been presented in connection with pressure drop considerations.

Because the packed tower is a continuous contacting device as compared to the step-wise plate tower, performance capacity is expressed as the number of transfer units, N , the height of the transfer unit, H.T.U., and mass transfer coefficients K_{Ga} and K_{La} . Figure 9-68 identifies the key symbols and constant flow material balance.

Number of Transfer Units, N_{OG} , N_{OL}

The transfer of mass between phases in a packed tower occurs either as essentially all gas film controlling, all liquid film controlling, or some combination of these mechanisms (see Figure 9-69). To express the ease (low number

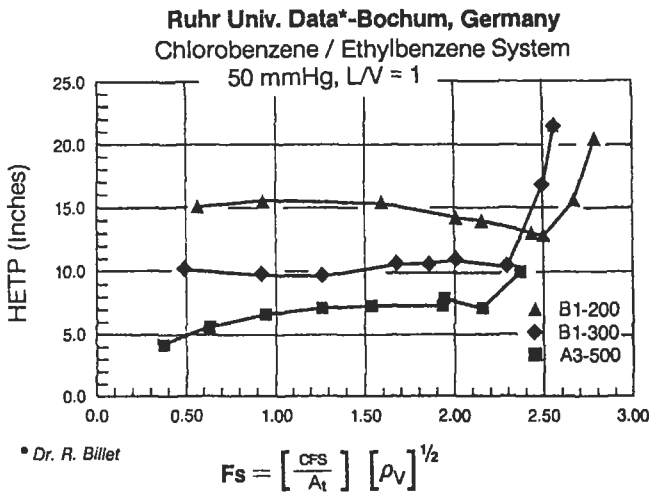


Figure 9-67. Representative HETP for Montz high-efficiency structured packings (several designs/styles) for a sheet metal packing. Used by permission of Nutter Engineering Co., Harsco Corp., Bull. B-1. Specifications and descriptions used were in effect when this publication was approved for printing. Nutter Engineering reserves the right to discontinue models or options at any time, or change specifications, equipment or designs without notice and without incurring obligation. Using any of this information for specific applications should be done in consultation with Nutter Engineering personnel.

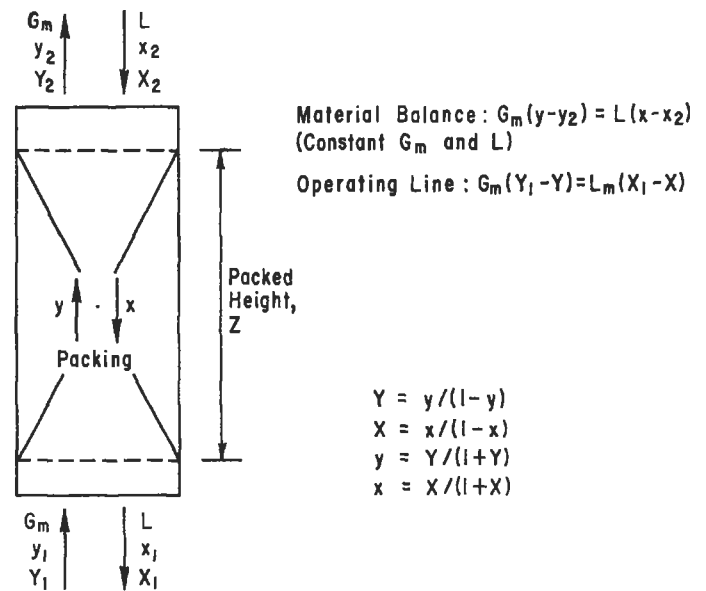


Figure 9-68. Counter-current packed tower symbols.

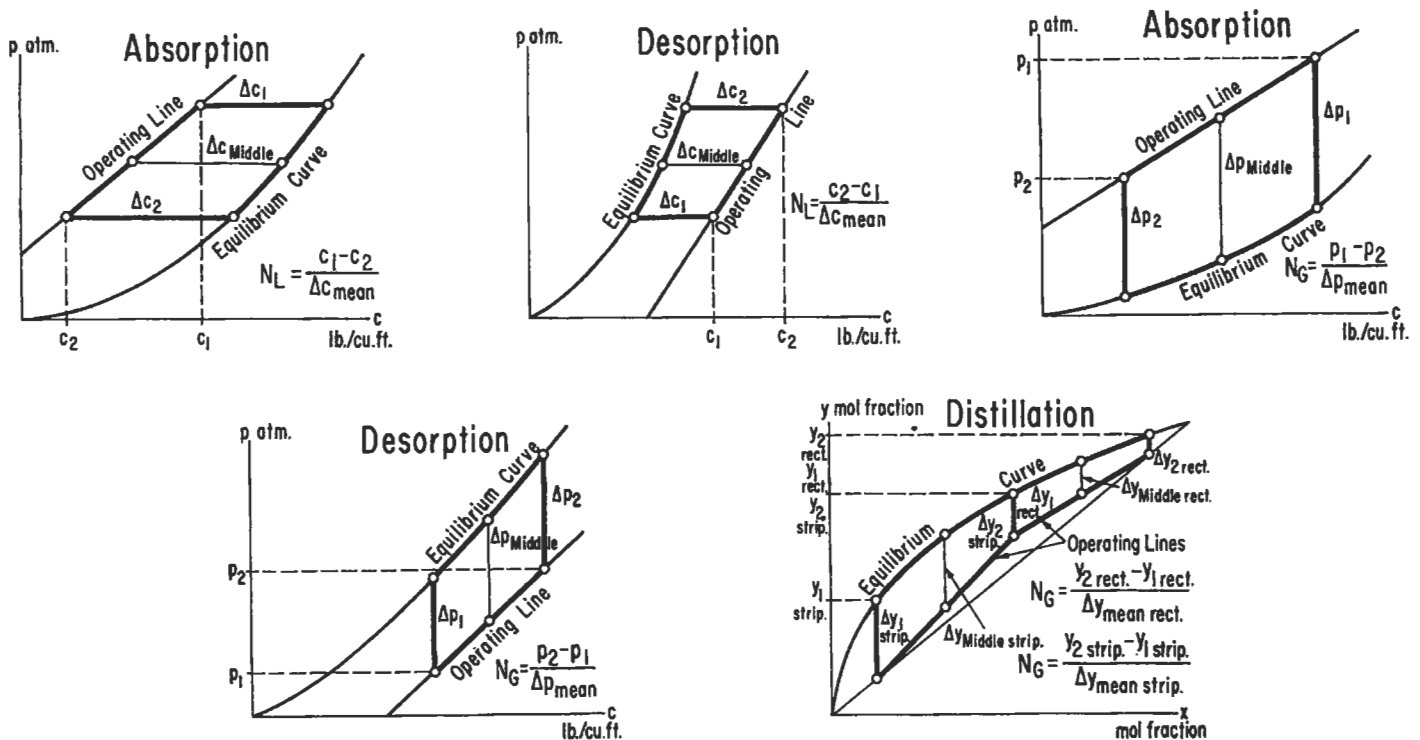


Figure 9-69. Mass transfer diagrams. The number of transfer units can be determined by the difference in concentration or vapor pressure, particularly over ranges where the equilibrium line is essentially straight. Used by permission of Czernann, J. J., Gyokhegyi, S. L., and Hay, J. J., *Petroleum Refiner*, V. 37, No. 4 (1958) p. 165; all rights reserved.

of transfer units) or difficulty of the transfer under the conditions of operation with respect to system equilibrium, the system is evaluated as to the number of transfer units N_{OG} or N_{OL} required. These can be determined experimentally and the data used for similar systems. However, it is also important to be in a position to estimate the number of transfer units for some foreign system when data are not available.

$$N_{OG} = \frac{Z}{H_{OG}} \text{ or } N_{OL} = \frac{Z}{H_{OL}} \quad (9-79)$$

where N_{OG} = number of transfer units, based on overall gas film coefficients

N_{OL} = number of transfer units, based on overall liquid film coefficients

Z = height of packing, ft

H_{OG} = height of transfer units, based on overall gas film coefficients, ft

H_{OL} = height of transfer unit, based on overall liquid film coefficients, ft

The transfer process is termed gas film controlling if essentially all of the resistance to mass transfer is in the gas film. This means that the gas is usually quite soluble in, or reactive with, the liquid of the system. If the system is liq-

uid film controlling, the gas is relatively insoluble in the liquid and the resistance to transfer is in the liquid film. Many systems are a combination of the two in various proportions. Without good data on such systems it is next to impossible to expect to accomplish an exact design of equipment, although satisfactory designs are possible. To have some guidelines, system information is presented in Table 9-39. Other data for different systems exist in the literature in a scattered fashion.

For (1) dilute solutions or (2) equal molar diffusion between phases (e.g., distillation)

$$N_{OG} = \int_{y_2}^{y_1} \frac{dy}{(y - y^*)} = \frac{y_1 - y_2}{\ln \frac{(y - y^*)_1}{(y - y^*)_2}} \quad (9-80)$$

where $(y - y^*)$ = driving force, expressed as mol fractions

y = mol fraction of one component (solute) at any point in the gas phases of the contacting system

y^* = mol fraction gas phase composition in equilibrium with a liquid composition, x

x = mol fraction in the liquid at the same corresponding point in the system as y

1, 2 = inlet and outlet conditions of system

Table 9-39
System Film Control*

Gas Film
1. Absorption of ammonia in water
2. Absorption of ammonia in aqueous ammonia
3. Stripping of ammonia from aqueous ammonia
4. Absorption of water vapor in strong acids
5. Absorption of sulfur trioxide in strong sulfuric acid
6. Absorption of hydrogen chloride in water
7. Absorption of hydrogen chloride in weak hydrochloric acid
8. Absorption of 5 vol. percent ammonia in acids
9. Absorption of sulfur dioxide in alkali solutions
10. Absorption of sulfur dioxide in ammonia solutions
11. Absorption of hydrogen sulfide in weak caustic
12. Evaporation of liquids
13. Condensation of liquids
Liquid Film
1. Absorption of carbon dioxide in water
2. Absorption of oxygen in water
3. Absorption of hydrogen in water
4. Absorption of carbon dioxide in weak alkali
5. Absorption of chlorine in water
Both Gas and Liquid Film
1. Absorption of sulfur dioxide in water
2. Absorption of acetone in water
3. Absorption of nitrogen oxide in strong sulfuric acid

*From: M. Leva, *Tower Packings and Packed Tower Design*, 2nd Ed. p. 91, U.S. Stoneware Co. (1953), by permission, now, Norton Chemical Process Products Corp.

If the system has more than two components, the calculations may be based on the component which varies the most in passing through the unit, or the component for which good data are available.

A large majority of the systems have operating lines and equilibrium curves which can be assumed as straight over the range covered by the design problem. For the conditions of a straight line equilibrium curve, $y^* = mx$, Colburn [10, 11] has integrated the relation above to obtain:

$$N = \frac{2.3 \log [(1 - P'')M + P'']}{1 - P''} \quad (9-81)$$

where N may be N_{OG} or N_{OL} depending on operation.

Table 9-40 identifies several important conditions that affect the values of P'' and M . These are extracted from Colburn's larger summary [11].

Figure 9-70 is a plot to aid in solving the equation for N (or N_{OG} or N_{OL}).

For constant temperature absorption, with no solute in the inlet liquid, $x_2 = 0$, and the abscissa becomes y_1/y_2 .

For Concentrated Solutions and More General Application

The following equation applies for diffusion in one direction (e.g., absorption, extraction, desorption) [74]:

$$N_{OG} = \int_{y_2}^{y_1} \frac{(1-y)_M dy}{(1-y)(y-y^*)} \quad (9-82)$$

$$N_{OG} = \int_{y_2}^{y_1} \frac{dy}{(y-y^*)} + 1/2 \ln \frac{(1-y_2)}{(1-y_1)} \quad (9-83)$$

or

$$N_{OG} = \int_{Y_2}^{Y_1} \frac{dY}{(Y-Y^*)} - 1/2 \ln \frac{1+Y_1}{1+Y_2} \quad (9-84)$$

or

$$N_{OG} = \int_{Y_2}^{Y_1} \frac{dY}{(Y-Y^*)} - 1.15 \log_{10} \frac{1+Y_1}{1+Y_2} \quad (9-85)$$

where $(1-y)_M$ = log mean average of concentration at the opposite ends of the diffusion process, $(1-y)$ in main gas body, and $(1-y^*)$ at the interface [74]

y = Concentration of solute in gas, mol fraction

y^* = Concentration of solute in gas in equilibrium with liquid, mol fraction

Y = Concentration of solute in gas, lb mol solute/lb mol solvent gas

Y^* = Concentration of solute in gas in equilibrium with liquid, lb mol solute/lb mol solvent gas

If the liquid film controls:

$$N_{OL} = \int_{x_2}^{x_1} \frac{dx}{(x^*-x)} + 1/2 \ln \frac{(1-x_2)}{(1-x_1)} \quad (9-86)$$

$$N_{OL} = \int_{X_2}^{X_1} \frac{dX}{(X^*-X)} - 1/2 \ln \frac{1+X_1}{1+X_2} \quad (9-87)$$

where x = concentration of solute in liquid, mol fraction

x^* = concentration of solute in liquid in equilibrium with gas, mol fraction

X = concentration of solute in liquid, lb mol solute/lb mol solvent

X^* = concentration of solute in liquid in equilibrium with the gas, lb mol solute/lb mol solvent

It is usually necessary to graphically integrate the first terms of the above equations, although some problems do allow for mathematical treatment.

Table 9-40
Values to Use With Transfer Equation and Figure 9-68

Condition of Operation	P''	M
<i>Absorption:</i>		
1. Constant mG_m/L_m	mG_m/L_m	$(y_1 - mx_2)/(y_2 - mx_2)$
2. Varying mG_m/L_m	m_2G_{m2}/L_{m2}	$\left(\frac{y_1 - m_2x_2}{y_2 - m_2x_2}\right) \left(\frac{1 - m_2G_m/L_m}{1 - y^*_1/y_1}\right)$
<i>Desorption (stripping):</i>		
3. Constant L_m/mG_m	L_m/mG_m	$(x_1 - y_2/m)(x_2 - y_2/m)$
4. Varying L_m/mG_m	L_{m2}/m_2G_{m2}	$\left(\frac{x_1 - y_2/m_2}{x_2 - y_2/m_2}\right) \left(\frac{1 - L_{m2}/m_2G_{m2}}{1 - x_1^*/x_1}\right)$
<i>Distillation, enriching¹</i>		
5. Constant mG_m/L_m		Same as 1
6. Varying mG_m/L_m stripping, closed steam ²		Same as 2
7. Constant L_m/mG_m	L_m/mG_m	$(x_1 - x_2/m)/(x_2 - x_2/m)$
8. Varying L_m/mG_m stripping, open steam ²	L_{m2}/m_2G_{m2}	$\left(\frac{x_1 - x_2/m_2}{x_2 - x_2/m_2}\right) \left(\frac{1 - L_{m2}/m_2G_{m2}}{1 - x_1^*/x_1}\right)$
9. Constant L_m/mG_m	L_m/mG_m	x_1/x_2
10. Varying L_m/mG_m	L_{m2}/m_2G_{m2}	$\left(\frac{x_1}{x_2}\right) \left(\frac{1 - L_{m2}/m_2G_{m2}}{1 - x_1^*/x_1}\right)$

*Equilibrium value

Subscripts 1 and 2 refer to the concentrated and dilute ends of the unit respectively

¹Concentrations and m are based on high boiler or "heavy key"

²Concentrations and m are based on low boiler or "light key"

m = slope of equilibrium line (mol-fraction solute in gas)/(mol-fraction solute in liquid)

By permission, A. P. Colburn, *Ind. Eng. Chem.* 33, 459 (1941). The American Chem. Soc., all rights reserved.

Example 9-9: Number of Transfer Units for Dilute Solutions

An existing 10-in. I.D. packed tower using 1-inch Berl saddles is to absorb a vent gas in water at 85°F. Laboratory data show the Henry's Law expression for solubility to be $y^* = 1.5x$, where y^* is the equilibrium mol fraction of the gas over water at compositions of x mol fraction of gas dissolved in the liquid phase. Past experience indicates that the H_{OG} for air-water system will be acceptable. The conditions are: (refer to Figure 9-68).

$$G'_1 = 200 \text{ mol gas/hr (ft}^2\text{)}$$

$$L'_2 = 500 \text{ mol water/hr (ft}^2\text{)}$$

$$y_1 = 0.03 \text{ (inlet)}$$

$$y_2 = 0.001 \text{ (outlet)}$$

$$x_2 = 0 \text{ (inlet)}$$

$$x_1 = ? \text{ (outlet)}$$

Determine the number of transfer units, and the packed tower height.

Material Balance

Dilute solutions, assume constant L' and G' .

$$\text{Gas phase change} = G_1 (y_1 - y_2) = 200 (y_1 - 0.001)$$

$$\text{Liquid phase change} = L_2 (x_2 - x_1) = 500 (0 - x_1)$$

Because the (-) sign has no significance, except to indicate the direction of mass change, use $500 (x_1)$.

Now, to use the simplified

$$N_{OG} = \int_{y_2}^{y_1} \frac{dy}{(y - y^*)} \quad (9-80)$$

Assume values of y_1 and solve the equated mass change for values of x .

$$200 (y_1 - 0.001) = 500 (x_1)$$

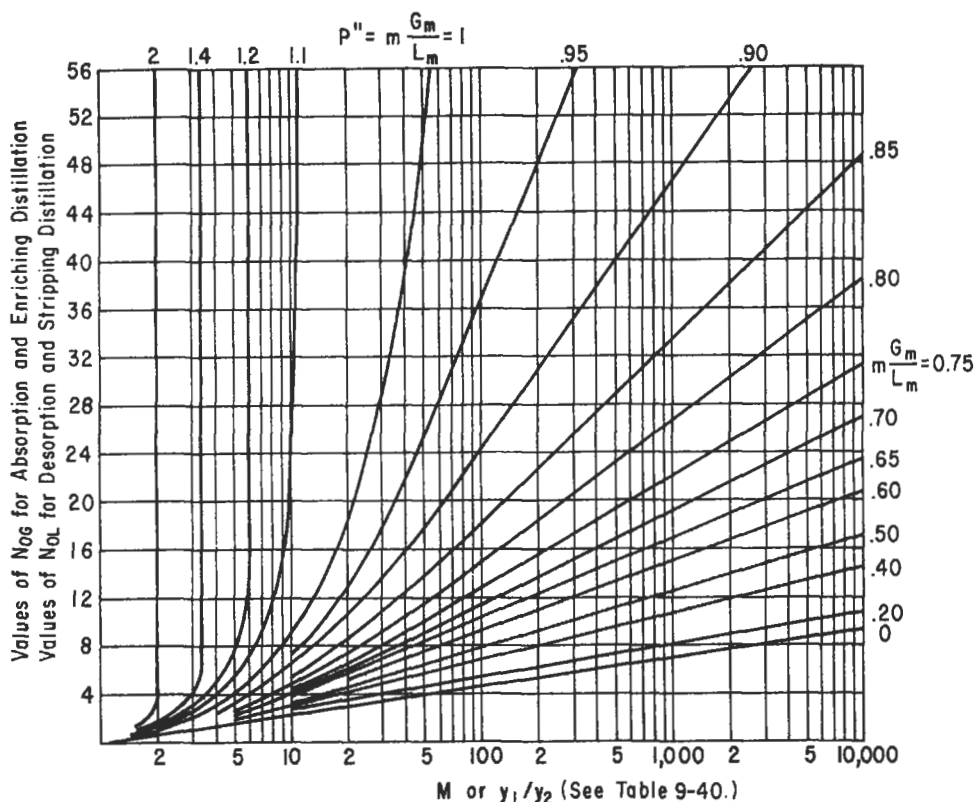


Figure 9-70. Colburn Plot for transfer units. Reproduced by permission of the American Chemical Society; Colburn, A. P., *Ind. Eng. Chem.* V. 33 (1941) p. 459; all rights reserved.

Assume y	Calculated x_1	Equilibrium y^*	$\left(\frac{1}{y - y^*}\right)$
0.03	0.0116	0.0174	79.4
0.025	0.0096	0.0144	94.4
0.02	0.0076	0.0114	116.4
0.015	0.0056	0.0084	151.4
0.01	0.0036	0.0054	217.
0.005	0.0016	0.0024	384.
0.001	0	0	1000.

Example: Calculate x , as illustrated for point $y = 0.015$

$$200(0.015 - 0.001) = 500 x_1$$

$$200(0.014) = 500 x_1$$

$$x_1 = \frac{200(0.014)}{500} = 0.0056$$

Calculate the equilibrium values, y^* , as illustrated for point of $x_1 = 0.0116$

$$y^* = 1.5(0.0116) = 0.0174$$

Calculate $1/(y - y^*)$ for point corresponding to: $x_1 = 0.0116$ where $y^* = 0.0174$

$$\frac{1}{y - y^*} = \frac{1}{0.03 - 0.0174} = \frac{1}{0.0126} = 79.4$$

Area Under Curve

Figure 9-71 is a summation of steps indicated, or the area can be circumscribed with a planimeter and evaluated.

Area = 6.27 units, then number of transfer units,
 $N_{OG} = 6.27$

Height of Transfer Unit

From data of Mehta and Parekh for 1-in. Berl Saddles [40],

$$H_{OG} = 0.86 \text{ ft}$$

Height of packed section:

$$Z = (6.27)(0.86) = 5.4 \text{ ft}$$

Total Packed Height Recommended

Process packed height	= 5.4 ft
Distribution packed height	= <u>2.00</u>
Total	7.4 ft

Use: 8.5 to 10 ft of 1-in. Berl saddles

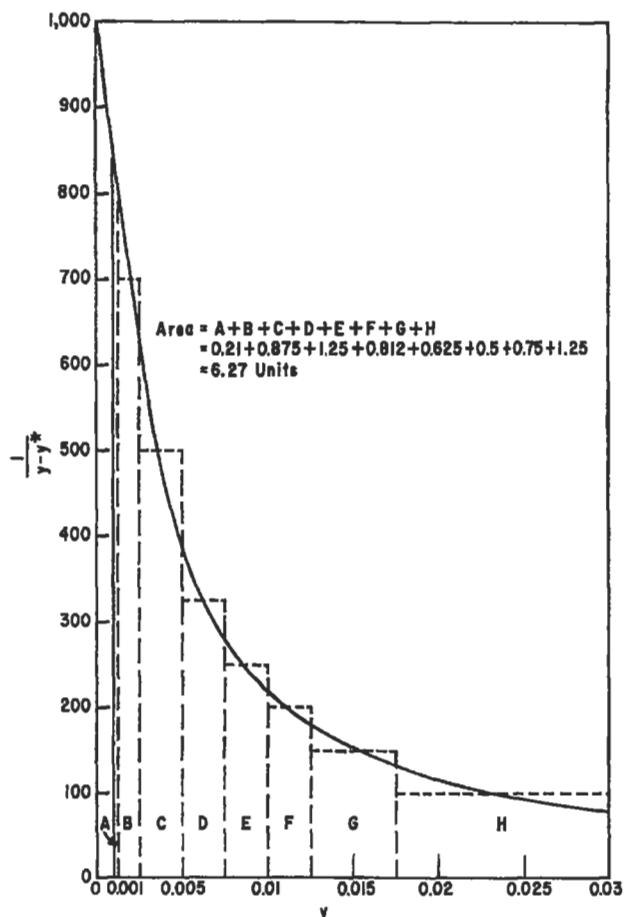


Figure 9-71. Graphical integration for Example No. 9-9.

To complete the design, the tower should be checked for loading and flooding conditions, and the pressure drop established. However, this procedure will not be repeated as it can be found elsewhere in this text.

Example 9-10: Use of Colburn's Chart for Transfer Units—Straight Line Equilibrium Curve, Figure 9-70 Constant Temperature Operation

Use the previous example on dilute solutions and solve by Colburn's Chart [11].

Abscissa: $y_1/y_2 = 0.03/0.001 = 30$, because $x_2 = 0$ (no dissolved solute gas in inlet water)

Parameter: $mG'/L' = (1.5)(200/500) = 0.6$

Note that m is the slope of the straight line equilibrium curve, $m = 1.5$

Reading chart: At $y_1/y_2 = 30$ and $mG'/L' = 0.6$
No. transfer units, $N = 6.4$

This compares with the value from graphical integration of 6.27 and is a good check.

If $N = 6.4$ were used for the tower:
 $= 6.4 (0.86) = 5.5$ ft minimum for process operations

Example 9-11: Number Transfer Units—Concentrated Solutions

Using the basic problem for dilute solutions, assume the following conditions for a higher concentration.

$G' = 200$ mol gas/hr (ft^2)
 $L' = 500$ mol water/hr (ft^2)
 $y_1 = 0.30$ (inlet)
 $y_2 = 0.01$ (outlet)
 $x_2 = 0$
 $y^* = 1.54$

Material Balance

Based on inert gas

$$\text{Gas phase change} = G' (1 - y_1) \left[\frac{y}{1 - y} - \frac{y_2}{1 - y_2} \right]$$

$$\left[\frac{y}{1 - y} - \frac{0.01}{1 - 0.01} \right]$$

Liquid phase change =

$$L' \left[\frac{x}{1 - x} - \frac{x_1}{1 - x_1} \right] = L' \left[\frac{x}{1 - x} - 0 \right]$$

These changes must be equal:

$$G (1 - 0.3) \left(\frac{y}{1 - y} - \frac{0.01}{0.99} \right) = L \left(\frac{x}{1 - x} \right)$$

Assume values of y and solve for corresponding values of x .

$$200(0.7) \left(\frac{y}{1 - y} - 0.0101 \right) = L \left(\frac{x}{1 - x} \right)$$

Let $y = 0.3$

$$200(0.7) \left[\left(\frac{0.3}{1 - 0.3} \right) - 0.0101 \right] = 500 \left(\frac{x}{1 - x} \right)$$

$$140(0.428 - 0.0101) = 500 \left(\frac{x}{1 - x} \right)$$

$$\frac{x}{1 - x} = \frac{58.5}{500} = 0.117$$

$x = 0.1048$

Calculate equilibrium y^* from values of x .

Assume that for this concentration range (this will usually not be same as for dilute solution tower):

$$y^* = 1.5x$$

$$y^* = 1.5 (.1048) = 0.157$$

Calculate $(1 - y)$:

$$1 - y = 1 - 0.30 = 0.70$$

Calculate $(1 - y^*)$:

$$1 - y^* = 1 - 0.157 = 0.843$$

Calculate $(1 - y)_M$, arithmetic average of non-diffusing gas concentration at ends of diffusing path:

$$(1 - y)_M = \frac{(1 - y) + (1 - y^*)}{2} = \frac{0.7 + 0.843}{2}$$

$$= 0.7715$$

Calculate $1/(y - y^*)$:

$$\frac{1}{y - y^*} = \frac{1}{0.30 - 0.157} = 7.0$$

Calculate $(1 - y)_M / (1 - y)(y - y^*)$:

$$= 0.7715(7.0) / 0.7 = 7.715$$

A plot of y versus $(1 - y)_M / (1 - y)(y - y^*)$ gives the number of transfer units as presented in the previous example. As a second solution:

$$N_{OG} = \int_{y_2}^{y_1} \frac{dy}{y - y^*} + 1/2 \ln \frac{1 - y_2}{1 - y_1}$$

From Figure 9-72 the area under the curve for y versus $1/(y - y^*)$ is 5.72 units = N_{OG} (approximate)

The correction is:

Assumed y	Calc. x	y^*	$1 - y$	$1 - y^*$	$(1 - y)_M$	$\frac{1}{y - y^*}$	$\frac{(1 - y)_M}{(1 - y)(y - y^*)}$
0.30	0.1048	0.157	0.70	0.843	0.7715	7.0	7.715
0.20	0.0631	0.0945	0.80	0.9055	0.8527	9.48	10.10
0.15	0.0446	0.0667	0.85	0.9333	0.8916	12.0	12.58
0.10	0.0276	0.0413	0.90	0.9587	0.9293	17.02	17.55
0.05	0.0142	0.0213	0.95	0.9787	0.9643	34.9	35.40
0.01	0.99	1.000	0.9950	100.0	100.50

$$1/2 \ln \frac{1 - y_2}{1 - y_1} = 1/2 \ln \frac{0.99}{0.70}$$

$$= 1/2 (0.345) = 0.172$$

Therefore:

$$N_{OG} = 5.72 + 0.172 = 5.89 \text{ transfer units}$$

Note that the graphical integration is never exact and hence the correction often makes little difference except for cases of curved equilibrium lines.

From Figure 9-72 the area under the curve, y versus $(1 - y)_M / (1 - y)(y - y^*)$ is only slightly larger than the y versus $1/y - y^*$ for this case. To avoid confusion the figure was only integrated for the latter. However, it could be performed for the former and the result should be very close to 5.89.

Gas and Liquid-phase Coefficients, k_G and k_L

Recent studies indicate that the individual film transfer coefficients may be correlated with good agreement for Raschig rings and Berl Saddles for aqueous and nonaqueous systems [67]:

$$j_D = \left[\frac{k_G M_M P_{BM}}{G} \right] [\mu_{Ga} / \rho_G D_v]^{0.667} = 1.195 \left[\frac{D_p G'}{\mu_{Ga} (1 - \epsilon)} \right]^{-0.36} \quad (9-88)$$

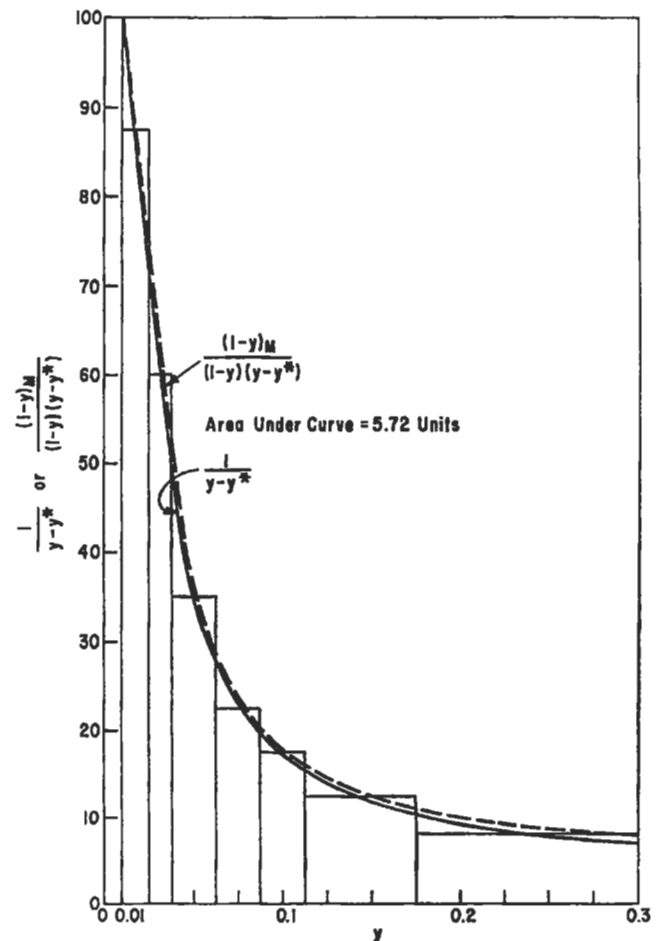


Figure 9-72. Graphical integration number of transfer units for Example 9-11.

This has been shown to correlate for a wide variety of tower packings, various operating conditions, and physical properties of the solute and inert gases. The k_G calculated must be used in conjunction with the effective interfacial areas determined by Shulman [65] Figure 9-47, to establish a reliable value for $k_G a$. Figure 9-47 should be used with the abscissa as $G/\sqrt{\rho}/0.075$ for inert gas other than air [67]:

$$k_G a = k_G(a)$$

$$\text{HTU (gas-Phase)} = G'/k_G a M_M P_{BM} \quad (9-89)$$

where D_v = diffusivity of solute in gas, ft²/hr
 k_G = gas-phase mass transfer coefficient lb mol/hr (ft²) (atm)
 M_M = mean molecular weight of gas, lb/lb mol
 P_{BM} = mean partial pressure of inert gas in the gas phase, atm
 μ_{G_a} = gas viscosity, lb/(hr) (ft)
 ρ_G = gas density, lb/ft³
 G' = superficial gas rate, lb/(hr)/(ft²)

$$\frac{1}{K_G a} = \frac{1}{k_G a} + \frac{1}{H' k_L a} = \frac{1}{k_G a} + \frac{m}{k_L a} = \frac{1}{H' K_L a} \quad (9-90)$$

$$\frac{1}{K_L a} = \frac{1}{k_L a} + \frac{H'}{k_G a} = \frac{1}{k_L a} + \frac{1}{m k_G a} \quad (9-91)$$

H' = Henry's law constant, lb mols/(ft³) (atm)
 k_L = liquid-phase mass transfer coefficient, lb mols/(hr) (ft²) (lb mols/ft³)

The relation

$$\frac{\text{vaporization}}{\text{absorption}} = \frac{(k_G a)_v}{(k_G a)_a} = 0.85 \frac{h_t}{h_o} \quad (9-92)$$

is reported to correlate $\pm 8\%$ based on data tested, and appears to be founded on a sound investigative program.

For the liquid phase based on Raschig ring and Berl saddle data [65]:

$$\frac{k_L D_P}{D_L} = 25.1 \left[\frac{D_P L'}{\mu_{L_a}} \right]^{0.45} \left[\frac{\mu_{L_a}}{\rho_L D_L} \right]^{0.5} \quad (9-93)$$

Use of k_G and k_L

1. From physical properties of system, determine k_G and k_L . If system is known or can be assumed to be essentially all gas or all liquid film controlling, then only the controlling k need be calculated. For greater accuracy, both values are recommended, because very few systems are more than 80% controlled by only one k .
2. Combine effective interfacial area to calculate $k_G a$ or $k_L a$.

3. Determine $K_G a$ by:

$$\frac{1}{K_G a} = \frac{1}{k_G a} + \frac{1}{H' k_L a} = \frac{1}{H' K_L a} \quad (9-94)$$

Height of a Transfer Unit, H_{OG} , H_{OL} , HTU

An earlier concept of height equivalent to a theoretical plate (HETP) for relating the height of packing to a unit of transfer known as the theoretical stage or plate has generally been dropped in favor of the "height of a transfer unit" HTU, and designated as H_{OG} or H_{OL} depending on whether it was determined from gas or liquid film data. HETP data for absorption and distillation is given in the section under packed tower distillation.

$$\frac{\text{HETP}}{H_{OG}} = \frac{(mG_m/L_m) - 1}{\ln(mG_m/L_m)}$$

Height of Overall Transfer Unit

For small changes in concentration and total number mols of gas and liquid remain essentially constant; applicable to all but very concentrated solutions. For the latter case see References 18 and 74.

$$H_{OG} = \frac{G_M}{K_G a P_{ave}} \quad (9-95A)$$

$$H_{OL} = \frac{L_m}{K_L a \rho_L} \quad (9-95B)$$

$$(\text{HTU})_{OG} = \frac{V'}{K_G P_{a_t} A} \quad (9-96)$$

$$Z = (\text{HTU})_{OG} (\text{NTU})_{OG} \quad (9-97)$$

Height of Individual Transfer Unit

For same conditions as (1.) Some data are reported as individual gas or liquid film coefficients or transfer unit heights. However, it is often possible to use it as overall data if the conditions are understood.

$$H_G = \frac{G_m}{k_G a P_{ave}} \quad (9-98)$$

$$H_L = \frac{L_m}{k_L a \rho_L} \quad (9-99)$$

$$H_{OG} = H_G + \frac{mG_m}{L_m} (H_L) = H_G + \frac{H_L}{A'} \quad (9-100)$$

$$H_{OL} = H_L + \frac{L_m}{mG} (H_G) = H_L + A' H_G \quad (9-101)$$

where $A' = L_m/mG_m$

For predominately liquid film controlling system, $A'H_G$ is almost negligible and $H_{OL} = H_L$; likewise for gas film controlling, H_L/A' is negligible and $H_{OG} = H_G$.

- where G_m = gas mass velocity, lb mol/(hr) (ft²)
- L_m = liquid mass velocity, lb mol/(hr) (ft²)
- K_{Ga} = overall gas mass-transfer coefficient, lb mol/(hr) (ft³) (atm)
- K_{La} = overall liquid mass-transfer coefficient, lb mol/(hr) (ft³) (lb mol/ft³)
- k_{Ga} = individual gas mass-transfer coefficient, lb mol/(hr) (ft³) (atm)
- k_{La} = individual liquid mass-transfer coefficient, lb mol/(hr) (ft³) (lb mol/ft³)
- P_{ave} = average total pressure in tower, atmospheres
- H_L = height of liquid film transfer unit, ft
- H_G = height of gas film transfer unit, ft
- a = effective interfacial area for contacting gas and liquid phases, ft²/ft³. Because this is very difficult to evaluate, it is usually retained as a part of the coefficient such as K_{Ga} , K_{La} , k_{Ga} , and k_{La} .
- V' = vapor flow rate, lb mol/hr

Estimation of Height of Liquid Film Transfer Units

The following relation is used in estimating liquid film transfer units [62]. For the proper systems H_L may be assumed to be equal to H_{OL} .

$$H_L = \phi (L'/\mu_{La})^j (\mu_{La}/\rho_L D_L)^{0.5}, \text{ ft} \tag{9-102}$$

- where $\mu_{La}/\rho_L D_L$ = Schmidt number
- H_L = height of transfer unit, ft
- L' = liquid rate, lb/(hr) (ft²)
- μ_L = viscosity of liquid, lb/(ft) (hr)
- D_L = liquid diffusivity, ft²/hr
- ϕ and j are constants given in Table 9-41.

Diffusivity values are given in Table 9-42.

Estimation of Height of Gas Film Transfer Units

The relation [61, 62, 63]

$$H_G = \frac{\alpha G^\beta}{L^\gamma} \left(\frac{\mu_{Ga}}{\rho_G D_G} \right)^{0.5} \tag{9-103}$$

describes a reasonable part of the gas film data. It allows the conversion of the ammonia-air-water data of Fellingner [27] to useful interpretation for other systems. Table 9-43 gives the constants for the equation.

α , β , γ = constants peculiar to packing for dilute and moderate concentrations [74]:

Table 9-41
Liquid Film Height of Transfer Unit*

Packing	ϕ	j	Range of L' Lb/hr (ft ²)
Raschig Rings (In.)			
¾	0.00182	0.46	400–15,000
½	0.00357	0.35	400–15,000
1	0.0100	0.22	400–15,000
1.5	0.0111	0.22	400–15,000
2	0.0125	0.22	400–15,000
Berl Saddles (In.)			
¾	0.00666	0.28	400–15,000
1	0.00588	0.28	400–15,000
1.5	0.00625	0.28	400–15,000
3 In. Partition rings, stacked staggered	0.0625	0.09	3,000–14,000
Spiral Rings, stacked staggered			
3-in. single spiral	0.00909	0.28	400–15,000
3-in. triple spiral	0.0116	0.28	3,000–14,000
Drip-point grids (continuous flue)			
Style 6146	0.0154	0.23	3,500–30,000
Style 6295	0.00725	0.31	2,500–22,000

*Reproduced by permission, Treybal, R. E., *Mass Transfer Operations*, McGraw-Hill Book Co., Inc. (1955), p. 237, using data of Sherwood, T. K. and Holloway, F. A. L. [62] and of Molstad, McKinney and Abbey [51], all rights reserved.

$$H_{OG} = H_G + \frac{mG}{L} (H_L) = H_G + \frac{H_L}{A} \tag{9-100}$$

$$H_{OL} = H_L + \frac{L}{mG} (H_G) = H_L + AH_G \tag{9-101}$$

Figure 9-73 presents some of the data of Fellingner [27] as presented in Reference 40 for H_{OG} for the ammonia-air-water systems. This data may be used with the Sherwood relations to estimate H_L and H_G values for other systems.

Estimation of Diffusion Coefficients of Gases

Good reliable diffusion data is difficult to obtain, particularly over a wide range of temperature. The Gilliland relation is [63]:

$$D_v = 0.0069 \frac{T^{3/2} \sqrt{1/M_A + 1/M_B}}{P(V_A^{1/3} + V_B^{1/3})^2}, \text{ sq. ft./hr} \tag{9-104}$$

- where T = absolute temperature, °R
- M_A , M_B = molecular weights of the two gases, A and B
- P = total pressure, atm

Table 9-42
Diffusion Coefficients of Gases and Liquids in Liquids at
68°F (Dilute Concentrations)

	Solvent	Diffusion Coefficient, D_L Ft ² /Hr (Multiply all Values by 10^{-5})
Gas		
Oxygen	Water	7.0
Carbon Dioxide	Water	5.82
Nitrous Oxide	Water	5.86
Ammonia	Water	6.83
Chlorine	Water	4.74
Bromine	Water	4.66
Hydrogen	Water	19.92
Nitrogen	Water	6.37
Hydrogen Chloride	Water	10.25
Hydrogen Sulfide	Water	5.47
Acetylene	Water	6.06
Liquid		
Sulfuric Acid	Water	6.72
Nitric Acid	Water	10.15
Methanol	Water	4.97
Sodium Chloride	Water	5.23
Sodium Hydroxide	Water	5.86

Note: Additional data are given in the reference, as well as the International Critical Tables.

From: Perry, J. H., *Chem. Engrs. Hndbk.* 3rd Ed. p. 540, McGraw-Hill Book Co., Inc. © (1950). By permission.

V_A, V_B = molecular volumes of gases, obtained by Kopp's law of additive volumes, cm³/gm mol at normal boiling point. See Table 9-44.

Diffusion coefficients are used to estimate K_{Ga} values for gas film controlling systems:

$$K_{Ga} (\text{unknown system}) = K_{Ga} (\text{known system})$$

$$\left[\frac{D_v \text{ unknown}}{D_v \text{ known}} \right]^{0.56} \quad (9-105)$$

Ammonia-air-water system data, Figure 9-73, is often used by converting H_{OG} (ammonia-air) to its corresponding K_{Ga} , and then substituting the above relation for the unknown K_{Ga} .

Example 9-12: Design of Ammonia Absorption Tower, Figures 9-74A and B

An inert gas process vent stream contains 91 lb/hr (5.35 mol/hr) ammonia. This is 5.7% (volume) of the total. The absorber is to operate at 150 psig and recover 99% of the inlet ammonia as aqua using 90°F water. Average vapor

Table 9-43
Gas Film Height of Transfer Unit [27, 50, 51]

Packing	α	β	γ	G'	L'
Raschig Rings (In.)					
½	2.32	0.45	0.47	200–500	500–1,500
1	7.00	0.39	0.58	200–800	400–500
	6.41	0.32	0.51	200–600	500–4,500
1.5	17.3	0.38	0.66	200–700	500–1,500
	2.58	0.38	0.40	200–700	1,500–4,500
2	3.82	0.41	0.45	200–800	500–4,500
Berl Saddles (In.)					
½	32.4	0.30	0.74	200–700	500–1,500
	0.811	0.30	0.24	200–700	1,500–4,500
1	1.97	0.36	0.40	200–800	400–4,500
1.5	5.05	0.32	0.45	200–1,000	400–4,500
3-In. Partition Rings (Stacked (Staggered)					
	650	0.58	1.06	150–900	3,000–10,000
Spiral Rings (stacked staggered)					
3-in. single spiral	2.38	0.35	0.29	130–700	3,000–10,000
3-in. triple spiral	15.6	0.38	0.60	200–1,000	500–3,000
Drip Point Grids (continuous flue)					
Style 6146	3.91	0.37	0.39	130–1,000	3,000–6,500
Style 6295	4.65	0.17	0.27	100–1,000	2,000–11,500

From the data of Fellinger [27] and of Molstad et. al [50, 51] as presented in Treybel, R. E. *Mass Transfer Operations*, p. 239, McGraw-Hill Book Co. Inc. © (1955), Ref. 74, by permission, all rights reserved.

mixture molecular weight = 11.6. Determine (a) the number of transfer units for the absorption (b) height of the transfer unit using 1-in. Berl saddles (c) the tower diameter and (d) the water rate.

Material Balance

Assume production of 8 wt % aqua. Then:

$$\text{Lb water/hour} = (0.99)(91) \left(\frac{0.92}{0.08} \right) = 1035$$

Entering water, X_2 , mol NH₃/mol H₂O = 0

Leaving water as aqua, X_1 , mol NH₃/mol H₂O

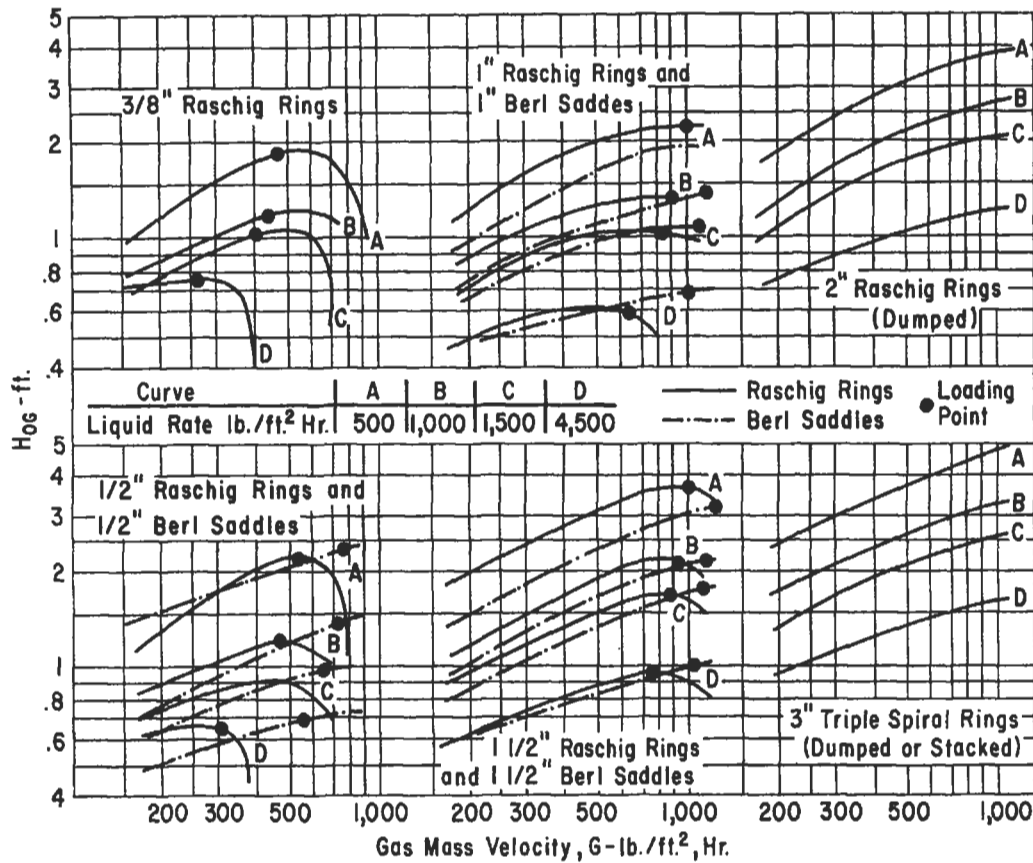


Figure 9-73. Fellingner's overall gas film mass transfer data for ammonia-water system. Used by permission of Leva, M. *Tower Packings and Packed Tower Design*, 2nd Ed. U.S. Stoneware Co. (now, Norton Chemical Process Products Corp.) (1953).

Table 9-44
Atomic and Molecular Volumes

Atomic Volume		Molecular	Volume
Carbon	14.8	H ₂	14.3
Hydrogen	3.7	O ₂	25.6
Chlorine	24.6	N ₂	31.2
Bromine	27.0	Air	29.9
Iodine	37.0	CO	30.7
Sulfur	25.6	CO ₂	34.0
Nitrogen	15.6	SO ₂	44.8
Nitrogen in primary amines	10.5	NO	23.6
Nitrogen in secondary amines	12.0	N ₂ O	36.4
Oxygen	7.4	NH ₃	25.8
Oxygen in methyl esters	9.1	H ₂ O	18.9
Oxygen in higher esters	11.0	H ₂ S	32.9
Oxygen in acids	12.0	COS	51.5
Oxygen in methyl ethers	9.0	Cl ₂	48.4
Oxygen in higher ethers	11.0	Br ₂	53.2
Benzene ring: subtract	15	I ₂	71.5
Naphthalene ring: subtract	30		

By permission, R. E. Treybal, *Mass-Transfer Operations*, p. 27, McGraw-Hill Book Co., Inc. (1955). Also see Ref. 63 for additional data.

$$= \frac{(5.35)(0.99)}{\left(\frac{1035}{18}\right)}$$

$$= 0.0921$$

Entering gas, Y₁, mol NH₃/mol inert gas

$$= \frac{5.35}{(5.35/0.057)(0.943)} = 0.0607$$

Leaving gas, Y₂, mol NH₃/mol inert gas

$$= (0.01)(.0607) = 0.000607$$

To calculate the equilibrium curve at 90°F (constant temperature) for the system aqua ammonia-ammonia-inert vapors follow the steps listed:

$$\text{Heat of solution } (-Q) = 45.8676 + n(286.103) - a' - nb', \text{ in kilojoules/g mole}$$

(text continued on page 356)

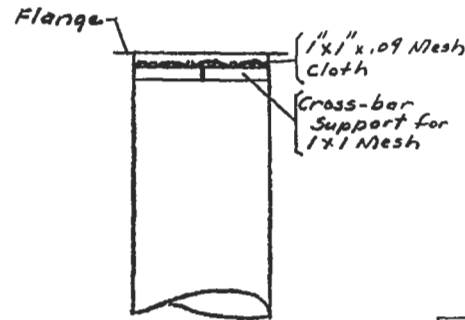
Job No. _____ _____ B/M No. _____	TOWER INTERNAL SPECIFICATIONS SPRAY OR PACKED TYPE COLUMNS	SPEC. DWG. NO. A- 2 Page 2 of 2 Pages Unit Price _____ No. Units 1 Item No. 7-63																				
Packing: <ul style="list-style-type: none"> (a) Size, Type & Thickness <u>1" Berl Saddles, Standard Weight</u> Bulk Density _____ (b) Height of Packing Sections: No. 1 <u>1'-0" of 1/2"</u> No. 2 <u>14'-0" of 1"</u> No. 3 _____ (c) Method of Packing (Wet) (Dry) <u>Flat into tower filled with water</u> (d) Packing Arrangement (Dumped) (Stacked) <u>Dumped</u> Type of Distributor Tray <u>Splash Plate, 4" Dia.</u> How Removed <u>out top</u> Type of Re-Distributor Tray <u>None</u> How Removed _____ Type of Packing Support(s) <u>75% open Hardware Cloth, 1x1 mesh</u> How Removed <u>At flanges</u> Packing removal Manways Located <u>Use flanges at support grid</u> Entrainment Separator: (Type, Size, Thickness) <u>None</u>																						
Spray Nozzles	<table border="1" style="width: 100%; border-collapse: collapse;"> <thead> <tr> <th style="width: 15%;">Bank No.</th> <th style="width: 20%;">No. of Nozzles</th> <th style="width: 15%;">Size</th> <th style="width: 20%;">Type</th> <th style="width: 30%;">Manufacturer</th> </tr> </thead> <tbody> <tr><td> </td><td> </td><td> </td><td> </td><td> </td></tr> <tr><td> </td><td> </td><td> </td><td> </td><td> </td></tr> <tr><td> </td><td> </td><td> </td><td> </td><td> </td></tr> </tbody> </table>		Bank No.	No. of Nozzles	Size	Type	Manufacturer															
Bank No.	No. of Nozzles	Size	Type	Manufacturer																		
MATERIALS OF CONSTRUCTION																						
Packing <u>unglazed porcelain</u> Distributor Tray <u>Carbon steel</u> Re-Distributor Tray _____ Packing Support <u>Carbon steel</u> Spray Nozzles _____																						
REMARKS																						
Packing on Supports: <ul style="list-style-type: none"> 1st. Layer Arrangement <u>1'-0" of 1/2" Berl saddles</u> <u>dumped</u> 2nd. Layer Arrangement <u>14'-0" of 1" Berl saddles</u> <u>dumped</u> 3rd. Layer Arrangement _____ Bulk of Packing Arrangement <u>See 2nd Layer.</u> 																						
		 <p style="font-size: small;"> Flange 1" x 1" x .09 Mesh Cloth Cross-bar Support for 1x1 Mesh </p>																				
By	Chk'd.	App.	Rev.	Rev.	Rev.																	
Date																						
P.O. To: _____																						

Figure 9-74B. Tower internal specifications, Spray or Packed Columns.

(text continued from page 353)

*n, g. moles H ₂ O	*-Q p.c.u./lb mole NH ₃	-Q Btu/lb NH ₃	x, mole fraction NH ₃	Lb. NH ₃ per 100# H ₂ O	*Adiabatic Temp. rise, °F
1	6,600	698	0.5	94.5	338
2.33	7,820	829	0.3	40.5	238
4	8,040	851	0.2	23.6	164
9	8,220	873	0.1	10.5	83
19	8,290	879	0.05	4.97	41.6
49	8,580	906	0.02	1.93	17.1

Data on heats of solution of ammonia taken from International Critical Tables Vol. V, pg. 213 [35] by Sherwood and Pigford (*Absorption and Extraction*, pg. 161, 2nd Ed., McGraw Hill Book Co., Inc.) Ref. 63*.

1. Assume values for Y, (0.012 for example) mol ammonia/mol of inert gas and read corresponding vapor pressure of ammonia from Figure 9-75 (curve Y) (= 102 mm). This figure was calculated from

$$Y = \frac{vp \text{ NH}_3}{\pi - vp \text{ NH}_3}$$

for a total pressure system at 164.7 psia (150 psig) and a temperature of 90°F with vapor pressures read from published data, Figure 9-76.

2. At the values of vapor pressure at 90°F (32.2°C) read the corresponding weight percent aqua ammonia (= 8%).
3. Convert this weight percent ammonia to lb mols ammonia/lb mol water by

$$\frac{\text{mol NH}_3}{\text{mol H}_2\text{O}} = \frac{(\text{wt}\%) (18)}{(100 - \text{wt}\% \text{ NH}_3) (17)}, (= 0.092 \text{ example})$$

4. Plot equilibrium curve (curve A) of Figure 9-77.

(at Y = 0.012, x = 0.092, example)

If the temperature rise over the temperature range is very high, then to operate at constant temperature requires internal cooling coils in the column, or other means of heat removal to maintain constant temperature operation. Usually this condition will require considerably less transfer units for the same conditions when compared to the adiabatic operation.

To calculate the equilibrium curve taking the heat of solution into account, i.e., operate adiabatically with liquid temperature variable, follow the steps:

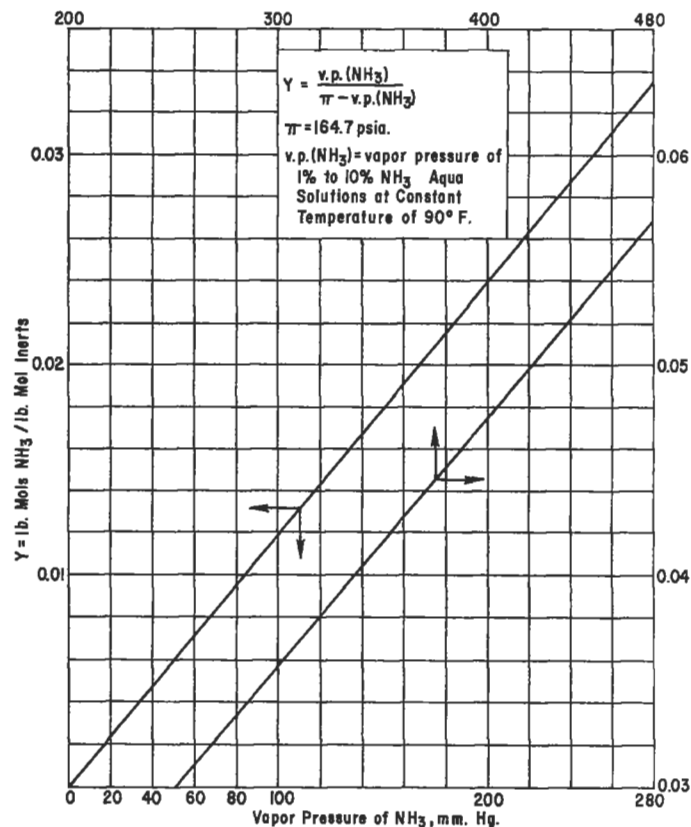


Figure 9-75. Ammonia vapor pressure-inerts data at a fixed pressure.

1. Assume a temperature rise (for example, 17.8°F) and read from Figure 9-78 (temp. rise) the lb NH₃/100 lb H₂O (= 2, example).
2. Convert this lb NH₃/100 lb H₂O to lb mol NH₃/lb mol H₂O by

$$\text{Lb NH}_3 / 100 \text{ lb H}_2\text{O} = \left(\frac{\text{mol NH}_3}{\text{mol H}_2\text{O}} \right) (100) \left(\frac{17}{18} \right)$$

(= 0.0215 lb mole NH₃ / lb mol H₂O)

3. Convert this (0.0215) lb mol NH₃/lb mol H₂O to weight percent NH₃ by step (3) of previous paragraph (= 1.95%).
4. Read aqua-ammonia vapor pressure curves at wt percent NH₃ and corrected temperature (base temperature plus rise) (= 90 + 17.8 = 107.8°F, e.g., or 41.1°C). Read 29.5 mm Hg as vapor pressure of ammonia, Figure 9-76.
5. Read "Y" curve, Figure 9-75 at value of vapor pressure to get Y (= 0.0035 lb mol NH₃/lb mol inerts).
6. Plot X (= 0.0215) and Y (= 0.0035) to get equilibrium curve, which accounts for this effect of heat of solution Curve B, (Figure 9-77).

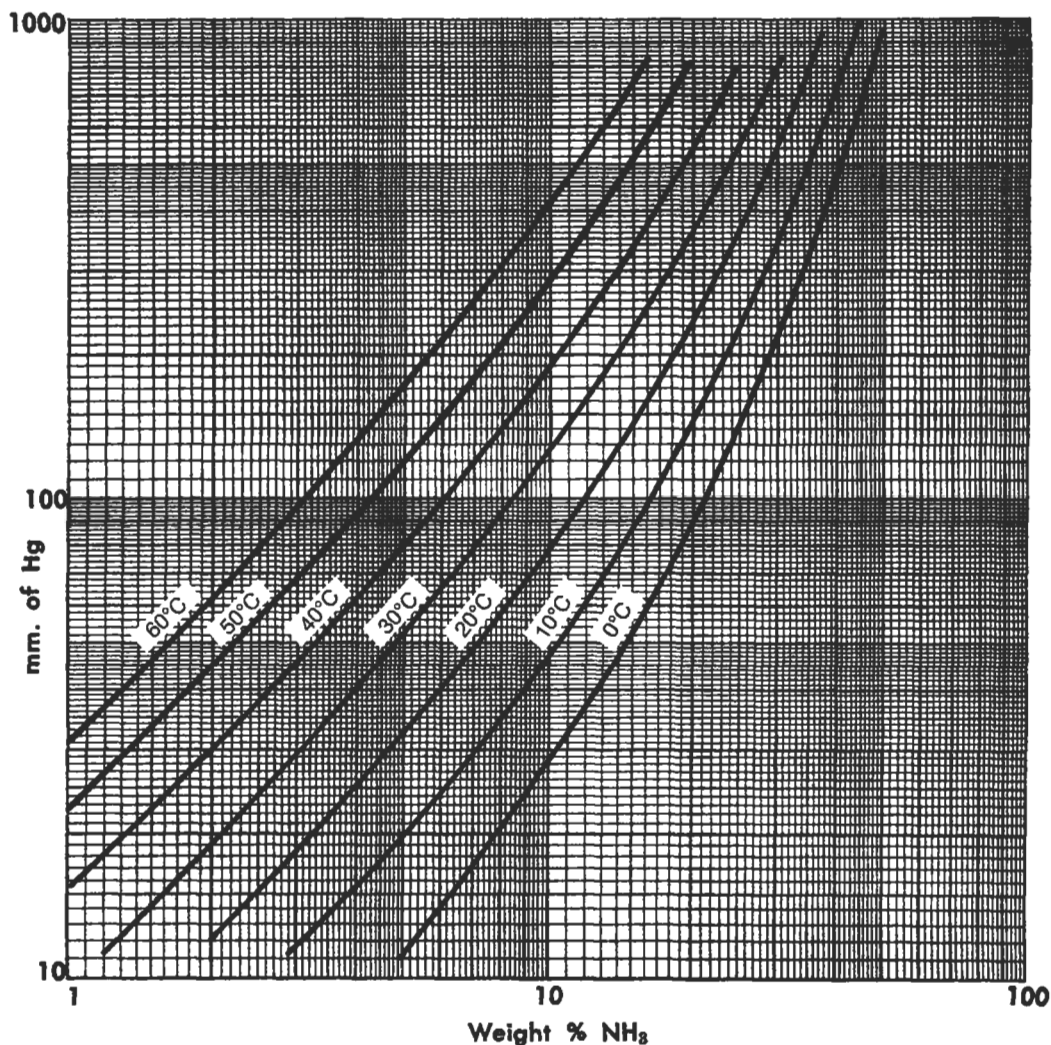


Figure 9-76. Partial pressure of ammonia over aqueous solutions of ammonia. Used by permission of Leva, M., *Tower Packings and Packed Tower Design*, 2nd Ed., U.S. Stoneware Co. (now, Norton Chemical Process Products Corp.) (1953).

Determine Number of Transfer Units, N

The number of transfer units is determined graphically by:

1. Bisecting the vertical distance (line C) of Figure 9-77 between the 8% aqua operating line and the equilibrium curve B.
2. Starting at Y_2 , draw horizontal line to line C. Extend this horizontal to right of C far enough to make "Y₂ to line C" equal to "line C to end," then step vertically to operating line, D. Move horizontally to line C, so that (a) (b) = (b) (c). Continue moving up the tower in this stepwise fashion.
3. At end, X_1Y_1 , if steps do not end at exact point, estimate fraction of vertical step required and report as fractional transfer unit.

This problem steps off six full transfer units and approximately $\frac{1}{3}$ of the seventh. Report as 6.33 units.

Performance Interpretation

The point X_1 represents 0.092 mol $\text{NH}_3/\text{mol H}_2\text{O}$, which is equivalent to 8 wt% ammonia solution. If a weaker product were desired fewer transfer units would be required.

Point (e) is the intersection of the equilibrium curve and the operating line and represents the equilibrium condition for tower outlet liquor, and the maximum liquor concentration.

Note that the 10% (wt) aqua product operating line is shown on the diagram, but such a concentration cannot be reached when operating at 150 psig. A greater pressure is required in order to lower the equilibrium curve.

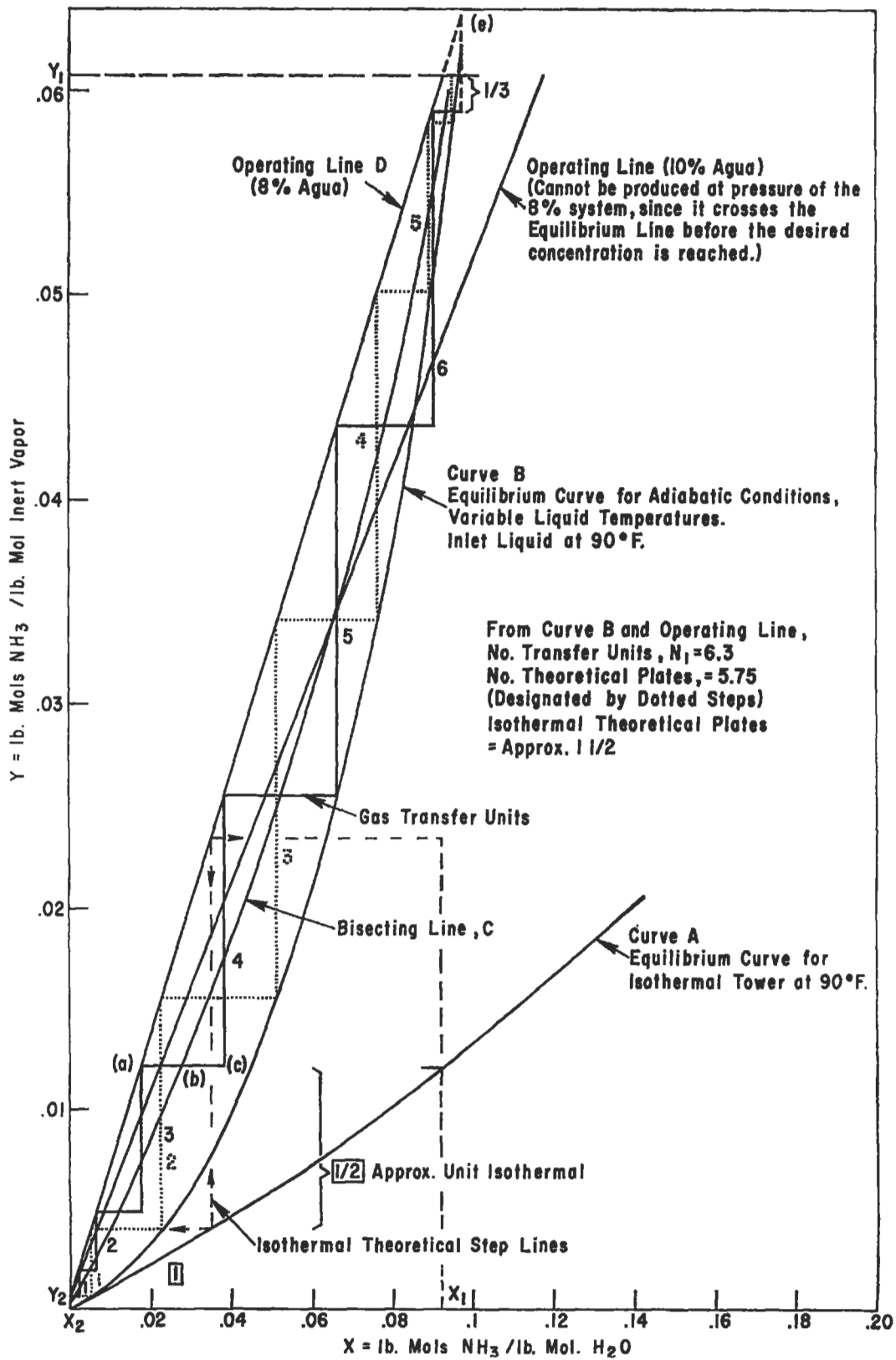


Figure 9-77. Equilibrium curves for ammonia-water; an operating system for production of 8% aqua (by weight) at total pressure of 150 psig.

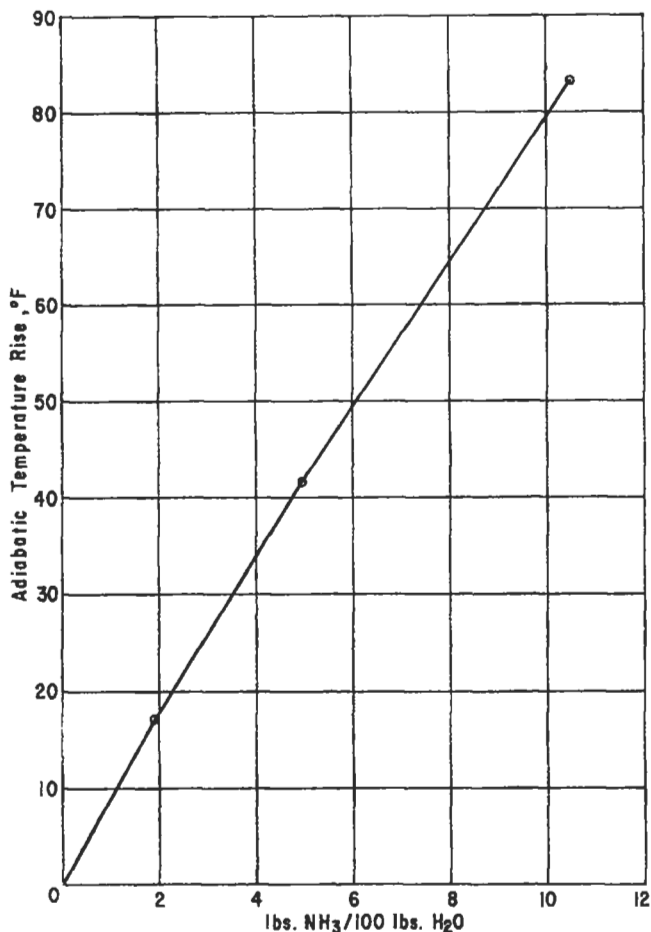


Figure 9-78. Temperature rise due to heat of solution, ammonia in water.

Curve A represents the equilibrium condition for water entering at 90°F, the gas entering saturated with water vapor at 90°F and isothermal tower operation.

Height of Transfer Unit

From Figure 9-73 the experimental H_{OG} may be picked based on ammonia from a mixture with air absorbing in water. Assume an 18 O.D. tower (pipe) which has an I.D. of 16.8 in.

$$\text{At inlet, } G' = \frac{5.35 (11.6)}{(.057) (1.553 \text{ ft}^2)} = 702 \text{ lb/hr (ft}^2\text{)}$$

$$\begin{aligned} \text{At outlet, } G' &= 702 - \frac{(0.99) (5.35) (17)}{1.553} \\ &= 702 - 57.8 = 644 \text{ lb/hr (ft}^2\text{)} \end{aligned}$$

$$\text{Avg } G' = \frac{702 + 644}{2} = 673 \text{ lb/hr (ft}^2\text{)}$$

$$\text{At inlet, } L' = \frac{1035}{1.553} = 666 \text{ lb/hr (ft}^2\text{)}$$

$$\text{At outlet, } L' = 666 + 57.8 = 724$$

$$\text{Avg } L' = \frac{666 + 724}{2} = 695 \text{ lb/hr (ft}^2\text{)}$$

$$\text{At, } L' = 695, G' = 673$$

$H_{OG} = 1.6$ ft (interpolated) based on ammonia-air-water system. The system under study has inerts other than air.

Tower Height Based on Air as Inert Gas in System

$$Z = NH_{OG}$$

$$Z = (6.33) (1.6) = 10.1 \text{ ft packing}$$

Tower Loading, Flooding, and Pressure Drop

Assume 18-in. O.D. steel pipe, 16.8-in. I.D., cross-section area is 1.553 ft².

$$\rho_L = 62.3 \text{ lb/ft}^3$$

$$\rho_G = \frac{11.6 (492) (164.7)}{359 (550) (14.7)} = 0.324 \text{ lb/ft}^3$$

$$\frac{a}{\epsilon^3} = 125 \text{ for 1-in. Berl saddles}$$

$$\mu^{0.2} = (0.77)^{0.2} = 0.949$$

$$\frac{L}{G} \left(\frac{\rho_G}{\rho_L} \right)^{0.5} = \frac{695}{673} \left(\frac{0.324}{62.3} \right)^{0.5} = 0.0744$$

$$\begin{aligned} \frac{G^2 \psi^2 \mu^{0.2}}{\rho_L \rho_G g_c} \left(\frac{a}{\epsilon^3} \right) &= \frac{(673/3600)^2 (62.3/62.3)^2 (0.949)}{(62.3) (0.324) (32.2)} (125) \\ &= 0.00635 \end{aligned}$$

Referring now to Figure 9-21D indicates that the tower would operate well below the loading zone at about 0.00635 (100)/.06 = 10.6% of the average loading condition. This is too low.

A new tower diameter can be assumed, or the limiting velocities can be calculated, and the diameter set from these. For illustration purposes, use the latter approach:

$$\text{Average gas rate} = (673) (1.553) = 1,047 \text{ lb/hr}$$

$$\text{Inlet gas rate} = (702) (1.553) = 1,090 \text{ lb/hr}$$

Average liquid rate = (695) (1.553) = 1,080 lb/hr

Outlet liquid rate = (724) (1.553) = 1,124 lb/hr

$$\frac{L}{G} \left(\frac{\rho_G}{\rho_L} \right)^{0.5} = \frac{1080}{1047} \left(\frac{0.324}{62.3} \right)^{0.5} = 0.0744$$

Because:

$$\frac{G^2 \psi^2 \mu^{0.2}}{\rho_L \rho_G g_c} \left(\frac{a}{\epsilon^3} \right) = \frac{V_g^2 \rho_G \mu^{0.2} \psi^2}{g_c \rho_L} \left(\frac{a}{\epsilon^3} \right)$$

where V_g = superficial gas velocity, ft/sec

Solve for V_g : at abscissa = 0.0744

Read Figure 9-21D at flooding, ordinate = 0.150

$$V_g^2 = \frac{(0.150)(32.2)(62.3)}{(0.324)(0.949)(1)(125)} = 7.83$$

V_g = 2.8 ft/sec flooding velocity

Read Figure 9-21D at upper loading, ordinate = 0.084

V_g = 2.1 ft/sec upper loading velocity

Base diameter on 50% of flooding

Operating velocity = 0.5 (2.8) = 1.4 ft/sec

$$\text{Gas flow rate} = \frac{(1047)}{(0.324)(3600)} = 0.896 \text{ ft}^3/\text{sec}$$

Required tower cross-sectional area at 50% of flooding:

$$\text{ft}^2 = \frac{0.896}{1.4} = 0.64$$

$$\text{Tower dia.} = \sqrt{(4/\pi)(0.64)} = 0.902 \text{ ft} = 10.8 \text{ in.}$$

If a standard 10-in. pipe is used (10.02-in. I.D.) the superficial velocity = $0.896/0.546 \text{ ft}^2 = 1.64 \text{ ft/sec}$.

$$\% \text{ of flooding} = 1.64 (100)/2.8 = 58.6\%$$

$$\% \text{ of upper loading} = 1.64 (100)/2.1 = 78.3\%$$

Pressure drop is approximately 0.5 in./ft packing height, Figure 9-21D.

This should be an acceptable operating condition, therefore, use tower diameter of 10-in. nominal Sch. 40 pipe. This pipe is satisfactory for 150 psig operating pressure (see Figures 9-74A and B).

Correcting Height of Transfer Unit for Inert Gases in System

$$\text{Diffusivity : } D_v = 0.0069 \frac{T^{3/2} \sqrt{1/M_A + 1/M_B}}{P(V_A^{1/3} + V_B^{1/3})^2}$$

T (for 90°F) = 90 + 460 = 550°R at liquid inlet

T (for 90 + 72°) = 162 + 460 = 622°R max. at liquid outlet

M_A = 17 for NH_3

M_B = 29 for air

$$P = 164.7/14.7 = 11.2 \text{ atm}$$

V_A = 26.7 for NH_3 from Table 9-44 (molecular volume) Note: The value of V_A is from Ref. 63. Molecular volume values vary between references.

V_B = 29.9 for air

Diffusion coefficient of NH_3 through air:

$$D_v = 0.0069 \frac{(550)^{3/2} \sqrt{1/17 + 1/29}}{11.2 [(26.7)^{1/3} + (29.9)^{1/3}]^2} = 0.065 \text{ ft}^2/\text{hr}$$

Diffusion coefficient of NH_3 through 3:1 H_2 - N_2 mixture gas:

M_A = 17 for NH_3

M_B = 11.2 for inert gas mixtures, less NH_3

V_A = 26.7 for NH_3

V_B = (0.75) (14.3) + (0.25) (31.2) = 18.5 for H_2 - N_2 mixture

Diffusion of ammonia through hydrogen—nitrogen inert gas:

$$D_v = 0.0069 \frac{(550)^{3/2} \sqrt{1/17 + 1/11.2}}{11.2 [(26.7)^{1/3} + (18.5)^{1/3}]^2}$$

$$D_v = 0.096 \text{ ft}^2/\text{hr}$$

For an ammonia-air system using mass rates in the tower the same as the H_2 - N_2 system: $G' = 1047/0.546 = 1920 \text{ lb/hr (ft}^2)$ and $L' = 1080/0.546 = 1980 \text{ lb/hr (ft}^2)$

From Figure 9-73 Extrapolated $H_{OG} = 0.95$ (this should be maximum to expect)

Then substituting, for ammonia-air mixture:

$$H_{OG} = \frac{G'}{K_G a P}$$

$$K_G a = \frac{1920 / (28.4 \text{ mol. wt of mixture})}{(0.95)(11.2)}$$

$$= 6.35 \text{ mol/hr (ft}^3\text{) (atm)}$$

Converting this to ammonia-H₂-N₂ mixture:

$$K_G a = 6.35 \left[\frac{0.096}{0.065} \right]^{0.56} = 7.9 \text{ mol/hr (ft}^3\text{) (atm)}$$

Then, substituting,

$$H_{OG} \text{ for this mixture} = \frac{(1920 / (11.2 \text{ mol wt H}_2\text{-N}_2 \text{ mixture}))}{(7.9)(11.2 \text{ atm})}$$

$$= 1.875 \text{ ft}$$

Tower Packing Height for Ammonia-Hydrogen-Nitrogen Mixture

$$Z = (1.875)(6.33) = 11.9 \text{ ft packing}$$

For 1-in. Berl saddles allow 2.0 ft for good liquid distribution through the packing from the top.

$$\text{Minimum packed bed depth} = 11.9 + 2.0 = 13.9 \text{ ft}$$

Use: 15 ft (or perhaps 18 ft to allow for variations in performance)

Expected Pressure Drop

Packing:	(15) (0.5 in/ft)	= 7.5 in.
Support:	(Grating type), approx.	= 1.0
Total drop		= 8.5 in. water

Inlet Liquid

For this small diameter tower, bring water into center of top of packing with a turned down 90° ell, placed 6–9 in. above packing.

Mass Transfer With Chemical Reaction

Many absorption processes involve some chemical reaction; however, it is fortunate that satisfactory correlation can be made without delving into the complexities of the reaction.

In many instances the gas being absorbed is to be recovered from the solution, and hence the effluent from the absorption must be treated. Often the application of heat

will release the gas, e.g., CO₂ from ethanolamine; however, in other cases chemical treatment must be used. In order to fully use the absorbent liquid, recycle systems must be established, and the economics of absorbent selection become of considerable importance, determining the size of the system in many cases. Because the absorption ability of the various combinations of gas and liquid vary rather widely and depend upon the system condition, it is often necessary to examine more than one absorbent for a given gas. The performance of several important systems is given in summary or reference form:

I. Carbon Dioxide or Sulfur Dioxide in Alkaline Solutions

$$K_G a = \frac{n}{Z A \Delta p_{lm} f_a} \quad (9-106)$$

where $K_G a$ = gas coefficient, lb mol/(hr) (ft³) (atm)

n = CO₂ (or SO₂) absorbed, lb mol/hr

A = tower cross-section area, ft²

Z = height of packed section in tower, ft

Δp_{lm} = log mean partial pressure of gas in inlet and exit gas streams, atm

f_a = fraction effective packing wetted

Design Procedure for Alkali-Absorbers

1. Calculate material balance, determining quantity of gas to be absorbed, and alkali required.
2. Estimate a tower diameter and establish its operating point from Figure 9-21. For initial trial set operating point at 50–60% of flood point system based on varying gas mass velocity at variable tower diameters for a fixed

$$\frac{L}{G} \left(\frac{\rho_G}{\rho_L} \right)^{0.5}$$
3. Estimate the effective fraction wetted packing area by Figure 9-46 or 9-43. As a general rule, try not to accept design if fraction wetted is less than 0.5. If it is less, adjust tower conditions to raise value, bearing in mind that this factor is based on scattered and very incomplete data.
4. Determine $K_G a$ based on inlet alkali normality and percent conversion to carbonate (for carbon dioxide).

K_Ga Data and Corrections [42, 69, 72]

The necessary data required to properly design a CO₂ scrubber are separated into three sections, depending upon the CO₂ concentration in the feed gas. Corrections

are necessary to convert "procedure based" information to the specific design basis of a given problem. The corrections outlined below are specific to the CO₂ concentration range being presented in the section.

Because there are not sufficient data to serve completely for all types and sizes of packing, it may be necessary to estimate K_{Ga} values by ratioing packing surface areas and making the other appropriate correction for the problem conditions.

1. Inlet CO₂ concentration, 100 to 1,000 ppm by volume

K_{Ga} : Use Figures 9-79A-E and Figure 9-80.

a. Increases with increase in liquid rate, L , to the 0.2

$$\text{power of the ratio, } K_{Ga} \propto \left(\frac{L_2}{L_1}\right)^{0.2}$$

b. Increases with increase in gas rate, G , to the 0.35

power of the rate ratio, up to a rate of 500 lb/hr (ft²). Above this rate the increase is reduced, being to the 0.15 power at rates near 1000 lb/hr (ft²).

$$K_{Ga} \propto \left(\frac{G_2}{G_1}\right)^{0.35} \quad \text{for } G = 1 \text{ to } 500$$

$$K_{Ga} \propto \left(\frac{G_2}{G_1}\right)^{0.15} \quad \text{for } G > 1000$$

c. Increases with increase in temperature to the 6.0 power of the absolute temperature ratio.

d. Decreases with increase in pressure to the 0.5 power of the absolute pressure ratio.

2. Inlet CO₂ concentration 1.5 to 5.0 mol%

K_{Ga} : Use Figures 9-80-82A-F.

a. Increases with increase in liquid rate, L , to the

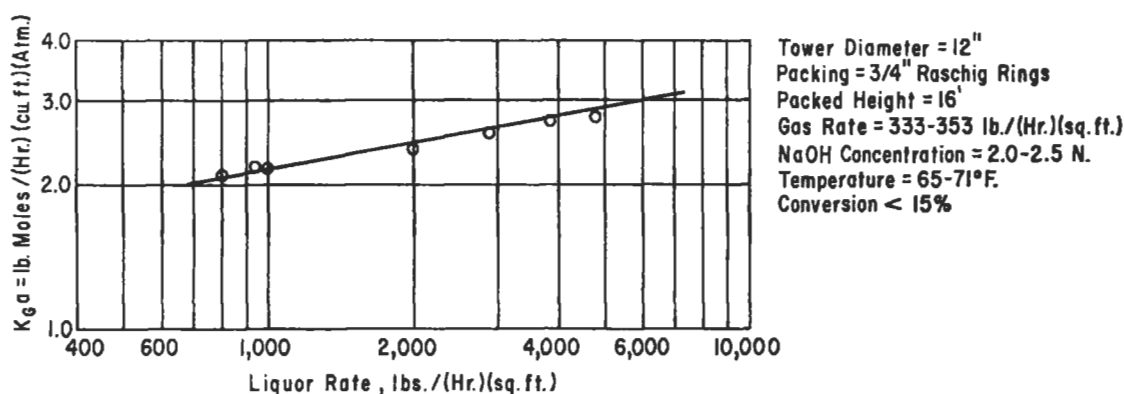


Figure 9-79A. CO₂ absorption from atmosphere; effect of liquor rate on K_{Ga} at atmospheric pressure. Reproduced by permission of the American Institute of Chemical Engineers, Spector, N. A., and Dodge, B. F., *Trans. A.I.Ch.E.*, V. 42 © (1946) p. 827; all rights reserved.

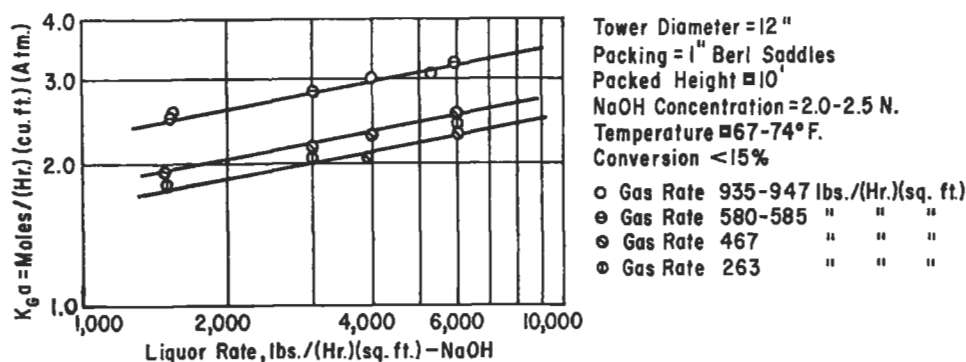


Figure 9-79B. CO₂ absorption from atmosphere; effect of liquor rate on K_{Ga} at atmospheric pressure and various gas rates. Reproduced by permission of the American Institute of Chemical Engineers, Spector, N. A., and Dodge, B. F., *Trans. A.I.Ch.E.*, V. 42 © (1946) p. 827; all rights reserved.

Packed Towers

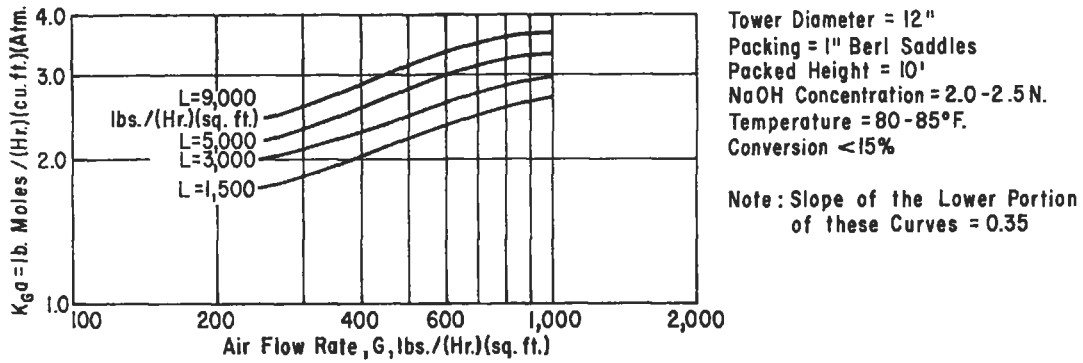


Figure 9-79C. CO₂ absorption from atmosphere; effect of gas rate on K_{Ga} at atmospheric pressure. Reproduced by permission of the American Institute of Chemical Engineers, Spector, N. A., and Dodge, B. F., *Trans. A.I.Ch.E.*, V. 42 © (1946) p. 827; all rights reserved.

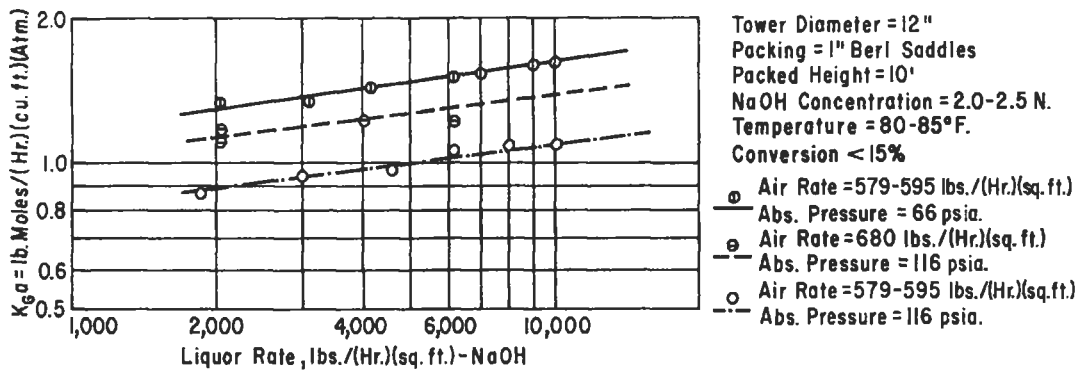


Figure 9-79D. CO₂ absorption from atmosphere; effect of flow rates on K_{Ga} at elevated pressure. Reproduced by permission of the American Institute of Chemical Engineers, Spector, N. A., and Dodge, B. F., *Trans. A.I.Ch.E.*, V. 42 © (1946) p. 827; all rights reserved.

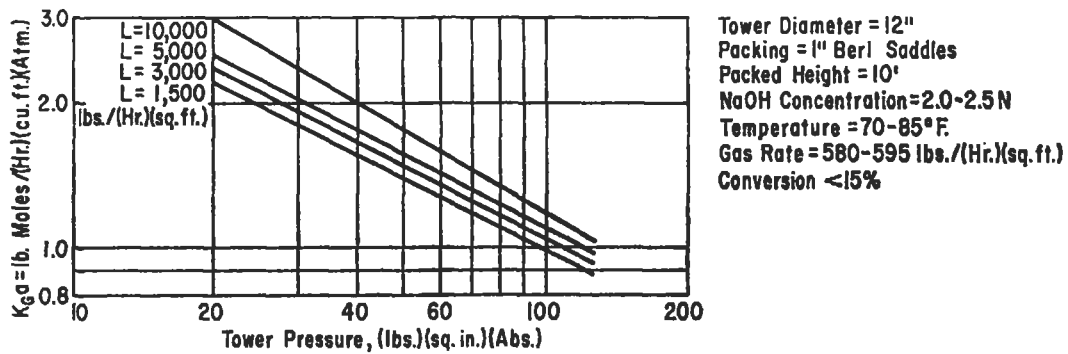


Figure 9-79E. CO₂ absorption from atmosphere; effect of tower pressure on K_{Ga} at various liquor rates. Reproduced by permission of the American Institute of Chemical Engineers, Spector, N. A., and Dodge, B. F., *Trans. A.I.Ch.E.*, V. 42 © (1946) p. 827; all rights reserved.

0.28 power of the rate ratio, $K_{Ga} \propto \left(\frac{L_2}{L_1}\right)^{0.28}$

b. No correction to gas rate, G, below loading. Above loading point, K_{Ga} increases with increase in gas rate G, to the 0.3 power of the rate ratio.

$K_{Ga} \propto \left(\frac{G_2}{G_1}\right)^{0.3}$ above loading

c. Effect of temperature and pressure same as section "1" above.

3. Inlet CO₂ concentration 5.0 to 10.0 mol%
K_{Ga}: Use Figures 9-80-82A-F.

a. Liquor rate correction follows section "2" above.
b. Increases with increase in gas rate, G, to the 0.15 power of rate ratio.

c. Effect of temperature and pressure same as section "1."

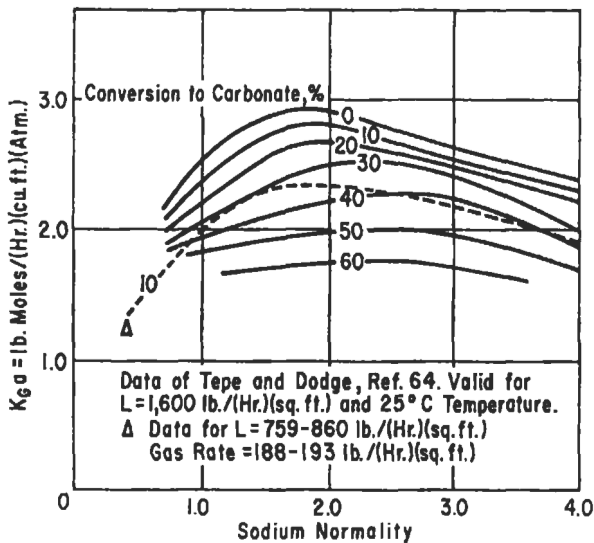


Figure 9-80. CO₂ absorption in sodium hydroxide (NaOH). Used by permission of Leva, M., *Tower Packings and Packed Tower Design*, 2nd Ed., U.S. Stoneware Co. (now, Norton Chemical Process Products Corp.) (1953).

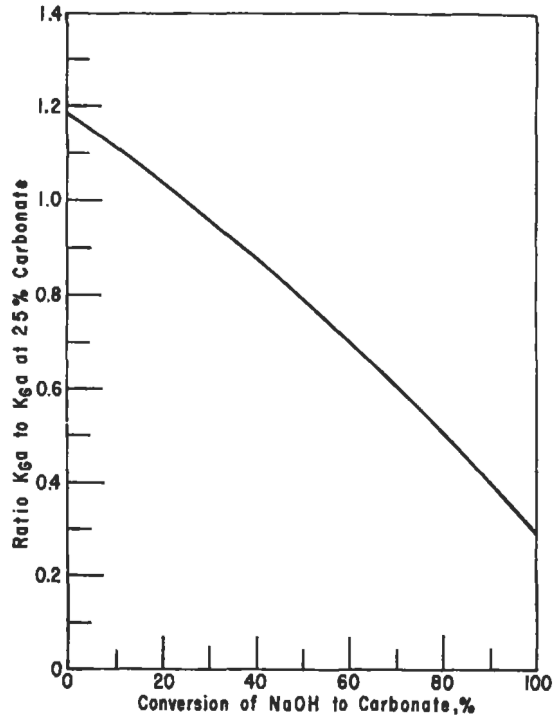


Figure 9-81. CO₂ absorption; effect of carbonate on K_{Ga}. Reproduced by permission of the American Institute of Chemical Engineers, Leva, M., *A.I.Ch.E. Jour.*, V. 1 © (1955) p. 224; all rights reserved.

e. Calculate height of packing required:

$$Z = \frac{n}{K_{Ga} (A) (\Delta p_{lm}) (f_a)}$$

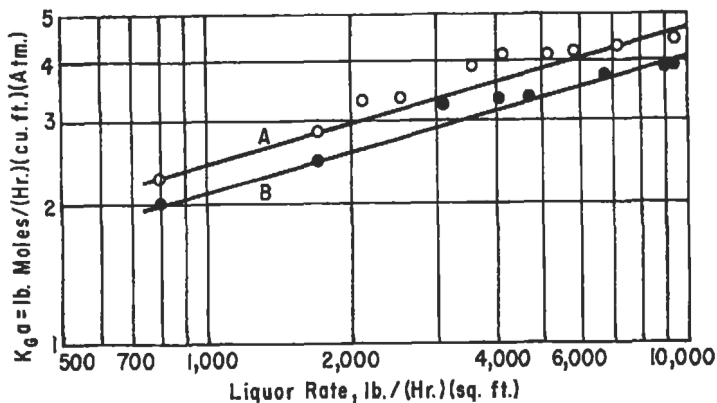
Calculate tower pressure drop from Figure 9-21 for packing, and Figures 9-37-41 for support and grids.

g. Make specification sheet.

Example 9-13. Design a Packed Tower Using Caustic to Remove Carbon Dioxide from a Vent Stream

A process stream containing mostly nitrogen and carbon dioxide is to be scrubbed with 10% (wt) NaOH for CO₂ removal, but not recovery. The requirements are:

- Inlet gas: CO₂ = 40.6 mol/hr
- Inerts = 365.4 mol/hr
- Avg mol wt = 20
- Temperature = 90°F
- Pressure = 35 psig = 49.7 psia
- Outlet gas: CO₂ = 0.1 mol%
- Inerts = 99.9 mol%
- Max. allowable pressure drop = 2 psi
- Liquid sp gr = 1.21



Curve	Symbol	Mean NaOH Concentration
A	○	1.94 - 2.05 Normal
B	●	0.95 - 1.10 Normal

Mean NaOH Concentration = 0.038 - 0.183 Normal.
 Gas Rate = 187-191 lb./(Hr.)(sq. ft.)
 Temperature = 78°F.

Figure 9-82A. CO₂ absorption; effect of liquor rate. Reproduced by permission of the American Institute of Chemical Engineers, Tepe, J. B., and Dodge, B. F., *Trans. A.I.Ch.E.*, V. 39 © (1943) p. 255; all rights reserved.

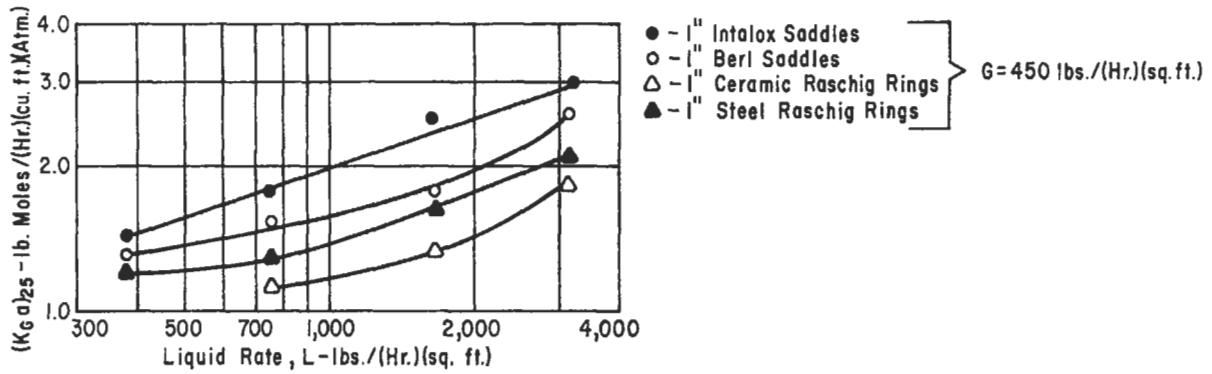


Figure 9-82B. CO₂ absorption; 1-in. packing data at constant gas rate. Reproduced by permission of the American Institute of Chemical Engineers, Leva, M., *A.I.Ch.E. Jour.*, V. 1 © (1955) p. 224; all rights reserved.

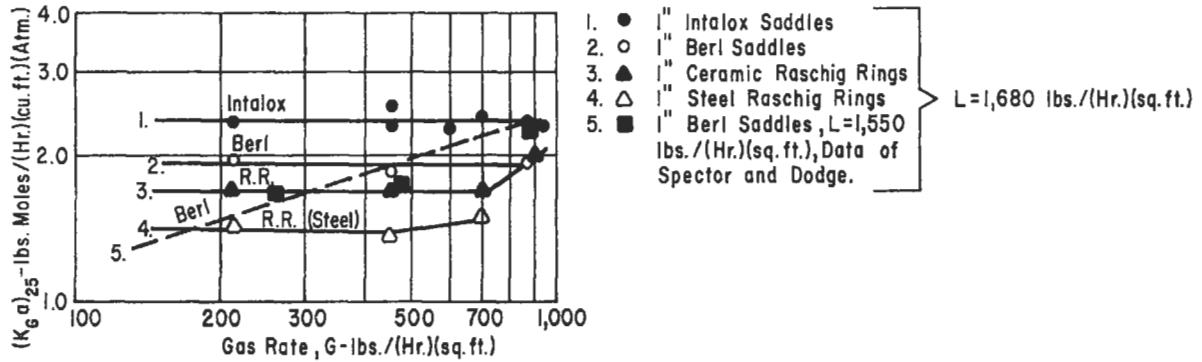


Figure 9-82C. CO₂ absorption; 1-in. packing data at constant liquid rate. Reproduced by permission of the American Institute of Chemical Engineers, Leva, M., *A.I.Ch.E. Jour.*, V. 1, No. 2 © (1955) p. 224; all rights reserved.

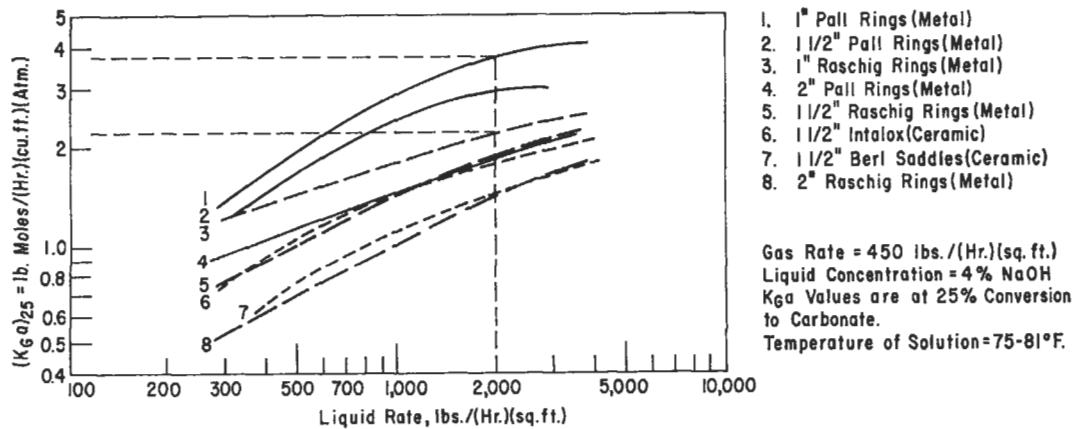


Figure 9-82D. $K_G a$ versus liquid rate for 4% sodium hydroxide (NaOH). Compiled from References 20 and 35.

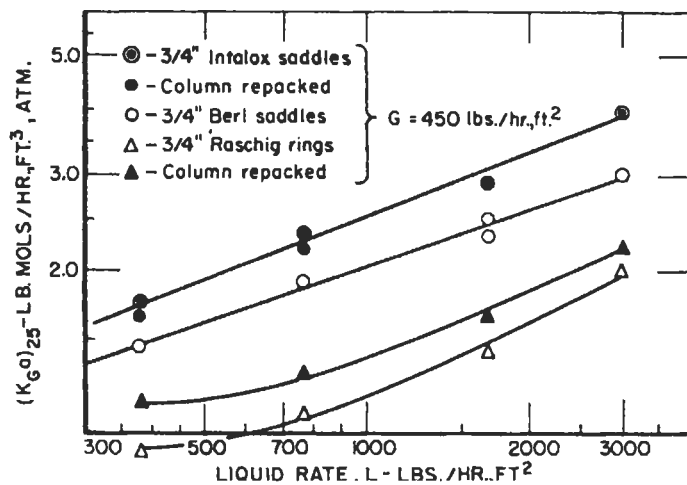


Figure 9-82E. $\frac{3}{4}$ -in. packing data for system carbon dioxide-sodium hydroxide, gas rate constant. Reproduced by permission of the American Institute of Chemical Engineers, Leva, M., *A.I.Ch.E. Jour.*, V. 1, No. 2 © (1955) p. 224; all rights reserved.

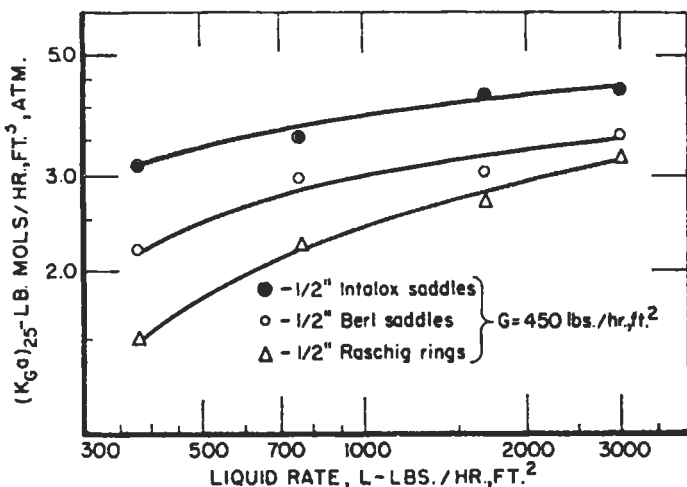
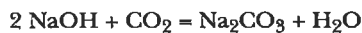


Figure 9-82F. $\frac{1}{2}$ -in. packing data for system carbon dioxide-sodium hydroxide, gas rate constant. Reproduced by permission of the American Institute of Chemical Engineers, Leva, M., *A.I.Ch.E. Jour.*, V. 1, No. 2 © (1955) p. 224; all rights reserved.

From a material balance; the NaOH required based on 25% conversion to Na_2CO_3 :



Lb 10% NaOH required/hr =

$$\frac{(40.6 \text{ mol CO}_2/\text{hr}) [(2) (40) \text{ lb NaOH/mol CO}_2]}{(0.1 \text{ wt fraction NaOH}) (0.25 \text{ conversion})}$$

= 129,000 lb/hr

Assume 3.5 ft I.D. Tower, use $\frac{1}{2}$ in. steel Raschig rings. At operating point

$$L' = \frac{129,000}{(\pi/4) (3.5)^2} = 13,470 \text{ lb/hr (ft}^2\text{)}$$

$$G' = \frac{(40.6 + 365.4) (20)}{(\pi/4) (3.5)^2} = 846 \text{ lb/hr (ft}^2\text{)}$$

$$G = 0.235 \text{ lb/sec (ft}^2\text{)}$$

$$\rho_G = \frac{(20) (35 + 14.7) (520)}{(379) (14.7) (550)} = 0.1688 \text{ lb/ft}^3$$

For Figure 9-21D

$$\frac{L}{G} \left(\frac{\rho_G}{\rho_L} \right)^{1/2} = \frac{13,470}{846} \left(\frac{0.1688}{1.21 (62.3)} \right)^{1/2} = 0.776$$

$$\frac{G^2 \psi^2 \mu^{0.2}}{\rho_G \rho_L g_c} \left(\frac{a}{\epsilon^3} \right) = \frac{(0.235)^2 (0.825)^2 (2.6)^2}{0.1688 (1.21) (62.3) (32.2)} \quad (110)$$

= 0.012

At flooding, ordinate = 0.0275, for abscissa = 0.776

At lower loading, ordinate = 0.012

Operating point = (0.012/0.0275) (100) = 43.8% of flood

This is only slightly lower than good practice, but because the operating point is at the lower loading point, continue with this selection. A smaller diameter tower might calculate to be a better choice. However, extreme caution must be used in designing too close to limits with packed towers. Very little of the data are exact, and often the range is not known.

Effective Wetted Packing

From Figure 9-43.

f_a = approx. 0.50 for ceramic material at $L'/G' = 15.9$

Because steel rings have thinner walls, it seems that the liquid should flow and wet this material a little better than ceramic.

Use $f_a = 0.6$

K_{GA} from Figure 9-82D uncorrected:

$$(K_{GA})_{25} = 1.9 \text{ lb. mol/hr (ft}^3\text{) (atm)}$$

The conditions for K_{GA} from Figure 9-82D are 4 wt% NaOH, which is 1 normal, and $G' = 450 \text{ lb/hr (ft}^2\text{)}$, $L' = 2,000 \text{ lb/hr (ft}^2\text{)}$, pressure = 14.7 psia. The $(K_{GA})_{25}$ is also for 25% conversion to carbonate.

Correct the K_{Ga} for pressure, normality of NaOH, and liquid rate:

There is not correction for gas rate at or below the loading point. Note that from Figure 9-80 the ratio of K_{Ga} at 1 normal and 2.5 normal solutions and for 25% conversion = 2.6/2.1.

$$K_{Ga} = (1.91) \left(\frac{13,470}{2000} \right)^{0.28} \left(\frac{14.7}{35 + 14.7} \right)^{0.5} \left(\frac{2.6}{2.1} \right)$$

$$K_{Ga} = 2.18 \text{ lb mol/hr (ft}^3\text{) (atm)}$$

Note: Because the solution temperature of data for Figure 9-82D is 75–81°F, it is assumed ambient, and no correction is made. If the operating temperature were higher or lower, then a temperature correction multiplier should be used above, with the absolute temperatures ratio being raised to the 6.0 power.

Log mean driving force, for CO_2 :

Inlet = 10%
Outlet = 0.1%

$$\Delta P_{lm} = \frac{[0.10 (49.7/14.7) - 0.001 (49.7/14.7)]}{\ln [0.10 (49.7/14.7)/(0.001) (49.7/14.7)]}$$

$$= 0.0726 \text{ atm}$$

Packing Height

$$Z = \frac{40.6 - 365.4 (0.001)/0.999}{(2.18) (0.0726) [(\pi/4) (3.5)^2] 0.6}$$

$$Z = 44.3 \text{ ft.}$$

Experience in caustic- CO_2 -steel Raschig ring systems indicates that the packing must be wetted better than the value of 60% (0.6); therefore a value of 0.85 is suggested.

then: Revised $Z = 44.3 (0.6/0.85) = 31.3 \text{ ft}$

Allowance for distribution at top = 2 ft

Allowance for redistribution at mid-point

= (2 ft) (2 sections) = 4 ft

Total packing height required = 31.3 + 2 + 4 = 37.3

Use 40 ft of packing.

Pressure Drop

From Figure 9-21C

$\Delta P = 0.38 \text{ in. H}_2\text{O/ft of packing}$

Total $\Delta P = (40) (0.38) = 15.2 \text{ in. H}_2\text{O}$

This is an acceptable figure

Arrangement

There are no data available on the liquid flow distribution vs. height for 1½-in. Raschig rings. Some information indicates that for 2-in. rings about 33% of the liquid is on the wall of a large tower after flowing through 20 ft of packed height, starting with good top liquid distribution.

To ensure good tower performance, use three 13 + ft packed sections of the 1½-in. Raschig rings. Two sections of 20 ft of packing would also probably perform satisfactorily, and be less expensive.

If Pall rings had been used, only two packed sections would be considered, because the general liquid distribution pattern is better. This would require a reevaluation of the performance, and a probable reduction in total packed height.

	1.5 in. Metal Pall Rings	1.5 Metal Raschig Rings
a/ε^3	25	110
Abscissa of Figure 9-21C	0.00272 (by ratio)	0.012
% Flood	$\frac{0.00272}{0.0275} (100) = 9.9\%$	43.8

On the basis of this better performance of the Pall ring, a smaller diameter tower *must* be selected and the tower reevaluated based on the new mass flow rates with this packing. The economics require that the higher packing cost, smaller tower diameter, new total packing volume, and tower pressure drop be considered.

II. NH_3 -Air- H_2O System

H_{OG} data of Fellingner [27] Figure 9-73.

K_{Ga} data of Dwyer and Dodge [21].

$$\frac{1}{K_{Ga}} = \frac{1}{\gamma G' \alpha L^b} + \frac{1}{H' j L^\tau} \text{ lb mol/hr (ft}^3\text{) (atm)}$$

Carbon Raschig rings:

Size, in.	γ	α	τ	b	j
½	0.0065	0.90	0.65	0.39	0.310
1	0.036	0.77	0.78	0.20	0.103
1½	0.014	0.72	0.78	0.38	0.093

(For average temperature of 85°F, $H' = 2.74 \text{ (lb mol/ft}^3\text{)/atm}$ in dilute NH_3 solution, $D = 9.8 \times 10^{-5}$, $\mu = 1.97$)

Effect of humidity of entering gas found to be minor.

K_{Ga} increases as the 0.45 power of packing superficial area, and decreases with increase in temperature °F as the 0.635 power of inverse water temperature ratio.

where H' = Henry's Law constant, (lb mol/ft³)/atm
 G' = gas rate, lb/hr (ft²)
 L' = liquid rate, lb/hr (ft²)

K_{Ga} and H_{OG} data of Wen [77], Figure 9-83
 For ceramic Berl saddles:

$$K_{Ga} = 0.0073 G_m^{0.655} L_m^{0.477} \quad (9-107A)$$

$$H_{OG} = 5.15 G_m^{0.400} L_m^{-0.520} \quad (9-107B)$$

where G_m = gas rate, lb mol/hr (ft²)
 L_m = liquid rate, lb mol/hr (ft²)

For ceramic Intalox saddles:

$$K_{Ga} = 0.0145 G_m^{0.688} L_m^{0.404} \quad (9-107C)$$

$$H_{OG} = 1.14 G_m^{0.316} L_m^{-0.315} \quad (9-107D)$$

Figure 9-84 shows effect of water temperature on K_{Ga} and H_{OG} .

III. SO₂-H₂O System (dilute gas)

K_{La} data of Whitney and Vivian [79]

Data for 1-in. ceramic Raschig rings, correlates reasonably well with 3-in. spiral tile and 1-in. coke.

$$\frac{1}{K_{La}} = \frac{H'}{0.028 (G')^{0.7} (L')^{0.25}} + \frac{1}{b(L')^{0.82}} \quad (9-108)$$

lb mol/hr (ft³) (lb mol/ft³)

Temperature °F	b	H', lb mol/ft ³ (atm)
50	0.034	0.163
60	0.038	0.130
80	0.048	0.090
90	0.056	0.076

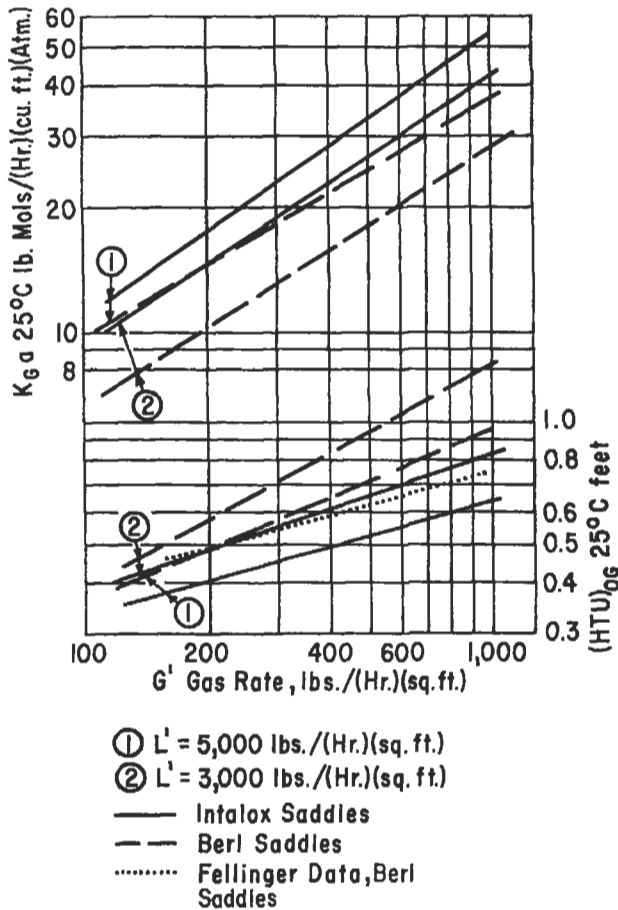


Figure 9-83. Ammonia-air-water absorption data of Wen, with ceramic packing. Used by permission of Chin-Yung, thesis, West Virginia University (1953).

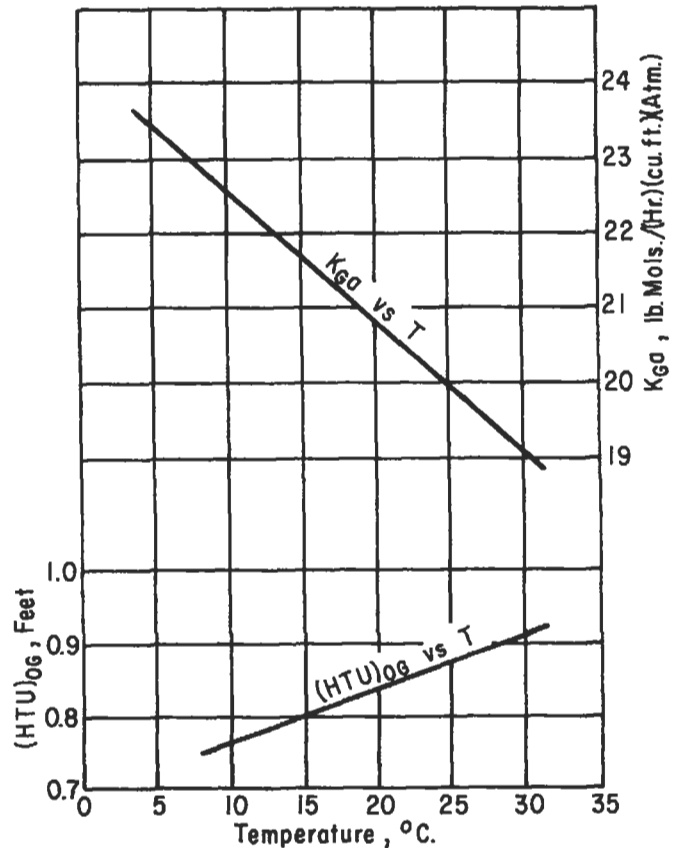


Figure 9-84. Effect of water temperature on ammonia absorption. Used by permission of Chin-Yung Wen, thesis, West Virginia University (1953).

where $K_L a$ = overall absorption coefficient, lb mol/hr (ft³) lb mol/ft³
 L = liquor rate, lb/hr (ft² of tower cross-section) G' is average gas rate of top and bottom of tower
 $H_{OL} = L'/\rho K_L a$, ft
 ρ = liquid density, lb/ft³
 H_{OL} = height of overall transfer unit in terms of liquid film, ft
 H' = Henry's Law constant, $c/p =$ lb mol/ft³ (atm)

Effects of temperature on $k_L a$:

$$k_L a \propto e^{0.023T}, T = ^\circ C$$

$k_L a$ is represented by the second term in the overall equation,

$$k_L a = b (L')^{0.82}$$

$k_L a$ = Liquid film absorption coefficient, lb mol/hr (ft³) lb mol/ft³ = 1/hr

Effect of temperature on $k_{CG} a$ = nil (assumed)

Reference 71 has excellent solubility data and absorption curves for the system.

IV. Cl₂-H₂O System (for dilute gas concentrations)

Chlorine has limited solubility in water, Figure 9-85. $K_L a$ and H_{OL} data of Vivian and Whitney, [76] Figure 9-86. Data for 1-in. ceramic Raschig rings.

$$K_L a = \frac{L' (C_1 - C_2)}{\rho Z \Delta C_{lm}} \tag{9-109A}$$

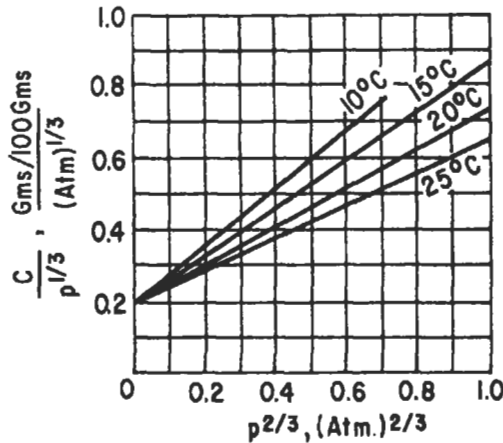


Figure 9-85. Solubility of chlorine in water. Reproduced by permission of the American Institute of Chemical Engineers, Vivian, J. E. and Whitney, R. P., *Chemical Engineering Progress*, V. 43 © (1947) p. 691; all rights reserved.

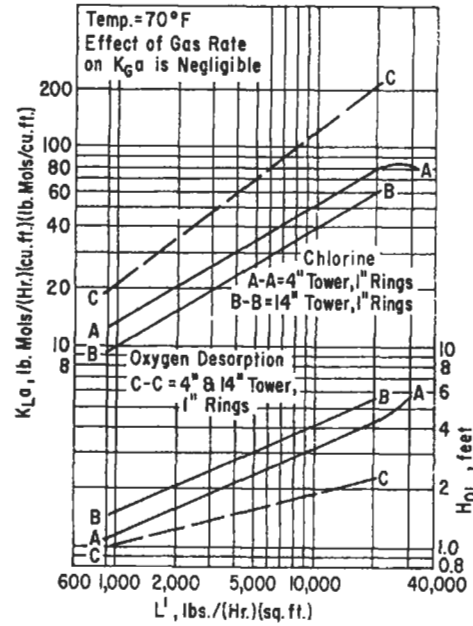


Figure 9-86. Effect of liquor rate on $K_L a$ and H_{OL} for chlorine and oxygen in water. Reproduced by permission of the American Institute of Chemical Engineers, Vivian, J. E. and Whitney, R. P., *Chemical Engineering Progress*, V. 43 © (1947) p. 691; all rights reserved.

$$H_L = \frac{L}{\rho K_L a}, \text{ ft.} \tag{9-109B}$$

$$K_L a \propto (L')^{0.6} \tag{9-109C}$$

$$K_L a \propto T^6 \text{ (of liquid, degrees absolute)}$$

where T = absolute liquid temperature, °R
 $K_L a$ = liquid coeff., lb mol/hr (ft³) (lb mol/cu ft³)
 L' = liquid rate, lb/hr (ft²)
 C_1 = concentration of chlorine in liquid, bottom of tower, lb mols/ft³
 C_2 = concentration of chlorine in liquid, top of tower, lb mols/ft³

V. Air-Water System

The system is used in humidification and dehumidification. However, grid and slat packings are more commonly used types.

The H_{CG} data of Mehta and Parekh [49] is compiled by Leva [39, 62] for the ring and saddle packing.

Sherwood and Holloway [61] also studied the desorption of oxygen from water.

VI. Hydrogen Chloride-Water System

The recovery of hydrogen chloride as well as the production of hydrochloric acid is effectively performed in

adiabatic type absorption towers. Uncooled or adiabatic towers can be used to produce 33.5 wt% acid and cooled towers will produce 35–36% acid with negligible vent losses [49] when using a feed gas containing 10–100% HCl. Due to the heat of absorption, heat dissipation must be taken care of by increasing the temperature of dilute acid product or as a combination of this plus removal as water vapor in the vent. It is important to recognize that acid strengths greater than the constant boiling mixture are made in this tower from gases containing less than 20% hydrogen chloride. The lower the inlet feed gas temperature, the lower will be the acid product temperature.

Van Nuys [75] gives excellent thermodynamic data for HCl. Figure 9-87 gives the equilibrium for the 100% HCl gas feed in an adiabatic tower, and Table 9-45 summarizes performance for two concentrations of feed gas. From the data it can be seen that it requires fewer theoretical plates to make 32% acid from 10% feed gas than from 100% gas and at the same time yield a vent containing only 0.01 weight% HCl.

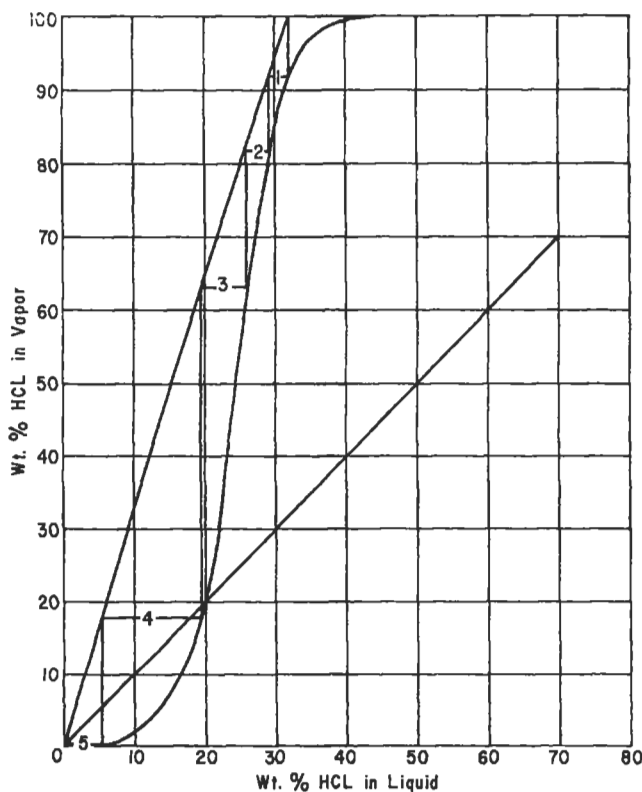


Figure 9-87. X-Y diagram for adiabatic absorption of HCl at 1 atmosphere. Reproduced by permission of the American Institute of Chemical Engineers, Oldershaw, C. F., Simenson, L., Brown, T. and Radcliffe, F. *Trans. Sect. Chemical Engineering Progress*, V. 43, No. 7 © (1947) p. 371; all rights reserved.

Table 9-45
Adiabatic Absorption of HCl Effect of Inert Gases

Operating Conditions		
Feed gas enters at equilibrium temperature at bottom of tower		
Make-up water enters at equilibrium temperature at top of tower		
Vent contains 0.1 wt. % HCl		
Theoretical Plates	Weight % in HCl in Product	
	10 Mol % HCl Feed	100 Mole % HCl Feed
2	26.5	20.5
4	32.0	30.5
6	33.8	32.8
10	34.7	34.0
∞	35.0	34.6

By permission; Oldershaw, C. F., Simenson, L., Brown, T., and Radcliffe, F. *Trans. Sect. Chem. Eng. Prog.*, 43, No. 7, p. 371 © (1947), all rights reserved.

In general about 18 ft of 1-in. Karbate® or other acid resistant Raschig rings will satisfactorily absorb HCl from a gas stream up to 100% and produce 32% HCl acid.

Figure 9-88 illustrates a falling film type absorber using water jacketed tubes in the cooler-absorber. The tails tower removes last traces of HCl in the vents. Figure 9-89 is a preliminary selection chart for this type of unit.

Distillation in Packed Towers

Packed towers are used in some distillation operations in preference to plate towers. Usually the selection requires an understanding of the fouling characteristics of fluids of the system. These towers have been used even in polymer forming operations. However, other contacting devices can be cleaned easier. For some processes the packed tower is much more effective as well as cheaper than a tray tower.

The more complicated separation for a three phase system is discussed by Harrison [134].

Height Equivalent to a Theoretical Plate (HETP)

Distillation operations can best be expressed in terms of equilibrium relations and theoretical plates. Therefore, one of the correlating factors for various packings is the height of packing equivalent to a theoretical plate for the separation. Data for effectively using this concept is extremely meager and apparently contains many uncertainties as far as general application is concerned. For this reason the use of HETP is not popular. When good correlations are developed to predict HETP without test data, then this can be an effective means of expressing packing heights in distillation. Most HETP data has been obtained

COOLER ABSORBER DIMENSIONS										
NO. OF TUBES	A OD	B	C	D	E	F	G ID	H PIPE ID	J ID	K ID
31	12 ³ / ₄	9	10 ¹ / ₂	9 ² / ₄	12	7	4	2	2	1
38	14	10	12	9 ¹ / ₄	13 ¹ / ₂	7 ¹ / ₂	4	3	3	1 ¹ / ₂
55	16	10	13 ¹ / ₂	8 ⁹ / ₄	15	7 ¹ / ₂	4	3	4	1 ¹ / ₂
74	18	10	14	8 ⁹ / ₄	15 ¹ / ₂	7 ¹ / ₂	4	3	4	1 ¹ / ₂
92	20	12	14 ³ / ₄	8 ⁹ / ₄	16 ¹ / ₂	8 ¹ / ₂	6	4	4	2
121	22	14	16 ¹ / ₂	8 ⁶ / ₄	19 ¹ / ₂	10	8	6	6	2
151	24	15	17 ³ / ₄	8 ⁶ / ₄	20	10	8	6	6	3
170	26	16	18 ¹ / ₄	8 ⁶ / ₄	20 ¹ / ₂	10	10	6	6	3
206	28	16	20 ¹ / ₄	8 ³ / ₄	22 ¹ / ₂	10	10	6	8	3
241	30	19	21	8 ³ / ₄	23 ¹ / ₂	11	12	8	8	4

TAILS TOWER DIMENSIONS							
TOWER SIZE ID	M OD	P	Q	R	S	T ID	U ID
8	9 ³ / ₄	21 ¹ / ₄	20 ⁷ / ₈	13 ³ / ₄	10 ⁷ / ₈	2 ¹ / ₂	1
10	13	22	21 ³ / ₈	14	10 ⁷ / ₈	3	1
12	15 ¹ / ₂	23	21 ⁵ / ₈	17	11 ¹ / ₈	4	2
16	19 ¹ / ₂	24	21 ⁵ / ₈	18	11 ⁵ / ₈	4	2
19	23 ¹ / ₂	30	27 ¹ / ₈	22	14 ³ / ₈	6	3
24	29	31	28 ¹ / ₈	22	15 ⁵ / ₈	8	4

For certain conditions, exchangers can be furnished with 12-foot long tubes. See selection chart.

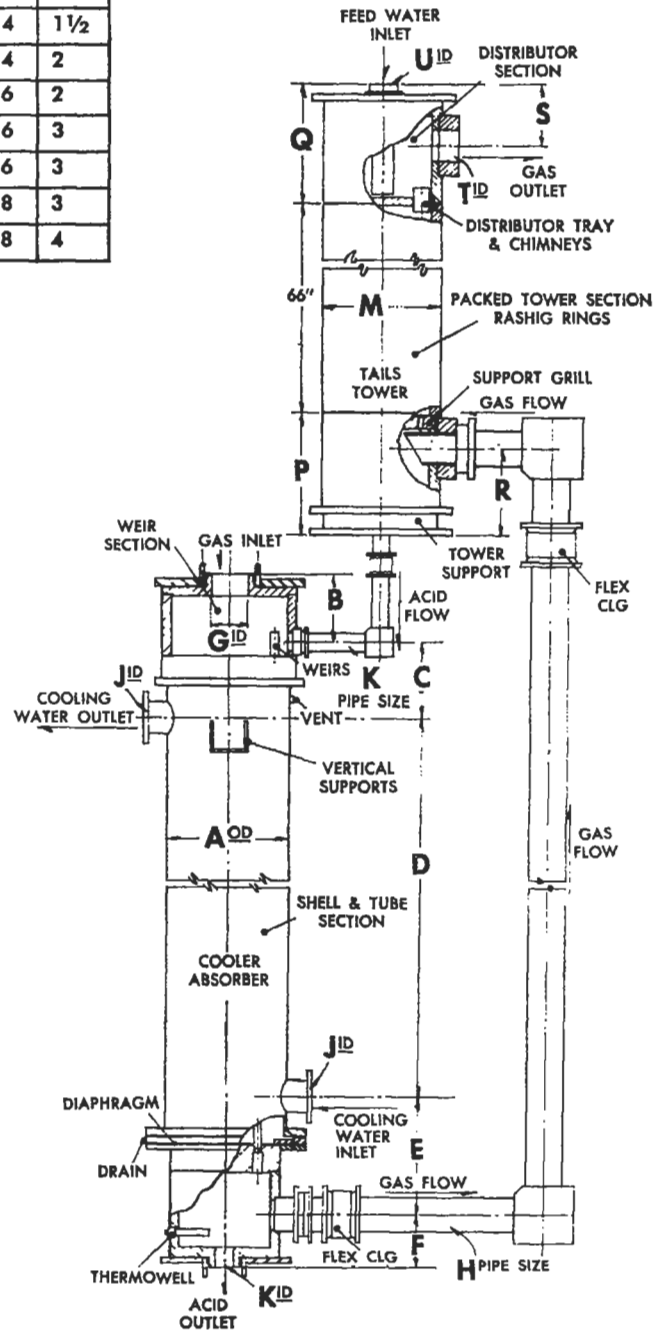
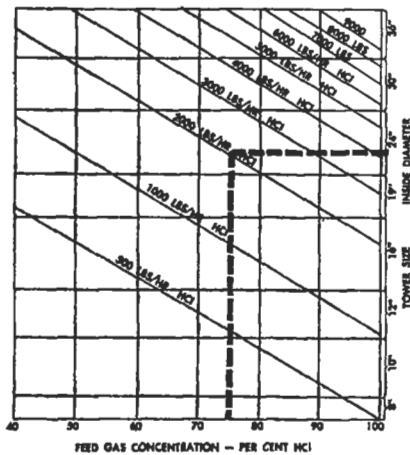
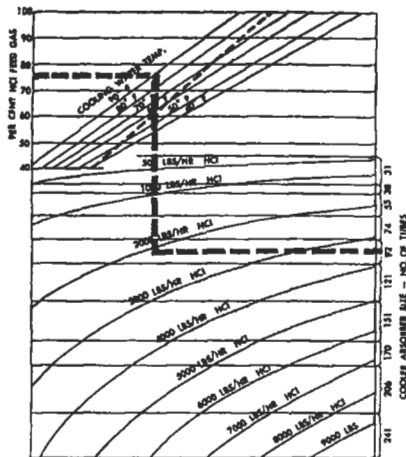


Figure 9-88. Graphite type HCl absorption tower. Used by permission of Falls Industries, Inc.

TAILS TOWER SELECTION CHART



COOLER ABSORBER SELECTION CHART



To select correct size tails tower and cooler absorber, to meet your specific requirements, follow the dotted line in the two charts. For example, using a 75% concentration of feed gas, 90° cooling water, and absorbing 2,000 lbs./hr. HCl; a 92 tube cooler absorber would be required in conjunction with a 24" diameter tower. To produce acid over 20° Be to 22° Be, use 12-foot long tubes in all instances where cooling water temperature falls to left of black dotted line in cooler absorber selection chart. Use 9-foot long tubes where temperature point is to the right of the dotted line.

Figure 9-89. Preliminary selection charts for HCl towers. Used by permission of Falls Industries, Inc.

on small diameter (often laboratory size) columns using very small packing, and operated at essentially total reflux, or on moderate sized columns, but with limited systems. The scale-up of such data to industrial sizes is questionable. When the designer does not have actual data from similar services (often broad classes of similarity may have to be assumed to arrive at what might be termed a reasonable and safe value for HETP), then it can be helpful to contact manufacturer's technical service departments for their recommendations (which they normally will

develop from application files). Keep in mind that the HETP is also unique to the packing size and configuration; therefore values obtained for one packing definitely do not accurately apply to another size or type. There is a rough relation, recognizing that the large size packing requires greater HETP than small size, but pressure drop is greater for the small packing.

There can be a significant difference between the conventional "particle" packing as represented in most of the illustrations of Figure(s) 9-6, and the HETP values for most of the structured packing in Figure(s) 9-6V-6OO and 9-6YFF. These later types (structured packing) offer HETP values varying from about 5 in. to 14 in., which are lower (greater efficiency) than the random particles at a minimum of 12 in. to as much as 36 in. Plots of HETP values for various packings have been presented in previous charts and discussions in this chapter.

Due to the unique HETP characteristics, it is important to consult the manufacturer on the specific system involved and operating conditions. Care must be exercised in selecting these or any other type of packing since plugging with suspended solids, polymer formation on surfaces, and similar mechanical problems can influence performance and life of the packing system.

Many correlations for HETP have been limited to Raschig rings or Berl saddles [25] both being the least efficient for mass transfer and pressure drop when compared to the more sophisticated designs represented in Figure 9-6. The guidelines given in a later paragraph are adequate for most of these applications.

Cornell, Knapp, and Fair [12, 13, 14] proposed the use of the transfer-unit concept for distillation, where:

$$H_{og} = H_g + m \left(\frac{G}{L} \right) H_l \quad (9-110)$$

where H_{og} = height of overall gas-phase transfer unit, ft
 H_g = height of gas phase transfer unit, ft
 H_l = height of a liquid-phase transfer unit, ft
 m = slope of equilibrium curve
 G = lb-mols gas/hour/ft²
 L = lb-mols liquid/hour/ft²

$$H_l = \phi C_p \left(\frac{\mu_1}{\rho_1 D_1} \right)^{0.5} \left(\frac{Z}{10} \right)^{0.15}$$

where ϕ = correlation from Figures 9-90 and 9-91 for a given packing
 C_p = correction factor for high gas rates, from Figure 9-92
 μ_1 = liquid viscosity, lb/ft (hr)
 ρ_1 = liquid density, lb/ft³
 D_1 = liquid-diffusion coefficient, ft²/hr
 Z = height of packing, ft

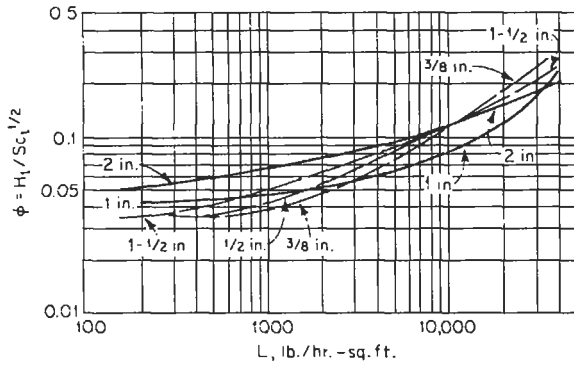


Figure 9-90. H_1 correlation for various sizes of Raschig rings, $Sc =$ Schmidt No. (N_{Sc}). Reproduced by permission of the American Institute of Chemical Engineers, Cornell, et al., *Chemical Engineering Progress*, V. 56, No. 8 © (1960) p. 68; all rights reserved.

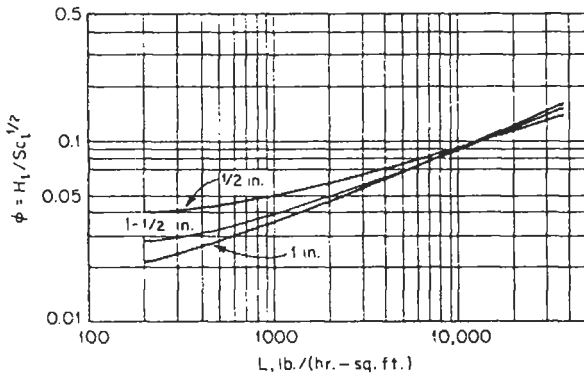


Figure 9-91. H_1 correlation for various sizes of Berl saddles. Reproduced by permission of the American Institute of Chemical Engineers, Cornell, et al., *Chemical Engineering Progress*, V. 56, No. 8 © (1960) p. 68; all rights reserved.

For Raschig Rings:

$$H_g = \frac{\psi S_{cg}^{0.5}}{(L_1 f_2 f_3)^{0.6}} \left(\frac{D}{12}\right)^{1.24} \left(\frac{Z}{10}\right)^{1/3} \quad (9-111)$$

For Berl Saddles:

$$H_g = \frac{\psi S_{cg}^{0.5}}{(L_1 f_2 f_3)^{0.5}} \left(\frac{D}{12}\right)^{1.11} \left(\frac{Z}{10}\right)^{1/3} \quad (9-112)$$

where $\psi =$ parameter for a given packing, from Figures 9-93 and 94

$S_{cg} =$ gas-phase Schmidt Number $= \mu_g / \rho_g D_g$

$\mu_g =$ gas viscosity, lb/ft (hr)

$\rho_g =$ gas density, lb/ft³

$D_g =$ gaseous diffusion coefficient, ft²/hr

$D =$ column diameter, in.

$Z =$ packed height, ft

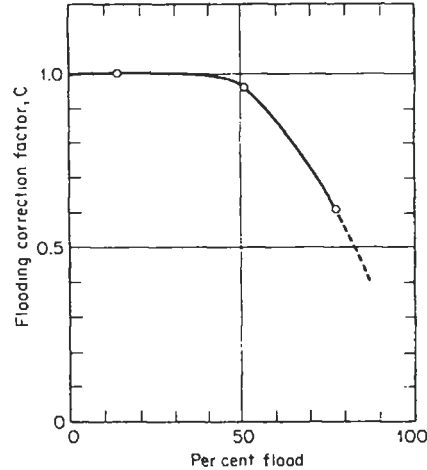


Figure 9-92. Liquid film correction factor for operation at high percent of flood. Reproduced by permission of the American Institute of Chemical Engineers, Cornell, et al., *Chemical Engineering Progress*, V. 56, No. 8 © (1960) p. 68; all rights reserved.

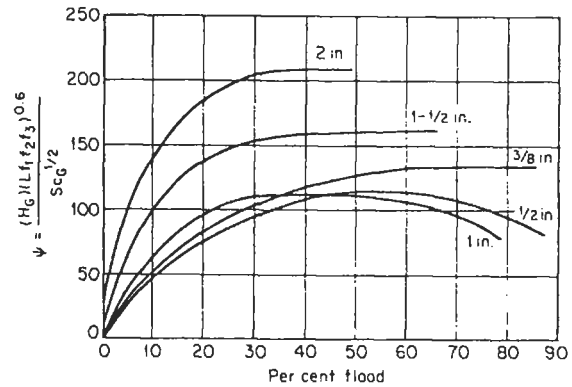


Figure 9-93. H_g correlation for various sizes of Raschig rings. Reproduced by permission of the American Institute of Chemical Engineers, Cornell, et al., *Chemical Engineering Progress*, V. 56, No. 8 © (1960) p. 68; all rights reserved.

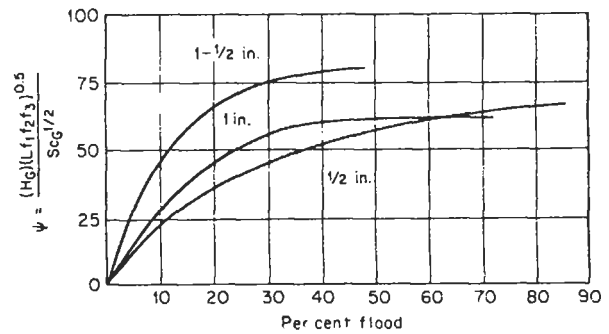


Figure 9-94. H_g correlation for various sizes of Berl saddles. Reproduced by permission of the American Institute of Chemical Engineers, Cornell, et al., *Chemical Engineering Progress*, V. 56, No. 8 © (1960) p. 68; all rights reserved.

$$f_1 = (\rho_1 / 2.42)^{0.16}$$

$$f_2 = (62.4 / \rho_1)^{1.25}$$

$$f_3 = (72.8 / \sigma)^{0.8}$$

μ_1 = liquid viscosity, lb/ft (hr)

ρ_1 = liquid density, lb/ft³

σ = surface tension, dynes/cm

In Reference 14, the authors modified the equations for H_g and H_1 as follows: (a) eliminate column diameter correction above 24 in. and (b) columns with *good* liquid distribution probably can allow elimination of the packing height correction.

Two separate investigators have evaluated the various correlation methods, and reported the Cornell, et al. method is significantly better than others. These were 1- and 2-in. metal Pall rings and 1-in. ceramic Intalox saddles [24] and 3/4-, 1 1/2-, and 3-in. Raschig rings [68].

Whitt [80] has correlated literature data of commercial size Raschig ring packing as shown in Figure 9-95. The range of plotted data is indicated, and the suggested design lines are good medians. The HTU values are for gas film controlling absorption systems, and the HETP data are for distillations at 760 mm Hg and below. These values should be usable for most pressure systems. The viscosity of the liquid ranged 0.35 to 1.0 centipoises. The equation for the HETP line is [34]:

$$\text{HETP} = 32 / \left(\frac{L'}{d_o \mu} \right)^{0.5} \quad (9-113)$$

and for HTU_G

$$\text{HTU}_G = 36 / \left(\frac{L'}{d_o \mu} \right)^{0.5} \quad (9-114)$$

In general, for the same liquid and vapor rates the HETP and HTU values for Berl saddles and others with a/ϵ^3 lower than Raschig rings should be lower. Correlating data is not available, except tests of Teller [71] which indicate 1-in. Berl saddles have HETP values 0.75 as compared to 0.85 for 1-in. Raschig rings.

The accuracy of establishing HETP values for new conditions in the same packing referenced to known values as suggested by Planovski [57] has not been tested by other literature references.

$$(\text{HETP})_{\text{new}} = (\text{HETP})_{\text{known}} P^* G_{\text{new}} / P_{\text{new}} G^* \quad (9-115)$$

*represents known conditions

P = system pressure, absolute

The operation of packed towers under vacuum conditions is not well defined in the literature. However, the work of Hands and Whitt [33] specifically evaluates several systems operating from 20 to 760 mm Hg abs. Their recommended limiting vapor velocity is

$$V_g = 0.065 (\rho_L / \rho_G)^{0.5}, \text{ ft/sec} \quad (9-116)$$

or

$$L_m = 0.334 (\text{Pressure, mm Hg. abs})^{0.5} \quad (9-117)$$

Operating values are recommended to be two-thirds of the limiting values. From the data it appears that entrainment (internal may be more significant than external) becomes a limiting factor before the flooding values predicted by Figure 9-21C or D.

Eckert [121, 122] and others have examined data and presented considerable tabulations of HETP and HTU val-

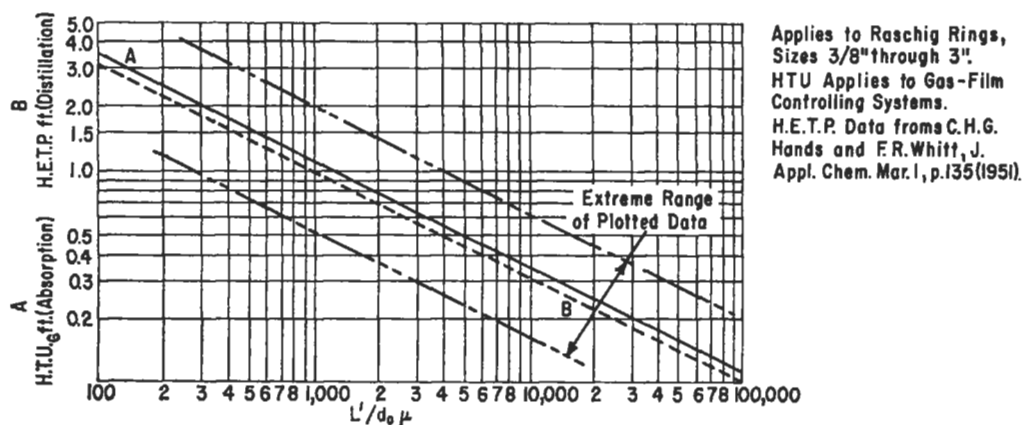


Figure 9-95. HETP and HTU correlation for tower random packings. Used by permission of Whitt, F. R., *British Chemical Engineering*, July (1955) p. 365; all rights reserved.

ues for random packing in various organic-water, polar organic, and hydrocarbon systems. Some of these are obsolete as of this publishing date due to the older type/style packing tested; however, the results still have value as a base reference and a recognition that the newer types/styles currently are more efficient, giving lower HETP and HTU values (the structured packing are discussed in a separate section of this chapter).

HETP Guide Lines

For industrial process equipment some general guide lines in this undefined area are (for particle packing)

1. Never use HETP less than 12 in. if tower is 12 in. dia. or larger; for general assumption, use HETP = 1.5 to 2.0 ft.
2. Use HETP = H_{OG} or H_{OL} if other data not available
3. Use HETP = Column diameter (over 12 in. dia.) if no other information available, up to 48 in. dia.

HETP values appear to vary somewhat within the process system of the distillation, while certainly varying with the size and style of packing. In general the larger, more open packing designs exhibit higher HETP values; while the smaller particle type packing and the compact styles exhibit significantly lower values for the same system. A brief guide to recent published values for various systems can be helpful in establishing the right order of magnitude for a system in design.

Kister [90] has tabulated published HETP data for a wide variety of process systems and proposes that using good experimental data to interpret for other systems can be just as effective (accurate) as calculated values using most mass transfer techniques.

Influences on HETP Values

Various authors [90] and researchers have published factors that influence the magnitude of HETP values. The lower the HETP value (i.e., number of feet (or inches) per theoretical plate/tray/stage) the more efficient is the packing (random or structured) for any particular separation system. Other influences include:

1. Packing surface area/unit packing volume increases resulting in more efficient packing performance (lower HETP). For structured packing the more narrow passage-way between sheet components results in more efficient performance [90].
2. Uniformity of packing surface on a specific random element of packing [90].

3. Uniformity of liquid (vapor) distribution increases packing performance efficiency.
4. Liquid and vapor loadings have little effect on HETP for random packing up to the point between loading and flooding.
5. For structured packings as loadings increase, HETP increases, and is more pronounced for wire-mesh types, and the effect is less for the corrugated sheet packings [90].
6. Pressures above 1 to 2 psia have small effects on HETP for random and structured packing. For high vacuum the data are not totally firm as to the consistency of effects, generally HETP increases (efficiency becomes lower). At high pressure above 200–300 psia structured packing HETP increases (lower efficiency) [90].

Transfer Unit

The transfer unit concept is also applicable to distillation in packed towers. Height of the packing required is:

$$Z = N_{OG} H_{OG} \quad (9-118)$$

For usual applications is rectifying where the number of transfer units N_{OG} is:

$$N_{OG} = \int_{y_1}^{y_2} \frac{dy}{y^* - y} \quad (9-119)$$

for stripping, usually:

$$Z = N_{OL} H_{OL} \quad (9-120)$$

The height of the transfer unit has not been satisfactorily correlated for application to a wide variety of systems. If pilot plant or other acceptable data are available to represent the system, then the height of packing can be safely scaled-up to commercial units. If such data are not available, rough approximations may be made by determining H_G and H_L as for absorption and combining to obtain an H_{OG} (Ref. 74, pg. 330). This is only very approximate. In fact it is because of the lack of any volume of data on commercial units that many potential applications of packed towers are designed as tray towers.

$$N_{OL} = \int_{x_1}^{x_2} \frac{dx}{x - x^*} \text{ for liquid concentration gradients } (9-121)$$

Based on the two resistance theory [127]

$$(HTU)_{OG} = (HTU)_G + (HTU)_L \quad (9-122)$$

If over a single stage, the equilibrium curve and the operating lines are assumed straight, then [127]:

$$\text{HETP} = (\text{HTU})_{\text{OG}} (\ln \lambda) / (\lambda - 1); \text{ for } \lambda \neq 1.0 \quad (9-123)$$

$$\text{HETP} = (\text{HTU})_{\text{OG}}; \text{ for } \lambda = 1.0 \quad (9-124)$$

L_M/G_M is the internal reflux ratio that is the slope of the operating line either in the rectifying or stripping sections. The value of L_M/G_M usually will not vary significantly from 1.0. $\lambda = mG_M/L_M$ is the ratio of the two slopes and remains close to 1.0 for different separation systems [127]. For these conditions $\text{HETP} \approx (\text{HTU})_{\text{OG}}$ and HETP becomes an important design variable. For $\alpha \gg 1.0$ for easy separations and λ is less than or much greater than 1.0. The authors cite the practical importance of their findings as. See Figures 9-96 and 9-97, which illustrate the effect on HETP of under-irrigating the bed by the distributor.

A minimum HETP or HTU represents a maximum separation efficiency with α representing the relative volatility, i.e., vapor and liquid phase compositions of the more volatile component in a binary system:

$$y = \alpha x [1 + (\alpha - 1)x]$$

The following examples are presented here by permission of the authors [127] and *Hydrocarbon Processing*:

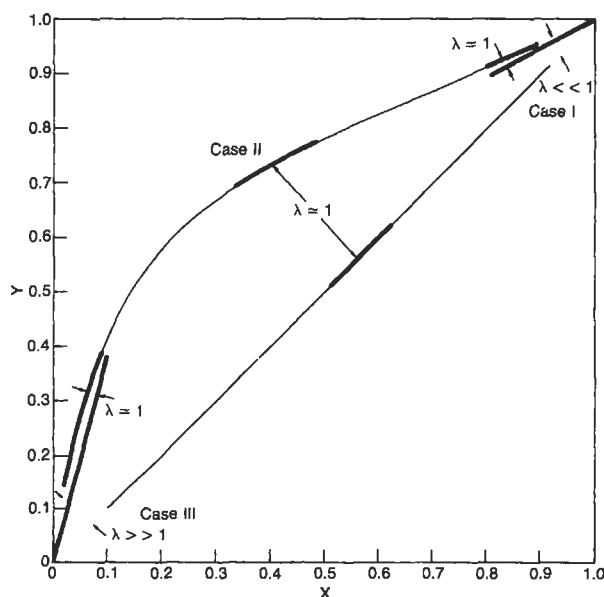


Figure 9-96. Vapor-liquid equilibrium showing λ and application cases referred to in the text. Used by permission, Koshy, T. D., and Rukovena, F. Jr., *Hydrocarbon Processing* V. 65, No. 5 (1986) p. 64; all rights reserved.

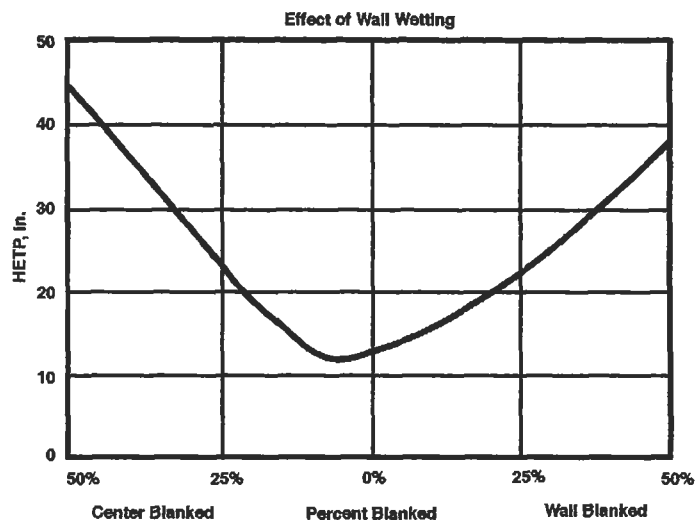


Figure 9-97. Effect of under-irrigating the wall area of a column using random packing. Note: % blanked refers to packing cross-sectional area not irrigated. At 0% blanked the best HETP is found. To the right of 0 towards the wall (50% blanked) the HETP becomes poorer until the wall is reached. For the center section (to the left) of the tower from the 0% to 50% of the center area of tower area blanked, the poorer HETP is again found. Reproduced by permission of the American Institute of Chemical Engineers, *Chemical Engineering Progress* Bonilla, J. A., V. 89, No. 3 (1993) p. 47; and by special permission of Fractionation Research, Inc.; all rights reserved.

Case I: γ is much less than 1. The circumstances when this happens are [127]:

- High purity of the more volatile component, i.e., $m \rightarrow 1/\alpha$.
- High reflux ratio, i.e., $L_M/G_M \rightarrow 1.0$.
- Both foregoing conditions mean $\lambda \rightarrow 1/\alpha$.

Case II. $\lambda = 1$. The following situations will produce this condition [127]:

- Very low reflux ratio for high purity rectification, i.e., $x \rightarrow 1.0$.
- Very high reflux ratio for high purity stripping, i.e., $x \rightarrow 0$.
- Total reflux for a symmetric separation. Note, the term "symmetric separation" is used here to mean that on a McCabe-Thiele diagram, the liquid phase compositions of the overhead product and bottom product are roughly equidistant from 0.5.

Case III. λ is much greater than 1. The circumstances when this occurs are [127]:

- High purity of bottoms products, i.e., $x \rightarrow 0$ and $m \rightarrow \alpha$
- Low L/V approaching total reflux, i.e., $L/V \rightarrow 1.0$
- Both foregoing conditions mean that $\lambda \rightarrow \alpha$.

where G_M = gas flow rate, kg-mols/hr, or lb mols/hr
 HETP = height equivalent to a theoretical plate, m, or ft
 HTU = height of a transfer unit, m or ft
 L_M = liquid rate, kg-mols/h, or lb mols/hr
 m = slope of the equilibrium line
 x = mol fraction of the more volatile component in the liquid phase
 y = mol fraction of the more volatile component in the vapor phase

Greek symbols

α = relative volatility between components 1 and 2
 $\lambda = m G_M / L_M$, ratio of the slopes of equilibrium and operating lines

Subscripts

G = gas phase
 L = liquid phase
 OG = overall gas phase

Packed column performance can use either the HETP or HTU concepts, the HTU is somewhat more complicated but no more correct than the HETP concept. The latter adapts itself to direct use from tray-by-tray digital computer calculations, and is thereby a little more direct.

The packed column has been quite useful in distillation, stripping, and absorptions processes and has become competitive with many types of distillation tray designs or types/styles.

Bolles and Fair [129] present an analysis of considerable data in developing a mass-transfer model for packed tower design; however, there is too much detail to present here.

Example 9-14: Transfer Units in Distillation

A benzene-toluene mixture is to be separated in a tower packed with 1-in. Berl saddles. The feed is 55.2 mol% (liquid feed, saturated), and an overhead of 90 mol% benzene, and bottoms of not more than 24 mol% benzene is desired. Using the data of Ref. 51 plotted in Figure 9-98, determine the number of transfer units in the rectifying and stripping sections using a reflux ratio (reflux to product, L/D) = 1.35.

Referring to Figure 9-98 for the graphical solution:

Rectifying section operating line slope =

$$\frac{R}{R+1} = \frac{1.35}{1.35+1} = 0.576$$

Note that point 7 can be determined by the intersection of the rectifying operating line and the feed condition line 8-7.

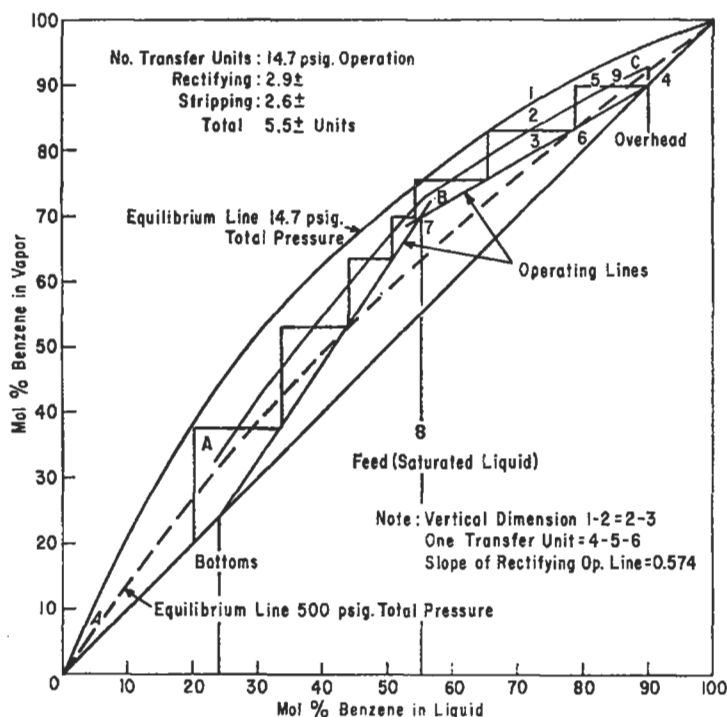


Figure 9-98. Vapor-liquid equilibrium (data only), benzene-toluene. Diagram notes for this text by this author. Reproduced by permission of the American Institute of Chemical Engineers, Griswold, J., Anders, D., and Klein, V. A., *Trans. A.I.Ch.E.* V. 39 © (1943) p. 223; all rights reserved.

Establish the location of the feed, bottoms and overhead compositions on the graph. Draw in the operating lines as for a distillation in a tray column.

To establish the transfer units draw in line A-B-C so that it is always half-way vertically between the equilibrium line and the operating line, making dimension 1-2 equal to 2-3. Begin drawing the transfer units at the overhead product 4, such that 4-9 equals 9-5, then drop vertically to the operating line and repeat the process always making the line A-B-C bisect the horizontal portion of the step. At the feed point re-start the stepwise process if the transfer unit step does not terminate at the feed point 7.

For this example, the number of transfer units is:

Rectifying:	2.9±
Stripping:	2.6±
Total	5.5± units

The reboiler for the column is in addition to this; however, the bottoms were specified as being the inlet from the reboiler. For most purposes the reboiler can be considered one additional transfer unit.

Alternate

An alternate method to determining the number of transfer units is the graphical integration of $dy/(y^* - y)$. The procedure is basically the same as for absorbers, that is:

1. For assumed values of x (mol fraction of component under consideration in liquid) from bottoms to overhead, read values of y (vapor under operating conditions corresponding to x) and values of y^* (vapor in equilibrium with x) from the equilibrium line.

2. Calculate $1/(y^* - y)$ at each selected point, thus:

x	y^*	y	$y^* - y$	$1/(y^* - y)$
0.24	0.44	0.24	0.20	5.0
0.30	0.52	0.328	0.192	5.21

3. Plot y , from y bottoms to y overhead versus $1/(y^* - y)$. The position of y -feed can be noted on the graph, and the integration so arranged as to reveal the split between rectifying and stripping transfer units. The total number by this method should check closely with the graphical step-wise method.

Height of Transfer Unit

The height of a transfer unit for this system is not available, therefore it may be *roughly* approximated by the method of additive H_G and H_L which is questionable at best, or the approximation of 2 ft for HTU may be used. The latter is just about as reliable as the former.

Then: height of tower packing, using 1-in. Berl saddles:

From transfer unit = (2) (5.5) =	11 ft
Allowances: for top distribution:	<u>2</u> ft
Sub-total	13 ft
Extra, 20%	<u>2.5</u> ft
Total Z,	15.5 ft
	use 16 ft

The tower must be designed for throughput—diameter determined and pressure drop established.

Check Theoretical Plate Basis

To determine HETP by approximate method, see Table 9-46 for benzene-toluene:

HETP = 1.0 to 1.5 ft

Select HETP = 1.25 ft

Safety factor suggested = 2, in any case a value not less than 1.25

Therefore use:

HETP = 24 in. = 2 ft

From Figure 9-98 it is evident that the number of theoretical plates and number of transfer units are not the same. When stepped off, the number of theoretical plates is 6+.

Height of packing = (6) (2) = 12 ft
 Allowance for distribution = 2 ft
 Total = 14 ft
 Use: 14-ft packing, 1-in. Berl saddles.

Because the 16 ft of packing by the HTU method is larger, this would be the recommended safe height to use.

For comparison, note the relative increase in the number of transfer units if the operation were at a higher pressure as shown by the dotted line for 500 psig.

Strigle [139] discusses packed column efficiency (HETP) in considerable detail. Most of his published data refers to work of Norton Chemical Process Products Corp.

A Norton [139] correlation for modern, random dumped packings used for distillation up to 200 psia is (use high performance internal distributors and supports) from surface tension of 4 dynes/cm but less than 33, and liquid viscosity of at least 0.83 to 0.08 cps but not greater:

$$\ln \text{HETP} = n - 0.187 \ln \sigma + 0.213 \ln(\mu) \quad (9 - 125)$$

Values of n in the equation for selected specific packings are given in Table 9-47 for random packing and Table 9-48 for structured packing.

Strigle presents typical separation efficiency ranges for Intalox[®] metal tower packing, for systems with relative volatility not greater than 2.0.

Packing size	HETP (ft)
#25	1.2 to 1.6
#40	1.5 to 2.0
#50	1.8 to 2.4

where σ = surface tension, dynes/cm

μ = liquid viscosity, centipoise

n = constant for HETP Equation 9-125

The summary of HETP values of Vital [142] for various types and sizes of packings are believed to be referenced to typical industrial distributors for the liquid. This variation can influence the value of HETP in any tabulation; the effect of distributor design is discussed in an earlier section of this chapter. Porter and Jenkins [143] developed a model to improve the earlier models of Bolles and Fair from about 25% deviation to about a 95% confidence using a 20% factor of safety [139].

Strigle [139] recommends: (See reference for related details):

Table 9-46
HETP Estimates for Distillation Applications

(Contact manufacturers for specific design recommendations)

System	Pressure Range If Known	General Packing Type/Style/Make	Estimating HETP* Ft or In. Marked
Iso-Octane/Toluene	100mm Hg	Hy-Pak No. 2	2.0-2.7
Same	740mm Hg	Hy-Pak No. 1	0.7-2.7
Para/Ortho Xylene	740mm Hg	Metal Intalox No. 25	0.8-1.3
Same	740mm Hg	Metal Intalox No. 40	1.3-1.55
Same	740mm Hg	Metal Intalox No. 50	1.75-2.15
Chlorinated HC	Vacuum	Metal Intalox No. 25	2
Chlorinated HC	Vacuum	Metal Intalox No. 40	2.4
Chlorinated HC	Vacuum	Metal Intalox No. 50	3.5
Iso-Octane/Toluene	740mm Hg	Pall Ring, 1 in. Metal	1.0-2.0
Iso-Octane/Toluene	740mm Hg	Pall Ring, 1½ in. Metal	0.75-1.0 (3.5)**
Iso-Octane/Toluene	740mm Hg	Pall Ring, 2 in. Metal	1.5-2.2
Methanol/Water	740mm Hg	Pall Ring, 1 in. Metal	0.65-0.8 (1.2)**
Isopropanol/Water	740mm Hg	Pall Ring, 1 in. Metal	0.6-1.5
Benzene/Toluene	740mm Hg	Pall Ring, 1 in. Metal	1.0-1.5
Acetone/Water	740mm Hg	Pall Ring, 1 in. Metal	0.9-1.2 (1.4)**
Same	—	Flexirings, 1 in. Metal	1.6-1.8 (2.3)**
Same	—	Flexirings, 2 in. Metal	1.8-2.2 (2.4)**
Same	—	Koch Sulzer Metal	0.45-0.9
Light Hydrocarbon	400 psia	Goodloe Metal	approx. 0.75
Propane/Butane	235 psia	Goodloe Metal	approx. 0.80
Chlorobenzene/ethylbenzene	50mm Hg	Montz structured metal	5 in.-17 in.
Chlorohexane/n-Heptane	1 atm	#2 Nutter Ring	22 in.-30 in.
Chlorohexane/n-heptane	5 psia	#2 Nutter Ring	25 in.-30 in.
Various sys.	vacuum	Goodloe metal, various	5 in.-8 in.
Iso-Octane/toluene	1 atm	Cascade Mini-ring, #3	22 in.-28 in.
Iso-Octane/toluene	1 atm	Cascade Mini-ring, #2	18 in.-24 in.
h-naphtha/light gas oil	unknown	Gempak, ½ in. crimp	13 in.-15 in.
h-naphtha/light gas oil	unknown	Gempak, 1 in. crimp	22 in.-27 in.
h-naphtha/light gas oil	unknown	Gempak, ¼ in. crimp	8 in.-10 in.
Ethylene dichloride/benzene	1 atm	ACS-X Mesh	4 in.-9 in.
Methylcyclohexane/toluene	1 atm	ACS-X-200 Mesh	3.5 in.-12 in.
Unknown	unknown	Koch structured Flexipac	17 in.
General/Average	unknown	Koch/Sulzer (R) structured	3 in.-9 in.
Ortho/para-	16mm Hg abs	Koch/Sulzer (R) structured	5 in.-16 in.
Ortho/para-	100mm Hg abs	Koch/Sulzer (R) structured	4.5 in.-8 in.

*Based on industrial data or commercial sized tests, note some values in inches.

**At very low gas rates.

Data for table compiled from respective manufacturer's published literature.

- For easy separations (less than 10 theoretical stages) a 20% design safety factor can be applied to a typical HETP value.
- For separations of 15 to 25 theoretical stages a 16% design safety factor should be applied to the HETP.
- For very difficult separations, the design HETP should be carefully evaluated by calculation and actual data when available.
- HETP values for random dumped packing have been found to be 25% greater at a greater viscosity than a lower viscosity, i.e., viscosity change from 0.15 cps to 0.44 cps.

Cooling Water With Air

Wood or plastic filled towers for cooling water by using air are quite economical for certain heat loads and geo-

Table 9-47
Constant n for HETP Correlation*, Random Packing

Tower Packing	Value of n
#25 IMTP® Packing	1.13080
#40 IMTP® Packing	1.37030
#50 IMTP® Packing	1.56860
1 in. Pall Ring	1.13080
1½ in. Pall Ring	1.39510
2 in. Pall Ring	1.65840
1 in. Intalox® Saddle	1.13080
1½ in. Intalox® Saddle	1.41570
2 in. Intalox® Saddle	1.72330

*Use with Equation 9-125.

**IMTP and Intalox are registered names of Norton Chemical Process Products Corp.

Used by permission from Strigle, R. F., Jr., *Packed Tower Design and Applications: Random and Structured Packings*; 2nd Ed. Gulf Pub. Co. (1994).

Table 9-48
Constant n for HETP Correlation* for Intalox Structured Packing

Packing Size	Value of n
1T	0.76830
2T	1.01280
3T	1.38680

*Use with Equation 9-125.

**IMTP and Intalox are registered names of Norton Chemical Process Products Corp.

Used by permission from Strigle, R. F., Jr., *Packed Tower Design and Applications: Random and Structured Packings*; 2nd Ed. Gulf Pub. Co. (1994).

graphical locations. The costs of installation and operation must be compared with once-through water costs at any location to arrive at a proper understanding of the advisability of the installation. The four commercial tower types are:

Atmospheric

This tower depends upon the atmospheric wind to blow horizontally (or nearly so) through the tower (Figure 9-99). These towers must be relatively open areas to receive the available wind from any particular direction. Wind velocities of 4.5 to 6.5 mph are necessary for reasonable operation. The towers operate in cross-flow of wind to falling water and range from 30–55% effective. They are not capable of producing water at a temperature much closer than 4°F of the entering air wet-bulb temperature. They require no fan, but do consume power to pump the water to the (relatively high) top of the tower. Ground area requirements may be large.

The spray-filled tower, Figure 9-100, is also an atmospheric type, containing no fill other than the water sprays and no fans. The water-air contact comes about due to the spray distribution system [144]. This design is often used where higher water temperatures are allowed, and the situations where excessive contaminants building up in the water would cause fouling of other direct contact heat transfer surfaces.

Natural Draft

This tower depends upon natural draft action the same as a chimney to draw cool air in at the bottom and expel it out the top as warm moist air (Figure 9-101). The action of the tower depends upon the atmospheric temperature; therefore, on a hot day the action of the tower may be less than on a cool day. These towers are relatively large, and require power for pumping the water to a point in the tower which is usually lower than for an atmospheric tower. There are no fan costs. Units have been built 310 ft high, base diameter 210 ft and a throat of 120 ft, widening to 134 ft in diameter at the top [30].

Forced Draft

This type of tower uses fans at the base to force air through the tower fill or packing (Figure 9-102). Due to the relatively low outlet air velocity, there is a tendency for discharged hot air to recirculate into the fan intake and reduce tower performance. The fan handles only atmospheric air thereby reducing its corrosion problem when compared to the fan on an induced draft tower. The tower size for the forced as well as the induced draft unit is considerably less than for an atmospheric or natural draft unit due to the higher heat transfer rates.

Induced Draft

This tower uses fans at the top of the tower to draw air in the base of the tower through the fill and out the fan discharge (Figures 9-103–105). In this type of mechanical draft tower the hot moist air discharges vertically (usually) to the atmosphere with such a velocity as to eliminate the possibility of recirculation of this air in at the base of the tower. This moist air is corrosive to the fan parts and therefore requires protection of coated plastic or special metal blades and sealed motors and reduction gears.

General Construction

Most cooling towers are built of redwood or cypress. However, special conditions and atmospheres dictate other types of construction.

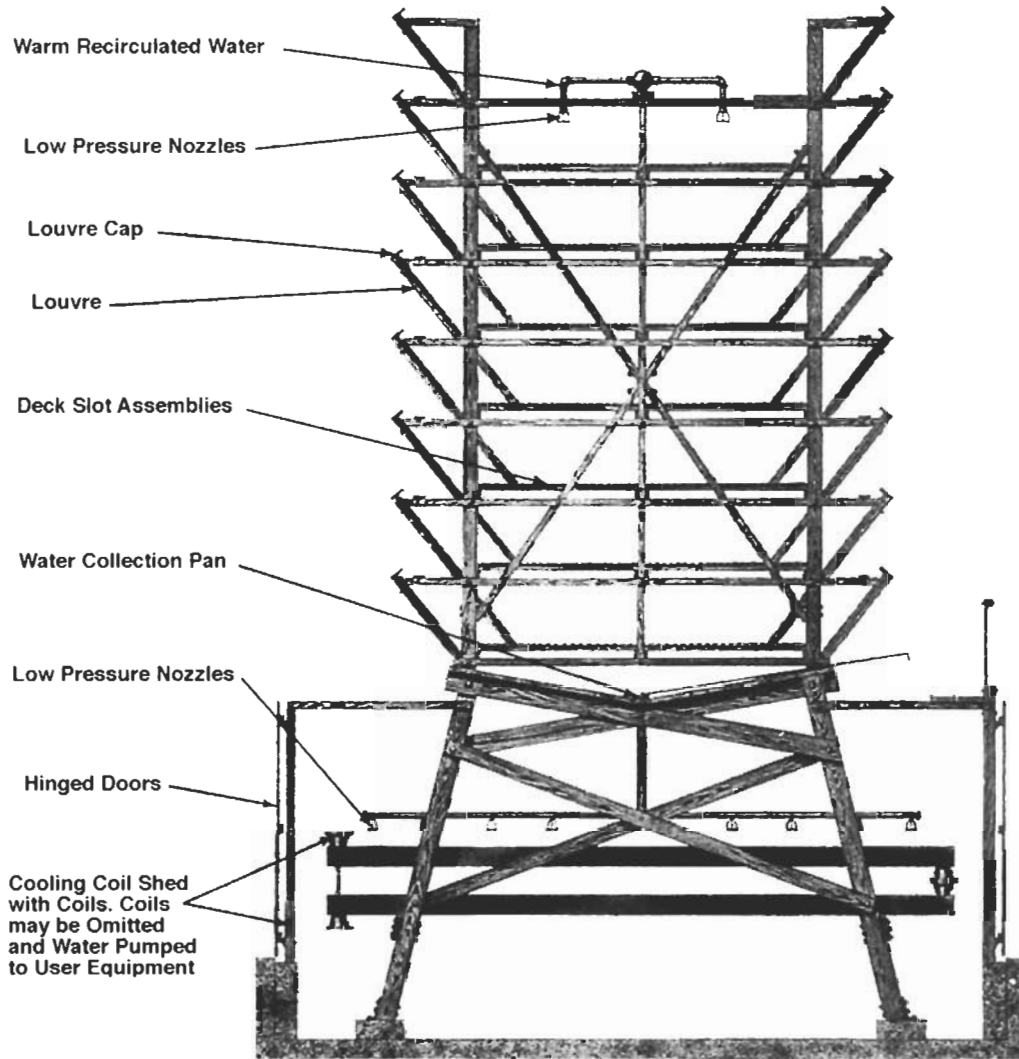


Figure 9-99. Atmospheric cooling tower. Used by permission of The Pritchard Corp. (now, Black and Veatch Pritchard).

Materials:

1. Framework
 - Heart redwood
 - Cypress
 - Galvanized steel
 - Brick or Concrete
2. Casing
 - Heart redwood
 - Cypress
 - Corrugated asbestos board, or some combination with redwood.
 - Brick or concrete block
3. Fill or Packing
 - Heart redwood
 - Cypress
 - Asbestos-cement boards or strips
 - Plastic sheet, grids or pieces
4. Drift Eliminators, same as 3.
5. Louvers, same as 3.
6. Miscellaneous Hardware
 - Monel, galvanized or other corrosion resistant metals
7. Fans and Drivers
 - Axial or propeller blade fans are either belt or gear driven. Some drivers are variable speed motors, and some fans have variable pitch blades. In special circumstances, steam turbine, gas or gasoline engine drivers are used. Gears should be carefully specified to avoid overload and should be specially sealed to prevent moisture entering the case.

Cooling Tower Terminology

Wet Bulb Temperature: the temperature of air at which it would saturate without a change in its heat content. It is

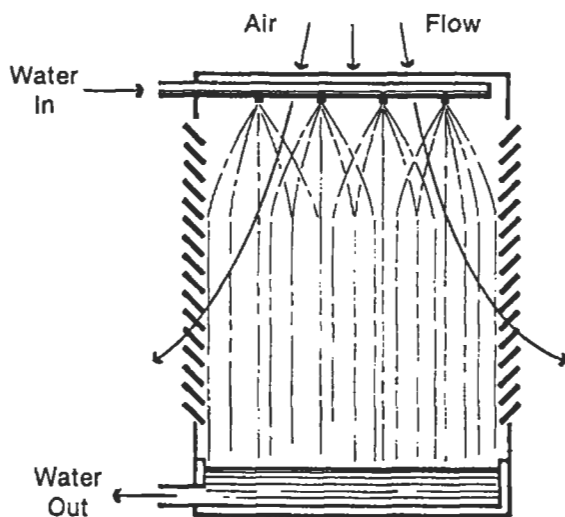


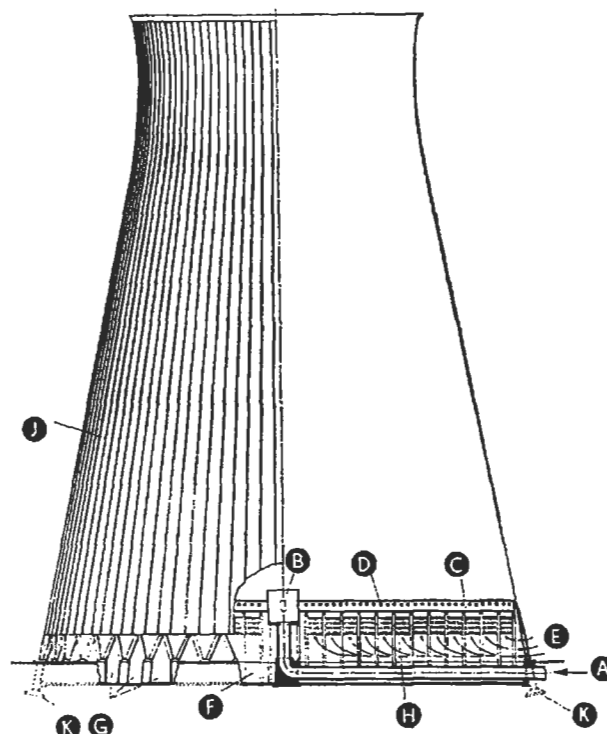
Figure 9-100. Atmospheric spray tower, air flow aspirated by pressure-spray water distribution system. Usually applied in small sizes. Used by permission of Hensley, John C. (ed), *Cooling Tower Fundamentals*, 2nd Ed. (1985), The Marley Cooling Tower Co., a United Dominion Company.

the theoretical minimum temperature to which water may be cooled in a cooling tower. However, in actuality this temperature can never be reached, but only approached. The selection of the proper wet bulb temperature is very critical, because it is the single most important factor in tower rating. The selected temperature should be high enough to include 95% of the maximum readings recorded during the time most critical or important in the cooling service.

If the temperature is too high, an expensive tower will be specified; and of course, if too low, the cooling load service will be required to sacrifice performance during the times when the wet bulb exceeds the specified value. At constant inlet humidity and constant rates for liquid, L' , and air, G' , the effect of changing wet bulb on the performance factor KaV/L' is only 1.2% with no trend dependent on rates [38].

Approach: the temperature difference between the tower cold water outlet temperature and the wet bulb temperature of the air. The smaller the approach the more difficult the cooling job, and the larger the required tower. For a fixed cold water temperature, changing the wet bulb temperature by one degree can make a significant difference in tower requirements. Usually an approach of 5°F is considered minimum.

Range: the temperature difference between the warm water into the tower and the cold water out. The range determines the heat load on the tower, which in turn reflects the requirements of the cooling water service. The



- A Hot water inlet main
- B Central Tank
- C Hot water channels
- D Asbestos distribution tubes
- E Air intake
- F Basin
- G Cold water outlet
- H Heat Exchanger
- J Tower Ribs
- K Foundation Footings

Figure 9-101. Component parts of modern natural draft tower. Used by permission of Hamon Cooling Towers, Inc.

average reduction in KaV/L' for each 10°F increase in hot water inlet temperature is 2% [38].

Drift Loss or Windage Loss: the amount of water lost from a tower as fine droplets entrained in the leaving air. For an atmospheric type tower this is usually 0.1–0.2% of the total water circulated. For mechanical draft towers it is usually less.

Make-up: the water required to be added to the system to make-up for losses by evaporation, drift loss, and blow-down.

Blow-down: the amount of water continuously or intermittently removed from the system to maintain a predetermined water analysis with respect to chemicals and dissolved gases. The build-up of solid or chemical

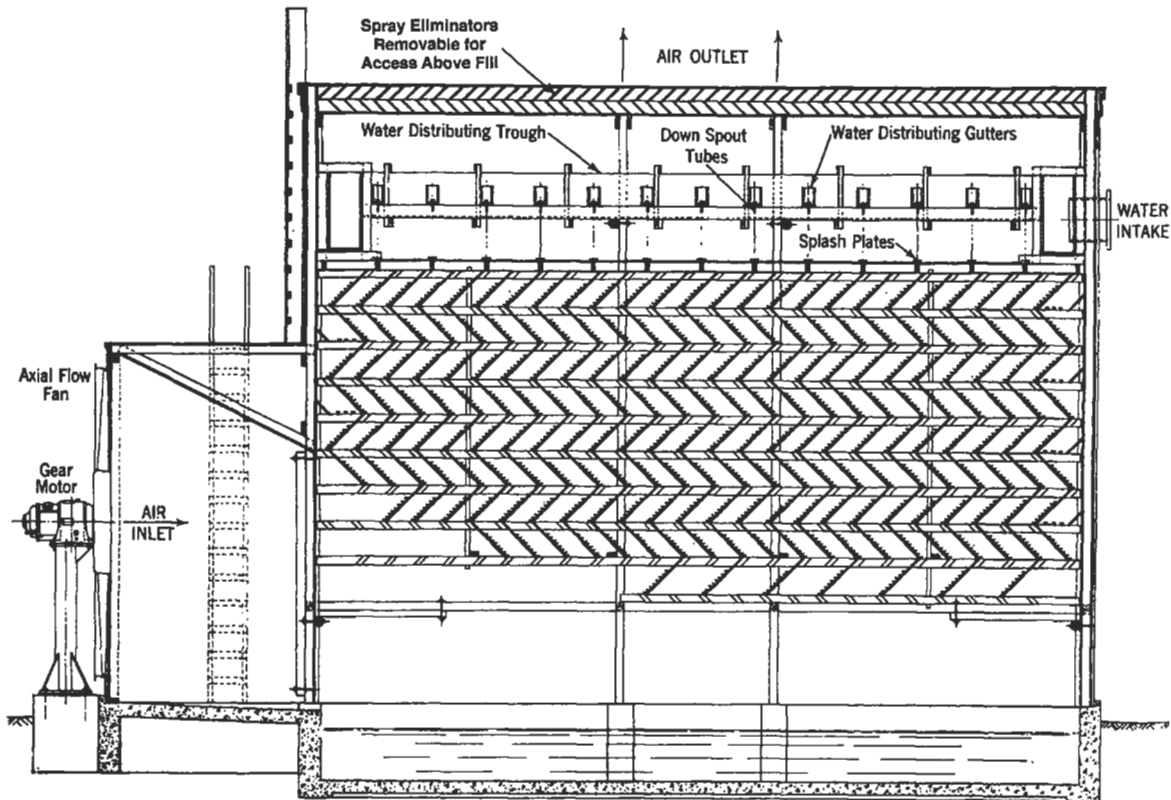


Figure 9-102. Cross-section of low-head forced-draft tower showing fan housing arrangement, filling, water distribution spray system and spray eliminators. Used by permission of Foster Wheeler Corp., Cooling Tower Dept.

concentration that will occur with continued evaporation and no blow-down can become very corrosive and harmful to metal and wood parts of the system. In addition, the deposition of salts on exposed surfaces and accumulation of sludge in the basin of the tower can influence performance as well as affect the life of the tower.

Recirculation: the portion of exit or outlet air from the tower that recirculates back to the inlet of the fresh air to the tower. To keep this low it is important to space towers away from each other as well as from any structures which can deflect the exit moist air back to the inlet. Due to recirculation the wet bulb temperature at the tower inlet may be different from that at a point 100 yards away. The recirculation of induced draft towers is usually less than forced draft due to the upward velocity of discharge of the air.

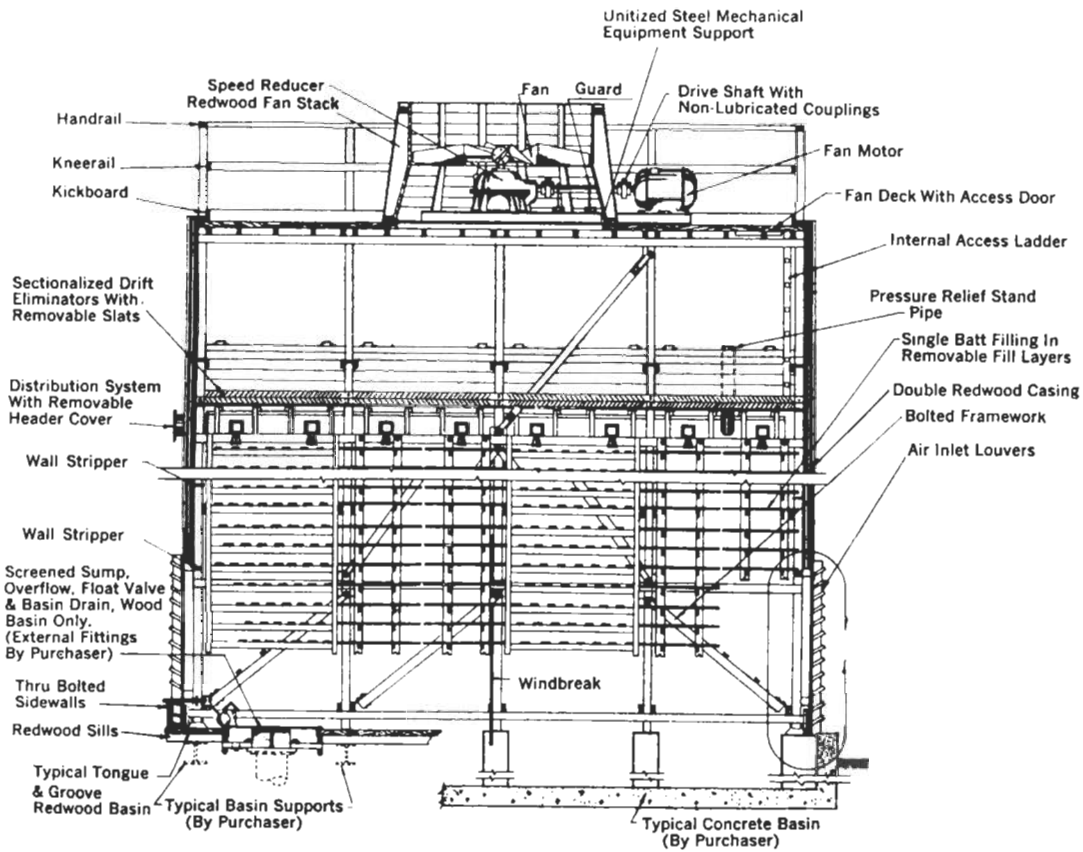
Normal recirculation in average installations for forced draft may run 3–10% of total inlet air, and 1–8% for induced draft towers, all depending upon the location and wind conditions during any day or season. Some towers can be arranged to have less than 1% recirculation. If conditions are suspected of being conducive to recirculation, it should definitely be allowed for in design of the tower. Recirculation increases the wet bulb temperature of entering air, increases the total air required (and hence size of

all equipment) in order to maintain a given tower performance.

Specifications

Specifications for performance rating are usually set by the process engineer with the rating selection performed by the cooling tower manufacturer. Each manufacturer has packing arrangements with known specific performance characteristics and has developed size modules for standard cells (usually 6 ft × 6 ft or 8 ft × 8 ft) together with the associated fan requirements. Some of this information is tabulated in general information form in the catalog literature. Specific economical ratings must consider the performance specified in light of the local application of the tower. To do otherwise can very often lead to excessive costs for this type of equipment. An informational specification sheet to be used by the process engineer is given in Figure 9-106.

Additional detailed information is available from the Cooling Tower Institute, including ATF-105 *Acceptance Test Procedure for Water-Cooling Towers*, STD-101 *CTI Grades of Redwood Lumber* [31], STD-102 'Structural Design Data' [70], and TSC-302 *Cooling Tower Wood Maintenance* [16].



Transverse Cross Section
One Fan per Cell

Figure 9-103A. Counterflow induced draft cooling tower. Used by permission of The Pritchard Corp. (now, Black and Veatch Pritchard).

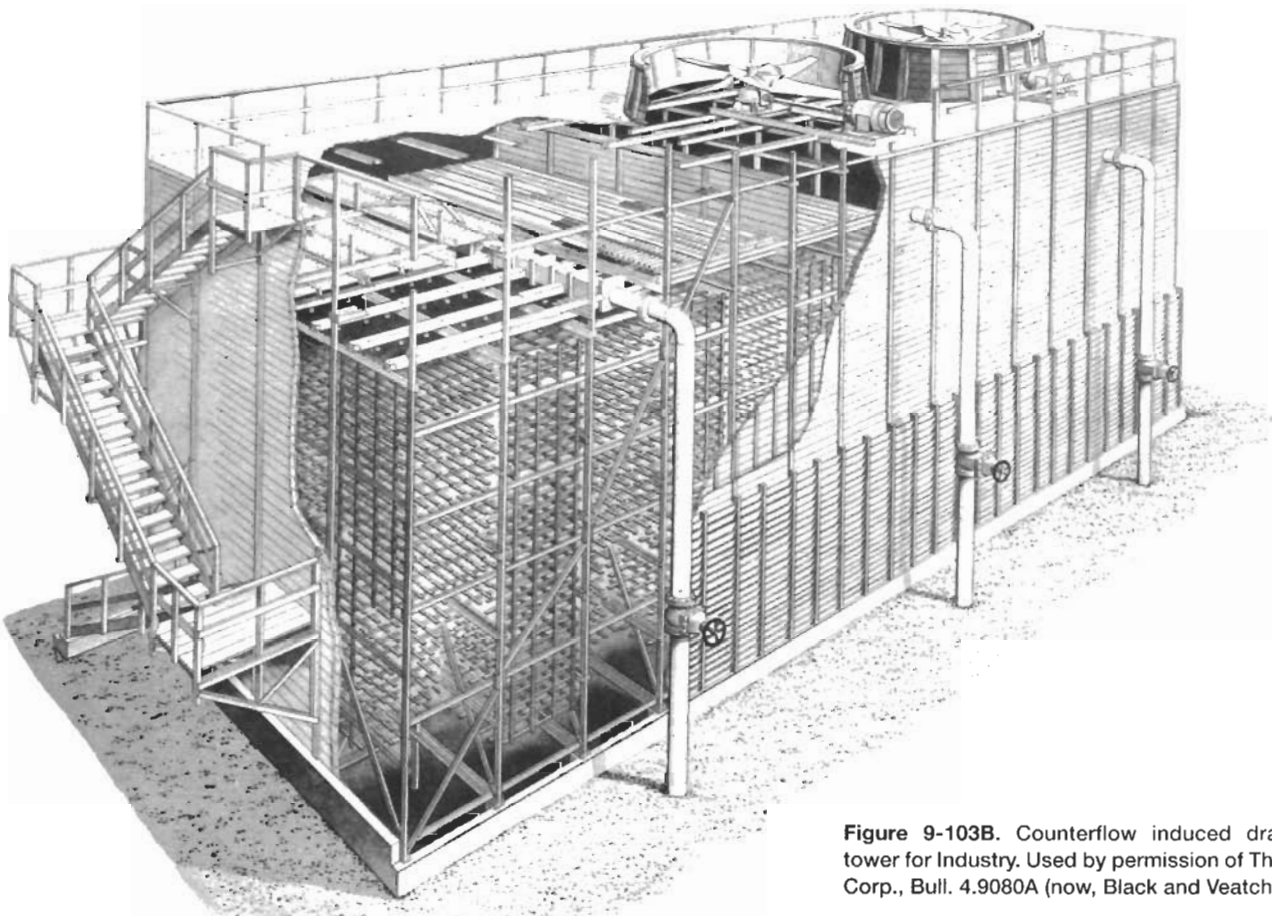


Figure 9-103B. Counterflow induced draft cooling tower for Industry. Used by permission of The Pritchard Corp., Bull. 4.9080A (now, Black and Veatch Pritchard).

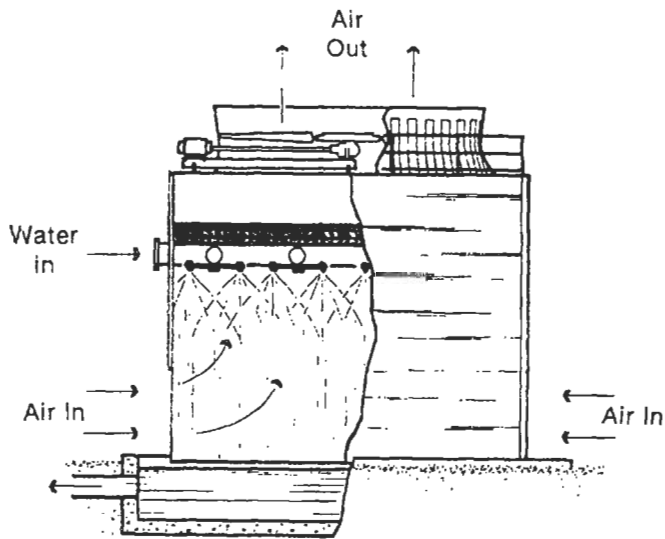


Figure 9-104. Spray-filled counterflow induced draft cooling tower. Used by permission of The Marley Cooling Tower, a United Dominion Co.

It is recommended that performance tests be specified and conducted in accordance with the Cooling Tower Institute procedure, as this gives the process engineer a standard of reference. Most cooling tower manufacturers are members of this Institute.

Manufacturer's bid proposals should include all of the information specified by the blanks on the specification sheet and in addition, details of construction, details regarding driver, gear, etc., and a guaranteed performance curve showing the effect of $\pm 10\%$ change in water quantity and lower wet bulb temperature, similar to Figure 9-107.

For rating by the manufacturer, the process engineer must specify and consider:

1. Water rate, gpm
2. Inlet water temperature, °F
3. Outlet cold water temperature, °F
4. Design wet bulb temperature, °F, for the location of construction of the tower.

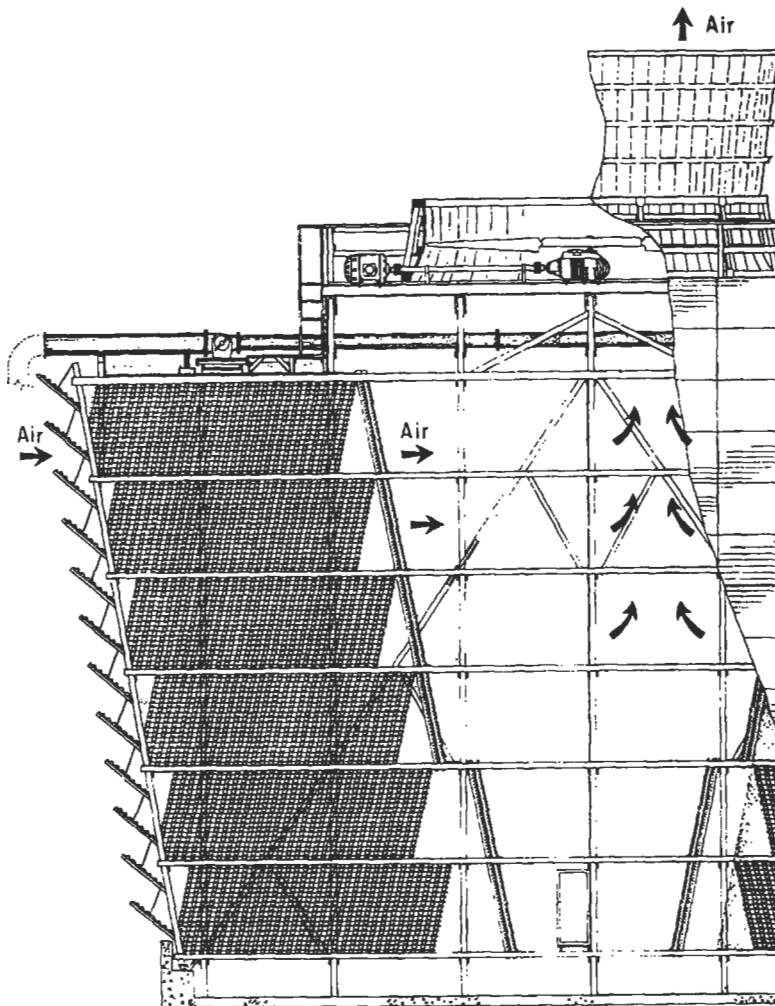


Figure 9-105. Cross-flow induced draft cooling tower. Used by permission of The Marley Cooling Tower, a United Dominion Co.

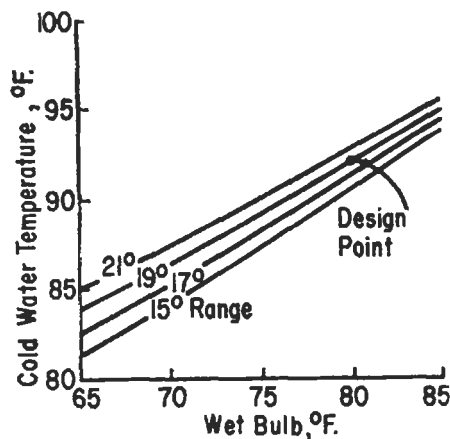


Figure 9-107. Typical performance for design gpm. Used by permission of Whitesell, J., *Chemical Engineering*, Jan. (1955) p. 187.

5. Water condition (sandy, oily, etc.) and type (river, canal, harbor, sea). The contaminating chemicals and/or minerals should be identified. Type of water treatment.
6. Drift loss or mist loss, usually maximum of 0.2% of design water flow rate.
7. External wind force or loading for standard design. Most designs are for 30 lb/ft², although specific geographical locations may require other specifications. Give minimum, and average wind velocities with compass direction for atmospheric and natural draft towers.
8. Geographical location; plant site location, general proximity to other structures and other factors relating to recirculation of exit air back to the inlet of the tower.
9. Type and specifications on fan driver, gear types, power voltage, phase, cycles. Motors should at least meet specifications equivalent to totally enclosed, fan cooled, or if in explosive hazardous area, TEFC Class I, Group D (except this not acceptable in hydrogen or acetylene atmosphere). Due to moisture conditions around this equipment, it should be protected against moisture penetration and corrosion.
10. Number, type, height, area requirements for cooling coils (if any) to be installed in tower basin by purchaser.
11. Power costs for fan and pump horsepower, approximate pump efficiency for water, and any special data peculiar to the economics of the installation. This will allow the manufacturer to select a tower giving consideration to the economic factors involved.
12. Items to be furnished by the purchaser, such as concrete basin, anchor bolts, electrical components,

external piping, material handling to job site. If the tower manufacturer is to perform a turn-key or package job, this should be specified, as in some instances the tower manufacturer may not be in a position to do this.

13. Fire protection if unit is to be allowed to stand dry for prolonged periods, or required by insurance.

Performance

The cooling tower cools hot water with cool air by counter-current (or cross-current) flow of the two fluids past each other in a tower filled with packing. This involves both mass and heat transfer. The water surface that exists on the tower packing is covered with an air film assumed to be saturated at the water temperature. The heat is transferred between this film and the main body of air by diffusion and convection. Detailed presentations of the development of cooling tower theory are given in References 39 and 46.

Figures 9-108 and 9-109 indicate the variables in tower performance. Also see Reference 150.

The packing or fill is arranged to prevent a droplet of water from falling the full height of the tower. As it falls it hits a packing member, splashes, forms a film, drops off and falls to hit the next packing member. The counter-current stream of air sweeps across these drops and films to effectively cool the water and humidify the air. As the water flows down through the tower its temperature may drop below the dry bulb temperature of the inlet air to the tower. It can never go below the inlet air wet bulb temperature, in fact, it just *approaches* this wet bulb. One of the controlling features in tower design and performance is how close these two temperatures, inlet air wet bulb and outlet water, are expected to operate. The driving force for the cooling is the difference in enthalpies of the film of air surrounding the water and that of the main body of the air.

The number of transfer units or tower characteristic is based on overall heat and mass transfer:

$$\int_{t_2}^{t_1} \frac{dt}{h' - h} = KaV/L' \quad (9-126)$$

where h' = enthalpy of saturated air film at bulk water temperature, Btu/lb

h = enthalpy of the main air stream, Btu/lb

t_1 = entering warm water temperature, °F, at top of tower

t_2 = outlet cool water temperature, °F, bottom of tower

t = bulk water temperature, °F

K = mass transfer coefficient, lb water/hr/ft²

a = contact area, ft²/ft³, tower volume

V = active cooling volume, ft²/ft³, of plan area

L' = water rate, lb/(hr) ft²

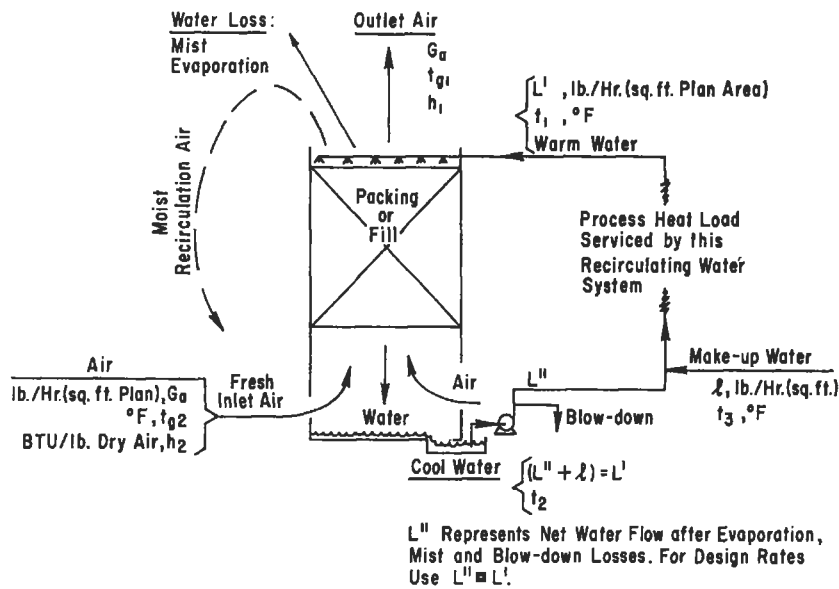


Figure 9-108. Diagram of counter current air-water cooling tower.

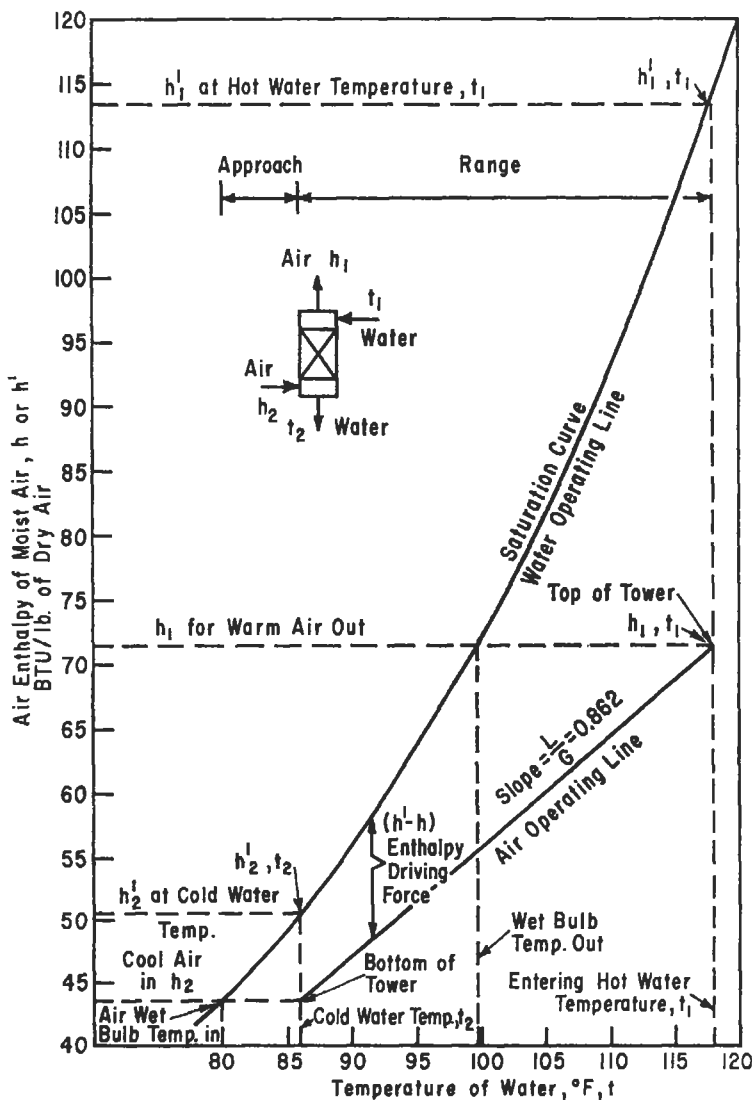


Figure 9-109. Driving force diagram for cooling tower.

Cooling tower data [15, 19, 46] has been plotted as KaV/L' vs. L'/G_a and indicates that the tower characteristic KaV/L' is a function of L'/G_a and not dependent on the value of G_a only, when using high voidage splash deck grid type packings. A few representative tower fill packings are shown in Figures 9-110A and B and performance characteristic values are shown in Figure 9-111. Figures 9-112 to 9-117 illustrate counterflow tower performance. The curves are satisfactory for close estimating, while exact data should be obtained from the manufacturers.

The fill illustrated in Figures 9-110A and B is typical of many cooling tower heat transfer evaporative cooling surfaces. The wooden splash type is the oldest in terms of length of usage, while the film types (some fabricated of plastic) have been in service about 40 years [148].

This latter type appears similar to some previously discussed, closely spaced structural packing, but is specifically designed for this application. Beyers [148] recommends film fill as the best choice if the water conditions of Table 9-49 are appropriate. For scaling or plugging water conditions, select splash fill.

Enthalpy of Air Operating Line

The enthalpy of air at any point on the operating line is [34]:

$$h_1^* = h_2 + (L'/G_a) (t_1 - t_2') \quad (9-127)$$

The equation for the line at terminal conditions is:

$$h_1 = h_2 + (L'/G_a) (t_1 - t_2) \quad (9-128)$$

where h_1^* = enthalpy of air at any temperature higher than inlet, Btu/lb dry air; note that h_1 is exit air

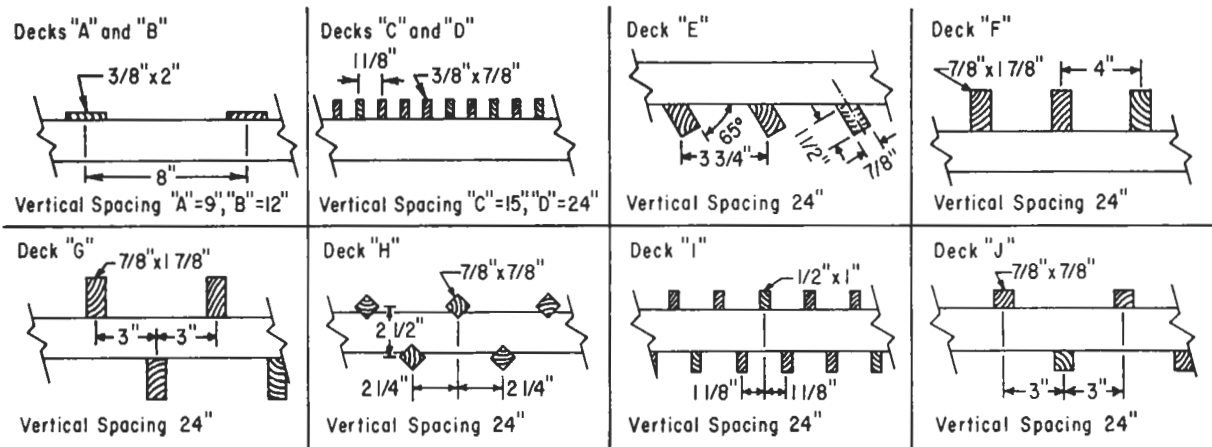


Figure 9-110A. Commercial cooling tower fill packing. Reproduced by permission of the American Institute of Chemical Engineers, Kelly, N. W., and Swenson, L. K., *Chemical Engineering Progress*, V. 52, No. 7 © (1956) p. 263; all rights reserved.

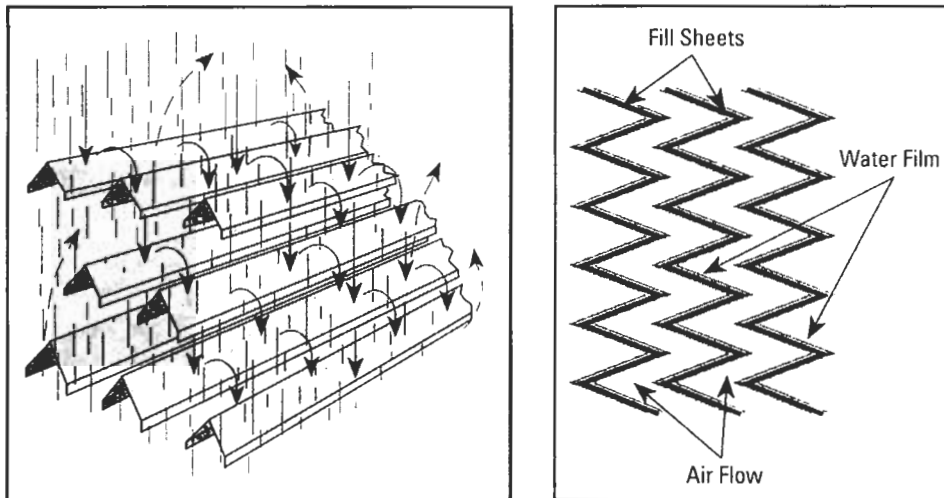


Figure 9-110B. Representative generic types of fill for cooling towers. Used by permission of the American Institute of Chemical Engineers, Beyer, A. H., *Chemical Engineering Progress*, V. 89, No. 7 © (1993); all rights reserved.

h_2 = enthalpy of inlet air to tower, equivalent to enthalpy of saturated air at wet bulb temperature, Btu/lb dry air, from *Moist Air Tables*, ASHVE Guide.

t_2' = any water temperature lower than inlet water temperature and higher than inlet air wet bulb temperature, °F

t_1 = inlet water temperature, °F

The effects of wet bulb, approach and range on mechanical draft cooling tower size is indicated in Figure 9-118.

The curves are necessarily the approximate midrange of a spread or band of the magnitude of the respective influences on the ground area. That is, the information is good for guidance as to the direction certain changes will take in the final selection. For example, the data are refer-

enced to a 70°F wet bulb and a 15°F approach, therefore, a change in wet bulb only to 75°F will indicate a tower requiring 90% of the ground area. If the approach changes too, then its correction must also be multiplied against the previous result, and the same handling applies to the wet bulb.

In examining the tower performance it is not the air temperature that sets the capacity, but the heat content or enthalpy of the air. Although the air temperature and wet bulbs at inlet may be different for two different inlet air conditions, it is still possible for the air to have the same enthalpy. Therefore, two different air streams of different conditions can produce the same effect on tower performance. The heat content or enthalpy of all air with the same wet bulb is the same, therefore it is clear that the wet bulb temperature is important and sets the performance.

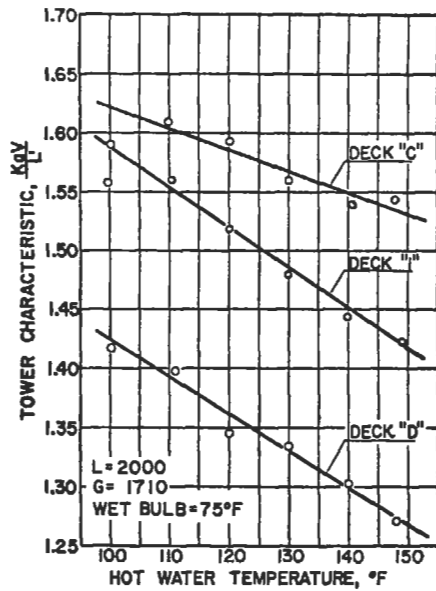


Figure 9-111. Typical effect of hot water temperature on tower characteristic, KaV/L' at constant L' , G_a wet bulb temperature and packed height. Note L and G shown in chart are hourly rates. Reproduced by permission of the American Institute of Chemical Engineers, Kelly, N. W., and Swenson, L. K., *Chemical Engineering Progress*, V. 52, No. 7 © (1956) p. 263; all rights reserved.

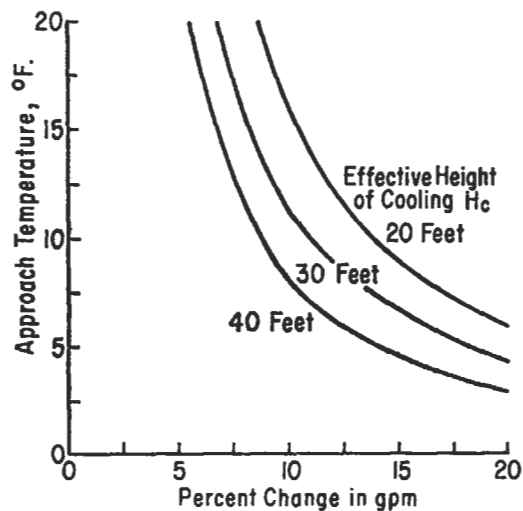


Figure 9-112. Percent change in gpm to produce 1°F change in approach. Used by permission of Whitesell, J., *Chemical Engineering*, Jan. (1955) p. 187, all rights reserved.

The data and information in the public literature are limited to performance evaluation of an existing cooling tower. It does not allow the design engineer in industry to actually design the height of tower packing or "fill." Even though the number of transfer units can be estimated (as in Reference 145), these numbers cannot be effectively used in design, because there are essentially no published

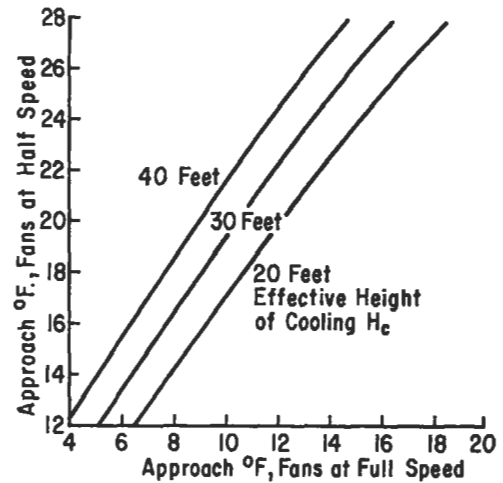


Figure 9-113. Effect of half-speed operation of fans. Used by permission of Whitesell, J., *Chemical Engineering*, Jan. (1955) p. 187, all rights reserved.

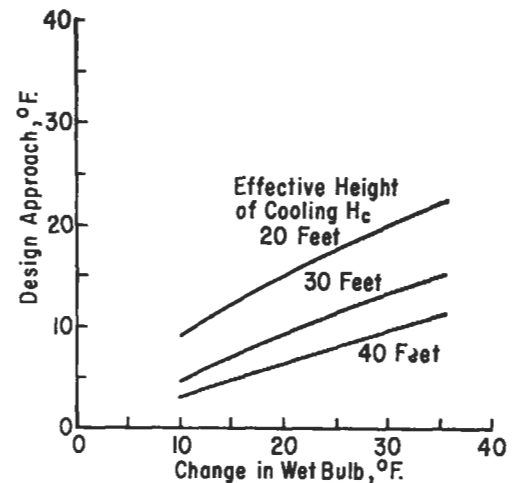


Figure 9-114. Decrease from approach for maintaining design water temperature. Used by permission of Whitesell, J., *Chemical Engineering*, Jan. (1955) p. 187, all rights reserved.

values for converting the gas mass transfer to square feet of effective contact tower filling, other than the proprietary data of the respective manufacturers [146]. Some data are available for relating the sizes of individual "cells" of respective manufacturers (a cell is a unit size containing x -number of square feet of fill surface distributed throughout y -number of vertical decks in the cell). These are not standard between the manufacturers, because the mass transfer of the respective fill varies with specific designs of contact surface between the water surface and the air-flow.

Mechanical draft towers are normally designed for L/G (liquid/gas rate) of 0.75 to 1.50 [147], and the values of KaV/L vary from 0.50 to 2.50.

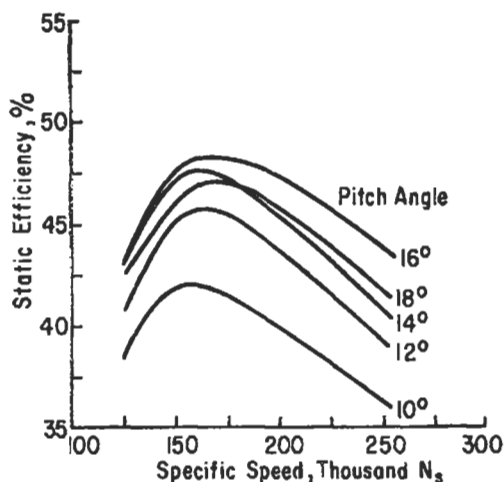


Figure 9-115. Fan efficiency versus specific speed for various blade settings of fans. Used by permission of Whitesell, J., *Chemical Engineering*, Jan. (1955) p. 187, all rights reserved.

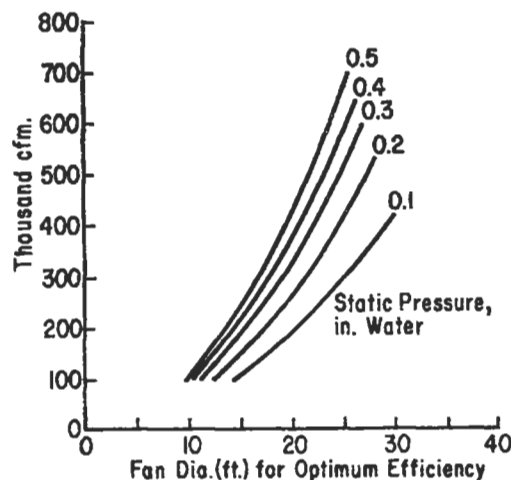


Figure 9-117. Diameter correlation for 16° pitch angle for fan blades. Used by permission of Whitesell, J., *Chemical Engineering*, Jan. (1955) p. 187, all rights reserved.

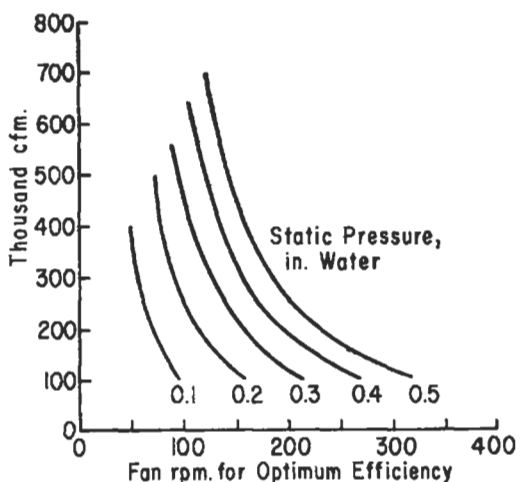


Figure 9-116. Rpm correlation for 16° pitch angle of fan blade. Used by permission of Whitesell, J., *Chemical Engineering*, Jan. (1955) p. 187, all rights reserved.

Recent studies indicate that the performance of all commonly used commercial high voidage packings can be correlated by [38, 146]:

$$KaV/L = \int_{t_1}^{t_2} \frac{dt_L}{i_L - i_G} \tag{9-129}$$

$$Ka V/L = 0.07 + A' N' (L'/G_a)^{-n'}$$

where L' = total water flow, lb/hr
 N' = no. of deck levels in tower
 t_1 = water temperature at bottom of tower, °F
 t_2 = water temperature at top of tower, °F
 t_L = water temperature of bulk of water, °F

- V = tower volume, ft³/ft² plan area
- i_G = enthalpy of air saturated at wet bulb temperature, Btu/lb dry air
- i_L = enthalpy of air saturated at bulk water temperature, Btu/lb dry air
- K = overall enthalpy transfer coefficient, lb/hr (ft² transfer area) (lb water/lb dry air)

This relates the tower characteristic to the number of packing decks in the tower and the L'/G_a ratio. Values of A' and n' are given in Table 9-50.

The simultaneous solution of Equation 9-127 involving the approach and cooling range and Equation 9-129 involving the number of packing decks (and thereby available surface area) yields the L'/G_a , which satisfies the specified performance. The accuracy of this combined with the data is within 5%. Equation 9-129 is essentially a straight line on log-log paper, so two points are sufficient to determine its position. The tediousness is involved in integrating the expression for the several enthalpy conditions involving approach and range that could satisfy the problem.

Ground Area vs. Height

The economics of forced and induced draft cooling tower operation require a study of fan and water pump horsepower and usually dictate a fan static pressure requirement not to exceed 0.75–1.0 in. of water. For atmospheric and natural draft towers the economics of pumping water are still very important. This means that the ground area must be so selected as to keep the height down while not dropping the unit rates so low that performance becomes poor. This then, is a balance of ground area versus total deck height. Pritchard [16] presents an

Table 9-49
Guidelines for Cooling Tower Recirculating Water (Normal Limits for Using Film Fill)

pH—Ideally 6.5–8.0; pH as low as 5.0 is acceptable if galvanized steel is not present.

Chlorides—Maximum 750 ppm (as NaCl) for galvanized steel; maximum 1,500 ppm for Type 300 stainless steel; maximum 4,000 ppm for Type 316 stainless steel; silicon bronze is the preferred material if chlorides exceed 4,000 ppm.

Calcium—In general, calcium (as CaCO₃) below 800 ppm should not result in calcium sulfate scale. In arid climates, however, the critical level may be much lower. For calcium carbonate scaling tendencies, calculate the Langelier Saturation Index or the Ryznar Stability Index.

Sulfates—If calcium exceeds 800 ppm, sulfates should be limited to 800 ppm, less in arid climates, to prevent scale. Otherwise, a sulfate level up to 5,000 ppm is acceptable.

Silica—Generally, limit silica to 150 ppm as SiO₂ to prevent silica scale.

Iron—Limit to 3 ppm. Note that excessive concentrations of iron may stain cooling tower components, but these stains are not the result of any rust or corrosion.

Manganese—Limit to 0.1 ppm.

Total Dissolved Solids (TDS)—Over 5,000 ppm can adversely affect thermal performance and may be detrimental to wood in the alternately wet/dry areas of the tower.

Suspended Solids—Limit to 150 ppm if the solids are abrasive. Avoid film fill if solids are fibrous, greasy, fatty, or tarry.

Oil and Grease—Over 10 ppm will cause noticeable thermal performance loss.

Nutrients—Nitrates, ammonia, oils, glycols, alcohols, sugars, and phosphates can promote growth of algae and slime. This growth can cause tower problems, particularly with film fill.

Ammonia—Limit to 50 ppm if copper alloys are present.

Organic Solvents—These can attack plastics and should be avoided.

Biological Oxygen Demand (BOD)—Limit BOD to 25 ppm, particularly if suspended solids exceed 25 ppm.

Sulfides—Should be limited to 1 ppm.

Langelier Saturation Index—Ideally, maintain between –0.5 and +0.5 A negative LSI indicates corrosion tendencies. A positive LSI indicates CaCO₃ scaling tendencies.

Reproduced by permission from American Institute of Chemical Engineers, Beyer, A. H., *Chem. Eng. Prog.*, Vol. 89, No. 7 © (1993), p. 42; all rights reserved.

estimating curve indicating that as packed height varies from 12–40 ft, the economics of ground area suggest a G_a of 2,000–1,400 respectively, being slightly less than a straight line function.

Pressure Losses

The tower pressure losses are: (1) tower packing or fill (70–80% of loss); (2) air inlet if induced draft; (3) mist eliminators at top; (4) air direction change losses and entrance to packing on forced draft units. These losses are a function of air velocity, number and spacing of packing decks, liquid rate and the relation between L' and G_a .

The pressure drop for a given number and type of packing deck is expressed [38]:

$$\Delta P' = N' B G_a^2 \left(\frac{0.0675}{\rho_G} \right) + N' C' \sqrt{S_F} (L) G_E^2 \left(\frac{0.0675}{\rho_G} \right) \quad (9-130)$$

Values of B , C' and S_F are given in Table 9-50. Pressure drop values, $\Delta P'/N'$, per individual deck range from 0.003–0.006 in. water for low L' and G_a rates to 0.03–0.06 in. water for high L' (3,500) and G_a (2,000) rates [19]. Values of G_E are taken from Figure 9-119. Typical pressure drop curve is shown in Figure 9-120.

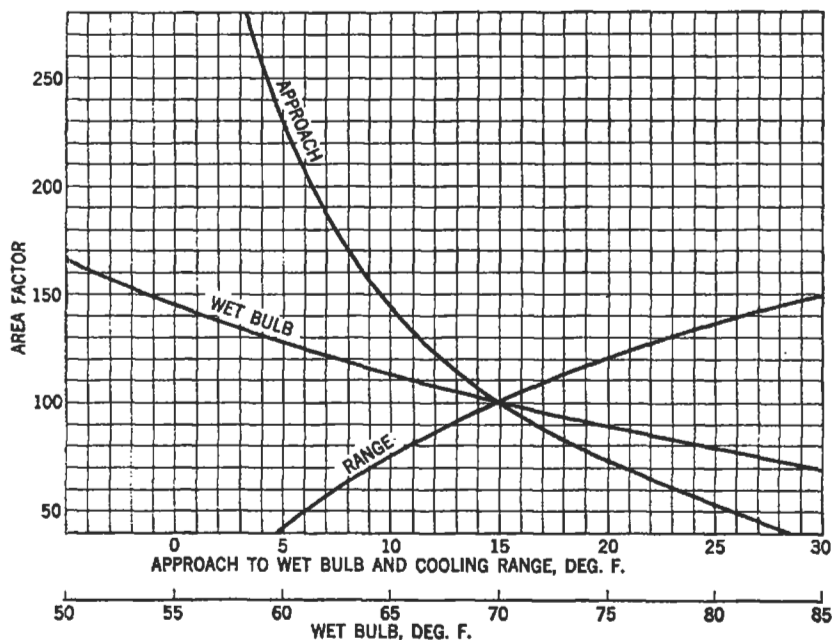
Pressure loss through wooden mist eliminators based on 0.0675 lb/ft³ air varies from 0.01 in. water at $G_a = 800$ to 0.07 at $G_a = 2,000$ as almost a straight line function [16]. These losses are based on the face area of the eliminators.

Pressure loss for inlet louvers based on two face velocity heads and 0.075 lb/ft³ air is given as 0.02 in. water for 400 ft/min face velocity to 0.32 in. water for 1,600 fpm, varying slightly less than a straight line [19].

Fan Horsepower for Mechanical Draft Tower

$$\text{BHP} = F p_{sa} / (6,356) (0.50) \quad (9-131)$$

where F = actual cfm at fan inlet, ft³/min
 p_s = total static pressure of fan, in. of water



Curve showing effect of wet bulb temperature, approach to wet bulb, and cooling range on cooling tower size. The normal tower is assumed to be designed for 15 degree cooling range and a 15 degree approach to a 70 degree wet bulb. If all other factors remain the same, reducing the approach to the wet bulb to 6.3 degrees will double the size of the tower; or decreasing the cooling range to 6.1 degrees will permit the use of a tower only half as large; or designing for a 53.7 degree wet bulb instead of a 70 degree wet bulb will require a tower 1-1/2 times as large because of the lower water absorbing capacity of colder air.

Figure 9-118. Effect of cooling tower performance variables on plan ground area required. Used by permission of Foster Wheeler Corp., Cooling Tower Dept.

Table 9-50
Values of A', n', B, C', and S_F

Deck Type	A'	n'	S _F , Ft	B	C'
				Mult. × 10 ⁻⁸	Mult. × 10 ⁻¹²
A	0.060	0.62	3.00	0.34	0.11
B	0.070	0.62	4.00	0.34	0.11
C	0.092	0.60	3.75	0.40	0.14
D	0.119	0.58	6.00	0.40	0.14
E	0.110	0.46	4.95	0.60	0.15
F	0.100	0.51	9.13	0.26	0.07
G	0.104	0.57	6.85	0.40	0.10
H	0.127	0.47	3.64	0.75	0.26
I	0.135	0.57	4.50	0.52	0.16
J	0.103	0.54	6.85	0.40	0.10

Used by permission: The American Institute of Chemical Engineers; Kelly, N. W. and Swenson, L. K., *Chem. Eng. Prog.*, Vol. 52 © (1956) p. 263 [38]; all rights reserved.

This relation includes a 50% static efficiency of the fan and gear losses, assuming a gear drive [19]. If belt driven the difference will not be great.

For study purposes the effects of performance as related to fan horsepower may be patterned after Figures 9-121 and 9-122. The conditions for actual air inlet conditions for an induced draft fan must be obtained from Equation 9-127 read from a diagram similar to Figure 9-109.

Economical tower sizes usually require fan horsepower between 0.05 and 0.08 hp/ft² of ground plan area [19], and motors larger than 75 hp are not often used due to

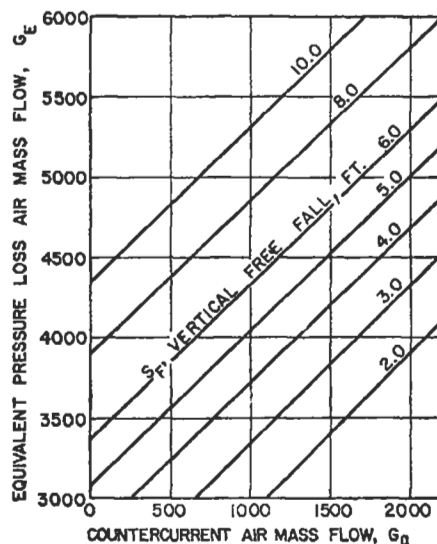


Figure 9-119. Values of equivalent air mass velocity. Reproduced by permission of the American Institute of Chemical Engineers, Kelly, N. W., and Swenson, L. K., *Chemical Engineering Progress*, V. 52, No. 7 © (1956) p. 263; all rights reserved.

inability to obtain the proper fans and gears in the space required.

Water Rates and Distribution

Water distribution must give uniform water flow over the tower packing. Many towers use a gravity feed system discharging the water through troughs and ceramic, metal

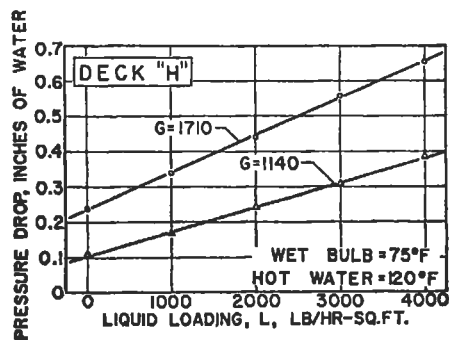


Figure 9-120. Typical effect of liquid loading on air pressure drop showing linear relationship; total deck height is 20 ft. Reproduced by permission of the American Institute of Chemical Engineers, Kelly, N. W., and Swenson, L. K., *Chemical Engineering Progress*, V. 52, No. 7 © (1956) p. 263; all rights reserved.

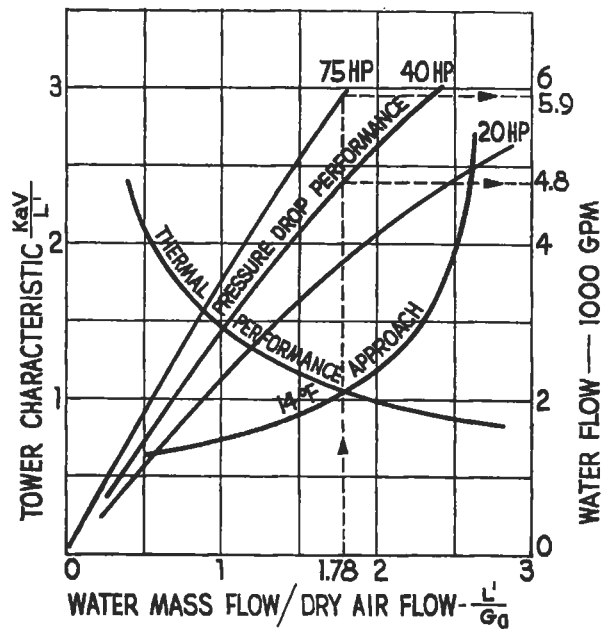


Figure 9-122. Plot illustrating combination of thermal and fan power characteristics to directly determine flow capacities of a given size. Used by permission of Groitein, E. E., *Combustion*, Nov. (1957).

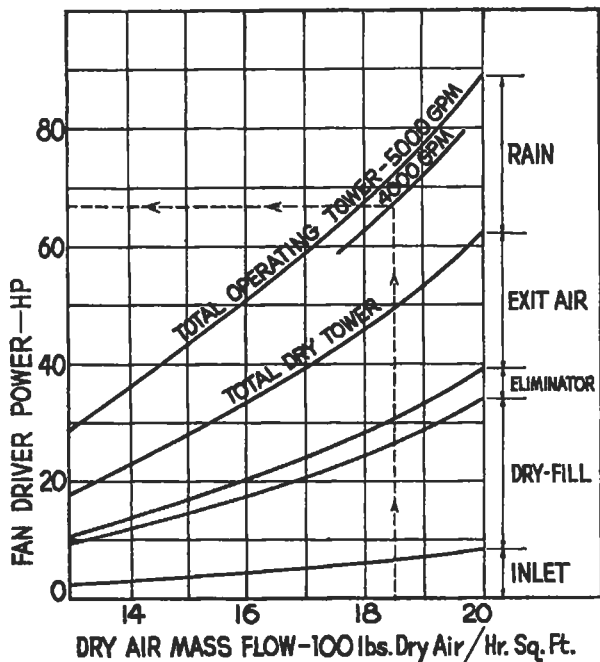


Figure 9-121. Fan power requirements for components of a typical counterflow induced draft cooling tower. Used by permission of Groitein, E. E., *Combustion*, Nov. (1957) p. 38.

or plastic nozzles. Other systems use pressure nozzles discharging upward, before falling back over the packing. This latter method requires more pumping head due to the pressure required at the nozzles. Water rates usually run from 1 to 3.5 gpm/ft² of ground plan area.

Blow-down and Contamination Build-up

As the circulating water evaporates in passing through the tower, the evaporated water vapor is pure. This leaves behind and creates a concentration effect for solids material dissolved in the remaining water. This concentration

can aggravate the heat transfer surfaces and develop corrosive conditions on many mechanical and structural parts of the tower. To control and limit this build-up, a certain amount of liquid is blown down to expel the concentrated material and this quantity is replaced with fresh make-up water. See Figure 9-123 for blow-down.

The level to which the contamination can concentrate in the circulating water is [144]:

$$C = \frac{E + D + B}{D + B} \tag{9-132}$$

$$\text{The rate of blow-down, } B = \frac{E - [(C - 1)(D)]}{(C - 1)} \tag{9-133}$$

where C = contaminant level in circulating water; number of concentration ratios

E = rate of evaporation, gpm (if not accurately known, evaporation can be approximated by multiplying total water rate in gpm times the cooling range (°F) times 0.0008).

$$E \text{ (est)} = (\text{gpm}_T) (CR) (0.0008) \tag{9-134}$$

where gpm_T = total cooling tower water flow rate, gpm, (incoming to be cooled by tower)
 DL = drift loss, water lost from tower system entrained in exhaust air stream, measured as (a) % of circulating water rate, gpm, or (b) more precise [144], an L/G parameter and drift becomes pounds of water per million pounds of exhaust air; for estimating:

$$DL = (\text{gpm}_T, \text{ as water flow rate}) (0.0002) \quad (9-135)$$

CR = cooling range, °F, difference between hot water into tower and cold water from the tower, °F

B = rate of blow-down, gpm. (Because an acceptable level of concentration has usually been predetermined, the operator is more concerned with the amount of blow-down necessary to maintain the concentration, Equation 9-132.)

L/G = ratio of total mass flow of water and dry air in cooling tower, lb/lb

Example: 9-15: Determining Approximate Blow-down for Cooling Tower (Used by permission of Marley Cooling Tower Co., Inc., from *Cooling Tower Fundamentals* [144])

“Assume that a given cooling tower is designed to reduce the incoming temperature of 10,000 gpm by 25°F (range). Then, assume that the level of chlorides in the make-up water is 250 ppm, and we do not want that level to go beyond 750 ppm in the circulating water. Allowable concentration ratio is 750/250 = 3. The approximate

evaporation rate would be 10,000 × 25 × 0.0008 = 200 gpm. The approximate drift rate would be 10,000 × 0.0002 = 2 gpm. Applying these values to Equation 9-133, blow-down would be:

$$\frac{200 - [(3 - 1) \times 2]}{(3 - 1)} = \frac{200 - (2 \times 2)}{2} = \frac{200 - 4}{2} = \frac{196}{2}$$

= 98 gpm, blow-down

“Even if the assumed evaporation and drift rates were perfectly accurate, the calculated blow-down rate of 98 gpm might still not be quite enough because of the effects of air-borne contaminants, which are usually incalculable. Once the approximate level of blow-down has been determined, the circulating water quality should be regularly monitored and appropriate adjustments made.

“Figure 9-123 is a plot of the percent of circulating water flow to be wasted in order to maintain various concentrations, based upon the approximate evaporation and drift rates indicated by Equations 9-134 and 9-135, expressed as percentages.

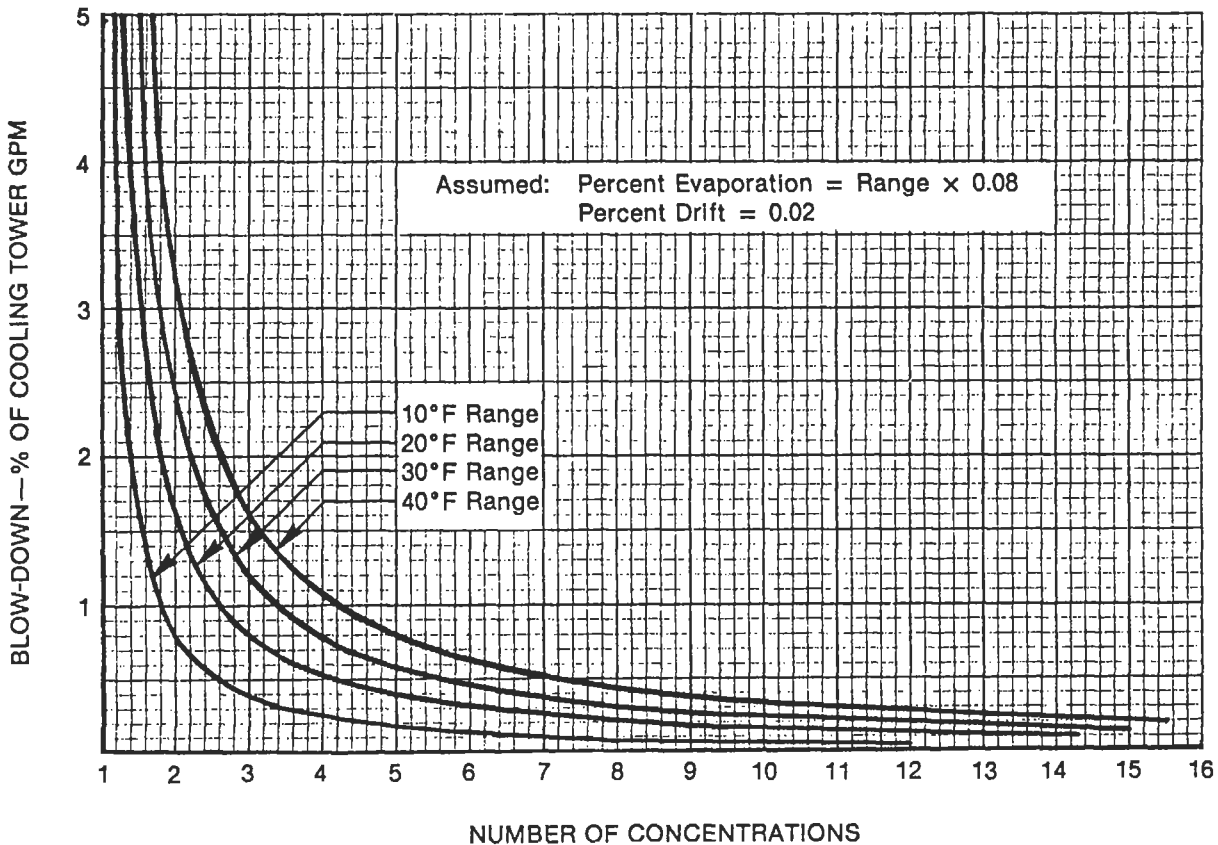


Figure 9-123. Cooling tower blow-down versus number of concentrations in circulating water; percent of total circulating water to be wasted to maintain various concentrations. Used by permission of Hensley, J. C. (ed.) *Cooling Tower Fundamentals*, 2nd Ed. (1985), The Marley Cooling Tower Co., a United Dominion Co.

"Despite the benefits of blow-down, however, chemical, electrostatic, or electronic treatment of the water is often required to prevent scale formation, corrosion, or biological growth. When treatment is required, or anticipated to be required, *the services of a reliable water treatment company should be obtained.*"

Brooke [234] provides calculation techniques using enthalpy of the air to determine water evaporated, air flow, and blow-down quantities.

Preliminary Design Estimate of New Tower

Refer to psychrometric chart, Figures 9-124A and B for basic considerations in establishing tower conditions.

1. Determine the inlet water temperature to the tower. This is approximately the outlet temperature from the cooling water load.
2. Determine the heat load to be performed by the tower, based on required water inlet and outlet temperatures and flow rates.
3. Establish the wet bulb temperature for the air at the geographical site of the tower. Use weather bureau records if other data are not available. Use caution, do not select a value too high.
4. Prepare a plot of the saturation curve for air-water. Establish the operating line by starting at the point set by the outlet cold water temperature and the enthalpy of air at the wet bulb temperature, and with a slope L'/G_a assumed between 0.9 and 2.7. See Figure 9-109.
5. Graphically integrate, by plotting $1/h'-h$ vs. t , reading $(h'-h)$ from the operating-equilibrium line plot for various values of temperature. See Figure 9-125.
6. The value of the integral is equal to the number of transfer units, so set it equal to Equation 9-129 and solve for the number of decks needed, N . Select the desired deck from Figures 9-110A and B and the constants A' and n from Table 9-50.
7. If the number of decks required is unreasonable from a height standpoint, the procedure must be repeated using a new assumed L'/G_a , or a new approach, or a new wet bulb temperature, or some combination of these.
8. For the assumed L'/G_a and known L' , calculate the required air rate G_a .

Alternate Preliminary Design of New Tower (after References 12 and 19)

1. Follow Steps (1), (2), and (3) of the procedure just outlined.

2. Refer to a plot of KaV/L' versus L'/G_a as in Figures 126A–G or in References 15 and 19. This saves the integration step, as this has been performed and calculated for a selection of reasonable wet bulb temperatures and temperature ranges. The curve to fit the design problem must be used.
3. Plot Equation 9-129 for two assumed L'/G_a values and an assumed number of checks on the plot of Figure 9-126C or its equivalent. The intersection with the approach curve gives the value of L'/G_a which satisfies the two Equations 9-118 and 9-129.
4. From the known liquid rate L' and the value of L'/G_a assumed, calculate the needed value of the air rate, G_a . This value converted to CFM at the fan inlet, together with the calculated pressure drop gives the fan horsepower requirements.

Performance Evaluation of Existing Tower [19]

1. Because the heat load, L' , G_a and temperatures are known for an operating tower, its performance as represented by the number of transfer units, or tower characteristics can be determined. Solve Equation 9-129 for KaV/L' , or use the modified Merkel diagram, Figure 9-127. This is the number of transfer units operating in the tower. For relative comparison of Ka values see Figure 9-128.
2. If it is desired to evaluate a change in performance on an existing tower, knowing the required conditions and numbers of decks and kind of packing, calculate KaV/L' for we assumed values of L'/G_a .
3. Following Reference 19, plot this on the appropriate curve (good up to altitudes of 3,000 ft) for KaV/L' vs. L'/G_a for the proper wet bulb, range and at the intersection of the straight line plot with the approach value selected or needed, read the L'/G_a required to meet the performance conditions.
4. Calculate the new G_a , assuming that L' is the important value known. If on the other hand, it is desired to determine just how much cooling can be obtained, then for a fixed air rate, calculate the L' that can be accommodated.

Example 9-16: Wood Packed Cooling Tower with Recirculation, Induced Draft

Perform the preliminary design on a cooling tower to establish its performance and size.

Required gpm = 5,000
 Inlet hot water = 110°F
 Outlet cold water = 85°F
 Wet bulb = 75°F
 Recirculation allowance = 3%

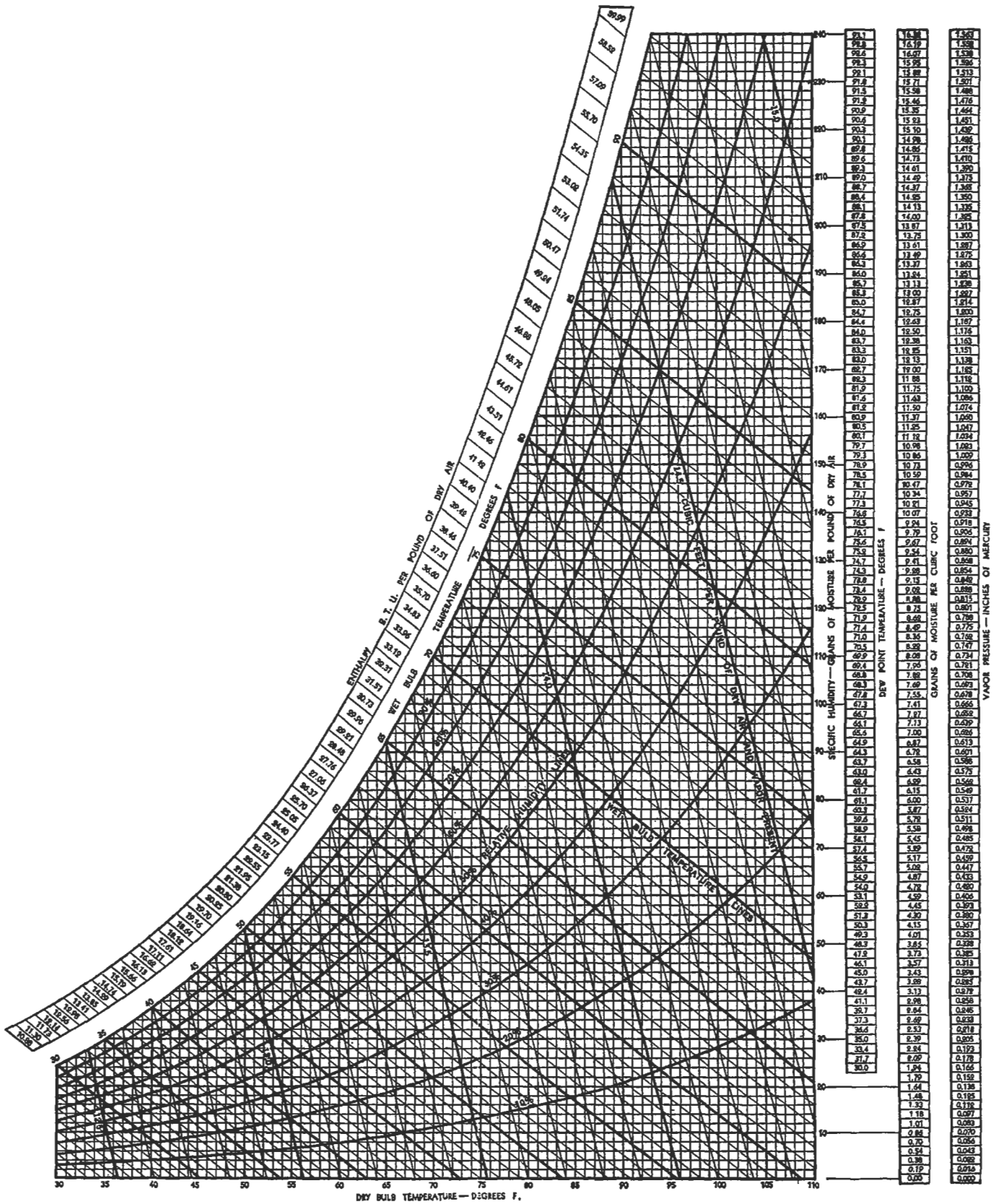


Figure 9-124A. Psychrometric chart, reference barometric pressure of 29.92 in. Hg. Used by permission of Westinghouse Electric Co., Sturtevant Div.

If any two properties of air are known, all others may be found.

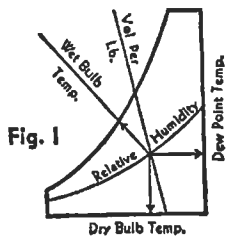


Fig. 1

Numerical values of properties may be read directly.

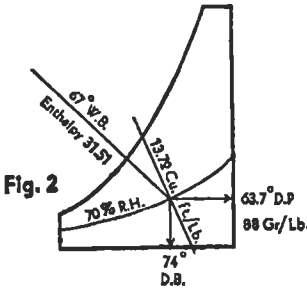


Fig. 2

SENSIBLE HEATING & COOLING is represented by a horizontal line between the limits of the process. All the properties of air change except the moisture content.

EXAMPLE:—Air initially at 90° D.B. is heated to 106° D.B.

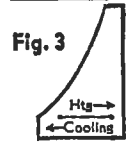


Fig. 3

	INITIAL	FINAL	INITIAL	FINAL
Dry bulb	90°	106°	Dew point	62.4
Wet bulb	71°	76°	Vap. pres.	0.562
Rel. hum.	40%	26.0%	Enthalpy	34.83
Grains/lb.	84	84	Cu. ft./lb.	14.12
				14.5

HUMIDIFYING & DEHUMIDIFYING with no change in dry bulb is represented by a vertical line between the limits of the process.

EXAMPLE:—Air at 90° D.B. and 84 GR./LB. is humidified without change of temperature to 128 GR./LB.

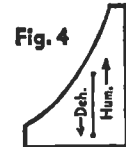


Fig. 4

	INITIAL	FINAL	INITIAL	FINAL
Dry bulb	90°	90°	Dew point	62.4
Wet bulb	71°	78°	Vap. pres.	0.562
Rel. hum.	40%	60%	Enthalpy	34.83
Grains/lb.	84	128	Cu. ft./lb.	14.12
				14.26

EVAPORATING COOLING is accomplished by passing air thru a spray or finely divided curtain of recirculated water, and is represented by a line of constant W. B. temperature. Sens. heat is absorbed in evaporation thereby increasing the moisture content while the total heat remains constant.

EXAMPLE:—Air at 90° D.B. and 40% rel. hum. is passed thru a spray of recirculated water. The water temp. will approach the W.B. temp. of the air which remains constant.

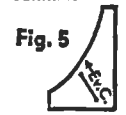


Fig. 5

	INITIAL	FINAL	INITIAL	FINAL
Dry bulb	90°	72°	Dew point	62.4
Wet bulb	71°	71°	Vap. pres.	.747
Rel. hum.	40%	95%	Enthalpy	34.83
Grains/lb.	84	112	Cu. ft./lb.	14.12
				13.74

TEMPERATURES OF A MIXTURE

Find the final wet and dry bulb temperatures of a mixture of 3000 C.F.M. at 60° D.B. and 46° W.B., and 5000 C.F.M. at 80° D.B. and 63° W.B. Read from constant volume lines on chart

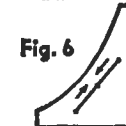


Fig. 6

3000 c.f.m.	60° d.b.	46° w.b.	13.17 cu. ft./lb.
5000 c.f.m.	80° d.b.	63° w.b.	13.85 cu. ft./lb.
3000		5000	
13.17	= 228 lbs./Min.	13.85	= 361 lbs./min.
228 + 361 = 589 total wt. of air per min.			

DRY BULB temperature of the mixture

$$\frac{228}{589} \times 60 = 23.25^\circ \quad \frac{361}{589} \times 80 = 49.10^\circ$$

$$23.25 + 49.10 = 72.35^\circ \text{ Final D.B.}$$

WET BULB temperature of the mixture

Enthalpy at 46° W.B. = 18.12, at 63° W.B. = 28.48

$$\frac{228}{589} \times 18.12 = 7.01 \quad \frac{361}{589} \times 28.48 = 17.45$$

$$7.01 + 17.45 = 24.46 \text{ Enthalpy of Mixture}$$

Corresponding W.B. Temp. = 57° Final W.B.

Figure 9-124B. Directions for using Figure 9-124A. Used by permission of Westinghouse Electric Corp., Sturtevant Div.

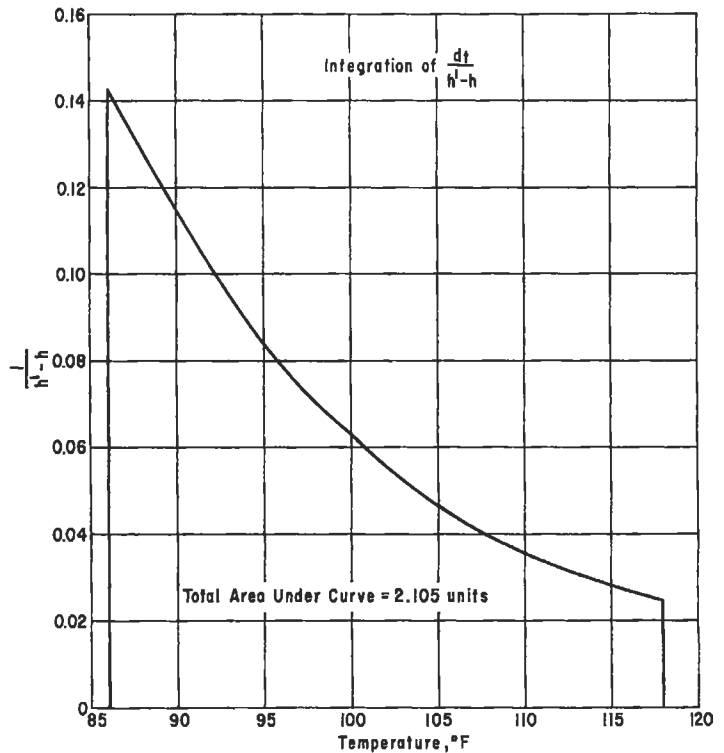


Figure 9-125. Graphical integration to determine number of transfer units.

Use alternate design procedure:

1. Range = 110 - 85 = 25°F
2. Wet bulb

Because recirculation is to be considered, the ambient wet bulb of 75°F must be corrected.

3. Solve Equation 9-129

$$KaV/L' = 0.07 + AN (L'/G_a)^{-n}$$

Select Deck "A":

Constants:

$$A' = 0.060$$

$$n = 0.62$$

$$L'/G_a = 1.00 \text{ assumed}$$

$$N' = 30, \text{ assumed number deck levels}$$

$$KaV/L' = 0.07 + 0.060 (30) (1.00)^{-0.62} = 1.87$$

Second solution of Equation 9-129 to determine line for plot:

$$L'/G_a = 2.0 \text{ assumed}$$

All other values remain the same.

$$KaV/L' = 0.07 + 0.060 (30) (2.0)^{-0.62} = 0.07 + (0.060) (30) (0.651)$$

$$KaV/L' = 1.24$$

(text continued on page 406)

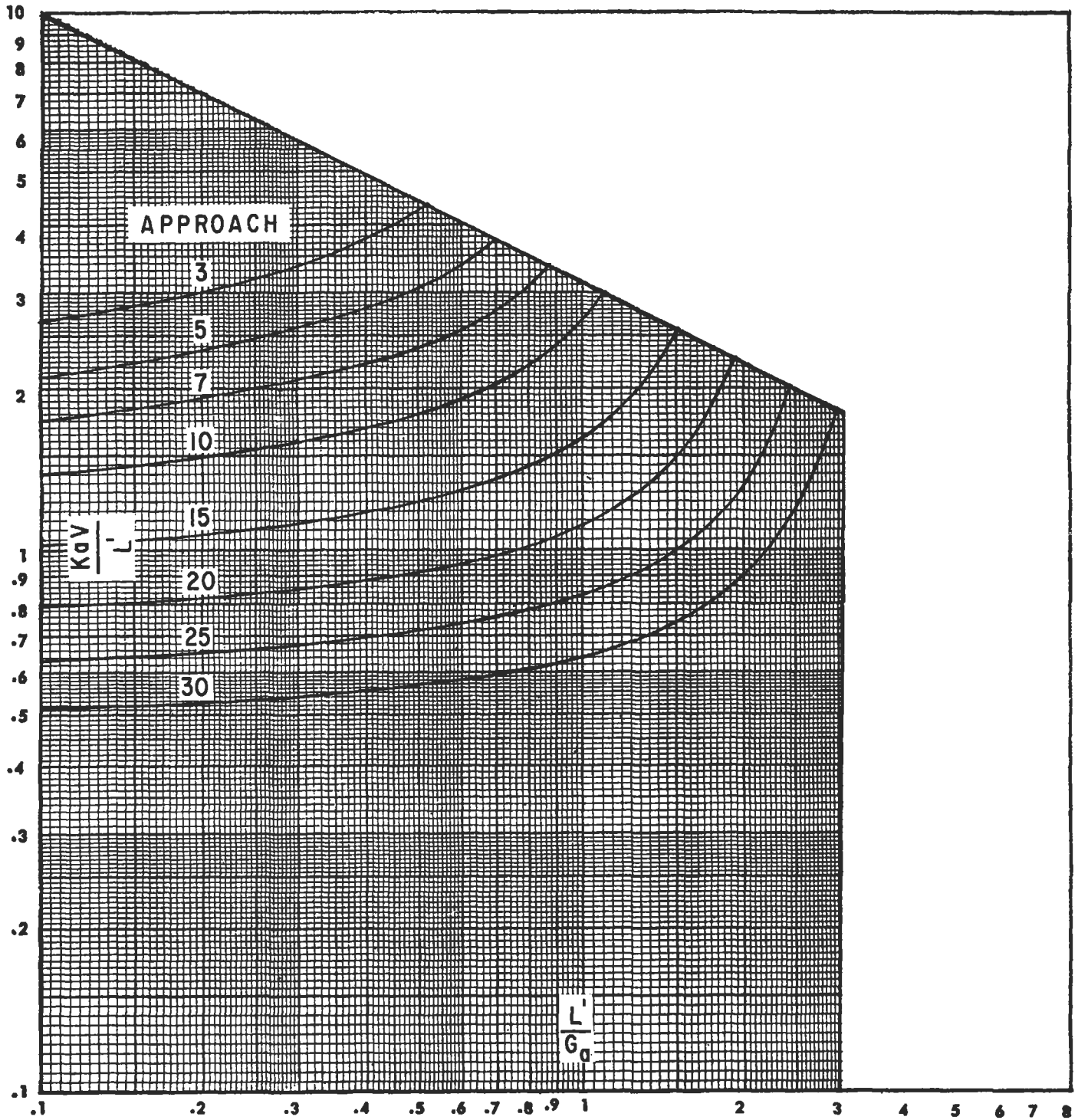


Figure 9-126A. 65°F wet bulb; 30°F range, counterflow cooling tower performance curves. Used by permission of *Counterflow Cooling Tower Performance*, The Pritchard Corp. (now, Black and Veatch Pritchard Corp.) (1957).

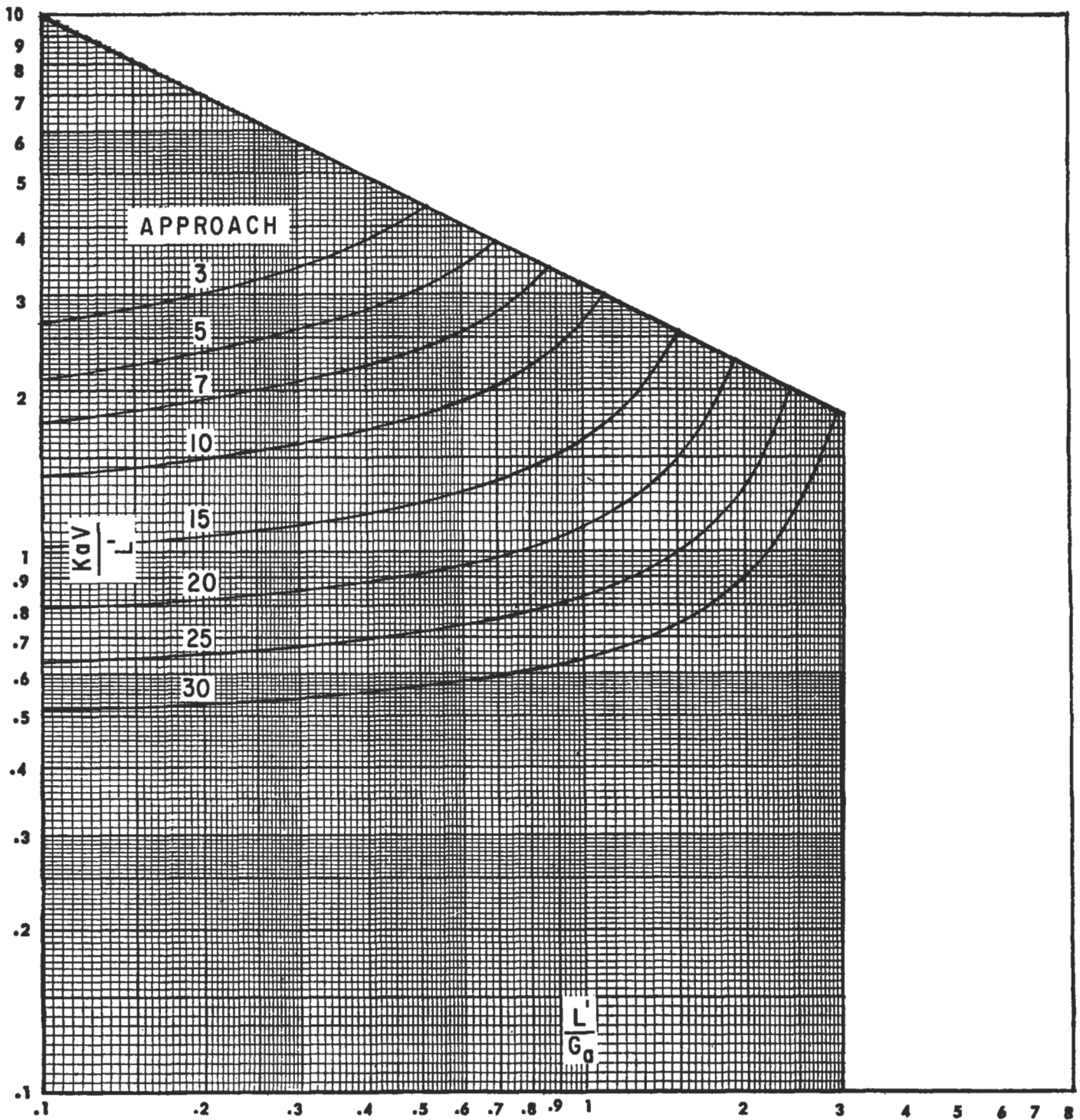


Figure 9-126B. 70°F wet bulb; 20°F range, counterflow cooling tower performance curves. Used by permission of *Counterflow Cooling Tower Performance*, The Pritchard Corp. (now, Black and Veatch Pritchard Corp.) (1957).

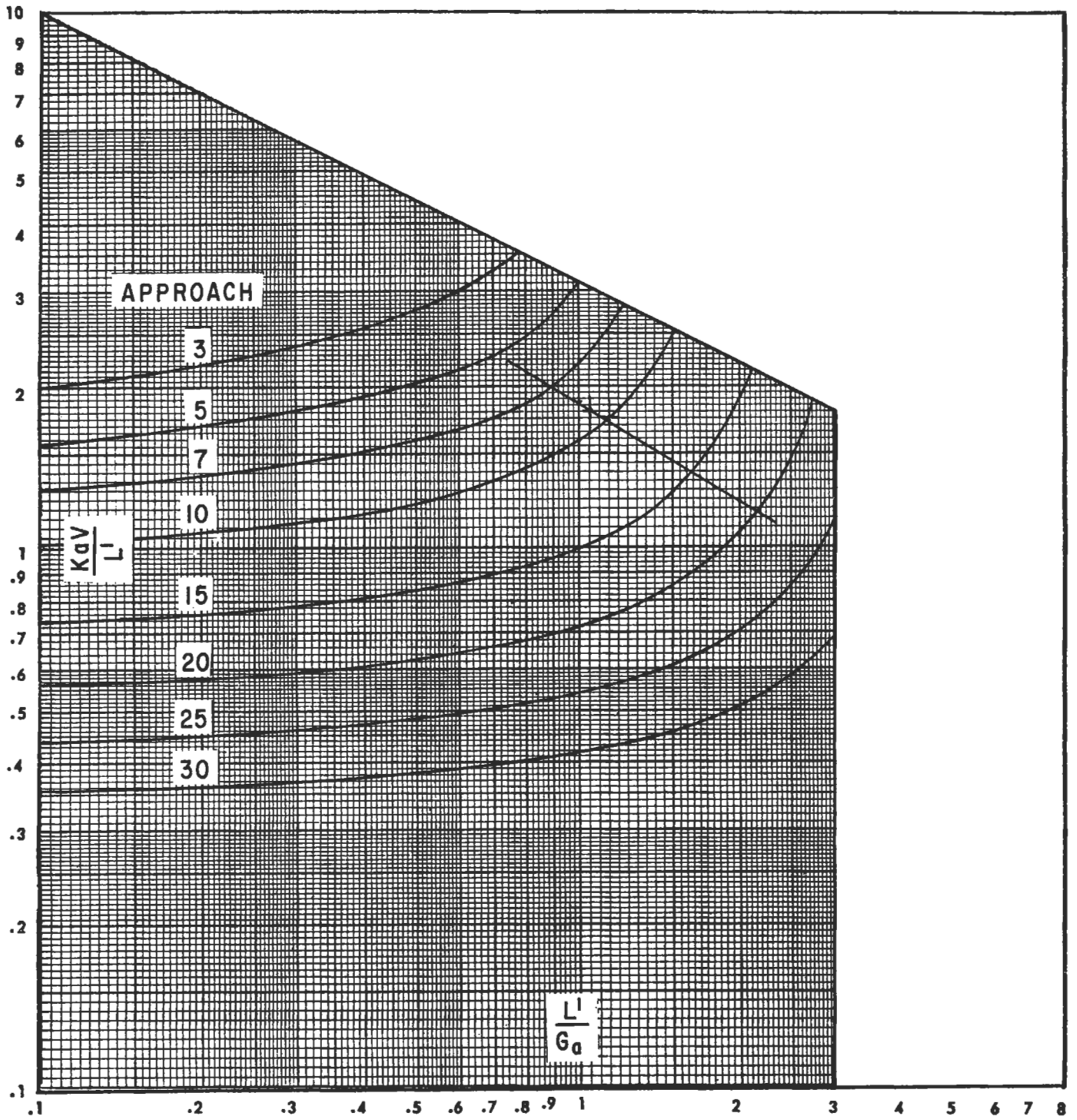


Figure 9-126C. 75°F wet bulb; 25°F range, counterflow cooling tower performance. Used by permission of *Counterflow Cooling Tower Performance*, The Pritchard Corp. (now, Black and Veatch Pritchard Corp.) (1957).

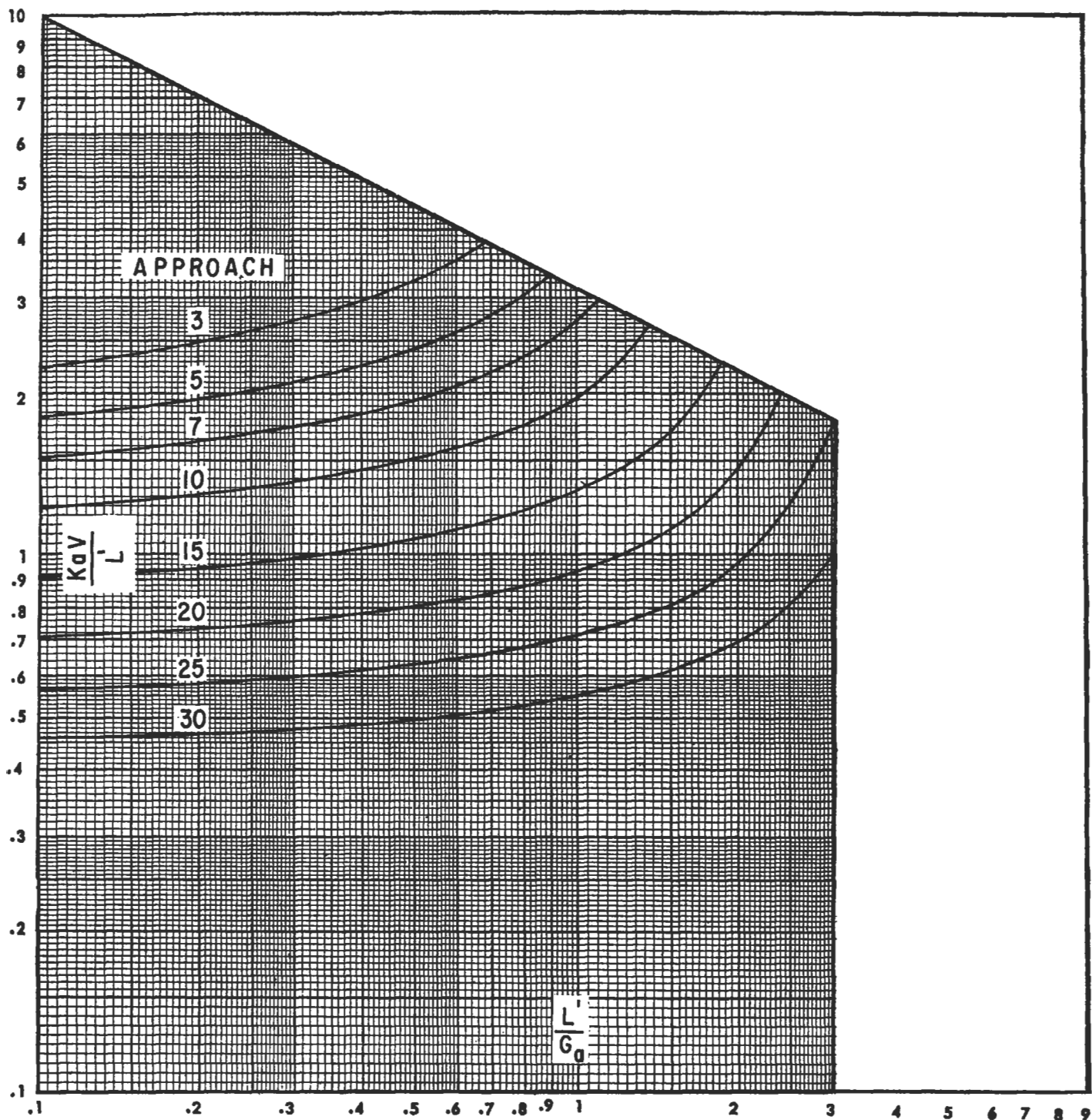


Figure 9-126D. 75°F wet bulb; 40°F range, counterflow cooling tower performance. Used by permission of Counterflow Cooling Tower Performance, The Pritchard Corp. (now, Black and Veatch Pritchard Corp.) (1957).

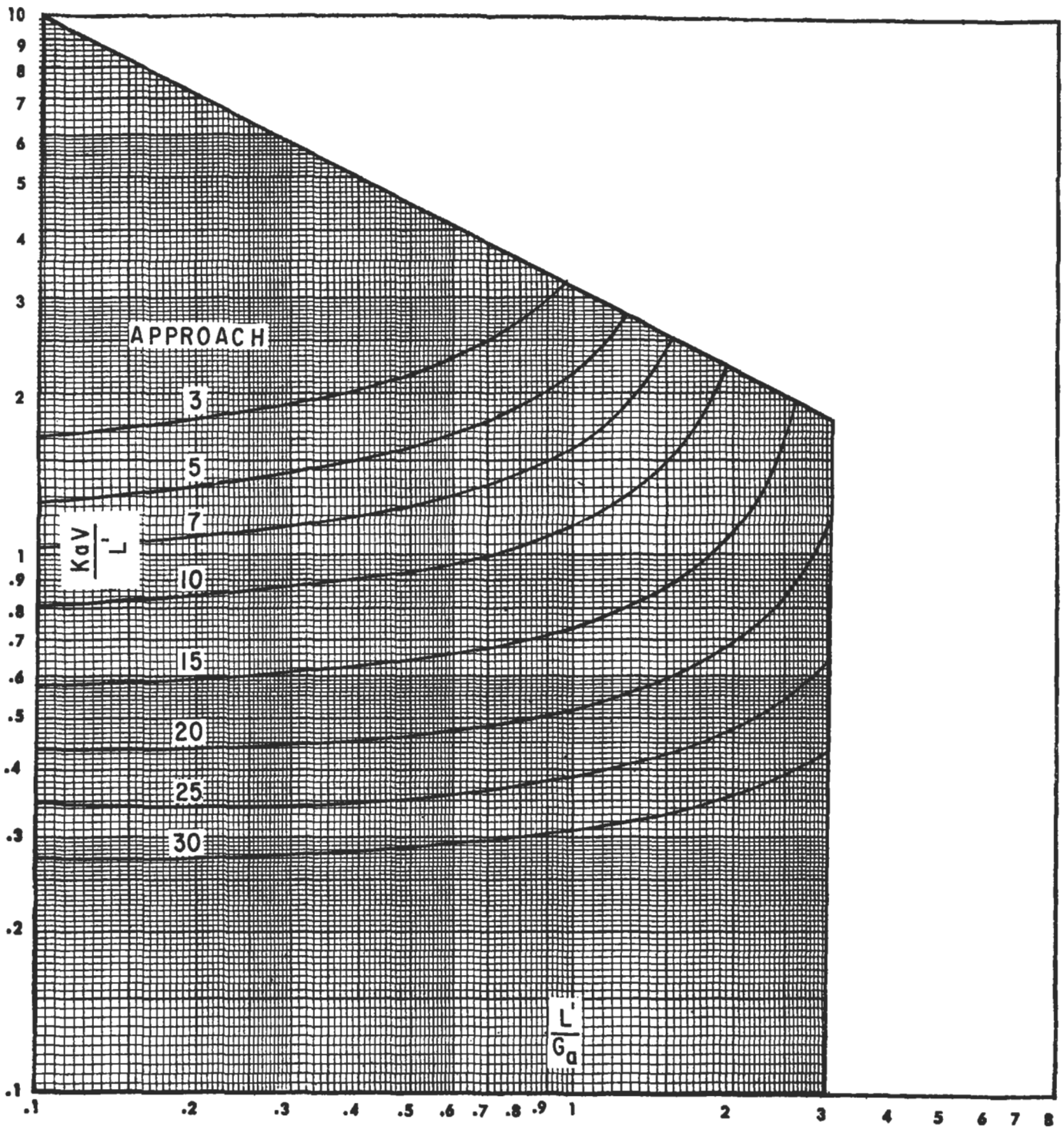


Figure 9-126E. 80°F wet bulb; 20°F range, counterflow cooling tower performance. Used by permission of *Counterflow Cooling Tower Performance*, The Pritchard Corp. (now, Black and Veatch Pritchard Corp.) (1957).

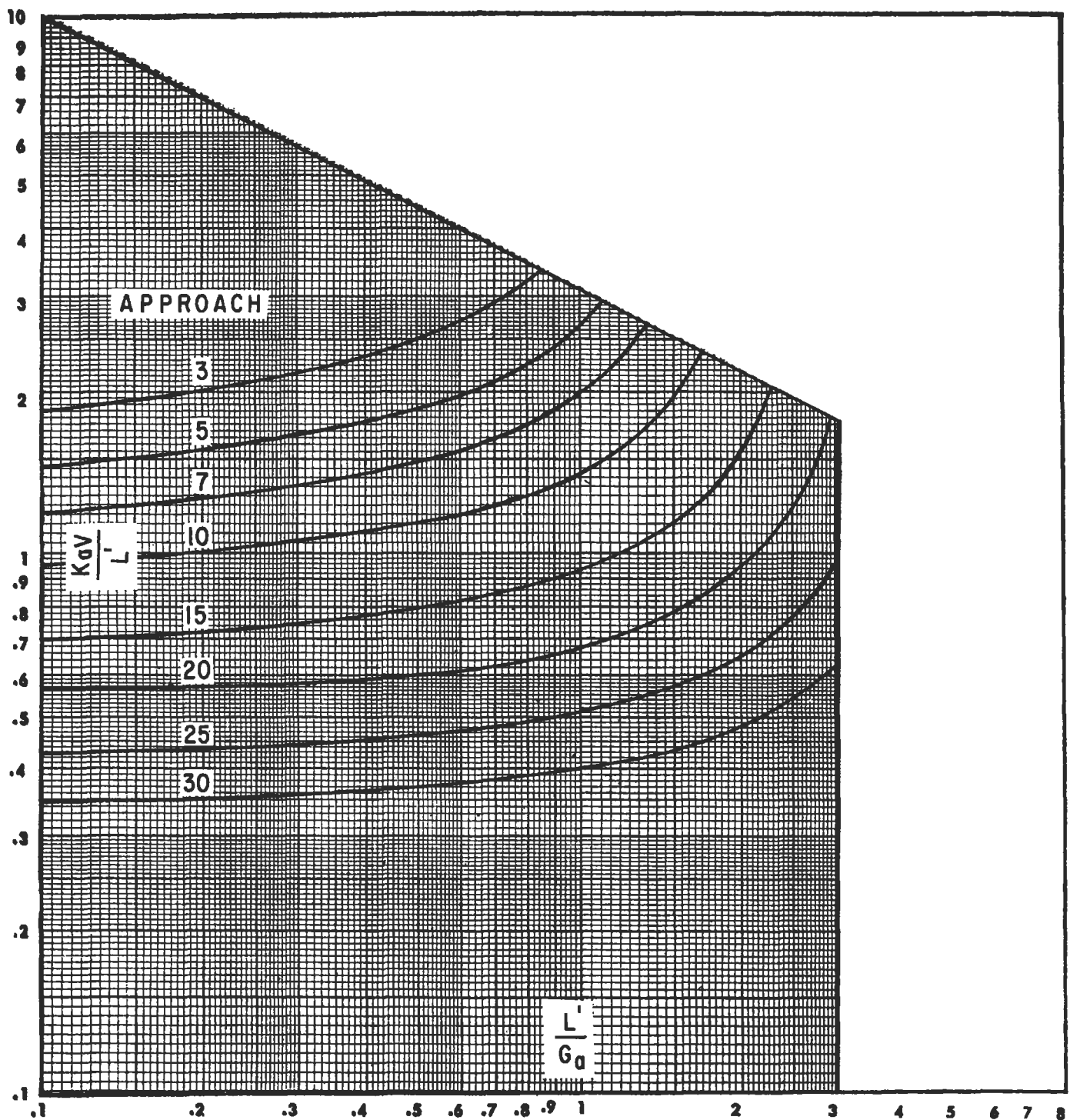


Figure 9-126F. 80°F wet bulb; 30°F range, counterflow cooling tower performance. Used by permission of *Counterflow Cooling Tower Performance*, The Pritchard Corp. (now, Black and Veatch Pritchard Corp.) (1957).

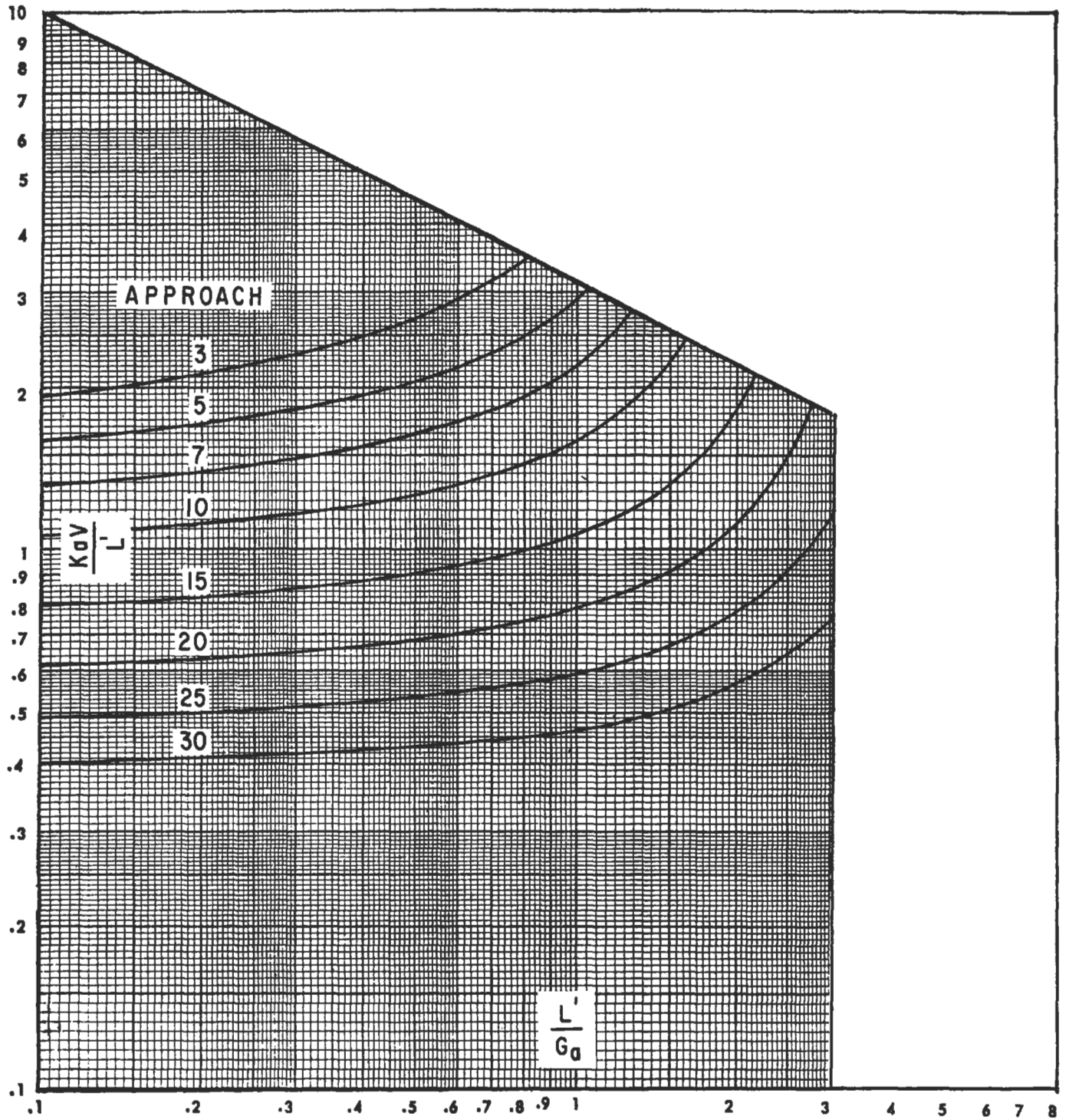


Figure 9-126G. 80°F wet bulb; 40°F range, counterflow cooling tower performance. Used by permission of *Counterflow Cooling Tower Performance*, The Pritchard Corp. (now, Black and Veatch Pritchard Corp.) (1957).

Note for use: Locate "cold water-cooling range" point and connect to selected wet bulb temperature of air. (Line 1.) Then, through L'/G_a draw line parallel to locate value of KaV/L' . (Line 2). The graph may be used in reverse to examine changing conditions on a given tower.

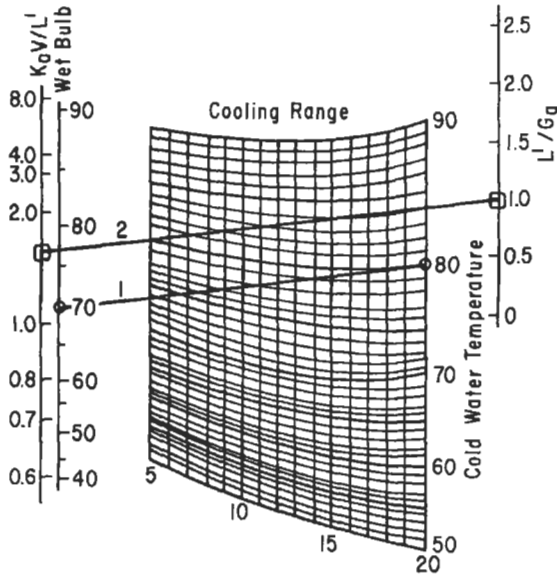


Figure 9-127. Calculation of KaV/L' factor. Used by permission of Brooke, M., *Refining Engineer*, May (1958) p. c-41; as reproduced from Woods and Betts, *The Engineer* (London), Mar. 17 and 24 (1950).

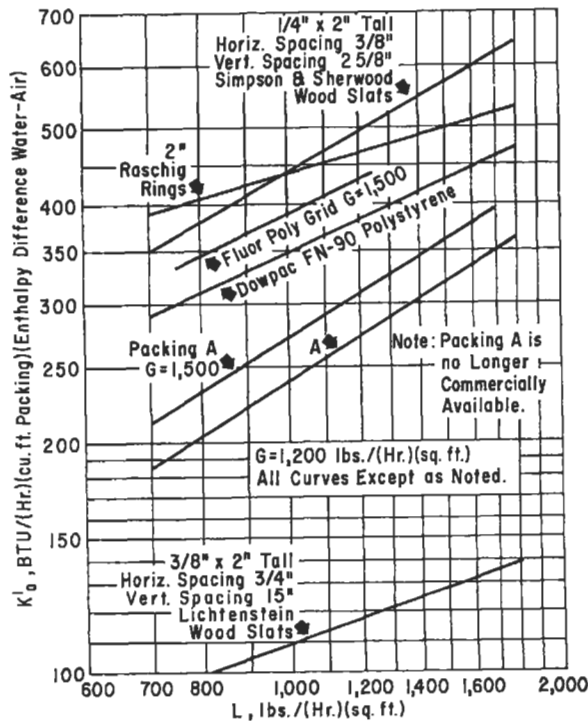


Figure 9-128. Comparison of cooling efficiency of several packing materials in terms of the coefficient of heat transfer $K'a$. Used by permission of Plastics Technical Service, The Dow Chemical Co., Midland Mich. with data added from Fuller, A. L., et al. *Chemical Engineering Progress*, V. 53, No. 10 (1957) p. 501; all rights reserved.

(text continued from page 398)

4. Plot points

$KaV/L' = 1.87$ and 1.24 on Figure 9-126C representing 75°F wet bulb, and 25°F range:
 For approach = $85^\circ - 75^\circ\text{F} = 10^\circ\text{F}$
 L'/G_a at intersection of straight line plot = 1.13
 This is L'/G_a required for 75°F wet bulb.
 Enthalpy of exit air, $h_1 = h_2 + (L'/G_a) (t_1 - t_2)$
 h_2 at $75^\circ\text{F} = 38.61$ Btu/lb dry air
 $h_1 = 38.61 + 1.13 (110 - 85)$
 $= 66.91$ Btu/lb dry air

Recirculation of 3%:

For 3% of air entering recirculated from the exit air, 97% comes from fresh air.

Enthalpy of recirculated air = 66.91
 Enthalpy of fresh air = 38.61

Average enthalpy of inlet mixture:

$= 0.97 (38.61) + 0.03 (66.91)$
 $= 39.41$ Btu/lb dry air

Refer now to "Moist Air" tables or other data of enthalpy vs. temperature:

At enthalpy = 39.41 Btu/lb dry air, read

Corresponding wet bulb temperature = 76°F (close)

New approach for tower design = $85^\circ - 76^\circ = 9^\circ\text{F}$, instead of the previous 10°F .

Referring back to plot of number of decks on KaV/L' vs. L'/G_a ,

Read at intersection of 9°F approach, $L'/G_a = 1.05$

5. Estimated G_a , for ground plan area

The assumed 30 decks on 9-in. spacing give a packed height of $(30-1) (9/12) = 21.8$ ft = 21 ft, 10 in. By approximate straight line interpolation given under "Ground Area Vs. Height":

$$\frac{40 \text{ ft} - 12 \text{ ft}}{40 \text{ ft} - 21.8 \text{ ft}} = \frac{2,000 - 1,400}{x}, G_a \text{ limit values are } 2,000 \text{ and } 1,400$$

$x = 390$ lb/hr (ft^2 ground area) incremental air rate
 Suggested $G_a = 1,400 + 390 = 1,790$ lb/hr (ft^2)

Then for $L'/G_a = 1.05$
 $L' = (1,790) (1.05) = 1,880$ lb/hr (ft^2)

For 5,000 gpm:
 lb/hr = $(5,000) (8.33 \text{ lb/gal}) (60)$
 $= 2,500,000$ lb/hr

$$\text{ft}^2 \text{ ground plan area} = \frac{2,500,000}{1,800} = 1,330$$

6. Cooling tower cells

Because cells are in modules of 6 ft, try combination of

$$30 \text{ ft} \times 24 \text{ ft} = 720 \text{ ft}^2$$

$$\text{Two cells} = 1,440 \text{ ft}^2$$

Using this area:

$$L' = \frac{2,500,000}{1,440} = 1,740 \text{ lb/hr (ft}^2\text{)}$$

$$G_a = \frac{1,740}{1.05} = 1,658 \text{ lb/hr (ft}^2\text{)}$$

This is about as close as can be estimated without manufacturer's data.

7. Pressure drop through packing

$$\Delta P' = N' B G_a^2 \left(\frac{0.0675}{\rho_G} \right) + N' C \sqrt{S_F} (L) G_E^2 \left(\frac{0.0675}{\rho_G} \right) \quad (9-130)$$

$$N' = 30$$

$$B = 0.34 \times 10^{-8}$$

$$C = 0.11 \times 10^{-12}$$

$$S_F = 3.00$$

$$G_a^2 = (1,658)^2 = 2,750,000$$

$$L' = 1740$$

$$G_E = 4,050 \text{ at } S_F = 3.0 \text{ and } G_a = 1,658 \text{ from Figure 9-119}$$

$$\rho_G = 0.07125 \text{ lb/ft}^3 \text{ avg. for tower}$$

$$\Delta P' = 30 (0.34 \times 10^{-8}) (2,750,000) \left(\frac{0.0675}{0.0712} \right) +$$

$$30 (0.11 \times 10^{-12}) \sqrt{3.0} (1,740) (4,050)^2 \left(\frac{0.0675}{0.0712} \right)$$

$$= 0.265 + 0.154 = 0.419 \text{ in. water}$$

This is an acceptable value.

For pressure drop comparisons of some fills, see Figure 9-129.

8. Pressure loss through louvers for induced draft tower

Assume louvers are along 24-ft dimension

Total louver face area

$$= (24) (2 \text{ cells}) (2 \text{ sides}) (6 \text{ ft high}) = 576 \text{ ft}^2$$

$$\text{ft}^2 \text{ tower ground area} = (24) (30) (2) = 1,440$$

$$\text{Air rate, lb/hr} = (1,658) (1,440) = 2,380,000$$

$$\text{cfm (at inlet)} = \frac{2,380,000}{(60) (0.075 \text{ lb/ft}^3)} = 530,000$$

Note the average value of $\rho_G = 0.07125$ could be used here.

$$\text{Face velocity through louvers} = \frac{530,000}{576} = 920 \text{ fpm}$$

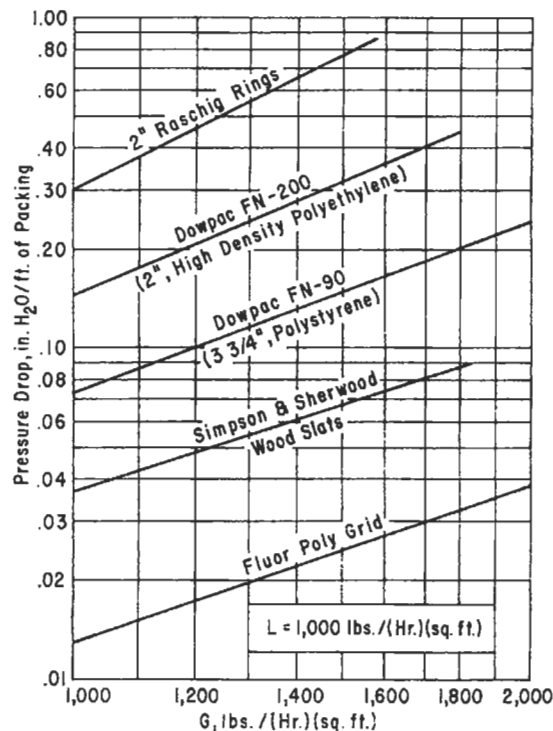


Figure 9-129. Comparison of pressure drops of several packing materials. Used by permission of Plastics Technical Service, The Dow Chemical Co., Midland Mich. with data added from Fuller, A. L., et al. *Chemical Engineering Progress*, V. 53, No. 10 (1957) p. 501; all rights reserved.

Louver pressure drop approximation from paragraph "Pressure Losses"

$$\frac{0.32 - 0.02}{x} = \frac{1,600 - 400}{1,600 - 920}$$

$$x = 0.17 \text{ in. water}$$

$$\text{Pressure loss} = 0.32 - 0.17 = 0.15 \text{ in. water}$$

Note that this value is high by 20-40% due to the approximation.

9. Pressure loss through mist eliminators

Approximation will give results on high side:

$$\frac{2,000 - 800}{2,000 - 1,658} = \frac{0.07 - 0.01}{x}$$

$$x = 0.0171 \text{ in. water}$$

$$\text{Pressure loss} = 0.07 - 0.02 = 0.05 \text{ in. water}$$

10. Total estimated static pressure loss

$$0.42 + 0.15 + 0.05 = 0.62 \text{ in. water}$$

This is an acceptable and reasonable value

11. Estimated fan brake horsepower

Assume gear drive

Air density at outlet = 0.067 lb/ft³ (close to 95% saturation at hot water temperature, induced draft fan condition).

$$\text{BHP} = \left(\frac{2,380,000}{0.067 (60)} \right) \frac{(0.62)}{(6356) (0.50)} = 115$$

This would be in at least two fans, one per cell.

$$\text{BHP/cell} = \frac{115}{2} = 57.5$$

Use 60 hp motor each.

Cooling Tower Based on Ka Data

The data on cooling water with air are usually presented in the literature as K_a values. In using this information the units should be checked very carefully.

1. Height of packing

$$Z = NL'/K'a \quad (9-131)$$

where K'_a = enthalpy coefficient of total heat transfer,
Btu/(hr) (ft³ tower packing volume)
(enthalpy difference between air and water)

2. Number of transfer units

$$N = \int_{t_2}^{t_1} \frac{dt}{h' - h} \quad (9-126)$$

3. $K'a$ Data

Figure 9-128 presents data for several packings in water cooling service.

4. Pressure Drop

Data is given in Figure 9-129 for water-air system.

Performance of Atmospheric and Natural Draft Towers

The evaluation of atmospheric and natural draft towers has not been completely presented in the detail comparable to mechanical draft towers. Some data are available in estimating form, but the evaluation of transfer rates is only adequate for estimating purposes [4]. The design of such towers by the process engineer must be made only after due consideration of this, and ample factor of safety should be included. Figure 9-130 presents general information on water loss due to wind on the tower.

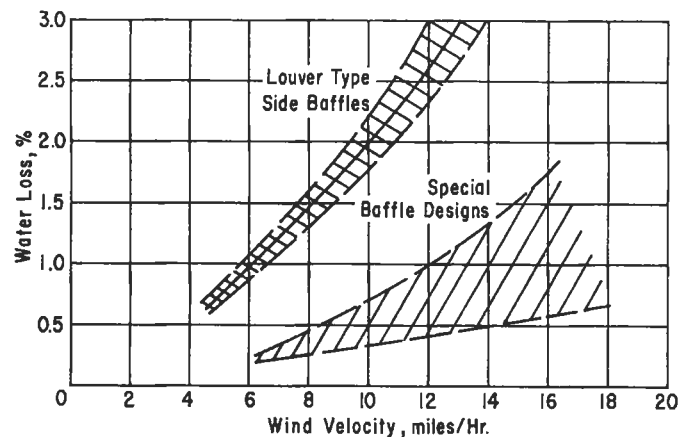


Figure 9-130. Atmospheric cooling tower; water loss for various wind velocities. Used by permission of Plastics Technical Service, The Dow Chemical Co., Midland Mich. with data added from Fuller, A. L., et al. *Chemical Engineering Progress*, V. 53, No. 10 (1957) p. 501; all rights reserved.

Nomenclature

- A = Tower cross-section, ft², or riser area, ft²
- A' = Constant in cooling tower performance equation, Equation 9-129, or in mass transfer = L_m/mG_m
- A_F = Final column inside net area, ft², or in. ²
- a = Surface area of an orifice, in. ²
- a = Effective interfacial area for contacting gas and liquid phases, ft²/ft³. Because this is very difficult to evaluate, it is usually retained as a part of the coefficient such as K_{Ga} or $K_L a$
- a = Area of transfer surface per unit of tower volume in water cooling towers, ft²/ft³, or, termed contact area
- α = Relative volatility between components 1 and 2
- A_0 = Column (tower) net inside operating area, ft²
- a/ε^3 = Packing factor, F , not equivalent to experimental values reported
- a' = Wetted packing surface, not necessarily same as effective interfacial surface area for contact, ft²/ft³
- a_t = Total specific packing surface area, ft²/ft³
- ACFM = Actual air volume, ft³/min, or = F
- B = Rate of blowdown, (cooling tower), gpm; or = constant in pressure drop equation for cooling tower
- BHP = Brake horsepower
- C = Concentration, lb mol/ft³
- C' = Constant in pressure drop equation for cooling towers
- C_0 = Capacity rating, ft/sec, or m/sec (Norton Chart)
- C_0 = Constant specific to a particular packing, also,

- C_1 = Constant specific to a particular packing.
 $C_3 = 7.4 \times 10^{-8}$
 $C_4 = 2.7 \times 10^{-5}$
 C_f = Vapor capacity factor, (vapor velocity) (vapor density)/(liquid - vapor density)^{0.5}
 C_{lm} = Log mean of the driving force at the top and bottom of tower
 C_p = Correction factor for high gas ratios, see Figure 9-92
 C_s = Capacity factor = C factor = C, ft/sec
 C_{sc} = Efficient capacity, ft/sec, or m/sec (Norton Chart)
 CR = Cooling range (cooling tower), °F
 c = Concentration of solution, lb solute/ft³ solution
 c, c_0, c_1, c_2, c_3 = Correlation constants
 D = Tower diameter, in. or ft as appropriate
 D_1 = Density of liquid, lb/ft³ = 1, or = L
 DL = Rate of drift loss (cooling tower), gpm
 D_L = Diffusivity of solute in liquid, ft²/hr; or = D_1
 D_g = Gaseous diffusion coefficient, ft²/hr
 D_p = Equivalent spherical diameter of particle as a sphere possessing same surface area as a piece of packing, ft
 D'_p = Nominal packing size, ft
 D_v = Diffusivity of solute in gas, ft²/hr
 D_v = Density of vapor, lb/ft³ = v
 d = Diameter of hole, in.; or orifice diameter, in.
 d_i = Individual packing piece inside diameter, in.
 d_o = Individual packing piece outside diameter, in.
 d_p = Equivalent spherical diameter of particle as a sphere possessing same surface area as a piece of packing, in.
 E = Rate of evaporation (cooling tower), gpm
 E = Overall column efficiency, %
 e = Base of natural logarithms
 F = Packing factor; experimentally determined, ft⁻¹
 F = Actual cfm at fan inlet
 F' = a/ϵ^3 , characteristic of packing size and shape, not packing factor
 FP = Flow parameter, = F-factor, = F
 F_p = Packing factor, empirical, dimensionless
 F_{pdt} = Dry-bed packing factor, dimensionless
 Fr_1 = Liquid Froude Number
 F_s = Superficial F-factor, $V_s (\rho_v)^{0.5}$, ft/sec (lb/ft³)^{0.5}
 f_a = Fraction of total packing area, a_t , wetted
 G = Superficial mass gas rate, lb/(sec) (ft² tower cross-section) or lb/hr, lb/sec, or lb/hr-ft², lb-mol/(sec) (ft²), depending on equation units
 G' = Superficial mass gas (vapor) rate, lb/(hr) (ft² tower cross-section, or lb/hr
 G'' = Gas rate, lb/sec
 G_a = Air mass velocity, lb dry air/(hr) (ft² of plan area)
 GA = Design vapor flow rate, lb/hr
 G_E = Equivalent mass air velocity for pressure drop between air and falling water drops, (lb/hr)/ft² of plan area, see Figure 9-119.
 G_f = Gas loading factor
 G_m = Gas molar mass velocity, lb mol/(hr) (ft²)
 G_h = Gas mass velocity, lb/(hr) (ft²)
 g_c, g = Acceleration of gravity, 32.2 ft/(sec) (sec)
 H, HTU = Height of a transfer unit, ft, or = differential head at orifice, ft liquid
 H' = Henry's Law constant, lb mol (ft³) (atm), or other units to suit system
 $HETP$ = Height equivalent to a theoretical plate, ft or in. when specified
 H_g = Height of individual gas film transfer unit, ft
 H_G = same as H_g
 H_l = Height of individual liquid film transfer unit, ft
 H_L = same as H_l
 H_{OG} = Height of transfer unit, based on overall gas film coefficients, ft or in. as specified
 H_{OL} = Height of transfer unit, based on overall liquid film coefficients, ft
 $(HTU)_{OG}$ = Height of gas phase transfer unit, ft or in.
 h = Enthalpy of the main air stream, Btu/lb
 h = Liquid height over orifice, in. liquid
 h' = Enthalpy of saturated air film at bulk water temperature, Btu/lb
 h_d = Vapor pressure drop across distributor, in. liquid
 h_1 = Liquid hold-up, ft³/ft³ packed tower volume
 h_o = Operating hold-up for any liquid, ft³/ft³ packing volume
 h_s = Static hold-up for any liquid, ft³/ft³ packing volume
 h_t = Total hold-up, ft³ liquid/ft³ packing volume
 h_1^* = Enthalpy of air at any temperature higher than inlet, Btu/lb dry air; note: h_1 = exit air
 h_2 = Enthalpy of inlet air to tower, equivalent to enthalpy of saturated air at wet bulb temperature, Btu/lb dry air from *Moist Air Tables*, ASHVE Guide
 h_{ow} = Operating hold-up for water, ft³/ft³ packing volume
 h_{sw} = Static hold-up for water, ft³/ft³ packing volume
 h_{tw} = Water hold-up, ft³ liquid/ft³ tower volume
 i_L = Enthalpy of air saturated at bulk water temperature, Btu/lb dry air
 i_G = Enthalpy of air saturated at wet bulb temperature, Btu/lb dry air
 j = Constant, Table 9-41
 K = Overall enthalpy transfer coefficient, lb/(hr) (ft² transfer area) (lb water/lb dry air); or, mass transfer coefficient, lb water/(hr) (ft²)
 K'_a = Enthalpy coefficient of total heat transfer, Btu/(hr) (ft³ tower packing volume) (enthalpy difference between air and water)
 K_G = Gas phase mass transfer coefficient, lb mol/(hr) (ft²) (atm)
 K_{Ga} = Overall gas mass transfer coefficient, lb mol/(hr) (ft³) (atm)
 K_L = Overall mass transfer coefficient based on liquid phase, lb mol/(hr) (ft²) (lb mol/ft³)
 K_{La} = Overall mass transfer coefficient based on liquid film controlling, lb mol (hr) (ft³) (lb mol/ft³)

- k_G = Gas-phase mass transfer coefficient, lb mol/(hr) (ft²) (atm)
 k_{GA} = Individual gas mass transfer coefficient, lb mol/(hr) (ft³) (atm)
 k_L = Liquid phase mass-transfer coefficient, lb mol/(hr) (ft²) (lb mol/ft³)
 k_{LA} = Individual liquid mass transfer coefficient, lb mol/(hr) (ft³) (lb mol/ft³)
 L = Liquid superficial mass rate, lb/(sec) (ft² tower cross-section), or lb/sec, depends on equation, or, lb mol/ft², or liquid rate, lb/sec-ft², or lb/hr-ft²
 L', L = Liquid (or water rate) superficial mass rate, lb/(hr) [ft² tower plan cross-section, when specified], or lb/hr
 L_c = Critical liquid rate for liquid continuous system, at which the packing becomes completely wetted and tower operation is in the liquid continuous range, lb/(hr) (ft²)
 L_f = Liquid loading factor
 L_h = Liquid mass velocity, lb/(hr) (ft²)
 L_M = Liquid mass rate, lb mol/(hr) (ft²), or lb mol/hr
 L_{min} = Minimum liquid wetting rate in packed tower, ft³/(hr) (ft² cross-section)
 l = Individual packing piece height (or length), in.
 m = Slope of equilibrium line, mol fraction
 M = Molecular weight of compound
 M_M = Mean molecular weight of gas, lb/lb mol
 MWR = Minimum wetting rate, liquid, ft³/(hr) (ft² cross-section)/ft² packing surface/(ft³ tower volume)
 MWR_G = Minimum wetting rate, gpm/ft², (Eq. 9-14)
 MWR_T = Minimum wetting rate, gpm/ft², constant, allowing for vertical height consumed by distribution/redistribution equipment, see Table 9-25
 N = Number of transfer units
 N' = Number of deck levels in cooling tower
 NO_G = Number of transfer units, based on overall gas film coefficients
 NO_L = Number of transfer units, based on overall liquid film coefficients
 $(NTU)_{OG}$ = Number of gas transfer units
 n = Moles absorbed or transferred, lb mol/hr; or,
 n = Number of holes in distributor
 n = Constant in cooling tower performance equation, or constant for Equation 9-125.
 P = Average total pressure in tower, atm or absolute units, or = P_{avg}
 ΔP_{pb} = Specific pressure drop through dry bed, in. water/ft packing
 P_{BM} = Mean partial pressure of inert gas in the gas phase, atm
 ΔP = Pressure drop, in. water/ft packed height, or in. of liquid; or pressure drop through risers, in. liquid.
 $\Delta P'$ = Air pressure loss, in. of water
 ΔP_{flood} = Pressure drop at flood point for all random packings, in. of water/ft of packing height
 ΔP_d = Dry bed pressure drop, in. water/ft packed height
 ΔP_w = Wet pressure drop, in. liquid/ft packed height (Nutter)
- p = Partial pressure of soluble gas, atm
 p_{lm} = Log mean partial pressure of gas in inlet and exit gas streams, atm
 p_s = Total static pressure of fan, in. of water
 Q = Liquid volumetric flow rate, gpm
 Q_c = Condenser duty, Btu/hr
 O_r = Reboiler duty, Btu/hr
 Re_g = Reynolds Number for gas/vapor
 \bar{S} = Tray spacing, in. (or ft when specified)
 S = Length of corrugation side (structured packing)
 S_F = Vertical free fall of water drops, ft
 Sc_g = Gas phase Schmidt Number
 T = Absolute temperature, °R = °F + 460
 t = Bulk water temperature, °F or t_L , if specified
 t_1 = Entering or inlet water temperature, or at bottom of tower, °F
 t_2 = Outlet water temperature, or at top of tower, °F
 t'_2 = Any water temperature lower than inlet water temperature and higher than inlet air wet bulb temperature, °F
 t_L = Water temperature of bulk water, °F
 u_g = Superficial velocity, based on cross-section area of empty column, ft/sec
 u_{maxIE} = Calculated or estimated maximum superficial vapor velocity, ft/sec
 u_{max} = Maximum vapor velocity for actual packing, ft/sec
 U_{gc} = Effective velocity of gas
 U_g = Superficial velocity of gas
 U_l = Superficial velocity of liquid
 V = Tower volume, ft³/ft² ground plan area; or active cooling volume, ft³/ft² plan area
 V = Horizontal liquid velocity, ft/sec (in distributor)
 V = Vapor rate, ft³/sec, or ft/sec
 V' = Vapor flow, lb mol/hr
 V_L = Liquid rate, gpm
 V_g = Superficial gas velocity, ft/sec
 V_A, V_B = Molecular volume of gases, obtained by Kopp's Law of additive volumes, cc/gm mole at normal boiling point, see Table 9-44.
 V_r = Reboiler vapor rate, lb/hr
 V_s = Superficial vapor velocity, ft/sec (or across tower cross-section)
 V_{SL} = Liquid velocity based on superficial tower area, gpm/ft²
 V_v = Vapor rate, ft³/sec
 X = Flow parameter (Norton Co.) = $F = FP$
 X = Concentration of solute in liquid, lb mol solute/lb mol solute free solvent (or stream)
 X^* = Concentration of solute in liquid, in equilibrium with the gas, lb mol solute/lb mol solvent
 x = Concentration of solute in liquid, mole fraction, or mol fraction of more volatile component in liquid phase
 X_1, X_2 = Curve fit coefficients for C_2 , Table 9-32
 X_3, X_4 = Curve fit coefficients for C_3 , Table 9-32
 x^* = Concentration of solute in liquid in equilibrium with gas, mol fraction
 Y = Concentration of solute in gas, lb mol solute/lb mol solute free (solvent) (stream)
 Y = Capacity parameter (Norton)

- Y* = Concentration of solute in gas in equilibrium with liquid, lb mol solute/lb mol solute free (solvent, stream)
 y = Mole fraction of solute in gas, or mol fraction of more volatile component in vapor phase
 y* = Mole fraction gas phase composition in equilibrium with a liquid composition, x
 Z = Height of packed section in tower, ft

Subscripts

- A, B = Refer to different items, gases, etc.
 a = Air
 f = Flooding condition, or flood
 G = Gas or vapor, v or V
 L = Liquid, or l
 OG = Overall gas phase
 V = Vapor, or v
 w = Water
 1 = Refers to inlet, or condition one (1)
 2 = Refers to outlet, or condition 2

Greek Symbols

- α = Relative volatility
 α_{lh} = Average relative volatility, light to heavy component
 α = Constant, or relative volatility between two components
 β = Constant
 ν = Constant
 λ = Ratio of two slopes (equilibrium and operating lines)
 π = Total absolute pressure, or 3.141, as appropriate for calculation
 Δ_M or Δ_{middle} = Driving force at middle position on gas or liquid basis.
 Δ_m or Δ_{mean} = Mean driving force on gas or liquid basis
 ε = Void fraction of packing under operating conditions; = void fraction of dry packing minus the total hold-up (not the free volume of dry packing)
 μ = Viscosity of liquid, centipoise
 μ' = Absolute viscosity, lb/sec/ft
 μ_a = Viscosity, lb/(hr) (ft)
 μ_l or μ_L = Viscosity of liquid, lb/(hr) (ft)
 μ_{Ga} = Gas viscosity, lb/(hr) (ft)
 ν = Kinematic viscosity, liquid; centistokes
 ρ = Density, lb/ft³
 ρ' = Liquid density, g/cc
 ρ_L = Liquid density, lb/ft³
 ρ_G = Gas density, lb/ft³
 σ = Surface tension, dynes/cm
 ψ = Ratio of density of water to density of new liquid (dimensionless); or parameter for a packing from Figures 9-21D, 9-93, and 9-94.
 \propto = Proportional to
 θ = Angle of flow channel from horizontal
 ϕ = For Equation 9-24, and Table 9-41, or Figure 9-90 or 9-91.

References

1. "Acceptance Test Procedure for Water-Cooling Towers, ATP-105," Cooling Tower Institute, Palo Alto, Calif.
2. *Air Conditioning Refrigerating Data Book*, 10th Ed. (1958), American Society of Heating, Refrigerating and Air-Conditioning Engineers, Inc., 234 Fifth Ave., New York 1, N.Y.
3. Baker, T., C. H. Chilton, and H. C. Vernon. "The Course of Liquor Flow Packed Towers," *Trans. Amer. Inst. Chem. Engrs.* 31, 296 (1935).
4. Bulletin, "Fluor Aerator Cooling Towers," The Fluor Corp. Ltd., Los Angeles, Calif. (1944).
5. Bulletin TP-54, Tower Packings, U.S. Stoneware Co., Akron, Ohio.
6. Bulletin S-29, Intalox Saddle Packing, The United States Stoneware Co., Akron, Ohio.
7. Campbell, J. M. and R. L. Huntington, "Heat Transfer and Pressure Drop in Fixed Beds of Spherical and Cylindrical Solids," *Pet. Ref.*, 30, 12, 127 (1951).
8. Chilton, C. H., "Drift or Mist Eliminator Loss," *Trans. Inst. Chem. Engrs.* 30, 235 (London) (1952).
9. Chilton, T. H. and A. P. Colburn, Part II, "Pressure Drop in Packed Tubes," *Trans. A.I.Ch.E.* 26, 178 (1931).
10. Colburn, A. P., "The Simplified Calculation of Diffusional Processes, General Considerations of Two Film Resistance," *Trans. A.I.Ch.E.* 35, 211 (1939).
11. Colburn, A. P., "Simplified Calculation of Diffusional Processes," *Ind. Eng. Chem.* 33, 459 (1941).
12. Cornell, Knapp, and Fair, *Chem. Engr. Progr.* 56 (7) (1960) p. 68.
13. Cornell, et al., *Chem Engr. Progr.*, (58) (8) 1960, p. 68.
14. Fair, J., *Chem Engr. Progr.*, 76, (15) (July 1969).
15. Cooling Tower Performance, Bulletin CT-43-2, Foster Wheeler Corp., New York, N.Y.
16. "Cooling Tower Wood Maintenance, TSC-302," Cooling Tower Institute, Palo Alto, Calif.
17. Cooper, C. M., R. J. Christl and L. C. Perry, "Packed Tower Performance at High Liquor Rates," *Trans. Amer. Inst. Chem. Engr.* 37, 979 (1941).
18. Coulson, J. M. and J. F. Richardson, *Chemical Engineering*, Vol. II, 719 (1955), McGraw-Hill Book Co., New York, N.Y.
19. "Counterflow Cooling Tower Performance," J. F. Pritchard and Co. of California, Kansas City, Mo. (1957).
20. Czermann, J. J., S. L. Gyokhegyi, and J. J. Hay, "Design Packed Towers Graphically," *Pet. Ref.* 37, No. 4, 165, (1958).
21. Dwyer, O. E., and B. F. Dodge, "Rate of Absorption of Ammonia by Water in a Packed Tower," *Ind. Eng. Chem.* 36, 485 (1941).
22. Eckert, J., U.S. Stoneware Co., private communication.
23. Eckert, J. S., E. H. Foote and R. L. Huntington, "Pall-Rings—New Type of Tower Packing," *Chem. Engr. Progress*, 54, No. 1, 70 (1958).
24. Eckert, R. G., and Walter, *Hydrocarbon Processing*, 43 (2) (1964) p. 107.
25. Ellis, *Chem. Engr. News*, 31 (44) (1953) p. 4613.
26. Elgin, J. C. and F. B. Weiss, "Liquid Hold-up and Flooding in Packed Towers," *Ind. Eng. Chem.* 31, 435 (1939).
27. Fellingner, L., Sc. D. Thesis, Mass. Inst. Technol. (1941).
28. Furnas, C. C. and F. Bellinger, "Operating Characteristics of Packed Columns," *Trans. A.I.Ch.E.* 34, 251 (1938).
29. Gambill, W. R., "How To Estimate Mass Transfer Factors," *Chem. Eng.*, Dec. p. 207 (1955).

30. Goitein, E. E., "Selection and Application of Cooling Towers," *Combustion*, Nov., p. 38 (1957).
31. "Grades of Redwood Lumber, Std.-101," Cooling Tower Institute, Palo Alto, Calif.
32. Griswold, J., D. Andres and V. A. Klein, "Determination of High Pressure Vapor-Liquid Equilibria. The Vapor-Liquid Equilibrium of Benzene-Toluene," *Trans. Amer. Inst. Chem. Engrs.* 39, 223 (1943).
33. Hands, C. H. G. and F. R. Whitt, "Design of Packed Distillation Columns II, Operating Vapor Rates for Packed Distillation Columns," *J. Appl. Chem.*, Jan. 1, p. 19 (1951).
34. Hands, C. H. G. and F. R. Whitt, "Design of Packed Distillation Columns IV. An Empirical Method For the Estimation of Column Height Using the H.E.T.P. Concept," *J. Appl. Chem.*, Mar. 1, p. 135 (1951).
35. *International Critical Tables*, Ed. W. Washburn, Editor, Vol. V, p. 213, National Research Council, McGraw-Hill Book Co., New York, N.Y.
36. Jesser, B. W. and J. C. Elgin, "Studies of Liquid Hold-up in Packed Towers," *Trans. Amer. Inst. Chem. Engrs.*, 39, No. 3 277 (1943).
37. Johnstone, H. F. and A. D. Singh, "Recovery of Sulfur Dioxide from Waste Gases," *Ind. Eng. Chem.*, 29, 286 (1937).
38. Kelly, N. W. and L. K. Swenson, "Comparative Performance of Cooling Tower Packing Arrangement," *Chem. Eng. Prog.*, 52, p. 265 (1956).
39. Kern, D., Q., *Process Heat Transfer*, 1st Ed., McGraw-Hill Book Co., Inc., New York, N.Y. (1950) p. 600.
40. Leva, M., "Tower Packings and Packed Tower Design," 2nd Ed. U.S. Stoneware Co., Akron, Ohio (1953).
41. Leva, M., *Chemical Engineering Progress Sym. Series No. 10*, 50, 151 (1954).
42. Leva, M., "Gas Absorption in Beds of Rings and Saddles," *A.I.Ch.E. Jour.*, No 2, p. 224 (1955).
43. Leva, M., "Flow Through Packings and Beds," *Chem. Eng.* 64, 261 (1957).
44. Leva, M., J. M. Lucas and H. H. Frahme, "Effect of Packing Supports on Mechanical Operation of Packed Towers," *Ind. Eng. Chem.* 46, No. 6, 1225 (1954).
45. Lerner, B. J., and C. S. Grove, Jr., "Critical Conditions of Two-Phase Flow in Packed Columns," *Ind. Eng. Chem.* 43, 1, p. 216 (1951).
46. Lichtenstein, S., "Performance and Selection of Mechanical Draft Cooling Towers," *Trans. Amer. Soc. Mech. Engrs.*, Oct. p. 779 (1943).
47. Lobo, W. E., L. Friend, F. Hashmall and F. Zenz, "Limiting Capacity of Dumped Tower Packings," *Trans. Amer. Inst. Chem. Engrs.* 41, 693 (1945).
48. Mass Transfer, Inc., "Absorption, Distillation Optimization," (1978) p. 14.
49. Menta and Parekh, M. S. Thesis Chemical Engineering, Mass. Inst. Technology, Cambridge, Mass. (1939).
50. Molstad, M. C., R. G. Abbey, A. R. Thompson, and J. F. McKinney, "Performance of Drip-Point Grid Tower Packings," *Trans. A.I.Ch.E.* 38, 387 (1942).
51. Molstad, M. C., J. F. McKinney and R. G. Abbey, "Performance of Drip-Point Grid Tower Packings," *Trans. Amer. Inst. of Chem. Engr.* Vol. 39, No. 5, 605 (1943).
52. Morris, R. and J. Jackson, *Absorption Towers*, Butterworth Scientific Publications (1953), London, England.
53. Murch, D. P., "Height of Equivalent Theoretical Plate in Packed Fractional Columns." *Ind. Eng. Chem.*, 45, 2616 (1953).
54. Norton Company, "Design Information for Packed Towers," Bulletin DC-11 (1977).
55. Otake, T. and K. Okada, "Liquid Hold-up in Packed Towers, Operating and Holdup Without Gas Flow," *Soc. Chem. Engrs. (Japan)* 17, No. 7, 176 (1953).
56. Oldershaw, C. F., L. Simenson, T. Brown and F. Radcliffe, "Absorption and Purification of Hydrogen Chloride from Chlorination of Hydrocarbons," *Chem. Eng. Prog. Trans. Section*, 43, No. 7, 371 (1947).
57. Planovski, Khimicheskay, *Prom.*, 45, No. 3, p. 16-20.
58. Robinson, C. S. and E. R. Gilliland, *Elements of Fractional Distillation*, 4th Ed. (1950) McGraw-Hill Book Co., Inc., New York, N.Y.
59. Sakiadis, B. C. and A. I. Johnson, "Generalized Correlation of Flooding Rates," *Ind. Eng. Chem.*, 46, 1229 (1954).
60. Sarchet, B. R., "Flooding in Packed Towers," *Trans. A.I.Ch.E.*, 38, No. 2, 293 (1942).
61. Sherwood, T. K. and F. A. L. Holloway, "Performance of Packed Towers—Experimental Studies of Absorption and Desorption," *Trans. Amer. Inst. Chem. Eng.*, 36, 21 (1940).
62. Sherwood, T. K. and F. A. L. Holloway, "Performance of Packed Towers, Liquid Flow Data For Several Packings," *Trans. Amer. Inst. Chem. Engrs.*, 36, 39 (1940).
63. Sherwood, T. K. and R. L. Pigford, *Absorption and Extraction*, 2nd Ed. (1952) McGraw-Hill Book Co., Inc., New York, N.Y. p. 161.
64. Shulman, H. L., C. F. Ullrich and N. Wells, "Performance of Packed Columns, Total, Static and Operating Holdups," *Amer. Inst. Chem. Engr. Jour.* 1, No. 2, 247 (1955).
65. Shulman, H. L., C. F. Ullrich, A. Z. Proulx and J. O. Zimmerman, "Wetted and Effective Interfacial Areas, Gas- and Liquid-phase Mass Transfer Rates," *A.I.Ch.E. Jour.* 1, No. 2, 253 (1955).
66. Shulman, H. L., C. F. Ullrich, N. Wells and A. Z. Proulx, "Holdup for Aqueous and Nonaqueous Systems," *A.I.Ch.E. Jour.* Vol. 1 No. 2, 259 (1955).
67. Shulman, H. L. and J. E. Margolis, "Performance of Packed Columns," *A.I.Ch.E. Jour.*, Vol. 3, 157 (1957).
68. Silvey and Keller, Proc. Intern. Symp. Dist. (Brighton, U.K.) (1970).
69. Spector, N. A., and B. F. Dodge, "Removal of Carbon Dioxide from Atmospheric Air," *Trans. Amer. Inst. Chem. Engrs.* 42, 827 (1946).
70. "Structural Design Data, Std-102," Cooling Tower Institute, Palo Alto, California.
71. Teller, A. J., "Packing Performance Below and Above Flooding," preprint copy prior to presentation at A.I.Ch.E. meeting 1953.
72. Tepe, J. B. and B. F. Dodge, "Absorption of Carbon Dioxide Sodium Hydroxide Solutions in a Packed Column," *Trans. Amer. Inst. Chem. Engrs.* 39, 255 (1943).
73. Tillson, Thesis, Mass. Inst. Technology, Cambridge, Mass. (1939).
74. Treyball, R. E. *Mass Transfer Operations*, McGraw-Hill Book Co., New York, N.Y. (1955).
75. Van Nuys, C. C., "Enthalpy and Heats of Dilution of the System HCl-H₂O," *Trans. Amer. Inst. Chem. Engrs.* 39, 663 (1943).
76. Vivian, J. E. and R. P. Whitney, "Absorption of Chlorine in Water," *Chem. Eng. Prog.*, Trans. Sect., 43, 691 (1947).
77. Chin-Yung Wen, "Ammonia Absorption in Beds of Saddles," Thesis, West Virginia University (1953).
78. Whitesell, Jack, "How To Evaluate Variable in Counterflow Cooling Towers," *Chem. Eng.* 62, Jan., p. 187 (1955).

79. Whitney, R. P. and J. E. Vivian, "Absorption of Sulfur Dioxide in Water," *Chem. Eng. Prog.* 45, 323 (1949).
80. Whitt, F. R., "A Correlation For Absorption Column Packings," *British Chem. Eng.*, July, p. 395 (1959).
81. Zenz, F. A., "What Every Engineer Should Know About Packed Tower Operations," *Chem. Eng.*, August, p. 176 (1953).
82. Strigle, R. F. Jr., *Random Packings and Packed Towers*, Gulf Publishing Co. Houston, Texas (1987).
83. Norton Chemical Process Products, "Intalox® High Performance Separation Systems," Bulletin IHP-1, Norton Chemical Process Products Corporation (1987).
84. Kunesh, J. G., L. L., Lahm, and T., Yanagi, "Liquid Distribution Studies in Packed Beds," *Ind. Eng. Chem. Res.* 26 (1987) p. 1845. Presented at A.I.Ch.E. meeting, Chicago, Nov. (1985).
85. Perry, D., D. E. Nutter, and A. Hale, "Liquid Distribution for Optimum Packing Performance," *Chem. Eng. Prog.*, Jan. (1990) p. 30.
86. Hoek, P. J., and F. J. Zuiderweg, *Chem. Eng. Res. Des.*, V. 64 (1986) 431.
87. Moore, F. D., "Distributor Design and the Effects on Tower Performance," Norton Chemical Process Products Corp. (1984).
88. Nutter, D. E., "Nutter Rings™, A Random Packed Developed for Consistent Performance," *Inst. of Chem. Engrs. Sym. Series No. 104*, (1987), p. A 129, Brighton, U.K.; also presented at A.I.Ch.E. Annual meeting, Miami Beach, Fla. Nov. (1986).
89. Perry, R. H., and D. Green, *Perry's Chemical Engineers Handbook*, 6th Ed. McGraw-Hill, Inc., New York, N.Y. (1984).
90. Kister, H. Z., *Distillation Design*, McGraw-Hill, Inc., New York, N.Y. (1992).
91. Kister, H. Z., *Distillation Operation*, McGraw-Hill, Inc. New York, N.Y. (1990).
92. Schmidt, R. I. *Chem. E. Sym. Fund.*, V. 6 (1967) p. 400.
93. Kister, H. Z. and D. R. Gill, "Predict Flood Point and Pressure Drop for Modern Random Packings," *Chem. Eng. Prog.*, V. 87, No. 2 (1991) p. 32.
94. Strigle, R. F., and F. Rukovena, "Packed Distillation Column Design," *Chem. Eng. Prog.*, V. 75 March (1979) p. 86.
95. Zenz, F. A., *Chem. Eng.*, Aug. (1953) p. 176.
96. Robbins, L. A., "Improve Pressure Drop Prediction with a New Correlation," *Chem. Eng. Prog.*, May (1991), p. 87.
97. Nutter Engineering, Harsco Corp. "Nutter Ring™ Random Packing," Bulletin NR-2, and private communication.
98. Nutter, D. E., private communication.
99. Nutter, D. E., and D. Perry, "Packing Capacity/Pressure Drop Models," presented A.I.Ch.E., New Orleans, La. (1988).
100. "Koch Sulzer Rectification Columns," Bulletin KS-1, Koch Engineering Co., Inc., Wichita, Kansas.
101. "Koch Flexipac® Structured Packing," Bulletin KFP-4, Koch Engineering Co., Inc.
102. "Intalox® High Performance Structured Packing," Bulletin IS-IR; Norton Chemical Process Products Corporation.
103. Martin, C. L., J. L. Bravo, and J. R. Fair, "Performance of Structured Packing in Distillation Service—Experimental and Modeling Results," presented at New Orleans, LA, A.I.Ch.E. Meeting, Mar. 7 (1988).
104. "A Family of Gempak® Packings for High Efficiency Fractionation," Bulletin 5140 (1993), Glitsch, Inc.
105. "Nutter Snap Grid™" Bulletin SG-1, Nutter Engineering Co., Harsco Corp.
106. "Koch Flexigrid Structural Packing," Bulletin KFG-2, Koch Engineering Co. Inc.
107. "Glitsch-Grid," Bulletin 217-5, 9-72, Glitsch, Inc.
108. Fair, J. R., and J. L. Bravo, "Distillation Columns Containing Structured Packing," *Chem. Eng. Prog.*, Jan. (1990) p. 19.
109. Billet, R., "Packed Column Analysis and Design," Glitsch, Inc. Dallas, Texas (1986), confidential in-house report, not available to this author.
110. Rukovena, F., "Effect of Pressure on Structured Packing Performance," presented at A.I.Ch.E. meeting, Houston, Texas.
111. Bravo, J. L., J. A. Rocha, and J. R. Fair, *Hydro. Processing*, V. 65, Jan. (1986) p. 45.
112. Stihlman, J., J. L. Bravo, and J. R. Fair, *Gas Separation Purification*, V. 3 (1989) p. 19.
113. Bravo, J. L., J. A. Rocha, and J. R. Fair, *Hydro. Processing*, V. 64, Jan. (1985) p. 91.
114. Hatfield, J. A., "High Efficiency Tower Packings and Responsive Control Schemes," *Chem. Processing*, Sept. (1988) p. 130.
115. Bravo, J. L., J. A. Rocha, and J. R. Fair, "Pressure Drop in Structured Packings," *Hydro. Processing*, V. 65, Mar. (1986) p. 45.
116. Shah, G. C., "Effectively Troubleshoot Structural Packing Distillation Systems," *Chem. Eng. Prog.*, V. 87, Apr. (1991) p. 49.
117. Dean, J. A., H. M. Turner, and B. C. Price, "How Packing Works in Dehydration," *Hydro. Processing*, V. 70, No. 4 (1991) p. 47.
118. Hausch, G. W., P. K. Quotson, and K. D. Seeger, "Structured Packing at High Pressure," *Hydro. Processing*, V. 71, No. 4 (1992) p. 67.
119. "Packings Growing Role in Distillation," *Chem. Week*, June 13 (1984) p. 18.
120. Hufton, J. R., J. L. Bravo, and J. R. Fair, "Scale-up of Laboratory Data for Distillation Columns Containing Corrugated Metal-type Structured Packing," *Ind. and Eng. Chem. Res.*, American Chem. Soc., V. 27, No. 11 (1988) p. 2096.
121. Eckert, L. S., "A New Look at Distillation Tower Packings Comparative Performance," *Chem. Eng. Prog.*, V. 59, No. 5 (1963) p. 76.
122. Eckert, J. S., "No Mystery in Packed-Bed Design," *Oil and Gas J.*, Aug. 24 (1970).
123. Billet, R., "Gauze-Packed Columns for Vacuum Distillation," *Chem. Eng.*, V. 79, No. 4 (1972) p. 68.
124. Hsu, Shih-liang, "Packing Pressure Drop Estimated," *Hydro. Processing*, V. 64, No. 7 (1985) p. 89.
125. Eckert, J. S., "Design Techniques for Sizing Packed Towers," *Chem. Eng. Prog.*, V. 57, No. 9 (1961) p. 54.
126. Kunesh, J. G., "Practical Tips on Tower Packing," *Chem. Eng.* V. 94, No. 18 (1987) p. 101.
127. Koshy, T. D. and F. Rukovena, "Reflux and Surface Tension Effects on Distillation," *Hydro. Processing*, V. 65, No. 5 (1986) p. 64.
128. Stadig, W. P., "Troubleshooting and Revamping Distillation Columns," *Chem. Processing*, Feb. (1989).
129. Bolles, W. L., and Fair, J. R., "Improved Mass-Transfer Model Enhances Packed-Column Design," *Chem. Eng.* V. 89, No. 14 (1982) p. 109.
130. Ward, H. C. and J. T. Sommerfield, "New Flooding Equation," *Hydro. Processing*, V. 61, Oct. (1982) p. 99.
131. Bonilla, J. A., "Don't Neglect Liquid Distributors," *Chem. Eng. Prog.*, V. 89, No. 3 (1993) p. 47.
132. Nutter, D. E., F. C. Silvey, and B. K. Stober, "Random Packing Performance in Light Ends Distillation," *Inst. of Chem. Engrs. (England)*, publication date not given.

133. Chen, G. K., "Packed Column Internals," *Chem. Eng.*, Mar. 5 (1984) p. 40.
134. Harrison, M. E., "Consider Three-phase Distillation in Packed Columns," *Chem. Eng. Progr.*, V. 86, No. 11 (1990) p. 80.
135. Bravo, J. L., "Effectively Fight Fouling of Packing," *Chem. Eng. Progr.*, V. 89, No. 4 (1993) p. 72.
136. Kister, H. Z., K. F. Larson and T. Yanagi, "How Do Trays and Packings Stack Up?" *Chem. Eng. Progr.*, V. 90, No. 2 (1994) p. 23.
137. Kister, H. Z., K. F. Larson, and T. Yanagi, "Capacity and Efficiency: How Trays and Packings Compare," A.I.Ch.E. Spring meeting, Mar. (1995).
138. Capps, R. W., "Consider the Ultimate Capacity of Fractionation Trays," *Chem. Eng. Progr.*, V. 89, No. 3 (1993) p. 37.
139. Strigle, R. F., Jr., *Packed Tower Design and Applications: Random and Structured Packings*, 2nd Ed. Gulf Pub. Co., Houston, Texas (1994).
140. Kaiser, V., "Correlate the Flooding of Packed Columns a New Way," *Chem. Eng. Progr.*, V. 90, No. 6 (1994) p. 55.
141. Nutter Engineering Co., Harsco Corp., Bulletin B-1, "High Efficiency Structured Packings."
142. Vital, T. J., et al. *Hydro Processing*, V. 63, No. 12 (1984) p. 95.
143. Porter, K. E. and J. D. Jenkins, *Institution of Chemical Engineers Symposium Series No. 56*, V. 3 (1979) p. 75.
144. Hensley, J. C. (ed.), *Cooling Tower Fundamentals*, 2nd Ed., The Marley Cooling Tower Co., a United Dominion Co., Kansas City, MO (1985).
145. Khodaparast, K. A., "Predict the Number of Transfer Units for Cooling Towers," *Chem. Eng. Progr.*, V. 88, No. 4 (1992) p. 67.
146. *Counter-flow Cooling Tower Performance*, J. F. Pritchard Co. of California (Pritchard Corp. is a Black and Veatch Co.) (1957).
147. Perry, R. H., and C. H. Chilton, *Chemical Engineers Handbook*, 5th, Ed., McGraw-Hill Book Co., Inc., New York, N.Y. (1973).
148. Beyer, A. H., "Choose the Right Cooling Tower Fill," *Chem. Eng. Progr.*, V. 89, No. 7 (1993), p. 42.
149. Brooke, M., "Tables Speed Cooling Tower Calculations," *Refining Engr.*, V. 29, No. 12 (1957) p. C-23.
150. Cheremisinoff, N. P. and P. N. Cheremisinoff, *Cooling Towers, Selection, Design and Practice*, Ann Arbor Science Publishers, Inc. (1981).
151. Rukovená, F. and T. D. Koshy, "Packed Distillation Tower Hydraulic Design Method and Mechanical Considerations," *Ind. and Eng. Chem. Res.*, Vol. 32, No. 10 (1993) p. 2400 (Used by permission, The American Chemical Society. All rights reserved.)
152. Rukovená, F., private communication.
153. Fitz, C. W., A. Shariat, and L. Spiegel, "Performance of Structured Packing at High Pressure," presented at AIChE Spring National Meeting, Houston, Texas, March (1995).
154. "Report of Tests of No. 2.5 Nutter Ring™ at Reduced Loadings, released to Nutter Engineering" per Fractionation Research, Inc. Note, author and date not given.
155. Zuiderweg, F. J. and D. E. Nutter, "On the Evidence of Vapor Backmixing in Packed Columns in the Case of High Pressure Distillation," copyright by Institution of Chemical Engineers. Note: undated and publication not given.
156. Nutter, D. E., F. C. Silvey, and B. K. Stober, "Random Packing Performance in Light Ends Distillation," copyright by Institution of Chemical Engineers, undated, and publication not given.
157. Kunesh, John G. and A. Shariat, "Packing Efficiency Testing on a Commercial Scale with Good Reflux Distribution," Fractionation Research, Inc., presented at AIChE Spring National Meeting, Houston, Texas, March (1993).

Bibliography

- Baker, W. J., "Direct Digital Control of Batch Processes Pays Off," *Chem. Eng.* Dec. 15, (1969) p. 121.
- Bannon, R. P. and S. Marple, Jr., "Heat Recovery in Hydrocarbon Distillation," *Chem. Eng. Progr.* 74, 7, p. 41 (1978).
- Biddulph, M. W. "Tray Efficiency is not Constant," *Hydrocarbon Processing*, Oct., (1977) p. 145.
- Billet, R. "Cost Optimization of Towers" *Chem. Eng. Progr.*, 66, 1, (1970) p. 41.
- Billet, R. "Development and Progress in the Design and Performance of Valve Trays," *British Chem. Eng.*, Apr. (1969).
- Bolles, W. L., "Distillation, The Solution of a Foam Problem," *Chem. Eng. Progr.* 63, 9, (1967) p. 48.
- Bowman, J. D., "Troubleshoot Packed Towers with Radioisotopes," *Chem. Eng. Progr.* V. 89, No. 9 (1993) p. 34.
- Bras, G. H. P., "Simplify Gas Cooling Tower Design," *Petroleum Refiner*, March 9(1956) p. 191.
- Broughton, D. B. and K. D. Uitti, "Estimate Tower For Naphtha Cuts," *Hydrocarbon Processing*, Oct., 109, (1971).
- Buckley, P. S., R. K. Cox and W. L. Luyben, "How to Use a Small Calculator In Distillation Column Design," *Chem. Eng. Progr.* 74, 6, (1978) p. 49.
- Chow, A., A. M. Fayon, and Bili Bauman, "Simulations Provide Blueprint For Distillation Operation," *Chem. Eng.* June 7 (1976) p. 1731.
- Coker, A. K., "Understand the Basics of Packed-Column Design," *Chem. Eng. Progr.* Nov. (1991) p. 93.
- Copigneaux, P., "Flooding in Packed Towers," *Hydro. Processing*, Feb. (1981) p. 99.
- "Distillation Tray Features Low ΔP , High Efficiency," *Chem. Engr.* Jan. 20 (1975).
- Douglas, J. M. "Rule-of-Thumb For Minimum Trays," *Hydrocarbon Processing*, Nov., (1977) p. 291.
- Eckhart, R. A. and A. Rose, "New Method For Distillation Prediction," *Hydrocarbon Processing*, May, (1968) p. 165.
- Eckert, J. S. and L. F. Walter, "Controlling Packed-Column Stills," *Chem. Eng.*, Mar. 30 (1964) p. 79.
- Economopoulos, A. P., "A Fast Computer Method For Distillation Calculations," *Chem. Eng.*, Apr. 24 (1978).
- Edmister, W. C., "Applied Hydrocarbon Thermodynamics, Part 49" *Hydrocarbon Processing*, May, 169, (1973).
- Edmister, W. C., *ibid*, "Part 46," Dec. 93 (1972).
- Eichel, F. G., "Capacity of Packed Columns in Vacuum Distillation," *Chem. Eng.* Sept. 12 (1966) p. 197.
- Ellerbe, R. W., "Batch Distillation Basics," *Chem. Eng.* May 28, (1973) p. 110.
- Ellerbe, R. W. "Steam-Distillation Basics," *Chem. Eng.*, Mar. 4, (1974) p. 105.
- Fair, J. R. and W. L. Bolles, "Modern Design of Distillation Columns," *Chem. Eng.* Apr. 22, (1968) p. 178.
- Frank, J. C., G. R. Geyer and H. Kehde, "Styrene-Ethyl-benzene Separation with Sieve Trays," *Chem. Eng. Progr.* 65, 2, (1969) p. 79.
- Frank, O., "Shortcuts For Distillation Design," *Chem. Eng.* Mar. 14, (1977) p. 111.
- Gallun, S. E. and C. D. Holland, "Solve More Distillation Problems, Part 5" *Hydrocarbon Processing*, Jan., 137, (1976).
- Garrett, G. R., R. H. Anderson and M. Van Winkle, "Calculation of Sieve and Valve Tray Efficiencies in Column Scale-up," *Ind. Eng. Chem., Process Des. Dev.* 16, 1, (1977) p. 79.
- Garvin, R. G. and E. R. Norton, "Sieve Tray Performance Under G S Process Conditions," *Chem. Eng. Progr.*, 64, 3, (1968) p. 99.

- Geyer, G. R. and P. E. Kline, "Energy Conservation Schemes For Distillation Process," *Chem. Eng. Progr.*, 72, 5, (1976) p. 49.
- Graf, "Correlations for Design and Evaluation of Packed Vacuum Towers," *Oil and Gas Jour.* May (1985).
- Guerreri, G., Bruno Peri, and F. Seneci, "Comparing Distillation Designs," *Hydrocarbon Processing*, Dec. (1972), p. 78.
- Haman, S. E. M. et al, "Generalized Temperature-Dependent Parameters of the Redlich-Kwong of State for Vapor-Liquid Equilibrium Calculations," *Ind. Eng. Chem. Process Des. Dev.* 16, 1, (1977) p. 51.
- Hanna, T., "Graphical Method, Find Mass Transfer Units," *Chem. Eng.* April 6 (1959), p. 127.
- Hanson, D. N. and J. Newman, "Calculation of Distillation Columns at the Optimum Feed Plate Location," *Ind. Eng. Chem. Process Des. Dev.* 16, 1, (1977) p. 223.
- Hattiangadi, U.S., "How to Interpret a Negative of Minimum Reflux Ratio," *Chem. Eng.*, May 18 (1970) p. 178.
- Helling, R. K., and M. A. Desjardin, "Get the Best Performance from Structured Packing," *Chem. Eng. Progress*, V. 90, No. 10, (1994) p. 62.
- Hess, F. E. et. al., "Solve More Distillation Problems," *Hydrocarbon Processing*, June, (1977) p. 183 May, (1977) p. 243.
- Holland, C. D., G. P. Pendon, and S. E. Gallun, "Solve More Distillation Problems," *Hydrocarbon Processing*, June, 101 (1975).
- Holland, C. D and G. P. Pendon, "Solve More Distillation Problems," *Hydrocarbon Processing*, July, (1974) p. 148.
- Huckabay, H. K. and R. L. Garrison, "Packed Tower Transfer Rate by Graphs," *Hydro. Processing*, June (1969), pg. 153.
- Kaiser, V., "Correlate the Flooding of Packed Columns a New Way," *Chem. Eng. Progress*, V. 90, No. 6 (1994), p. 55.
- Kemp, D. W., and D. G. Ellis, "Computer Control of Fractionation Plants," *Chem. Eng.* Dec. 5, 115, (1975).
- Kern, R. "Layout Arrangements For Distillation Columns," *Chem. Eng.*, Aug. 15, (1977) p. 153.
- Kister, H. Z. and I. D. Doig, "Entrainment Flooding Prediction," *Hydrocarbon Processing*, Oct. (1977) p. 150.
- Koppel, P. M., "Fast Way to Solve Problems For Batch Distillations," *Chem. Eng.* Oct. 16, 109, (1972).
- Leach, M. J., "An Approach to Multiphase Vapor-Liquid Equilibria," *Chem. Eng.* May 23, (1977) p. 137.
- Lemieux, E. J., "Data for Tower Baffle Design," *Hydro. Processing*, Sept. (1983) p. 106.
- Lenoir, J. M. and C. R. Koppay, "Need Equilibrium Ratios? Do it Right," *Hydrocarbon Processing*, Vol. 46, 249 (1967).
- Lenoir, J. M., "Predict Hash Points Accurately," *Hydrocarbon Processing*, Jan., 95 (1975).
- Leva, M., "Reconsider Packed-Tower Pressure-Drop Correlations," *Chem. Eng. Progress*, V. 88, No. 1 (1992), p. 65.
- Lieberman, N. P., "Packing Expands Low-Pressure Fractionators," *Hydro. Processing*, V. 63, No. 4 (1984) p. 143.
- Lieberman, N. P., "Change Controls to Save Energy," *Hydrocarbon Processing*, Feb., (1978) p. 93.
- Loud, G. D. and R. C. Waggoner, "The Effects of Interstage Backmixing on the Design of a Multicomponent Distillation Column," *Ind. Eng. Chem. Process Des. & Dev.*, 17, 2, (1978) p. 149.
- Luyben, W. L., "Azeotropic Tower Design by Graph," *Hydrocarbon Processing*, Jan., (1973) p. 109.
- Maas, J. H., "Optimum-Feed-Stage Location in Multicomponent Distillations," *Chem. Eng.*, Apr. 16, (1973) p. 96.
- Mapstone, G. E., "Reflux Versus Trays by Chart," 47, 5, (1968) p. 169.
- Martinez-Ortiz, J. A., and D. B. Manley, "Direct Solution of the Isothermal Gibbs-Duhem Equation for Multicomponent Systems," *Ind. Eng. Chem. Process Des. Dev.*, 17, 3, (1978) p. 346.
- McWilliams, M. L., "An Equation to Relate K-Factors to Pressure and Temperature," *Chem. Eng.*, Oct. 29, (1973) p. 138.
- Michell, S. J., "Designing a Gas-Cooling Tower," *British Chem Eng.*, July (1958).
- Mix, T. J., et. al., "Energy Conservation In Distillation," *Chem. Eng. Progr.*, Apr. (1978) p. 49.
- Nemunaitis, R. R., "Sieve Trays? Consider Viscosity," *Hydrocarbon Processing*, Nov., 235 (1971).
- Osburn, J. O., "Transfer Unit Simplifies Calculations," *Chem. Eng.* Aug. 11 (1958) p. 147.
- Petterson, W. C. and T. A. Wells, "Energy-Saving Schemes in Distillation," *Chem. Eng.*, Sept. 26, (1977) p. 79.
- Pfeiffer, E. L., "Preliminary Cooling Tower Selection," Foster Wheeler Corp., Bul. CT-49-6, reprinted from *Chem. Eng.* (date not given).
- Prater, N. H., "Designing Stripping Columns" *Petroleum Refiner*, V. 33, No. 2 (1954) p. 96.
- Rao, A. K., "Prediction of Liquid Activity Coefficients," *Chem. Eng.* May 9, (1977) p. 143.
- Robbins, L. A., "Improve Pressure-Drop Prediction with a New Correlation," *Chem. Eng. Progress*, V. 87, No. 5 (1991), p. 87.
- Robinson, D. B., et. al. "Capability of the Peng-Robinson Programs," *Hydrocarbon Processing*, Apr. (1978) p. 95.
- Ross, S. "Mechanisms of Foam Stabilization and Antifoaming Action," *Chem. Eng. Progr.* 63, 9, (1967) p. 41.
- Scheiman, A. D. "Find Minimum Reflux By Heat Balance," *Hydrocarbon Processing*, Sept. (1969) p. 187.
- Shah, G. C., "Troubleshooting Distillation Columns," *Chem. Eng.* July 31, (1978) p. 70.
- Shinsky, F. G., "Energy Conserving Control Systems For Distillation Units," *Chem. Engr. Progr.* 72, 5, (1976) p. 73.
- Silverman, N. and D. Tassios, "The Number of Roots in the Wilson Equation and its Effect on Vapor-Liquid Equilibrium Calculations," *Ind. Eng. Chem., Process Des. Dev.*, 16, 1, (1977) p. 13.
- Sommerville, R. F., "New Method Gives Quick, Accurate Estimate of Distillation Costs," *Chem. Eng.*, May 1, (1972) p. 71.
- Strigle, R. F., Jr., "Understand Flow Phenomena in Packed Columns," *Chem. Eng. Progress*, V. 89, No. 8 (1993), p. 79.
- Thorngren, J. T., "Valve Tray Flooding Generalized," *Hydrocarbon Processing*, 57, 8, (1978) p. 111.
- Tierney, Jr., L. F. Stuzman and R. L. Daileader, "Mass Transfer in Packed Towers," *Ind. Eng. Chemistry* V. 46, Aug. (1954) p. 1594.
- Treybal, R. E. "A Simple Method For Batch Distillation," *Chem. Eng.*, Oct. 5, (1970) p. 95.
- Van Winkle, M. and W. G. Todd, "Minimizing Distillation Costs via Graphical Techniques," *Chem. Eng.*, Mar. 6, (1972) p. 105.
- Wade, H. L. and C. J. Ryskamp, "Tray Flooding Sets Crude Thruput," *Hydrocarbon Processing*, Nov. (1977) p. 281.
- Wheeler, D. E., "Design Criteria For Chimney Trays," *Hydrocarbon Processing*, July, (1968) p. 119.
- Wichterle, I. R. Kobayashi, and P. S. Chapple, "Caution! Pinch Point in Y-X Curve," *Hydrocarbon Processing*, Nov. 233, (1971).
- York, J. L., L. T. Barberio, M. Samyn, F. A. Zenz, and J. A. Zenz, "Solve All Column Flows with One Equation," *Chem. Eng. Prog.*, Oct. (1992) p. 93.
- Zanker, A. "Nomograph Replaced Gilliland Plot," *Hydrocarbon Processing*, May, (1977), p. 263.

A-1. (Continued). Alphabetical Conversion Factors

TO CONVERT	INTO	MULTIPLY BY	TO CONVERT	INTO	MULTIPLY BY
feet of water	kgs/sq meter	304.8	grains (troy)	grains (avdp)	1.0
feet of water	pounds/sq ft	62.43	grains (troy)	grams	0.06480
feet of water	pounds/sq in.	0.4335	grains (troy)	ounces (avdp)	2.0833×10^{-3}
feet/min	cms/sec	0.5080	grains (troy)	pennyweight (troy)	0.04167
feet/min	feet/sec	0.01667	grains/U.S. gal	parts/million	17.118
feet/min	kms/hr	0.01829	grains/U.S. gal	pounds/million gal	142.86
feet/min	meters/min	0.3048	grains/Imp. gal	parts/million	14.286
feet/min	miles/hr	0.01136	grams	dynes	980.7
feet/sec	cms/sec	30.48	grams	grains	15.43
feet/sec	kms/hr	1.097	grams	joules/cm	9.807×10^{-5}
feet/sec	knots	0.5921	grams	joules/meter (newtons)	9.807×10^{-3}
feet/sec	meters/min	18.29	grams	kilograms	0.001
feet/sec	miles/hr	0.6818	grams	milligrams	1,000.
feet/sec	miles/min	0.01136	grams	ounces (avdp)	0.03527
feet/sec/sec	cms/sec/sec	30.48	grams	ounces (troy)	0.03215
feet/sec/sec	kms/hr/sec	1.097	grams	poundals	0.07093
feet/sec/sec	meters/sec/sec	0.3048	grams	pounds	2.205×10^{-3}
feet/sec/sec	miles/hr/sec	0.6818	grams/cm	pounds/inch	5.600×10^{-3}
feet/100 feet	per cent grade	1.0	grams/cu cm	pounds/cu ft	62.43
Foot — candle	Lumen/sq. meter	10.764	grams/cu cm	pounds/cu in	0.03613
foot-pounds	Btu	1.286×10^{-3}	grams/cu cm	pounds/mil-foot	3.405×10^{-7}
foot-pounds	ergs	1.356×10^7	grams/liter	grains/gal	58.417
foot-pounds	gram-calories	0.3238	grams/liter	pounds/gal	8.345
foot-pounds	hp-hrs	5.050×10^{-7}	grams/liter	pounds/cu ft	0.062427
foot-pounds	joules	1.356	grams/liter	parts/million	1,000.0
foot-pounds	kg-calories	3.24×10^{-4}	grams/sq cm	pounds/sq ft	2.0481
foot-pounds	kg-meters	0.1383	gram-calories	Btu	3.9683×10^{-3}
foot-pounds	kilowatt-hrs	3.766×10^{-7}	gram-calories	ergs	4.1868×10^7
foot-pounds/min	Btu/min	1.286×10^{-3}	gram-calories	foot-pounds	3.0880
foot-pounds/min	foot-pounds/sec	0.01667	gram-calories	horsepower-hrs	1.5596×10^{-4}
foot-pounds/min	horsepower	3.030×10^{-5}	gram-calories	kilowatt-hrs	1.1630×10^{-6}
foot-pounds/min	kg-calories/min	3.24×10^{-4}	gram-calories	watt-hrs	1.1630×10^{-3}
foot-pounds/min	kilowatts	2.260×10^{-5}	gram-calories/sec	Btu/hr	14.286
foot-pounds/sec	Btu/hr	4.6263	gram-centimeters	Btu	9.297×10^{-8}
foot-pounds/sec	Btu/min	0.07717	gram-centimeters	ergs	980.7
foot-pounds/sec	horsepower	1.818×10^{-3}	gram-centimeters	joules	9.807×10^{-3}
foot-pounds/sec	kg-calories/min	0.01945	gram-centimeters	kg-cal	2.343×10^{-8}
foot-pounds/sec	kilowatts	1.356×10^{-3}	gram-centimeters	kg-meters	10^{-5}
Furlongs	miles (U.S.)	0.125			
furlongs	rods	40.0			
furlongs	feet	660.0			
	G				
gallons	cu cms	3,785.0	Hand	Cm.	10.16
gallons	cu feet	0.1337	hectares	acres	2.471
gallons	cu inches	231.0	hectares	sq feet	1.076×10^3
gallons	cu meters	3.785×10^{-3}	hectograms	grams	100.0
gallons	cu yards	4.951×10^{-3}	hectoliters	liters	100.0
gallons	liters	3.785	hectometers	meters	100.0
gallons (liq. Br. Imp.)	gallons (U.S. liq.)	1.20095	hectowatts	watts	100.0
gallons (U.S.)	gallons (Imp.)	0.83267	henries	millihenries	1,000.0
gallons of water	pounds of water	8.3453	Hogsheads (British)	cubic ft.	10.114
gallons/min	cu ft/sec	2.228×10^{-3}	Hogsheads (U.S.)	cubic ft.	8.42184
gallons/min	liters/sec	0.06308	Hogsheads (U.S.)	gallons (U.S.)	63
gallons/min	cu ft/hr	8.0208	horsepower	Btu/min	42.44
gausses	lines/sq in.	6.452	horsepower	foot-lbs/min	33,000.
gausses	webers/sq cm	10^{-8}	horsepower	foot-lbs/sec	550.0
gausses	webers/sq in.	6.452×10^{-8}	horsepower (metric)	horsepower	0.9863
gausses	webers/sq meter	10^{-4}	(542.5 ft lb/sec)	horsepower (metric)	1.014
gilberts	ampere-turns	0.7958	horsepower	(542.5 ft lb/sec)	
gilberts/cm	amp-turns/cm	0.7958	horsepower	kg-calories/min	10.68
gilberts/cm	amp-turns/in	2.021	horsepower	kilowatts	0.7457
gilberts/cm	amp-turns/meter	79.58	horsepower (boiler)	watts	745.7
Gills (British)	cubic cm.	142.07	horsepower (boiler)	Btu/hr	33.479
gills	liters	0.1183	horsepower-hrs	kilowatts	9.803
gills	pints (liq.)	0.25	horsepower-hrs	Btu	2,547.
Grade	Radian	.01571	horsepower-hrs	ergs	2.6845×10^{13}
Grains	drams (avoirdupois)	0.03657143	horsepower-hrs	foot-lbs	1.98×10^6
				gram-calories	641,190.
				joules	2.684×10^6

A-1. (Continued). Alphabetical Conversion Factors

TO CONVERT	INTO	MULTIPLY BY	TO CONVERT	INTO	MULTIPLY BY
horsepower-hrs	kg-calories	641.1	kilograms/sq cm	inches of mercury	28.96
horsepower-hrs	kg-meters	2.737×10^5	kilograms/sq cm	pounds/sq ft	2,048.
horsepower-hrs	kilowatt-hrs	0.7457	kilograms/sq cm	pounds/sq in.	14.22
hours	days	4.167×10^{-2}	kilograms/sq meter	atmospheres	9.678×10^{-5}
hours	weeks	5.952×10^{-3}	kilograms/sq meter	bars	98.07×10^{-6}
Hundredweights (long)	pounds	112	kilograms/sq meter	feet of water	3.281×10^{-3}
Hundredweights (long)	tons (long)	0.05	kilograms/sq meter	inches of mercury	2.896×10^{-3}
Hundredweights (short)	ounces (avoirdupois)	1600	kilograms/sq meter	pounds/sq ft	0.2048
Hundredweights (short)	pounds	100	kilograms/sq meter	pounds/sq in.	1.422×10^{-3}
Hundredweights (short)	tons (metric)	0.0453592	kilograms/sq mm	kgs/sq meter	10^6
Hundredweights (short)	tons (long)	0.0446429	kilogram-calories	Btu	3.968
			kilogram-calories	foot-pounds	3,088.
	I		kilogram-calories	hp-hrs	1.560×10^{-3}
inches	centimeters	2.540	kilogram-calories	joules	4,186.
inches	meters	2.540×10^{-2}	kilogram-calories	kg-meters	426.9
inches	miles	1.578×10^{-5}	kilogram-calories	kilojoules	4.186
inches	millimeters	25.40	kilogram-calories	kilowatt-hrs	1.163×10^{-3}
inches	mils	1,000.0	kilogram meters	Btu	9.294×10^{-3}
inches	yards	2.778×10^{-2}	kilogram meters	ergs	9.804×10^7
inches of mercury	atmospheres	0.03342	kilogram meters	foot-pounds	7.233
inches of mercury	feet of water	1.133	kilogram meters	joules	9.804
inches of mercury	kgs/sq cm	0.03453	kilogram meters	kg-calories	2.342×10^{-3}
inches of mercury	kgs/sq meter	345.3	kilogram meters	kilowatt-hrs	2.723×10^{-6}
inches of mercury	pounds/sq ft	70.73	kilolines	maxwells	1,000.0
inches of mercury	pounds/sq in.	0.4912	kiloliters	liters	1,000.0
inches of water (at 4°C)	atmospheres	2.458×10^{-3}	kilometers	centimeters	10^5
inches of water (at 4°C)	inches of mercury	0.07355	kilometers	feet	3,281.
inches of water (at 4°C)	kgs/sq cm	2.540×10^{-3}	kilometers	inches	3.937×10^4
inches of water (at 4°C)	ounces/sq in.	0.5781	kilometers	meters	1,000.0
inches of water (at 4°C)	pounds/sq ft	5.204	kilometers	miles	0.6214
inches of water (at 4°C)	pounds/sq in.	0.03613	kilometers	millimeters	10^4
International Ampere	Ampere (absolute)	.9998	kilometers	yards	1,094.
International Volt	Volts (absolute)	1.0003	kilometers/hr	cms/sec	27.78
International volt	Joules (absolute)	1.593×10^{-19}	kilometers/hr	feet/min	54.68
International volt	Joules	9.654×10^4	kilometers/hr	feet/sec	0.9113
			kilometers/hr	knots	0.5396
	J		kilometers/hr	meters/min	16.67
joules	Btu	9.480×10^{-4}	kilometers/hr	miles/hr	0.6214
joules	ergs	10^7	kilometers/hr/sec	cms/sec	27.78
joules	foot-pounds	0.7376	kilometers/hr/sec	ft/sec/sec	0.9113
joules	kg-calories	2.389×10^{-4}	kilometers/hr/sec	meters/sec/sec	0.2778
joules	kg-meters	0.1020	kilometers/hr/sec	miles/hr/sec	0.6214
joules	watt-hrs	2.778×10^{-4}	kilowatts	Btu/min	56.92
joules/cm	grams	1.020×10^4	kilowatts	foot-lbs/min	4.426×10^4
joules/cm	dynes	10^7	kilowatts	foot-lbs/sec	737.6
joules/cm	joules/meter (newtons)	100.0	kilowatts	horsepower	1.341
joules/cm	poundals	723.3	kilowatts	kg-calories/min	14.34
joules/cm	pounds	22.48	kilowatts	watts	1,000.0
			kilowatt-hrs	Btu	3,413.
	K		kilowatt-hrs	ergs	3.600×10^{13}
kilograms	dynes	980,665.	kilowatt-hrs	foot-lbs	2.655×10^4
kilograms	grams	1,000.0	kilowatt-hrs	gram-calories	859,850.
kilograms	joules/cm	0.09807	kilowatt-hrs	horsepower-hrs	1.341
kilograms	joules/meter (newtons)	9.807	kilowatt-hrs	joules	3.6×10^4
kilograms	poundals	70.93	kilowatt-hrs	kg-calories	860.5
kilograms	pounds	2.205	kilowatt-hrs	kg-meters	3.671×10^3
kilograms	tons (long)	9.842×10^{-4}	kilowatt-hrs	pounds of water	
kilograms	tons (short)	1.102×10^{-3}	kilowatt-hrs	evaporated from and	
kilograms/cu meter	grams/cu cm	0.001		at 212° F.	3.53
kilograms/cu meter	pounds/cu ft	0.06243	kilowatt-hrs	pounds of water raised	
kilograms/cu meter	pounds/cu in.	3.613×10^{-5}		from 62° to 212° F.	22.75
kilograms/cu meter	pounds/mil-foot	3.405×10^{-10}		feet/hr	6,080.
kilograms/meter	pounds/ft	0.6720	knots	kilometers/hr	1.8532
Kilogram/sq. cm.	Dynes	980,665	knots	nautical miles/hr	1.0
kilograms/sq cm	atmospheres	0.9678	knots	statute miles/hr	1.151
kilograms/sq cm	feet of water	32.81	knots		

(Continued on next page)

A-1. (Continued). Alphabetical Conversion Factors

TO CONVERT	INTO	MULTIPLY BY	TO CONVERT	INTO	MULTIPLY BY
knots	yards/hr	2,027.	microhms	ohms	10^{-6}
knots	feet/sec	1.689	microliters	liters	10^{-6}
	L		Microns	meters	1×10^{-4}
league	miles (approx.)	3.0	miles (naut.)	feet	6,080.27
Light year	Miles	5.9×10^{12}	miles (naut.)	kilometers	1.853
Light year	Kilometers	9.46091×10^{13}	miles (naut.)	meters	1,853.
lines/sq cm	gausses	1.0	miles (naut.)	miles (statute)	1.1516
lines/sq in.	gausses	0.1550	miles (statute)	yards	2,027.
lines/sq in.	webers/sq cm	1.550×10^{-9}	miles (statute)	centimeters	1.609×10^5
lines/sq in.	webers/sq in.	10^{-8}	miles (statute)	feet	5,280.
lines/sq in.	webers/sq meter	1.550×10^{-5}	miles (statute)	inches	6.336×10^4
links (engineer's)	inches	12.0	miles (statute)	kilometers	1.609
links (surveyor's)	inches	7.92	miles (statute)	meters	1,609.
liters	bushels (U.S. dry)	0.02838	miles (statute)	miles (naut.)	0.8684
liters	cu cm	1,000.0	miles (statute)	yards	1,760.
liters	cu feet	0.03531	miles/hr	cms/sec	44.70
liters	cu inches	61.02	miles/hr	feet/min	88.
liters	cu meters	0.001	miles/hr	feet/sec	1.467
liters	cu yards	1.308×10^{-3}	miles/hr	kms/hr	1.609
liters	gallons (U.S. liq.)	0.2642	miles/hr	kms/min	0.02682
liters	pints (U.S. liq.)	2.113	miles/hr	knots	0.8684
liters	quarts (U.S. liq.)	1.057	miles/hr	meters/min	26.82
liters/min	cu ft/sec	5.886×10^{-4}	miles/hr	miles/min	0.1667
liters/min	gals/sec	4.403×10^{-3}	miles/hr/sec	cms/sec/sec	44.70
lumens/sq ft	foot-candles	1.0	miles/hr/sec	feet/sec/sec	1.467
Lumen	Spherical candle power	.07958	miles/hr/sec	kms/hr/sec	1.609
Lumen	Watt	.001496	miles/hr/sec	meters/sec/sec	0.4470
Lumen/sq. ft.	Lumen/sq. meter	10.76	miles/min	cms/sec	2,682.
lux	foot-candles	0.0929	miles/min	feet/sec	88.
	M		miles/min	kms/min	1.609
maxwells	kilolines	0.001	miles/min	knots/min	0.8684
maxwells	webers	10^{-8}	miles/min	miles/hr	60.0
megalines	maxwells	10^6	mil-feet	cu inches	9.425×10^{-4}
megohms	microhms	10^{12}	milliers	kilograms	1,000.
megohms	ohms	10^6	Millimicrons	meters	1×10^{-9}
meters	centimeters	100.0	Milligrams	grains	0.01543236
meters	feet	3.281	milligrams	grams	0.001
meters	inches	39.37	milligrams/liter	parts/million	1.0
meters	kilometers	0.001	millihenries	henries	0.001
meters	miles (naut.)	5.396×10^{-4}	milliliters	liters	0.001
meters	miles (stat.)	6.214×10^{-4}	millimeters	centimeters	0.1
meters	millimeters	1,000.0	millimeters	feet	3.281×10^{-3}
meters	yards	1.094	millimeters	inches	0.03937
meters	varas	1.179	millimeters	kilometers	10^{-4}
meters/min	cms/sec	1.667	millimeters	meters	0.001
meters/min	feet/min	3.281	millimeters	miles	6.214×10^{-7}
meters/min	feet/sec	0.05468	millimeters	yards	39.37
meters/min	kms/hr	0.06	millimeters	yards	1.094×10^{-3}
meters/min	knots	0.03238	millimeters	cu ft/sec	1.54723
meters/min	miles/hr	0.03728	millimeters	centimeters	2.540×10^{-3}
meters/sec	feet/min	196.8	millimeters	feet	8.333×10^{-5}
meters/sec	feet/sec	3.281	millimeters	inches	0.001
meters/sec	kilometers/hr	3.6	millimeters	kilometers	2.540×10^{-8}
meters/sec	kilometers/min	0.06	millimeters	yards	2.778×10^{-3}
meters/sec	miles/hr	2.237	millimeters	cu ft/min	1.5
meters/sec	miles/min	0.03728	millimeters	cubic cm.	0.059192
meters/sec/sec	cms/sec/sec	100.0	millimeters	cubic cm.	0.061612
meters/sec/sec	ft/sec/sec	3.281	millimeters	degrees	0.01667
meters/sec/sec	kms/hr/sec	3.6	millimeters	quadrants	1.852×10^{-4}
meters/sec/sec	miles/hr/sec	2.237	millimeters	radians	2.909×10^{-4}
meter-kilograms	cm-dynes	9.807×10^7	millimeters	seconds	60.0
meter-kilograms	cm-grams	10^5	millimeters	kilograms	10.0
meter-kilograms	pound-feet	7.233	millimeters	kilometers	10.0
microfarad	farads	10^{-6}	millimeters	kilowatts	10.0
micrograms	grams	10^{-6}	millimeters		
microhms	megohms	10^{-12}		N	
			nepers	decibels	8.686
			Newton	Dynes	1×10^5

A-1. (Continued). Alphabetical Conversion Factors

TO CONVERT	INTO	MULTIPLY BY	TO CONVERT	INTO	MULTIPLY BY
O					
OHM (International)	OHM (absolute)	1.0005	pounds (troy)	ounces (avdp.)	13.1657
ohms	megohms	10^{-6}	pounds (troy)	ounces (troy)	12.0
ohms	microhms	10^6	pounds (troy)	pennyweights (troy)	240.0
ounces	drams	16.0	pounds (troy)	pounds (avdp.)	0.822857
ounces	grains	437.5	pounds (troy)	tons (long)	3.6735×10^{-4}
ounces	grams	28.349527	pounds (troy)	tons (metric)	3.7324×10^{-4}
ounces	pounds	0.0625	pounds (troy)	tons (short)	4.1143×10^{-4}
ounces	ounces (troy)	0.9115	pounds of water	cu feet	0.01602
ounces	tons (long)	2.790×10^{-5}	pounds of water	cu inches	27.68
ounces	tons (metric)	2.835×10^{-5}	pounds of water	gallons	0.1198
ounces (fluid)	cu inches	1.805	pounds of water/min	cu ft/sec	2.670×10^{-4}
ounces (fluid)	liters	0.02957	pound-foot	cm-dynes	1.356×10^9
ounces (troy)	grains	480.0	pound-foot	cm-grams	13,825.
ounces (troy)	grams	31.103481	pound-foot	meter-kgs	0.1383
ounces (troy)	ounces (avdp.)	1.09714	pounds/cu ft	grams/cu cm	0.01602
ounces (troy)	pennyweights (troy)	20.0	pounds/cu ft	kgs/cu meter	16.02
ounces (troy)	pounds (troy)	0.08333	pounds/cu ft	pounds/cu in.	5.787×10^{-4}
Ounce/sq. inch	Dynes/sq. cm.	4309	pounds/cu ft	pounds/mil-foot	5.456×10^{-9}
ounces/sq in.	pounds/sq in.	0.0625	pounds/cu in.	gms/cu cm	27.68
P					
Parsec	Miles	19×10^{12}	pounds/cu in.	kgs/cu meter	2.768×10^4
Parsec	Kilometers	3.084×10^{13}	pounds/cu in.	pounds/cu ft	1,728.
parts/million	grains/U.S. gal	0.0584	pounds/cu in.	pounds/mil-foot	9.425×10^{-4}
parts/million	grains/Imp. gal	0.07016	pounds/ft	kgs/meter	1.488
parts/million	pounds/million gal	8.345	pounds/in.	gms/cm	178.6
Pecks (British)	cubic inches	554.6	pounds/mil-foot	gms/cu cm	2.306×10^6
Pecks (British)	liters	9.091901	pounds/sq ft	atmospheres	4.725×10^{-4}
Pecks (U.S.)	bushels	0.25	pounds/sq ft	feet of water	0.01602
Pecks (U.S.)	cubic inches	537.605	pounds/sq ft	inches of mercury	0.01414
Pecks (U.S.)	liters	8.809582	pounds/sq ft	kgs/sq meter	4.882
Pecks (U.S.)	quarts (dry)	8	pounds/sq ft	pounds/sq in.	6.944×10^{-3}
pennyweights (troy)	grains	24.0	pounds/sq in.	atmospheres	0.06804
pennyweights (troy)	ounces (troy)	0.05	pounds/sq in.	feet of water	2.307
pennyweights (troy)	grams	1.55517	pounds/sq in.	inches of mercury	2.036
pennyweights (troy)	pounds (troy)	4.1667×10^{-3}	pounds/sq in.	kgs/sq meter	703.1
pints (dry)	cu inches	33.60	pounds/sq in.	pounds/sq ft	144.0
pints (liq.)	cu cms.	473.2	Q		
pints (liq.)	cu feet	0.01671	quadrants (angle)	degrees	90.0
pints (liq.)	cu inches	28.87	quadrants (angle)	minutes	5,400.0
pints (liq.)	cu meters	4.732×10^{-4}	quadrants (angle)	radians	1.571
pints (liq.)	cu yards	6.189×10^{-4}	quadrants (angle)	seconds	3.24×10^5
pints (liq.)	gallons	0.125	quarts (dry)	cu inches	67.20
pints (liq.)	liters	0.4732	quarts (liq.)	cu cms	946.4
pints (liq.)	quarts (liq.)	0.5	quarts (liq.)	cu feet	0.03342
Planck's quantum	Erg — second	6.624×10^{-27}	quarts (liq.)	cu inches	57.75
Poise	Gram/cm. sec.	1.00	quarts (liq.)	cu meters	9.464×10^{-4}
Pounds (avoirdupois)	ounces (troy)	14.5833	quarts (liq.)	cu yards	1.238×10^{-3}
poundals	dynes	13,826.	quarts (liq.)	gallons	0.25
poundals	grams	14.10	quarts (liq.)	liters	0.9463
poundals	joules/cm	1.383×10^{-3}	R		
poundals	joules/meter (newtons)	0.1383	radians	degrees	57.30
poundals	kilograms	0.01410	radians	minutes	3,438.
poundals	pounds	0.03108	radians	quadrants	0.6366
pounds	drams	256.	radians	seconds	2.063×10^5
pounds	dynes	44.4823×10^4	radians/sec	degrees/sec	57.30
pounds	grains	7,000.	radians/sec	revolutions/min	9.549
pounds	grams	453.5924	radians/sec	revolutions/sec	0.1592
pounds	joules/cm	0.04448	radians/sec/sec	revs/min/min	573.0
pounds	joules/meter (newtons)	4.448	radians/sec/sec	revs/min/sec	9.549
pounds	kilograms	0.4536	radians/sec/sec	revs/sec/sec	0.1592
pounds	ounces	16.0	revolutions	degrees	360.0
pounds	ounces (troy)	14.5833	revolutions	quadrants	4.0
pounds	poundals	32.17	revolutions	radians	6.283
pounds	pounds (troy)	1.21528	revolutions/min	degrees/sec	6.0
pounds	tons (short)	0.0005	revolutions/min	radians/sec	0.1047
pounds (troy)	grains	5,760.	revolutions/min	revs/sec	0.01667
pounds (troy)	grams	373.24177			

(Continued on next page)

A-2. Physical Property Conversion Factors

Acceleration of gravity = 32.172 ft./sec./sec.
= 980.6 cm./sec./sec.

Electrical conductance;

1 mho = 1 ohm⁻¹
= 10⁻⁶ megamho
= 10⁶ micromho

Heat Value of Fuel

Lower heating value
= Higher heating value - 10.3 (9H₂ + H₂O), Btu/lb.

where: H₂ = weight % hydrogen in fuel

H₂O = weight % water vapor in fuel

GPM = (pounds/hour) / (500 × Sp.Gr.)

Velocity, feet/sec. = $\frac{0.321 \text{ (GPM)}}{\text{(Flow Area, sq.in.)}}$

Head, feet = 2.31 (Pressure or head, psi) / Sp.Gr.

Brake horsepower, BHP = $\frac{\text{(GPM)} \text{ (Sp.Gr.)} \text{ (Head, feet)}}{3960 \text{ (Efficiency, fraction)}}$

Weight/Volume (avoirdupois unless otherwise stated)

Density of sea water = 1.025 grams/cc.

1 gram-molecular volume of a gas at 760 mm Hg and 0° C. = 22.4 liters

1 U. S. gallon = (8.34 × Sp.Gr. of fluid), pounds

Weight of one cu.ft. liquid = (62.32 pounds × Sp.Gr. of fluid), pounds/cu.ft.

1 pound avoirdupois = 1.2153 pound apothecaries'

1 grain avoirdupois = 1 grain troy = 1 grain apothecaries' weight

Air Analysis*

	By Weight %	By Volume %
Nitrogen	75.47	78.2
Oxygen	23.19	21.0

* Neglects trace gases such as argon, xenon, helium, krypton and assumes dry basis.

Gas Constants, (R), Universal

R = 0.0821 (atm) (liter) / (g-mol) (°K)
= 1.987 (g-cal.) / (g-mol) (°K)
= 1.987 Btu / (lb.-mol) (°R)
= 1.987 (Chu) / (lb.-mol) (°K)
= 8.314 joules / (g-mol) (°K)
= 1,546 (ft.) (lb.force) / (lb.-mol) (°R)

= 10.73 (lb.-force/sq. in abs.) (cu.ft.) / (lb.-mol) (°R)
= 18,510 (lb.-force/sq.in.) (cu.in.) / (lb.-mol) (°R)
= 0.7302 (Atm) (cu.ft.) / (lb.-mol) (°R)

R₁ = R/mol.wt. gas

where: R₁ = individual gas constant

Avogadro Constant, N_a = 6.02252 × 10²³ molecules/mol

Density, Vapor or Gases (Ideal), ρ

$$\rho = \left(\frac{\text{mol. wt., vapor}}{359} \right) \left(\frac{14.7 + p}{14.7} \right) \left(\frac{460 + 32}{460 + ^\circ\text{F}} \right), \text{ lbs./cu.ft.}$$

where: p = gage pressure at actual condition, psig

°F = fahrenheit temperature at actual condition

$$\rho = \frac{144 P}{R_1 T}, \text{ pounds/cu.ft.}$$

where: P = absolute pressure, pounds/sq. in. abs.

T = absolute temperature, °Rankine, °R

o = standard conditions (0° C & 760 mm Hg)

$$\bar{V} = \bar{V}_o \left(\frac{P_o}{P} \right) \left(\frac{T}{T_o} \right)$$

P°V = 1543 nT; P° = PSF abs.; V = cu. ft.

T = °R; n = Lb. moles

$$\text{cu.ft.} = \frac{\text{lb}}{\text{MW}} (359) \left(\frac{273 + ^\circ\text{C}}{273} \right) \left(\frac{14.7}{p + 14.7} \right) \text{ at } p, ^\circ\text{C}$$

Specific Volume, Gas or Vapor

$$\bar{V} = 1/\rho, \text{ cu.ft./pound}$$

Velocity of sound in dry air @ 0° C. and 1 atm. = 1,089 ft./sec.

Density of dry air @ 0° C. and 1 atm.

= 0.001293 gm/cu.cm.

= 0.0808 lb./cu.ft.

Viscosity (Dynamic)

1 Poise = 1 gram/cm.-sec. = 1 dyne-sec./sq.cm.
= 0.1 kg/meter-sec.

1 Poise × 100 = Centipoise (μ)

Poise × 2.09 × 10⁻³ = slugs/ft.-sec.

= pounds (force)-sec./sq.ft.

Poise × 0.10 = pascal-sec.

(Continued on next page)

A-2.

(Continued). Physical Property Conversion Factors

$$\text{Poise} \times 0.0672 = \text{pounds (mass)/(ft.-sec.)} \\ = \text{poundal-sec./sq.ft.}$$

$$\text{Poise} \times 0.10 = \text{Newton-sec./sq. meter}$$

$$\text{Centipoise} \times 0.01 = \text{gm./cm.-sec.}$$

$$\text{Centipoise} \times 6.72 \times 10^{-4} = \text{pound/ft.-sec.}$$

$$\text{Centipoise} \times 2.4 = \text{pound/ft.-hr.}$$

$$\text{Millipoise} \times 1000 = \text{poise}$$

$$\text{Micropoise} \times 1,000,000 = \text{poise}$$

$$\text{Slugs/ft.-sec.} \times 47,900 = \text{centipoise}$$

$$1 \text{ centistoke} = 1.076 \times 10^{-5} \text{ ft.}^2/\text{sec.}$$

$$1 \text{ centipoise (cp)} = 0.01 \text{ gm./cm. sec.}$$

$$\text{Slugs/ft.-sec.} \times 32.2 = \text{pounds (mass)/ft.-sec.}$$

$$\text{Pounds/ft.-sec.} \times 3600 = \text{lb./ft.-hr.}$$

$$\text{Pounds (mass)/ft.-sec.} \times 1487 = \text{centipoise}$$

$$\text{Pounds (mass)/ft.-sec.} \times 0.0311 = \text{slugs/ft.-sec.} \\ = \text{pounds (force)-sec./sq.ft.}$$

$$\text{Viscosity of air @ } 68^\circ \text{ F.} = 180.8 \times 10^{-6} \text{ poise}$$

$$\text{Viscosity of water @ } 66^\circ \text{ F} = 0.010087 \text{ poise}$$

Viscosity (Kinematic)

Kinematic viscosity,

$$\text{centistokes} \times 1.076 \times 10^{-5} = \text{ft.}^2/\text{sec.}$$

$$\text{Kinematic viscosity, centistokes } (\nu) = \frac{\text{Dynamic viscosity, centipoise}}{\text{Fluid density, gm./cu.cm.}}$$

$$= \frac{\text{Centipoise}}{\text{Sp.Gr. of liquid relative to water at } 39.2^\circ \text{ F. (} 4^\circ \text{ C.)}}$$

$$\text{Centistokes} \times 0.01 = \text{stokes, sq.cm./sec.}$$

$$\text{Centistokes} \times 1.076 \times 10^{-5} = \text{sq.ft./sec.}$$

$$\text{Centistokes} \times 0.01 = \text{Stokes, sq.cm./sec.}$$

Thermal Conductivity (through a homogeneous material)

$$\frac{\text{Btu (ft.)}}{(\text{sq.ft.}) (\text{°F.}) (\text{hr.})} \times 4.134 \times 10^{-3} = \frac{(\text{g.-cal.}) (\text{cm.})}{(\text{sq.cm.}) (\text{°C.}) (\text{sec.})}$$

$$\times 1.200 \times 10 = \frac{(\text{Btu}) (\text{in.})}{(\text{sq.ft.}) (\text{°F.}) (\text{hr.})}$$

$$\times 3.518 \times 10^{-3} = \frac{(\text{kilowatt hrs.}) (\text{in.})}{(\text{sq.ft.}) (\text{°F.}) (\text{hr.})}$$

$$\frac{(\text{g.-cal.}) (\text{cm.})}{(\text{sq.cm.}) (\text{°C.}) (\text{hr.})} \times 8.063 \times 10^{-1} = \frac{\text{Btu (in.)}}{(\text{sq.ft.}) (\text{°F.}) (\text{hr.})}$$

$$\times 6.719 \times 10^{-2} = \frac{\text{Btu (ft.)}}{(\text{sq.ft.}) (\text{°F.}) (\text{hr.})}$$

$$\frac{(\text{g.-cal.}) (\text{cm.})}{(\text{sq.cm.}) (\text{°C.}) (\text{sec.})} \times 2.903 \times 10^3 = \frac{\text{Btu (in.)}}{(\text{sq.ft.}) (\text{°F.}) (\text{hr.})}$$

$$\times 8.063 \times 10^{-1} = \frac{\text{Btu (in.)}}{(\text{sq.ft.}) (\text{°F.}) (\text{sec.})}$$

$$\times 8.506 \times 10^2 = \frac{(\text{joules}) (\text{in.})}{(\text{sq.ft.}) (\text{°F.}) (\text{sec.})}$$

Specific Gravity (Liquid)

$$s = \frac{\rho \text{ of liquid @ } 60^\circ \text{ F.*}}{\rho \text{ of water @ } 60^\circ \text{ F.*}}$$

* or at other specified temperature

Oil

$$s \text{ at } 60^\circ \text{ F./} 60^\circ \text{ F.} = \frac{141.5}{131.5 + \text{degrees API}}$$

Liquids Lighter Than Water

$$s \text{ @ } 60^\circ \text{ F./} 60^\circ \text{ F.} = \frac{140}{130 + \text{degrees Baume'}}$$

Liquids Heavier Than Water

$$s \text{ @ } 60^\circ \text{ F./} 60^\circ \text{ F.} = \frac{145}{145 - \text{degrees Baume'}}$$

Specific Gravity (Gases)

$$S_g = \frac{R \text{ of air}}{R \text{ of gas}} = \frac{53.3}{R \text{ of gas}}, \text{ where } R = \text{gas constant}$$

$$S_g = \frac{\text{mol. wt. (gas)}}{\text{mol. wt. (air)}} = \frac{\text{mol. wt. (gas)}}{29}$$

Density, Liquid ρ

$$\text{Density liquid, } \rho = (62.3 \text{ lb./cu. ft. water}) (\text{Sp. Gr. liquid}), \\ \text{pounds /cu. ft.}$$

Metric

$$1 \text{ gram} = 10 \text{ decigrams} \\ = 100 \text{ centigrams} \\ = 1,000 \text{ milligrams} \\ = 1,000,000 \text{ microgram} \\ = 0.001 \text{ kilogram} \\ = 10^{-6} \text{ megagram}$$

$$1 \text{ liter} = 10 \text{ deciliters} = 1.0567 \text{ liquid quarts}$$

$$10 \text{ liters} = 1 \text{ dekaliter} = 2.6417 \text{ liquid gallons}$$

$$10 \text{ dekaliters} = 1 \text{ hectoliter} = 2.8375 \text{ U. S. bushels}$$

(Continued on next page)

A-2. (Concluded). Physical Property Conversion Factors

1 meter = 10 decimeters = 39.37 inches
 = 100 centimeters
 = 1,000 millimeters
 = 1,000,000 microns = 1,000,000 micrometers
 = 1/1,000 kilometer
 = 10^{10} Angstrom units

10 millimeters = 1 centimeter = 0.3937 inches
 10 centimeters = 1 decimeter = 3.937 inches
 25.4 millimeters = 1 inch

Specific Heat

$$\begin{aligned} \frac{(\text{gram-cal.})}{(\text{gram})(^{\circ}\text{C.})} \times 1.8 &= \frac{\text{Btu}}{(\text{pound})(^{\circ}\text{C.})} \\ &\times 1.0 = \frac{\text{Btu}}{(\text{pound})(^{\circ}\text{F.})} \\ &\times 4.186 = \frac{\text{joules}}{(\text{gram})(^{\circ}\text{C.})} \\ &\times 1055 = \frac{\text{joules}}{(\text{pound})(^{\circ}\text{F.})} \\ &\times 1.163 \times 10^{-3} = \frac{\text{kilowatt-hours}}{(\text{kilogram})(^{\circ}\text{C.})} \\ &\times 2.930 \times 10^{-4} = \frac{\text{kilowatt-hours}}{(\text{pound})(^{\circ}\text{F.})} \end{aligned}$$

Specific heat of water at 1 atm. = 0.238 cal./gm-°C.
 Btu/lb. - °F. \times 0.2390 = Btu/lb. - °R

Heat Transfer Coefficient

$$\begin{aligned} &\text{PCU}/(\text{hr.})(\text{sq. ft.})(^{\circ}\text{C.}) \times 1.0 \\ &= \text{Btu}/(\text{hr.})(\text{sq. ft.})(^{\circ}\text{F.}) \end{aligned}$$

$$\begin{aligned} &\text{Kg-cal.}/(\text{hr.})(\text{sq. m.})(^{\circ}\text{C.}) \times 0.2048 \\ &= \text{Btu}/(\text{hr.})(\text{sq. ft.})(^{\circ}\text{F.}) \\ &\text{G-cal.}/(\text{sec.})(\text{sq. cm.})(^{\circ}\text{C.}) \times 7,380 \\ &= \text{Btu}/(\text{hr.})(\text{sq. ft.})(^{\circ}\text{F.}) \\ &\text{Watts}/(\text{sq. in.})(^{\circ}\text{F.}) \times 490 = \text{Btu}/(\text{hr.})(\text{sq. ft.})(^{\circ}\text{F.}) \end{aligned}$$

Energy Units

$$\begin{aligned} \text{Pound-Centigrade-Unit(PCU)} &\times 1.8 = \text{Btu} \\ &\times 0.45359 = \text{calorie} \\ &\times 1400.4 = \text{ft.-lb.} \\ &\times 0.0005276 = \\ &\quad \text{kilowatt-hr.} \\ &\times 1899.36 = \text{joules} \end{aligned}$$

$$\begin{aligned} \text{Calories} &\times 3.9683 = \text{Btu} \\ &\times 3091.36 = \text{ft.-lb.} \\ &\times 0.001559 = \text{horsepower-hr.} \\ &\times 0.001163 = \text{kilowatt-hr.} \\ &\times 4187.37 = \text{joules} \end{aligned}$$

Pressure

$$\begin{aligned} 1 \text{ mm Hg} &= 1,333 \text{ dynes/sq. cm.} \\ 750 \text{ mm Hg} &= 10 \text{ dynes/sq. cm.} = 1 \text{ megabar @ } ^{\circ}\text{C.} \\ &\text{and } g = 980.6 \end{aligned}$$

A-3. Synchronous Speeds

$$\text{Synchronous Speed} = \frac{\text{Frequency} \times 120}{\text{No. of Poles}}$$

FREQUENCY				FREQUENCY		
Poles	60 cycle	50 cycle	25 cycle	Poles	60 cycle	50 cycle
2	3600	3000	1500	42	171.4	142.9
4	1800	1500	750	44	163.6	136.4
6	1200	1000	500	46	156.5	130.4
8	900	750	375	48	150	125
10	720	600	300	50	144	120
12	600	500	250	52	138.5	115.4
14	514.3	428.6	214.3	54	133.3	111.1
16	450	375	187.5	56	128.6	107.1
18	400	333.3	166.7	58	124.1	103.5
20	360	300	150	60	120	100
22	327.2	272.7	136.4	62	116.1	96.8
24	300	250	125	64	112.5	93.7
26	276.9	230.8	115.4	66	109.1	90.9
28	257.1	214.3	107.1	68	105.9	88.2
30	240	200	100	70	102.9	85.7
32	225	187.5	93.7	72	100	83.3
34	211.8	176.5	88.2	74	97.3	81.1
36	200	166.7	83.3	76	94.7	78.9
38	189.5	157.9	78.9	78	92.3	76.9
40	180	150	75	80	90	75

Courtesy Ingersoll-Rand Co.

A-4. Conversion Factors

Units of Length	Multiply units in left column by proper factor below							
	in.	ft.	yd.	mile	mm.	cm.	m.	km.
1 inch	1	0.0833	0.0278	—	25.40	2.540	0.0254	—
1 foot	12	1	0.3333	—	304.8	30.48	0.3048	—
1 yard	36	3	1	—	914.4	91.44	0.9144	—
1 mile	—	5280	1760	1	—	—	1609.3	1.609
1 millimeter	0.0394	0.0033	—	—	1	0.100	0.001	—
1 centimeter	0.3937	0.0328	0.0109	—	10	1	0.01	—
1 meter	39.37	3.281	1.094	—	1000	100	1	0.001
1 kilometer	—	3281	1094	0.6214	—	—	1000	1

(1 micron = 0.001 millimeter)

Courtesy Ingersoll-Rand Co.

(Continued on next page)

A-4. (Continued). Conversion Factors

Units of Weight	Multiply units in left column by proper factor below						
	grain	oz.	lb.	ton	gram	kg.	metric ton
1 grain	1	—	—	—	0.0648	—	—
1 ounce	437.5	1	0.0625	—	28.35	0.0283	—
1 pound	7000	16	1	0.0005	453.6	0.4536	—
1 ton	—	32,000	2000	1	—	907.2	0.9072
1 gram	15.43	0.0353	—	—	1	0.001	—
1 kilogram	—	35.27	2.205	—	1000	1	0.001
1 metric ton	—	35,274	2205	1.1023	—	1000	1

Units of Density	Multiply units in left column by proper factor below				
	lb/cu. in.	lb/cu. ft.	lb/gal.	g/cu. cm.	g/liter
1 pound/cu. in.	1	1728	231.0	27.68	27,680
1 pound/cu. ft.	—	1	0.1337	0.0160	16.019
1 pound/gal.	0.00433	7.481	1	0.1198	119.83
1 gram/cu. cm.	0.0361	62.43	8.345	1	1000.0
1 gram/liter	—	0.0624	0.00835	0.001	1

Units of Area	Multiply units in left column by proper factor below						
	sq. in.	sq. ft.	acre	sq. mile	sq. cm.	sq. m.	hectare
1 sq. inch	1	0.0069	—	—	6.452	—	—
1 sq. foot	144	1	—	—	929.0	0.0929	—
1 acre	—	43,560	1	0.0016	—	4047	0.4047
1 sq. mile	—	—	640	1	—	—	259.0
1 sq. centimeter	0.1550	—	—	—	1	0.0001	—
1 sq. meter	1550	10.76	—	—	10,000	1	—
1 hectare	—	—	2.471	—	—	10,000	1

Units of Volume	Multiply units in left column by proper factor below							
	cu. in.	cu. ft.	cu. yd.	cu. cm.	cu. meter	liter	U.S. gal.	Imp. gal.
1 cu. inch	1	—	—	16.387	—	0.0164	—	—
1 cu. foot	1728	1	0.0370	28,317	0.0283	28.32	7.481	6.229
1 cu. yard	46,656	27	1	—	0.7646	764.5	202.0	168.2
1 cu. centimeter	0.0610	—	—	1	—	0.0010	—	—
1 cu. meter	61,023	35.31	1.308	1,000,000	1	999.97	264.2	220.0
1 liter	61.025	0.0353	—	1000.028	0.0010	1	0.2642	0.2200
1 U.S. gallon	231	0.1337	—	3785.4	—	3.785	1	0.8327
1 Imperial gallon	277.4	0.1605	—	4546.1	—	4.546	1.201	1

(Continued on next page)

A-4. (Concluded). Conversion Factors

Units of Pressure	Multiply units in left column by proper factor below						
	lb/sq. in.	lb/sq. ft.	Int. at.	kg/cm ²	mm Hg at 32°F	in. Hg at 32°F	ft. water at 39.2°F
1 pound/sq. in.	1	144	—	0.0703	51.713	2.0359	2.307
1 pound/sq. ft.	0.00694	1	—	—	0.3591	0.01414	0.01602
1 Intern. atmosphere	14.696	2116.2	1	1.0333	760	29.921	33.90
1 kilogram/sq. cm.	14.223	2048.1	0.9678	1	735.56	28.958	32.81
1 millimeter-mercury— 1 torr (torricelli)—	0.0193	2.785	—	—	1	0.0394	0.0446
1 inch mercury	0.4912	70.73	0.0334	0.0345	25.400	1	1.133
1 foot water	0.4335	62.42	—	0.0305	22.418	0.8826	1

Units of Energy	Multiply units in left column by proper factor below					
	ft.-lb.	Btu	g. cal.	Joule	kw-hr.	hp-hr.
1 foot-pound	1	0.001285	0.3240	1.3556	—	—
1 Btu	778.2	1	252.16	1054.9	—	—
1 gram calorie	3.0860	0.003966	1	4.1833	—	—
1 Int. Joule	0.7377	0.000948	0.2390	1	—	—
1 Int. kilowatt-hour	2,655,656	3412.8	860,563	—	1	1.3412
1 horsepower-hour	1,980,000	2544.5	641,617	—	0.7456	1

Units of Specific Energy	Multiply units in left column by proper factor below				
	absolute Joule/g	Int. Joule/g	cal/g	Int. cal/g	Btu/lb.
1 absolute Joule/gram	1	0.99984	0.23901	0.23885	0.42993
1 Int. Joule/gram	1.000165	1	0.23904	0.23892	0.43000
1 calorie/gram	4.1840	4.1833	1	0.99935	1.7988
1 Int. calorie/gram	4.1867	4.1860	1.00065	1	1.8000
1 Btu/lb.	2.3260	2.3256	0.55592	0.55556	1

Units of Power (rates of energy use)	Multiply units in left column by proper factor below								
	hp	watt	kw	Btu/min.	Btu/hr.	ft-lb/sec.	ft-lb/min.	g. cal/sec.	metric hp
1 horsepower	1	745.7	0.7475	42.41	2544.5	550	33.000	178.2	1.014
1 watt	—	1	0.001	0.0569	3.413	0.7376	44.25	0.2390	0.00136
1 kilowatt	1.3410	1000	1	56.88	3412.8	737.6	44,254	239.0	1.360
1 Btu per minute	—	—	—	1	60	12.97	778.2	4.203	0.0239
1 metric hp	0.9863	735.5	0.7355	41.83	2509.6	542.5	32.550	175.7	1

Units of Refrigeration	Multiply units in left column by factor below					
	Btu(IT)/min.	Btu(IT)/hr.	kg cal/hr.	ton (U.S.) comm	ton (BRIT.) comm	frigorie/hr.
1 ton (U.S.) comm	200	12,000	3025.9	1	0.8965	3025.9
1 ton (Brit) comm	223.08	13,385	3375.2	1.1154	1	3375.2
1 frigorie/hr.	0.06609	3.9657	1	0.0003305	0.0002963	1

Note:—Btu is International Steam Table Btu(IT). 1 frigorie = 1 kg cal (Not IT).

A-5. Temperature Conversion

NOTE: The center column of numbers in boldface refers to the temperature in degrees, either Centigrade or Fahrenheit, which it is desired to convert into the other scale. If converting from Fahrenheit to Centigrade degrees, the equivalent temperature will be found in the left column; while if converting from degrees Centigrade to degrees Fahrenheit, the answer will be found in the column on the right.

Centigrade	Fahrenheit	Centigrade	Fahrenheit	Centigrade	Fahrenheit	Centigrade	Fahrenheit	
-273.17	-459.7	-20.6	-5	23.0	11.1	52	125.6	
-268	-450	-17.8	0	32.0	11.7	53	127.4	
-262	-440				12.2	54	129.2	
-257	-430	-17.2	1	33.8	12.8	55	131.0	
-251	-420	-16.7	2	35.6	13.3	56	132.8	
-246	-410	-16.1	3	37.4				
-240	-400	-15.6	4	39.2	13.9	57	134.6	
-234	-390	-15.0	5	41.0	14.4	58	136.4	
		-14.4	6	42.8	15.0	59	138.2	
-229	-380	-13.9	7	44.6	15.6	60	140.0	
-223	-370	-13.3	8	46.4	16.1	61	141.8	
-218	-360				16.7	62	143.6	
-212	-350	-12.8	9	48.2	17.2	63	145.4	
-207	-340	-12.2	10	50.0	17.8	64	147.2	
-201	-330	-11.7	11	51.8				
-196	-320	-11.1	12	53.6	18.3	65	149.0	
-190	-310	-10.6	13	55.4	18.9	66	150.8	
		-10.0	14	57.2	19.4	67	152.6	
-184	-300	-9.4	15	59.0	20.0	68	154.4	
-179	-290	-8.9	16	60.8	20.6	69	156.2	
-173	-280				21.1	70	158.0	
-169	-273	-459.4	-8.3	62.6	21.7	71	159.8	
-168	-270	-454	-7.8	64.4	22.2	72	161.6	
-162	-260	-436	-7.2	66.2				
-157	-250	-418	-6.7	68.0	22.8	73	163.4	
-151	-240	-400	-6.1	69.8	23.3	74	165.2	
			-5.6	71.6	23.9	75	167.0	
-146	-230	-382	-5.0	73.4	24.4	76	168.8	
-140	-220	-364	-4.4	75.2	25.0	77	170.6	
-134	-210	-346			25.6	78	172.4	
-129	-200	-328	-3.9	77.0	26.1	79	174.2	
-123	-190	-310	-3.3	78.8	26.7	80	176.0	
-118	-180	-292	-2.8	80.6				
-112	-170	-274	-2.2	82.4	27.2	81	177.8	
-107	-160	-256	-1.7	84.2	27.8	82	179.6	
			-1.1	86.0	28.3	83	181.4	
-101	-150	-238	-0.6	87.8	28.9	84	183.2	
-96	-140	-220	0.0	89.6	29.4	85	185.0	
-90	-130	-202			30.0	86	186.8	
-84	-120	-184	0.6	91.4	30.6	87	188.6	
-79	-110	-166	1.1	93.2	31.1	88	190.4	
-73.3	-100	-148.0	1.7	95.0				
-67.8	-90	-130.0	2.2	96.8	31.7	89	192.2	
-62.2	-80	-112.0	2.8	98.6	32.2	90	194.0	
			3.3	100.4	32.8	91	195.8	
-59.4	-75	-103.0	3.9	102.2	33.3	92	197.6	
-56.7	-70	-94.0	4.4	104.0	33.9	93	199.4	
-53.9	-65	-85.0			34.4	94	201.2	
-51.1	-60	-76.0	5.0	105.8	35.0	95	203.0	
-48.3	-55	-67.0	5.6	107.6	35.6	96	204.8	
-45.6	-50	-58.0	6.1	109.4				
-42.8	-45	-49.0	6.7	111.2	36.1	97	206.6	
-40.0	-40	-40.0	7.2	113.0	36.7	98	208.4	
			7.8	114.8	37.2	99	210.2	
-37.2	-35	-31.0	8.3	116.6	37.8	100	212.0	
-34.4	-30	-22.0	8.9	118.4	40.6	105	221	
-31.7	-25	-13.0			43.3	110	230	
-28.9	-20	-4.0	9.4	120.2	46.1	115	239	
-26.1	-15	5.0	10.0	122.0	48.9	120	248	
-23.3	-10	14.0	10.6	123.8	51.7	125	257	
							260	
							130	266
							135	275
							140	284
							145	293
							150	302
							155	311
							160	320
							165	329
							170	338
							175	347
							180	356
							185	365
							190	374
							195	383
							200	392
							205	401
							210	410
							212	414
							215	419
							220	428
							225	437
							230	446
							235	455
							240	464
							245	473
							250	482
							255	491
							260	500
							265	509
							270	518
							275	527
							280	536
							285	545
							290	554
							295	563
							300	572
							310	590
							320	608
							330	626
							340	644
							350	662
							360	680
							370	698
							380	716
							390	734
							400	752
							410	770
							420	788
							430	806
							440	824
							450	842
							460	860
							470	878
							480	896
							490	914
							500	932

The formulas at the right may also be used for converting Centigrade or Fahrenheit degrees into the other scales.

$$\text{Degrees Cent., } ^\circ\text{C} = \frac{5}{9} (^{\circ}\text{F} + 40) - 40$$

$$\text{Degrees Fahr., } ^\circ\text{F} = \frac{9}{5} (^{\circ}\text{C} + 40) - 40$$

$$= \frac{5}{9} (^{\circ}\text{F} - 32)$$

$$= \frac{9}{5} \text{ } ^\circ\text{C} + 32$$

$$\text{Degrees Kelvin, } ^\circ\text{K} = ^\circ\text{C} + 273.2$$

$$\text{Degrees Rankine, } ^\circ\text{R} = ^\circ\text{F} + 459.7$$

A-6. Altitude and Atmospheric Pressures

Altitude above Sea Level			Temperature**		Barometer*		Atmospheric Pressure	
Feet*	Miles	Meters*	°F	°C	Inches Hg Abs.	mm Hg Abs.	PSIA	Kg/sq cm Abs.
-5000	—	-1526	77	25	35.58	903.7	17.48	1.229
-4500	—	-1373	75	24	35.00	889.0	17.19	1.209
-4000	—	-1220	73	23	34.42	874.3	16.90	1.188
-3500	—	-1068	71	22	33.84	859.5	16.62	1.169
-3000	—	-915	70	21	33.27	845.1	16.34	1.149
-2500	—	-763	68	20	32.70	830.6	16.06	1.129
-2000	—	-610	66	19	32.14	816.4	15.78	1.109
-1500	—	-458	64	18	31.58	802.1	15.51	1.091
-1000	—	-305	63	17	31.02	787.9	15.23	1.071
-500	—	-153	61	16	30.47	773.9	14.96	1.052
0	—	0	59	15	29.92	760.0	14.696	1.0333
500	—	153	57	14	29.38	746.3	14.43	1.015
1000	—	305	55	13	28.86	733.0	14.16	.956
1500	—	458	54	12	28.33	719.6	13.91	.978
2000	—	610	52	11	27.82	706.6	13.66	.960
2500	—	763	50	10	27.32	693.9	13.41	.943
3000	—	915	48	9	26.82	681.2	13.17	.926
3500	—	1068	47	8	26.33	668.8	12.93	.909
4000	—	1220	45	7	25.84	656.3	12.69	.892
4500	—	1373	43	6	25.37	644.4	12.46	.876
5000	0.95	1526	41	5	24.90	632.5	12.23	.860
6000	1.1	1831	38	3	23.99	609.3	11.78	.828
7000	1.3	2136	34	1	23.10	586.7	11.34	.797
8000	1.5	2441	31	-1	22.23	564.6	10.91	.767
9000	1.7	2746	27	-3	21.39	543.3	10.50	.738
10,000	1.9	3050	23	-5	20.58	522.7	10.10	.710
15,000	2.8	4577	6	-14	16.89	429.0	8.29	.583
20,000	3.8	6102	-12	-24	13.76	349.5	6.76	.475
25,000	4.7	7628	-30	-34	11.12	282.4	5.46	.384
30,000	5.7	9153	-48	-44	8.903	226.1	4.37	.307
35,000	6.6	10,679	-66	—	7.060	179.3	3.47	.244
40,000	7.6	12,204	-70	-57	5.558	141.2	2.73	.192
45,000	8.5	13,730	-70	-57	4.375	111.1	2.15	.151
50,000	9.5	15,255	-70	-57	3.444	87.5	1.69	.119
55,000	10.4	16,781	-70	-57	2.712	68.9	1.33	.0935
60,000	11.4	18,306	-70	-57	2.135	54.2	1.05	.0738
70,000	13.3	21,357	-67	-55	1.325	33.7	.651	.0458
80,000	15.2	24,408	-62	-52	†8.273 ⁻¹	21.0	.406	.0285
90,000	17.1	27,459	-57	-59	5.200 ⁻¹	13.2	.255	.0179
100,000	18.9	30,510	-51	-46	3.290 ⁻¹	8.36	.162	.0114
120,000	22.8	36,612	-26	-48	1.358 ⁻¹	3.45	—	—
140,000	26.6	42,714	4	-16	5.947 ⁻²	1.51	—	—
160,000	30.4	48,816	28	-2	2.746 ⁻²	†6.97 ⁻¹	—	—
180,000	34.2	54,918	19	-7	1.284 ⁻²	3.26 ⁻¹	—	—
200,000	37.9	61,020	-3	-19	5.846 ⁻³	1.48 ⁻¹	—	—
220,000	41.7	67,122	-44	-42	2.523 ⁻³	6.41 ⁻²	—	—
240,000	45.5	73,224	-86	-66	9.955 ⁻⁴	2.53 ⁻²	—	—
260,000	49.3	79,326	-129	-90	3.513 ⁻⁴	8.92 ⁻³	—	—
280,000	53.1	85,428	-135	-93	1.143 ⁻⁴	3.67 ⁻³	—	—
300,000	56.9	91,530	-127	-88	3.737 ⁻⁵	9.49 ⁻⁴	—	—
400,000	75.9	122,040	—	—	6.3 ⁻⁷	1.60 ⁻⁵	—	—
500,000	94.8	152,550	—	—	1.4 ⁻⁷	3.56 ⁻⁶	—	—
600,000	114	183,060	—	—	5.9 ⁻⁸	1.50 ⁻⁶	—	—
800,000	152	244,080	—	—	1.6 ⁻⁸	4.06 ⁻⁷	—	—
1,000,000	189	305,100	—	—	5.1 ⁻⁹	1.30 ⁻⁷	—	—
1,200,000	228	366,120	—	—	2.0 ⁻⁹	5.08 ⁻⁸	—	—
1,400,000	266	427,140	—	—	8.2 ⁻¹⁰	2.08 ⁻⁸	—	—
1,600,000	304	488,160	—	—	3.8 ⁻¹⁰	9.65 ⁻⁹	—	—
1,800,000	342	549,180	—	—	1.8 ⁻¹⁰	4.57 ⁻⁹	—	—
2,000,000	379	610,200	—	—	9.2 ⁻¹¹	2.34 ⁻⁹	—	—

Data from NASA Standard Atmosphere (1962).

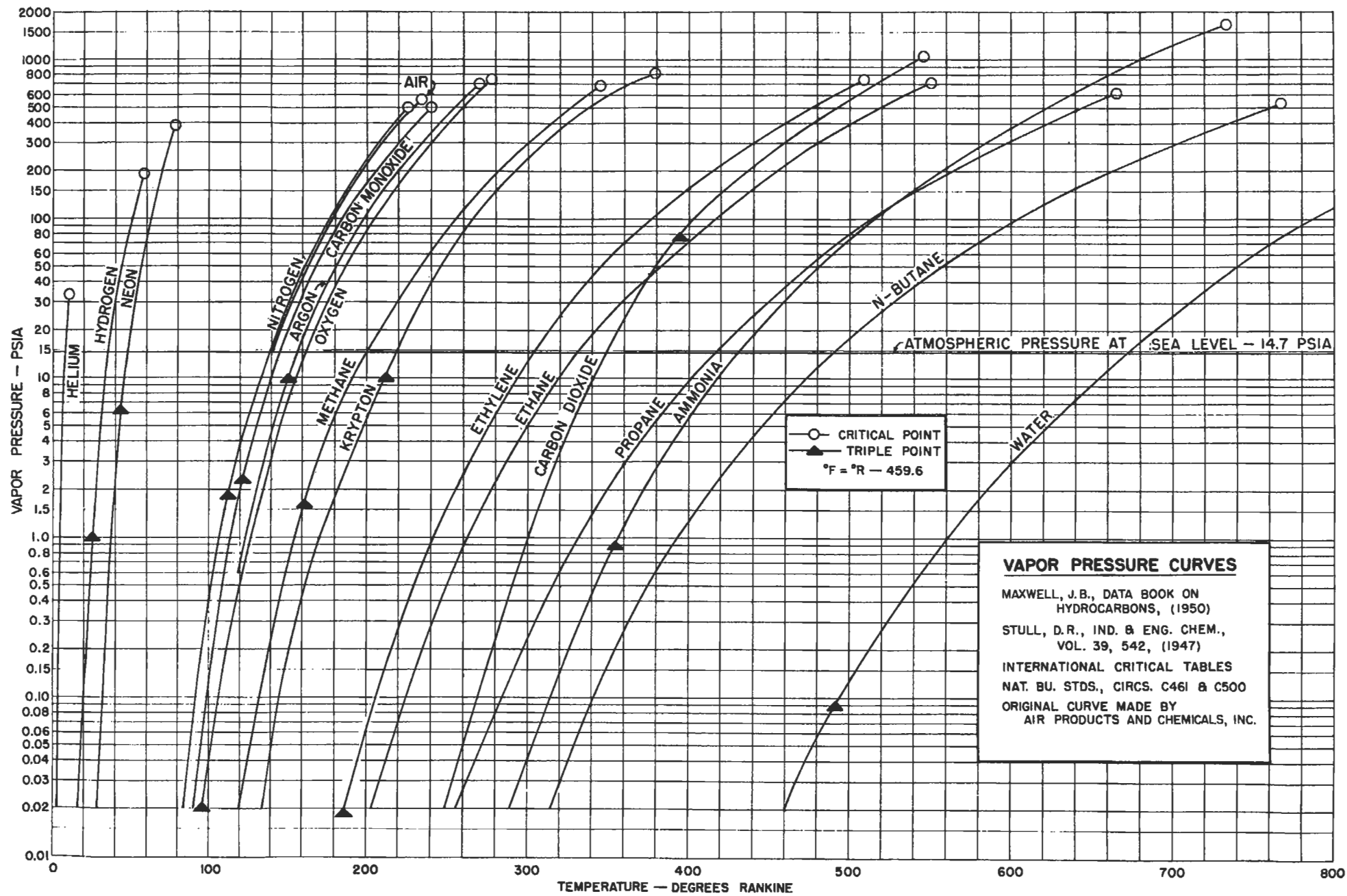
*Temperature and barometer are approximate for negative altitudes.

**Temperatures are average existing at 40° latitude and are rounded to even numbers.

†Negative exponent shows number of spaces the decimal point must be moved to the left.

Courtesy Ingersoll-Rand Co.

A-7.
Vapor Pressure Curves. (Courtesy Ingersoll-Rand Co.)



VAPOR PRESSURE CURVES
 MAXWELL, J.B., DATA BOOK ON
 HYDROCARBONS, (1950)
 STULL, D.R., IND. & ENG. CHEM.,
 VOL. 39, 542, (1947)
 INTERNATIONAL CRITICAL TABLES
 NAT. BU. STDS., CIRC. C461 & C500
 ORIGINAL CURVE MADE BY
 AIR PRODUCTS AND CHEMICALS, INC.

A-8. Pressure Conversion Chart

BY FACTOR TO OBTAIN →

MULTIPLY GIVEN NUMBER OF	GIVEN	lb/in ²	in H ₂ O (at +39.2°C)	cm H ₂ O (at +4°C)	in Hg (at +32°F)	mm Hg (Torr) (at 0°C)	dynes/cm ² (1 μ bar)	newton/m ² (PASCAL)	kgm/cm ²	bar	atm. (A _n)	lb/ft ²	ft H ₂ O (at +39.2°C)
	lb/in ²	1.0000	2.7890x10 ¹	7.0308x10 ¹	2.0380	5.1715x10 ¹	6.8948x10 ⁴	6.8948x10 ³	7.0306x10 ⁻²	6.8947x10 ⁻²	6.8045x10 ⁻²	1.4400x10 ²	2.3067
	in H ₂ O (at +39.2°C)	3.6127x10 ⁻²	1.0000	2.5400	7.3554x10 ⁻²	1.8683	2.4908x10 ³	2.4908x10 ²	2.5399x10 ⁻³	2.4908x10 ⁻³	2.4582x10 ⁻³	5.2022	8.3333x10 ⁻²
	cm H ₂ O (at +4°C)	1.4223x10 ⁻²	0.3937	1.0000	2.8958x10 ⁻²	0.7355	9.8064x10 ²	9.8064x10 ¹	9.9997x10 ⁻⁴	9.8064x10 ⁻⁴	9.6781x10 ⁻⁴	2.0481	3.2808x10 ⁻²
	in Hg (at +32°F)	4.9116x10 ⁻¹	1.3596x10 ¹	3.4532x10 ¹	1.0000	2.5400x10 ¹	3.3864x10 ⁴	3.3864x10 ³	3.4532x10 ⁻²	3.3864x10 ⁻²	3.3421x10 ⁻²	7.0727x10 ¹	1.1330
	mm Hg (Torr) (at 0°C)	1.9337x10 ⁻²	5.3525x10 ⁻¹	1.3595	3.9370x10 ⁻²	1.0000	1.3332x10 ³	1.3332x10 ²	1.3595x10 ⁻³	1.3332x10 ⁻³	1.3158x10 ⁻³	2.7845	4.4605x10 ⁻²
	dynes/cm ² (1 μ bar)	1.4504x10 ⁻⁵	4.0147x10 ⁻⁴	1.0197x10 ⁻³	2.9530x10 ⁻⁵	7.5006x10 ⁻⁴	1.0000	1.0000x10 ⁻¹	1.0197x10 ⁻⁶	1.0000x10 ⁻⁶	9.8692x10 ⁻⁷	2.0886x10 ⁻³	3.3456x10 ⁻⁵
	newton/m ² (PASCAL)	1.4504x10 ⁻⁴	4.0147x10 ⁻³	1.0197x10 ⁻²	2.9530x10 ⁻⁴	7.5006x10 ⁻³	1.0000x10 ¹	1.0000	1.0197x10 ⁻⁵	1.0000x10 ⁻⁵	9.8692x10 ⁻⁶	2.0885x10 ⁻²	3.3456x10 ⁻⁴
	kgm/cm ²	1.4224x10 ¹	3.9371x10 ²	1.00003x10 ³	2.8959x10 ¹	7.3556x10 ²	9.8060x10 ⁵	9.8060x10 ⁴	1.0000	9.8060x10 ⁻¹	9.678x10 ⁻¹	2.0482x10 ³	3.2809x10 ¹
	bar	1.4504x10 ¹	4.0147x10 ²	1.0197x10 ³	2.9530x10 ¹	7.5006x10 ²	1.0000x10 ⁶	1.0000x10 ⁵	1.0197	1.0000	9.8692x10 ⁻¹	2.0885x10 ³	3.3456x10 ¹
	atm. (A _n)	1.4896x10 ¹	4.0679x10 ²	1.0333x10 ³	2.9921x10 ¹	7.6000x10 ²	1.0133x10 ⁶	1.0133x10 ⁵	1.0332	1.0133	1.0000	2.1162x10 ³	3.3900x10 ¹
	lb/ft ²	6.9445x10 ⁻³	1.9223x10 ⁻¹	4.882x10 ⁻¹	1.4139x10 ⁻²	3.591x10 ⁻¹	4.7880x10 ²	4.7880x10 ¹	4.8824x10 ⁻⁴	4.7880x10 ⁻⁴	4.7254x10 ⁻⁴	1.0000	1.6019x10 ⁻²
	ft H ₂ O (at +39.2°C)	4.3352x10 ⁻¹	1.2000x10 ¹	3.0480x10 ¹	8.826x10 ⁻¹	2.2419x10 ¹	2.9890x10 ⁴	2.9890x10 ³	3.0479x10 ⁻²	2.9890x10 ⁻²	2.9499x10 ⁻²	6.2427x10 ¹	1.0000

A-9.
Vacuum Conversion

Torr	Absolute Pressure		Inches Hg (Abs.)	Psia	Vacuum* Inches Hg
	Microns Hg	Mm Hg			
		762	30.00	14.74	—
		750	29.53	14.50	0.47
		700	27.56	13.54	2.44
		650	25.59	12.57	4.41
		600	23.62	11.60	6.38
		550	21.65	10.64	8.35
		500	19.68	9.67	10.32
		450	17.72	8.70	12.28
		400	15.75	7.74	14.25
		350	13.78	6.77	16.22
		300	11.81	5.80	18.19
		250	9.84	4.84	20.16
		200	7.84	3.87	22.13
		150	5.91	2.900	24.09
		100	3.94	1.934	26.06
		50	1.97	.967	28.03
		40	1.57	.774	28.43
		30	1.181	.580	28.82
		20	0.787	.3868	
		10	0.394	.1934	
		5	.197	.0967	
		4	.158	.0774	
		3	.1181	.0580	
		2	.0787	.0387	
1.0	1000	1	.0392	.0193	
0.5	500	0.50	.0197		Low Vacuum
1 × 10 ⁻¹	100	0.10	.0039		
5 × 10 ⁻²	50	0.050			
1 × 10 ⁻²	10	0.010			
5 × 10 ⁻³	5	0.005			
1 × 10 ⁻³	1	0.001			
1 × 10 ⁻⁴					High Vacuum
1 × 10 ⁻⁶ to					
1 × 10 ⁻⁸					Very High Vac.
1 × 10 ⁻⁹ to					
1 × 10 ⁻⁹					Ultra High Vac.
and beyond					

*Refers to 30" Barometer

Conversion Factors:

1 millimeter = 1000 microns
1 Torr = 1 mm Hg Abs.

1 inch Hg = 25.4 mm Hg
1 atmosphere = 14.7 pounds per sq. in. = 760 mm Hg = 29.92 in. Hg

A-10. Decimal and Millimeter Equivalents of Fractions

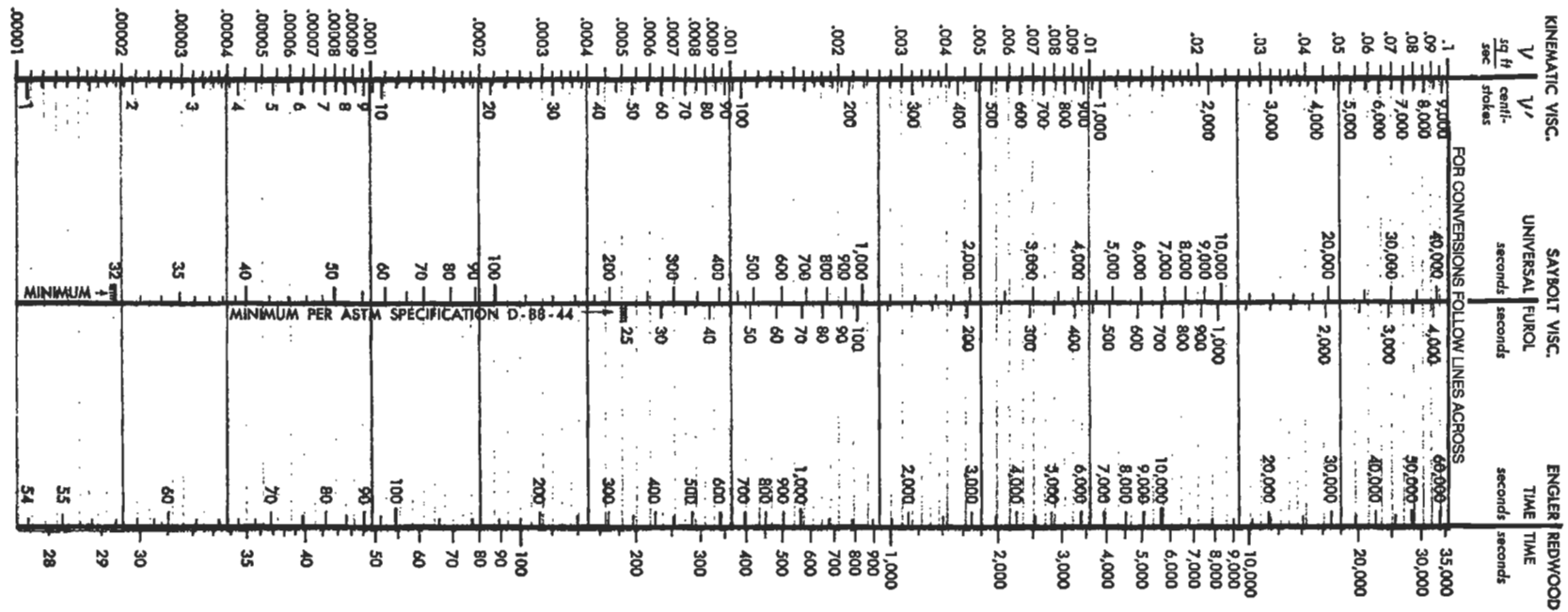
Inches		Milli- meters	Inches		Milli- meters
Fractions	Decimals		Fractions	Decimals	
1/64	.015625	.397	33/64	.515625	13.097
1/32	.03125	.794	17/32	.53125	13.494
3/64	.046875	1.191	35/64	.546875	13.891
1/16	.0625	1.588	9/16	.5625	14.288
5/64	.078125	1.984	37/64	.578125	14.684
3/32	.09375	2.381	19/32	.59375	15.081
7/64	.109375	2.778	39/64	.609375	15.478
1/8	.125	3.175	5/8	.625	15.875
9/64	.140625	3.572	41/64	.640625	16.272
5/32	.15625	3.969	21/32	.65625	16.669
11/64	.171875	4.366	43/64	.671875	17.066
3/16	.1875	4.763	11/16	.6875	17.463
13/64	.203125	5.159	45/64	.703125	17.859
7/32	.21875	5.556	23/32	.71875	18.256
15/64	.234375	5.953	47/64	.734375	18.653
1/4	.250	6.350	3/4	.750	19.050
17/64	.265625	6.747	49/64	.765625	19.447
9/32	.28125	7.144	25/32	.78125	19.844
19/64	.296875	7.541	51/64	.796875	20.241
5/16	.3125	7.938	13/16	.8125	20.638
21/64	.328125	8.334	33/64	.828125	21.034
11/32	.34375	8.731	27/32	.84375	21.431
23/64	.359375	9.128	35/64	.859375	21.828
3/8	.375	9.525	7/8	.875	22.225
25/64	.390625	9.922	37/64	.890625	22.622
13/32	.40625	10.319	29/32	.90625	23.019
27/64	.421875	10.716	39/64	.921875	23.416
7/16	.4375	11.113	15/16	.9375	23.813
29/64	.453125	11.509	61/64	.953125	24.209
15/32	.46875	11.906	31/32	.96875	24.606
31/64	.484375	12.303	63/64	.984375	25.003
1/2	.500	12.700	1	1.000	25.400

A-11. Particle Size Measurement

Meshes/Lineal Inch US and ASTM Std. Sieve No.	Actual Opening		Meshes/Lineal Inch US and ASTM Std. Sieve No.	Actual Opening	
	Inches	Microns		Inches	Microns
10	.0787	2000	170	.0035	88
12	.0661 1/6	1680	200	.0029	74
14	.0555	1410		.0026	65
16	.0469 3/64	1190	230	.0024	62
18	.0394	1000	270	.0021	53
20	.0331 1/32	840		.0020	50
25	.0280	710	325	.0017	44
30	.0232	590		.0016	40
35	.0197 1/64	500	400	.00142	36
40	.0165	420		.00118	30
45	.0138	350	550	.00099	25
50	.0117	297	625	.00079	20
60	.0098	250		.00059	15
70	.0083	210	1,250	.000394	10
80	.0070	177	1,750	.000315	8
100	.0059	149	2,500	.000197	5
120	.0049	125	5,000	.000099	2.5
140	.0041	105	12,000	.0000394	1

* 1 micron (μ) = 1 micrometer (μm), new National Bureau of Standards terminology
 1 micron = one-millionth of a meter
 Inches × 25,400 = microns or micrometers
 Reference ASTM E 11-70

A-12. Viscosity Conversions. (By permission, Tube Turns Div., Chemetron Corp., Bull. TT 725.)



Appendix

To convert other units into kinematic viscosity in English units v (sq ft per sec) or in Metric units v' (centistokes), use the chart or the formulas to the right:

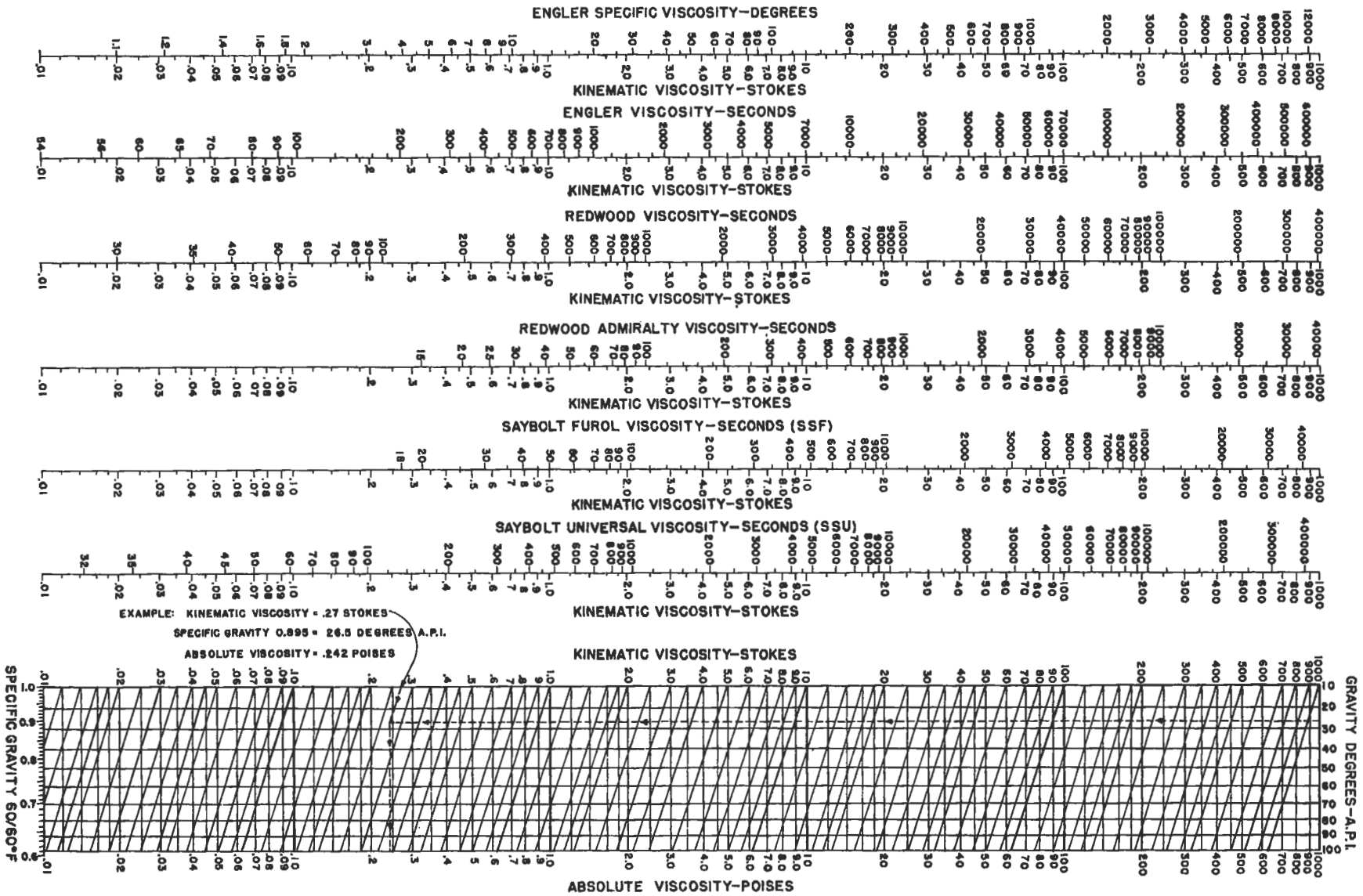
To convert:	into centistokes (v')	into sq ft per sec (v)
from Metric units (centistokes)	$v = 0.000\ 010\ 76\ v'$
from English units (sq ft per sec)	$v' = 92\ 900\ v$
from Saybolt Universal (seconds)	see Table I in ASTM Spec. D-446-39 (plotted for basic temperature 100 F)	converted from ASTM Spec. D-446-39
from Saybolt Furol (seconds)	see Table I in ASTM Spec. D-666-44 (plotted for std temp of 122 F)	converted from ASTM Spec. D-666-44
from Engler (seconds)	$v' = 0.147\ \text{Engler} - \frac{374}{\text{Engler}}$	$v = 0.000\ 001\ 58\ \text{Engler} - \frac{0.00403}{\text{Engler}}$
from Redwood standard (seconds)	$v' = 0.260\ \text{Redwood} - \frac{171.5}{\text{Redwood}}$	$v = 0.000\ 002\ 80\ \text{Redwood} - \frac{0.00185}{\text{Redwood}}$
from absolute viscosity	$v' = \frac{\text{centipoises}}{\text{density}}$	$v = 32.2\ \mu \frac{(\text{lb sec per sq ft})}{\rho (\text{lb per cu ft})}$

To convert degrees API and Baumé into Specific Gravity, use the formulas to the right:

Liquids lighter than water (API Formula)	Liquids heavier than water (U.S. Bureau of Stds.)
Specific gravity 60/60F = $\frac{141.5}{131.5 + \text{Degrees API}}$	Specific gravity = $\frac{145}{145 - \text{Degrees Baumé}}$

A-13.

Viscosity Conversions. (Courtesy Kinney Vacuum Div., The New York Air Brake Co.)



**Appendix
A-14.
Commercial Wrought Steel Pipe Data
(Based on ANSI B36.10 wall thicknesses)**

	Nominal Pipe Size Inches	Outside Diameter Inches	Thick-ness Inches	Inside Diameter		Inside Diameter Functions (In Inches)				Transverse Internal Area	
				d Inches	D Feet	d ²	d ³	d ⁴	d ⁵	a Sq. In.	A Sq. Ft.
Schedule 10	14	14	0.250	13.5	1.125	182.25	2460.4	33215.	448400.	143.14	0.994
	16	16	0.250	15.5	1.291	240.25	3723.9	57720.	894660.	188.69	1.310
	18	18	0.250	17.5	1.4583	306.25	5359.4	93789.	1641309.	240.53	1.670
	20	20	0.250	19.5	1.625	380.25	7414.9	144590.	2819500.	298.65	2.074
	24	24	0.250	23.5	1.958	552.25	12977.	304980.	7167030.	433.74	3.012
	30	30	0.312	29.376	2.448	862.95	25350.	744288.	21864218.	677.76	4.707
Schedule 20	8	8.625	0.250	8.125	0.6771	66.02	536.38	4359.3	35409.	51.85	0.3601
	10	10.75	0.250	10.25	0.8542	105.06	1076.9	11038.	113141.	82.52	0.5731
	12	12.75	0.250	12.25	1.021	150.06	1838.3	22518.	275855.	117.86	0.8185
	14	14	0.312	13.376	1.111	178.92	2393.2	32012.	428185.	140.52	0.9758
	16	16	0.312	15.376	1.281	236.42	3635.2	55894.	859442.	185.69	1.290
	18	18	0.312	17.376	1.448	301.92	5246.3	91156.	1583978.	237.13	1.647
	20	20	0.375	19.250	1.604	370.56	7133.3	137317.	2643352.	291.04	2.021
	24	24	0.375	23.25	1.937	540.56	12568.	292205.	6793832.	424.56	2.948
	30	30	0.500	29.00	2.417	841.0	24389.	707281.	20511149.	660.52	4.587
Schedule 30	8	8.625	0.277	8.071	0.6726	65.14	525.75	4243.2	34248.	51.16	0.3553
	10	10.75	0.307	10.136	0.8447	102.74	1041.4	10555.	106987.	80.69	0.5603
	12	12.75	0.330	12.09	1.0075	146.17	1767.2	21366.	258304.	114.80	0.7972
	14	14	0.375	13.25	1.1042	175.56	2326.2	30821.	408394.	137.88	0.9575
	16	16	0.375	15.25	1.2708	232.56	3546.6	54084.	824801.	182.65	1.268
	18	18	0.438	17.124	1.4270	293.23	5021.3	85984.	1472397.	230.30	1.599
	20	20	0.500	19.00	1.5833	361.00	6859.0	130321.	2476099.	283.53	1.969
	24	24	0.562	22.876	1.9063	523.31	11971.	273853.	6264703.	411.00	2.854
	30	30	0.625	28.75	2.3958	826.56	23764.	683201.	19642160.	649.18	4.508
Schedule 40	1/8	0.405	0.068	0.269	0.0224	0.0724	0.0195	0.005242	0.00141	0.057	0.00040
	1/4	0.540	0.088	0.364	0.0303	0.1325	0.0482	0.01756	0.00639	0.104	0.00072
	3/8	0.675	0.091	0.493	0.0411	0.2430	0.1198	0.05905	0.02912	0.191	0.00133
	1/2	0.840	0.109	0.622	0.0518	0.3869	0.2406	0.1497	0.09310	0.304	0.00211
	3/4	1.050	0.113	0.824	0.0687	0.679	0.5595	0.4610	0.3799	0.533	0.00371
	1	1.315	0.133	1.049	0.0874	1.100	1.154	1.210	1.270	0.864	0.00600
	1 1/4	1.660	0.140	1.380	0.1150	1.904	2.628	3.625	5.005	1.495	0.01040
	1 1/2	1.900	0.145	1.610	0.1342	2.592	4.173	6.718	10.82	2.036	0.01414
	2	2.375	0.154	2.067	0.1722	4.272	8.831	18.250	37.72	3.355	0.02330
	2 1/2	2.875	0.203	2.469	0.2057	6.096	15.051	37.161	91.75	4.788	0.03322
	3	3.500	0.216	3.068	0.2557	9.413	28.878	88.605	271.8	7.393	0.05130
	3 1/2	4.000	0.226	3.548	0.2957	12.59	44.663	158.51	562.2	9.886	0.06870
	4	4.500	0.237	4.026	0.3355	16.21	65.256	262.76	1058.	12.730	0.08840
	5	5.563	0.258	5.047	0.4206	25.47	128.56	648.72	3275.	20.006	0.1390
6	6.625	0.280	6.065	0.5054	36.78	223.10	1352.8	8206.	28.891	0.2006	
	8	8.625	0.322	7.981	0.6651	63.70	508.36	4057.7	32380.	50.027	0.3474
	10	10.75	0.365	10.02	0.8350	100.4	1006.0	10080.	101000.	78.855	0.5475
	12	12.75	0.406	11.938	0.9965	142.5	1701.3	20306.	242470.	111.93	0.7773
	14	14.0	0.438	13.124	1.0937	172.24	2260.5	29666.	389340.	135.28	0.9394
	16	16.0	0.500	15.000	1.250	225.0	3375.0	50625.	759375.	176.72	1.2272
	18	18.0	0.562	16.876	1.4063	284.8	4806.3	81111.	1368820.	223.68	1.5533
	20	20.0	0.593	18.814	1.5678	354.0	6659.5	125320.	2357244.	278.00	1.9305
	24	24.0	0.687	22.626	1.8855	511.9	11583.	262040.	5929784.	402.07	2.7921
Schedule 60	8	8.625	0.406	7.813	0.6511	61.04	476.93	3725.9	29113.	47.94	0.3329
	10	10.75	0.500	9.750	0.8125	95.06	926.86	9036.4	88110.	74.66	0.5185
	12	12.75	0.562	11.626	0.9688	135.16	1571.4	18268.	212399.	106.16	0.7372
	14	14.0	0.593	12.814	1.0678	164.20	2104.0	26962.	345480.	128.96	0.8956
	16	16.0	0.656	14.688	1.2240	215.74	3168.8	46544.	683618.	169.44	1.1766
	18	18.0	0.750	16.500	1.3750	272.25	4492.1	74120.	1222982.	213.83	1.4849
	20	20.0	0.812	18.376	1.5313	337.68	6205.2	114028.	2095342.	265.21	1.8417
	24	24.0	0.968	22.064	1.8387	486.82	10741.	236994.	5229036.	382.35	2.6552
Schedule 80	1/8	0.405	0.095	0.215	0.0179	0.0462	0.00994	0.002134	0.000459	0.036	0.00025
	1/4	0.540	0.119	0.302	0.0252	0.0912	0.0275	0.008317	0.002513	0.072	0.00050
	3/8	0.675	0.126	0.423	0.0353	0.1789	0.0757	0.03200	0.01354	0.141	0.00098
	1/2	0.840	0.147	0.546	0.0455	0.2981	0.1628	0.08886	0.04852	0.234	0.00163
	3/4	1.050	0.154	0.742	0.0618	0.5506	0.4085	0.3032	0.2249	0.433	0.00300
	1	1.315	0.179	0.957	0.0797	0.9158	0.8765	0.8387	0.8027	0.719	0.00499
	1 1/4	1.660	0.191	1.278	0.1065	1.633	2.087	2.6667	3.409	1.283	0.00891

A-14.
(Continued). Commercial Wrought Steel Pipe Data
(Based on ANSI B36.10 wall thicknesses)

	Nominal Pipe Size	Outside Diameter	Thick-ness	Inside Diameter		Inside Diameter Functions (In Inches)				Transverse Internal Area	
				Inches	Feet	d ²	d ³	d ⁴	d ⁵	α	λ
Schedule 80—cont.	1½	1.900	0.200	1.500	0.1250	2.250	3.375	5.062	7.594	1.767	0.01225
	2	2.375	0.218	1.939	0.1616	3.760	7.290	14.136	27.41	2.953	0.02050
	2½	2.875	0.276	2.323	0.1936	5.396	12.536	29.117	67.64	4.238	0.02942
	3	3.5	0.300	2.900	0.2417	8.410	24.389	70.728	205.1	6.605	0.04587
	3½	4.0	0.318	3.364	0.2803	11.32	38.069	128.14	430.8	8.888	0.06170
	4	4.5	0.337	3.826	0.3188	14.64	56.006	214.33	819.8	11.497	0.07986
	5	5.563	0.375	4.813	0.4011	23.16	111.49	536.38	2583.	18.194	0.1263
	6	6.625	0.432	5.761	0.4801	33.19	191.20	1101.6	6346.	26.067	0.1810
	8	8.625	0.500	7.625	0.6354	58.14	443.32	3380.3	25775.	45.663	0.3171
	10	10.75	0.593	9.564	0.7970	91.47	874.82	8366.8	80020.	71.84	0.4989
	12	12.75	0.687	11.376	0.9480	129.41	1472.2	16747.	190523.	101.64	0.7058
	14	14.0	0.750	12.500	1.0417	156.25	1953.1	24414.	305176.	122.72	0.8522
	16	16.0	0.843	14.314	1.1928	204.89	2932.8	41980.	600904.	160.92	1.1175
	18	18.0	0.937	16.126	1.3438	260.05	4193.5	67626.	1090518.	204.24	1.4183
	20	20.0	1.031	17.938	1.4948	321.77	5771.9	103536.	1857248.	252.72	1.7550
	24	24.0	1.218	21.564	1.7970	465.01	10027.	216234.	4662798.	365.22	2.5362
Schedule 100	8	8.625	0.593	7.439	0.6199	55.34	411.66	3062.	22781.	43.46	0.3018
	10	10.75	0.718	9.314	0.7762	86.75	807.99	7526.	69357.	68.13	0.4732
	12	12.75	0.843	11.064	0.9220	122.41	1354.4	14985.	165791.	96.14	0.6677
	14	14.0	0.937	12.126	1.0105	147.04	1783.0	21621.	262173.	115.49	0.8020
	16	16.0	1.031	13.938	1.1615	194.27	2707.7	37740.	526020.	152.58	1.0596
	18	18.0	1.156	15.688	1.3057	246.11	3861.0	60572.	950250.	193.30	1.3423
	20	20.0	1.281	17.438	1.4532	304.08	5302.6	92467.	1612438.	238.83	1.6585
	24	24.0	1.531	20.938	1.7448	438.40	9179.2	192195.	4024179.	344.32	2.3911
Schedule 120	4	4.50	0.438	3.624	0.302	13.133	47.595	172.49	625.1	10.315	0.07163
	5	5.563	0.500	4.563	0.3802	20.82	95.006	433.5	1978.	16.35	0.1136
	6	6.625	0.562	5.501	0.4584	30.26	166.47	915.7	5037.	23.77	0.1650
	8	8.625	0.718	7.189	0.5991	51.68	371.54	2671.	19202.	40.59	0.2819
	10	10.75	0.843	9.064	0.7553	82.16	744.66	6750.	61179.	64.53	0.4481
	12	12.75	1.000	10.750	0.8959	115.56	1242.3	13355.	143563.	90.76	0.6303
	14	14.0	1.093	11.814	0.9845	139.57	1648.9	19480.	230137.	109.62	0.7612
	16	16.0	1.218	13.564	1.1303	183.98	2495.5	33849.	459133.	144.50	1.0035
18	18.0	1.375	15.250	1.2708	232.56	3546.6	54086.	824804.	182.66	1.2684	
20	20.0	1.500	17.000	1.4166	289.00	4913.0	83521.	1419857.	226.98	1.5762	
24	24.0	1.812	20.376	1.6980	415.18	8459.7	172375.	3512313.	326.08	2.2645	
Schedule 140	8	8.625	0.812	7.001	0.5834	49.01	343.15	2402.	16819.	38.50	0.2673
	10	10.75	1.000	8.750	0.7292	76.56	669.92	5862.	51291.	60.13	0.4176
	12	12.75	1.125	10.500	0.8750	110.25	1157.6	12155.	127628.	86.59	0.6013
	14	14.0	1.250	11.500	0.9583	132.25	1520.9	17490.	201136.	103.87	0.7213
	16	16.0	1.438	13.124	1.0937	172.24	2260.5	29666.	389340.	135.28	0.9394
	18	18.0	1.562	14.876	1.2396	221.30	3292.0	48972.	728502.	173.80	1.2070
	20	20.0	1.750	16.5	1.3750	272.25	4492.1	74120.	1222981.	213.82	1.4849
	24	24.0	2.062	19.876	1.6563	395.06	7852.1	156069.	3102022.	310.28	2.1547
Schedule 160	½	0.840	0.187	0.466	0.0388	0.2172	0.1012	0.04716	0.02197	0.1706	0.00118
	¾	1.050	0.218	0.614	0.0512	0.3770	0.2315	0.1421	0.08726	0.2961	0.00206
	1	1.315	0.250	0.815	0.0679	0.6642	0.5413	0.4412	0.3596	0.5217	0.00362
	1¼	1.660	0.250	1.160	0.0966	1.346	1.561	1.811	2.100	1.057	0.00734
	1½	1.900	0.281	1.338	0.1115	1.790	2.395	3.205	4.288	1.406	0.00976
	2	2.375	0.343	1.689	0.1407	2.853	4.818	8.138	13.74	2.241	0.01556
	2½	2.875	0.375	2.125	0.1771	4.516	9.596	20.39	43.33	3.546	0.02463
	3	3.50	0.438	2.624	0.2187	6.885	18.067	47.41	124.4	5.408	0.03755
	4	4.50	0.531	3.438	0.2865	11.82	40.637	139.7	480.3	9.283	0.06447
	5	5.563	0.625	4.313	0.3594	18.60	80.230	346.0	1492.	14.61	0.1015
	6	6.625	0.718	5.189	0.4324	26.93	139.72	725.0	3762.	21.15	0.1469
	8	8.625	0.906	6.813	0.5677	46.42	316.24	2155.	14679.	36.46	0.2532
	10	10.75	1.125	8.500	0.7083	72.25	614.12	5220.	44371.	56.75	0.3941
	12	12.75	1.312	10.126	0.8438	102.54	1038.3	10514.	106461.	80.53	0.5592
	14	14.0	1.406	11.188	0.9323	125.17	1400.4	15668.	175292.	98.31	0.6827
	16	16.0	1.593	12.814	1.0678	164.20	2104.0	26961.	345482.	128.96	0.8956
18	18.0	1.781	14.438	1.2032	208.45	3009.7	43454.	627387.	163.72	1.1369	
20	20.0	1.968	16.064	1.3387	258.05	4145.3	66590.	1069715.	202.67	1.4074	
24	24.0	2.343	19.314	1.6095	373.03	7204.7	139152.	2687582.	292.98	2.0346	

(Concluded). Commercial Wrought Steel Pipe Data
(Based on ANSI B36.10 wall thicknesses)

Nominal Pipe Size Inches	Outside Diameter Inches	Thick-ness Inches	Inside Diameter		Inside Diameter Functions (In Inches)				Transverse Internal Area	
			d Inches	D Feet	d ²	d ³	d ⁴	d ⁵	A Sq. In.	A Sq. Ft.
Standard Wall Pipe										
1/8	0.405	0.068	0.269	0.0224	0.0724	0.0195	0.00524	0.00141	0.057	0.00040
1/4	0.540	0.088	0.364	0.0303	0.1325	0.0482	0.01756	0.00639	0.104	0.00072
3/8	0.675	0.091	0.493	0.0411	0.2430	0.1198	0.05905	0.02912	0.191	0.00133
1/2	0.840	0.109	0.622	0.0518	0.3869	0.2406	0.1497	0.0931	0.304	0.00211
3/4	1.050	0.113	0.824	0.0687	0.679	0.5595	0.4610	0.3799	0.533	0.00371
1	1.315	0.133	1.049	0.0874	1.100	1.154	1.210	1.270	0.864	0.00600
1 1/4	1.660	0.140	1.380	0.1150	1.904	2.628	3.625	5.005	1.495	0.01040
1 1/2	1.900	0.145	1.610	0.1342	2.592	4.173	6.718	10.82	2.036	0.01414
2	2.375	0.154	2.067	0.1722	4.272	8.831	18.250	37.72	3.355	0.02330
2 1/2	2.875	0.203	2.469	0.2057	6.096	15.051	37.161	91.75	4.788	0.03322
3	3.500	0.216	3.068	0.2557	9.413	28.878	88.605	271.8	7.393	0.05130
3 1/2	4.000	0.226	3.548	0.2957	12.59	44.663	158.51	562.2	9.886	0.06870
4	4.500	0.237	4.026	0.3355	16.21	65.256	262.76	1058.	12.730	0.08840
5	5.563	0.258	5.047	0.4206	25.47	128.56	648.72	3275.	20.006	0.1390
6	6.625	0.280	6.065	0.5054	36.78	223.10	1352.8	8206.	28.891	0.2006
8	8.625	0.277	8.071	0.6725	65.14	525.75	4243.0	34248.	51.161	0.3553
	8.625S	0.322	7.981	0.6651	63.70	508.36	4057.7	32380.	50.027	0.3474
10	10.75	0.279	10.192	0.8493	103.88	1058.7	10789.	109876.	81.585	0.5666
	10.75	0.307	10.136	0.8446	102.74	1041.4	10555.	106987.	80.691	0.5604
	10.75S	0.365	10.020	0.8350	100.4	1006.0	10080.	101000.	78.855	0.5475
12	12.75	0.330	12.090	1.0075	146.17	1767.2	21366.	258300.	114.80	0.7972
	12.75S	0.375	12.000	1.000	144.0	1728.0	20736.	248800.	113.10	0.7854

Extra Strong Pipe										
1/8	0.405	0.095	0.215	0.0179	0.0462	0.00994	0.002134	0.000459	0.036	0.00025
1/4	0.540	0.119	0.302	0.0252	0.0912	0.0275	0.008317	0.002513	0.072	0.00050
3/8	0.675	0.126	0.423	0.0353	0.1789	0.0757	0.03201	0.01354	0.141	0.00098
1/2	0.840	0.147	0.546	0.0455	0.2981	0.1628	0.08886	0.04852	0.234	0.00163
3/4	1.050	0.154	0.742	0.0618	0.5506	0.4085	0.3032	0.2249	0.433	0.00300
1	1.315	0.179	0.957	0.0797	0.9158	0.8765	0.8387	0.8027	0.719	0.00499
1 1/4	1.660	0.191	1.278	0.1065	1.633	2.087	2.6667	3.409	1.283	0.00891
1 1/2	1.900	0.200	1.500	0.1250	2.250	3.375	5.062	7.594	1.767	0.01225
2	2.375	0.218	1.939	0.1616	3.760	7.290	14.136	27.41	2.953	0.02050
2 1/2	2.875	0.276	2.323	0.1936	5.396	12.536	29.117	67.64	4.238	0.02942
3	3.500	0.300	2.900	0.2417	8.410	24.389	70.728	205.1	6.605	0.04587
3 1/2	4.000	0.318	3.364	0.2803	11.32	38.069	128.14	430.8	8.888	0.06170
4	4.500	0.337	3.826	0.3188	14.64	56.006	214.33	819.8	11.497	0.07986
5	5.563	0.375	4.813	0.4011	23.16	111.49	536.6	2583.	18.194	0.1263
6	6.625	0.432	5.761	0.4801	33.19	191.20	1101.6	6346.	26.067	0.1810
8	8.625	0.500	7.625	0.6354	58.14	443.32	3380.3	25775.	45.663	0.3171
10	10.75	0.500	9.750	0.8125	95.06	926.86	9036.4	88110.	74.662	0.5185
12	12.75	0.500	11.750	0.9792	138.1	1622.2	19072.	223970.	108.434	0.7528

Double Extra Strong Pipe										
1/2	0.840	0.294	0.252	0.0210	0.0635	0.0160	0.004032	0.00102	0.050	0.00035
3/4	1.050	0.308	0.434	0.0362	0.1884	0.0817	0.03549	0.01540	0.148	0.00103
1	1.315	0.358	0.599	0.0499	0.3588	0.2149	0.1287	0.07711	0.282	0.00196
1 1/4	1.660	0.382	0.896	0.0747	0.8028	0.7193	0.6445	0.5775	0.630	0.00438
1 1/2	1.900	0.400	1.100	0.0917	1.210	1.331	1.4641	1.611	0.950	0.00660
2	2.375	0.436	1.503	0.1252	2.259	3.395	5.1031	7.670	1.774	0.01232
2 1/2	2.875	0.552	1.771	0.1476	3.136	5.554	9.8345	17.42	2.464	0.01710
3	3.500	0.600	2.300	0.1917	5.290	12.167	27.984	64.36	4.155	0.02885
3 1/2	4.000	0.636	2.728	0.2273	7.442	20.302	55.383	151.1	5.845	0.04059
4	4.500	0.674	3.152	0.2627	9.935	31.315	98.704	311.1	7.803	0.05419
5	5.563	0.750	4.063	0.3386	16.51	67.072	272.58	1107.	12.966	0.09006
6	6.625	0.864	4.897	0.4081	23.98	117.43	575.04	2816.	18.835	0.1308
8	8.625	0.875	6.875	0.5729	47.27	324.95	2234.4	15360.	37.122	0.2578

A-15.
Stainless Steel Pipe Data
(Based on ANSI B36.19 wall thicknesses)

Nominal Pipe Size	Outside Diameter	Thick-ness	Inside Diameter		Inside Diameter Functions (In Inches)				Transverse Internal Area	
			<i>d</i>	<i>D</i>	<i>d</i> ²	<i>d</i> ³	<i>d</i> ⁴	<i>d</i> ⁵	<i>a</i>	<i>A</i>
Inches	Inches	Inches	Inches	Feet					Sq. In.	Sq. Ft.
Schedule 5 S										
1/2	0.840	0.065	0.710	0.0592	0.504	0.358	0.254	0.1804	0.396	0.00275
3/4	1.050	0.065	0.920	0.0767	0.846	0.779	0.716	0.659	0.664	0.00461
1	1.315	0.065	1.185	0.0988	1.404	1.664	1.972	2.337	1.103	0.00766
1 1/4	1.660	0.065	1.530	0.1275	2.341	3.582	5.480	8.384	1.839	0.01277
1 1/2	1.900	0.065	1.770	0.1475	3.133	5.545	9.815	17.37	2.461	0.01709
2	2.375	0.065	2.245	0.1871	5.040	11.31	25.40	57.03	3.958	0.02749
2 1/2	2.875	0.083	2.709	0.2258	7.339	19.88	53.86	145.9	5.764	0.04003
3	3.500	0.083	3.334	0.2778	11.12	37.06	123.6	411.9	8.733	0.06065
3 1/2	4.000	0.083	3.834	0.3195	14.70	56.36	216.1	828.4	11.545	0.08017
4	4.500	0.083	4.334	0.3612	18.78	81.41	352.8	1529.	14.750	0.1024
5	5.563	0.109	5.345	0.4454	28.57	152.7	816.2	4363.	22.439	0.1558
6	6.625	0.109	6.407	0.5339	41.05	263.0	1685.	10796.	32.241	0.2239
8	8.625	0.109	8.407	0.7006	70.68	594.2	4995.	41996.	55.512	0.3855
10	10.750	0.134	10.482	0.8375	109.9	1152.	12072.	126538.	86.315	0.5994
12	12.750	0.156	12.438	1.0365	154.7	1924.	23933.	297682.	121.50	0.8438
Schedule 10 S										
1/8	0.405	0.049	0.307	0.0256	0.0942	0.0289	0.00888	0.00273	0.074	0.00051
1/4	0.540	0.065	0.410	0.0342	0.1681	0.0689	0.02826	0.01159	0.132	0.00092
3/8	0.675	0.065	0.545	0.0454	0.2970	0.1619	0.08822	0.04808	0.233	0.00162
1/2	0.840	0.083	0.674	0.0562	0.4543	0.3062	0.2064	0.1391	0.357	0.00248
3/4	1.050	0.083	0.884	0.0737	0.7815	0.6908	0.6107	0.5398	0.614	0.00426
1	1.315	0.109	1.097	0.0914	1.203	1.320	1.448	1.589	0.945	0.00656
1 1/4	1.660	0.109	1.442	0.1202	2.079	2.998	4.324	6.235	1.633	0.01134
1 1/2	1.900	0.109	1.682	0.1402	2.829	4.759	8.004	13.46	2.222	0.01543
2	2.375	0.109	2.157	0.1798	4.653	10.04	21.65	46.69	3.654	0.02538
2 1/2	2.875	0.120	2.635	0.2196	6.943	18.30	48.21	127.0	5.453	0.03787
3	3.500	0.120	3.260	0.2717	10.63	34.65	112.9	368.2	8.347	0.05796
3 1/2	4.000	0.120	3.760	0.3133	14.14	53.16	199.9	751.5	11.11	0.07712
4	4.500	0.120	4.260	0.3550	18.15	77.31	329.3	1403.	14.26	0.09899
5	5.563	0.134	5.295	0.4413	28.04	148.5	786.1	4162.	22.02	0.1529
6	6.625	0.134	6.357	0.5298	40.41	256.9	1633.	10382.	31.74	0.2204
8	8.625	0.148	8.329	0.6941	69.37	577.8	4813.	40083.	54.48	0.3784
10	10.750	0.165	10.420	0.8683	108.6	1131.	11789.	122840.	85.29	0.5923
12	12.750	0.180	12.390	1.0325	153.5	1902.	23566.	291982.	120.6	0.8372
Schedule 40 S										
1/8 to 12	Values are the same, size for size, as those shown on the facing page for Standard Wall Pipe (heaviest weight on 8, 10, and 12-inch sizes).									
Schedule 80 S										
1/8 to 12	Values are the same, size for size, as those shown on the facing page for Extra Strong Pipe.									

A-16. Properties of Pipe

Tabulated below are the most generally required data used in piping design. This table is believed to be the most comprehensive published up to this time. Many thicknesses traditionally included in such tables have been omitted because of their having become obsolete through disuse and lack of coverage by any Standard.

Sizes and thicknesses listed herein are covered by the following Standards:—

- 1) American National Standard Institute B36.10
- 2) American National Standard Institute B36.19
- 3) American Petroleum Institute Standard API 5L
- 4) American Petroleum Institute Standard API 5LX
- 5) New United States Legal Standard for Steel Plate Gauges.

Sizes and thicknesses to which no Standard designation applies are largely the more commonly used dimensions to which Taylor Forge Electric Fusion Welded Pipe is produced for a wide variety of applications including river crossings, penstocks, power plant and other piping.

All data is computed from the *nominal* dimensions listed and the effect of tolerances is not taken into account. Values are computed by application of the following formulas:

Radius of Gyration: $R = \frac{\sqrt{D^2 + d^2}}{4}$
 Moment of Inertia: $I = R^2 A$
 Section Modulus: $Z = \frac{I}{0.5 D}$

ANSI American National Standards Institute

Pipe Size	Nominal	Designation	Wall Thickness	Inside Diam. d	Weight per Foot	Wt. of Water per Ft. of Pipe	Sq. Ft. Outside Surface per Ft.	Sq. Ft. Inside Surface per Ft.	Transverse Area in. ²	Area of Metal in. ²	Moment of Inertia in. ⁴	Section Modulus in. ³	Radius of Gyration in.
	Outside Diam. D								a	A	I	Z	R
1/8	.405	10S	.049	.307	.186	.0320	.106	.0804	.0740	.0548	.00090	.00440	.1270
		Std.	.068	.269	.244	.0246	.106	.0705	.0568	.0720	.00106	.00530	.1215
		X-Stg.	.095	.215	.314	.0157	.106	.0563	.0364	.0925	.00122	.00600	.1146
1/4	.540	10S	.065	.410	.330	.0570	.141	.1073	.1320	.0970	.00280	.01030	.1695
		Std.	.088	.364	.424	.0451	.141	.0955	.1041	.1250	.00331	.01230	.1628
		X-Stg.	.119	.302	.535	.0310	.141	.0794	.0716	.1574	.00378	.01395	.1547
3/8	.675	10S	.065	.545	.423	.1010	.177	.1427	.2333	.1245	.00590	.01740	.2160
		Std.	.091	.493	.567	.0827	.177	.1295	.1910	.1670	.00730	.02160	.2090
		X-Stg.	.126	.423	.738	.0609	.177	.1106	.1405	.2173	.00862	.02554	.1991
1/2	.840	10S	.083	.670	.671	.1550	.220	.1764	.3568	.1974	.01430	.03410	.2692
		Std.	.109	.622	.850	.1316	.220	.1637	.3040	.2503	.01710	.04070	.2613
		X-Stg.	.147	.546	1.087	.1013	.220	.1433	.2340	.3200	.02010	.04780	.2505
		160	.138	.464	1.310	.0740	.220	.1220	.1706	.3836	.02213	.05269	.2402
3/4	1.050	XX-Stg.	.294	.252	1.714	.0216	.220	.0660	.0499	.5043	.02424	.05772	.2192
		10S	.083	.884	.857	.2660	.275	.2314	.6138	.2522	.02970	.05660	.3430
		Std.	.113	.824	1.130	.2301	.275	.2168	.5330	.3326	.03704	.07055	.3337
1	1.315	X-Stg.	.154	.742	1.473	.1875	.275	.1948	.4330	.4335	.04479	.08531	.3214
		160	.219	.612	1.940	.1280	.275	.1607	.2961	.5698	.05270	.10038	.3041
		XX-Stg.	.308	.434	2.440	.0633	.275	.1137	.1479	.7180	.05792	.11030	.2840
1 1/4	1.660	10S	.109	1.097	1.404	.4090	.344	.2872	.9448	.4129	.07560	.1150	.4282
		Std.	.133	1.049	1.678	.3740	.344	.2740	.8640	.4939	.08734	.1328	.4205
		X-Stg.	.179	.957	2.171	.3112	.344	.2520	.7190	.6388	.10560	.1606	.4066
1 1/4	1.660	160	.250	.815	2.850	.2261	.344	.2134	.5217	.8364	.12516	.1903	.3868
		XX-Stg.	.358	.599	3.659	.1221	.344	.1570	.2818	1.0760	.14050	.2136	.3613
		10S	.109	1.442	1.806	.7080	.434	.3775	1.633	.5314	.1606	.1934	.5499
		Std.	.140	1.380	2.272	.6471	.434	.3620	1.495	.6685	.1947	.2346	.5397
1 1/4	1.660	X-Stg.	.191	1.278	2.996	.5553	.434	.3356	1.283	.8815	.2418	.2913	.5237
		160	.250	1.160	3.764	.4575	.434	.3029	1.057	1.1070	.2833	.3421	.5063
		XX-Stg.	.382	.896	5.214	.2732	.434	.2331	.6305	1.5340	.3411	.4110	.4716

Courtesy Taylor Forge Division, Energy Products Group, Gulf and Western Mfg. Co., by permission.

A-16.
(Continued). Properties of Pipe

Nominal		Designation	Wall Thickness	Inside Diam.	Weight per Foot	Wt. of Water per Ft. of Pipe	Sq. Ft. Outside Surface per Ft.	Sq. Ft. Inside Surface per Ft.	Transverse Area in. ²	Area of Metal in. ²	Moment of Inertia in. ⁴	Section Modulus in. ³	Radius of Gyration in.
Pipe Size	Outside Diam.												
	D												
				d					e	A	I	Z	R
1½	1.900	10S Std.	.109 .145	1.682 1.610	2.085 2.717	.9630 .8820	.497 .497	.4403 .4213	2.221 2.036	.613 .800	.2469 .3099	.2599 .3262	.6344 .6226
		X-Stg. 160	.200 .281	1.500 1.337	3.631 4.862	.7648 .6082	.497 .497	.3927 .3519	1.767 1.405	1.068 1.430	.3912 .4826	.4118 .5080	.6052 .5809
		XX-Stg.	.400	1.100	6.408	.4117	.497	.2903	.950	1.885	.5678	.5977	.5489
2	2.375	10S Std.	.109 .154	2.157 2.067	2.638 3.652	1.583 1.452	.622 .622	.5647 .5401	3.654 3.355	.775 1.075	.5003 .6657	.4213 .5606	.8034 .7871
		X-Stg.	.218	1.939	5.022	1.279	.622	.5074	2.953	1.477	.8679	.7309	.7665
		-- 160	.250 .344	1.875 1.687	5.673 7.450	1.196 .970	.622 .622	.4920 .4422	2.761 2.240	1.669 2.190	.9555 1.162	.8046 .9790	.7565 .7286
XX-Stg.	.436	1.503	9.029	.769	.622	.3929	1.774	2.656	1.311	1.1040	.7027		
2½	2.875	10S Std.	.120 .203	2.635 2.469	3.53 5.79	2.360 2.072	.753 .753	.6900 .6462	5.453 4.788	1.038 1.704	.9878 1.530	.6872 1.064	.9755 .9474
		X-Stg. 160	.276 .375	2.323 2.125	7.66 10.01	1.834 1.535	.753 .753	.6095 .5564	4.238 3.547	2.254 2.945	1.924 2.353	1.339 1.638	.9241 .8938
		XX-Stg.	.552	1.771	13.69	1.067	.753	.4627	2.464	4.028	2.871	1.997	.8442
3	3.500	10S	.120	3.260	4.33	3.62	.916	.853	8.346	1.272	1.821	1.041	1.196
		API	.125	3.250	4.52	3.60	.916	.851	8.300	1.329	1.900	1.086	1.195
		API	.156	3.188	5.58	3.46	.916	.835	7.982	1.639	2.298	1.313	1.184
		API	.188	3.125	6.65	3.34	.916	.819	7.700	1.958	2.700	1.545	1.175
		Std.	.216	3.068	7.57	3.20	.916	.802	7.393	2.228	3.017	1.724	1.164
		API	.250	3.000	8.68	3.06	.916	.785	7.184	2.553	3.388	1.936	1.152
API	.281	2.938	9.65	2.94	.916	.769	6.780	2.842	3.819	2.182	1.142		
X-Stg. 160	.300	2.900	10.25	2.86	.916	.761	6.605	3.016	3.892	2.225	1.136		
XX-Stg.	.438 .600	2.624 2.300	14.32 18.58	2.34 1.80	.916 .916	.687 .601	5.407 4.155	4.214 5.466	5.044 5.993	5.044 5.993	2.882 3.424	1.094 1.047	
3½	4.000	10S	.120	3.760	4.97	4.81	1.047	.984	11.10	1.46	2.754	1.377	1.372
		API	.125	3.750	5.18	4.79	1.047	.982	11.04	1.52	2.859	1.430	1.371
		API	.156	3.688	6.41	4.63	1.047	.966	10.68	1.88	3.485	1.743	1.360
		API	.188	3.624	7.71	4.48	1.047	.950	10.32	2.27	4.130	2.065	1.350
		Std.	.226	3.548	9.11	4.28	1.047	.929	9.89	2.68	4.788	2.394	1.337
		API	.250	3.500	10.02	4.17	1.047	.916	9.62	2.94	5.201	2.601	1.329
API	.281	3.438	11.17	4.02	1.047	.900	9.28	3.29	5.715	2.858	1.319		
X-Stg.	.318	3.364	12.51	3.85	1.047	.880	8.89	3.68	6.280	3.140	1.307		
XX-Stg.	.636	2.728	22.85	2.53	1.047	.716	5.84	6.72	9.848	4.924	1.210		
4	4.500	10S	.120	4.260	5.61	6.18	1.178	1.115	14.25	1.65	3.97	1.761	1.550
		API	.125	4.250	5.84	6.15	1.178	1.113	14.19	1.72	4.12	1.829	1.548
		API	.156	4.188	7.24	5.97	1.178	1.096	13.77	2.13	5.03	2.235	1.537
		API	.188	4.124	8.56	5.80	1.178	1.082	13.39	2.52	5.86	2.600	1.525
		API	.219	4.062	10.02	5.62	1.178	1.063	12.96	2.94	6.77	3.867	1.516
		Std.	.237	4.026	10.79	5.51	1.178	1.055	12.73	3.17	7.23	3.214	1.510
		API	.250	4.000	11.35	5.45	1.178	1.049	12.57	3.34	7.56	3.360	1.505
		API	.281	3.938	12.67	5.27	1.178	1.031	12.17	3.73	8.33	3.703	1.495
		API	.312	3.876	14.00	5.12	1.178	1.013	11.80	4.11	9.05	4.020	1.482
		X-Stg. 120	.337	3.826	14.98	4.98	1.178	1.002	11.50	4.41	9.61	4.271	1.477
--	.438 .500	3.624 3.500	19.00 21.36	4.47 4.16	1.178 1.178	.949 .916	10.32 9.62	5.59 6.28	11.65 12.77	5.177 5.676	5.177 5.676	1.444 1.425	
160	.531	3.438	22.60	4.02	1.178	.900	9.28	6.62	13.27	5.900	5.900	1.416	
XX-Stg.	.674	3.152	27.54	3.38	1.178	.826	7.80	8.10	15.28	6.793	6.793	1.374	

A-16.
(Continued). Properties of Pipe

Nominal		Designation	Wall Thickness	Inside Diam. d	Weight per Foot	Wt. of Water per Ft. of Pipe	Sq. Ft. Outside Surface per Ft.	Sq. Ft. Inside Surface per Ft.	Transverse Area	Area of Metal	Moment of Inertia	Section Modulus	Radius of Gyration
Pipe Size	Outside Diam. D								in. ²	in. ²	in. ⁴	in. ³	in.
								a	A	I	Z	R	
5	5.563	10S	.134	5.295	7.77	9.54	1.456	1.386	22.02	2.29	8.42	3.028	1.920
		API	.156	5.251	9.02	9.39	1.456	1.375	21.66	2.65	9.70	3.487	1.913
		API	.188	5.187	10.80	9.16	1.456	1.358	21.13	3.17	11.49	4.129	1.902
		API	.219	5.125	12.51	8.94	1.456	1.342	20.63	3.68	13.14	4.726	1.891
		Std.	.258	5.047	14.62	8.66	1.456	1.321	20.01	4.30	15.16	5.451	1.878
		API	.281	5.001	15.86	8.52	1.456	1.309	19.64	4.66	16.31	5.862	1.870
		API	.312	4.939	17.51	8.31	1.456	1.293	19.16	5.15	17.81	6.402	1.860
		API	.344	4.875	19.19	8.09	1.456	1.276	18.67	5.64	19.28	6.932	1.849
		X-Stg.	.375	4.813	20.78	7.87	1.456	1.260	18.19	6.11	20.67	7.431	1.839
		120	.500	4.563	27.10	7.08	1.456	1.195	16.35	7.95	25.74	9.253	1.799
160	.625	4.313	32.96	6.32	1.456	1.129	14.61	9.70	30.03	10.800	1.760		
XX-Stg.	.750	4.063	38.55	5.62	1.456	1.064	12.97	11.34	33.63	12.090	1.722		
6	6.625	12 Ga.	.104	6.417	7.25	14.02	1.734	1.680	32.34	2.13	11.33	3.42	2.31
		10S	.134	6.357	9.29	13.70	1.734	1.660	31.75	2.73	14.38	4.34	2.29
		8 Ga.	.164	6.297	11.33	13.50	1.734	1.649	31.14	3.33	17.38	5.25	2.28
		API	.188	6.249	12.93	13.31	1.734	1.639	30.70	3.80	19.71	5.95	2.28
		6 Ga.	.194	6.237	13.34	13.25	1.734	1.633	30.55	3.92	20.29	6.12	2.27
		API	.219	6.187	15.02	13.05	1.734	1.620	30.10	4.41	22.66	6.84	2.27
		API	.250	6.125	17.02	12.80	1.734	1.606	29.50	5.01	25.55	7.71	2.26
		API	.277	6.071	18.86	12.55	1.734	1.591	28.95	5.54	28.00	8.46	2.25
		Std.	.280	6.065	18.97	12.51	1.734	1.587	28.90	5.58	28.14	8.50	2.24
		API	.312	6.001	21.05	12.26	1.734	1.571	28.28	6.19	30.91	9.33	2.23
API	.344	5.937	23.09	12.00	1.734	1.554	27.68	6.79	33.51	10.14	2.22		
API	.375	5.875	25.10	11.75	1.734	1.540	27.10	7.37	36.20	10.90	2.21		
X-Stg.	.432	5.761	28.57	11.29	1.734	1.510	26.07	8.40	40.49	12.22	2.19		
- -	.500	5.625	32.79	10.85	1.734	1.475	24.85	9.63	45.60	13.78	2.16		
120	.562	5.501	36.40	10.30	1.734	1.470	23.77	10.74	49.91	15.07	2.15		
160	.719	5.187	45.30	9.16	1.734	1.359	21.15	13.36	58.99	17.81	2.10		
XX-Stg.	.864	4.897	53.16	8.14	1.734	1.280	18.83	15.64	66.33	20.02	2.06		
8	8.625	12 Ga.	.104	8.417	9.47	24.1	2.26	2.204	55.6	2.78	25.3	5.86	3.01
		10 Ga.	.134	8.357	12.16	23.8	2.26	2.188	54.8	3.57	32.2	7.46	3.00
		10S	.148	8.329	13.40	23.6	2.26	2.180	54.5	3.94	35.4	8.22	3.00
		8 Ga.	.164	8.297	14.83	23.4	2.26	2.172	54.1	4.36	39.1	9.06	2.99
		API	.188	8.249	16.90	23.2	2.26	2.161	53.5	5.00	44.5	10.30	2.98
		6 Ga.	.194	8.237	17.48	23.1	2.26	2.156	53.3	5.14	45.7	10.60	2.98
		API	.203	8.219	18.30	23.1	2.26	2.152	53.1	5.38	47.7	11.05	2.98
		API	.219	8.187	19.64	22.9	2.26	2.148	52.7	5.80	51.3	11.90	2.97
		3 Ga.	.239	8.147	21.42	22.6	2.26	2.133	52.1	6.30	55.4	12.84	2.96
		20	.250	8.125	22.40	22.5	2.26	2.127	51.8	6.58	57.7	13.39	2.96
30	.277	8.071	24.70	22.2	2.26	2.115	51.2	7.26	63.3	14.69	2.95		
API	.312	8.001	27.72	21.8	2.26	2.095	50.3	8.15	70.6	16.37	2.94		
Std.	.322	7.981	28.55	21.6	2.26	2.090	50.0	8.40	72.5	16.81	2.94		
API	.344	7.937	30.40	21.4	2.26	2.078	49.5	8.94	76.8	17.81	2.93		
API	.375	7.875	33.10	21.1	2.26	2.062	48.7	9.74	83.1	19.27	2.92		
60	.406	7.813	35.70	20.8	2.26	2.045	47.9	10.48	88.8	20.58	2.91		
API	.438	7.749	38.33	20.4	2.26	2.029	47.2	11.27	94.7	21.97	2.90		
X-Stg.	.500	7.625	43.39	19.8	2.26	2.006	45.6	12.76	105.7	24.51	2.88		
100	.594	7.437	50.90	18.8	2.26	1.947	43.5	14.96	121.4	28.14	2.85		
- -	.625	7.375	53.40	18.5	2.26	1.931	42.7	15.71	126.5	29.33	2.84		
120	.719	7.187	60.70	17.6	2.26	1.882	40.6	17.84	140.6	32.61	2.81		
140	.812	7.001	67.80	16.7	2.26	1.833	38.5	19.93	153.8	35.65	2.78		
XX-Stg.	.875	6.875	72.42	16.1	2.26	1.800	37.1	21.30	162.0	37.56	2.76		
160	.906	6.813	74.70	15.8	2.26	1.784	36.4	21.97	165.9	38.48	2.76		

A-16.

(Continued). Properties of Pipe

Nominal		Designation	Wall Thickness	Inside Diam. d	Weight per Foot	Wt. of Water per Ft. of Pipe	Sq. Ft. Outside Surface per Ft.	Sq. Ft. Inside Surface per Ft.	Transverse Area	Area of Metal	Moment of Inertia	Section Modulus	Radius of Gyration
Pipe Size	Outside Diam. D								a	A	I	Z	R
10	10.750	12 Ga.	.104	10.542	11.83	37.8	2.81	2.76	87.3	3.48	49.3	9.16	3.76
		10 Ga.	.134	10.482	15.21	37.4	2.81	2.74	86.3	4.47	63.0	11.71	3.75
		8 Ga.	.164	10.422	18.56	37.0	2.81	2.73	85.3	5.45	76.4	14.22	3.74
		10S	.165	10.420	18.65	36.9	2.81	2.73	85.3	5.50	76.8	14.29	3.74
		API	.188	10.374	21.12	36.7	2.81	2.72	84.5	6.20	86.5	16.10	3.74
		6 Ga.	.194	10.362	21.89	36.6	2.81	2.71	84.3	6.43	89.7	16.68	3.73
		API	.203	10.344	22.86	36.5	2.81	2.71	84.0	6.71	93.3	17.35	3.73
		API	.219	10.310	24.60	36.2	2.81	2.70	83.4	7.24	100.5	18.70	3.72
		3 Ga.	.239	10.272	28.05	35.9	2.81	2.69	82.9	7.89	109.2	20.32	3.72
		20	.250	10.250	28.03	35.9	2.81	2.68	82.6	8.26	113.6	21.12	3.71
		API	.279	10.192	31.20	35.3	2.81	2.66	81.6	9.18	125.9	23.42	3.70
		30	.307	10.136	34.24	35.0	2.81	2.65	80.7	10.07	137.4	25.57	3.69
		API	.344	10.062	38.26	34.5	2.81	2.63	79.5	11.25	152.3	28.33	3.68
		Std.	.365	10.020	40.48	34.1	2.81	2.62	78.9	11.91	160.7	29.90	3.67
		API	.438	9.874	48.28	33.2	2.81	2.58	76.6	14.19	188.8	35.13	3.65
		X-Stg.	.500	9.750	54.74	32.3	2.81	2.55	74.7	16.10	212.0	39.43	3.63
		80	.594	9.562	64.40	31.1	2.81	2.50	71.8	18.91	244.9	45.56	3.60
		100	.719	9.312	77.00	29.5	2.81	2.44	68.1	22.62	286.2	53.25	3.56
		--	.750	9.250	80.10	29.1	2.81	2.42	67.2	23.56	296.2	55.10	3.54
		120	.844	9.062	89.20	27.9	2.81	2.37	64.5	26.23	324.3	60.34	3.51
140	1.000	8.750	104.20	26.1	2.81	2.29	60.1	30.63	367.8	68.43	3.46		
160	1.125	8.500	116.00	24.6	2.81	2.22	56.7	34.01	399.4	74.31	3.43		
12	12.750	12 Ga.	.104	12.542	14.1	53.6	3.34	3.28	123.5	4.13	82.6	12.9	4.47
		10 Ga.	.134	12.482	18.1	53.0	3.34	3.27	122.4	5.31	105.7	16.6	4.46
		8 Ga.	.164	12.422	22.1	52.5	3.34	3.25	121.2	6.48	128.4	20.1	4.45
		10S	.180	12.390	24.2	52.2	3.34	3.24	120.6	7.11	140.4	22.0	4.44
		6 Ga.	.194	12.362	26.0	52.0	3.34	3.23	120.0	7.65	150.9	23.7	4.44
		API	.203	12.344	27.2	52.0	3.34	3.23	119.9	7.99	157.2	24.7	4.43
		API	.219	12.312	29.3	51.7	3.34	3.22	119.1	8.52	167.6	26.3	4.43
		3 Ga.	.239	12.272	32.0	51.3	3.34	3.21	118.3	9.39	183.8	28.8	4.42
		20	.250	12.250	33.4	51.3	3.34	3.12	118.0	9.84	192.3	30.2	4.42
		API	.281	12.188	37.4	50.6	3.34	3.19	116.7	11.01	214.1	33.6	4.41
		API	.312	12.126	41.5	50.1	3.34	3.17	115.5	12.19	236.0	37.0	4.40
		30	.330	12.090	43.8	49.7	3.34	3.16	114.8	12.88	248.5	39.0	4.39
		API	.344	12.062	45.5	49.7	3.34	3.16	114.5	13.46	259.0	40.7	4.38
		Std.	.375	12.000	49.6	48.9	3.34	3.14	113.1	14.58	279.3	43.8	4.37
		40	.406	11.938	53.6	48.5	3.34	3.13	111.9	15.74	300.3	47.1	4.37
		API	.438	11.874	57.5	48.2	3.34	3.11	111.0	16.95	321.0	50.4	4.35
		X-Stg.	.500	11.750	65.4	46.9	3.34	3.08	108.4	19.24	361.5	56.7	4.33
		60	.562	11.626	73.2	46.0	3.34	3.04	106.2	21.52	400.5	62.8	4.31
		--	.625	11.500	80.9	44.9	3.34	3.01	103.8	23.81	438.7	68.8	4.29
		80	.688	11.374	88.6	44.0	3.34	2.98	101.6	26.03	475.2	74.6	4.27
--	.750	11.250	96.2	43.1	3.34	2.94	99.4	28.27	510.7	80.1	4.25		
100	.844	11.062	108.0	41.6	3.34	2.90	96.1	31.53	561.8	88.1	4.22		
--	.875	11.000	110.9	41.1	3.34	2.88	95.0	32.64	578.5	90.7	4.21		
120	1.000	10.750	125.5	39.3	3.34	2.81	90.8	36.91	641.7	100.7	4.17		
140	1.125	10.500	140.0	37.5	3.34	2.75	86.6	41.08	700.7	109.9	4.13		
--	1.250	10.250	153.6	35.8	3.34	2.68	82.5	45.16	755.5	118.5	4.09		
160	1.312	10.126	161.0	34.9	3.34	2.65	80.5	47.14	781.3	122.6	4.07		
--	1.375	10.000	167.2	34.0	3.34	2.62	78.5	49.14	807.2	126.6	4.05		
--	1.500	9.750	180.4	32.4	3.34	2.55	74.7	53.01	853.8	133.9	4.01		

A-16.
(Continued). Properties of Pipe

Nominal		Designation	Wall Thickness	Inside Diam. d	Weight per Foot	Wt. of Water per Ft. of Pipe	Sq. Ft. Outside Surface per Ft.	Sq. Ft. Inside Surface per Ft.	Transverse Area in. ²	Area of Metal in. ²	Moment of Inertia in. ⁴	Section Modulus in. ³	Radius of Gyration in.
Pipe Size	Outside Diam. D								a	A	I	Z	R
14	14.000	10 Ga.	.134	13.732	20	64.2	3.67	3.59	148.1	5.84	140.4	20.1	4.90
		8 Ga.	.164	13.672	24	63.6	3.67	3.58	146.8	7.13	170.7	24.4	4.89
		6 Ga.	.194	13.612	29	63.1	3.67	3.56	145.5	8.41	200.6	28.7	4.88
		API	.210	13.580	31	62.8	3.67	3.55	144.8	9.10	216.2	30.9	4.87
		API	.219	13.562	32	62.6	3.67	3.55	144.5	9.48	225.1	32.2	4.87
		3 Ga.	.239	13.522	35	62.3	3.67	3.54	143.6	10.33	244.9	35.0	4.87
		10	.250	13.500	37	62.1	3.67	3.54	143.0	10.82	256.0	36.6	4.86
		API	.281	13.438	41	61.5	3.67	3.52	141.8	12.11	285.2	40.7	4.85
		20	.312	13.375	46	60.8	3.67	3.50	140.5	13.44	314.9	45.0	4.84
		API	.344	13.312	50	60.3	3.67	3.48	139.2	14.76	344.3	49.2	4.83
		Std.	.375	13.250	55	59.7	3.67	3.47	137.9	16.05	372.8	53.2	4.82
		40	.438	13.124	63	58.5	3.67	3.44	135.3	18.66	429.6	61.4	4.80
		X-Stg.	.500	13.000	72	57.4	3.67	3.40	132.7	21.21	483.8	69.1	4.78
		60	.594	12.812	85	55.9	3.67	3.35	129.0	24.98	562.4	80.3	4.74
		--	.625	12.750	89	55.3	3.67	3.34	127.7	26.26	588.5	84.1	4.73
		80	.750	12.500	107	51.2	3.67	3.27	122.7	31.22	687.5	98.2	4.69
		--	.875	12.250	123	51.1	3.67	3.21	117.9	36.08	780.1	111.4	4.65
		100	.938	12.124	131	50.0	3.67	3.17	115.5	38.47	820.5	117.2	4.63
		--	1.000	12.000	139	49.0	3.67	3.14	113.1	40.84	868.0	124.0	4.61
		120	1.094	11.812	151	47.5	3.67	3.09	109.6	44.32	929.8	132.8	4.58
--	1.125	11.750	155	47.0	3.67	3.08	108.4	45.50	950.3	135.8	4.57		
140	1.250	11.500	171	45.0	3.67	3.01	103.9	50.07	1027.5	146.8	4.53		
--	1.375	11.250	186	43.1	3.67	2.94	99.4	54.54	1099.5	157.1	4.49		
160	1.406	11.188	190	42.6	3.67	2.93	98.3	55.63	1116.9	159.6	4.48		
--	1.500	11.000	200	41.2	3.67	2.88	95.0	58.90	1166.5	166.6	4.45		
16	16.000	10 Ga.	.134	15.732	23	84.3	4.19	4.12	194.4	6.68	210	26.3	5.61
		8 Ga.	.164	15.672	28	83.6	4.19	4.10	192.9	8.16	256	32.0	5.60
		--	.188	15.624	32	83.3	4.19	4.09	192.0	9.39	294	36.7	5.59
		6 Ga.	.194	15.612	33	83.0	4.19	4.09	191.4	9.63	301	37.6	5.59
		API	.219	15.562	37	82.5	4.19	4.07	190.2	10.86	338	42.3	5.58
		3 Ga.	.239	15.522	40	82.0	4.19	4.06	189.2	11.83	368	45.9	5.57
		10	.250	15.500	42	82.1	4.19	4.06	189.0	12.40	385	48.1	5.57
		API	.281	15.438	47	81.2	4.19	4.04	187.0	13.90	430	53.8	5.56
		20	.312	15.375	52	80.1	4.19	4.03	185.6	15.40	474	59.2	5.55
		API	.344	15.312	57	80.0	4.19	4.01	184.1	16.94	519	64.9	5.54
		Std.	.375	15.250	63	79.1	4.19	4.00	182.6	18.41	562	70.3	5.53
		API	.438	15.124	73	78.2	4.19	3.96	180.0	21.42	650	81.2	5.51
		X-Stg.	.500	15.000	83	76.5	4.19	3.93	176.7	24.35	732	91.5	5.48
		--	.625	14.750	103	74.1	4.19	3.86	170.9	30.19	893	111.7	5.44
		60	.656	14.688	108	73.4	4.19	3.85	169.4	31.62	933	116.6	5.43
		--	.750	14.500	122	71.5	4.19	3.80	165.1	35.93	1047	130.9	5.40
		80	.844	14.312	137	69.7	4.19	3.75	160.9	40.14	1157	144.6	5.37
		--	.875	14.250	141	69.1	4.19	3.73	159.5	41.58	1192	149.0	5.35
		--	1.000	14.000	160	66.7	4.19	3.66	153.9	47.12	1331	166.4	5.31
		100	1.031	13.938	165	66.0	4.19	3.65	152.6	48.49	1366	170.7	5.30
--	1.125	13.750	179	64.4	4.19	3.60	148.5	52.57	1463	182.9	5.27		
120	1.219	13.562	193	62.6	4.19	3.55	144.5	56.56	1556	194.5	5.24		
--	1.250	13.500	197	62.1	4.19	3.53	143.1	57.92	1586	198.3	5.23		
--	1.375	13.250	215	59.8	4.19	3.47	137.9	63.17	1704	213.0	5.19		
140	1.438	13.124	224	58.6	4.19	3.44	135.3	65.79	1761	220.1	5.17		
--	1.500	13.000	232	57.4	4.19	3.40	132.7	68.33	1816	227.0	5.15		
160	1.594	12.812	245	55.9	4.19	3.35	129.0	72.10	1893	236.6	5.12		

A-16.
(Continued). Properties of Pipe

Nominal		Designation	Wall Thickness	Inside Diam. d	Weight per Foot	Wt. of Water per Ft. of Pipe	Sq. Ft. Outside Surface per Ft.	Sq. Ft. Inside Surface per Ft.	Transverse Area in. ² a	Area of Metal in. ² A	Moment of Inertia in. ⁴ I	Section Modulus in. ³ Z	Radius of Gyration in. R
Pipe Size	Outside Diam. D												
18	18.000	10 Ga.	.134	17.732	26	107.1	4.71	4.64	246.9	7.52	300	33.4	6.32
		8 Ga.	.164	17.672	31	106.3	4.71	4.63	245.3	9.19	366	40.6	6.31
		6 Ga.	.194	17.612	37	105.6	4.71	4.61	243.6	10.85	430	47.8	6.29
		3 Ga.	.239	17.522	45	104.5	4.71	4.59	241.1	13.34	526	58.4	6.28
		10	.250	17.500	47	104.6	4.71	4.58	241.0	13.96	550	61.1	6.28
		API	.281	17.438	49	104.0	4.71	4.56	240.0	14.49	570	63.4	6.27
		20	.312	17.375	59	102.5	4.71	4.55	237.1	17.36	679	75.5	6.25
		API	.344	17.312	65	102.0	4.71	4.53	235.4	19.08	744	82.6	6.24
		Std.	.375	17.250	71	101.2	4.71	4.51	233.7	20.76	807	89.6	6.23
		API	.406	17.188	76	100.6	4.71	4.50	232.0	22.44	869	96.6	6.22
		30	.438	17.124	82	99.5	4.71	4.48	229.5	24.95	963	107.0	6.21
		X-Stg.	.500	17.000	93	98.2	4.71	4.45	227.0	27.49	1053	117.0	6.19
		40	.562	16.876	105	97.2	4.71	4.42	224.0	30.85	1177	130.9	6.17
		--	.625	16.750	116	95.8	4.71	4.39	220.5	34.15	1290	143.2	6.14
		60	.750	16.500	138	92.5	4.71	4.32	213.8	40.64	1515	168.3	6.10
		--	.875	16.250	160	89.9	4.71	4.25	207.4	47.07	1730	192.3	6.06
		80	.938	16.124	171	88.5	4.71	4.22	204.2	50.23	1834	203.8	6.04
		--	1.000	16.000	182	87.2	4.71	4.19	201.1	53.41	1935	215.0	6.02
		--	1.125	15.750	203	84.5	4.71	4.12	194.8	59.64	2133	237.0	5.98
		100	1.156	15.688	208	83.7	4.71	4.11	193.3	61.18	2182	242.3	5.97
		--	1.250	15.500	224	81.8	4.71	4.06	188.7	65.78	2319	257.7	5.94
		120	1.375	15.250	244	79.2	4.71	3.99	182.7	71.82	2498	277.5	5.90
		--	1.500	15.000	265	76.6	4.71	3.93	176.7	77.75	2668	296.5	5.86
		140	1.562	14.876	275	75.3	4.71	3.89	173.8	80.66	2750	305.5	5.84
160	1.781	14.438	309	71.0	4.71	3.78	163.7	90.75	3020	335.5	5.77		
20	20.000	10 Ga.	.134	19.732	28	132.6	5.24	5.17	305.8	8.36	413	41.3	7.02
		8 Ga.	.164	19.672	35	131.8	5.24	5.15	303.9	10.22	503	50.3	7.01
		6 Ga.	.194	19.612	41	131.0	5.24	5.13	302.1	12.07	592	59.2	7.00
		3 Ga.	.239	19.522	50	129.8	5.24	5.11	299.3	14.84	725	72.5	6.99
		10	.250	19.500	53	130.0	5.24	5.11	299.0	15.52	759	75.9	6.98
		API	.281	19.438	59	128.6	5.24	5.09	296.8	17.41	846	84.6	6.97
		API	.312	19.374	66	128.1	5.24	5.08	295.0	19.36	937	93.7	6.95
		API	.344	19.312	72	127.0	5.24	5.06	292.9	21.24	1026	102.6	6.95
		Std.	.375	19.250	79	126.0	5.24	5.04	291.1	23.12	1113	111.3	6.94
		API	.406	19.188	85	125.4	5.24	5.02	289.2	24.99	1200	120.0	6.93
		API	.438	19.124	92	125.1	5.24	5.01	288.0	26.95	1290	129.0	6.92
		X-Stg.	.500	19.000	105	122.8	5.24	4.97	283.5	30.63	1457	145.7	6.90
		40	.594	18.812	123	120.4	5.24	4.93	278.0	36.15	1704	170.4	6.86
		--	.625	18.750	129	119.5	5.24	4.91	276.1	38.04	1787	178.7	6.85
		60	.812	18.376	167	114.9	5.24	4.81	265.2	48.95	2257	225.7	6.79
		--	.875	18.250	179	113.2	5.24	4.78	261.6	52.57	2409	240.9	6.77
		--	1.000	18.000	203	110.3	5.24	4.71	254.5	59.69	2702	270.2	6.73
		80	1.031	17.938	209	109.4	5.24	4.80	252.7	61.44	2771	277.1	6.72
		--	1.125	17.750	227	107.3	5.24	4.65	247.4	66.71	2981	298.1	6.68
		--	1.250	17.500	250	104.3	5.24	4.58	240.5	73.63	3249	324.9	6.64
		100	1.281	17.438	256	103.4	5.24	4.56	238.8	75.34	3317	331.7	6.63
		--	1.375	17.250	274	101.3	5.24	4.52	233.7	80.45	3508	350.8	6.60
		120	1.500	17.000	297	98.3	5.24	4.45	227.0	87.18	3755	375.5	6.56
		140	1.750	16.500	342	92.6	5.24	4.32	213.8	100.33	4217	421.7	6.48
160	1.969	16.062	379	87.9	5.24	4.21	202.7	111.49	4586	458.6	6.41		

A-16.
(Continued). Properties of Pipe

Nominal		Designation	Wall Thickness	Inside Diam.	Weight per Foot	Wt. of Water per Ft. of Pipe	Sq. Ft. Outside Surface per Ft.	Sq. Ft. Inside Surface per Ft.	Transverse Area	Area of Metal	Moment of Inertia	Section Modulus	Radius of Gyration
Pipe Size	Outside Diam.								a	A	I	Z	R
	D												
22	22.000	8 Ga.	.164	21.672	38	159.9	5.76	5.67	368.9	11.25	671	61.0	7.72
		6 Ga.	.194	21.612	45	159.0	5.76	5.66	366.8	13.29	790	71.8	7.71
		3 Ga.	.239	21.522	56	157.7	5.76	5.63	363.8	16.34	967	87.9	7.69
		API	.250	21.500	58	157.4	5.76	5.63	363.1	17.18	1010	91.8	7.69
		API	.281	21.438	65	156.5	5.76	5.61	361.0	19.17	1131	102.8	7.68
		API	.312	21.376	72	155.6	5.76	5.60	358.9	21.26	1250	113.6	7.67
		API	.344	21.312	80	154.7	5.76	5.58	356.7	23.40	1373	124.8	7.66
		API	.375	21.250	87	153.7	5.76	5.56	354.7	25.48	1490	135.4	7.65
		API	.406	21.188	94	152.9	5.76	5.55	352.6	27.54	1607	146.1	7.64
		API	.438	21.124	101	151.9	5.76	5.53	350.5	29.67	1725	156.8	7.62
		API	.500	21.000	115	150.2	5.76	5.50	346.4	33.77	1953	177.5	7.61
		--	.625	20.750	143	146.6	5.76	5.43	338.2	41.97	2400	218.2	7.56
		--	.750	20.500	170	143.1	5.76	5.37	330.1	50.07	2829	257.2	7.52
		--	.875	20.250	198	139.6	5.76	5.30	322.1	58.07	3245	295.0	7.47
		--	1.000	20.000	224	136.2	5.76	5.24	314.2	65.97	3645	331.4	7.43
		--	1.125	19.750	251	132.8	5.76	5.17	306.4	73.78	4029	366.3	7.39
--	1.250	19.500	277	129.5	5.76	5.10	298.6	81.48	4400	400.0	7.35		
--	1.375	19.250	303	126.2	5.76	5.04	291.0	89.09	4758	432.6	7.31		
--	1.500	19.000	329	122.9	5.76	4.97	283.5	96.60	5103	463.9	7.27		
24	24.000	8 Ga.	.164	23.672	42	190.8	6.28	6.20	440.1	12.28	872	72.7	8.43
		6 Ga.	.194	23.612	49	189.8	6.28	6.18	437.9	14.51	1028	85.7	8.42
		3 Ga.	.239	23.522	61	188.4	6.28	6.16	434.5	17.84	1260	105.0	8.40
		10	.250	23.500	63	189.0	6.28	6.15	435.0	18.67	1320	110.0	8.40
		API	.281	23.438	71	187.0	6.28	6.14	431.5	20.94	1472	122.7	8.38
		API	.312	23.376	79	186.9	6.28	6.12	430.0	23.20	1630	136.0	8.38
		API	.344	23.312	87	185.0	6.28	6.10	426.8	25.57	1789	149.1	8.36
		Std.	.375	23.250	95	183.8	6.28	6.09	424.6	27.83	1942	161.9	8.35
		API	.406	23.188	102	183.1	6.28	6.07	422.3	30.09	2095	174.6	8.34
		API	.438	23.124	110	182.1	6.28	6.05	420.0	32.42	2252	187.7	8.33
		X-Stg.	.500	23.000	125	181.0	6.28	6.02	416.0	36.90	2550	213.0	8.31
		30	.562	22.876	141	178.5	6.28	5.99	411.0	41.40	2840	237.0	8.28
		--	.625	22.750	156	175.9	6.28	5.96	406.5	45.90	3137	261.4	8.27
		40	.688	22.624	171	174.2	6.28	5.92	402.1	50.30	3422	285.2	8.25
		--	.750	22.500	186	172.1	6.28	5.89	397.6	54.78	3705	308.8	8.22
		--	.875	22.250	216	168.6	6.28	5.82	388.8	63.57	4257	354.7	8.18
60	.969	22.062	238	165.8	6.28	5.78	382.3	70.04	4652	387.7	8.15		
--	1.000	22.000	246	164.8	6.28	5.76	380.1	72.26	4788	399.0	8.14		
--	1.125	21.750	275	161.1	6.28	5.69	371.5	80.85	5302	441.8	8.10		
80	1.219	21.562	297	158.2	6.28	5.65	365.2	87.17	5673	472.8	8.07		
--	1.250	21.500	304	157.4	6.28	5.63	363.1	89.34	5797	483.0	8.05		
--	1.375	21.250	332	153.8	6.28	5.56	354.7	97.73	6275	522.9	8.01		
--	1.500	21.000	361	150.2	6.28	5.50	346.4	106.03	6740	561.7	7.97		
100	1.531	20.938	367	149.3	6.28	5.48	344.3	108.07	6847	570.6	7.96		
120	1.812	20.376	429	141.4	6.28	5.33	326.1	126.30	7823	651.9	7.87		
140	2.062	19.876	484	134.4	6.28	5.20	310.3	142.10	8627	718.9	7.79		
160	2.344	19.312	542	127.0	6.28	5.06	293.1	159.40	9457	788.1	7.70		
26	26.000	8 Ga.	.164	25.672	45	224.4	6.81	6.72	517.6	13.31	1111	85.4	9.13
		6 Ga.	.194	25.612	54	223.4	6.81	6.70	515.2	15.73	1310	100.7	9.12
		3 Ga.	.239	25.522	66	221.8	6.81	6.68	511.6	19.34	1605	123.4	9.11
		API	.250	25.500	67	221.4	6.81	6.68	510.7	19.85	1646	126.6	9.10
		API	.281	25.438	77	220.3	6.81	6.66	508.2	22.70	1877	144.4	9.09
API	.312	25.376	84	219.2	6.81	6.64	505.8	25.18	2076	159.7	9.08		

A-16.
(Continued). Properties of Pipe

Nominal		Designation	Wall Thickness	Inside Diam. d	Weight per Foot	Wt. of Water per Ft. of Pipe	Sq. Ft. Outside Surface per Ft.	Sq. Ft. Inside Surface per Ft.	Transverse Area	Area of Metal	Moment of Inertia	Section Modulus	Radius of Gyration		
Pipe Size	Outside Diam.								a	A	I	Z	R		
	D														
26 cont.	26.000	API	.344	25.312	94	218.2	6.81	6.63	503.2	27.73	2280	175.4	9.07		
		API	.375	25.250	103	217.1	6.81	6.61	500.7	30.19	2478	190.6	9.06		
		API	.406	25.188	111	216.0	6.81	6.59	498.3	32.64	2673	205.6	9.05		
		API	.438	25.124	120	214.9	6.81	6.58	495.8	35.17	2874	221.1	9.04		
		API	.500	25.000	136	212.8	6.81	6.54	490.9	40.06	3259	250.7	9.02		
		--	.625	24.750	169	208.6	6.81	6.48	481.1	49.82	4013	308.7	8.98		
		--	.750	24.500	202	204.4	6.81	6.41	471.4	59.49	4744	364.9	8.93		
		--	.875	24.250	235	200.2	6.81	6.35	461.9	69.07	5458	419.9	8.89		
		--	1.000	24.000	267	196.1	6.81	6.28	452.4	78.54	6149	473.0	8.85		
		--	1.125	23.750	299	192.1	6.81	6.22	443.0	87.91	6813	524.1	8.80		
		--	1.375	23.250	362	184.1	6.81	6.09	424.6	106.37	8088	622.2	8.72		
		--	1.500	23.000	393	180.1	6.81	6.02	415.5	115.45	8695	668.8	8.68		
		30	30.000	8 Ga.	.164	29.672	52	299.9	7.85	7.77	691.4	15.37	1711	114.0	10.55
				6 Ga.	.194	29.612	62	298.6	7.85	7.75	688.6	18.17	2017	134.4	10.53
3 Ga.	.239			29.522	76	296.7	7.85	7.73	684.4	22.35	2474	165.0	10.52		
API	.250			29.500	79	296.3	7.85	7.72	683.4	23.37	2585	172.3	10.52		
API	.281			29.438	89	295.1	7.85	7.70	680.5	26.24	2897	193.1	10.51		
10	.312			29.376	99	293.7	7.85	7.69	677.8	29.19	3201	213.4	10.50		
API	.344			29.312	109	292.6	7.85	7.67	674.8	32.04	3524	235.0	10.49		
API	.375			29.250	119	291.2	7.85	7.66	672.0	34.90	3823	254.8	10.48		
API	.406			29.188	130	290.7	7.85	7.64	669.0	37.75	4132	275.5	10.46		
API	.438			29.124	138	288.8	7.85	7.62	666.1	40.68	4442	296.2	10.45		
20	.500			29.000	158	286.2	7.85	7.59	660.5	46.34	5033	335.5	10.43		
30	.625			28.750	196	281.3	7.85	7.53	649.2	57.68	6213	414.2	10.39		
--	.750			28.500	234	276.6	7.85	7.46	637.9	68.92	7371	491.4	10.34		
--	.875			28.250	272	271.8	7.85	7.39	620.7	80.06	8494	566.2	10.30		
--	1.000	28.000	310	267.0	7.85	7.33	615.7	91.11	9591	639.4	10.26				
--	1.125	27.750	347	262.2	7.85	7.26	604.7	102.05	10653	710.2	10.22				
--	1.250	27.500	384	257.5	7.85	7.20	593.9	112.90	11682	778.8	10.17				
--	1.375	27.250	421	252.9	7.85	7.13	583.1	123.65	12694	846.2	10.13				
--	1.500	27.000	457	248.2	7.85	7.07	572.5	134.30	13673	911.5	10.09				
32	32.000	API	.250	31.500	85	337.8	8.38	8.25	779.2	24.93	3141	196.3	11.22		
		API	.281	31.438	95	336.5	8.38	8.23	776.2	28.04	3525	220.3	11.21		
		API	.312	31.376	106	335.2	8.38	8.21	773.2	31.02	3891	243.2	11.20		
		API	.344	31.312	116	333.8	8.38	8.20	770.0	34.24	4287	268.0	11.19		
		API	.375	31.250	127	332.5	8.38	8.18	766.9	37.25	4656	291.0	11.18		
		API	.406	31.188	137	331.2	8.38	8.16	764.0	40.29	5025	314.1	11.17		
		API	.438	31.124	148	329.8	8.38	8.15	760.8	43.43	5407	337.9	11.16		
		API	.500	31.000	168	327.2	8.38	8.11	754.7	49.48	6140	383.8	11.14		
		--	.625	30.750	209	321.9	8.38	8.05	742.5	61.59	7578	473.6	11.09		
		--	.750	30.500	250	316.7	8.38	7.98	730.5	73.63	8990	561.9	11.05		
		--	.875	30.250	291	311.5	8.38	7.92	718.6	85.53	10368	648.0	11.01		
		--	1.000	30.000	331	306.4	8.38	7.85	706.8	97.38	11680	730.0	10.95		
		--	1.125	29.750	371	301.3	8.38	7.79	695.0	109.0	13003	812.7	10.92		
		--	1.250	29.500	410	296.3	8.38	7.72	680.5	120.7	14398	899.9	10.88		
--	1.375	29.250	450	291.2	8.38	7.66	671.9	132.2	15526	970.4	10.84				
--	1.500	29.000	489	286.3	8.38	7.59	660.5	143.7	16752	1047.0	10.80				

A-16.
(Concluded). Properties of Pipe

Nominal		Designation	Wall Thickness	Inside Diam. d	Weight per Foot	Wt. of Water per Ft. of Pipe	Sq. Ft. Outside Surface per Ft.	Sq. Ft. Inside Surface per Ft.	Transverse Area	Area of Metal	Moment of Inertia	Section Modulus	Radius of Gyration		
Pipe Size	Outside Diam.								a	A	I	Z	R		
	D														
34	34.000	API	.250	33.500	90	382.0	8.90	8.77	881.2	26.50	3773	221.9	11.93		
		API	.281	33.438	101	380.7	8.90	8.75	878.2	29.77	4230	248.8	11.92		
		API	.312	33.376	112	379.3	8.90	8.74	874.9	32.99	4680	275.3	11.91		
		API	.344	33.312	124	377.8	8.90	8.72	871.6	36.36	5147	302.8	11.90		
		API	.375	33.250	135	376.2	8.90	8.70	867.8	39.61	5597	329.2	11.89		
		API	.406	33.188	146	375.0	8.90	8.69	865.0	42.88	6047	355.7	11.87		
		API	.438	33.124	157	373.6	8.90	8.67	861.7	46.18	6501	382.4	11.86		
		API	.500	33.000	179	370.8	8.90	8.64	855.3	52.62	7385	434.4	11.85		
		--	.625	32.750	223	365.0	8.90	8.57	841.9	65.53	9124	536.7	11.80		
		--	.750	32.500	266	359.5	8.90	8.51	829.3	78.34	10829	637.0	11.76		
		--	.875	32.250	308	354.1	8.90	8.44	816.8	90.66	12442	731.9	11.71		
		--	1.000	32.000	353	348.6	8.90	8.38	804.2	103.6	14114	830.2	11.67		
		--	1.125	31.750	395	343.2	8.90	8.31	791.6	116.1	15703	923.7	11.63		
		--	1.250	31.500	437	337.8	8.90	8.25	779.2	128.5	17246	1014.5	11.58		
		--	1.375	31.250	479	332.4	8.90	8.18	766.9	140.9	18770	1104.1	11.54		
		--	1.500	31.000	521	327.2	8.90	8.11	754.7	153.1	20247	1191.0	11.50		
		36	36.000	--	.164	35.672	63	433.2	9.42	9.34	999.3	18.53	2975	165.3	12.67
				--	.194	35.612	74	431.8	9.42	9.32	996.0	21.83	3499	194.4	12.66
				--	.239	35.522	91	429.6	9.42	9.30	991.0	26.86	4293	238.5	12.64
				API	.250	35.500	96	429.1	9.42	9.29	989.7	28.11	4491	249.5	12.64
				API	.281	35.438	107	427.6	9.42	9.28	986.4	31.49	5023	279.1	12.63
API	.312			35.376	119	426.1	9.42	9.26	982.9	34.95	5565	309.1	12.62		
API	.344			35.312	131	424.6	9.42	9.24	979.3	38.56	6127	340.4	12.60		
API	.375			35.250	143	423.1	9.42	9.23	975.8	42.01	6664	370.2	12.59		
API	.406			35.188	154	421.6	9.42	9.21	972.5	45.40	7191	399.5	12.58		
API	.438			35.124	166	420.1	9.42	9.19	968.9	48.93	7737	429.9	12.57		
API	.500			35.000	190	417.1	9.42	9.16	962.1	55.76	8785	488.1	12.55		
--	.625			34.750	236	411.1	9.42	9.10	948.3	69.50	10872	604.0	12.51		
--	.750			34.500	282	405.3	9.42	9.03	934.7	83.01	12898	716.5	12.46		
--	.875			34.250	329	399.4	9.42	8.97	921.2	96.60	14906	828.1	12.42		
--	1.000			34.000	374	393.6	9.42	8.90	907.9	109.9	16851	936.2	12.38		
--	1.125			33.750	419	387.8	9.42	8.83	894.5	123.3	18766	1042.6	12.34		
--	1.250			33.500	464	382.1	9.42	8.77	881.3	136.5	20624	1145.8	12.29		
--	1.375			33.250	509	376.4	9.42	8.70	868.2	149.6	22451	1247.3	12.25		
--	1.500			33.000	553	370.8	9.42	8.64	855.3	162.6	24237	1346.5	12.21		
42	42.000			--	.250	41.500	112	586.4	10.99	10.86	1352.6	32.82	7126	339.3	14.73
				--	.375	41.250	167	579.3	10.99	10.80	1336.3	49.08	10627	506.1	14.71
		--	.500	41.000	222	572.3	10.99	10.73	1320.2	65.18	14037	668.4	14.67		
		--	.625	40.750	276	565.4	10.99	10.67	1304.1	81.28	17373	827.3	14.62		
		--	.750	40.500	331	558.4	10.99	10.60	1288.2	97.23	20689	985.2	14.59		
		--	.875	40.250	385	551.6	10.99	10.54	1272.3	113.0	23896	1137.9	14.54		
		--	1.000	40.000	438	544.8	10.99	10.47	1256.6	128.8	27080	1289.5	14.50		
		--	1.125	39.750	492	537.9	10.99	10.41	1240.9	144.5	30193	1437.8	14.45		
		--	1.250	39.500	544	531.2	10.99	10.34	1225.3	160.0	33233	1582.5	14.41		
		--	1.375	39.250	597	524.4	10.99	10.27	1209.9	175.5	36240	1725.7	14.37		
		--	1.500	39.000	649	517.9	10.99	10.21	1194.5	190.8	39181	1865.7	14.33		

A-17. Equation of Pipes

The table below gives the number of pipes of one size required to equal in delivery other larger pipes of same length and under same conditions. The upper portion above the diagonal line of stars pertains to "standard" steam and gas pipes, while the lower portion is for pipes of the ACTUAL internal diameters given. The figures given in the table opposite the intersection of any two sizes is the number of the smaller-sized pipes required to equal one of the larger. Thus, it requires 29 standard 2-inch pipes to equal one standard 7-inch pipe.

STANDARD STEAM AND GAS PIPES

Dia.	1/2	3/4	1	1 1/2	2	2 1/2	3	4	5	6	7	8	9	10	11	12	13	14	15	16	17	Dia.
1/2	***	2.27	4.88	15.8	31.7	52.9	96.9	205	377	(620)	918	1292	1767	2488	3014	3786	4904	5927	7321	8535	9717	1/2
3/4	2.60	***	2.05	6.97	14.0	23.3	42.5	90.4	166	273	405	569	779	1096	1328	1668	2161	2615	3226	3761	4282	3/4
1	7.55	2.90	***	3.45	6.82	11.4	20.9	44.1	81.1	133	198	278	380	536	649	815	1070	1263	1576	1837	2092	1
1 1/2	24.2	9.30	3.20	***	1.26	3.34	6.13	13.0	23.8	39.2	58.1	81.7	112	157	190	239	310	375	463	539	614	1 1/2
2	54.8	21.0	7.25	2.26	***	1.67	3.06	6.47	11.9	19.6	29.0	40.8	55.8	78.5	95.1	119	155	187	231	269	307	2
2 1/2	102	39.4	13.6	4.23	1.87	***	1.83	3.87	7.12	11.7	17.4	24.4	33.4	47.0	56.9	71.5	92.6	112	138	161	184	2 1/2
3	170	65.4	22.6	7.03	3.11	1.66	***	2.12	3.89	6.39	9.48	13.3	20.9	23.7	31.2	39.1	50.6	61.1	75.5	88.0	100	3
4	376	144	49.8	15.5	6.87	3.67	2.21	***	1.84	3.02	4.48	6.30	8.61	12.1	14.7	18.5	23.9	28.9	35.7	41.6	47.4	4
5	686	263	90.9	28.3	12.5	6.70	4.03	1.83	***	1.65	2.44	3.43	4.69	6.60	8.00	10.0	13.0	15.7	19.4	22.6	25.8	5
6	1116	429	148	46.0	20.4	10.9	6.56	2.97	1.63	***	1.48	2.09	2.85	4.02	4.86	6.11	7.91	9.56	11.8	13.8	15.6	6
7	1707	656	226	70.5	31.2	16.6	10.0	4.54	2.49	1.51	***	1.41	1.93	2.71	3.28	4.12	5.34	6.45	7.97	9.31	10.6	7
8	2435	936	322	101	44.5	23.8	14.3	6.48	3.54	2.18	1.43	***	1.35	1.93	2.33	2.92	3.79	4.57	5.67	6.60	7.52	8
9	3335	1281	440	137	60.8	32.5	19.5	8.85	4.85	2.98	1.95	1.37	***	1.41	1.71	2.14	2.77	3.35	4.14	4.83	5.50	9
10	4393	1688	582	181	80.4	42.9	25.8	11.7	6.40	3.93	2.57	1.80	1.32	***	1.21	1.52	1.97	2.38	2.94	3.43	3.91	10
11	5642	2168	747	233	103	55.1	33.1	15.0	8.22	5.05	3.31	2.32	1.70	1.28	***	1.26	1.63	1.88	2.43	2.83	3.22	11
12	7087	2723	938	293	129	69.2	41.6	18.8	10.3	6.34	4.15	2.91	2.13	1.61	1.26	***	1.30	1.57	1.93	2.26	2.58	12
13	8657	3326	1146	358	158	84.5	50.7	23.0	12.6	7.75	5.07	3.56	2.60	1.98	1.53	1.22	***	1.21	1.49	1.74	1.98	13
14	10600	4070	1403	438	193	103	62.2	28.2	15.4	9.48	6.21	4.35	3.18	2.41	1.88	1.50	1.22	***	1.24	1.44	1.64	14
15	12824	4927	1698	530	234	126	75.3	34.1	18.7	11.5	7.52	5.27	3.85	2.92	2.27	1.81	1.48	1.21	***	1.17	1.35	15
16	14978	5758	1984	619	274	146	88.0	39.9	21.8	13.4	8.78	6.15	4.51	3.41	2.66	2.12	1.73	1.42	1.18	***	1.14	16
17	17537	6738	2322	724	320	171	103	46.6	25.6	15.7	10.3	7.20	5.27	3.99	3.11	2.47	2.03	1.66	1.37	1.17	***	17
18	20327	7810	2691	840	317	198	119	54.1	29.6	18.2	11.9	8.35	6.11	4.63	3.60	2.87	2.35	1.92	1.59	1.36	1.16	18
20	26676	10249	3532	1102	487	260	157	70.9	38.9	23.9	15.6	10.9	8.02	6.07	4.73	3.76	3.08	2.52	2.03	1.78	1.52	20
24	42624	16376	5644	1761	778	416	250	113	62.1	38.2	25.0	17.5	12.8	9.70	7.55	6.01	4.92	4.02	3.32	2.84	2.43	24
30	75453	28990	9990	3117	1378	736	443	201	110	67.6	44.2	31.0	22.7	17.2	13.4	10.7	8.72	7.14	5.88	5.03	4.30	30
36	120100	46143	15902	4961	2193	1172	705	319	175	108	70.4	49.3	36.1	27.3	21.3	16.9	13.9	11.3	9.37	8.01	6.85	36
42	177724	68282	23531	7341	3245	1734	1044	473	259	159	104	73.0	53.4	40.5	31.5	25.1	20.5	16.8	13.9	11.9	10.1	42
48	249351	95818	33020	10301	4554	2434	1465	663	363	223	146	102	75.0	56.8	44.2	35.2	28.8	23.5	19.4	16.6	14.2	48
Dia.	1/2	3/4	1	1 1/2	2	2 1/2	3	4	5	6	7	8	9	10	11	12	13	14	15	16	17	

By permission, Buffalo Tank Div., Bethlehem Steel Corp.

A-18.
(Continued). Circumferences and Areas of Circles
(Advancing by eighths)

Dia.	Circum.	Area*	Dia.	Circum.	Area*
29 1/2	93.070	689.30	36 1/4	113.097	1017.9
29 3/4	93.462	695.13	36 1/2	113.490	1025.0
29 7/8	93.855	700.98	36 3/4	113.883	1032.1
			36 7/8	114.275	1039.2
30 1/8	94.248	706.86	36 7/8	114.668	1046.3
30 1/4	94.640	712.76	36 5/8	115.061	1053.5
30 1/2	95.033	718.69	36 1/2	115.454	1060.7
30 3/4	95.426	724.64	36 3/4	115.846	1068.0
30 7/8	95.819	730.62	36 7/8	116.239	1075.2
			37 1/8	116.632	1082.5
31 1/8	96.211	736.62	37 1/4	117.024	1089.8
31 1/4	96.604	742.64	37 1/2	117.417	1097.1
31 1/2	96.997	748.69	37 3/4	117.810	1104.5
			37 7/8	118.202	1111.8
31 3/8	97.389	754.77	37 7/8	118.596	1119.2
31 1/2	97.782	760.87	37 7/8	118.988	1126.7
31 3/4	98.175	766.99			
31 7/8	98.567	773.14	38 1/8	119.381	1134.1
			38 1/4	119.773	1141.6
32 1/8	98.959	779.31	38 1/2	120.166	1149.1
32 1/4	99.353	785.51	38 3/4	120.559	1156.6
32 1/2	99.746	791.73	38 7/8	120.951	1164.2
32 3/4	100.138	797.98	38 7/8	121.344	1171.7
			38 7/8	121.737	1179.3
32 7/8	100.531	804.25	38 7/8	122.129	1186.9
33 1/8	100.924	810.54			
33 1/4	101.316	816.86	39 1/8	122.522	1194.6
33 1/2	101.709	823.21	39 1/4	122.915	1202.3
33 3/4	102.102	829.58	39 1/2	123.308	1210.6
33 7/8	102.494	835.97	39 3/4	123.700	1217.7
			39 7/8	124.093	1225.2
34 1/8	102.887	842.39	39 7/8	124.486	1232.4
34 1/4	103.280	848.83	39 7/8	124.878	1240.0
			39 7/8	125.271	1248.8
34 3/4	103.673	855.30			
34 7/8	104.065	861.79	40 1/8	125.664	1256.6
			40 1/4	126.056	1264.5
35 1/8	104.458	868.31	40 1/2	126.449	1272.4
35 1/4	104.851	874.85	40 3/4	126.842	1280.3
35 1/2	105.243	881.41	40 7/8	127.235	1288.2
35 3/4	105.636	888.00	40 7/8	127.627	1296.2
35 7/8	106.029	894.62	40 7/8	128.020	1304.2
			40 7/8	128.413	1312.2
36 1/8	106.421	901.26			
36 1/4	106.814	907.92	41 1/8	128.805	1320.3
36 1/2	107.207	914.61	41 1/4	129.198	1328.3
36 3/4	107.600	921.32	41 1/2	129.591	1336.4
36 7/8	107.992	928.06	41 3/4	129.983	1344.5
			41 7/8	130.376	1352.7
37 1/8	108.385	934.82	41 7/8	130.769	1360.8
37 1/4	108.778	941.61	41 7/8	131.161	1369.0
37 1/2	109.170	948.42	41 7/8	131.554	1377.2
37 3/4	109.563	955.25			
37 7/8	109.956	962.11	42 1/8	131.947	1385.4
38 1/8	110.348	969.00	42 1/4	132.340	1393.7
38 1/4	110.741	975.91			
38 1/2	111.134	982.84	42 1/2	132.733	1402.0
38 3/4	111.527	989.80	42 3/4	133.126	1410.3
38 7/8	111.919	996.78	42 7/8	133.519	1418.6
39 1/8	112.312	1003.8			
39 1/4	112.705	1010.8			

*Approximate area sufficiently accurate for practical purposes, including estimating.

A-18.
(Continued). Circumferences and Areas of Circles
(Advancing by eighths)

Dia.	Circum.	Area*	Dia.	Circum.	Area*
48 5/8	152.760	1857.0	55 1/4	172.788	2375.8
48 3/4	153.153	1866.5	55 1/2	173.180	2386.6
48 7/8	153.545	1876.1	55 3/4	173.573	2397.5
			55 7/8	173.966	2408.3
49 1/8	153.938	1885.7	55 7/8	174.358	2419.2
49 1/4	154.331	1895.4	55 7/8	174.751	2430.1
49 1/2	154.723	1905.0	55 7/8	175.144	2441.1
49 3/4	155.116	1914.7	55 7/8	175.536	2452.0
49 7/8	155.509	1924.4			
50 1/8	155.902	1934.2	56 1/8	175.929	2463.0
50 1/4	156.294	1943.9	56 1/4	176.322	2474.0
50 1/2	156.687	1953.7	56 1/2	176.715	2485.0
			56 3/4	177.107	2496.1
50 3/4	157.080	1963.5	56 3/4	177.500	2507.2
50 7/8	157.472	1973.3	56 3/4	177.893	2518.3
			56 3/4	178.285	2529.4
51 1/8	157.865	1983.2	56 3/4	178.678	2540.6
51 1/4	158.258	1993.1			
51 1/2	158.650	2003.0	57 1/8	179.071	2551.8
51 3/4	159.043	2012.9	57 1/4	179.463	2563.0
51 7/8	159.436	2022.8	57 1/2	179.856	2574.2
			57 3/4	180.249	2585.4
51 7/8	159.829	2032.8	57 3/4	180.642	2596.7
			57 3/4	181.034	2608.0
51 7/8	160.221	2042.8	57 3/4	181.427	2619.4
51 7/8	160.614	2052.8	57 3/4	181.820	2630.7
51 7/8	161.007	2062.9			
51 7/8	161.399	2073.0	58 1/8	182.212	2642.1
51 7/8	161.792	2083.1	58 1/4	182.605	2653.5
51 7/8	162.185	2093.2	58 1/2	182.998	2664.9
51 7/8	162.577	2103.3	58 1/2	183.390	2676.4
51 7/8	162.970	2113.5	58 1/2	183.783	2687.8
			58 1/2	184.176	2699.3
52 1/8	163.363	2123.7	58 1/2	184.569	2710.9
52 1/4	163.756	2133.9	58 1/2	184.961	2722.4
52 1/2	164.148	2144.2			
52 3/4	164.541	2154.5	59 1/8	185.354	2734.0
52 7/8	164.934	2164.8	59 1/4	185.747	2745.6
52 7/8	165.326	2175.1	59 1/2	186.139	2757.2
52 7/8	165.719	2185.4	59 1/2	186.532	2768.8
52 7/8	166.112	2195.8	59 1/2	186.925	2780.5
			59 1/2	187.317	2792.2
53 1/8	166.504	2206.2	59 1/2	187.710	2803.9
53 1/4	166.897	2216.6	59 1/2	188.103	2815.7
53 1/2	167.290	2227.0			
53 3/4	167.683	2237.5	60 1/8	188.496	2827.4
53 7/8	168.075	2248.0	60 1/4	188.888	2839.2
53 7/8	168.468	2258.5	60 1/2	189.281	2851.0
53 7/8	168.861	2269.1	60 1/2	189.674	2862.9
53 7/8	169.253	2279.6	60 1/2	190.066	2874.8
			60 1/2	190.459	2886.6
54 1/8	169.646	2290.2	60 1/2	190.852	2898.6
54 1/4	170.039	2300.8	60 1/2	191.244	2910.5
54 1/2	170.431	2311.5			
54 3/4	170.824	2322.1	61 1/8	191.637	2922.5
54 7/8	171.217	2332.8	61 1/4	192.030	2934.5
54 7/8	171.610	2343.5			
54 7/8	172.002	2354.3			
54 7/8	172.395	2365.0			

*Approximate area, sufficiently accurate for practical purposes, including estimating.

A-18.
(Continued). Circumferences and Areas of Circles
(Advancing by eighths)

Dia.	Circum.	Area*	Dia.	Circum.	Area*
67 1/2	212.058	3578.5	80.	251.327	5026.5
5/8	212.450	3591.7	1/8	251.720	5042.3
3/4	212.843	3605.0	1/4	252.113	5058.0
7/8	213.236	3618.3	2/8	252.506	5073.8
68.	213.628	3631.7	3/8	252.898	5089.5
1/8	214.021	3645.0	4/8	253.291	5105.4
1/4	214.414	3658.4	5/8	253.684	5121.2
3/8	214.806	3671.8	6/8	254.076	5137.1
1/2	215.199	3685.3	7/8	254.469	5153.0
5/8	215.592	3698.7	81.	254.862	5168.9
3/4	215.984	3712.2	1/8	255.254	5184.9
7/8	216.377	3725.7	1/4	255.647	5200.8
69.	216.770	3739.3	3/8	256.040	5216.8
1/8	217.163	3752.8	4/8	256.433	5232.8
1/4	217.555	3766.4	5/8	256.825	5248.9
3/8	217.948	3780.0	6/8	257.218	5264.9
1/2	218.341	3793.7	7/8	257.611	5281.0
5/8	218.733	3807.3	82.	258.003	5297.1
3/4	219.126	3821.0	1/8	258.396	5313.3
7/8	219.519	3834.7	1/4	258.789	5329.4
70.	219.911	3848.5	3/8	259.181	5345.6
1/8	220.304	3862.2	4/8	259.574	5361.8
1/4	220.697	3876.0	5/8	259.967	5378.1
3/8	221.090	3889.8	6/8	260.359	5394.3
1/2	221.482	3903.6	7/8	260.752	5410.6
5/8	221.875	3917.5	83.	261.145	5426.9
3/4	222.268	3931.4	1/8	261.538	5443.3
7/8	222.660	3945.3	1/4	261.930	5459.6
71.	223.053	3959.2	3/8	262.323	5476.0
1/8	223.446	3973.1	4/8	262.716	5492.4
1/4	223.838	3987.1	5/8	263.108	5508.8
3/8	224.231	4001.1	6/8	263.501	5525.3
1/2	224.624	4015.2	7/8	263.894	5541.8
5/8	225.017	4029.2	84.	264.286	5558.3
3/4	225.409	4043.3	1/8	264.679	5574.8
7/8	225.802	4057.4	1/4	265.072	5591.4
72.	226.195	4071.5	3/8	265.465	5607.9
1/8	226.587	4085.7	4/8	265.857	5624.5
1/4	226.980	4099.8	5/8	266.250	5641.2
3/8	227.373	4114.0	6/8	266.643	5657.8
1/2	227.765	4128.2	7/8	267.035	5674.5
5/8	228.158	4142.5	85.	267.428	5691.2
3/4	228.551	4156.8	1/8	267.821	5707.9
7/8	228.944	4171.1	1/4	268.213	5724.7
73.	229.336	4185.4	3/8	268.606	5741.5
1/8	229.729	4199.7	4/8	268.999	5758.3
1/4	230.122	4214.1	5/8	269.392	5775.1
3/8	230.514	4228.5	6/8	269.784	5791.9
1/2	230.907	4242.9	7/8	270.177	5808.8
5/8	231.300	4257.4	86.	270.570	5825.7

*Approximate area, sufficiently accurate for practical purposes, including estimating.

A-18.
(Continued). Circumferences and Areas of Circles
(Advancing by eighths)

Dia.	Circum.	Area*	Dia.	Circum.	Area*
86 1/4	270.962	5842.6	92 1/2	290.597	6720.1
3/8	271.355	5859.6	5/8	290.990	6738.2
1/2	271.748	5876.5	3/4	291.383	6756.4
5/8	272.140	5893.5	7/8	291.775	6774.7
87.	272.533	5910.6	93.	292.168	6792.9
1/8	272.926	5927.6	1/8	292.561	6811.2
1/4	273.319	5944.7	1/4	292.954	6829.5
3/8	273.711	5961.8	3/8	293.346	6847.8
1/2	274.104	5979.0	1/2	293.739	6866.1
5/8	274.497	5996.0	5/8	294.132	6884.5
3/4	274.889	6013.2	3/4	294.524	6902.9
7/8	275.282	6030.4	7/8	294.917	6921.3
88.	275.675	6047.6	100.	295.310	6939.8
1/8	276.067	6064.9	1/8	295.702	6958.2
1/4	276.460	6082.1	1/4	296.095	6976.7
3/8	276.853	6099.4	3/8	296.488	6995.3
1/2	277.246	6116.7	1/2	296.881	7013.8
5/8	277.638	6134.1	5/8	297.273	7032.4
3/4	278.031	6151.4	3/4	297.666	7051.0
7/8	278.424	6168.8	7/8	298.059	7069.6
89.	278.816	6186.2	101.	298.451	7088.2
1/8	279.209	6203.7	1/8	298.844	7106.9
1/4	279.602	6221.1	1/4	299.237	7125.6
3/8	279.994	6238.6	3/8	299.629	7144.3
1/2	280.387	6256.1	1/2	300.022	7163.0
5/8	280.780	6273.7	5/8	300.415	7181.8
3/4	281.173	6291.2	3/4	300.807	7200.6
7/8	281.565	6308.8	7/8	301.200	7219.4
89.	281.958	6326.4	102.	301.593	7238.2
1/8	282.351	6344.1	1/8	301.986	7257.1
1/4	282.743	6361.7	1/4	302.378	7276.0
3/8	283.136	6379.4	3/8	302.771	7294.9
1/2	283.529	6397.1	1/2	303.164	7313.8
5/8	283.921	6414.9	5/8	303.556	7332.8
3/4	284.314	6432.6	3/4	303.949	7351.8
7/8	284.707	6450.4	7/8	304.342	7370.8
90.	285.100	6468.2	103.	304.734	7389.8
1/8	285.492	6486.0	1/8	305.127	7408.9
1/4	285.885	6503.9	1/4	305.520	7428.0
3/8	286.278	6521.8	3/8	305.913	7447.1
1/2	286.670	6539.7	1/2	306.305	7466.2
5/8	287.063	6557.6	5/8	306.698	7485.3
3/4	287.456	6575.5	3/4	307.091	7504.5
7/8	287.848	6593.5	7/8	307.483	7523.7
91.	288.241	6611.5	104.	307.876	7543.0
1/8	288.634	6629.6	1/8	308.269	7562.2
1/4	289.027	6647.6	1/4	308.661	7581.5
3/8	289.419	6665.7	3/8	309.054	7600.8
1/2	289.812	6683.8	1/2	309.447	7620.1
5/8	290.205	6701.9	5/8	309.840	7639.5

*Approximate area, sufficiently accurate for practical purposes, including estimating.

A-18.

**(Continued). Circumferences and Areas of Circles
(Advancing by eighths)**

Dia.	Circum.	Area*	Dia.	Circum.	Area*
105. $\frac{1}{8}$	329.87	8659	111 $\frac{1}{2}$	349.50	10844
$\frac{1}{4}$	330.26	8679	$\frac{3}{8}$	349.90	10867
$\frac{1}{2}$	330.65	8700	$\frac{1}{2}$	350.29	10890
$\frac{3}{8}$	331.05	8721	$\frac{5}{8}$	350.68	10913
$\frac{1}{2}$	331.44	8741	$\frac{3}{4}$	351.07	10936
$\frac{5}{8}$	331.83	8762	$\frac{7}{8}$	351.47	10960
$\frac{3}{4}$	332.22	8783	118.	351.86	10983
$\frac{7}{8}$	332.62	8804	$\frac{1}{8}$	352.25	11007
106. $\frac{1}{8}$	333.01	8825	$\frac{1}{4}$	352.65	11030
$\frac{1}{4}$	333.40	8845	$\frac{3}{8}$	353.04	11053
$\frac{1}{2}$	333.80	8866	$\frac{1}{2}$	353.43	11076
$\frac{3}{8}$	334.19	8887	$\frac{3}{4}$	353.82	11099
$\frac{1}{2}$	334.58	8908	$\frac{5}{8}$	354.22	11122
$\frac{3}{4}$	334.97	8929	$\frac{7}{8}$	354.61	11146
$\frac{7}{8}$	335.37	8950	113.	355.00	11169
107. $\frac{1}{8}$	335.76	8971	$\frac{1}{8}$	355.39	11193
$\frac{1}{4}$	336.15	8992	$\frac{1}{4}$	355.79	11216
$\frac{1}{2}$	336.54	9014	$\frac{3}{8}$	356.18	11240
$\frac{3}{8}$	336.94	9035	$\frac{1}{2}$	356.57	11263
$\frac{1}{2}$	337.33	9056	$\frac{3}{4}$	356.96	11287
$\frac{5}{8}$	337.72	9077	$\frac{7}{8}$	357.35	11310
$\frac{3}{4}$	338.12	9098	120.	357.74	11334
$\frac{7}{8}$	338.51	9119	$\frac{1}{8}$	358.14	11357
108. $\frac{1}{8}$	338.90	9140	$\frac{1}{4}$	358.54	11381
$\frac{1}{4}$	339.29	9161	$\frac{3}{8}$	358.93	11404
$\frac{1}{2}$	339.69	9183	$\frac{1}{2}$	359.32	11428
$\frac{3}{8}$	340.08	9204	$\frac{3}{4}$	359.71	11451
$\frac{1}{2}$	340.47	9225	$\frac{5}{8}$	360.11	11475
$\frac{3}{4}$	340.86	9246	$\frac{7}{8}$	360.50	11499
$\frac{7}{8}$	341.26	9268	121.	360.89	11522
109. $\frac{1}{8}$	341.65	9289	$\frac{1}{8}$	361.28	11546
$\frac{1}{4}$	342.04	9310	$\frac{1}{4}$	361.68	11570
$\frac{1}{2}$	342.43	9331	$\frac{3}{8}$	362.07	11594
$\frac{3}{8}$	342.83	9353	$\frac{1}{2}$	362.46	11618
$\frac{1}{2}$	343.22	9374	$\frac{3}{4}$	362.86	11642
$\frac{5}{8}$	343.61	9396	$\frac{7}{8}$	363.25	11666
$\frac{3}{4}$	344.01	9417	122.	363.64	11690
$\frac{7}{8}$	344.40	9439	$\frac{1}{8}$	364.03	11714
110. $\frac{1}{8}$	344.79	9460	$\frac{1}{4}$	364.43	11738
$\frac{1}{4}$	345.18	9481	$\frac{3}{8}$	364.82	11762
$\frac{1}{2}$	345.58	9503	$\frac{1}{2}$	365.21	11786
$\frac{3}{8}$	345.97	9525	$\frac{3}{4}$	365.60	11810
$\frac{1}{2}$	346.36	9546	$\frac{5}{8}$	366.00	11834
$\frac{3}{4}$	346.75	9568	$\frac{7}{8}$	366.39	11858
$\frac{7}{8}$	347.15	9589	123.	366.78	11882
111. $\frac{1}{8}$	347.54	9611	$\frac{1}{8}$	367.18	11907
$\frac{1}{4}$	347.93	9633	$\frac{1}{4}$	367.57	11931
$\frac{1}{2}$	348.33	9655	$\frac{3}{8}$	367.96	11956
$\frac{3}{8}$	348.72	9677	$\frac{1}{2}$	368.35	11980
$\frac{1}{2}$	349.11	9698	$\frac{3}{4}$	368.75	

*Approximate area, sufficiently accurate for practical purposes, including estimating.

A-18.

**(Continued). Circumferences and Areas of Circles
(Advancing by eighths)**

Dia.	Circum.	Area*	Dia.	Circum.	Area*
123 $\frac{5}{8}$	388.38	12004	136 $\frac{1}{4}$	408.41	13273
$\frac{3}{4}$	388.77	12028	$\frac{3}{8}$	408.80	13299
$\frac{7}{8}$	389.17	12052	$\frac{1}{2}$	409.19	13324
124. $\frac{1}{8}$	389.56	12076	$\frac{5}{8}$	409.59	13350
$\frac{1}{4}$	389.95	12101	$\frac{3}{4}$	409.98	13375
$\frac{3}{8}$	390.34	12125	$\frac{1}{2}$	410.37	13401
$\frac{1}{2}$	390.74	12150	$\frac{5}{8}$	410.76	13426
$\frac{3}{4}$	391.13	12174	$\frac{7}{8}$	411.16	13452
$\frac{7}{8}$	391.52	12199	137.	411.55	13478
125. $\frac{1}{8}$	391.92	12223	$\frac{1}{4}$	411.94	13504
$\frac{1}{4}$	392.31	12248	$\frac{3}{8}$	412.34	13529
$\frac{1}{2}$	392.70	12272	$\frac{1}{2}$	412.73	13555
$\frac{3}{8}$	393.09	12297	$\frac{3}{4}$	413.12	13581
$\frac{1}{2}$	393.49	12321	$\frac{5}{8}$	413.51	13607
$\frac{3}{4}$	393.88	12346	$\frac{7}{8}$	413.91	13633
$\frac{7}{8}$	394.27	12370	138.	414.30	13659
126. $\frac{1}{8}$	394.66	12395	$\frac{1}{8}$	414.69	13685
$\frac{1}{4}$	395.06	12419	$\frac{1}{4}$	415.08	13711
$\frac{1}{2}$	395.45	12444	$\frac{3}{8}$	415.48	13737
$\frac{3}{4}$	395.84	12469	$\frac{1}{2}$	415.87	13763
$\frac{5}{8}$	396.23	12494	$\frac{3}{4}$	416.26	13789
$\frac{7}{8}$	396.63	12518	$\frac{7}{8}$	416.66	13815
127. $\frac{1}{8}$	397.02	12543	$\frac{1}{8}$	417.05	13841
$\frac{1}{4}$	397.41	12568	$\frac{1}{4}$	417.44	13867
$\frac{1}{2}$	397.81	12593	133.	417.83	13893
$\frac{3}{8}$	398.20	12618	$\frac{1}{2}$	418.23	13919
$\frac{1}{2}$	398.59	12643	$\frac{3}{8}$	418.62	13946
$\frac{3}{4}$	398.98	12668	$\frac{1}{2}$	419.01	13972
$\frac{5}{8}$	399.38	12693	$\frac{3}{4}$	419.40	13999
$\frac{7}{8}$	399.77	12718	$\frac{7}{8}$	419.80	14025
128. $\frac{1}{8}$	400.16	12743	$\frac{1}{8}$	420.19	14051
$\frac{1}{4}$	400.55	12768	$\frac{1}{4}$	420.58	14077
$\frac{1}{2}$	400.95	12793	134.	420.97	14103
$\frac{3}{8}$	401.34	12818	$\frac{1}{2}$	421.37	14130
$\frac{1}{2}$	401.73	12843	$\frac{3}{8}$	421.76	14156
$\frac{3}{4}$	402.13	12868	$\frac{1}{2}$	422.15	14183
$\frac{5}{8}$	402.52	12893	$\frac{3}{4}$	422.55	14209
$\frac{7}{8}$	402.91	12919	$\frac{7}{8}$	422.94	14236
129. $\frac{1}{8}$	403.30	12944	$\frac{1}{8}$	423.33	14262
$\frac{1}{4}$	403.70	12970	$\frac{1}{4}$	423.72	14288
$\frac{1}{2}$	404.09	12995	135.	424.12	14314
$\frac{3}{8}$	404.48	13020	$\frac{1}{2}$	424.51	14341
$\frac{1}{2}$	404.87	13045	$\frac{3}{8}$	424.90	14367
$\frac{3}{4}$	405.27	13070	$\frac{1}{2}$	425.29	14394
$\frac{5}{8}$	405.66	13096	$\frac{3}{4}$	425.69	14420
$\frac{7}{8}$	406.05	13121	$\frac{7}{8}$	426.08	14447
130. $\frac{1}{8}$	406.44	13147	$\frac{1}{8}$	426.47	14473
$\frac{1}{4}$	406.84	13172	$\frac{1}{4}$	426.87	14500
$\frac{1}{2}$	407.23	13198	136.	427.26	14527
$\frac{3}{8}$	407.62	13223	$\frac{1}{2}$	427.65	14553
$\frac{1}{2}$	408.02	13248	$\frac{3}{8}$		

*Approximate area, sufficiently accurate for practical purposes, including estimating.

A-18.
(Continued). Circumferences and Areas of Circles
(Advancing by eighths)

Dia.	Circum.	Area *	Dia.	Circum.	Area *
142 1/2	447.68	15949	155. 1/8	486.95	18869
3/8	448.07	15977	1/4	487.34	18900
1/2	448.46	16005	3/8	487.73	18930
5/8	448.86	16033	1/2	488.13	18961
143. 1/8	449.25	16061	5/8	488.52	18991
1/4	449.64	16089	1/2	488.91	19022
3/8	450.03	16117	3/8	489.30	19052
1/2	450.43	16145	1/2	489.70	19083
5/8	450.82	16173	5/8	490.09	19113
1/2	451.21	16201	1/4	490.48	19144
3/4	451.61	16229	1/2	490.88	19174
7/8	452.00	16258	3/4	491.27	19205
144. 1/8	452.39	16286	1/2	491.66	19235
1/4	452.78	16314	5/8	492.05	19266
3/8	453.18	16342	1/2	492.45	19297
1/2	453.57	16371	3/4	492.84	19328
5/8	453.96	16399	157. 1/8	493.23	19359
1/2	454.35	16428	1/4	493.62	19390
3/4	454.75	16456	1/2	494.02	19421
7/8	455.14	16485	3/4	494.41	19452
145. 1/8	455.53	16513	1/2	494.80	19483
1/4	455.93	16542	5/8	495.20	19514
3/8	456.32	16570	1/2	495.59	19545
1/2	456.71	16599	3/4	495.98	19576
5/8	457.10	16627	158. 1/8	496.37	19607
1/2	457.50	16656	1/4	496.76	19638
3/4	457.89	16684	1/2	497.15	19669
7/8	458.28	16713	3/8	497.55	19701
146. 1/8	458.67	16742	1/2	497.94	19732
1/4	459.07	16770	5/8	498.34	19763
3/8	459.46	16799	1/2	498.73	19794
1/2	459.85	16827	3/4	499.12	19825
5/8	460.24	16856	159. 1/8	499.51	19856
1/2	460.64	16885	1/4	500.30	19887
3/4	461.03	16914	1/2	500.69	19919
7/8	461.42	16943	5/8	501.09	19950
147. 1/8	461.82	16972	1/2	501.48	19982
1/4	462.21	17000	3/8	501.87	20013
3/8	462.60	17029	1/2	502.26	20044
1/2	462.99	17058	5/8	502.66	20075
5/8	463.39	17087	160. 1/8	503.05	20106
1/2	463.78	17116	1/4	503.45	20138
3/4	464.17	17145	1/2	503.83	20169
7/8	464.56	17174	3/4	504.22	20201
148. 1/8	464.96	17203	1/2	504.62	20232
1/4	465.35	17232	5/8	505.01	20264
3/8	465.74	17262	1/2	505.41	20295
1/2	466.14	17291	3/4	505.80	20327
5/8	466.53	17321	161. 1/8	506.19	20358
1/2	466.92	17350	1/4	506.58	20390

*Approximate area, sufficiently accurate for practical purposes, including estimating.

A-18.
(Continued). Circumferences and Areas of Circles
(Advancing by eighths)

Dia.	Circum.	Area *	Dia.	Circum.	Area *
161 1/4	506.58	20421	173 3/4	545.85	23711
3/8	506.98	20453	1/8	546.25	23745
1/2	507.37	20484	174. 1/8	546.64	23779
5/8	508.15	20516	1/4	547.03	23813
1/2	508.55	20548	3/8	547.82	23848
162. 1/8	508.94	20580	1/2	548.21	23882
1/4	509.33	20612	5/8	548.60	23917
3/8	509.73	20644	1/2	549.00	23951
1/2	510.12	20675	3/4	549.39	23985
5/8	510.51	20707	175. 1/8	549.78	24019
1/2	510.90	20739	1/4	550.17	24053
3/4	511.30	20771	1/2	550.57	24087
7/8	511.69	20803	3/8	550.96	24122
163. 1/8	512.08	20835	1/2	551.35	24156
1/4	512.47	20867	5/8	551.74	24191
3/8	512.87	20899	1/2	552.14	24225
1/2	513.26	20931	3/4	552.53	24260
5/8	513.65	20964	176. 1/8	552.92	24294
1/2	514.04	20996	1/4	553.31	24329
3/4	514.44	21028	1/2	553.71	24363
7/8	514.83	21060	3/8	554.10	24398
164. 1/8	515.22	21092	1/2	554.49	24432
1/4	515.62	21124	5/8	554.89	24467
3/8	516.01	21157	1/2	555.28	24501
1/2	516.40	21190	3/4	555.67	24536
5/8	516.79	21222	177. 1/8	556.06	24571
1/2	517.18	21254	1/4	556.46	24606
3/4	517.58	21287	1/2	556.85	24640
7/8	517.97	21319	3/8	557.24	24675
165. 1/8	518.36	21351	1/2	557.63	24710
1/4	518.76	21383	5/8	558.03	24745
3/8	519.15	21416	1/2	558.42	24780
1/2	519.54	21448	3/4	558.81	24815
5/8	519.94	21481	178. 1/8	559.21	24850
1/2	520.33	21513	1/4	559.60	24885
3/4	520.72	21546	1/2	559.99	24920
7/8	521.11	21578	3/8	560.38	24955
166. 1/8	521.51	21610	1/2	560.78	24990
1/4	521.90	21642	5/8	561.17	25025
3/8	522.29	21675	1/2	561.56	25060
1/2	522.68	21707	3/4	561.95	25095
5/8	523.08	21740	179. 1/8	562.35	25130
1/2	523.47	21772	1/4	562.74	25165
3/4	523.86	21805	1/2	563.13	25200
7/8	524.26	21838	3/8	563.53	25236
167. 1/8	524.65	21871	1/2	563.92	25271
1/4	525.04	21904	5/8	564.31	25307
3/8	525.43	21937	1/2	564.70	25342
1/2	525.83	21969	3/4	565.10	25377
5/8	526.22	22002	179. 1/8	565.50	25412

*Approximate area, sufficiently accurate for practical purposes, including estimating.

A-18.
(Continued). Circumferences and Areas of Circles
(Advancing by eighths)

Dia.	Circum.	Area*	Dia.	Circum.	Area*
180. 1/8	565.49	25447	192 1/2	604.76	29103
1/4	565.88	25482	5/8	605.15	29141
3/8	566.27	25518	3/4	605.54	29179
1/2	566.67	25553	7/8	605.94	29217
5/8	567.06	25589			
3/4	567.45	25624	193.	606.33	29255
7/8	567.84	25660	1/8	606.72	29293
	568.24	25695	1/4	607.11	29331
181. 1/8	568.63	25730	3/8	607.51	29369
1/4	569.02	25765	1/2	607.90	29407
3/8	569.42	25801	5/8	608.29	29445
1/2	569.81	25836	3/4	608.58	29483
5/8	570.20	25872	7/8	609.08	29521
3/4	570.59	25908			
7/8	570.99	25944	200. 1/8	609.47	29559
	571.38	25980	1/4	609.86	29597
182. 1/8	571.77	26016	3/8	610.26	29636
1/4	572.16	26051	1/2	610.65	29674
3/8	572.56	26087	5/8	611.05	29713
1/2	572.95	26122	3/4	611.43	29751
5/8	573.34	26158	7/8	611.83	29789
3/4	573.74	26194			
7/8	574.13	26230	201. 1/8	612.29	29827
	574.52	26266	1/4	612.61	29865
183. 1/8	574.91	26302	3/8	613.00	29903
1/4	575.31	26338	1/2	613.40	29942
3/8	575.70	26374	5/8	613.79	29980
1/2	576.09	26410	3/4	614.18	30019
5/8	576.48	26446	7/8	614.57	30057
3/4	576.88	26482			
7/8	577.27	26518	202. 1/8	614.97	30096
	577.66	26554	1/4	615.36	30134
184. 1/8	578.05	26590	3/8	615.75	30172
1/4	578.45	26626	1/2	616.15	30210
3/8	578.84	26663	5/8	616.54	30249
1/2	579.23	26699	3/4	616.93	30287
5/8	579.63	26736	7/8	617.32	30326
3/4	580.02	26772			
7/8	580.41	26808	203. 1/8	617.72	30364
	580.80	26844	1/4	618.11	30403
185. 1/8	581.20	26880	3/8	618.50	30442
1/4	581.59	26916	1/2	618.89	30481
3/8	581.98	26953	5/8	619.29	30519
1/2	582.37	26989	3/4	619.68	30558
5/8	582.77	27026	7/8	620.08	30596
3/4	583.16	27062			
7/8	583.55	27099	204. 1/8	620.47	30635
	583.95	27135	1/4	620.86	30674
186. 1/8	584.34	27172	3/8	621.25	30713
1/4	584.73	27208	1/2	621.64	30752
3/8			5/8	622.04	30791
1/2			3/4	622.44	30830
5/8			7/8	622.83	30869
3/4				623.22	30908
7/8				623.62	30947
				624.01	30986

*Approximate area, sufficiently accurate for practical purposes, including estimating.

A-18.
(Concluded). Circumferences and Areas of Circles
(Advancing by eighths)

Dia.	Circum.	Area*	Dia.	Circum.	Area*
198 3/4	624.40	31025	204 7/8	643.63	32966
1/8	624.79	31064			
199. 1/8	625.18	31103	205. 1/8	644.03	33006
1/4	625.58	31142	3/8	644.82	33046
3/8	625.97	31181	1/2	645.21	33087
1/2	626.36	31220	5/8	645.61	33127
5/8	626.76	31260	3/4	646.01	33168
3/4	627.15	31299	7/8	646.39	33208
7/8	627.54	31338			
	627.94	31377	212. 1/8	646.78	33249
200. 1/8	628.32	31416	1/4	647.17	33289
1/4	628.72	31455	3/8	647.57	33329
3/8	629.11	31495	1/2	647.96	33369
1/2	629.51	31534	5/8	648.35	33410
5/8	629.90	31574	3/4	648.75	33450
3/4	630.29	31613	7/8	649.14	33491
7/8	630.58	31653			
	631.08	31692	213. 1/8	649.53	33572
201. 1/8	631.46	31731	1/4	650.31	33613
1/4	631.86	31770	3/8	650.71	33654
3/8	632.26	31810	1/2	651.10	33694
1/2	632.65	31849	5/8	651.50	33735
5/8	633.05	31889	3/4	651.90	33775
3/4	633.43	31928	7/8	652.28	33816
7/8	633.83	31968			
	634.29	32007	214. 1/8	652.57	33898
202. 1/8	634.60	32047	1/4	653.45	33939
1/4	635.00	32086	3/8	653.85	33980
3/8	635.40	32126	1/2	654.25	34020
1/2	635.79	32166	5/8	654.64	34061
5/8	636.18	32206	3/4	655.04	34102
3/4	636.57	32246	7/8	655.42	34143
7/8	636.97	32286			
	637.36	32326	215. 1/8	655.82	34184
203. 1/8	637.74	32366	1/4	656.28	34225
1/4	638.15	32405	3/8	656.59	34266
3/8	638.54	32445	1/2	656.99	34307
1/2	638.93	32485	5/8	657.39	34348
5/8	639.32	32525	3/4	657.78	34389
3/4	639.72	32565	7/8	658.17	34430
7/8	640.11	32605			
	640.50	32645	216. 1/8	658.56	34472
204. 1/8	640.88	32685	1/4	658.96	34513
1/4	641.28	32725	3/8	659.35	34554
3/8	641.67	32766	1/2	659.73	34595
1/2	642.07	32806	5/8	659.73	34636
5/8	642.46	32846	3/4	660.14	34677
3/4	642.85	32886	7/8	660.53	34719
7/8	643.24	32926			
			217. 1/8	660.92	34760
			1/4	661.31	34802
			3/8	661.71	34843
			1/2	662.10	34885
			5/8	662.49	34926
			3/4		
			7/8		

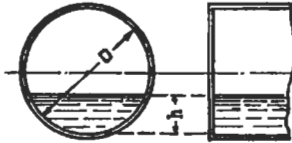
*Approximate area, sufficiently accurate for practical purposes, including estimating.

A-19. (Concluded). Capacities of Cylinders and Spheres

Diam. in Feet	Cu. Ft. per Foot of Cylinder	Gallons per Foot of Cylinder	42 Gallon Barrels per Foot of Cylinder	Sphere Surface in Sq. Ft.	Sphere Volume in Cu. Ft.	Diam. in Feet	Cu. Ft. per Foot of Cylinder	Gallons per Foot of Cylinder	42 Gallon Barrels per Foot of Cylinder	Sphere Surface in Sq. Ft.	Sphere Volume in Cu. Ft.
126	12469	93274	2220.8	49876	1047394	138	14957	111887	2664.0	59828	1376055
126 1/4	12519	93645	2229.6	50074	1053641	138 1/4	15011	112293	2673.6	60045	1383547
126 1/2	12568	94016	2238.5	50273	1059913	138 1/2	15066	112699	2683.3	60263	1391067
126 3/4	12618	94388	2247.3	50471	1066209	138 3/4	15120	113107	2693.0	60481	1398613
127	12668	94761	2256.2	50671	1072531	139	15175	113514	2702.7	60699	1406187
127 1/4	12718	95134	2265.1	50870	1078877	139 1/4	15229	113923	2712.5	60917	1413788
127 1/2	12768	95508	2274.0	51071	1085248	139 1/2	15284	114333	2722.2	61136	1421416
127 3/4	12818	95883	2282.9	51271	1091645	139 3/4	15339	114743	2732.0	61356	1429072
128	12868	96259	2291.9	51472	1098066	140	15394	115154	2741.8	61575	1436755
128 1/4	12918	96635	2300.8	51673	1104513	140 1/4	15449	115565	2751.6	61795	1444466
128 1/2	12969	97013	2309.8	51875	1110985	140 1/2	15504	115978	2761.4	62016	1452204
128 3/4	13019	97390	2318.8	52077	1117481	140 3/4	15559	116391	2771.2	62237	1459970
129	13070	97769	2327.8	52279	1124004	141	15615	116805	2781.1	62458	1467763
129 1/4	13121	98148	2336.9	52482	1130551	141 1/4	15670	117219	2790.9	62680	1475584
129 1/2	13171	98528	2345.9	52685	1137124	141 1/2	15725	117634	2800.8	62902	1483433
129 3/4	13222	98909	2355.0	52889	1143723	141 3/4	15781	118050	2810.7	63124	1491310
130	13273	99291	2364.1	53093	1150347	142	15837	118467	2820.6	63347	1499214
130 1/4	13324	99673	2373.2	53297	1156996	142 1/4	15893	118885	2830.6	63570	1507146
130 1/2	13376	100056	2382.3	53502	1163671	142 1/2	15948	119303	2840.5	63794	1515107
130 3/4	13427	100440	2391.4	53707	1170371	142 3/4	16005	119722	2850.5	64018	1523095
131	13478	100824	2400.6	53913	1177098	143	16061	120142	2860.5	64242	1531111
131 1/4	13530	101209	2409.7	54119	1183850	143 1/4	16117	120562	2870.5	64467	1539156
131 1/2	13581	101595	2418.9	54325	1190627	143 1/2	16173	120983	2880.6	64692	1547228
131 3/4	13633	101982	2428.1	54532	1197431	143 3/4	16230	121405	2890.6	64918	1555329
132	13685	102369	2437.4	54739	1204260	144	16286	121828	2900.7	65144	1563458
132 1/4	13737	102757	2446.6	54947	1211116	144 1/4	16343	122251	2910.7	65370	1571615
132 1/2	13789	103146	2455.9	55155	1217997	144 1/2	16399	122675	2920.8	65597	1579800
132 3/4	13841	103536	2465.1	55363	1224904	144 3/4	16456	123100	2931.0	65824	1588014
133	13893	103926	2474.4	55572	1231838	145	16513	123526	2941.1	66052	1596256
133 1/4	13945	104317	2483.7	55781	1238797	145 1/4	16570	123952	2951.2	66280	1604527
133 1/2	13998	104709	2493.1	55990	1245783	145 1/2	16627	124379	2961.4	66508	1612826
133 3/4	14050	105102	2502.4	56200	1252795	145 3/4	16684	124807	2971.6	66737	1621154
134	14103	105495	2511.8	56410	1259833	146	16742	125235	2981.8	66966	1629511
134 1/4	14155	105889	2521.2	56621	1266898	146 1/4	16799	125665	2992.0	67196	1637896
134 1/2	14208	106284	2530.6	56832	1273988	146 1/2	16856	126095	3002.3	67426	1646310
134 3/4	14261	106679	2540.0	57044	1281106	146 3/4	16914	126525	3012.5	67656	1654752
135	14314	107075	2549.4	57256	1288249	147	16972	126957	3022.8	67887	1663224
135 1/4	14367	107472	2558.9	57468	1295420	147 1/4	17029	127389	3033.1	68118	1671724
135 1/2	14420	107870	2568.3	57680	1302616	147 1/2	17087	127822	3043.4	68349	1680253
135 3/4	14473	108268	2577.8	57893	1309840	147 3/4	17145	128256	3053.7	68581	1688811
136	14527	108667	2587.3	58107	1317090	148	17203	128690	3064.0	68813	1697398
136 1/4	14580	109067	2596.8	58321	1324366	148 1/4	17262	129125	3074.4	69046	1706015
136 1/2	14634	109468	2606.4	58535	1331670	148 1/2	17320	129561	3084.8	69279	1714660
136 3/4	14687	109869	2615.9	58750	1339000	148 3/4	17378	129998	3095.2	69513	1723334
137	14741	110271	2625.5	58965	1346357	149	17437	130435	3105.6	69746	1732038
137 1/4	14795	110674	2635.1	59180	1353741	149 1/4	17495	130873	3116.0	69981	1740771
137 1/2	14849	111078	2644.7	59396	1361152	149 1/2	17554	131312	3126.5	70215	1749533
137 3/4	14903	111482	2654.3	59612	1368590	149 3/4	17613	131751	3136.9	70450	1758325
						150	17671	132192	3147.4	70686	1767146

A-20. Tank Capacities, Horizontal Cylindrical— Contents of Tanks with Flat Ends When Filled to Various Depths

Diameter of tank inches	Full tank	Depth of liquid, in inches = h																			
		3"	6"	9"	12"	15"	18"	21"	24"	27"	30"	33"	36"	39"	42"	45"	48"	51"	54"	57"	60"
12"	5.88	1.15	2.94
18"	13.22	1.45	3.86	6.61
24"	23.50	1.70	4.60	8.05	11.75
30"	36.72	1.91	5.23	9.27	13.72	18.36
36"	52.88	2.12	5.79	10.34	15.43	20.85	26.44
42"	71.97	2.28	6.31	11.31	16.07	23.07	29.47	35.99
48"	94.01	2.45	6.78	12.20	18.38	25.10	32.20	39.54	47.00
54"	118.98	2.60	7.22	13.04	19.68	26.97	34.72	42.80	51.08	59.49
60"	146.89	2.75	7.64	13.82	20.91	28.72	37.06	45.82	54.87	64.11	73.44
66"	177.73	2.89	8.04	14.56	22.07	30.37	39.28	48.65	58.39	68.41	78.59	88.86
72"	211.52	3.02	8.42	15.26	23.17	31.92	41.36	51.32	61.71	72.45	83.41	94.54	105.76
78"	248.24	3.15	8.78	15.94	24.21	33.41	43.34	53.86	64.87	76.27	87.97	99.90	111.97	124.13
84"	287.90	3.26	9.12	16.57	25.24	34.85	45.24	56.29	67.87	79.91	92.30	104.98	117.85	130.87	143.05
90"	330.49	3.43	9.46	17.20	26.20	36.21	47.05	58.61	70.75	83.39	96.43	109.81	123.45	137.28	151.23	165.25
96"	376.02	3.50	9.79	17.80	27.13	37.52	48.81	60.84	73.52	86.73	100.39	114.44	128.79	143.40	158.17	173.06	188.01
102"	424.50	3.61	10.10	18.37	28.01	39.00	50.49	62.99	76.18	89.94	104.20	118.89	133.92	149.25	164.81	180.53	196.37	212.25
108"	476.10	3.71	10.39	18.94	28.90	40.03	52.14	65.09	78.74	93.04	107.87	123.17	138.87	154.80	171.19	187.71	204.37	221.14	238.05
114"	530.25	3.78	10.74	19.49	29.75	41.22	53.73	67.10	81.24	96.05	111.43	127.31	143.63	160.33	177.33	194.60	212.05	229.65	247.37	265.13
120"	587.54	3.81	10.98	20.02	30.57	42.39	55.26	69.06	83.65	98.95	114.87	131.32	148.25	165.58	183.27	201.24	219.46	237.87	256.43	275.08	293.77

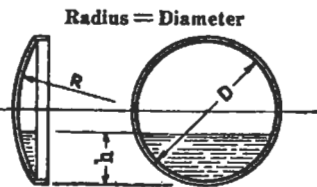


To ascertain the contents of a tank over one-half full: Let h = depth of unfilled portion. Find from the table the quantity corresponding to a depth h . Subtract this quantity from the contents of a full tank.

Contents in U.S. gallons per 1 foot of length.
By permission, The Permutit Co., Inc., Data Book, 1953.

A-21. Tank Capacities, Horizontal Cylindrical— Contents of Standard Dished Heads When Filled to Various Depths

Diameter of head inches	Full head	Depth of liquid, in inches = h																			
		3"	6"	9"	12"	15"	18"	21"	24"	27"	30"	33"	36"	39"	42"	45"	48"	51"	54"	57"	60"
12"	0.40	0.05	0.20
18"	1.36	0.07	0.32	0.68
24"	3.22	0.08	0.41	0.95	1.61
30"	6.30	0.10	0.49	1.18	2.10	3.15
36"	10.88	0.11	0.56	1.39	2.54	3.92	5.44
42"	17.28	0.12	0.63	1.59	2.94	4.64	6.57	8.64
48"	25.79	0.13	0.68	1.75	3.31	5.29	7.62	10.19	12.89
54"	36.72	0.14	0.74	1.90	3.84	5.91	8.60	11.65	14.95	18.36
60"	50.37	0.14	0.82	2.07	3.98	6.49	9.54	13.03	16.87	20.96	25.18
66"	67.04	0.15	0.83	2.19	4.25	6.98	10.35	14.30	18.68	23.43	28.42	33.52
72"	87.04	0.16	0.88	2.32	4.52	7.47	11.15	15.48	20.38	25.74	31.46	37.43	43.52
78"	110.66	0.17	0.93	2.44	4.79	7.97	11.94	16.65	22.02	27.97	34.39	41.16	48.20	55.33
84"	138.22	0.18	0.98	2.59	5.07	8.44	12.60	17.78	23.60	30.11	37.19	44.75	52.67	60.83	69.11
90"	170.01	0.18	1.00	2.68	5.33	8.91	13.44	18.86	25.12	32.18	39.90	48.22	56.99	66.14	75.52	85.00
96"	206.32	0.20	1.07	2.83	5.59	9.36	14.14	19.90	26.60	34.17	42.52	51.53	61.13	71.22	81.66	92.34	103.16
102"	247.48	0.22	1.14	3.01	5.89	9.87	14.92	21.01	28.11	36.18	45.19	54.91	65.31	76.29	87.73	99.56	111.59	123.74
108"	293.77	0.20	1.13	3.03	6.04	10.21	15.50	21.93	29.47	38.03	47.56	57.97	69.14	81.05	93.53	106.47	119.76	133.26	146.88
114"	345.51	0.21	1.16	3.12	6.25	10.55	16.06	22.80	30.70	39.73	49.81	60.88	72.85	85.61	99.05	113.07	127.56	142.41	157.51	172.75
120"	402.27	0.21	1.19	3.23	6.47	10.93	16.68	23.70	31.96	41.43	52.04	63.73	76.40	89.95	104.32	119.39	135.04	151.15	167.62	184.32	201.13



To ascertain the contents of a head over one-half full: Let h = depth of unfilled portion. Find from the table the quantity corresponding to a depth h . Subtract this quantity from the contents of a full head.

Contents in U.S. gallons for one head only. This table is only approximate, but close enough for practical use.
By permission, The Permutit Co., Inc., Data Book, 1953.

Miscellaneous Formulas
(Courtesy of Chicago Bridge and Iron Co.)

1. Area of Roofs.

Umbrella Roofs:

D = diameter of tank in feet.

Surface area in } { = 0.842 D² (when radius = diameter)
square feet } { = 0.882 D² (when radius = 0.8 diameter)

Conical Roofs:

Surface area in } { = 0.787 D² (when pitch is ¾ in 12)
square feet } { = 0.792 D² (when pitch is 1½ in 12)

2. Average weights.

Steel -490 pounds per cubic foot—specific gravity 7.85

Wrought iron -485 pounds per cubic foot—specific gravity 7.77

Cast iron -450 pounds per cubic foot—specific gravity 7.21

1 cubic foot air or gas at 32° F., 760 m.m. barometer = molecular weight x 0.0027855 pounds.

3. Expansion in steel pipe = 0.78 inch per 100 lineal feet per 100 degrees Fahr. change in temperature = 0.412 inch per mile per degree Fahr. temperature change.

4. Linear coefficients of expansion per degree increase in temperature:

	Per Degree Fahrenheit	Per Degree Centigrade
STRUCTURAL STEEL—A-7		
70° to 200° F.....	0.0000067	—
21.1° to 93° C.....	—	0.0000121
STAINLESS STEEL—TYPE 304		
32° to 932° F.....	0.0000102	—
0° to 500° C.....	—	0.0000184
ALUMINUM		
-76° to 68° F.....	0.0000120	—
-60° to 20° C.....	—	0.0000216

5. To determine the net thickness of shells for horizontal cylindrical pressure tanks:

$$T = \frac{6 PD}{S}$$

P = working pressure in pounds per square inch

D = diameter of cylinder in feet

S = allowable unit working stress in pounds per square inch

T = Net thickness in inches

Resulting net thickness must be corrected to gross or actual thickness by dividing by joint efficiency.

6. To determine the net thickness of heads for cylindrical pressure tanks:

(6a) Ellipsoidal or Bumped Heads:

$$T = \frac{6 PD}{S}$$

T, P and D as in formula 5

(6b) Dished or Basket Heads:

$$T = \frac{10.6P(MR)}{S}$$

T, S and P as in formula 5

MR = principal radius of head in feet

Resulting net thickness of heads is both net and gross thickness if one piece seamless heads are used, otherwise net thickness must be corrected to gross thickness as above.

Formulas 5 and 6 must often be modified to comply with various engineering codes, and state and municipal regulations. Calculated gross plate thicknesses are sometimes arbitrarily increased to provide an additional allowance for corrosion.

7. Heads for Horizontal Cylindrical Tanks:

Hemi-ellipsoidal Heads have an ellipsoidal cross section, usually with minor axis equal to one half the major axis—that is, depth = ¼ D, or more.*Dished or Basket Heads* consist of a spherical segment normally dished to a radius equal to the inside diameter of the tank cylinder (or within a range of 6 inches plus or minus) and connected to the straight cylindrical flange by a "knuckle" whose inside radius is usually not less than 6 per cent of the inside diameter of the cylinder nor less than 3 times the thickness of the head plate. Basket heads closely approximate hemi-ellipsoidal heads.*Bumped Heads* consist of a spherical segment joining the tank cylinder directly without the transition "knuckle." The radius = D, or less. This type of head is used only for pressures of 10 pounds per square inch or less, excepting where a compression ring is placed at the junction of head and shell.

Surface Area of Heads:

(7a) Hemi-ellipsoidal Heads:

$$S = \pi R^2 [1 + K^2(2-K)]$$

S = surface area in square feet

R = radius of cylinder in feet

K = ratio of the depth of the head (not including the straight flange) to the radius of the cylinder

The above formula is not exact but is within limits of practical accuracy.

(7b) Dished or Basket Heads:

Formula (7a) gives surface area within practical limits.

(7c) Bumped Heads:

$$S = \pi R^2 (1 + K^2)$$

S, R, and K as in formula (7a)

Volume of Heads:

(7d) Hemi-ellipsoidal Heads:

$$V = \frac{2}{3} \pi K R^3$$

R = radius of cylinder in feet

K = ratio of the depth of the head (not including the straight flange) to the radius of the cylinder

(7e) Dished or Basket Heads:

Formula (7d) gives volume within practical limits.

(7f) Bumped Heads:

$$V = \frac{1}{2} \pi K R^3 (1 + \frac{1}{3} K^2)$$

V, K and R as in formula (7d)

Note: K in above formulas may be determined as follows:

Hemi-ellipsoidal heads—K is known

$$\text{Dished Heads—} K = M - \sqrt{(M-1)(M+1-2m)}$$

$$\text{Bumped Heads—} K = [M - \sqrt{M^2-1}]$$

MR = principal radius of head in feet

mR = radius of knuckle in feet

R = radius of cylinder in feet

$$M = \frac{MR}{R} \quad m = \frac{mR}{R}$$

For bumped heads m = 0

8. Total volume or length of shell in cylindrical tank with ellipsoidal or hemispherical heads:

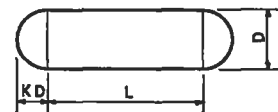
V = Total volume

L = Length of cylindrical shell

KD = Depth of head

$$V = \frac{\pi D^3}{4} (L + 1\frac{1}{2} KD)$$

$$L = (V \div \frac{\pi D^3}{4}) - 1\frac{1}{2} KD$$



A-22.

(Continued). Miscellaneous Formulas

9. Volume or contents of partially filled horizontal cylindrical tanks:

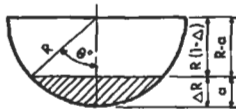
(9a) Tank cylinder or shell (straight portion only)

$$Q = R^2 L \left[\left(\frac{\pi \Theta}{180} \right) - \sin \Theta \cos \Theta \right]$$

Q = partially filled volume or contents in cubic feet

R = radius of cylinder in feet

L = length of straight portion of cylinder in feet



The straight portion or flange of the heads must be considered a part of the cylinder. The length of flange depends upon the diameter of tank and thickness of head but ranges usually between 2 and 4 inches.

a = Δ R = depth of liquid in feet

$$\Delta = \frac{a}{R} = \text{a ratio}$$

$$\cos \Theta = 1 - \Delta, \text{ or } \frac{R-a}{R}$$

Θ = degrees

(9b) Hemi-ellipsoidal Heads:

$$Q = \frac{3}{4} V \Delta^3 (1 - \frac{1}{3} \Delta)$$

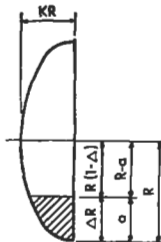
Q = partially filled volume or contents in cubic feet

V = total volume of one head per formula (7d)

$$\Delta = \frac{a}{R} = \text{a ratio}$$

a = Δ R = depth of liquid in feet

R = radius of cylinder in feet



(9c) Dished or Basket Heads:

Formula (9b) gives partially filled volume within practical limits, and formula (7d) gives V within practical limits.

(9d) Bumped Heads:

Formula (9b) gives partially filled volume within practical limits, and formula (7f) gives V.

Note: To obtain the volume or quantity of liquid in partially filled tanks, add the volume per formula (9a) for the cylinder or straight portion to twice (for 2 heads) the volume per formula (9b), (9c) or (9d) for the type of head concerned.

10. Volume or contents of partially filled hemi-ellipsoidal heads with major axis vertical:

Q = Partially filled volume or contents in cubic feet

V = Total volume of one head per formula (7d)

R = Radius of cylinder in feet

(10a) Upper Head:

$$Q = 1\frac{1}{2} V \Delta (1 - \frac{1}{3} \Delta^2)$$

$$\Delta = \frac{a}{KR} = \text{a ratio}$$

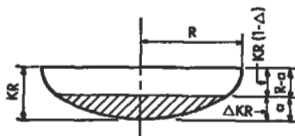
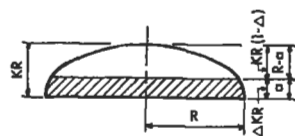
a = Δ KR = depth of liquid in feet

(10b) Lower Head:

$$Q = 1\frac{1}{2} V \Delta^3 (1 - \frac{1}{3} \Delta)$$

$$\Delta = \frac{a}{KR} = \text{a ratio}$$

a = Δ KR = depth of liquid in feet



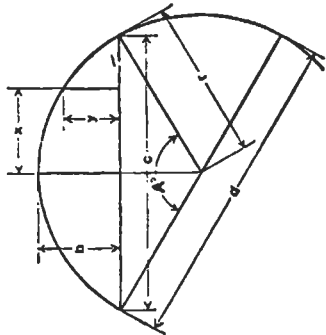
A-23.
Decimal Equivalents in Inches, Feet and Millimeters

In. Equiv. for Decimal of In.	Decimals	Millimeter Equiv. for Decimal of In.	In. Equiv. for Decimal of Ft.
1/64	.0156	0.397	3/16
1/32	.0313	0.794	3/8
3/64	.0469	1.191	9/16
1/16	.0625	1.588	3/4
5/64	.0781	1.984	15/16
3/32	.0938	2.381	1 1/8
1/4	.1094	2.778	1 1/4
1/8	.1250	3.175	1 1/2
9/64	.1406	3.572	1 5/8
5/32	.1563	3.969	1 3/4
11/64	.1719	4.366	2 1/8
3/16	.1875	4.763	2 1/4
13/64	.2031	5.159	2 3/8
7/32	.2188	5.556	2 1/2
15/64	.2344	5.953	2 5/8
1/4	.2500	6.350	3
17/64	.2656	6.747	3 1/8
9/32	.2813	7.144	3 1/4
19/64	.2969	7.541	3 3/8
5/16	.3125	7.938	3 1/2
21/64	.3281	8.334	3 5/8
11/32	.3438	8.731	4 1/8
23/64	.3594	9.128	4 1/4
3/8	.3750	9.525	4 3/8
25/64	.3906	9.922	4 1/2
13/32	.4063	10.319	4 3/4
27/64	.4219	10.716	5 1/8
7/16	.4375	11.113	5 1/4
29/64	.4531	11.509	5 3/8
15/32	.4688	11.906	5 1/2
31/64	.4844	12.303	5 3/4
1/2	.5000	12.700	6
33/64	.5156	13.097	6 1/8
17/32	.5313	13.494	6 1/4
35/64	.5469	13.891	6 3/8
9/16	.5625	14.288	6 1/2
37/64	.5781	14.684	6 3/4
19/32	.5938	15.081	6 5/8
39/64	.6094	15.478	7 1/8
5/8	.6250	15.875	7 1/4
41/64	.6406	16.272	7 1/2
21/32	.6563	16.669	7 3/8
43/64	.6719	17.066	7 1/2
11/16	.6875	17.463	7 3/4
45/64	.7031	17.859	7 5/8
23/32	.7188	18.256	8 1/8
47/64	.7344	18.653	8 1/4
3/4	.7500	19.050	9
49/64	.7656	19.447	9 1/8
25/32	.7813	19.844	9 1/4
51/64	.7969	20.241	9 3/8
13/16	.8125	20.638	9 1/2
53/64	.8281	21.034	9 3/4
27/32	.8438	21.431	9 5/8
55/64	.8594	21.828	10 1/8
7/8	.8750	22.225	10 1/4
57/64	.8906	22.622	10 1/2
29/32	.9063	23.019	10 3/4
59/64	.9219	23.416	10 5/8
15/16	.9375	23.813	10 3/4
61/64	.9531	24.209	11 1/8
31/32	.9688	24.606	11 1/4
63/64	.9844	25.003	11 3/8
1	1.0000	25.400	12

(By permission of Buffalo Tank Div., Bethlehem Steel Corp.)

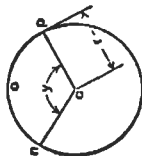
PROPERTIES OF THE CIRCLE

- Circumference = $0.28318 r = 3.14159 d$
- Diameter = 0.31831 circumference
- Area = $3.14159 r^2$
- Arc $a = \frac{\pi r A^\circ}{180^\circ} = 0.017453 r A^\circ$
- Angle $A^\circ = \frac{180^\circ a}{\pi r} = 57.29578 \frac{a}{r}$
- Radius $r = \frac{4 b^2 + c^2}{8 b}$
- Chord $c = 2 \sqrt{2 br - b^2} = 2 r \sin \frac{A}{2}$
- Rise $b = r - \frac{1}{2} \sqrt{4 r^2 - c^2} = \frac{c}{2} \tan \frac{A}{4}$
 $= 2 r \sin^2 \frac{A}{4} = r + y - \sqrt{r^2 - x^2}$
 $y = b - r + \sqrt{r^2 - x^2}$
 $x = \sqrt{r^2 - (r + y - b)^2}$



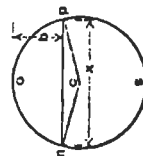
Diameter of circle of equal periphery as square = 1.27324 side of square
 Side of square of equal periphery as circle = 0.78540 diameter of circle
 Diameter of circle circumscribed about square = 1.41421 side of square
 Side of square inscribed in circle = 0.70711 diameter of circle

CIRCULAR SECTOR



- r = radius of circle
- y = angle ncp in degrees
- Area of Sector ncpo = $\frac{1}{2}$ (length of arc ncp $\times r$)
 $=$ Area of Circle $\times \frac{y}{360}$
 $= 0.0087266 \times r^2 \times y$

CIRCULAR SEGMENT



- r = radius of circle
- x = chord
- b = rise
- Area of Segment ncp = Area of Sector ncpo - Area of triangle ncp
 $= \frac{1}{2}$ (Length of arc ncp $\times r$) - $x(r - b)$
- Area of Segment nsp = Area of Circle - Area of Segment ncp

VALUES FOR FUNCTIONS OF π

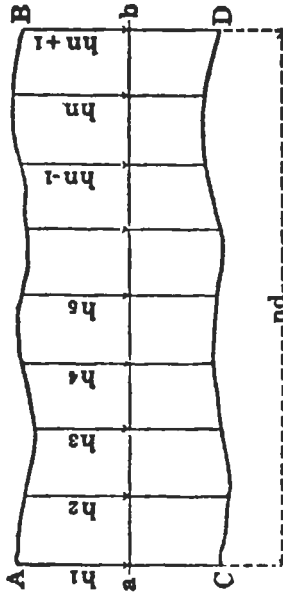
- $\pi = 3.14159265359$, $\log = 0.4971499$
- $\pi^2 = 9.8696044$, $\log = 0.9942998$
- $\frac{1}{\pi} = 0.3183099$, $\log = \bar{1}.5028501$
- $\sqrt{\frac{1}{\pi}} = 0.5641896$, $\log = \bar{1}.7514281$
- $\pi^3 = 31.0062767$, $\log = 1.4914497$
- $\frac{1}{\pi^3} = 0.1013212$, $\log = \bar{1}.0057002$
- $\frac{\pi}{180} = 0.0174533$, $\log = \bar{2}.2418774$
- $\sqrt{\pi} = 1.7724539$, $\log = 0.2465749$
- $\frac{1}{\sqrt{\pi}} = 0.0322515$, $\log = \bar{2}.5085503$
- $\frac{180}{\pi} = 57.2957795$, $\log = 1.7581228$

A-24. (Continued).

AREA OF PLANE FIGURES

- Triangle:** Base $\times \frac{1}{2}$ perpendicular height.
 $\sqrt{s(s-a)(s-b)(s-c)}$
 $s = \frac{1}{2}$ sum of the three sides a, b and c .
- Trapezium:** Sum of area of the two triangles.
- Trapezoid:** $\frac{1}{2}$ sum of parallel sides \times perpendicular height.
- Parallelogram:** Base \times perpendicular height.
- Regular Polygon:** $\frac{1}{2}$ sum of sides \times inside radius.
 $\pi r^2 = 0.78540 \times \text{dia.}^2 = 0.07958 \times \text{circumference}^2$
 $\pi r^2 A^\circ = 0.0087266 r^2 A^\circ = \text{arc} \times \frac{1}{2}$ radius.
- Sector of Circle:** $\frac{r^2}{2} \left(\frac{\pi A^\circ}{180} - \sin A^\circ \right)$
 $\times 1.12838$
- Circle of same area as square:** diameter = side
- Square of same area as circle:** side = diameter $\times 0.88623$
- Ellipse:** Long diameter \times short diameter $\times 0.78540$
- Parabola:** Base $\times \frac{3}{8}$ perpendicular height.

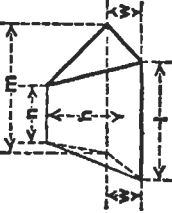
Irregular plane surface



Divide any plane surface A, B, C, D, along a line a-b into an even number, n , of parallel and sufficiently small strips, d , whose ordinates are $h_1, h_2, h_3, \dots, h_n$, then for section ABCD, considering contours between three ordinates as parabolic curves, then for section ABCD,

$$\text{Area} = \frac{d}{3} \left[h_1 + h_n + 4(h_2 + h_4 + \dots + h_n) + 2(h_3 + h_5 + \dots + h_{n-1}) \right]$$
 or, approximately, Area = Sum of ordinates \times width, d .

VOLUME OF A WEDGE



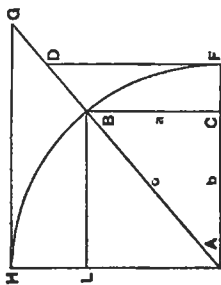
This formula is useful in obtaining the contents of special, wedge-shaped, tank bottoms.

$$\text{Volume} = \frac{wh}{6} (l + m + n)$$

TRIGONOMETRIC FORMULAS

Radius AF = 1

$\sin^2 A + \cos^2 A = \sin A \operatorname{cosec} A$
 $\cos A \sec A = \tan A \cot A$
 $\frac{\cos A}{\cot A} = \frac{1}{\operatorname{cosec} A} = \cos A \tan A = \sqrt{1 - \cos^2 A} = BC$
 $\frac{\sin A}{\tan A} = \frac{1}{\sec A} = \sin A \cot A = \sqrt{1 - \sin^2 A} = AC$
 $\frac{\sin A}{\cos A} = \frac{1}{\cot A} = \sin A \sec A = FD$
 $\frac{\cos A}{\sin A} = \frac{1}{\tan A} = \cos A \operatorname{cosec} A = HG$
 $\frac{\tan A}{\sin A} = \frac{1}{\cos A} = \tan A \sec A = AD$
 $\frac{\cot A}{\cos A} = \frac{1}{\sin A} = \cot A \operatorname{cosec} A = AG$



RIGHT ANGLED TRIANGLES

$a^2 = c^2 - b^2$
 $b^2 = c^2 - a^2$
 $c^2 = a^2 + b^2$



Known	Required		
a, b	$\tan A = \frac{a}{b}$ $\tan B = \frac{b}{a}$	$\frac{a}{\sin A} = \frac{b}{\sin B}$	$\sqrt{a^2 + b^2}$
a, c	$\sin A = \frac{a}{c}$	$\frac{a \cot A}{\sin A}$	$\frac{a \sqrt{c^2 - a^2}}{2}$
A, a	$90^\circ - A$	$b \tan A$	$\frac{a^2 \cot A}{2}$
A, b	$90^\circ - A$	$c \sin A$	$\frac{b^2 \tan A}{2}$
A, c	$90^\circ - A$	$c \cos A$	$\frac{c^2 \sin 2A}{4}$

OBLIQUE ANGLED TRIANGLES



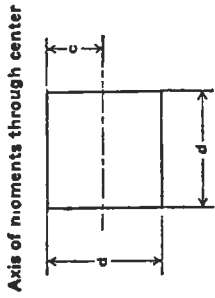
$a^2 = b^2 + c^2 - 2bc \cos A$
 $b^2 = a^2 + c^2 - 2ac \cos B$
 $c^2 = a^2 + b^2 - 2ab \cos C$

$s = \frac{a+b+c}{2}$

Known	Required		
a, b, c	$\cos \frac{1}{2} A = \sqrt{\frac{s(s-b)}{bc}}$	$\cos \frac{1}{2} C = \frac{a \sin B}{\sin A}$	$\frac{a \sin C}{\sin A}$
a, A, B	$\sin B = \frac{b \sin A}{a}$	$180^\circ - (A+B)$	$\frac{b \sin C}{\sin B}$
a, b, A	$\sin B = \frac{b \sin A}{a}$	$\sqrt{a^2 + b^2 - 2ab \cos C}$	$\frac{ab \sin C}{2}$
a, b, C	$\tan A = \frac{a \sin C}{b - a \cos C}$	$\sqrt{s(s-a)}$	$\sqrt{s(s-a)(s-b)(s-c)}$

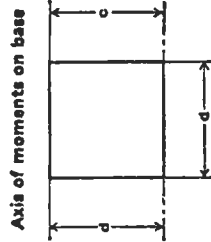
PROPERTIES OF SECTIONS

SQUARE



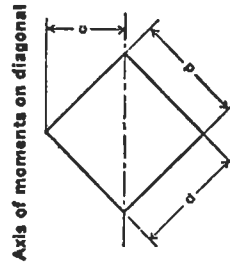
$A = d^2$
 $c = \frac{d}{2}$
 $I = \frac{d^4}{12}$
 $S = \frac{d^3}{6}$
 $r = \frac{d}{\sqrt{12}} = .288675 d$

SQUARE



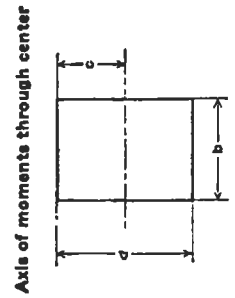
$A = d^2$
 $c = d$
 $I = \frac{d^4}{3}$
 $S = \frac{d^3}{3}$
 $r = \frac{d}{\sqrt{3}} = .577350 d$

SQUARE



$A = d^2$
 $c = \frac{d}{\sqrt{2}} = .707107 d$
 $I = \frac{d^4}{12}$
 $S = \frac{d^3}{6\sqrt{2}} = .117851 d^3$
 $r = \frac{d}{\sqrt{12}} = .288675 d$

RECTANGLE



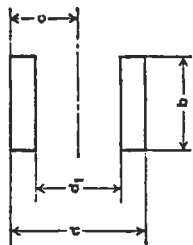
$A = bd$
 $c = \frac{d}{2}$
 $I = \frac{bd^3}{12}$
 $S = \frac{bd^2}{6}$
 $r = \frac{d}{\sqrt{12}} = .288675 d$

A-24.
(Continued).

PROPERTIES OF SECTIONS

EQUAL RECTANGLES

Axis of moments through center of gravity



$$A = b(d - d_1)$$

$$c = \frac{d}{2}$$

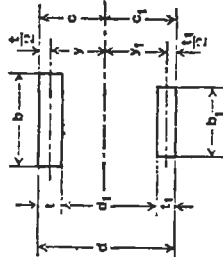
$$I = \frac{b(d^3 - d_1^3)}{12}$$

$$S = \frac{b(d^2 - d_1^2)}{6d}$$

$$r = \sqrt{\frac{d^3 - d_1^3}{12(d - d_1)}}$$

UNEQUAL RECTANGLES

Axis of moments through center of gravity



$$A = bt + b_1t_1$$

$$c = \frac{\frac{1}{2}bt^2 + b_1t_1(d - \frac{1}{2}t_1)}{A}$$

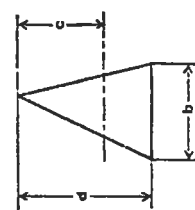
$$I = \frac{bt^3}{12} + bty^2 + \frac{b_1t_1^3}{12} + b_1t_1y_1^2$$

$$S = \frac{I}{c} \quad S_1 = \frac{I}{c_1}$$

$$r = \sqrt{\frac{I}{A}}$$

TRIANGLE

Axis of moments through center of gravity



$$A = \frac{bd}{2}$$

$$c = \frac{2d}{3}$$

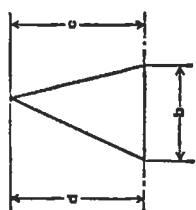
$$I = \frac{bd^3}{36}$$

$$S = \frac{bd^2}{24}$$

$$r = \frac{d}{\sqrt{18}} = .235702 d$$

TRIANGLE

Axis of moments on base



$$A = \frac{bd}{2}$$

$$c = d$$

$$I = \frac{bd^3}{12}$$

$$S = \frac{bd^2}{12}$$

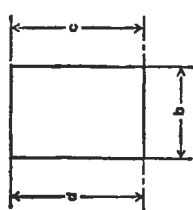
$$r = \frac{d}{\sqrt{6}} = .408248 d$$

A-24.
(Continued).

PROPERTIES OF SECTIONS

RECTANGLE

Axis of moments on base



$$A = bd$$

$$c = \frac{d}{2}$$

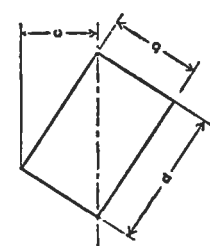
$$I = \frac{bd^3}{3}$$

$$S = \frac{bd^2}{3}$$

$$r = \frac{d}{\sqrt{3}} = .577350 d$$

RECTANGLE

Axis of moments on diagonal



$$A = bd$$

$$c = \frac{bd}{\sqrt{b^2 + d^2}}$$

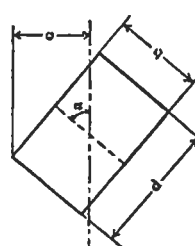
$$I = \frac{b^2d^3}{6(b^2 + d^2)}$$

$$S = \frac{b^2ds}{6\sqrt{b^2 + d^2}}$$

$$r = \frac{bd}{\sqrt{6(b^2 + d^2)}}$$

RECTANGLE

Axis of moments any line through center of gravity



$$A = bd$$

$$c = \frac{b \sin a + d \cos a}{2}$$

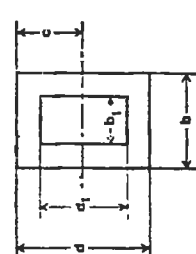
$$I = \frac{bd(b^2 \sin^2 a + d^2 \cos^2 a)}{12}$$

$$S = \frac{bd(b^2 \sin^2 a + d^2 \cos^2 a)}{6(b \sin a + d \cos a)}$$

$$r = \sqrt{\frac{b^2 \sin^2 a + d^2 \cos^2 a}{12}}$$

HOLLOW RECTANGLE

Axis of moments through center



$$A = bd - b_1d_1$$

$$c = \frac{d}{2}$$

$$I = \frac{bd^3 - b_1d_1^3}{12}$$

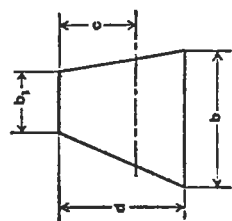
$$S = \frac{bd^2 - b_1d_1^2}{6d}$$

$$r = \sqrt{\frac{bd^3 - b_1d_1^3}{12A}}$$

A-24.
(Continued).

PROPERTIES OF SECTIONS

TRAPEZOID
Axis of moments through center of gravity



$$A = \frac{d(b + b_1)}{2}$$

$$c = \frac{d(2b + b_1)}{3(b + b_1)}$$

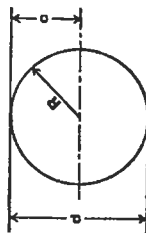
$$I = \frac{d^3 (b^2 + 4bb_1 + b_1^2)}{36(b + b_1)}$$

$$S = \frac{d^2 (b^2 + 4bb_1 + b_1^2)}{12(2b + b_1)}$$

$$r = \frac{d}{6(b + b_1)} \sqrt{2(b^2 + 4bb_1 + b_1^2)}$$

CIRCLE

Axis of moments through center



$$A = \frac{\pi d^2}{4} = \pi R^2 = .785398 d^2 = 3.141593 R^2$$

$$c = \frac{d}{2} = R$$

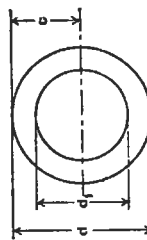
$$I = \frac{\pi d^4}{64} = \frac{\pi R^4}{4} = .049087 d^4 = .785398 R^4$$

$$S = \frac{\pi d^3}{32} = \frac{\pi R^3}{4} = .098175 d^3 = .785398 R^3$$

$$r = \frac{d}{4} = \frac{R}{2}$$

HOLLOW CIRCLE

Axis of moments through center



$$A = \frac{\pi(d^2 - d_1^2)}{4} = .785398 (d^2 - d_1^2)$$

$$c = \frac{d}{2}$$

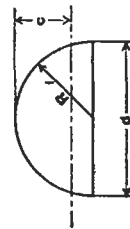
$$I = \frac{\pi(d^4 - d_1^4)}{64} = .049087 (d^4 - d_1^4)$$

$$S = \frac{\pi(d^3 - d_1^3)}{32d} = .098175 \frac{d^3 - d_1^3}{d}$$

$$r = \frac{\sqrt{d^2 + d_1^2}}{4}$$

HALF CIRCLE

Axis of moments through center of gravity



$$A = \frac{\pi R^2}{2} = 1.570796 R^2$$

$$c = R \left(1 - \frac{4}{3\pi}\right) = .575587 R$$

$$I = R^4 \left(\frac{\pi}{8} - \frac{8}{9\pi}\right) = .109757 R^4$$

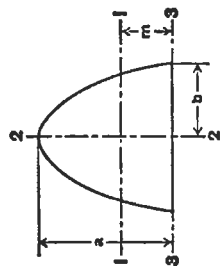
$$S = \frac{R^3 (9\pi^2 - 64)}{24(3\pi - 4)} = .190687 R^3$$

$$r = R \frac{\sqrt{9\pi^2 - 64}}{6\pi} = .264336 R$$

A-24.
(Continued).

PROPERTIES OF SECTIONS

PARABOLA



$$A = \frac{4}{3} ab$$

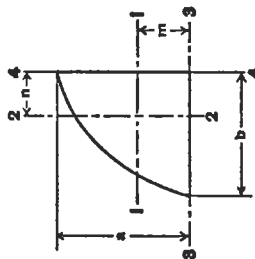
$$m = \frac{2}{5} a$$

$$I_1 = \frac{16}{175} a^3 b$$

$$I_2 = \frac{4}{15} ab^3$$

$$I_3 = \frac{32}{105} a^2 b$$

HALF PARABOLA



$$A = \frac{2}{3} ab$$

$$m = \frac{2}{5} a$$

$$n = \frac{3}{8} b$$

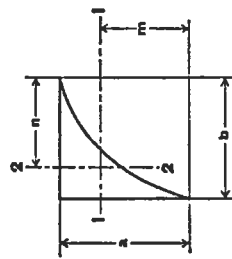
$$I_1 = \frac{8}{175} a^3 b$$

$$I_2 = \frac{19}{480} ab^3$$

$$I_3 = \frac{16}{105} a^2 b$$

$$I_4 = \frac{2}{15} ab^3$$

COMPLEMENT OF HALF PARABOLA



$$A = \frac{1}{3} ab$$

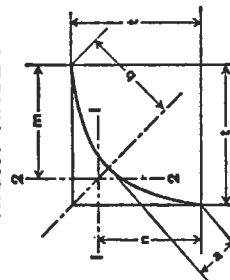
$$m = \frac{7}{10} a$$

$$n = \frac{3}{4} b$$

$$I_1 = \frac{37}{2100} a^3 b$$

$$I_2 = \frac{1}{30} ab^3$$

PARABOLIC FILLET IN RIGHT ANGLE



$$a = \frac{t}{2\sqrt{2}}$$

$$b = \frac{t}{\sqrt{2}}$$

$$A = \frac{1}{6} t^2$$

$$m = n = \frac{4}{5} t$$

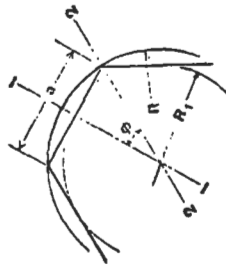
$$I_1 = I_2 = \frac{11}{2100} t^4$$

A-24.
(Concluded).

PROPERTIES OF SECTIONS

REGULAR POLYGON

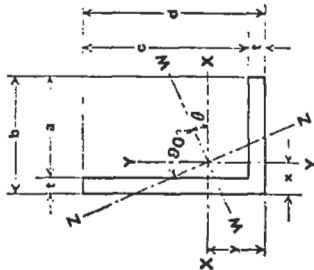
Axis of moments through center



n = Number of sides
 ϕ = $\frac{180^\circ}{n}$
 a = $2\sqrt{R^2 - R_1^2}$
 R = $\frac{a}{2 \sin \phi}$
 R_1 = $\frac{a}{2 \tan \phi}$
 A = $\frac{1}{4} n a^2 \cot \phi = \frac{1}{2} n R_1^2 \sin 2\phi = n R_1^2 \tan \phi$
 $I_1 = I_2$ = $\frac{A(6R^2 - a^2)}{24}$ = $\frac{A(12R_1^2 + a^2)}{48}$
 $r_1 = r_2$ = $\sqrt{\frac{6R^2 - a^2}{24}}$ = $\sqrt{\frac{12R_1^2 + a^2}{48}}$

ANGLE

Axis of moments through center of gravity

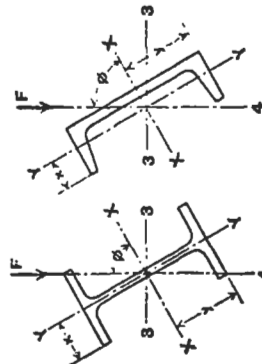


$\tan 2\phi$ = $\frac{2K}{I_y - I_x}$
 A = $t(b+c)$ $x = \frac{b^2 + ct}{2(b+c)}$ $y = \frac{dt + at}{2(b+c)}$
 K = Product of Inertia about X-X & Y-Y = $\frac{abcdt}{4(b+c)}$
 I_x = $\frac{1}{3} (t(d-y)^2 + by^2 - a(y-t)^2)$
 I_y = $\frac{1}{3} (t(b-x)^2 + dx^2 - c(x-t)^2)$
 I_z = $I_x \sin^2 \phi + I_y \cos^2 \phi + K \sin 2\phi$
 I_w = $I_x \cos^2 \phi + I_y \sin^2 \phi - K \sin 2\phi$

K is negative when heel of angle, with respect to c.g., is in 1st or 3rd quadrant, positive when in 2nd or 4th quadrant.

BEAMS AND CHANNELS

Transverse force oblique through center of gravity



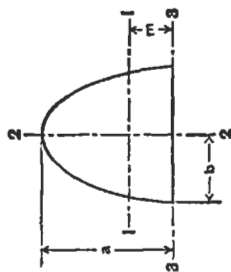
I_s = $I_x \sin^2 \phi + I_y \cos^2 \phi$
 I_e = $I_x \cos^2 \phi + I_y \sin^2 \phi$
 M = $\left(\frac{Y}{I_x} \sin \phi + \frac{X}{I_y} \cos \phi \right)$

where M is bending moment due to force F. Extreme fiber assumed same as for case $\phi=0$. If not, locate extreme fiber and find f by usual method.

A-24.
(Continued).

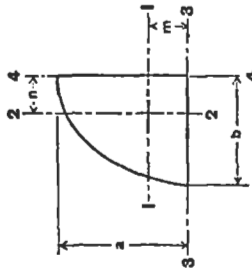
PROPERTIES OF SECTIONS

*** HALF ELLIPSE**



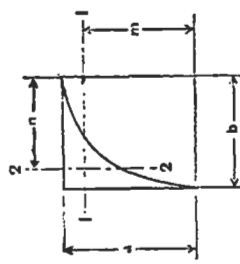
A = $\frac{1}{2} \pi ab$
 m = $\frac{4a}{3\pi}$
 I_1 = $a^3 b \left(\frac{\pi}{8} - \frac{8}{9\pi} \right)$
 I_2 = $\frac{1}{8} \pi ab^3$
 I_3 = $\frac{1}{8} \pi a^2 b$

*** QUARTER ELLIPSE**



A = $\frac{1}{4} \pi ab$
 m = $\frac{4a}{3\pi}$
 n = $\frac{4b}{3\pi}$
 I_1 = $a^3 b \left(\frac{\pi}{16} - \frac{4}{9\pi} \right)$
 I_2 = $ab^3 \left(\frac{\pi}{16} - \frac{4}{9\pi} \right)$
 I_3 = $\frac{1}{16} \pi a^2 b$
 I_4 = $\frac{1}{16} \pi ab^2$

*** ELLIPTIC COMPLEMENT**



A = $ab \left(1 - \frac{\pi}{4} \right)$
 m = $\frac{a}{6 \left(1 - \frac{\pi}{4} \right)}$
 n = $\frac{b}{6 \left(1 - \frac{\pi}{4} \right)}$
 I_1 = $a^3 b \left(\frac{1}{3} - \frac{\pi}{16} - \frac{1}{36 \left(1 - \frac{\pi}{4} \right)} \right)$
 I_2 = $ab^3 \left(\frac{1}{3} - \frac{\pi}{16} - \frac{1}{36 \left(1 - \frac{\pi}{4} \right)} \right)$

* To obtain properties of half circle, quarter circle and circular complement substitute $a = b = R$.

A-25. Wind Chill Equivalent Temperatures on Exposed Flesh at Varying Velocity

Temperature, F	WIND VELOCITY (MILES PER HOUR)										
	45	35	25	20	15	10	5	3	2	1	0
90	89.5	89	88.5	88	88.75	87.5	87	86	84.5	83	
82	81	80.5	80	79.5	78	76	74	72.5	70	60	
72	71	69.5	68	67	65	60	57	53.5	47.5	23	
63	61	59	57	55	52	44.5	39	34.5	20	-11	
51	49	47	45	42.5	38	28	18.5	11	0	-27	
41	39	36	34	30.5	25	11	0	-9	-23.5	-38	
30	28	25	23	18	11	-5	-16.5	-40	Below -40	Below -40	
20	18	14	11	6	-2	-19	-40	Below -40	do	do	
10	7.5	3	0	-6	-15	-35	Below -40	do	do	do	
0	-2.5	-8	-12	-18	-29	Below -40	do	do	do	do	
-11	-14	-18	-23	-30	Below -40	do	do	do	do	do	
-21	-24	-30	-35	Below -40	do	do	do	do	do	do	
-32	-35	-40	-40				do	do	do	do	

Instructions for use of the table:

- (1) First obtain the temperature and wind velocity forecast data.
- (2) Locate the number at the top corresponding to the expected wind speed (or the number closest to this).
- (3) Read down this column until the number corresponding to the expected temperature (or the number closest to this) is reached.
- (4) From this point follow across to the right on the same line until the last number is reached under the column marked zero (0) wind speed.
- (5) This is the equivalent temperature reading. Example: weather information gives the expected temperature (at a given time, such as midnight) to be 35°F, and the expected wind speed (at the same time, midnight) to be 20 miles per hour (mph). Locate the 20 mph column at the top, follow down this column to the number nearest to 35°F. The nearest number is 34°F. From this point, move all the way to the right on the same line and find the last number, which is -38°F. This means that with a temperature of 35°F, and a windspeed of 20 mph the rate of cooling of all exposed flesh is the same as -38°F, with no wind.

do means ditto.

Reproduced by permission of the Department of the Army.

A-26. Impurities in Water

U. S. Systems of Expressing Impurities

- 1 grain per gallon = 1 grain calcium carbonate (CaCO₃) per U. S. gallon of water
 1 part per million = 1 part calcium carbonate (CaCO₃) per 1,000,000 parts of water
 1 part per hundred thousand . . = 1 part calcium carbonate (CaCO₃) per 100,000 parts of water

Foreign Systems of Expressing Impurities

- 1 English degree (or °Clark) . . = 1 grain calcium carbonate (CaCO₃) per British Imperial gal. of water
 1 French degree = 1 part calcium carbonate (CaCO₃) per 100,000 parts of water
 1 German degree = 1 part calcium oxide (CaO) per 100,000 parts of water

Conversions

CONVERSION TABLE (Expressed to 3 Significant Figures)	Parts CaCO ₃ per Million (ppm)	Parts CaCO ₃ per Hundred Thousand (Pts./100,000)	Grains CaCO ₃ per U.S. Gallon (gpg)	English Degrees or ° Clark	French Degrees — ° French	German Degrees — ° German	Milli-equivalents per Liter or Equivalents per Million
1 Part per Million	1.	.1	.0583	.07	.1	.0560	.020
1 Part per Hundred Thousand	10.0	1.	.583	.7	1.	.560	.20
1 Grain per U. S. Gallon	17.1	1.71	1.	1.2	1.71	.958	.343
1 English or Clark Degree	14.3	1.43	.833	1.	1.43	.800	.286
1 French Degree	10.	1.	.583	.7	1.	.560	.20
1 German Degree	17.9	1.79	1.04	1.24	1.79	1.	.357
1 Milli-equivalent per Liter or 1 Equivalent per Million	50.	5.	2.92	3.60		2.80	1.

By permission, The Permutit Co., Inc., Data Book, 1953.

A-27. Water Analysis Conversions for Units Employed: Equivalents

WATER ANALYSIS UNITS CONVERSION TABLE (Expressed to 3 Significant Figures)	Parts per Million (ppm)	Milligrams per Liter (mgm/L)	Grams per Liter (grms/L)	Parts per Hundred Thousand (Pta./100,000)	Grains U.S. Gallon (gm/U.S. gal)	Grains per British Imp. Gallon	Kilograins per Cubic Foot (Kgr/cu. ft.)
1 Part per Million	1.	1.	.001	.1	.0583	.07	.0004
1 Milligram per Liter	1.	1.	.001	.1	.0583	.07	.0004
1 Gram per Liter	1000.	1000.	1.	100.	58.3	70.	.436
1 Part per Hundred Thousand	10.	10.	.01	1.	.583	.7	.00436
1 Grain per U.S. Gallon	17.1	17.1	.017	1.71	1.	1.2	.0075
1 Grain per British Imp. Gallon	14.3	14.3	.014	1.43	.833	1.	.0062
1 Kilograin per Cubic Foot	2294.	2294.	2.294	229.4	134.	161.	1.

NOTE: In practice, water analysis samples are measured by volume, not by weight and corrections for variations in specific gravity are practically never made. Therefore, parts per million are assumed to be the same as milligrams per liter and hence the above relationships are, for practical purposes, true.

By permission, The Permutit Co., Inc., Data Book, 1953.

A-28. Parts Per Million to Grains Per U. S. Gallon

A. To convert parts per million of hardness to grains per U. S. gallon, divide by the factor 17.1.

B. To convert grains per U. S. gallons to parts per million of hardness, multiply by the factor 17.1.

Example:

$$1. \frac{242 \text{ parts/million}}{17.1} = 14.1 \text{ grains/U. S. gallon}$$

$$2. 24.3 \text{ grains/U. S. gallon} \times 17.1 = 416 \text{ parts/million}$$

Equivalents

Water analyses may also be expressed as:

- (1) Equivalents per million (epm) = $\frac{\text{No. of ppm of substance present}}{\text{Equivalent weight of substance}}$
- (2) Milli equivalents per liter (meq/l) = Equivalents per million
- (3) Parts per million expressed as CaCO₃ = No. of ppm CaCO₃ equivalent to No. of ppm of substance present
- (4) Fiftieths of equivalents per million (epm/50) = $\frac{\text{No. of ppm of substance present} \times 50}{\text{Equivalent weight of substance}}$

NOTES: Numerically (1) and (2) are equal.
Numerically (3) and (4) are equal.

Section XXIII contains equivalent weights of a number of substances.
Section XXIII contains factors for converting various substances to CaCO₃.
Section XXIII contains factors for various chemical conversions.

By permission, The Permutit Co., Inc., Data Book, 1953.

A-29.
Formulas, Molecular and Equivalent Weights, and Conversion
Factors to CaCO₃ of Substances Frequently Appearing
in the Chemistry of Water Softening

Substance	Formula	Molecular weight	Equivalent weight	Multiplying Factor Considering molecular wt. of CaCO ₃ as 100.	
				Substance to CaCO ₃ equivalent	CaCO ₃ equivalent to substance
Aluminum	Al	27.0	9.0	5.56	0.18
Aluminum Chloride	AlCl ₃	133.	44.4	1.13	0.89
Aluminum Chloride	AlCl ₃ ·6H ₂ O	241.	80.5	0.62	1.61
Aluminum Sulfate	Al ₂ (SO ₄) ₃ ·18H ₂ O	666.4	111.1	0.45	2.22
Aluminum Sulfate	Al ₂ (SO ₄) ₃ (anhydrous)	342.1	57.0	0.88	1.14
Aluminum Hydrate	Al(OH) ₃	78.0	26.0	1.92	0.52
Alumina	Al ₂ O ₃	101.9	17.0	2.94	0.34
Sodium Aluminate	Na ₂ Al ₂ O ₄	163.9	27.3	1.83	0.55
Ammonium Alum	Al ₂ (SO ₄) ₃ (NH ₄) ₂ SO ₄ ·24H ₂ O	906.6	151.1	0.33	3.02
Potassium Alum	Al ₂ (SO ₄) ₃ K ₂ SO ₄ ·24H ₂ O	948.8	156.1	0.32	3.12
Ammonia	NH ₃	17.0	17.0	2.94	0.34
Ammonium (Ion)	NH ₄ ⁺	18.0	18.0	2.78	0.36
Ammonium Chloride	NH ₄ Cl	53.5	53.5	0.94	1.07
Ammonium Hydroxide	NH ₄ OH	35.1	35.1	1.43	0.70
Ammonium Sulfate	(NH ₄) ₂ SO ₄	132.	66.1	0.76	1.32
Barium	Ba	137.4	68.7	0.73	1.37
Barium Carbonate	BaCO ₃	197.4	98.7	0.61	1.97
Barium Chloride	BaCl ₂ ·2H ₂ O	244.3	122.2	0.41	2.44
Barium Hydroxide	Ba(OH) ₂	171.	85.7	0.59	1.71
Barium Oxide	BaO	153.	76.7	0.65	1.53
Barium Sulfate	BaSO ₄	233.4	116.7	0.43	2.33
Calcium	Ca	40.1	20.0	2.50	0.40
Calcium Bicarbonate	Ca(HCO ₃) ₂	162.1	81.1	0.62	1.62
Calcium Carbonate	CaCO ₃	100.08	50.1	1.00	1.00
Calcium Chloride	CaCl ₂	111.0	55.5	0.90	1.11
Calcium Hydrate	Ca(OH) ₂	74.1	37.1	1.35	0.74
Calcium Hypochlorite	Ca(ClO) ₂	143.1	35.8	0.70	1.43
Calcium Oxide	CaO	56.1	28.0	1.79	0.56
Calcium Sulfate	CaSO ₄ (anhydrous)	136.1	68.1	0.74	1.36
Calcium Sulfate	CaSO ₄ ·2H ₂ O (gypsum)	172.2	86.1	0.58	1.72
Calcium Nitrate	Ca(NO ₃) ₂	164.1	82.1	0.61	1.64
Calcium Phosphate	Ca ₃ (PO ₄) ₂	310.3	51.7	0.97	1.03
Carbon	C	12.0	3.00	16.67	0.06

Chlorine (Ion)	Cl	36.6	36.6	1.41	0.71
Copper (Cupric)	Cu	63.6	31.8	1.57	0.64
Copper Sulfate (Cupric)	CuSO ₄	160.	80.0	0.63	1.60
Copper Sulfate (Cupric)	CuSO ₄ ·5H ₂ O	250.	125.	0.40	2.50
Iron (Ferrous)	Fe ⁺⁺	55.8	27.9	1.79	0.55
Iron (Ferric)	Fe ⁺⁺⁺	55.8	18.6	2.69	0.37
Ferrous Carbonate	FeCO ₃	116.	57.9	0.86	1.16
Ferrous Hydroxide	Fe(OH) ₂	89.9	44.9	1.11	0.90
Ferrous Oxide	FeO	71.8	35.9	1.39	0.72
Ferrous Sulfate	FeSO ₄ (anhydrous)	151.9	76.0	0.66	1.52
Ferrous Sulfate	FeSO ₄ ·7H ₂ O	278.0	139.0	0.36	2.78
Ferrous Sulfate	FeSO ₄ (anhydrous)	151.9	151.9	oxidation	
Ferric Chloride	FeCl ₃	162.	54.1	0.93	1.08
Ferric Chloride	FeCl ₃ ·6H ₂ O	270.	90.1	0.56	1.80
Ferric Hydroxide	Fe(OH) ₃	107.	35.6	1.41	0.71
Ferric Oxide	Fe ₂ O ₃	160.	26.6	1.88	0.53
Ferric Sulfate (Ferric)	Fe ₂ (SO ₄) ₃	399.9	66.7	0.76	1.33
Ferrous or Ferric	Fe or Fe ⁺⁺	55.8	55.8	oxidation	
Ferrous Sulfate	FeSO ₄	151.9	151.9	oxidation	
Fluorine	F	19.0	19.0	2.66	0.38
Hydrogen (Ion)	H	1.01	1.01	50.0	0.02
Iodine	I	127.	127.	0.40	2.54
Lead	Pb	207.	104.	0.48	2.08
Magnesium	Mg	24.3	12.2	4.10	0.24
Magnesium Oxide	MgO	40.3	20.2	2.48	0.40
Magnesium Bicarbonate	Mg(HCO ₃) ₂	146.3	73.2	0.68	1.46
Magnesium Carbonate	MgCO ₃	84.3	42.2	1.19	0.84
Magnesium Chloride	MgCl ₂	95.2	47.6	1.05	0.95
Magnesium Hydrate	Mg(OH) ₂	58.3	29.2	1.71	0.58
Magnesium Nitrate	Mg(NO ₃) ₂	148.3	74.2	0.67	1.48
Magnesium Phosphate	Mg ₃ (PO ₄) ₂	262.9	43.8	1.14	0.88
Magnesium Sulfate	MgSO ₄	120.4	60.2	0.83	1.20
Manganese (Manganous)	Mn ⁺⁺	54.9	27.5	1.82	0.55
Manganese (Manganic)	Mn ⁺⁺⁺	54.9	18.3	2.73	0.37
Manganese Chloride	MnCl ₂	125.8	62.9	0.80	1.26
Manganese Dioxide	MnO ₂	86.9	21.7	2.30	0.43
Manganese Hydrate	Mn(OH) ₂	89.0	44.4	1.13	0.89
Manganic Oxide	Mn ₂ O ₃	158.	26.3	1.90	0.53
Manganous Oxide	MnO	70.9	35.5	1.41	0.71

By permission, The Permutit Co., Inc., Data Book, 1953.

(continued on next page)

A-29.
(Concluded). Formulas, Molecular and Equivalent Weights, and
Conversion Factors to CaCO₃ of Substances Frequently
Appearing in the Chemistry of Water Softening

Substance	Formula	Molecular weight	Equivalent weight	Multiplying Factor Considering molecular wt. of CaCO ₃ as 100.	
				Substance to CaCO ₃ equivalent	CaCO ₃ equivalent to substance
Nitrate (Ion)	NO ₃	62.0	62.0	0.81	1.24
Nitric Acid	HNO ₃	63.0	63.0	0.79	1.26
Nitrogen (Valence 3)	N ^{'''}	14.0	4.67	10.8	0.093
Nitrogen (Valence 5)	N ^{''''}	14.0	2.80	17.9	0.056
Oxygen	O	16.0	8.00	6.25	0.16
Phosphorus (Valence 3)	P ^{'''}	31.0	10.3	4.76	0.21
Phosphorus (Valence 5)	P ^{''''}	31.0	6.20	8.83	0.12
Potassium	K	39.1	39.1	1.28	0.78
Potassium Carbonate	K ₂ CO ₃	138.	69.1	0.72	1.38
Potassium Chloride	KCl	74.6	74.6	0.67	1.49
Potassium Hydroxide	KOH	56.1	56.1	0.88	1.12
Silver Chloride	AgCl	143.3	143.3	0.35	2.87
Silver Nitrate	AgNO ₃	169.9	169.9	0.29	3.40
Silica	SiO ₂	60.1	30.0	1.67	0.60
Silicon	Si	28.1	7.03	7.14	0.14
Sodium	Na	23.0	23.0	2.18	0.46
Sodium Bicarbonate	NaHCO ₃	84.0	84.0	0.60	1.68
Sodium Bisulfate	NaHSO ₄	120.	120.	—	—
Sodium Bisulfite	NaHSO ₃	104.	104.	—	—
Sodium Carbonate	Na ₂ CO ₃	106.	53.0	0.94	1.06
Sodium Carbonate	Na ₂ CO ₃ · 10H ₂ O	286.	143.	0.85	2.86
Sodium Chloride	NaCl	58.5	58.5	0.85	1.17
Sodium Hypochlorite	NaClO	74.5	37.3	0.67	1.49
Sodium Hydroxide	NaOH	40.0	40.0	1.25	0.80
Sodium Nitrate	NaNO ₃	85.0	85.0	0.59	1.70
Sodium Nitrite	NaNO ₂	69.0	34.5	0.73	1.38
Sodium Oxide	Na ₂ O	62.0	31.0	1.61	0.62
Tri-sodium Phosphate	Na ₃ PO ₄ · 12H ₂ O (18.7% P ₂ O ₅)	380.2	126.7	0.40	2.53
Tri-sodium Phos. (anhydrous)	Na ₃ PO ₄ (43.2% P ₂ O ₅)	164.0	54.7	0.91	1.09
Di-sodium Phosphate	Na ₂ HPO ₄ · 12H ₂ O (19.8% P ₂ O ₅)	358.2	119.4	0.42	2.39
Di-sodium Phos. (anhydrous)	Na ₂ HPO ₄ (50% P ₂ O ₅)	142.0	47.3	1.06	0.95
Mono-sodium Phosphate	NaH ₂ PO ₄ · H ₂ O (51.4% P ₂ O ₅)	138.1	46.0	1.09	0.92
Mono-sod. phos. (anhydrous)	NaH ₂ PO ₄ (59.1% P ₂ O ₅)	120.0	40.0	1.25	0.80
Meta-Phosphate (Hagan)	NaPO ₃ (69% P ₂ O ₅)	102.0	34.0	1.47	0.68
Sodium Sulfate	Na ₂ SO ₄ · 10H ₂ O	322.1	161.1	0.31	3.22
Sodium Sulfate	Na ₂ SO ₄	142.1	71.0	0.70	1.42
Sodium Thiosulfate	Na ₂ S ₂ O ₃	158.1	158.1	0.63	1.59
Sodium Tetrathionate	Na ₂ S ₄ O ₆	270.2	135.1	0.37	2.71
Sodium Sulfite	Na ₂ SO ₃	126.1	63.0	0.79	1.27
Sulfur (Valence 2)	S ^{''}	32.1	16.0	3.13	0.32
Sulfur (Valence 4)	S ^{''''}	32.1	8.02	6.25	0.16
Sulfur (Valence 6)	S ^{''''''}	32.1	5.34	9.10	0.11
Sulfur Dioxide	SO ₂	64.1	32.0	—	—
Tin	Sn	119.	119.	—	—
Water	H ₂ O	18.0	9.00	5.56	0.18
Zinc	Zn	65.4	32.7	1.54	0.65
ACID RADICALS					
Bicarbonate	HCO ₃	61.0	61.0	0.82	1.22
Carbonate	CO ₃	60.0	30.0	1.67	0.60
Carbon Dioxide	CO ₂	44.0	22.0	2.27	0.44
Chloride	Cl	35.5	35.5	1.41	0.71
Iodide	I	126.9	126.9	0.40	2.54
Nitrate	NO ₃	62.0	62.0	0.81	1.24
Hydrate	OH	17.0	17.0	2.94	0.34
Phosphate	PO ₄	95.0	31.7	1.68	0.63
Phosphorous Oxide	P ₂ O ₅	142.0	23.7	2.11	0.47
Sulfide	S	32.1	16.0	3.11	0.32
Sulfate	SO ₄	96.1	48.0	1.04	0.96
Sulfur Trioxide	SO ₃	80.1	40.0	1.25	0.80
ACIDS					
Hydrogen	H	1.0	1.0	50.00	0.02
Acetic Acid	HC ₂ H ₃ O ₂	60.1	60.1	0.83	1.20
Carbonic Acid	H ₂ CO ₃	62.0	31.0	1.61	0.62
Hydrochloric Acid	HCl	36.5	36.5	1.37	0.73
Phosphoric Acid	H ₃ PO ₄	98.0	32.7	1.68	0.65
Sulfurous Acid	H ₂ SO ₃	82.1	41.1	1.22	0.82
Sulfuric Acid	H ₂ SO ₄	98.1	49.0	1.02	0.98
Hydrogen Sulfide	H ₂ S	—	—	—	—
Manganous Acid	H ₂ MnO ₃	104.9	52.5	0.95	1.05

A-30. Grains Per U.S. Gallons— Pounds Per 1000 Gallons

- A. To convert grains per U. S. gallons to pounds per 1000 gallons multiply by the factor 0.143.
- B. To convert pounds per 1000 gallons to grains per U. S. gallons multiply by the factor 7.0.

Example:

1. 4.5 grains/U. S. gallon $\times 0.143 = 0.644$ lbs./1000 gals.
2. 0.5 lbs./1000 gallons $\times 7.0 = 3.5$ grains/U. S. gal.

A-31. Parts Per Million— Pounds Per 1000 Gallons

- A. To convert parts per million to pounds per 1000 gallons divide by the factor 120.
- B. To convert pounds per 1000 gallons to parts per million multiply by the factor 120.

Example:

1. $\frac{39 \text{ parts/million}}{120} = 0.325$ lbs./1000 gals.
2. $0.167 \text{ lbs./1000 gals.} \times 120 = 20$ parts/million

A-32. Coagulant, Acid, and Sulfate—1 ppm Equivalents

1 Ppm Name of Chemical	1 Ppm. Formula of Chemical	ppm Alkalinity Reduction	ppm SO ₂ as CaCO ₃ Increase	ppm Na ₂ SO ₄ Increase	ppm CO ₂ Increase	ppm Total Solids Increase
Filter Alum	Al ₂ (SO ₄) ₃ · 18H ₂ O	0.45	0.45	0.64	0.40	0.16
Ammonia Alum	Al ₂ (SO ₄) ₃ · (NH ₄) ₂ SO ₄ · 24H ₂ O	0.33	0.44	0.63	0.29	0.27
Potash Alum	Al ₂ (SO ₄) ₃ · K ₂ SO ₄ · 24H ₂ O	0.32	0.43	0.60	0.28	0.30
Copperas (ferrous sulfate)	FeSO ₄ · 7H ₂ O	0.36	0.36	0.51	0.31	0.13
Chlorinated Copperas	FeSO ₄ · 7H ₂ O + (½Cl ₂)	0.54	0.36	0.51	0.48	0.18
Ferric Sulfate (100% Fe ₂ (SO ₄) ₃)	Fe ₂ (SO ₄) ₃	0.75	0.75	1.07	0.66	0.27
Sulfuric Acid—98%	H ₂ SO ₄	1.00	1.00	1.42	0.88	0.36
Sulfuric Acid—93.2% (66° Be)	H ₂ SO ₄	0.95	0.95	1.35	0.84	0.34
Sulfuric Acid—77.7% (60° Be)	H ₂ SO ₄	0.79	0.79	1.18	0.70	0.28
Salt Cake—95%	Na ₂ SO ₄	—	0.66	0.95	—	1.00

By permission, The Permutit Co., Inc., Data Book, 1953.

A-33. Alkali and Lime—1 ppm Equivalents

Name 1 Ppm	Formula 1 Ppm	Alkalinity A Increase ppm	Free CO ₂ Reduction ppm	T.H. as CaCO ₃ Increase ppm
Sodium Bicarbonate	NaHCO ₃	0.60	—	—
Soda Ash (56% Na ₂ O = 89.16% Na ₂ CO ₃)	Na ₂ CO ₃	0.94	0.41	—
Caustic Soda (76% Na ₂ O = 98.06% NaOH)	NaOH	1.23	1.08	—
Chemical Lime (Quicklime—Usually 99% CaO)	CaO	1.61	1.41	1.61
Hydrated Lime (Usually 93% Ca(OH) ₂)	Ca(OH) ₂	1.28	1.11	1.28

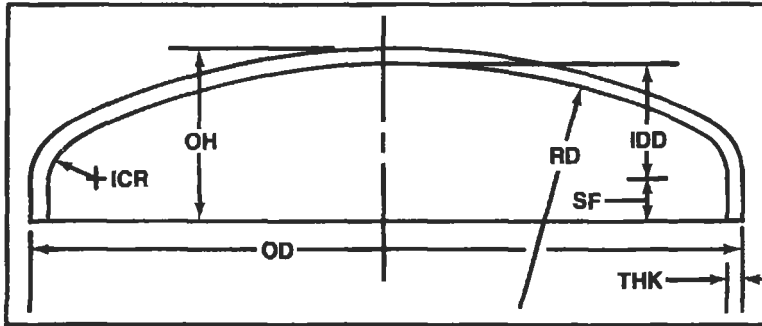
By permission, The Permutit Co., Inc., Data Book, 1953.

A-34. Sulfuric, Hydrochloric Acid Equivalent

Name	Formula	Specific Gravity 60°/60°F.	Concentration	Grams/Liter	CaCO ₃ Equivalent to one lb. Acid		
					Libs.	Grains	
Sulfuric Acid	60° Be	H ₂ SO ₄	1.7059	77.67%	1325	.7926	5348
Sulfuric Acid	66° Be	H ₂ SO ₄	1.8354	93.19%	1710	.9509	6657
Sulfuric Acid	88%	H ₂ SO ₄	1.8407	98.00%	1804	1.0000	7000
Hydrochloric Acid	18° Be	HCl	1.1417	27.92%	319	.8831	2682

By permission, The Permutit Co., Inc., Data Book, 1953.

A-35.



**ASME FLANGED AND DISHED HEADS
IDD CHART**

- OD - Outside Diameter
- THK - Thickness
- OH - Overall Height
- SF - Straight Flange
- RD - Radius of Dish
- ICR - Inside Corner Radius
- IDD - Inside Depth of Dish

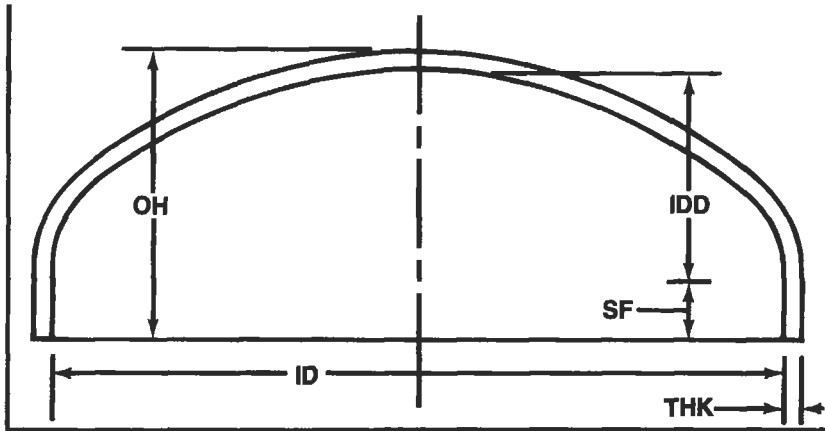
For "Overall Height" add length of straight flange to IDD given, plus thickness of material.

Use when **RD EQUALS DIAMETER**

OD	THK ICR	3/16"	1/4"	5/16"	3/8"	7/16"	1/2"	9/16"	5/8"	3/4"	7/8"	1"	
12	3/4	1.95	1.92	2.00	2.09								
14	3/4	2.29	2.26	2.27	2.35								
16	1	2.63	2.60	2.57	2.62								
18	1 1/4	2.97	2.94	2.91	2.88								
20	1 1/4	3.31	3.28	3.25	3.22								
22	1 1/4	3.73	3.75	3.67	3.64								
24	1 1/4	4.00	3.97	3.93	3.90								
26	2 1/4	4.72	4.69	4.66	4.63								
28	2 1/4	4.99	4.96	4.92	4.89								
30	2 1/4	5.25	5.22	5.19	5.16								
32	2 1/4	5.52	5.48	5.45	5.42								
34	2 1/4	5.78	5.75	5.72	5.69								
36	2 1/4	6.05	6.02	5.98	5.95								
38	3	6.78	6.74	6.71	6.68	6.65	6.62	6.59	6.56	6.53	6.50	6.44	6.38
40	3	7.04	7.01	6.98	6.95	6.91	6.88	6.85	6.82	6.79	6.76	6.70	6.64
42	3	7.31	7.27	7.24	7.21	7.18	7.15	7.12	7.08	7.05	7.02	6.96	6.90
44	2	7.57	7.54	7.51	7.47	7.44	7.41	7.38	7.35	7.32	7.29	7.22	7.16
46	3	7.84	7.80	7.77	7.74	7.71	7.68	7.64	7.61	7.58	7.55	7.49	7.43
48	3	8.10	8.07	8.04	8.00	7.97	7.94	7.91	7.88	7.85	7.81	7.75	7.69
50	3	8.37	8.34	8.30	8.27	8.24	8.21	8.17	8.14	8.11	8.08	8.02	7.95
52	3 3/4	9.09	9.06	9.03	8.99	8.96	8.93	8.90	8.87	8.84	8.80	8.74	8.68
54	3 3/4	9.35	9.32	9.29	9.26	9.23	9.19	9.16	9.13	9.10	9.07	9.01	8.94
56	3 3/4	9.62	9.59	9.56	9.52	9.49	9.46	9.43	9.40	9.36	9.33	9.27	9.21
58	3 3/4	9.89	9.85	9.82	9.79	9.76	9.72	9.69	9.66	9.63	9.60	9.53	9.47
60	3 3/4	10.15	10.12	10.09	10.05	10.02	9.99	9.96	9.93	9.89	9.86	9.80	9.74
62	3 3/4	10.42	10.39	10.35	10.32	10.29	10.26	10.22	10.19	10.16	10.13	10.06	10.00
64	4 1/4	10.99	10.95	10.92	10.89	10.86	10.83	10.79	10.76	10.73	10.70	10.64	10.57
66	4 1/4	11.25	11.22	11.19	11.16	11.12	11.09	11.06	11.03	10.99	10.96	10.90	10.84
68	4 1/4	11.52	11.49	11.45	11.42	11.39	11.36	11.32	11.29	11.26	11.23	11.16	11.10
70	4 1/4	11.78	11.75	11.72	11.69	11.65	11.62	11.59	11.56	11.53	11.49	11.43	11.37
72	4 1/4	12.35	12.32	12.29	12.26	12.22	12.19	12.16	12.13	12.10	12.06	12.00	11.94
74	4 1/4	12.62	12.59	12.55	12.52	12.49	12.46	12.43	12.39	12.36	12.33	12.27	12.20
76	4 1/4	12.89	12.85	12.82	12.79	12.76	12.72	12.69	12.66	12.63	12.59	12.53	12.47
78	4 1/4	13.15	13.12	13.09	13.05	13.02	12.99	12.96	12.92	12.89	12.86	12.80	12.73
80	5	13.57	13.54	13.50	13.47	13.44	13.41	13.37	13.34	13.31	13.28	13.21	13.15
82	5	13.84	13.80	13.77	13.74	13.70	13.67	13.64	13.61	13.57	13.54	13.48	13.41
84	5 1/4	14.56	14.52	14.49	14.46	14.43	14.39	14.36	14.33	14.30	14.27	14.20	14.14
86	5 1/4	14.82	14.79	14.76	14.72	14.69	14.66	14.63	14.60	14.56	14.53	14.47	14.40
88	5 1/4	15.09	15.05	15.02	14.99	14.96	14.92	14.89	14.86	14.83	14.80	14.73	14.67
90	5 1/4	15.35	15.32	15.29	15.26	15.22	15.19	15.16	15.13	15.09	15.06	15.00	14.93
92	5 1/4	15.62	15.59	15.55	15.52	15.49	15.46	15.42	15.39	15.36	15.33	15.26	15.20
94	5 1/4	15.89	15.85	15.82	15.79	15.75	15.72	15.69	15.66	15.62	15.59	15.53	15.46
96	6 1/4	16.61	16.57	16.54	16.51	16.48	16.44	16.41	16.38	16.35	16.32	16.25	16.19
98	6 1/4	16.87	16.84	16.81	16.77	16.74	16.71	16.68	16.64	16.61	16.58	16.52	16.45
100	6 1/4	17.14	17.10	17.07	17.04	17.01	16.97	16.94	16.91	16.88	16.85	16.78	16.72
102	6 1/4	17.40	17.37	17.34	17.31	17.27	17.24	17.21	17.18	17.14	17.11	17.05	16.98
104	6 1/4	17.67	17.64	17.60	17.57	17.54	17.51	17.47	17.44	17.41	17.38	17.31	17.25
106	6 1/4	17.94	17.90	17.87	17.84	17.80	17.77	17.74	17.71	17.67	17.64	17.58	17.51
108	6 1/4	18.20	18.17	18.14	18.10	18.07	18.04	18.00	17.97	17.94	17.91	17.84	17.78
110	7 1/4	18.92	18.89	18.86	18.82	18.79	18.76	18.73	18.69	18.66	18.63	18.57	18.50
112	7 1/4	19.19	19.15	19.12	19.09	19.06	19.02	18.99	18.96	18.93	18.89	18.83	18.77
114	7 1/4	19.45	19.42	19.39	19.36	19.32	19.29	19.26	19.23	19.19	19.16	19.10	19.03
116	7 1/4	19.72	19.69	19.65	19.62	19.59	19.56	19.52	19.49	19.46	19.43	19.36	19.30
118	7 1/4	19.99	19.95	19.92	19.89	19.85	19.82	19.79	19.76	19.72	19.69	19.63	19.56
120	7 1/4	20.25	20.22	20.19	20.15	20.12	20.09	20.05	20.02	19.99	19.96	19.89	19.83

On Application

A-35.



**ELLIPTICAL HEADS
(2:1 RATIO)**

- ID - Inside Diameter
- THK - Thickness
- OH - Overall Height
- SF - Straight Flange
- IDD - Inside Depth of Dish

- X - STANDARD
- I - INQUIRE

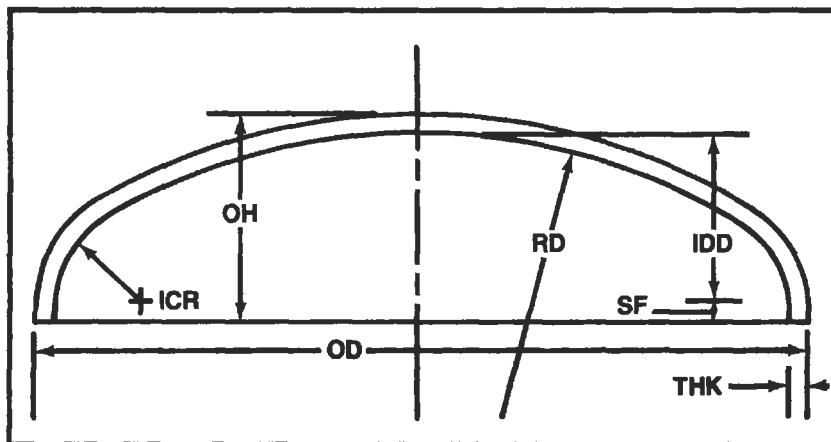
SIZES AND THICKNESSES OF HEADS

THK \ ID	3/16	1/4	9/16	3/8, 7/16	1/2, 9/16, 5/8	11/16, 3/4, 13/16	7/8, 1	1 1/4, 1 1/8	1 3/8	1 1/2, 1 5/8, 1 3/4	1 7/8	2	2 1/4, 2 1/2, 2 3/4	3	3 1/4	3 1/2	3 3/4	4, 4 1/4, 4 1/2	4 3/4	5, 5 1/4	5 1/2	5 3/4	6	6 1/2	7	8	THK \ ID	
6	X	X	X	X	X	X	X	I	I	I																	6	
8	X	X	X	X	X	X	X	X	X	I																		8
10	X	X	X	X	X	X	X	X	X	X	X	X																10
12	X	X	X	X	X	X	X	X	X	X	X	X	X	X	I													12
14	X	X	X	X	X	X	X	X	X	X	X	X	X	X	I													14
16	X	X	X	X	X	X	X	X	X	X	X	X	X	X	I													16
18	X	X	X	X	X	X	X	X	X	X	X	X	X	X	I													18
20	X	X	X	X	X	X	X	X	X	X	X	X	X	X	I													20
22	X	X	X	X	X	X	X	X	X	X	X	X	X	X	X													22
24	X	X	X	X	X	X	X	X	X	X	X	X	X	X	X	X	I											24
30	X	X	X	X	X	X	X	X	X	X	X	X	X	X	X	X	I											30
36	X	X	X	X	X	X	X	X	X	X	X	X	X	X	X	X	X	X										36
42	X	X	X	X	X	X	X	X	X	X	X	X	X	X	X	X	X	X	X	X								42
48	X	X	X	X	X	X	X	X	X	X	X	X	X	X	X	X	X	X	X	X	I							48
54	X	X	X	X	X	X	X	X	X	X	X	X	X	X	X	X	X	X	X	X	X	I	I					54
60	X	X	X	X	X	X	X	X	X	X	X	X	X	X	X	X	X	X	X	X	X	X	X	X	X	I	I	60
66		X	X	X	X	X	X	X	X	X	X	X	X	X	X	X	X	X	X	X	X	X	X	X	X	I	I	66
72		X	X	X	X	X	X	X	X	X	X	X	X	X	X	X	X	X	X	X	X	X	X	X	X	I	I	72
78			X	X	X	X	X	X	X	X	X	X	X	X	X	X	X	X	X	X	X	X	X	X	X	I	I	78
84				X	X	X	X	X	X	X	X	X	X	X	X	X	X	X	X	X	X	X	X	X	X	I	I	84
90				X	X	X	X	X	X	X	X	X	X	X	X	X	X	X	X	X	X	X	X	X	X	I	I	90
96				X	X	X	X	X	X	X	X	X	X	X	X	X	X	X	X	X	X	X	X	X	X	I	I	96
102				X	X	X	X	X	X	X	X	X	X	X	X	X	X	X	X	X	X	X	X	X	X	I	I	102
108				X	X	X	X	X	X	X	X	X	X	X	X	X	X	X	X	X	X	X	X	X	X	I	I	108
114				X	X	X	X	X	X	X	X	X	X	X	X	X	X	X	X	X	X	X	X	X	X	I	I	114
120				X	X	X	X	X	X	X	X	X	X	X	X	X	X	X	X	X	X	X	X	X	X	I	I	120

Elliptical
(2:1 Ratio)

By permission, Hackney-Brighton, a division of Trinity Industries.

A-35.



80-10® HEADS

- OD — Outside Diameter
- THK — Thickness
- OH — Overall Height
- SF — Straight Flange
- RD — Radius of Dish
- ICR — Inside Corner Radius
- IDD — Inside Depth of Dish

Meeting all A.S.M.E. Unfired Pressure Vessel Code requirements, the 80-10® Head permits significantly higher pressures than other configurations selected for the same service. The 80-10® Head is named for its unique dimensions—the dish radius equals 80% of the head diameter and the inside corner radius equals 10% of the head diameter. These dimensions compare to 100% and 6% respectively for A.S.M.E. F&D Heads.

Figure 1.

INTERNAL PRESSURE COMPARISON

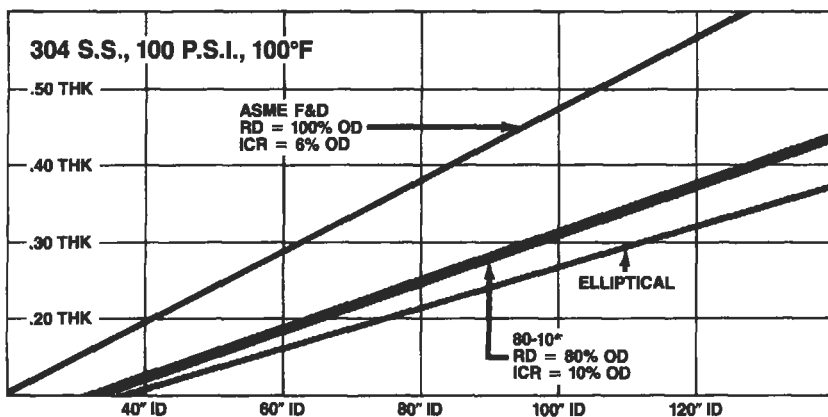
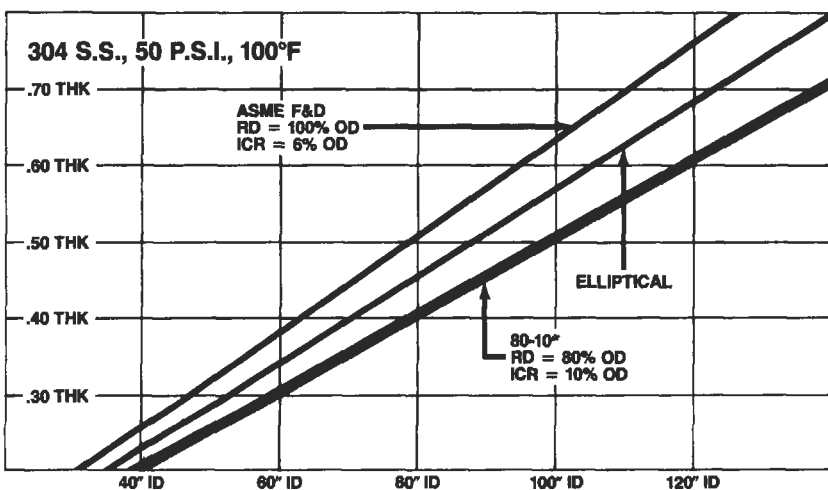


Figure 2.

EXTERNAL PRESSURE COMPARISON



By permission, Hackney-Brighton, Division of Trinity Industries.

Index

- Absorbers, intercooling, 116
- Absorption, 108
 - calculation procedure, 108, 109
 - component absorption, 108
 - diagram, 110
 - Edmister method, 112
 - efficiency, 118
 - fraction absorbed, 108
 - lean oil requirement, 112
 - procedure, 109, 113
 - rich oil, 108
 - theoretical trays, 108
 - trays for specified absorption, 109, 113
- Absorption and stripping efficiency, 118
- Absorption equilibrium curve, 117
- Absorption factor, 108
 - chart for E_a and E_s , 112
- Actual number trays, plates, stages, 85
- Adjacent keys, constant overflow, 94
- Air-water system, 369
- Akers and Wade multicomponent tray-by-tray, 87, 92
- Allowable mass velocity, tower design, 136
- American Institute of Chemical Engineers tray efficiency, 41
- Ammonia-air-water system, 367
 - absorption data, 368
 - effect of water temperature, 368
- Ammonia partial pressure over aqueous solution, 357
- Ammonia solution temperature rise, heats of solution, 359
- Ammonia vapor pressure-inerts data, 356
- Ammonia-water equilibrium curve, 358
- Ammonia-water overall gas film mass transfer, 353
- Ammonia-water Ponchon distillation, 66
- Atomic and molecular volumes, 353
- Azeotropes, 12–14
- Baffle tray columns, 213
 - mass transfer efficiency, example, 215
 - performance, 214
 - pressure drop, 214
 - tray arrangement, 213, 214
- Ballast ring, 238
- Batch distillation, 45
 - constant α with trays, reflux, 47
 - constant reflux, after Block, 51
 - constant reflux ratio, fixed trays, 48, 50
 - diagram, 46
 - differential, simple batch, 46
 - fixed theoretical trays, constant reflux ratio, variable overhead, 48
 - minimum reflux diagram, 49
 - Raleigh equation, 47, 53
 - simple, no trays, 55
 - vapor boil-up, fixed trays, 53
 - variable reflux rate, fixed theoretical plates, 50
 - variable reflux ratio, various theoretical plates, 49, 51
- Benzene-toluene mixture, 27, 33, 35
 - transfer units, 377
- Benzene-toluene vapor-liquid equilibrium transfer units, 377
- Berl saddles, 237
- Binary mixture, fractionation, minimum reflux, 29
- Binary mixtures, 3
- Binary systems, 15
 - minimum reflux at infinite plates, 23
 - solution for trays, L/D , 23
- Boiling point diagram, 27
- Brown and Martin operating reflux, 83
- Bubble cap(s), 122, 123, 155
 - cap and riser comparison dimensional data, 141–143
 - layout, 134
 - performance, diagram, 126
 - shroud ring, 156
 - slot dimensions, 158
 - slot performance, 160
 - slot seals, 158
 - typical 4-in. pressed, 134
 - typical styles, design details, 140
- Bubble cap tray design guide, 138
- Bubble cap trays, 122, 123
 - “C” factor chart for diameter, 135

- cap area by tray type, 138
- cartridge assembly, 125
- design, 124
- design guide, 138
- effect of liquid and vapor loads, 155
- effect of liquid gradient on vapor distribution, 157
- layouts, 130, 133, 137
- schematic arrangement, 125
- sieve and bubble cap flooding comparison, 192
- tower diameter, 126
- turndown ratio, 155
- Bubble cap trays, performance design, 155, 156
 - blowing, 158
 - bottom tray seal pan, 170
 - bubble cap pressure drop constant, 167
 - cap slots, 160
 - capacity vs. vapor-liquid loads, 156
 - composite tower assembly, 219
 - coning, 158
 - correction for wet pressure drop, 167
 - downcomer pressure drop, 167
 - downcomer slot seal, 170
 - dry tray pressure drop, 167
 - effect of liquid gradient on vapor, 157
 - effect of vapor load on cap slots, 157
 - entrainment, 158, 169
 - example bubble cap tray design, 171
 - flexibility, 157
 - flooding, 157
 - flooding comparison, sieve and bubble cap, 192
 - free height in downcomer, 170
 - inlet weir, 170
 - liquid gradient, 161
 - charts, 162–165
 - correction, 166
 - liquid height in downcomer, 168
 - liquid height over outlet weir, 158, 159
 - overdesign, 158
 - pulsing, 157
 - riser and reversal pressure drop, 166
 - Bolles design, 166
 - modified Dauphine design, 166
 - slot opening, caps, 160
 - slot seals, 158
 - spacing of trays, 168
 - stability, 157
 - throw over outlet segmental weir, 170
 - total pressure drop through tray, 158, 167
 - vapor distribution, 171
 - weir correction factor, segmental, 159
- Bubble cap typical tray details, 139, 146
 - general purpose design details, 154
- Bubble point, 15, 16
- Carbon dioxide absorption, effect on carbonate K_{g_a} , 364, 365
- Carbon dioxide in alkaline solution, 361
 - absorption in sodium hydroxide, 364
 - design procedure alkaline absorbers, 361
 - from atmosphere, 362, 363
 - K_{g_a} data and corrections, 361
 - sulfur dioxide in alkaline solutions, 361
- Chempak®, 240
- Chlorine-water system (dilute gas), 367
 - effect of liquor, rate, 369
 - solubility in water, 369
- Chou and Yaws multicomponent method, 81
- Colburn minimum reflux, pinch temperatures, 74
 - minimum factors, 78
- Column performance, 104
- Condensers, 2, 19, 20
 - partial, 20
 - total, 19, 20
 - x-y diagram, 20
- Contacting trays, 123
- Convergence pressure, 4, 6–9
- Cooling tower(s), 379ff.
 - blow-down, 395
 - design/operating terminology, 382
 - air pressure drop, 394
 - alternate design of new tower, 396
 - approach, 382
 - atmospheric cooling tower water loss, 408
 - blow-down, 382, 394
 - characteristic performance charts, 399–405
 - comparison cooling efficiency of packing, 406
 - contamination build-up, 394
 - drift loss or windage loss, 382
 - fan power required, 394
 - graphical integration transfer units, 398
 - make-up, 382
 - performance evaluation of existing tower, 396
 - pressure drop comparison, 407
 - range, 382
 - recirculation, 383
 - tower characteristics vs. fan power, 394
 - water rates, 393
 - effect of performance variables on ground area, 393
 - fan performance, 391
 - general construction, 380
 - ground area vs. height, 391
 - packing efficiency, 406
 - pressure drop comparison, 407
 - specifications, 383
 - form, 386
 - terminology, 381
 - types, 380–385
 - atmospheric, 380–382
 - forced draft, 380, 383
 - induced draft, 380, 384, 385
 - natural draft, 380, 381
 - spray filled, 385
 - typical performance, 387
 - design gpm, 387
 - diagram of counter-current tower, 388
 - driving force diagram, 388
 - effect of change in gpm on approach, 390
 - effect of half-speed operation of fans, 390
 - effect of hot water temperature, 390
 - enthalpy of air operating line, 388
 - fan horsepower, 392
 - fan performance, 391

- guide for recirculating water for film fill, 392
- pressure loss, 392
- tower characteristic, 387
- tower fill, 389
- transfer units, 388, 396
- water loss, atmospheric tower, 380
- Cooling water with air, 379
- Counterflow cooling tower performance, 399–405
- Dalton's Law, 2, 3, 26
 - combined with Raoult's Law, 2
- DePriester K-value light hydrocarbon systems, 10, 11
- Dew point, 15, 16
- Diagnostic study of column performance, 104
- Diffusion coefficient for gases, 351
 - table, gases/liquids and liquid/liquid, 352
- Distillation, 1
 - downcomer, 135
 - heat balance, 63
 - key components, 68
 - nomenclature, 2, 102, 121, 221
 - operating diagrams, 21
 - operating pressures, 18, 19
 - in packed towers, 370, 379
 - Ponchon-Savarit method, binary, unequal molal overflow, 63, 64
 - process performance, 1
 - schematic tower/column arrangement, 2
 - short-cut, multicomponent, 72
 - tray specification data sheet, FRI, 220
 - underwood multicomponent, 71
- Distillation in packed towers, 370
 - HETP estimates various systems and packing, 379
- Distribution, packed towers, 246ff.
 - effects of liquid maldistribution, 266, 267
 - guide for selection, 264
 - liquid, 246, 254, 260–265
 - number of flow or drip points, 265, 266
 - patterns, 267
 - redistribution, illustration, 271
- Distribution of liquid, effect of under-irrigating wall, packed towers, 376
- Distributor pan, packed towers, 257
 - guide for selection, 264
 - multipan, 262, 263
 - orifice pan, 262
 - pipe orifice header, 265
 - spray nozzle, 263, 264
 - spray pipes/headers, 261, 265
 - trough, 261, 265
 - weir flow, 261
- Downcomer, distillation, 135
 - free height, 170
 - liquid height, 168
 - pressure drop, 167
 - residence time, 169
 - seal, 168
 - suggested velocities in, table, 169
- Drikamer and Bradford tray efficiency, 41
- Drip point tile, pressure drop, 293–295
- Drip points recommended, liquid, packed towers number, 265
 - table, points/ft² random packing, 266
- Dual flow tray, 123
- Edmister method, 112
- Effect of packing on CO₂-sodium hydroxide system, 366
- Effective absorption and stripping factors, 114
- Efficiency, absorption and stripping, 118
 - table, 118
- Efficiency, comparative, sieve vs. bubble cap, 44
 - Effect of liquid mixing on tray, 45
 - Effect of vapor mixing on tray, 45
- Efficiency correlations, 41
- Entrainment
 - bubble cap trays, 169
 - comparison, 191
 - sieve tray, correction, 177
- Entrainment flooding, sieve trays, 187, 189
 - Fair's method, 188, 189
- Equilibrium, basic considerations, 1
- Equilibrium, hydrocarbon, 4
- Erbar, Joyner, and Maddox improved Underwood method, 91
- Estimating multicomponent recoveries, 85
 - Non-key components, 86
 - Yaw's method, 85
- Ethanol-water diagram, minimum reflux, 52
- Examples
 - absorption of hydrocarbon with lean oil, 114
 - alternate evaluation of tower condition, 315
 - baffle tray column mass transfer, 215
 - batch distillation, constant reflux, 51
 - batch distillation, vapor boil-up, fixed trays, 53
 - binary batch differential distillation, 54
 - boiling point curve and equilibrium, 26
 - bubble cap tray design, 171
 - bubble point and dew point, 17
 - change performance with change in existing tower packing, 315
 - Colburn equation, minimum reflux ratio, 76
 - Colburn minimum reflux, pinch temperature, 74
 - component absorption, fixed tray tower, 119
 - continuous steam flash, 61
 - design of ammonia absorption tower, 352
 - performance interpretation, 357
 - design packed tower removing carbon dioxide w/caustic, 364
 - determining blow-down for cooling tower, 395
 - estimated multicomponent recoveries, Yaw's method, 87
 - estimating distillation tray efficiency, 42
 - evaluation tower condition and pressure drop, 313
 - Fair's recommended tower diameter, 199
 - flash vaporization, hydrocarbon mixture, 27
 - flashing composition, 17
 - graphical design, binary system, 33
 - heavy gas oil fractionation using Gempak®, 331
 - hydrocarbon stripper, 302
 - K-values, 27
 - Koch-Sulzer packing tower sizing, 326
 - minimum reflux ratio, Underwood equation, 73
 - minimum theoretical plates at total reflux, 38

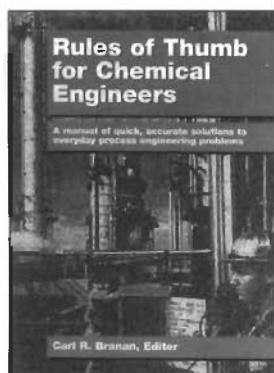
- minimum trays, Winn's method, 24
- multicomponent batch distillation, 55
- multicomponent design by Yaw's method, 70
- multicomponent steam flash, 59
- multicomponent study of reflux ratio, 99
- number of transfer units for concentrated solution, 348
- number of transfer units for dilute solution, 346
- number of trays for specified absorption, 118
- open steam stripping of heavy rich oil, 62
- operating reflux ratio, 84
- operation at low rate, random liquid hold-up, 320
- perforated plate, no downcomers, 206
- Ponchon-Savarit unequal overflow design charts, 65
- Raoult's Law, 14
- relative volatility estimate, Wagle's method, 29
- Scheibel-Montross minimum reflux, 80
- sieve tray design with downcomer, 195
- solve Gilliland's equation, 32
- stacked packing pressure drop, 316
- stripping dissolved organics from water, method of Li and Hsiao, 100
- thermal condition of feed, 35
- transfer units in distillation, 377
- tray-by-tray, multicomponent mixture using computer, 95
- tray-to-tray design multicomponent mixture, 90
- wood-packed cooling tower, induced draft, 396
- Fair's method, dry sieve tray pressure drop, 181
- Fan horsepower, cooling towers, 392
- Feed thermal condition, 20
 - diagram, 21
- Feed tray location, 85
- Fenske equation, 22
- Fenske minimum theoretical trays at total reflux, 80
- Fenske-Underwood-Gilliland multicomponent trays, 72
- Flash vaporization, 15
- Flashing composition, 17
- Flexiring®, 238, 240
- Flood point, random packing, 288
 - Kister's study, 288
- Flooding, sieve trays, maximum hole velocity, 193
- Flooding correlation, Sherwood chart, 283
- Flooding on perforated support plates, 314
- Foaming liquid systems, 280
- Fraction absorbed, 108
- Fractional entrainment, 190
- Fractionation Research, Inc. (FRI), 122, 176
- Francis weir formula, 159
- Fugacity, \bar{v} , 12
- Gas and liquid-phase coefficients, 349
- Gas Processors Suppliers Association, 4
- Gilliland plot, plates vs. reflux ratio, 30
 - nomogram, 31
- Glitsch Ballast valve tray, 123
- Glitsch Cascade®, 241
- Glitsch Nye tray, 124
- Graphical integration
 - batch distillation, 52, 54
 - transfer units, 348, 349
 - cooling tower, 398
- Grid packing, metal, 347, 348
 - Glitsch-Grid™, 338
 - comparison performance charts, 339
 - Koch Flexigrid®, 335
 - comparison capacities with random packing, 337
 - pressure drop charts, 337
 - Norton Intalox® Grid, 247
 - Nutter Snap-Grid®, 247, 335
 - HETP, 335
 - pressure drop, 337
- Hausbrand vapor pressure diagram, steam distillation, 58
- Heat balance, distillation, 63
 - adjacent key system, 94
 - Ponchon-Savarit method, 63–65
- Heats of absorption, 116
- Height of gas film transfer unit, estimate, 351
 - diffusion coefficient of gases, 351, 352
- Height of individual transfer unit, 350
- Height of liquid film transfer unit estimate, 351
- Height of overall transfer unit, 350
- Henry's Law, 3, 4
- HETP (height equivalent to a theoretical plate), 370–377
 - charts, 373
 - correlation equation, 372, 378
 - correlation factor "n" for HETP, 380
 - estimates for distillation, 379
 - HETP and HTU correlation, random packing, 374
 - HETP guidelines, use, selection, 375
 - influence on, 375
 - relationship to HTU, 376
 - typical operating and design, 288
- HETP random packing comparison, 280
 - typical operating and design chart, 288
- Hold-down grids, 269, 271
 - bed limiters, 269
- Hold-up, liquid, ceramic tower packings, 316
- Horton-Franklin method, 113
- Hutchinson, A.J.L., 117
- Hydrocarbon absorption and stripping, 108
- Hydrogen chloride-water system, 369
 - adiabatic absorption of, effect of inert gases, 370
 - graphite absorption tower, 371
 - preliminary selection charts, 372
- Hy-Pak®, 238
 - x-y diagram adiabatic absorption, 370
- Ideal systems, 2
- Intalox saddles, 237–238
- Interfacial area, effective (random), 320
 - random ceramic packing, 321
- Jaeger Tri-Paks®, 241
- K-Factor hydrocarbon equilibrium, 4, 6
- Key components, multicomponent, 68
 - estimating chart, recovery, 86
 - heavy, 68
 - light, 68
- Kister, H.Z., 188
 - chart, 299
 - correlation pressure drop, 287, 298
- Koch Fleximax®, 240, 241

- Koch Flexitray®, (valve tray), 123
- Koch HcKp, 240
- Kremser-Brown-Sherwood method, 108
- Lean oil requirement(absorption), 112
- Lessing rings, 237
- Liquid distribution into packed tower, 231
- Liquid distribution patterns, packed tower, 267
 - effect of maldistribution on efficiency, 218
 - illustration, 271
 - redistribution, 267, 269
- Liquid hold-up, random packing, 317
- Loading and flooding regions, random packing, 310
 - liquid rate, liquid continuous mode (packing), 311
 - pressure drop at flooding, 311
 - pressure drop below and at flood point, continuous range, 311
- Mass and heat transfer, 343
- Mass transfer diagram, types of operation, 344
- Mass transfer equation, 345
 - function values to use with equation, 346
- Mass transfer with chemical reaction, 361
- Materials of construction, random packing, 280
- Maximum operating capacity (MOC), random packing, 299
 - comparison of various packings, 300
 - Strigle's table, 300
- McCabe-Thiele diagram, 3
 - Binary mixture, 3
- Mechanical arrangement, distillation tower, 2
- Mechanical designs for tray performance, 122
- Mechanical tolerances for construction self-supporting towers, 218
 - composite tray assembly, 219
- Metal VSR®, 239
- Minimum plates at total reflux, 21
- Minimum reflux ratio, infinite plates, 29
- Minimum total trays, 22
- Minimum trays, total reflux, constant volatility, 80
- Montz-Nutter structured packing, 246, 342
- Multicomponent distillation, 68
 - Akers and Wade method, 87, 92
 - algebraic plate-to-plate method, 70
 - Chou and Yaws multicomponent method, 81–89
 - key components, 68
 - minimum reflux ratio, 68
 - minimum reflux ratio/infinite plates, 68
 - tray-by-tray, 87
 - Underwood algebraic method, 71
 - Yaw's short-cut method, 6
- Murphree tray efficiency, 41–43
- Nomenclature
 - distillation
 - absorption and stripping, 121
 - mechanical designs, tray performance, 221
 - process performance, 2, 102
 - packed towers, 408–411
- Non-ideal systems, 5
- Norton Intalox®, 241
- Norton trays
 - bubble cap tray, 124
 - valve tray, 124
- Norton's packing capacity chart, IMTP® random metal packing, non-foaming, 287
- Norton's pressure drop correlation for IMTP® random packing, 286
- Nutter MVG tray, 123
- Nutter Ring®, 239
- O'Connell tray efficiency, 41
- Open steam stripping, 62
- Operating line, equilibrium diagram, 3
- Packed tower mass transfer countercurrent diagram and symbols, 343
- Packed towers, 230ff.
 - basic features, 230
 - bell and spigot ceramic construction, 234, 235
 - brick and membrane-lined shell, 232, 233
 - distillation in, 370
 - distribution, 246ff.
 - distributor pan, 257
 - drip points, recommended, 265–266
 - grid, 231, 248, 249
 - packing supports, 236
 - random packing, 234
 - reinforced plastic shell construction, 236
 - rubber-lined, 232, 233
 - shell, 234
 - structured packing, 234
 - typical arrangement internal components, cross-section, 234, 235
- Packing, fouling, 280
- Packing, random, recommended design capacity and pressure drop, 292
- Packing data
 - Berl saddles, ceramic, 250
 - metal, 251
 - Chempak®, metal, 253
 - cross partition tile, ceramic, 251
 - Drip point tile, ceramic, 253
 - Hy-Pak™, metal, 252
 - Intalox®, ceramic, 251
 - Lessing rings, metal, 250
 - ceramic, 250
 - Pall rings, metal, 252
 - plastic, 252
 - Raschig rings, ceramic, 248
 - carbon, 249
 - metal, 249
 - Super Intalox®, ceramic, 252
 - plastic, 252
 - Tellerette, plastic, 252
- Packing factors, wet and dumped, random, 289–291
 - flooding vs. packing factors, 291
 - special packing, 292
- Packing installation, 270
 - dumped, 270, 272
 - stacked, 270, 272

- Packing performance, random
 - capacity basis for design, 300
 - capacity parameter, 282
 - comparison at flood, tray vs. packing, 273
 - contacting efficiency, HETP, HTU, $K_g a$, 276
 - design efficiency and capacity, various packings, 300
 - efficiency, random vs. structural, 274
 - flooding capacity, 273
 - flow parameters, 282
 - fouling, 280
 - fraction packing wetted, 317
 - generalized correlation, loading, flooding pressure drop, 284
 - generalized pressure drop correlation(s), 283–285
 - HETP, 274
 - comparison at design point, various packing, 302
 - comparison of 2-ft rings, 280
 - Kister correlation, 299
 - liquid hold-up, 307
 - liquid hold-up variation with surface tension, 318
 - loading point/loading region, 282
 - minimum liquid wetting rates, 281
 - minimum rate, 281
 - wetting rates vs. surface conditioning, 281
 - Norton's packing capacity correlation for IMTP® metal, 287
 - packing size for various column diameters, 271, 279, 297
 - pressure drop, 280
 - comparison, valve tray vs. Nutter ring®, 276
 - design and guide, 293–298
 - relative performance characteristics, 277
 - Sherwood flooding correlation, 283
 - static hold-up, 318
 - Strigle's latest generalized pressure drop correlation, 286
 - Strigle's maximum operating capacity, 299
 - surface tension effects, 289
 - typical HETP curve, operating and design relationship, 288
 - typical performance comparison, random vs. structural, 279, 280
- Packing related to column diameter (random), 279
- Packing service application, 254
- Packing supports, 236, 256–259
 - flooding on perforated supports, 314
 - pressure drop in various designs, 313
- Packing type application, 255
- Packing vs. trays
 - capacity at flood, 273
 - FRI studies, 273
 - guidelines, 272
 - Kister studies, 273
 - practical packing, 273
 - practical tray, 273
- Packing wetted area (random), 320
- Pall rings, 237–238
- Perforated plates (sieve) without downcomers, 202
 - calculation: summary, 202–206
 - dump point, load point, 204
 - efficiency, 204
 - tray layout, 202
 - vapor and liquid rates for tray activation, 205
- Perforated sieve plates/trays, 196
 - number holes in plate, 196
 - percent open hole area, 196
- Perforated trays with downcomers, 122, 123
- Perforated trays without downcomers (dual flow), 122, 123
- Performance structured packings, 323
 - Size selection
 - ACS woven knitted mesh, 323–325
 - Glitsch Gempac® structured packing, 331, 335, 336
 - Koch Flexipac® structured packing, 328–329
 - Koch Sulzer woven wire packing, 325, 327
 - Norton Intalox® structured packing, 328–331
- Pinch conditions, x-y diagram, 32
- Ponchon-Savarit binary mixture, 63
 - graphical method, 63–67
 - performance/design charts, 64–66
 - unequal overflow distillation, 65
- Prausnitz, 5
- Pressure, distillation operating, 18
 - algorithm for establishing, 19
- Pressure drop, bubble cap tray, 167
- Pressure drop, design guide random packing, 293–298
 - drip point tile, 293–295
- Pressure drop, random packing, 283–286
 - across packing supports and redistribution plates, 312, 313
 - comparison of various packings, 300
 - constants below flooding region, 312
 - correlation at flood point, 310
 - Norton's proprietary correlation (GPDC) for metal IMTP packing only, 286
 - Strigle's correlation, (GPDC), 286
- Pressure drop, sieve tray with downcomers, 182
 - Fair's method, 182
 - Hughmark and O'Connell method, 182
 - through downcomer, 183
 - total wet tray, 182
- Proprietary valve tray design, 207–211
 - comparison valve tray pressure drop, 210
 - correlation of aerated tray liquid pressure drop chart, 209
 - dry tray pressure drop, 208
 - materials used for valves, 209
 - typical operating valve tray pressure drop, 208
- Psychrometric chart for air, 397–398
- Radial liquid spreading coefficients, 268
- Random packing, 234ff.
 - loading/flooding regions, 310
 - materials of construction, 280
 - maximum operating capacity, 299
 - packing types, shapes, 237–242
 - Ceramic, 237
 - Metal, 237–241
 - Plastic, 238–242
 - proprietary design guidelines
 - Glitsch Cascade metal Mini-Ring®, 309
 - Norton metal Intalox IMTP®, 301–302
 - Nutter Ring™, 305–308

- Raoult's Law, 2
 - combined with Dalton's Law, 2
- Rauschert Hiflow®, 241
- Recovery, multicomponent system, 85–86
 - Yaw's method, 88
- Redistribution of liquid, 267, 269
 - wall wipers, 269, 270
- References
 - distillation/absorption/mechanical tray design, 223
 - packed towers, 411–414
- Reflux
 - Colburn minimum, pinch temperature, 74
 - Fenske equation, 22
 - minimum chart, 23
 - minimum plates, 21, 23
 - operating, Brown and Martin, 83
 - theoretical trays relationship, 40
 - total, 21, 23
 - vs. trays, Gilliland, 31
- Reflux ratio
 - effects on overhead and bottoms, chart, 99
 - minimum infinite plates, 29
 - theoretical plates, chart, 30
- Relative volatility, 22
 - quick estimate, 28
- Residence time in downcomer, 169
 - rich oil, 108
- Robbin's pressure drop correlation, 297
- Robinson and Gilliland, 63
- Scheibel-Montross multicomponent system, 79
- Schematic tower arrangement with performance
 - nomenclature, 2
- Seal pan, bottom tray, 154
- Sieve and bubble tray flooding comparison, 192
- Sieve tray vapor cross-flow channeling, 194, 195
- Sieve trays, 122
 - arrangement with downcomer, 126
 - layout, 127
 - tray spacing, 177
- Sieve trays with downcomers, 174ff.
 - aeration factor, 180
 - alternate downcomer weirs, 178
 - composite tower assembly, 219
 - design, 187
 - calculations, 195, 199
 - hole velocity, 193
 - downcomer, 177
 - dry tray pressure drop, 181
 - dynamic liquid seal, 182
 - effective liquid head, with downcomer, 182
 - entrainment calculations, 178
 - entrainment flooding, 187
 - equivalent hole diameter, 184
 - Fair method, dry tray, 181
 - Fair method entrainment flooding, 188, 189
 - fractional entrainment, 190
 - free height in downcomer, 183
 - friction factor for froth crossflow, 180
 - graphical correlation ultimate capacity, 212
 - height of liquid over outlet weir, 179
 - hydraulic gradient, 179, 180
 - liquid backup, or height in downcomer, 183
 - maximum hole velocity, flooding, 193
 - minimum vapor velocity, weep point, 183
 - number holes in plate, 196
 - percent open hole area, 196
 - pressure drop through downcomer, 183
 - selection guide, 175
 - static liquid seal on tray, submergence, 181
 - terminology, 175, 176
 - total wet tray pressure drop, 182
 - tower diameter, 176, 197
 - tray components, 175
 - tray hydraulics, 179
 - tray stability, 193, 194
 - typical operating curves, 179
 - vs. bubble cap trays, 44
 - weep point velocity, 186
 - weeping calculations, correlations, 183, 184
 - weeping comparison Koch valves and sieve trays, 185
- Souders-Brown, 176
- Specification data sheet, 220
 - process tray performance, 220
 - mechanical tray performance, 220
- Specification form for tower details (shell), 354
 - internal tower detail, spray or packed, 355
- Spray distributor, 263, 264
- Static hold-up, 318
 - effects of surface tension, density, viscosity, 319
- Steam distillation, 57
 - calculations, 57, 58
 - continuous differential, 60
 - continuous flash, 59, 60
 - Hausbrand vapor pressure chart, 58
 - open live steam, with trays, 60
 - open stem stripping diagram, 62
 - phase rule, 57
- Stripping, 110–111
- Stripping dissolved organics from water, method of Li and Hsiao, 100
- Stripping tower using air, 102
- Structured packing, 242–247, 322, 337
 - packing types, shapes, etc., 242–247
 - ACS knitted wire mesh, 243
 - features, 322
 - Glitsch Gempak®, corrugated metal, 245
 - Goodloe wiremesh (Glitsch, Inc.), 242
 - Koch ceramic Flexiramic®, 247
 - Koch Flexipac®, 244
 - Koch-Sulzer corrugated sheets, 244
 - Metal Max-Pak™, corrugated sheets, 245
 - Montz-Nutter™, corrugated metal, 246
 - Norton Intalox® wire gauze, 245
 - Nutter BHS™ expanded metal textured, 246
 - Panapak, 242

- Spraypak, 242
- York-twist™, 243
- performance features, 242–247, 323, 337
 - capacity correlation for structured Intalox®, 331
 - characteristics comparison table, 340
 - comparison of flooding data charts, 340
 - comparison of structured gauze vs. Pall rings, 341
 - flooding, 337
 - guidelines for structured packings, 342
 - HETP for Montz-Nutter® packing, chart, 343
 - pressure drop, 338
 - at flood vs. loading, 341
 - for Montz-Nutter® packing, 343
 - scale-up, 342
- Sulfur dioxide-water system (dilute gas), 368
- Support, packing, 236, 256–259
- Teller Rosette, 242
- Theoretical trays at operating (actual) reflux, 3, 30, 83, 85
- Thermal condition of feed, 20
- Total reflux, minimum plates, 21
- Tower diameter, sieve trays, 176
- Tower specifications, 215
 - composite tower-tray assembly, 219
 - mechanical internal specifications, tray columns, 217
 - mechanical specifications form, trays, 216
 - mechanical tolerances for construction, 218
- Tower/column diameter, 275, 292, 293, 300
 - Brown-Souders tower diameter, 197
 - bubble cap, 126
 - calculations, 126, 129, 130, 195
 - sieve trays, 176
- Transfer unit relationship to HETP, 375, 376
- Transfer units, 343, 375
 - Colburn plot, 347
 - concentrated solutions, 345
 - cooling towers, 387
 - general applications, 345
 - graphical integration, 348, 349
 - liquid film control, 345
 - number, 343, 344
 - overall mass transfer, ammonia-water, 353
 - relationship to HETP, 376
 - system film control, 345
 - use of k_G and k_L , 349
 - vapor-liquid diagram for benzene-toluene transfer units, 377
- Tray-by-tray multicomponent distillation, 87, 90
- Tray designs for liquid paths (bubble cap), 137
- Tray efficiency, 40, 41
 - AIChE distillation tray efficiency, 41
 - effects of vapor mixing and liquid respectively on tray efficiency, 45
 - Murphree, 41, 42
 - Sieve vs. bubble cap, 44
- Tray layout, 131, 133, 154
 - bottom seal pan, 154
 - bubble cap layout form, 144, 145
 - bubble cap typical design details, 139, 146–153
 - liquid weep, drainage, 154
 - Nutter valve, 129
 - sieve tray with downcomers, 126, 127, 174, 195
 - sieve tray without downcomer, 205
 - spacing, 168
- Tray liquid drainage, 154
- Tray performance, mechanical designs, 122
- Tray stability, sieve charts, 193, 194
- Tray types, 122
 - bubble cap, 122, 123
 - comparison of major contacting, 123
 - sieve or perforated, 122, 123
- Tray types for liquid paths (bubble cap), 137
 - classification of tray areas, 137
 - guide for tray type selection, 137
- Troubleshooting, distillation tray, predictive maintenance, 101, 220, 221
- Underwood algebraic distillation, 71
 - adjacent key systems, 71
 - improved alternate method, 71
 - minimum reflux ratio, example, 73
 - procedure, 71
 - split-key system, constant volatility, 72
 - variable α , adjacent keys, 71
- Unequal molal overflow, distillation, 63
- Vapor distribution, bubble cap, 171
- Vapor-liquid equilibrium curve, 3
- Weep holes, 154
- Weep point, sieve trays with downcomers
 - calculations, 184
 - correlations, 184, 286
 - minimum vapor velocity, 183
 - performance comparison, 186
 - velocity, 186
 - weeping correlations, 183
- Weeping correlations, Koch valve tray, 184, 186
 - chart comparison with sieve trays, 185, 186
 - weep point velocity, 186
 - weir height performance comparison, 186
- Weeping correlations for sieve trays w/downcomers
 - calculations, 184
 - charts, 183
- Weirs, 134
 - bottom tray seal pan, 170
 - correction factor for segmental, 159
 - height liquid over, 159
 - inlet, 170
 - length, design chart, 155
 - throw over outlet segmental, 170
- Wetted packing, fraction, 317
- Winn, F.W., 24, 25
- x-y diagram, benzene-toluene, 26
- x-y diagram, ethanol-water, 73
- Yaw's recovery of non-key components, 86
- Yaw's short-cut multicomponent distillation, 69



RULES OF THUMB FOR CHEMICAL ENGINEERS

Carl Branan, Editor

Packed full of useful information, this volume helps you solve field engineering problems with its hundreds of common sense techniques, shortcuts, and calculations. The safety chapter covers lowers explosive limit and flash, flammability, as well as static charge.

1994. 368 pages, figures, tables, charts, appendixes, index, large-format flexible cover.
ISBN 0-88415-162-X
#5162 \$79 £57

GAS PURIFICATION

Fifth Edition

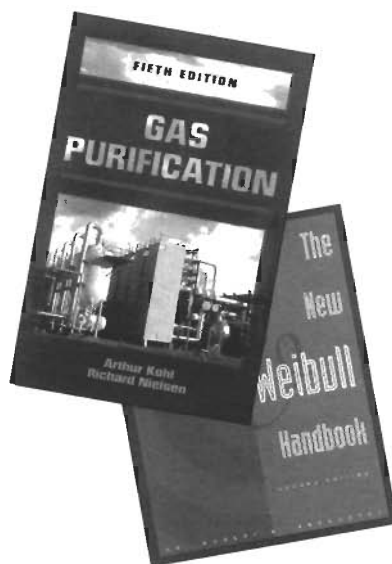
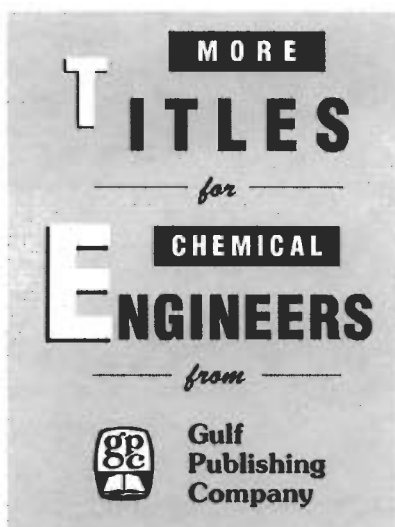
Arthur Kohl and Richard Nielsen

With its practical process and equipment design descriptions, this is the most complete, authoritative engineering treatment of gas and dehydration purification processes available. This new edition covers all the noteworthy advances in the field.

1997. 1,344 pages, figures, photos, graphs, tables, index, 6" x 9" hardcover. ISBN 0-88415-220-0
#5220 \$195 £157



<http://www.gulfpub.com>



Visit Your Favorite Bookstore

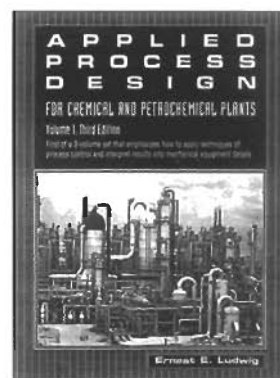
Or order directly from:

Gulf Publishing Company
P.O. Box 2608 • Dept. MR
Houston, Texas 77252-2608
713-520-4444 • FAX: 713-525-4647

Send payment plus \$11.95 (\$15.55 if the order is \$100 or more, \$17.95 for orders of \$150 or more) shipping and handling or credit card information. CA, IL, PA, TX, and WA residents must add sales tax on books and shipping total.

Prices and availability subject to change without notice.

Thank you for your order!



APPLIED PROCESS DESIGN FOR CHEMICAL AND PETROCHEMICAL PLANTS

Volumes 1, 2, and 3

Ernest E. Ludwig

This top reference shows you how to apply the techniques of process design and how to interpret results into mechanical equipment details.

Volume 1: Third Edition

1995. 630 pages, figures, photos, graphs, tables, charts, index, 8-3/8" x 10-7/8" hardcover.
ISBN 0-88415-025-9
#5025 \$150 £94

Volume 2: Third Edition

1997. 484 pages, figures, photos, graphs, tables, charts, index, 8-3/8" x 10-7/8" hardcover.
ISBN 0-88415-101-8
#5101 \$150 £94

Volume 3: Second Edition

1983. 506 pages, figures, photos, graphs, tables, charts, author and subject indexes, 8-3/8" x 10-7/8" hardcover. ISBN 0-87201-754-0
#1754 \$95 £60

THE NEW WEIBULL HANDBOOK

Second Edition

Robert B. Abernethy

This second edition includes the author's latest research findings, most notably, which numerical method is best and when. Special methods, such as Weibayes, are presented with actual case studies.

1996. 252 pages, figures, tables, 8 1/2" x 11" lay-flat paperback. ISBN 0-88415-507-2
#5507 \$89 £63

Applied Process Design for Chemical and Petrochemical Plants

Volume 2 Third Edition

Now in a new, completely revised third edition, Volume 2 further establishes the status of this 3-volume classic as an indispensable reference for design engineers in the chemical and petrochemical industries.

This latest edition covers the technical performance and mechanical details of converting chemical and petrochemical processes into the appropriate hardware for distillation and packed towers. It incorporates recent advances and major innovations in distillation contacting devices and features new generations of packing. In addition, this new edition reflects the significant progress that has been made in process design techniques in recent years.

Volume 2's example calculation techniques guide in the preparation of preliminary and final rating designs. In some instances, the book includes manufacturers' procedures and notes clearly indicate when manufacturers should verify results.

Throughout the text, new illustrations and rating charts provide the process designer/engineer with greater latitude in evaluating processes and selecting hardware for different applications. To give the designer new ways to verify calculations, Volume 2 includes important findings from recent literature to illustrate alternate design methods.

The references and bibliography are updated and substantially expanded.

All three volumes of **Applied Process Design for Chemical and Petrochemical Plants** serve engineers by providing organized design procedures, equipment suitable for application selection, and charts in readily usable form. Process engineers, designers, and operators will find more chemical petrochemical plant design data in:

Volume 1/Third Edition, which covers process planning, scheduling, and flow-sheet design, fluid, flow, pumping of liquids, mechanical separations, mixing of liquids, ejector and vacuum systems, and pressure-relieving devices.

Volume 3/Second Edition, which covers heat transfer, refrigeration systems, compression surge drums, and mechanical drivers.

Ernest E. Ludwig, P.E., is a Fellow of the American Institute of Chemical Engineers and a past member of the American Society of Mechanical Engineers. A registered professional chemical engineer in Louisiana, he specializes in plant design, operations, and management in the chemical and petrochemical industry and focuses on controlling industrial fires and explosions.

Product #5101



Gulf Professional Publishing

an imprint of Butterworth-Heinemann

<http://www.gulfp.com>

ISBN 0-88415-101-8



50000



9 780884 151012

